



OLLSCOIL NA GAILLIMHE  
UNIVERSITY OF GALWAY

**Croke Park, Dublin, Ireland  
9-10 October, 2024**

**44<sup>th</sup> AIVC Conference  
12<sup>th</sup> TightVent Conference  
10<sup>th</sup> venticool Conference**

**Retrofitting the Building Stock:  
Challenges and Opportunities for  
Indoor Environmental Quality**

**PROCEEDINGS**

**Supporting Organizers:**



## **Conference scope**

In a world striving to achieve carbon neutrality by 2050, it is imperative to strike a balance that sustains both our environment as well as the health and comfort of the individuals inhabiting buildings. Considering that 90% of the current buildings are projected to remain in the year 2050, retrofitting the existing building stock is paramount to reaching decarbonisation goals.

From the perspective of climate goals, reducing energy use in the built environment via energy retrofit and climate neutral newly constructed buildings are critical. However, it is crucial to prioritise indoor environmental quality when reducing energy usage to meet climate targets. Well-designed and executed retrofits are needed to reduce carbon emissions while ensuring healthy indoor environments. Building retrofit professionals, energy conservation experts, ventilation system designers & installers, and indoor air quality specialists must collaborate on innovative solutions to achieve these multifaceted objectives. AIVC 2024 will serve as a multidisciplinary platform to address the emerging challenges by exchanging cutting-edge ideas, research findings, policies and industrial experiences.

Since its 40<sup>th</sup> year of operation and annual Conference, the AIVC board has been offering authors the opportunity for a peer review of their paper. The procedure is twofold including 2 separate calls for abstracts & papers depending on whether the authors are interested in the peer review of their papers or not.

The papers which have been peer reviewed are indicated in the table of contents.

## Editors

Peter Wouters (*INIVE*), Arnold Janssens (*INIVE/Ghent University*), Maria Kapsalaki (*INIVE*)

## Scientific Committee

### Australia

Riccardo Paolini University of New South Wales

### Austria

Peter Holzer Institute of Building Research & Innovation ZT-GmbH

### Belgium

Hilde Breesch KU Leuven

Samuel Caillou Buildwise

Arnold Janssens Ghent University

Jelle Laverge Ghent University

Peter Wouters INIVE

### China

Zhengtao Ai Hunan University

Guoqiang Zhang Hunan University

### Denmark

Alireza Afshari Aalborg University

Bjarne Olesen Technical University of Denmark

Carsten Rode Technical University of Denmark

Pawel Wargocki Technical University of Denmark

### France

Gaëlle Guyot Cerema

Valérie Leprince Cerema

Adeline Melois Cerema

Bassam Moujalled Cerema

Laure Mouradian CETIAT

### Germany

Gunnar Grün Fraunhofer-Institut für Bauphysik IBP

### Hungary

Laszlo Fulop University of Pecs

Zoltan Magyar Budapest University of Technology and Economics

### Ireland

Marie Coggins NUI Galway

Hala Hassan NUI Galway

Marion Jammet Irish Green Building Council

Simon Jones Air Quality Matters

James McGrath Maynooth University

Michelle McDermott Occupational Hygiene Society of Ireland

Asit Kumar Mishra University College Cork &

Technical University of Denmark

Adam O'Donovan Munster Technological University

Paul O'Sullivan Munster Technological University

Susan Vickers Cluid Housing

### Italy

Michele Zinzi ENEA

Marco Simonetti Politecnico di Torino

### Japan

Yoshihiko Akamine  
Takao Sawachi  
Hiroshi Yoshino

**Netherlands**

Wouter Borsboom  
Willem de Gids  
Jaap Hogeling

**New Zealand**

Manfred Plagmann  
Yu Wang

**Norway**

Kari Thunshelle

**Republic of Korea**

Dong Hwa Kang  
Yun Gyu Lee

**Spain**

Pilar Linares Alemparte

Sonia García Ortega

**Sweden**

Jan-Olof Dalenbäck

**United Kingdom**

Benjamin Jones  
Maria Kolokotroni

**United States of America**

Andrew Persily  
Max Sherman  
Ian Walker  
Don Weekes

NILIM  
Building Research Institute  
Tohoku University

TNO  
ventGuide  
REHVA

BRANZ  
BRANZ

SINTEF Byggforsk

University of Seoul  
Korea Institute of Construction Technology

The Eduardo Torroja institute for Construction Science-  
CSIC  
The Eduardo Torroja institute for Construction Science-  
CSIC

Chalmers University of Technology

University of Nottingham  
Brunel University London

NIST  
LBNL  
LBNL  
IEQ-GA

ISSN: 3041-5128  
ISBN: 978-2-930471-68-6  
EAN: 9782930471686

# Conference Organizers

## **INIVE (International Network for Information on Ventilation and Energy performance)**

[INIVE](#) (International Network for Information on Ventilation and Energy Performance) was created in 2001. The main reason for founding INIVE was to set up a worldwide acting network of excellence in knowledge gathering and dissemination. At present, INIVE has as member organisations [Buildwise](#), [CETIAT](#), [Ghent University](#), [Fraunhofer – IBP](#), [KU Leuven](#)).

INIVE has multiple aims, including the collection and efficient storage of relevant information, providing guidance and identifying major trends, developing intelligent systems to provide the world of construction with useful knowledge in the area of energy efficiency, indoor environment, ventilation and airtightness of buildings. Building energy- and environmental performance regulations are another major area of interest for the INIVE members, especially in relation to the implementation of the European Energy Performance of Buildings Directive. With respect to the dissemination of information, INIVE aims for the widest possible distribution of information.

INIVE is coordinating and/or facilitating various international projects, e.g. the Air Infiltration and Ventilation Centre – [AIVC](#), [Dynastec](#), the Indoor Environmental Quality – Global Alliance – [IEQ-GA](#), the [TightVent Europe platform](#), and the [venticool](#) platform. INIVE has also coordinated the ASIEPI project (01/10/2007 – 31/03/2010) dealing with the evaluation of the implementation and impact of the EU Energy Performance of Buildings Directive, the QUALICheck project and platform aiming towards improved compliance and quality of the works for better performing buildings, the European portal on Energy Efficiency – [BUILD UP](#) and the EPBD feasibility study 19a.



## **AIVC**

The AIVC ([www.aivc.org](http://www.aivc.org)) activities are supported by the following countries: Australia, Belgium, China, Denmark, France, Ireland, Italy, Japan, Netherlands, New Zealand, Norway, Republic of Korea, Spain, Sweden, UK and USA.

Created in 1979, the Air Infiltration and Ventilation Centre ([www.aivc.org](http://www.aivc.org)) is one of the projects/annexes running under the International Energy Agency's Energy in Buildings and Communities Programme. With the support of 16 member countries as well as key experts and associations (IEQ-GA, REHVA, IBPSA, ISIAQ), the AIVC offers industry and research organisations technical support aimed at better understanding the ventilation challenges and optimising energy efficient ventilation

Since 1980, the annual AIVC conferences have been the meeting point for presenting and discussing major developments and results regarding infiltration and ventilation in buildings.

AIVC combines forces with the TightVent Europe and venticool platforms aiming at facilitating exchanges and progress on airtightness and ventilative cooling issues, which are major topics of this conference.



## **TightVent Europe**

The [TightVent Europe](#) ‘Building and Ductwork Airtightness Platform’ was launched in January 2011. TightVent Europe aims at facilitating exchanges and progress on building and ductwork airtightness issues, including the organization of conferences, workshops and webinars. It fosters experience sharing as well as knowledge production and dissemination on practical issues such as specifications, design, execution, control, etc., taking advantage of the lessons learnt from pioneering work while keeping in mind the need for adequate ventilation. In September 2012, the TightVent Airtightness Associations Committee (TAAC) was also launched with the primary goal of promoting reliable testing/inspection and reporting procedures. TAAC gathers both TightVent partners and TAAC members (experts or representatives of airtightness testers in their countries).

TightVent Europe has been initiated by INIVE (International Network for Information on Ventilation and Energy Performance) with at present the financial and/or technical support of the following partners: [Lindab](#), [MEZ-TECHNIK](#), [Retrotec](#), [Acin Instrumenten](#), [BCCA](#), [BlowerDoor GmbH](#), [Build Test Solutions](#), [dooApp](#), [Soudal](#), [Eurima](#), [Gonal](#), [SIGA](#) and [BPIE](#).



## **venticool**

[venticool](#) is the international ventilative cooling platform launched in October 2012 to accelerate the uptake of ventilative cooling by raising awareness, sharing experience and steering research and development efforts in the field of ventilative cooling. In 2020, venticool decided to broaden its scope towards resilient ventilative cooling.

The platform supports better guidance for the appropriate implementation of resilient ventilative cooling strategies as well as adequate credit for such strategies in building regulations.

The platform philosophy is to pull resources together and to avoid duplicating efforts to maximize the impact of existing and new initiatives. venticool joins forces with international projects (in particular [IEA EBC Annex 62](#) (ventilative cooling), [IEA EBC annex 80](#) (Resilient cooling for buildings) and more recently [IEA EBC annex 87](#) (Energy and Indoor Environmental Quality Performance of Personalised Environmental Control Systems) as well as organizations with significant experience and/or well identified in the field of ventilation and thermal comfort like [AIVC](#) and [REHVA](#).

venticool was initiated by INIVE (International Network for Information on Ventilation and Energy Performance) with the financial and/or technical support of the following partners: [Agoria](#), [Velux](#), [Reynaers Aluminium](#), [WindowMaster](#), [Active House](#), [CIBSE nvg](#), [Eurowindoor](#) and [REHVA](#).



## **Maynooth University**

[Maynooth University](#), situated just 25 kilometres outside Dublin, Ireland, is a globally recognised institution. Located in Ireland's only university town, its distinctive features and character owe much to its unique history and heritage. Established as an autonomous university in 1997, its roots trace back to the foundation of the Royal College of St. Patrick in 1795, boasting a rich heritage of over 200 years in education and scholarship. In the 2022 Times Higher Education (THE) Best Young University Rankings, Maynooth University was ranked #1 in Ireland and 85th globally.

Maynooth University is a place of lively contrasts – a modern institution, dynamic, rapidly growing, research-led, and engaged, yet grounded in historic academic strengths and scholarly traditions. Today, the university embodies a unique blend of modernity and tradition. Maynooth University's Strategic Plan for 2023-2028 focuses on research beacons, 'Health and Wellbeing,' 'Sustainability and Climate Change,' 'Data and Digital Transformation,' and 'Society and Public Policy.'

The university's distinctive, collegial culture encourages an interdisciplinary research approach, a quality evident in the contributions of its world-class academics. Together, they tackle some of society's most fundamental challenges, making Maynooth University a vibrant hub of innovation and intellectual exploration.



## **University of Galway**

The [University of Galway](#) was established in 1845 and is currently ranked in the top 2% of universities in the world, among the top 100 in Europe and in the top 50 in the world for progress in line with the UN Sustainable Development Goals.

The University of Galway is a bilingual university (English and Irish), comprised of four colleges, 18 schools and five research institutes, with around 20,000 students, including around 3,000 international students. The University has been accredited with an Athena SWAN Institutional Bronze Award, and 11 out of the 18 schools hold individual Athena SWAN Awards. The University has more than 2,500 staff, and research collaborations with 4,675 international institutions in 137 countries. The University of Galway has 133,000 alumni, 98% of graduates are in employment or further study within six months.

SEAI is funded by the Government of Ireland through the Department of the Environment, Climate and Communications.



OLLSCOIL NA GAILLIMHE  
UNIVERSITY OF GALWAY

## SEAI

[SEAI](#) is Ireland's national energy authority investing in, and delivering, appropriate, effective, and sustainable solutions to help Ireland's transition to a clean energy future. We work with Government, homeowners, businesses, and communities to achieve this, through expertise, funding, educational programmes, policy advice, research, and the development of new technologies.

SEAI is funded by the Government of Ireland through the Department of the Environment, Climate and Communications.



## Supporting Organizers





## Event sponsors

The conference organizers are grateful to the following companies for their support to this event

### *TightVent Partners*



### *Venticool Partners*



### *Other Sponsors/ Exhibitors*



# Table of Contents

<b>Breathing Better: Evaluating the Impact of Personalized Ventilation in Daycare Baby Beds</b>	21
<i>Hailin Zheng, Marcel Loomans, Shalika Walker, Zhijian Wang, Wim Zeiler</i>	
<b>Building airtightness for renovations Leaflets (Germany)</b>	31
<i>Stefanie Rolfsmeier</i>	
<b>Achieving suitable airflow rate in New Zealand classrooms: a CFD approach to inform on potential retrofitting solutions</b>	35
<i>Mikael Boulic, Pierre Bombardier, Andrew Russell, David Waters, Angelo Cuyo, Hennie van Heerden, Jean-Richard Templier, Robyn Phipps</i>	
<b>On the impact of night ventilation through motorized windows on the energy and thermal performance of office buildings</b>	49
<i>Michele Zinzi, Martina Botticelli, Sabrina Romano, Stefano Agnoli</i>	
<b>Exploring the impact of the urban modified albedo on the indoor temperature and the ventilative cooling potential in a typical Italian residential building</b>	59
<i>Michele Zinzi, Stefano Agnoli, Sabrina Romano, Anna Maria Siani, Serena Falasca</i>	
<b>Cognitive well-being in classrooms: A holistic investigation into Indoor Environmental Quality in New Zealand primary schools</b>	69
<i>Lara Tookey, Mikael Boulic, Ilaria Stura, Wyatt Page, Pawel Wargocki, Hennie van Heerden</i>	
<b>Particle concentration and indoor air quality in naturally ventilated patient rooms-A field study in a hospital building in Bucharest, Romania</b>	81
<i>Mohamed Elsayed, Natalia Lastovets, Ville Silvonen, Anni Luoto, Topi Rönkkö, Piia Sormunen</i>	
<b>Performance optimization of an office building with a dynamic façade system</b>	91
<i>Zhijian Wang, Magdalena Hajdukiewicz, Pieter-Jan Hoes, Marcel G.L.C. Loomans</i>	
<b>Exploring the use of TABS and Peak-Shift Control in Office Buildings</b>	101
<i>Honoka Kyojuka, Kiyoto Koga, Yasuyuki Shiraishi, Arash Erfani, Dirk Saelens</i>	
<b>Proposal of a design method for radiant ceiling cooling system using CFD analysis</b>	108
<i>Rio Matsumoto, Jianan Liu, Yasuyuki Shiraishi, Fujio Tamura, Daiki Yamashina, Masahiro Yamamoto, Sae Senda</i>	
<b>Ventilation performance in cultural centres in Flanders</b>	115
<i>Niels De Kempeneer, Mart Verlaek, Sophie De Mulder, Gitte Schreurs, Maja Mampaey, Karen Van Campenhout</i>	
<b>Evaluating the Long-term Performance of Air Barrier Systems in Modern Buildings</b>	125
<i>Sean O'Brien, David Artigas</i>	

<b>Ventilation guidelines for Flemish childcare and psychological care centres</b>	135
<i>Quinten Carton, Douaa Al-Assaad, Liesje Van Gelder, Maarten De Strycker, Hilde Breesch</i>	
<b>Semantics-based expert system for fault detection in air handling units</b>	145
<i>Sebastian Blechmann, Hannah Görigk, Rita Streblow, Dirk Müller</i>	
<b>Health-Equivalent Energy Efficiency Factor, combined metric of harm and energy use</b>	155
<i>Klaas De Jonge</i>	
<b>Numerical performance evaluation of ventilation systems for energy-efficient retrofitting of existing houses in France</b>	165
<i>Louison Boulier, Daniela Mortari, Bassam Moujalled, Nolwenn Hurel, Gaëlle Guyot, Franck Alessi, Ophélie Ouvrier Bonnaz, Mélina Echivard, Sylvain Berthault</i>	
<b>Effects of closed vertical void on natural ventilation in double-loaded apartment building</b>	176
<i>Tetsu Kubota, Hayato Shima, Hanief Sani, Nikhil Kumar, Haruka Kitagawa, Takashi Asawa, Muhammad Nur Fajri Alfata</i>	
<b>The Impact of Simplified Window and Exhaust Fan Assumptions on Model-Based Predictions of Inter-Zonal Air Flow and Contaminant Transport in Multifamily Buildings</b>	184
<i>Iain S. Walker, Brennan D. Less, Cara H. Lozinsky, Núria Casquero-Modrego, Michael D. Sohn</i>	
<b>Application strategies and effectiveness of CO<sub>2</sub> signal lights for improving indoor air quality in classrooms</b>	194
<i>Simon Beck, Gabriel Rojas</i>	
<b>Performance evaluation of humidity controlled decentralized ventilation systems in social housing in Chile</b>	209
<i>Gilles Flamant, Waldo Bustamante, Arnold Janssens, Jelle Laverge</i>	
<b>Airborne transmission in a meeting room with mixing and displacement ventilation</b>	220
<i>Risto Kosonen, Weixin Zhao, Simo Kilpeläinen, Juha Jokisalo</i>	
<b>A novel method for the characterization of infiltration airflow using infrared thermography</b>	227
<i>Diego Tamayo-Alonso, Irene Poza-Casado, M.Á. Padilla-Marcos, Lida Mercado, Alberto Meiss</i>	
<b>Control of airborne particle concentrations in a meeting room with stand-alone air cleaners: influence of type, airflow rate, flow pattern and position in the room</b>	234
<i>Mirela Robitu, Alain Ginestet, Benoît Golaz, Dominique Pugnet, Lionel Boiteux, Jean-Marc Thiebaut</i>	

<b>Direct adiabatic cooling systems – Resilience to climate change for industrial building applications in a Mediterranean climate</b>	244
<i>Antoine Breteau, Patrick Salagnac, Jean-Marie Caous, Emmanuel Bozonnet</i>	
<b>Experimental and simulation analysis of different natural ventilation scenarios and their relation with IAQ in office buildings</b>	254
<i>Giannis Papadopoulos, Ioannis Sakellaris, Evangelos I. Tolis, John G. Bartzis,, Giorgos Panaras</i>	
<b>Assessing the level of adaptation to heat waves in Parisian housing</b>	264
<i>Letizia Roccamena, Jean-Marie Alessandrini, Pierrick Gervasi, Julien Guilhot, Georgios Kyriakodis, Simon Molesin, Maeva Sabre, Wenjuan Wei</i>	
<b>Air Pressure Differences over the Building Envelope: Case Studies</b>	274
<i>Lara Deprez, Kevin Verniers, Ivan Pollet, Niek-Jan Bink, Jelle Laverge</i>	
<b>Evaluating the IAQ and energy performance of two types of ventilation systems in multifamily buildings</b>	284
<i>Zohreh Kiani, Ali Alexander Nour Eddine, Kévin Taurines, Kátia Cordeiro Mendonça, Marc Abadie</i>	
<b>Comprehensive analysis of indoor air quality in a real home using low-cost sensors</b>	288
<i>Marc Olivier Abadie, Kátia Cordeiro Mendonça</i>	
<b>Summertime Resilience in an L-Shaped Long-Term Care Facility with Mixed Natural Ventilation and Pressurized Corridors</b>	298
<i>Chang Shu, Lili Ji, Justin Berquist, Liang Grace Zhou</i>	
<b>Assessment of SARS-CoV- and other IAQ parameters in Belgian elderly care homes</b>	307
<i>Sarah L. Paralovo, Annelies Asteur, Borislav Lazarov, Boudewijn Catry, Koenraad Van Hoorde, Maarten Spruyt, Katrien Latour, Marianne Stranger</i>	
<b>The Influence of Outdoor Conditions on Indoor Air Quality: Case Study of Norwegian Schools</b>	317
<i>Iselin Ørbek Eide, Christer Eskedal, Kai Gustavsen, Kent Hart, Azimil Gani Alam, Guangyu Cao</i>	
<b>Impact of filter class and airflow control on the indoor airborne particles in a nursery school</b>	328
<i>Mirela Robitu, Alain Ginestet, Dominique Pugnet, Jean-Hugues Salazar</i>	
<b>Data Analysis of Indoor Air Quality and Thermal Comfort in Dwellings in Santiago, Chile</b>	338
<i>Constanza Molina, Benjamin Jones, Ignacio Garrido, Gioberti Morantes</i>	

<b>The protection from harm to populations of people provided by Exposure Limit Values</b>	344
<i>Benjamin Jones, Gioberti Morantes, Constanza Molina, Max Sherman, James A. McGrath</i>	
<b>Challenges in measurement for clean air in public indoor environment</b>	351
<i>Ralph Krause, Ralf Heidenreich</i>	
<b>The relationship between airtightness and summertime infiltration rates</b>	356
<i>Ben M. Roberts, David Allinson, Kevin J. Lomas</i>	
<b>Intervention study of climate correlation model predictions for occupant control of indoor environment</b>	363
<i>Maria Kolokotroni, May Zune, Thet Paing Tun, Ilia Christantoni, Dimitra Tsakanika, Dorota Stawowczyk, Tristan de Kerchove d'Exaerde</i>	
<b>IAQ-label for Belgian public spaces: Monitoring in 11 public spaces</b>	373
<i>Klaas De Jonge, Arnold Janssens</i>	
<b>Test facility for building envelope leakage type analysis and improvement of acoustic and thermographic airtightness measurement methods</b>	381
<i>Markus Diel, Björn Schiricke, Johannes Pernpeintner</i>	
<b>RENOVAIR: Study of the evolution of airtightness, ventilation, comfort and indoor air quality in 7 energy renovation operations of social housing in France</b>	392
<i>Andrés Litvak, Eddy Handtschoewercker</i>	
<b>Experimental study on the dehumidification performance of a window-type liquid desiccant ventilation system</b>	402
<i>Jabin Goo, Woo Hyoung Lee, Hyo Beom Jung, Dong Hwa Kang, Hyun Wook Park, Dong Hee Choi</i>	
<b>Optimization of airflow rate in a displacement-ventilated room to minimize particle inhalation risk and control energy consumption</b>	405
<i>Alicia Murga, Haruki Nakagawa, Rahul Bale, Makoto Tsubokura</i>	
<b>Adaptive comfort technology for temperature control in balanced ventilation systems</b>	408
<i>Bart Cremers</i>	
<b>Uncertainty of IAQ and energy performance schemes for residential smart ventilation</b>	416
<i>Baptiste Poirier, Gaelle Guyot, Monika Woloszyn</i>	
<b>Assessment of thermal environment and thermal comfort in air traffic control towers</b>	427
<i>Bassam Moujalled, Fabrice Richieri, Adeline Mollard, Mathilde Hostein</i>	

<b>Assessment of in-situ aging and maintenance impact on Relative Humidity-Controlled Mechanical Extract Ventilation (RH-MEV) Systems: A Case study in multifamily social housing buildings</b>	437
<i>Juan Rios, Marc Legree, Adeline Mélois, Ambre Marchand Moury</i>	
<b>Evaluation of the impact of window use on the heating energy use and IEQ in dwellings based on simulations</b>	446
<i>Silke Verbruggen, Arnold Janssens, Jelle Laverge</i>	
<b>Literature Review on Windows Airtightness Performances: Insights and Gaps</b>	454
<i>Martin Prignon</i>	
<b>Exploring the Effect of Post-Pandemic Behaviour of Occupants on Indoor Air Quality and Comfort Conditions in Existing Residential Buildings in Turkiye</b>	467
<i>Büşra Karadeniz Akkoç, Gülsu Ulukavak Harputlugil</i>	
<b>Assessment of PM2.5 particulate matter exposure under different ventilation and air filtration strategies in a kindergarten</b>	470
<i>J. L. Sánchez-Jiménez, M. Ruiz de Adana</i>	
<b>Proposal of a More Reliable Model and Procedures for Estimating Operational Leakage in Air Systems.</b>	480
<i>Federico Pedranzini</i>	
<b>Experimental assessment of a resilient air-cooling system under extreme heat events in southern European climate conditions</b>	492
<i>María Jesús Romero-Lara, Francisco Comino, Manuel Ruiz de Adana</i>	
<b>Examining the Impact of Improving the Airtightness of the Building Envelopes on Differential Pressures and Contaminant Dispersion in Temporary Negative Pressure Isolation Rooms</b>	502
<i>Jooyeon Roh, Shinhye Lee, Wonseok Lee, Sejin Lee, Myoung-souk Yeo</i>	
<b>Trends in Indoor Environmental Quality in Non-Domestic Energy-Efficient Buildings in Ireland: The BENEFIT Project</b>	505
<i>Jorge Fernandes, Miriam Byrne, Adam Collison, James A. McGrath</i>	
<b>Design and performance verification methods for naturally ventilated buildings from the experience of ABC 21 EU Project</b>	508
<i>Izabella Milto, Silvia Erba, Andrea Sangalli, Guilherme Carrilho da Graça, François Garde, Lorenzo Pagliano</i>	
<b>Estimation of Airborne Particle Removal Efficiency in Personal Isolation Room based on Full-scale Experiment</b>	526
<i>Shinhye Lee, Hyunmin Kim, Jooyeon Roh, Myoung-souk Yeo</i>	
<b>Temperature, Relative humidity and Indoor Air Quality in office buildings and their subjective evaluation</b>	529
<i>Yoshinori Honma, Kei Shimonosono, Kenichi Azuma, Dai Shimazaki, Kenichi Kobayashi, Michiko Bando, Naoe Nishihara</i>	

<b>Measurements in Greece of installed windows and comparison between the given air permeability classification and the classification applied to the building envelope</b>	539
<i>Theodoros Sotirios Tountas</i>	
<b>Numerical simulation guided design of novel experimental chamber used to assess the effectiveness of ventilation strategies with hygro-regulated air terminals</b>	546
<i>Jean Paul Harrouz, Bassam Moujalled, Michel Ondarts, Benjamin Golly, Adeline Mélois, Gaëlle Guyot, Jérémy Depoorter</i>	
<b>Assessment of Airborne Cross-infection Risk Across Various Body Orientations in Indoor Airflow Environments</b>	558
<i>Hee Won Shin, Hyun Wook Park, Jae Hyun Park, Dong Hwa Kang</i>	
<b>Proposal for improving the linear regression method and uncertainty calculation in building airtightness tests</b>	560
<i>Benedikt Kölsch, Valérie Leprince</i>	
<b>Optimizing the design of retirement homes concerning the indoor environment, energy efficiency, and climate change resiliency</b>	569
<i>Julie Lindgaard Hald, Daria Zukowska-Tejsen, Jakub Kolarik</i>	
<b>Room integrity tests and registration of the actual situation regarding the fire protection and holding times in fire compartments in Greece</b>	572
<i>Theodoros Sotirios Tountas</i>	
<b>Performance 2 project - Analysis of the interactions between the Humidity-based DCV systems and IAQ in homes 15 years after their construction</b>	577
<i>Adeline Mélois, Ambre Marchand Moury, Juan Rios, Marc Legrée, Jérémy Depoorter, Sylvain Rebières, Gaëlle Guyot</i>	
<b>Review and analysis of existing diagnostic methods for characterizing air transfers in existing homes</b>	587
<i>Imane Mannan, Adeline Mélois, Bassam Moujalled, Luke Smith, Christopher Wood, Xiaofeng Zheng</i>	
<b>Evaluation of Indoor Environmental Quality and Thermal Environment in Airtight Energy-Efficient Naturally Ventilated Dwellings</b>	597
<i>Ibrahim Alhindawi, James McGrath, Divyanshu Sood, James O'Donnell, Miriam Byrne</i>	
<b>A Longitudinal Study to Assess Indoor Environmental Quality in Airtight Energy-Efficient Naturally Ventilated Dwellings</b>	600
<i>Ibrahim Alhindawi, James McGrath, Divyanshu Sood, James O'Donnell, Miriam Byrne</i>	
<b>Are Irish Low Energy School Designs Resilient Against Overheating?</b>	603
<i>Elahe Tavakoli, Adam O'Donovan, Paul D. O'Sullivan</i>	

<b>Experimental evaluation of the bidirectional filtration efficiency of respirators and face masks against airborne particles during cyclic breathing</b> <i>Dennis Derwein, Tobias Maria Burgholz, Kai Rewitz, Dirk Müller</i>	613
<b>Assessment of the indoor/outdoor dynamic of some air pollutants in three buildings located in the valley city of Chambéry, France</b> <i>Diana Decilap, Gaëlle Guyot, Jean-Luc Besombes, Benjamin Golly</i>	621
<b>Leakage in Large-Building Duct Systems: Modelling the Savings for Various Applications</b> <i>Mark Modera, Mahmood Farzaneh Gord</i>	627
<b>Performance of smart ventilation in residential buildings: a literature review</b> <i>Yu Wang, Daniela Mortari, Manfred Plagmann, Nathan Mendes, Gaëlle Guyot</i>	637
<b>IEQ and energy performance of residential smart ventilation strategies in France</b> <i>Raïssa Andrade, Gaëlle Guyot</i>	648
<b>Particulate matter in UK school classrooms – building an evidence base for improving classroom air quality</b> <i>Alice Handy, Henry Burridge, the SAMHE consortium</i>	653
<b>Utilization of ventilation systems to maintain selected environmental comfort parameters at the required level</b> <i>Małgorzata Basińska, Joanna Kubiak, Michał Michalkiewicz</i>	656
<b>Quantifying ventilation rates in heterogeneous rooms based on point measurements of carbon dioxide</b> <i>Joshua Finneran, Henry C Burridge</i>	659
<b>Incomplete resistance; ventilation, mould growth and built in furniture in a 1930's Dublin clinker concrete apartment building</b> <i>Gearóid Carvilla, Joseph Little, Andrew Lundberg</i>	662
<b>Log-normal distribution for radon measurements in one room</b> <i>J. Kubiak, M. Basińska</i>	665
<b>On the estimate and reduction of the zero-flow pressure estimation uncertainty in fan pressurization measurement</b> <i>Martin Prignon, Christophe Delmotte, Benedikt Kölsch</i>	672
<b>A Pre-Post Retrofit Evaluation on Indoor Air Quality and Comfort in Classrooms and Offices: Pre-Retrofit Findings</b> <i>Adam Collison, Miriam Byrne, James A. McGrath</i>	684
<b>Assessing the Prediction of Human CO2 Emissions for IAQ Applications</b> <i>Oluwatobi Oke, Andrew Persily</i>	687



<b>Applying a composite indoor environmental quality indicator to Danish office spaces: The TAIL rating scheme</b>	694
<i>Asit K Mishra, Dania T Pharaon, Ida B Feldskou, Lina F Præstegaard, Pawel Wargocki</i>	
<b>Thermal comfort of adolescent children in classrooms: Some reflections on the state-of-the-art</b>	697
<i>Asit K Mishra, Pawel Wargocki, Eilis J O'Reilly</i>	
<b>Estimating the health impact of exposure to indoor PM2.5 concentrations in Irish deep energy retrofitted residential dwellings – ARDEN</b>	700
<i>Hala Hassan, Asit Kumar Mishra, Hilary Cowie, Marie Coggins</i>	
<b>Filling the Indoor Air Quality Data Gap: Research Challenges and Opportunities</b>	704
<i>Gráinne McGill, Marco-Felipe King, James McGrath, Douglas Booker</i>	
<b>Balanced ventilation - energy efficient and healthy</b>	707
<i>Piet Jacobs, Wim Kornaat, Wouter Borsboom</i>	
<b>Indoor air quality post deep energy retrofit in social homes in Ireland (HAVEN)</b>	714
<i>Marie Coggins, Daniel Norton, Asit Kumar Mishra, Victoria Hogan, Nina Wemken, Hala Hassan, Medeina Macenaite</i>	
<b>Calibration methodology for combined heating and ventilation models</b>	717
<i>Wouter Borsboom, Ruud van der Linden</i>	
<b>Perceptions of thermal comfort following deep energy retrofit in social homes in Ireland (HAVEN)</b>	727
<i>Victoria Hogan, Daniel Norton, Asit Kumar Mishra, Nina Wemken, Hilary Cowie, Marie Coggins</i>	
<b>Investigating the Impacts of New Energy Renovation Strategies on Indoor Environmental Quality</b>	730
<i>Buddila Wijeyesekera, Miriam Byrne, James O'Donnell, Reihaneh Aghamolaei, James A. McGrath</i>	
<b>Decarbonization Within the Path of Sustainable Development Goals</b>	733
<i>Constanza Molina</i>	
<b>Retrofitting and Ventilation: Challenges, Benefits and Lessons Learnt</b>	735
<i>James A. McGrath</i>	
<b>Impact of dust build-up on building airtightness durability: preliminary results of the Durabilitair2 project</b>	737
<i>Andrés Litvak, Eddy Handschoewercker, Sylvain Berthault, Romain Mathieu</i>	
<b>On the potential of HAMSTER's bi-climatic chamber for testing building component airtightness durability</b>	739
<i>Martin Prignon</i>	

<b>Research on airtightness durability in Norway</b> <i>Tore Kolstad Linløkken, Bozena Dorota Hrynyszyn</i>	742
<b>The Recast Energy Performance of Buildings Directive: a green light for clean air?</b> <i>Ciarán Cuffe</i>	745
<b>What do we know about the current state of indoor air in buildings and associated human health effects?</b> <i>Corinne Mandin</i>	746
<b>Perfect Mixing or Imperfect Terminology</b> <i>Andrew Persily</i>	748
<b>Guidance on damp and mould: understanding and addressing the health risks in the home</b> <i>Sani Dimitroulopoulou</i>	749
<b>Risk mitigation for indoor air quality on example of construction products</b> <i>Ana Maria Scutaru</i>	751
<b>How a harm budget can be used to regulate Indoor Air Quality in Dwellings</b> <i>Benjamin Jones, Gioberttti Morantes, Constanza Molina, Max Sherman</i>	754
<b>Methodology to define new performance indicator for ventilation regulation in France</b> <i>Valérie Leprince, Baptiste Poirier</i>	757
<b>Assessing IAQ in existing residential buildings within a performance-based regulatory framework through a predictive model</b> <i>Sonia García-Ortega, Pilar Linares-Alemparte</i>	762
<b>The importance of performance-based regulations for residential ventilation. State of the art</b> <i>Gaëlle Guyot, Valérie Leprince</i>	765
<b>The IAQ performance-based regulation in Spain: description, identified problems for its application, and foreseen changes</b> <i>Pilar Linares-Alemparte, Sonia García-Ortega</i>	768
<b>Challenges and opportunities arising from different ventilation approaches: controlled experiments conducted at the Canadian Centre for Housing Technology</b> <i>Liang Grace Zhou, Yunyi Ethan Li, Janet Gaskin, Patrique Tardif</i>	776
<b>Field study measurements evaluating radon concentrations under different ventilation scenarios</b> <i>Janet Gaskin, Yunyi Ethan Li, Marcel Brascoupé, Liang Grace Zhou</i>	779
<b>Passive sumps as a method of reducing radon levels in Irish dwellings</b> <i>Alison Dowdall</i>	787

<b>Quantify Factors Influencing Radon Flux in Dwellings</b>	789
<i>Mohsen Pourkiaei, Miriam Byrne, Patrick Murphy, James A. McGrath</i>	
<b>A novel indicator to assess thermal resilience of buildings to overheating</b>	791
<i>Abantika Sengupta, Douaa Al Assaad, Hilde Breesch, Marijke Steeman</i>	
<b>Exploring the effect of different measures on thermal resilience: implications for design of HVAC systems and energy use</b>	801
<i>Debora Resta, Bert Lemmens, Hilde Breesch, Abantika Sengupta, Douaa Al-assaad, Steven Delrue, Joost Declercq, Marijke Steeman</i>	
<b>Impact of solar shading &amp; ventilative cooling control strategies on the resilience of residential buildings to overheating</b>	817
<i>Ivan Pollet, Frederik Losfeld, Steven Delrue</i>	
<b>ReCOVer++ project: wrap up</b>	827
<i>Hilde Breesch, Douaa Al Assaad, Abantika Sengupta, Marijke Steeman</i>	
<b>How to design a resilient building? Lessons learnt from an architectural view</b>	829
<i>Joost Declercq, Martijn Holvoet</i>	
<b>Indoor Thermal Resilience in Irish Schools, Office and Healthcare Buildings</b>	835
<i>Adam O' Donovan, Elahe Tavakoli, Paul D. O'Sullivan</i>	
<b>Overall outcomes from the project and next steps</b>	836
<i>Adam O' Donovan, Paul D. O'Sullivan</i>	
<b>Overheating Mitigation Policy: Current Trends &amp; Future Outlook</b>	837
<i>Paul D. O'Sullivan, Adam O' Donovan</i>	
<b>Effect of Personalized Environmental Control Systems on Occupants' Health, Comfort and Productivity</b>	838
<i>Mariya Bivolarova, Dolaana Khovalyg, Bjarne W. Olesen</i>	
<b>Personalized environmental control systems (PECS): Overview of applications, technology classification and KPIs</b>	841
<i>Kai Rewitz, Joyce Kim, Fatemeh Nabilou, Kehinde Bayode, Dirk Müller</i>	
<b>Personalized environmental control systems (PECS): Overview of evaluation methods</b>	844
<i>Douaa Al Assaad, Ilaria Pigliautile</i>	
<b>Policy Strategies and Market Perspective of Personalized Environmental Control Systems</b>	846
<i>Rajan Rawal, Bjarne Olesen, Ongun Berk Kazanci, Arsen Krikor Melikov</i>	
<b>Building ventilation requirements and inspection in Belgium</b>	849
<i>Arnold Janssens, Laura De Jonge, Maarten De Strycker, Liesje Van Gelder</i>	
<b>Trends in building ventilation requirements and inspection in France</b>	859
<i>Valérie Leprince, Gaëlle Guyot, Laure Mouradian</i>	

<b>Trends in building ventilation requirements and inspection in Ireland</b> <i>Marie Coggins, Brian McIntyre, Simon Jones, James McGrath</i>	862
<b>Trends in building ventilation requirements and inspection in Spain</b> <i>Pilar Linares-Alemparte, Sonia García-Ortega, Fernando Feldman</i>	864
<b>Design of ventilative cooling systems using Ventilative cooling standards; design steps and corresponding flow diagram</b> <i>Beat Frei, Paul D O'Sullivan</i>	872
<b>A comprehensive overview of ventilative cooling and its role in the standardization</b> <i>Christoffer Plesner, Jannick K. Roth</i>	876
<b>Early Stage Design of VC: A standardised approach to improve robustness and avoid vulnerability lock-in at the later design stages</b> <i>Paul O'Sullivan</i>	881

# Breathing Better: Evaluating the Impact of Personalized Ventilation in Daycare Baby Beds

Hailin Zheng<sup>\*</sup>, Marcel Loomans, Shalika Walker, Zhijian Wang, Wim Zeiler

*Eindhoven University of Technology, Eindhoven, the Netherlands*

*\*Corresponding author: [h.zheng1@tue.nl](mailto:h.zheng1@tue.nl)*

*Presenting author: underline First & Last name*

## ABSTRACT

Daycare centers (DCCs) are pivotal in early childhood development, serving as a primary indoor environment for young children. A notable feature of DCCs, especially in the Netherlands, is the use of semi-enclosed baby beds for children aged 0-4 years. These beds provide safety and comfort but pose challenges in maintaining healthy air quality due to their enclosed design, which is critical given infants' vulnerability to pollutants and extended daytime sleep. Prior research has indicated the need to improve the air quality in these beds, and suggested using personalized ventilation (PV) as a potential solution.

Therefore, the current study builds on this by examining the effectiveness of PV in semi-enclosed baby beds, addressing limitations of earlier research such as fixed air supply rates directed towards the wall side. Utilizing a full-scale bedroom setup with a breathing thermal baby model, it evaluated the impact of three PV airflow directions (wall-side, head-side, cover-side), five ventilation rates (21, 37, 55, 65, 75 m<sup>3</sup>/h), and three sleep positions (supine, lateral-to-corridor, and lateral-to-wall) on bed-level air quality. For comparative purposes, a control scenario employing the MV (mixing ventilation) strategy at the ventilation rate of 55 m<sup>3</sup>/h was also examined. The experimental setup, including 23 CO<sub>2</sub> sensors, provided an in-depth analysis of CO<sub>2</sub> levels at various scales, with 34 experimental cases conducted across different ventilation modes, airflow directions, rates, and sleeping positions.

The results re-confirmed the superior effectiveness of PV in mitigating exposure of metabolic CO<sub>2</sub> emissions over the conventional MV strategy under the same ventilation rates. Moreover, the study noted that increased ventilation rates typically corresponded with lower CO<sub>2</sub> levels, although the optimal rate varied depending on the specific PV strategy and sleeping position. Notably, the PV head-side strategy consistently recorded the lowest inhaled CO<sub>2</sub> concentrations, highlighting its capability in effectively removing metabolic CO<sub>2</sub> emissions.

In conclusion, this research underscores the crucial role of PV in improving air quality in DCC baby beds. It demonstrates PV's ability to optimize air quality at lower rates, suggesting energy efficiency benefits. These insights are vital for developing customized ventilation solutions in daycare environments, and advancing the understanding of bed-level air quality optimization using diverse PV strategies.

## KEYWORDS

Daycare Center; Indoor Air Quality; Personalized Ventilation; Inhaled Air Quality; Semi-enclosed Baby Bed.

## 1 INTRODUCTION

Daycare centers (DCCs) are the first educational programs for the social development of young children (infants and toddlers) prior to primary school ages, serving as the indoor environments to which they are most exposed, aside from their homes [1]. Naptimes for young children are key daily activities distinguishing DCCs from other educational facilities like schools [2], with many featuring densely populated bedrooms to accommodate this [3-6]. A notable solution for these accommodations is the semi-enclosed baby bunk bed (see **Figure 1b**), designed for 0-4-year-olds in DCCs [7]. There are three key features of this bed: safety features that prevent infant falls, a sheltered design that provides psychological comfort, and its compact size that allows for easy placement in small spaces. These features contribute to its global popularity. Notably, over 95,000 units are utilized in Dutch DCCs across more than 9,000 locations [7].

As the main occupants in DCCs, infants and toddlers are especially vulnerable to air pollutants due to their rapid and incomplete physiological development. Also, in semi-enclosed sleeping environments, young children are not able to actively control their surroundings as they are under the asleep state. Even worse, the source-proximity effect may become dominant in the bed-level environment. For example, the bed-level concentrations of volatile organic compounds (VOCs) from bedding materials can be significantly higher than in the bulk room air [8-10]. All of these factors point to the need for the investigation of ventilation conditions inside the semi-enclosed baby beds.

However, the current literature on this subject is scant. There is an existing study [11] where CO<sub>2</sub> dispersion and inhalation from a breathing thermal baby model in a semi-enclosed bed was investigated under standard room-level mixing ventilation. The findings concluded inadequate ventilation conditions at the bed level. Building on this, a subsequent study [12] explored the effectiveness of three ventilation strategies—mixing ventilation (MV), displacement ventilation (DV), and personalized ventilation (PV)—in improving air quality at the bed level. Employing a full-scale setup of a typical Dutch DCC bedroom [13], the study assessed ventilation performance through CO<sub>2</sub> dispersion and inhalation metrics, demonstrating PV's superior ability to reduce inhaled CO<sub>2</sub> concentrations compared to MV and DV. However, this study limited its scope to limited air supply rates and a singular direction of air supply (specifically, a PV setup directed only towards the wall side), leaving the effectiveness of bed-level ventilation under varied air supply directions and volumes unexplored.

The current study, therefore, aims to bridge this research gap by thoroughly investigating the effectiveness of PV setups inside semi-enclosed baby beds. It aims to study the effect of three variables: different PV airflow directions, ventilation rates, and sleeping positions. In terms of novelty, this study is the first, in a full-scale setup, to research the ventilation effectiveness of different PV configurations inside the semi-enclosed baby beds under a controlled indoor environment.

## 2 METHODS

### 2.1 A full-scale bedroom setup and a breathing thermal baby model

In this follow-up study, the same full-scale bedroom setup (see **Figure 1**) and the breathing thermal baby model (BTBM) (see **Figure 2**) were utilized, as described in the previous studies [11, 12]. Briefly, a field survey of 17 Dutch DCCs (including 68 bedrooms) informed the experimental design, capturing essential data on bedroom features, bed density, ventilation specifics, and typical occupant characteristics [13]. This led to constructing a 4.2m x 2.7m x 2.5m bedroom setup, featuring six baby bunk beds with used mattresses from a participating DCC, arranged in a bilateral layout that mirrors one of the common configurations (38%) found in the survey. The constructed bedroom, made of plastic films and wooden frames, is placed in a climate-controlled chamber to ensure an adiabatic environment, isolating the experiment from external temperature influences.

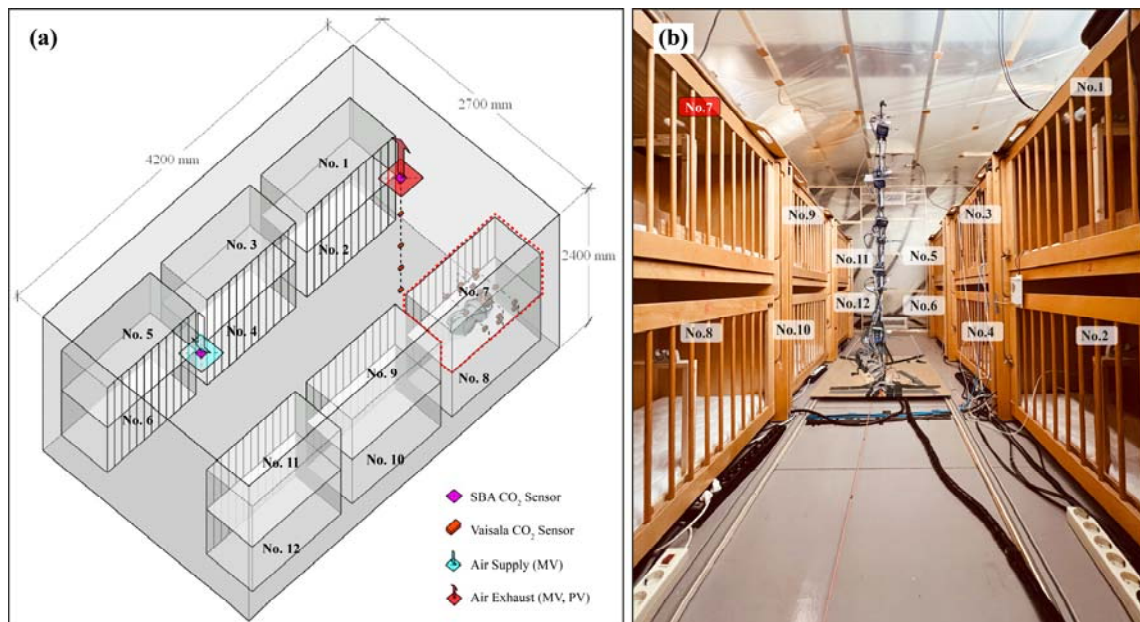


Figure 1: Experimental setup. (a) Axonometric schematic of the full-scale bedroom, including 12 beds (from No.1 to No.12) and sensor placement. (b) A picture of the on-site bedroom.

In terms of the BTBM, it was developed to mimic the sleeping body of a baby, generating heat and simulating breathing patterns. This model, representing a 30-month-old infant, featured a torso wrapped in an electric heating layer to produce a heat output of  $45 \text{ W/m}^2$ , matching the average metabolic rate of sleeping toddlers [14, 15]. An infrared image (see **Figure 2**) confirmed the BTBM's surface temperature at around  $36.5 \text{ }^\circ\text{C}$ , aligning with real toddler skin temperatures during sleep [16]. The BTBM's breathing mechanism comprised inhalation and exhalation systems, alternating through a digital timer controlling two valves. Both systems simulated realistic tidal volumes (123 ml), with exhalation and inhalation facilitated by simplified mouth and nose pathways. The exhaled airflow, mixed to achieve a CO<sub>2</sub> concentration of around 50000 ppm [17, 18], was delivered through the mouth, angled towards the chest to replicate natural breathing in sleep. Inhalation was similarly directed, with CO<sub>2</sub> levels continuously monitored by a Vaisala sensor (for the specification, see **Section 2.1**). The study simulated a 30-month-old's respiration rate at 30 breaths per minute [19], with each breath cycle consisting of 1-second inhalation and 1-second exhalation.

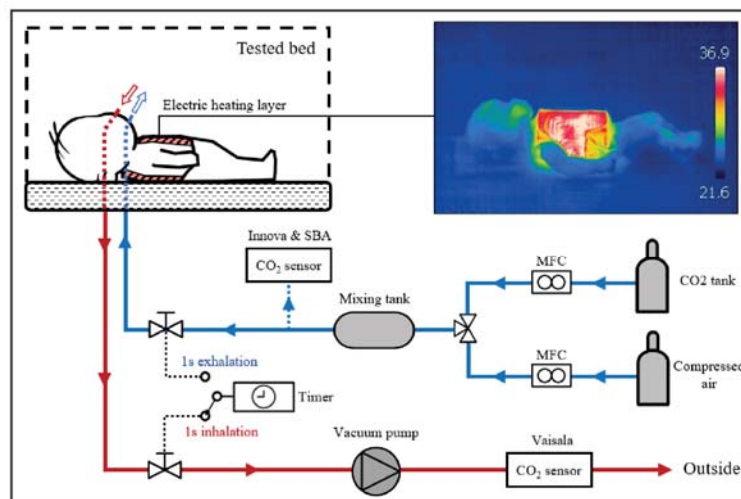


Figure 2: A schematic of the thermal and breathing simulation system of a baby model (BTBM), adapted from the prior study [11].

## 2.2 Instrumentation's specifications and placement

To evaluate bed-level and room-level ventilation, CO<sub>2</sub> was used as a tracer gas. 25 CO<sub>2</sub> sensors were placed at strategic locations to measure exhaled, inhaled, and dispersed CO<sub>2</sub> levels at bed and bedroom level. Four types of CO<sub>2</sub> measurement devices were deployed due to specific requirements for measurement range, conditions, and accuracy:

- (1) An Innova Photoacoustic Gas Monitor setup, with a reported accuracy of  $\pm 1.5\%$ , used at a ca. 42-second measurement interval to verify exhaled air CO<sub>2</sub> concentration at 50000 ppm (see **Figure 2**) and measure real-time room air exchange rates through SF<sub>6</sub> gas dosing.
- (2) Three SBA-5 CO<sub>2</sub> gas analyzers, accurate within 1% of span concentration, monitored CO<sub>2</sub> levels at 1-second interval in the air ducts to assess the supply and exhaust air quality (see **Figure 1a**), as well as the exhaled air (see **Figure 2**).
- (3) 21 Vaisala CO<sub>2</sub> Probes provided 1-second readings within the room and inside a bed, capturing CO<sub>2</sub> distribution at various heights, as well as for the exhaled air measurement (see **Figure 2** and **Figure 3**). The accuracy of Vaisala was documented as  $\pm 40$  ppm in the range of 0-3000 ppm,  $\pm 2\%$  of reading in the range of 3000-10000 ppm, and  $\pm 3.5\%$  of reading in the range of 10000-30000 ppm.

Before the experiments, all sensors underwent factory and laboratory calibrations to ensure accuracy, followed by a cross-calibration process to align readings across the different devices. This calibration confirmed an overall measurement uncertainty of 50 ppm.

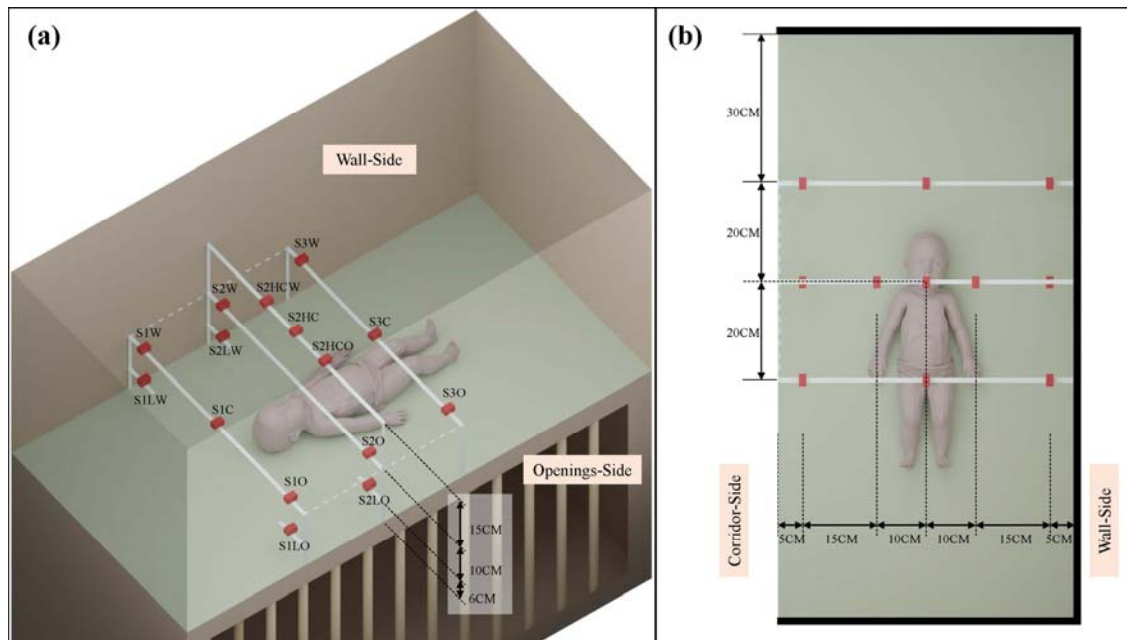


Figure 3: Experimental setup. (a) Axonometric schematic of the full-scale bedroom, including 12 beds (from No.1 to No.12) and sensor placement. (b) A picture of the on-site bedroom.

## 2.3 PV setup and experimental conditions

The PV setup (see **Figure 4b**), featuring an air supply interface measuring 45 x 40 cm (length\*height), is designed to deliver a consistent distribution of airflow across its surface. The setup allows for adjustable ventilation rates by modulating the power supplied to the unit, facilitating a tailored approach to study the impact of different airflows on the bed-level ventilation performance.



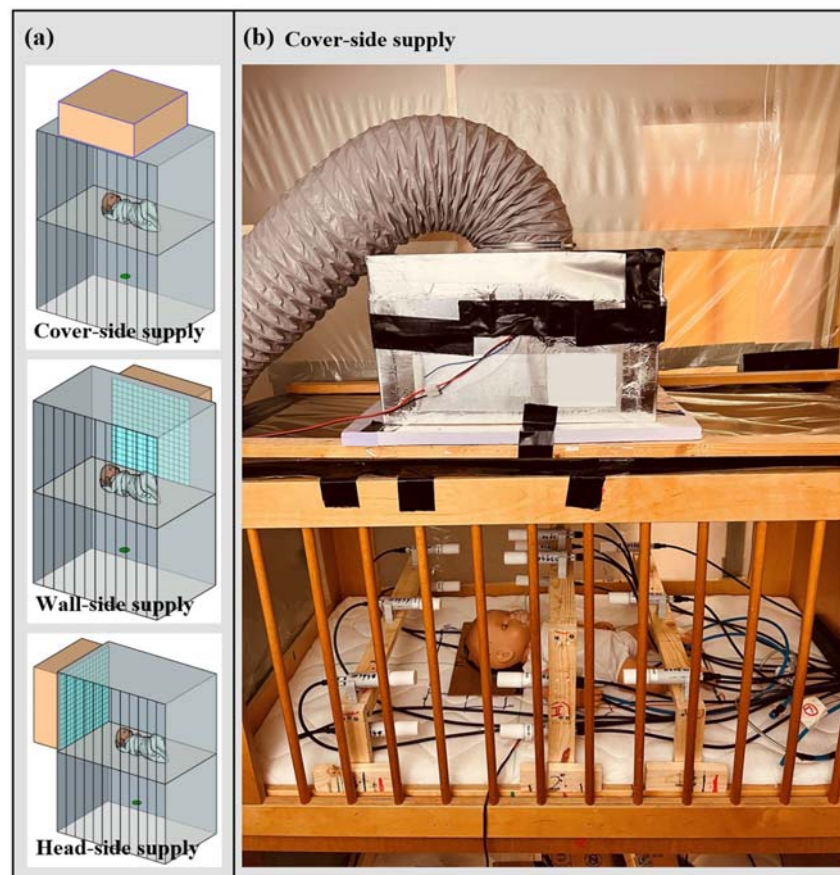


Figure 4: Experimental setup. (a) Axonometric schematic of the full-scale bedroom, including 12 beds (from No.1 to No.12) and sensor placement. (b) A picture of the on-site bedroom.

Table 1: Overview of 34 experiments categorized by combinations of experimental conditions.

Ventilation Mode	PV Location Placed	Ventilation Rate	Sleep Position	Test Run Time *	
MV	-	55 m <sup>3</sup> /h	Supine	1	
		55 m <sup>3</sup> /h	Lateral-to-Wall	1	
		55 m <sup>3</sup> /h	Lateral-to-Corridor	2	
PV	Wall-side	55 m <sup>3</sup> /h	Supine	1	
		55 m <sup>3</sup> /h	Lateral-to-Wall	1	
		55 m <sup>3</sup> /h	Lateral-to-Corridor	1	
	Head-side	27, 37, 55 m <sup>3</sup> /h	Supine	2	
		21, 37, 55, 65, 75 m <sup>3</sup> /h	Lateral-to-Wall	2	
		55 m <sup>3</sup> /h	Lateral-to-Corridor	1	
	Cover-side	21, 37, 55, 65, 75 m <sup>3</sup> /h	21, 37, 55, 65, 75 m <sup>3</sup> /h	Supine	2
			21, 37, 55, 65, 75 m <sup>3</sup> /h	Lateral-to-Wall	2
			55, 65, 75 m <sup>3</sup> /h	Lateral-to-Corridor	2

**Notes:** \* In the scenario described as ‘MV’ (Mixing Ventilation), the indicated ventilation rate was solely provided by a single ceiling air supply diffuser (see **Figure 1a**), while in the ‘PV’ (Personalized Ventilation) case, the supply of air was exclusively provided through the PV setup (see **Figure 2**). The ‘Test Run Time’ column in this table primarily indicates the number of experimental runs conducted under a specific ventilation rate of 55 m<sup>3</sup>/h for each sleeping position and ventilation mode combination. For ventilation rates other than 55 m<sup>3</sup>/h (as listed under the ‘PV Location Placed’ category), each experimental condition was tested only once.

Notably, the baby model was positioned in the No.7 bed (see **Figure 1**). This choice was necessitated by the dimensions of the PV setup, which could not be accommodated in the smaller space of other beds inside the climate chamber.

As shown in **Table 1**, the experimental design encompassed three supply airflow directions (cover-side, wall-side, head-side, also see **Figure 4a**), five ventilation rates (21, 37, 55, 65, 75 m<sup>3</sup>/h), and three sleep positions (supine, lateral-to-corridor, and lateral-to-wall). It should be mentioned that the selection of the lowest ventilation rate (21 m<sup>3</sup>/h) was based on the operational capacity of the PV setup with the lowest power, while the selection of the highest rates (75 m<sup>3</sup>/h) was aimed at the supplied air velocity to be within 0.2 m/s for comfort considerations [20-22]. For comparative purposes, a control scenario employing mixing ventilation (MV) at the ventilation rate of 55 m<sup>3</sup>/h was also examined.

## 2.4 Experimental procedure and data analysis

The experimental procedures, as followed the protocols established in the prior study [11], ensured that each measurement reached a steady state for accurate CO<sub>2</sub> quantification. Data analysis was processed using Python 3.8.8 with the following key steps:

- (1) Measurements from various instruments were averaged into 1-minute averages using pandas' DataFrame.resample.mean method.
- (2) Equilibrium in indoor air distribution was determined by analyzing sensor data over a 10-minute period for consistency using the Shapiro-Wilk test for normality and either one-way ANOVA or Kruskal-Wallis H Test for statistical differences, with a significance level of 0.05.
- (3) Actual CO<sub>2</sub> concentration variations were isolated by subtracting the stable background supply air CO<sub>2</sub> level (average 418 ppm) from sensor readings.
- (4) Experimental repeatability was checked by comparing the absolute difference in CO<sub>2</sub> concentrations between repeated tests to a 50 ppm threshold (the uncertainty of CO<sub>2</sub> measurements).
- (5) Steady-state values for each sensor were calculated from 10-minute averages in each case.

## 3 RESULTS AND DISCUSSION

All tests showed no significant differences ( $p$ -value > 0.05) in CO<sub>2</sub> concentrations across the last 10-minute measurements, indicating that a steady state was reached in each case. The reproductivity test confirmed that the median of absolute differences in CO<sub>2</sub> concentrations between repeated cases for each sensor was below 50 ppm, demonstrating good experimental repeatability. Consequently, data from six repeated cases were averaged to represent a single case based on the steady-state data of each sensor.

### 3.1 Bed-level CO<sub>2</sub> spatial distribution

**Figure 5** presents the CO<sub>2</sub> spatial distribution at bed level for all cases under ventilation rate of 55 m<sup>3</sup>/h. The CO<sub>2</sub> distribution can be visually compared in four ventilation strategies and three different sleep positions. Two main aspects that are generally applicable to most cases in **Figure 5** are pointed out as follows:

- (1) Under the same sleep position, the MV mode generally registered the highest CO<sub>2</sub> concentration around the baby model within the bed, compared to others three PV modes. This demonstrated that PV mode has better ventilation effectiveness to remove the metabolic CO<sub>2</sub> emissions from the semi-enclosed bed than MV mode.
- (2) Under the same ventilation strategies, a significant difference in CO<sub>2</sub> spatial distribution inside the baby bed was observed among the three sleep positions investigated. This

confirms that the CO<sub>2</sub> distribution pattern within the breathing zone is affected by the babies' posture [11, 23].

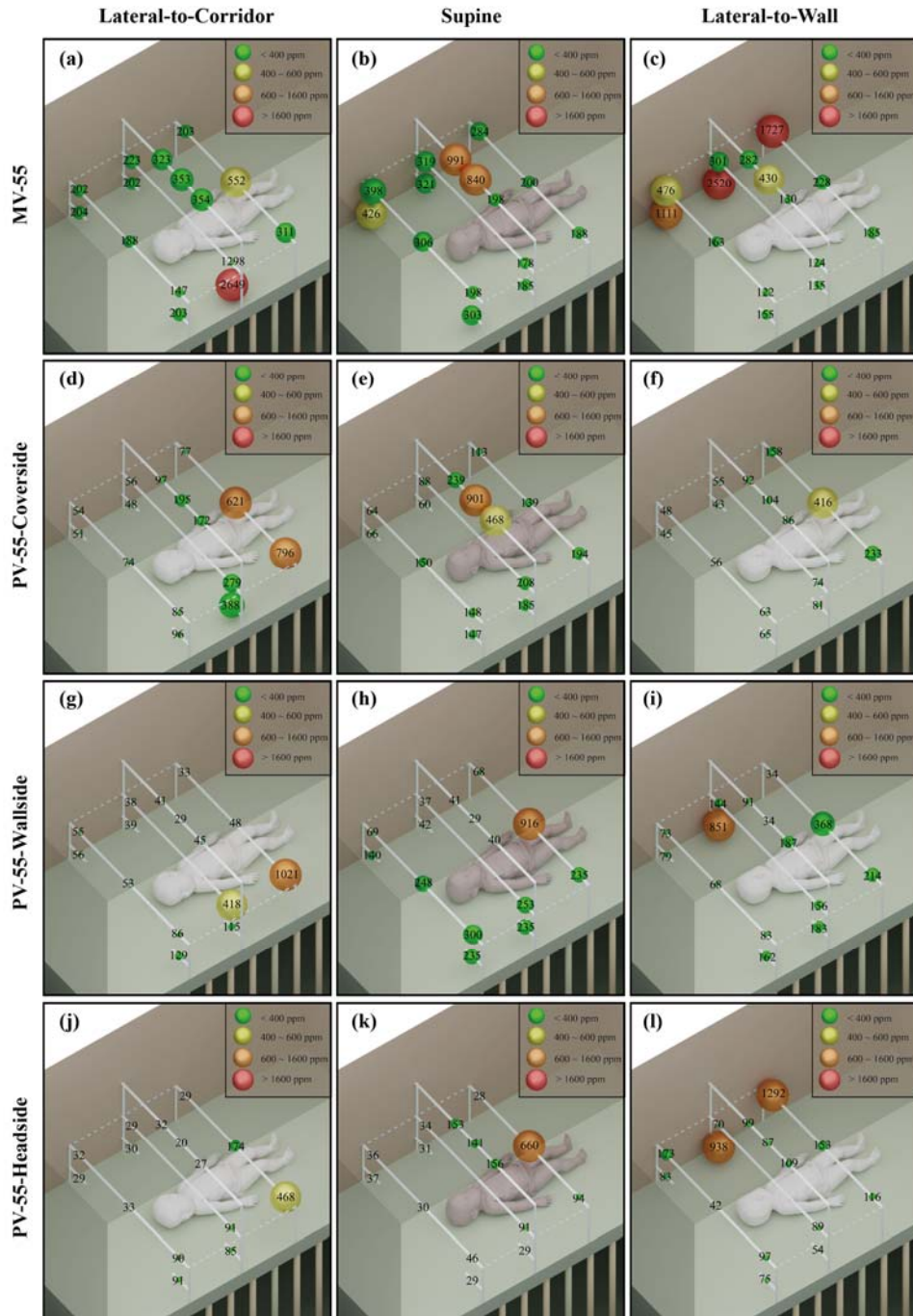


Figure 5: CO<sub>2</sub> dispersion (values above the background level: 418 ppm) inside the No.7 bed in all cases under the ventilation rates of 55 m<sup>3</sup>/h.

### 3.2 Effect of different PV strategies

Results from **Figure 6** indicate CO<sub>2</sub> concentrations measurements at different locations, considering inhaled air, in-bed mean, and exhaust air at the same ventilation rate of 55 m<sup>3</sup>/h for the comparison of MV and the other three PV strategies. Key findings can be drawn from the figure:

- (1) The exhaust air CO<sub>2</sub> concentrations were consistent across all strategies, underpinning the robustness of the experimental setup. This consistency is attributed to the same settings in CO<sub>2</sub> emission rates and ventilation rates, ensuring a stable baseline for comparison.
- (2) MV resulted in the highest CO<sub>2</sub> levels in both inhaled and in-bed measurements compared to the PV strategies. Particularly for inhaled air, MV's values were noticeably elevated (up to 1392 ppm above the background level), suggesting that PV strategies are more effective in diluting CO<sub>2</sub> concentrations within the breathing zone over MV.
- (3) PV head-side consistently recorded the lowest inhaled CO<sub>2</sub> concentrations across all positions, suggesting an enhanced capability for removing metabolic CO<sub>2</sub> emissions. Notably, in the lateral-to-wall position, PV head-side reduced inhaled CO<sub>2</sub> to as low as 53 ppm above the background level, demonstrating a better improvement in inhaled air quality compared to the other PV strategies.

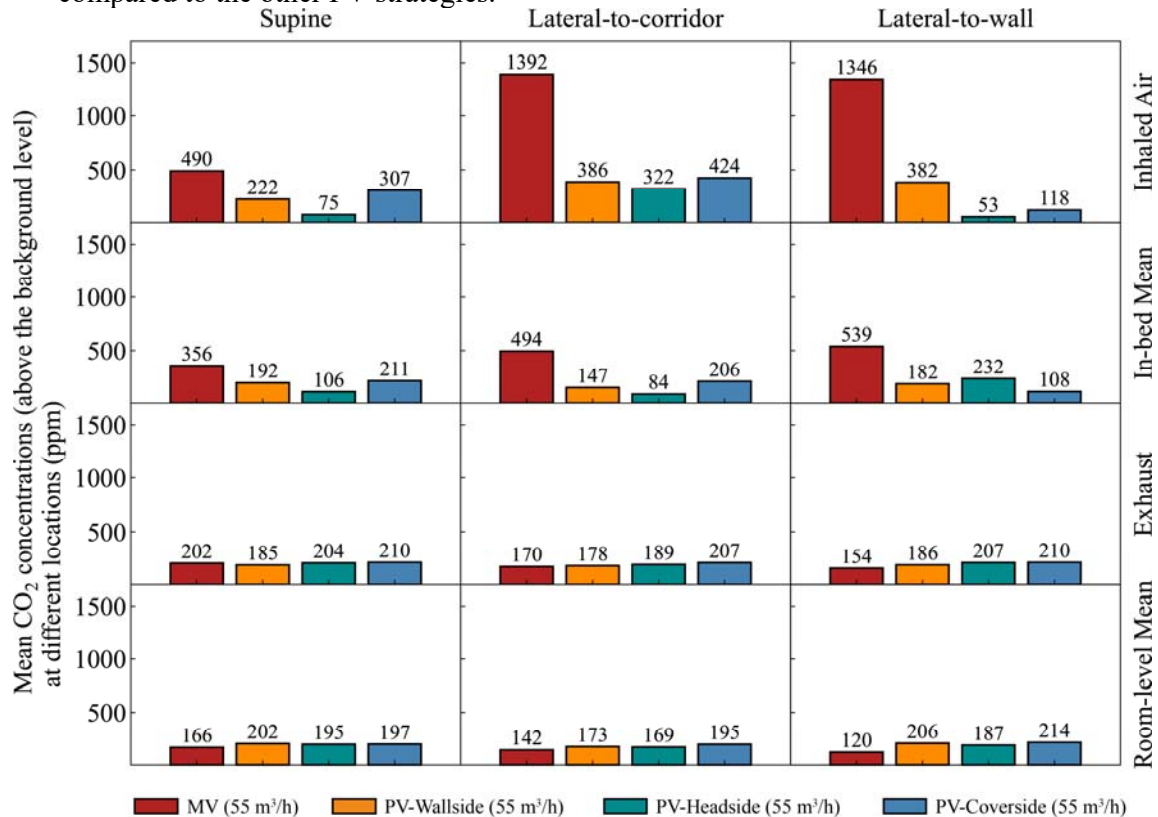


Figure 6: Comparative CO<sub>2</sub> concentrations (values above the background level: 418 ppm) across four different ventilation strategies and three sleep positions at a uniform ventilation rate of 55 m<sup>3</sup>/h.

### 3.3 Effect of different ventilation rates

Additionally, **Figure 7** presents CO<sub>2</sub> concentration levels at two different locations for two PV strategies —PV head-side and PV cover-side— under varying ventilation rates (21, 37, 55, 65, 75 m<sup>3</sup>/h) and three different sleeping positions, revealing that:

- (1) Generally, increased ventilation rates correlate with lower CO<sub>2</sub> concentrations at different measurement points across different sleep positions and ventilation strategies.
- (2) The PV head-side strategy tends to perform better at lower ventilation rates, while the PV-cover-side strategy requires higher rates to achieve similar dilution effects.
- (3) However, the relationship is not linear, and some positions show a plateau or increase in CO<sub>2</sub> concentrations at higher ventilation rates, indicating that the optimal rate may vary by position and strategy.

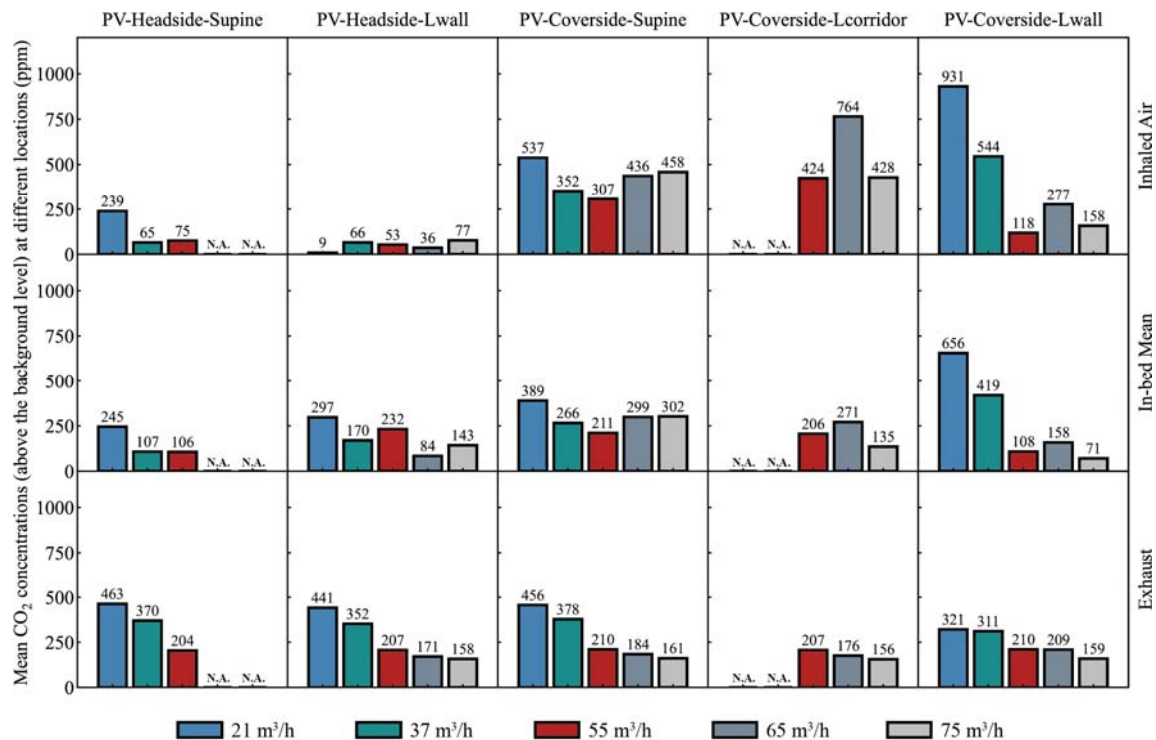


Figure 7: CO<sub>2</sub> concentrations (values above the background level: 418 ppm) at different measurement points (inhaled, in-bed, and exhaust air) for two ventilation strategies (PV head-side and PV cover-side) under three different sleeping positions and ventilation rate (21, 37, 55, 65, 75 m<sup>3</sup>/h).

## 4 CONCLUSIONS

Ventilation in semi-enclosed baby beds requires improvement, and fortunately, there are feasible solutions available. The study examined the effectiveness of personalized ventilation (PV) strategies within a semi-enclosed baby bed in a typical daycare center environment. This study confirms that PV can more efficiently enhance inhaled and bed-level air quality for young children compared to traditional ventilation methods. Using a detailed setup with varied airflow directions and rates, the PV head-side strategy proved to be most efficient at lower flow rates, optimizing inhaled air quality and suggesting potential for energy savings. The results also indicate that while increased PV ventilation rates typically improve bed-level air quality, the optimal ventilation rate is influenced by the specific strategy and sleeping position. This emphasizes the need for tailored ventilation solutions for infants in daycare centers.

## 5 ACKNOWLEDGEMENTS

Dr. Arjen de Jong from AirTulip is acknowledged for providing us with personalized ventilation setup from New York and assisting us in the experimental preparations. We are also grateful to the Building Physics and Services Laboratory team for their support.

## 6 REFERENCES

1. Zheng, H., et al., *Laboratory evaluation of low-cost air quality monitors and single sensors for monitoring typical indoor emission events in Dutch daycare centers*. *Environment International*, 2022. **166**: p. 107372.
2. Zhang, Y., P.K. Hopke, and C. Mandin, *Handbook of Indoor Air Quality*. 2022: Springer Nature Singapore Pte Ltd.

3. Basinska, M., M. Michalkiewicz, and K. Ratajczak, *Impact of physical and microbiological parameters on proper indoor air quality in nursery*. Environment International, 2019. **132**: p. 105098.
4. Roda, C., et al., *Assessment of indoor environment in Paris child day care centers*. Environ Res, 2011. **111**(8): p. 1010-7.
5. Sander, I., et al., *Allergen quantification in surface dust samples from German day care centers*. Journal of Toxicology and Environmental Health - Part A: Current Issues, 2016. **79**(22-23): p. 1094-1105.
6. Onishchenko, A., et al., *RADON MEASUREMENTS IN KINDERGARTENS IN URAL REGION (RUSSIA)*. Radiation protection dosimetry, 2017. **177**(1-2): p. 112-115.
7. Capi Education BV. *Capi Education for Bed*. 2022; Available from: [https://www.capi-education.com/?s=bed&post\\_type=product](https://www.capi-education.com/?s=bed&post_type=product).
8. Boor, B.E., et al., *Human exposure to indoor air pollutants in sleep microenvironments: A literature review*. Building and Environment, 2017. **125**: p. 528-555.
9. Liang, Y. and Y. Xu, *Emission of phthalates and phthalate alternatives from vinyl flooring and crib mattress covers: The influence of temperature*. Environmental Science and Technology, 2014. **48**(24): p. 14228-14237.
10. Jr, E.J.F., et al., *Modeling indoor air concentrations near emission sources in imperfectly mixed rooms*. Journal of the Air & Waste Management Association, 1996. **46**(9): p. 861-868.
11. Zheng, H., et al., *Bed-level ventilation conditions in daycare centers*. Building and Environment, 2023: p. 110638.
12. Zheng, H., et al., *Bedroom ventilation performance in daycare centers under three typical ventilation strategies*. Building and Environment, 2023. **243**: p. 110634.
13. Wang, Z., et al. *A survey of indoor air quality conditions in bedrooms of Dutch daycare centers*. 18th Healthy Buildings Europe Conference 2023; Available from: [https://pure.tue.nl/ws/portalfiles/portal/301657351/Wang\\_1312\\_A\\_1\\_.pdf](https://pure.tue.nl/ws/portalfiles/portal/301657351/Wang_1312_A_1_.pdf).
14. Hull, D., et al., *Individual variation in sleeping metabolic rates in infants*. Archives of disease in childhood, 1996. **75**(4): p. 288-291.
15. Hull, D., et al., *Metabolic rate of sleeping infants*. Archives of disease in childhood, 1996. **75**(4): p. 282-287.
16. Garcia-Souto, M. and P. Dabnichki, *Core and local skin temperature: 3–24 months old toddlers and comparison to adults*. Building and Environment, 2016. **104**: p. 286-295.
17. Kierat, W., et al., *Towards enabling accurate measurements of CO2 exposure indoors*. Building and Environment, 2022. **213**: p. 108883.
18. ISO, *ISO 8996:2021-Ergonomics of the thermal environment — Determination of metabolic rate*. 2021, ISO.
19. Fleming, S., et al., *Normal ranges of heart rate and respiratory rate in children from birth to 18 years of age: a systematic review of observational studies*. Lancet, 2011. **377**(9770): p. 1011-8.
20. Dongmei, P., et al., *Air-conditioning for sleeping environments in tropics and/or sub-tropics – A review*. Energy, 2013. **51**: p. 18-26.
21. Zhu, S., W. Cai, and J.D. Spengler, *Control of sleep environment of an infant by wide-cover type personalized ventilation*. Energy and Buildings, 2016. **129**: p. 69-80.
22. Cao, G., et al., *A review of the performance of different ventilation and airflow distribution systems in buildings*. Building and Environment, 2014. **73**: p. 171-186.
23. Pantelic, J., et al., *Personal CO2 cloud: laboratory measurements of metabolic CO2 inhalation zone concentration and dispersion in a typical office desk setting*. Journal of Exposure Science & Environmental Epidemiology, 2020. **30**(2): p. 328-337.

# Building airtightness for renovations Leaflets (Germany)

Stefanie Rolfsmeier

*BlowerDoor GmbH, Zum Energie- und Umweltzentrum 1, 31832 Springe, Germany,  
rolfsmeier@blowerdoor.de*

## SUMMARY

The WTA-Leaflets (International Association for Science and Technology of Building Maintenance and Monuments Preservation", (WTA)) provide recommendations on how a defined quality of building airtightness can be achieved when renovating existing buildings. These recommendations are guidelines that support planners, builder and quality inspectors involved in construction in their implementation.

The leaflet series consists of 3 parts:

- Part 1 (WTA-Leaflet 6-9) defines the required level of airtightness for renovated buildings and building elements. Moreover, basic planning rules are formulated.
- Part 2 (WTA-Leaflet 6-10) gives information about planning details, sources of errors, construction options as well as methods to check the quality.
- Part 3 (WTA-Leaflet 6-11) focuses on suitable methods for airtightness testing with leak detection of existing and renovated buildings, including the building preparation and the best times for testing.

The leaflets are expected to be published at the end of 2024 / beginning of 2025.

## KEYWORDS

Airtightness, existing buildings, refurbishment, planning, air permeability test, quality control, airtightness concept

## 1 AIRTIGHTNESS IN EXISTING BUILDINGS

In Germany, the requirements for the airtightness of buildings are widely accepted and are applied to new buildings. In comparison, this is rarely the case when renovating existing buildings, although there is significant potential for saving energy.

A good airtightness of the building envelope protects the construction against condensation due to convection, reduces energy consumption due to uncontrolled air exchange and increases comfort by preventing draughts.

The current revision of the WTA leaflet series from 2015 [Vogel] is intended to help focus attention once again on the need for a defined quality of airtightness, even in existing buildings. The developments of recent years in the field of processing and new airtightness materials will be brought up to date. The leaflets are scheduled to be published at the end of 2024 or beginning of 2025.

The aim is to achieve an airtightness after a renovation or extension of existing buildings that is comparable to that of a new building. In cases where the "new building standard" cannot be achieved, the aim is to achieve the best possible quality. Controlled mechanical ventilation is also taken into consideration for a demand-oriented air exchange rate in order to prevent, among other things, the entry of humid indoor air into the construction via individual leaks in the air barrier.

These leaflets have been updated to the best of the knowledge and belief by experts with many years of experience in the areas of planning, production and measurement in the field of airtightness in new and existing buildings, without any claim to completeness.

The leaflet series consists of three parts:

- Part 1: General principles of planning (WTA Leaflet 6-9)
- Part 2: Detailed planning and execution (WTA Leaflet 6-10)
- Part 3: Measuring Procedure (WTA Leaflet 6-11)

### 1.1 Part 1: General principles of planning (WTA-Leaflet 6-9)

In Part 1, methods are presented for determining a level for the airtightness for an existing building or building component in the case of renovation and basic planning rules are explained.

To ensure that a building renovation is successful in improving the thermal insulation and airtightness of the building envelope, it is essential to first analyze the existing building. In addition to the building inspection, an airtightness measurement (single-point measurement) with leak detection is recommended. Based on this, an airtightness requirement for the renovated building can be defined and the air barrier planned.

To assess the quality of the airtightness of the existing building envelope, the air permeability  $q_{E50}$  is used as the key value, because it is independent of the surface/volume ratio of the building. It is used to describe the leakage rate at 50 Pa in relation to one square meter of building envelope.

The primary goal when making changes to the building envelope is to improve the quality of the air barrier. In order to be able to set requirements (target value or limit value) for the air permeability, four cases (Figure 1) are considered:

Figure 1: (1) Existing building (2) Partial renovation (3) Extension to existing building (4) Complete renovation (note on the graphic: lines with dots = not renovated; solid line = refurbished or new)



#### *Case 1: Checking the airtightness of the existing building (Figure 1, Case 1)*

The air permeability of the existing building envelope is determined by a single-point measurement. This is the basis for further decisions and planning.

#### *Case 2: Renovation parts of the building envelope (Figure 1, Case 2)*

In the case of partial renovation of the building envelope, the target air permeability for the entire building is determined using a calculation formula based on the measured permeability for the unrenovated envelope areas and the air permeability at new-build level for the renovated envelope areas.

#### *Case 3: Extension of the heated building volume (Figure 1, Case 3)*

For newly added parts of the building, the aim is to achieve the level of a new building. The target air permeability for the entire building is determined using a calculation formula based



on the measured permeability for the unrenovated envelope areas and the desired air permeability for the new envelope areas.

*Case 4: Full renovation (Figure 1, Case 4)*

If the building is completely renovated, the requirements of new buildings will be applied.

Components (e.g. windows or doors) that are to be retained for historical reasons are treated separately.

It is clearly stated that a ventilation concept is required when improving the airtightness of a building so that a defined air exchange can take place and, among other things, indoor air humidity can be extracted in a controlled way.

The leaflet lists data from previous experience for the air permeability and air exchange rates of existing buildings. It also presents specific target values / limit values for full renovations, depending on the desired building quality (e.g. Building Energy Act standard or passive house standard).

## **1.2 Part 2: Detailed planning and execution (WTA- Leaflet 6-10)**

Part 2 provides information on planning details, sources of errors, execution options and methods for verifying the quality achieved. It is based on the basic planning principles of Part 1.

Detailed information is provided on the planning and execution of the air barrier of the heat-transferring building envelope such as roof surfaces, exterior walls and basement ceilings, among others. Different constructions (masonry, timber construction, etc.), the position of the air barrier, e.g. in the roof construction or stairwells to unheated basements, are presented based on current developments and risks during implementation are examined in detail. The installation of the air barrier when replacing windows and external doors is shown, as well as the handling of bonding and sealings, taking into account the nature of new and existing bases. Reference is also made to the need for quality assurance and quality control during the installation of the air barrier.

## **1.3 Part 3: Measuring Procedure (WTA- Leaflet 6-11)**

Part 3 explains suitable methods for measuring the airtightness of existing buildings, including a description of the preparation of the building and the best times to do tests.

In addition to the "final measurement" with measurement of the air permeability after completion of the renovation, two further testing times are suggested: the first test before and the second during the renovation.

*Measurement 1: Before the renovation as a status analysis*

This inspection is important in order to obtain an overview of the existing air permeability of the building envelope and the qualities of the individual air barriers. The focus is on leakage detection at approx. 50 Pa negative pressure, so a simple single-point test with an estimate of the air permeability  $q_{E50}$  is sufficient. This investigation is the essential basis for planning the air barrier.

*Measurement 2: During the renovation - quality controls*

This inspection at a negative pressure of approx. 50 Pa during the renovation process is used to check the planned air barrier for defects. If leaks are detected, they can be eliminated quickly and easily at this phase of construction and plans and installations can be adapted if problems arise. With a simple single-point measurement, it is possible to document the air permeability at the time of measurement.

*Measurement 3: After the renovation - final measurement*

After finishing the building envelope, the final measurement is carried out according to DIN EN ISO 9972. The test result is compared with the target air permeability. At the time of this measurement, the air barriers are often covered and no longer accessible. Improvement is only possible at an extremely high effort.

This leaflet provides further information on, among other things, guard zone tests that prevent internal airflows between adjacent building sections, as well as on sectional measurements for large buildings or buildings that cannot be measured as a single unit due to their complexity or the construction process.

## 2 REFERENCES

- DIN EN ISO 9972:2018-12 (20218). *Thermal performance of buildings - Determination of air permeability of buildings - Fan pressurization method*
- Vogel, L. (2013). WTA-Merkblatt „Luftdichtheit im Bestand – Anforderungen an Planung und Ausführung“. Tagungsreader BUILDAIR 2013
- WTA-Merkblatt 6-9 (2015). *Luftdichtheit im Bestand - Teil 1 - Grundlagen der Planung*. Wissenschaftlich-Technische Arbeitsgemeinschaft für Bauwerkserhaltung und Denkmalpflege e.V.
- WTA-Merkblatt 6-9 (unpublished revision). *Luftdichtheit im Bestand - Teil 1 - Grundlagen der Planung*. Wissenschaftlich-Technische Arbeitsgemeinschaft für Bauwerkserhaltung und Denkmalpflege e.V.
- WTA-Merkblatt 6-10 (2015). *Luftdichtheit im Bestand - Teil 2: Detailplanung und Ausführung*. Wissenschaftlich-Technische Arbeitsgemeinschaft für Bauwerkserhaltung und Denkmalpflege e.V.
- WTA-Merkblatt 6-10 (unpublished revision). *Luftdichtheit im Bestand - Teil 2: Detailplanung und Ausführung*. Wissenschaftlich-Technische Arbeitsgemeinschaft für Bauwerkserhaltung und Denkmalpflege e.V.
- WTA-Merkblatt 6-11 (2015). *Luftdichtheit im Bestand - Teil 3 - Messung der Luftdichtheit*. Wissenschaftlich-Technische Arbeitsgemeinschaft für Bauwerkserhaltung und Denkmalpflege e.V.
- WTA-Merkblatt 6-11 (unpublished revision). *Luftdichtheit im Bestand - Teil 3 - Messung der Luftdichtheit*. Wissenschaftlich-Technische Arbeitsgemeinschaft für Bauwerkserhaltung und Denkmalpflege e.V.

# Achieving suitable airflow rate in New Zealand classrooms: a CFD approach to inform on potential retrofitting solutions.

Mikael Boulic<sup>1\*</sup>, Pierre Bombardier<sup>2</sup>, Andrew Russell<sup>3</sup>, David Waters<sup>4</sup>, Angelo Cuyo<sup>5</sup>, Hennie van Heerden<sup>1</sup>, Jean-Richard Templier<sup>2</sup> and Robyn Phipps<sup>6</sup>

*1 School of Built Environment, Massey University  
Auckland Campus, Auckland, New Zealand*

*2 Faure QEI, ATRIX Group, France*

*\*Corresponding author: m.boulic@massey.ac.nz*

*3 Proctor Group Australia, Australia*

*4 APL Window Solutions, New Zealand*

*5 Dynamic Composite Technologies Pty Ltd,  
Australia*

*6 Faculty of Architecture and Design Innovation,  
Victoria University of Wellington, New Zealand*

## ABSTRACT

During the COVID-19 pandemic, besides sanitising, masking, and increasing social distancing, opening classroom windows was the NZ Ministry of Education's main requirement for reopening schools. However, a pre-COVID-19 survey showed that only a third of the NZ teachers opened windows during teaching time. Achieving a suitable ventilation level could not rely on humans to open windows. Heating, Ventilation, and Air Conditioning (HVAC) systems are not affordable for most NZ schools. Consequently, an alternative and affordable ventilation method that could be retrofitted is needed to increase the airflow rate. In this project, we investigated the benefit of using trickle ventilators with connection (or not) to extraction fans in three NZ locations (Auckland, Wellington and Dunedin). The computational fluid dynamic (CFD) approach allowed us to test different scenarios for ventilation performances, such as single-sided trickle ventilators versus cross-ventilation scenarios, modelling with or without extractor fans. We carried out an aerodynamic simulation of the airflows to visualise the trajectory of the flows and check the air velocity and temperature in the classroom volume where the students are located. The results for the Wellington case study (no extractor fan used) showed a suitable airflow rate in summer when the trickle ventilators were fully open. However, the trickle ventilators' effective area was reduced in winter, and insufficient air entered the classroom. In addition, despite good air mixing assisted by the inverter heat pump use in winter, there were still a few areas where the air was not well-mixed. These areas experiencing a lower mixing rate could create some "CO<sub>2</sub> pockets", reducing the extraction of pollutants or viruses. Acknowledging COVID-19 and its lasting impacts on NZ schools and families, we must better prepare for future learning disruptions. By investigating different cases simulated by CFD software, we compared different scenarios to improve ventilation performance in the classroom. Following the CFD project, we plan to deploy some sensors to monitor the temperature, relative humidity and CO<sub>2</sub> in Auckland, Wellington and Dunedin classrooms and validate our modelling findings. This study will assist the NZ Ministry of Education retrofit classrooms for a healthy environment.

## KEYWORDS

Computational Fluid Dynamic (CFD), IAQ, ventilation, occupied primary schools

## 1 INTRODUCTION

Children spend the second largest proportion of their time at school. Half of the school stock in New Zealand (NZ) was built before 1970, and nearly all classrooms depend entirely on natural ventilation via open windows. This dependence on occupants for airing does not always guarantee an adequate ventilation rate. Surveys showed that only 30% of NZ teachers open windows during teaching time (Gully, 2015; Liaw, 2015; Boulic, 2019). In addition, classrooms

have a higher density of occupants than most other building types. Due to the high density of occupants and reliance on natural ventilation, providing an acceptable ventilation rate during the winter in the school environment could be challenging.

A lack of ventilation will increase pollutants and moisture levels in the classroom (Sadrizadeh, 2022). It is also well established that a poorly ventilated classroom will favour the transmission of viruses like SARS-CoV-2, even if social distancing is respected (Correia, 2020; Dai, 2020). The literature shows some associations between moderate levels of heat stress and CO<sub>2</sub> in classrooms and children's cognitive performance (Palacios Temprano, 2020).

As NZ teachers seldom open windows, there is a need to find an alternative solution to assist them in airing in the classrooms. Smart ventilation could assist in providing more ventilation in the classroom when needed (Guyot 2018). In a previous study, we tested trickle ventilators connected to extraction fans in an Australian apartment. The results showed trickle ventilators connected to an extraction fan (continuous extraction) could be a classroom ventilation option (Boulic, 2023).

Our approach will use Computational Fluid Dynamics (CFD) to evaluate three ventilation configurations for winter and summer across three NZ locations. We will first test the performance of cross ventilation (airflow enters the classroom through the trickle ventilators) with no extractor fan. The results from this first configuration are presented in this paper. Our second and third tests will evaluate the ventilation performance under a continuous extraction regime (8 litres per second per child, NZS 4303:1990) with the air entering the classroom either from one or both sides. Our study aims to investigate the airflow velocity, temperature distribution and ventilation efficiency in winter and summer seasons.

## 2 MATERIALS AND METHODS

### 2.1 Description of the classroom and ventilation strategies

#### Case study locations

The rationale for selecting these three locations (Auckland, Wellington and Dunedin) is the large temperature and wind gradients across the three NZ cities. Auckland is exposed to a subtropical climate with warm, humid summers and mild winters (Chappell, 2013). Wellington region experiences stronger winds than other parts of New Zealand (Chappell, 2014). Dunedin, located in the southern part of the South Island, is characterised by cool coastal breezes (Macara 2015). Figure 1 shows the locations of these three cities (Auckland, Wellington and Dunedin).



Figure 1: Location of the three cities (Auckland, Wellington and Dunedin) selected for the modelling  
**Modelled classroom building**

Figure 2 shows the 3D model of the two-classroom building imported into the CFD program. This 160.4 m<sup>2</sup> floor building comprises two identical classrooms of 80.2 m<sup>2</sup> each (11.3 m x 7.1

m), an average area for NZ primary schools (MOE, 2024). The building has a mono-pitch skillion roof (ceiling height between 2.7 m and 3.5 m) and is made of Metra Wall™ (panels constructed from NZ pine wood fibre and resin with a 640 kg/m<sup>3</sup> density, BRANZ, 2021). A NZ building company (Builtsmart, Huntly, NZ) uses this plan to deliver prefabricated classrooms to the NZ Ministry of Education.

Figure 2 shows that the building comprises two identical classrooms side by side (mirror). This design allowed us to run two CFD simulations (summer and winter) simultaneously, display the differences on the same graph, and explore more case studies in a shorter time due to the high computing needs to conduct CFD simulations. The classroom furniture is distributed as in a typical NZ classroom. Each classroom has five tables with five students (25 total). The NZ median class size is 25 students (PPTA, 2024). The building faces the north (south hemisphere) for optimal solar gain during the school day (9 am – 3 pm). Each classroom has four windows (thermally broken aluminium frame and double glazed,  $U_w = 2.0 \text{ W/m}^2\cdot\text{K}$ ) and one door.

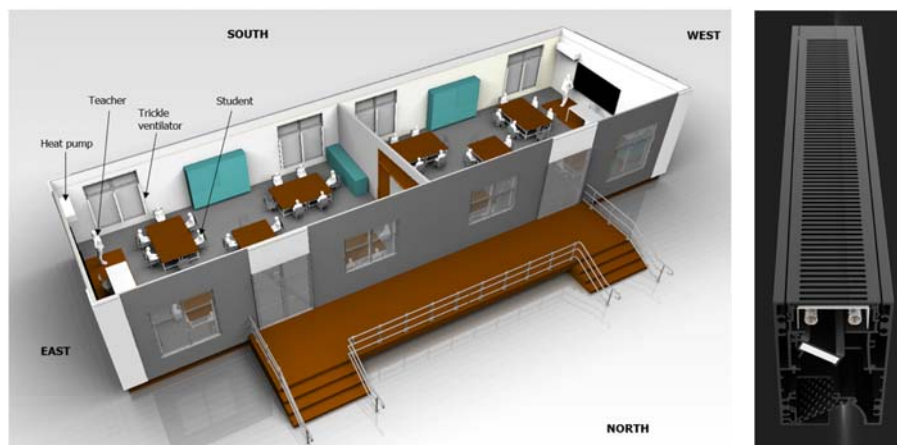


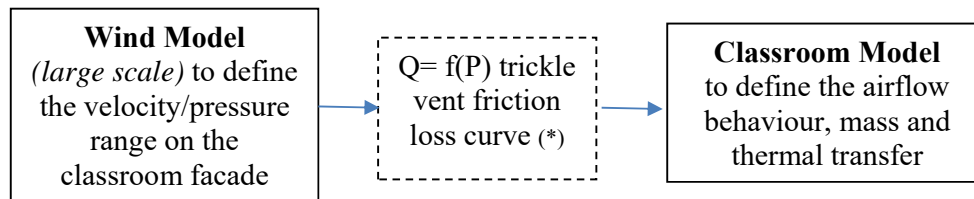
Figure 2: The 3D model of the two-classroom building imported into the CFD program (left) and the trickle ventilator (APL Ventient SCW-SH1500) installed vertically on the classroom windows (right).

### Ventilation system

The original classroom relies on occupants to open windows for airing. In our study, we installed three vertical trickle ventilators (Figure 2, right) on each of the four windows (one trickle ventilator on each jamb and one on the mullion), making twelve trickle ventilators per classroom. All twelve trickle ventilators are the same size (1500 mm by 55 mm with a 64.4 cm<sup>2</sup> effective open area when fully open). The trickle ventilator incorporates a passive wind dampener to manage water ingress and draughts associated with high wind gusts and a filter for coarse particles. The trickle ventilator has an acoustic treatment to mitigate the effects of outside noise. Discussions with a few NZ teachers reported that outside noise was a significant factor that prevented teachers from opening windows during teaching (Tookey L, 2024, personal communication). This trickle ventilator includes a shape memory alloy adapting the opening to external temperature (fully open above 18°C and one-third open under 12°C external temperature). A fan extractor will be installed on the classroom ceiling to assist with ventilation and test the impact of continuous ventilation on CO<sub>2</sub> levels. The fan flow rate (749 m<sup>3</sup>/h) follows the NZS 4303:1990 minimum requirements of 8 litres per second per child/teacher, assuming 25 children and one teacher per classroom. This fan is rated 42dB(A) at 3 m and suits the learning environment. The air will enter the classroom via the trickle ventilators and be extracted via the ceiling fan extractor. As there are twelve trickle ventilators per classroom, we assumed each ventilator would have a mean airflow of 17.3 L/s (equivalent to 62.4 m<sup>3</sup>/h).

## 2.2 Conceptual framework

Figure 3 shows our two-step process. The first step, the "Wind Model", defines the velocity range on the input face of the trickle ventilators for the main wind direction. The "Wind Model" results will be implemented in the second step, the "Classroom Model". The velocity profile obtained in the "Wind Model" will be combined with the "Fan Q/P equation" to define the airflow behaviour in the classroom. The "Wind Model" is a steady-state model, while the "Classroom Model" will be a transient model simulated over 90 minutes (average teaching period at the primary school level).



(\*) Trickle vent friction loss formula for our configuration is  $Q = 97.7 (\Delta P/9.8)^{0.53}$

Figure 3: Conceptual framework of the CFD simulations

## 2.3 Wind boundary conditions

We implemented the wind data (meteorological station data measured at 10 m high) in the "Wind Model" for the three selected locations (Grey Lynn for Auckland, Wellington Airport/Lyall Bay for Wellington, and Forbury for Dunedin). Figure 4 shows the monthly wind direction in Auckland (top), Wellington (middle) and Dunedin (bottom). For Auckland, the January 2014 - March 2024 data was averaged. For Wellington, the June 2004 - March 2024 data was averaged. For Dunedin, the January 2014 to March 2024 data was averaged. We selected one month in summer (January) and one month in winter (July) in NZ (south hemisphere) for our CFD simulations.

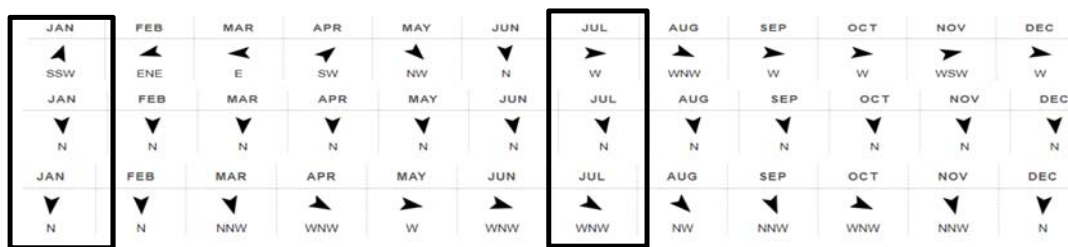


Figure 4: Dominant wind direction in Auckland Grey Lynn (top), Wellington Lyall Bay (middle) and Dunedin St Clair/Forbury Park (bottom) (Source Windfinder.com)

In Auckland, the wind predominates from the South/South-West during January (summer) and the West during July (winter). In Wellington, the wind predominates from the North during January (summer) and North during July (winter). In Dunedin, the wind predominates from the North during January (summer) and the West/North-West in July (winter).

Table 1 presents the averaged wind velocity and temperatures over the summer and winter. The wind velocity is twice as high for Wellington than Auckland and Dunedin for winter. In a subtropical climate, Auckland experiences higher temperatures than Wellington and Dunedin. In winter, Dunedin, located in the southern part of the South Island, is characterised by cool coastal breezes. These three cities show a significant gradient of temperature and wind that should cover most NZ locations.

Table 1: Average wind speed (m/s) and temperatures for Auckland, Wellington and Dunedin in summer and winter (Source: Windfinder.com and Weatherspark.com)

	Season	Auckland (Grey Lynn)	Wellington (Airport)	Dunedin (Forbury)
Average wind speed (m/s)	Summer	3.6	6	6
	Winter	2.8	7.2	3.3
Average temperature (°C)	Summer	23.0	19.0	19.0
	Winter	9.0	7.0	5.0

### Heat sources and heat transfer

The preliminary simulation did not consider solar gain from the north-facing glazing surfaces but considered the heat gain from the children (100 W) and the teacher (157 W), as stated in Gao (2023). The heat loss for walls (88.6 W/K), windows (116.5 W/K), roof (21 W/K), and floor (50.3 W/K) were provided by the prefab module designer. In addition, one wall-mounted inverter heat pump (Mitsubishi DXK33) was used only in winter to heat the room. Consequently, we expect a higher air mixing effect in winter than in summer, which will help de-stratify the air that tends to make thermal layers (entering cold air and staying at the bottom of the classroom).

## 2.4 CFD modelling approach

The general equations used in this CFD simulation can be found in Versteeg et al. (2007). These equations are based on the mass, energy, and momentum conservation laws. The CFD modelling was undertaken using a commercial CFD software, scSTREAM (Cradle CFD part of Hexagon Manufacturing Intelligence, Hexagon AB Group, Sweden).

### Turbulence models

CFD employs turbulence models to simulate fluid motion and the appearance of eddies. These turbulence models are specific to different situations, and a significant research effort has been dedicated to their development (Stevanovic, 2009). In ventilation studies, air turbulence is usually described using the Reynolds-Averaged-Navier-Stokes (RANS) equations (Yakhot, 1986; Lu et al., 2019). Derived from the RANS equations, several models have been developed, like the ReNormalization Group (RNG) K-epsilon turbulence model. This model is commonly used for airflow simulation to study building cross-ventilation and agrees well with experimental data (K. Kosutova et al., 2019).

### Computational grid and convergence criteria

scSTREAM has a finite volume discretisation scheme. The computational grid is a structured hexahedral mesh defined following CFD good practices (Sørensen et al. 2003). A sensitivity analysis was run after refining the volumes where considerable pressure or velocity gradients were expected, and then the grid convergence was obtained. The solver convergence was assessed by meeting residual error convergence criteria ( $10^{-6}$  level). The final mesh includes 8 million nodes for the models described.

## 2.5 Scenarios considered

### Occupants, activities, and carbon dioxide generation rate

Figure 2 shows that each classroom is occupied by 25 children (10 years old) and one teacher (female, 40 years old). The occupants are undertaking light activities (MET 1.5). Table 2 shows the two occupant categories' CO<sub>2</sub> generation rate (L/s).

Table 2: Carbon dioxide generation rate (L/s) at MET 1.5: sitting tasks, light effort (Persily et al., 2017)

Occupants	Generation rate (L/s) at MET 1.5
Female (40 years old)	0.0045
Child (10 years old)	0.0037

In our study, we assume that the CO<sub>2</sub> is generated at a constant rate. The CFD simulation keeps the outside CO<sub>2</sub> background level constant (0 ppm). The results will be increased by 419.3 ppm, the current outside CO<sub>2</sub> level in NZ (NIWA, 2024).

In our modelling, we considered three case studies:

**Case study 1 - Cross ventilation without extraction fan:** The airflow enters the classroom through the six trickle ventilators due to the difference in pressure between the outside and inside compartments (extractor fan disabled). This scenario is valid as most NZ classrooms lack extraction fans. For this case study, we expect the pressure difference between the inside and outside will usually not provide enough airflow to achieve the recommended 8 litres per second per child (Nzs 4303: 1990).

**Case study 2 - single-side ventilation with extraction fan:** The fan Q/P curve controls the extracted airflow. Under a continuous extraction regime (8 litres per second per child/teacher – 749 m<sup>3</sup>/h for the 26 occupants), the air flowing through the six trickle ventilators (north-facing windows only) will be influenced by the dynamic pressure applied due to the wind force on the classroom facade.

**Case study 3 - double-side ventilation with extraction fan:** The fan curve controls the extracted airflow. Under a continuous extraction regime (8 litres per second per child/teacher – 749 m<sup>3</sup>/h for the 26 occupants), the air flows through the 12 trickle ventilators (north and south facade).

### 3 RESULTS AND DISCUSSION

#### 3.1 Wellington Wind Model (Summer case): wind velocity on the classroom facade

Figure 5 shows a large-scale model for the Wellington school during summer. The dimensions of the Wind model are defined considering the building height (4.5 m) and the surface blockage on the plane perpendicular to the wind direction (200 m width (44H) and 50 m height (11H), 8 million nodes). On the windward side of the building (the north-facing side in our simulation), the velocity ranges from 0 to 8.0 m/s, with a reference input velocity of 6 m/s at 10 m (Table 1). A similar profile will be observed for the Dunedin classroom; both sites have a dominant northern wind with an average wind velocity of 6 m/s at 10m (Table 1).



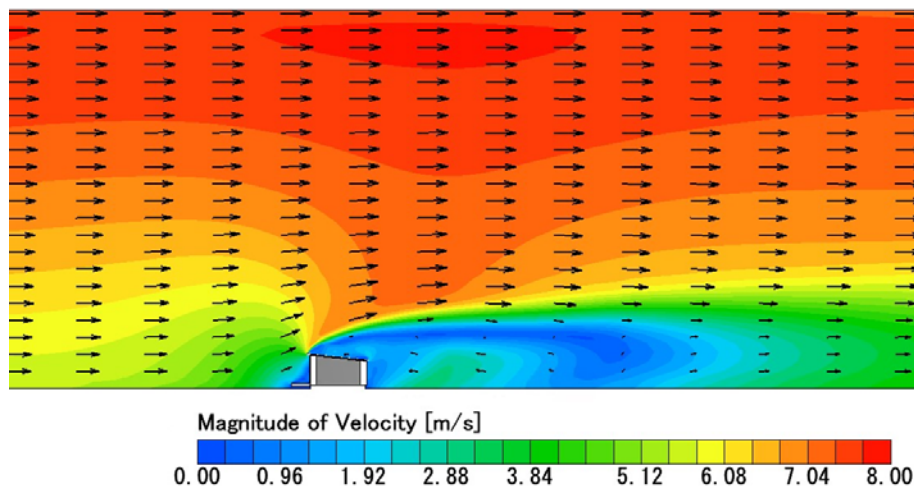


Figure 5: Wind velocity on the Wellington classroom façade in summer

Figure 5 shows a 2 m/s velocity near the windows where the trickle ventilators are located. The five additional simulations were undertaken (three locations/two seasons in total), and the pressure results are reported in Table 3.

Table 3 reports the pressure applied to the trickle ventilators and the flow rate entering the trickle vents. These results were obtained by averaging ten points along the length of each of the six trickle ventilators on the dominant wind façade (average of 60 values).

	Auckland summer	Auckland winter	Dunedin summer	Dunedin winter	Wellington summer	Wellington winter
<b>Pressure applied to the façade [Pa]</b>						
North façade	-5.83	-3.07	22.0	-0.88	22.00	31.23
South façade	3.14	-2.85	-5.84	-3.88	-5.84	-8.88
$\Delta P/2$	4.49	0.11	13.92	1.50	13.92	20.05
<b>Flow Rate [m<sup>3</sup>/h]</b>						
Flow rate deduced for each trickle ventilator	64.6	9.1	117.7	36.1	117.7	142.8
Total flow rate per classroom (input from six trickle ventilators fully open)	387.5	54.7	706.0	216.6	706.0	856.8
Percentage of achievement (749 m <sup>3</sup> /h recommended level)	52%	7%	94%	29%	94%	114%

Table 3 Mean dynamic pressures and corresponding flow rates applied to the trickle ventilators

Table 3 shows lower pressures applied to the Auckland classroom facades than in Dunedin and Wellington. As expected, Wellington showed higher pressures for both summer and winter than Auckland and Dunedin.

NZS4303:1990 recommends 8 litres per second per child. Assuming 25 children and one teacher per classroom, the minimum air flow rate is 749 m<sup>3</sup>/h to ventilate the classroom and keep the CO<sub>2</sub> level below 1000 ppm. Table 3 (last row) shows the achievement percentage across the six trickle ventilators (assuming the trickle ventilators fully open).

For the Auckland classroom, 52% and 7% of the recommended air flow rates were achieved in summer and winter, respectively. Regarding Dunedin's results, the airflow was almost sufficient

(94%) in the summer season. However, only 29% of the recommended flow rate entered the classroom in winter. For the Wellington case study, the airflow rate was close to the recommended level for summer (94%) and exceeded the recommended level in winter (114%).

The air enters at 19°C and 7°C in summer and winter, respectively (Table 1). We expect the summer airflow profiles through the trickle ventilators for the air at 19 °C (same temperature as room temperature) will follow a 45° angle. In contrast, the winter airflow profiles through the trickle ventilators for the air at 7°C (intake temperature is 12°C cooler than the 19°C room temperature) should quickly fall to the floor (Boulic, 2023). They could create discomfort for children sitting close to the windows.

It should be noted that these winter results were simulated with the trickle ventilators fully open. However, this assumption is only valid when the outside temperature is above 18°C, which was not the case in winter. The trickle ventilator will be only a third open when the outside temperature is below 12°C. So, the winter achievement should be divided by three. In summary, Wellington and Dunedin could achieve the recommended ventilation rate only in summer when using the trickle ventilators without a fan extractor. None of the three winter simulations achieved the recommended level of ventilation (effective open area reduced to a third of the full opening).

Building Bulletin 101 (BB101, 2006) recommend trickle ventilators with a minimum effective area of 0.192 m<sup>2</sup> to satisfy the classroom ventilation requirement in the case of single-sided ventilation. This is five times the effective area we used in our study (0.04 m<sup>2</sup> with six trickle ventilators fully open). Still, we had a case of double-sided ventilation, which should be more efficient than single-sided ventilation. A study carried out in a Wellington school over four days in late summer (March 2022) showed that more than five air changes per hour (twice higher than the recommended ventilation rate) were achieved with approximately 1.5 m<sup>2</sup> effective window opening in a cross-ventilation setting and under a wind velocity between 1.2 m/s and 3.5 m/s (Aniebietabasi et al. 2022). The size of the effective area of the trickle ventilator is important, and in our case study 1, it was insufficient in winter (lower effective area) and with low wind velocity. The wind velocity (creating the pressure difference) also impacts the ventilation rate. Cornaro et al. (2013) reported a higher ventilation rate with a 3.2 m/s average wind velocity entering the trickle ventilators than a lower 1.3 m/s wind average velocity. In our Case Study 1, a velocity of 2.0 m/s (Wellington summer) provided around 94% of the recommended level with the trickle ventilator fully open. The literature supports our results that wind velocity combined with a large effective area of trickle ventilators (at least 0.05 m<sup>2</sup>) will be needed to achieve the recommended ventilation rate when no extraction fan is used (BB101, 2006; Biler, 2018). In summary, we demonstrated that achieving a suitable air flow rate in a classroom environment with the sole operation of trickle vents (no extraction fan) was not possible in winter but was close to the requirement (94%) in the summer season for Dunedin and Wellington. An extraction fan connected to the trickle ventilators will be tested in Case Study 2 and Case Study 3.

### **3.2 Wellington classroom CFD model during winter and summer.**

#### **Airflow path and ventilation efficiency - no usage of the extractor fan (Case Study 1).**

In Case Study 1, the airflow enters the classroom through the trickle ventilators due to the difference in pressure between the outside and inside compartments (extractor fan disabled). The building comprises two identical classrooms. This will allow us to run two CFD simulations (winter and summer) simultaneously. Figure 6 shows the airflow path for the

classroom located in Wellington during winter (left) and summer (right). The dominant wind was North for both summer (January) and winter (July), as reported in Figure 4.

In winter, the inverter heat pump (Mitsubishi DXK33) is operated to keep the classroom in the thermal comfort zone ( $20^{\circ}\text{C} \pm 2^{\circ}\text{C}$ ). The inverter heat pump is not operated for cooling during the summer season. In Figure 6 (left), the inverter heat pump created the green streamlines.

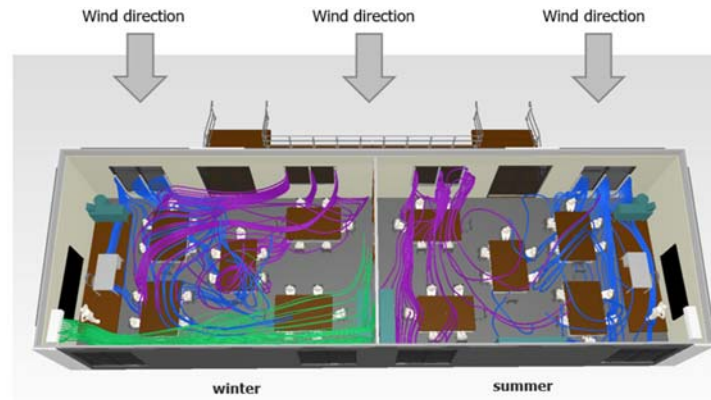


Figure 6: Air streamlines for the air entering from the North facade (cross ventilation)

For the summer case, we can notice fewer streamlines around the middle table (Figure 6, right). This result is expected as the middle table is not aligned with the trickle ventilator axis. Figure 6 shows that the inverter heat pump contributes to the winter air mixing in the classroom (the heat pump is not used in summer for cooling). The air streamlines are more disturbed during the winter case than the summer case. We can also notice that the furniture located in the left top corner (winter) and in the right top corner (summer) disturbed the streamlines.

Figure 7 shows the magnitudes of the velocity (m/s). Figure 7 (left) shows two seasons' positions on the vertical axis (air column). Figure 7 (right) shows the velocity plan 1.5 m from the floor, representing the children's breathing zone.

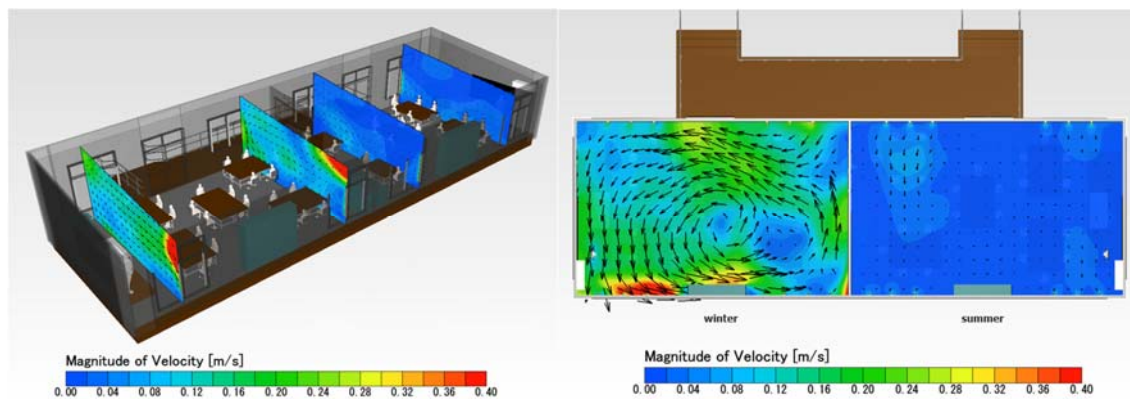


Figure 7: Magnitude of the velocity (left, vertical plan; right, 1.5 m from the floor)

Figure 7 confirms that the inverter heat pump contributes to air mixing during winter. The air moves at a velocity of 0.20 m/s in the centre of the room during the winter season. In contrast, the classroom has a much lower air velocity (0.05 m/s) during the summertime (lower buoyancy due to a lower difference in inside/outside temperatures). Despite the good mixing of air (0.20 m/s) in most parts of the classroom (inverter heat pump), we can notice a few areas with lower air velocity (0.05 m/s). These areas experiencing a lower mixing rate could create some “CO<sub>2</sub>

pockets” (Boulic, 2023). This hypothesis will be confirmed by our model investigating the impact of the airflow on the CO<sub>2</sub> concentration generated by the occupants.

### Temperature distribution - no usage of the extractor fan (Case Study 1).

Figure 8 shows the temperature distribution (°C). Figure 8 (left) shows two seasons' positions on the vertical axis (air column). Figure 8 (part) shows the temperature distribution 1.5 m from the floor (children's breathing zone). In winter, the input temperature is 7°C, while the summer input temperature is 19°C (Table 1).

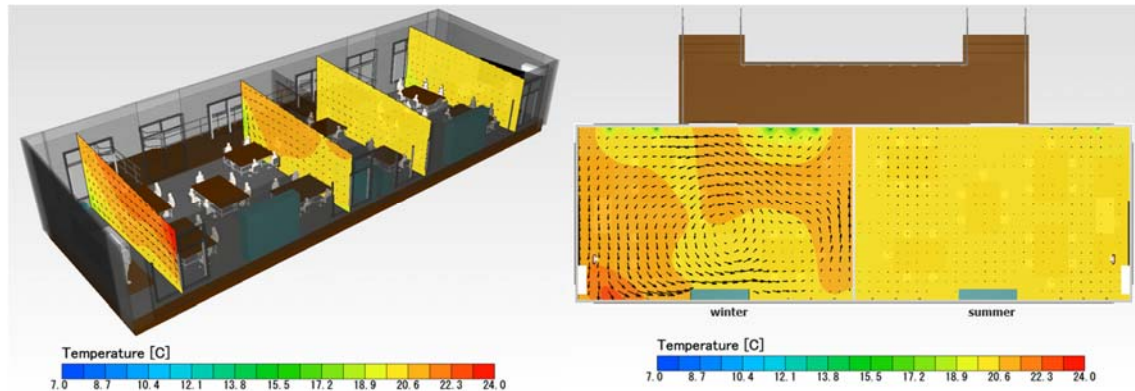


Figure 8: Temperature distribution (left, vertical plan; right, at 1.5 m from the floor)

Figure 8 (left) shows the winter case's temperature gradient from floor to ceiling and homogenous temperature distribution (well-mixed column) during the summer. A ceiling fan could be installed to homogenise the classroom air volume, mainly during winter (destratification).

Figure 8 (right) shows the cold air (7°C) entering the classroom through the six trickle ventilators for winter (blue spots). We need to confirm that intake air, which is 12°C cooler than the 19°C room temperature, will not create discomfort for children sitting close to the windows. This cold air trajectory is expected to be unidirectional downwards from the trickle ventilators (due to the temperature difference).

The trickle ventilators are equipped with a shape memory alloy spring, which will change the opening to external temperature (fully open above 18°C and one-third open under 12°C external temperature). Therefore, with an outside temperature of 7°C, the incoming flow rate could be reduced from 856.8 m<sup>3</sup>/h to 282.7 m<sup>3</sup>/h (66 % decrease), representing only 38% of the recommended flow rate. Reducing the effective open area of the trickle vent will reduce the ventilation rate and potentially impact pollutant distribution and virus transmission.

This section focused on the airflow path and the temperature distribution in the Wellington classroom for Case Study 1. We will repeat the modelling for Auckland and Dunedin and then move to Case Study 2 (continuous extraction regime of 749 m<sup>3</sup>/h with an air intake through the six trickle ventilators) and Case Study 3 (continuous extraction regime of 749 m<sup>3</sup>/h with an air intake through the 12 trickle ventilators).

We also plan to investigate the distribution of CO<sub>2</sub> in the classroom when CO<sub>2</sub> is used as a proxy for the ventilation rate. We will use the CO<sub>2</sub> generated by the classroom occupants over 90 minutes as a tracer gas. We will also investigate the potential creation of “CO<sub>2</sub> pockets” due to a lack of air mixing in some parts of the classroom. We will run the simulations for the three cities and the three case studies. When no extractor fan is used (Case Study 1), we expect to find a higher concentration of CO<sub>2</sub> in Auckland and Dunedin classrooms than in Wellington

classrooms due to the lower air velocity input. We also expect to find a higher CO<sub>2</sub> concentration in winter than in summer due to a decrease in trickle ventilators' efficient areas. Using an extraction fan (8 litres per second per child) should reduce the CO<sub>2</sub> concentration to the recommended level. A Finish study shows that the cold outdoor temperature makes opening windows for airing in winter more challenging. The same study recommends a mechanical ventilation strategy and a reduced classroom density (number of children per m<sup>2</sup>) to preserve indoor air quality in winter for cold climates (Uotila et al., 2023).

For temperate climates, a Spanish winter study (8°C to 12°C outside temperature) shows that after 10 minutes of cross ventilation (flush method), the CO<sub>2</sub> level decreases by 300 ppm (from 1000 ppm to 700 ppm) with a classroom temperature loss from 21.5°C to 19.5°C (Rey-Hernández, 2023).

For tropical climates, Seng Theng Ang et al. (2023) used CFD to simulate airflow and thermal comfort in a school. They showed that airing through louvres only does not sufficiently decrease the temperature, but using a windcatcher to extract the hot air through the roof provided potential chilliness to the occupants. Elmualim's study (2006) supports these findings as a windcatcher system can assist in reducing indoor temperature and mitigate summertime overheating. This method could be useful for Auckland and Northland NZ classrooms located in subtropical climates.

#### **4 LIMITATIONS AND SUGGESTIONS FOR FUTURE WORK**

This study focuses on the behaviour of different ventilation scenarios for a selected average classroom. However, it should be noted that variable configurations (room geometry, position of the tables, number of children and room volume) and wind conditions could vary. Furthermore, we neglected the infiltration rate for the building envelope, considering that they were negligible in the overall air flow trajectories.

This paper focused on the airflow path and the temperature distribution in the Wellington classroom for Case Study 1. We will repeat the modelling for Auckland and Dunedin and then move to Case Study 2 (continuous extraction regime of 8 litres per second per child with an air intake through the six trickle ventilators) and Case Study 3 (continuous extraction regime of 8 litres per second per child with an air intake through the 12 trickle ventilators).

We also plan to investigate the distribution of CO<sub>2</sub> in the classroom. We will use the CO<sub>2</sub> generated by the classroom occupants over 90 minutes as a tracer gas. The CO<sub>2</sub> level is used as a proxy for the air change rate following the NZS4303:1990 (ASHRAE 62: 1989) threshold. However, the classroom's CO<sub>2</sub> level should not be considered an overall indoor air quality indicator (Persily, 2020).

#### **5 CONCLUSION**

An appropriate ventilation rate is needed to provide children with a healthy classroom environment. Classroom occupants tend not to open windows during teaching, so an alternative solution is needed, which could retrofit existing windows and install an extraction fan.

In three NZ locations (Auckland, Wellington and Dunedin), our project investigated a suitable ventilation solution (trickle ventilators disconnected/connected to an extraction fan). This paper reported findings for the Wellington classroom with the disconnected extractor fan. This case study was selected because Wellington experiences the highest wind velocity level in NZ, so the highest pressure is applied to the classroom facade, and potentially, there should be a higher air intake. The results showed that the air was well-mixed in the classroom in summer (no temperature difference between inside and outside). Our CO<sub>2</sub> model must confirm that enough

flow rate can be provided to the classroom in summer. However, the trickle ventilators' effective area was reduced in winter, and insufficient air entered the classroom. In addition, despite good air mixing assisted by the inverter heat pump use, there were still a few areas where the air was not well-mixed. A ceiling fan could be installed to assist in the air mixing. The literature supports our results that wind velocity (at least 2 m/s at the trickle ventilator level) combined with a large effective area of trickle ventilators (at least 0.05 m<sup>2</sup>) will be needed to achieve the recommended ventilation rate when no extraction fan is used. It will be advised to connect the trickle ventilators to the fan extractor to increase the ventilation rate throughout the year. Following the CFD project, we will deploy sensors to monitor the temperature, relative humidity and CO<sub>2</sub> in Auckland, Wellington and Dunedin classrooms to validate the modelling findings.

## 6 REFERENCES

Aniebietabasi, A., Longley, I., Chen, J., MacKenzie, S., Sutherland, A., Jermy, M., Phipps, R., Gronert, R. (2022) The effectiveness of natural ventilation: a case study of a typical New Zealand classroom with simulated occupation. The New Zealand Ministry of Education, Wellington, New Zealand <https://assets.education.govt.nz/public/Documents/School/Property-and-transport/Ventilation-in-school-buildings/effectiveness-of-natural-ventilation.pdf>

BB101 (2006). Building Bulletin 101. Ventilation of school buildings, Version 1.4, 2006. Education and Skill Funding Agency.

Biler, A., Unlu Tavit, A., Su, Y., Khan, N. (2018). A Review of Performance Specifications and Studies of Trickle Vents. Buildings, 8, 152. <https://doi.org/10.3390/buildings8110152>

Boulic, M., Bombardier, P., Zaidi, Z., Russell, A., Waters, D., van Heerden, A. (2023). Using trickle ventilators coupled to fan extractor to achieve a suitable airflow rate in an Australian apartment: A nodal network approach connected to a CFD approach, Energy and Buildings, 304, 113828, ISSN 0378-7788, <https://doi.org/10.1016/j.enbuild.2023.113828>.

Boulic, M., Wang, Y., Phipps, R., Chitty, C., Cunningham, C., Moses, A., Weyers, R., Jang-Jaccard, J., Olivares, G., Shekar, A., Longley, I., Tookey, L., Ponder-Sutton, A., Waters, D., (2019) Project: Using a low-cost sensor platform to explore the indoor environment in New Zealand schools <https://d39d3mj7qio96p.cloudfront.net/media/documents/BRANZ-RN-Indoor Air Quality 5.pdf>

BRANZ (2021) Metra Panel System Appraisal #364 <https://www.branz.co.nz/appraisal-codemark-certificates/metra-panel-system/>

Chappell, P.R. (2013). The climate and weather of Auckland. NIWA Science and Technology Series 60, 40 pp.

Chappell, P.R. (2014). The climate and weather of Wellington. NIWA Science and Technology Series 65, 44 pp.

Cornaro, C., Paravicini, A., and Cimini, A. (2013) Monitoring Indoor Carbon Dioxide Concentration and Effectiveness of Natural Trickle Ventilation in a Middle School in Rome, Indoor and Built Environment, 22:2, 445 – 455.

Correiax, G., Rodrigues, L., Gameiro da Silva, M., Gonçalves, T., (2020). Airborne route and bad use of ventilation systems as non-negligible factors in SARS-CoV-2 transmission. *Med Hypotheses*.141:109781. <https://doi:10.1016/j.mehy.2020.109781>

Dai, H., Zhao, B., (2020). Association of the infection probability of COVID-19 with ventilation rates in confined spaces. *Build Simul*. 13(6):1321-1327. <https://doi:10.1007/s12273-020-0703-5>

Elmualim, A.A. (2006). Effect of damper and heat source on wind catcher natural ventilation performance. *Energy and Buildings*, 38: 939–948.

Gao, S., Yang, L., Li, Y., Liu, S., Zhang, H., Arens, E., Zhai, Y., (2023) Metabolic rate in children and adolescents: Tabulate values for common activities and comparisons with standards and adult values, *Building and Environment*, 244, 110804, ISSN 0360-1323, <https://doi.org/10.1016/j.buildenv.2023.110804>.

Gully, F. (2015). *Windows and Doors in Schools: A study of low-decile primary schools in Auckland (Final Year Project Report)*. Auckland, NZ: Massey University.

Guyot, G., Sherman, M., Walker, I., (2018) Smart ventilation energy and indoor air quality performance in residential buildings: A review, *Energy and Buildings*, 165, 416-430, ISSN 0378-7788, <https://doi.org/10.1016/j.enbuild.2017.12.051>

Kosutova, K., van Hooff, T., Vanderwel, C., Blocken, B., Hensen, J., (2019) Cross-ventilation in a generic isolated building equipped with louvers: Wind-tunnel experiments and CFD simulations, *Building and Environment*, 154, 263-280, ISSN 0360-1323, <https://doi.org/10.1016/j.buildenv.2019.03.019>

Liaw, F. (2015). *Doors and Windows Needs for School (Final Year Project Report)*. Auckland, NZ: Massey University.

Lu, J., Zhu S., Kim M. K., Srebric J. (2019). A Review of CFD Analysis Methods for Personalized Ventilation (PV). *Indoor Built Environments, Sustainability*, 11, 4166.

Macara, G.R. (2015). *The climate and weather of Otago*. NIWA Science and Technology Series 67, 44 pp

MOE (2024) Ministry of Education – Te Tahuu o te Matauranga. Plan and build a new teaching space. Wellington, New Zealand. <https://www.education.govt.nz/school/funding-and-financials/funding/teaching-space-funding/plan-and-build-a-new-teaching-space/>

NIWA (2024) Daily CO<sub>2</sub> measurements from NIWA's atmospheric monitoring station at Baring Head, New Zealand <https://niwa.co.nz/climate/research-projects/carbonwatchnz/dailyco2measurements>

NZS4303:1990 Ventilation for acceptable indoor air quality. New Zealand Standard, Wellington, New Zealand.

Palacios Temprano, J., Eichholtz, P., Willeboordse, M., Kok, N., (2020). Indoor environmental quality and learning outcomes: protocol on large-scale sensor deployment in schools. *BMJ Open*; 10:e031233. doi:10.1136/bmjopen-2019-031233

Persily, A. et al. (2017). Carbon dioxide generation rates for building occupants. *Indoor Air*, 27(5): 868–879.

Persily, A. (2020). Quit Blaming ASHRAE Standard 62.1 for 1000 ppm CO<sub>2</sub>, in the 16<sup>th</sup> Conference of the International Society of Indoor Air Quality & Climate (Indoor Air 2020), Seoul, Korea.

PPTA (2024) <https://www.ppta.org.nz/news-and-media/class-size-average-class-size-and-pupil-teacher-ratio-truth-lies-and-government-statistics/#:~:text=The%20most%20common%20class%20size,smallest%20had%20a%20single%20student.>

Rey-Hernández, J.M., Arroyo-Gómez, Y., San José-Alonso, J.F., Rey-Martínez, F.J. (2023) Assessment of natural ventilation strategy to decrease the risk of COVID-19 infection at a rural elementary school, *Heliyon*, Volume 9, Issue 7, e18271, ISSN 2405-8440, <https://doi.org/10.1016/j.heliyon.2023.e18271>

Sadrizadeh, S., Yao, R., Yuan, F., Awbi, H., Bahnfleth, W., Bi, Y., Cao, G., Croitoru, C., de Dear, R., Haghghat, F., Kumar, P., Malayeri, M., Nasiri, F., Ruud, M., Sadeghian, P., Wargocki, P., Xiong, J., Yu, W., Li, B., (2022). Indoor air quality and health in schools: a critical review for developing the roadmap for the future school environment. *Journal of Building Engineering*, 57, 2022, 104908, ISSN 2352-7102, <https://doi.org/10.1016/j.job.2022.104908>.

Seng Theng Ang, A., Chin Voon Sia, C., Lee Yeu, Y., Hing Chong, K., Seng Chia, C., and Joseph, A. (2023). Natural Ventilation and Indoor Air Quality in Domestic School Building: CFD Simulation and Improvement Strategies. *CFD Letters*, 16(3), 1–14. <https://doi.org/10.37934/cfdl.16.3.114>

Sørensen, D.N., Nielsen, P.V. (2003). Quality control of computational fluid dynamics in indoor Environments, *Indoor Air*; 13: 2–17.

Stevanovic, Z., Mumovic, D., Kavgic, M. (2009). Indoor Air Quality and Ventilation Modelling in Mumovic, D., & Santamouris, M. (Eds.). *A handbook of sustainable building design and engineering: An integrated approach to energy, health and operational performance* (1st ed.). Routledge.

Uotila, U., and Saari, A. (2023), "Determining ventilation strategies to relieve health symptoms among school occupants", *Facilities*, Vol. 41 No. 15/16, pp. 1-20. <https://doi.org/10.1108/F-10-2021-0101>

Versteeg, H. K., Malalasekera, W. (2007). *An introduction to computational fluid dynamics: The finite volume method*. Harlow, Essex, England; Pearson Education Ltd.

Yakhot, V., Orszag, S.A., (1986). Renormalisation group analysis of turbulence. I. Basic theory. *Journal of Scientific Computing*, 1, 3–51.



# On the impact of night ventilation through motorized windows on the energy and thermal performance of office buildings

Michele Zinzi<sup>\*1</sup>, Martina Botticelli<sup>1</sup>, Sabrina Romano<sup>1</sup>, Stefano Agnoli<sup>2</sup>

*1 ENEA TERIN ICER  
Via Anguillarese 301  
00123 Rome, Italy*

*2 ENEA ISER  
Via Enrico Fermi, 45,  
00044 Frascati (RM), Italy*

*\*Corresponding author: michele.zinzi@enea.it*

## ABSTRACT

Global and local climate changes affect the energy performance of buildings, especially during the warm season, with relevant increase of cooling uses in mechanically cooled buildings and discomfort hours in naturally ventilated ones. The ventilative cooling is proved to be a promising strategy to tackle this threat, however installing new ventilation systems in existing buildings is challenging in technical and economic terms. The strategy can be also pursued by motorized windows duly operated. This solution is tested in a living lab in the northern outskirts of Rome, Italy. The living lab consists of seven rooms of an office building, planned to be upgraded to more four rooms and services during the present year. The energy and environmental performances of the living lab are continuously monitored and operated by a smart energy management system. Four of the seven rooms are equipped with motorized windows to provide free cooling and adequate indoor air quality through the implementation of different control rules. These windows are 200cm wide and 160cm high, the width of the manually and monetized sashes are 130 and 67.5cm, respectively. The latter opens/closes thanks a developing chain (30cm long) that allows 30° as maximum angle opening. As the living lab is expanding in the number of rooms, new solutions are screened to exploit the free cooling potential for windows to be replaced. Field measurements were carried out to assess the impact of night ventilation under real operative conditions, as well as to calibrate the living lab model in TRNSYS 17. In this study, starting from the calibrated model, a parametric analysis is carried out to evaluate the impact of different aperture angles of the motorized sash on the ventilative cooling potential. Simulations are run for the case of the active cooling installed in the office rooms. Based on the numerical analyses outcomes, the partner industries designed a prototypal windows, in which the developing chain is stretched so to allow 45° opening angle of the motorized sash. The new windows are currently under production, and it is planned to be installed and tested on site in summer 2024.

## KEYWORDS

Energy performance, night ventilation, dynamic simulation, advanced windows

## 1 INTRODUCTION

As in most European countries, the energy renovation of the building stock is a crucial issue to meet the environmental objective set at Italian and international level (MiSE, 2019). The issue is of particular relevance in Italy, due to the age and the obsolescence of a relevant part of existing buildings (MiSE, 2020). Despite the first target has been to reduce the space heating use for decades, it is now necessary to tackle the recent explosion of space cooling uses, due to thermal comfort expectations by a large portion of the population not able to afford mechanical cooling systems before, as well as increase of the demand induced by global and local overheating phenomena, as the urban heat island.

The trend is bound to increase in most part of the world in the coming years (IEA, 2018). This framework created the condition for international collaborations aimed at identifying and quantifying solutions for efficient cooling, as done under the Energy and Buildings Community

of the International Energy Agency; among the studied ones, the ventilative cooling emerged as one of the most promising passive cooling strategy in several climatic regions (Holzer, 2023). This strategy can be applied by naturally cooling down the building during the cooler hours of the day, typically at night and in the first hours of the morning. Ventilative cooling can be optimised when mechanical ventilation systems are installed, unfortunately most of the existing buildings, either residential or not, are not in such conditions. Windows, and other envelope components, can be thus used to pursue the night ventilation (Hee, 2015).

More in general, windows and transparent surfaces deeply affect the building energy and environment performances (Vanhoutteghem, 2015; Valladares-Rendón, 2017) and the replacement or upgrade of existing fenestration systems is one the most effective solutions to improve the thermal response of the building during the heating and cooling season. During the latter, thermal loads are affected by solar gains through transparent components; consequently, the solar protection is an important solution to achieve energy efficiency, thermal and visual comfort (Al-Masrani, 2019). In addition, dynamic aperture of the building envelope may mitigate the indoor thermal environment via natural ventilation, according to the specific climatic conditions and building use (Zhang, 2021; Chiesa 2015).

Automated dynamic windows can be operated to optimise the thermal response of the building, and, at the same time, ensure comfort conditions for the occupants (Psomas, 2017). Benefits of this technology were quantified in field and numerical studies, aimed at improving the performance of an office building by modulating solar gains and night ventilation through automated windows managed by a smart energy management system (Botticelli, 2023). The here presented study starts from those findings and analyses window design alternatives to increase the ventilative cooling potential and increase the energy and thermal performance of the building.

## 2 MATERIALS AND METHOD

The activity, here presented, resumes the results achieved in (Botticelli, 2023) and develop a process to upgrade the advanced windows installed in the F40 building of the Casaccia Research Centre of ENEA, as well as to quantify the impact on the built environment. The work is carried out in the following steps:

- Description of the reference building and recap of the model calibration;
- Detailed description of the current windows system and possible upgrade aimed at enhance ventilative cooling;
- Modelling of the new windows' configuration for single side ventilation;
- Numerical analyses to assess the impact of the technology on the building cooling energy performance.

The base case is the building without any night ventilation (windows closed) and the alternatives are compared against both, the base case and the current windows' configuration. The results are then analysed to identify the most effective window aperture configuration as a function of the cooling potential and the technological limitations for the window motorization.

### 2.1 Description of the building and recap of the model calibration

The test building dates back to the late 80s of the past century. It was a state of art building at those time, in fact the structure is in reinforced concrete and the walls have a double layer of clay bricks with thermal insulation in between, scoring  $0.50 \text{ W/m}^2\text{K}$  thermal transmittance.. The case study is the Living Lab of the building consisting of seven rooms at the second of the three floors; they are west oriented and the dimensions are: width 3.90 m, depth 4.34 m, height 3.20 m. Each room has a hole-in-a-wall window 200 cm wide and 160 cm high, with a window to floor and window to wall are ration of 0.19 and 0.26, respectively. Rooms host one or two

workers, with flexible working schedule, mostly in the 08:00-18:00 range. The seven rooms have identical rooms at the lower and upper level with identical thermal regime. The lay-out of the living lab with indicated rooms and window type is reported in Figure 1.



Figure 1: Lay-out of the ENEA living lab. The figure show the office number and the window typology in each room

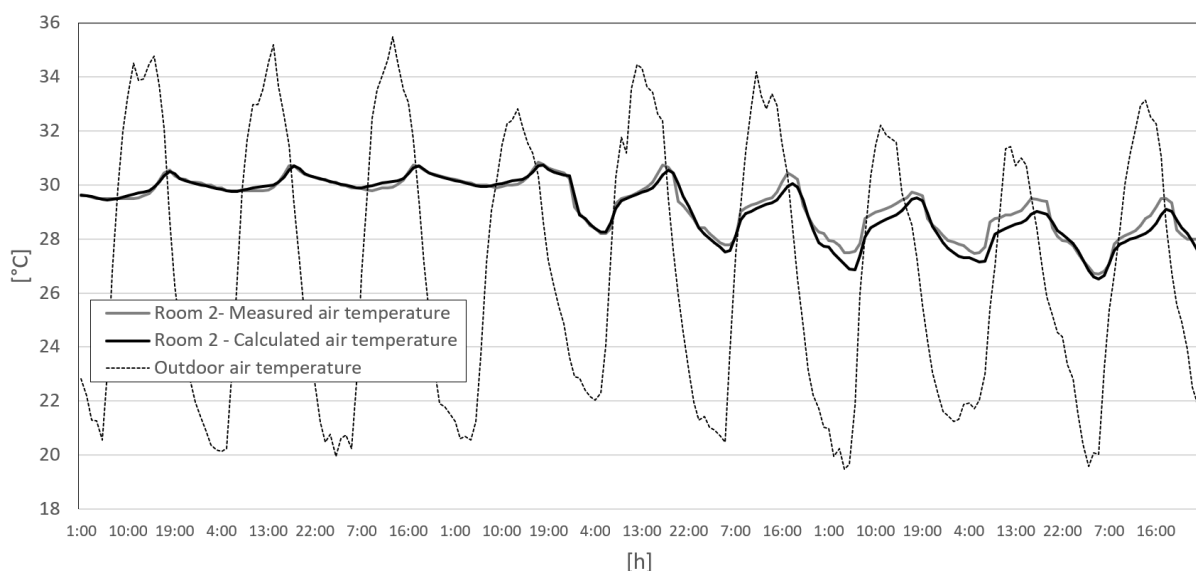


Figure 2: Comparison of measured and calculated air temperature in an exemplary room during 9 days in August 2020. The first 4 days the windows are closed, next the windows are automatically opened during the night-time hours

Rooms 5, 6 and 7 have original windows (W1), equipped with double glazing units with no-thermal break aluminium frame and an external blind for solar control. Rooms 1 and 2 have new windows (W3) with triple glazing unit with low-emissivity solar selective coating and argon in the two gaps, and the frame is in aluminium with thermal breaks. Room 3 and 4 have windows (W2) as W3 but with a double glazing unit. W2 and W3 have moveable venetian blinds in the air gap and a motorized sash. Figure 2 reports an exemplary comparison of the measured and the calculated air temperature, in a TRNSYS calibrated model against thermal free-floating and active cooling conditions according. Accuracy of the temperature sensor  $0.5^{\circ}\text{C}$  in the range of measured temperatures. Figures 2 also reports the outdoor air temperature during the monitoring period.

According to the procedures defined in (ASHRAE, 2002), a thermal model is calibrated when the coefficient of variation of the root means square error is lower than 30% in hourly data are used; in our previous exercise the indicator was slightly above 2% only, in full compliance with the reference method. Full details about measures and calculations can be found in (Botticelli, 2023; Zinzi, 2023).

## 2.2 Detailed window description and new design options

The new windows (W1 and W2) were designed and installed in the living lab in the framework of a joint activity with shading and fenestration systems manufacturers. The cooperation aimed at testing the potential of advanced dynamic windows in improving the energy performance of an existing building, thanks to the presence of the smart energy management system installed in the building, able to activate the venetian shading system and the sash opening of the windows to ensure solar protection during the day and ventilative cooling at night.

The graph in Figure 2 shows the impact of the window opening from 9pm until 7am (next day) on the temperature level in that exemplary room. Comparing the temperature profile with the windows closed (first four days in the graph) with that of the days with night ventilation it was observed that the maximum temperature reduction was not greater than 1.5°C. In agreement with the manufacturers, it was decided to study new configurations of the windows to enhance the ventilative cooling potentials.

The current new windows have two sashes, see Figure 3, and the net openable areas are as follows: the one on the left is manually operated and is 130cm wide and 154cm high, and the one on the right that is 65cm wide and 154cm high. The latter is motorized and it is activated either by the push-button on the sash or remotely by the building smart system. The motorized opening takes place thanks to a developing-chain, whose maximum length is 30 cm and allows 26cm of maximum aperture – image on the right of Figure 3.

Increasing the ventilation potential is, thus, intimately linked to the length of the chain, which rule the sash opening. Increasing the latter has a number of technical restraints; one of them would be related to the higher position of the button (not-ergonomic), other ones cannot be disclosed because of industrial property. To asses in details the impact of the windows and sash configuration, it was decided to analyse the impact of different apertures configurations on the energy and thermal performance of the calibrated model.



Figure 3: Front view of the new window, left, with the push-button indicated on the right sash; detail of the motorized chain to open/close the sash on the right.

### 3 CALCULATION

The living lab was implemented in the well known software TRNSYS 17, a model able to calculate the thermal response of buildings and solar systems in transient regime. The overall simulation is carried out by several calculation routines (called Types), each of them with a specific calculation task, and appropriately link each other. The model here used is that calibrated and applied for energy performance analyses in the aforementioned publications. The following routines were used:

- weather data reader, where local measured air temperature, relative humidity and wind speed are inputted (data used for simulation are those from Ciampino Airport as reported in the Meteorom international database);
- solar processing, where the solar irradiation is calculated for whatever façade starting from the local measured global horizontal irradiation;
- sky temperature calculation routing, to calculate the radiative heat transfer between the building elements and the sky;
- psychometrics to calculate the characteristic of the moisted air;
- building descriptor, where the characteristic of the envelope, energy systems, gains/losses, occupancy are described;
- ad-hoc routine to model the solar shading occupancy, shading and ventilation schedule;
- ad-hoc routine to model the single side ventilation induced by the window opening.

#### 3.1 Thermo-physics characteristics of the building

Each room of the living lab is treated as a thermal zone; all the boundary zones (corridor and rooms above and below) were monitored so they thermal conditions are used as known input. The external wall has U-value  $0.5 \text{ W/m}^2\text{K}$  U value; the vertical and horizontal internal structures have U-value 1.6 and  $1.67 \text{ W/m}^2\text{K}$ , respectively. Once calibrated, the model was simplified for the sake of the calculation effort, using the window W2 in all the rooms; its main properties are: U-value  $1.4 \text{ W/m}^2\text{K}$ , g-value of the glazing system 0.35, light transmittance of the glazing system 0.69, the solar properties with the shading activated change as a function of the sun position and the lamellae tilt. With the objective of focusing on the ventilative cooling potential, occupancy and internal gains were simplified and assigned a constant 300W during the occupancy hours from 08:00 until 18:00.

The simulation is run for the cooling season only in line with the scope of the study. Each room is equipped with a direct-expansion air conditioning unit with 4.03 Energy Efficiency Ratio (EER) and 2.5kW as peak power. The summer set-point are  $26^\circ\text{C}$  and 55%, and the system run on daily basis during the occupancy hours; the air conditioning is switched-off during the week-end, when the offices are empty. When the night ventilation is activated, fixed 0.1 ACH is considered as infiltration, while the ventilation rates at night are calculated according to the procedure defined in the next sub-section.

Concerning the dynamic behaviour of the windows, the shading systems are activated when the global solar irradiation raised above  $150 \text{ W/m}^2$  and they are retracted when the irradiation drops below  $100 \text{ W/m}^2$ ; for the sake of calculation times the lamellae are not varying the tilt according to the solar position but are kept fixed with  $45^\circ$  tilt against the. The night ventilation is ensured by opening the automated sash when the indoor temperature is  $2^\circ\text{C}$  higher than the external one, and they close when the temperature difference is below  $0.5^\circ\text{C}$ .

### 3.2 Natural ventilation through window model

As mentioned above, the external flow rate due to the single-side opening of windows was calculated according to the empiric model developed in (Warren, 1985), which resulted to be sufficiently accurate for the specific case study, as reported in the previous sections. The model provides two equations to calculate the flow rate through the window aperture due to stack effect (1) and to wind (2):

$$Q_s = A \cdot \frac{C_d}{3} \cdot (\Delta\theta \cdot g \cdot \frac{h}{\theta})^{0.5} \quad (1)$$

$$Q_w = 0.025 \cdot A \cdot w_R \quad (2)$$

Being:

$Q$ (m <sup>3</sup> /s)	air flow rate for stack effect (s) and wind (w)
$A$ (m <sup>2</sup> )	area of the aperture, being $h$ the height of the aperture and $b$ its width
$C_d$ (-)	coefficient of discharged assumed 0.61 for sharp edged windows
$g$ (m/s <sup>2</sup> )	acceleration of gravity
$\theta$ (K)	mean of the internal and external absolute air temperature
$\Delta\theta$ (K)	difference between internal and external air temperature
$w_R$ (m/s)	wind velocity at reference height

At a given time step, the flow rate entering the room is the greater value between the two obtained with the equations 1 and 2.

Given the objective of the study, we run a set of simulation for different values of the aperture, keeping fixed the height of 154cm and progressively increasing the width of the aperture, starting from the initial value 26cm maximum current opening allowed by the chain and progressively increasing it by 5cm. The geometry of the apertures and the opening to floor area ration for the different chain length is reported in Table 1, together with the results on the building energy performance.

## 4 RESULTS

The simulations were run for the cooling season and, in particular, they focused on the three hottest months (June, July, August); the performance, in terms of total energy and energy intensity, of the building as a function of the windows opening geometry are reported in Table 1. Figure 4 shows the cooling savings achievable by the different opening sizes of the window with respect to the base case (no night ventilation) and the incremental savings achievable with respect to the current aperture. It can be observed that the current window configuration leads to 2% to aperture to floor area ratio. The additional increase of the chain length by 5cm produces about 5% increase of the aperture to floor area ratio, peaking 4.4% for the maximum chain length (0.51m).

The results report the absolute final energy uses, as well as the energy savings compared with the base case (no night ventilation), whose initial cooling energy is 37.4kWh/m<sup>2</sup> per year. The energy uses as a function of the window opening do not follow a linear correlation, in fact the relative energy savings progressively decrease with the increase of the aperture. The best approximation is reached by a cubic interpolation function, scoring an R<sup>2</sup> of 1. From the simulation results, it can be observed that the window opening with the current aperture halves (57%) the initial energy use, reaching 70% energy savings with the greatest window opening (aperture 0.74m<sup>2</sup>). Comparing to the base case, increasing the chain length from 36 to 51cm

brings 5% ( $1.8\text{kWh/m}^2$ ) as additional savings. Increasing the aperture width of 10cm provides an absolute cooling reduction of  $3.1\text{kWh/m}^2$ , corresponding to 20% additional savings respect to the current aperture. An additional 15cm of the chain length would provide only  $1.5\text{kWh/m}^2$  cooling use reduction.

Table 1: Window aperture geometry and energy performance for the identified configurations

Chain length [m]	Aperture area [m <sup>2</sup> ]	Aperture to floor area ratio [%]	Energy [kWh]	Energy intensity [kWh/m <sup>2</sup> ]
0.00	0.00	0.0	4558	37.4
0.26	0.35	2.1	1983	16.3
0.31	0.43	2.5	1762	14.5
0.36	0.51	3.0	1613	13.2
0.41	0.59	3.5	1510	12.4
0.46	0.66	3.9	1445	11.9
0.51	0.74	4.4	1386	11.4

It is observed also that the prevailing ventilation forcing is the stack effect for the current configuration, this ventilation mode applies for 67% of the period. Increasing the size of the opening, a slight increment of the wind effect is observed, even if the stack effect remains the prevalent ventilation mode in all configuration; in fact, the stack effect occurrence drops to 62% for the  $0.66\text{m}^2$  aperture.

The current aperture provides 2.5ACH on average (0.6 and 8.2 as minimum and maximum, respectively) during the opening hours. The  $0.51$  and  $0.66\text{m}^2$  apertures provide 3.4 and 4.3ACH on average, with a relative increase compared to the current configuration by 40% and 75%, respectively; in both cases the maximum rates peak well above 10ACH.

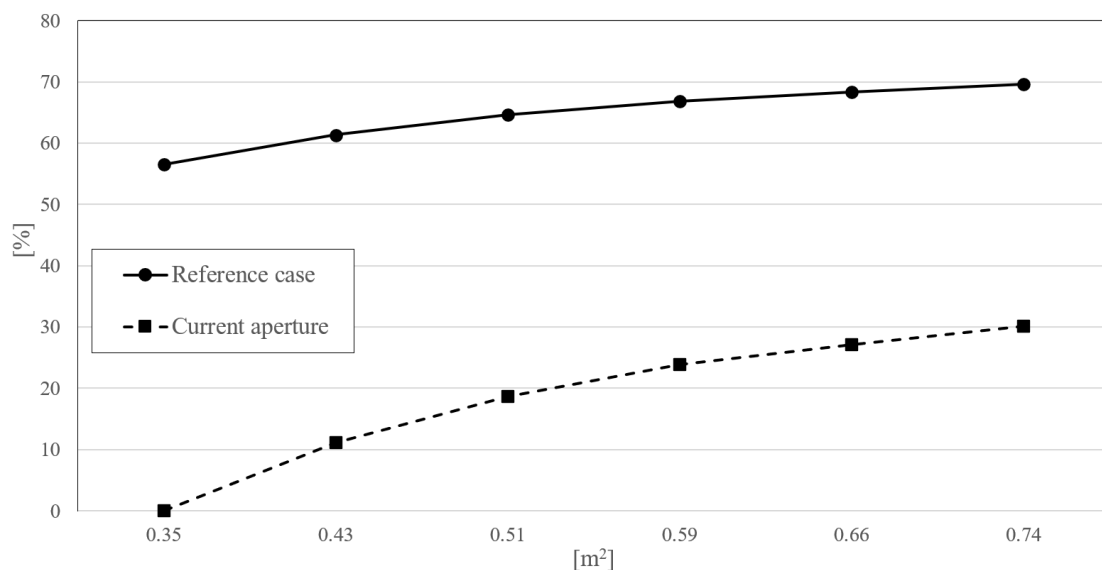


Figure 4: Relative energy savings for different aperture areas; they are calculated with respect to the base case (no night ventilation) and to the current aperture.

As exemplary case, Figure 5 reports the ACHs as a function different aperture areas for an entire week in mid-August. The plots well depict the relation between the two variables and also show the air exchange peaks due to the sudden increase of the wind. It can be also observed that the chosen rule keeps the window opened not only during the night-time, but also during the morning hours. In addition, the increase of indoor temperature, due to the absence of active cooling during the week end, keeps the window opened for entire days, thus mitigating the overheating risk in thermal free floating conditions.

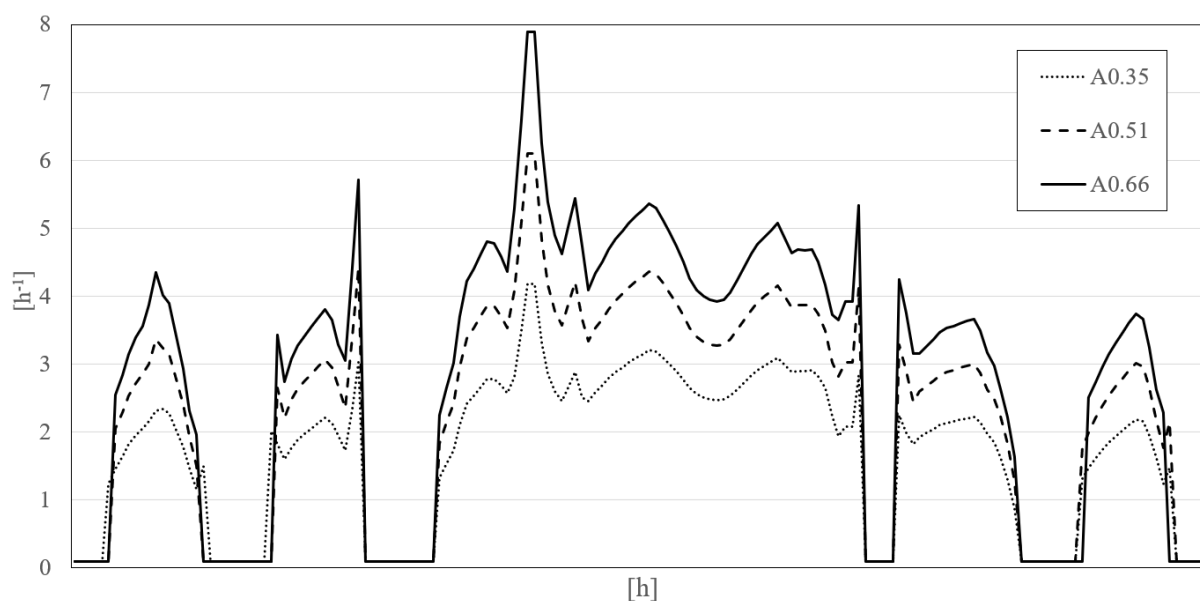


Figure 5: Air exchange per hour for different aperture sizes during a week in mid July

## 5 CONCLUSIONS

This study aimed at assessing the potential of natural ventilation provided by advanced fenestration systems, whose aperture can be managed via a building energy management system to enhance ventilative cooling by night opening. Starting on previous studies, focus was here to provide insight on ventilation potential to upgrade the design of these innovative windows, in particular on the mechanical parts that rule the aperture size. The calculation work was based on a model validated against field measurements and, with the given input, it was found that the current aperture provides 57%; additional savings, up to 70%, can be reached increasing the aperture up to  $0.74\text{m}^2$ . Increasing the area, however, implies to substantially increase the metal chain that ensure the automated opening of the moveable sash of the window; this is critical, especially for the usual window sizes (total height up to 170cm). According to the study, increasing the length of chain by 10cm provides more than  $3\text{kWh/m}^2$  energy savings, with 20% incremental saving respect to the current chain. Further stretching provides lower savings and does not justify the mechanical implications needed to upgrade the current motorization window design.

## 6 ACKNOWLEDGEMENTS

Research funded by Project 1.7 “Technologies for the efficient penetration of the electric vector in the final uses” within the “Electrical System Research” Programme Agreements 22-24 between ENEA and the Ministry of Environment (PTR 22-24).

The authors thank Pellini s.p.a. and Schuco Italia s.r.l. for the valuable support in the design and production phase of the fenestration systems.

## 7 REFERENCES

Al-Masrani, S. M., & Al-Obaidi, K. M. (2019) Dynamic shading systems: A review of design parameters, platforms and evaluation strategies, *Automation in Construction*, Volume 102, Pages 195-216, <https://doi.org/10.1016/j.autcon.2019.01.014.18>



- ASHRAE (2002) Measurement of Energy and Demand Savings, Guideline 14-2002
- Botticelli, M., Agnoli, S., Romano, S., Zinzi, M. (2023). Exploiting Passive Cooling in Office Buildings with Advanced Automated Glazing Systems: Preliminary Analyses from a Field Study. In: Wang, L.L., et al. Proceedings of the 5th International Conference on Building Energy and Environment. COBEE 2022. Environmental Science and Engineering. Springer, Singapore. [https://doi.org/10.1007/978-981-19-9822-5\\_55](https://doi.org/10.1007/978-981-19-9822-5_55)
- Chiesa, G., & Grosso, M. (2015) Geo-climatic applicability of natural ventilative cooling in the Mediterranean area, *Energy and Buildings*, Volume 107, Pages 376-391, <https://doi.org/10.1016/j.enbuild.2015.08.043>.
- Hee, W.J., Alghoul, M.A., Bakhtyar, B., Elayeb, O., Shameri, M.A., Alrubaih, M.S., Sopian, K. (2015) The role of window glazing on daylighting and energy saving in buildings, *Renewable and Sustainable Energy Reviews*, Volume 42, <https://doi.org/10.1016/j.rser.2014.09.020>.
- Holzer, P., et al. (2023) Resilient Cooling of Buildings – State of the Art Review, *International Energy Agency EBC Annex 80*, doi: 10.52776/COXK4763
- IEA – International Energy Agency (2018) The Future of Cooling -Opportunities for energy-efficient air conditioning, Technology report.
- MiSE - Italian Ministry for the Economic Development (2019) Piano Nazionale Integrato per l'Energia e il Clima.
- MiSE - Italian Ministry for the Economic Development (2020) Strategia per la Riquilificazione Energetica del Parco Immobiliare Nazionale.
- Psomas, T., Fiorentini, M., Kokogiannakis, G., Heiselberg, Per. (2017) Ventilative cooling through automated window opening control systems to address thermal discomfort risk during the summer period: Framework, simulation and parametric analysis, *Energy and Buildings*, Volume 153, Pages 18-30, <https://doi.org/10.1016/j.enbuild.2017.07.088>.
- Valladares-Rendón, L.G., Schmid, G., Lo, S-H. (2017) Review on energy savings by solar control techniques and optimal building orientation for the strategic placement of façade shading systems, *Energy and Buildings*, Volume 140, Pages 458-479, <https://doi.org/10.1016/j.enbuild.2016.12.073>.
- Vanhoutteghem, L., Skarning, G.C., Hviid, C.A., Svendsen, S. (2015) Impact of façade window design on energy, daylighting and thermal comfort in nearly zero-energy houses, *Energy Build*, 102, pp. 149-156, doi:10.1016/j.enbuild.2015.05.018.
- Warren, P.R., Parkins, L.M. (1985) Single-sided ventilation through open windows. In Conf. proc. Thermal Performance of the Exterior Envelopes of Buildings, ASHRAE, Florida. ASHRAE, 1985, p. 20.
- Zhang, H., Yang, D., Tam, V. W.Y., Tao, Y., Zhang, G., Setunge, S., Shi, L. (2021) A critical review of combined natural ventilation techniques in sustainable buildings, *Renewable*

and Sustainable Energy Reviews, Volume 141, 110795,  
<https://doi.org/10.1016/j.rser.2021.110795>.

Zinzi, M., & Chiesa, G. (2023) Model comparison and demonstration in controlled conditions, Deliverable D4.3 of the Energy flexible DYnamic building Certification Project, Project no. 893945

# Exploring the impact of the urban modified albedo on the indoor temperature and the ventilative cooling potential in a typical Italian residential building

Michele Zinzi<sup>\*1</sup>, Stefano Agnoli<sup>1</sup>, Sabrina Romano<sup>1</sup>, Anna Maria Siani<sup>2</sup>, Serena Falasca<sup>2</sup>

*1 ENEA  
Via Anguillarese 301  
00123 Rome, Italy*

*\*Corresponding author: michele.zinzi@enea.it*

*2 Department of Physics, "Sapienza" University of Rome"  
Piazzale Aldo Moro, 5,  
00185 Rome, Italy*

## ABSTRACT

Urban heat island, with the associated urban overheating, is a well-documented phenomenon, which demonstrates the hazard related to local climate change and the related negative impacts at environment, economic, social and public health level, with heavier consequences on the low income and more fragile segment of the population. The phenomenon takes origin by the positive thermal balance in the urban built environment mainly, depending on the synergic effect of different causes. It is also associated with a typical atmospheric circulation, playing a significant role in local dispersion processes. The interaction of local and global climate change exacerbates the thermal quality of cities, with more frequent and more intense extreme events, being the heat waves the most relevant. Several solutions exist to counteract urban overheating, and three main categories are identified: blue (water), green (vegetation) and white (materials) technologies. The present study investigates the potential of ventilative night cooling improvement in residential buildings in the city of Rome, Italy, by dynamic analyses carried out at mesoscale and building level. Initially the land and atmospheric models of the city are implemented in the Weather Research and Forecasting model, in a next phase the whole model was validated against the near surface temperature and wind speed ground measurements. Then, a number of different albedo scenario is defined and simulations are run for the hottest months (July and August) of the year 2020. The so obtained weather data set are used as input to simulate the thermal performance of a typical residential Italian buildings using TRNSYS 17 software, with a dedicated routine based on a simplified model to take into account the contribution of the natural ventilation. The operative temperature is the key performance indicator for the analyses and the number of discomfort hours, calculated according to the relevant standard, are used to quantify the impact of the urban modified albedo on the thermal response of residential buildings.

## KEYWORDS

Mesoscale simulation, night ventilation, thermal comfort, building energy simulation

## 1 INTRODUCTION

Urban heat island, with the associated urban overheating, is a well-documented phenomenon, which demonstrates the hazard related to local climate change and the related negative impacts at environment, economic, social and public health level, with heavier consequences on the low income and more fragile segment of the population. The phenomenon takes origin by the positive thermal balance in the urban built environment mainly, depending on the synergic effect of different causes: absorption and storage of solar irradiation by the construction surfaces, the anthropogenic heat, the reduced evapotranspiration and surface permeability due to the lack green and natural areas, change and reduction of urban ventilation (Oke et al., 1991). It is also associated with a typical atmospheric circulation, playing a significant role in local dispersion processes (Falasca et al., 2013). The interaction of local and global climate change

exacerbates the thermal quality of cities, with more frequent and more intense extreme events, being the heat waves the most relevant (Perkins, 2015).

Several solutions exist to counter urban overheating, and three main categories are identified: blue (water), green (vegetation) and white (materials) technologies (Akbari et al., 2015). The latter solution gained interest in the past three decades with the development of the cool materials, characterised by high albedo (also called solar reflectance, when referred to specific materials rather than to large areas) and thermal emissivity, which minimise the solar irradiation absorbed by the construction surface and easily dissipate the residual stored heat by radiation (Santamouris et al., 2017). Cool roofs use white or selective cool coloured materials, being the latter characterised by a very high reflectance in the near-infrared range while keeping the design colour in the visible range. The benefit of the technology is well documented by numerical analyses and field studies (Testa & Krarti, 2017). Mesoscale simulations have been recently introduced to predict the mitigation impact of higher albedo materials in cities, trying to understand potentials and risks of the application at large scale (Falasca et al., 2019).

The impact of different urban albedo scenario on the improvement of the cooling energy performance of a residential building was analysed by dynamic analyses carried out at mesoscale and building level for the City of Rome (Italy) in (Falasca et al., 2024). The objective of this study is to carry out a similar analysis for residential buildings without active cooling and naturally ventilated. As per in the previous study, the application of an innovative configuration of the Weather Research and Forecasting (WRF) model was specifically implemented for the city of Rome. In addition, the observation period was here extended to two entire months to cover the hottest period of summer.

## 2 MATERIALS AND METHOD

The study is structured in the following phases:

- I. Implementation of the city land and atmospheric model, and successive validation against the measured air temperature and wind speed in a selected site.
- II. Identification of the modified urban albedo scenarios in line with (Falasca et al., 2024), next the meso-scale simulations for the reference and the variant scenarios are run for the months of July and August 2020.
- III. Identification and modelling of the reference building and of the natural ventilation strategies, and thermal calculation of the building in thermal free floating condition in transient regime.
- IV. Calculation of the indoor operative temperature for all the building configuration, and assessment of the change in the indoor thermal comfort conditions due to heat mitigation caused by the increase of the urban albedo.

### 2.1 The case study area

Rome, the capital and largest city of Italy, is in the middle of the Mediterranean basin, and it belongs to the Csa class (Mediterranean climate) according to the Köppen-Geiger climate classification. It is one of the largest Mediterranean metropolises with 2.85 million inhabitants, peaking 4.6 million if all the metropolitan area is considered. The municipality extension is about 1290 km<sup>2</sup> and a density of about 2200 inhab./km<sup>2</sup>.

The green areas within the city borders account to more than 60% of all territory, which is exceptionally high in comparison with the other metropolis of the region. Such areas are, however, essentially located in the extreme periphery of the municipality, while urban green areas account only for the 3.1% of the city surface. This aspect, as well as the complex, dense and stratified urban texture, makes the city highly vulnerable to urban heat island and overheating (Zinzi et al., 2018).

## 2.2 The reference urban setting and its variants

A reference case and three variants simulating the application of high albedo materials in the urban area of Rome are defined and then simulated through the Weather Research and Forecasting model (WRF, described in detail in Section 3.1). The reference case is based on the database present in the WRF model for the footprint share of green areas, pavements and roof within the city boundaries. The model includes the buildings and streets' size as a function of urban typologies, as well as the solar reflectance (albedo) of the construction materials for the current urban dataset. The latter is reported in Table 1 with the values of the three variants. Reflectance values for V3 correspond to state of the art solutions available on the market, such as light grey concrete, treated with light coloured aggregates and binder, for pavements and white coating and tiles for roof. Intermediate values are selected accordingly: V1 doubles the reference values, next the increase in reflectance are 0.1 and 0.2 for urban surfaces and roofs, respectively. To be noted that thermal properties of materials (e.g., albedo, thermal emissivity) are the same throughout the built area, regardless of the urban typologies (for more details see Section 3.1); the thermal emissivity is 0.9 in all cases, as it is very high for all the construction materials but metals, thus it does not change for the selected scenarios.

The calculations of the building thermal response are carried out using the four weather data data-set, referring to the reference case and to the three identified modified urban albedo scenarios.

Table 1: Albedo of roofs and pavements of the reference case and variants

Scenario	Road/Pavement Albedo	Roof Albedo
Reference	0.15	0.2
V1	0.3	0.4
V2	0.4	0.6
V3	0.5	0.8

## 2.3 The reference building and the night ventilation strategy

The building used for this study is part of the set of reference buildings used in Italy for the studies related to the implementation of the European Energy Performance of Buildings Directive. It was selected because its geometrical features are often found in Rome for buildings of different periods, from Middle Age until nowadays. The building has three identical floors, each of them with two flats of the same size, as inferred from Figure 1. Each apartment has 89m<sup>2</sup> net floor area and 242m<sup>3</sup> volume, the net floor height is 2.7m. The windows area is 17m<sup>2</sup>, accounting to about 20% of the apartment surface, and they are distributed across the three different orientations for each apartment, but with limited apertures on the north façade, according to the prevalent national design criteria.

Table 2: Main thermi-physical properties of the building envelope components

Envelope component	U [W/m <sup>2</sup> K]	HT [kJ/K]
Vertical wall	0.29	330
Roof	0.26	221
Ground floor	0.29	635
Window	1.85	---

Despite the majority of residential building in the consolidated urban area is still not thermally insulated, the study focuses on new and energy renovated buildings, in order to explore the

performance that can be expected in the near future according to the forthcoming energy requirements. The main thermo-physical parameters (thermal transmittance  $U$  and heat capacity  $HT$ ) are reported in Table 2.

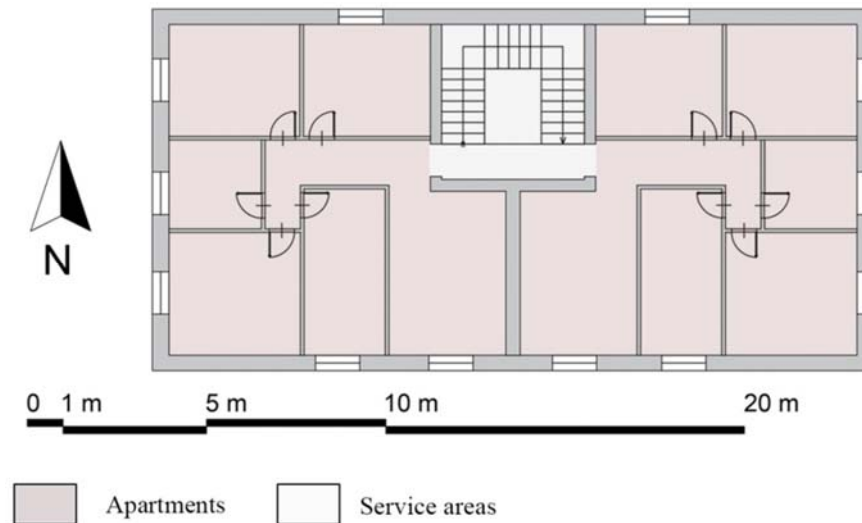


Figure 1: Reference building floor-plan

Other relevant characteristics of the reference building were defined in accordance with the relevant requirements of the Italian building code for the assessment of the energy performance of buildings (Decreto Ministero dello Sviluppo Economico, 2015; UNI, 2014). In particular, the following settings are defined for the thermal model of the building:

- internal sensible heat gains (occupancy, lighting and appliances)  $5 \text{ W/m}^2$ ;
- internal latent heat gains (occupancy and appliances)  $2.5 \text{ W/m}^2$ ;
- $g$ -value 0.60 for low- $e$  double glazing unit of the insulated configuration;
- the external solar protection - 0.7 shading coefficient – is activated during daytime.

Concerning the natural ventilation strategies, the approach is to limit the air exchange per hour (ACH) to  $0.5 \text{ h}^{-1}$  during daytime hours (08:00–20:00) and increase the natural ventilation rate during night-time hours (20:00–08:00 of the next morning). For the night ventilation fixed values are selected for the calculation: 1, 2, 3 and 5.

#### 2.4 The observation period and the performance indicator

The analysis was carried out for July and August 2020, period that accounts for about two third of the cooling energy use in Rome. Numerical output of the reference case for temperature at 2 meters height and wind speed at 10 meters height is used for the validation of the model. The dataset from the meso-scale simulations to be supplied to the building model includes hourly values of: air temperature and relative humidity at 2 meters height, wind speed at 10 meters height, global horizontal solar irradiation.

The thermal comfort in thermal free floating is assessed using the operative temperature as main performance indicator. This indicator is defined as the arithmetic mean of the air and mean radiant temperature for compact thermal zones (calculated starting from the temperature surfaces of the thermal zone), as is the case of the simulated apartments.

### 3 CALCULATION

This section reports the main contents of the calculation exercises, referring to the meso-scale analysis and to the building thermal assessment.

#### 3.1 The meso-scale atmospheric calculation

The Weather Research and Forecasting (WRF) model is a state-of-the-art mesoscale numerical weather prediction system suitable for multiple applications, both research and operational (Skamarock et al., 2019). Its operation is based on the integration of Euler equations on a three-dimensional calculation grid, defined by the user from different points of view, such as geographical coverage, horizontal and vertical spatial resolution. In this application, the urban area of Rome is simulated at 500 m through a two-way nesting technique with a total of four nested domains with a growing spatial horizontal resolution starting from 13.5 km (Figure 2a). The vertical resolution, increasing from the bottom to the top of the domain, is approximately 12 m near the ground. Grid cells land use is categorized according to the MODIS database and urban cells are further classified in terms of morphology according to the Local Climate Zones (Stewart and Oke, 2012) based on the WUDAPT database (Ching et al., 2018; Demuzere et al., 2022). Figure 2b shows the non-urban areas and the LCZs present in Rome according to these datasets. The physical setup is based on the revised MM5 surface layer scheme, the Noah Land Surface Model, the Bougeault-Lacarrère Planetary Boundary Layer scheme coupled with the Building Effect Parameterization scheme, the Single-Moment 6-class microphysics scheme, the RRTM and the Dudhia schemes for long and short wave respectively (Skamarock et al., 2019). Initial and boundary conditions are the final operational global analysis data of the National Center for Environmental Prediction ( $0.25^\circ \times 0.25^\circ$ , every 6 hours) (NCEP, 2015).

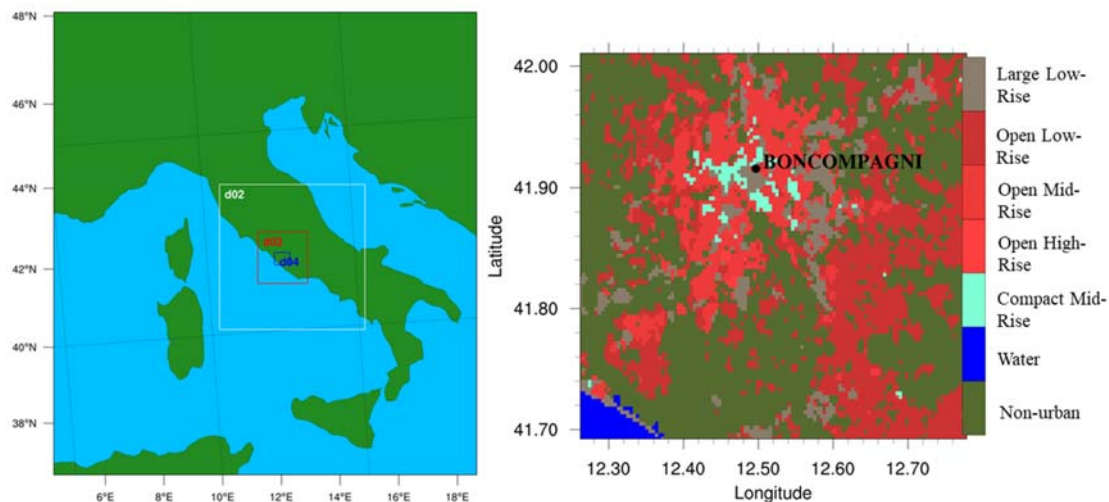


Figure 2: Geographical areas covered by the WRF nested domains (left); non-urban land use and Local Climate Zones in the domain over Rome (right). The black dot identifies the Boncompagni ARPA station whose weather records are compared with the WRF results.

#### 3.2 The building thermal calculation

TRNSYS 17, a spread and validated model for thermal analyses in transient regime, was used for the building performance analysis. The model work as different routines properly linked each other, and each with a specific calculation task. Each TRNSYS 17 project consists of several routines linked together, each with a specific calculation task. The project implemented

for this analysis include: a) the data reader for Generic Data Files, where the outdoor air temperature, relative humidity and velocity are inputted; b) the radiation processor to calculate the solar irradiation at every incidence angle, starting from the inputted global horizontal irradiation; c) the psychometrics routine to calculate moist air properties; d) the effective sky temperature to calculate the long-wave radiation exchange, v) the Multi-Zone building model; e) the slab on grade, to model the heat transfer to soil below the building.

The simulation is run for the 62 days of July and August on hourly basis. The output is the air, mean radiant and operative temperature in each apartment. Next section report and discuss the results of the average of the operative temperature calculated in the six apartments, for the sake of brevity and because the results do not significantly the various flats.

## 4 RESULTS

### 4.1 The meso-scale calculation results

Two-months long WRF simulations have been performed for the four cases described in Table 1. In order to evaluate the performances of the WRF configuration applied here, hourly time series of temperature at 2 meters height and wind speed at 10 meters height of the reference case have been extrapolated corresponding to the Boncompagni site of the ARPA (Italian acronym for Regional Agency for Environmental Protection) Lazio and then compared to the records acquired by the ARPA Lazio weather station (Figure 3). WRF performances are quantified throught some common statistical parameters (i.e., bias, Pearson correlation coefficient, Root Mean Square Error) whose values show a very good reliability of the model (Table 3), slightly lower for the wind speed consistently with a well known feature of WRF (Ribeiro et al., 2021). The comparison of wind profiles confirm the worse ability of WRF to simulate wind as a well-known limitation of the model. This is due to a greater sensitivity of the wind to parameterizations of turbulent exchanges that occur in the atmospheric boundary layer and which cannot be resolved explicitly.

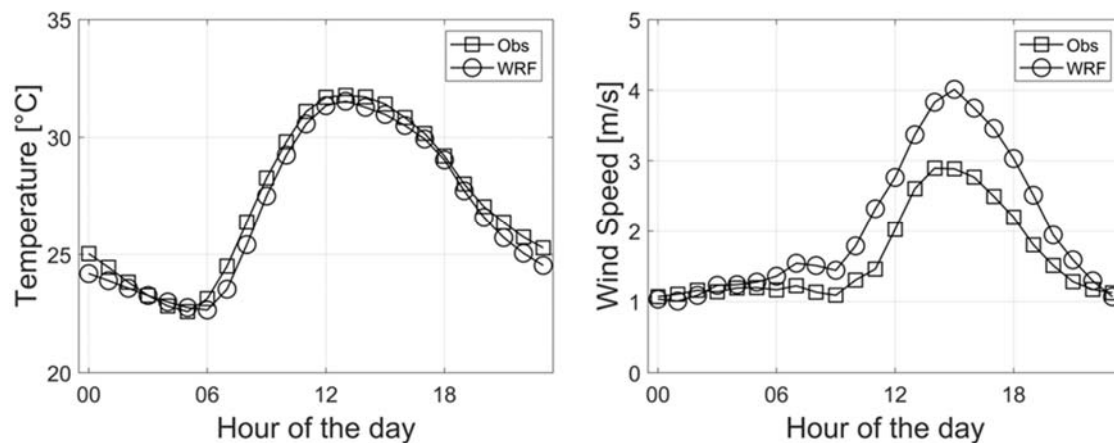


Figure 3: Comparison between average daily cycles of observations and numerical results of the reference case for air temperature (left) and wind speed (right) at the Boncompagni ARPA site.

Table 4 reports, as exemplary case, the maximum, average and minimum air temperature values calculated for the four scenarios. It can be noted that the albedo has a relevant impact on the maximum temperature, dropping by 1.7°C from the reference to the third scenario; conversely, the impact on the minimum values is limited to  $\pm 0.2^\circ\text{C}$ . The average values show a progressive reduction of 0.2°C for all the modified albedo scenarios, peaking 0.6°C for the third variant.



Finally, Figure 4 shows the hourly profiles, averaged for the monitoring period and referring to the current configuration and the identified scenarios.

Table 3: Statistical parameters used for validation of WRF in this study

Statistical Parameter	Air Temperature	Wind Speed
	[°C]	[m/s]
Bias	-0.52	0.43
Correlation coefficient	0.94	0.79
Root Mean Square Error	1.22	0.95

Table 4: Air temperature results for the different configuration

Scenario	T max [°C]	T average [°C]	Tmin [°C]
Reference	35.4	26.2	18.4
V1	34.9	26.0	18.6
V2	34.4	25.8	18.4
V3	33.7	25.6	18.2

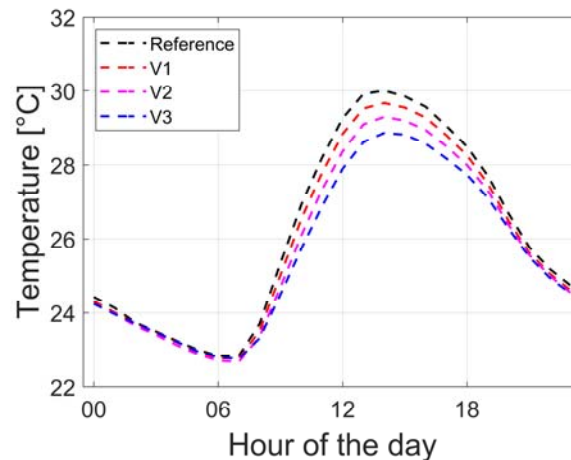


Figure 4: Hourly profiles of the air temperature, averaged for the monitoring period. Plots report the reference case and the three selected variants

## 4.2 The thermal comfort results

Relevant results of the simulation set are reported in Table 5. They include the maximum, average and minimum operative temperature for each scenario. The results include the number of hours above some relevant threshold values (28, 29, and 30°C); they were included as the discomfort hours calculated according to the relevant standard for adaptive comfort (last column) resulted to be quite low (CEN, 2007). Observing the absolute values of the operative temperature for the same ACH, it is noted that the variation of albedo has a low impact, with temperature reductions not greater than 0.3°C. In addition, in some cases, the minimum temperatures slightly increase in a modified albedo case with respect to the reference (see the variant 3 case). More impactful is the increase of the ventilation rate, as the average temperature drop is 0.9-1.0°C and 1.5°C for 3 and 5 ACH respectively.

Changes are also scarcely relevant taking into account the unmet comfort hours, which peak 68 (corresponding to 5% of the total hours of the calculation period) in the reference case with the lowest night ventilation rate. Increasing the night ventilation to 2 ACH, still a quite low value,

the unmet hours account for 2% of the period in the reference case and 1% in all the albedo variants configurations.

The results change if the number of hours exceeding some reference threshold values are observed. In the reference case 28, 29, and 30°C are reached in 74, 36, and 9% hours of the period. Taking the 29°C as reference, it is observed that the occurrence is practically the same for the albedo variant 1 but it drops to 28 and 24% for the scenarios 2 and 3 respectively. The impact of the first albedo variant is confirmed also for the other ventilation rates; the albedo variant 2 shows a noticeable improvement with respect to the reference case, while the further increase of the urban albedo does not provide significant advancement in terms of temperature drops.

Table 5: Albedo of roofs and pavements of the reference case and variants

Weather	NACH [h <sup>-1</sup> ]	T max [°C]	T av [°C]	T min [°C]	T>28°C [h]	T>29°C [h]	>30°C [h]	Unmet h. [h]
Reference	1	31.4	28.6	25.2	1104	541	139	68
Reference	2	31.0	28.1	24.4	832	277	51	29
Reference	3	30.6	27.7	23.9	593	163	27	10
Reference	5	30.1	27.1	23.0	326	71	3	0
V1	1	31.3	28.6	25.6	1077	514	130	60
V1	2	30.9	28.1	24.9	812	267	40	21
V1	3	30.5	27.7	24.3	590	164	23	5
V1	5	30.0	27.1	23.6	327	74	2	0
V2	1	31.3	28.4	25.1	1003	412	92	48
V2	2	30.8	27.9	24.4	716	203	36	18
V2	3	30.5	27.5	23.8	504	124	17	2
V2	5	30.0	26.9	23.0	252	49	1	0
V2	1	31.2	28.4	25.3	957	360	86	45
V2	2	30.7	27.8	24.6	660	196	35	17
V3	3	30.4	27.4	24.1	441	119	17	2
V3	5	29.9	26.9	23.3	225	47	0	0

It is thus interesting to compare the reference case and the variant 2 in more detail. The effect of the modified albedo is to reduce very high indoor temperatures (above 30°C) by 34%, as the hours drop from 139 to 92; this result is relevant as the occurrence of such peak values is 9% of the all period. The operative temperature is higher than 28°C in many hours of the period, whatever the night ventilation rate might be; the effect of the albedo is here a reduction of such hours in the range between 14% (2 ACH) and 23% (5 ACH). Also noticeable is reduction for temperature above 29°C, which happens in few hundreds of hours in the reference case; in fact, it is in the 24-27% range for air exchange between 1 and 3h<sup>-1</sup>.

## 5 CONCLUSIONS

This study aimed at demonstrating the impact of the urban modified albedo to enhance thermal comfort conditions in residential building in the city of Rome, Italy. Meso-scale simulation showed the positive impact on the reduction of maximum and average air temperature: 1.5° and 0.6°C, respectively. The results were used to feed a dynamic building model to calculate the impact on the indoor heat mitigation and thermal comfort for different night ventilation strategies.

It was observed that the impact on average operative temperature and discomfort hours according to the relevant standard procedure was quite limited. Observing the occurrence of high temperature values (>28°C), it was instead found that the impact of the modified albedo can be relevant (reduction of hours >24%) for equivalent ACH values. In general, the impact of the night ventilation is predominant in mitigating the indoor environment; however, it must be reminded that high ventilation rates cannot be easily achieved in densely built areas in

buildings without mechanical ventilation, as it is the case for Rome and the majority of dwellings in Italy.

Next steps will explore this issue, approaching the natural ventilation also according to prevailing micro-climatic conditions; in addition, the study demonstrates the need of more accurate analyses on the discomfort hours calculated according to the existing standard, especially during extended hot periods, as they happen in the European Mediterranean region. In fact, internal studies in office buildings showed that air temperature values above 28°C are not tolerated by the vast majority of people, which appears in contrast with the adaptive method of the above cited standard.

## 6 ACKNOWLEDGEMENTS

Research funded by Project 1.7 “Technologies for the efficient penetration of the electric vector in the final uses” within the “Electrical System Research” Programme Agreements 22-24 between ENEA and the Ministry of Environment (PTR 22-24).

Serena Falasca gratefully acknowledges fellowship funding from MUR (Ministero dell’Università e della Ricerca) under PON “Ricerca e Innovazione” 2014-2020 (D.M. 1062/2021).

We acknowledge the CINECA award under the ISCRA initiative, for the availability of high-performance computing resources and support.

The computing resources and the related technical support used for this work have been provided also by CRESCO/ENEAGRID High Performance Computing infrastructure and its staff (F. Iannone et al., "CRESCO ENEA HPC clusters: a working example of a multifabric GPFS Spectrum Scale layout," 2019 International Conference on High Performance Computing & Simulation (HPCS), Dublin, Ireland, 2019, pp. 1051-1052, doi: 10.1109/HPCS48598.2019.9188135.). see <http://www.cresco.enea.it/english> for information.

The authors gratefully acknowledge ARPA Lazio for providing weather data.

## 7 REFERENCES

Akbari, H., et al. (2015). Local climate change and urban heat island mitigation techniques – the state of the art. *Journal of Civil Engineering and Management*, 22.

CEN (2007) EN 15251:2008 - Indoor environmental input parameters for design and assessment of energy performance of buildings addressing indoor air quality, thermal environment, lighting and acoustics.

Ching, J., Mills, G., Bechtel, B., See, L., Feddema, J., Wang, X., Ren, C., Brousse, O., Martilli, A., Neophytou, M., Mouzourides, P., Stewart, I., Hanna, A., Ng, E., Foley, M., Alexander, P., Aliaga, D., Niyogi, D., Shreevastava, A., Theeuwes, N. (2018). Wudapt: An urban weather, climate, and environmental modeling infrastructure for the anthropocene. *Bulletin of the American Meteorological Society*, 99(9), 1907–1924. <https://doi.org/10.1175/BAMS-D-16-0236.1>

Demuzere, M., Argüeso, D., Zonato, A., & Kittner, J. (2022). W2w: A python package that injects wudapt’s local climate zone information in wrf. *Journal of Open Source Software*, 7(76), 4432. <https://doi.org/10.21105/joss.04432>

Falasca, S., Ciancio, V., Salata, F., Golasi, I., Rosso, F., & Curci, G. (2019). High albedo materials to counteract heat waves in cities: An assessment of meteorology, buildings energy needs and pedestrian thermal comfort. *Building and Environment*, 163.

Falasca, S., Moroni, M. and A. Cenedese, (2013). Laboratory simulations of an urban heat island in a stratified atmospheric boundary layer. *Journal of Visualization*, 16.

Falasca, S., Siani, A.M., Agnoli, S., Zinzi, M. (2024) Impact of the urban modified albedo on the energy performance of buildings. The case of Rome, Italy. Oral presentation accepted at *The 37<sup>th</sup> PLEA Conference - (Re)thinking resilience*, 25-28 June 2024, Wroclaw, Poland.

Ministero dello Sviluppo Economico (2015) Decreto del 26 giugno 2015. Applicazione delle metodologie di calcolo delle prestazioni energetiche e definizione delle prescrizioni e dei requisiti minimi degli edifici.

National Centers For Environmental Prediction/National Weather Service/NOAA/U.S. Department Of Commerce. (2015). Ncep gdas/fnl 0.25 degree global tropospheric analyses and forecast grids [dataset]. <https://doi.org/10.5065/D65Q4T4Z>

Oke, T.R., Johnson, G.T., Steyn, D.G. and I.D. Watson, (1991). Simulation of Surface Urban Heat Islands under 'Ideal' Conditions at Night - Part 2: Diagnosis and Causation, *Boundary Layer Meteorology*, 56.

Perkins, E. S., (2015). A review on the scientific understanding of heatwaves—Their measurement, driving mechanisms, and changes at the global scale, *Atmospheric Research*, Volumes 164–165, 2015, Pages 242-267.

Ribeiro, I., Martilli, A., Falls, M., Zonato, A., Villalba, G., 2021. Highly resolved WRF-BEP/BEM simulations over Barcelona urban area with LCZ. *Atmospheric Research* 248, 105220. <https://doi.org/10.1016/j.atmosres.2020.105220>

Santamouris, M., Ding, L., Fiorito, F., Oldfield, P., Osmond, P., Paolini, R., Prasad, D., & Synnefa, A. (2017). Passive and active cooling for the outdoor built environment – Analysis and assessment of the cooling potential of mitigation technologies using performance data from 220 large scale projects. *Solar Energy*, 154.

Skamarock, W. C., Klemp, J. B., Dudhia, J., Gill, D. O., Liu, Z., Berner, J., Wang, W., Powers, J. G., Duda, M. G., Barker, D. M., & Huang, X.-Y. (2019). A description of the advanced research wrf model version 4. UCAR/NCAR. <https://doi.org/10.5065/1DFH-6P97>

Stewart, I. D., & Oke, T. R. (2012). Local climate zones for urban temperature studies. *Bulletin of the American Meteorological Society*, 93(12), 1879–1900. <https://doi.org/10.1175/BAMS-D-11-00019.1>

Testa, J., and M. Krarti, (2017). A review of benefits and limitations of static and switchable cool roof systems. *Renewable and Sustainable Energy Reviews*, 77.

UNI (2011) UNI/TS 11300-1:2014 - Prestazioni energetiche degli edifici - Parte 1: Determinazione del fabbisogno di energia termica dell'edificio per la climatizzazione estiva ed invernale.

Zinzi, M., Carnielo, E., Mattoni, B. (2018) On the relation between urban climate and energy performance of buildings. A three-years experience in Rome, Italy. *Applied Energy*, Volume 221, 2018, Pages 148-160.

# Cognitive well-being in classrooms: A holistic investigation into Indoor Environmental Quality in New Zealand primary schools

Lara Tookey<sup>\*1</sup>, Mikael Boulic<sup>1</sup>, Ilaria Stura<sup>2</sup>, Wyatt Page<sup>3</sup>,  
Pawel Wargocki<sup>4</sup> and Hennie van Heerden<sup>1</sup>

<sup>1</sup>Massey University  
School of Built Environment,  
Auckland, New Zealand  
\*l.tookey@massey.ac.nz

<sup>2</sup> University of Turin  
Applied Physics for Neuroscience  
Turin ,Italy

<sup>3</sup>Massey University  
School of Health Sciences,  
Wellington, New Zealand

<sup>4</sup>Technical University of Denmark  
Department of Environmental and Resource  
Engineering Indoor Environment,  
Denmark

## Abstract

Children spend about 80-90% of their time indoors, making the quality of indoor environments (IEQ) crucial, particularly since children are more susceptible to pollutants due to their developing bodies and higher relative air intake per body weight. This study examines the influence of various indoor environmental conditions on cognitive performance in primary school students. Data collected over the first three weeks from a total eight-week cognitive study are analysed, focusing on the impact of thermal comfort and CO<sub>2</sub> levels as proxies for ventilation.

Classroom environments were categorised into three conditions: 'TEST 1' (moderate CO<sub>2</sub>, temperature, and humidity), 'TEST 2' (elevated CO<sub>2</sub>, optimal temperature), and 'TEST 3' (higher CO<sub>2</sub> and temperature). The findings are based on Shapiro-Wilk normality tests, linear regression, ANOVA, and Kruskal-Wallis tests across three cohorts (RM5, RM6, RM7). Results show that 'TEST 1' conditions generally support standard cognitive performance, while 'TEST 3' conditions, characterised by elevated CO<sub>2</sub> and temperature, negatively impact working memory and attention. 'TEST 2' conditions present mixed results, suggesting that even minor changes in environmental factors can influence cognitive outcomes.

Overall, the study highlights the necessity of maintaining optimal indoor environments to support cognitive functions and academic performance. Sensitivity to environmental conditions varies among cohorts, indicating that personalised approaches to environmental management may be required to optimise learning conditions.

## Keywords

Please provide a maximum of five keywords which cognitive performance, thermal comfort, CO<sub>2</sub> levels, ventilation, primary school classroom environment

## 1 INTRODUCTION

Children spend 80-90% of their time indoors, making the quality of indoor environments (IEQ) crucial for their health and learning. Children are more vulnerable to pollutants as their bodies are still developing and they inhale more air relative to their body weight than adults. Poor indoor conditions can negatively impact children's health and educational outcomes, especially during critical stages of cognitive growth (Salthammer, et al., 2016; Temprano, et al., 2020; Thoua, et al., 2022)

Classroom occupancy and design significantly influence IEQ. Typical classrooms hold 17-30 students in spaces of 40-80 m<sup>2</sup>, providing 2.27-3.63 m<sup>2</sup> per student. High-density classrooms can compromise air quality, thermal comfort, and noise levels. Effective ventilation and climate control are essential to maintain a healthy learning environment (Hama, et al., 2023; Sadrizadeh, 2022)

Schools often have higher occupant densities than offices, stressing the need for optimal IEQ to support cognitive function and academic performance. The sporadic use of school buildings complicates maintaining stable IEQ, underscoring the need for reliable ventilation and climate control during operational hours to ensure a beneficial learning environment (EPA, 2016).

Overall, maintaining high IEQ in schools is vital for promoting students' cognitive development, academic success, and overall well-being.

## 2. IMPACT OF IEQ ON ACADEMIC PERFORMANCE AND COGNITIVE FUNCTION

We will explore how thermal comfort and CO<sub>2</sub> levels, as proxies for ventilation, impact cognitive development in educational settings. Understanding these key aspects of IEQ is crucial for enhancing students' cognitive functions and academic performance. This examination highlights the need for optimal indoor environments to support cognitive well-being and academic success.

### 2.1 Thermal comfort

Commonality between the research outputs from Wargocki and Wyon (2013) and Haverinen-Shaughnessy et al. (2015) pointed to the positive correlation between lower classroom temperatures and improved student performance.

Both studies investigate the impact of thermal conditions within the classroom setting on the cognitive performance of children, focusing particularly on the effects of temperature reduction on academic outcomes. Wargocki and Wyon (2013) identified a dose-response relationship indicating that a 1°C drop in classroom temperature could potentially enhance performance speed in arithmetic and language tasks by 4% for 10-12-year-old students.

Similarly, Haverinen-Shaughnessy et al. (2015) examined the influence of classroom temperatures on fifth-grade students' academic performance. Their findings suggest that a reduction in temperature within the 20–25 °C range is associated with significant improvements in mathematics scores, and to a variable extent, in science and reading scores as well.

Jiang's 2018 study in rural Northwest China incorporated adaptive theory by considering the participants' thermal preferences in various temperature conditions ranging from 10 °C to 20 °C. The study acknowledged that occupants could adapt to their environment, indicated by the 12-year-old participants reporting thermal neutrality at 14.5 °C — a temperature that reflects local climatic norms and clothing practices, with an insulation value of 1.55 clo. A notable 80% of the children described a sense of comfort at 14 °C. The adaptive theory is further supported by the observation that attention test accuracy peaked under slightly cool conditions, suggesting that students had adapted to their environment to maintain focus and cognitive function. Although perception and comprehension did not show substantial differences across the temperature spectrum, deduction tasks were most accurately performed in the cooler settings, underlining the adaptability of cognitive functions to preferred thermal conditions.

On the flip side, Fadillah et al. (2020) found through their study in Indonesia that an optimal warmer room temperature around 29 °C enhanced concentration levels, challenging the cooler preferences observed in Jiang's study. This outcome aligns with adaptive theory, which posits that cognitive performance is influenced by individuals adapting to their prevailing thermal environment, which in this case, is the tropical climate of Indonesia. Hence, students performed better at this higher temperature, which was more in line with their acclimatisation and thermal comfort zone. These differing findings between the two studies exemplify the adaptive theory's premise that people's thermal comfort and performance levels are relative to their customary environments, indicating that thermal preferences and their cognitive effects are not universal but context dependent.

## **2.2 CO<sub>2</sub> as proxy for ventilation**

Coley et al. (2007) found a negative correlation between elevated CO<sub>2</sub> levels and the Power of Attention in educational settings. The "Power of Attention" cognitive function refers to an individual's capacity to concentrate on a particular task or piece of information while filtering out distractions and irrelevant information. This cognitive function is critical for learning and processing information effectively, particularly in environments like classrooms where focus and the ability to follow instructions are essential.

As CO<sub>2</sub> concentrations rose from an average of 690 parts per million (ppm) to 2909 ppm, there was approximately a 5% decrease in students' attentiveness. This implies that as the quality of air in the classroom deteriorated due to higher CO<sub>2</sub> levels, students' ability to maintain focus on the teacher's instructions declined. High CO<sub>2</sub> levels in the air can lead to a variety of physiological and cognitive effects, such as drowsiness, lethargy, and a diminished ability to concentrate—factors that are critical to the Power of Attention. When students are less able to pay attention, their cognitive resources are spread thin, and they may find it challenging to stay engaged with the lesson, absorb new information, and perform academically.

Therefore, the study by Coley et al. emphasises the importance of maintaining good IEQ in learning environments to ensure that the Power of Attention in students is not compromised, thereby allowing for optimal learning conditions.

Commonality was found between this study and three others, showing a clear link between better ventilation, which typically corresponds to lower CO<sub>2</sub> levels, and improved cognitive function and academic performance in students.

Haverinen-Shaughnessy et al. (2011) show a quantitative relationship between increased ventilation rates and the success rate of language and mathematics tests, implying that better

air quality, which is often reflected by lower CO<sub>2</sub> concentrations, supports cognitive performance. The subsequent study by Haverinen-Shaughnessy et al. (2015) also supports this by showing enhancement in mathematics scores with increased ventilation rates, further substantiating the notion that adequate ventilation is crucial for maintaining cognitive functions that are essential for learning and test-taking. The research by Petersen et al. (2015) added to these findings by demonstrating improvements across various cognitive performance tests when ventilation rates were increased in classrooms.

Collectively, these studies affirm the hypothesis that improved indoor air quality, primarily due to increased ventilation, is associated with better attention, cognitive performance, and academic outcomes. They all point towards the importance of environmental conditions in the learning process, particularly the role that CO<sub>2</sub> levels and ventilation play in affecting students' ability to focus, process information, think critically, and ultimately, succeed academically.

This study has been conducted in accordance with the following standards and guidelines. The World Health Organisation (WHO) recommends maintaining a temperature range of 18°C to 24°C during school hours when classrooms are occupied. The American Society of Heating, Refrigerating and Air-Conditioning Engineers (ASHRAE) suggests that the ideal relative humidity (RH) should be between 40% and 60% if the temperature is set within the 18°C to 24°C range. The New Zealand Standard for Ventilation and Air Quality (NZS 4303:1990) specifies that CO<sub>2</sub> levels in indoor environments should remain below 1000 ppm to ensure acceptable air quality. Furthermore, the New Zealand Ministry of Education's 2017 guidelines emphasise the importance of managing indoor air quality (IAQ) and thermal comfort in classrooms, stating that CO<sub>2</sub> levels should be maintained well below 1000 ppm.

Recognising IEQ's pivotal role in education, this research study quantifies cognitive function changes due to variations in thermal comfort and CO<sub>2</sub> levels as a proxy for ventilation. The research design includes continuous monitoring of thermal comfort and CO<sub>2</sub> levels as a proxy for ventilation, and cognitive metrics across multiple classrooms. For this paper, cognitive function is limited to concentration, reasoning and short-term memory.

### **3. THE NEW ZEALAND CONTEXT**

In Auckland, a mild, temperate maritime climate predominates, with average summertime (December to February) daytime temperatures ranging from 20 to 25 °C, and winter (June to August) daytime temperatures spanning from 11 to 15 °C, as reported by NIWA (2023a). Primary school students attend classes from 09:00 to 15:00, Monday through Friday.

According to Swarbrick (2012), the bulk of NZ's school infrastructure was built in the 1950s and 1960s. These structures were intentionally crafted for natural air circulation, consisting of single-story, timber-framed buildings equipped with large, single-glazed windows that could be opened to usher in daylight and airing for ventilation. Notably, these buildings were constructed without insulation, a feature that only became a NZ standard requirement in 1978.

### **4. RESEARCH METHODOLOGY.**

The chosen primary school, built in 1965, is in the temperate climate of North Shore, Auckland, which experiences an average annual temperature of 15.6°C and receives around 1,231 mm of



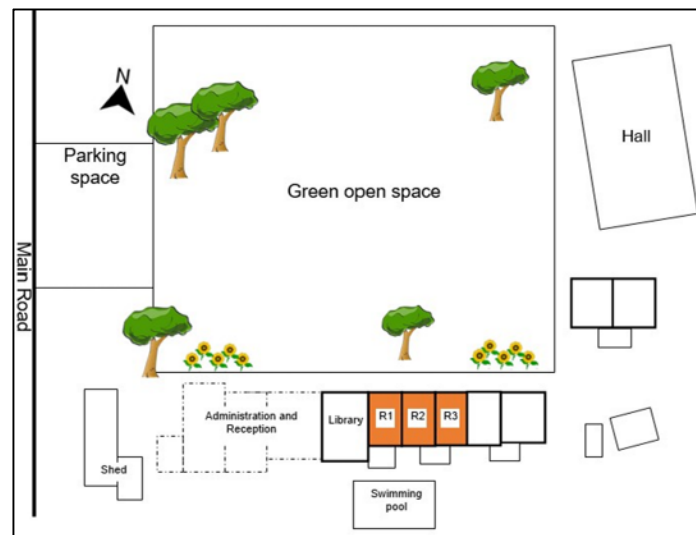
rainfall, according to NIWA's (2023b) report. As depicted in **Figure 1**, the school caters to 160 children between the ages of 5 and 11 in multi-age group classes. The facility includes seven classrooms of equal floor area and a library space. All classrooms are situated on the first floor and feature doors on the North side that open directly to the play area. The classrooms facilitate cross ventilation through windows on both the North (front) and South (back) sides, with louvres installed on the upper section of the north wall that typically remain slightly ajar to enable natural airing. The specific classes involved in this research study are denoted in orange on **Figure 1** and are identified as RM1-RM3 to uphold confidentiality. RM1 is approximately 90 m from the Main Road, which helps to reduce auditory disturbances.

#### 4.1 Ethics protocol

The study was conducted in accordance with the Massey University Human Ethics (High Risk) protocols, as outlined in the approval document SOA 21/53.

#### 4.2 Self-administered online cognitive tests

Creyos, formerly known as Cambridge Brain Sciences (CBS), offers a comprehensive web-enabled platform for cognitive assessments. This platform enables users to self-administer well-validated neuropsychological tests, modified for remote usage as highlighted by Hampshire, Highfield, Parkin & Owen (2012). Each task dynamically adjusts in complexity in reaction to the user's performance, as explained by Thienel, Borne, et al. (2023).




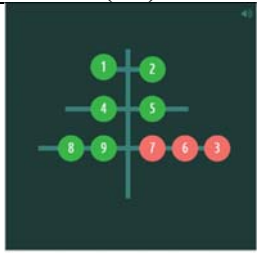
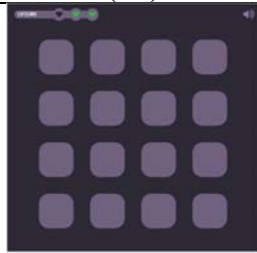

**Figure 1:** Site Map of School and Location and Study Classrooms

The tests provided by Creyos have undergone rigorous validation across numerous studies, with research cohorts ranging from the healthy population to individuals with medical conditions, as shown in work by Levine et al. (2013), Brenkel et al. (2017), as well as Nichols, Wild, Owen & Soddu (2021). Past research has also employed these tests to investigate the cognitive effects of indoor thermal conditions (Ko et al., 2020; Barbic et al., 2019; Luo et al., 2023).

**Table 1** provides an overview of the selected four tasks which have been designed to evaluate concentration, reasoning, and short-term memory. The tasks featured include:

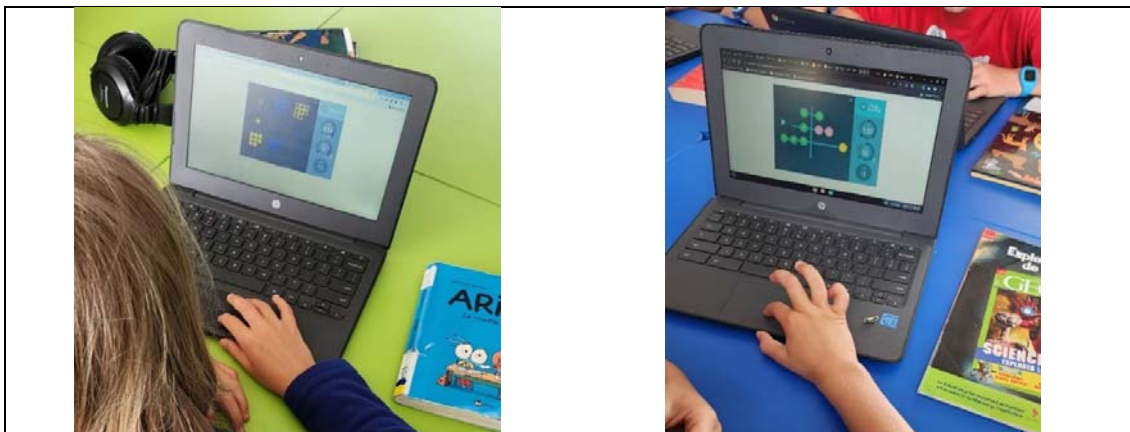
- Double Trouble (DT): Evaluates concentration by requiring users to respond to stimuli in situations that challenge their ability to stay focused. Real-life equivalent: Ignoring background conversations while trying to concentrate on a task.
- Spatial Planning (SP): Evaluates the user's ability to develop and execute a plan through specific tasks. Real-life equivalent: Strategically packing items into the trunk of your car to ensure everything fits.
- Spatial Span (SS): Tests short-term memory by asking users to recall spatial sequences. Real-life related activity Following a set of dance moves.
- Odd One Out (OOO): Assesses deductive reasoning by challenging users to identify the item that doesn't belong in a given set. Real-life equivalent: Determining the truth of a situation based on a set of given facts.

**Table 1:** Four Neurocognitive Tasks from Creyos

Double trouble (DT)	Spatial planning (SP)	Spatial span (SS)	Odd one out (OOO)
			

### 4.3 Test administration and procedure

Prior to the commencement of the testing session, the researcher offered a comprehensive briefing on the tasks ahead. Each task was introduced to the students with the aid of screenshots and verbal instructions tailored to their age group, enhancing the clarity of the on-screen prompts. Students had the option to go through an online tutorial to familiarise themselves with the tasks, after which they engaged with the 'gamified' tests (as depicted in **Figure 2**). The entire sequence of tasks was designed to be completed within a time frame of approximately 15 to 20 minutes.



**Figure 2:** Students Undertaking 'Gamified' Online Creyos Tests

In this study aimed at discerning the effects of the classroom environment on student cognitive function, the Principal Investigator avoided prescribing seating arrangements to the students.

Instead, they were advised to select their seats based on personal comfort (as shown in **Figure 3**). Understanding that a natural setting was crucial for the accuracy of the research, the PI chose not to alter the classroom's status quo; thus, the positions of windows and doors remained unchanged for the first two tests. This approach allowed for a more authentic assessment of the environment's impact on cognitive performance.



**Figure 3:** Students Personal Seating Choices during Cognitive Test

#### **4.4 Internal environmental conditions for the tests**

The tests were run under three different environmental conditions.

- 'Test One' hypothesis: The students' cognitive function in a standard classroom setting, without any deliberate modifications to thermal comfort or CO<sub>2</sub> levels, will serve as a baseline measure and reflect typical learning conditions.
- 'Test Two' hypothesis: "Marginally increasing the temperature with a heater while keeping the windows open will have a negligible impact on students' cognitive performance compared to the baseline conditions.
- 'Test Three' hypothesis: Closing windows and doors while continuing to use a heater will affect students' cognitive performance due to altered thermal comfort and CO<sub>2</sub> levels.

### **5. RESULTS**

The data presented in this report is from the first three of twelve weeks of cognitive studies. The size of the population undergoing the cognitive tests exhibits a slight fluctuation over time. This variation can be attributed to occasions when students must depart before the completion of the tests, either to attend additional English for Speakers of Other Languages (ESOL) or Maths testing or because they are summoned to the principal's office, among other reasons. Such a condition was anticipated and accepted before initiating the testing.

The field study results for examining the three different environmental scenarios were:

- 'TEST 1' conditions: Featured CO<sub>2</sub> concentrations around 608 ppm, an ambient temperature of 21.4 °C, and a relative humidity (RH) of 54.2%.
- 'TEST 2' scenario: Included CO<sub>2</sub> concentrations close to 707 ppm, with an indoor temperature of 23.3 °C and a RH of 51.5%.

- ‘TEST 3’ scenario: Presented elevated CO<sub>2</sub> levels at roughly 1437 ppm, with the temperature inside at 24.2 °C and a RH of 47.6%.

**Table 2** summarises the results of the Shapiro-Wilk normality test conducted on the data obtained from cognitive tests under three different classroom environment conditions each with different levels of thermal comfort and carbon dioxide concentration.

**Table 2: Shapiro-Wilk Normality Test Results for Cognitive Tests Across Different Classroom Environment Conditions**

		SHAPIRO-WILK								
		TEST 1 <i>p</i> -value			TEST 2 <i>p</i> -value			TEST 3 <i>p</i> -value		
	Study size	RM5	RM6	RM7	RM5	RM6	RM7	RM5	RM6	RM7
<b>DT</b>	194	0.1029	0.4567	<b>0.0087</b>	0.2067	0.185	0.0555	0.5096	0.7727	0.1068
<b>SP</b>	200	0.973	0.2749	<b>8.91E-05</b>	0.7661	0.7829	0.7485	0.9985	0.516	0.187
<b>SS</b>	197	<b>0.0023</b>	<b>0.0002</b>	<b>6.86E-05</b>	0.0502	<b>0.0003</b>	0.0614	0.4326	0.0804	<b>0.013</b>
<b>OOO</b>	182	0.1107	0.3314	0.564	0.549	0.9421	<b>3.77E-05</b>	0.7968	0.5727	0.5436

In synthesising this information, findings suggest that the environment might have differential impacts on cognitive test performance, and these impacts vary depending on both the cognitive domain of the test and the cohort. Furthermore, the sensitivity to environmental conditions, especially noticeable in RM7 across multiple tests and conditions, could be of particular interest and might warrant additional investigation into factors that could explain this cohort's unique responses to the test environments.

**Table 3** provides the results from linear regression analyses.

**Table 3: Linear Regression Results for Cognitive Test Scores Under Different Classroom Environmental Conditions**

		LINEAR MODEL					
		‘TEST 1’		‘TEST 2’		‘TEST 3’	
		Coefficient	<i>p</i> -value	Coefficient	<i>p</i> -value	Coefficient	<i>p</i> -value
<b>DT</b>		13.429	<b>2.00E-16</b>	3.218	0.1739	5.327	0.0315
<b>SP</b>		18.5882	<b>2.00E-16</b>	0.9216	0.507	2.1777	0.128
<b>SS</b>		na	na	na	na	na	na
<b>OOO</b>		6.837	<b>2.00E-16</b>	-1.5178	0.106	0.3258	0.735

In the ‘TEST 2’ condition, none of the tests (**Table 3**) showed a statistically significant association with the cognitive scores, since all *p*-values exceeded the 0.05 threshold. The DT test had a *p*-value close to the significance cut-off, which may imply a possible, but not statistically confirmed, weak positive relationship. On the contrary, the OOO test exhibited a negative coefficient (-1.5178), which, despite not being statistically significant (*p*-value of 0.106), could suggest that worse performance is associated with the ‘TEST 2’ condition, warranting further investigation.

For the ‘TEST 3’ condition, the DT test showed a statistically significant relationship, albeit the coefficient is smaller (5.327) than in the ‘TEST 1’ condition, which suggests that while there is still a positive effect, it may be weaker. The SP and OOO tests did not demonstrate a

statistically significant relationship in this environment, as indicated by  $p$ -values of 0.128 and 0.735, respectively, which are above the conventional significance level of 0.05.

Overall, the implication of these findings could be that the ‘TEST 1’ environmental condition is more conducive to better cognitive performance in primary school students compared to the conditions represented by ‘TEST 2’ and ‘TEST 3’.

From **Table 4** ANOVA results for the different cognitive tests and environmental conditions, several deductions can be made:

**Table 4:** ANOVA Results for Cognitive Test Scores Based on Environmental Type and Room Factor

ANOVA										
EnvironType						RoomFactor				
	df	Sum of Squares	Mean Square	F-value	$p$ -value	df	Sum of Squares	Mean Square	F-value	$p$ -value
<b>DT</b>	2	965	482.3	2.78	0.06	2	2819	1409.3	8.12	0.00041
<b>SP</b>	2	155	77.34	1.23	0.29	2	575	287.68	4.57	0.0115
<b>SS</b>	na	na	na	na	na	na	na	na	na	na
<b>OOO</b>	2	95	47.39	1.78	0.17	2	141	70.74	2.66	0.0729

The DT and SP tests show significant differences in performance across environmental conditions, but not due to room factors. The OOO test does not show significant differences across environmental conditions. This underscores the impact of environmental factors on certain cognitive tasks and suggests areas for further research.

After completing a Kruskal-Wallis test for Spatial Span for Rooms RM5, RM6, and RM7, several inferences can be made:

- The Kruskal-Wallis test for all three rooms indicates no significant differences in cognitive scores across different classroom environment conditions.  $P$ -values for RM6 (0.8618), RM5 (0.667), and RM7 (0.4041) all exceed the 0.05 significance threshold.

## 6. DISCUSSION

Analysing the impact of environmental parameters on cognitive test results within specific conditions raises intriguing discussions. In ‘TEST 1’ conditions where CO<sub>2</sub>, temperature, and humidity levels are moderate, the environment is thought to support standard cognitive performance. However, deviations from this norm in test scores could stem from factors beyond the environment, considering the overall comfort levels should not significantly impair cognitive functions.

On the other hand, the ‘TEST 3’ scenario, characterised by higher CO<sub>2</sub> levels and increased temperature, presents a contrasting picture. Elevated CO<sub>2</sub> levels have been linked to decreased cognitive functioning, while discomfort from higher temperatures may further impact cognitive performance. Notable deviations from normality, particularly evident in RM7's Spatial Span test under ‘TEST 3’ conditions ( $p = 0.013$ ), suggest a potential influence on working memory and attention due to environmental stressors. In comparison, the ‘TEST 2’ scenario, featuring elevated CO<sub>2</sub> levels but optimal temperatures, offers a nuanced perspective. Cognitive

performance in this setup is expected to surpass that of the 'TEST 3' condition but may slightly trail the levels seen in the normal condition. For example, the significant deviation in RM7's Odd One Out performance ( $p = 3.77E-05$ ) points towards a potential impact on pattern recognition and logical reasoning within this context.

These findings prompt thoughtful discussions on the multifaceted relationship between environmental conditions and cognitive performance. They highlight the intricate interplay between environmental factors and cognitive functions, underscoring the need for comprehensive assessments to better understand the complexities involved in cognitive testing within varying environmental contexts.

Overall, the three different environmental conditions present a range of CO<sub>2</sub> concentrations, temperatures, and humidity levels that can aid in understanding the nuances of how such factors may interact and affect cognitive outcomes in school settings. The subtle differences in cognitive test performance between these conditions, as indicated by the Shapiro-Wilk test results, could suggest that even small environmental changes are impactful.

## 7. CONCLUSIONS

Therefore, if you were in RM7 and experienced 'TEST 1' conditions, you could expect to maintain standard cognitive performance across most tasks. However, under 'TEST 3' conditions in the same room, you might notice impaired attention and memory, likely due to higher CO<sub>2</sub> levels and increased temperatures. Under 'TEST 2' conditions, you would experience mixed results; although the performance might be better than 'TEST 3' conditions, it still wouldn't be as optimal as in 'TEST 1'.

Similarly, if you were in another room, such as RM5, under 'TEST 1' conditions, your cognitive performance might also be stable. However, elevated CO<sub>2</sub> levels and increased temperatures ('TEST 3') would likely lead to reduced cognitive performance. Like in RM7, a mixed performance would be observed under 'TEST 2' conditions.

The key takeaway is that moderate environmental conditions (like those in 'TEST 1') generally support better cognitive performance. Elevated CO<sub>2</sub> levels and higher temperatures (like in 'TEST 3') tend to negatively impact cognitive functioning. Nevertheless, individual responses can vary, highlighting the importance of considering physical classroom settings, student characteristics, and instructional methods in educational research and practice. Future efforts should aim to optimize classroom conditions to enhance academic performance and cognitive function.

The analyses underscore the complexity of how environmental factors such as CO<sub>2</sub> levels, temperature, and humidity interact to influence cognitive performance. The findings highlight that even small changes in environmental conditions can have measurable effects on cognitive outcomes, although these effects vary depending on the specific cognitive domain and cohort. It does also suggest that other factors, possibly including individual student characteristics or instructional methods, contribute significantly to cognitive performance. Additionally, the specific room in which tests are conducted has a substantial impact on cognitive scores, underscoring the importance of considering physical classroom settings in educational research and practice.

## 8. REFERENCES

- Brenkel, M., Shulman, K., Hazan, E., Herrmann, N., & Owen, A. M. (2017). Assessing capacity in the elderly: comparing the MoCA with a novel computerized battery of executive function. *Dementia and geriatric cognitive disorders extra*, 7(2), 249-256.
- Coley, D. A., Greeves, R., & Saxby, B. K. (2007). The effect of low ventilation rates on the cognitive function of a primary school class. *International Journal of Ventilation*, 6(2), 107-112.
- Environmental Protection Agency (EPA, 2016). Volatile organic compounds' impact on indoor air quality. Health effects. Retrieved from [https://www.epa.gov/indoor-air-quality-iaq/volatile-organic-compounds-impact-indoor-air-quality#Health\\_Effects](https://www.epa.gov/indoor-air-quality-iaq/volatile-organic-compounds-impact-indoor-air-quality#Health_Effects)
- Fadillah, M. F., Muslim, E., & Pane, F. E. S. (2020, May). Analysis of environmental factors effect on cognitive performance and stress level in elementary school students. In *AIP Conference Proceedings* (Vol. 2227, No. 1). AIP Publishing.
- Hama, S., Kumar, P., Tiwari, A., Wang, Y., & Linden, P. F. (2023). The underpinning factors affecting the classroom air quality, thermal comfort and ventilation in 30 classrooms of primary schools in London. *Environmental Research*, 236, 116863.
- Hampshire, A., Highfield, R. R., Parkin, B. L., & Owen, A. M. (2012). Fractionating human intelligence. *Neuron*, 76(6), 1225-1237. [10.1016/j.neuron.2012.06.022](https://doi.org/10.1016/j.neuron.2012.06.022)
- Haverinen-Shaughnessy, U., Moschandreas, D. J., & Shaughnessy, R. J. (2011). Association between substandard classroom ventilation rates and students' academic achievement. *Indoor air*, 21(2), 121-131.
- Haverinen-Shaughnessy, U., & Shaughnessy, R. J. (2015). Effects of classroom ventilation rate and temperature on students' test scores. *PloS one*, 10(8), e0136165.
- Jiang, J., Wang, D., Liu, Y., Xu, Y., & Liu, J. (2018). A study on pupils' learning performance and thermal comfort of primary schools in China. *Building and Environment*, 134, 102-113.
- Levine, B., Bacopulos, A., Anderson, N. D., Black, S. E., Davidson, P. S., Fitneva, S. A., & Hampshire, A. (2013, December). Validation of a novel computerized test battery for automated testing. In *Canadian Stroke Congress. Canadian Stroke Congress* (Vol. 2013, pp. E196-E196).
- Nichols, E. S., Wild, C. J., Owen, A. M., & Soddu, A. (2021). Cognition across the lifespan: Investigating age, sex, and other sociodemographic influences. *Behavioural Sciences*, 11(4), 51.
- Petersen, S., Jensen, K. L., Pedersen, A. L. S., & Rasmussen, H. S. (2016). The effect of increased classroom ventilation rate indicated by reduced CO<sub>2</sub> concentration on the performance of schoolwork by children. *Indoor Air*, 26(3), 366-379.
- Sadrizadeh, S., Yao, R., Yuan, F., Awbi, H., Bahnfleth, W., Bi, Y., ... & Li, B. (2022). Indoor air quality and health in schools: A critical review for developing the roadmap for the future school environment. *Journal of Building Engineering*, 57, 104908.
- Salthammer, T., Uhde, E., Schripp, T., Schieweck, A., Morawska, L., Mazaheri, M., ... & Kumar, P. (2016). Children's well-being at schools: Impact of climatic conditions and air pollution. *Environment International*, 94, 196-210.
- Swarbrick, N. (2012). Primary and secondary education – School administration and funding in Te Ara the Encyclopaedia of New Zealand <http://www.TeAra.govt.nz/en/primary-and-secondary-education>
- Temprano, J. P., Eichholtz, P., Willeboordse, M., & Kok, N. (2020). Indoor environmental quality and learning outcomes: protocol on large-scale sensor deployment in schools. *BMJ open*, 10(3), e031233.

- Thienel, R., Borne, L., Faucher, C., Robinson, G., Fripp, J., Giorgio, J., ... & Lupton, M. K. (2023). Can an online battery match in-person cognitive testing in predicting age-related cortical changes. *Alzheimer's & Dementia*, *19*, e074476.
- Thoua, C., Cooper, E., Stamp, S., Mavrogianni, A., & Mumovic, D. (2022). Indoor Air Quality in Schools. In *Handbook of Indoor Air Quality* (pp. 1891-1933). Singapore: Springer Nature Singapore.
- Wargoeki, P., & Wyon, D. P. (2013). Providing better thermal and air quality conditions in school classrooms would be cost-effective. *Building and Environment*, *59*, 581-589.



# Particle concentration and indoor air quality in naturally ventilated patient rooms-A field study in a hospital building in Bucharest, Romania

The Role of Portable Air Purifiers in Reducing Particle Concentration in Patient Rooms

Mohamed Elsayed <sup>\*1</sup>, Natalia Lastovets<sup>1</sup>, Ville Silvonen <sup>2</sup>, Anni Luoto<sup>1,3</sup>, Topi Rönkkö <sup>2</sup>, Piia Sormunen<sup>1,3</sup>

*1 Tampere University, Faculty of Built Environment  
Korkeakoulunkatu 5  
33720 Tampere, Finland*

*\*Corresponding author: mohamed.elsayed@tuni.fi*

*2 Aerosol Physics Laboratory, Faculty of  
Engineering and Natural Sciences, Tampere  
University  
Korkeakoulunkatu 6  
33720 Tampere, Finland*

*3 Granlund Oy  
Malminkaari 21  
00700 Helsinki, Finland*

## ABSTRACT

In response to the COVID-19 pandemic, there has been a significant emphasis on improving indoor air quality (IAQ), particularly within hospital buildings. Despite developments in integrated central advanced mechanical ventilation and filtration technologies in new hospital buildings, challenges persist in installing them in existing and old hospital buildings relying on traditional natural ventilation. In this context, portable air purifiers have been developed and utilised in hospital facilities as a solution to reduce airborne particulate matter (PM) concentrations and the potential airborne infection risk. However, there have been a limited number of IAQ studies in hospital buildings due to the unique operational environments of hospitals and the associated risks for researchers while conducting in-situ research in hospital facilities, especially in naturally ventilated hospital buildings. This has resulted in a knowledge gap concerning the measured effectiveness of portable air purifiers in traditionally naturally ventilated hospital buildings. To address this gap, a one-week measurement campaign was conducted at a naturally ventilated hospital building in Bucharest, Romania. The campaign aimed to assess PM concentrations before and after utilizing portable air purifier units in two distinct patient rooms — an intensive care unit (ICU) and an isolation room. Additionally, the study involved measuring various aspects of indoor environmental quality (IEQ) parameters, including CO<sub>2</sub> levels, temperature, and relative humidity. Values of measured parameters were used for infection risk calculation. The effectiveness of the air purifier units was determined by comparing indoor and outdoor (I/O) PM concentration ratios before and after using the air purifiers. PM measurement results indicated a significant reduction in PM<sub>2.5</sub> I/O ratios of (78% - 93%) with air purifier use. The findings from the infection risk assessment highlight the potential benefits associated with the employment of portable air purifiers featuring high-efficiency particulate air (HEPA) filters in reducing PM concentration and increasing the total Air Changes per Hour (ACH) in naturally ventilated patient rooms.

## KEYWORDS

Hospital natural ventilation, infection risk, portable air purifying technologies, indoor air quality, airborne particulate matter

## 1 INTRODUCTION

Following the COVID-19 global pandemic, there has been significant emphasis on maintaining good indoor air quality (IAQ) and minimizing cross-infection risks within hospital buildings (Agarwal et al. 2021). IAQ in hospital buildings is influenced by indoor and outdoor air pollution, human activities, and ventilation systems (Roberts et al. 2022). Various ventilation systems, including mechanical, natural, and hybrid systems, are utilized to provide fresh and clean air for patients, medical teams, and visitors (Jung et al. 2015). While natural ventilation provides fresh air with low energy consumption compared to advanced mechanical ventilation systems (Olsson 2017), its effectiveness in maintaining consistent airflow, supporting air filtration and purification, and regulating air temperature and humidity is often inferior to advanced mechanical ventilation systems (Edwards et al. 2024). Moreover, the quality of the delivered air through natural ventilation is affected by various factors such as outdoor air pollution level, wind speed, indoor space arrangement, exhaust shaft placement, and opening size, etc., (Almhafdy et al. 2024). Contemporary mechanical ventilation and filtration technologies, on the other hand, overcome the issues with natural ventilation, and when properly designed, they effectively and efficiently maintain good IAQ (Wu, Rong, and Luhung 2018). However, while it is easy to implement advanced mechanical and filtration systems in new hospital buildings, challenges persist in installing them in existing and old hospital buildings that rely on traditional natural ventilation (Gilkeson et al. 2013).

In Romania, there are 543 hospitals in the country, 488 of them are in urban areas (Petre et al. 2023). Previous research highlighted the relatively higher risk of all-cause mortality due to polluted air and particularly particulate matter (PM) concentrations from vehicle emissions in urban areas in Romania (Bodor, Szép, and Bodor 2023). This risk is higher in naturally ventilated buildings in which pollution source control is difficult, and outdoor air PM pollutants could penetrate the building through openings, envelope, and ventilation shafts (Chamseddine and El-Fadel 2015). New hospital buildings equipped with advanced mechanical ventilation and filtration systems have been designed to uphold and maintain IAQ by eliminating particles that may carry air pollutants (Nourozi et al. 2023). The construction of new hospitals in the public sector in Romania in the last 30 years is very rare (Mihăilă et al. 2020). In addition, there was an increase in hospital mortality cases from 24.7% in 2014 to 31.4% in 2019 of the total mortality in Romania. 62.5% of these cases were reported in hospitals in urban areas (Vlădescu, Ciutan, and Musat 2019). This could be influenced, among other factors, by air pollution (Ab Manan, Aizuddin, and Hod 2018).

In this context, previous studies emphasized the benefits of using air purifiers to reduce PM concentrations and lower the probability of infection risk associated with airborne pathogens in naturally ventilated buildings such as homes, schools, and office buildings (Salmons-Smith et al. 2023). However, because of the heightened inherent risks linked to conducting in-situ research in hospital facilities and their unique operational environments (Jiang et al. 2024), there have been a limited number of IAQ studies in hospital buildings especially in Romania (Ackley et al. 2024). As a result, there is a knowledge gap concerning the measured effectiveness of air purifiers in traditionally naturally ventilated hospital buildings in Romania. To address this gap, a one-week measurement campaign was conducted in two distinct patient rooms in a naturally ventilated hospital building in Bucharest – an ICU room and an isolation room. The study aimed to assess IAQ by monitoring PM<sub>2.5</sub> (particles < 2.5 μm in diameter) mass concentrations before and after utilizing portable air purifier units. The effectiveness of the air purifier units was determined by comparing indoor and outdoor (I/O) PM concentration ratios before and after using the air purifiers. Additionally, the study involved measuring various aspects of indoor environmental quality parameters, including CO<sub>2</sub> levels, temperature, and relative humidity. Measured parameters were used for infection risk calculation.

## 2 MATERIALS/METHODS

### 2.1 Case study description

The two buildings (main building and the isolation ward) hosting the two investigated rooms are part of a larger complex, housing various medical facilities in addition to teaching and research laboratories, and administration, located in the heart of Bucharest city. The complex was constructed in different stages between 1921 and 1941 and underwent renovation between 1950 and 2000, when the use of concrete construction and brick walls was a common practice. Technical information about the buildings was collected through site visits, walkthrough investigations, and a review of architectural and technical drawings provided by the technical team. The ICU room (25.38 m<sup>2</sup>) is in the ICU department on the second floor of a four-story main hospital building. The department consists of one main hallway dividing the ICU rooms on opposite sides (north, and south), the investigated ICU room faces north - see [Figure 1](#).

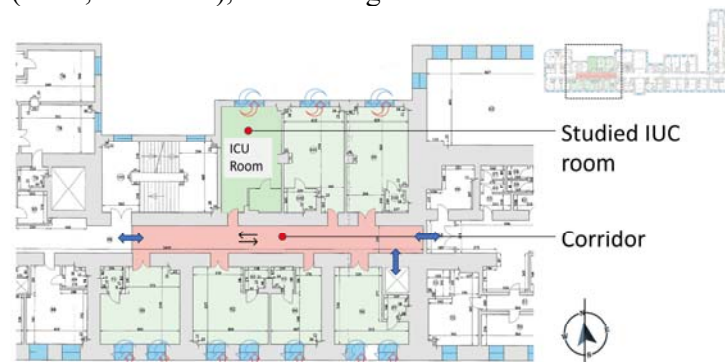


Figure 1: ICU department floor plan - studied room facing north.

The isolation department, located on the second floor of a four-story building, includes an enclosed hallway that divides the isolation patient rooms on both sides of the building, east-west. The isolation patient room under investigation (13.60 m<sup>2</sup>) faces east - see [Figure 2](#).

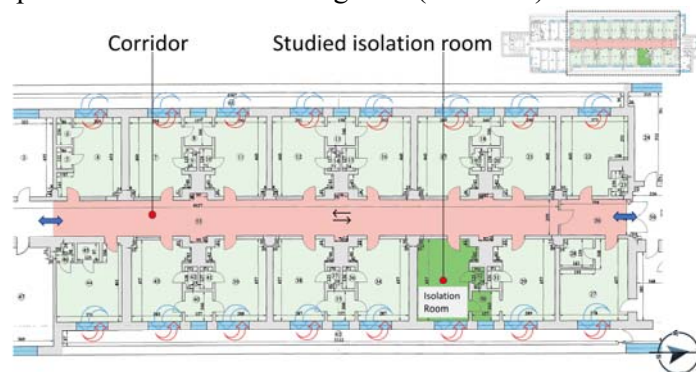


Figure 2: Isolation department floor plan - studied isolation room facing east.

Both buildings were naturally ventilated, with fresh air infiltrating through the openings (i.e., windows and doors), and exhaust air being removed through exhaust shafts. According to the hospital protocol, windows were manually opened every two hours and for fifteen minutes. The investigated rooms were heated by water radiators located under the windows and connected to the central heating system of each building. The designed capacity of the two investigated rooms was for two patients; however, during the monitoring campaign, both rooms housed only one patient. The monitoring campaign lasted for five days during the wintertime (13-17 February 2023). A portable air purifier unit (Air purifier Kuulas+) from ISEC was utilised for each room during the monitoring period - see [section 2.4](#) for more information about air purifier units.

## 2.2 Research methodology

The study followed six steps (see [Figure 3](#)). In [Step One](#), a preliminary visit to the ICU and the isolation rooms was conducted. The objective was to gather information on each room's geometric characteristics, overall layout, and arrangement of medical appliances. Additionally, details regarding the positioning of heating radiators, dimensions of openings, existing furniture, and information about available electrical sockets were collected and documented. This information was used in strategically planning the optimal placement of monitoring instruments and the portable air purifier unit (Mousavi, Khademi, and Taaffe 2020). Moreover, explicit verbal consent was obtained from the participating patient and/or the doctor in charge during this phase.

In [Step Two](#), all instrument sensors were attached to a tripod at varying heights in a specifically designated empty room provided by the staff for this purpose (see [section 2.3](#)). The goal was to simplify the deployment of sensors in the investigated rooms efficiently, with minimal disruption to patients and personnel, while reducing the exposure time for researchers entering the room to minimize the potential infection risk. On [Step Three](#), the monitoring instruments and the portable air purifier unit were transferred to the patient rooms and positioned according to the pre-visit observations in [Step One](#). In [Step Four](#), monitoring took place over a span of two days without turning on the portable air purifier units. [Step Five](#) involved a subsequent visit by the research team to retrieve measured data from the sensors, reset sensors for the following monitoring period, and turn on the air purifier units. In the final step, [Step Six](#), a concluding visit was conducted to retrieve all data and take sensors away after disinfecting them. On each visit to the investigated rooms, the prescribed disinfection protocol mandated by the hospital was applied to the instrument tools brought to the room as well as the research team members.

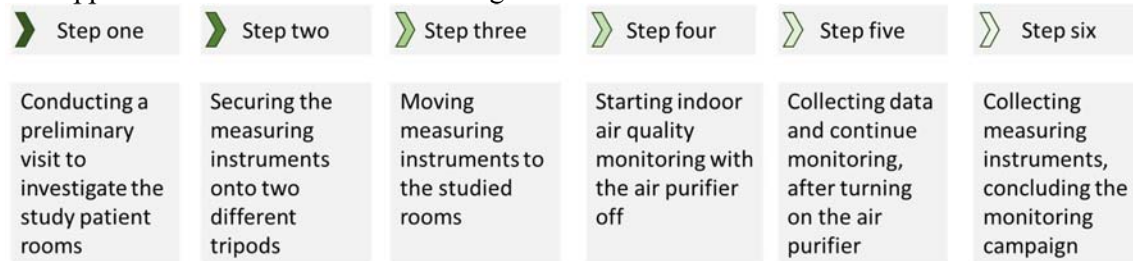


Figure 3: Case study monitoring campaign steps.

## 2.3 Indoor and outdoor measurements

For the indoor air measurements, sensors were attached to a tripod in each room at a different height (150, 100, and 50 cm). The tripod was positioned near the patient bed, approximately 100 – 150 cm away from the patient's head and 50-100 cm from the adjacent wall (see [Figure 4](#)), following the recommendations of Mousavi et al. (2020), and Yun and Licina (2023), for optimal particle exposure capturing. For the PM<sub>2.5</sub> mass concentration measurement, a miniaturized optical particle counter (OPC-N3 from Alphasense) was attached to the tripod at a height of 150 cm. It operated with a one-second resolution in accordance with the European standard EN 481 and previous studies (Kaur and Kelly 2023). For carbon dioxide (CO<sub>2</sub>) concentrations, HOBO data logger MX1102 was attached to the tripod at a height of 150 cm, the MX1102 sensor also measured indoor air temperature (T) and relative humidity (RH%). Two HOBO data loggers MX1101 were attached to the tripod at the height of 100, and 50 cm to measure the air temperature and RH%. The data from all HOBO data loggers were used for building the simulation model and infection risk assessment. The temperature measurement range of the HOBO sensors is from -20 to +70 °C, with an accuracy of ± 0.21 °C. The range for RH% was 1-95 %, with an accuracy of ± 2.0 %, and the range for CO<sub>2</sub> measurement from

0 to 5000 parts per million (ppm), with an accuracy of  $\pm 50$  ppm at 25 °C (Onset 2022). The monitoring resolution for all HOBO sensors was set to one-minute based on recommendations from previous in-situ measurement campaigns to capture sudden variations possibly linked to human activities, such as window or door openings (Elsayed et al. 2023). The outdoor instruments including OPC and HOBO MX2301A were positioned on the second-floor balcony on the western side of the isolation department building. Sensors were positioned within a specifically designated outdoor enclosure to protect them from adverse weather conditions (Schery 2001). Patients were located in nearby buildings, but their rooms were at the same height from the ground level as the second floor, where the PM levels were measured.

Prior to the measurement campaign, a comprehensive testing procedure was executed at the Technical Research Centre of Finland ([www.vttresearch.com](http://www.vttresearch.com)). The testing phase aimed to establish a baseline for sensor performance, enabling robust comparisons throughout the study (Clements and Duvall 2022). The PM sensors' performance was assessed using a reference instrument (Fidas® Frog from Palas), while the HOBO sensors' performance was evaluated against TESTO 6051 from TESTO.

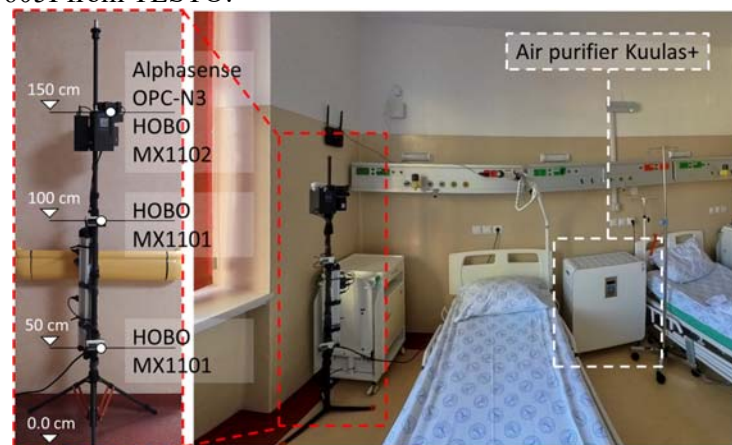


Figure 4: Indoor sensors and air purifier placement-Isolation room.

#### 2.4 Air purifier intervention and infection risk assessment

Portable air purifier (Kuulas+) with a Clean Air Delivery Rate (CADR) of 320m<sup>3</sup>/h was installed in the two investigated rooms. The air purifier was placed next to the patient bed and was operating at 60% power, providing CADR of 192m<sup>3</sup>/h. Each individual unit is outfitted with three distinct filters. The initial filter, a coarse filter, serves to eliminate sizable dust particles, thereby averting the potential obstruction of the subsequent active carbon filter. The active carbon filter is designed to mitigate odours, as well as reduce the concentration of chemical and gaseous compounds in the air. Lastly, a HEPA filter is incorporated, demonstrating efficacy in the removal of 99.97% of dust and pollen particles with a size exceeding 0.3  $\mu\text{m}$  (ISEC n.d.).

Wells-Riley model was used for the calculation of the probability of infection transmission (Lastovets et al., 2023). This model has been extensively used in studies of indoor air quality and ventilation design, and it is applicable to influenza and COVID-19, using quanta emission rates as an indicator of infection doses that affect infection transmission probabilities (Noakes and Sleigh 2008). The analysis focused on scenarios devoid of facial masks, with emission rates ranging from 2 to 10 quanta per hour per person. These simulations considered a setting with one infectious and one susceptible individual consistently present. The study further explored the effect of incorporating an air purifier (ISEC Kuulas) in naturally ventilated conditions. This comprehensive approach allowed for evaluating different ventilation and air purification strategies in reducing infection risks within hospital settings.

### 3 RESULTS AND DISCUSSION

#### 3.1 Indoor and outdoor particulate matter

Figure 5 a represents the monitored indoor and outdoor PM<sub>2.5</sub> concentration as a 30-minute average for the investigated rooms. Throughout the monitoring period (i.e., 5 days), both before and after turning on the air purifier unit, the indoor PM<sub>2.5</sub> mass concentration in the ICU room remained lower than the outdoor concentration and was within the WHO global air quality guidelines (i.e., a 24-hour average concentration of 15 µg/m<sup>3</sup>) (WHO 2021). After turning on the air purifier unit in the ICU, the PM<sub>2.5</sub> concentration decreased, reaching the lowest value of 1.0 µg/m<sup>3</sup>. On the other hand, in the isolation room and before turning on the air purifier unit, the PM<sub>2.5</sub> mass concentration was close to the WHO guidelines, with some spikes in concentration in the afternoon and evening, reaching 30-minute average concentrations of up to 87 µg/m<sup>3</sup>. After turning on the air purifier, the indoor PM<sub>2.5</sub> concentration in the isolation room was below the recommended concentration of 15 µg/m<sup>3</sup>. However, two short spikes were noticed in concentration on the 16<sup>th</sup> of February, reaching 30-minute average concentrations of up to 26 µg/m<sup>3</sup>. The reason behind these spikes was not further investigated; however, it might be caused by the cleaning protocol conducted by staff preparing the room for the next patient, which includes using cleaning products and opening the window. Both factors could have an influence on the indoor PM<sub>2.5</sub> concentration, as concluded from previous studies (Chamseddine and El-Fadel 2015). On the same day (i.e., the 16<sup>th</sup> of February), two spikes were observed in the isolation room, which could be caused by window opening or human activities. However, with the absence of the outdoor PM<sub>2.5</sub> concentration at the time of these spikes, it was not possible to correlate these spikes to the outdoor PM<sub>2.5</sub> concentration. Nevertheless, the daily check on the instrument revealed that data loss remains a problem within situ monitoring (Ministry for the Environment 2009), and it is one of the limitations of this study.

To further investigate the impact of the utilisation of air purifiers on indoor PM<sub>2.5</sub> concentrations, the I/O PM<sub>2.5</sub> ratio was calculated both before and after using the air purifiers. A notable median reduction in the I/O ratio of 78% and 93% was observed in the ICU and isolation room, respectively (see Figure 5 b). Despite using the same air purifier model and applying same power settings, various factors may have contributed to different PM<sub>2.5</sub> reduction values in the two rooms, such as room orientation, infiltration rate, and volume (Chen et al. 2022). High levels of PM concentration in the air, especially fine particles like PM<sub>2.5</sub>, contains toxic and harmful substances as well as pathogenic microorganisms such as bacteria and viruses, which can induce and aggravate human respiratory diseases, thereby affecting the probability of contracting an airborne infection (Abdin and Mahmoud, 2024). The demonstrated decrease in PM<sub>2.5</sub> underscores the potential benefits of employing portable air purifiers equipped with HEPA filters for mitigating PM concentration in hospital patient rooms. This approach has the potential to reduce the risk of airborne pathogen infections, as further detailed in section 3.3.

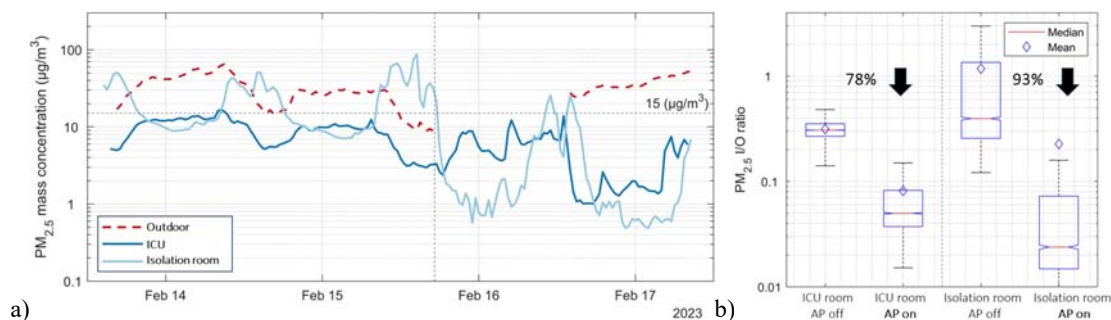


Figure 5: a) PM<sub>2.5</sub> mass concentration time series. The vertical dotted line represents the time when air purifiers were turned on and the horizontal dotted line marks the WHO guideline value of 15 µg/m<sup>3</sup> (24-hour average), b) PM<sub>2.5</sub> mass concentration indoor to outdoor ratios - ICU, and isolation room.

### 3.2 Indoor air temperature and CO<sub>2</sub> concentration

Both the ICU and isolation room featured traditional natural ventilation. As previously mentioned, the windows in each room were manually opened by hospital staff for fifteen minutes every two hours. In the ICU room (78.7m<sup>3</sup>), there was a variation in indoor air temperature at different heights, indicating heat stratification, with an average difference of 1.5 °C. The average recorded indoor air temperature in the ICU room was 23.4°C, while the maximum recorded outdoor air temperature was 9 °C, and the minimum recorded outdoor air temperature -3 °C. Conversely, in the isolation room (42m<sup>3</sup>), the indoor air temperature exhibited greater stability with less heat stratification phenomenon with an average recorded indoor air temperature of 22 °C (see Figure 6). However, both rooms were equipped with a wall-mounted radiator for heating, technical information about the temperature set point and heating schedule was not available.

Regarding CO<sub>2</sub> concentration, for 64% and 67% of the monitoring time for the isolation room and the ICU room respectively, the CO<sub>2</sub> levels remained below the recommended threshold value of 800 ppm by the World Health Organization (WHO) and the REHVA guidelines (REHVA 2021; WHO 2021). However, there were spikes in the CO<sub>2</sub> concentration in both rooms, the spikes lasted for longer periods in the isolation room than in the ICU room (see Figure 6). Several factors could have contributed to the elevated CO<sub>2</sub> levels in the isolation room, including orientation, room volume, and human activities. The lowest CO<sub>2</sub> concentrations in both rooms occurred during the day (afternoon and evening), while elevated concentrations were observed from midnight until morning. This could be attributed to less frequent window opening during the night. However, it was not possible to monitor window opening during the campaign, hindering confirmation of this potential causation.

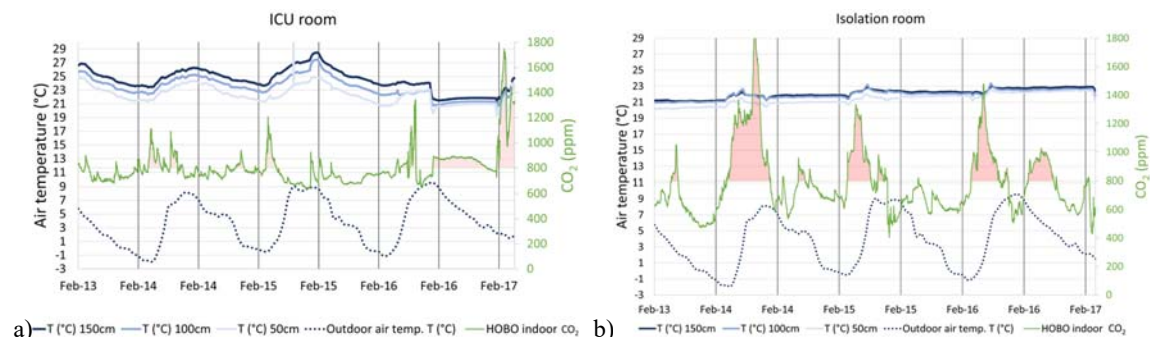


Figure 6: Indoor & outdoor air temperature and indoor CO<sub>2</sub> concentration; a) ICU room, b) Isolation room.

### 3.3 Air purifier intervention and infection risk assessment

Figure 7 shows how infection rates increase over time in both ICU and Isolation room using natural ventilation, air purifiers, and different infectious dose rates. For both scenarios, the ICU room (Figure 7 a) and the isolation room (Figure 7 b), the probability of infection is calculated from zero and increases rapidly within the first few hours, showing the rapid spread of infection in an enclosed space. Predictably, with natural ventilation alone the infection probability is the highest. The slope of the increase is steeper in the Isolation room, due to it having approximately half the volume compared to the ICU room, which allows for faster accumulation of infectious aerosols. In the studied cases, air purifiers almost halves infection estimated infection probability and can be efficient even in scenarios with high quanta emission rates.

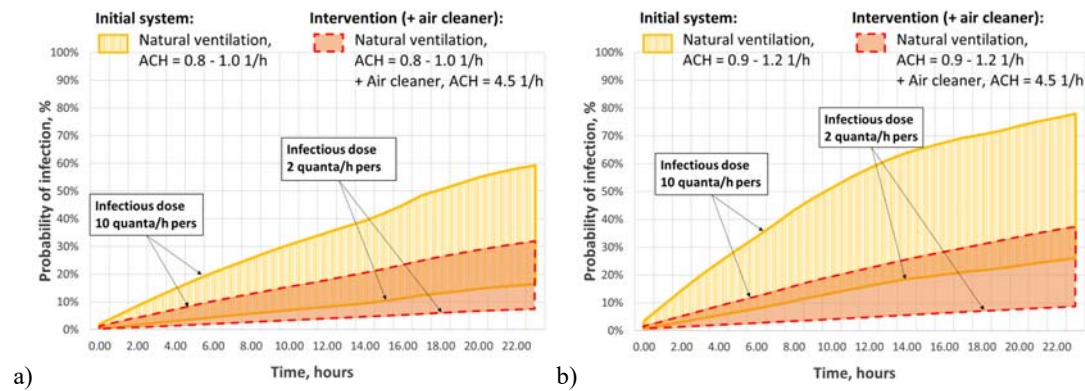


Figure 7: Infection risk probability within a day of exposure with and without air cleaners in a) ICU room, b) Isolation room.

#### 4 CONCLUSIONS

The study investigated some aspects of indoor environmental quality (IEQ) and the potential benefits of using portable air purifiers in a naturally ventilated hospital building. By measuring Particulate Matter (PM<sub>2.5</sub>) concentration before and after the use of the portable air purifier, a reduction in PM<sub>2.5</sub> I/O ratios of 78% to 93% were observed in the two investigated hospital rooms, an Intensive Care Unit (ICU) room, and an isolation patient room, respectively. Regarding indoor air temperature, the average recorded indoor air temperature in the ICU room was 23.4°C, and 22°C in the isolation room, while the average outdoor air temperature was -3°C. The temperature was more stable in the isolation room (42m<sup>3</sup>), with less heat stratification phenomenon. However, in the ICU room (78.7m<sup>3</sup>), there was a variation in indoor air temperature at different heights, with an average difference of 1.5°C every 50cm between (50cm-150cm). The CO<sub>2</sub> concentrations in the isolation room and the ICU room remained below the World Health Organization (WHO) recommended value of 800 parts per million (ppm) for 64% and 67% of the monitoring time (five days), respectively. Different room volumes could have contributed to the lower CO<sub>2</sub> concentrations in the ICU room compared to the isolation room, among other possible factors such as occupant behaviour and window opening. The infection risk assessment reveals that using portable air purifiers with HEPA filters in hospitals can significantly reduce the risk of airborne infections. The air purifiers can complement natural ventilation, lower the immediate risk of infection, and enhance indoor air quality, creating safer environments for patients and healthcare workers.

#### 5 ACKNOWLEDGEMENTS

This study was supported by the Business Finland project E3 Excellence in Pandemic Response and Enterprise Solutions - ([www.pandemicresponse.fi](http://www.pandemicresponse.fi)). The authors extend their heartfelt gratitude to the Hospital team in Romania for their invaluable cooperation.



## 6 REFERENCES

- Ab Manan, Norfazillah, Azimatun Noor Aizuddin, and Rozita Hod. 2018. "Effect of Air Pollution and Hospital Admission: A Systematic Review." *Annals of Global Health* 84(4):670–78. doi: 10.29024/aogh.2376.
- Ackley, Aniebietabasi, Oludolapo Ibrahim Olanrewaju, Oluwatobi Nurudeen Oyefusi, Wallace Imoudu Enegbuma, Toba Samuel Olaoye, Atamewan Eugene Ehimatie, Edidiong Ukpong, and Paulina Akpan-Idiok. 2024. "Indoor Environmental Quality (IEQ) in Healthcare Facilities: A Systematic Literature Review and Gap Analysis." *Journal of Building Engineering* 108787. doi: 10.1016/j.job.2024.108787.
- Agarwal, Nehul, Chandan Swaroop Meena, Binju P. Raj, Lohit Saini, Ashok Kumar, N. Gopalakrishnan, Anuj Kumar, Nagesh Babu Balam, Tabish Alam, Nishant Raj Kapoor, and Vivek Aggarwal. 2021. "Indoor Air Quality Improvement in COVID-19 Pandemic: Review." *Sustainable Cities and Society* 70(April):102942. doi: 10.1016/j.scs.2021.102942.
- Almhafdy, Abdulbasit, Hussein Z. Korany, Saleem S. AlSaleem, and Shi-Jie Cao. 2024. "Airflow Distribution in Hospital Isolation Rooms with Different Ventilation and Exhaust Vent Configurations." *Indoor and Built Environment* 33(1):23–37. doi: 10.1177/1420326X231177460.
- Bodor, Katalin, Róbert Szép, and Zsolt Bodor. 2023. "Examination of Air Pollutants and Their Risk for Human Health in Urban and Suburban Environments for Two Romanian Cities: Brasov and Iasi." *Heliyon* 9(11). doi: 10.1016/j.heliyon.2023.e21810.
- Chamseddine, A., and M. El-Fadel. 2015. "Exposure to Air Pollutants in Hospitals: Indoor–Outdoor Correlations." Pp. 707–16 in Vol. 168.
- Chen, Chiu-Fan, Chun-Hsiang Hsu, Yu-Jung Chang, Chao-Hsien Lee, and David Lin Lee. 2022. "Efficacy of HEPA Air Cleaner on Improving Indoor Particulate Matter 2.5 Concentration." *International Journal of Environmental Research and Public Health* 19(18):11517. doi: 10.3390/ijerph191811517.
- Clements, Andrea, and Rachelle Duvall. 2022. "The Enhanced Air Sensor Guidebook." (September).
- Edwards, Alexander J., Marco-Felipe King, Martín López-García, Daniel Peckham, and Catherine J. Noakes. 2024. "Assessing the Effects of Transient Weather Conditions on Airborne Transmission Risk in Naturally Ventilated Hospitals." *Journal of Hospital Infection*. doi: 10.1016/j.jhin.2024.02.017.
- Elsayed, Mohamed, Sofie Pelsmakers, Lorenza Pistore, Raúl Castaño-Rosa, and Piercarlo Romagnoni. 2023. "Post-Occupancy Evaluation in Residential Buildings: A Systematic Literature Review of Current Practices in the EU." *Building and Environment* 236(February). doi: 10.1016/j.buildenv.2023.110307.
- Gilkeson, C. A., M. A. Camargo-Valero, L. E. Pickin, and C. J. Noakes. 2013. "Measurement of Ventilation and Airborne Infection Risk in Large Naturally Ventilated Hospital Wards." *Building and Environment* 65:35–48. doi: 10.1016/j.buildenv.2013.03.006.
- ISEC. n.d. "Air Purifier Kuulas+." Retrieved December 28, 2023 (<https://www.sisailmaverkkokauppa.fi/kuulas-plus-ilmanpuhdistin/>).
- Jiang, Chuan, Zhijian Liu, Xia Xiao, Haiyang Liu, Junzhou He, Rui Rong, Jingwei Liu, Zhenzhe Huang, and Yongxin Wang. 2024. "Controlling Airborne Pathogen within Fangcang Shelter Hospitals: Aerodynamic Analysis of Bioaerosols Released from Various Locations through Experiment and Simulation." *Building and Environment* 252. doi: 10.1016/j.buildenv.2024.111263.
- Jung, Chien Cheng, Pei Chih Wu, Chao Heng Tseng, and Huey Jen Su. 2015. "Indoor Air Quality Varies with Ventilation Types and Working Areas in Hospitals." *Building and Environment* 85:190–95. doi: 10.1016/j.buildenv.2014.11.026.

- Kaur, Kamaljeet, and Kerry E. Kelly. 2023. "Laboratory Evaluation of the Alphasense OPC-N3, and the Plantower PMS5003 and PMS6003 Sensors." *Journal of Aerosol Science* 171(December 2022):106181. doi: 10.1016/j.jaerosci.2023.106181.
- Mihăilă, Dragoș, Cornel Demeter, Dragoș Bocan, and Cristina Tănasă. 2020. *Characteristics of a Newly Built General Hospital in Romania*.
- Ministry for the Environment. 2009. *Good Practice Guide for Air Quality Monitoring and Data Management*.
- Mousavi, Ehsan, Amin Khademi, and Kevin Taaffe. 2020. "Optimal Sensor Placement in a Hospital Operating Room." *IISE Transactions on Healthcare Systems Engineering* 10(3):212–27. doi: 10.1080/24725579.2020.1790698.
- Noakes, Catherine J., and P. Andrew Sleigh. 2008. "Applying the Wells-Riley Equation to the Risk of Airborne Infection in Hospital Environments : The Importance of Stochastic and Proximity Effects." *Indoor Air* 17–22.
- Nourozi, Behrouz, Aneta Wierzbicka, Runming Yao, and Sasan Sadrizadeh. 2023. "A Systematic Review of Ventilation Solutions for Hospital Wards: Addressing Cross-Infection and Patient Safety." *Building and Environment* 110954. doi: 10.1016/j.buildenv.2023.110954.
- Olsson, Daniel. 2017. *History of Ventilation*.
- Onset. 2022. "ONSET." Retrieved October 24, 2022 (<https://www.onsetcomp.com/>).
- Petre, Ion, Flavia Barna, Daniela Gurgus, Laurentiu Cezar Tomescu, Adrian Apostol, Izabella Petre, Cristian Furau, Miruna Lucia Năchescu, and Anca Bordianu. 2023. "Analysis of the Healthcare System in Romania: A Brief Review." *Healthcare (Switzerland)* 11(14).
- REHVA. 2021. *REHVA COVID-19 Guidance Document*.
- Roberts, Ben M., Raymond Kasei, Samuel Nii, Ardey Codjoe, Ebenezer Forkuo Amankwaa, Samuel N. A. Codjoe, Ebenezer F Amankwaa, Katherine V Gough, Karim Abdullah, Peter Mensah, and Kevin J. Lomas. 2022. "Comparing Indoor Air Quality in Naturally Ventilated and Air-Conditioned Hospitals in the Tropics." (October):2022.
- Salmonsmith, Jacob, Andrea Ducci, Ramanarayanan Balachandran, Liwei Guo, Ryo Torii, Catherine Houlihan, Ruth Epstein, John Rubin, Manish K. Tiwari, and Laurence B. Lovat. 2023. "Use of Portable Air Purifiers to Reduce Aerosols in Hospital Settings and Cut down the Clinical Backlog." *Epidemiology and Infection* 151. doi: 10.1017/S0950268823000092.
- Schery, Stephen D. 2001. "Aerosol Measurement." Pp. 171–216 in.
- Vlădescu, Cristian, Marius Ciutan, and Simon Musat. 2019. "Time Trends in Inhospital Mortality. A Retrospective Study in Romania 2014-2019." *Romanian Journal of Legal Medicine* 27(4):399–404. doi: 10.4323/rjlm.2019.399.
- WHO. 2021. "WHO Global Air Quality Guidelines." *Particulate Matter (PM2.5 and PM10), Ozone, Nitrogen Dioxide, Sulfur Dioxide and Carbon Monoxide* 1–360.
- Wu, Yan, Jiahui Rong, and Irvan Luhung. 2018. "Influence of Air Conditioning and Mechanical Ventilation (ACMV) Systems on Indoor Microbial Aerosols." *Kexue Tongbao/Chinese Science Bulletin* 63(10):920–30. doi: 10.1360/N972017-01114.
- Yun, Seoyeon, and Dusan Licina. 2023. "Optimal Sensor Placement for Personal Inhalation Exposure Detection in Static and Dynamic Office Environments." *Building and Environment* 241(June):110459. doi: 10.1016/j.buildenv.2023.110459.

# Performance optimization of an office building with a dynamic façade system

Zhijian Wang\*<sup>1</sup>, Magdalena Hajdukiewicz<sup>1,2</sup>, Pieter-Jan Hoes<sup>1</sup>, Marcel G.L.C. Loomans<sup>1</sup>

<sup>1</sup> Eindhoven University of Technology  
Groene Loper 3  
Eindhoven, Netherlands

<sup>2</sup> University of Galway  
University Road,  
Galway, Ireland

\*Corresponding author: z.wang7@tue.nl

## ABSTRACT

Buildings account for a substantial portion of global energy consumption, and heating, ventilation and air conditioning (HVAC) systems are responsible for approximately 40% of the buildings' energy consumption. A building façade, with HVAC, has a great influence on the internal environment. An optimization of the façade design and operation can help improve building energy efficiency. This research utilized building energy simulation to assess and optimize the operational strategy for a dynamic façade system (including natural ventilation and shading functions) in an office building. The work focused on building energy demand based on a validated simulation model. Several parameters in the model were recalibrated, based on an existed simulation model, by historical weather and building operation data, resulting in a yearly mean absolute error of 2.1% in heating and cooling energy demand. The model then was used to study different dynamic façade control strategies. Based on the base model, different control strategies of shading and natural ventilation were designed, and the control parameter (solar irradiation) for the shading system was optimized, with energy efficiency as a performance indicator. Based on monthly energy demand data, a combined strategy model was selected. It was found that utilizing an optimized strategy for natural ventilation through the dynamic façade resulted in 14.9% energy-saving when compared to the case without natural ventilation. Next, a parameter study was carried out on the combined strategy model. Notably, natural ventilation airflow rate and occupancy density parameters showed less impact on the total energy demand, while the occupancy density had a significant impact on the ratio between the heating and cooling energy demand. Additionally, the parameter study confirmed the energy saving potential of applying a wider range of cooling and heating setpoints. The results of this research confirmed the significant energy-saving potential for the dynamic façade system, consisting of a natural ventilation and shading. Performance optimization of the investigated dynamic façade can be found by combining the control strategy for both control elements of the façade system, to deal best with the (Dutch) seasonal changes in weather conditions. Furthermore, with various building operation goals, such as cooperating with long-term energy storage systems or providing thermal comfort, the research suggests flexibly in arranging the occupancy and HVAC setpoints.

## KEYWORDS

Dynamic façade, natural ventilation, ventilation strategy, energy performance, thermal comfort

## 1 INTRODUCTION

Buildings account for 40% of global energy consumption, and over 30% of CO<sub>2</sub> emissions (Ni et al. 2023). To meet occupants' thermal comfort needs, the heating, ventilation, and air conditioning systems (HVAC) systems account for 40% of building energy consumption (Costa et al. 2013). The exterior wall of a building is known as the building façade. It plays a significant role in architectural design and serves as a protective barrier against changes in the outside environment, which can greatly affect the indoor conditions in buildings according to different façade materials and geometries (Wonorahardjo et al. 2022). Thus, a rationally designed building façade can help to reduce building energy demand.

Actively adaptive, or dynamic, building façades are designed with integrated features that allow for various manipulations, such as openable windows and building-integrated dynamic shading systems (Alkhatib et al. 2021). The openable windows enable the flow of natural ventilation and the dynamic shading systems allow control of solar irradiance inside the building, which have potential to save energy consumed by operation (Bamdad et al. 2022). Tognon (Tognon et al. 2023) evaluated the ability of natural ventilation to save cooling energy consumption by openable windows. The cooling demand decreased significantly by utilizing openable windows, which was up to 30% in a warm climate like Italy and 11% in a cold climate such as Finland. Lemarchand (Lemarchand, et al., 2014) designed a photovoltaic window with adjustable transmission, which could control and reduce the solar radiation into a building from 80% to 5% and adjust the indoor thermal condition to achieve energy efficiency and thermal comfort. However, most studies have focused on one dynamic technology, and only a few studies have investigated the energy saving potential of dynamic façades with multiple functions. This research aims to explore the effect of a dynamic façade system, with natural ventilation and shading, on the operation of a modern office building. Through computational simulation based on experimental and measured data, this research aims to evaluate the energy saving potential on heating and cooling consumption while maintaining thermal comfort of the occupants.

## **2 METHOD**

The research firstly includes experimental measurements to investigate the effect of natural ventilation systems in the office building. Based on that, a basic simulation model developed and calibrated using historical building operation data (Bognár et al. 2022), was used in this research. The dynamic façade operation strategies were developed and analysed using the calibrated model, and parameter study was further implemented.

### **2.1 Experimental study**

Figure 1 shows a model of an office room where the experiment was carried out to investigate the effect of natural ventilation. The office was located on the ninth floor of an educational office building and had a typical layout representing offices in the building. The room was equipped with a mechanical ventilation system, and a façade of floor-to-ceiling windows facing East side, including an openable window for natural ventilation purposes. In the experiment, the air change per hour rate (ACH) in the room was regarded as the index to evaluate the performance of ventilation. A gas analyser (INNOVA 1512, LumaSense Technologies A/S, Ballerup, Denmark) in combination with a multipoint sampler and dozer (INNOVA 1403, LumaSense Technologies A/S, Ballerup, Denmark) were employed to measure the ACH. The experiment took place on 15<sup>th</sup> September 2023. The ACH was measured when windows are opened and closed.

### **2.2 Simulation model**

The simulation model focused on the tenth floor of an educational building, as shown in Figure 2. The simulation model inherited the basic setup from the study of Bognár et al. (2022). In that work, the model was calibrated by annual cooling and heating energy consumption from September 2020 to August 2021, which was the only available data at that time. The research presented here incorporated the natural ventilation experiment results into the simulation model of Bognár. This is achieved by switching the original natural ventilation method in the model to a scheduled method with constant parameters of infiltration and natural ventilation. Therefore, the infiltration ACH parameter in the simulation model was fitted again based on the energy consumption data. Also, since the model of Bognár was without occupancy due to Covid-19

constriction, to study the effect of natural ventilation of the dynamic façade system with normal occupancy condition, the weather data and occupancy condition of year 2022 (from January to December) was updated as boundary conditions and model inputs. Afterwards, the updated simulation model was validated by comparing the Mean Absolute Error (MAE) of indoor temperature between measurement and simulation.

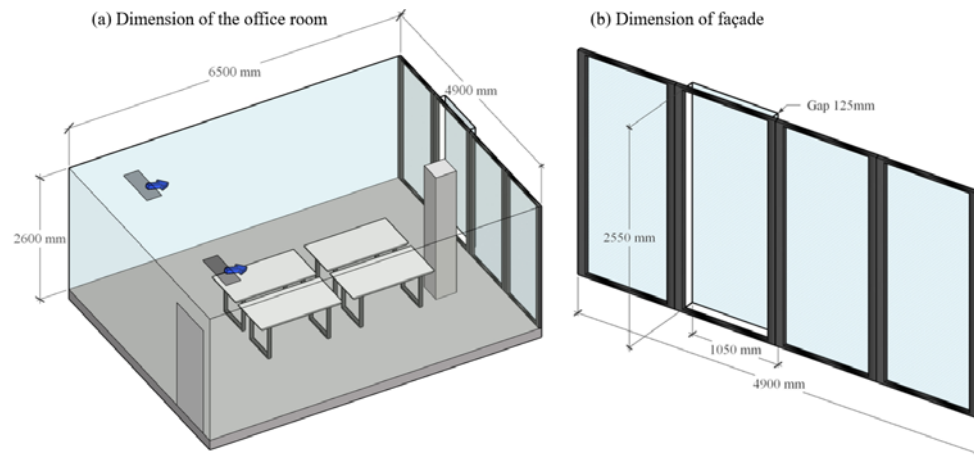


Figure 1: Geometry of the office room and façade system

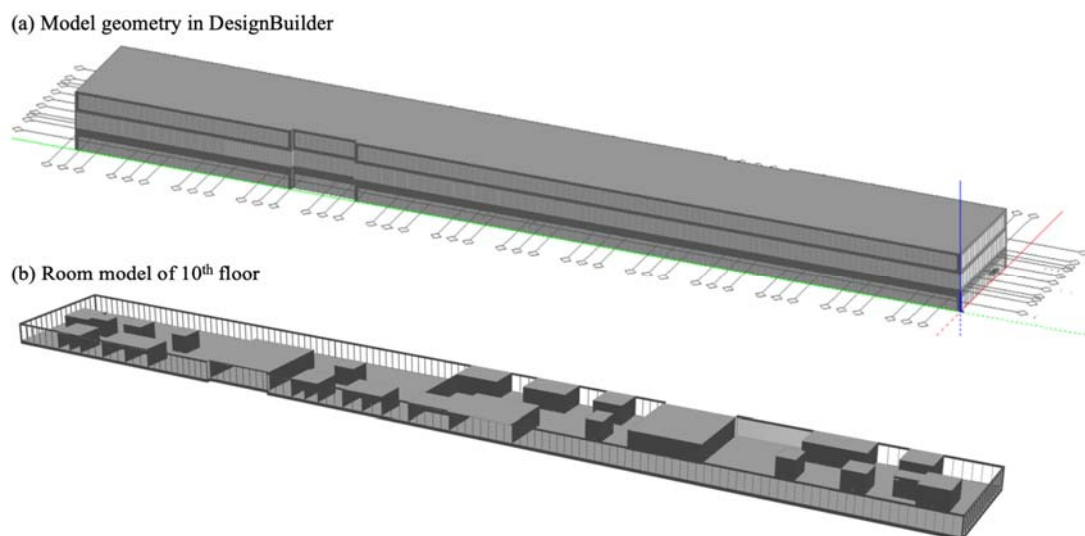


Figure 2: Model of the building

### 2.3 Dynamic façade system strategies

The simulation of the dynamic façade system was set up in EnergyPlus [ref]. Figure 3 shows the dynamic façade system operation logic for the real-life scenario and the simulation tool and. In the real-life case, a button can be activated when the weather conditions are favourable for the occupant to open the window manually. The weather factors include wind speed and precipitation factors. Opening the window will cause the whole shading blinds in the room to go up. In the simulation tool, the natural ventilation system only operates when it is set as available. When the natural ventilation system is enabled during a specific period, and the indoor temperature exceeds  $23^{\circ}\text{C}$ , with a minimum  $1^{\circ}\text{C}$  higher compared to the outdoor dry bulb temperature, the system will be activated. The operation logic for the simulation tool does not consider the wind and precipitation factors.

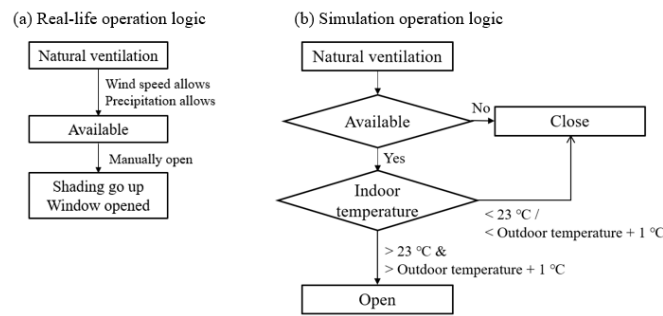


Figure 3: Operation logic of dynamic façade system

Five operational strategies were considered for the façade system and developed in the EnergyPlus simulation. General information about each strategy and the optimization process is shown in Figure 4.

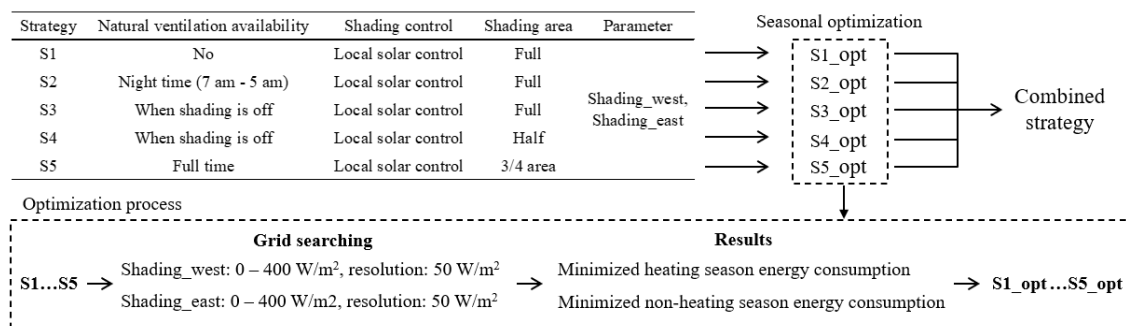


Figure 4: Strategies information and optimization process

Strategy S1 had no natural ventilation function as a control group. In S2, the natural ventilation system offered night cooling only, which was available between 7 pm to 5 am the next day. S3 was developed since the openable window could not be opened when the shading blinds went down. Thereby, for each room, the natural ventilation system was available when the local solar radiation was below the threshold and shading blinds went up. Besides, S4 generated a similar control strategy as S3, where the shading could only be half-opened (considering objects accidentally placed under the windows could damage the shading system). It was observed that when natural ventilation was on, the shading system in the room was turned off. Since only one out of four windows was openable, it was worth exploring the energy saving potential of a case, S5, where the openable windows with natural ventilation are fully independent from the solar radiance control while the rest of the windows (three quarters) can still response to solar radiance index. In the proposed five strategies the shading system was controlled by two local solar radiance indexes, surface outside face incident solar radiation rate per area for the East and West walls, called Shading\_east and Shading\_west. The two local solar radiance indexes were optimized for each specific case, regarding minimizing the total heating and cooling energy demand. The optimization used a grid search method. The range of the two parameters was between 0 to 400 W/m<sup>2</sup> (resolution of 50 W/m<sup>2</sup>). Besides, given the fact that the typical heating season in the Netherlands is from 1<sup>st</sup> October to 30<sup>th</sup> April (Yang et al., 2020), the local Indexes in strategy should be optimized for a heating season and a non-heating season separately. In the end, the lowest energy demand case in each month would be combined into a combined-strategy case.

## 2.4 Parameter study

To study the impact of several parameters, three parameter studies were implemented based on the simulation model of combined strategy in Chapter 3.2, with the optimized shading thresholds. More specifically, firstly, the experiment of natural ventilation was implemented in a limited period. The ACH of natural ventilation through an opening connected to the atmosphere will be influenced by not only stack effect but also wind speed. Meanwhile, the occupancy condition in the model follows a ratio curve ranged from 0 to 100% of the input occupancy density value. However, the highest occupancy density value in each day may vary for different reasons, like education schedule. Besides, the heating and cooling setpoints in the simulation model were kept as fixed values. It is illustrated, according to the adaptive thermal comfort theory, that a wider range of temperature can be considered in a naturally ventilated indoor environment (de Dear and Brager 1998), since the occupancy accept wider temperature ranges in that case. As a result, the range of the heating and cooling setpoints can be wider since the building is naturally ventilated. Thus, the natural ventilation parameter, occupancy density, and heating and cooling setpoints in the combined strategy case have been further studied based on the original setup. The variable of the parameter study is as shown in Table 1. The study variants marked with a star are the original variants in the simulation model. In parameter study 1, the ventilation airflow rate was the variable, the airflow rate was calculated according to different ACH in the measured room. In parameter study 2, as mentioned previously, the highest occupancy in each day of simulation was determined by 50% of the number of seats on the floor. The ratio was adjusted to generate different occupancy conditions. In parameter study 3, the heating and cooling setpoints were adjusted accordingly, to provide a wider range than the original case. In each parameter study case, only one variable was changed. The combination of parameters was not studied.

Table 1: Variable in each parameter study

<i>Parameter study 1</i>	Experimental ACH (1/h)	<i>Parameter study 2</i>	Occupancy ratio (%)	<i>Parameter study 3</i>	Cooling/heating setpoints (°C)
<i>NV0</i>	0	<i>Occ0</i>	0	<i>SP22/23*</i>	22/23
<i>NV1</i>	1	<i>Occ25</i>	25	<i>SP24/21</i>	24/21
<i>NV3</i>	3	<i>Occ50*</i>	50	<i>SP25/20</i>	25/20
<i>NV5*</i>	5	<i>Occ75</i>	75		
<i>NV7</i>	7	<i>Occ100</i>	100		
<i>NV9</i>	9				

## 3 RESULTS

### 3.1 Air exchange rate and basic model setup

The experiments included two steady state stages of measurement, window closed, and window opened. With the room dimension 6.5 x 4.9 x 2.6m, the ACH and airflow rate could be calculated accordingly. The ACH measured with opened window was 7.59/h. The ACH with closed window was 2.36/h. Thus, the experiment results of ACH and airflow rate for the natural ventilation were assessed at 5.23/h and 432.85m<sup>3</sup>/h, while for mechanical ventilation 2.36/h and 195.42 m<sup>3</sup>/h were assumed. As introduced, due to the typical layout of the experiment room, the result was regarded as the universal performance of ventilation in the building. Specifically, in the simulation model, the ACH difference caused by each activated openable window was rounded to ACH of 5/h for the investigated room, corresponding to 414 m<sup>3</sup>/h for each open window.

The simulation model was developed by Bognár (Bognár et al. 2022). In the current model, the natural ventilation method in the model was switched to a scheduled method to utilize the experimental results in the simulation model. This required a re-calibration of the model infiltration parameter. The infiltration ACH value was fitted to 0.088/h. The simulation model with fitted infiltration predicts an annual cooling energy demand of 23,688 kWh and heating energy demand of 75,656 kWh, compared to measured values of 23,346 kWh for cooling and 75,527 kWh for heating. Afterwards, the boundary condition of the simulation model, i.e., occupancy condition, and number of openable windows were updated according to the conditions of year 2022. The calculated occupancy density is 0.04 people/m<sup>2</sup>, which was calculated from 50% of the maximum seat number and was applied to the whole floor during working time. The number of openable windows in each zone is also set in the model. As for model validation, the measured and simulated indoor temperature were compared. The MAE of the monthly indoor temperature is 0.72°C and the MAE of hourly indoor temperature is 1.06°C. According to the study of Pachano & Bandera (2021), this result is acceptable. As a result, the basic model was considered valid for further dynamic façade strategy study.

### 3.2 Dynamic façade strategy study

Table 2 shows the optimized values of local solar shading thresholds of each strategy in two in the heating and non-heating season. Table 3 shows the highest and lowest energy demand value of each simulation case, including heating and cooling energy demand. The optimized threshold values shows that the solar radiance thresholds to control the shading system were generally lower in the non-heating season than in the heating season, since the solar radiation was a significant heat source in the building. In the non-heating season, a lower solar threshold leads to better building envelope insulation from the solar radiance and lower cooling energy demand. In cases where shading system and natural ventilation system were independent, including S1, S2, and S5, the thresholds for the shading system in the non-heating season reached the lowest possible value, 0 W/m<sup>2</sup>. This means that the shading blinds went down when there was any solar radiation present and only went up during night. From the results, one may deduce that, in the non-heating season, the heat dissipation from human body and equipment, and heat conducted by building materials are already sufficient to generate a cooling demand. Extra solar radiation will only add to the building cooling demand and cause extra energy demand. On the other hand, a higher threshold for the shading system in the heating season allows the building to gain more heat and thereby consume less heating energy. As a result, almost all cases have the highest possibly threshold in the heating season of 400 W/m<sup>2</sup>.

Figure 5 (a) shows the monthly heating and cooling energy demand of each strategy. Among all cases, with S1 as the control group, S3 shows the highest annual energy saving potential, which was 13,087 kWh per year. Based on the results of the previous section a combination of monthly strategies could be considered to further explore the energy saving potential of the dynamic façade system in the building. Figure 5 (b) shows the result of the strategy with combined monthly lowest energy demand strategies, where S3 has the lowest energy demand from April to October, S4 has the lowest energy demand from November to February, and S5 has the lowest energy demand in March. The annual energy demand of the combined strategy is 86,781 kWh, compared to S1 (101918 kWh), an energy saving ratio of 14.9% was reached.



Table 2: The optimized results of each dynamic façade operation strategies

Seasonal threshold	S1		S2		S3		S4		S5	
	Heating	Non-heating	Heating	Non-heating	Heating	Non-heating	Heating	Non-heating	Heating	Non-heating
Shading_east (W/m <sup>2</sup> )	400	0	400	0	400	150	400	150	400	0
Shading_west (W/m <sup>2</sup> )	350	0	400	0	400	250	400	200	400	0

Table 3: The highest and lowest energy demand value of simulation results for each case

Energy consumption (kWh)	S1		S2		S3		S4		S4	
	Highest	Lowest	Highest	Lowest	Highest	Lowest	Highest	Lowest	Highest	Lowest
Heating season	54804	54279	54626	53973	54594	53752	53114	52414	53270	52920
Non heating season	51743	46799	43537	39951	37298	35080	47351	43221	46615	44079

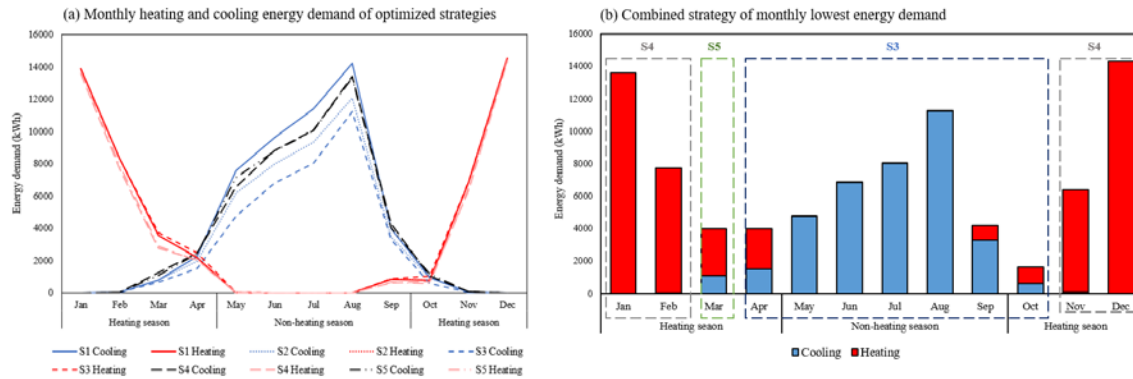


Figure 5: Monthly energy demand in each optimized strategy and the combined strategy with monthly minimized energy demand

### 3.3 Parameter study

Figure 6 shows the results of three parameter studies. The highlighted columns show the simulation model results for the original setup in each parameter study.

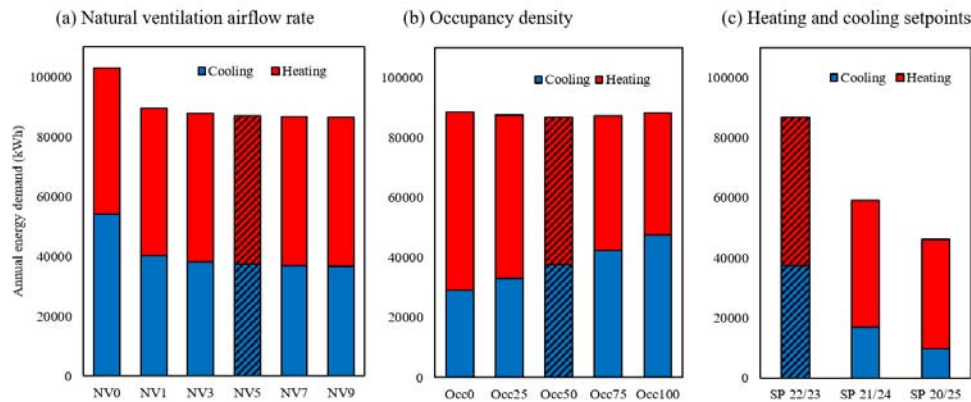


Figure 6: Annual energy demand in each parameter study case

Figure 6 shows, for parameter study 1, that the annual heating energy demand is higher and annual cooling energy demand is lower when a natural ventilation airflow rate is present. A higher natural ventilation ACH will lead to more cooling power, though sensitivity to the natural ventilation airflow rate is small. Comparing NV1 (89505 kWh) with NV0 (102818kWh), disabling natural ventilation results in a 14.9% increase in energy demand. The energy demand of NV9 (86462 kWh) is only 3.4% (3034 kWh) lower than NV1. It is concluded that, in the original simulation model (NV5), the natural ventilation was already sufficient for providing cooling. The influence of wind, represented by a higher natural ventilation ACH rate, affects

the simulation results less. In parameter study 2, a higher occupancy density leads to more cooling energy demand and less heating energy demand because of the heat power generated by occupancy. However, as they compensate each other, the total annual energy demand is influenced less by the occupancy density. The Occ50 case (86781kWh) has the lowest annual energy demand. Compared with that, the annual energy demand of Occ0 case and Occ100 case is only 2.1% and 1.6% higher. However, the difference in ratio of heating and cooling annual energy demand is more significant. With occupancy density from lower to higher, the ratio of cooling annual energy demand in the total annual energy demand is 33%, 38%, 43%, 49%, 54%, respectively. Besides, it is learnt from parameter study 3 that a wider temperature range will lead to a significantly lower monthly heating and cooling energy demand. This is because a wider range of setpoint will allow for a more flexible indoor temperature and thus the heating and cooling demand both are relaxed. Following the results shown in Figure 6, the energy saving ratios of the SP 21/24 and SP 20/25 cases, as compared to SP 22/23, are 32% and 47%, respectively.

#### 4 DISCUSSION

This study indicates that solar radiation has a large effect on building energy consumption. Furthermore, implementing dynamic façade systems with adjustable local solar radiance thresholds that change with the season can have a high energy saving potential. In the studied building, lower thresholds are recommended to be used in the non-heating season to reduce cooling energy demand, while higher thresholds are recommended to be used in the heating season to utilize solar energy and minimize heating energy demand. Also, when cooperating with the natural ventilation system, different thresholds for each surface of the building can be considered to make the best use of natural ventilation and solar radiation.

However, this study only focused on solar shading as the control factor in the aspect of energy demand. In real-life, indoor environmental quality includes additional factors, such as thermal and visual comfort and indoor air quality, etc. Those factors will also influence the occupancy's willingness to control the dynamic facades. The solar index setting in the model does not consider the comfort issue caused by strong solar radiance, since a higher threshold might lead to less thermal comfort (Matsuda et al., 2023) and an over-illuminated indoor environment (Derbas & Voss, 2023).

Combining natural ventilation strategies can be considered to optimize energy demand throughout the year. The heating and cooling loads show seasonal characteristics (Lin et al. 2022). It is worth considering implementing strategies that consume less energy each season to achieve significant energy savings during the operating year.

Based on the parameter studies, widening the range of heating and cooling setpoints can be considered, to create more flexible indoor temperature control. This can result in significant energy savings, especially when natural ventilation is integrated (Ke et al. 2019). It also aligns with the increased need for energy flexibility (Papachristou et al. 2021). Besides, critically managing occupancy in the building should be considered. The heating system in the building is cooperating with a seasonal energy storage system to utilize the heating and cooling demand of the building and reach energy saving goals. The influence of occupants on heating and cooling energy demand could be utilized. Also, according to the parameter study of natural ventilation airflow rate, the presence (or availability) of natural ventilation has enormous influence on energy saving (14.9% energy saved). However, the increasing of natural ventilation airflow rate shows less impact (only 3.4% energy saved when increasing the ACH ninefold).

The research was focused on the energy demand. As mentioned before, there may be indoor environment quality conditions that benefit from the operation of natural ventilation, which have not been considered in the simulation tool, e.g., thermal comfort and indoor air quality (Sas-Wright and Clark 2023). These reasons may affect the energy effectiveness of the natural ventilation solution in the target building. In future study, these factors could be included in the simulation model to provide a more complete evaluation of the dynamic façade system.

## 5 CONCLUSIONS

This research aims to evaluate the effect of a novel dynamic façade system operation on energy demand in an office building, with a specific focus on heating and cooling systems. By experimentally investigating the impact of the dynamic façade on natural ventilation airflow rates, a calibrated and valid simulation model was developed. Based on actual operational needs, this research investigated the evaluation of energy demand with various dynamic façade operational strategies, which were optimized based on local solar radiation indexes and seasonal variations. A combined strategy model yielded a potential energy-saving ratio of 14.9% compared to a model without natural ventilation, which emphasized the importance of utilizing natural ventilation. The study indicates that the presence of natural ventilation contributes significantly to energy saving in the building. Also, the occupancy density had a great impact on the heating and cooling energy demand balance. Furthermore, a wider range of heating and cooling setpoints has a significant energy saving effect. Considering the occupants could adapt to a wider range of indoor temperatures in a naturally ventilated space, a wider thermal comfort adaptive temperature range is recommended to be considered for building operation to save energy. Meanwhile, the study recognized the need for further investigations and the consideration of additional factors in assessing dynamic façade system performance. It is acknowledged that some factors for dynamic façade operation were not considered in the research. Future studies will focus on additional indoor environmental parameters and operating factors of the dynamic façade system to better optimize the operational strategies of the dynamic façade system in the Atlas building.

## 6 ACKNOWLEDGEMENTS

The authors would like to acknowledge the financial support from the European Union's MSCA PF FaceINQ project (grant agreement no.101066362). We extend our gratitude to all the people who assisted and supported this research. The Real Estate and Atlas Living Lab are acknowledged for sharing data and assisting us implementing the measurement experiments. The technical staff of the Building Physics and Services lab at the Built Environment department are acknowledged for preparing the experimental equipment. Ádám Bognár is acknowledged for providing calibrated simulation model and further advice. The authors acknowledge the Academic Committee for Design of the Department of Mechanical Engineering, Eindhoven University of Technology, for financing the conference cost.

## 7 REFERENCES

- Alkhatib, H., P. Lemarchand, B. Norton, and D. T. J. O’Sullivan. 2021. “Deployment and Control of Adaptive Building Facades for Energy Generation, Thermal Insulation, Ventilation and Daylighting: A Review.” *Applied Thermal Engineering* 185:116331.
- Bamdad, Keivan, Soha Matour, Nima Izadyar, and Sara Omrani. 2022. “Impact of Climate Change on Energy Saving Potentials of Natural Ventilation and Ceiling Fans in Mixed-Mode Buildings.” *Building and Environment* 209:108662.

- Bognár, Ádám, Pieter-Jan Hoes, Twan van Hooff, and Marcel G. L. C. Loomans. 2022. "Practical Experiences from the Implementation of Extensive Sensoring in a Modern Building." *CLIMA 2022 Conference*.
- Carlucci, F., K. Negendahl, and F. Fiorito. 2023. "Energy Flexibility of Building Systems in Future Scenarios: Optimization of the Control Strategy of a Dynamic Shading System and Definition of a New Energy Flexibility Metric." *Energy and Buildings* 289:113056.
- Costa, Andrea, Marcus M. Keane, J. Ignacio Torrens, and Edward Corry. 2013. "Building Operation and Energy Performance: Monitoring, Analysis and Optimisation Toolkit." *Applied Energy* 101:310–16.
- de Dear, Richard, and G. S. Brager. 1998. "Developing an Adaptive Model of Thermal Comfort and Preference."
- Ke, Yujie, Yin Yin, Qiuting Zhang, Yutong Tan, Peng Hu, Shancheng Wang, Yichao Tang, Yang Zhou, Xinglin Wen, Shaofan Wu, Timothy J. White, Jie Yin, Jinqing Peng, Qihua Xiong, Dongyuan Zhao, and Yi Long. 2019. "Adaptive Thermochromic Windows from Active Plasmonic Elastomers." *Joule* 3(3):858–71.
- Lemarchand, P., J. Doran, and B. Norton. 2014. "Smart Switchable Technologies for Glazing and Photovoltaic Applications." *Energy Procedia* 57:1878–87.
- Lin, Hongyu, Qingyou Yan, Xueting Li, Jialu Dang, Shenbo Yang, De Gejirifu, Lujin Yao, and Yao Wang. 2022. "Multi-Energy Coordinated and Flexible Operation Optimization and Revenue Reallocation Models for Integrated Micro Energy System Considering Seasonal and Daily Load Characteristics of Different Buildings." *Energy Reports* 8:12583–97.
- Ni, Shenyang, Neng Zhu, Yingzhen Hou, and Zhiyuan Zhang. 2023. "Research on Indoor Thermal Comfort and Energy Consumption of Zero Energy Wooden Structure Buildings in Severe Cold Zone." *Journal of Building Engineering* 67:105965.
- Papachristou, Christina, Pieter-Jan Hoes, M. G. L. C. Loomans, T. A. J. van Goch, and J. L. M. Hensen. 2021. "Investigating the Energy Flexibility of Dutch Office Buildings on Single Building Level and Building Cluster Level." *Journal of Building Engineering* 40:102687.
- Sas-Wright, Troye, and Jordan D. Clark. 2023. "Numerical Assessment of Indoor Air Quality in Spaces in the United States Designed with the ASHRAE 62.1–2019 Natural Ventilation Procedure." *Building and Environment* 243:110671.
- Tognon, Giacomo, Marco Marigo, Michele De Carli, and Angelo Zarrella. 2023. "Mechanical, Natural and Hybrid Ventilation Systems in Different Building Types: Energy and Indoor Air Quality Analysis." *Journal of Building Engineering* 76:107060.
- Wonorahardjo, Surjamanto, Inge Magdalena Sutjahja, Y. Mardiyati, Heri Andoni, Rizky Amalia Achsani, S. Steven, Dixon Thomas, Ekrem Tunçbilek, Müslüm Arıcı, Nadiya Rahmah, and Suwardi Tedja. 2022. "Effect of Different Building Façade Systems on Thermal Comfort and Urban Heat Island Phenomenon: An Experimental Analysis." *Building and Environment* 217:109063.

# Exploring the use of TABS and Peak-Shift Control in Office Buildings

Honoka Kyojuka<sup>1</sup>, Kiyoto Koga<sup>2</sup>, Yasuyuki Shiraishi<sup>1</sup>, Arash Erfani<sup>3</sup>  
and Dirk Saelens<sup>3, 4</sup>

*1 The University of Kitakyushu  
1-1 Hibikino, Wakamatsu-ku, Kitakyusyu-shi,  
Fukuoka, Japan 808-0135  
e-mail address: f4mbb008@eng.kitakyu-u.ac.jp*

*2 TAKENAKA CORPORATION  
4-1-13 Honmachi, Chuo-ku, Osaka-shi,  
Osaka, Japan 541-0053*

*3 KU Leuven  
Kasteelpark Arenberg 40,  
3001 Leuven, Belgium*

*4 EnergyVille  
Thor Park 8310,  
3600 Genk, Belgium*

## ABSTRACT

Thermally activated building systems (TABS) are gaining attention as a means of realizing comfort and energy efficiency in office spaces. TABS use the building mass for heat dissipation and the storage part of the building to save energy, improve comfort, and shift peak energy consumption. However, the thermal response is slow due to the large thermal capacity. Therefore, in this study, we propose a method for optimizing the operation of TABS by applying Adaptive Model Predictive Control (AMPC) combined with sequential updating of the predictive model through online estimation. Furthermore, we verify the feasibility of Demand-Response (DR) implementation using the proposed method. From the results, AMPC was shown to reduce the control error compared to MPC and to reduce computational load compared to Nonlinear MPC (NLMPC). We also confirmed that DR control using AMPC can suppress TABS operation during the hours of 8:00 - 10:00 and 16:00 - 18:00 when electricity demand is high, while maintaining PMV within  $\pm 0.3$  and ensuring energy efficiency.

## KEYWORDS

TABS, MPC, IDEAS, DR, thermal storage, online estimation

## 1 INTRODUCTION

In recent years, thermally activated building systems (TABS), which use the structure of a building to dissipate or store heat, have been attracting attention as a means for achieving a thermal environment that realizes both comfort and energy savings in office spaces. TABS are expected to offer a variety of advantages, including high comfort, energy savings, and shifting peak energy consumption, by utilizing the high thermal capacity of the building. However, high thermal capacity means slow thermal response, making it desirable to introduce dynamic control methods. In a previous study<sup>1), 2)</sup>, we proposed a method for optimizing model predictive control (MPC) by combining load forecasting with machine learning. The method however leaves room for further study, such as shifting peak electricity demand through heat storage and improving control performance using nonlinear MPC (NLMPC)<sup>3), 4)</sup>. Because the thermal response of TABS is nonlinear, when the nonlinear predictive model is used for NLMPC, high controllability can be expected for complex behaviour of the controlled object as well as a reference is needed here. However, the nonlinear model has various limitations, including the need for a large amount of training data, the time required to model the target system, and the difficulty of obtaining a solution within the sampling time for large and computationally demanding systems.

Therefore, we propose adaptive MPC (AMPC)<sup>5), 6)</sup> as a control method for TABS, specifically by combining sequential updating of the predictive model with online estimation. Using this

method, the possibility of individual TABS control and DR control with TABS is verified through a co-simulation with Dymola and MATLAB/Simulink (Figure 1). In addition, comparative verification between AMPC, regular MPC and NLMPC will also be performed.

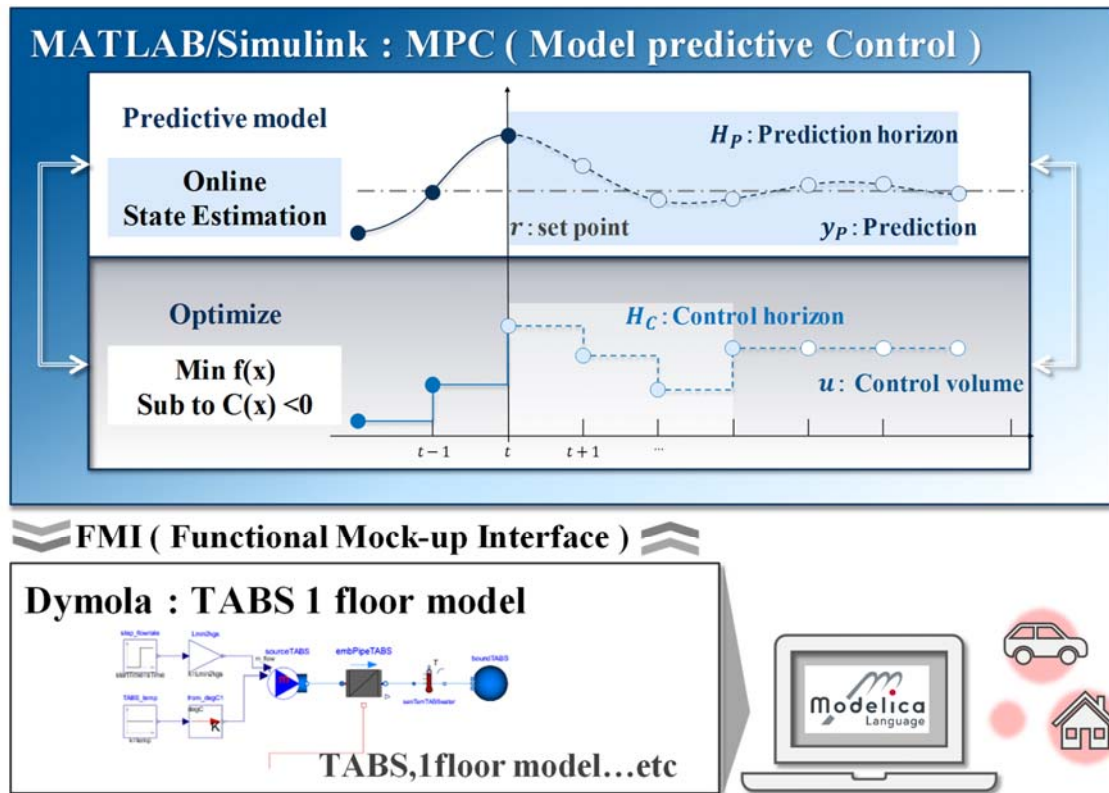


Figure 1: Outline of this study

## 2 ANALYSIS OVERVIEW

### 2.1 Overview of control methods

In this study, MPC-based control is performed on TABS. MPC is a control method that sequentially determines the optimal level of operation at the current time while predicting future response. However, since it is necessary to predict the future behaviour of the controlled variable at each sample time, the prediction model that expresses the dynamic causal relationship between the manipulated variable and the controlled variable is required. On the other hand, the thermal behaviour of TABS (changes in ceiling surface temperature and room temperature) is a nonlinear phenomenon. So, when using MPC to operate TABS, NLMPC with the nonlinear prediction model could be implemented. However, when modelling large nonlinear systems, the complexity of the optimization problem is a concern due to the consideration of model parameters and the huge amount of training data required. In contrast, AMPC sequentially updates the parameters of the linear prediction model online by using the input/output data at each time. AMPC has some advantages: the modelling is possible even in the absence of prior data, the computational load is low, and the system can cope with unexpected disturbances. Therefore, in this study, MPC, NLMPC, and AMPC are verified as control methods for TABS, with the transfer function (TF)<sup>7)</sup> model, the nonlinear autoregressive exogenous (NLARX)<sup>8)</sup>, and the recursive ARX (RARX)<sup>9)</sup> model used as the respective prediction models. The TF model represents the relationship between the input data and output data of the controlled by object. In this study, The TF model is identified from the step response with the TABS operation amount (water-supply flow rate). The TABS operation

amount is used as the input data and the ceiling surface temperature is used as the output data. It is then converted into a state-space representation and used as a dynamical model for MPC. The NLARX model is also extension of the linear ARX model to the nonlinear case. The linear ARX model is a model that incrementally linearly predicts the variable to be forecast from its own historical time series data of other external input variables. The RARX model is the linear ARX model that is sequentially updated from the input/output data of the control target. In this study, the sequential least squares method is applied as the estimation method. A Kalman Filter (KF) is employed as the online model parameter estimation algorithm in this study.

## 2.2 Analysis model

Figure 2 shows the model of the analyzed floor. The analysis target is a one-floor model<sup>2)</sup> of TABS created in Dymola<sup>10)</sup>, a modelica-based<sup>11)</sup> composite physical-modelling tool. In this study, the target heating, ventilation, and air conditioning system and the building model were constructed using IDEAS<sup>12)</sup>.

## 2.3 Analysis conditions

Tables 1 and 2 show the Dymola and MPC analysis conditions. The analysis period was assumed to be August and the duration was 1 week each for the initialization period and the primary analysis. In the Dymola model, the schedules of occupancy are given according to the loading schedule shown in Figure 3. Specifically, the loads of Light and OA (office automation) shown in Figure 3 were predicted by the random forest model, while state estimation was performed using the KF. The target value of the ceiling surface temperature was analysed by Dymola in advance and set to  $24.5^{\circ}\text{C} \pm 0.3^{\circ}\text{C}$ , which is considered to be within the comfort zone. The required ventilation air volume ( $480\text{m}^3/\text{h}$ ) is treated by a desiccant outside air handling unit and then supplied by a floor outlet ventilation system.

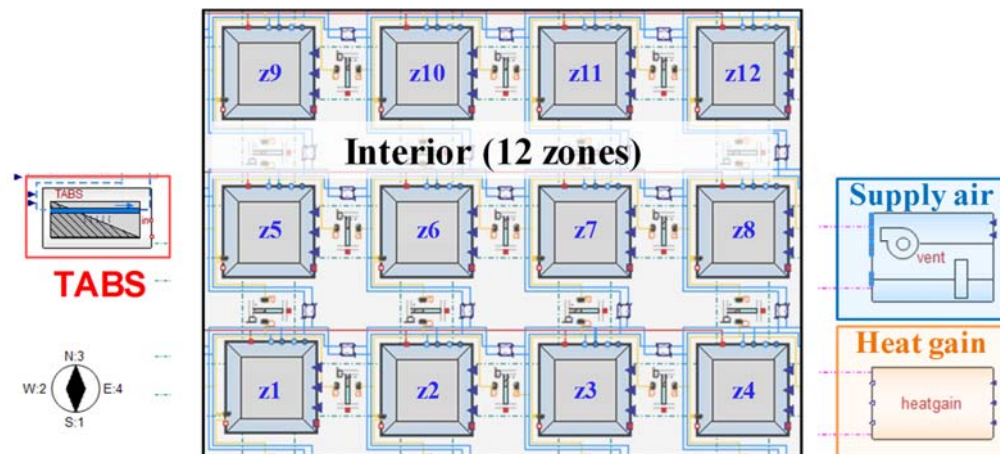


Figure 2: Analysis model (1 floor)

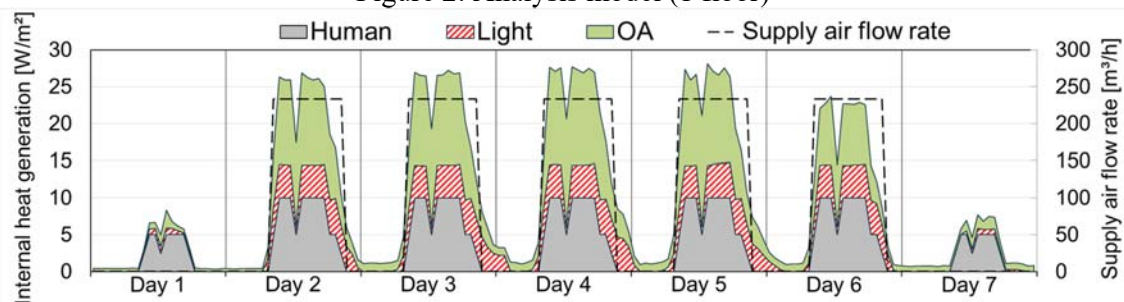


Figure 3: The loading schedule

Tables 1: Analysis conditions of Dymola

Weather data		Tokyo, Japan <sup>13)</sup>
TABS	Water supply, Temperature	5L/min, 16°C
Ventilation	Flow rate, Supply temperature	30m <sup>3</sup> /h·person, 23°C
Heat generation	Human	10W/m <sup>2</sup>
	OA	15W/m <sup>2</sup>
	Lighting	5W/m <sup>2</sup>
Boundary condition under the ceiling and floor		23°C

Tables 2: Analysis conditions of MPC

Predictive Model		TF, NLARX, RARX
Algorithm		Effective Constraint Solver (KWIK)
Sample time		1step = 3,600s
Prediction horizon		24step
Heat generation		Predicted by RF, KF
Constraints	$u$ [L/min]	$0 \leq u \leq 5$
	$\Delta u$ [L/min]	$-5 \leq \Delta u \leq 5$
	$y$ [°C]	$24.2 \leq y \leq 24.8$ (Weekday Work Hours)

## 2.4 Cases

Table 3 shows the details of the analyzed cases: in Case 1, comparative verification of control performance is performed using MPC, NLMPC, and AMPC; in Case 2, optimal control is performed by AMPC and DR-AMPC, with constraints on the ceiling surface temperature during weekday occupancy in consideration of the actual operation. In all cases, on/off control was used during the initialization period.

Tables 3: Analysis case

Case	comparison items	control method	cost function	constraint
Case1-1	Control performance	MPC	Minimize temperature error	-
Case1-2		NLMPC		
Case1-3		AMPC		
Case2-1	Energy saving performance	AMPC	Minimize water supply flow rate	Office hour: 24.5°C ± 0.3°C
Case2-2		DR-AMPC		Office hour: 24.5°C ± 0.3°C Water supply restrictions during times of increased demand (8:00 - 10:00, 16:00 - 18:00)

## 3 ANALYSIS RESULTS

### 3.1 Case1: Control performance verification

Figure 4 shows the root mean square error of the ceiling surface temperatures and the target for each zone in Case 1. In Case 1-1, the error variation is large, while in Case 1-2, the control error is smaller. Case 1-3 resulted in a slight increase in control error compared with Case 1-2 but had a higher accuracy compared with Case1-1. The computation time for NLMPC and AMPC was about 49.3 and 33.1 times longer than MPC, respectively. AMPC reduced the computation



time by 32.8% compared with NLMPC. Therefore, this study examined DR control considering the actual operation with AMPC applied to reduce the computational load.

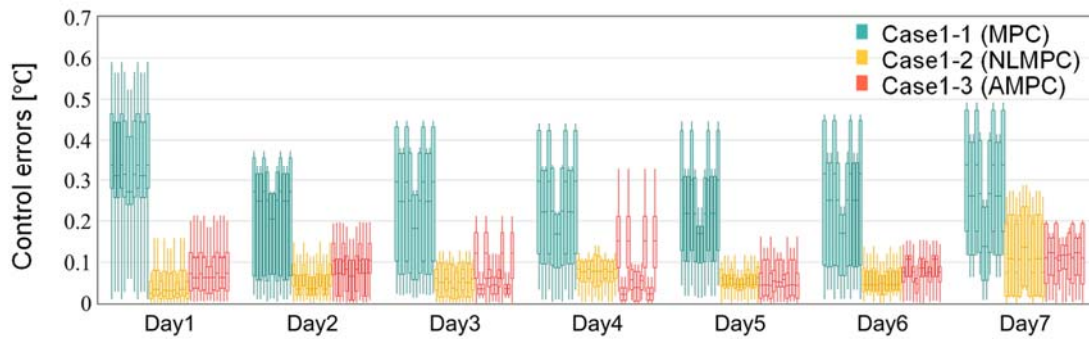


Figure 4: RMSE of the ceiling surface temperatures and the target in Case 1

### 3.2 Case2: Verification of DR methods

Figures 5 and 6 show the time variations of the ceiling surface temperature and water flow rate, respectively, for Case 2. In all cases, the control satisfied the constraint conditions. Figure 6 also shows that in Case 2-2, the water supply was restricted during high-demand hours (8:00–10 and 16:00–18:00) in consideration of DR, which resulted in a reduction in water supply during certain hours. The right side of Figure 6 shows the percentage of the total weekly water supply flow for Case2-1 and Case2-2 when Case 1-1 was set as 100%. It shows that the water supply flow rate is approximately 95%, which means that the water supply flow rates were generally the same before and after implementing DR control. Figure 7 shows the time variation of PMV in Case 2. The PMV values of all cases were generally 0.00–0.25, indicating that comfort was maintained. From the above results, it was confirmed that employing AMPC for one floor of a typical office with TABS installed enables TABS operation considering DR while maintaining energy savings and comfort.

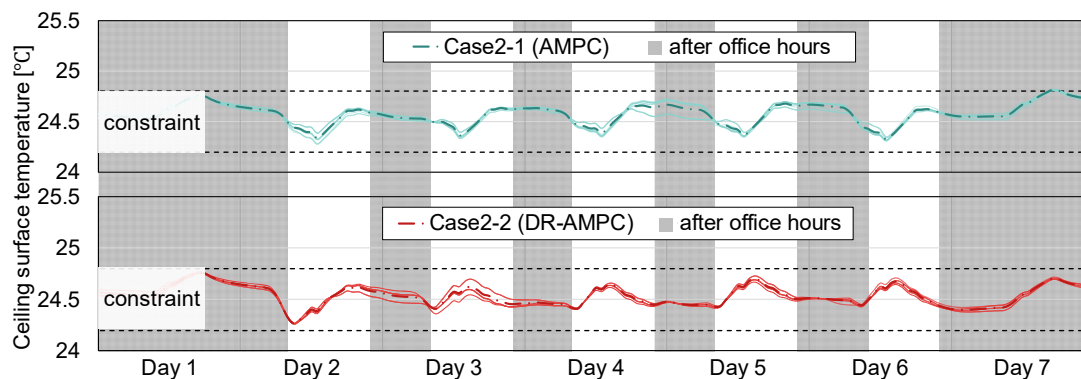


Figure 5: Change over time of the ceiling surface temperature in Case 2

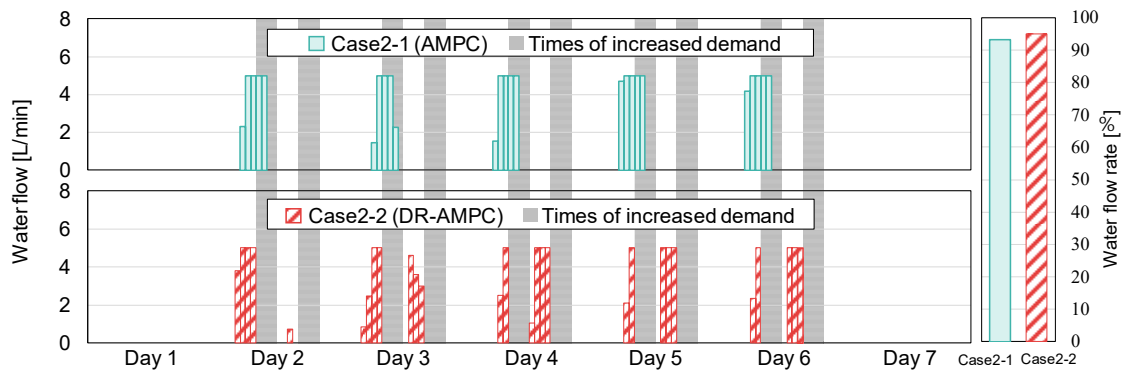


Figure 6: Change over time of the water flow rate in Case 2

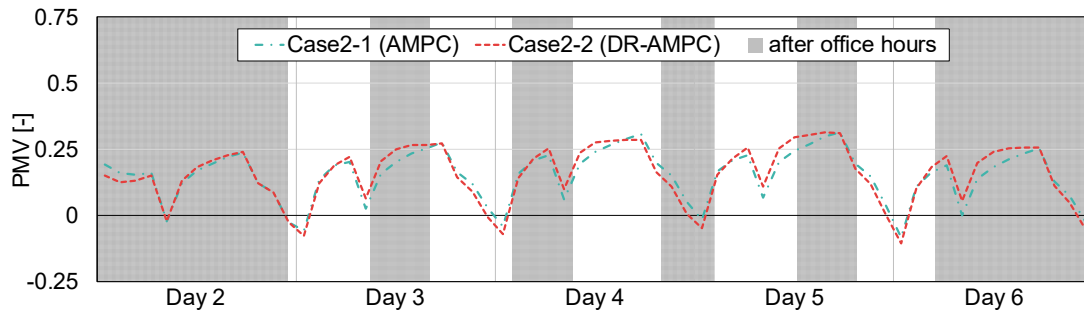


Figure 7: Change over time of PMV in Case 2

#### 4 CONCLUSIONS

In this study, comparative verification of MPC, NLMPC, and AMPC for TABS was performed to assess control and energy savings, computational load, and DR control. As a result, we confirmed that DR control using AMPC enables DR-aware TABS operation while maintaining energy savings and comfort. AMPC also reduced the computational load by 32.8% compared with NLMPC while reducing the control error by about 66.7% compared with MPC. Verification of simulation results by comparison with actual measurement results is a future challenge.

#### 5 REFERENCES

- 1) Koga, K. et al.: Optimal control of TABS using a combined method of MPC and heat load prediction. *Jpn Archit Rev*, 2023
- 2) Koga, K.: Optimal control of TABS in hot and humid regions. 42nd AIVC - 10th TightVent - 8th venticool Conference - Rotterdam, Netherlands - 5-6 October 2022
- 3) MathWorks Home Page. "Nonlinear MPC - MATLAB & Simulink", <https://jp.mathworks.com/help/mpc/ug/nonlinear-mpc.html>
- 4) Chao, Pan. et al.: Nonlinear model predictive control of chiller plant demand response with Koopman bilinear model and Krylov-subspace model reduction, *Control Engineering Practice*, Vol.147, 105936, 2024 (DOI: <https://www.sciencedirect.com/science/article/pii/S0967066124000960> )
- 5) MathWorks Home Page. "Adaptive MPC - MATLAB & Simulink", <https://jp.mathworks.com/help/mpc/ug/adaptive-mpc.html>
- 6) Zihao, Zhao. et al.: Adaptive model predictive control of a heat pump-assisted solar water heating system, *Energy and Buildings*, Vol.300, 113682, 2023 (DOI: <https://www.sciencedirect.com/science/article/pii/S037877882300912X> )
- 7) MathWorks Home Page. "Transfer Function Models - MATLAB & Simulink", <https://jp.mathworks.com/help/ident/transfer-function-models.html>
- 8) MathWorks Home Page. "What are Nonlinear ARX Models? - MATLAB & Simulink", <https://jp.mathworks.com/help/ident/ug/what-are-nonlinear-arx-models.html>
- 9) MathWorks Home Page. "recursiveARX - MATLAB & Simulink",

- <https://jp.mathworks.com/help/ident/ref/recursiveax-system-object.html>
- 10) Dassault Systèmes: Dymola, <https://www.3ds.com/ja/products-services/catia/products/dymola/>
  - 11) Modelica Association: Modelica Language, <https://modelica.org/modelicalanguage.html>
  - 12) IDEAS: Modelica library, <https://github.com/open-ideas/IDEAS>
  - 13) EnergyPlus: Weather Data, <https://energyplus.net/weather>

## **ACKNOWLEDGMENT**

This work was supported by JSPS KAKENHI Grant Numbers 20KK0102 and 23K22923.

# Proposal of a design method for radiant ceiling cooling system using CFD analysis

Rio Matsumoto<sup>1</sup>, Jianan Liu<sup>1</sup>, Yasuyuki Shiraishi<sup>1</sup>, Fujio Tamura<sup>2</sup>,  
Daiki Yamashina<sup>2</sup>, Masahiro Yamamoto<sup>2</sup> and Sae Senda<sup>2</sup>

*1 The University of Kitakyushu  
1-1 Hibikino, Wakamatsu, Kitakyushu, Fukuoka  
808-0135, Japan*

*Email : f4mbb023@eng.kitakyu-u.ac.jp*

*2 AXS Satow Inc.,  
AXS Building, 2-10-12 Yokoami, Sumida, Tokyo.  
130-0015, Japan*

## ABSTRACT

In recent years, the adoption of water-based radiant ceiling cooling systems has been increasing in Japan with the aim of realizing comfort and energy savings. Conventionally, when designing radiant cooling systems, the target operative temperature for the indoor thermal environment is set, but these are usually combined with convection air conditioning system, which do not always achieve the target value during summer cooling. In addition, several parameters must be assumed at the design stage, originally not only operative temperature, but also temperatures of uncooled surface and radiant panel surface, etc. Therefore, it may not be possible to achieve the expected indoor thermal environment under the design conditions, which may affect the estimation of the cooling capacity of radiant panels and the calculation of the number of panels required.

This study proposes a new design method that incorporates CFD analysis based on the conventional design method suggested by ASHRAE. By incorporating CFD analysis, several parameters can be determined at the same time under the assumed environment. In addition, determination of the optimal cooling capacity of radiant panels can be used to realize the target operative temperature by feedback control utilizing the results of CFD analysis. Therefore, in this study, the proposed method was used to redesign a real office with a radiant ceiling cooling system, and the effectiveness of the proposed method was evaluated. The results showed that the cooling capacity of radiant panels can be updated and that the number of panels required can be reduced without compromising indoor thermal comfort.

## KEYWORDS

Radiant Ceiling Cooling System, Design Method, CFD Analysis, Operative Temperature

## 1 INTRODUCTION

In recent years, radiant cooling systems [1][2] have been increasingly adopted for offices and other applications because of their high comfort and energy-saving performance. Usually, panel cooling capacity diagrams are used in the design of radiant cooling systems, and it is necessary to set the target operative temperature (OT) for the indoor thermal environment. However, because radiant cooling systems are combined with convection air conditioning systems with the aim of preventing condensation on panel surfaces, especially during summer cooling, it is not always possible to achieve the target OT. Air temperature is also subject to the influence of the surrounding environment, so the processing heat load due to ventilation and convection air conditioning systems also includes a certain error, i.e., difference from expected value.

To solve the above problems, this study sought to establish an elaborate method for designing a radiant ceiling cooling system utilizing Computational Fluid Dynamics (CFD) analysis. This paper proposes a design method and investigates its effectiveness, using actual summer measurement data of an office building with a radiant ceiling cooling system.

## 2 A DESIGN METHOD USING CFD ANALYSIS

We propose a design method that incorporates feedback control using CFD analysis based on the conventional design method proposed by American Society of Heating, Refrigerating and Air-Conditioning Engineers (ASHRAE) [3], which assumes the influence of the cooling capacity of radiant panels on the indoor thermal environment and its use with convection air conditioning system.

Figure 1 shows the proposed design flow of the radiant ceiling cooling system. The two new steps added to the conventional design method are marked in red boxes. In conventional design method, OT is calculated and evaluated in a later process, but this design method assumes steady state conditions and determines the assumed operating temperature ( $OT^*$ ), assuming air temperature = OT. In this study, OT is calculated as the average of air temperature and mean radiation temperature (MRT). Next, based on the indoor heat load and required ventilation volume, the processing heat load (total heat) by convection air conditioning and radiant cooling systems (sensible heat) are calculated. Determine the cooling capacity of radiant panels based on the temporary processing heat load by radiant cooling and determine the required panel area. Conventional design methods then determine minimum permissible effective cooling panel surface temperature and the area-weighted average uncooled surface temperature (AUST). The calculation of AUST is based on the simplified assumption that temperature of uncooled surface is air temperature. AUST is used to calculate MRT and even OT to assess the indoor thermal environment and determine panel area. Whereas this design method incorporates CFD analysis to predict the indoor thermal environment distribution that reproduces the real phenomena in detail. Specifically, it is possible to calculate and determine several parameters at once, which originally had to be assumed at the design stage, such as the cooling capacity of radiant panels and temperature of radiant panels surface, reflecting the effect of temperature of uncooled surface and convection air conditioning system. Therefore, the method is expected to improve the design errors that occur in conventional design methods. The results of the comparison of each parameter with conventional methods are presented in Chapter 4.

Furthermore, after determining the outline of convection air conditioning and radiant cooling systems, the layout of radiant panels is determined and CFD analysis is performed in the verification assuming steady-state conditions. From the results of the CFD analysis, the analytical value ( $OT_{ci}$ ) is compared with the assumed operative temperature ( $OT^*$ ), and the cooling capacity of radiant panels is revised and updated until the assumed value and the analytical value are almost in agreement. Finally, based on the determined the cooling capacity of radiant panels, the water supply temperature is determined using a panel cooling capacity diagram, and the design flow is completed.

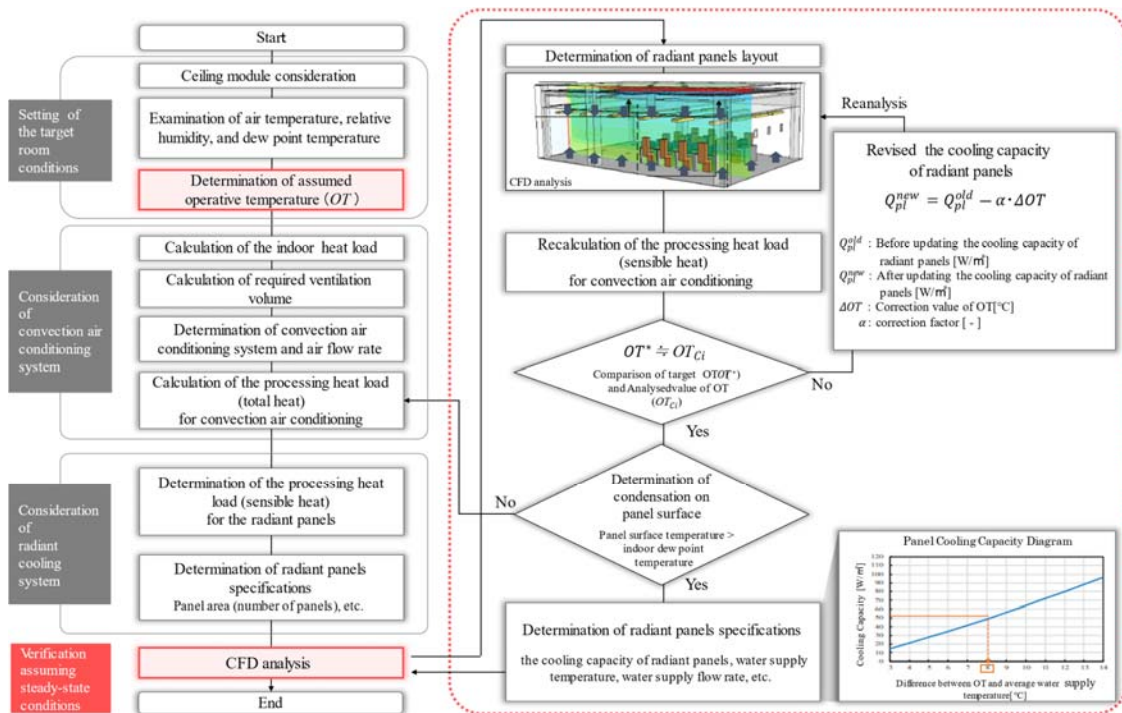


Figure 1: The proposed design flow of the radiant ceiling cooling system

### 3 OVERVIEW OF THE SUBJECT FACILITY AND CFD ANALYSIS MODEL

#### 3.1 Subject facility

The building is a city hall completed in June 2022 (Fig. 2). This study focuses on an area of the third floor used as office space, where a radiant ceiling cooling system is installed (Fig. 3).



Figure 2: Building exterior

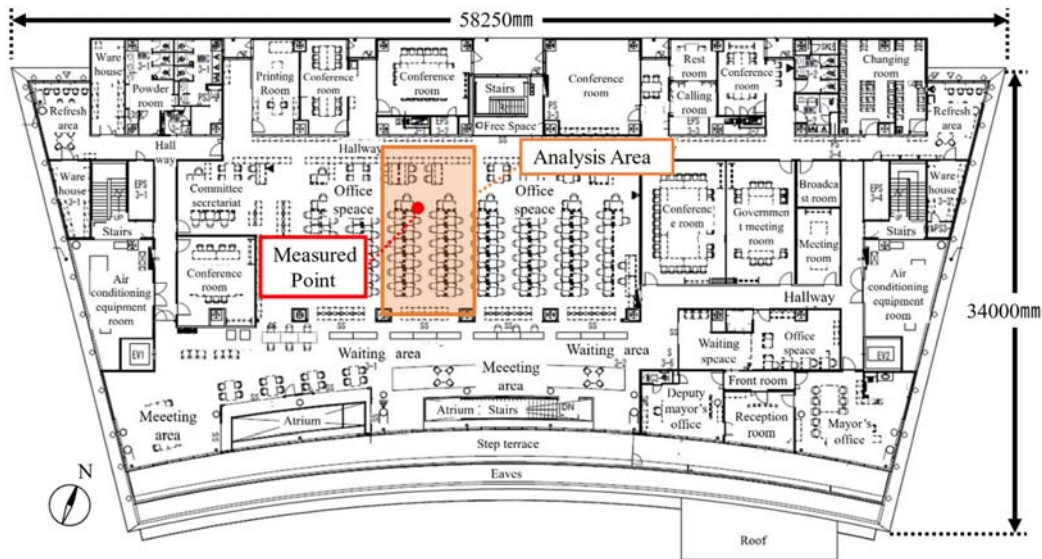


Figure 3: Floor plan

### 3.2 CFD analysis model and analysis conditions

The analysis model of the target area is shown in Fig. 4, the analysis model of the radiant panels in Fig. 5 and the analysis conditions in Table 1. Sixty-eight ceiling radiation panels (total area: 48.96 m<sup>2</sup>, ceiling coverage ratio: 53%) were installed in the area analysed. During office hours, outside air is supplied at a constant temperature and flow rate from three air outlets (supply outdoor air : SOA). Return air (RA) is also taken in at a constant flow rate at the return air outlet. The difference between SOA and RA is exhaust (as exhaust air: EA) in the toilet via the common space north of the office.

The modelling of radiant panels was simplified to reduce the computational load of the analysis. The chilled water pipes were changed to 1 mm panels with the physical properties of water, and the processing heat load of the chilled water was given as the analysis condition for that panel. The thickness of the aluminium panel was set to 10 mm. However, the thermal capacity of the panel was set to be the same as that of a 1 mm thick panel, and the thermal conductivity in the thickness direction was set so that the thermal resistance value of the panel in the thickness direction was set to be the same as that of 1 mm thick aluminium.

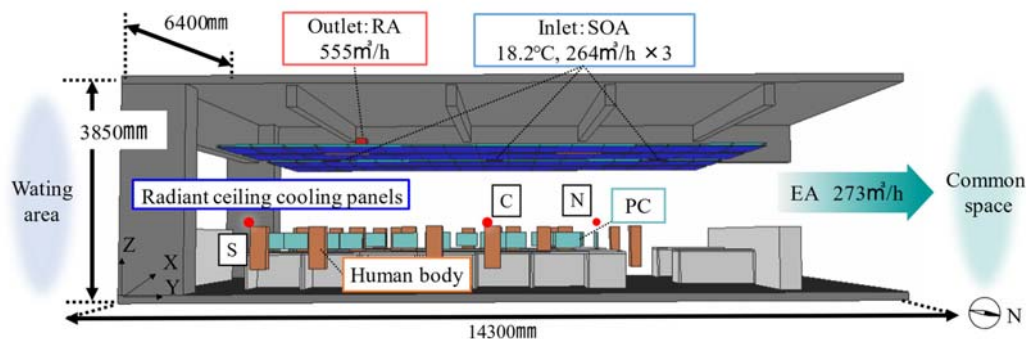


Figure 4: Analysis model

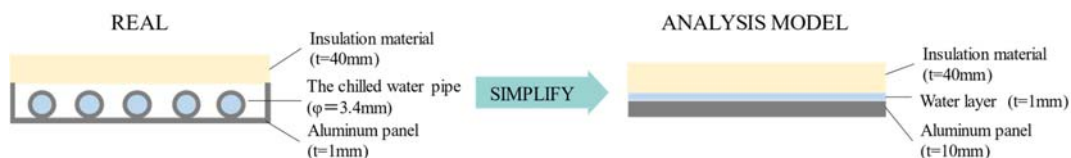


Figure 5: Radiant ceiling cooling panels model

Table 1: Analysis conditions for CFD analysis

<b>Domain</b>	6.4m(X)×14.3m(Y)×4.15m(Z)	
<b>Mesh</b>	125(X)×279(Y)×81(Z)= 2,824,875	
<b>Inlet boundary conditions</b>	[Present System]	Temperature: 18.2□, Velocity: 264*3 m <sup>3</sup> /h $k_{in1}=(U_{in1}/10)^2, \epsilon_{in1}=C_{\mu}^{3/4} \cdot k_{in1}^{3/2}/l_{in1}$
	[Case 1]	Temperature: 18.2□, Velocity: 264*3 m <sup>3</sup> /h $k_{in2}=(U_{in2}/10)^2, \epsilon_{in2}=C_{\mu}^{3/4} \cdot k_{in2}^{3/2}/l_{in2}$
	[Case 2]	Temperature: 20.0□, Velocity: 200*3 m <sup>3</sup> /h $k_{in3}=(U_{in3}/10)^2, \epsilon_{in3}=C_{\mu}^{3/4} \cdot k_{in3}^{3/2}/l_{in3}$
<b>Outlet boundary conditions</b>	RA	Velocity: 555m <sup>3</sup> /h
	North Side	[Present System] 237m <sup>3</sup> /h
		[Case 1] 237m <sup>3</sup> /h
	[Case 2] 55m <sup>3</sup> /h	
<b>Turbulence model</b>	Linear Low Reynolds turbulence model	
<b>Advection scheme</b>	QUICK	
<b>Wall boundary conditions</b>	Velocity	Analytical wall function
	Temperature	Logarithmic law
<b>Indoor heat load</b>	Human (20 person): 69W/person, Lighting (2 lights): 398W/unit, PC (20 units): 75W/unit	

$U_{in1}, U_{in2}, U_{in3}$ : Outlet air wind speed [m/s],  $k_{in1}, k_{in2}, k_{in3}$ : Outlet air turbulence energy [m<sup>2</sup>/s<sup>2</sup>],  $\epsilon_{in1}, \epsilon_{in2}, \epsilon_{in3}$ : Dissipation rate of  $k_{in}$  [m<sup>2</sup>/s<sup>3</sup>],  $C_{\mu1}, C_{\mu2}, C_{\mu3}$ : Model constant (=0.09) [-],  $l_{in1}, l_{in2}, l_{in3}$ : Length scale [m]

## 4 OVERVIEW OF THE SUBJECT FACILITY AND CFD ANALYSIS MODEL

### 4.1 Verification of the prediction accuracy of the analysis model

Figure 6 shows predictive validation results of the analysis model in vertical air temperature distribution. This analysis evaluated the prediction accuracy of the analysis model by comparing the vertical air temperature distribution, using the data of the subject office, which was measured in the summer. The assumed number of occupants was set to 20 based on the actual measurement data. From the results of the prediction accuracy verification, root mean square error (RMSE) of the vertical air temperature distribution was 0.30°C, which indicated sufficient prediction accuracy.

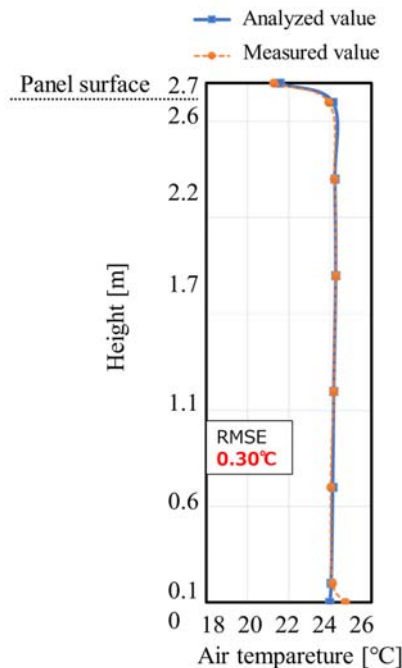




Figure 6: Predictive validation results of the analysis model in vertical air temperature distribution

#### 4.2 Thermal environment evaluation by CFD analysis

The indoor thermal environment was assessed by the occupant area mean OT in the office and the predicted mean vote (PMV). The metabolic rate and the clothing insulation when calculating PMV were 1.2 met and 0.6 clo, respectively, which are common values in summer. The relative humidity was assumed to be 50% because no humidity measurements were performed in this study. PMV was also calculated from the average of three points (S, C, and N) of the room's central sensor (Fig. 4; height, 1.1 m).

The average OT of the workspace was 24.5°C, resulting in a generally uniform the indoor thermal environment. PMV was 0.15, which was confirmed to be within the comfortable range. However, in the present operation, the assumed cooling capacity of radiant panels was only 54% of the rated cooling capacity. Therefore, it was suggested that the number of radiant panels could be reduced, and the processing heat load ratio by radiant cooling could be increased.

#### 4.3 Redesign of radiant cooling system using the proposed method

In this section, case studies on the redesign of radiant cooling system are carried out (Table 2). In Case 1, the present blowout conditions were maintained, and the minimum number of panels (44 panels) were installed. The calculated panel reductions were dummy panels and were evenly distributed within the laying area. In Case 2, the blowout conditions were relaxed to increase the processing heat load ratio by radiant cooling. First, considering comfort, the assumed OT was set at 24.4°C (PMV corresponds to approximately  $\pm 0$ ). Next, the assumed cooling capacity of radiant panels determined was input into the CFD analysis as an initial value, and the convergence calculation was started. However, the convergence calculation was terminated because PMV was 0.05, reaching the target value (Table 3).

The heat balance before and after the redesign is shown in Figure 7. Case 1 shows that 24 radiant panels can be reduced while maintaining the indoor thermal environment. In addition, the processing heat load ratio by radiant panels increased by 26% when comparing the current situation with Case 2. Furthermore, a comparison of the initial and final convergence values of Case 1 shows the processing heat load by radiant panels from 1,958 to 1,657W through convergence calculations performed in the CFD analysis. These results suggest that the proposed method may have high design accuracy regarding comfort and energy saving.

Comparing the analysis results of the conventional design method and the proposed method in Case 1, the air temperature was updated from 24.4°C to 24.3°C, OT from 23.1°C to 24.4°C, temperature of radiant panels surface from 17.3°C to 19.8°C and AUST from 24.2°C to 24.9°C. Furthermore, it was confirmed that air temperature  $\neq$  AUST.

Table 2: Analysis case with redesign

	Blowoff temperature [°C]	Blowoff flow rate [m <sup>3</sup> /h]	Number of panels	The assumed cooling capacity of radiant panels [W/m <sup>2</sup> ]
Case1	18.2	792	44	52.32
Case2	20.0	600	68	53.32

Table 3: Convergence results of CFD analysis

	The cooling capacity of radiant panels [W/m <sup>2</sup> ]	Air temperature [°C]	MRT [°C]	OT [°C]	PMV [-]
Initial Assumed Value	61.84	24.40	24.40	24.40	0
Final Convergence value	52.32	24.31	24.42	24.37	+0.05

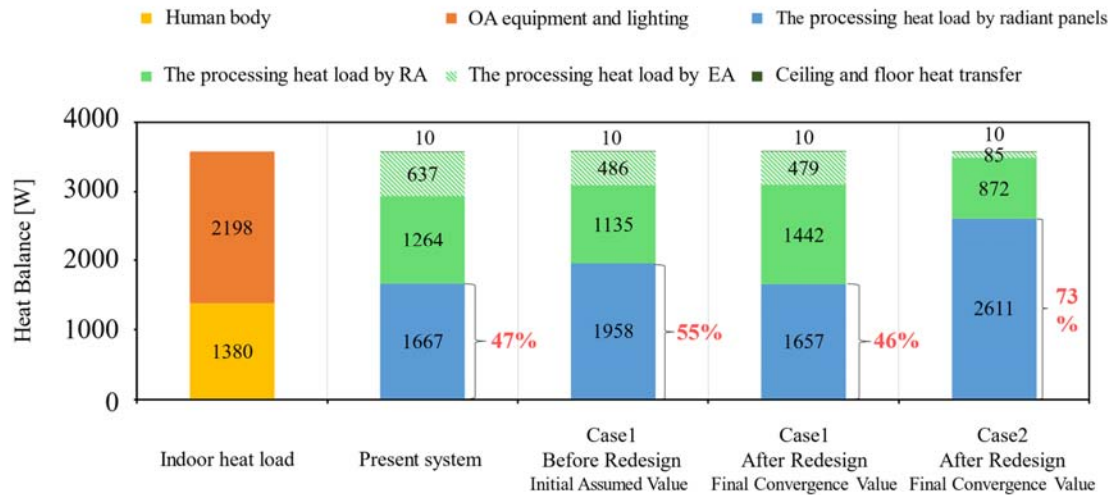


Figure 7: Heat balance before and after convergence calculation

## 5 CONCLUSIONS

A design method for radiant ceiling cooling system that incorporate CFD analysis into the conventional ASHRAE design method was proposed. Using the proposed design method to redesign an actual building, it was possible to reduce the number of radiant panels without compromising indoor comfort, in addition to improving the processing heat load ratio by radiant cooling. In the future, the effectiveness of the proposed method will be verified by increasing the number of cases in which it is adapted to real properties.

## 6 REFERENCES

- [1] ISO 11855(all parts).(2024).“Building environment design” - Design, dimensioning, installation and control of embedded radiant heating and cooling systems
- [2] ISO 18566 (all parts).(2019) “Building environment design” - Design, test methods and control of hydronic radiant heating and cooling panel systems
- [3] ASHRAE.(2012) “2012 ASHRAE Handbook HVAC System and Equipment” SI edition-Ch.6 Panel Heating and Cooling, American Society of Heating Refrigerating and Air-Conditioning Engineers

# Ventilation performance in cultural centres in Flanders

Niels De Kempeneer<sup>1</sup>, Mart Verlaek<sup>1</sup>, Sophie De Mulder<sup>\*1</sup>, Gitte Schreurs<sup>1</sup>,  
Maja Mampaey<sup>1</sup>, Karen Van Campenhout<sup>1</sup>

*1 Department of Environment & Spatial Development  
Flanders*

*Koning Albert II-laan 20  
1000 Brussels, Belgium*

*\*Corresponding author:  
sophie.demulder@vlaanderen.be*

## ABSTRACT

Ventilation impacts the quality of the indoor environment. Indoor air quality (IAQ) contributes to the overall personal exposure of occupants of a building to certain pollutants and is therefore an important environmental determinant of health. Research shows that European citizens spend on average 90% of their time indoors. The Flemish government, and more specifically the Flemish Department of Environment & Spatial Development, has been conducting research on IAQ in homes and schools to inform and develop policy since 2007. In 2019, the Environment and Health research team at the Flemish Department of Environment & Spatial Development, together with VITO (Flemish Institute for Technological Research) developed a sensor box with innovative and high-quality sensor technology — indoor@box, which allows continuous, real-time measurement of several pollutants and parameters. This makes it possible to communicate results real time, to collect a lot of data over longer periods and to make links with other data (e.g. weather, questionnaires, occupancy rates).

With these indoor@boxes, the Flemish Department of Environment & Spatial Development has been conducting various measurement campaigns in (semi-)public buildings where many people gather or stay, such as schools, sports centres, residential care centres and cultural centres, since 2020. The analysis mainly focuses on CO<sub>2</sub> measurements and ventilation performance. The reports aim at providing concrete advice that considers the specific situation of the building, so that the ventilation improves. In addition, the research gives advice to the policy, which uses existing health guidelines that were important during the COVID-19 pandemic (e.g. in terms of CO<sub>2</sub> values in (semi)public buildings). The research allows to check whether those guidelines are feasible and effective for the different sectors. Ventilation performance can be assessed thanks to a thorough technical screening of the ventilation systems in place.

This paper elaborates on the campaign in ten different cultural centres in Flanders and Brussels, which varied in size, building type, ventilation system and audience capacity (2022). Overall, the cultural centres' ventilation systems are unable to meet the CO<sub>2</sub> guidelines at higher occupancies. The thorough technical screening uncovered that having a ventilation system with sufficient flow rate pulse, in relation to the maximum capacity of the event space does not always guarantee desirable CO<sub>2</sub> values. Additional parameters have an influence, e.g. settings of the ventilation system, activity degree and flow rate per person (m<sup>3</sup>/hr/person), composition of the audience, maintenance and management of the system...The combination of CO<sub>2</sub> measurements and technical screenings complement each other well, showing where improvements are needed, and how the ventilation performance can be improved. In the future, the findings from this research could be summarised and incorporated into technical guidelines.

## KEYWORDS

public buildings, CO<sub>2</sub> measurements, ventilation performance, policy guidelines, indoor air quality

## 1 INTRODUCTION

Indoor air quality (IAQ) contributes to the overall personal exposure of occupants of a building to certain pollutants and is therefore an important environmental determinant of health (Superior Health Council, 2017). Research shows that Europeans spend on average 90% of their time indoors (Fernandes et al., 2009). This makes healthy indoor air quality highly important. The performance of (mechanical) ventilation impacts the quality of the indoor environment. By performance, we mean (1) the ventilation effectiveness that indicates how efficiently the airborne pollutant is being removed from the room and (2) how efficiently the fresh air is being distributed in the room through air exchange efficiency (Atkinson et al., 2009). In this research we assessed the performance of the ventilation systems by in depth technical screenings of the systems: we gathered information on the settings, and air flow measurements and made other calculations.

Indoor air quality encompasses many parameters and pollutants, but this specific focuses on CO<sub>2</sub> levels as a proxy for ventilation effectiveness in ten different cultural centres in Flanders and Brussels. We used our sensor device, the indoor@box, to measure the CO<sub>2</sub> values. These results were linked to other parameters such as actual and maximum occupation of the space, settings of the ventilation system, and air flow measurements and calculations. Combining these different aspects allows us to draw conclusions about the performance of the ventilation systems. Next to discussing the global results, this paper aims to understand how CO<sub>2</sub> measurements during events can be related to the ventilation system, the settings, the nominal capacity and the actual occupancy of the room.

### 1.1 Previous research

Since 2007, the Department of Environment & Spatial Development of Flanders has been conducting research regarding indoor air quality in homes and schools to give concrete advice to the participants and to inform policy. With the emergence of new technology such as sensors and the ability to transmit more data, the Department of Environment & Spatial Development designed several sensor boxes in 2019 in collaboration with VITO (Flemish Institute for Technological Research) (Lazarov et al., 2019). These sensor boxes, named the indoor@boxes, allow real-time measurements of several indoor air pollutants and components to be transmitted, such as particulate matter (PM), carbon dioxide (CO<sub>2</sub>), carbon monoxide (CO), nitrogen dioxide (NO<sub>2</sub>), volatile organic compounds (VOC), temperature and relative humidity. Moreover, the indoor@boxes allow for data to be collected over longer periods of time. They are calibrated annually.

As described in previous work the COVID-19 pandemic between 2020 and 2022 generated a big focus in Belgium and in Flanders on CO<sub>2</sub> values and how efficiently ventilation is carried out (De Mulder et al., 2023). The general guideline values during the COVID-19 pandemic were derived from health guidelines: if the CO<sub>2</sub> concentration is below 900 ppm (or not more than 500 ppm higher than the outdoor concentration), we consider the room well ventilated (Taskforce Ventilatie van het coronacommissariaat, 2021). In practice, 900 ppm for an adult engaged in standard light activity corresponds with a ventilation flow rate of 40 m<sup>3</sup>/h/person of fresh outdoor air. For values between 900 and 1200 ppm, measures need to be taken to fall back below 900 ppm. Exceedances above 1200 ppm are in principle not allowed and immediate action or evacuation is required to improve the CO<sub>2</sub> concentration. CO<sub>2</sub> values are considered a good proxy to monitor the quality of the indoor air, the ventilation and aeration, and an important preventive measure to limit potential contamination via airborne

transmission of viruses. The guidelines of 900 ppm and 1200 ppm CO<sub>2</sub> values have been used in our research to get a picture of ventilation performance.

The Department of Environment & Spatial Development has been conducting various measurement campaigns in (semi-)public buildings where many people gather or stay, such as schools, sports centres, residential care centres and cultural centres. The research has resulted in several overarching insights. For instance, ventilation behaviour plays an important role when it comes to indoor air quality. Additionally, the technical aspects of the ventilation are important. While installing the sensor boxes, we noticed that people on site — regardless of the type of sector — often have little knowledge about the presence of a ventilation system, the way it works, or when its last maintenance took place. Based on our findings, we conclude that investing in demand-controlled (mechanical) ventilation — a system that measures and monitors CO<sub>2</sub> values — contributes to improved air quality and consistently lowers CO<sub>2</sub> concentrations in the indoor environment, and therefore helps to reduce airborne viral transmission. But other technical factors of the ventilation also remain important, such as maintenance and proper dimensioning and management of the ventilation system, with an adequate relation to occupancy and activity.

In this paper, we focus on the measurements that were conducted in cultural centres, and more specifically on the relation between the CO<sub>2</sub> measurements during events, the (settings of) ventilation system, and the actual occupancy of the room. This measurement campaign goes further than previous research since a technical screening of the mechanical ventilation system was carried out between two measurement periods. Each cultural centre received a detailed ventilation report with recommendations. The intention was that cultural centres would make certain adjustments based on the screening, and that in the second measurement the effect would be reflected in the CO<sub>2</sub> values. But in practice, we saw that culture centres were unable to adjust their systems in the interim period. Therefore, data from the two measurement periods are analysed together as one dataset. Additionally, data were gathered concerning activities, occupancy and calculated corresponding ventilation flow rate in m<sup>3</sup>/h/person and placed into relation with the measured CO<sub>2</sub> concentrations in the indoor air.

## **2 MATERIALS AND METHOD**

### **2.1 Research in ten cultural centres in Flanders and Brussels**

In this paper, we define "cultural centres" as all types of public event buildings where cultural events take place such as theatre, concerts and performing arts. In Flanders and Brussels, most cities or towns have at least one cultural centre. Each of these buildings differ in terms of location, size, venue capacity, age of construction, and type of activities. Almost all cultural centres are polyvalent in terms of activities: music performances (classical, pop, DJ,...), theatre, comedy, exhibitions, cinema, standing or sitting activities, and so on. Often, a cultural centre consists of several halls or event spaces which, again, differ from each other. Globally, there are spaces for performances, for supporting activities (e.g. bar, cloak room, entrance hall,...) and spaces that combine both performance and supporting activities (e.g. bar/foyer, entrance hall/ticket office...). This paper organises in Table 1 the different spaces within the ten cultural centres based on mutual differences and similarities. Table 1 shows (1) the

location of the cultural centres<sup>1</sup>, (2) the type of space where the measurements took place<sup>2</sup> (3) the type of ventilation system in place in the different spaces, where “no ventilation” means that based on a visual check no natural ventilation system could be detected, (4) the number of activities that took place in the first and second measurement period, (5) the maximum audience capacity of the event space (people sitting (sit.) or standing (st.)), (6) the control of the ventilation system, (7) the efficiency of the air exchange in the different spaces, based on technical measurements and expert technical opinion. This information was synthesized in a descriptive way with two categories “optimal” and “not optimal” and (8) the measured flow rate pulse (m<sup>3</sup>/h).

The categorisation of the different spaces where measurements took place are the following: 17 performances spaces, 5 supporting spaces and 4 spaces that combined performance and supporting activities. 17 spaces have a mechanically balanced ventilation system, a mechanical ventilation system or a system with mechanical extraction (predominantly with timer control). For 5 spaces it was unknown whether ventilation systems were present. Additionally, there are 4 spaces where there was no mechanical ventilation system present, and one performance space with no ventilation system.

The indoor@boxes were used for two measurement periods, each time for approximately two weeks: once during May and June, and once during October, November and December 2022. In total, we measured the CO<sub>2</sub> levels during approximately 290 events. In-between these two measurement periods, the spaces with mechanical ventilation were screened for the ventilation systems’ characteristics and air flow rate, e.g. control of the ventilation system according to EN 13779:2004, measured flow rate pulse in m<sup>3</sup>/h fresh air according to NBN EN 12792, NBN EN 13779 and EN12599 for ventilation duct measurement and an assessment of the efficiency of air exchange based on the location of pulsion and extraction points. It is important to note that this research’s sample of buildings and performance spaces is too small to make generalisations for all cultural event centres in Flanders and Brussels. Nevertheless, the data suffice to formulate several descriptive statements.

Table 1: Main characteristics of the cultural centres, the spaces and the ventilation types.

(1) Location cult. centre	(2) Type of space in cultural centre	(3) Ventilation system of space	(4) No. activities (period 1 + 2)	(5) Max. capacity people	(6) Control of vent. System	(7) Efficiency of air exchange	(8) Measured flow rate pulse (m <sup>3</sup> /h)
1. Capital	1. Perform.	Mech. bal.	11 + 11	1000 / 2000	Timer control	Not optimal	62336
	2. Perform.	Mech. bal.	4 + 5	100 / 300	Timer contr.	Not optimal	13316
	3. Combi.	Mech. bal.	11 + 11	NA	Timer contr.	Not optimal	6375
2. Town	1. Perform.	Mech. bal.	2 + 8	428 sit.	Manual	Optimal	1752
	2. Support.	NA	2 + 8	NA	NA	NA	NA
3. Town	1. Perform.	Mech. bal.	2 + 10	329 sit.	Timer contr.	Optimal	4640
	2. Support.	NA	3 + 10	NA	NA	NA	NA
4. Town	1. Perform.	Mech. bal.	7 + 9	402 sit.	Timer contr.	Not optimal	14971
	2. Support.	NA	7 + 9	NA	NA	NA	NA
5. City	1. Perform.	Mech. bal.	3 + 14	290 / 670	Timer contr.	Not optimal	13876
	2. Combi.	Mech. bal.	3 + 4	150 st.	Timer contr.	NA	1124
6. City	1. Perform.	Mech. bal.	4 + 8	288 sit.	Timer contr.	NA	11041

<sup>1</sup> Cities are defined as urban areas with more than 50000 inhabitants and towns as urban areas with more than 5000 inhabitants in 2019

<sup>2</sup> Additional information about the volume of the space has been considered, but is not required, as the Flemish policy is based on CO<sub>2</sub> values per person.

	2. Perform.	Mech. bal.	4 + 16	940 sit.	Timer contr.	NA	25756
	3. Combi.	Mech. extr.	5 + 12	NA	Timer contr.	NA	NA
	4. Perform.	Mech. bal.	3 + 9	803 sit.	Timer & direct	NA	24514
7. Town	1. Support.	Mech. bal.	1	NA	Timer contr.	NA	2251
	2. Perform.	No mech. ventilation	2 + 3	144 sit.	NA* <sup>3</sup>	NA*	NA
	3. Combi.	No mech. ventilation	1	NA	NA*	NA*	NA
8. Town	1. Perform.	Mech. bal.	2 + 5	480 st.	Manual	Optimal	8791
	2. Perform.	No vent.	2 + 5	391 sit.	NA*	NA*	NA
9. City	1. Perform.	Mech. bal.	3 + 9	127 sit.	Direct cont.	Optimal	5091
	2. Support.	No mech. ventilation	4 + 4	NA	NA*	NA*	NA
	3. Perform.	No mech. ventilation	6 + 3	130 sit.	NA*	NA*	NA
10. City	1. Perform.	Mech. bal.	5 + 4	650 sit.	Direct cont.	Optimal	29794
	2. Perform.	Mech. vent.	2 + 2	400 st.	NA	NA	10950
	3. Perform.	NA	4 <sup>4</sup>	200 sit.	NA	NA	NA

## 2.2 Measurements indoor@box: ventilation efficiency using CO<sub>2</sub> levels

For the research in cultural centres, the indoor@box was used. Although the box can monitor different pollutants, only the CO<sub>2</sub> measurement results were used. The assumption is that the higher the CO<sub>2</sub> concentration, the higher the concentration of bioaerosols (microdroplets produced by breathing) that can contain microorganisms such as bacteria and viruses, that can spread via airborne transmission in addition to contact transmission and droplet transmission. Additionally, CO<sub>2</sub> concentration is a good indicator of the efficiency of ventilation and aeration in function of its occupancy (Geyskens & Stranger, 2016).

One or more indoor@boxes were placed in the different spaces of the ten cultural centres. The indoor@box transmits an interval measurement of the CO<sub>2</sub> concentration every three minutes to the data platform where they are available for analysis. The platform also allows real-time monitoring of the measurements to intervene, if necessary, when the CO<sub>2</sub> concentration becomes too high. Measurements by the boxes provide data points that can be checked against the guidelines of 900 and 1.200 ppm. If, during an event, CO<sub>2</sub> concentration exceeds 900 ppm (or 500 ppm above outside air concentration), ventilation capacity as delivered at that time is insufficient given the current occupancy and action is required. Concentrations above 1.200 ppm are not acceptable from a health perspective. This study reports in what percentage of data points, during events, CO<sub>2</sub> exceeds 900 ppm (Table 2), as well as how many events per space have exceedances of 900 ppm (Table 2).

For the ten cultural centres, additional data has been obtained on the nature of the events, the occupancy (tickets sold), and the start and end time of the event. Unfortunately, not all cultural centres were able to provide this information. However, it is important for the analysis to delineate the duration of the event: at times without spectators, CO<sub>2</sub> levels are low, while during events they evidently rise. For this, an algorithm was used in which all sudden sharp increases in CO<sub>2</sub> concentrations are counted as events, if such increases happen after people enter the venue. The end of the show is defined to be after a significant decrease in

<sup>3</sup> “NA\*” stands for “Not Applicable”, as it does not concern a mechanical ventilation, whereas “NA” stands for “Not Available”. In this case it was not possible to measure the flow rate pulse because the ducts were not accessible or did not exist over enough straight sections.

<sup>4</sup> For that room we only have measurements for the second period, because only then were performances scheduled.

peak values. Each defined start of an event is combined with the consequential end, defined by said decrease in CO<sub>2</sub> values, with a minimum time-limit of 30 minutes, and a maximum of 8 hours. This means that the events reported for the cultural centres in column “No. of activities” of Table 1 do not always fully concur with the events from the algorithm<sup>5</sup>.

### 2.3 Screening of the ventilation infrastructure

In the halls with a mechanical ventilation system, the performance of the system was analysed via air flow measurements (grille and or duct measurements). The mixing section, if installed, was switched off during the measurements, except in performance spaces 6.2 and 6.4, where the mixing section was at 30%. The air groups and how they are operated were analysed. Pulsion, extraction points and energy recovery were mapped for each space partly to assess the efficiency of air exchange, this included regulation by valves. The type of air filtration and the condition of the filters were also assessed. Pulsion and extraction flow rate were also examined to control balance (Table 1). For this study, only the spaces with a mechanical system were screened, as this system defines how the ventilation of the space happens. We only include here the following aspects of the screening for further analysis: the operation of the system, the efficiency of air exchange, and the flow rate.

### 2.4 Screening of the ventilation effectiveness using flow rate and occupancy

Information was requested from cultural centres on the maximum occupancy of the spaces. The occupancy per activity was also queried in each cultural centre for each space. This information helps to determine whether the ventilation system can provide sufficient flow rate for the nominal capacity (N) and real occupancy of the hall. The measured flow rate of the mechanical ventilation system ( $Q_{mech}$  determined in m<sup>3</sup>/hr fresh air) was used to calculate, based on both actual and maximum possible occupancy, the flow rate per person (m<sup>3</sup>/hr/person). To achieve 900 ppm (N<sub>900</sub>), a flow rate of 40 m<sup>3</sup>/hr/person (V<sub>900</sub>) is needed for 1.200 ppm (N<sub>1200</sub>) it becomes 25 m<sup>3</sup>/hr/person (V<sub>1200</sub>), these values are for a MET (activity degree) equal to 1,63 (Taskforce Ventilatie van het coronacommissariaat, 2021):

$$N_{900} = \frac{Q_{mech}}{V_{900}} \quad \text{or} \quad N_{1200} = \frac{Q_{mech}}{V_{1200}} \quad (1)$$

If these values are not met, then the maximum occupancy possible with the measured ventilation flow rate is determined. In addition, the flow rate necessary to achieve 900 or 1200 ppm with the actual occupancy is determined. The efficiency of air exchange is considered in this analysis.

## 3 RESULTS

In ten cultural centres, it has been investigated whether (1) each room’s ventilation system was technically able to meet the guidelines of 900 and 1200 ppm at full room capacity (calculated with an airflow of 40 m<sup>3</sup>/h/pp for 900 ppm, and 25 m<sup>3</sup>/h/pp for 1200 ppm), and whether (2) the CO<sub>2</sub> values that were measured with the indoor@boxes during events corresponded with the technical specifications of the ventilation systems.

---

<sup>5</sup> A fault margin can occur when, for instance, people enter a room without performances (e.g. for a rehearsal) and cause for the CO<sub>2</sub> to rise significantly. The algorithm will note this as an event. On the other hand, if the ventilation systems work properly during the performance, or if there is a small audience at the event, no significant CO<sub>2</sub> rise occurs. This will not be registered as an event by the algorithm. This fault margin is acceptable as in principle all situations above 900 ppm should be avoided.



Table 2: Main results of the CO<sub>2</sub> measurements, occupancy and ventilation flow rate per space in relation to general health guidelines.

(1) No. space and location	(2) Percentage of time of CO <sub>2</sub> >900ppm during events (Min. /Max.), based on indoor@box	(3) Max. audience capacity	(4) Nominal capacity (N900 / N1.200), based on measured flow rate pulse	(5) Sufficient ventilation flow at max. aud. capacity (900 ppm / 1.200 ppm)	(6) Min. amount of people when measured CO <sub>2</sub> >900 ppm (events with known occupancy)	(7) Percentage of events with CO <sub>2</sub> >900 ppm, based on indoor @box	(8) P1/P99 of CO <sub>2</sub> , based on indoor @box
1.1	0 / 74	2000	1558/2493	No / Yes	1312	79	552 / 2940
1.2	0 / 68	300	333 / 533	Yes / Yes	35	31	541 / 1672
1.3	0 / 81	NA	159 / 255	NA	653	96	547 / 2571
2.1	0 / 77	428	394 / 630	No / Yes	151	50	622 / 1182
2.2	0 / 94	NA	NA	NA	NA	54	879 / 1104
3.1	0 / 49	329	116 / 186	No / No	100	60	480 / 1607
3.2	9 / 63	NA	NA	NA	NA	75	524 / 2158
4.1	0 / 100	402	374 / 599	No / Yes	165	73	2463 / 5008
4.2	0 / 98	NA	NA	NA	108	22	723 / 1743
5.1	0 / 73	670	347 / 555	No / No	NA	63	600 / 2008
5.2	4 / 100	150	28 / 45	No / No	NA	100	1361/2832
6.1	0 / 83	288	276 / 442	No / Yes	150	67	781 / 1568
6.2	0 / 53	940	644 / 1030	No / Yes	850	19	560 / 1175
6.3	0 / 34	NA	NA	NA	60	92	519 / 1967
6.4	0 / 0	803	613 / 981	No / Yes	NA	0	566 / 798
7.1	0 / 65	NA	56 / 90	NA	NA	14	634 / 2048
7.2	0 / 54	144	NA	NA	NA	60	502 / 2541
7.3	0 / 76	NA	NA	NA	NA	63	501 / 1355
8.1	3 / 21	480	220 / 352	No / No	85	100	547 / 1098
8.2	20 / 93	391	NA	NA	80	100	848 / 1663
9.1	NA	127	127 / 204	Yes / Yes	NA	NA	NA
9.2	0 / 78	NA	NA	NA	NA	71	710 / 2337
9.3	0 / 84	130	NA	NA	NA	78	751 / 3025
10.1	0 / 75	650	745 / 1192	Yes / Yes	70	80	469 / 1725
10.2	0 / 76	400	274 / 438	No / Yes	200	75	546 / 2451
10.3	0 / 81	200	NA	NA	NA	80	568 / 2399

Table 2 summarizes the main results from the research. The table shows (1) the spaces that have been investigated (for more details see Table 1), (2) the minimum and maximum percentage of time that a measured event exceeded 900 ppm based on indoor@box measurements, (3) the maximum audience capacity, based on the space's design/available space, (4) the maximum (nominal) audience capacity of the space (for 900 and for 1200 ppm), based on the measured flow rate pulse, (5) whether there is sufficient ventilation capacity to ensure CO<sub>2</sub> values below 900 or 1200 ppm when the room is at full capacity, (6) the minimum amount of visitors that were present when an exceedance of 900 ppm was measured during an event (based on events with known capacity), (7) the percentage of events when the indoor@boxes measured CO<sub>2</sub> levels that exceeded 900 ppm and (8) the maximum P1 and P99 of all the events where the indoor@boxes measured CO<sub>2</sub> values<sup>6</sup>. Based on Table 1, Table 2 and the other gathered and analysed data, we summarise the findings in 3 points, using specific spaces as illustrations.

<sup>6</sup> We choose P1 and P99 because maximum values matter in this study, but we still want to exclude certain anomalies in the data (e.g. someone coughing on the sensor).

### 3.1 Global CO<sub>2</sub> results compared to the general health guidelines

When looking at all the measured events in all cultural centres, some insights can be gathered. With the exception of one performance space (6.4)<sup>7</sup>, all performance spaces had CO<sub>2</sub> exceedances of the 900 ppm threshold during at least one event. The threshold of 900 ppm in the CO<sub>2</sub> levels has been exceeded during 68% of the measured events. The highest value that has been measured during an event is 5046 ppm. The measurements show that, on average, the CO<sub>2</sub> values in an event space exceed 900 ppm between 1 and 70% of the duration of the event, with several events that have exceedances during more than 90% of the time. Most measured events significantly exceeded general health (and COVID-19 pandemic guidelines).

### 3.2 Ventilation at full audience capacity

For 14 of the measured spaces, enough data were available to calculate whether the flow rate pulse of the ventilation system that is present would (theoretically) suffice when the space is at full audience capacity. To ensure CO<sub>2</sub> values below 900 ppm at full audience capacity, only 3 spaces (performance spaces 1.2, 9.1, and 10.1) turned out to have sufficient ventilation capacity. This means that in almost 80% of the cases, the ventilation system is under-dimensioned or incapable to keep CO<sub>2</sub> values below 900 ppm at full audience capacity. In these cases, the maximum audience capacity of the performance spaces is between 4% and 65% higher than the ventilation system would allow, with a peak of 81% (performance space 5.2). To ensure CO<sub>2</sub> values that remain below 1200 ppm, the ventilation systems of 10 performance spaces suffice. In the remaining 4 spaces, where the dimensioning of the ventilation system cannot guarantee values below 1200 ppm, a serious under dimensioning or a measured flow rate that is too low can often be seen, where an additional 17% to 70% of air flow will be needed before meeting the 1200 ppm threshold. Some spaces also have an over dimensioned ventilation system, with numbers that range from 4% (performance space 6.1), to 11% (performance space 1.2) and 13% (performance space 10.1) additional capacity of air flow. One room (performance space 9.1) has a ventilation system that is perfectly dimensioned for its maximum audience capacity.

### 3.3 Ventilation systems linked to audience capacity and CO<sub>2</sub> results

One of the initial hypotheses of this research was that the results of the CO<sub>2</sub> measurements during events would be directly related to the ventilation system, the settings and the actual occupancy of the room. In practice, CO<sub>2</sub> values turned out to be the result of a more complex interplay of numerous factors, some of which were not always clear. This complexity can be illustrated by some examples. Our sample size of event spaces with well-dimensioned ventilation systems is quite small (4 spaces): the analysis does not allow for generalisations. However, it is notable that none of these rooms were able to keep CO<sub>2</sub> values below 900 ppm during events. Technical aspects such as efficiency of air exchange play a role, as does the type of activity and the engagement of the public. Performance space 1.2, for instance, theoretically has a proper dimensioning of its ventilation system to keep CO<sub>2</sub> values below 900 ppm at full capacity. With a maximum capacity of 300 people for the room, and a nominal capacity of 333 people to remain under 900 ppm based on the ventilation system, there is an over dimensioning of 11%. For the CO<sub>2</sub> values to remain under 1200 ppm, the over dimensioning is even 78%. However, during the two measuring periods in this performance space, 31% of the events exceeded the threshold of 900 ppm between 5 and 68% of their

---

<sup>7</sup> This can be explained because the maximum capacity was not reached: there was only an audience of 400 people present, while there is space for 803 people.

duration. Exceedances of 900 ppm were already measured with an audience of only 35 people. These results may be explained by the fact that the settings of the ventilation system are not optimal. In terms of efficiency of air exchange, the ventilation system is not optimal (see Table 1).

Another example of theoretically good dimensioning of the ventilation system is performance space 10.1. With a maximum audience capacity of 650 and a nominal capacity of 745 to stay below 900 ppm CO<sub>2</sub> values, there is an oversizing of 13%. During the measurement periods, with about 635 tickets sold, the performance space was almost at maximum capacity, but well below nominal capacity. However, the CO<sub>2</sub> measurements indicate that in 80% of the events there is an exceedance of 900 ppm, varying between 0 and 75% of the event duration. In almost 50% of the events, there are also exceedances of 1200 ppm. Exceedances of 900 ppm happen even at an actual capacity of 70 people. According to the technical data, the ventilation system is optimal in terms of efficiency of air exchange (see Table 1). This is not in line with expectations, which may require further investigation, including regarding the activity degree and the need of fresh air per person.

Out of the 16 performance and combination spaces (with a known mechanical ventilation system), 11 are calculated not to have sufficient flow rate at maximum occupancy for 900 ppm. They are expected to give high CO<sub>2</sub> values for longer periods of times at high room occupancy. Overall, this seems to be the case, 3 performance and combination spaces (5.2, 8.1, 8.2) have exceedances of the 900-ppm limit at 100% of their events, and 6 spaces (1.3, 4.1, 5.2, 8.2, 9.3, 10.3) have at least one event with more than 80% of the event duration exceeding 900 ppm. Three spaces, which perform better than the others are worth discussing briefly. The first performance space, 6.2, has a mechanically balanced ventilation system, a maximum seating capacity of 940 and a nominal capacity of 644. Unfortunately, there are no technical data about the efficiency of air exchange for this space. During the measurement periods, several events were fully booked. However, it is only at a capacity of 850 people that exceedances of the 900-ppm value were noted. So, although the ventilation system does not perform at maximum capacity of 940 people, it seems that the ventilation system is self-adjusting according to the audience occupancy. Technical screening of the ventilation system and CO<sub>2</sub> measurements seem to complement each other, to get a good grasp of the ventilation performance. The second performance space is 6.4, which is already discussed briefly. It is equipped with a mechanically balanced ventilation system and is the only performance space without exceedances of the 900-ppm level. This is probably due to the lack of audience: this space has a capacity of 803 people, and a nominal capacity of 613, but during the measurement periods, only a maximal of 400 tickets per event were sold. However, it shows that a reduced capacity of audience can, in certain cases, be beneficial for the CO<sub>2</sub> levels. This finding contrasts with previous paragraph where some spaces still had exceedances of the CO<sub>2</sub> levels, even when maximum capacity is not reached. At last, the third performance space (8.1) has a mechanically balanced ventilation system and shows exceedances of 900 ppm CO<sub>2</sub> level at all events, but only for a short amount of time (only 3-21% of the events duration), which is, compared to the other spaces, remarkably shorter. This suggests that the ventilation system only kicks in after some time. It is worth noting though, that this space was not at maximal capacity with only 85 people playing brass instruments, while the maximum capacity is 480 and the nominal capacity 220.

#### 4 CONCLUSIONS

In general, the research has shown that most cultural centres struggle to meet the general health guidelines to maintain CO<sub>2</sub> concentrations below 900 ppm. Even when the maximum audience

capacity of the space is not met, the guideline of 900 ppm is often exceeded. This means that there is clearly room for improvement when it comes to ventilation performance. Each cultural house received an individual report with recommendations from the study, which they can take further.

Measuring CO<sub>2</sub> values remains a good and easy indicator to determine whether an event space is adequately ventilated. Especially if you consider that in cultural centres the intensity of the activity, the composition of the audience (children/adults, sitting/standing) can vary greatly. This research simultaneously showed that having a ventilation system with sufficient flow rate pulse, in relation to the maximum capacity of the room does not always guarantee desirable CO<sub>2</sub> values. Additional parameters that can have an influence — and therefore should not be neglected — are, for instance, the settings of the ventilation system, the intensity of the activity in the room, the composition of the audience, the maintenance of the system, and so on. One aspect to investigate further is determining the activity degree and the need of fresh air per person.

To determine whether a ventilation system is performing properly, the screening of the ventilation infrastructure offers great added value. Several parameters determine the proper performance: installation and setting (e.g. flow rate pulse), correct use and maintenance. A screening identifies these parameters and concrete improvements can be made where necessary (e.g. maintenance of ventilation grids). In the next step, the findings from this research could summarised and incorporated into technical guidelines. The results will be shared with all policy levels as a basis for policy development too.

## 5 ACKNOWLEDGEMENTS

We wish to thank Joris Pieters, data scientist at Keyrus, warmly for his help with data analysis, the engineering office AirX, for the technical screenings, and the ten participating cultural centres.

## 6 REFERENCES

- Atkinson, J., Chartier, Y., Pessoa-Silva, C., & et al (eds), (2009). *Natural Ventilation for Infection Control in Health-Care Settings*. World Health Organization.
- De Mulder, S., Goethals, M., Verlaek, M., Gommé, L., De Kempeneer, N., Van Hoof, T., Mampaey, M., Van Haver, P., Teughels, C., Van Haute, G., & Van Campenhout, K. (2023). Living and Working in a Healthy Environment: How Sensor Research in Flanders can Help Measure and Monitor Exposure to Certain Environmental Factors. *KEEP ON PLANNING FOR THE REAL WORLD Climate Change Calls for Nature-Based Solutions and Smart Technologies*, 10.
- Fernandes, E. D. O., Jantunen, M., Carrer, P., Seppanen, O., Harrison, P. T. C., & Kephelopoulos, S. (2009). *ENVIE - Co-ordination Action on Indoor Air Quality and Health Effects—Final Activity Report*. <https://doi.org/10.13140/RG.2.2.28314.85447>
- Geyskens, F., & Stranger, M. (2016). *Milieu en Gezondheid en Binnenhuis—Vraag om advies m.b.t. CO2 als indicator voor een gezond binnenmilieu, studie uitgevoerd in opdracht van Het Departement LNE, Dienst Milieu en Gezondheid* (p. 36).
- Lazarov, B., Elen, B., Spruyt, M., & Stranger, M. (2019). *Long-term monitoring of environmental pollutants in the indoor climate of various housing types* (p. 83).
- Taskforce Ventilatie van het coronacommissariaat. (2021). *Aanbevelingen voor de praktische implementatie en bewaking van ventilatie en binnenluchtkwaliteit*

# Evaluating the Long-term Performance of Air Barrier Systems in Modern Buildings

Sean O'Brien<sup>\*1</sup>, David Artigas<sup>1</sup>

*1 Simpson Gumpertz & Heger Inc.  
525 Seventh Avenue, 22nd Floor  
New York, NY 10018 USA*

*\*Corresponding author: smobrien@sgh.com*

## ABSTRACT

The durability of air barrier systems is a topic that is rarely discussed during the design phase of most projects. An unfortunate amount of effort is spent on drawing details and specifying products with the sole intention of meeting energy code requirements, with much less thought being given to how those systems actually will be constructed and possibly worse – how those systems will fare over time.

Air barrier systems are very complex and involve a wide variety of components. Windows, doors, walls, foundations, and roofs all need to work together, since even small breaches in the building air barrier can significantly reduce performance. But with so many different systems, all of which are composed of different types of materials, the risk of both physical and chemical incompatibilities between air barrier materials or poor weatherability is high. Unfortunately, many of these problems only will manifest after construction of the building is complete. The point of failure is likely to go unnoticed, as membranes lose adhesion, sealants fail, or expanding foam shrinks away from its substrate within walls that are concealed by interior finishes and exterior cladding or at small joints or concealed in assemblies.

This paper reviews previous research related to the long-term durability of air barrier systems, focusing on wall membranes and fenestration systems. It also discusses energy modelling of a typical large building at varied air leakage rates to show the associated potential impacts to building energy use. These results show that, as an industry, current energy code requirements are both reasonable and achievable with modern materials and industry knowledge. Instead of energy losses, deterioration of the building materials due to a poorly performing air barrier may be of greater concern.

## KEYWORDS

Air barriers, Air leakage, Energy performance, Fenestration

## 1 INTRODUCTION

An “air barrier” as defined by the energy conservation building codes in the United States of America (energy codes) is a continuous membrane or combination of different interconnected membranes that have been tested according to different industry standards (depending on the type of material or system) as having very low air permeability or leakage when subjected to differential pressure across the membrane (we use the term “membrane” loosely in this sentence to mean a continuous planar component within the exterior walls or roofs). The current energy codes require a continuous air barrier around the building’s thermal enclosure to limit energy loss from air leakage through the walls and roofs, the reason being that indoor conditioned air leaking out or unconditioned outdoor air leaking in both increase the amount of energy that the mechanical systems must use to maintain interior setpoints. While the need for an air barrier may seem logical as a way to improve buildings’ energy efficiency and knowledge of the importance of an air barrier within the enclosure dates back several decades,

at least as far as the 1930s (Beals, 2016), most US energy codes did not require a continuous air barrier as part of the building enclosure until 2010 (ASHRAE, 2010) and 2012 (ICC, 2011), although the Canadian building code first required an air barrier in 1985 (NRCC, 1985). Around this time, the United States Department of Energy published data showing that it estimated that air infiltration in buildings accounted for approximately 7% of total building energy use (DOE, 2014) but did not differentiate by building type or use.

While required by the energy codes (presumably for energy conservation reasons), a continuous air barrier also is an important component to help manage water vapor flow through the building enclosure. In fact, much of the older historical literature that discusses the importance of a continuous air barrier does so in the context of mitigating condensation, frost, efflorescence, biological growth, etc., with brief mention of it also being important for energy efficiency (Quirouette, 1985; Peterson & Hendricks, 1988 are examples). However, some historical authors do discuss building air leakage in the context of energy loss, noting that it can contribute as much as 40% of the total heat loss in single-family detached houses (Tamura, 1975) and that air leakage through the building enclosure must be considered when designing mechanical systems (Handegord, 1979). Using energy modelling, Sherman and Matson estimate that relying on “loose” air infiltration to provide ventilation to single-family homes, rather than mechanical ventilation or “controlled” infiltration according to ASHRAE standards, resulted in \$2.4 billion in energy costs annually for the United States as a whole in 1997, but did not estimate the effect on individual buildings (Sherman & Matson, 1997). We did not find much other data (either from field measurements or energy models) that estimates or quantifies the energy loss associated with air leakage through building enclosures in our review of the literature, despite most studies stating that air leakage increases energy consumption as a given.

In our review of the literature, most historical studies focused on small/single-family construction, with less attention paid to the air leakage performance of commercial or larger multi-family construction. More recent research has evaluated the airtightness of mid-rise and high-rise construction and found that it typically meets or exceeds energy code requirements (Sherman & Chan, 2004). Sherman and Chan state that research by others found that 42% of air leakage through high-rise building enclosures is through windows, 26% is through doors, and 6% through opaque walls and roofs, with the remainder through vertical shafts, but again, no estimate of air leakage’s effect on energy consumption (Sherman & Chan, 2004).

A study of whole-building air leakage testing of 276 new buildings of different construction types, heights, and uses built between 2009 and 2019 in the United States found that, on average, the buildings were below the maximum allowable air leakage in the energy codes (2.0 L/sm<sup>2</sup> at 75 Pa pressure differential). However, the study also found that, on average, buildings of a “mixed-use” type (commercial plus residential) showed air leakage approximately 40% greater than allowed by code and some individual buildings showed air leakage from 50% to more than double that allowed by code (Marceau & Shrode, 2019). This study did not analyse the energy loss due to air leakage, but it does show that even new buildings built under energy codes that require a continuous air barrier still may not meet the code-prescribed maximum air leakage. Reviewing data from whole-building air leakage testing of 267 buildings (some older, some new), one study found air leakage rates as high as over 10 L/sm<sup>2</sup> at a pressure differential of 50 Pa, but again, these authors did not analyse the energy loss due to air leakage. Citing research by others, the authors do state that the ratio of air infiltration to mechanical air exchange can vary greatly, ranging from almost nothing to

0.8 (Price et al, 2006). Another study in 2005 investigated air leakage in commercial buildings and found the average air leakage to be 7.9 L/sm<sup>2</sup> (Emmerich & Persily, 2005).

Buildings are built at a point in time, but they must provide good performance over their entire service life. A material or system that provides good resistance to air leakage at the time of construction must continue to do so over the building's lifetime for the building to still be an air barrier. Recognising the importance of air barrier durability, two French research projects, Durabilit'air and Durabilit'air2 attempted to evaluate and develop testing protocols for the long-term durability and performance of air barriers based on a review of the literature, experiments, and field data (Leprince et al, 2017; Litvak, 2022). One study of building air leakage in recently constructed single-family houses in France with different types of air barriers that was part of the Durabilit'air project found that air leakage generally increases over the first two years of service then generally stabilises (Moujalled et al, 2019). A study of single-family homes in the United States found that air leakage increased by approximately 25% twelve to thirteen years after construction, and that houses that had undergone air-sealing retrofits showed an increase in air leakage of approximately 12% six to seven years after implementing the retrofits (Chan et al, 2015).

However, it is not just the individual materials that comprise the air barrier that must continue to perform, it also is the transitions between these materials that must provide long-term performance. For example, both the wall and the roof on a building may be in good condition and airtight, but an open joint between the two due to poor installation or materials with poor weatherability can result in significant air leakage over time.

## 2 AIR BARRIER SYSTEMS

Many different types of materials and systems can be part of the building's air barrier. The energy codes list prescriptive materials and systems that these codes consider an air barrier, which are in the following general categories:

- Sheet or fluid-applied membranes.
- Fenestration systems.
- Foam insulation (board or spray-applied).
- Mass assemblies (e.g., concrete, fully-grouted concrete masonry).
- Rigid board materials (e.g., plywood, gypsum wallboard).

Note that the energy codes accept materials that are installed on the interior side and on the exterior side of the wall or roof deck as part of the building's air barrier. The energy codes allow other materials to be used as an air barrier if they have test results from an accredited agency showing that the materials have air permeance of 0.02 L/sm<sup>2</sup> under a pressure differential of 75 Pa when tested according to ASTM E2178 – Standard Test Method for Determining Air Leakage Rate and Calculation of Air Permeance of Building Materials. The energy codes do not have any requirements for long-term performance testing of the air barrier materials or air leakage of the building, so an air barrier product that fails within a few years of installation does not violate the energy code.

## 3 DURABILITY OF MEMBRANE AIR BARRIERS

We focus our discussion of air barrier durability in this paper on two of the primary air barrier types for wall assemblies in modern buildings – membrane air barriers and fenestration systems. We use the term “durability” as including both a material's or system's chemical

and UV stability and its reliability to perform as intended. For example, a mechanically-fastened membrane air barrier that falls off of its substrate within a wall cavity may be intact and chemically stable, but it no longer functions reliably as an air barrier.

### 3.1 Membrane Air Barriers

Membrane air barriers can be loose sheets of polyethylene or spunbonded polyethylene fibres (taped at seams and terminations), adhered sheets, or fluid-applied products. The adhered sheet and fluid applied products can have low water vapor permeability or high water vapor permeability. Adhered sheet products with low water vapor permeability have the longest track record of reliable field performance; water vapor-permeable adhered sheet products and fluid-applied products with both low and high water vapor permeability have a shorter track record of field service (approximately 10 to 15 yrs).

Citing research by others, Sherman and Chan state that spunbonded polyethylene air barriers can fail at joints when exposed to high service temperatures (Sherman & Chan, 2004). Wissink et al (colleagues of these authors) describe observed in-service failures of recently installed fluid-applied air barriers, including blistering, loss of adhesion, dissolution, tearing, and network cracking. The authors performed laboratory testing of both low and high vapor-permeable fluid-applied air barrier products from different manufacturers, subjecting samples to adhesion, elongation, and water immersion testing both in an unconditioned state and after conditioning the samples with UV and condensation cycling and freeze/thaw cycling. They found that most tested products met the industry standard for adhesion and elongation (200%) both before and after conditioning, but most samples absorbed significant amounts of water during immersion testing (higher values showing an increase in weight of 20% to over 200%) or deteriorated during immersion (broke apart, dissolved, etc.). The authors note that prolonged exposure to water should be expected for air barriers (which often also are the wall's waterproofing membrane), so deterioration after water immersion is a particular concern for these products. They also note that the products that showed worse results after water immersion in their testing correlated to products that they observed to have greater incidence of failure (e.g., blistering, reverting to a fluid-like state, debonding from the substrate) in service (Wissink et al, 2012; Wissink et al, 2014). Their field observations and laboratory testing both showed that materials that may perform well upon initial installation or meet energy code requirements for laboratory-certified performance can quickly lose their air-resistive properties and have reduced function as an air barrier.

Quirouette describes a mechanically-fastened polyethylene sheet wall air barrier that had pulled away from its substrate and collapsed within the wall cavity due to cyclical positive and negative wind pressure causing it to pull off of the wall, an example of the membrane itself being durable but deficiencies in its installation causing it to fail in service (Quirouette, 1989). Lux and Brown describe open seams and transitions to other systems in the air barrier on a building that allowed significant air leakage, another example of the air barrier material itself not degrading but poor detailing significantly impairing its function (Lux & Brown, 1989).

In contrast to the failures and issues described above, GCP Applied Technologies, Inc. (a waterproofing and air/vapor barrier membrane manufacturer) tested samples of their self-adhered rubberized asphalt below-grade waterproofing membrane (which is very similar in composition to their sheet-applied air barrier systems) that had been in service for at least fifteen years and found that the material still met or exceed all published performance data. Given that a below-grade application likely is more severe than an above-grade application



(prolonged exposure to hydrostatic head pressure or chemicals), this study shows that materials with a longer record of successful in-service performance can be more reliable than newer materials (GCP Applied Technologies, Inc., 2023).

### 3.2 Fenestration Systems

Because the glass in fenestration systems has negligible air permeability, air leakage through fenestration systems typically occurs in the joints between the glass and the sash or frame, joints between the sash and frame, joints within the sash and frame, or the joint between the fenestration and the surrounding wall system. Fenestration products must be tested by an accredited testing agency to show that their products meet energy code air leakage requirements, but that test is performed in a laboratory on a representative window sample, not on each window that a manufacturer produces. The energy codes typically do not have requirements for field testing of installed fenestration systems to confirm that the installed condition meets the code requirements for air leakage, but AAMA's voluntary test standards for field testing of installed fenestration allows the air leakage of the installed system to exceed its rated performance by 50%. These standards also only require newly-installed fenestration systems to meet this performance for the first six months of service (AAMA, 2014; FGIA 2021).

A study in 1980 tested 192 newly-installed residential windows in the field found that 40% of the windows had air leakage that exceeded their rating by as much as a factor of almost two and that, on average, window air leakage resistance decreased by 29% in the time between manufacture and installation (Weidt & Weidt, 1980). A study in 1985 subjected newly-manufactured windows to accelerated weathering in a laboratory and found that the air leakage could increase by a factor of almost two over time (Kerhli, 1985). We have not found other, more recent published information on the long-term performance of fenestration systems, but the general conclusions of these previous studies stand today – that fenestration systems' resistance to air leakage can decrease over time as gaskets and seals shrink, expand, harden, or debond, as frame and sash joints open (again due to cyclical thermal expansion and contraction), due to “wear and tear” from general use and weathering, or due to issues with their original manufacture and installation.

In addition to the windows themselves, their integration with the surrounding wall systems must also be detailed and installed to limit air leakage. One study found that air leakage due to poor sealing around the window perimeter in resulted in air leakage that was two times or greater than the air leakage through the window itself (Louis & Nelson, 1995). Another study of air leakage through window perimeter joints found leakage rates of approximately 0.32 to 0.61 L/s per meter of joint length (Weidt & Weidt, 1980).

## 4 ENERGY MODELLING

We performed energy modelling of a large (approximately 55,000 m<sup>2</sup>) building using the eQUEST v3.65 building energy simulation tool. For our models, we used an idealized typical multifamily residential building, complying with the 2018 International Energy Conservation Code (IECC) and varied the air leakage rate through the enclosure based upon the previous research discussed above (ICC, 2018).

While air leakage rates for buildings and materials are typically given at a pressure differential of approximately 75 Pa, roughly equivalent to the stalling pressure of an 11.2 m/s wind speed, in reality the typical pressure differential across a building enclosure will be

much lower. To account for this, we adjusted leakage rates down to a wind speed of 4.5 m/s using the methodology in ASHRAE Standard 90.1-2016, Normative Appendix G (ASHRAE, 2016). This provides a more reasonable air leakage rate for a typical building than the typical test pressures. Actual air leakage rates will vary based on the specific construction, wind speeds and exposures, but for the purposes of this analysis the ASHRAE-modified leakage rate is sufficient for comparison purposes (as we are not attempting to predict the actual energy use of a specific, real-world building, only analyse the energy effects of varying air leakage through the building enclosure).

We found that when the air leakage rate in the modelled building is doubled from the typical U.S. and ICC code-prescribed rate (maximum 2.0 L/sm<sup>2</sup>), the corresponding increase in annual building energy use is still relatively small, in the range of 2-3%. This doubling is consistent with our above-mentioned literature review which found published research showing a doubling of air leakage in many windows over time, albeit very conservative. Going beyond that and increasing 5fold produces larger changes in energy use, around 6%, but this level of leakage would require complete failure of fenestration systems or near-total loss of airtightness in membrane air barriers. We ran a similar case considering the difference between a building built to Passive House standards (0.6 air changes per hour) and an IECC-compliant building as described above and found similar results – only about a 3% increase in space conditioning energy use. These results are relatively consistent with industry findings that, years ago when air leakage was not even considered in the energy codes, energy losses due to air leakage were extremely high so even moderate changes to leakage rates produces significant savings. Decades of research, building science education, and improvements to the energy codes have reduced the air leakage for typical new construction and produced good reductions in energy use. The results presented here show that the industry now is approaching the point of diminishing returns on air leakage, where even a factor of two on an “airtight” building might mean a leakage rate of 2 L/sm<sup>2</sup> instead of 1 L/sm<sup>2</sup>. High in multiplier but still low in overall magnitude, as opposed to going from a poorly constructed building with a leakage rate of 10 L/sm<sup>2</sup> down to something closer to current energy code norms.

Our analysis and findings show that a reduction in air barrier performance over time (barring significant deterioration or loss of performance) may not result in a significant energy penalty since the change in overall air leakage magnitude is relatively small. It also helps to validate the current U.S. energy code leakage rates as reasonable targets for air leakage, as the difficulty of improving on current standards is simply not justified by the resulting energy savings.

## **5 OTHER ISSUES WITH POOR AIR BARRIER DURABILITY**

In addition to the potential energy losses associated with deterioration of the air barrier, a deteriorated air barrier can lead to other, more readily apparent damage. Given that some deterioration of the air barrier may not result in significant energy loss (as described above), the potential for this damage may be the primary concern when considering air barrier deterioration. These products often also function as the waterproofing membrane and vapor retarder on the walls, so deficiencies in the air barrier can lead to damage from water leakage or water vapor diffusion. Leaking air also carries humidity, so air leakage can lead to condensation on or within wall or roof assemblies. Figures 1 through 6 show examples of deficiencies in installed air barriers and the types of damage that can result from air or water leakage through the air barrier that the authors and their colleagues have observed firsthand on newly-built buildings.



Figure 1: Breach in fluid-applied air barrier



Figure 2: Breach in fluid-applied air barrier



Figure 3: Corrosion on metal framing due to air leakage causing condensation

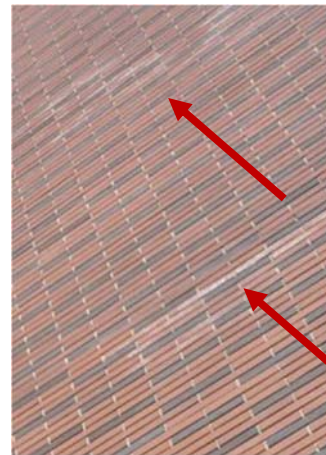


Figure 4: Efflorescence on brick masonry due to air leakage



Figure 5: Mold growth on interior wall and damaged carpet due to air and water leakage



Figure 6: Mold growth on wall due to air and water leakage

## 6 CONCLUSIONS

Designers and builders have a great variety of air barrier products, materials, and systems from which to select when designing and constructing a building. As with other building components, an established record of durable and reliable performance should be one of the

first considerations when selecting the air barrier, because it must be able to function for the entire service life of the building. Materials that are newer to the market may be more cost-effective initially or advertise stellar performance but carry more risk without a record of performance.

Our research and energy modelling show that a complete lack of an air barrier (or an air barrier that is deteriorated to the point of no longer functioning) or lack of continuity between the different air barrier components on a building can result in modest air leakage and resulting energy losses for larger multi-family commercial-type construction. With improvements to design and construction standards for air barrier materials and their installation and the energy codes now requiring a continuous air barrier, research by others and our energy modelling results show that the current energy code requirement of maximum 2.0 L/sm<sup>2</sup> both is achievable and reasonable in terms of energy performance. Attempting to lower this standard can have diminishing returns and must be considered in the context of other environmental concerns that it may cause (e.g., more raw materials, embodied energy, carbon production, etc.) from the research and development, production, and shipping of higher-performing materials or waste from installed systems that cannot meet a more stringent standard and must be removed and replaced. As building enclosure and mechanical systems develop, it will no doubt become easier to achieve lower (e.g., Passive House) levels of air leakage and realize additional savings. But for a typical modern building, dramatic reductions in air leakage alone (in the absence of improvements to the thermal envelope, ventilation, and mechanical systems) is not the most productive pathway to energy savings and must be considered in terms of costs (both monetary and environmental) versus benefit.

Given that the industry may have reached a point of balance between permitted air leakage and energy performance, a greater concern for air barrier durability may be damage to the building that could result from their deterioration or improper detailing. Air leakage, water leakage, and vapor diffusion through a deteriorated or poorly installed air barrier (which also often is the waterproofing and vapor retarder on the building) can cause significant damage to other building components. Again, in the context of the environment, damaged materials must be removed and replaced, all of which require raw materials and energy to manufacture, ship, and install the replacement materials. When we consider the environmental impacts of air barrier durability, these considerations must have equal or possibly greater weight to energy loss due to air leakage.

## 7 REFERENCES

- American Architectural Manufacturers Association [AAMA]. (2014). *AAMA 503.14 Voluntary Specification for Field Testing of Newly Installed Storefronts, Curtain Walls and Sloped Glazing Systems*. American Architectural Manufacturers Association.
- American Society of Heating, Refrigerating and Air-Conditioning Engineers [ASHRAE]. (2010). *Standard 90.1 Energy Standard for Buildings Except Low-Rise Residential Buildings*. Atlanta: American Society of Heating, Refrigerating and Air-Conditioning Engineers.
- American Society of Heating, Refrigerating and Air-Conditioning Engineers [ASHRAE]. (2016). *Standard 90.1 Energy Standard for Buildings Except Low-Rise Residential Buildings*. Atlanta: American Society of Heating, Refrigerating and Air-Conditioning Engineers.

- Beals, W. (2016). Air Barriers for Metal Buildings. *Insulation Outlook*, February 2016, 26-30.
- Chan, W. R., I. S. Walker, & M. H. Sherman (2015). Durable Airtightness in Single-Family Dwellings: Field Measurements and Analysis. Ernest Orlando Lawrence Berkeley National Laboratory, Environmental Energy Technologies Division.
- Emmerich S. J. & A. K. Persily. (2005). Airtightness of commercial buildings in the US. *Proceedings from the 26th Air Infiltration and Ventilation Centre Conference: Ventilation in Relation to the Energy Performance of Buildings*. INIVE EEIG.
- Fenestration and Glazing Industry Alliance [FGIA]. (2021). *AAMA 502-21 Voluntary Specification for Field Testing of Newly Installed Fenestration Systems*. Fenestration and Glazing Industry Alliance.
- GCP Applied Technologies., Inc. (2023). TL-0012 — BITUTHENE Longevity Technical Letter. <http://www.gcpat.com/solutions/products/bituthene-post-applied-waterproofing/tl-0012-bituthene-longevity-technical> (accessed 6 June 2024).
- International Code Council, Inc. [ICC]. (2011). *2012 International Energy Conservation Code*. International Code Council, Inc.
- International Code Council, Inc. [ICC]. (2018). *2018 International Energy Conservation Code*. International Code Council, Inc.
- Handegord, G. O. (1979). Building Research Note, No. BRN-151 The Need for Improved Airtightness in Buildings. National Research Council of Canada.
- Kerhli, D. (1985). *Window Air Leakage Performance as a Function of Differential Temperatures and Accelerated Aging*. Rochester: Schlegel Corporation.
- Leprince, V., B. Moujalled, & A. Litvak (2017). Durability of building airtightness, review and analysis of existing studies, *Proceedings from the 38th AIVC Conference "Ventilating healthy low-energy buildings", Nottingham, UK, 13-14 September 2017*.
- Litvak, A. (2022). Lesson learnt and new protocol for the Durabilit'air project: laboratory measurements. *Proceedings from the 42nd AIVC - 10th TightVent - 8th venticool Conference - Rotterdam, Netherlands - 5-6 October 2022*.
- Louis, M. J. & P. E. Nelson. (1995). Extraneous Air Leakage from Window Perimeters. *Air Flow Performance of Building Envelopes, Components, and Systems, ASTM STP 1255*, Mark P. Moreda and Andrew K. Persily, Eds. Philadelphia: American Society for Testing and Materials, 108-122.
- Lux, M. E. & W. C. Brown. (1989). Air Leakage Control, *Proceedings Building Science Insight 1986: An Air Barrier for the Building Envelope, Institute for Research in Construction, National Research Council Canada*, 13-19.
- Marceau, M. & A Shrode. (2019). Analysis and Lessons Learned from Whole-Building Air Leakage Testing of 276 Buildings, *Thermal Performance of the Exterior Envelopes of Whole Buildings XIV International Conference*.

- Moujalled, B., S. Berthault, A. Litvak, V. Leprince, & G. Frances (2019). Assessment of long-term and mid-term building airtightness durability: field study of 61 French low energy single-family dwellings, *Proceedings of the 40th AIVC - 8th TightVent - 6th venticool Conference - Ghent, Belgium - 15-16 October 2019*.
- National Research Council of Canada [NRCC]. (1985). *National Building Code of Canada*. Ottawa: National Research Council of Canada.
- Peterson, R. A. & L. T. Hendricks. (1988). Exterior Wall Airtightness and the Role of Air Barriers and Vapor Retarders. Cold Climate Housing Information Centre. CD-FO-3569, Minnesota Extension Service, University of Minnesota.
- Price, P. N., A. Shehabi, R. W. Chan, & A. J. Gadgil. (2006). *Indoor-outdoor Air Leakage of Apartments and Commercial Buildings*. California Energy Commission, PIER.
- Quirouette, R. L. (1985). Building Practice Note No. 54 The Difference Between a Vapour Retarder and an Air Barrier. National Research Council Canada, Division of Building Research.
- Quirouette, R. L. (1989). The Air Barrier Defined. National Research Council, Institute for Research in Construction, Proceedings of Buildings, Science Insight '86, 1-5.
- Sherman, M. & N. Matson. (1997). Residential Ventilation and Energy Characteristics. Unites States, N. p.
- Sherman, M. H. & R. Chan. (2004). Building Airtightness: Research and Practice. Lawrence Berkeley National Laboratory. LBNL Report #: LBNL-53356.
- Tamura, G. T. (1975). Measurement of Air Leakage Characteristics of House Enclosures. *ASHRAE Transactions*, 81(1), 202-208.
- United States Department of Energy [DOE]. (2014). Windows and Building Envelope Research and Development February 2014. United States Department of Energy.
- Weidt, J. & J. Weidt. (1980). *Air Leakage of Newly Installed Residential Windows*. Lawrence Berkeley Laboratory.
- Wissink, K. S., L. R. Kellet, & S. S. Ruggiero. (2012). Testing Fluid-applied Air and Water Barriers. *Construction Specifier*, 65(12), 70-80.
- Wissink, K. S., L. K. Bashaw, & S. S. Ruggiero. (2014). Comparative Analysis of Fluid-applied Air Barrier Products, *Building Walls Subject to Water Intrusion and Accumulation: Lessons from the Past and Recommendations for the Future*, STP 1549, Jeff Erdly and Paul Johnson, Eds. West Conshohocken: ASTM International, 1-15.

# Ventilation guidelines for Flemish childcare and psychological care centres

Quinten Carton<sup>1</sup>, Douaa Al-Assaad<sup>\*1</sup>, Liesje Van Gelder<sup>2</sup>, Maarten De Strycker<sup>2</sup>, Hilde Breesch<sup>1</sup>

*1 KU Leuven, Department of Civil Engineering, Building Physics and Sustainable Design, Ghent Campus  
Gebroeders de Smetstraat 1  
9000 Ghent, Belgium*

*2 BCCA  
Hermeslaan 9  
1831 Diegem, Belgium*

*\*Corresponding author: douaa.al-assaad@kuleuven.be*

## ABSTRACT

Since the COVID-19 pandemic, governments have expressed the need for practical ventilation guidelines to maintain acceptable indoor air quality (IAQ) in the public care sector, where vulnerable groups reside. The aim of this paper is to establish such guidelines dedicated to old and newly built psychological care homes and child day care centres in Flanders (Belgium). For each sector, a representative simulation model was designed in Modelica. Inputs for building and system characteristics, and occupant behaviour were gathered via an online survey and assessed via a stakeholder group, representing each sector. Afterwards, multiple simulation scenarios, varying building and system characteristics (e.g., ventilation system type, control, flow rate, window opening area) and occupant behaviours (e.g., window opening frequency and duration, occupancy density) were tested. The impact of each simulation scenario on the CO<sub>2</sub>-concentrations exceedance hours and energy use were evaluated. Based on the simulation results, appropriate ventilation strategies offering acceptable IAQ conditions were determined. Finally, the feasibility of each ventilation strategy was discussed with the stakeholder groups and the guidelines were translated into practical instructions for building facility managers in the public care sector of Flanders.

## KEYWORDS

Ventilation guidelines, indoor air quality, energy use, care facilities, occupant behaviour

## INTRODUCTION

Nowadays, individuals spend approximately 90% of their time indoors, engaging in daily activities for work or recreation. Thus, it is crucial that existing and newly constructed buildings prioritize the creation of optimal levels of indoor environmental quality, especially thermal comfort and indoor air quality (IAQ). This is even more imperative in the case of vulnerable groups having fragile or already compromised health, that spend even more time indoors and are most susceptible to building-related health outcomes. This includes infants and children in childcare centres, elderly people in retirement homes and disabled individuals in specialized care facilities. As recently evidenced by field measurements, questionnaires and clinical tests in 50 nursing homes across Europe, there is a direct relationship between respiratory symptoms and exposure to indoor air pollutants (Bentayeb et al., 2015). A meta-analysis of 10 European birth cohorts found associations between pneumonia in early childhood and exposure to pollutants (MacIntyre et al., 2014). This shows the vulnerability of current care facilities and the lack of proper ventilation measures put in place to protect its inhabitants.

Thus, indoor air pollution is a major global public health problem that requires increasing efforts in research and policy making, especially when it comes to the design and operation of existing ventilation systems. So far, EU standards recommend ventilation rates for human occupancy to satisfy certain indoor air classifications. This cannot always guarantee good IAQ under typical expected conditions and has proven itself to be completely insufficient in the face of disruptive events such as the COVID-19 pandemic. The latter had a great negative impact on care facilities world-wide which were already vulnerable. In Belgium alone, 42% of

COVID-19 deaths occurred in care facilities and nursing homes (Comas-herrera et al., 2020). Quick fix solutions in buildings with common gathering areas included increasing ventilation rates in tandem with a more vigorous monitoring of the IAQ. This yields an increase in energy usage (e.g., 15%) without a guarantee of improved IAQ at a time where saving energy is a priority in the EU (Krarti & Aldubyan, 2021; Pease et al., 2021). Moreover, such solutions are not an option for care facilities as most are public buildings with limited budgets. In these cases, facility managers often rely on counter-intuitive opening of windows and doors without paying much regard to the operation of building HVAC systems, energy usage, interzonal airflows, wind, type of rooms and activities. While such strategies can sometimes improve IAQ, they are often random and unreliable. Therefore, care facilities can benefit from clear and simple ventilation guidelines that can guarantee an acceptable level of IAQ without unnecessary energy usage throughout the year.

Thus, the aim of the current work is to establish in coordination with the Preventive Health Policy Division and the Flemish Infrastructure fund for personal affairs (VIPA) of the Flemish department of care ; ventilation guidelines for different types of care sectors in Flanders, Belgium: (i) elderly care homes, (ii) childcare facilities for children between 0 – 3 years of age, (iii) psychological care centres for mentally disadvantaged individuals, (iv) local service centres, (v) care centres for physically disabled individuals, and (vi) rehabilitation centres. These guidelines are meant to help facility managers of care sector buildings in their decision-making regarding facility operations. To reach this aim, a performance assessment of current ventilation designs in existing care facilities was conducted via simulations of representative cases of such buildings in Flanders. The assessment considered the realistic usage profile of the premises by conducting qualitative surveys across a wide range of care facilities in Flanders. The guidelines give simplified recommendations about the adequate opening of windows in tandem with the ventilation system while accounting for energy use. While the guidelines were established for different facility types and multiple space ventilation systems variations, for the sake of brevity, **the results that will be presented in this work will focus on childcare (CCC) and psychological care centres (PCC) and a mechanical exhaust system.**

## METHODS

Firstly, a data collection campaign was performed to construct representative simulation models of the corresponding buildings. This was done by conducting surveys in each of the sectors to gather descriptive information pertaining to the usage of the buildings (i.e., occupancy schedules, activities, density, window usage and opening, ventilation systems) and analysing building plans to determine a representative typology (i.e., spaces and geometry, window locations). A literature study on existing national standards and legislation in each sector was conducted to gather information regarding current buildings and systems and make appropriate assumptions. Afterwards, meetings with stakeholders from each sector were organized to validate the initial assumptions. Secondly, the reference simulation models of the buildings were defined together with a set of simulation scenarios (e.g. variations in window opening schedules, size, occupancy densities, ventilation system operations) to conduct. The impact of each simulation scenario on the CO<sub>2</sub>-concentrations exceedance hours and energy use was evaluated and ventilation guidelines were finally established from the simulation results. Though not the most representative indicator on cumulative exposure, the CO<sub>2</sub>-concentrations exceedance hours was chosen due to its simplicity and to easily communicate the resulting guidelines with the stakeholders and personnel of the PCC and CCC.

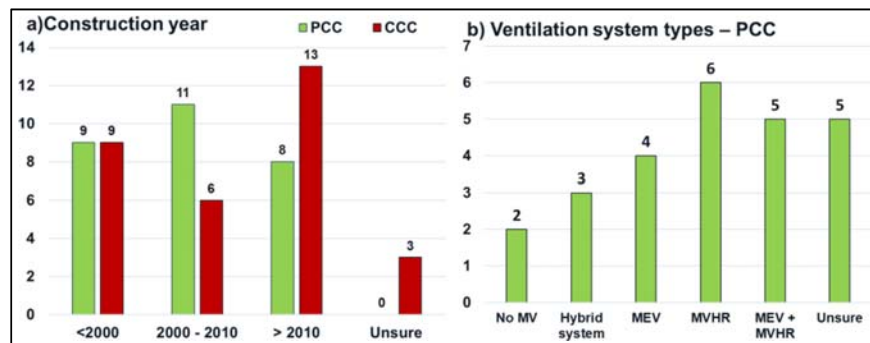


## Step 1: Data collection

### Online surveys

Online surveys were distributed among technical personnel of PCC and CCCC facilities. The survey aimed to gain year-round insights into (1) building and system characteristics (e.g., building age distribution, type of ventilation system and operation, solar shading and operation) and (2) occupant behaviour (e.g., occupancy schedules, window opening, control over heating and cooling setpoints). The surveys were designed and distributed via the software “Qualtrics” (Qualtrics, 2005). Stakeholders, representing multiple care facilities, distributed the survey among their members. In total, 25 and 31 respondents completed the surveys on their PCC or CCC facility, respectively. In the case of the PCC, the responses comprised 18 different facilities and 28 buildings. Figure 1a shows the results for the building construction year of both the PCC and CCC facilities. The distribution shows that both old and more recent buildings are commonly present in both facilities. Older constructions follow the older EPB standards before 2010 (Vlaanderen, 2006) while newer constructions follow the newer EPB standards that require a more energy performant building (Vlaanderen, 2022). These standards were used to model the building envelope characteristics.

Figure 1b presents the responses on the type of ventilation system present in the PCC facilities. A majority indicated that the facility was equipped with a balanced mechanical ventilation system with heat recovery (i.e., **MVHR**). The second highest response were respondents unsure about the ventilation system in their facility and respondents indicating that their facility was equipped with both a MVHR and mechanical exhaust ventilation (i.e., **MEV**). In the facilities with both system types, the multi-occupied spaces were equipped with a MVHR, while the personal bedroom had a MEV. A minority of the respondents indicated that their facility lacked a mechanical ventilation system (no MV) or comprised of a hybrid system, combining natural and mechanical ventilation.



**Figure 1.** Survey results regarding a) building construction year, b) ventilation system types

Input from a large-scale survey in CCC facilities performed by VITO (Geyskens et al., 2023) was also used in the set-up of the reference simulation models. The results of the large-scale survey indicated that older CCC facilities were mostly not equipped with a mechanical ventilation system or equipped with an exhaust-only ventilation system (**MEV**). In newly built CCC facilities, exhaust-only or balanced mechanical ventilation system were present (**MEV**, **MVHR**). These systems were operated according to a schedule of 7:00 to 22:00.

In the PCC, the exhaust fans in the bathrooms connected to the sleeping rooms were always operated in case of occupancy in the bedrooms. In newer constructions, the smart humidity and CO<sub>2</sub> driven demand-controlled variable air volume (VAV) version of systems C and D could also be found (referred to as **MEV+ and MVHR+**) in common areas. In older and newer constructions of both CCC and PCC facilities, ventilation rates of 22 m<sup>3</sup>/h and 36 m<sup>3</sup>/h

per person were considered in the common rooms respectively. For the case of PCC, ventilation rates of 50 m<sup>3</sup>/h and 75 m<sup>3</sup>/h were considered in the bathrooms adjoint to the bedrooms in older and newer constructions respectively.

As for shading, for both CCC and PCC, older constructions were not equipped with any active solar shading device but rather overhangs and were not equipped with any cooling strategy. Newer CCC and PCC had automated external solar shading device and a split cooling end unit in common areas operated by the facility managers in case indoor temperatures exceed 26°C during hot summer months. According to the surveys, occupants had no control over the operation of the shading or cooling device. Radiators were used for heating in older and new constructions.

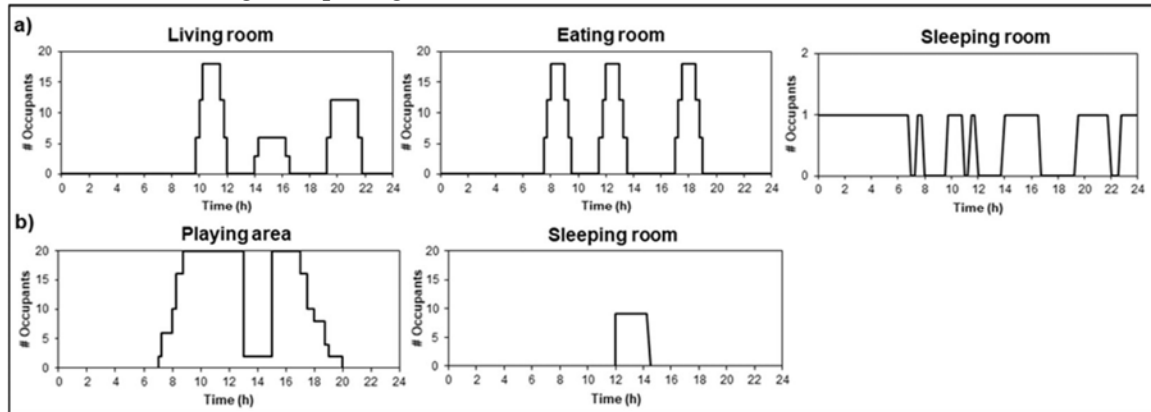
**Table 1.** Summary of ventilation systems and rates in a) PCC and b) CC

<b>a) PCC sector</b>		
	<b>Old construction</b>	<b>New construction</b>
<b>Ventilation system types</b>	MEV in all rooms with a ventilation rate of 22 m <sup>3</sup> /h per person with fans operating between 7:00 – 22:00 in multi-occupied spaces. A ventilation rate of 50 m <sup>3</sup> /h in WC adjoint to bedrooms via a door with grills. Fans operate during occupancy	MEV/MEV+, MVHR/MVHR+ in all rooms or MVHR/MVHR+ in multi-occupied spaces and MEV in sleeping rooms. Ventilation rate of 36 m <sup>3</sup> /h per person in multi-occupied spaces operating between 7:00 – 22:00 for systems MEV/MVHR. CO <sub>2</sub> -setpoint of 900ppm active in MEV+ and MVHR+. A ventilation rate of 75 m <sup>3</sup> /h in WC adjoint to bedrooms via a door with grills. Fans operate during occupancy
<b>b) CCC sector</b>		
	<b>Old construction</b>	<b>New construction</b>
<b>Ventilation system types</b>	No mechanical ventilation (only window operation for ventilation)	MEV/MEV+, MVHR/MVHR+ in all rooms. Same rates per person as PCC and same control

Occupancy schedules varied depending on room usage and the type of sector. **Figure 2** shows representative occupancy schedules for PCC and CCC sectors. In the PCC, the common room had a maximum occupant density of 5 m<sup>2</sup> per person. It was in usage three times a day in the mornings, afternoons and evenings for three hours at a time. The dining room was used during mealtimes (breakfast, lunch, dinner) at a constant maximum occupancy density of 5 m<sup>2</sup> per person. The sleeping rooms were constantly occupied during nighttime and intermittently throughout the day depending on the preferences of occupants. In the PCC, occupants stayed regularly in their rooms. In the CCC, 9 children were allowed in one sleeping room at a time. The kids slept mostly in the afternoon for three hours. For the rest of the day, they were in the playing area in 2 groups at a time (18 children and 2 care takers). Parents would normally pick up their kids from 17:00 onwards.

Window opening was managed by the facility personnel and opening behaviours depended on the season and varied within the different sectors according to multiple scenarios. In winter season, windows were either kept closed most of the time, or opened 1 hour in the morning for the sake of ventilation. In multi-occupied areas, windows were also opened after peak activity hours to purge polluted air perceived as stuffy by occupants. In summer season, windows were opened more frequently. They were either open the whole day or closed during

the day and open at night. **Table 2** shows the assumed window opening scenarios that are inclusive of the range of opening behaviour.



**Figure 2.** Occupancy schedules for a) PCC and b) CCC sectors

**Table 2.** Window opening scenarios: a) PCC and b) CCC sectors

<b>a) PCC sector</b>			
	<b>Room type</b>	<b>Heating season</b>	<b>Cooling season</b>
<b>Scenario A</b>	Common	Closed all day	Open at night
	Sleeping	Open 1h in the morning	Open at night
<b>Scenario B</b>	Common & sleeping	Open 1h in the morning	Full day open
<b>Scenario C</b>	Living	Open after activities for 1h	Open during the day, closed at night
	Eating	Open after meals for 1h	Open during the day, closed at night
	Sleeping	Open 1h in the morning	Open 1h in the morning
<b>b) CCC sector</b>			
		<b>Heating season</b>	<b>Cooling season</b>
<b>Scenario 1</b>	Common & sleeping	Closed all day	Closed all day
<b>Scenario 2</b>	Common	Open 1h in the morning	Open during activities
	Sleeping	Open 1h in the morning	Open 1h before and after occupancy
<b>Scenario 3</b>	Common	Open 1h in the morning and during activities	Open full day
	Sleeping	Open 1h in the morning and 1h before and after occupancy	Open full day
<b>Scenario 4</b>	Common & sleeping	Open full day	Open full day

## Building plans

A set of building plans from representative psychological care homes (PCC) and childcare centres (CCC) were delivered by VIPA and analysed. In Belgium, older and new constructions are commonly present when it comes to the care sector. Thus, both were considered in the analysis of the building plans and the formulation of the guidelines. The analysis consisted of determining a representative layout and geometry of the different rooms of interest, window positioning and areas, building orientations and layouts. For the PCC sector, a representative layout of older and new constructions consists of a common area room used for recreation and oriented South (average conditioned floor area  $A_c$  of 90 m<sup>2</sup>) with one external façade. It has south oriented manually operable windows with a window to floor ratio (WFR) of 7%. Opposite to it and connected by a narrow hallway is a dining room ( $A_c = 128$  m<sup>2</sup>) with one external façade having north oriented windows and a WFR of 16%. Located on either side of the hallway; are the residents' bedrooms with connected bathrooms ( $A_c = 20$  m<sup>2</sup>). The bedrooms have west-oriented windows with a WFR of 8%. As for the CCC, older constructions consist of a playing area ( $A_c = 54$  m<sup>2</sup>) and sleeping rooms ( $A_c = 22.5$  m<sup>2</sup>) with external façades facing south (WFR = 9%) and connected by an internal wall. Newly constructed CCCs have additionally an internal sleeping room ( $A_c = 22.5$  m<sup>2</sup>) connected to the playing area via a hallway.

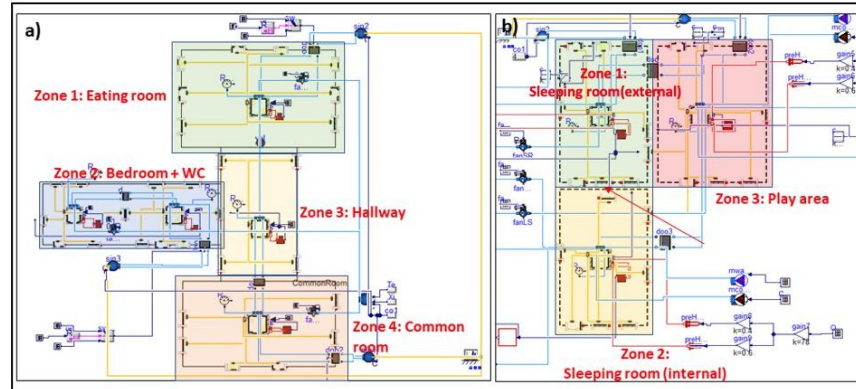
## Literature review

Current ventilation regulation requires that both residential and non-residential buildings in Belgium are equipped with a ventilation system capable of guaranteeing acceptable IAQ conditions, i.e., IDA class 3 in standard EN 13779 (European Committee for Standardization, 2007). However, practical guidelines on the operation of ventilation systems or opening of windows to maintain acceptable IAQ conditions are still missing. The Flemish decree on IEQ sets reference values for indoor temperature (Vlaamse Overheid, 2018). The decree advised an indoor temperature in multi-occupied spaces between 20°C-24°C and 22°C-26°C during heating and cooling season, respectively. The EPB guidelines were used to inform the building envelope construction (i.e., insulation, glazing, air tightness) for older and newer buildings in each sector. Since ventilation system design was based on CO<sub>2</sub>, two thresholds are normally applied, i.e., 1200ppm and 900ppm. The first represented the maximum allowed CO<sub>2</sub>-concentration during normal conditions. The latter corresponded to the target CO<sub>2</sub>-concentration during normal circumstances and the maximum CO<sub>2</sub>-concentration during periods of increased risk of respiratory infections (e.g., flu season, pandemic). Both thresholds were used as references levels for IAQ in Belgian legislation (Federale Overheidsdienst Werkgelegenheid - Arbeid en Sociaal overleg, 2022).

## Step 2: Simulation models and performance assessment

Based on the building plans, existing guidelines and data collected from the online surveys, representative simulation models of the PCC and CCC sectors were developed using the Modelica language in the Dymola environment (Dassault Systèmes, 2024) as shown in **Figure 3**. The model was built using pre-validated components from the integrated district energy and systems (IDEAS) library (i.e., zones, envelope components, windows, HVAC systems)(Jorissen et al., 2018). Note that the window opening behaviour was modelled in Modelica with operable windows. The wind pressure coefficients were calculated using the correlation of (Swami & Chandra, 1987). Yearly simulations were conducted using the RADAUII solver with a time step of 15 minutes. The simulation scenarios included varying the ventilation systems and rates and window opening scenarios according to **Tables 1** and **2**. The IAQ was evaluated based on the CO<sub>2</sub>-concentrations exceedance hours, which gave a percentage (%) of occupied time that the CO<sub>2</sub>-concentrations were above the two thresholds.

The energy use (heating, cooling, fan electricity use) was also computed and used as a benchmark to formulate the guidelines.

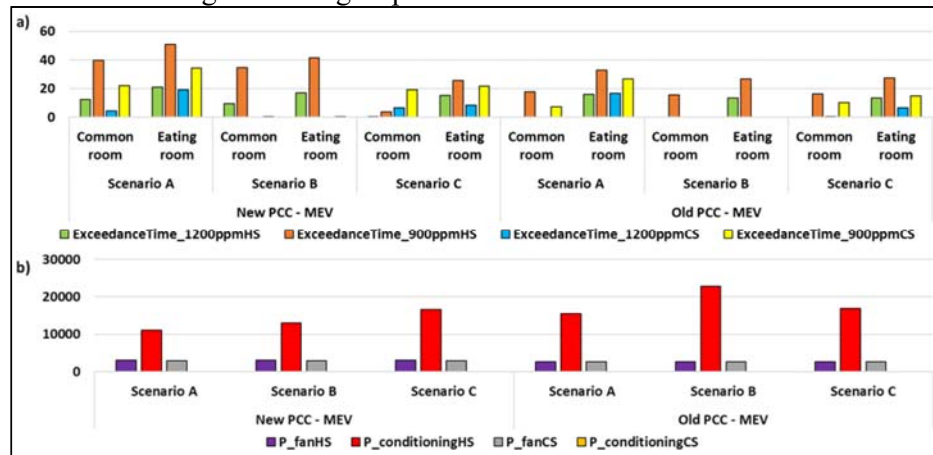


**Figure 3.** Modelica models of a) PCC and b) CCC sectors

## RESULTS

### Psychological care homes (PCC)

**Figure 4** represents the simulation results for the old and new PCC buildings for scenarios A, B and C (**Table 2**) for MEV. As expected, older constructions with lower ventilation rates had more IAQ problems than newer constructions and the IAQ in the heating season was worse than in the cooling season due to less frequent and shorter window opening. Thus, recommended window opening behaviour is dependent on the construction year and season type. For a threshold of 1200 ppm in the heating season, common rooms in old PCC would benefit from more frequent window opening according to **scenario B** which offers a compromise between IAQ and energy use (**Figure 4b**). Another option would be more efficient occupancy management (i.e., occupy premises in smaller groups at a time). For a stricter threshold of 900 ppm in the heating season in case of disease circulation and a heightened contamination risk, a less energy efficient **scenario C** is required despite it causing a 30% increase in energy use. The difference in heating energy usage between the old and new facilities was due to a higher heating setpoint active in the new PCC facilities.

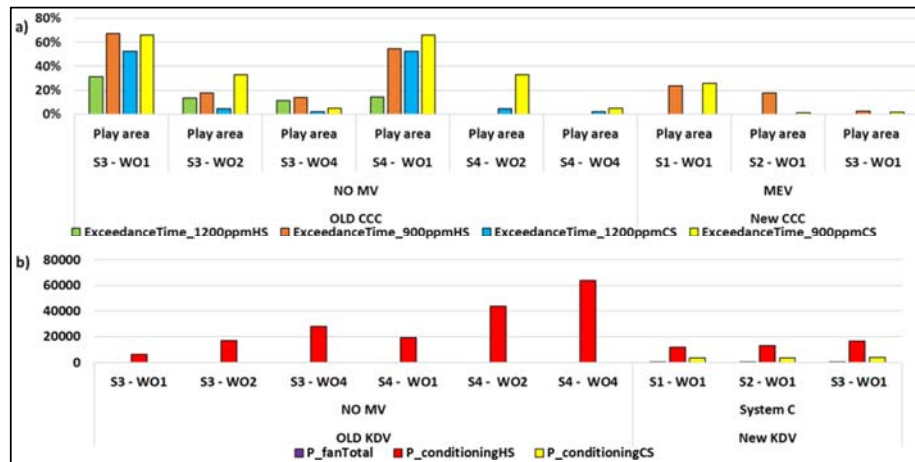


**Figure 4.** a) Exceedance time of CO<sub>2</sub>-concentration [% occupied time], b) Energy usage [kWh] in the PCC sector. Results are shown for heating season (HS) and cooling season (CS)

### Child day care centres (CCC)

**Figure 5** shows the simulation results for the old CCC without mechanical ventilation and the new CCC with a ventilation system type C for window opening scenarios S1, S2, S3 and S4 (**Table 2**). In the case of the old CCC, three different window opening areas (Mourkos et al., 2020) are tested, i.e., 1m<sup>2</sup> (WO1), 2m<sup>2</sup> (WO2), 4m<sup>2</sup> (WO4). In the old CCC, windows must be

frequently opened to maintain an acceptable IAQ. Windows with an opening area of 2m<sup>2</sup> must be opened a full day during heating season in order to avoid an exceedance in CO<sub>2</sub>-concentration of 1200 and 900ppm. Due to unfavourable wind conditions during cooling season, a larger window opening area of 4m<sup>2</sup> is necessary to minimize the exceedance of CO<sub>2</sub>-concentrations. **Figure 5b** shows a high increase in heating energy usage for scenario 4 in comparison to scenario 3 (+ 162%), therefore, lowering the allowed occupancy in the room would be a more suitable solution. No additional window opening is necessary in the new CCC when CO<sub>2</sub>-concentrations must be below 1200ppm. In case a threshold of 900ppm is applied, windows must be opened 1hour in the morning and during activities during heating season. During cooling season, the windows should be opened a full day to remain below the 900ppm threshold.



**Figure 5.** a) Exceedance time of CO<sub>2</sub>-concentration [% occupied time], b) Energy usage [kWh] in the CCC sector. Results are shown for heating season (HS) and cooling season (CS)

## CONCLUSIONS

**Table 3** summarises the resulting guidelines per facility (i.e., PCC or CCC), season (i.e., heating or cooling season) and required IAQ threshold (i.e., 900 or 1200ppm). In case the characteristics of a care facility differ from the assumed space properties and occupancy profile, it is advised to verify the suitability of the guidelines with CO<sub>2</sub> measurements. The ventilation guidelines for CCC facilities will be checked with the results of field measurement campaigns performed by VITO in the future.

**Table 3.** Practical ventilation guidelines

a) PCC: Old facility – Ventilation type C			
1200 ppm		900 ppm	
Heating season	Cooling season	Heating season	Cooling season
The current ventilation flow rate is insufficient. Open windows after activities in the space or decrease the allowed occupancy in the room.	The current ventilation flow rate is insufficient. Keep windows open all day and night. In case of a heat wave, it is advised to keep windows closed and to decrease the allowed occupancy in the room.	The current ventilation flow rate is insufficient. Opening windows is not sufficient. Decrease the allowed occupancy and/or occupancy duration in the room.	The current ventilation flow rate is insufficient. Keep windows open all day and night. In case of a heat wave, it is advised to keep windows closed and to decrease the allowed occupancy in the room.
b) PCC: New facility – Ventilation type C			
1200 ppm		900 ppm	
Heating season	Cooling season	Heating season	Cooling season

The current ventilation flow rate is sufficient. No additional measures are necessary.	The current ventilation flow rate is sufficient. No additional measures are necessary.	The current ventilation flow rate is insufficient. Opening windows is not sufficient. Decrease the allowed occupancy and/or occupancy duration in the room.	The current ventilation flow rate is insufficient. Keep windows open all day and night. In case of a heat wave, it is advised to keep windows closed and to decrease the allowed occupancy in the room.
<b>c) CCC: Old facility – No mechanical ventilation</b>			
<b>1200 ppm</b>		<b>900 ppm</b>	
<b>Heating season</b>	<b>Cooling season</b>	<b>Heating season</b>	<b>Cooling season</b>
The current ventilation flow rate is insufficient. Open windows with an opening area of 2m <sup>2</sup> the whole day or decrease the allowed occupancy in the room.	The current ventilation flow rate is insufficient. Open windows with an opening area of 2m <sup>2</sup> the whole day. In case of a heat wave, it is advised to keep windows closed and to decrease the allowed occupancy in the room.	The current ventilation flow rate is insufficient. Open windows with an opening area of 2m <sup>2</sup> the whole day or decrease the allowed occupancy in the room.	The current ventilation flow rate is insufficient. Open windows with an opening area of 4m <sup>2</sup> the whole day. In case of a heat wave, it is advised to keep windows closed and to decrease the allowed occupancy in the room.
<b>d) CCC: New facility – Ventilation type C</b>			
<b>1200 ppm</b>		<b>900 ppm</b>	
<b>Heating season</b>	<b>Cooling season</b>	<b>Heating season</b>	<b>Cooling season</b>
The current ventilation flow rate is sufficient. No additional measures are necessary.	The current ventilation flow rate is sufficient. No additional measures are necessary.	The current ventilation flow rate is insufficient. Open windows with an opening area of 1m <sup>2</sup> 1 hour in the morning and during activities.	The current ventilation flow rate is insufficient. Open windows with an opening area of 2m <sup>2</sup> during activities. In case of a heat wave, it is advised to keep windows closed and to decrease the allowed occupancy in the room.

## ACKNOWLEDGEMENTS

The authors acknowledge the support of the Preventive Health Policy Division and the Flemish Infrastructure fund for personal affairs (VIPA) of the Flemish department of care. This study was financed by the Flemish government via the project ‘Vlaamse Veerkracht’ (project number: VV045).

## REFERENCES

- Bentayeb, M., Norback, D., Bednarek, M., Bernard, A., Cai, G., Cerrai, S., Eleftheriou, K. K., Gratiou, C., Holst, G. J., Lavaud, F., Nasilowski, J., Sestini, P., Sarno, G., Sigsgaard, T., Wieslander, G., Zielinski, J., Vieg, G., & Annesi-Maesano, I. (2015). Indoor air quality, ventilation and respiratory health in elderly residents living in nursing homes in Europe. *European Respiratory Journal*, 45(5), 1228–1238. <https://doi.org/10.1183/09031936.00082414>
- Comas-herrera, A., Zalakaín, J., Lemmon, E., Litwin, C., Hsu, A. T., Schmidt, A. E., & Arling, G. (2020). Mortality associated with COVID-19 in care homes: international evidence. In

*International Long-term Care Policy Network.*  
<https://www.ecdc.europa.eu/sites/default/files/documents/Increase-fatal-cases-of-COVID-19->

- Dassault Systèmes. (2024). *Dymola*. <https://www.3ds.com/products/catia/dymola>
- European Committee for Standardization. (2007). *NBN EN 13779: Ventilatie voor niet-residentiële gebouwen - Prestatie-eisen voor ventilatie- en luchtbehandelingsystemen*.
- Federale Overheidsdienst Werkgelegenheid - Arbeid en Sociaal overleg. (2022). *Codex over het welzijn op het werk*. <https://werk.belgie.be/nl/themas/welzijn-op-het-werk/algemene-beginselen/codex-over-het-welzijn-op-het-werk>
- Geyskens, F., Lazarov, B., & Stranger, M. (2023). *Rapport settinganalyse Kinderdagverblijven Deel I: Online survey 2023*.
- Jorissen, F., Reynders, G., Baetens, R., Picard, D., Saelens, D., & Helsens, L. (2018). Implementation and verification of the ideas building energy simulation library. *Journal of Building Performance Simulation*, 11(6), 669–688. <https://doi.org/10.1080/19401493.2018.1428361>
- Krarti, M., & Aldubyan, M. (2021). Review analysis of COVID-19 impact on electricity demand for residential buildings. *Renewable and Sustainable Energy Reviews*, 143(January), 110888. <https://doi.org/10.1016/j.rser.2021.110888>
- MacIntyre, E. A., Gehring, U., Mölter, A., Fuertes, E., Klümper, C., Krämer, U., Quass, U., Hoffmann, B., Gascon, M., Brunekreef, B., Koppelman, G. H., Beelen, R., Hoek, G., Birk, M., de Jongste, J. C., Smit, H. A., Cyrus, J., Gruzieva, O., Korek, M., ... Heinrich, J. (2014). Air pollution and respiratory infections during early childhood: An analysis of 10 European birth cohorts within the ESCAPE project. *Environmental Health Perspectives*, 122(1), 107–113. <https://doi.org/10.1289/ehp.1306755>
- Mourkos, K., McLeod, R. S., Hopfe, C. J., Goodier, C., & Swainson, M. (2020). Assessing the application and limitations of a standardised overheating risk-assessment methodology in a real-world context. *Building and Environment*, 181, 107070. <https://doi.org/10.1016/j.buildenv.2020.107070>
- Pease, L. F., Wang, N., Salsbury, T. I., Underhill, R. M., Flaherty, J. E., Vlachokostas, A., Kulkarni, G., & James, D. P. (2021). Investigation of potential aerosol transmission and infectivity of SARS-CoV-2 through central ventilation systems. *Building and Environment*, 197(October 2020), 107633. <https://doi.org/10.1016/j.buildenv.2021.107633>
- Qualtrics. (2005). *Qualtrics*. <https://www.qualtrics.com/>
- Swami, M. V., & Chandra, S. (1987). *Procedures for calculating natural ventilation airflow rates in buildings*.
- Vlaamse Overheid. (2018). *Vlaams Binnenmilieubesluit*.
- Vlaanderen. (2006). *EPB-eisen bij bouwaanvraag/melding van 2006 tot en met 2009*. <https://www.vlaanderen.be/epb-pedia/epb-plichtig-toepassing-en-eisen/epb-eisentabellen-per-aanvraagjaar/epb-eisen-bij-bouwaanvraag-melding-van-2006-tot-en-met-2009>
- Vlaanderen. (2022). *EPB-eisen bij bouwaanvraag/melding in 2022*. <https://www.vlaanderen.be/epb-pedia/epb-plichtig-toepassing-en-eisen/epb-eisentabellen-per-aanvraagjaar/epb-eisen-bij-bouwaanvraag-melding-in-2022>



# Semantics-based expert system for fault detection in air handling units

Sebastian Blechmann<sup>1\*</sup>, Hannah Görigk<sup>1</sup>, Rita Streblow<sup>1</sup>, Dirk Müller<sup>1</sup>

*1 RWTH Aachen University, E.ON Energy Research Center, Institute for Energy Efficient Buildings and Indoor Climate  
Mathieustr. 10  
52074 Aachen, Germany*

*\*Corresponding author: sebastian.blechmann@eonerc.rwth-aachen.de*

## ABSTRACT

Heating, ventilation and air conditioning systems, e.g., air handling units (AHUs), play a key role in modern building energy systems (BES) as they account for a high share of the energy usage, e.g., 30 % within the U.S. commercial building sector. Unfortunately, many faults occur during the operation of AHUs leading to higher energy usage and the need for expert personnel monitoring the according plants. The latter is a time-consuming task and is assisted by fault detection systems nowadays. While there are many different approaches to detect faults in air handling units, this paper presents an approach based on semantic knowledge.

For this approach, an ontology for fault detection and diagnosis (FDD) in AHUs is developed. The FDD ontology describes which components, e.g., temperature sensors or valves, can face what kinds of faults. Hence, the FDD ontology contains generic knowledge and is interoperable and reusable. Furthermore, generic semantic fault rules based on the air handling performance assessment rules (APAR) are developed.

For this generic concept, the actual information about the examined plants, their configuration, sensors, actuators, and controls are stored in a knowledge graph based on existing ontologies, like Brick Schema.

For the evaluation of the fault rules, the configuration of the plants is queried and rules get activated if the necessary components needed for evaluation of the rules are present. Afterwards, the according time series data for rule evaluation are fetched for analysis, following the linked data principle - in this work from a cloud platform. Depending on the analysis result, fault messages are gathered in a list and sorted according to their incidence to allow a certain prioritization for maintenance personnel. The fault notation follows a unified schema allowing personnel to understand and locate the faults fast.

The developed approach is validated using historical data of a real AHU on our premises. We inject faults into the historical data, e.g., drift, stuck, bias, fouling, abnormal, and frozen. The results indicate a high rate of fault detection, e.g., average accuracy of 99.3 %, precision of 97.85, sensitivity of 95.6 %, and Matthews Correlation Coefficient of 98.4 %. Therefore, the approach is considered valid for fault detection in AHUs.

In the future, it is planned to implement more complex faults, e.g., valve needle separated from drive or control faults. Furthermore, the semantic enriched plant configuration shall be used to improve the discovery of fault-symptom relationships.

The presented approach has the big advantage that the knowledge about air handling units and their faults needs to be formulated only once, leveraging semantic knowledge. Therefore, this generic solution can be used for diverse AHU configurations potentially reducing FDD development efforts.

## KEYWORDS

Fault detection and diagnosis (FDD), FDD Ontology, Air Handling Unit (AHU), Fault Component Relationship (FCR), Rule-based FDD

## 1 INTRODUCTION

Building energy systems (BES) are still responsible for a high energy share, e.g., heating, ventilation and air conditioning (HVAC) systems still account for 30 % of the energy usage (Goetzler et al. 2017). Yet, during the operation of BES, on average 245 faults occur per month and building (Crowe et al. 2023). One common approach to detect faults and, where possible,

their causes during their operation is the use of fault detection and diagnosis (FDD) systems. A study by Kramer et al. (Kramer et al. 2020) shows median savings of 6 % in building energy usage in using FDD systems in the first year after installation of the FDD system. Knowledge-based FDD approaches use expert knowledge, e.g., rules to detect abnormalities. In current FDD approaches, manufacturers usually use their own proprietary FDD software, data structure, and fault naming (Chen et al. 2021). This data heterogeneity leads to longer application development time and maintenance personnel need more time to get familiar with faults in a BES due to the absence of a standard for FDD report format. This culminates in the fact that some “fault messages can only be interpreted by FDD tool developers” (Chen et al. 2021).

According to Gallaher et al. (Gallaher et al. 2004), insufficient data interoperability costs \$15.8 billion per year in the U. S. capital facilities industry. The issue of syntactic interoperability can be solved by the use of protocol-translating gateways or middleware structures, e.g., cloud platforms. But the issue of semantic interoperability remains. One way to overcome this issue is the use of semantic metadata models enabling operational cost reduction (Bergmann et al. 2022), e.g., in FDD applications. There are already metadata models formalizing semantic descriptions in the building energy sector, all focusing on their very own area, e.g., Brick Schema (Brick) (Balaji et al. 2018) modeling components in BES, like HVAC systems, e.g., air handling units (AHUs), lighting, floors, and rooms. Chen et al. (Chen et al. 2021) created a taxonomy to describe the fault nature, fault component, fault type, fault location, and fault equipment to provide a unified description for fault naming in HVAC systems. The authors provide some examples of possible fault-component (FCR) or fault-symptom relationships (FSR). However, the taxonomy itself does not provide distinct FCR or FSR. Furthermore, in contrast to ontologies, taxonomies do not provide formal descriptions in common standardized language, like the resource description framework (RDF) (Cyganiak et al. 2014).

There are already a few ontology-based expert approaches for FDD in BES: During the development of the proposed FDD ontology, a similar, independently developed approach was published by Hwang et al. (Hwang, Akinci, and Berges 2023). While the authors follow the same approach in modeling and relating certain faults to certain Brick components enabling FSR, they do not use unified fault naming conventions, fault types, or fault locations. Furthermore, faults like malfunctioning, stuck, leakage, fouling, and block are modeled for components like valves, coils, pumps, dampers, and fans by the authors. Yet, common sensor faults are not modeled. In another approach by Pruvost et al. (Pruvost, Wilde, and Engel-Rosenblatt 2023), the authors create an ontology, re-using parts from Brick. They use a rule-based approach to detect faults and risks in the operation of BES. They model symptomatic faults, like simultaneous heating and cooling, overheating, or too low temperatures. Yet, they do not model sensor or actuator faults as such and do not model FCR or FSR. To close this gap, we develop a rule-based expert system for FDD in BES using semantic information based on formalized knowledge. For this, we design an FDD ontology, reusing concepts from Brick, to formalize the modeling of faults and their possible relations according to the taxonomy by Chen et al. (Chen et al. 2021). Additionally, we apply the air handling unit performance assessment rules (APAR) (Schein et al. 2006) to detect faults in the operation of AHUs. We inject faulty data in the historical data of a real AHU and develop a fault detection application written in Python to detect these faults based on the formal knowledge in the FDD ontology. The latter is saved in a fault report for all detected faults to assist maintenance personnel in locating and prioritizing faults.

The remainder is structured as follows:

In chapter 2, we summarize faults and FDD systems in BES. In chapter 3, we describe and evaluate existing metadata models and ontologies for BES followed by the proposed FDD ontology. In chapter 4, we present the used FDD metrics and our use case: A rule-based FDD

application on the base of the APAR using knowledge from the FDD ontology. Chapter 5 gives an overview of the results including their discussion. Last, we draw conclusions from this work followed by an outlook in chapter 6.

## 2 FAULTS AND FDD SYSTEMS IN THE BUILDING ENERGY DOMAIN

There are many faults detected in the operation of BES and they account for a high share of energy consumption in buildings (Crowe et al. 2022; Kramer et al. 2020). However, different studies develop their own fault naming convention and FCR.

Crowe et al. (Crowe et al. 2023) analyze FDD data from 317 buildings in regard to faults in the operation of the BES. The authors originally find 1563 uniquely named faults, apply the unified taxonomy from Chen et al. (Chen et al. 2021), and narrow down the number of unique faults to 182. The taxonomy allows the representation of equipment, e.g., AHU, the component location, e.g., supply air, the component type, e.g., temperature sensor, and last the fault nature, e.g., frozen. Furthermore, the taxonomy allows the classification of faults in condition-based (CB), behavior-based (BB), and outcome-based (OB) faults. Frank et. al (Frank et al. 2019) define a CB fault as a fault that leads to an undesired physical condition inside the plant though they do not always cause faulty behavior. One could argue that these kinds of faults are the “root cause” of other types of faults. An example would be a stuck valve. BB faults are defined by their impact on the behavior of the plant. Often, they do not cause the fault but rather show fault “symptoms”. A typical BB fault is simultaneous heating and cooling. OB faults are defined by the overall impact on the metrics of the plant, e.g., high cooling water consumption.

Kim et al. (Kim et al. 2021) analyze 26 different studies regarding fault occurrences in buildings and define 18 types of equipment with each up to 8 different types of faults. Leong (Leong 2019) names fault natures similar to the already discussed taxonomy. The author presents typical faults and components in which they could occur.

Comparing the presented studies, it becomes clear that, there are approaches for unified fault naming in HVAC systems but there is no standard yet. Furthermore, on the one hand, there is no complete list of faults available. On the other hand, the heterogeneous naming schema for faults makes it difficult to have an unambiguous mapping of possible faults to components (Kim et al. 2021).

According to Matetić et al. (Matetić et al. 2022), there are four different categories for FDD approaches: knowledge-based, data-based, physics-based, and hybrid.

In this work, we focus on the use of knowledge-based FDD systems and their wide applicability based on expert knowledge, e.g., formulated in rules. A ruleset often used in FDD expert systems in BES is the set of AHU Performance Assessment Rules (APAR) first described by House et al. (House, Vaezi-Nejad, and Whitcomb 2001). They provide 28 expert rules focussing on temperature control in AHUs depending on the operational state of the plant. These generic rules can find a variety of faults while only depending on eleven sensors in the plant.

To express the connection between the APAR, the components needed for their evaluation, and CB and BB faults, we develop an FDD ontology which is described in the following chapter.

## 3 MODELING OF BES COMPONENTS AND FAULTS

### 3.1 Existing metadata models and naming schemas

Semantic metadata models such as Brick, SAREF (Daniele, den Hartog, and Roes 2015), and Project Haystack (“Project Haystack” 2014) can improve the interpretability and interoperability of an FDD System, enabling the widespread use of fault detection across different BES. Even though there is a multitude of semantic metadata models in the building

sector, no existing description can represent a whole BES. Furthermore, there is no standardization between the models and the same object may exist with different descriptions in different models (Bergmann et al. 2022).

An often-used model is Brick which, amongst other things, models BES components in HVAC systems and thermal zones (Balaji et al. 2018). With the current Brick release version 1.3, Brick neither models faults of BES components nor supports FCR or FSR. However, an addition to Brick has been proposed recently by Hwang et al. (Hwang, Akinci, and Berges 2023): Fault-Symptom Brick (FSBrick), which tries to close the gap by adding faults and FCR to Brick. For fault naming, the authors follow the naming conventions defined by Chen et al. (Chen et al. 2021) in their unified taxonomy for HVAC faults. FSBrick has been developed in parallel to the work at hand and was published recently. It is a very promising approach, however, it does not yet model sensor faults, fault types, or fault locations.

Another ontology is proposed by Pruvost et al. (Pruvost, Wilde, and Enge-Rosenblatt 2023). Reusing parts of Brick and other metadata models, they create a set of ontologies aggregated as SENSE ontology which covers symptomatic faults but does not model sensor or actuator faults. The aforementioned taxonomy proposed by Chen et al. (Chen et al. 2021) covers naming conventions for equipment, faults, and fault locations in order to make faults easy to locate and fix. They introduce a fault name convention that is distinct, reproducible, and, if built upon a standardized knowledge base, applicable to other BES. However, in contrast to ontologies, taxonomies prescribe the fault structure and relationships to certain components but do not describe them in a standardized format, like RDF, allowing knowledge inference.

As heterogenous and incomplete fault mapping proves difficult to make different BES and FDD interoperable and easy to use for maintenance personnel we develop our own hierarchical ontology describing the concepts mentioned above. We apply the taxonomy by Chen et al. as the main structure and naming schema while adding information about BES components and their associated faults based on findings of Leong et al. and Kim et al. (Leong 2019; Kim et al. 2021).

### 3.2 Proposed FDD ontology

Due to the shortcomings of current metadata models and their fault coverage combined with the purpose of formally expressing unified fault nature, fault types, fault location, and FCR, we decided to create an FDD ontology in RDF syntax to express these factors in one ontology.

For describing the relationships and entities of components and equipment, structures of Brick are reused. All components' data points are modeled as Brick Points, which makes internal naming conventions irrelevant as they are distinctly identified by their Brick type. Furthermore, we assign possible FCR (`fdd:hasPotentialFault`), a link to historical data (`ref:hasTimeseriesReference`), and the location of the component (`fdd:hasSection`). Lastly, we create a link to expert rules needing measurements of these components or equipment in order to be executed (`fdd:requiresComponent`). The last definition is important to determine the number of rules in a ruleset that fulfill all criteria to be used for fault detection in a plant. For possible FSR, we currently relate rules to certain components based on prior work from Schein (Schein 2006) (`fdd:affectedBy`). The exact modeling of FSR is important and yet out of scope of this paper. Figure 1 shows a modeling example of an AHU supply air temperature sensor.

In future work, it needs to be evaluated how our approach can be aligned with FSBrick to represent FSR in more detail. Whenever possible, the naming of entities and faults is identical to the taxonomy by Chen et al. to avoid ambiguity.

Using the advantages of inferred knowledge in knowledge graphs using RDF syntax, not all relationships have to be added manually. A reasoner can be used to infer relationships and connections automatically if certain information about a component is known. For example, the assignment of a section to a sensor or an FCR is automatically assigned based on the

corresponding Brick component definition. Furthermore, it can be validated which APAR rules are applicable by checking whether the required components are available. When not all requirements are met, the rule cannot be executed for fault detection in the according plant. When all requirements are met, a rule gets marked activated for this plant. With the presented FDD ontology and its formalized knowledge, it is possible to create a detailed fault report to make fault localization and fixing as time-efficient and easy as possible.

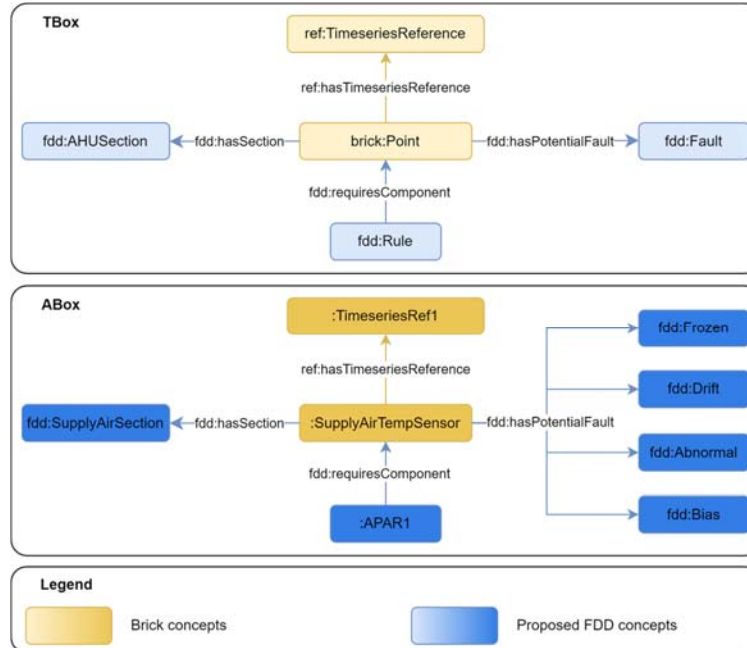


Figure 1: Supply air temperature sensor used in rule 1 of the APAR modeled with the developed FDD ontology.

**Disclaimer:** The ontology presented corresponds to the status as of 1 July 2024 and is still under development.

## 4 USE CASE

### 4.1 FDD application and experiments

The semantic information of a real AHU on our premises, see figure 2, is modeled with Brick and the proposed FDD ontology. The information is stored in a knowledge graph and can be queried from a graph database.

To detect faults in the operation of an AHU, we develop a rule-based FDD application written in Python. The FDD application runs in a loop and checks for possible faults every run. In the FDD application, the APAR set is included. Equation 1 shows rule 1 of the APAR, checking if the supply air temperature ( $T_{sa}$ ) is smaller than the sum of the mixed air temperature ( $T_{ma}$ ) and a delta of the supply air fan ( $T_{sf}$ ) minus a plant-specific tolerance factor ( $\epsilon_T$ ).

$$T_{sa} < T_{ma} + \Delta T_{sf} - \epsilon_T \quad (1)$$

To validate the rule, historical data from the according data points of the AHU are evaluated. They are fetched from a cloud platform following the linked data principle.

In each iteration of the FDD application loop with a fixed time period ( $\Delta t$ ), in this work 30 minutes, it follows the link towards historical data, fetches it, and evaluates each activated

rule. Before a rule is evaluated, the fetched historical data pass a Hampel filter to find potential outliers.

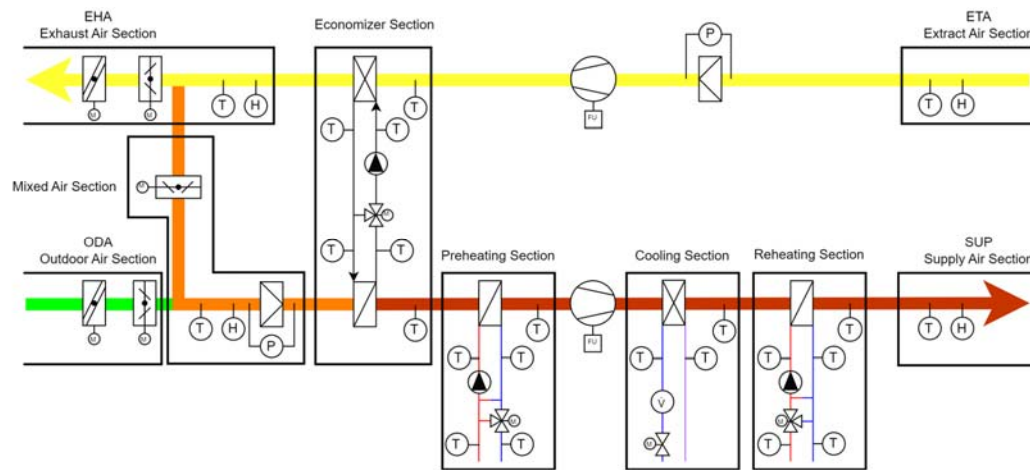


Figure 2: Schematic of used AHU and the proposed sections for fault location assessment.

For validation of the proposed implementation, faulty data is injected into the historical data of the plant before it is fetched by the FDD application. As a reference scenario, untampered historical data is analyzed to exclude possible pre-existing faults from the actual experiments at hand. As proof of concept, a temperature sensor and a valve are chosen as representatives for sensors and actuators, and faults are injected in five experiments at a certain time step ( $t_{\text{fault}}$ ). Experiment 0 is the reference scenario. In experiment 1, drift and stuck faults are injected, in experiment 2, fouling, offset, and frozen faults are injected. In experiment 3, a bias fault is injected while in experiment 4, a combination of drift, stuck, and bias are injected. Last, in experiment 5, a combination of fouling, abnormal, frozen, and bias is injected. The faulty data is injected at the beginning of each experiment ( $t_{\text{fault}}=0$ ) with a data resolution ( $t$ ) for each experiment of 1 s. All experiments are stopped after a total time frame of 4 h since the AHU operates statically and this work serves just as a proof of concept. This leads to a total amount of data in each experiment of 14,400 per data point.

The actual implementation of each fault is demonstrated in table 1 where each value can be replaced according to the fault description. Depending on the injected fault, the value is replaced by a constant change (e.g.,  $x_{(t)} \pm 2\text{K}$  as offset) or by an increasing or decreasing change dependent on the current time ( $t$ ) divided by the inspected time period ( $\Delta t$ ). The experiments are then evaluated using the metrics from the following section.

Table 1: Fault description for injected faults.

Fault component	Injected faults	Fault description for $t \geq t_{\text{fault}}$	Fault component	Injected fault	Fault description for $t \geq t_{\text{fault}}$
Sensor	Frozen	$x_{(t)} = x_{(t-t_{\text{fault}})}$	Valve	Stuck	$x_{(t)} = x_{(t-t_{\text{fault}})}$
	Offset	$x_{(t)} \pm 2\text{K}$		Fouling	$-x_t * (0.12 * t) / \Delta t$
	Drift	$\pm x_t * (0.12 * t) / \Delta t$			

## 4.2 Metrics

For the validation of the FDD application, confusion matrices can be used. For that, it can be distinguished between false-positives (FP), false-negatives (FN), true-positives (TP), and true-negatives (TN) predictions over all predictions ( $n_{\text{pred}}$ ). With this, the following metrics are calculated:

$$Accuracy = \frac{TP+TN}{n_{pred}} \quad (2)$$

$$Precision = \frac{TP}{TP+FP} \quad (3)$$

$$Recall = \frac{TP}{TP+FN} \quad (4)$$

$$F_1 = \frac{2*TP}{2*TP+FP+FN} = \frac{2*Recall*Precision}{Precision+Recall} \quad (5)$$

$$MCC = \frac{TP*TN - FP*FN}{\sqrt{(TP+FP)*(TP+FN)*(TN+FP)*(TN+FN)}} \quad (6)$$

Accuracy, precision, and recall (equations 2-4) are classical metrics in binary classification, living in the range [0, 1]. The commonly used F1-score (equation 5) ranges in [0, 1] with F1 = 0 standing for all positive samples misclassified and F1 = 1 for perfect classification. We also take the Mathews Correlation Coefficient (MCC) (Matthews 1975), living in the range [-1, 1], into consideration (equation 6). An MCC = 1 represents perfect classification, MCC = 0 represents random classification, and MCC = -1 represents perfect misclassification. The F1-score does not consider imbalances in the dataset, e.g., if there are way more positive than negative data, in contrast, the MCC does consider such imbalances (Chicco and Jurman 2020) and is therefore taken into account in this study.

For the fault report, we calculate the cumulative sum chart (CUSUM) (Trojanová et al. 2009). The CUSUM represents how often and for how long faults occur. It can be calculated according to equation (7). Here, the fault incidence ( $R_i(t)$ ) rises each time step a fault is detected and decreases every time step the fault is not detected anymore. It is calculated by the maximum of 0 and the binary fault state ( $m(f_i, s_j)$ ) minus a constant (k) plus the previous fault incidence. It is taken as a metric for maintenance personnel to observe and assess detected faults and the duration for which they have persisted; the higher the CUSUM for a fault ( $i$ ), the longer the according fault persists.

$$R_i(t) = \max(0, m(f_i, s_j) - k + R_i(t - 1)) \quad (7)$$

We use the CUSUM as an indicator for fault incidence which will be displayed in the fault report next to information like the detected fault, fault type, affected component, fault location, faulty and reference values, and the detection time.

## 5 RESULTS AND DISCUSSION

The metrics indicate a high rate of fault detection, e.g., average accuracy of 99.3 %, precision of 97.85, sensitivity of 95.6 %, and MCC of 98.4 % over all five experiments. Although the FDD algorithm checks for self-injected faults, it does not deliver perfect results. This is due to the fact that some parameters, e.g., the specific tolerance parameter of rule 1, are not chosen perfectly and some faults interfere with each other so that they cannot be isolated and detected easily. The parameters need fine-tuning for each plant. Still, the inference of different faults is not yet properly examined. As mentioned, there are already approaches examining FSR modeling certain BB faults to possible CB faults, e.g., for the APAR (Schein 2006), or alarms to component faults, e.g., based on Brick (FSBrick) that can be modeled and aligned in the FDD ontology in the future. Yet, this is out of scope of this paper and needs thorough discussions of

the particular faults. Additionally, further rule sets to detect more complex faults, e.g., a valve needle separated from drive or control faults, can be implemented and analyzed over a longer time frame. Nevertheless, the presented approach is considered a proof of concept for FDD in the presented framework with self-injected faults as the high majority of the injected faults is found based on knowledge derived from the FDD ontology.

As per the fault report, the detected faults are logged in a CSV file and can be displayed in a simple column structure as depicted in table 2. Following the structure of the fault taxonomy by Chen et al., this fault report can distinctly identify faults and aid to locate them quickly. Furthermore, the detected faults can be prioritized based on their incidence, fault type, and faulty values. This is a huge advantage for maintenance personnel since digging through unstructured documents to understand the fault message and locating the actual faulty component are not necessary anymore.

Furthermore, FDD algorithm development engineers can re-use the knowledge from the presented FDD ontology. This saves time and cost in the development of FDD applications. However, the presented metrics only cover the actual FDD and not the portability to other plants. The work at hand delivers a proof of concept of an FDD ontology being used for knowledge-based FDD in a single AHU. Therefore, the approach shall be validated for the use on the other plant configurations in future work, e.g., using a combination of experiments and simulations. This way, fault inferences and the modeling of FSR can actually be examined. In doing so, the idea of the ontology to represent generic, re-usable knowledge can be validated.

Table 2: Exemplary fault report filled with dummy components and values.  
(BB = behavior-based, CB = condition-based, i = incidence, n = index)

n	time	component	fault	type	section	i	faulty values
1	10:00	SATsen	Abnormal	BB	SupplyAirSection	0.7	„value“: 18.4, „setpoint“: 21
2	10:00	RHValve	Stuck	CB	ReheatingSection	0.7	„value“: 19, „setpoint“: 28
1	10:30	SATsen	Abnormal	BB	SupplyAirSection	1.4	„value“: 18.5, „setpoint“: 21
2	10:30	RHValve	Stuck	CB	ReheatingSection	1.4	„value“: 19, „setpoint“: 90

## 6 CONCLUSIONS

Ontologies bear huge potential towards data interoperability and interpretability. Although approaches to standardize semantic metadata schemas in BES exist, faults, their relationships to certain components, as well as fault types and locations are not formally described in ontologies. This is why we presented an FDD ontology and used its information in a rule-based FDD application to detect faults and their characteristics in the operation of an AHU. We injected faults in the historical operational data of the AHU and used the widely applied APAR for the actual FDD. We were able to detect most of the injected faults and create a fault report based on the knowledge modeled in the ontology. This way, maintenance personnel can prioritize faults based on their incidence and type while also locating faults with the given information. Moreover, the ontology allows FDD application development engineers to re-use the concepts presented in this work and adapt them to their use cases. However, the presented ontology is only a small part of the necessary changes to make FDD more usable. For future work, information on how faults affect each other needs thorough discussion and proper modeling, e.g., which BB fault can relate to which CB fault. This is particularly important considering the fact that faults can influence each other making the fault detection of the root cause fault even more difficult. This can be modeled with FSR. Furthermore, the metrics presented in this work only cover the aspect of the actual FDD itself, which is important for



showing the functionality of the approach, but not the portability of the ontology. As the generic knowledge is already formulated, this could be achieved by applying the presented approach to other plants, e.g., with different configurations in future studies reducing time and cost for FDD development. This way the generic sense of this approach can be validated and might open up ways for automatic FDD.

It is planned to publish the proposed FDD ontology with the World Wide Web Consortium.

## 7 ACKNOWLEDGEMENTS

We gratefully acknowledge the financial support by the German Federal Ministry for Economic Affairs and Climate Action (BMWK), promotional reference 03EN1030B.

## 8 REFERENCES

- Balaji, Bharathan, Arka Bhattacharya, Gabriel Fierro, Jingkun Gao, Joshua Gluck, Dezhi Hong, Aslak Johansen, et al. 2018. “Brick : Metadata Schema for Portable Smart Building Applications.” *Applied Energy* 226 (September):1273–92. <https://doi.org/10.1016/j.apenergy.2018.02.091>.
- Bergmann, Harry, Cory Mosiman, Avijit Saha, Selam Haile, William Livingood, Steve Bushby, Gabe Fierro, et al. 2022. “Semantic Interoperability to Enable Smart, Grid-Interactive Efficient Buildings,” January. <https://escholarship.org/uc/item/1325d5j3>.
- Chen, Yimin, Guanqing Lin, Eliot Crowe, and Jessica Granderson. 2021. “Development of a Unified Taxonomy for HVAC System Faults.” *Energies* 14 (17): 5581. <https://doi.org/10.3390/en14175581>.
- Chicco, Davide, and Giuseppe Jurman. 2020. “The Advantages of the Matthews Correlation Coefficient (MCC) over F1 Score and Accuracy in Binary Classification Evaluation.” *BMC Genomics* 21 (1): 6. <https://doi.org/10.1186/s12864-019-6413-7>.
- Crowe, Eliot, Yimin Chen, Jessica Granderson, Hayden Reeve, Lucas Troup, David Yuill, Yuxuan Chen, and Lawrence Berkeley National Laboratory. 2022. “What We Learned From Analyzing 18 Million Rows of Commercial Buildings’ HVAC Fault Data.” <https://escholarship.org/uc/item/8d378066>.
- Crowe, Eliot, Yimin Chen, Hayden Reeve, David Yuill, Amir Ebrahimifakhar, Yuxuan Chen, Lucas Troup, Amanda Smith, and Jessica Granderson. 2023. “Empirical Analysis of the Prevalence of HVAC Faults in Commercial Buildings.” *Science and Technology for the Built Environment* 29 (10): 1027–38. <https://doi.org/10.1080/23744731.2023.2263324>.
- Cygniak, Richard, David Wood, Markus Lanthaler, Graham Klyne, Jeremy J. Carroll, and Brian McBride. 2014. “RDF 1.1 Concepts and Abstract Syntax.” February 25, 2014. <https://www.w3.org/TR/2014/REC-rdf11-concepts-20140225/>.
- Daniele, L. M., F. T. H. den Hartog, and J. B. M. Roes. 2015. “Created in Close Interaction with the Industry: The Smart Appliances REference (SAREF) Ontology.” *Formal Ontologies Meet Industry : Proceedings 7th International Workshop on Formal Ontologies Meet Industry, FOMI 2015, 5 August 2015, Berlin, Germany*, 100. [https://doi.org/10.1007/978-3-319-21545-7\\_9](https://doi.org/10.1007/978-3-319-21545-7_9).
- Frank, Stephen, Guanqing Lin, Xin Jin, Rupam Singla, Amanda Farthing, and Jessica Granderson. 2019. “A Performance Evaluation Framework for Building Fault Detection and Diagnosis Algorithms.” *Energy and Buildings* 192 (June):84–92. <https://doi.org/10.1016/j.enbuild.2019.03.024>.
- Gallaher, Michael P., Alan C. O’Connor, John L. Dettbarn, Jr., and Linda T. Gilday. 2004. “Cost Analysis of Inadequate Interoperability in the U.S. Capital Facilities Industry.”

- NIST GCR 04-867. National Institute of Standards and Technology. <https://doi.org/10.6028/NIST.GCR.04-867>.
- Goetzler, William, Richard Shandross, Jim Young, Oxana Petritchenko, Decker Ringo, Sam McClive, and Building Technologies Office Corporate. 2017. “Energy Savings Potential and RD&D Opportunities for Commercial Building HVAC Systems.” DOE/EE--1703, 1419622. <https://doi.org/10.2172/1419622>.
- House, John M., Hossein Vaezi-Nejad, and J. Michael Whitcomb. 2001. “An Expert Rule Set for Fault Detection in Air-Handling Units.” *ASHRAE Transactions* 107 (ASHRAE Transactions-2001 Winter Meeting, Atlanta, GA, Volume 107, Part 1): 858–74.
- Hwang, Min Young, Burcu Akinci, and Mario Berges. 2023. “FSBrick: An Information Model for Representing Fault-Symptom Relationships in HVAC Systems.” In *Proceedings of the 10th ACM International Conference on Systems for Energy-Efficient Buildings, Cities, and Transportation*, 69–78. BuildSys '23. Istanbul, Turkey: Association for Computing Machinery. <https://doi.org/10.1145/3600100.3623729>.
- Kim, Janghyun, Kim Trenbath, Jessica Granderson, Yimin Chen, Eliot Crowe, Hayden Reeve, Sarah Newman, and Paul Ehrlich. 2021. “Research Challenges and Directions in HVAC Fault Prevalence.” *Science and Technology for the Built Environment* 27 (5): 624–40. <https://doi.org/10.1080/23744731.2021.1898243>.
- Kramer, Hannah, Guanjing Lin, Claire Curtin, Eliot Crowe, and Jessica Granderson. 2020. “Proving the Business Case for Building Analytics,” October. <https://doi.org/10.20357/B7G022>.
- Leong, Cheng Yew. 2019. “Fault Detection and Diagnosis of Air Handling Unit: A Review.” Edited by Lim Meng Hee. *MATEC Web of Conferences* 255:06001. <https://doi.org/10.1051/mateconf/201925506001>.
- Matetić, Iva, Ivan Štajduhar, Igor Wolf, and Sandi Ljubic. 2022. “A Review of Data-Driven Approaches and Techniques for Fault Detection and Diagnosis in HVAC Systems.” *Sensors* 23 (1): 1. <https://doi.org/10.3390/s23010001>.
- Matthews, B. W. 1975. “Comparison of the Predicted and Observed Secondary Structure of T4 Phage Lysozyme.” *Biochimica et Biophysica Acta (BBA) - Protein Structure* 405 (2): 442–51. [https://doi.org/10.1016/0005-2795\(75\)90109-9](https://doi.org/10.1016/0005-2795(75)90109-9).
- “Project Haystack.” 2014. Project Haystack Home. May 2014. <https://project-haystack.org/>.
- Pruvost, Hervé, Andreas Wilde, and Olaf Enge-Rosenblatt. 2023. “Ontology-Based Expert System for Automated Monitoring of Building Energy Systems.” *Journal of Computing in Civil Engineering* 37 (1): 04022054. [https://doi.org/10.1061/\(ASCE\)CP.1943-5487.0001065](https://doi.org/10.1061/(ASCE)CP.1943-5487.0001065).
- Schein, Jeffrey. 2006. “Results from Field Testing of Embedded Air Handling Unit and Variable Air Volume Box Fault Detection Tools.” NIST IR 7365. Gaithersburg, MD: National Institute of Standards and Technology. <https://doi.org/10.6028/NIST.IR.7365>.
- Schein, Jeffrey, Steven T. Bushby, Natascha S. Castro, and John M. House. 2006. “A Rule-Based Fault Detection Method for Air Handling Units.” *Energy and Buildings* 38 (12): 1485–92. <https://doi.org/10.1016/j.enbuild.2006.04.014>.
- Trojanová, J., J. Vass, K. Macek, J. Rojiček, and P. Stluka. 2009. “Fault Diagnosis of Air Handling Units.” *IFAC Proceedings Volumes* 42 (8): 366–71. <https://doi.org/10.3182/20090630-4-ES-2003.00061>.

# Health-Equivalent Energy Efficiency Factor, combined metric of harm and energy use

Klaas De Jonge <sup>\*1,2</sup>

*1 Ghent University, Department of Architecture and Urban Planning*

*Jozef Plateastraat 22  
9000 Ghent, Belgium*

*2 Flanders Research Foundation (FWO)*

*Leuvenseweg 38  
1000 Brussel, Belgium*

*\*Corresponding author: klaas.dejonge@UGent.be*

## ABSTRACT

The inclusion of health-based performance indicators and metrics in ventilation system design and research is a widely discussed topic in recent years. This is due to increased awareness about the health implication of indoor air quality and due to the need for innovative ventilation system control (smart ventilation) to limit building energy use.

The main target of most smart ventilation systems on the market today is limiting the building energy use while maintaining a comfortable indoor environment. The health aspect is therefore often overlooked although it would lead to a dilemma is ventilation system optimization: to what extent does achieving energy saving justify an increase in the concentration levels of unhealthy pollutants?

The rationale behind a new metric is introduced that combines and quantifies the combined performance of energy saving and a harm based metric of a smart ventilation system compared to a chosen reference as the ratio between the energy use indicator of the smart ventilation system and the energy use of the reference line at equal harm: The Health-Equivalent energy efficiency factor. The used reference can be either a pre-defined ventilation concept (e.g. continuous ventilation) or based on energy and health targets.

Eight smart ventilation strategies are modelled, simulated, and analysed and for each, the health-equivalent energy efficiency factor is calculated using two possible references. The first reference-line is defined by the base continuous ventilation system simulated at 10%, 50% and 100% of the nominal flow rate,  $\eta_{\text{system}}$ . The second reference-line is a straight line connecting two extreme, theoretical scenarios: (1) which energy use is acceptable for a situation with *no harm* and (2) what is the minimum target of harm for a situation *without any energy use*,  $\eta_{\text{linear}}$ .

Based on the results and insights gained while applying the metric,  $\eta_{\text{linear}}$  is preferred as it results in more versatile and more widely applicable metric. The application of the metric shows that only one of the smart ventilation systems under investigation is unable to provide health-equivalent indoor air quality energy efficient based on both  $\eta_{\text{system}}$  and  $\eta_{\text{linear}}$ . The performance of the nominal reference system C (mechanical extract ventilation) is unacceptable based on  $\eta_{\text{linear}}$ .

## KEYWORDS

Health performance, Energy efficiency, Smart ventilation, Performance-based design

## 1 INTRODUCTION

The inclusion of health-based performance indicators and metrics in ventilation system design and research is a widely discussed topic in recent years. This is due to increased awareness concerning the health implication of indoor air quality (Morantes et al. 2022; Liu et al. 2023; Asikainen et al. 2016; De Jonge and Laverge 2022) and due to the need for innovative ventilation system control (smart ventilation) to limit building energy use (De Jonge, Ghijssels, and Laverge 2023; Guyot et al. 2019). Recently, also on a legislative level the (public) health implication of indoor air quality, ventilation systems and how they are controlled has gained importance with the topic of health being addressed in the drafts of the EN15665 and EN 16798-1-3 standards, the health based equivalence approach adopted in the ASHRAE 62.2 standard (Sherman, Walker, and Logue 2012) and the explicit inclusion of indoor environmental quality in the new EPBD directive advocating for improving energy efficiency and indoor environmental quality in parallel when buildings are renovated (Council of the European Union - General Secretariat of the Council 2023).

This context creates a need for practical indicators used by Indoor Air Quality (IAQ) management system designers or R&D to be able to decide on optimal solutions with regards to both the energy use and health implication, which are often of conflicting interest (e.g. for continuous airflow ventilation systems, increasing the overall ventilation airflow rates typically lowers the health impact but increases the related energy use). This type of indicator could potentially become part of national implementation of the new EPBD directive or other legislative or standardisation initiatives.

This paper outlines and applies an indicator specifically developed to support the decision making in health-focused IAQ-management system design and control. The results of this paper are part of a larger study that describes a consistent set of indicators that also address other focus points of IAQ-management (e.g. comfort, acute health effects, mold prevention) (De Jonge 2023).

## 2 HEALT-EQUIVALENT ENERGY EFFICIENCY FACTOR

### 2.1 Rationale

#### 2.1.1 Health impact indicator

The proposed health impact indicator is the chronic population health effect attributable to the exposure to the indoor air. This impact can be expressed in terms of Disability-Adjusted Life-Years (DALYs), which is a well known and widely used metric of harm (C. J. Murray 1994; C. J. L. Murray et al. 1996). For this research the health impact indicator was derived from simulated individual exposure concentration data using combined Building Energy Simulation and Indoor Air Quality (BES-IAQ) dynamic simulation and by use of the novel dynamic DALYs concept (De Jonge and Laverge 2022).

Other health effects like acute health effects should be accounted for using acute exposure limits (e.g. AEGL, DNEL). To limit the health effects from exposure to spores from mold, a source control strategy is proposed where mold-growth is prevented. A separate indicator is included in the larger consistent set of indicators to limit this risk (De Jonge 2023) but is not further discussed in this paper.

#### 2.1.2 System energy use indicator

The definition of the energy use indicator depends partly on the methods and models used for the estimation of the performance and consist of the most representative sum of energy use. The proposed method is the use of dynamic combined BES-IAQ dynamic models as they allow for a prediction of the building heating energy use which includes the direct and indirect impact

of IAQ-management systems on the building heating energy use as well as dynamic variation of outdoor condition (e.g. higher impact of ventilation on the energy demand when outdoor temperatures are low; higher natural infiltration rates when indoor-outdoor temperature difference are higher; thermal performance of heat exchangers and by-pass systems). The electric fan energy use associated with the air handling unit makes up the second part of the energy use indicator.

### 2.1.3 Combined metric

For each IAQ-management system, the associated health impact indicator and system energy use indicator can be determined. However, as previously mentioned, two IAQ-management strategies can result in conflicting results where the first solution has a minimal impact on health and a high energy use indicator while the latter has a low associated energy use but a higher impact on health. To aid the decision making in such case, the health-equivalent energy efficiency factor can be determined.

This factor is the ratio between the energy use indicator of the IAQ management strategy and the energy use of the reference line at equal harm.

This concept extends on the approach used in support of the current Belgian EPB legislation that applied a similar method to determine the comfort equivalent energy efficiency for smart ventilation control strategies (Caillou et al. 2014).

## 2.2 Definition

For a system with relative indicators  $[E_{\text{sys}}, D_{\text{sys}}]$ :

$$\eta = \frac{E_{\text{sys}}}{E_{\text{sys,ref}}(D_{\text{sys}})} \quad (1)$$

With

- $\eta$  [-] Health equivalent energy efficiency factor
- $E_{\text{sys}}$  [kwh] System relative energy use indicator value
- $E_{\text{sys,ref}}(D_{\text{sys}})$  [kwh] Reference relative energy use indicator value for  $D_{\text{sys}}$
- $D_{\text{sys}}$  [yr] System relative health indicator value

Figure 1 illustrates how the health-equivalent energy efficiency factor is derived from a plot where energy use indicator is the x-axis and health impact indicator is the y-axis. One IAQ-management strategy shows as one point on the plot.

From an energy-efficiency point of view, systems that lie above their respective reference line should not be allowed to market as its use only contributes negatively to the relative energy efficiency. In other words, they are not pareto-optimal with regards to their reference systems.

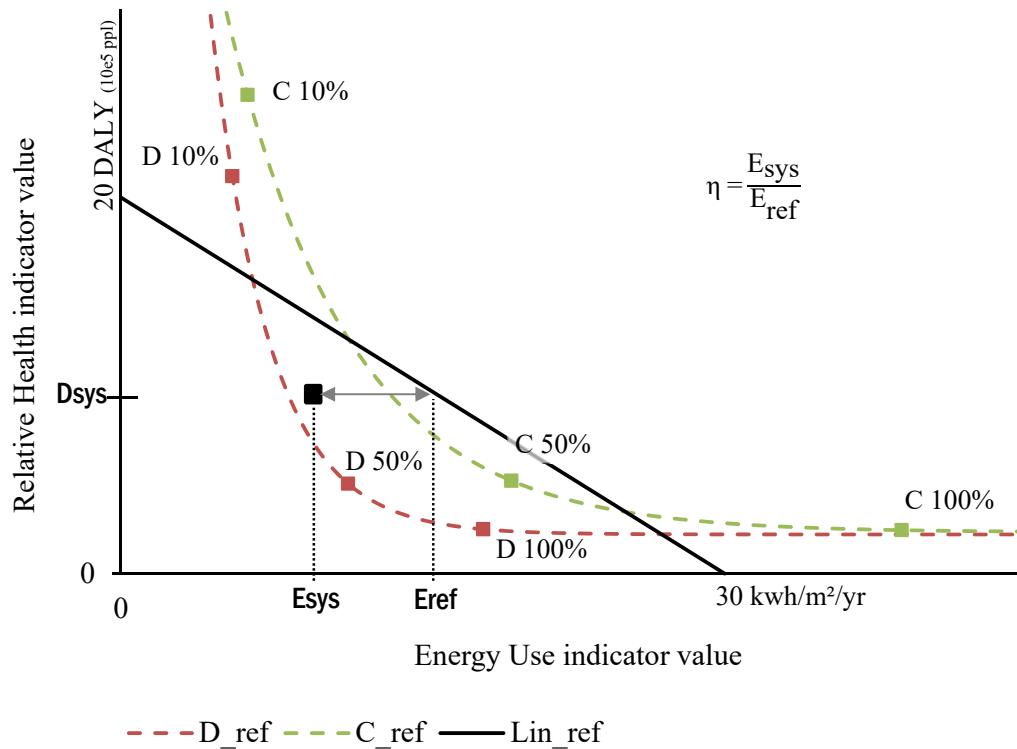


Figure 1 Plot graphically explaining the principle of the health-equivalent energy efficiency factor and the different investigated reference lines. The full line represents a linear reference line based on two target values. The dotted lines represent two reference lines based on simulations of two continuous airflow Belgian standard systems (system C- MEV and system D with heat recovery -MVHR).

### 2.3 Reference lines

The references show as continuous lines on Figure 1. The choice of reference has an important impact on the results and should be well considered. Two options for the reference lines were investigated and will be discussed:

1. The use of reference IAQ-strategies
2. The use of targets for health-impact and energy use.

#### 2.3.1 Reference systems

In line with the methods for comfort-equivalent energy efficiency factors, the reference line can be based on a reference system (Caillou et al. 2014),  $\eta_{system}$ .

In Belgium the NBN D50-001 describes four types of ventilation systems (BIN 1991). These systems, operated with a continuous and constant airflow rate (without any smart control strategies) can serve as reference systems. The IAQ-strategy under investigation can then be compared to the reference line defined by the ‘standard system’ which is conceptually most alike.

The reference lines shown in Figure 1 (dotted lines) are defined by means of the unique exponential decay function that cross three point: the results for the standard nominal ventilation system C and system D at 100%, 50% and 10% nominal airflow rate.

The used equation is as follows:

$$D_{\text{sys,ref}}(E_{\text{sys,ref}}) = Ae^{B \cdot E_{\text{sys,ref}} + C} \quad (2)$$

With

- $D_{\text{sys,ref}}$  [kwh] Reference system relative health indicator value
- $E_{\text{sys,ref}}$  [kwh] Reference system relative energy use indicator value
- A, B, C [varies] Derived parameters,  $A > 0$ ,  $B < 0$  and  $C > 0$

Although the installation of a ventilation system is required in Belgium, it is not mandatory for the building users to operate the system at full capacity (100% nominal flow rate). Therefore, these lines represent the actual possible outcomes of the energy-use indicator and the health-impact indicator that can be expected of a standard compliant system.

If the health-equivalent energy efficiency factor is below 1, this indicates that the proposed IAQ-strategy (e.g. a smart control) is more energy-efficient efficient in safe-guarding an indoor air quality achievable by the chosen reference system.

One issue with this approach is that the factor is directly tied to the prescriptive continuous ventilation system legislation (for Belgium: NBN D50-001) and thus, that the performance of the nominal systems is satisfactory, which is not necessarily the case, especially given the age of the standard (1991).

A second issue is that not for each IAQ-management strategy, the ‘conceptually most alike system’ is clear and requires additional simulations/models and analysis to define the reference line. For smart ventilation systems that do not intervene too much in the design of the system components or expected flow patterns, the choice is clear. But for other IAQ-management strategies like the use of stand-alone aircleaning, the chosen reference could be debated.

A third issue is that because of changing references, the results obtained by means of different reference systems lose the ability to be easily compared.

### 2.3.2 Targets

An alternative approach that counters the issues raised for the reference system approach is to define only one reference line based on targets for energy efficiency and health impact,  $\eta_{\text{linear}}$ . This would yield a truly performance-based approach. Any IAQ-strategy strategy, type of ventilation system, design flow rates applied to the same situation could be compared.

Note that the values set as targets will inherently be coupled with the decision on which pollutants to consider as part of the health-impact indicator and which energy fluxes are included in the energy-use indicator.

The reference line shown in Figure 1 (continuous line) connects a set number DALYs at a theoretical point of zero energy use and a maximum energy use at a theoretical point of 0 DALYs. The points are defined by [0;20] and [30;0]. The second point being the total theoretical maximum energy use of the households set at a target of 30kwh/m<sup>2</sup>/yr/household. The first point was derived by setting the maximum allowable harm of IAQ to harm as  $\pm 0.1\%$  of the total burden of disease in Belgium for 2019 (Devleesschauwer, Scohy, and Van Den Borre 2023).

If the health-equivalent energy efficiency factor is below 1, this indicates that the proposed IAQ-strategy (e.g. a smart control) can provide IAQ that meets both targets, and we can state that this is achieved in an acceptably energy efficient manner. As a designer, you can increase the health-equivalent energy efficiency by decreasing the energy use and/or by decreasing the health impact indicator (e.g. source control)

The main issue with this approach is that it requires the definition of the targets which is a matter of (public) debate and (political) decision and touches upon questions like: “what is acceptable risk?” (Morantes et al. 2023).

However, if this is successful, a target driven approach allows to easily compare any technological solution or combination of solutions which makes it the more versatile solution.

### 3 APPLICATION & RESULTS

To illustrate the developed metric, it is applied to eight smart ventilation systems. Four systems are based on the Belgian standard MEV system (NBN D50-001 – system C). The system airflow rates and other design decisions follow the standard, but the airflow rates are varied between a minimum of 10% and maximum of 100% of the nominal airflow rates according to rule-based controls linked to CO<sub>2</sub>, RH and/or presence sensors. Likewise for the other four systems but then based on the Belgian standard MVHR (NBN D50-001 – system D with heat recovery if possible). Table 1 summarizes the different control strategies of the smart ventilation systems. The case-study building is a typical Belgian apartment which has been used for several previous studies on smart ventilation performance in Belgium (Caillou et al. 2014; Laverge and Janssens 2013).

Table 1 Summary of the investigated smart ventilation control strategies

System	Description/Notable feature	Control algorithms	
		Sensors	Controls
C1	Local exhaust only, CO <sub>2</sub> only in kitchen	CO <sub>2</sub> in kitchen, RH in bathroom and service room, Presence in Toilet	Extract airflow rates vary room-to-room based on the sensor in that room
C2	Local exhaust only, CO <sub>2</sub> in all dry spaces	CO <sub>2</sub> in kitchen, Living room and bedrooms, RH in bathroom and service room, Presence in Toilet	Extract rates vary room-to-room based on the sensor in that room AND increase of all extract airflow rates based on MAX CO <sub>2</sub> level.
C3	2-zone (bedrooms - living) with additional mechanical exhausts in dry spaces	CO <sub>2</sub> in kitchen, Living room and bedrooms, RH in bathroom and service room, Presence in Toilet	Extract rates vary room-to-room based on the sensor in that room (including additional extract points in bedrooms and living). AND MIN CO <sub>2</sub> determines which zone is limited to 10% nominal flowrate.
C4	Automatic trickle vents	CO <sub>2</sub> in kitchen, Living room and bedrooms, RH in bathroom and service room, Presence in Toilet	Like C1 but with an automatic control of the trickle-vent opening area based on local CO <sub>2</sub> concentration.
D5	As C1, but with mechanical supply	CO <sub>2</sub> in kitchen, RH in bathroom and service room, Presence in Toilet	Extract airflow rates vary room-to-room based on sensor in that room. The supply airflow rates are varied to keep the total supply and total extract airflow rates equal.
D6	1-Zone (P-controller)	CO <sub>2</sub> in Living room and bedrooms, RH in kitchen, bathroom, service room and Toilet	MAX RH decides minimum whole house ventilation rate based on a proportional controller AND Supply airflow rates vary room-to-room based on the sensor in that room. Total extract and total supply airflow rates are kept equal.
D7	2-zone (bedrooms - living) nominal supply in dry spaces	CO <sub>2</sub> in Living room and bedrooms, RH in kitchen, bathroom, service room and Toilet	MAX RH decides minimum whole house ventilation rate based on a proportional controller AND MAX CO <sub>2</sub> decides the supply airflow rates and which zone is supplied. (The other limited to 10%) Total extract and total supply airflow rates are kept equal.
D8	Decentralized supply (no heat recovery)	CO <sub>2</sub> in Living room and bedrooms, RH in kitchen, bathroom, service room and Toilet	Extract and Supply airflow rates varied room-to-room based on sensor in that room. Total extract and total supply airflow rates are kept equal.



### 3.1 Results

The simulations were done using a combination of the open-source IDEAS Modelica library (Jorissen et al. 2018; De Jonge et al. 2021) and proprietary Modelica libraries for airflow modelling and the modelling of sources and sinks of pollutants and moisture buffering. The combination provides a combined model for BES-IAQ simulations. Table 2 includes the results for all eight smart ventilation systems as well as the results for the continuous reference systems at full nominal airflow rate. To acquire the data for each of the tested smart controls, 10 simulations were done with changing households to lower the influence of this parameter on the results (De Jonge, Ghijsels, and Laverge 2023).

Table 2 Energy indicator value, Health indicator value and derived health-equivalent energy efficiency factors for all investigated systems.

System	Energy	Health	$\eta$		
			$\eta_{\text{system}}$	$\eta_{\text{linear}}$	
	kWh/m <sup>2</sup>	yr/yr		[-]	[-]
C <sub>nom</sub>	39.8	2.3	C <sub>nom</sub>	1	<u>1.46</u>
D <sub>nom,hr85</sub>	18.5	2.4	D <sub>nom,hr85</sub>	1	0.68
C1	13.1	7.8	C <sub>nom</sub>	0.85	0.70
C2	28.8	3.2	C <sub>nom</sub>	<u>1.11</u>	<u>1.12</u>
C3	14.9	6.7	C <sub>nom</sub>	0.89	0.73
C4	11.3	8.8	C <sub>nom</sub>	0.78	0.65
D5 <sub>hr85</sub>	7.9	9.1	D <sub>nom,hr85</sub>	0.91	0.47
D6 <sub>hr85</sub>	8.4	7.8	D <sub>nom,hr85</sub>	0.90	0.45
D7 <sub>hr85</sub>	7.3	10.9	D <sub>nom,hr85</sub>	0.91	0.52
D8	12.3	8.1	-	-	0.67

\*<sub>hr85</sub> indicates that this system includes a heat recover system with a constant efficiency of 85%; <sub>nom</sub> indicates that it is the nominal system operated at the full nominal airflow rate.

Figure 2 shows the health-equivalent energy efficiency factor for all systems. If the reference system is used to calculate the factor, it is only used to compare with the chosen reference and with systems that use the same reference.

For the system C based ventilation system controls, C4 obtains the best health-equivalent energy efficiency factor while system C2 obtains the worst with a  $\eta_{\text{system}}$  reaching above 1. This indicates that the simple control strategy of system C2 is not able to perform better than the prescribed Belgian standard system C.

For the system D based ventilation system controls, D5, D6 and D7 score very much alike with  $\eta_{\text{system}}$  equal to 0.91, 0.90 and 0.91 respectively. For system D8,  $\eta_{\text{system}}$  could not be calculated as results from a correct reference system that is conceptually close (mechanical supply and extraction without heat recovery) were not available.

If the fixed target approach is used, for all systems a health-equivalent energy efficiency factor can be calculated and can be compared. This illustrates that as this approach can achieve a truly performance-based approach. In case of the target reference approach, the health-equivalent energy efficiency factor combines the performance of the heat recovery and the smart controls.

This also explains why  $\eta_{\text{linear}}$  for the smart MVHR systems achieve the best scores. System C2 still performs the worst, it is not capable of energy efficiently providing health equivalent IAQ.

Note that the nominal systems do not obtain an  $\eta_{\text{linear}}$  score of 1. Here, for instance, does the nominal reference system C fail the pragmatic limit of  $\eta_{\text{linear}} > 1$ , and thus should not be allowed from a combined health and energy point of view. Nominal system D with heat exchanger, D<sub>85</sub>, is able to meet the target with  $\eta_{\text{linear}}=0.68$ . Here I would like to repeat that the linear target line is shown as an example of a straightforward, possible, approach but that other target points or ‘shapes’ can also be considered.

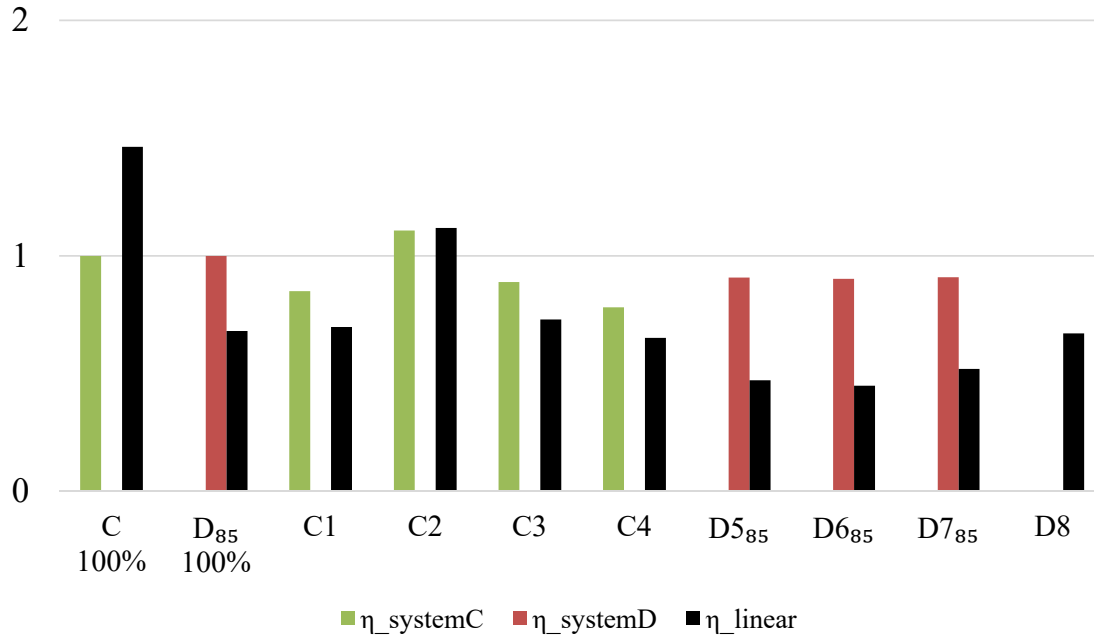


Figure 2 The different available Health-equivalent energy efficiency factors for each smart ventilation system and two reference systems (100%)

#### 4 CONCLUSIONS

The health-equivalent energy efficiency factor is a metric developed to combine two indicators for the performance of IAQ-management strategies, namely the system energy use indicator and the health impact indicator into one indicator that can be used to score the overall performance of the system. Two possible methods to come to the proposed metric are described and evaluated. Based on the results and insights gained while applying the metric, the approach where the reference line is defined by means of target values is preferred as it results in more versatile and more widely applicable metric. The application of the metric shows that only one of the smart ventilation systems under investigation is not able to provide health-equivalent indoor air quality energy efficient. The performance of the nominal reference system C would score unsatisfactory for  $\eta_{\text{linear}}$ .

#### 5 ACKNOWLEDGEMENT

The author, K. De Jonge, would like to acknowledge FWO and Ghent University for respectively funding and hosting this work as former SB PhD fellow of Flanders research foundation, FWO (1SA7619N).

#### 6 REFERENCES

Asikainen, Arja, Paolo Carrer, Stylianos Kephelopoulos, Eduardo de Oliveira Fernandes, Pawel Wargocki, and Otto Hänninen. 2016. ‘Reducing Burden of Disease from Residential

- Indoor Air Exposures in Europe (HEALTHVENT Project)’. *Environmental Health* 15 (S1). <https://doi.org/10.1186/s12940-016-0101-8>.
- Belgisch Instituut voor Normalisatie. 1991. ‘Ventilatievoorzieningen in Woongebouwen (NBN D50-001)’. Belgisch Staatsblad.
- Caillou, Samuel, Nicolas Heijmans, Jelle Laverge, and Arnold Janssens. 2014. ‘Méthode de calcul PER: Facteurs de réduction pour la ventilation à la demande’, 141.
- Council of the European Union - General Secretariat of the Council. 2023. ‘Proposal for a DIRECTIVE OF THE EUROPEAN PARLIAMENT AND OF THE COUNCIL on the Energy Performance of Buildings (Recast) - Preparation for the Trilogue’. [https://www.rehva.eu/fileadmin/user\\_upload/2023/ST-11501-2023-INIT\\_en.pdf](https://www.rehva.eu/fileadmin/user_upload/2023/ST-11501-2023-INIT_en.pdf).
- De Jonge, Klaas. 2023. ‘Holistic Performance Assessment of Residential Ventilation Systems’. PhD dissertation, Gent: Ghent University.
- De Jonge, Klaas, Janneke Ghijsels, and Jelle Laverge. 2023. ‘Energy Savings and Exposure to VOCs of Different Household Sizes for Three Residential Smart Ventilation Systems with Heat Recovery’. *Energy and Buildings* 290 (July): 113091. <https://doi.org/10.1016/j.enbuild.2023.113091>.
- De Jonge, Klaas, Filip Jorissen, Lieve Helsen, and Jelle Laverge. 2021. ‘Wind-Driven Air Flow Modelling in Modelica: Verification and Implementation in the IDEAS Library’. In *Proceedings of the 17th IBPSA Conference*, 17:1099–1106. Building Simulation. IBPSA. <https://doi.org/10.26868/25222708.2021.30165>.
- De Jonge, Klaas, and Jelle Laverge. 2022. ‘Time-Resolved Dynamic Disability Adjusted Life-Years Estimation’. *Indoor Air* 32 (11): e13149. <https://doi.org/10.1111/ina.13149>.
- Devleeschauwer, Brecht, Aline Scohy, and Laura Van Den Borre. 2023. ‘BeBOD Estimates of Mortality and Years of Life Lost, 2004-2019’. Zenodo. <https://doi.org/10.5281/ZENODO.7573531>.
- Guyot, Gaëlle, Iain Walker, Max Sherman, Pilar Linares, Sonia Garcia Ortega, and Samuel Caillou. 2019. ‘VIP 39: A Review of Performance-Based Approaches to Residential Smart Ventilation’. *Ventilation Information Paper*, no. 39 (March). <https://www.aivc.org/resource/vip-39-review-performance-based-approaches-residential-smart-ventilation>.
- Jorissen, F., G. Reynders, R. Baetens, D. Picard, D. Saelens, and L. Helsen. 2018. ‘Implementation and Verification of the IDEAS Building Energy Simulation Library’. *Journal of Building Performance Simulation* 11 (6): 669–88. <https://doi.org/10.1080/19401493.2018.1428361>.
- Laverge, J., and A. Janssens. 2013. ‘Optimization of Design Flow Rates and Component Sizing for Residential Ventilation’. *Building and Environment* 65 (July): 81–89. <https://doi.org/10.1016/j.buildenv.2013.03.019>.
- Liu, Ningrui, Wei Liu, Furong Deng, Yumeng Liu, Xuehuan Gao, Lin Fang, Zhuoru Chen, et al. 2023. ‘The Burden of Disease Attributable to Indoor Air Pollutants in China from 2000 to 2017’. *The Lancet Planetary Health* 7 (11): e900–911. [https://doi.org/10.1016/S2542-5196\(23\)00215-2](https://doi.org/10.1016/S2542-5196(23)00215-2).
- Morantes, Gioberti, Benjamin Jones, Constanza Molina, and Max Sherman. 2023. ‘A Harm Budget Approach to Indoor Air Quality Acceptability’. n . Glasgow: CIBSE.
- Morantes, Gioberti, Benjamin Jones, Max Sherman, and Constanza Molina. 2022. *Health Impacts of Indoor Air Contaminants Determined Using the DALY Metric*.
- Murray, C. J. 1994. ‘Quantifying the Burden of Disease: The Technical Basis for Disability-Adjusted Life Years.’ *Bulletin of the World Health Organization* 72 (3): 429–45.
- Murray, Christopher J. L., Alan D. Lopez, World Health Organization, World Bank, and Harvard School of Public Health. 1996. ‘The Global Burden of Disease: A Comprehensive Assessment of Mortality and Disability from Diseases, Injuries, and

- Risk Factors in 1990 and Projected to 2020 : Summary'. World Health Organization.  
<https://apps.who.int/iris/handle/10665/41864>.
- Sherman, Max H., Iain S. Walker, and Jennifer M. Logue. 2012. 'Equivalence in Ventilation and Indoor Air Quality'. *HVAC&R Research* 18 (4): 760–73.  
<https://doi.org/10.1080/10789669.2012.667038>.

# Numerical performance evaluation of ventilation systems for energy-efficient retrofitting of existing houses in France

Louison Boulrier<sup>\*1</sup>, Daniela Mortari<sup>2</sup>, Bassam Moujalled<sup>2</sup>, Nolwenn Hurel<sup>2</sup>,  
Gaëlle Guyot<sup>2</sup>, Franck Alessi<sup>1</sup>, Ophélie Ouvrier Bonnaz<sup>1</sup>, Méлина Echivard<sup>3</sup>,  
Sylvain Berthault<sup>2</sup>

1 CEA

INES - Institut National de l'Energie Solaire  
73370 Le Bourget du Lac, France

\*Corresponding author: [louison.boulrier@cea.fr](mailto:louison.boulrier@cea.fr)

2 CEREMA

46 Rue Saint-Théobald,  
38080 L'Isle-d'Abeau, France

3 Dorémi Rénovation

1 Rue Marc Seguin,  
26300 Alixan, France

## ABSTRACT

More and more single-family houses are being retrofitted to achieve better energy efficiency levels. In this retrofitting process, the building envelope's airtightness is usually improved, and a ventilation system becomes necessary to create and sustain a healthy indoor air quality (IAQ). However, in France, as in many other western countries, ventilation requirements exist for new dwellings but not for residential retrofitting. Ventilation professionals as well as inhabitants are facing a lack of knowledge, recommendations and decision tools to choose, design, and install the most efficient system in retrofitted houses. The work presented in this paper was carried out as part of the French JUSTAIR national research project (2022-2025) which aims to tackle this issue.

A consultation of ventilation stakeholders and a review of the scientific literature were performed to identify the most commonly used ventilation systems for individual house retrofitting in France and to develop a methodology for assessing the performance of such systems. The performance is assessed by a numerical approach using the NIST's multizone software CONTAM. As a first step of this project, numerical models of the various ventilation systems are created based on a specific test case: a 100 m<sup>2</sup> experimental single-family house of two stories, representative of the French building stock. Only the ventilation terminal devices, filters and heat exchangers are modelled to simulate the ventilation systems. The calculation is performed in winter, under a French south-eastern climate, and the indoor temperature is considered as constant.

This paper presents the selected 8 ventilation systems with a potential for single-family house retrofitting, including commonly installed systems (balanced and exhaust mechanical systems, with and without humidity control) as well as more emerging systems (thermodynamic, decentralized and balanced without supply ducts). The methodology for the performance evaluation of these systems is also detailed, with in particular the indicators identified to assess the physical performance and the scenarios used for the model: occupation, pollutants and humidity emissions.

Finally, the results of the numerical study are presented with the simulation of the 8 ventilation systems applied to the test case building and a performance comparison based on a set of eight indicators. In the next steps, three of the studied ventilation systems will be implemented in the experimental house for the model's validation. The validated models will be used to perform sensitivity analysis under different configurations and climate conditions.

## KEYWORDS

Ventilation, retrofitting, indoor air quality, energy efficiency, performance

## 1 INTRODUCTION

Generally, people spend more than 90% of their time indoors, considering the time at home, at work, at school, and so on (Ortiz et al., 2020). However, the indoor environments to which people are exposed not always provide a good air quality, and can cause negative effects for health, productivity and comfort (Guyot et al., 2018; Ortiz et al., 2020). The improvements to reach energy efficiency in buildings can aggravate these effects.

To achieve the requirements set by energy-efficiency programs, many countries have focused on the renovation of the housing stock. Retrofitted buildings tend to be air-tighter and more thermally insulated generating problems related to humidity, pollutants and overheating. In this context, ventilation plays an important role to create and sustain a healthy indoor air quality (IAQ). Meanwhile, in France, as in many other western countries, ventilation requirements exist in regulation for new dwellings but not for residential retrofitting. Hence, the professionals as well as inhabitants involved in renovation currently are facing a lack of knowledge, recommendations and decision tools to choose, design, and install the most efficient and suitable system in retrofitted houses.

In order to tackle this issue, the ongoing research project JUSTAIR (2022-2025) aims at developing and testing the tools needed to draw up a future technical reference framework for ventilation in the renovation of single-family homes. This project is divided in four subtasks that comprises (1) the analysis of households and building professionals feedbacks, (2) the identification of relevant ventilation strategies in renovation, (3) the development of a numerical methodology for evaluating their global performance, integrating at least the IAQ, the risks of condensation for the building, heating needs and electricity consumption, and finally (4) test the strategies experimentally.

The work presented in this paper was carried out as part of the subtask 3, focusing on the numerical evaluation of the global performance of the ventilation strategies. Several important aspects influence the choice of a ventilation system and must be included in the concept of global performance. They are, without hierarchy: IAQ, humidity, energy consumption, thermal comfort, acoustic comfort (both external and internal noise including registers and casing), total cost (covering purchase, installation, maintenance, servicing, and filter component replacement), durability of system components and performance, installation feasibility and aesthetics, as well as maintenance and design considerations.

Almost all of the residential mechanical ventilation system in France installed in buildings built after 1983 has humidity-based control (Jardinier et al., 2018; Leprince et al., 2023; Mélois et al., 2019). This system proved to be very effective in controlling humidity in buildings, however, its effectiveness in mitigating other pollutants is still under investigation. In addition, to optimize energy performance, the innovation possibilities are limited due to the prescriptive regulations (Leprince et al., 2023). As an alternative, it has been developed a performance-based approach for ventilation system regulation to evaluate the ability of a ventilation system in providing good IAQ and avoiding risks for occupant's health (Leprince et al., 2023; Poirier et al., 2023).

When working with performance-based approach for ventilation, several questions arise regarding which pollutants and/or relevant parameters should be used in the calculation of performance indicators, which indicators should be used, how to define the relevant input data and at what level of detail should be used to model air flows and pollutants throughout the house. These questions were previously raised by Poirier (Poirier et al., 2023) in the context of the design stage. In this article, we want to obtain these answers for the renovation scenario.

In this context, the objective of this study is to compare eight ventilation strategies used in single-family house retrofitting, including commonly installed systems (Jardinier et al., 2018; Poirier et al., 2023, 2022) as well as emerging systems and identify which ones are suitable for

renovation and later test them experimentally. The results were evaluated in terms of the indicators defined to assess indoor air pollution, humidity and energy consumption.

## 2 METHOD

### 2.1 Case study

#### 2.1.1 House

The case study is an experimental low-energy house located in the city of Chambéry in the south-eastern France, characterized by a temperate oceanic climate (Cfb according to the Köppen classification) (Schreck et al., 2024). It is a 128m<sup>2</sup> single-family house comprising two stories and an unused attic space, typical of French houses, as illustrated in Figure 1.

The first floor features a spacious living room with an open kitchen, and a toilet (WC1), while the second floor accommodates three bedrooms, a bathroom and a second toilet (WC2). The air tightness under 4 Pa Q4Pa-surf is 0.9 m<sup>3</sup> h<sup>-1</sup>m<sup>-2</sup> per external surface unit.

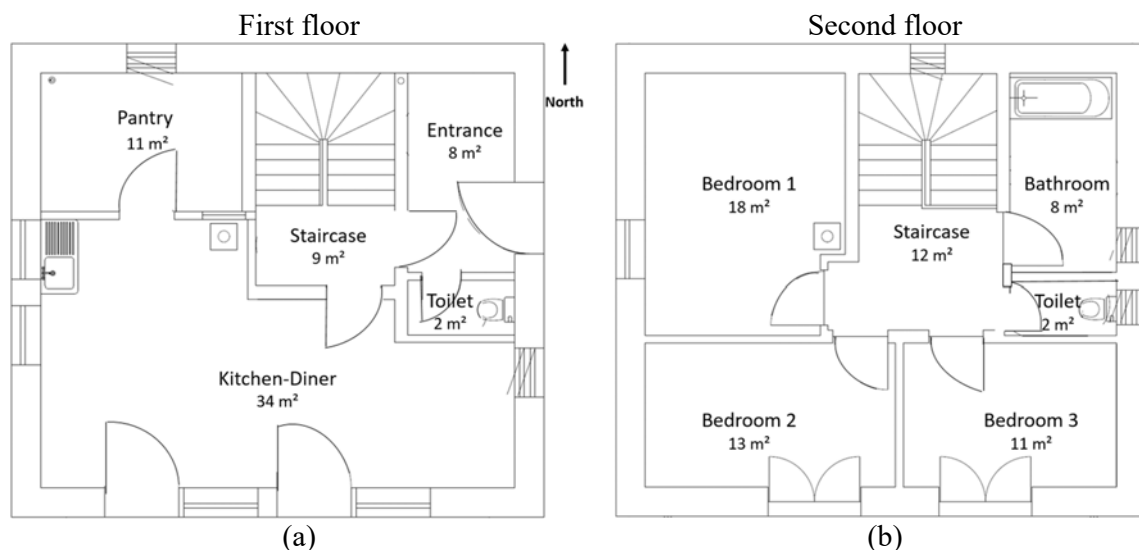


Figure 1: Plan of the house used in simulation (a) first floor and (b) second floor.

#### 2.1.2 Ventilation systems

After consulting ventilation stakeholders and performing a literature review to identify the most commonly used ventilation systems for individual house retrofitting in France, eight systems were selected and are described as follow:

1. Mechanical exhaust only ventilation with humidity control (EV-rh-b): Exhaust Air Terminal Device (ATD) with humidity control in the wet rooms and air inlets with humidity control on the facades in the living room and the bedrooms. Described by Jardinier (Jardinier et al., 2018)
2. Mechanical exhaust only ventilation with humidity control (EV-rh-a): Exhaust Air Terminal Device (ATD) with humidity control in the wet rooms and air inlets without control on the facades in the living room and the bedrooms.
3. Mechanical balanced ventilation with constant air volume (BV-cav): Constant airflow supply in bedrooms and living room and constant airflow exhausts in bathroom, kitchen and WC. Supply ATD is equipped with a PM<sub>2.5</sub> filter (e65)
4. Demand-controlled mechanical supply with humidity control (SV-rh): Supply air Terminal Device (ATD) in the living room at the first floor (60% of total flow) and in the circulation area at the second floor (40% of total flow), controlled by relative

- humidity. The supply ATD is equipped with a PM<sub>2.5</sub> filter (e65) and provides an airflow varying from 120 m<sup>3</sup> h<sup>-1</sup> for RH<30% to 280 m<sup>3</sup> h<sup>-1</sup> RH >70%. Air outlets without controls are located on the façades in each room.
5. Decentralized mechanical balanced ventilation with heat recovery and humidity control (DBV-rh): Room-based mechanical balanced ventilation with heat recovery. Supply and exhaust in the same device, installed one in the living room and another in the circulation area. The air flow is controlled by the RH measured in the living room and in the circulation area, varying from 15 m<sup>3</sup> h<sup>-1</sup> for RH<30% to 70 m<sup>3</sup> h<sup>-1</sup> for RH >70%.
  6. Mechanical balanced ventilation without supply duct with CO<sub>2</sub> control (BV-nsd-CO<sub>2</sub>): Supply air is centralized at the first floor using a Flair unit system (high-performance fan with heat exchanger), controlled by the CO<sub>2</sub> concentration measured in the circulation area. The supply air flow varies from 50 m<sup>3</sup> h<sup>-1</sup> for [CO<sub>2</sub>] <600 ppm to 200 m<sup>3</sup> h<sup>-1</sup> for [CO<sub>2</sub>] >1000 ppm. Fan coils draw in air above bedroom doors and discharge it to the circulation area. The extraction is located in the wet rooms and is proportional to the supply flow, splitted in 35% in kitchen, 35% in the bathroom, 15% in WC1 and 15% in WC2.
  7. Mechanical balanced ventilation with constant air volume coupled with heat pump (BVHP-cav): Constant air supply in bedrooms (40 m<sup>3</sup>/h in bedroom 1 and 20 m<sup>3</sup>/h in bedroom 2 and 3) and living room (130 m<sup>3</sup>/h), and constant air extraction in bathroom (30 m<sup>3</sup>/h), Kitchen (120 m<sup>3</sup>.h<sup>-1</sup>) and WC (30 m<sup>3</sup> h<sup>-1</sup>). Supply ATD is equipped with a PM<sub>2.5</sub> filter (e65).
  8. Distributed Mechanical Ventilation (DEV-rh60): Independent exhaust ATD in kitchen, bathroom and WC (ON/OFF when RH>60%) and air inlets with humidity control on the facades in bedrooms and living room.

## 2.2 Evaluation approach

The ventilation performance was assessed by a numerical approach using CONTAM. The two-stories single family house was modelled using 12 zones, represented by each room including the attic space, with the kitchen-diner modelled as a single zone. A 10-min time step calculation was performed in winter, from October 1<sup>st</sup> (00:00 a.m.) to May 31<sup>st</sup> (12:00 p.m.), with the weather conditions of Chambéry, and a constant indoor temperature at 20°C.

Only the ventilation terminals, filters and heat exchangers were modelled to simulate the ventilation systems.

The variable wind pressure at the building was calculated from the weather data. The wind pressure modifier coefficient was determined as 0.36 according to CONTAM manual, resulting from a power law used, considering the terrain characteristics as suburban type (0.6) and the house elevation 8.5 m. The pressure coefficients were based on EN 15242, varying from 0.5 on the upwind facades to - 0.7 on the downwind facades.

The infiltration was assumed to be pressure driven by a power-law model  $Q = C(dP)^n$ , where  $C$  is the flow coefficient and  $n$  is the flow exponent, being estimated as  $4.97e^{-5} \text{ m}^3 \cdot \text{s}^{-1} \cdot \text{Pa}^n$  and 0.67, respectively. This infiltration level corresponds to an air tightness level Q4Pa-surf of 0.9 m<sup>3</sup> h<sup>-1</sup>m<sup>-2</sup> per external surface unit. The Q4Pa-surf is the airflow rate at 4 Pa divided by the envelope surface area excluding lowest floor (Moujalled and Mélois, 2023). For the wall leakage, two relative elevations were considered (1/3 and 2/3 of the ceiling height of the zone). The doors and windows were considered closed, with a 85-cm<sup>2</sup> leakage area for the interior doors, corresponding to a 1-cm undercut. No other leakage through the interior wall were considered.

We assumed outdoor constant concentrations of 9.4 µg.m<sup>-3</sup> for PM<sub>2.5</sub>, 2.9 µg.m<sup>-3</sup> for formaldehyde and 400 ppm for CO<sub>2</sub> (Poirier *et al.*, 2021).



## 2.2.1 Input parameters for simulation

The detailed inputs scenarios for pollutant emissions and occupancy schedules are presented in Table 1.

Table 1: Input data for occupants schedules and pollutant emissions scenario

Occupants schedules			
Room/Occupants	Occupants 1 and 2	Occupant 3	Occupant 4
Kitchen and living (5h30/occupant)	7:00-8:30 12:00-14:00 19:00-21:00	6:20-8:30 12:00-14:00 19:00-20:20	6:20-8:30 12:00-14:00 19:00-19:40 20:20-21:00
Bathroom (40 min/occupant)	6:20-7:00 (WC1 and 2)	20:20-21:00	19:40-20:20
Bedroom (9h20/occupant)	21:00-6:20 ( <b>Bedroom 1</b> )	21:00-6:20 ( <b>Bedroom 2</b> )	21:00-6:20 ( <b>Bedroom 3</b> )
Pollutants and humidity emissions scenarios*			
Bio effluents (occupied room)	CO <sub>2</sub>	Awake: 18 L.h <sup>-1</sup> /person	6:20 – 21:00
		Asleep: 15 L.h <sup>-1</sup> /person	21:00-6:20
	Humidity	Awake: 55 g.h <sup>-1</sup> /person	6:20 – 21:00
		Asleep: 40 g.h <sup>-1</sup> /person	21:00-6:20
Cooking (kitchen)	PM <sub>2.5</sub>	2.55 mg.min <sup>-1</sup>	6:20 -6:35, 12:00 – 12:30 and 19:00 – 19:40
	Humidity	1512 g.h <sup>-1</sup>	6:20 -6:35
		2268 g.h <sup>-1</sup>	12:00 – 12:30
		2844 g.h <sup>-1</sup>	19:00 – 19:40
Shower (bathroom)	Humidity	1440 g.h <sup>-1</sup>	10 min/person at 6:20 (occ1),6:40 (occ2), 19:40 (occ4) and 20:20 (occ3)
Laundry (kitchen)	Humidity - wash machine	252 g.h <sup>-1</sup>	5 times a week, 2h/time- Mondays, Tuesdays, Wednesdays, Saturdays and Sundays, at 19:00h
	Humidity – dryer (naturally) (living room?)	136.8 g.h <sup>-1</sup>	5 times a week, 1h/time - Mondays, Tuesdays, Wednesdays, Saturdays and Sundays, at 21:00h
Building-related emission (all rooms)	Formaldehyde	23.6 µg.h <sup>-1</sup> .m <sup>-2</sup>	Continuous in all rooms, per m <sup>2</sup> of floor space

\*(Poirier et al., 2021)

## 2.2.2 Key-performance indicators

For evaluating the physical performance, we proposed a reduced set of IAQ performance indicators as output data. The methodology for calculating the IAQ indicators is detailed by Poirier (Poirier *et al.*, 2021).

1. E\_CO<sub>2</sub> – CO<sub>2</sub> cumulative exposure concentration above the reference concentration of 1000 ppm and divided by the time of exposure, calculated for the occupants (ppm).
2. E\_RH - Percentage of time in which relative humidity is outside the range [40-60%] considering health risks for all rooms in the building during occupied hours (%).
3. E\_RH70: Percentage of time in which relative humidity is above 70% in all rooms, considering condensation risk (%).

4.  $E_{\text{HCHO}}$  - Long-term cumulative exposure to formaldehyde, calculated for the occupants and divided by the time of exposure ( $\mu\text{g}\cdot\text{m}^{-3}$ ).
5.  $E_{\text{PM2.5}}$  - Long-term cumulative exposure to  $\text{PM}_{2.5}$ , calculated for the occupants and divided by the time of exposure ( $\mu\text{g}\cdot\text{m}^{-3}$ ).
6.  $\text{Energy}_{\text{tot}}$  – This energy indicator is the sum of the heat loss due to air changes (including the heat recovery for BV) and the electrical consumption of the fans (kWh).
7.  $\text{Cons}_{\text{Fan}}$  – Electric consumption due to the ventilation system operation ( $\text{kWh}_{\text{el}}\cdot\text{m}^{-2}$ )
8.  $q_{v,\text{mean}}$  - The mean air flow rate extracted/supplied by the mechanical ventilation system ( $\text{m}^3\cdot\text{h}^{-1}$  or  $\text{vol}\cdot\text{h}^{-1}$ ).

### 3 RESULTS

#### 3.1.1 Comparison of the behaviour of ventilation systems

Figure 2 shows the variation in total flowrate for all systems throughout the day of 01/02. These flowrates and control strategies were defined for each system based on respective technical documentation or after consultation with ventilation constructors.

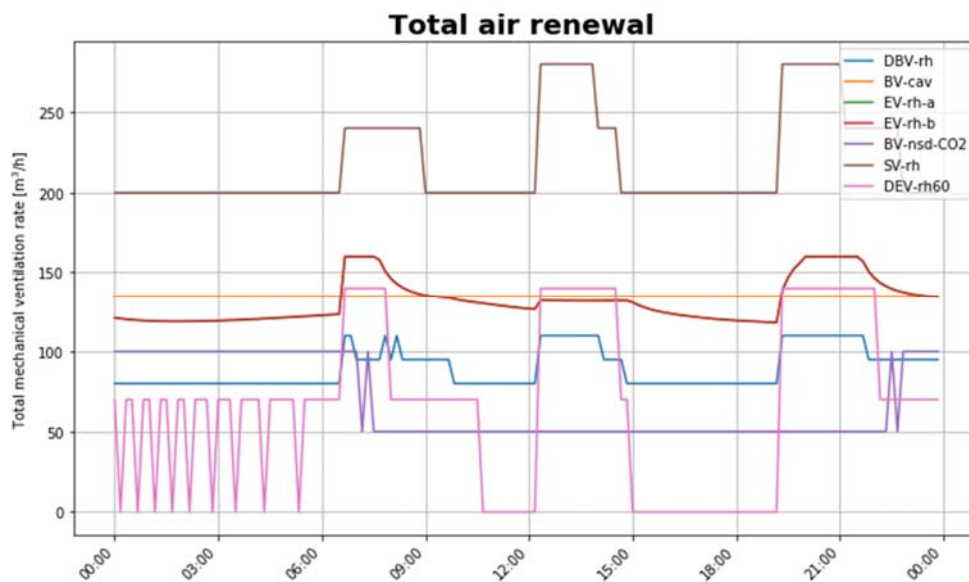


Figure 2: Total flowrate for all systems throughout the day February 1<sup>st</sup>.

BVHP-cav is not represented in this section, as its behaviour is the same as BV-cav: only the energy consumption differs due to the use of a heat pump in the case of BVHP-cav.

Airflow rates vary significantly across different systems. With the exception of BV-cav, which maintains a constant airflow rate of  $140 \text{ m}^3 \text{ h}^{-1}$ , all other systems exhibit variable airflow rate profiles. These profiles maintain a constant base value (ranging from  $0 \text{ m}^3 \text{ h}^{-1}$  for DEV-rh60 up to  $200 \text{ m}^3 \text{ h}^{-1}$  for SV-rh), with peak values occurring during periods of occupants' activities such as cooking or showering (ranging from  $70 \text{ m}^3 \text{ h}^{-1}$  for DBV-rh up to  $280 \text{ m}^3 \text{ h}^{-1}$  for SV-rh). The dynamics of variation vary according to the control strategy ( $\text{CO}_2$  or RH). SV-rh exhibit the highest rates among all the systems at all time. DEV-rh60 shows the lowest rates during the base hours, while DBV-rh and BV-nsd- $\text{CO}_2$  show the lowest rates during peak hours. EV-rh-a and EV-rh-b present very similar trends in the whole study: the exhaust flowrates are the same for both, the only difference is the amount of air entering the building through the air inlets, and its distribution among the different rooms.

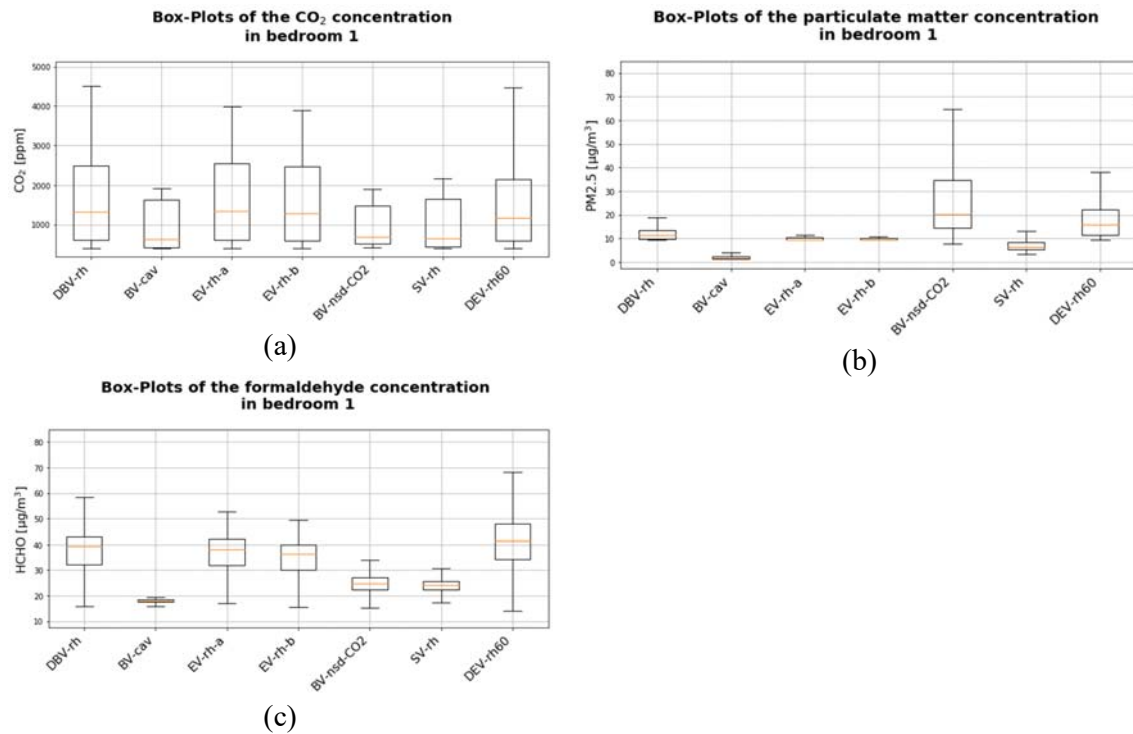


Figure 3: Comparison of (a) CO<sub>2</sub> concentration in ppm, (b) PM<sub>2.5</sub> concentration in  $\mu\text{g}\cdot\text{m}^{-3}$  and (c) formaldehyde concentration in  $\mu\text{g}\cdot\text{m}^{-3}$  in bedroom 1 obtained for each ventilation system.

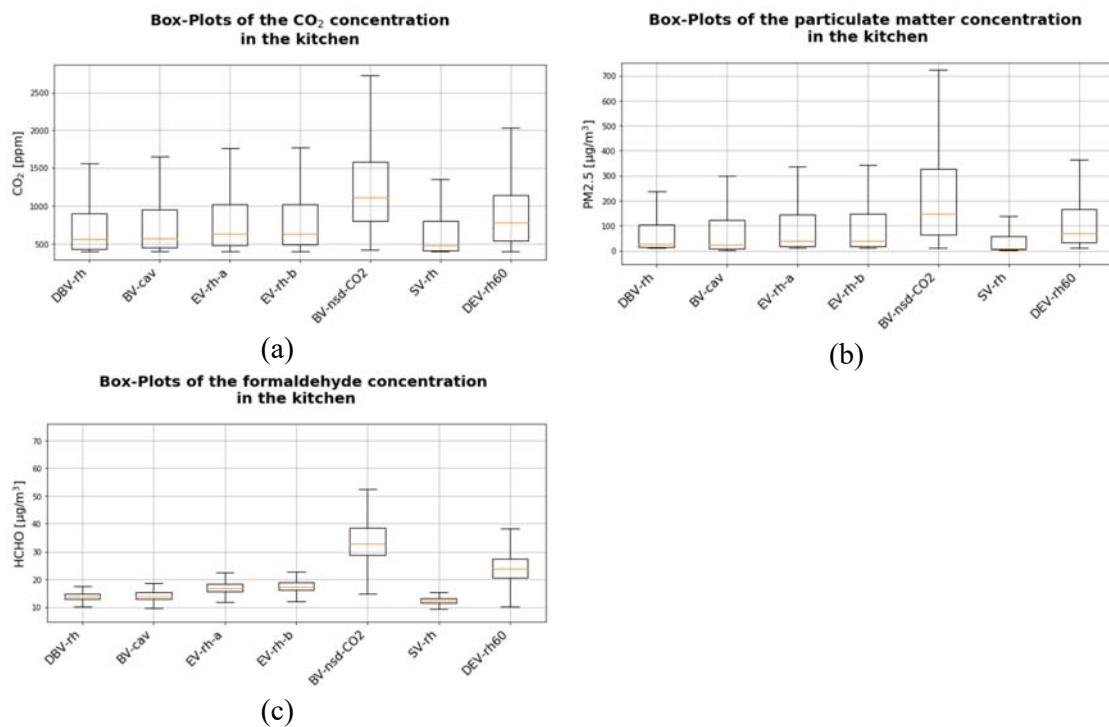


Figure 4: Comparison of (a) CO<sub>2</sub> concentration in ppm, (b) PM<sub>2.5</sub> concentration in  $\mu\text{g}\cdot\text{m}^{-3}$  and (c) formaldehyde concentration in  $\mu\text{g}\cdot\text{m}^{-3}$  in kitchen obtained for each ventilation system.

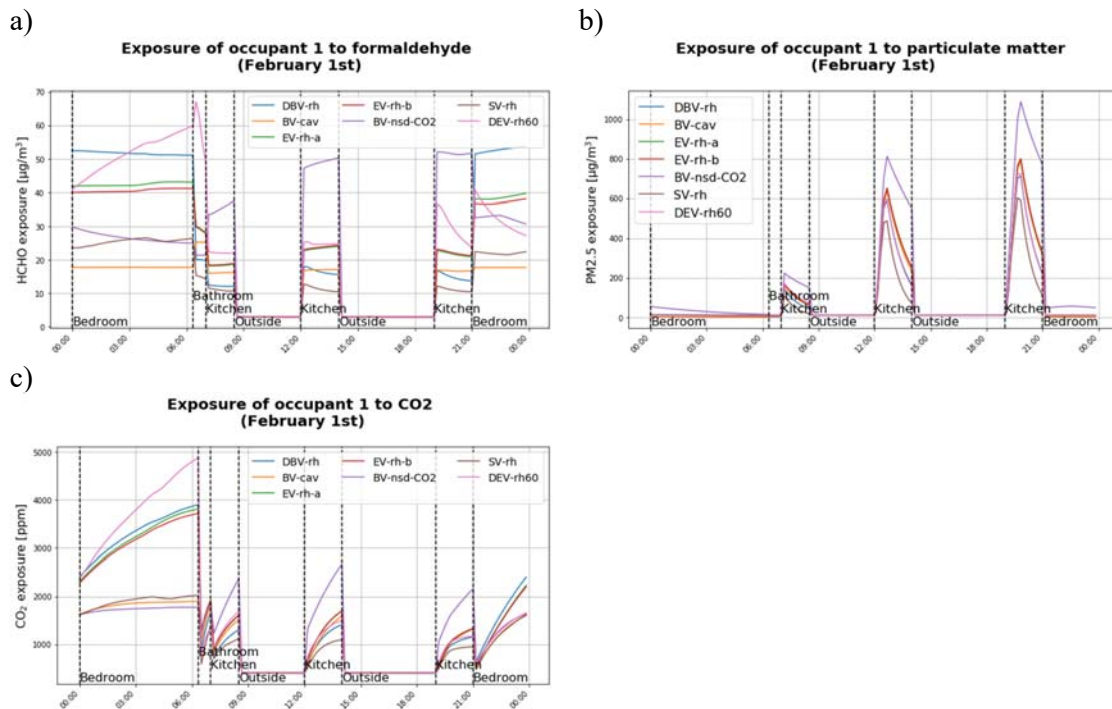


Figure 5: Occupant 1 exposure to (a) formaldehyde, (b) PM<sub>2.5</sub> and (c) CO<sub>2</sub> throughout the day February 1st.

Figure 3 and Figure 4 illustrate the boxplots of the pollutant concentrations in the main bedroom and the kitchen respectively, and Figure 5 the typical profile of occupant1 exposure during a single day. The exposure to formaldehyde is higher in the bedrooms than in other rooms (except for BV-nsd-CO<sub>2</sub>). BV-cav, SV-rh and BV-nsd-CO<sub>2</sub> have quite stable levels, the other systems show important variations over time due to the variation of air flowrate according to humidity and CO<sub>2</sub> level.

The outdoor concentration in PM<sub>2.5</sub> being fixed to very low level in these calculations, the exposure to particles matter is only due to the cooking activities. A strong increase of the PM<sub>2.5</sub> exposure is observed at each cooking period, this peak is then quickly balanced by the air changes, with a peak value and a slope that depend on the considered system.

For all systems (except BV-nsd-CO<sub>2</sub>), the moment of highest exposure to CO<sub>2</sub> is at night. Indeed, the CO<sub>2</sub> emitted by the occupants themselves by metabolic activity concentrates all night long. In comparison, the exposure in the kitchen is roughly half-way smaller than the highest one reached in the bedroom. We can notice that none of the considered systems is able to remove the CO<sub>2</sub> as fast as it is emitted.

### 3.1.2 Analysis of the performance

Table 2: Analysis of the performance indicators for all ventilation systems.

	EV-rh-b	BV-cav	BVHP-cav	BV-nsd-CO2	DBV-rh	SV-rh	DEV-rh60
E_CO2 [ppm]	246.1	42.9	42.9	47.9	243.0	149.7	191.3
E_RH [%]	66.2	65.1	65.1	70.8	65.6	66.6	62.5
E_RH70 [%]	23.6	21.6	21.6	48.6	18.5	19.3	24.4
E_HCHO [ $10^5$ $\mu\text{g}\cdot\text{h}/\text{m}^3$ ]	3.6	2.2	2.2	3.5	3.6	3.4	4.3
E_PM25 [ $10^5$ $\mu\text{g}\cdot\text{h}/\text{m}^3$ ]	16.2	14.5	14.5	24.2	14.7	12.2	17.5
Energy_loss [ $\text{kWh}_{\text{th}}/\text{m}^2$ ]	109.1	11.8	5.4	4.9	12.3	180.6	36.4
Cons_fan [ $\text{kWh}_{\text{el}}/\text{m}^2$ ]	0.9	2.6	2.6	0.8	0.7	1.1	0.8
$q_{v\_mean}$ [vol/h]	0.34	0.39	0.39	0.19	0.22	0.58	0.17

We can observe in Table 2 that no system is superior to all others for all indicators, even though the balanced ventilation systems BV-cav and BVHP-cav present good results overall.

All systems present poor results in terms of air humidity: the relative humidity in occupied rooms is outside the range [40-60%] around 70% of the time for all systems. On the contrary, all systems (except BV-nsd-CO<sub>2</sub>) trespass 70% relative humidity less than 20% of the time. The exposure to formaldehyde and particulate matter varies from simple to double depending on the considered system.

For better readability of Table 2, the indicators for the ventilation system EV-rh-a are not represented as they are all very similar to EV-rh-b. Indeed, despite the difference of air inlets (and with similar air outlets and fan), the flowrates are similar in both cases as can be seen on Figure 2. This similar air renewal induces very similar IAQ and energy consumption indicators. The energy loss due to air renewal (Energy\_loss) shows great variation: the balanced ventilation associated to a heat pump (BVHP-cav) and the balanced ventilation without supply duct with CO<sub>2</sub> control (BV-nsd-CO<sub>2</sub>) lead to about 5  $\text{kWh}\cdot\text{m}^{-2}$  consumption over the heating period, whereas the exhaust-only system EV-rh-b leads to more than 109  $\text{kWh}\cdot\text{m}^{-2}$  consumption, and more than 180  $\text{kWh}\cdot\text{m}^{-2}$  for the supply ventilation SV-rh over the same period. These results must be taken with a pinch of salt, as no thermal simulation was performed. Neither the thermal loss through the walls nor the solar gains are taken into account. This difference in energy consumption is notably due to the presence or not of a heat recovery unit (and to a heat pump for BVHP-cav). Another factor which contributes to explain this energy consumption variation is the difference in *mean total air changes*  $q_{v\_mean}$ , which range from 0.17  $\text{vol}\cdot\text{h}^{-1}$  only for DEV-rh60, to 0.58  $\text{vol}\cdot\text{h}^{-1}$  for SV-rh.

The electric consumption due to the ventilation system operation Cons\_fan is very small compared to the loss due to air renewal, especially for the system which does not include a heat exchanger. For the balanced ventilation systems, this consumption represents up to 33% of the Energy\_loss (for BVHP-cav) due to both a smaller Energy\_loss with the heat exchanger, and a high electrical consumption due to the operation of two fans and a significant pressure drop through the heat exchanger.

## 4 CONCLUSION

This paper presents a numerical performance evaluation of ventilation systems, based on a methodology which was developed considering ad-hoc benchmark and review of the scientific literature.

This simulation work results in the computation of IAQ and energy indicators in winter period for eight ventilation systems, among which very usual ones in the French context but also more innovative ones.

According to the simulations, the ventilation systems lead to various performance levels for these indicators. All systems present advantages and limitations: depending on the room, the

moment of the day and the pollutant considered -or the energy consumed or the heat loss by air changes, all systems seem alternatively better or less performant than others.

The upcoming work within the scope of the JUSTAIR project will involve enriching the simulation model. This enhancement will notably include constructing a thermo-aeraulic coupling to account for temperature changes, enabling thus simulations to be performed during the summer period. Additionally, the set of indicators will be enriched by incorporating thermal comfort and total cost considerations.

Another crucial step of the project will be the installation and testing of 3 different ventilation systems in the experimental house on which the present simulations are based. Pollutant emissions similar to the scenarios presented in this paper will be implemented and a set of sensors will be installed and monitored to evaluate the actual performance of these systems in operation.

These further steps will enhance the understanding and comparison of all the studied ventilation systems.

## **5 ACKNOWLEDGEMENTS**

The authors would like to thank ADEME (Ecological Transition Agency - Auvergne-Rhône-Alpes) for its support through the grant number N°2204D0013.

## 6 REFERENCES

- Guyot, G., Sherman, M.H., Walker, I.S., 2018. Smart ventilation energy and indoor air quality performance in residential buildings: A review. *Energy and Buildings*, 165, 416–430.
- Jardinier, E., Parsy, F., Guyot, G., Berthin, S., 2018. Long-term durability of humidity-based demandcontrolled ventilation: results of a ten years monitoring in residential buildings, in: 39th AIVC Conference “Smart Ventilation for Buildings”, Antibes Juan-Les-Pins, France, 18-19 September 2018.
- Leprince, V., Poirier, B., Guyot, G., 2023. How to create a performance-based regulation on ventilation – the French Experience. Presented at the 43rd AIVC - 11th TightVent - 9th venticool Conference - Copenhagen, Denmark - 4-5 October 2023.
- Mélois, A.B., Moujalled, B., Guyot, G., Leprince, V., 2019. Improving building envelope knowledge from analysis of 219,000 certified on-site air leakage measurements in France. *Build. Environ.* 159, 106145. <https://doi.org/10.1016/j.buildenv.2019.05.023>
- Moujalled, B., Mélois, A., 2023. VIP 45.6: Trends in building and ductwork airtightness in France. <https://www.aivc.org/resource/vip-456-trends-building-and-ductwork-airtightness-france>
- Ortiz, M., Itard, L., Bluysen, P.M., 2020. Indoor environmental quality related risk factors with energy-efficient retrofitting of housing: A literature review. *Energy Build.* 221, 110102. <https://doi.org/10.1016/j.enbuild.2020.110102>
- Poirier, B., Guyot, G., Geoffroy, H., Woloszyn, M., Ondarts, M., Gonze, E., 2021. Pollutants emission scenarios for residential ventilation performance assessment. A review. *J. Build. Eng.* 42, 102488. <https://doi.org/10.1016/j.job.2021.102488>
- Poirier, B., Guyot, G., Woloszyn, M., 2023. Development of Performance-Based Assessment Methods for Conventional and Smart Ventilation in Residential Buildings. Presented at the 41st AIVC/ASHRAE IAQ- 9th TightVent - 7th venticool Conference - Athens, Greece - 4-6 May 2022, <https://www.aivc.org/resource/development-performance-based-assessment-methods-conventional-and-smart-ventilation>.
- Poirier, B., Jakub, K., Gaëlle, G., Woloszyn, M., 2022. Design of residential ventilation systems using performance-based evaluation of Indoor Air Quality: application to a Danish study case. *E3S Web Conf.* 362, 09004. <https://doi.org/10.1051/e3sconf/202236209004>
- Schreck, C., Rouchier, S., Fouquier, A., Machefert, F., Wurtz, E., 2024. In situ air change rate estimation from metabolic CO2 measurement. Summer experimental campaign in a single-family test house. *Build. Environ.* 259, 111646. <https://doi.org/10.1016/j.buildenv.2024.111646>

# Effects of closed vertical void on natural ventilation in double-loaded apartment building

Tetsu Kubota<sup>\*1</sup>, Hayato Shima<sup>1</sup>, Hanief Sani<sup>1</sup>, Nikhil Kumar<sup>1</sup>, Haruka Kitagawa<sup>2</sup>, Takashi Asawa<sup>3</sup>, Muhammad Nur Fajri Alfata<sup>4</sup>

*1 Graduate School of Advanced Science and Engineering, Hiroshima University  
1-5-1 Kagamiyama, Higashi-Hiroshima, 739-8529,  
Japan*

*\*Corresponding author: tetsu@hiroshima-u.ac.jp  
3 School of Environment and Society, Tokyo Institute of Technology, 4259 Nagatsuta-cho, Midori-ku, Yokohama, Kanagawa, 226-8502, Japan*

*2 Institute of Technology, Shimizu Cooperation  
3-4-17 Etchujima, Koto-ku, Tokyo, 135-8530, Japan*

*4 Directorate for Settlements and Housing Engineering Development, Ministry of Public Works and Housing, Indonesia  
Jl. Panyawungan, Cileunyi Wetan, Kabupaten, Bandung 40393, Indonesia*

## ABSTRACT

We proposed a new design of an affordable apartment with a closed-vertical void to improve the indoor natural ventilation especially for the leeward side of the building and constructed a full-scale experimental house in Indonesia in 2020. This paper analyses the effects of the proposed ventilation system through field measurements in the experimental house. In the experimental house, the vertical-closed void with a width of 2.85 m was designed between the two rows of units. A pilotis was provided on the ground floor and a wind fin was attached to the bottom of the vertical void. The rooftop of the void was basically closed. First, vertical and horizontal distributions of wind velocities were measured at 125 points placed inside and outside the void with various window/door-opening conditions in 2022. Second, the volumetric flow rates (VFRs) for the void space as well as leeward units were measured through a tracer gas decay method and based on the measured inlet wind velocities respectively in 2023. The average wind velocity ratio,  $\overline{WVR}$  at the inlet of the pilotis was approximately 2.4 times higher than that in front of the building at the same height (reference point) due to the venturi effect. However, the increased winds did not reach the upper floor of the leeward units sufficiently even when the fin size was increased. Opening conditions of windows/doors significantly affected the wind velocity distribution in and around the void. Sufficient levels of VFR were obtained even in the upper floor of leeward units due to the increased static pressure inside the closed void. The proposed ventilation system would be able to provide sufficient cross ventilation to the double-loaded apartment buildings entirely with the increase in static pressure even for a mid-rise building.

## KEYWORDS

Natural ventilation, Void, Field measurement, Tracer gas method, Hot-humid climate

## 1 INTRODUCTION

Affordable housing is highly demanded in the Global South in response to the rapid rise of middle-class in urban areas. Meanwhile, these countries are also required to meet low-carbon targets such as the Paris Agreement. To date, most affordable apartments in the Global South are constructed with a double-loaded corridor system because south-facing orientation is not necessarily a strong design requirement unlike those in the northern hemisphere (Prasetya et al., 2023). In the case of double-loaded apartments, rows of occupied units are located on both sides of the building from the single central corridor, and therefore poor environmental conditions, such as daylighting and natural ventilation, often take place (Bardhan et al., 2018; Lueker et al., 2020).

One of the natural ventilation strategies to cope with the above-mentioned environmental issues is to incorporate an internal void within such a double-loaded apartment—



### Abbreviations

ACH	Air changes per hour
CFD	Computer fluid dynamics
VRF	Volumatic flow rate
WVR	Wind velocity ratio

this will divide the single central corridor into two single-loaded corridor systems. In fact, approximately 34% of the existing public apartments in Indonesia were equipped with vertical voids, although the percentage of those with voids tends to decline in recent years (Prasetya et al., 2023). All of the above-mentioned internal voids were opened-vertical voids where the rooftop of the voids is opened to the sky. These opened voids may create upward winds inside the voids caused by the negative pressure created on the rooftop due to the separated winds. These upward winds would improve cross ventilation from the outdoors to the indoor units for both sides of the building. On the other hand, we proposed a new alternative design of affordable apartments with a closed-vertical void to improve the indoor natural ventilation especially for the leeward side of the building (Kumar et al., 2021, 2022). Kumar et al. (2021) proved that the new closed-vertical void apartment design may be prior to that of the conventional opened-void apartment, at least for the natural ventilation performance on the leeward side of the building. Fig. 1 illustrates the ventilation concept of the proposed alternative building design that incorporates a closed-vertical void. The proposed design has a pilotis on the ground floor and a closed-vertical void with a slit-shaped wind fin attached to the vertical void's edge on the leeward side. The idea of the proposed design was to create a positive pressure region inside the closed-vertical void by combining the venturi effect and wind fin. To analyse the resultant ventilation performance, we then constructed a full-scale experimental house in the city of Tegal, Indonesia in 2020. This paper analyses the effects of the proposed ventilation system through field measurements in the experimental house.

## 2 METHODS

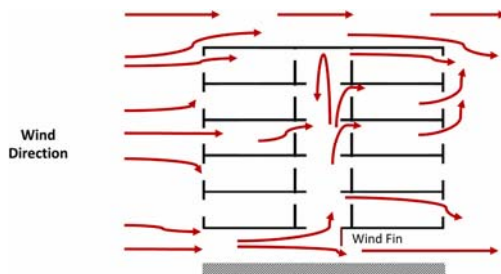


Fig. 1. Natural ventilation concept of the proposed apartment building with a closed-vertical void (Kumar et al., 2022).

Table 1. Measurement cases for the 1<sup>st</sup> experiment.

Case	Window and door	Penthouse window	Fin size
1.1	✓	✓	Large
1.2	-	✓	Large
1.3	✓	-	Large
1.4	-	-	Large
1.5	-	-	Small

✓: Open, -: Close



Fig. 2. Experimental house in Tegal, Indonesia.

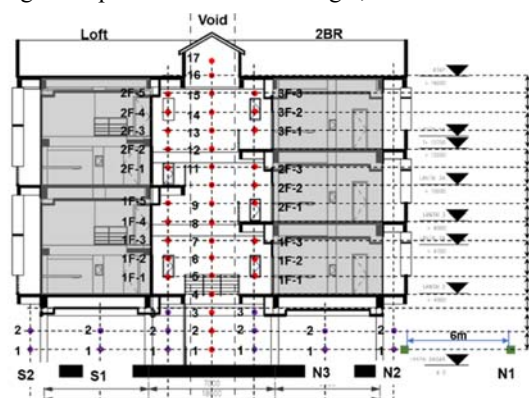


Fig. 3. Measuring positions of anemometers.

## 2.1 Full-scale experimental house in Tegal

The experimental house is an apartment building with a total floor area of approximately 2,000 m<sup>2</sup> (Fig. 2). The northern side consists of six standard units (3 stories, 52.4 m<sup>2</sup>/unit) with a floor-to-ceiling height of 3.05 m, whereas the southern side is composed of six loft units (2 stories, 63.2 m<sup>2</sup>/unit) with a larger height (5.15 m). The vertical-closed void with a width of 2.85 m is located between the two rows of units. The size (height) of the wind fin is manually changeable. On the rooftop of the vertical void, there is a penthouse to secure natural lighting. Louver windows are designed for the penthouse to exhaust the excessive heat. The experimental house is located approximately 800 m south from the northern coastal line of the Java island (6.86°S, 109.12°E), and therefore a sea breeze prevails from the north during the afternoon on sunny days. The design and construction of this experimental house are detailed in Alfata et al. (2023).

## 2.2 Wind velocity distributions

The 1<sup>st</sup> field experiment was conducted during the dry season from June to July 2022. Outdoor air temperature ranged from 22.5-33.2 °C with an average of 27.5 °C, whereas relative humidity ranged from 36-98%. Outdoor wind velocity at 1 m above ground was averaged at 1.21 m/s (up to 7.6 m/s) during daytime and at 0.69 m/s (up to 8.7 m/s) during night-time. Vertical and horizontal distributions of wind velocities were measured at multiple points shown in Fig. 3. A total of 122 anemometers (KOA Windgraphy (hot-wire anemometer); Kamomax Model 6333 and 0976-03 (thermal anemometer)) were placed in and around the vertical void, whereas three 2D ultrasonic anemometers (YOUNG Model 86000) were placed inside and outside the pilotis. A weather station was placed on the rooftop (21 m above the ground level). The experiment was conducted in five cases with changing window/door opening conditions and size of the wind fin (Table 1). The measured wind velocities were normalized to wind velocity ratio (WVR) by Eq. 1.

$$WVR = V_m / U_o \quad (1)$$

Table 2. Measurement cases for the 2<sup>nd</sup> experiment.

Case	Standard units (windward)		Loft units (leeward)		
	1N1 2N1 3N1	1N2 2N2 3N2	1S1 2S1	1S2 2S2	1S3 2S3
2.1	✓	✓	✓	✓	✓
2.2	✓	-	-	✓	-
2.3	-	-	-	✓	-
2.4	-	-	-	✓2S2	-
2.5	-	-	-	✓1S2	-

✓: Open, -: Close

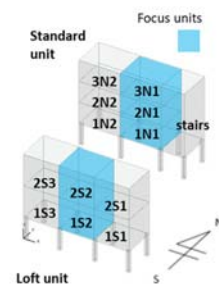


Fig. 4. Measuring positions of dust meters and anemometers.

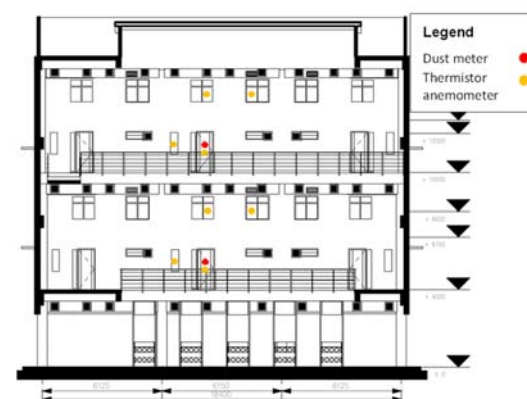


Fig. 5. Measuring positions of anemometers: North section of the leeward loft units.

Where  $V_m$  is the measured wind velocities (m/s) and  $U_o$  is the wind velocities recorded at the 2D ultrasonic anemometer (at 1 m above the ground) at 6 m north from the building (m/s) (N1 in Fig. 3).

$\overline{WVR}$  represents the temporal average value of  $WVR$ . We analysed the  $WVR$ s under the daytime prevailing wind direction of NNE, allowing  $30^\circ$  deviations on each side, with a wind velocity of more than 1 m/s at the above-mentioned reference anemometer. The wind velocities at the middle section were analysed in this paper.

### 2.3 Flow rate measurement

The 2<sup>nd</sup> field experiment was conducted during the dry season in September 2023. Outdoor air temperature ranged from 22.5-33.7 °C with an average of 26.9 °C, whereas relative humidity was averaged at 63.9%. Outdoor wind velocity at 1.5 m above ground was averaged at 1.37 m/s during daytime and at 0.88 m/s during night-time. As before, we analysed wind velocities under the daytime prevailing wind direction of NNE  $\pm 30^\circ$  with a wind velocity of more than 1 m/s at the reference point. Here, the volumetric flow rate (VFR) for the vertical void space was measured through a tracer gas decay method using a fog machine (ANTARI Z-1000 II), where propylene glycol gas was used. The concentration of smoke was measured using a digital dust meter (Shibata LD-5R) in a corridor space at 1.5 m above the floor in front of the leeward units (Fig. 4). The measurement was carried out in five cases with various opening conditions during the daytime prevailing wind directions, i.e., north winds (Table 2). The louver windows on the penthouse were opened throughout this measurement. During the measurement, the opening of the void was closed with a cover, while the fog machine filled the void with smoke. Once the concentration was equal between the 1<sup>st</sup> and 2<sup>nd</sup> floors of the leeward side, the cover was opened and the decay of smoke concentration was recorded until it became the normal level. The measured values were calibrated by comparing them with those measured by the CO<sub>2</sub> decay method afterward.

Wind velocities were measured at the centres of every opening (windows and doors) of the selected leeward units (1S2 and 2S2) (Kamomax Model 6333 and 0976-03), whereas wind velocities and directions were measured in the corridor and void spaces (Fig. 5). The reference values were obtained 6 m north of the building (YOUNG Model 86000). The  $VFR_{unit}$  for the leeward units (1S2 and 2S2) was calculated based on the measured wind velocities at the inlet openings. All the  $VFR_{unit}$  values were normalized as  $VFR_0$  based on the reference value,  $VFR_{ref}$  as follows:

$$VFR_0 = VFR_{unit}/VFR_{ref} \quad (2)$$

$$VFR_{ref} = A_{void} V_{ref} \quad (3)$$

Where  $A_{void}$  is the cross-sectional area of the inlet of the vertical void (m<sup>2</sup>) and  $V_{ref}$  is the temporal average wind velocity measured at the reference point during the measurement (m/s).

## 3 RESULTS AND DISCUSSION

### 3.1 Wind velocity distributions

Fig. 6 shows the results of comparisons between open windows/doors (Cases 1.1 and 1.3) and closed windows/doors (Cases 1.2 and 1.4), respectively. The conditions of penthouse windows were different between Cases 1.1 & 1.2 (opened) and Cases 1.3 & 1.4 (closed). In all cases, it can be seen that the wind velocities were increased at the inlet of the pilotis due to the venturi effect.  $\overline{WVR}$  at the inlet (N2) was approximately 2.4 times higher than the reference point in most cases. In the pilotis,  $\overline{WVR}$  ranges from 1.2-2.4 on the windward side, while those on the leeward side range from 0.2-1.8. When the windows and doors were opened, the wind velocities

were increased not only on the windward side of the building, but also on the leeward side. The increase in  $\overline{WVR}$  can be seen in the vertical void, particularly at the internal corridor spaces of the leeward units.  $\overline{WVR}$ s in the void in Cases 1.1 and 1.3 are approximately 1.6 times higher than those in Cases 1.2 and 1.4.

When the windows/doors are opened, the volume of inflows to the indoor spaces will be largely increased. The increased inflows are provided from the windward units as well as pilotis to the vertical void and then to the leeward units. This increased inflows simply improved

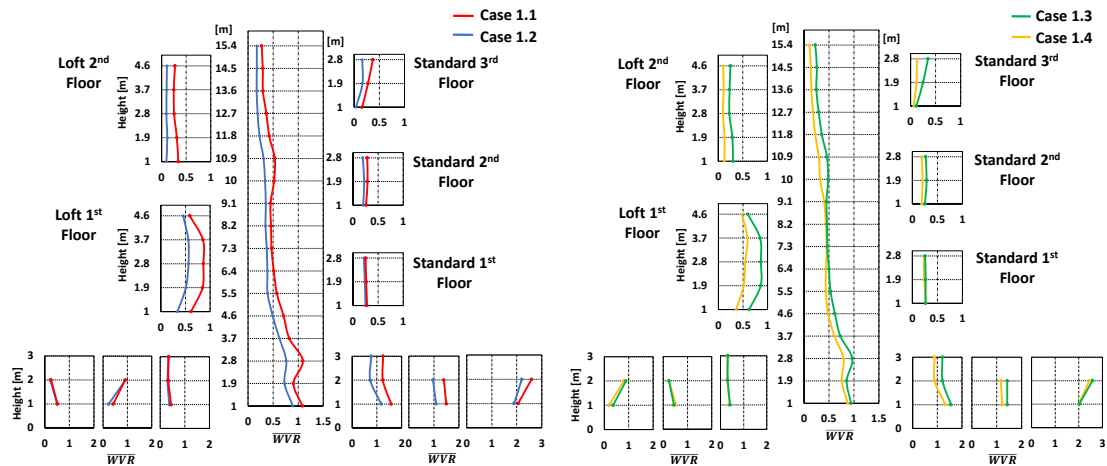


Fig. 6.  $\overline{WVR}$  with changes in window/door opening conditions; (a) with penthouse open, (b) with penthouse closed.

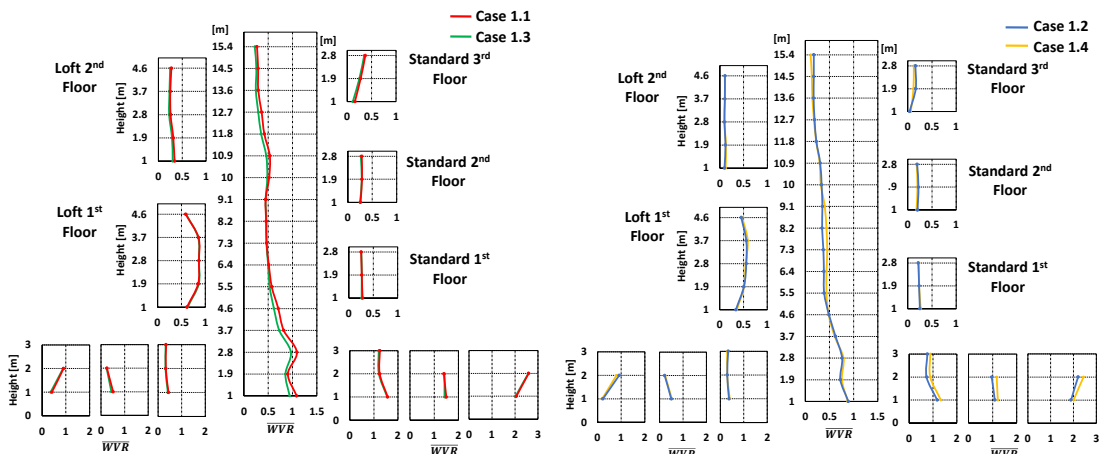


Fig. 7.  $\overline{WVR}$  with changes in penthouse window-opening conditions; (a) with windows/doors open, (b) with windows/doors closed.

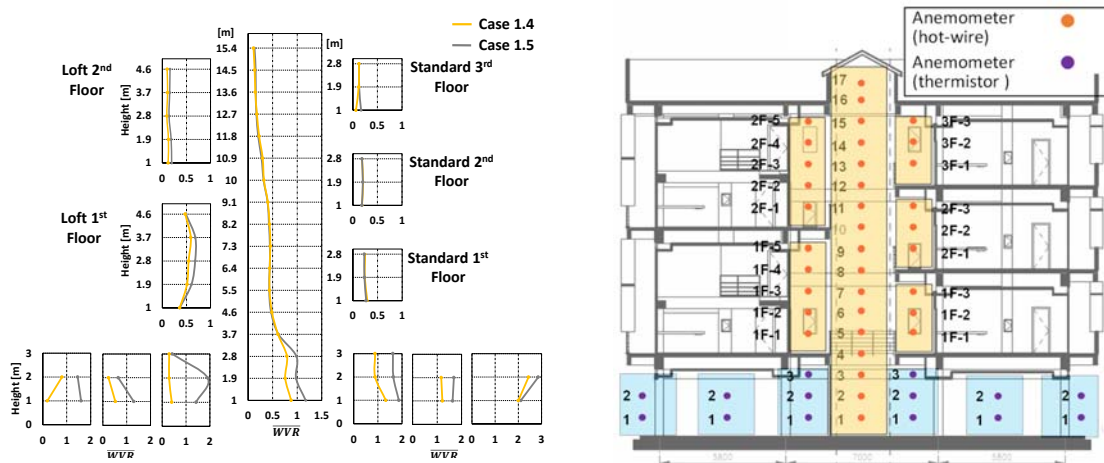


Fig. 8.  $\overline{WVR}$  with changes in fin size.

the wind velocities inside the building. However, the increased inflows from the pilotis did not reach the upper floor and therefore the wind velocities inside the void significantly decreased with height regardless of the window opening conditions. The internal corridor also obstructed the wind flow towards the 2<sup>nd</sup> floor of the loft units.

Fig. 7 depicts the results of comparisons between open and closed louver windows of the penthouse. The conditions of windows and doors were different between Cases 1.1 & 1.3 (opened) and Cases 1.2 & 1.4 (closed). Overall, the increase in  $\overline{WVR}$ s is not observed except for a lower part (at 1.0–4.6 m) and upper part (at 10.9–13.6 m) of the void in Case 1.1. This is mainly because the wind-forced ventilation is dominant in the present natural ventilation system rather than those based on the temperature difference, and the increase in inflow volume did not reach the upper part of the building sufficiently as discussed before.

Fig. 8 shows the results of comparison between the large size of the wind fin (Case 1.4) and that of the small size (Case 1.5). The wind fin was 4 m by 12 m for the large size and approximately 2.4 m by 12 m for the small size (see Fig. 2). As shown in Fig. 8,  $\overline{WVR}$ s in pilotis are higher in most measuring points when the fin size was small. This is because the cross section of the pilotis was increased with the small size of the fin. The volume of inflows to the void was reduced as the size of the fin reduced and thus the wind pressure (i.e. static pressure) inside the void should be decreased accordingly. However, the increase in fin size did not result in the increase in wind velocity. Instead,  $\overline{WVR}$ s were increased by up to 0.12 in Case 1.5 (small fin) at the internal corridor of the 1<sup>st</sup> floor loft unit (leeward side) because of the increased wind velocities of the inflow from the pilotis.

### 3.2 Flow rate measurement

Fig. 9 depicts the vertical distributions of averaged wind velocities measured at the openings at four different levels on the corridor side of the leeward units. It should be noted that the wind velocities at the lower level of the 1<sup>st</sup> floor loft unit received stronger winds than the outdoor reference values especially when the window/doors were opened (Cases 2.1–2.3, 2.5). Similarly, the wind velocities at the 2<sup>nd</sup> floor units were almost equal but slightly increased in Case 2.2 compared with Case 2.3 when the windows/doors of the windward units were opened. As seen

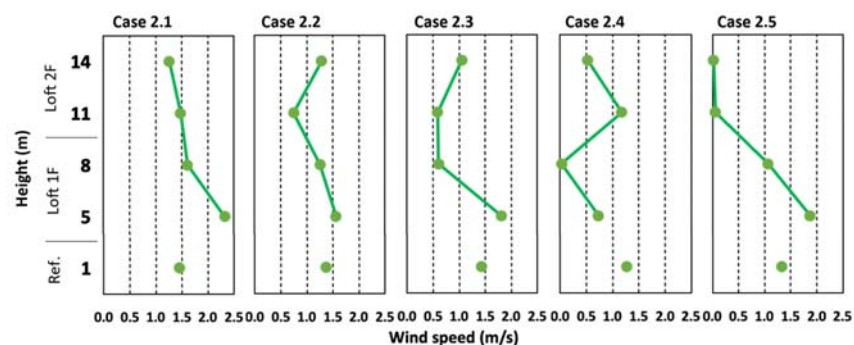


Fig. 9. Vertical distributions of wind velocities on the corridor side of the leeward units.

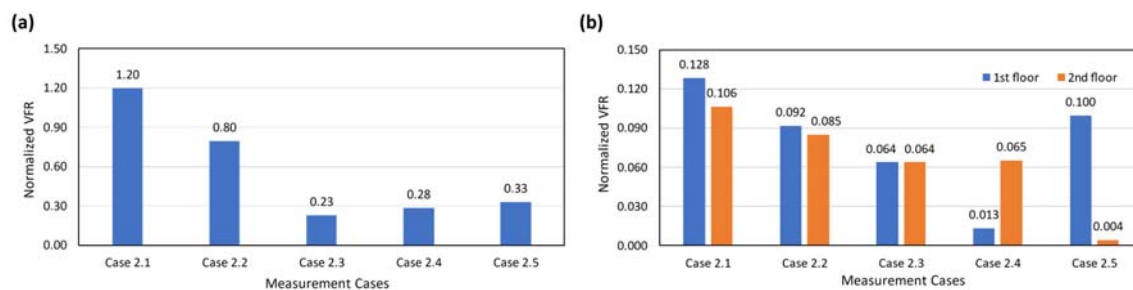


Fig. 10. Normalized volumetric flow rates in (a) vertical void and (b) leeward loft units.

in the above-mentioned measurement, window/door-opening increased the wind velocities for most spaces in and around the void (see Fig. 6).

Fig. 10 presents the results of *VFR* measurements. As shown in Fig. 10a, the *VFR* for the void was maximized (1.20) when all the windows/doors were opened in Case 2.1, which is equivalent to approximately 193 ACH (times/h). As expected, the opening conditions of the windward units affected the *VFR* of the void. However, even when the windows/doors were closed on the windward side, sufficient *VFRs* of approximately 0.23-0.33 were obtained through the inflows from the pilotis (Cases 2.3-2.5), which are approximately 36.6-48.2 ACH. As indicated in Fig. 10b, *VFRs* of the leeward units were largest in Case 2.1 (all windows/doors opened), followed by Case 2.2 (windward units were opened) and Case 2.3 (windward units were closed). It can be seen that among Cases 2.1-2.3, *VFRs* for the 1<sup>st</sup> floor leeward unit received larger values than those for the 2<sup>nd</sup> floor unit, but similar levels of *VFRs* were obtained even on the upper floor of the leeward units unlike the wind velocity distributions. It can be seen that approximately 11% of *VFR* of the void entered the 1<sup>st</sup> floor loft unit, whereas approximately 8.8% went to the 2<sup>nd</sup> floor loft unit in Case 2.1. This means that about 81% of *VFR* went to other spaces in this case. Similarly, in Case 2.2, approximately 12% went to the 1<sup>st</sup> floor loft unit and about 11% went to the 2<sup>nd</sup> floor unit. When the windows and doors of the windward units were closed in Case 2.3, approximately 28% of *VFRs* of the void entered the respective units (1<sup>st</sup> floor and 2<sup>nd</sup> floor), while the rest, approximately 44% or less might go back to the pilotis and a small amount passed through the penthouse's louver windows.

Similar results were obtained in the previous CFD simulation studies (Kumar et al., 2021, 2022). Kumar (2022) conducted a parametric study for a similar type of apartment building with a closed-vertical void. The results showed that the mass flow rates were slightly larger for the 1<sup>st</sup> floor leeward unit compared to the upper floors except for the top floor. An isolated vortex was created inside the closed void space and streamlines went back to the pilotis. The increase in wind speed was also observed near the corridor-side external wall of the lower leeward units in the CFD simulation results as seen in Figs. 6-8. Overall, it can be said that the results of the previous CFD simulations (Kumar et al., 2021, 2022) well replicate the present measurement results.

#### 4 CONCLUSIONS

The venturi effect was clearly observed at the pilotis. However, the increased winds did not reach the upper floor of the leeward units sufficiently even when the fin size was increased. Opening conditions of windows and doors significantly affected the wind velocity distribution in and around the void, though those of penthouse were negligible. Sufficient levels of *VFR* can be obtained even in the upper floor of leeward units due to the increased static pressure inside the closed void. Furthermore, the *VFR* of the lower floor of leeward units received slightly larger *VFRs* not only due to the increase in the overall static pressure but also in the wind velocities (i.e., dynamic pressure) for the specific areas. The proposed ventilation system would be able to provide sufficient cross ventilation to the double-loaded apartment buildings entirely with the increase in static pressure even for a mid-rise building. Moreover, the previous CFD simulation results well replicated the present measurement results.

#### 5 ACKNOWLEDGEMENTS

This research was partially supported by the SATREPS in collaboration with JST and JICA (JPMJSA1904), YKK AP Inc. and Asahi Glass Foundation. The experimental house in Tegal was constructed based on the financial support mainly by Nichias Corporation. The field measurements were conducted jointly with the Ministry of Public Works and Housing, Indonesia, and YKK AP Indonesia.

## 6 REFERENCES

- Alfata, M.N.F., Trihamdhani, A.R., Kubota, T., Asawa, T. (2023) Development of Low-Carbon Affordable Apartments in the Hot and Humid Climate of Indonesia: Construction of a Full-Scale Experimental House, *Environmental Science and Engineering*, 2537-2546.
- Bardhan, R., Debnath, R., Malik, J., Sarkar, A. (2018) Low-income housing layouts under socio-architectural complexities: a parametric study for sustainable slum rehabilitation, *Sustain. Cities Soc.* 41 (2018) 126–138.
- Kumar, N., Bardhan, R., Kubota, T., Tominaga, Y., Shirzadi, M. (2022) Parametric study on vertical void configurations for improving ventilation performance in the mid-rise apartment building, *Build. Environ.* 215, 108969.
- Kumar, N., Kubota, T., Tominaga, Y., Shirzadi, M., Bardhan, R. (2021) CFD simulations of wind-induced ventilation in apartment buildings with vertical voids: effects of pilotis and wind fin on ventilation performance, *Build. Environ.* 194, 107666.
- Lueker, J., Bardhan, R., Sarkar, A., Norford, L. (2020) Indoor air quality among Mumbai's resettled populations: comparing Dharavi slum to nearby rehabilitation sites, *Build. Environ.* 167 (2020) 106419.
- Prasetya, A., Ho, A.D., Kubota, T. (2023) Analysis of typical layout of apartment buildings in Indonesia, *Buildings*, 13(6), 1387.

# The Impact of Simplified Window and Exhaust Fan Assumptions on Model-Based Predictions of Inter-Zonal Air Flow and Contaminant Transport in Multifamily Buildings

Iain S. Walker<sup>1</sup>, Brennan D. Less<sup>1</sup>, Cara H. Lozinsky<sup>1,2</sup>,  
Núria Casquero-Modrego<sup>\*1</sup>, Michael D. Sohn<sup>3</sup>

<sup>1</sup> Residential Building Systems Group, Lawrence Berkeley National Laboratory, Berkeley, CA 94720, USA <i>*corresponding author: nuriacm@lbl.gov</i>	<sup>2</sup> Civil and Environmental Engineering Department, Carleton University, Ottawa, ON, Canada
<sup>3</sup> Energy Analysis and Environmental Impacts Division, Lawrence Berkeley National Laboratory Berkeley, CA 94720, USA	

## ABSTRACT

In residential buildings, the indoor air quality can be significantly affected by ventilation measures initiated by occupants, including the operation of windows and in-unit exhaust fans in kitchens and bathrooms. The outcome of these measures can be highly variable and difficult to accurately characterize in building simulation frameworks. Consequently, many simulations simplify these factors by disregarding window opening behaviours and using fixed schedules for exhaust fan operation across all residential units. To determine if these simplifications are reasonable and estimate the magnitude of changes in air flow and contaminant transport, this study used coupled CONTAM and EnergyPlus models to simulate airflow, contaminant transport, and controls in multifamily dwellings. The coupled models parametrically varied climate zone, building airtightness, and mechanical ventilation system types. The study focused on two key occupant behaviours: (1) operating kitchen and bathroom exhausts on different schedules in individual dwelling units, and (2) scheduling open windows on ground and top floors. The findings show that the simplified assumptions regarding uniform in-unit exhaust fan operation and window operation had a minimal impact on inter-unit air flow and contaminant transport simulations across a broad range of building airtightness and mechanical ventilation system types. Staggering exhaust fan operation schedules had close to zero effect on average inter-unit air flow with maximum changes of about 1 L/s (2 cfm). For contaminant transport, the changes in concentrations were typically much less than 1%, compared to baseline assumptions. These findings suggest that for buildings with tight construction it is reasonable for most modelling and simulation efforts to ignore the effects of non-uniform exhaust fan operation and window opening.

## KEYWORDS

Occupant behaviour; compartmentalization; multifamily buildings; CONTAM; EnergyPlus

## 1 INTRODUCTION

In multifamily residential buildings, occupants can supplement dwelling unit ventilation by opening windows and/or operating in-unit exhaust fans. Window operation increases the air change rate of the dwelling unit, diluting contaminants from indoor emission sources. In-unit exhaust fan operation also helps to improve indoor air quality (IAQ) by capturing contaminant emissions from indoor sources (e.g., humidity from showering/bathing and humidity and contaminants from cooking and heating) and exhausting them before they mix with the indoor air. While window and exhaust fan operation can be motivated by dissatisfaction with the IAQ, occupant behaviours are not easily predictable. Window operation behaviours can be influenced by indoor and/or outdoor climate, time of day, perceived air quality, building



orientation/construction, adequacy of ventilation and/or space conditioning systems, occupant activities, and security, among others (Fabi et al., 2012; Andersen et al., 2013). Exhaust fan operation is also highly variable and does not always track perfectly with indoor emission events (Lozinsky et al., 2023). In simulation studies, it is common to make simplifying assumptions regarding occupant behaviours, either assuming no window and/or exhaust fan operation, or using fixed schedules. The impact of occupant behaviours in whole building energy simulations has been extensively studied (Fabi et al., 2012; D’Oca et al., 2014; Sorgato et al., 2016). These studies consistently show that variations in occupant behaviour profiles have significant effects on energy consumption. While field studies on single-family homes have demonstrated that window and exhaust fan operations can alter air flow patterns and air change rates (Howard-Reed et al., 2002; Wallace et al., 2002; Nazaroff, 2021), the impact of occupant behaviours in multi-zone air flow simulations remains less thoroughly documented.

This study presents a sensitivity analysis, to evaluate the impact of window and exhaust fan operation on air flow and contaminant transport in multifamily buildings using coupled CONTAM/EnergyPlus simulations. The study parametrically varied building type (mid-rise, high-rise), climate zone, dwelling unit air leakage rate, and mechanical ventilation system type.

## 2 METHODOLOGY

This analysis utilized a simulation framework previously developed in a project that assessed compartmentalization and ventilation system performance in multifamily buildings. The following provides an abridged description of the methodology. For more details, refer to (Walker et al., 2024).

### 2.1 Prototype Buildings and Simulation Framework

The building geometry, building envelope, heating, ventilation, and air conditioning (HVAC) equipment were modelled based on the Pacific Northwest National Laboratory (PNNL) mid-rise multifamily prototype model used in energy code analysis (Department of Energy (DOE), 2023). This prototype is a four-storey building, with eight dwelling units per floor, a common corridor, with a stairwell and elevator shafts on each end of the corridor (Figure 1). Additionally, a high-rise version of this building type was simulated, comprising twenty storeys, each with the floor plan shown in Figure 1. Each dwelling unit was modelled as a single zone, leaving out any interior partitions.

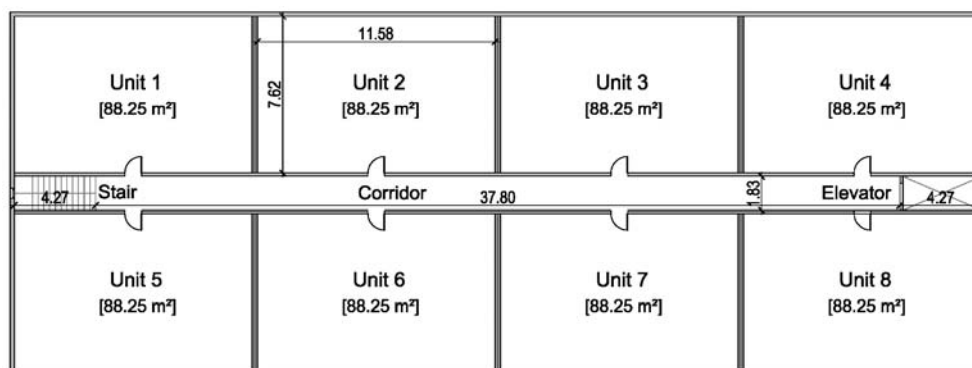


Figure 1: Layout of a prototypical building floor for the mid-rise and high-rise common corridor simulations.

During co-simulation, EnergyPlus provided CONTAM with zone temperatures, humidity ratios, ventilation system air flows, weather data, contaminant source generation rates, and other model parameters at each time step. CONTAM returned the infiltration and zone-to-zone

air flows, along with the concentrations of the contaminants of interest. Simulations were run at a 3-minute time-step, although outputs were recorded at hourly intervals. The short time step was essential for adequate representation of short time-scale events such as cooking and intermittent exhaust fans operation and to minimize time step lag by co-simulation introduced between EnergyPlus and CONTAM. For a detailed description of the coupling process, refer to (Dols et al., 2016) and (Justo Alonso et al., 2022).

## 2.2 Climate Zone

We simulated three EnergyPlus climate zones (CZs) to cover the range of conditions across the continental United States: CZ 2A (Hot humid, Tampa, FL), CZ 4A (Mixed humid, New York, NY), and CZ 7 (Very Cold/International Falls, MN). The hourly Typical Meteorological Year 3 (TMY3) weather data were linearly interpolated by EnergyPlus within each hour to accommodate the 3-minute time steps used in the simulations.

## 2.3 Ventilation System Types

In this study we considered three whole dwelling ventilation system types (Table 1): (1) Unit Balanced HRV; (2) Unit Exhaust, Corridor Supply; and (3) Unit Supply. Dwelling unit mechanical fan flow rates met the minimum calculated requirement of 27.5 L/s (58 cfm) based on ASHRAE 62.2-2019 (ASHRAE, 2019b). For the Unit Balanced HRV and Unit Supply cases, the corridor on each floor was supplied with outdoor air at a minimum rate of 19.2 L/s (41 cfm), based on ASHRAE 62.1 requirements for common corridors (ASHRAE, 2019a). For the Unit Exhaust with Corridor Supply cases, the corridor supply air flow rate was 220 L/s (466 cfm), which includes the 19.2 L/s (41 cfm) for the corridor and 27.5 L/s/dwelling unit (58 cfm per dwelling unit). The Unit Balanced HRV cases included sensible heat recovery at 70%. For further details on in-unit exhaust operation schedules, refer to Section 2.6 and Table 3.

Table 1: Whole dwelling ventilation system air flow rates.

Ventilation System Type	Dwelling Exhaust Flow L/s (cfm)	Dwelling Supply Flow L/s (cfm)	Corridor Supply Flow L/s (cfm)
Unit Balanced HRV	27.5 (58)	27.5 (58)	19.2 (41)
Unit Exhaust, Corridor Supply	27.5 (58)	0	220 (466)
Unit Supply	0	27.5 (58)	19.2 (41)

## 2.4 Air Leakage Pathways

The analysis included three dwelling unit air leakage rates: (1) “Leaky”: 5.1 L/s<sub>50</sub>/m<sup>2</sup> (1.0 cfm<sub>50</sub>/ft<sup>2</sup>); (2) “Typical Practice”: 1.0 L/s<sub>50</sub>/m<sup>2</sup> (0.20 cfm<sub>50</sub>/ft<sup>2</sup>); and (3) “Tight”: 0.25 L/s<sub>50</sub>/m<sup>2</sup> (0.05 cfm<sub>50</sub>/ft<sup>2</sup>). Leakage areas were distributed to the different dwelling unit surfaces based on field studies that measured partition-level air leakage rates in low- and high-rise multifamily buildings (Bohac et al., 2007, 2020; Ricketts, 2014; Lozinsky & Touchie, 2023): 2.5% to each party wall, 10% to each floor or ceiling surface, 45% to the corridor wall and 30% to exterior wall surfaces. Each element of the building envelope's leakage was treated using the power law formulation in CONTAM, with a discharge coefficient (C<sub>d</sub>) of 1.0, flow exponent (n) of 0.67, and a reference pressure of 4 Pa. Interior door leakage paths were treated as orifices using the power law formulation in CONTAM (C<sub>d</sub> = 0.60 and n = 0.50 at 4 Pa). The elevator and stairwell doors had leakage areas of 300 cm<sup>2</sup> (46.5 in<sup>2</sup>) and 200 cm<sup>2</sup> (31.0 in<sup>2</sup>), respectively. Dwelling unit entry door undercuts for Unit Balanced HRV and Unit Supply cases were assumed to be 13 cm<sup>2</sup> (2.0 in<sup>2</sup>) (Tian et al., 2020), while the Unit Exhaust, Corridor Supply had door undercuts of 210 cm<sup>2</sup> (32.6 in<sup>2</sup>) (Peter Moffatt et al., 1998).

## 2.5 Contaminant Emission

The models included three types of contaminants: carbon dioxide (CO<sub>2</sub>), formaldehyde (CH<sub>2</sub>O), and particulate matter with a diameter less than 2.5 microns (PM<sub>2.5</sub>). Details regarding indoor emission rates/sources and outdoor concentrations are listed in Table 2.

Table 2: Dwelling units Indoor emission rates and outdoor concentrations.

Contaminant	Indoor Dwelling Unit Emission Rates	Outdoor Concentration
CO <sub>2</sub> *	Sleeping: 6.5 mg/s (adult), 4 mg/s (child) Awake: 10 mg/s (adult), 6.5 mg/s (child) (Emmerich et al., 2005)	400 ppm
CH <sub>2</sub> O	Calculated based on zone air temperature, relative humidity and ventilation rate (Zhao et al., 2022).	2 ppb
PM <sub>2.5</sub>	Cooking: 0.0416 mg/s** Occupant-generated emissions: 0.00007 mg/s (Chan et al., 2020)	Hourly, diurnal concentrations calculated from U.S.E.P.A. monitoring station for Sussex, DE (Site 1002)***
*CO <sub>2</sub> generation assumes each dwelling is occupied 24 hours of the day with two adults and two children (occupants spent 16 h awake and 8 h sleeping) **Cooking emission rates were reduced by 50% in the models, to account for exhaust fan capture efficiency ***Mean concentration = 8.1 µg/m <sup>3</sup> . This site was selected as a typical outdoor PM <sub>2.5</sub> profile.		

The models assumed no particle filtration in the mechanical ventilation systems. Interior and exterior leakage pathways were modelled with a 50% removal efficiency for PM<sub>2.5</sub>, to account for penetration losses, while the particulate deposition rate was modelled at 0.6/h. We simulated two types of indoor contaminants: (1) global contaminants; and (2) shadow contaminants. Both contaminant types followed the identical emission rates and schedules described previously. Global contaminants were uniformly emitted in every dwelling unit to characterize indoor contaminant concentrations from typical occupant activities. These contaminants were not specific to individual units, meaning that we did not track their origin or movement. In contrast, shadow contaminants were emitted in Unit 2 (Figure 1) on three levels in each building type: levels 1, 3 and 4 in the mid-rise building; and levels 1, 11 and 20 in the high-rise building. These contaminants were labelled with a unique identifier to facilitate independent tracking from the global contaminants. This classification allowed us to characterize the impact of compartmentalization on inter-unit contaminant transport.

## 2.6 Exhaust Fan and Window Operation Schedules (Sensitivity Analysis)

The baseline simulation scenarios assumed the default exhaust fan operation schedule (Table 3) across all dwelling units. The variable exhaust fan schedule scenarios used three different profiles as follows: Profile 1 used the default exhaust fan operation schedule, while Profile 2 shifted all exhaust fan operation events forward by 30 minutes. Profile 3 rescheduled the showering event to 19:00 – 19:30 and increased the bathroom fan flow rate to 50 L/s (106 cfm), omitted the morning cooking event, shifted the mid-day cooking event forward by 60 minutes to 12:45 – 13:15, moved the evening cooking activity forward by 30 minutes and extended its duration by 30 minutes (18:30 – 19:00), and used the same scheduling and fan flow rate for the laundry event as Profile 1. The total fan air flow was the same for all three profiles. The profiles were assigned to dwelling units in a continuous rotation (e.g., Profile 1 was assigned to units 1ap1, 1ap4, 1ap7, etc; Profile 2 to units 1ap2, 1ap5, 1ap8, etc; and Profile 3 to units 1ap3, 1ap6; 2ap1, etc) to ensure both horizontal and vertical variability. Consistent with the baseline model assumptions, both the default and variable exhaust fan simulation cases assumed no window operation.

In baseline simulations we did not assume window operation. For window operation cases we assumed all dwelling units on the ground and top floors had their windows open. In both

scenarios, the open windows had an opening area of 0.38 m<sup>2</sup> (4.04 ft<sup>2</sup>) in each unit. The two cases of no window opening and all window at the top and bottom of the buildings represent the operational extremes providing an expected range of performance. Both the baseline and “top/bottom open” window operation simulations assumed the default exhaust fan operation schedule.

Table 3: Default exhaust fan operation schedule.

Start and End Times	Activities	Kitchen Fan L/s (cfm)	Bathroom Fan L/s (cfm)	Laundry Fan L/s (cfm)
07:00 – 07:30	Showering	0	25 (53)	0
07:30 – 08:00	Cooking and Showering	50 (106)	25 (53)	0
11:45 – 12:15	Cooking	50 (106)	0	0
18:00 – 18:30	Cooking	50 (106)	0	0
21:30 – 22:00	Laundry	0	0	37.5 (79)

### 3 RESULTS

#### 3.1 Direct Air Flow from Adjacent Units

Air flow between dwelling units is a necessary precursor to the transport of contaminants between dwelling units. This study assessed the air flow directly from adjacent dwelling units throughout multifamily buildings (for mid- and high-rise buildings). Previous research has established that “From Unit” air flows (air flows from units that are adjacent to each other) are generally dominated by vertical air flows and are uniform throughout the building. The exception is for the ground floor, which has no units below and therefore negligible inflow from other units (Walker et al., 2024).

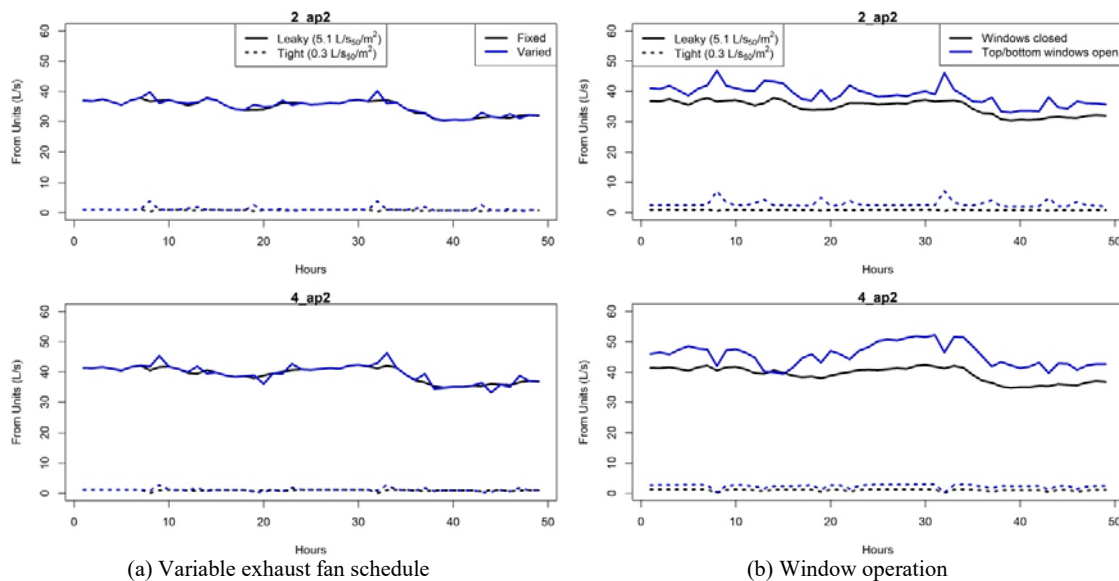


Figure 2: Occupant activity schedule and window operation impacts from adjacent units for the mid-rise common corridor prototype.

Figure 2a and Figure 2b show hourly mean “From Unit” air flows for Unit 2 on Floors 2 and 4, over a 48-hour period in January (winter) for the variable exhaust fan schedules and window operation cases, respectively. The example results are for Corridor Supply, Unit Exhaust ventilation in CZ7 for the mid-rise common corridor prototype. “Leaky” and “Tight” dwelling cases are compared with solid and dashed lines respectively. Baseline cases (i.e., fixed occupant activity schedules and closed windows) are compared with varied occupant activity schedules

in adjacent units and open windows on the top and bottom floors by line colour (i.e., black and blue lines, respectively).

The variations in variable exhaust fan schedules and window operation showed relatively minor impacts on air flow from other units. Variable exhaust fan schedules had minimal changes in air flow from adjacent units in both the “Leaky” and “Tight” dwellings, with maximum “From Unit” air flow changes coincident with changed fan operation of about 5 L/s (11 cfm) for the Leaky case and 2.5 L/s (5 cfm) for the tight case, with similar effects observed on the 2<sup>nd</sup> and 4<sup>th</sup> floors. Typical changes are close to zero. Window operation caused a consistent increase in air flow from other units with a greater absolute increase in air flow observed in the “Leaky” buildings (about 5 L/s (11 cfm) compared to 1-2 L/s (0.5-1 cfm) for tight construction).

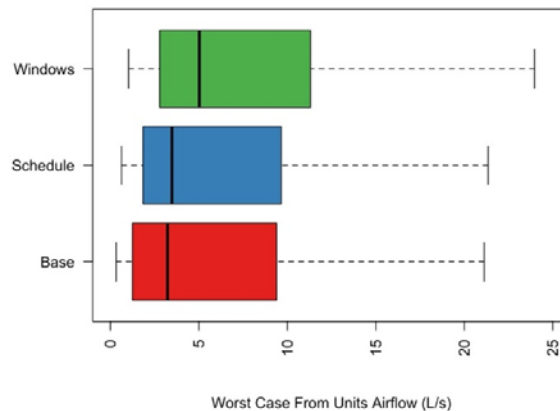


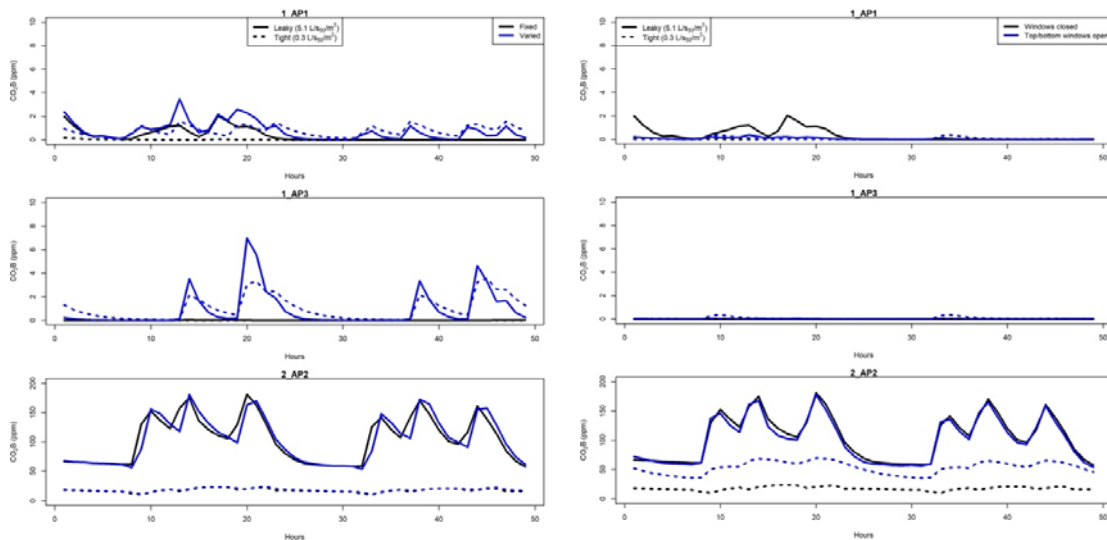
Figure 3: Annual mean “From Unit” air flows in worst-case dwellings from every simulation case. Boxplots are coloured according to the simulation case—baseline, variable exhaust fan schedules and window operation. Distributions show the annual average values for the worst-case dwelling unit in each building.

As shown by the time-series results from select buildings and dwellings, building operation assumptions have minimal impacts on hourly mean air flow directly from adjacent dwelling units. For the annual impacts on a whole building level, Figure 3 shows the distribution across all simulated buildings of the worst-case “From Unit” air flows for any given dwelling unit. These distributions are compared for the baseline (red colour), variable exhaust fan schedule (blue colour) and window operation (green colour) cases across all simulated climate zones, building types, leakage levels, and ventilation system types. Overall, both open windows and varied exhaust fan schedules increase the “From Unit” air flow, with windows having a somewhat greater impact (~2 L/s (~4 cfm)) compared with the variable exhaust fan schedules (<1 L/s (<2 cfm)). These are small fractions of the dwelling unit air flows of 27.5 L/s (58 cfm). The building prototype (i.e., mid- and high-rise) had minimal impacts on the results. These worst case air flow changes are a small percentage of the whole dwelling mechanical system flow of 27.5 L/s (58 cfm), with typical changes being even smaller. Other ventilation system results are very similar.

### 3.2 Contaminant Transport

The study evaluated the impacts of building operation on inter-dwelling contaminant transport using the shadow contaminant analysis described in the methodology. Figure 4 shows the bottom shadow CO<sub>2</sub> concentration (i.e., shadow CO<sub>2</sub> released in Unit 2 on the 1<sup>st</sup> floor) in the three directly adjacent units (i.e., Units 1 and 3 on the 1<sup>st</sup> floor, and Unit 2 on the 2<sup>nd</sup> floor) for two days in January. These example results are for the case of Corridor Supply, Unit Exhaust ventilation in CZ7 for the mid-rise common corridor prototype. “Leaky” and “Tight” building cases are compared with solid and dashed lines, while fixed and variable exhaust fan schedules

are indicated by blue and black line colouring. Note the differing y-axis scales in the bottom plot panes for the dwelling unit directly above the source dwelling unit (2\_ap2). For comparison, the peak CO<sub>2</sub> in the source dwelling unit was about 700 ppm at times corresponding to the peak concentrations in Figure 4.



(a) Variable exhaust fan schedule impacts on shadow contaminant concentrations of CO<sub>2</sub>. (b) Window operation impacts on shadow contaminant concentrations of CO<sub>2</sub>.

Figure 4: Shadow contaminant concentrations of CO<sub>2</sub> in zones directly adjacent to the shadow contaminant source zone (1\_ap2)

Horizontal and vertical transport of shadow CO<sub>2</sub> increased between the baseline and varied building operation schedule cases during emission events (e.g., cooking). For horizontally attached dwelling units, the increases were not significant: at most, ~3 ppm for the “Tight” case and 5-6 ppm for the “Leaky” case, and far less than this on average. This was typically less than 1% change in the total CO<sub>2</sub> concentration in these units. For the dwelling unit above the source zone (i.e., 2\_ap2, bottom plot pane) there was CO<sub>2</sub> transport for the “Leaky” case, where CO<sub>2</sub> peaks were evident from cooking events in the dwelling unit below. The typical increase in total CO<sub>2</sub> due to shadow CO<sub>2</sub> was about 5-10%, assuming baseline conditions. The effect of window opening and variable fan schedules are hard to discern, particularly for the fan schedule changes where sometimes CO<sub>2</sub> transport increased and at other times decreased. For the “Tight” case in this dwelling unit (2\_ap2), the variable fan schedules did not show any change in CO<sub>2</sub> concentrations, but window opening consistently increased shadow CO<sub>2</sub> concentrations by 20-50 ppm. For other dwelling units in the building *not directly attached* to a dwelling unit emitting a shadow contaminant, the increases in concentration of shadow contaminant were negligible at much less than 1% for the peak events shown in Figure 4, and even smaller when averaged over a year.

Inter-unit air flow (and contaminant transport) is predominantly driven by stack effect in these building simulations (Walker et al., 2024), particularly for the examples shown here for the coldest climate zone. These generally insignificant changes in air flows and concentrations are because the inter-unit pressure differences induced by the variable exhaust fan and window operations tend to be smaller than the background stack effect driving the inter-unit air flow. Similar results were observed for the units directly adjacent to the middle and top shadow source zones and were unaffected by the building prototype (i.e., mid-rise vs. high-rise).

While the example time series data are useful for observing trends and allow us to observe how air flows and concentrations change with different time-scheduled events, it is important to look at results for the full dataset covering all weather, different ventilation systems and both building prototypes. While the time-series results generally showed small effects on average, it can be instructive to examine the peak short-term results. To examine short-term effects and to better observe any differences, we searched the results for the occurrences where differences in concentrations caused by the fan schedules and window openings were the greatest: i.e., the worst-case results. Figure 5 shows the annual worst-case *non-source zone* CO<sub>2</sub> concentrations from each simulation case, for each shadow contaminant source location (i.e., how much of the shadow contaminant accumulates in adjacent zones). The variable exhaust fan schedules did not have a meaningful effect for shadow contaminants released near the bottom or middle of the building, but roughly doubled the transport of shadow contaminants released at the top of the building, with a median increase of 5 to 10 ppm above baseline cases. Open windows led to higher shadow CO<sub>2</sub> concentrations in zones adjacent to the source zone on bottom and top floors, but not near the middle of the building (~10 ppm increase in median, compared to baseline). This is likely driven by our model assumptions, which assumed open windows on the bottom and top floors. This would greatly increase infiltration/exfiltration rates near the top and bottom of the building, but would have minimal impact on the middle of the building. Evenly distributing the window openings across the full height of the building would likely have tempered this effect. For both the variable exhaust fan schedule and window operation cases, the increased inter-unit contaminant transport was typically less than 15 ppm (<3% of the total dwelling unit CO<sub>2</sub> concentrations).

#### 4 SUMMARY AND CONCLUSIONS

This study explored the impacts of varied exhaust fan schedules and window operation on predictions of air flow and contaminant transport between dwelling units in multifamily buildings. We performed parametric, annual simulations for mid- and high-rise multifamily buildings with three types of envelope leakages (“Leaky”, “Typical Practice” and “Tight”), three climate zones, three ventilation system types, and two building heights using a co-simulation framework that combined EnergyPlus and CONTAM. The air flow results showed close to zero change in average “From Unit” flow for changing fan schedules, with worst case changes less than 1 L/s (2 cfm). Open windows had consistent increases in “From Unit” flow of about 2 L/s (4 cfm) with tight construction being lower in the range of 1-2 L/s (2-4 cfm). These air flow changes are a small percentage of the whole dwelling mechanical system flow of 27.5 L/s (58 cfm). For contaminant transport, the changes in concentrations were typically much less than 1%. The exception is for the “Tight” case in the dwelling unit directly above the source unit, where window opening consistently increased shadow CO<sub>2</sub> concentrations by 20-50 ppm. Window operation had a larger impact on air flow and contaminant transport, compared to varied exhaust fan schedules; however, there was a height-based effect, induced by window opening locations. Different window operation assumptions may produce slightly different results. This analysis provides support for the use of static and simplified approaches to scheduling activities and window operation in simulation assessments of airflow and air quality in multi-zone buildings.

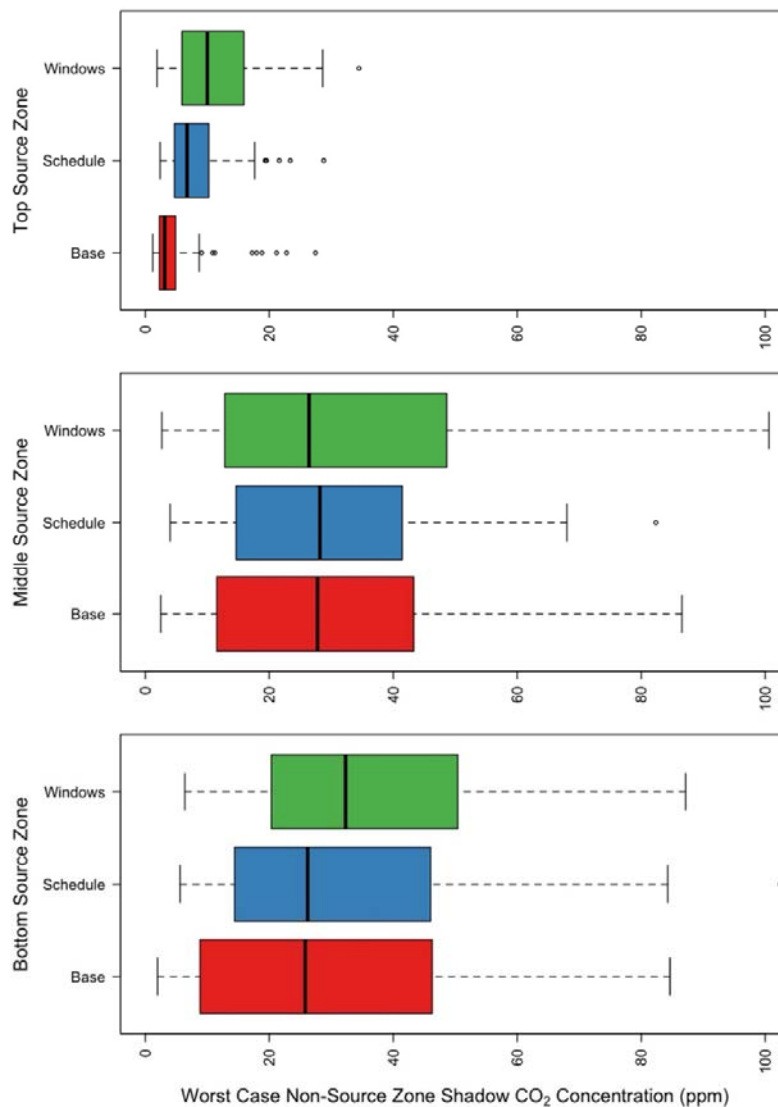


Figure 5: Annual worst-case non-source zone shadow CO<sub>2</sub> concentration. Boxplots are coloured according to the simulation case—baseline, varied activity schedules and window operation. Distributions show the annual average values for the worst-case dwelling unit in each building.

## 5 ACKNOWLEDGEMENTS

This work was supported by the Assistant Secretary for Energy Efficiency and Renewable Energy, Building Technologies Office, of the U.S. Department of Energy under Contract No. DE-AC0205CH11231.

## 6 REFERENCES

- Andersen, R., Fabi, V., Toftum, J., Corgnati, S. P., & Olesen, B. W. (2013). Window opening behaviour modelled from measurements in Danish dwellings. *Building and Environment*, *69*, 101–113. <https://doi.org/10.1016/j.buildenv.2013.07.005>
- ASHRAE. (2019a). *ANSI/ASHRAE Standard 62.1: Ventilation for Acceptable Indoor Air Quality*. <https://doi.org/10.1201/9780849338960.ch6>
- ASHRAE. (2019b). *ANSI/ASHRAE Standard 62.2: Ventilation and Acceptable Indoor Air Quality in Residential Buildings*.



- Bohac, D. L., Hewett, M. J., Fitzgerald, J. E., & Grimsrud, D. (2007). Measured Change in Multifamily Unit Air Leakage and Airflow Due to Air Sealing and Ventilation Treatments. *Buildings X: Thermal Performance of the Exterior Envelopes of Whole Buildings.*, 14.
- Bohac, D. L., Sweeney, L., Davis, R., Olson, C., & Nelson, G. (2020). *Energy Code Field Studies: Low-Rise Multifamily Air Leakage Testing*. US DOE. [https://www.mncee.org/sites/default/files/report-files/LRMF\\_AirLeakageTesting\\_FinalReport\\_2020-07-06.pdf](https://www.mncee.org/sites/default/files/report-files/LRMF_AirLeakageTesting_FinalReport_2020-07-06.pdf)
- Chan, W. R., Kim, Y.-S., Less, B., Singer, B., & Walker, I. (2020). *Ventilation and Indoor Air Quality in New California Homes with Gas Appliances and Mechanical Ventilation (2001200R1)*. LBNL. <https://doi.org/10.20357/B7QC7X>
- Department of Energy (DOE). (2023). *Prototype Building Models*. Building Energy Codes Program. <https://www.energycodes.gov/prototype-building-models>
- D'Oca, S., Fabi, V., Corgnati, S. P., & Andersen, R. K. (2014). Effect of thermostat and window opening occupant behavior models on energy use in homes. *Building Simulation*, 7(6), 683–694. <https://doi.org/10.1007/s12273-014-0191-6>
- Dols, W. S., Emmerich, S. J., & Polidoro, B. J. (2016). Coupling the multizone airflow and contaminant transport software CONTAM with EnergyPlus using co-simulation. *Building Simulation*, 9(4), 469–479. <https://doi.org/10.1007/s12273-016-0279-2>
- Emmerich, S. J., Howard-Reed, C., & Gupte, A. (2005). *Modeling the IAQ impact of HHI interventions in inner-city housing (NIST IR 7212; p. NIST IR 7212)*. National Institute of Standards and Technology. <https://doi.org/10.6028/NIST.IR.7212>
- Fabi, V., Andersen, R. V., Corgnati, S., & Olesen, B. W. (2012). Occupants' window opening behaviour: A literature review of factors influencing occupant behaviour and models. *Building and Environment*, 58, 188–198. <https://doi.org/10.1016/j.buildenv.2012.07.009>
- Howard-Reed, C., Wallace, L. A., & Ott, W. R. (2002). The Effect of Opening Windows on Air Change Rates in Two Homes. *Journal of the Air & Waste Management Association*, 52(2), 147–159. <https://doi.org/10.1080/10473289.2002.10470775>
- Justo Alonso, M., Dols, W. S., & Mathisen, H. M. (2022). Using Co-simulation between EnergyPlus and CONTAM to evaluate recirculation-based, demand-controlled ventilation strategies in an office building. *Building and Environment*, 211, 108737. <https://doi.org/10.1016/j.buildenv.2021.108737>
- Lozinsky, C. H., Stopps, H., & Touchie, M. F. (2023). In-situ performance of a pressurized corridor ventilation system: A long-term study in a high-rise multi-unit residential building. *Journal of Building Engineering*, 70, 106320. <https://doi.org/10.1016/j.jobe.2023.106320>
- Lozinsky, C. H., & Touchie, M. F. (2023). Quantifying suite-level airtightness in newly constructed multi-unit residential buildings using guarded suite-level air leakage testing. *Building and Environment*, 236, 110273. <https://doi.org/10.1016/j.buildenv.2023.110273>
- Nazaroff, W. W. (2021). Residential air change rates: A critical review. *Indoor Air*, 31(2), 282–313. <https://doi.org/10.1111/ina.12785>
- Peter Moffatt, Ian Theaker, & Craig Wray. (1998). *Field Testing to Characterize Suite Ventilation in Recently Constructed Mid- and High Rise Residential Buildings* [Research Report]. Canada Mortgage and Housing Corporation. [https://publications.gc.ca/collections/collection\\_2011/schl-cmhc/nh18-1/NH18-1-177-1998-eng.pdf](https://publications.gc.ca/collections/collection_2011/schl-cmhc/nh18-1/NH18-1-177-1998-eng.pdf)
- Ricketts, L. (2014). *A Field Study of Airflow in a High-Rise Multi-Unit Residential Building* [M.A.Sc. Thesis]. University of Waterloo.
- Sorgato, M. J., Melo, A. P., & Lamberts, R. (2016). The effect of window opening ventilation control on residential building energy consumption. *Energy and Buildings*, 133, 1–13. <https://doi.org/10.1016/j.enbuild.2016.09.059>
- Tian, X., Fine, J., & Touchie, M. (2020). The Impact of Sweeps and Weather Stripping on Suite Door Air Tightness. *ASHRAE Transactions*, 126(1).
- Walker, I. S., Less, B. D., Lozinsky, C. H., Lorenzetti, D., Casquero-Modrego, N., & Sohn, M. D. (2024). Compartmentalization and ventilation system impacts on air and contaminant transport for multifamily buildings. *International Journal of Ventilation*, 1–28. <https://doi.org/10.1080/14733315.2024.2333669>
- Wallace, L. A., Emmerich, S. J., & Howard-Reed, C. (2002). Continuous measurements of air change rates in an occupied house for 1 year: The effect of temperature, wind, fans, and windows. *Journal of Exposure Science & Environmental Epidemiology*, 12(4), 296–306. <https://doi.org/10.1038/sj.jea.7500229>
- Zhao, H., Walker, I. S., Sohn, M. D., & Less, B. (2022). A Time-Varying Model for Predicting Formaldehyde Emission Rates in Homes. *International Journal of Environmental Research and Public Health*, 19(11), 6603. <https://doi.org/10.3390/ijerph19116603>

# Application strategies and effectiveness of CO<sub>2</sub> signal lights for improving indoor air quality in classrooms

Simon Beck<sup>\*1</sup>, Gabriel Rojas<sup>1</sup>

*1 University of Innsbruck and Digital Science Center  
Innrain 52  
6020 Innsbruck, Austria*

*\*Corresponding author: simon.beck@uibk.ac.at*

## ABSTRACT

Improving air quality in existing classrooms can be difficult if retrofitting a mechanical ventilation system is considered too expensive or cannot be implemented due to other reasons, e.g., heritage protection. Especially in the cold winter months, window airing initiated by pupils or teachers is often not sufficient. To address this issue, a possible approach involves the incorporation of CO<sub>2</sub> feedback devices (or CO<sub>2</sub> traffic lights) into classrooms, which serve to visually and sometimes acoustically alert occupants when CO<sub>2</sub> concentrations get too high, signalling the need for a higher outdoor air change rate. Different types of CO<sub>2</sub> feedback devices and strategies are investigated, looking at threshold values, the CO<sub>2</sub> sensors used, and their precision within existing studies, standards, and commercially available devices. In the scope of an ongoing Citizen Science project in ten Austrian schools, a typical CO<sub>2</sub> sensor light application strategy is tested in a subset of the investigated classrooms and evaluated under real-world conditions by monitoring CO<sub>2</sub> concentrations before and after its implementation, as well as a comparison to a control group. Analysis is done by comparing CO<sub>2</sub> levels at different outside temperatures and applying statistical tests such as the Welch t-Test and Mann-Whitney-U-Test. Covariances are investigated using the ANCOVA test. The comparison of CO<sub>2</sub> levels under different outdoor temperatures shows improvements after implementation of the visual feedback at lower ambient temperatures, suggesting that CO<sub>2</sub> traffic lights can be a valid intervention for classrooms. This is partly supported by the comparison to the control group, which showed unchanged air quality up to 9°C outdoor temperature when looking at a hypothetical intervention. The study concludes that the visual feedback system appears to be effective in reducing CO<sub>2</sub> levels in classrooms during colder periods, although long-term effects and potential behavioural changes require further investigation, including the effect on thermal comfort and energy use. Limitations include potential habituation to the equipment and the late intervention date, which affect interpretation due to seasonal differences in weather or behaviour. Future research could explore the removal of the CO<sub>2</sub> traffic lights after prolonged use to observe changes in behaviour in a reverse manner.

## KEYWORDS

Indoor Air Quality, Schools, CO<sub>2</sub> Traffic Light, Ventilation, Intervention

## 1 INTRODUCTION

Window airing in educational buildings might not ensure optimal indoor air quality (IAQ) due to the trade-off between maintaining thermal comfort and indoor air quality, particularly in the colder seasons. This problem is still widespread in Austrian schools (Beck et al., 2023; Brandl et al., 2001; Hohenblum et al., 2008; Humhal, 2014; Knotzer & Venus, 2013), since there is a reluctance to install mechanical ventilation systems in schools, mainly because of the high cost or heritage protection of the buildings. As a result, alternative measures such as CO<sub>2</sub> traffic lights have gained attraction as a cost-effective and minimally invasive solution to this challenge. The effectiveness of such air quality feedback devices has merely been investigated, and reported results are inconclusive (Heebøll et al., 2018; Wargocki & Da Silva, 2015), probably because their effectiveness is dependent on the particular users to ensure proper

window operation. There is also the question of whether such devices will become less effective over time when the “novelty” effect has vanished.

Recognising that poor air quality can have a significant impact on student wellbeing and academic performance (e.g., Simons et al., 2010; Wargocki, 2015), there is growing interest in implementing real-time feedback mechanisms to monitor and improve IAQ. Since many indoor air contaminants cannot be reliably detected with human senses, the use of low-cost sensors might help with identifying ventilation needs. CO<sub>2</sub> concentration serves as an indicator for assessing contamination with bio-effluents and is therefore often used as a tool to evaluate ventilation (ASHRAE, 2022). By providing visual or acoustic signals based on CO<sub>2</sub> levels, these systems prompt occupants to sufficiently ventilate spaces, thereby helping to mitigate potential health risks associated with prolonged exposure to harmful indoor pollutants.

However, the lack of standardised guidelines for such feedback devices, together with variations in acceptable CO<sub>2</sub> thresholds within applicable standards (e.g., EN 16798-1, 2024; ÖNORM H 6039, 2023), underlines the need for systematic investigation of their effectiveness. To fill this gap, this study examines the effects of a specific variant of CO<sub>2</sub> traffic lights installed in 19 classrooms across Tyrol, Austria. These classrooms have been subject to continuous monitoring for approximately three months before the intervention (March 2024) and one month after the intervention. Within this longitudinal experiment, changes within classrooms using visual CO<sub>2</sub> feedback were analysed and compared to classrooms without such devices.

This research is part of the DIGIdat (2022) project, which focuses on assessing air quality in ten schools in Tyrol, Austria. Five of those schools that rely on window airing as the main ventilation method were chosen to implement the CO<sub>2</sub> traffic lights into their daily use. As part of the citizen science nature of the DIGIdat project, sensor maintenance was carried out by students in the classrooms studied. In addition, educational materials, including posters and instructional videos, were provided to support the effective use of the CO<sub>2</sub> traffic lights. In previous measurements, CO<sub>2</sub> concentrations of up to 5000 ppm were found in classrooms with window airing. (Beck et al., 2023)

## 1.1 Existing Studies

The literature search included databases such as Google Scholar, ScienceDirect, ResearchGate, Wiley Online Library, and Taylor & Francis Online. Different synonyms, such as “CO<sub>2</sub> signal lights”, “CO<sub>2</sub> traffic lights”, and “visual air quality feedback” were used. The search focused primarily on the school context. Only a small number of studies were found, and some of them were mostly of descriptive nature, considering the possibility of intervention for public buildings in general (Dunst, 2022) or the development of a do-it-yourself CO<sub>2</sub> traffic light (Dey et al., 2021; Wejner & Wilke, 2023) as well as a description of the underlying physics (Höfner & Schütze, 2021).

As a more general approach, a red warning light was introduced in the experiments of Geelen et al. (2008) in combination with advice on how to handle the signals. In this study, the feedback device was installed for one week, where it showed a reduction of the average CO<sub>2</sub> concentrations in the classroom, whereas it was stated that the long-term effect might not be given. The effect of a visual feedback device was evaluated in the work of Wargocki & Da Silva (2015), where they found that the window opening behaviour was affected and the CO<sub>2</sub> concentrations were reduced with the interventions, as it also increased the energy consumption of the school in the heating season. A similar intervention was researched in the study of Heebøll et al. (2018). They found that while the feedback device led to the windows being opened for a longer period of time during classroom usage, it did not significantly reduce the CO<sub>2</sub> levels. A different signal light, which displayed the feedback in a nine-step colour transition (green to yellow to red), was used in the work of Toftum et al. (2016). There the

“visual CO<sub>2</sub> display” helped to reduce the time in the classroom with concentrations over 1000 ppm by 40 - 60%. Another air quality feedback signal was tested by Avella et al. (2021), which in addition to CO<sub>2</sub> levels, also considers temperature and humidity as relevant inputs for the signal colour. The AI-based algorithm that decides if the light should be green, yellow, or red was not further described. They found that the effect of the visual feedback is heavily dependent on users, and the device has the best effect in mild temperatures with higher willingness for window airing. An overview of these studies and the applied CO<sub>2</sub> concentration for the visual feedback signal colours is displayed in Table 1.

Table 1: CO<sub>2</sub> Limits for signal light colour and sensor information

Source	Feedback	Limit [ppm]		CO <sub>2</sub> Sensor	
		Green - Yellow	Yellow - Red	Name	Accuracy
(Geelen et al., 2008)	Visual		1200*	Atal ATV-8002	± 75ppm
(Wargocki & Da Silva, 2015)	Visual	1000	1600	Vaisala GM20D	± 30ppm+2%
(Toftum et al., 2016)	Visual	1000	1600	Vaisala GMW22	± 100ppm+2%
(Heebøll et al., 2018)	Visual	1000	1600	Vaisala GMW22	± 100ppm+2%
(Avella et al., 2021)	Visual			Senseair K30	± 30ppm+3%
(Dey et al., 2021)	Visual	800	1200	Sensirion SCD30	± 30ppm+3%
(Höfner & Schütze, 2021)	Vis./Acoustic	750	1000	Sensirion SCD30	± 30ppm+3%
(Dunst, 2022)	Visual	1000	2000		
(Wejner & Wilke, 2023)	Visual			Winsen MS-Z14A	± 50ppm+5%

\* Only red warning light

There is no consensus on the limits of the different warning signals in the existing studies. Based on the three levels of warning, the limit from green to yellow is between 750 and 1000 ppm, which should indicate that additional ventilation would now be beneficial, and the limit from yellow to red is between 1000 and 2000 ppm, which should prompt the immediate opening of windows.

## 1.2 Applicable standards

No standards or guidelines addressing air quality feedback systems as an airing aid are known to the authors. To decide on the most suitable limits for the warning signals, the applicable norms for CO<sub>2</sub> concentration limits in classrooms are investigated - here with focus on Austria. In general, the European standard for the energy performance of buildings, EN 16798-1 (2024), states input parameters for classrooms for the maximum CO<sub>2</sub> concentration at a value of 500 ppm above outdoor levels, which with today's outdoor levels is calculated to be 900 to 1000 ppm inside. The Austrian standard, ÖNORM H 6039 (2023), covering ventilation systems specifically for school and educational buildings, sets an upper limit for classrooms at 1000 ppm and for other spaces in schools at 1400 ppm, both calculated as the arithmetic mean over the duration of one lesson (usually 50 min). These limits are similar to ISO 16000-1 (2004). The so-called MAK value (maximum workplace concentration), the legally binding threshold limit value (TLV) for occupational exposure in Austria, is set at 5000 ppm for CO<sub>2</sub> and is therefore not relevant for evaluating ventilation requirements.

Outside of Austria, the lower threshold for appropriate air quality in schools is set similarly. In Germany, the recommendation of the German Federal Environmental Agency is as well at 1000 ppm absolute CO<sub>2</sub> concentration (UBA, 2017). Older versions of the ASHRAE Standard 62.1 (2018) display that a concentration in indoor spaces of less than 700 ppm above outdoor levels will likely satisfy the majority of occupants with respect to human bio-effluents, which was removed in more recent versions of the standard. The UK states for non-dwellings that an absolute CO<sub>2</sub> concentration of 1500 ppm is a sign of poor ventilation (The Building

Regulations 2010 Part F, 2022), and in China, the absolute CO<sub>2</sub> concentration is limited to 1000 ppm (GB/T 18883, 2023) as an average over eight hours.

For the CO<sub>2</sub> traffic light used in this study, the thresholds of the warning signals are chosen to be in accordance with the guidelines for the assessment of indoor air of the Federal Ministry in Austria, which set the limit for rooms with cognitive activities at 1000 ppm and the limit for rooms with permanent stay at 1400 ppm (Tappler, 2024).

### 1.3 Market analysis

To compare research and standards with commercially available CO<sub>2</sub> traffic lights, 26 devices were looked at, and their datasheet specifications were analysed. Of the given devices, ten have connectivity features that enable the use of IOT (internet of things) functions, and eight of them have a display to show the CO<sub>2</sub> measurements in addition to the warning signal light. Twelve devices have an extra acoustic signal when the concentrations surpass certain limits. In general, sensing is based on the NDIR (non-dispersive infrared) principle, and the available devices specify accuracies in the range of  $\pm 30$  ppm+3% to  $\pm 50$  ppm+5%. The calibration of the sensors follows mostly some auto-calibration algorithm or a manual method, where the devices must be (regularly) exposed to outdoor air. At least two of the traffic light devices measure other indoor air pollutants, such as fine particulate matter, nitrogen oxides, or volatile organic compounds. A summary of the data collected within the extended Google search is displayed in Table 2.

Table 2: Summary of 26 commercially available CO<sub>2</sub> feedback devices (March 2024)

Parameter	Price [€]	CO <sub>2</sub> threshold [ppm]			Max. CO <sub>2</sub> sensor reading [ppm]
		Good	Tolerable	Bad	
Minimum	55.00	750	1000	1200	2000
Mean	176.73	911	1552	2400	
Median	179.67	1000	1500	2650	5000
Maximum	309.00	1000	2000	3000	40000

## 2 METHOD

The primary objective of this study is to evaluate the effectiveness of CO<sub>2</sub> feedback devices in improving indoor air quality in classrooms with window airing as the sole ventilation method. To compare the non-randomised subject classrooms this study uses a quasi-experimental design and was carried out over a period of five months. The primary hypothesis is that classrooms equipped with these devices will be ventilated more sufficiently and therefore maintain lower CO<sub>2</sub> levels over the occupation period.

Within the project DIGIdat, five Tyrolean (Austria) schools were chosen to implement CO<sub>2</sub> traffic lights as an intervention to improve indoor air quality. The other five schools that participate in the project did not activate any feedback signals and only took part in the awareness campaign. The Tyrolean climate can be classified as warm-summer humid continental climate (Dfb) according to Köppen & Geiger, and therefore the given school buildings usually deal with an extended heating season from October to April. Altogether, 61 classrooms are equipped with sensor kits, which measure air quality and thermal comfort parameters in 60 s intervals over multiple months. Within each classroom, ca. three sensor kits that were built using the platform senseBox (2023) measure temperature, humidity, carbon dioxide, fine particulate matter, and volatile organic compounds and send their data via Wi-Fi to the online database for environmental measurements called openSenseMap (OpenSenseLab, 2023).

The measurements for the school year 2023/24 started in November/December 2023 and are still ongoing. Around the beginning of March (approx. after three months of measurements), the sensor kits in sixteen classrooms were upgraded to include visual feedback depending on the current CO<sub>2</sub> concentration. The upgrade was implemented by activating the LED included in the senseBox MCU. The programming was partially done by the pupils within a 2-hour workshop as part of the DIGIdat project. The code was verified and complemented by the scientific team to ensure its proper function. Apart from the project given devices, one school additionally installed their own CO<sub>2</sub> traffic lights in three classrooms, which the IT teacher had designed, assembled, and programmed with his students. Their self-made devices follow a very similar colour control strategy as the provided ones, with slightly lower threshold values (600 ppm and 1300 ppm) as anchors for the colour mapping and an additional purple colour for very high CO<sub>2</sub> levels.

The measurements after the intervention are still ongoing, but the data for the herein presented analysis ends on April 19, 2024, after one and a half months of measurements. The intervention is supported by a video on air quality and the usage of CO<sub>2</sub> traffic lights, as well as complementary posters in the investigated classrooms. All devices are maintained by the students of one particular class per school, which has had a programming workshop as part of the citizen science of project DIGIdat. A list of the subset of all classrooms which are supported by CO<sub>2</sub> traffic lights is given in Table 3. Only classrooms with window-airing as their sole ventilation method were chosen for the following analysis. The pupils in the given classrooms are approximately 12 to 16 years old and in most cases one teacher is present in the classrooms during lessons.

Table 3: List of rooms that are supported by CO<sub>2</sub> feedback devices

Room	Type	Active Kits	Standard Ventilation	Measurement Start	Intervention Date	Volume [m <sup>3</sup> ]	Operable windows	Max N° of pupils	
SC01	EG-07	classroom	3	window-airing	10.11.2023	07.03.2024	253	6	23
	EDV-2	informatics	2	window-airing	23.11.2023	07.03.2024	330	1	27
	EG-14	classroom	3	window-airing	10.11.2023	07.03.2024	166	2	18
	TW-2	handicraft	2	window-airing	23.11.2023	07.03.2024	107	2	11
	EG-04	classroom	3	window-airing	10.11.2023	07.03.2024	182	6	20
SC02*	105	classroom	3	window-airing	06.12.2023	04.03.2024	172	9	21
	201	classroom	3	window-airing	06.12.2023	22.02.2024	192	9	25
	NG106	classroom	3	window-airing	06.12.2023	06.03.2024	173	3	24
SC03	OG1011	classroom	5	window-airing	22.11.2023	29.02.2024	127	6	-
	OG1007	classroom	4	mechanical	22.11.2023	29.02.2024	239	8	-
SC04	R2.05	classroom	3	window-airing	11.12.2023	06.03.2024	248	3	30
	R2.19	classroom	3	mechanical	15.01.2024	06.03.2024	257	3	26
	R1.22	classroom	3	mechanical	11.12.2023	06.03.2024	245	2	27
	R3.08	classroom	3	window-airing	11.12.2023	06.03.2024	225	3	27
	WER2	handicraft	1	window-airing	11.12.2023	06.03.2024	173	5	15
SC05	EG08	classroom	3	overflow	28.11.2023	06.03.2024	206	4	-
	R2.3	classroom	3	window-airing	28.11.2023	06.03.2024	214	4	-
	R2.13	classroom	3	window-airing	28.11.2023	06.03.2024	214	4	-
	Sal29	classroom	3	mechanical	28.11.2023	06.03.2024	176	1	-

\* installed their own CO<sub>2</sub> traffic lights

## 2.1 Control strategy of warning signal

Due to variations in threshold values among CO<sub>2</sub> feedback devices on the market, a new control strategy is introduced to represent the market average while also adhering to relevant standards and guidelines. The chosen threshold aligns with the guideline for assessing indoor air provided by the Austrian Ministry for Climate Action, Environment, Energy, Mobility, Innovation and Technology (Tappler, 2024). The feedback signal used within this investigation

is a small LED, which shows a colour range from green over yellow to red. A mathematical dependency of the underlying RGB values of the LED was found for the measured CO<sub>2</sub> concentration on the device. The functions for the red and green parts of the RGB value are based on the limit for spaces with cognitive tasks at 1000 ppm and the limit for spaces with permanent stay at 1400 ppm (see formulas for  $\beta_1$  and  $\beta_2$ ). The formulas for the RGB values, with red, green, and blue values in the number range from 0 to 255 and the CO<sub>2</sub> concentration in parts per million (ppm), are the following:

$$\begin{bmatrix} R \\ G \\ B \end{bmatrix} = \begin{bmatrix} 0 \leq (\alpha \times CO_2 - \beta_1) \leq 255 \\ 0 \leq (-\alpha \times CO_2 + \beta_2) \leq 255 \\ 0 \end{bmatrix} \text{ with } \alpha = 0.25$$

The constants are defined by  $\beta_1 = 255 - 1400 \times \alpha$  and  $\beta_2 = 255 + 1000 \times \alpha$ . This results in a gradient from RGB (5,255,0) at 400 ppm to RGB (255,5,0) at 2000 ppm. The full colour range with the according values is displayed in Figure 1.

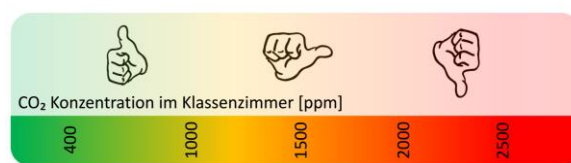


Figure 1: Colour range of CO<sub>2</sub> feedback signal

## 2.2 Positioning and housing

The sensor kits in each classroom, which are also used as CO<sub>2</sub> traffic lights, are mounted at a height of approx. 110 cm above the floor and positioned in the front (next to blackboard), the back (opposite side of blackboard) and the interior side wall (typically opposite the exterior wall with windows). The sensor height is matched with the breathing level of the students, and the positioning considers appropriate distance to windows, doors, and sources of pollution according to ISO 16000-1 (2004).

To protect the sensor kit from shocks and other environmental influences except from the air in the classroom, it is enclosed in a 3D-printed housing that has a separate chamber for the air quality and temperature sensors to reduce the heat flux from the processing unit. Despite this effort, the readings of the temperature sensors are inconsistently higher (up to 1° Celsius) than reference measurements. Three different CO<sub>2</sub> concentrations and their corresponding warning light are shown in Figure 2.



Figure 2: Example of the feedback colours at three different CO<sub>2</sub> levels of the used device

### 2.3 Sensor specifications and error adjustment

The sensor kits include, next to other air quality sensors, the SCD30 (Sensirion, 2020) for the CO<sub>2</sub> measurements (range: 0 – 10000 ppm, accuracy:  $\pm 30$  ppm +3%) and the BME680 (Bosch Sensortec, 2022) for temperature (range: -40 – 85 °C, accuracy:  $\pm 1$  °C). In fall 2023, the sensors were tested and compared before installation using high-grade reference measurement devices for CO<sub>2</sub> and temperature. Additionally, the CO<sub>2</sub> sensors were calibrated at a pressure of 950 hPa and temperature of 22°C at 1012 ppm using a calibration gas (synthetic air with specific carbon dioxide concentration). The auto-calibration function of the SCD30 was deactivated, and the data was pressure corrected in post-processing according to the school location's height. Measurement redundancy was provided by three measurement devices per classroom, and the readings are averaged within each timestep to weaken potential effects stemming from drifting of single sensors or unrealistic spikes, e.g. from “interested” students breathing directly onto the sensor.

### 2.4 Data Handling

Since the large amount of data is saved wirelessly via the openSenseMap (OpenSenseLab, 2023), the measurements were not disturbed during operation. One day at the beginning of the measurement campaign and around the intervention date were excluded from the dataset used in this paper so that boundary artefacts can be prevented. To complement missing data readings from the external sensors positioned within the DIGIdat project, ambient air temperature data from the nearest official weather station was retrieved from the GeoSphere Austria Data Hub (2024). Holidays and weekends were also omitted from the analysis. Data handling and statistical analysis were conducted using Python.

## 3 RESULTS OF STATISTICAL ANALYSIS

For evaluating the effect of the CO<sub>2</sub> traffic lights, two methods of comparison were employed. The focus of this analysis is the CO<sub>2</sub> concentration in each classroom between 9:00 to 12:00 on each school day, and since the air quality measurements from previous project phases showed a strong dependency of the CO<sub>2</sub> levels on the outside temperature, the data was categorised into 2 °C temperature bins. The two methods of comparison include:

- Pre- and post-intervention for CO<sub>2</sub> distribution within the studied classrooms
- Intervention and control group for CO<sub>2</sub> distribution with hypothetical intervention



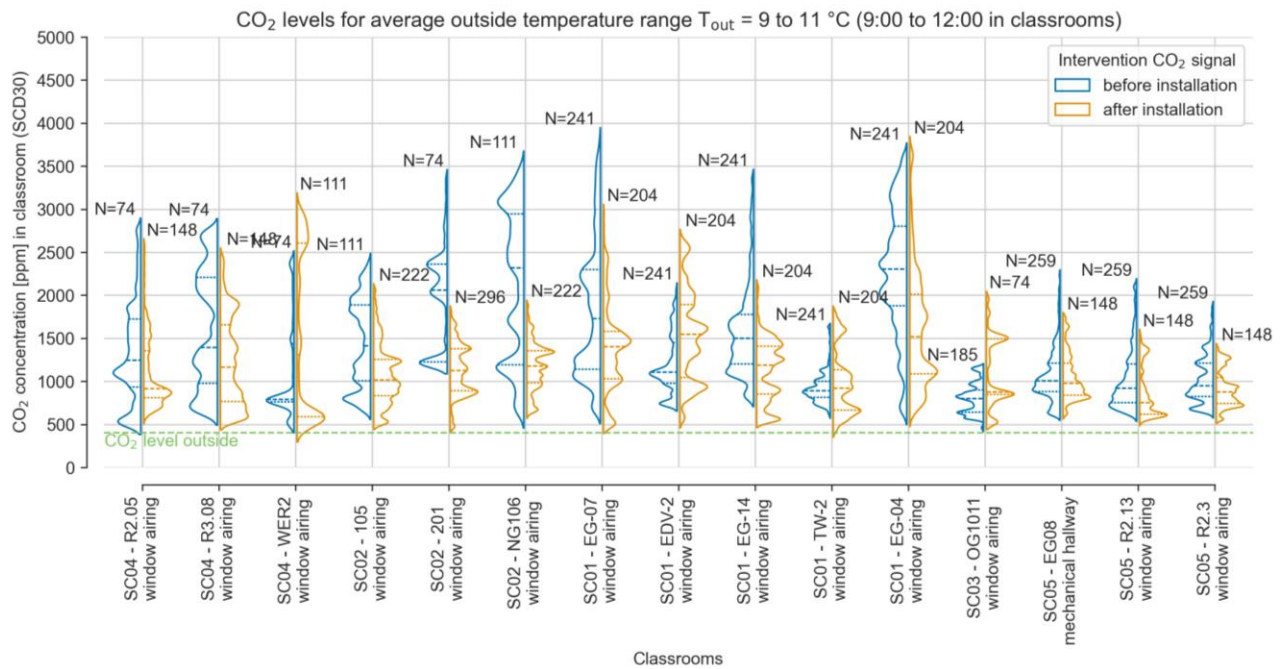


Figure 3: CO<sub>2</sub> concentrations from 9:00 to 12:00 before and after installation of the visual feedback device

As an example of the datasets for each classroom, Figure 3 shows the pre- and post-intervention (CO<sub>2</sub> traffic light installation) violin plots for temperature bin [9, 11] °C. A data point corresponds to the average of all sensors within a classroom over 5 minutes, which represents up to fifteen sensor readings for CO<sub>2</sub> and temperature. As the information on classroom occupancy was not complete up to this point, only readings from 9:00 to 12:00 were considered, chosen because this is the time when classrooms are most likely to be occupied.

### 3.1 Temperature dependency

To check for a difference between the dependency on the outside temperature before and after the intervention, CO<sub>2</sub> concentrations of all classrooms with their corresponding outside temperature are plotted (Figure 4) with a regression line and mean root square error (RMSE). Those datapoints represent the mean values for all measurements from 9:00 to 12:00 of each day and classroom.

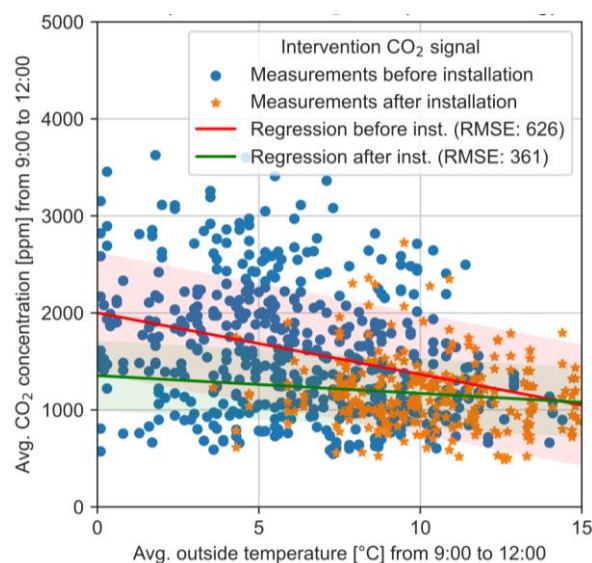


Figure 4: Correlation of outside temperature and inside CO<sub>2</sub> concentrations for classrooms with window airing

Similar to the previous study (Beck et al., 2023), the plot shows a strong temperature dependency of the average CO<sub>2</sub> levels in the classrooms without intervention. After installation of the device, the data shows a smaller dependency on outside temperatures. This is supported by the Spearman test, in which the null hypothesis states that the underlying data is not correlated. The resulting p-values are ca. 8e-12 before intervention and 0.047 after intervention. The regression lines only include data with outside temperatures from 0 to 15 °C, as this was the range with a reasonable amount of data points. Therefore, the results must be interpreted with caution, as the dataset after the intervention is smaller and within only a subset of the temperature range. According to the Shapiro-Wilk-Test, both datasets (before and after) are not normally distributed but follow a fitted Weibull distribution best. The p-values for the Kolmogorov-Smirnov test hypothesis, that the data is drawn from the Weibull distribution (determining the goodness of fit), are 0.79 (before intervention) and 0.09 (after intervention). The authors are not aware of a widely accepted test to compare the regression lines pre- and post-intervention with Weibull-distributed data; therefore, the ANCOVA (analysis of covariance) test was performed. The results of the ANCOVA test are shown in Table 4.

Table 4: Main results of ANCOVA to test the intervention effect

Parameter	Sum of squares	F-value	p-value (uncorrected)
Intervention	6.8e+06	22.34	2.70e-06
Avg. T <sub>out</sub>	2.4e+07	79.44	2.90e-18

The data indicates a significant effect of the intervention but an even stronger effect of outside temperature on the CO<sub>2</sub> concentrations in the classrooms, with p-values well below a significance level of  $\alpha = 0.01$ .

To support this, the data was again summarised and plotted within the temperature bins, and their differences were checked using Welch's t-test (on ranked datapoints, RWT) and the Mann-Whitney-U-Test (MWU). Those tests were chosen because of the non-normality of the data distribution. The null hypothesis of both tests is that the CO<sub>2</sub> concentration after the intervention is not significantly smaller than before. Figure 5 shows the violin distribution curves before and after the installation of the CO<sub>2</sub> traffic lights in different temperature bins, which had enough data points to be statistically meaningful. The threshold of statistical significance due to the nature of the one-sided test is set at  $\alpha = 0.005$ .

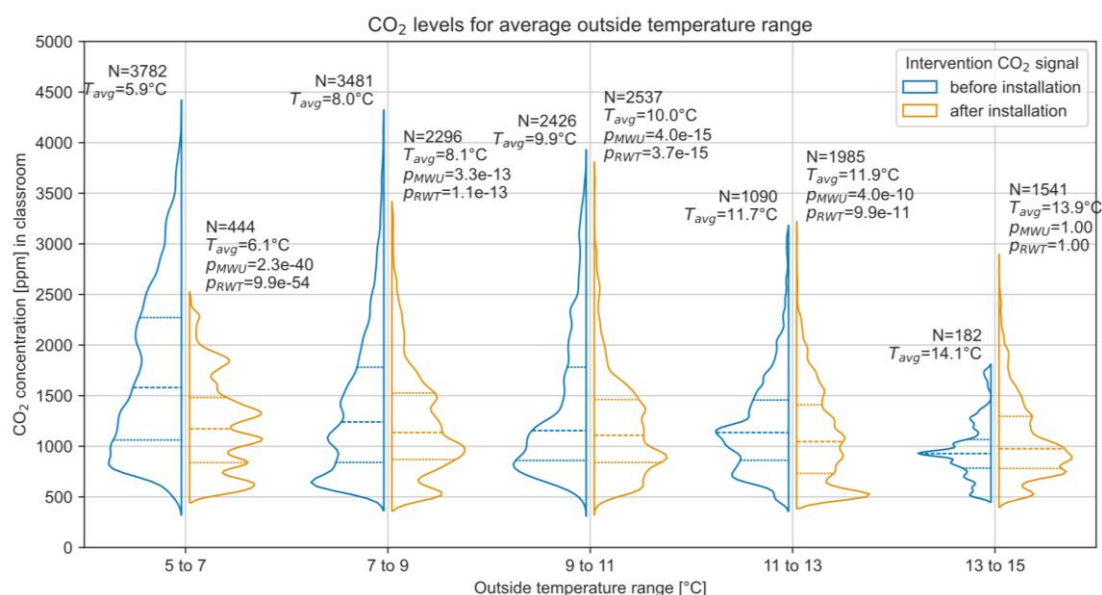


Figure 5: CO<sub>2</sub> concentration distribution for different outside temperature ranges

The p-values as shown in Figure 5 show a significantly smaller CO<sub>2</sub> concentration in classrooms in all temperature bins except for the bin from 13 to 15 °C.

### 3.2 Comparison to control group

To assess if the results are biased due to differing weather characteristics, in particular ambient temperature, the dataset is compared to a control group, which had the same awareness campaign but no visual feedback devices available. In this comparison, the control group was assigned a hypothetical intervention around a similar date, when the CO<sub>2</sub> traffic lights were installed in the intervention classrooms, namely at the beginning of March. The correlation between outside temperatures and inside CO<sub>2</sub> levels is shown in Figure 6. No major difference can be interpreted by visual inspection before and after the hypothetical intervention. Analysis using the Spearman test results in correlation coefficients of -0.29 (p: 6e-6) before and -0.27 (p: 0.0026) after the reference date, indicating a significant correlation between CO<sub>2</sub> concentration and ambient temperature for both periods. The ANCOVA test shows a similar picture (see Table 5). The given uncorrected p-value and F-value show a significant difference before and after the intervention date. However, it must be mentioned that this analysis does not quantify the magnitude and direction in which the correlation coefficients differ and that the observed difference in magnitude is small.

Table 5: Main results of ANCOVA to test control group with hypothetical intervention

Parameter	Sum of squares	F-value	p-value (uncorrected)
Hypothetical intervention	3.3e+06	12.41	4.79e-04
Avg. T <sub>out</sub>	8.3e+07	31.11	4.58e-08

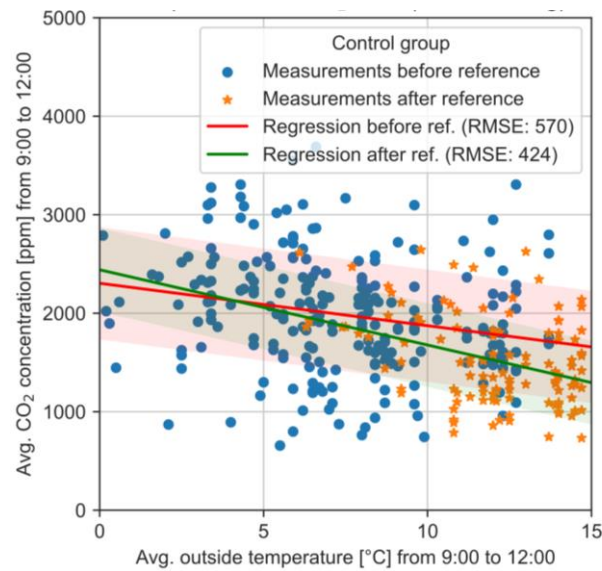


Figure 6: Correlation of outside temperature and inside CO<sub>2</sub> concentrations for classrooms (control group)

Violin plots for the control group (see Figure 7) in the different outside temperature ranges show that the CO<sub>2</sub> levels after reference are not lower during periods with lower ambient temperatures. The given p-values for the control group indicate that significantly lower CO<sub>2</sub> values after the reference date occur only in temperature bins with temperatures above 9 °C.

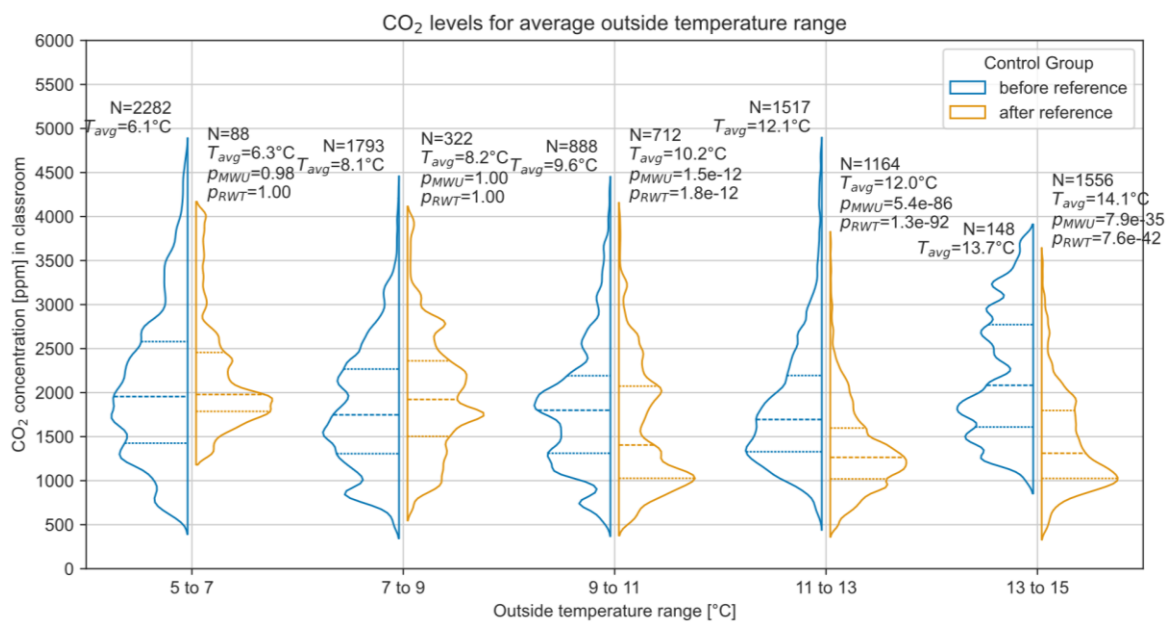


Figure 7: CO<sub>2</sub> concentration distribution for different outside temperature ranges (control group)

#### 4 DISCUSSION AND CONCLUSION

This paper investigates whether there is a positive effect of CO<sub>2</sub> traffic lights on reducing CO<sub>2</sub> levels in the subject classrooms. The statistical analysis shows, according to two different comparison approaches, that the ventilation strategy using visual feedback improves the CO<sub>2</sub> levels in the classrooms under the given circumstances.

- 1) The difference between classrooms with or without CO<sub>2</sub> feedback signals is statistically significant at lower ambient temperatures (below 9 °C) when comparing before and after the intervention and shows no difference in the control group. At higher

ambient temperatures, these differences become small and/or are not significant. The question is, however, whether this effect will be visible over a longer period of time as pupils and teachers get used to the presence of such equipment. Other limiting factors of this study are the late date of the intervention, with generally warmer ambient temperatures after the intervention, and the fact that only schools with a presumable interest in air quality are taking part in this citizen science project. Five of the fifteen herein analysed classrooms have the additional bias of being actively involved in programming the feedback devices. Therefore, the willingness to ventilate according to the CO<sub>2</sub> traffic light might be higher than in other classrooms. It is also important to mention that the intervention has to be seen in the context of an awareness campaign, which was necessary to show affected teachers and students how to deal with the visual feedback. Another experiment should investigate the effect of visual feedback without proper information about its use.

- 2) A review of existing studies, standards, and the market shows that there are several approaches to the design of CO<sub>2</sub> traffic lights and thresholds for warning signals (usually green, yellow, and red). Therefore, a mathematical approach was considered to link the colour scheme to the thresholds given by the regulations in Austria.

As the measurement campaign is still ongoing, the long-term effect of the CO<sub>2</sub> traffic lights will be monitored and analysed with a more complete data set. Another interesting approach would be to test the difference of removing an active CO<sub>2</sub> traffic light after a longer period of use to see if there is a change in behaviour after this "negative" intervention. Based on the current data, the visual feedback system seems to be a valid approach to reducing CO<sub>2</sub> levels in classrooms.

Despite the effect, it must be considered, that the energy consumption for heating is probably higher due to a higher air change rate using the traffic light system. This trade-off between good air quality and the energy efficiency of the school building itself was not evaluated in this work and requires further investigation. E.g., mechanical ventilation systems with heat recovery might be able to alleviate this trade-off.

## **5 ACKNOWLEDGEMENTS**

Project DIGIdat is funded by the Sparkling Science Programme of the Austrian Agency for Education and Internationalisation (OEAD) and the Federal Ministry of Education, Science and Research Austria (BMBWF). We also want to deeply acknowledge the dedicated engagement of all involved students and teachers.

## 6 REFERENCES

- ASHRAE. (2022, February 2). *Position Document on Indoor Carbon Dioxide*.
- ASHRAE Standard 62.1 (2018, February 21). *Ventilation for Acceptable Indoor Air Quality* (ANSI/ASHRAE Standard 62.1-2016). American Society of Heating, Refrigerating and Air-Conditioning Engineers, Inc.
- Avella, F., Gupta, A., Peretti, C., Fulici, G., Verdi, L., Belleri, A., & Babich, F. (2021). Low-Invasive CO<sub>2</sub>-Based Visual Alerting Systems to Manage Natural Ventilation and Improve IAQ in Historic School Buildings. *Heritage*, 4(4), 3442–3468. <https://doi.org/10.3390/heritage4040191>
- Beck, S., Rojas, G., Krois, E., Goreth, S., & Hechenberger, C. (2023). Indoor air quality in Austrian classrooms: Assessing different ventilation strategies with a citizen science approach. In *43rd AIVC Conference, 11th TightVent Conference, 9th venticool Conference*, Copenhagen.
- Bosch Sensortec. (2022). *BME680 Datasheet: Digital low power gas, pressure, temperature & humidity sensor*. <https://www.bosch-sensortec.com/media/boschsensortec/downloads/datasheets/bst-bme680-ds001.pdf>
- Brandl, A., Tappler, P., Twrdik, F., & Damberger, B. (2001). Untersuchungen raumlufthygienischer Parameter in oberösterreichischen Schulen. *6. AGÖF Fachkongress Nürnberg 20.-21.09.2001: Umwelt, Gebäude & Gesundheit*. <http://www.innenraumanalytik.at/newsletter/brandl.pdf>
- The Building Regulations 2010 Part F (2022, June 15). *Ventilation - Volume 2: Buildings other than dwellings*.
- Dey, T., Elsen, I., Ferrein, A., Frauenrath, T., Reke, M., & Schiffer, S. (2021). CO<sub>2</sub> Meter: A do-it-yourself carbon dioxide measuring device for the classroom. In F. Makedon (Ed.), *Proceedings of the 14th Pervasive Technologies Related to Assistive Environments Conference* (pp. 292–299). ACM. <https://doi.org/10.1145/3453892.3462697>
- DIGIdat. (2022). *Digitale Datenanalyse trifft Bildung für nachhaltige Entwicklung: Forschungsprojekt zur Analyse for Raumlufqualität in Tiroler Schulen*. Sparkling Science 2.0. <https://digidat.at/>
- Dunst, M. (2022). *Lüftungsanlagen in öffentlichen Gebäuden*. Springer Fachmedien Wiesbaden. <https://doi.org/10.1007/978-3-658-35752-8>
- EN 16798-1 (2024, March 1). *Energy performance of buildings - Ventilation for buildings* (ÖNORM EN 16798-1:2024-03). Austrian Standards International.
- GB/T 18883 (2023, February 1). *Standards for Indoor Air Quality* (GB/T 18883-2022).
- Geelen, L. M. J., Huijbregts, M. A. J., Ragas, A. M. J., Bretveld, R. W., Jans, H. W. A., van Doorn, W. J., Evertz, S. J. C. J., & van der Zijden, A. (2008). Comparing the effectiveness of interventions to improve ventilation behavior in primary schools. *Indoor Air*, 18(5), 416–424. <https://doi.org/10.1111/j.1600-0668.2008.00542.x>
- GeoSphere Austria Data Hub. (2024). *Messstationen Stundendaten v2*.
- Heebøll, A., Wargocki, P., & Toftum, J. (2018). Window and door opening behavior, carbon dioxide concentration, temperature, and energy use during the heating season in classrooms with different ventilation retrofits—ASHRAE RP1624. *Science and Technology for the Built Environment*, 24(6), 626–637. <https://doi.org/10.1080/23744731.2018.1432938>

- Höfner, S., & Schütze, A. (2021). Air Quality Measurements and Education: Improving Environmental Awareness of High School Students. *Frontiers in Sensors*, 2, Article 657920. <https://doi.org/10.3389/fsens.2021.657920>
- Hohenblum, P., Fröhlich, M., Moosmann, L., Scharf, S., Uhl, M., Gundacker, C., Hutter, H.- P., Kundi, M., Jansson, M., & Tappler, P. (2008). *LUKI - Luft und Kinder: Einfluss der Innenraumluft auf die Gesundheit von Kindern in Ganztagschulen - Endbericht (Kurzfassung). Report / Umweltbundesamt: [N.F.] 181*. Umweltbundesamt. <https://permalink.obvsg.at/AC07056099>
- Humhal, C. (2014, November 18). *Optimierte Unterrichtsräume in Kärntner Pflichtschulen*. 5. Innenraumtag. [http://raumluft.linux47.webhome.at/fileadmin/dokumente/2014\\_Humhal.pdf](http://raumluft.linux47.webhome.at/fileadmin/dokumente/2014_Humhal.pdf)
- ISO 16000-1 (2004, July 1). *Indoor Air - Part 1: General aspects of sampling strategies* (ISO 16000-1:2004). International Organization for Standardization.
- Knotzer, A., & Venus, D. (2013). *School vent cool: Lüftung, passive Kühlung und Strategien für hochwertige Schulsanierungen* (Berichte aus Energie- und Umweltforschung No. 29). [https://nachhaltigwirtschaften.at/resources/hdz\\_pdf/berichte/endbericht\\_1329\\_schoolventcool.pdf](https://nachhaltigwirtschaften.at/resources/hdz_pdf/berichte/endbericht_1329_schoolventcool.pdf)
- ÖNORM H 6039 (2023, February 1). *Lüftungstechnische Anlagen - Kontrollierte mechanische Be- und Entlüftung von Schul-, Unterrichts- oder Gruppenräumen sowie Räumen mit ähnlicher Zweckbestimmung* (ÖNORM H 6039:2023-02). Austrian Standards International.
- OpenSenseLab. (2023). *OpenSenseMap*. <https://opensensemap.org/>
- senseBox. (2023). *Home / senseBox.de*. <https://sensebox.de/>
- Sensirion. (2020). *Datasheet Sensirion SCD30 Sensor Module: CO2, humidity, and temperature sensor*. [https://sensirion.com/media/documents/4EAF6AF8/61652C3C/Sensirion\\_CO2\\_Sensors\\_SCD30\\_Datasheet.pdf](https://sensirion.com/media/documents/4EAF6AF8/61652C3C/Sensirion_CO2_Sensors_SCD30_Datasheet.pdf)
- Simons, E., Hwang, S.- A., Fitzgerald, E. F., Kielb, C., & Lin, S. (2010). The impact of school building conditions on student absenteeism in Upstate New York. *American Journal of Public Health*, 100(9), 1679–1686. <https://doi.org/10.2105/AJPH.2009.165324>
- Tappler, P. (2024, March 8). *Richtlinie zur Bewertung der Innenraumluft – Kohlenstoffdioxid als Lüftungsparameter*. Bundesministerium für Klimaschutz, Umwelt, Energie, Mobilität.
- Toftum, J., Wohlgemuth, M. M., Christensen, U. S., Bekö, G., & Clausen, G. (2016). Managed airing behaviour and the effect on pupil perceptions and indoor climate in classrooms. In *Indoor Air*, Ghent.
- UBA. (2017). *Anforderungen an Lüftungskonzeptionen in Gebäuden - Teil 1: Bildungseinrichtungen*. Umweltbundesamt Deutschland.
- Wargocki, P. (2015). Ventilation, indoor air quality and learning in schools. *AIVC Conference*, 949–958.
- Wargocki, P., & Da Silva, N. A. F. (2015). Use of visual CO2 feedback as a retrofit solution for improving classroom air quality. *Indoor Air*, 25(1), 105–114. <https://doi.org/10.1111/ina.12119>

Wejner, M., & Wilke, T. (2023). Air quality: An inexpensive CO<sub>2</sub> indicator for the classroom with LabPi. *CHEMKON*, 30(2), 64–67.  
<https://doi.org/10.1002/ckon.202100036>



# Performance evaluation of humidity controlled decentralized ventilation systems in social housing in Chile

Gilles Flamant<sup>\*1,2</sup>, Waldo Bustamante<sup>1</sup>, Arnold Janssens<sup>2</sup>, and Jelle Laverge<sup>2</sup>

*1 Centre for Sustainable Urban Development  
(CEDEUS)  
Pontificia Universidad Católica de Chile  
El Comendador 1916  
Santiago, RM, 7520245, Chile*

*2 Research Group Building Physics, Ghent  
University, Sint-Pietersnieuwstraat 41  
B-9000 Gent, Belgium*

*\*Corresponding author: gilles.flamant@uc.cl*

## ABSTRACT

More than 70% of the dwellings in Chile were built before 2000, when the use of thermal insulation in the roofs of residential buildings became mandatory. This explains why less than 2% of dwellings are considered energy efficient. Social housing is no exception. Several studies have shown poor thermal performance of the envelope of social housing throughout the country, with low levels of thermal comfort and indoor air quality that affect the health of its occupants. Retrofitting programs for social housing launched by the government in recent years have implemented more rigorous thermal standards, along with the installation of humidity controlled decentralized mechanical exhaust ventilation systems. However, it is not known whether such ventilation system can effectively guarantee air quality in homes.

This study evaluated the indoor air quality and ventilation heat losses of a typical social house in Chile equipped with a humidity-controlled ventilation system using the airflow and pollutant transport calculation software CONTAM. It was shown that such a system does not at all guarantee the indoor air quality, especially in the bedrooms during the night hours. Several alternative ventilation systems and strategies were identified and evaluated. Two of them showed good performance in terms of indoor air quality while limiting ventilation heat losses, for the moderate and high occupancy profiles considered in this study. They include demand-based ventilation using CO<sub>2</sub> concentration detection. The first system is based on the extended cascade ventilation principle, while the second includes the addition of an exhaust system specific to bedrooms. They reduce the ventilation heat losses by about 32% and 37% on average, respectively, compared to a continuously operating ventilation system, while ensuring an equivalent level of indoor air quality.

By proposing better solutions than those currently used in social housing, this study will contribute to the development of public policies aimed at improving the comfort and health of social housing occupants while limiting the dwelling's energy use.

## KEYWORDS

Mechanical exhaust ventilation, demand-based control, indoor air quality, ventilation heat losses, social housing.

## 1 INTRODUCTION

More than 70% of the dwellings in Chile were built before 2000, when the use of thermal insulation in the roofs of residential buildings became mandatory. This explains why, according to OECD figures, less than 2% of dwellings are considered energy efficient (OECD, 2014). Social housing is no exception. Several studies have shown that the thermal performance of the envelope of social housing is poor throughout the country, leading to problems of surface condensation on walls, high heat losses in winter and low levels of thermal comfort for their occupants (de la Barrera et al., 2021; Vives et al., 2023). In addition, social housing also has indoor air quality (IAQ) problems that affect the health of its occupants. The above shows the enormous challenge and the need to renovate existing housing in order to achieve adequate standards of habitability, better comfort, wellbeing and quality of life for its occupants. Retrofitting programs for social housing launched by the government in recent years have implemented more rigorous thermal standards, along with the installation of decentralized mechanical exhaust ventilation systems (MINVU, 2017). Exhaust fans in wet rooms are usually activated when the light is turned on, by means of a manual ON/OFF switch or based on the relative humidity level of the room.

Previous studies have shown that the control strategy based on relative humidity was less suited to maintain the IAQ compared to a constant flow exhaust ventilation (e.g. Laverge et al., 2011). Based on the analysis of monitoring data, Pecceu et al. concluded that relative humidity seemed to be a poor control variable for detecting people in demand-controlled ventilation (Pecceu et al., 2018). A comparison of different ventilation control algorithms showed that control based only on relative humidity in humid spaces was not effective (Caillou et al., 2014). However, to date, no study in Chile has shown the performance of this type of humidity-based control for the specific outdoor climates found in Chile and how it could be improved.

The aim of this study was to evaluate the IAQ and ventilation heat losses of a typical social housing unit in Chile equipped with the most common humidity-controlled decentralized ventilation system currently in use. In a subsequent phase, alternative ventilation strategies and solutions were proposed, evaluated, and compared with the base case solution. Given the importance of simple, robust and cost-effective ventilation solutions, especially for social housing, only relatively simple solutions based on existing decentralized ventilation systems were considered in this study. Such ventilation solutions are also easier to implement in renovation projects than more complex centralized systems. All systems were evaluated using the airflow and pollutant transport calculation software CONTAM.

## 2 METHODS

### 2.1 Description of the case-study

The dwelling under investigation is a one-story detached social house with a total floor area of 43m<sup>2</sup>, which is typical for Chilean social houses. It consists of a living-dining room with an open kitchen, two bedrooms, and a bathroom, as shown in Figure 1. It is assumed that bedroom 1 faces north. The house is fitted with exhaust fans in wet rooms (bathroom, kitchen) that are activated when the light is turned on, by means of a manual ON/OFF switch or based on the relative humidity level of the room, and with supply vents in the dry rooms (living room and bedrooms) sized to provide 25 m<sup>3</sup>/h per person at 10Pa (category II in EN16798-1) (CEN, 2019). The total exhaust airflow is 176 m<sup>3</sup>/h, with 50 m<sup>3</sup>/h in the bathroom and 126 m<sup>3</sup>/h in the

kitchen (Flamant et al., 2023). Figure 1 shows the location of the two exhaust fans and supply vents.

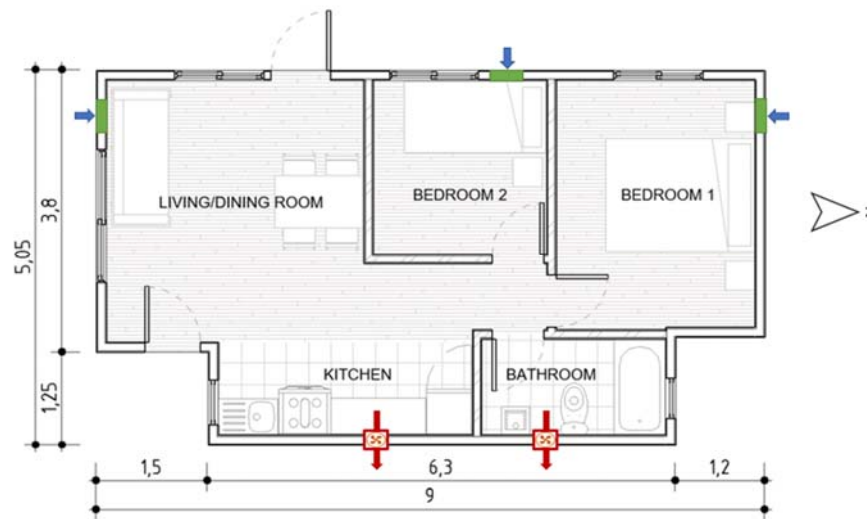


Figure 1: Layout of the house investigated in this study. Air inlets are pictured in green and exhaust fans in red.

## 2.2 Climatic data

This study considers two sets of climatic data (IWEC datafile) corresponding to the two main cities in Chile: Santiago and Concepción. Despite being classified under the same climate type 'Csb' according to the Köppen classification, the two cities exhibit clear differences. Santiago, located in the central valley, has a Mediterranean climate with mild temperatures. Concepción is a coastal town with a maritime climate characterised by heavy rainfall and high levels of air relative humidity during the winter. Table 1 presents the monthly average air temperature, air relative humidity and wind speed for the heating period considered in this study, which spans from May 1 to September 30. The average absolute humidity during this period is approximately 0.0054 kg/kg in Santiago and 0.0066 kg/kg in Concepción.

Table 1 : climatic data considered in this study

Month	Santiago			Concepción		
	Temp. [°C]	RH [%]	Wind sp. [m/s]	Temp. [°C]	RH [%]	Wind sp. [m/s]
May	12.8	61	2.4	11.3	88	3.1
June	8.5	70	1.8	9.7	88	3.2
July	8.4	75	1.7	9.2	86	3.9
August	10.1	67	2.4	10.1	84	4.3
September	13.2	64	2.7	10.8	80	4.1

## 2.3 Model and assumptions

To evaluate the performances of the ventilation systems and strategies considered in this study, simulations were performed using the multizone airflow network model CONTAM. A 5-minute timestep was used for the calculation and the outputs. The wind pressure on each building surface was calculated using wind pressure coefficients from the Swami and Chandra model (Florida Solar Energy Center, 1987) and a wind speed modifier coefficient to account for 'suburban' terrain. We assume an airtightness of the building envelope  $n_{50}$  of  $5h^{-1}$ , which is the

number of air changes per hour for a pressure difference of 50 Pa between indoor and outdoor.  $n_{50}=5$  is the compulsory value for new and renovated houses in some cities in Chile where *Air Quality Management Plans* (PDA) are in force (Ministerio del Medio Ambiente, 2020). This value has also been recommended in the proposal to update the thermal building code in Chile (MINVU, 2020). The air leakage is uniformly distributed over all vertical walls exposed to the ambient environment. Airflow paths were located at 3 different heights of each wall - top, middle and bottom - and modelled using the power law model with a flow exponent of 0.65. All internal doors are closed with an undercut of 1cm. Supply vents were modelled as a one-way flow using a power law with exponent  $n$  equal to 0.5. The indoor air temperature is set at 18°C in all rooms throughout the entire simulation period.

A family of 4 people is assumed considering two 40-year-old adults, and 5- and 10-year-old children. Occupants produce moisture by breathing and sweating according to their level of activity. Metabolism moisture emissions rates of 55 g/h for an awake adult, and 40 g/h for a sleeping adult were considered (CEN, 2006). Taking into account a 25% reduction in moisture production for children (Johansson et al., 2015), the following rates were used: 41 g/h for an awake child, and 30 g/h for a sleeping child. Based on a literature review, the quantity of water vapor generated by the different household activities is indicated in Table 2.

Table 2 : Total water vapor generation by the household activities

Activity	Rate	Duration	Frequency	Total amount (g/day)	Location
Shower	250 g/event	5 min/event	1 event/ pers./day	1000	Bathroom
Cooking	2380 g/day	60 min/day	3 meals, every day	2380	Kitchen
Dishwashing	450 g/day	25 min	3 washings/day (3 meals), every day	450	Kitchen

The carbon dioxide emission rate from human respiration is (Persily & de Jonge, 2017):

- Adult: 18 L/h for an awake person, and 12 L/h for a sleeping person
- Child: 14 L/h for an awake person, and 7 L/h for a sleeping person

Two daily occupancy profiles were developed, specifying the location and activity of each household member of the family in the dwelling every 15 minutes, as shown in Figure 2. The first one corresponds to a high (permanent) occupancy of the house, the other to a moderate occupancy. The two profiles were built by taking into account the ‘*Use of Time National Survey*’ conducted in 2015 in Chile, which provided some activity data from a randomly selected group of 15,312 households (Molina et al., 2021).

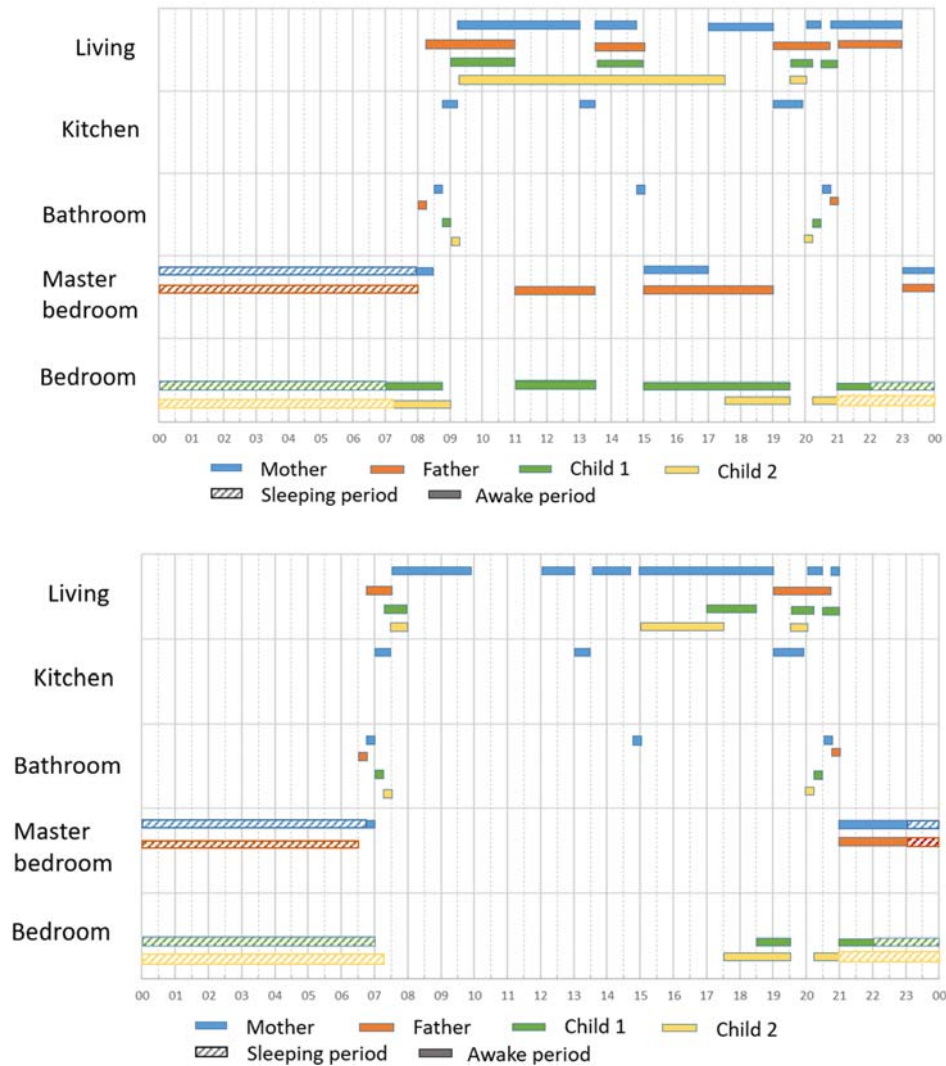


Figure 2: Occupancy profiles. Above: high occupancy, down: moderate occupancy.

## 2.4 Ventilation systems evaluated

Seven different ventilation systems were simulated. Some of them were evaluated with different settings. Table 3 provides a brief explanation for each of them.

System A is a decentralized ventilation system that corresponds to the base configuration (see §2.1), but assuming continuous operation 24/7: the exhaust fans in the kitchen and bathroom extract the maximum airflow rates every moment of the day. This system serves as the reference case. System B is the most commonly installed system today in new or retrofitted houses in Chile, where exhaust fans are activated when the relative humidity of the indoor air exceeds a setpoint (ON-OFF mode). The bathroom fan also detects the presence of the occupant and continues to operate for 15 minutes after the occupant leaves the room. Three RH setpoints were considered: RH = 70% (B1), 65% (B2) and 60% (B3). System C is similar to B, but with the additional requirement that the exhaust fans operate continuously every hour of the night (22h-7h) to provide ventilation during sleeping hours. The exhaust fans in System D can operate at two different speeds to provide different airflow rates. When operating at normal speed, System D is the same as B1, but it maintains a minimum exhaust airflow rate equal to half of

the maximum value when operating at low speed. Systems E and F are identical to B1, but with an additional centralized exhaust system for the two bedrooms only. The maximum total airflow of the exhaust system is 100 m<sup>3</sup>/h, with 50 m<sup>3</sup>/h per bedroom. This exhaust system operates only during the night for system E and based on the average CO<sub>2</sub> concentration over the bedrooms for system F, with a flowrate directly proportional to the CO<sub>2</sub> concentration. System G operates according to the *extended cascade ventilation principle* (Rojas et al., 2015) and has no supply air inlet in the living room. The bathroom fan is activated based on the relative humidity of the air, similar to B1. The kitchen fan has two speeds. The high-speed setting corresponds to the maximum airflow rate of 126 m<sup>3</sup>/h. It runs all night to maintain a minimum airflow in the bedrooms and when the CO<sub>2</sub> concentration in the open kitchen (equivalent to the one in the living) exceeds 1000 ppm during the day. The low-speed setting runs the rest of the time, corresponding to 1/3 of the maximum value to guarantee a minimal ventilation rate in the house.

Table 3 : List of the ventilation systems compared in the study

ID	Description
A	ON, 100% of the time
B1	ON/OFF, RH=70% in both bathroom and kitchen & presence detection in the bathroom
B2	ON/OFF, RH=65% in both bathroom and kitchen & presence detection in the bathroom
B3	ON/OFF, RH=60% in both bathroom and kitchen & presence detection in the bathroom
C1	ON/OFF, RH=70% in both bathroom and kitchen & presence detection in the bathroom + ON 100% during night (clock)
C2	ON/OFF, RH=65% in both bathroom and kitchen & presence detection in the bathroom + ON 100% during night (clock)
D	2 speeds (low/normal), RH=70% in both bathroom and kitchen & presence detection in the bathroom + Minimum airflow = ½ maximum value.
E	ON/OFF, RH=70% in both bathroom and kitchen & presence detection in the bathroom + centralized exhaust system only for bedrooms operating at 100% during the night (clock)
F	ON/OFF, RH=70% in both bathroom and kitchen & presence detection in the bathroom + centralized exhaust system only for bedrooms with airflow proportional to CO <sub>2</sub> concentration in bedrooms
G	'Extended' cascade ventilation. Bathroom: ON/OFF, RH=70% & presence detection. Kitchen: ON 100% during night (clock) and when CO <sub>2</sub> concentration > 1000 ppm during day + Minimum airflow = 1/3 maximum value.

## 2.5 Assessment criteria

The ventilation systems were evaluated based on the following criteria:

1. Ventilation and infiltration heat losses during the heating period from May 1 to September 30 (kWh). In the remainder of this document, the term "Ventilation Losses" is used to refer to "Ventilation and Infiltration Losses".
2. CO<sub>2</sub> cumulative exceeding exposure above 1000 ppm, assuming an outdoor concentration of 400 ppm, expressed as ppm.h per hour of occupancy. CO<sub>2</sub> is a good marker of occupant-related emissions, including bio-effluents and odours. It characterizes the perceived indoor air quality experienced by building occupants and is good indicator of ventilation rate per person (Poirier et al., 2021). Complementary indicators are needed, however, to achieve a comprehensive air quality assessment.
3. Risk of mould growth, supposed to occur when the monthly average relative humidity on a typical thermal bridge with a temperature factor of 0.7 exceeded 80% (Caillou et al., 2014).

### 3 RESULTS AND DISCUSSION

#### 3.1 Climate of Santiago

Figure 3 shows the exceeding CO<sub>2</sub> exposure above 1000 ppm versus the ventilation losses for the different ventilation systems investigated in this study, for the moderate occupancy scenario. As a 'reference case', ventilation system A allows to guarantee a good IAQ with a low exceeding CO<sub>2</sub> exposure, but at the expense of high ventilation heat losses due to the continuous air exhaust. Despite the continuous operation of the system, the design values for supply airflow are not reached in the bedrooms due to the influence of air leakage and wind forces (Flamant et al., 2023). This results in CO<sub>2</sub> concentrations that are slightly above 1000 ppm during the night, mainly in the bedroom 1. Systems B, the most commonly installed systems today, show the worst performance in terms of IAQ, with high CO<sub>2</sub> concentrations mainly in the two bedrooms during the night, as shown in Figure 4. The HR-based algorithm is effective to evacuate the water vapour peaks from the household activities in the kitchen and bathroom, but is not suitable to remove the pollutants generated by the occupants in the bedrooms. In addition, Systems B1 and B2 do not meet the criterion for the risk of mould growth. Compared to systems B, System C allows for a significant reduction of excess CO<sub>2</sub> exposure, especially in the bedrooms, by enforcing continuous ventilation during the night. The bathroom and kitchen exhaust fans in System C2 operate 58% and 61% of the time, respectively, compared to 51% and 30% in System B2. Such an increase in the use of exhaust fans also results in much higher ventilation losses. Maintaining a minimum exhaust airflow rate (in this case half of the maximum value) throughout the whole day (System D) improves the IAQ compared to Systems B, but without reaching the performance of Systems C. The additional installation of a dedicated exhaust system for the bedrooms – Systems E & F -, in addition to the bathroom and kitchen exhaust fans, offers the highest performance in terms of IAQ, with a ~50% reduction in ventilation losses compared to the reference case A. The *cascade ventilation system* G offers another interesting alternative in terms of IAQ and energy. The continuous use of the kitchen exhaust fan during the night maintains a low CO<sub>2</sub> concentration in the bedrooms, and the absence of air intake in the living room reduces the ventilation heat losses in this room compared to the other systems studied. Thanks to its daytime CO<sub>2</sub>-based detection, the kitchen/living fan adjusts the ventilation flow rate according to the needs of the room. This System G has the advantage of not requiring the installation of an additional exhaust system. However, it requires a more sophisticated detection and control system than the exhaust fans usually used. It is particularly suitable for the house configuration considered in this study, with a kitchen opened onto the living room (Rojas et al., 2015). With the exception of Systems B1 and B2, all other systems meet the criterion for the risk of mould growth. It must be noted that the control parameters of the various ventilation solutions were selected following a limited optimization process; it is possible that further optimization may lead to even more favourable results.

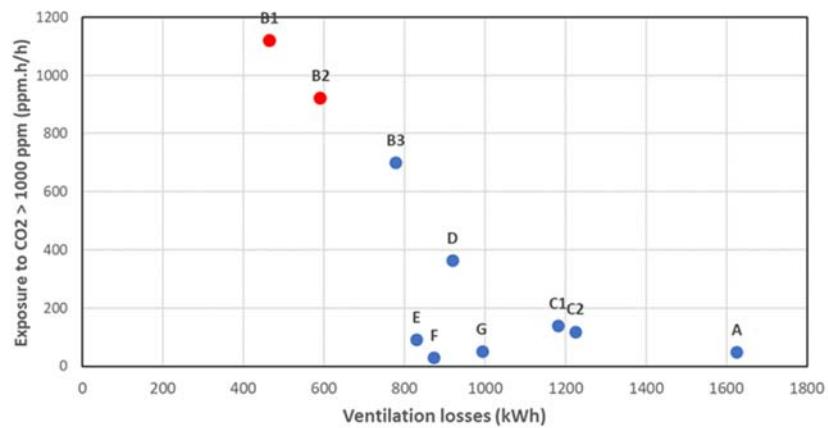


Figure 3: Exposure to CO<sub>2</sub> vs ventilation losses (kWh) for the different ventilation systems under analysis. Moderate occupancy. Climate of Santiago.

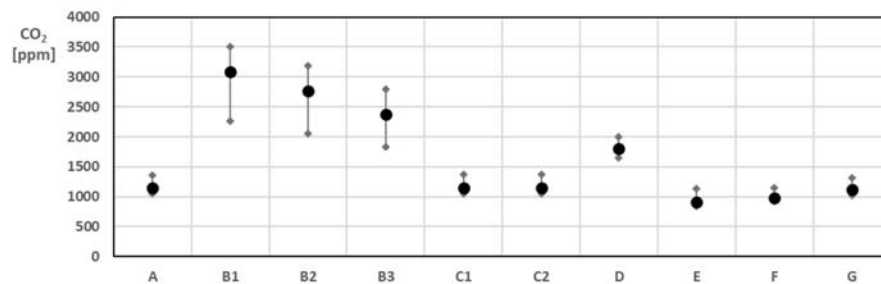


Figure 4: Minimum, mean and maximum values of CO<sub>2</sub> concentration in bedroom 1 during the night hours for the different ventilation systems under analysis. Moderate occupancy. Climate of Santiago.

Figure 5 illustrates the exposure to CO<sub>2</sub> versus ventilation losses for the different ventilation systems, but this time for the high occupancy scenario of the house. Compared to the case of moderate occupancy, the main difference concerns the performance of the clock-based control systems (night hours), i.e. Systems C and E. Both systems fail to maintain air quality in bedrooms and living rooms during the day. Only Systems F and G perform well for both occupancy scenarios.

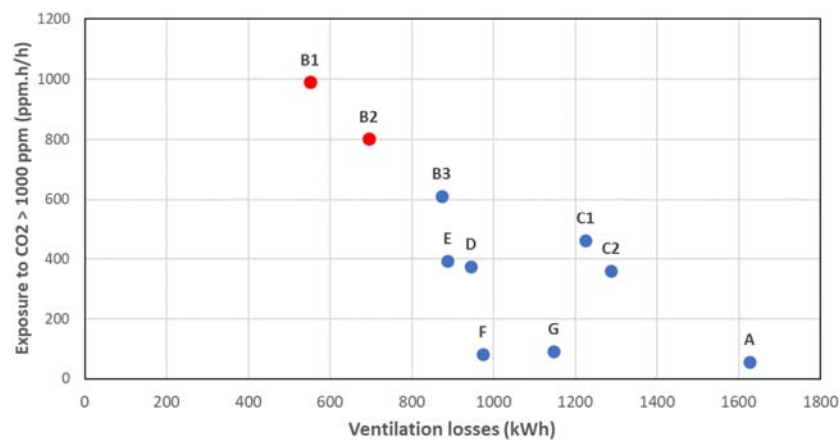


Figure 5: Exposure to CO<sub>2</sub> vs ventilation losses (kWh) for the different ventilation systems under analysis. High occupancy. Climate of Santiago.



### 3.2 Climate of Concepción

Figure 6 shows the exposure to CO<sub>2</sub> versus ventilation losses for the climate of Concepción in the case of the high occupancy scenario. The points are closer together in terms of excess CO<sub>2</sub>. Indeed, since the absolute humidity of the outdoor air in Concepción is higher than in Santiago, the ventilation systems, whose control is based on the relative humidity of the indoor air, have to run longer to maintain a given RH level. This leads to an improvement in indoor air quality at the expense of higher ventilation losses. None of the systems B meets the criterion for the risk of mould growth. Systems C1, D, E and F, whose control is partly based on RH=70%, also present a risk, but this can be avoided by lowering the RH setpoint to a lower level (e.g. RH=65%). Again, systems F and G offer the best performance in terms of IAQ, with energy savings of about 25% compared to reference case A.

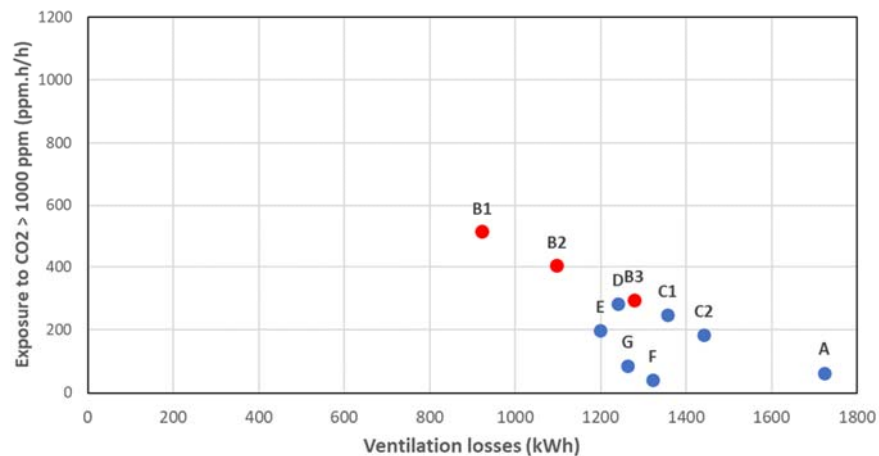


Figure 6: Exposure to CO<sub>2</sub> vs ventilation losses (kWh) for the different ventilation systems under analysis. High occupancy. Climate of Concepción.

## 4 CONCLUSIONS

This study showed that a decentralized ventilation system controlled by the relative humidity of the indoor air does not at all guarantee the IAQ in the dwelling under consideration, particularly in the bedrooms during the night hours. This finding is particularly important given that this system is currently the most widely used in Chile in both new construction and renovation projects. The study identified and evaluated several alternative ventilation systems and strategies that significantly improved IAQ. In particular, two systems showed good performance in terms of IAQ while limiting ventilation heat losses, for the two occupancy profiles considered. They include demand ventilation control based on local CO<sub>2</sub> concentration detection. The first is based on the *extended cascade ventilation principle*, while the second involves the addition of an exhaust system specific to bedrooms. They reduce the ventilation heat losses by about 32% and 37% on average, respectively, compared to a ventilation system operating continuously, while ensuring an equivalent level of IAQ. Further research will focus on evaluating a wider variety of cost-effective ventilation systems and strategies, for a series of typical social housing typologies. Air quality will be assessed not only in terms of CO<sub>2</sub> concentration, but also considering other pollutants such as formaldehyde and particulate matter PM<sub>2.5</sub>.

## 5 ACKNOWLEDGEMENTS

This work was funded by the National Research and Development Agency (ANID), Chile, under research grant FONDECYT 1221666. The authors also gratefully acknowledge the research support provided by CEDEUS, ANID FONDAP 1522A0002.

## 6 REFERENCES

- Caillou, S., Heijmans, N., Laverge, J., & Janssens, A. (2014). *Méthode de calcul PER : Facteurs de réduction pour la ventilation à la demande*.
- CEN. (2006). *CEN/TR 14788, Ventilation for buildings - Design and dimensioning of residential ventilation system*.
- CEN. (2019). *EN 16798-1:2019, Energy performance of buildings - Ventilation for buildings - Part 1: Indoor environmental input parameters for design and assessment of energy performance of buildings addressing indoor air quality, thermal environment, lighting and acou*.
- de la Barrera, F., Rivera, M. I., Barraza, C., Durán, C., & Pavez, J. (2021). La Temperatura Importa: Confortabilidad De La Vivienda Social En San Pedro De La Costa 1. *Síntesis de Investigación*. <https://doi.org/10.7764/cedeus.si.13>
- Flamant, G., Bustamante, W., Janssens, A., & Laverge, J. (2023). Impact of the building airtightness and natural driving forces on the operation of an exhaust ventilation system in social housing in Chile. *43rd AIVC, 11th TightVent, 9th Venticool Conference, 43*, 585–593.
- Florida Solar Energy Center. (1987). *Procedure for Calculating Natural Ventilation Airflow Rates in Buildings*.
- Johansson, P., Pallin, S., & Shahriari, P. D. M. (2015). *Risk Assessment Model Applied on Building Physics: Statistical Data Acquisition and Stochastic Modeling of Indoor Moisture Supply in Swedish Multi-family Dwellings*.
- Laverge, J., Van Den Bossche, N., Heijmans, N., & Janssens, A. (2011). Energy saving potential and repercussions on indoor air quality of demand controlled residential ventilation strategies. *Building and Environment, 46*(7). <https://doi.org/10.1016/j.buildenv.2011.01.023>
- Ministerio del Medio Ambiente. (2020). *Planes de prevención y/o descontaminación atmosférica (PPDA)*. <https://ppda.mma.gob.cl>
- MINVU. (2017). D.S. N° 18. Programa de regeneración de conjuntos habitacionales de viviendas sociales. In *Ministerio de Vivienda y Urbanismo (DS 18)*.
- MINVU. (2020). *Propuesta de actualización de la reglamentación térmica, Art. 4.1.10 de la OGUC (Consulta Simplificada)*.
- Molina, C., Jones, B., Hall, I. P., & Sherman, M. H. (2021). CHAARM: A model to predict uncertainties in indoor pollutant concentrations, ventilation and infiltration rates, and associated energy demand in Chilean houses. *Energy and Buildings, 230*, 110539.
- OECD. (2014). *Chile's Pathway to Green Growth: Measuring progress at local level*.
- Pecceu, S., Caillou, S., & Gaever, R. Van. (2018). Demand controlled ventilation : relevance of humidity based detection systems for the control of ventilation in the spaces occupied by persons. *39th AIVC Conference "Smart Ventilation for Buildings", Antibes Juan-Les-Pins, France, 18-19 September 2018*.
- Persily, A., & de Jonge, L. (2017). Carbon dioxide generation rates for building occupants. *Indoor Air, 27*(5). <https://doi.org/10.1111/ina.12383>
- Poirier, B., Guyot, G., Woloszyn, M., Geoffroy, H., Ondarts, M., & Gonze, E. (2021). Development of an assessment methodology for IAQ ventilation performance in

- residential buildings: An investigation of relevant performance indicators. In *Journal of Building Engineering* (Vol. 43). <https://doi.org/10.1016/j.jobbe.2021.103140>
- Rojas, G., Pfluger, R., & Feist, W. (2015). Cascade ventilation—Air exchange efficiency in living rooms without separate supply air. *Energy and Buildings*, *100*, 27–33.
- Vives, A., González, F., Orlando, L., Baeza, F., & Valdebenito, R. (2023). *ESTUDIO RUCAS, Regeneración Urbana Calidad de vida y Salud, Informe final*.

# Airborne transmission in a meeting room with mixing and displacement ventilation

Risto Kosonen<sup>\*1,2</sup>, Weixin Zhao<sup>1</sup>, Simo Kilpeläinen<sup>1</sup>, Juha Jokisalo<sup>1</sup>

<sup>1</sup> Aalto University  
Sähkömiehentie 4

P.O. Box 14400 FI-00076, Finland

\*Corresponding author: [risto.kosonen@aalto.fi](mailto:risto.kosonen@aalto.fi)

<sup>2</sup> Nanjing Tech University

College of Urban Construction

P.O. Box 76, No. 200 North Zhongshan Rd  
210009, Nanjing, China

Presenting author: Risto Kosonen

## ABSTRACT

The main purpose of this study is to analyse the effects of heat gain, airflow rate, air distribution, and the location of an infector on the airborne transmission and infection probability in a meeting room. In a six-person meeting room the droplet nuclei of an infected person were simulated with tracer gas (SF<sub>6</sub>) generated by a thermal breathing manikin. An overhead perforated duct (OPD) and low velocity unit (LVU) were used and their performance was compared. With OPD, the average contaminant removal efficiency in the breathing zone was quite uniformly between 0.9 and 1.1. With LVU, the average contaminant removal efficiency varied greatly between 0.2 and 10.1. The airborne generation was assumed to be 5 quantum/h by an infected person. The infection probability for every exposed person was found to be quite uniform with OPD, 1.4% with a heat gain and air flow rate of 38 W/m<sup>2</sup> and 61 l/s and 0.9% with a heat gain and air flow rate of 60 W/m<sup>2</sup> and 116 l/s after three hours' exposure. However, variation of the infection probability with LVU was significant and the highest risk reached 4%. The infection probability was lower if the exposed person was farther from the infector, or in the case of OPD if the infector was near the exhaust. With LVU, the infection probability depended on the airflow rate and the relative distance between the supply unit and the exposed person.

## KEYWORDS

Airborne transmission, air distribution, heat gain, meeting room, tracer gas

## 1 INTRODUCTION

It is important to understand the mechanism of aerosol particles transmission in the occupied space and methods to reduce the risk of cross infection. By increasing the airflow rate, it is possible to reduce the infection risk in many cases. However, an increase of the airflow could increase the concentration level of aerosol particles locally (Memarzadeh and Xu, 2012). From the energy-efficiency point of view, it is not always the most optimal manner to reduce the infection risk. Recently it has been clearly proven that airflow distribution methods have a significant effect on the personal exposure to indoor air pollutants (Li et al., 2007). Thus, it is possible to reduce the infection risk with suitable air distribution and without increasing the total airflow rate.

Two main categories of air distribution are displacement ventilation and mixing ventilation. In mixing ventilation, the outdoor air is supplied at a high velocity outside the occupied zone, such as near or at the ceiling. This promotes good mixing with uniform temperature and pollution distribution in the occupied zone. In displacement ventilation, the principle is to replace but not to mix the room air with supply air, where the clean and cold air is utilizing convection flows of heat gains. To prevent the transmission of exhaled air, the ventilation approach should rely on source and air distribution control rather than on dilution, i.e., supplying large volumes of clean conditioned air. This includes organizing the airflow pattern from clean zone toward less clean zones inside the occupied space followed by efficient polluted air removal.

In a previous study (Su et al, 2021), the infection risk was numerically investigated for mixing and displacement ventilation systems in an office space. With displacement ventilation, the infection probability was 0.74% after four hours with 10.5 quantum/h by an infected person, which is lower than in well-mixed conditions (2.9 %). This indicated the buoyancy-driven air distribution methods may have good performance at preventing cross-infection. However, the infection risk is sensitive to the location of the infector with displacement ventilation (Batlle et al., 2021), depending on whether the infector is near or far from the air supply diffuser. Moreover, other factors such as the heat gain from equipment and solar heat gains were not considered in the study.

This paper presents analyse of airborne transmission and infection risk using overhead perforated duct (OPD) and low velocity unit (LVU) under different heat gain conditions and airflow rates. The infection risk is affected by the location of the infector in the room.

## 2 METHODS

The experiments were conducted in a full-scale test room, where a stable indoor climate can be maintained. The dimensions of the test room were 5.50 m (length), 3.80 m (width), and 3.60 m (height) from the floor to the ceiling. The heat gains used in the test room are summarized in **Error! Reference source not found.**

### 2.1 Thermal chamber and air distribution

A meeting table for six persons was placed in the middle of the room. The length and width of the meeting table was 5.2 m x 0.8 m. One breathing thermal manikin, one heated dummy, and 4 persons simulated by heated cylinders were placed around the table. The mixing air distribution was implemented with an overhead perforated duct (OPD) in the ceiling zone. The

perforated duct was extended for the entire length of the room and the supplied airflow was downwards toward the direction of the floor. The diameter of the perforated duct was 200 mm and the total length was 5.5 m. The displacement air distribution was achieved with a low velocity unit (LVU). A rectangular perforated low velocity unit was installed in the middle of the wall opposite the door on the floor. The width and height of the low velocity unit was 1140 mm x 550 mm.

Table 1: Heat gains, airflow rates and design parameters under two heat gain levels.

		Heat gain and cooling load balance	
Total heat flux	W/m <sup>2</sup>	<b>60</b>	<b>38</b>
Floor area	m <sup>2</sup>	21	21
Total heat gain	W	1253	805
Manikin	W	80	80
Dummy	W	85	85
4 Cylinder dummies	W	4*80=320	4*80=320
2 Laptops	W	2*40=80	2*40=80
2 Lights	W	2*45=90	2*45=90
Heated Window panels	W	133	105
Solar load at floor	W	420	0
Equipment of manikin	W	45	45
Supply air flow rate	L/s	116	61
Air change rate	1/h	5.5	2.9
Supply air temperature	°C	16	14
Design room air temperature	°C	25	25
Cooling load	W	-1253	-805

## 2.2 Experimental conditions

The operative temperature was controlled at  $25 \pm 1$  °C at a height of 1.1 m. The supply air temperature was kept at 14 °C with 38 W/m<sup>2</sup> and 16 °C with 60 W/m<sup>2</sup>. The exhaust air temperature was around 25 °C. The supplied airflow rates were 116 l/s and 61 l/s with the 60 W/m<sup>2</sup> and 38 W/m<sup>2</sup> to be balanced with the total heat gain used. A thermal breathing manikin was used to simulate an infected sitting person in the room space, and one heated dummy and four heated cylinders represented the exposed persons. The breathing cycle of the manikin consisted of 2.5 s inhalation, 1 s break, 2.5 s exhalation and 1 s break.

To investigate the behaviour of gaseous indoor-emitted pollutants, a tracer gas can be used to simulate droplet nuclei from the exhaled air and to study the effect of the air distribution on the local concentration levels. In the previous study, it was demonstrated that the tracer gas technique is applicable to analysing airborne transmissions in air distribution studies (Ai et al.,

2020). The tracer gas concentration in the inhaled air of exposed persons and exhaled air infector was measured by Multi-gas Sampler and Monitor. This equipment took air samples via plastic tubes in the breathing zone and analysed the components in the air. In this study, tracer SF<sub>6</sub> was released by exhaling through the nose of the thermal manikin with a pulmonary ventilation rate of 6 l/min. This was dosed directly into the artificial lung of the infector. The dosing rate was 2 ml/s, resulting in a contaminant concentration of the exhaled flow around 20,000 ppm. The breathing air of the manikin was heated to a setpoint of 35 °C and humidified to a level of 85%. During the experiment, continuous tracer gas measurements using a multi-gas sampler and monitor were taken at 7 locations, including the breathing zone of the 5 exposed persons, and at the exhaust and supply duct. The distance between two face-to-face persons' noses was 1.2 m and between two side-by-side persons it was 1.05 m. To investigate the effect of the infector's location on the exposure level, the manikin was placed at 4 different locations in each case as shown in **Error! Reference source not found.** and the exhaust point was near P4. A Wells–Riley model was used that assumed that the whole room volume was fully-mixed and in steady-state conditions.

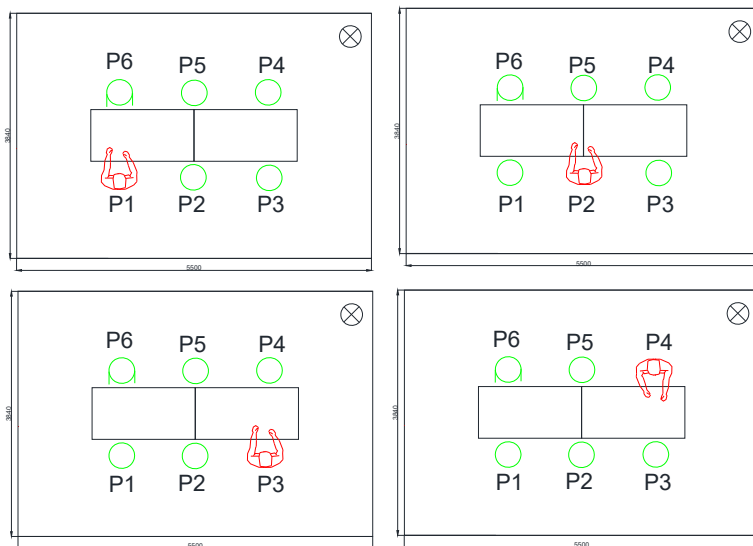


Figure 1: The locations of the infector (red breathing thermal manikin) in the test room.

### 3 RESULTS

#### 3.1 Airborne transmission

**Error! Reference source not found.** shows the tracer gas distribution at different measured locations when the manikin was at P1 and the dummy at P6. The tracer gas concentration was increased with time and reached a steady state after 60 min and 34 min at the exhaust with an

airflow rate of 61 l/s and 116 l/s, respectively. After the tracer gas concentration at the exhaust reached a stable level, the average concentration in the room with OPD was 21.3 ppm and 11.3 ppm with a heat gain of 38 W/m<sup>2</sup> and 60 W/m<sup>2</sup>, respectively. The average contaminant removal efficiency [35] was 0.9 and 1.1 with an airflow rate of 61 l/s and 116 l/s, respectively. Therefore, the air distribution was mixed well in the whole space.

With OPD, the concentration distribution was quite uniform at each location, and the average standard deviation was only 0.3 to 0.6 ppm. However, the tracer gas distribution varied spatially and temporally with LVU. After the concentration reached steady state conditions at the exhaust point, the minimum concentration was 2.0 ppm, but a maximum value of 52.3 ppm occurred in the breathing zone. The highest standard deviation was 11.2 ppm. Therefore, the horizontally supplied airflow from LVU created a varied air movement, especially close to the opposite wall. Additionally, fluctuations of the concentration at P6 increased with a higher airflow rate.

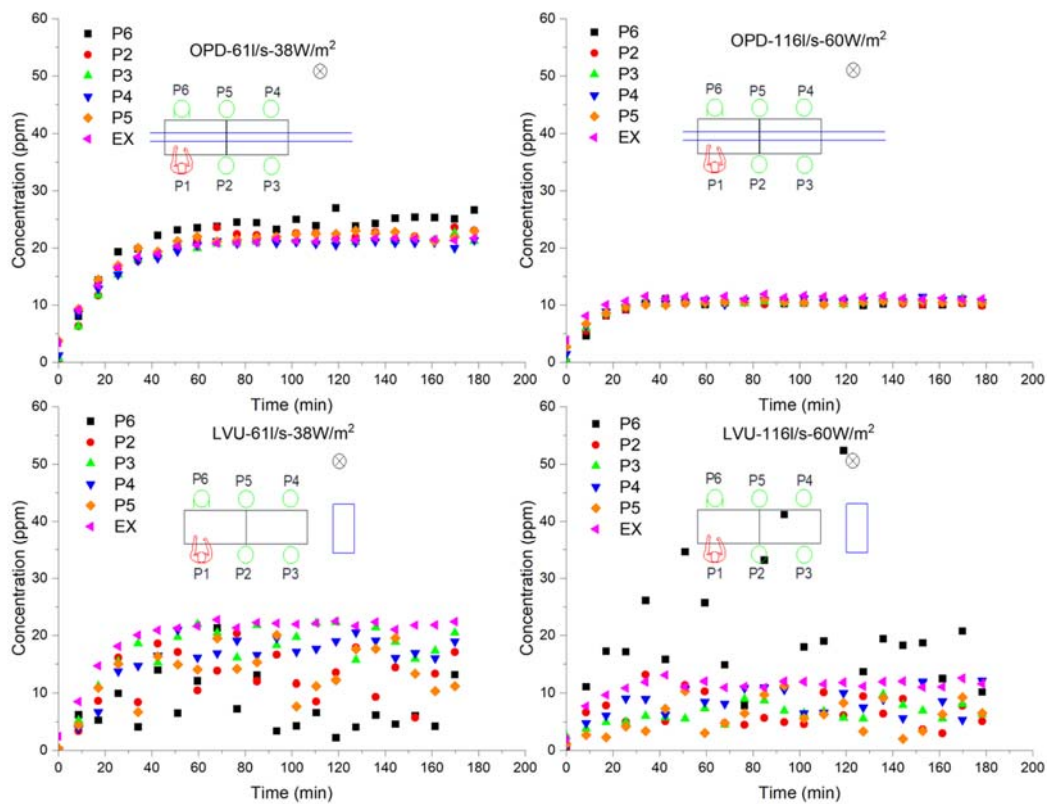


Figure 2: The concentration distribution of tracer gas at different locations when the manikin was at P1 with OPD and LVU with two heat gains of 38 W/m<sup>2</sup> and 60 W/m<sup>2</sup>.



### 3.2 Infection probability

**Error! Reference source not found.** shows the infection probability variations for different exposed persons when the infector changed its location. When the airflow rate was increased from 61 l/s to 116 l/s with OPD, the average infection probability was reduced by 35% after three hours (from 1.4% to 0.9%). Therefore, the airflow rate level had a significant effect on the infection probability with OPD. The average infection probability in the room was decreased from 1.1% to 0.9% when the airflow rate was increased from 61 l/s to 116 l/s with LVU. Therefore, the increasing airflow rate with LVU reduced the exposure risk by 16%.

With a heat gain of 38 W/m<sup>2</sup>, the average infection risk was 1.4% and 1.2% with OPD and LVU, respectively. The average performance of LVU is superior to OPD. With a heat gain of 60 W/m<sup>2</sup>, the average infection risk was quite similar (0.9%) with OPD and LVU. However, with LVU, there were large differences and fluctuations. The highest standard deviation reached 1.4%. The average standard deviation with LVU was 0.7% and 0.6% with heat gains of 38 W/m<sup>2</sup> to 60 W/m<sup>2</sup>, respectively. The corresponding value was only 0.1% with OPD.

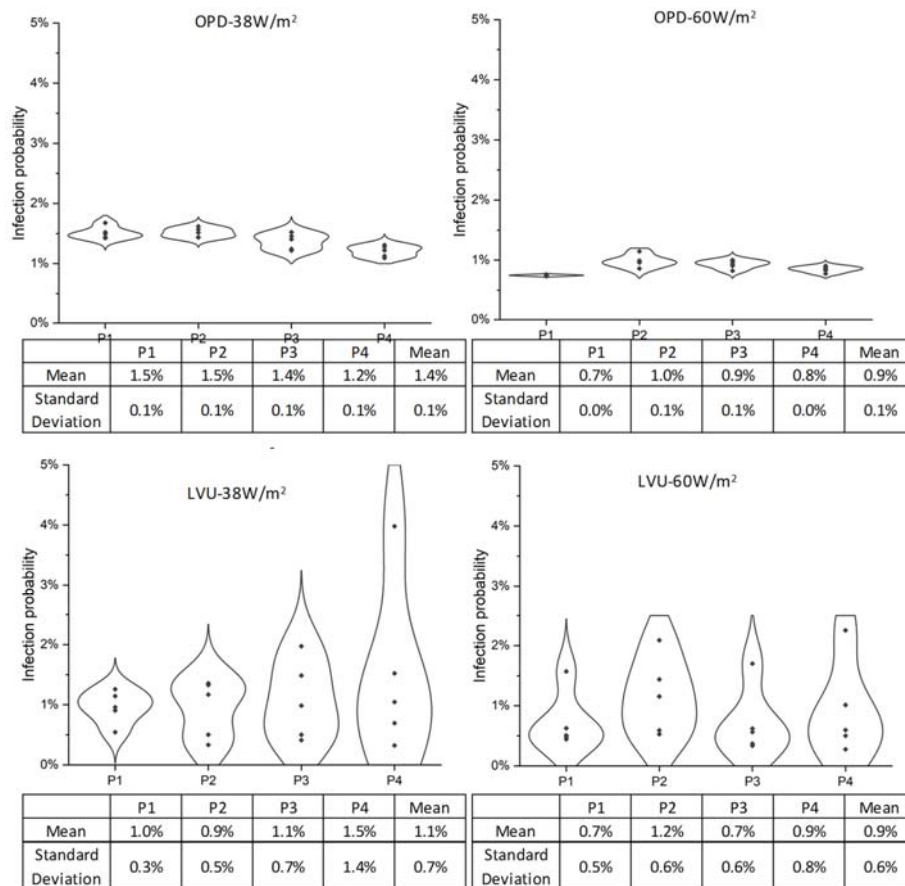


Figure 3: The infection probability with OPD and LVU in the test room.

## 4 CONCLUSIONS

The infection probability in the meeting room was investigated by full-scale tests. Air distribution methods with an overhead perforated duct (OPD) and low velocity unit (LVU) were analyzed under two heat gain levels (38 W/m<sup>2</sup> and 60 W/m<sup>2</sup>) and two airflow rates (61 l/s and 116 l/s). The following findings can be concluded:

- With OPD, the average contaminant removal efficiency was between 0.9 and 1.1. However, with LVU, the average contaminant removal efficiency varied spatial and temporal between 0.2 and 10.1.
- The infection probability was quite uniform (SD=0.1%) with the OPD, especially at a higher heat gain level. The variation of infection probability with LVU was significant. The highest standard deviation reached 1.4%.
- The highest risk was reached at 4% with LVU when the infector was located near the supply unit. The lowest risk was only 0.3%. Therefore, both best and worst situations were achieved with LVU, indicating that it can offer (in this specific case) superior performance to OPD if properly designed.
- When the infector sat near the exhaust, the infection probability was the smallest with 38 W/m<sup>2</sup>. Therefore, the proper air distribution combined with local exhaust is most effective for source removal.

## 5 ACKNOWLEDGEMENTS

The study was supported by SUOJAILMA project funded by the Finnish Work Environment Fund (Grant No. 210099).

## 6 REFERENCES

- Ai Z., Mak C.M, Gao N. and Niu J. (2020). *Tracer gas is a suitable surrogate of exhaled droplet nuclei for studying airborne transmission in the built environment*. Building Simulation, Springer, 2020: 489–496
- Li Y., Leung G.M., Tang J.W., Yang X., Chao C.Y, Lin J.Z., Lu J.W., Nielsen P.V., Niu J. and Qian H (2007). *Role of ventilation in airborne transmission of infectious agents in the built environment-a multidisciplinary systematic review*. Indoor Air 17 2–18.
- Memarzadeh F. and Xu W. (2012). *Role of air changes per hour (ACH) in possible transmission of airborne infections*. Build. Simul. 5 15–28.  
<https://doi.org/10.1007/s12273-011-0053-4>.
- Su W., Yang B., Melikov A., Liang C., Lu Y., Wang F., Li A., Lin Z., Li X., Cao G. and Kosonen R. (2021). *Infection probability under different air distribution patterns*. Building and Environment (2021) 108555.

# A novel method for the characterization of infiltration airflow using infrared thermography

Diego Tamayo-Alonso<sup>1</sup>, Irene Poza-Casado<sup>1</sup>, M.Á. Padilla-Marcos<sup>1</sup>, Lida Mercado<sup>1</sup>, Alberto Meiss<sup>1</sup>

*1 GIR Arquitectura & Energía, Dpto. Construcciones  
Arquitectónicas I.T. y M.M.C.T.E., E.T.S  
Arquitectura, Universidad de Valladolid (Spain)*

*\*Corresponding author: [diego.tamayo@uva.es](mailto:diego.tamayo@uva.es)  
Presenting author: underline First & Last name*

## ABSTRACT

Controlling air infiltration is crucial to ensure thermal comfort, optimal performance of ventilation systems, and the overall energy efficiency of buildings. The quantification of the overall airtightness of the building envelope, often conducted through pressurization tests, has been widely used. In addition, IR thermography is a valuable complementary tool for identifying and locating air leakage paths.

A methodology to characterize leakage flows based on the bi-dimensional temperature array has been previously developed. This method was proved to be useful, but the total test time is very extensive because several image captures must be performed for to compose a three-dimensional array. This paper presents an optimized methodology where the measuring device is the three-dimensional matrix, obtaining in this way the three-dimensional image of the airflow with a single capture. The objective of this study is to optimize the characterization process of the infiltration airflow using IR thermography, reducing time, and improving its application in practice.

This work opens multiple research lines, for example, the use of the presented methodology coupled with machine learning to estimate the airflow or the characterization of the air distribution of ventilation systems' air inlets.

## KEYWORDS

IR thermography, air infiltration, airtightness, leakage paths, leakages.

## 1 INTRODUCTION

Infrared (IR) Thermography is a technique that enables the measurement of an object's temperature without physical contact (Sarawade & Charniya, 2018). In the construction industry, this technology is increasingly used to identify thermal irregularities, leakages, and humidity issues in building envelopes (Kirimtat & Krejcar, 2018) and assess their impact on energy loss (González-Aguilera et al., 2013). Some researchers combine temperature monitoring with IR cameras to observe how temperatures change throughout the day within structural imperfections. This approach helps avoid errors resulting from interpreting single data points by associating each type of error with an IR representation instead (Fox et al., 2015; Lehmann et al., 2013). Additionally, images of the same defect from both inside and outside of buildings have been studied in order to compare any differences between them (Fox et al., 2016).

The application of IR thermography in detecting and measuring air infiltration has been the subject of previous research and (Barreira et al., 2017; Lerma et al., 2018; Royuela-del-Val et al., 2019). Some authors have identified crack parameters by analysing surface temperatures on the infiltration plane, (Dufour et al., 2009; Liu et al., 2018).

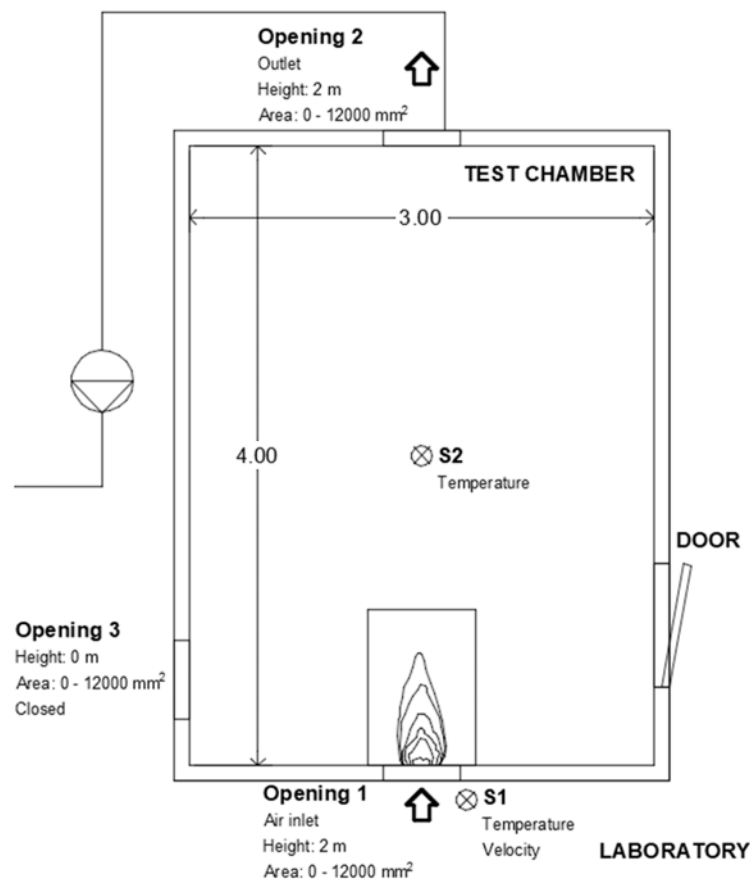
Additionally, IR thermography combined with neural networks has been used to predict airflows based on temperature changes along the air leakage path (Royuela-del-Val et al., 2019). In the same line, Gil-Valverde et al., (2021) proposed a new technique that involved a reduction of the Coanda effect, improving the accuracy and obtaining as a result a three-dimensional characterization of the infiltrating airflows (Gil-Valverde et al., 2021).

This paper presents a step forward based on tests performed in a controlled environment with the objective of obtaining optimized results with a single IR capture. In this way, the possibility of error due to temperature changes during the measuring period is reduced.

## 2 METHODOLOGY

### 2.1 Equipment and laboratory experimental set-up

The tests were carried out in the Laboratory of Ventilation located in the School of Architecture of the University of Valladolid. This laboratory has a controlled test chamber with a size of 3.0 m x 4.0 m x 2.5 m (height). Three openings can be configured as inlet or outlet (Figure 1).

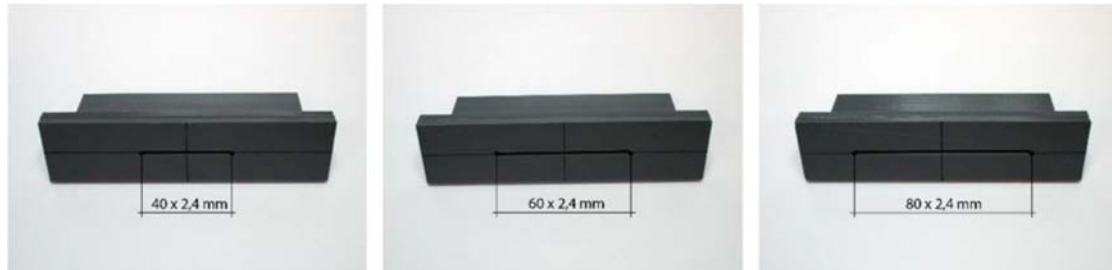


**Figure 1.** Test chamber configuration floor plan.

The test chamber was set up with the inlet (Opening 1) and exhaust (Opening 2) positioned opposite each other to ensure balanced airflow perpendicular to the wall where the incoming airflow opening was located. To induce air movement, a fan connected to a frequency variator for control purposes was used to create negative pressure inside the chamber. Additionally, the

electric underfloor radiant system with low thermal inertia was activated to maintain approximately 5 °C temperature difference between the interior (S2) and exterior of the test chamber (S1), thus ensuring accurate boundary conditions. A Lambert radiator was placed under the inlet to mitigate any thermal radiation caused by the heating system.

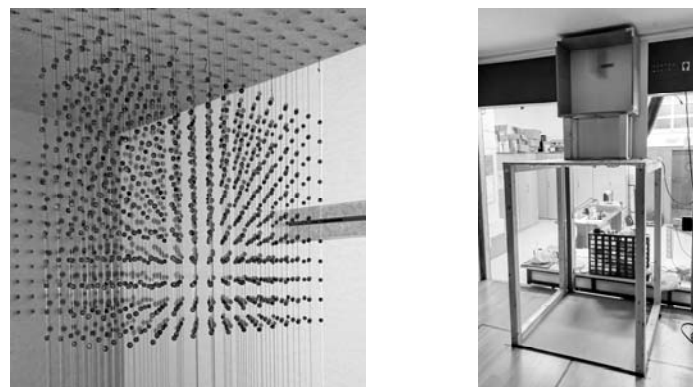
Three different interchangeable air inlets produced through additive 3D printing were used to ensure precise dimensions of the Opening 1. All inlets shared identical heights but varied in width, resulting in three different air inlet areas (Figure 2).



**Figure 2.** Incoming airflow openings a) A1. 40 mm x 2.4 mm (96 mm<sup>2</sup>) b) A2. 60 mm x 2.4 mm (144 mm<sup>2</sup>) c) A3. 80 mm x 2.4 mm (192 mm<sup>2</sup>)

The monitorization of the airflow through the test chamber and other parameters as the temperature and velocity of the inlet air was done by a data acquisition system composed of a multisensory data logger, two high-precision temperature sensors (accuracy  $\pm 0.1\text{K}$ ), a thermal mass flow sensor (accuracy  $\leq 3\%$ ) and a differential pressure sensor.

The sensible device was a 3D matrix of balls. Each ball works like a temperature sensor, so these balls switched their temperatures by the air temperature. When the temperatures were established, we take a thermal image. The thermal images were captured with an IR camera with a resolution IR of 320 x 240 pixels. These balls were printed with a 3D resin printer. The resin used was black and its emissivity  $\epsilon=0.95$ . The 3D matrix had 20 mm of separation in the three dimensions (Figure 3).



**Figure 3.** a) 3D Matrix b) Set-up of the experiment

## 2.2 Experimental design and data processing

During the tests, IR thermal images were captured when the temperatures were stabilized. Unlike other methods (Gil-Valverde et al., 2021) what it needed a lot of thermal images for to

obtain a **tridimensional** characterization, and therefore it took a long time to stabilize temperatures between each image, now only one thermal image was taken for each setup. This greatly reduces data collection time because we only need waiting the time to stabilized the temperatures one time. Also, all the points were measured at the same time, which avoided the need to adjust temperatures between samples.

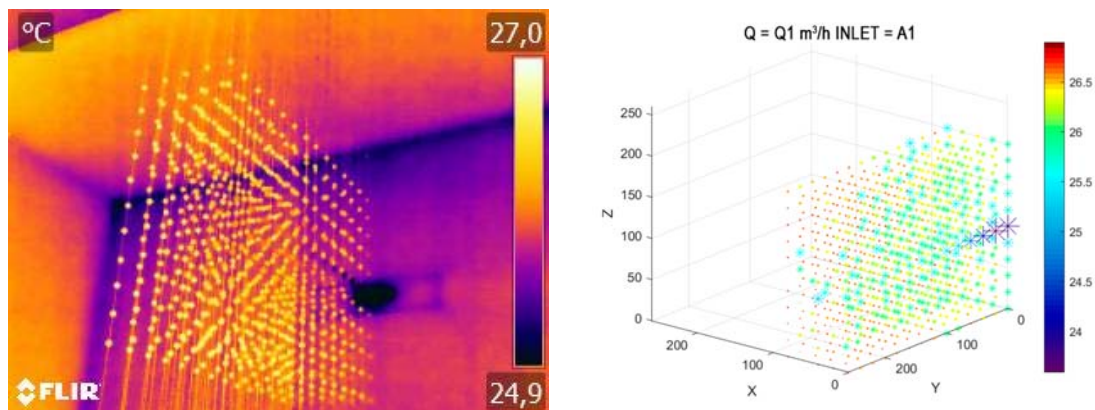
The location of the camera was essential for the automation of temperature extraction. Therefore, the camera position, as well as its setup, remained unchanged to guarantee the visualization of the points in the central axis of the opening. Only one-half of the airflow was studied assuming a symmetrical pattern (Gil-Valverde et al., 2021).

The tests were performed considering three different flow rates (Q1, Q2, and Q3) per opening (A1, A2, and A3). The following data were also registered for each IR thermal image: indoor temperature ( $T_{int}$ ), outdoor temperature ( $T_{ext}$ ), temperature gradient ( $\Delta T$ ), air flow rate (Q), pressure differential ( $\Delta P$ ), medium air velocity at the opening, inferred from the airflow rate (V), and the opening dimensions, according to the Continuity Law of Fluids (Table 1).

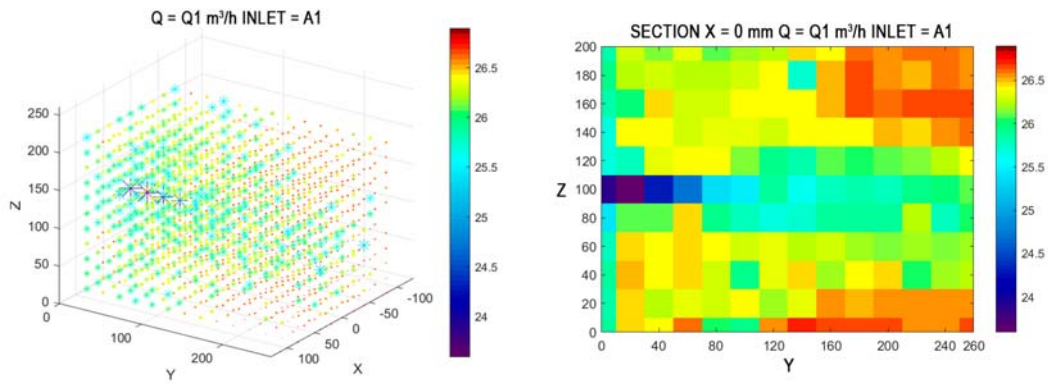
Table 1: Data registered during the tests

	A1-Q1	A1-Q2	A1-Q3	A2-Q1	A2-Q2	A2-Q3	A3-Q1	A3-Q2	A3-Q3
Q (m <sup>3</sup> /h)	1.4	2.4	3.8	2.2	3.1	5.1	2.7	4.7	5.7
$\Delta P$ (Pa)	1.6	10.8	36.00	1.28	4.8	35.3	0.9	10.4	34.8
$T_{int}$ (°C)	26.1	26.3	26.0	26.0	25.3	25.4	24.9	24.6	24.7
$T_{ext}$ (°C)	20.9	21.0	20.9	20.5	20.3	20.2	19.7	19.6	19.5
$\Delta T$ (°C)	5.2	5.3	5.1	5.5	5.0	5.2	5.2	5.0	5.2
V (m/s)	3.9	7.1	10.9	4.2	6.0	9.9	3.9	6.8	8.2

The first step was to identify the points to be extracted from the image by creating a mapping of the "pixels" and the points of one-half of the 3D matrix. The viewpoint is very important to view most of the balls. In this set, only 3.7% of the balls were hidden, moreover, these hidden balls belonged, in this case, to areas away from the airflow, so they did not interfere with the measurement. The second step involved the processing of all the images with MATLAB. The temperature values of the previously selected points were extracted. After that, the 3D representation of the whole matrix and every plan section in the edges X, Y, and Z is obtained (Figure 5).



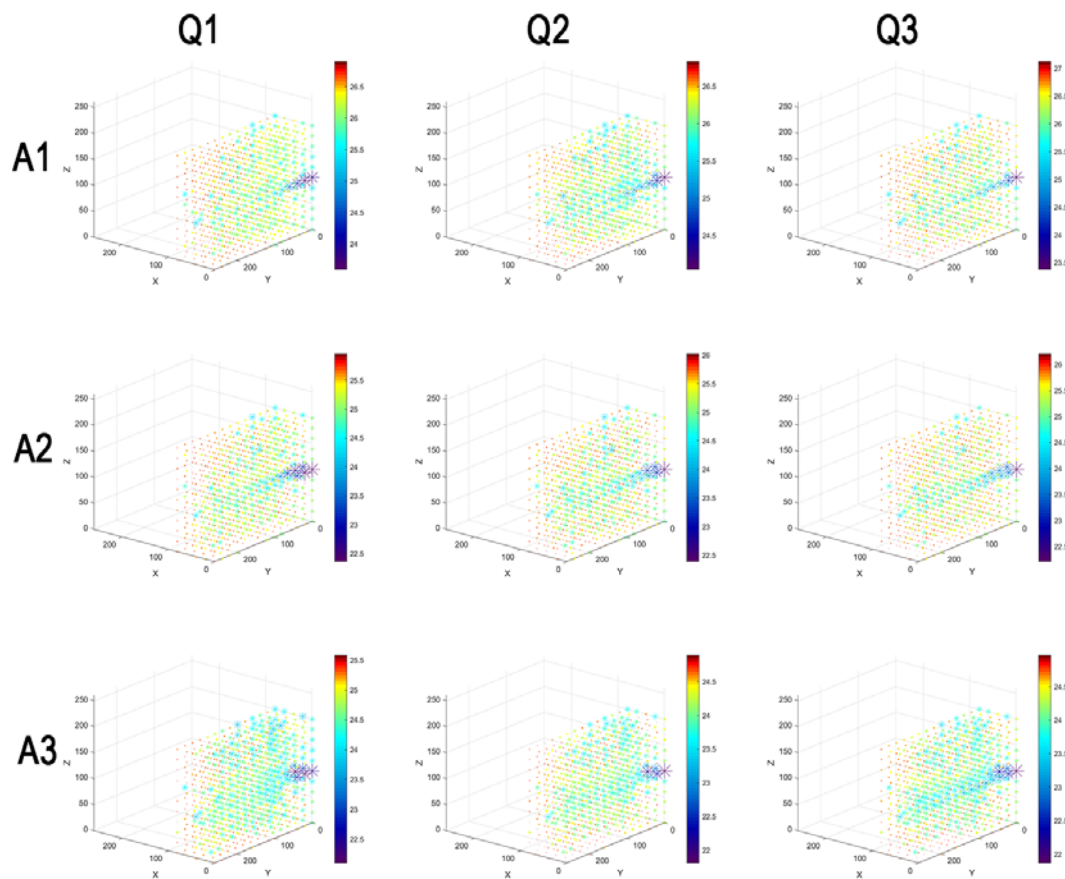
**Figure 4.** Images of the airflow A1-Q1. a) Thermal image b) 3D representation of half the airflow



**Figure 5.** Images of the airflow A1-Q1. a) Complete 3D representation b) Measurement of plane ZY at 0 mm from the opening's axis

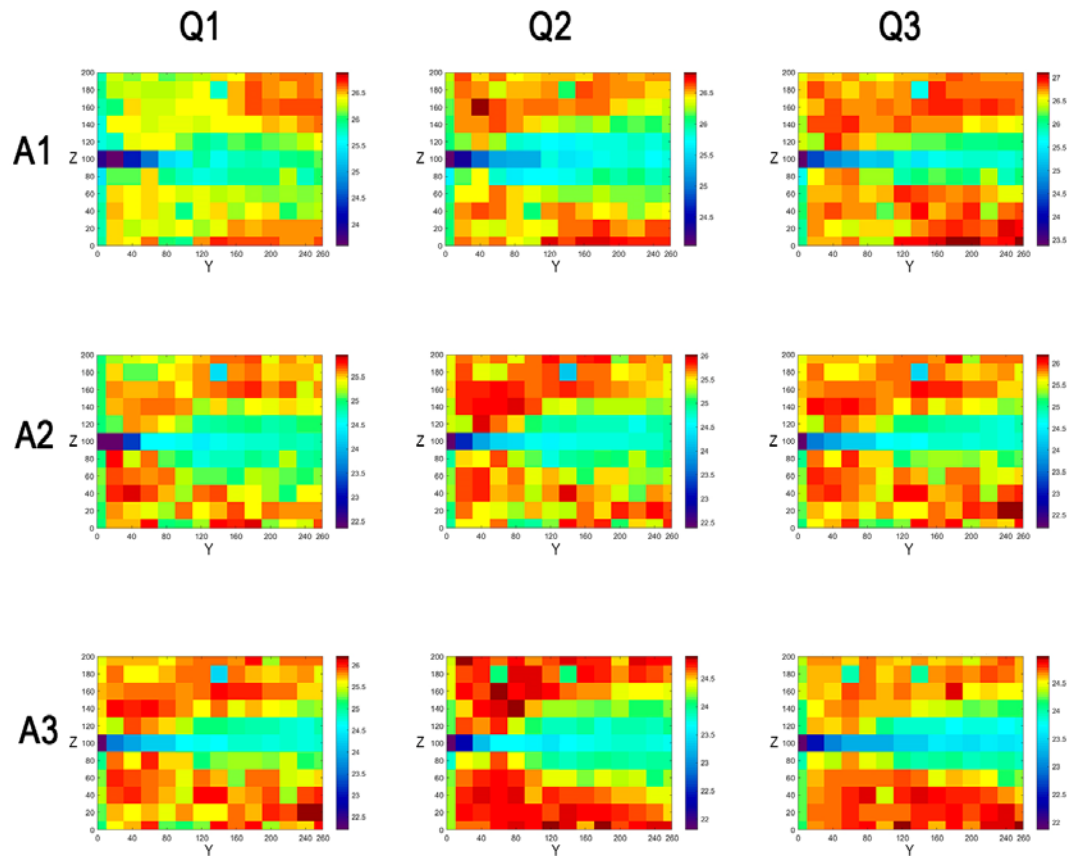
### 3 RESULTS

The following graphs were created by combining the different openings and airflows resulting from only one IR thermal image, along with the post-processing of the captures (see Figure 6). The variation in the airflow path can be observed based on the parameters.



**Figure 6.** Three-dimensional representation of one-half of the airflow a) A1-Q1 b) A1-Q2 c) A1-Q3 d) A2-Q1 e) A2-Q2 f) A2-Q3 g) A3-Q1 h) A3-Q2 i) A3-Q3

It can be observed how the airflow changes with the size of the inlet and the airflow rate. As an example, the results obtained for the measurement plane on the inlet axis can be seen in Figure 7. We can see how at an opening, as the flow rate increases, the flow appears to stretch due to the increased velocity of the air. If we look at the lower flow rate (Q1) it appears that the air has a slight tendency to go down, due to the lower velocity, and that being cold air, due to the lower density, it tends to go down. At the other flow rates this phenomenon will also occur, but as the air exits at a higher velocity, this occurs outside the measurement area.



**Figure 7.** Measurement plane ZY at 0 mm from the opening's axis a) A1-Q1 b) A1-Q2 c) A1-Q3 d) A2-Q1 e) A2-Q2 f) A2-Q3 g) A3-Q1 h) A3-Q2 i) A3-Q3

#### 4 CONCLUSIONS

This paper presents an optimized technique for the characterization of airflows through controlled air inlets. In contrast with previous methods, which required a lot of data collection time, the advantage is that only one IR thermal image is needed for each airflow condition, and that makes it possible to transfer the method to a real situation in a building. Also, the need for a single thermal image avoids uncertainties regarding pressure and temperature changes during the measurement or even camera location variation due to limited battery life.

This method to characterize airflows opens new possibilities about several research lines such as the quantification of leakages, the in-situ evaluation of the operating regime of ventilation grids, or the validation of CFD systems.



## 5 REFERENCES

- Barreira, E., Almeida, R. M. S. F., & Moreira, M. (2017). An infrared thermography passive approach to assess the effect of leakage points in buildings. *Energy and Buildings*, *140*, 224–235. <https://doi.org/10.1016/j.enbuild.2017.02.009>
- Dufour, M. B., Derome, D., & Zmeureanu, R. (2009). Analysis of thermograms for the estimation of dimensions of cracks in building envelope. *Infrared Physics and Technology*, *52*(2–3), 70–78. <https://doi.org/10.1016/j.infrared.2009.01.004>
- Fox, M., Coley, D., Goodhew, S., & De Wilde, P. (2015). Time-lapse thermography for building defect detection. *Energy and Buildings*, *92*, 95–106. <https://doi.org/10.1016/j.enbuild.2015.01.021>
- Fox, M., Goodhew, S., & De Wilde, P. (2016). Building defect detection: External versus internal thermography. *Building and Environment*, *105*, 317–331. <https://doi.org/10.1016/j.buildenv.2016.06.011>
- Gil-Valverde, R., Tamayo-Alonso, D., Royuela-del-Val, A., Poza-Casado, I., Meiss, A., & Padilla-Marcos, M. Á. (2021). Three-dimensional characterization of air infiltration using infrared thermography. *Energy and Buildings*, *233*, 110656. <https://doi.org/10.1016/J.ENBUILD.2020.110656>
- González-Aguilera, D., Lagüela, S., Rodríguez-Gonzálvez, P., & Hernández-López, D. (2013). Image-based thermographic modeling for assessing energy efficiency of buildings façades. In *Energy and Buildings* (Vol. 65, pp. 29–36). <https://doi.org/10.1016/j.enbuild.2013.05.040>
- Kirimtat, A., & Krejcar, O. (2018). A review of infrared thermography for the investigation of building envelopes: Advances and prospects. *Energy and Buildings*, *176*, 390–406. <https://doi.org/10.1016/j.enbuild.2018.07.052>
- Lehmann, B., Ghazi Wakili, K., Frank, T., Vera Collado, B., & Tanner, C. (2013). Effects of individual climatic parameters on the infrared thermography of buildings. *Applied Energy*, *110*, 29–43. <https://doi.org/10.1016/j.apenergy.2013.03.066>
- Lerma, C., Barreira, E., & Almeida, R. M. S. F. (2018). A discussion concerning active infrared thermography in the evaluation of buildings air infiltration. *Energy and Buildings*, *168*, 56–66. <https://doi.org/10.1016/j.enbuild.2018.02.050>
- Liu, W., Zhao, X., & Chen, Q. (2018). A novel method for measuring air infiltration rate in buildings. In *Energy and Buildings* (Vol. 168, pp. 309–318). <https://doi.org/10.1016/j.enbuild.2018.03.035>
- Royuela-del-Val, A., Padilla-Marcos, M. Á., Meiss, A., Casaseca-de-la-Higuera, P., & Feijó-Muñoz, J. (2019). Air infiltration monitoring using thermography and neural networks. *Energy and Buildings*, *191*, 187–199. <https://doi.org/10.1016/J.ENBUILD.2019.03.019>
- Sarawade, A. A., & Charniya, N. N. (2018). Infrared Thermography and its Applications: A Review. *2018 3rd International Conference on Communication and Electronics Systems (ICCES)*, *Icces*, 280–285. <https://doi.org/10.1109/CESYS.2018.8723875>

# Control of airborne particle concentrations in a meeting room with stand-alone air cleaners: influence of type, airflow rate, flow pattern and position in the room

Mirela Robitu<sup>1</sup>, Alain Ginestet<sup>\*1</sup>, Benoît Golaz<sup>1</sup>, Dominique Pugnet<sup>1</sup>, Lionel Boiteux<sup>1</sup>, Jean-Marc Thiebaut<sup>1</sup>

*1 CETIAT*

*Domaine Scientifique de la Doua, 25 avenue des Arts, 69100 Villeurbanne, France*

*\*Corresponding author: alain.ginestet@cetiat.fr*

## ABSTRACT

The objective of this study is to assess the ability to mitigate the airborne particle concentration in a mechanically ventilated meeting room with stand-alone air cleaners (ACs) as function of the amount and type of devices, the total airflow rate, the location(s) of the device(s) in the room and their flow pattern. Six commercially available ACs, selected to be representative of the French market, are included in the study, each featuring distinct airflow patterns for both air inlet and outlet. The intrinsic performances of the ACs have been measured according to the French standard (NF B 44-200, 2016). Their filtration efficiencies are close to 100%, as expected with HEPA filter, the airflow rates targeted for this study, 80, 200 and 400 m<sup>3</sup>/h corresponding to respectively 1, 2.5 and 5 volume per hour (vol/h), are attained. Nevertheless, the airflow rate is 20 to 50% lower than values declared by the manufacturers. The sound power level as well as the operating power of the air cleaners have also been measured.

Numerical 3D simulation (CFD) was used to assess 66 configurations of ACs in the room. The airflow pattern, the air velocity, the particle concentration as function of time and at different locations in the room at breathing zone were calculated. The cleaning efficiency represented by the particle concentration after 16 minutes AC operating divided by the initial concentration was determined. When the AC is placed in a corner behind a wall (a common placement), the performance is lower compared to other locations in the room. As the total airflow rate increases, the cleaning efficiency increases (C16/C0 decreases). The differences in particle concentrations across the room when an AC is used are weak at 5 vol/h but become larger at 2.5 vol/h. Airborne particle concentrations within the room are more homogeneous with the ceiling-type ACs. Also, most of the studied ACs have sound power levels exceeding 50 dB(A) above 200 m<sup>3</sup>/h, which can lead to noise nuisance for occupants. 9 of the 66 simulated configurations were also assessed through experimental measurements of airborne particle concentrations using low-cost particle sensors (0.3 to 5 µm range).

## KEYWORDS

Stand-alone air cleaner, performance, numerical simulation, measurement, indoor air quality

## 1 INTRODUCTION

In the industrialized countries, people spend most of their time indoors (at home, at work, at school, for shopping and in public transportation). They are exposed to various harmful airborne substances being in gaseous (CO<sub>2</sub>, CO, VOCs, NO<sub>x</sub>, etc.) or in particulate (fine particles) form. These airborne indoor pollutants come from indoors and outdoors and their level mainly depends on the air change rate, people and indoors activities. The use of stand-alone air cleaners (ACs) can mitigate the exposure of people to airborne indoor pollutants if the buildings where they live, or stay, are not well ventilated or even if there is no ventilation system. An AC can also be used for complementing the ventilation system which always needs to be implemented first; this was recalled during the recent COVID-19 pandemic by French authorities (Haut Conseil de la Santé Publique (HCSP, 2021), Institut National de Recherche et de Sécurité (INRS, 2020)). Airborne fine particles are especially considered because they are harmful (they

can penetrate deep into the respiratory tract and the bloodstream) and most of the commercially available ACs are designed to treat particles. The most widely used technique is mechanical filtration implemented with HEPA filters (NF EN 1822-1, 2019) but electrostatic precipitation, ionization, photocatalysis, cold plasma are also available.

Numerous studies in the literature underscore the potential of ACs in the control of the airborne particle concentrations in commercial and residential buildings. For example, in the United States, it has been shown by Carmona *et al.* (Carmona, et al., 2022) that utilizing ACs with HEPA filter (at a flowrate of 850 m<sup>3</sup>/h) positioned at the centre of the classrooms resulted in indoors ultrafine airborne particle concentrations being ten times lower than outdoors levels, whereas this ratio was only halved without AC usage. In the study of Duill *et al.* (Duill, Schulz, Jain, & van Wachen, 2023), 2 small ACs (3 to 4 units used simultaneously) and 4 large ACs (only 1 unit utilized at a time), equipped with HEPA filters, were deployed within a rectangular classroom. It was shown that the decay rate increases when the total airflow rate increases. With the 2 large ACs, the particle concentration was divided by 10 after 30 minutes, which means a decay rate of 4.6 h<sup>-1</sup>; this result was obtained with a sound level lower than 40 dB(A). With the 2 small ACs the same result was obtained, albeit at higher sound level (40 dB(A) was reached at 3.1 to 3.4 h<sup>-1</sup>). The decay rate was the same at the 2 different measuring points located along the length of the classroom regardless of the tested ACs. Moreover, the decay rate was higher when the clean air was released upward and horizontally by the AC (highlighting the impact of the flow pattern). In the study of Curtius *et al.* (Curtius, Grandin, & Schrod, 2021), 4 identical ACs equipped with HEPA filter (total 1026 m<sup>3</sup>/h, 5.5 vol/h) were installed within a non-ventilated classroom. It was observed that the particle concentration (0.01 to 10 µm) measured at 5 different positions decreases by 95% after 37 minutes and this decrease is similar at the 4 positions; also, there is little influence on the particle size. Furthermore, in a study by Kähler *et al.* (Kähler, Hain, & Fuchs, 2023), conducted in a meeting room, an AC equipped with an HEPA filter (with air inlet at the bottom and outlet at the top on 4 sides, inclined at 25° to the vertical axis) was placed both at the centre of the room and in a corner. The results show that the cleaning efficiency increases with airflow, the aerosol particle concentration decay rate  $k$  increases from 2.9 to 3.3 h<sup>-1</sup> at 600 m<sup>3</sup>/h to 5.7 to 6.3 h<sup>-1</sup> at 1500 m<sup>3</sup>/h, depending on the position of the measuring point. Furthermore, the presence of occupants does not significantly affect the cleaning efficiency. However, a slight enhancement in efficiency was observed when the room contains chairs and tables, with airflow preferably directed above the tables. Moreover, cleaning efficiency was found to be higher in square rooms compared to rectangular ones, with significantly higher efficiency near the AC in the latter case.

A lot of the available studies in this field lack comprehensive documentation, particularly regarding details such as buildings specifications, ventilation system, and AC types.

Our study focuses on the ability to mitigate the airborne particle concentrations in a mechanically ventilated meeting room with ACs equipped with HEPA filter as function of different factors, such as the number and type of AC devices, total airflow rates, airflow patterns, and AC placement(s). Through systematic experimentation and simulations, our study aims to provide valuable insights into the most effective strategies for utilizing ACs in tertiary buildings to improve indoor air quality by reducing airborne fine particle concentrations.

## 2 METHOD

Simulations and measurements were carried out to evaluate the efficiency of ACs in a CETIAT meeting room. The ACs selected were subjected to experimental tests to determine their intrinsic performances, which was necessary for the CFD simulations. Low-cost particle sensors were used for the measurements. Initially, these sensors were placed near each other to assess the consistency of the measured values and to calibrate them if any discrepancies were detected. Subsequently, these sensors were used in the measurement campaign to verify the

overall performance of certain ACs in the meeting room and to validate the numerical simulations. The following sections describe the ACs selected, the methods used to assess intrinsic and overall performance, and the simulation model.

## 2.1 The studied stand-alone air cleaners (ACs)

Six ACs equipped with HEPA filter (as illustrated in Figure 1) were selected for the study. This selection includes four mobile units: three floor types (designated as C, D, and F) and one table type (labeled as B). Additionally, two fix units were included: ceiling-type models (identified as A and E). This selection is made to ensure representation of commercially available products on the French market and to include a variety of flow patterns, characterized by different air inlet and outlet positions synthesized in Table 1. The main characteristics of the ACs are provided in Table 2.

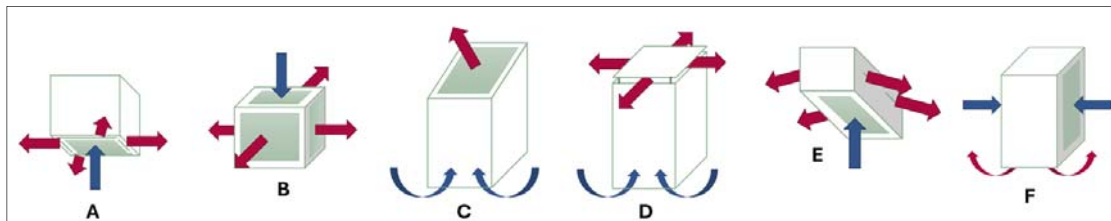


Figure 1: The six stand-alone air cleaners (ACs) studied

Table 1: Position of inlet and outlet of the 6 studied AC models

Model	A	B	C	D	E	F
Inlet	Bottom face	Top face	Floor level	Floor level	Bottom face	Two opposite side faces
Outlet	Horizontal on all four sides	Horizontal on all four side faces	Upward inclined at 45°	Horizontal at the top in all directions	Horizontal, on two long vertical sides	Floor level

Table 2: Main characteristics of the six stand-alone air cleaners (AC) studied

Unit	A	B	C	D	E	F
Type	Ceiling	Floor	Floor	Floor	Ceiling	Floor
Dimensions (cm)*	59/60/36	42/43/40	45/37/96	69/67/113	59/89/30	34/34/72
Main filter**	H14	H14	H13	H14	H14	H14
Air flow rate (m <sup>3</sup> /h)***	200 max	1000 max	200 to 900	1200 max	300 max	37 to 433

\* Length/Width/Height; \*\* As per EN 1822-1 (2019); \*\*\* Manufacturer's data

## 2.2 Measurement of the intrinsic performances of the stand-alone air cleaners (ACs)

The intrinsic performances of the ACs have been measured according to the French standard (NF B 44-200, 2016). This standard provides a method for measuring specified product performances especially airflow, particulate matter removal efficiency, electric operating power, and sound power level. It references EN ISO 5801 (2017) for airflow measurement and EN ISO 3743-1 (2010) for sound power level measurement. For assessing particulate matter removal efficiency, the AC under test is installed within a test duct, its inlet placed upstream, and its outlet placed downstream utilizing a specially designed separator plate. An auxiliary fan

is used to equalize pressure between the AC's upstream and downstream sections, reproducing real operating conditions. Particles of DEHS (Di-Ethyl-Hexyl-Sebacat) are continuously injected upstream, and concentration measurements are taken upstream and downstream of the AC.

### 2.3 Meeting room

For this study, a meeting room located at CETIAT was chosen. The room is rectangular, measuring 7.9 m x 4.7 m, with a total volume of 80 m<sup>3</sup>, and is mechanically ventilated at approximately 1.5 vol/h. It features two exhaust valves (outlets) positioned on the ceiling and 3 fresh air inlets located above the windows (refer to Figure 2 a)). The room is furnished with tables, chairs, cupboards, and fan coil units (VC). For simplification of the geometry, the chairs are not included in the room model.

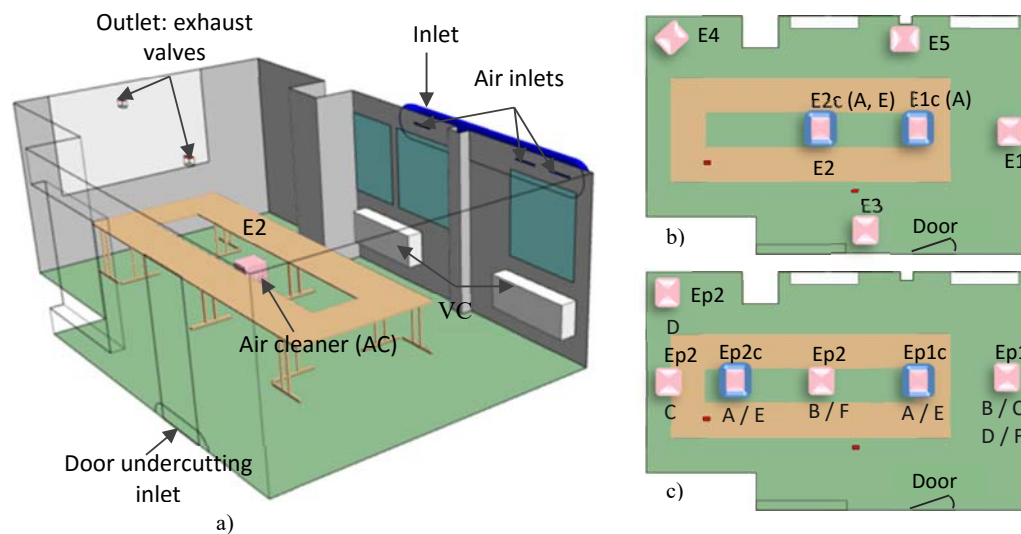


Figure 2: Views of the meeting room: geometry and boundary conditions (a)); AC simulation positions with one unit (b)) and with two units (c))

### 2.4 Numerical simulation method

A stationary three-dimensional computational fluid dynamics (CFD) modeling of the AC within the meeting room was conducted to assess cleaning efficiency relative to various factors including airflow rate, AC positioning, device quantity and type, and air flow pattern. A commercial CFD software was employed to conduct the simulations. The computational domain reproduces the full-scale meeting room with the AC installed (refer to Figure 2 a)). The mesh features a refined mesh near the air inlets and outlets including a boundary-layer grid near the wall surfaces and a coarser mesh elsewhere in the computational domain. The final volume mesh grid comprises approximately 10.2 million of polyhedral elements. Flow pattern simulations employed steady Navier-Stokes equations with a two-layer  $k-\epsilon$  turbulence model, integrating all  $y^+$  wall treatment. A Eulerian species model was utilized to simulate aerosol particle dispersion, with CO<sub>2</sub> serving as the tracer gas. This approach is applicable for modeling particles with diameters less than 5  $\mu\text{m}$ , which remain suspended in the air for many hours (Castellini, Faulkner, Zuo, Lorenzetti, & Sohn, 2022); (Noakes, Fletcher, Beggs, Sleight, & Kerr, 2004)).

For each AC, simulations were conducted for nearly five different positions and two airflow rates corresponding to 1 or 2.5 air changes per hour (ACH), as well as 5 ACH of the room volume. One type of AC at a time was positioned at locations E1 to E5 on the floor, (ACs B, C, D and F) or table (AC B), and at the positions E1c and E2c on the ceiling (AC A) as shown in Figure 2 b) and 2 c). AC E was positioned in the center of the ceiling, in position E1c, the air outlet flows in the direction of the width of the room and in position E2c in the direction of the length of the room. Additionally, configurations with two ACs were simulated, with their positions labeled as "Ep" on Figure 2c).

The inlet and outlet air boundary conditions were set as "Velocity Inlet" while the door undercutting inlet was set as a reference pressure condition. The inlet and outlet of the ACs were set as velocity inlets corresponding to airflow rates of 1 or 2.5 ACH and 5 ACH. The particle concentration at the AC outlet equaled that at the inlet, which was reduced by the experimentally obtained AC efficiency. For each scenario, an initial calculation of steady-state airflow fields was conducted. Subsequently, transient simulations were initiated to model particle concentration in the room as the ACs operated for 60 minutes. These simulations employed a 2-minute time step, allowing observation of concentration level changes over time.

## 2.5 Experimental method

The airborne particle concentrations within the meeting room were measured with low-cost particle sensors. These sensors continuously count particles as function of their size, ranging from 0.3  $\mu\text{m}$  up to more than 5  $\mu\text{m}$ . Particles are classified in 5 channels: 0.3-0.5  $\mu\text{m}$ , 0.5-1.0  $\mu\text{m}$ , 1.0-2.5  $\mu\text{m}$ , 2.5-5.0  $\mu\text{m}$  and > 5.0  $\mu\text{m}$ . Nine sensors were used indoors: one positioned near one of the 2 air outlets and eight evenly spaced over the tables at a height of 1.2 m. The particle concentration was recorded every 10 seconds and expressed in number per cubic meter of air. Before measurements within the meeting room, the nine particle sensors were compared to assess whether the measurements are consistent when placed in the same location. This experience has been done in an office room at CETIAT, where an AC was used to vary particle concentration and to ensure that the sensors are compared over a wide airborne particle concentration. While the sensors give very different values (with a factor of around 2 between the lowest and the highest values), they record the same trend when the particle concentration decreases (AC on) or increases (AC off). As the sensors are supposed to provide the same data, it was decided to adjust the values of the other 8 sensors to match those of the PS9 sensor. Linear regression analyses were performed between each of the 8 other sensors and the PS9 sensor ( $R^2 > 0.99$ ) to determine the correction factor. This correction methodology was subsequently applied to measurements done within the meeting room (refer to paragraph 3.3).

## 3 RESULTS AND DISCUSSION

The intrinsic performances of the stand-alone air cleaners (ACs), simulations and measurements results are presented in this paragraph. For the simulations and measurements, the results are principally expressed as the ratio between the particle concentration after 16 minutes of operation (C16) and the initial concentration (C0). By focusing the analysis on this 16-minute performance metric, the results shed light on a key aspect of the AC' real-world effectiveness in improving indoor environments where people are present.

### 3.1 Intrinsic performances of the ACs

Figure 3 a) and b) display the measured airflow and sound power level, respectively. The results show that the targeted airflows for this study, ranging from 80 to 400  $\text{m}^3/\text{h}$ , were successfully achieved. However, it's noteworthy that the measured airflows for all ACs were observed to be

below the manufacturer's declared data (refer to Figure 3 a)). Acoustic pressure level measurements (Figure 3 b)) reveal that most of the ACs generate more than 50 dB(A) when operating above 200 m<sup>3</sup>/h. While this has no impact on particulate matter removal, it raises the question of noise acceptability for users. Such levels of noise can become annoying in environments as a meeting room, offices, and especially bedrooms.

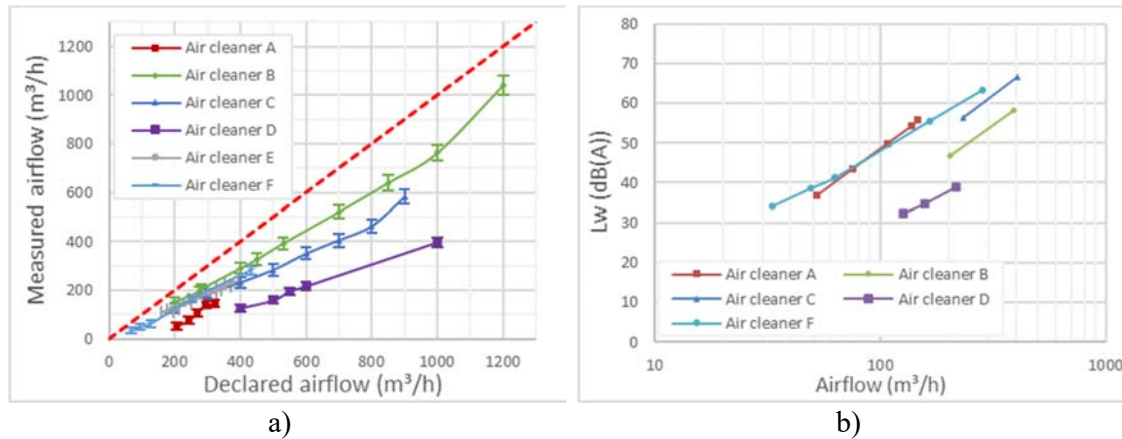


Figure 3: Intrinsic performance measurements results. Air flow (a)), sound power level ( $L_w$ ) (b))

The particulate matter removal efficiency obtained exceeds 99% for all ACs, with only one exception where it was around 95%. These results align with expectations for HEPA filters. Upon examination of the AC with the lower efficiency, a leak was revealed between the filter and the mounting frame. However, this isolated incident does not undermine the overall effectiveness of HEPA filters.

### 3.2 Simulations results

Figures 4 through 6 present the simulation results. Figures at left show the results for the floor and table ACs, while Figures at right display the results for the ceiling mounted ACs. Figure 4 shows the particle concentration  $C_{16}/C_0$  in the meeting room for the different ACs positioned at location E2, as a function of the airflow rate expressed in air changes per hour (vol/h). The results show that increasing the airflow rate led to a significant reduction in particle concentration in the room after 16 minutes of AC operation. For the floor ACs, increasing the airflow rate from 2.5 to 5 vol/h resulted in a 31% decrease in the  $C_{16}/C_0$  ratio (see Figure 5a)). For the ceiling mounted ACs, increasing the airflow rate from 1 to 2.5 vol/h led to a 25% decrease in the  $C_{16}/C_0$  ratio (see Figure 5a)).

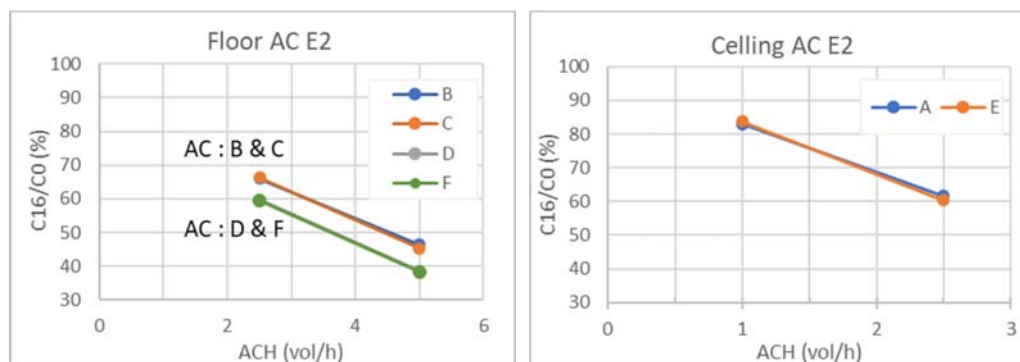


Figure 4: Impact of the ACH on the particle concentration after 16 minutes of AC operation

In summary, the results show that higher airflow rates through the AC, whether floor or ceiling mounted, led to more effective reduction of particle concentrations in the meeting room over a 16-minute period. A slightly superior performance was observed when increasing airflow for floor AC. However, it is important to note that increasing the AC airflow rate does not necessarily translate to a proportionate improvement in air cleaning efficiency, underscoring the importance of judiciously selecting the type of AC and airflow rate setting based on the specific needs of the indoor environment.

Figure 5 illustrates the particle concentrations  $C_{16}/C_0$  ratio, in the meeting room with single and two units of each type of AC. The results are shown for the floor ACs operating at an airflow rate of 5 vol/h and the ceiling mounted ACs operating at 2.5 vol/h. The results show that increasing the number of floor AC from 1 to 2 had varying effects on the performance of different models. For some ACs, like B and C, the particle removal efficiency was improved with the additional AC. For others, like D and F, a performance decrease is noted when going from 1 to 2 ACs. Increasing the number of ceiling mounted ACs from 1 to 2 units did not have a significant impact on the particle removal performance for both ACs models A and E. In summary, the data suggests that the AC type and the number of units deployed can impact the overall particle concentration reduction achieved in the space. The optimal configuration appears to depend on the specific AC models being used.

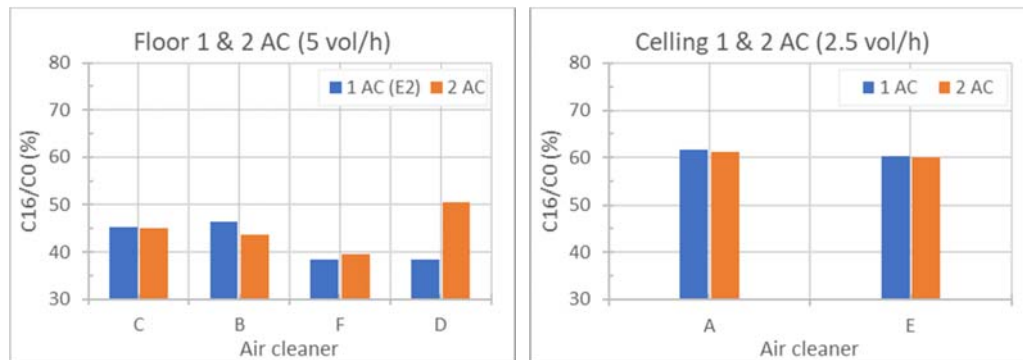


Figure 5: Impact of the AC number on the particle concentration after 16 minutes of AC operation

Figure 6 displays the  $C_{16}/C_0$  ratio for the ACs positioned in locations E1 to E5 within the meeting room. The results show that the location of the floor ACs within the room had a significant impact on their particle removal performance. Location E2 seemed to be the most favourable position, while location E4 generally resulted in the higher  $C_{16}/C_0$  ratios for the different AC models.

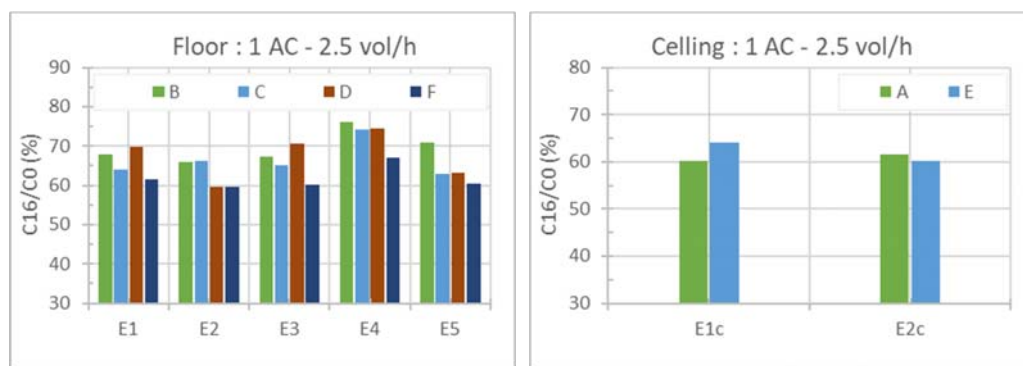


Figure 6: Impact of the AC position on the particle concentration after 16 minutes of AC operation



For the AC C, the better performance was achieved in location E5, with a C16/C0 ratio of 63%. For the ceiling AC A, the location E1c seems to be better, with C16/C0 slightly lower than in location E2c. For the AC E, the location E2c is better than the location Ec1. The results highlight that, factors such as airflow patterns, room geometry, and potential obstructions in the space can influence the effectiveness of in-room ACs. Careful consideration of the placement of these devices is important to optimize their performance in reducing airborne particle levels.

### 3.3 Measurements results

The measurements were conducted for 9 configurations amongst the 66 studied through numerical simulations. An example of the results of such measurements is presented in Figure 7, with measurements taken on February 28 and 29, 2024. For this example, the AC D was positioned in location E1. Its airflow rate was set at 200 m<sup>3</sup>/h (equivalent to 2.5 vol/h). The AC was alternatively turned on and off, and it results in short decreases and increases of the particle concentration over time.

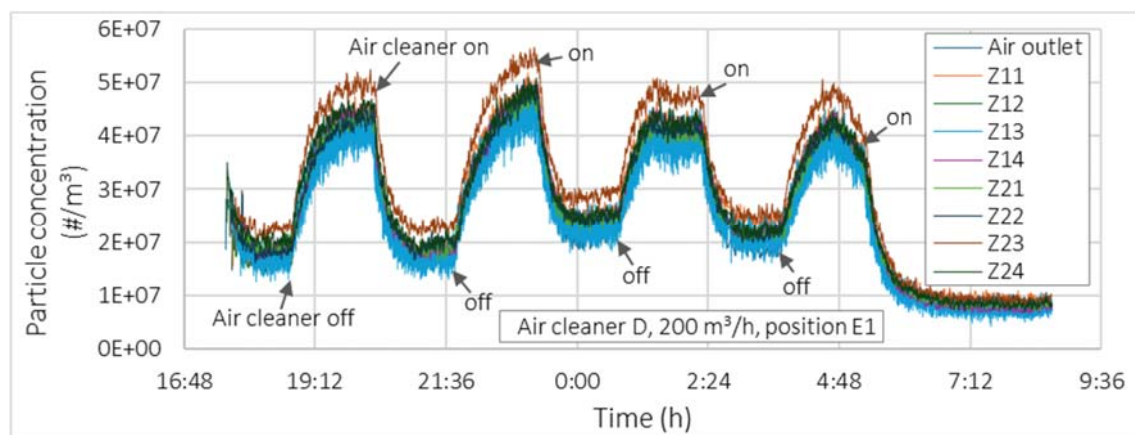


Figure 7: Particle concentration (0.3 – 0.5  $\mu\text{m}$ ) in the meeting room with the AC D at position E1

Figure 8 presents the particle concentration after 16 minutes (C16) compared to the initial concentration (C0) in box plot form, including both experimental (Meas) and simulation (Simul) results. A lower C16/C0 ratio means a higher decrease in particle concentrations. The box plots are built based on data obtained from 8 sensors uniformly spaced over the tables at a height of 1.2 m for the measurements. For the simulations, the box plots are derived from the volume average of 8 breath zones extending up to the tables.

The experimental results show that increasing the airflow rate of the AC leads to a higher decrease of the overall particle concentration. Specifically, the mean C16/C0 ratio ranges between 63 and 72% at 2.5 vol/h, between 58 and 60% at 3.5 vol/h, and between 41 and 55% at 5 vol/h, depending on the AC type and its location within the room. Similar trends are obtained by simulations. Specifically, the concentration (C16/C0) ranges between 63% and 73% at 2.5 vol/h, decreases to 53% at 3.5 vol/h, and ranges between 44% and 55% at 5 vol/h (refer to the preceding paragraph and Figure 8).

The height of the box plot indicates the homogeneity of the concentrations between the 8 points: a smaller box plot suggests that the impact of the AC is homogenous between the points, while a higher box plot means less uniformity, with some areas being better cleaned than others. The results, shown in Figure 8, highlight that the decrease in particle concentration varies for the

different areas of the room, indicating that effectiveness of the AC is influenced by airflow patterns.

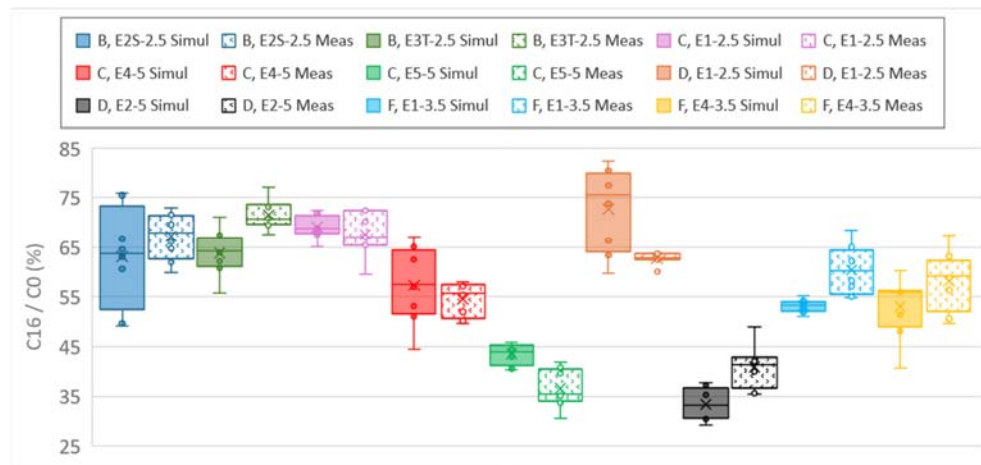


Figure 8: Normalized particle concentration ( $C_{16}/C_0$ ) after 16 minutes of ACs operation

The simulations (CFD) and experimental data of the particle concentrations after 16 minutes of the ACs use show close values but some differences are observed and may be explained for different reasons:

- Differences in flow patterns. The CFD simulations assume constant inlet airflow rates, with 88% of the total extracted flow coming from the outside via the “Inlet” and 12% coming from the corridor. However, the actual inlet airflow rates from outdoors and corridor are not measured, and this assumption may not accurately reflect the actual inlet airflow rates.
- Differences in meeting room layout. The CFD simulation does not consider the chairs in the meeting room, which can impact airflow and particle dispersion.
- Differences in measurement methods. The particle concentrations are measured at single points whereas the CFD simulation considers particle concentration integrated values over a rectangular zone leading to potential discrepancies.
- Assumptions regarding outdoor and corridor particle concentrations: CFD simulation assume constant outdoors and corridor particle concentrations, which may fluctuate over time, during the measurements campaign.

#### 4 CONCLUSIONS

Our parametric study has allowed to a better understanding of the ways to implement stand-alone air cleaners (ACs) equipped with HEPA filter in a meeting room. The simulation results show that when the total airflow rate involved by 1 or 2 stand-alone air cleaners (ACs) increases, the cleaning efficiency increases, and the airborne particle concentration obtained after 16 minutes of ACs use decreases.

When the AC is positioned at the centre of the room, higher performances levels are obtained. Inversely, when the AC is in a corner behind a wall, the performances are lower compared to other positions of ACs in the room. The differences in particle concentrations across the room when an AC is used are weak at 5 vol/h but become larger at 2.5 vol/h; airborne particle concentrations within the room are more homogeneous with the ceiling-type ACs.

Out of the 66 configurations studied through simulation, nine were assessed using experimental particle concentration measurements with low-cost particle sensors (between 0.3 and 5  $\mu\text{m}$ ). The overall air cleaning efficiency tendencies observed experimentally are in line with those

obtained by simulation. However, comparing air cleaning efficiencies across the room is more difficult due to different hypotheses in simulation and measurements.

Most of the ACs have sound power levels exceeding 50 dB(A) above 200 m<sup>3</sup>/h, which can cause noise nuisance for occupants; thus, this parameter must be considered.

This study is limited to a single rectangular meeting room, and additional studies in various types of indoor spaces are necessary to establish guidelines for the implementation of stand-alone air cleaners in tertiary buildings. Future research directions include investigating the effectiveness of stand-alone ACs in mitigating the airborne particle concentration within a non-ventilated larger, square-shaped meeting room.

## 5 ACKNOWLEDGEMENTS

This study has been sponsored by the French heating, air conditioning and air handling system manufacturers which are members of CETIAT. The authors are grateful to AAF, CAMFIL, DELTA NEU, ERLAB, FRANCE AIR and INTERFILTRE for supplying the stand-alone air cleaners (ACs) used for the study.

## 6 REFERENCES

- Carmona, N., Seto, E., Gould, T., Rasyid, E., Shirai, J., & Austin, E. (2022). Indoor air quality intervention in schools: effectiveness of a portable HEPA filter deployment in five schools impacted by roadway and aircraft pollution. *Atmosphere*, 13(10).
- Castellini, J., Faulkner, C., Zuo, W., Lorenzetti, D., & Sohn, M. (2022). Assessing the use of portable air cleaners for reducing exposure to airborne diseases in a conference room with thermal stratification. *Building and Environment*, 207(B).
- Curtius, J., Grandin, M., & Schrod, J. (2021). Testing mobile air purifiers in a school classroom: Reducing the airborne transmission risk for SARS-CoV-2. *Aerosol Science and Technology*, 55(5).
- Duill, F., Schulz, F., Jain, A., & van Wachen, B. (2023). Comparison of portable and large mobile air cleaners for use in classrooms and the effect of increasing filter loading on particle number concentration reduction efficiency. *Atmosphere*, 14(9).
- Haut Conseil de la Santé Publique (HCSP, 2. (2021). *Avis relatif au recours à des unités mobiles de purification de l'air dans le cadre de la maîtrise de la diffusion du SARS-CoV-2 dans les espaces clos*. Haut Conseil de la Santé Publique.
- Institut National de Recherche et de Sécurité (INRS, 2. (2020). *Covid-19 et prévention en entreprise - L'INRS met en garde contre certains dispositifs dits "anti-Covid-19"*.
- Kähler, C., Hain, R., & Fuchs, T. (2023). Assessment of mobile air cleaners to reduce the concentration of infectious aerosol particles indoors. *Atmosphere*, 14(4).
- NF B 44-200. (2016). *Independent air purification devices for tertiary sector and residential applications - Test methods - Intrinsic performances (in French)*, 24p.
- NF EN 1822-1. (2019). *High efficiency air filters (EPA, HEPA and ULPA) – Part 1: Classification, performance testing, marking*.
- Noakes, C., Fletcher, L., Beggs, C., Sleight, P., & Kerr, K. (2004). Development of a numerical model to simulate the biological inactivation of airborne microorganisms in the presence of ultraviolet light. *Journal of Aerosol Science*, 35(4), 489-507.

# Direct adiabatic cooling systems – Resilience to climate change for industrial building applications in a Mediterranean climate

Antoine Breteau<sup>\*1,2</sup>, Patrick Salagnac<sup>1</sup>, Jean-Marie Caous<sup>2</sup>, Emmanuel Bozonnet<sup>1</sup>

*1 LaSIE (UMR 7356), La Rochelle Université  
Av.M.Crépeau, La Rochelle  
17042, France*

*2 BLUETEK  
Z.I Nord les Pins, Luynes  
17042, France*

\*Corresponding author: [antoine.breteau@univ-lr.fr](mailto:antoine.breteau@univ-lr.fr)

## ABSTRACT

This paper presents an analysis of the resilience to climate change of a direct adiabatic cooling system integrated within an industrial building. The system is a solution that utilizes humidified porous material to lower the air temperature without requiring external energy. In this study, the system is evaluated for two typical climate periods (historical and future) for a Mediterranean climate, using indicators of energy performance, thermal comfort and water consumption. The results reveal that compared to the reference case, the system reduces indoor overheating almost similarly between the typical historical climate (76%) and typical future climate (71%). In addition, climate change would increase total system energy consumption by 40% and double water consumption. However, climate change increases the performance of the system, particularly with regard to the reduction of interior overheating in relation to the energy consumption of the fan (+90%) and the volume of water evaporated (+19%). To finish, the system is resilient in the face of climate change, even if this is 38% weaker between typical historical and future climate.

## KEYWORDS

Passive cooling, adiabatic cooling, comfort, resilience

## 1 INTRODUCTION

On 12 January 2024, the World Meteorological Organisation (WMO) officially declared that 2023 had been the warmest year on record. The average annual temperature across the world was 1.5 °C above pre-industrial levels (WMO 2024). Human activities are increasing the phenomenon of rising temperatures, particularly the intensive use of air conditioning. This solution, which is becoming increasingly popular for cooling buildings during heat peaks (Batiweb 2023), is also one of the problematic factors exacerbating global warming (Salamanca et al. 2014). Air conditioning accounts for 12% of the building sector's greenhouse gas emissions (PROMEE 2023). To tackle the impact of global warming and reduce the use of air conditioners, passive adiabatic cooling methods are being developed.

Adiabatic cooling is emerging as a promising solution to address environmental challenges, particularly in ensuring resilient building cooling amidst climate change, as suggested by the work of Annex 80 of the International Energy Agency (IEA) (Zhang et al. 2021). Unlike traditional air conditioners, this technology avoids the use of refrigerants and consumes considerably less electrical energy (Ford et al. 1998; McKenzie et al. 2013). Adiabatic cooling systems cool building interiors by harnessing the energy from water evaporation produced by the passage of hot, dry air through a wet porous material (Watt 1997). This isenthalpic process requires minimal external energy for the water pump and fan. Direct adiabatic systems supply cool and humid air to the building, while indirect adiabatic systems prevent moisture buildup

by using an air heat exchanger (Xuan et al. 2012). The combination of both direct and indirect approaches is more complex, though this allows to dynamically optimize the system performance (PROFEEL 2021).

These systems are particularly effective in hot, dry climates (Chiesa et al. 2017). Our previous studies have demonstrated the effectiveness of direct adiabatic systems in reducing overheating inside buildings (Breteau et al. 2022; 2023). In terms of energy performance, these systems are often considered as a robust and practical alternative for cooling industrial buildings, due to the low energy consumption of direct adiabatic systems (Kowalski et Kwiecień 2020), although water consumption is an aspect to be taken into account (Sahai 2012; Kowalski et Kwiecień 2020).

The aim of this paper is to examine the resilience of a direct adiabatic system integrated into an industrial building in response to climate change, specifically in a Mediterranean climate context. We compare the system performances for the both historical (before 2020) and mid-term (around 2050) periods. We then analyse the behavior of the system, highlighting the different operation phases. Finally, we give a detailed analysis of the direct adiabatic system performance, regarding thermal comfort and resilience indicators.

## 2 CASE STUDY

### 2.1 Typical industrial building

The building studied is a warehouse-type industrial building, consisting of a steel structure with a floor area of  $36 \times 36 \text{ m}^2$  and a height of 8 m (Figure 1).

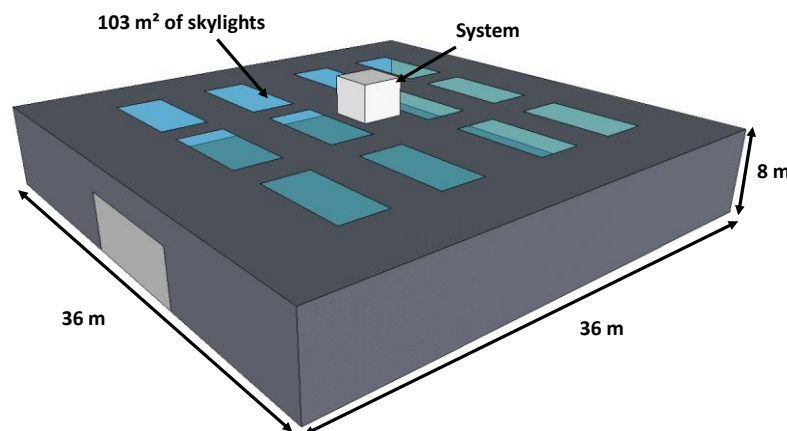


Figure 1 : Geometry of the industrial building

The building stores merchandises (paperboard, metal and pallets box) on metal shelves whose inertia is considered as an internal mass. The vertical walls and roof are made up of two 2 mm thick steel claddings covering a 5 cm thick layer of rock wool. The floor consists of an uninsulated 20 cm concrete slab. The building has  $103 \text{ m}^2$  of skylights evenly distributed across the roof (8% of the roof surface). The building has an air permeability equivalent to  $2.6 \text{ m}^3 \cdot \text{h}^{-1} \cdot \text{m}^{-2}$  (under 4 Pa) without a ventilation system, but a hygienic flow rate of  $45 \text{ m}^3 \cdot \text{h}^{-1} \cdot \text{occ}^{-1}$  has been set up to comply with standards. It is designed to accommodate an occupancy density of  $60 \text{ m}^2 \cdot \text{occ}^{-1}$  during opening hours, from 7 a.m to 10 p.m. every day except Sunday. For ventilation and cooling, the building uses a direct adiabatic cooling system.

## 2.2 Direct evaporative cooling system

We have developed a numerical model and integrated into the thermal simulation software for buildings (TRNSYS©) based on the saturation efficiency  $\epsilon_{wb}$ , see equation (1).

$$\epsilon_{wb} = 100 \frac{T_{AO} - T_{AS}}{T_{AO} - T_{wb,AO}} \quad (1)$$

with  $T_{AO}$ ,  $T_{AS}$ , and  $T_{wb,AO}$  respectively the outside air temperature, the supply air temperature and the wet bulb temperature of the outside air.

The system reduces the dry bulb temperature of the outside air to its wet bulb temperature by means of the energy of evaporation of the water produced as the air passes through a porous material.

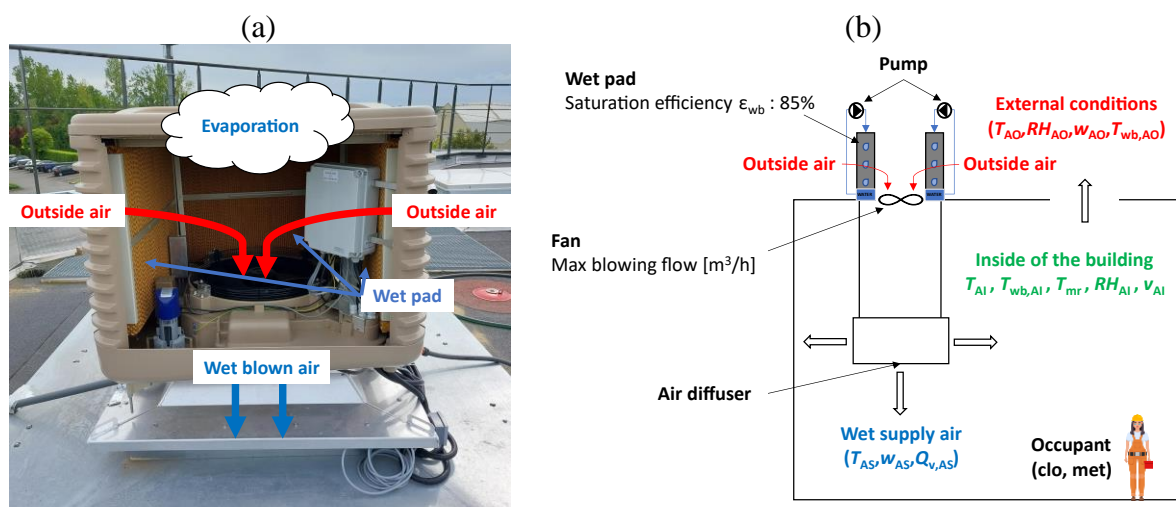


Figure 2 : direct adiabatic system (a), and system integration onto the building (b)

An adiabatic box (Figure 2) is composed of several wet media with a saturation efficiency of 85%, a fan (12 000 m<sup>3</sup>/h for this box), and a water pump. This box is installed on the roof of the building (Figure 2), and can operate either in free-cooling mode (fan only), or in adiabatic mode (with humidification). The regulation of both modes of the system remains similar, where the fan adjusts its airflow based on a proportional band of 2 °C with different temperature conditions (Table 1).

Table 1 : Indoor and outdoor temperature conditions

Air temperature conditions	Free cooling conditions		Adiabatic conditions	
	Indoor ( $T_{AI}$ )	Outdoor ( $T_{AO}$ )	Indoor ( $T_{AI}$ )	Outdoor ( $T_{wb,AO}$ )
Occupancy hours	> 22 °C	< $T_{AI}$	> 24 °C	< $T_{AI}$
Unoccupied hours	> 19 °C	< $T_{AI}$	> 28 °C	< $T_{AI}$

In free-cooling mode, this proportional band applies between the indoor temperature ( $T_{AI}$ ) and a set indoor target temperature, as well as the outdoor temperature ( $T_{AO}$ ). In adiabatic mode, however, the proportional band applies between the indoor temperature ( $T_{AI}$ ) and a target temperature, and also with the outdoor wet-bulb temperature ( $T_{wb,AO}$ ). This control makes it possible to optimise the use of the cooling potential offered between the outdoor and indoor conditions.

In this study, the resilience of the system was assessed regarding the historical climate (1990 – 2019) versus the mid-term climate change (2040 – 2069). We used the typical weather files (TMY) generated from the hourly historical weather data and the mid-term future climate from Cordex data (Machard et al. 2020). The method considers the high emissions scenario for future climate change.

The sizing of the direct adiabatic system is crucial for our study in terms of energy performance in dynamic mode, and is highly dependent on the location of the building. To this end, we determined the optimum steady-state airflow rate, taking into account typical outdoor conditions for the climate studied and the equivalent indoor temperature ( $SET^*$ ) obtained from different airflow rates of the direct adiabatic system. As the efficiency of the system is not 100%, the cooling effect tends towards an asymptotic ideal value, and we have chosen the cooling effect of 2/3 to define the maximum fan airflow rate. Sizing the system for a Mediterranean climate (Carpentras) resulted in a maximum airflow of 22 000 m<sup>3</sup>/h (2.1 ACH).

### 2.3 Key Performance Indicators (KPI)

In this article, various comfort, performance and resilience indicators were used. To assess indoor thermo(hydric) comfort, the  $T_{op}$  and  $SET^*$  indicators were chosen.

The  $SET^*$  temperature is defined as an operating temperature of a reference environment that would cause the same physiological responses as the real environment. The  $SET^*$  is defined as the equivalent of the dry temperature of an isothermal environment at 50% relative humidity where the occupants would have standardised clothing for the activity under consideration, which would have the same thermal constraint (skin temperature) and the same thermoregulatory constraint (skin humidity) as in a reference environment (Gagge, Fobelets, et Berglund 1986).

Indoor thermo(hydric) discomfort was assessed by the number of degree-hours above the limit temperature ( $T_{i,lim}$ ).  $T_{i,lim}$  values for  $T_{op}$  and  $SET^*$  were determined by an equivalence method using the PMV indicator (Zare et al. 2018). We chose a PMV indicator equal to 0 (neutral thermal sensation) and the following parameters:  $v_{AI} = 0.2$  m/s; metabolism 1.4 met; clothing 0.5 clo. According to the psychometric comfort diagram (ASHRAE 2013), an operating temperature  $T_{op}$  of 26 °C has a  $SET^*$  equivalence of 28 °C.

The system's performance was assessed using indicators to reduce internal overheating, based on water consumption ( $\Delta SETH/V_w$ ) (2) and fan energy consumption ( $\Delta SETH/C_{fan}$ ) (3).

$$\frac{\Delta SETH}{V_w} = \frac{SETH_{ref} - SETH_{sys}}{V_w} \quad (2)$$

$$\frac{\Delta SETH}{C_{fan}} = \frac{SETH_{ref} - SETH_{sys}}{C_{fan}} \quad (3)$$

with  $\Delta SETH$ ,  $C_{fan}$  and  $V_w$  respectively the reduction in internal overheating by the system, the fan energy consumption and the volume of water evaporated.

The system resilience was analysed using the  $\alpha$  indicator, which assesses a building ability to withstand the impacts of climate change and the resulting risk of overheating (4). This is determined by the slope of the regression between the  $IOD$  and the  $AWD$  (Hamdy et al. 2017).  $IOD$  quantifies interior overheating relative to a limit ( $T_{lim} = 26$  °C) and  $AWD$  is used to quantify the severity of outdoor thermal conditions relative to a base temperature ( $T_b = 26$  °C).

$$\alpha = \frac{IOD}{AWD} \quad (4)$$

If  $\alpha < 1$  then the building is able to eliminate external thermal stress in the long term and if  $\alpha > 1$  then the building is unable to eliminate external thermal stress in the long term.

### 3 RESULTS AND DISCUSSIONS

#### 3.1 Climate data

Climate data (temperature and relative humidity) of the historical (left) and future (right) climate are displayed on a heatmap with the days on the x-axis and the times of day on the y-axis (Figure 3).

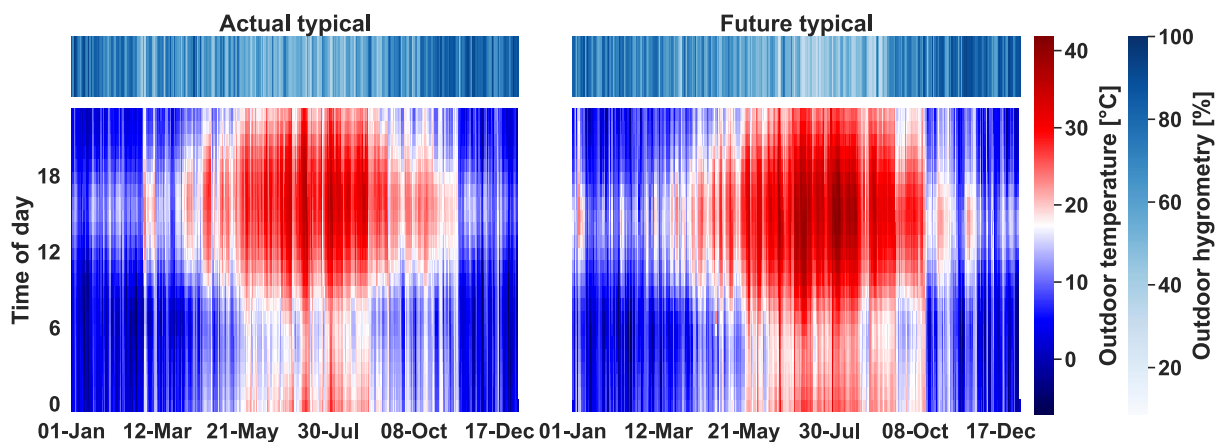


Figure 3 : Outdoor conditions

Figure 3 shows the disparity between historical and future climate. The analysis reveals an increase in night-time temperatures in the future climate scenario compared with historical data. Although the seasonal trend remains stable, with periods of intense heat from late May to early October, the average annual temperature rises significantly in the future scenario, showing an increase of 2 °C. Maximum temperatures rise from 37 °C in the historical period to 41 °C in the future period. At the same time, average relative humidity over the year falls by 2 points in the future scenario.

#### 3.2 System operation

The study examined the behaviour of the system by analysing variations in water consumption and changes in free-cooling (green) and adiabatic (purple) operating modes over historical and future climate periods. These results are presented in the form of a heatmap showing the percentage of fan flow for each mode by color intensity as a function of time of day (y-axis) and day of year (x-axis) (Figure 4).



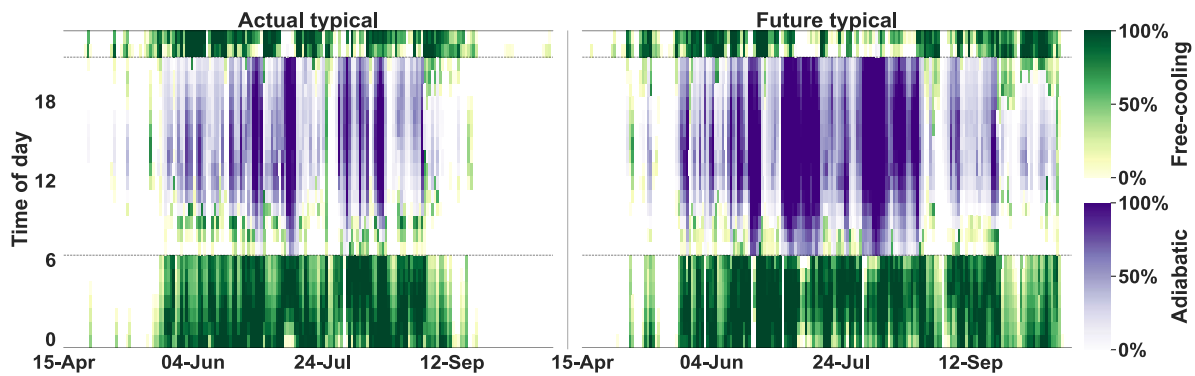


Figure 4 : The operation of both modes

Figure 4 indicates that free-cooling is generally used during periods when the building is not occupied, while adiabatic cooling is used during periods of occupancy, especially when free-cooling has not lowered the indoor temperature sufficiently. However, for the typical future period, the times when free-cooling was used during occupancy are now considered to be in adiabatic mode due to the increase in outdoor and indoor temperatures. Quantitatively, there was a 53% increase in the number of hours of operation in adiabatic mode and a 16% increase in free-cooling mode between the typical historical and future meteorological periods.

The increase in running time has led to significant changes in energy consumption. Pump consumption increased by 53%, from 43 kWh to 66 kWh, while total annual energy consumption increased by 40%, from 7 013 kWh to 9 812 kWh. The quantity of water evaporated more than doubled, from 75 m<sup>3</sup> to 161 m<sup>3</sup>. Including emptying cycles, it went from 143 m<sup>3</sup> to 220 m<sup>3</sup> per year.

### 3.3 Thermal comfort and system performance

Thermo(hydr)ic comfort was analysed using  $SET^*$ . The results represent indoor overheating with a color gradient based on its intensity. The days of the year are depicted on the x-axis, and the hours of the day on the y-axis. For each climate period, the upper figure illustrates indoor overheating without the system, while the lower figure represents indoor overheating with the system (Figure 5).

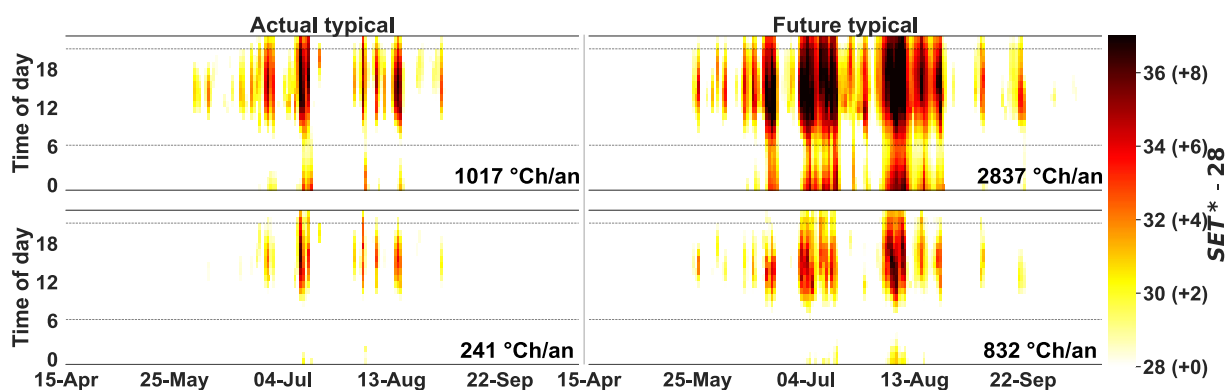


Figure 5 : Internal overheating ( $SET^* - SET^*_{lim}$ )

In the absence of the system, in a future climate, there is a clear increase in the duration and intensity of daily overheating periods, particularly in July and August. The number of degree hours in the future climate is almost three times that of the historical climate, largely due to external inputs. It is also notable that the system effect on reducing indoor discomfort decreases

according to future climate. The observed reduction is 76% (from 1 017 °Ch to 241 °Ch) for the historical climate, compared with 71% (from 2 837 °Ch to 818 °Ch) for the future period.

Then we compare the multiple aspects of the system performances for both typical historical and typical future climate, which we synthesized in a radar chart (Figure 6 - left) for the relative performances (reference without system 0%), and a table (Figure 6 - right) for the absolute performances (absolute values without system in brackets). The relative performance maxima (100%) have been specifically set for  $\Delta SETH/V_w$  and  $\Delta SETH/C_{fan}$  indicators, given the maximum performance that we obtained for these two indicators with the help of simulations in a set of various locations (historical and future climates). Hence, we obtained the maximum performance for Singapore location ( $\Delta SETH/V_w = 35.26 \text{ °Ch/m}^3$ , and  $\Delta SETH/C_{fan} = 0.85 \text{ °Ch/kWh}$ ) for Singapore. The other indicator maxima are consistent with the parameters, i.e., 100% performance in degree-hour ( $DH$ ) reduction means that  $DH = 0 \text{ °Ch}$ .

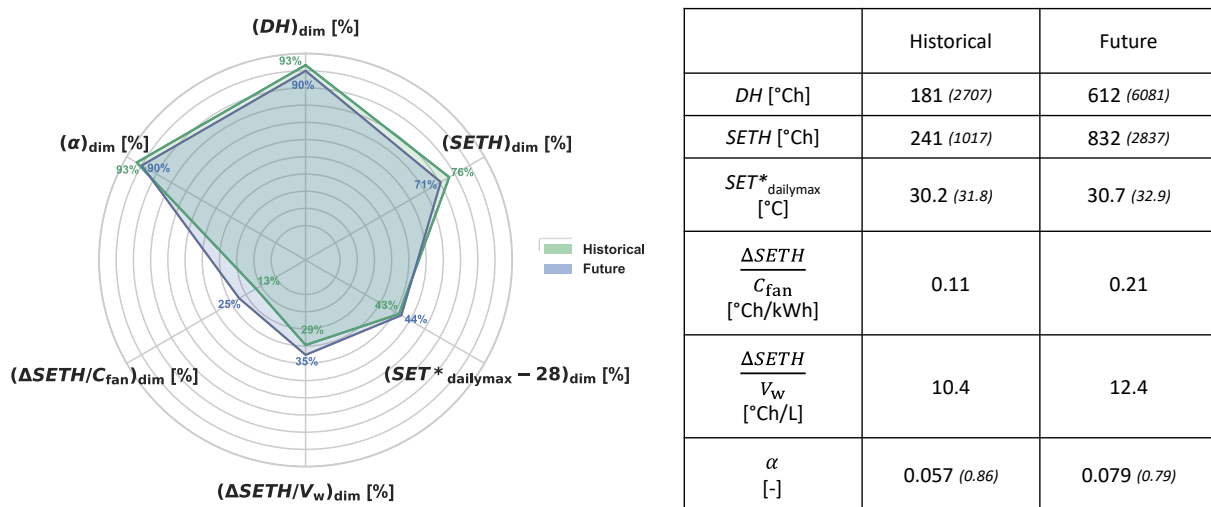


Figure 6 : System performance for two climate periods

Figure 6 show that the system performs equally well in historical and future climate conditions. The relative values obtained compared with the reference case (without system) show little difference in the system impact on reducing indoor overheating between the two climate periods. Nevertheless, the performance results ( $\Delta SETH/V_w$  and  $\Delta SETH/C_{fan}$ ) show that the system has a better impact in future climate conditions with respectively 12 and 6 points more reduction than in the historical climate. In absolute terms, we can see that the number of degree hours ( $DH$ ) remains high for the typical future period (612 °Ch), more than 3 times higher than the typical historical period (181 °Ch). This phenomenon is more significant when we look at the  $SETH$ , which is due to the increase in outdoor temperatures at night and during the day. As a result, the maximum daily average occupancy of  $SET^*$  for the year is 30.7 °C for the future period and 30.2 °C for the historical period. It can also be seen that the system is well adapted to climate change, particularly by observing the resilience indicator  $\alpha$ , which remains low ( $\alpha < 1$ ), despite taking into account a typical future climate scenario.

Finally, we note that the reduction of internal overheating relative to fan consumption ( $\Delta SETH/C_{fan}$ ) is better for the future period (0.21 °Ch/kWh) than for the historical period (0.11 °Ch/kWh). The trend is similar if we relate the reduction of internal overheating to the volume of water evaporated ( $\Delta SETH/V_w$ ); we observe a 19% increase in this gain between the historical period (10.4 °Ch/L) and the future period (12.4 °Ch/L).

These results indicate that without a system, in both climate scenarios, the building is able to eliminate external thermal stress in the long term. However, this phenomenon is accentuated in the presence of the system. In terms of reducing indoor overheating, the system performs similarly between historical and future climate conditions. However, when this reduction is

related to the system consumption (water and fan), the system performance is better in future climate conditions. The system should be more efficient in the years to come, when outdoor conditions are more important.

#### 4 CONCLUSION

The aim of this study was to assess the ability of a direct adiabatic cooling system integrated into an industrial building, located in a mediterranean climate, to meet the challenges of climate change. The results demonstrated the resilience and efficiency of the system under projected future climate conditions. Analysis of the system behaviour revealed an increase in the operating time of the adiabatic and free-cooling systems to face the increased external heat input, resulting in higher fan energy consumption and higher water consumption. In a future climate, the system adapted to maintain its effectiveness in mitigating indoor overheating compared with historical climate data. Despite an increase in the severity of external thermal conditions, the resilience indicator remained low. Finally, the system performed better under future climate conditions, with a significant reduction in indoor overheating compared with the energy consumption of the fan (+90%) and the volume of water evaporated (+19%).

#### 5 REFERENCES

- ASHRAE. 2013. « ANSI/ASHRAE Standard 55-2013 ».
- Batiweb. 2023. « PAC : un marché en demi-teinte ». Batiweb. 2023. <https://www.batiweb.com/actualites/vie-des-societes/www.batiweb.com>.
- Breteau, Antoine, Patrick Salagnac, Emmanuel Bozonnet, Mathieu Carage, et Jean-Marie Caous. 2022. « Evaluation des performances énergétiques d'un système de rafraîchissement adiabatique intégré au sein d'un bâtiment industriel ». In *Colloque International Franco-Québécois en Energie Ville et Transition face aux défis climatiques et énergétiques*, 164-69. Ville et Transition face aux défis climatiques et énergétiques. Paris, France. <https://hal.archives-ouvertes.fr/hal-03718248>.
- Breteau, Antoine, Patrick Salagnac, Emmanuel Bozonnet, Mathieu Carage, et Jean-Marie Caous. 2023. « Comparaison d'indicateurs dans l'analyse du confort intérieur d'un bâtiment industriel équipé d'un système de rafraîchissement adiabatique direct ». In *31ème Congrès Français de la Société Française de Thermique "Thermique et Agroressources"*, 127. Reims, France: Société Française de Thermique. <https://doi.org/10.25855/SFT2023-127>.
- Chiesa, Giacomo, Nora Huberman, David Pearlmutter, et Mario Grosso. 2017. « Summer Discomfort Reduction by Direct Evaporative Cooling in Southern Mediterranean Areas ». *Energy Procedia*, 8th International Conference on Sustainability in Energy and Buildings, SEB-16, 11-13 September 2016, Turin, Italy, 111 (mars): 588-98. <https://doi.org/10.1016/j.egypro.2017.03.221>.
- Ford, Brian, Nimish Patel, Parul Zaveri, et Mark Hewitt. 1998. « Cooling without Air Conditioning: The Torrent Research Centre, Ahmedabad, India ». *Renewable Energy, Renewable Energy Energy Efficiency, Policy and the Environment*, 15 (1): 177-82. [https://doi.org/10.1016/S0960-1481\(98\)00150-5](https://doi.org/10.1016/S0960-1481(98)00150-5).
- Gagge, A., A. Fobelets, et L. Berglund. 1986. « A standard predictive index of human response to the thermal environment ». *Ashrae Transactions* 92 (1): 709-31.

Hamdy, Mohamed, Salvatore Carlucci, Pieter-Jan Hoes, et Jan L. M. Hensen. 2017. « The Impact of Climate Change on the Overheating Risk in Dwellings—A Dutch Case Study ». *Building and Environment* 122 (septembre): 307-23. <https://doi.org/10.1016/j.buildenv.2017.06.031>.

Kowalski, Piotr, et Dariusz Kwiecień. 2020. « Evaluation of Simple Evaporative Cooling Systems in an Industrial Building in Poland ». *Journal of Building Engineering* 32 (novembre). <https://doi.org/10.1016/j.jobee.2020.101555>.

Machard, Anaïs, Christian Inard, Jean-Marie Alessandrini, Charles Pelé, et Jacques Ribéron. 2020. « A Methodology for Assembling Future Weather Files Including Heatwaves for Building Thermal Simulations from the European Coordinated Regional Downscaling Experiment (Euro-Cordex) Climate Data ». *Energies* 13 (13): 3424. <https://doi.org/10.3390/en13133424>.

Mckenzie, Erica, Theresa Pistochini, Frank Loge, et Mark Modera. 2013. « An investigation of coupling evaporative cooling and decentralized graywater treatment in the residential sector ». *Building and Environment* 68 (octobre): 215-24. <https://doi.org/10.1016/j.buildenv.2013.07.007>.

PROFEEL. 2021. « Les solutions de rafraîchissement adiabatique dans les bâtiments tertiaires en rénovation ». *Profeel* (blog). 2021. <https://programmeprofeel.fr/ressources/guide-les-solutions-de-rafraichissement-adiabatique-dans-les-batiments-tertiaires-en-renovation/>.

PROMEE. 2023. « La climatisation représente 5% des émissions de CO2 du bâtiment ». Promee. 2023. <http://promee.fr/actualites/conseils/la-climatisation-represente-5-des-emissions-de-co2-du-batiment>.

Sahai, Rashmi. 2012. « Addressing Water Consumption of Evaporative Coolers with Greywater », juillet. <https://escholarship.org/uc/item/6gz5q7mx>.

Salamanca, F., M. Georgescu, A. Mahalov, M. Moustou, et M. Wang. 2014. « Anthropogenic Heating of the Urban Environment Due to Air Conditioning ». *Journal of Geophysical Research: Atmospheres* 119 (10): 5949-65. <https://doi.org/10.1002/2013JD021225>.

Watt, John R. 1997. *Evaporative Air Conditioning Handbook*. 3rd ed. Lilburn, GA, Upper Saddle River, NJ: Fairmont Press.

WMO. 2024. « L'OMM confirme que 2023 bat le record mondial de températures ». Organisation Météorologique Mondiale. 12 janvier 2024. <https://wmo.int/fr/media/news/lomm-confirme-que-2023-bat-le-record-mondial-de-temperatures>.

Xuan, Y. M., F. Xiao, X. F. Niu, X. Huang, et S. W. Wang. 2012. « Research and Application of Evaporative Cooling in China: A Review (I) – Research ». *Renewable and Sustainable Energy Reviews* 16 (5): 3535-46. <https://doi.org/10.1016/j.rser.2012.01.052>.

Zare, Sajad, Naser Hasheminejad, Hossein Elahi Shirvan, Rasoul Hemmatjo, Keyvan Sarebanzadeh, et Saeid Ahmadi. 2018. « Comparing Universal Thermal Climate Index (UTCI) with Selected Thermal Indices/Environmental Parameters during 12 Months of the Year ». *Weather and Climate Extremes* 19 (mars): 49-57. <https://doi.org/10.1016/j.wace.2018.01.004>.

Zhang, Chen, Ogun Berk Kazanci, Ronnen Levinson, Per Heiselberg, Bjarne W. Olesen, Giacomo Chiesa, Behzad Sodagar, et al. 2021. « Resilient Cooling Strategies- a Critical Review and Qualitative Assessment ». *Energy and Buildings*, juillet, 111312. <https://doi.org/10.1016/j.enbuild.2021.111312>.

# Experimental and simulation analysis of different natural ventilation scenarios and their relation with IAQ in office buildings

Giannis Papadopoulos<sup>1</sup>, Ioannis Sakellaris<sup>1,2</sup>, Evangelos I. Tolis<sup>1</sup>, John G. Bartzis<sup>1,2</sup>, Giorgos Panaras<sup>1</sup>

*1 Mechanical Engineering Department  
University of Western Macedonia  
50100, Kozani  
Greece*

*\*Corresponding author: gpanaras@uowm.gr*

*2 Atmospheric Chemistry & Innovative Technologies  
Laboratory, Institute of Nuclear & Radiological  
Sciences  
& Technology, Energy & Safety, National Centre for  
Scientific Research “Demokritos”,  
15310 Agia Paraskevi, Attiki, Greece*

## ABSTRACT

Following the pandemic of Covid-19, the scientific interest in ventilation rate of buildings, and especially in spaces with high occupancy, has increased. The creation of a healthy and acceptable internal environment, especially at workplaces is considered necessary, both to deal with the sick building syndrome, or the spread of various diseases, as well as to improve the comfort of employees. In the proposed work, the experimental investigation of the indoor environment in naturally ventilated office buildings, located in Kozani, Western Macedonia, Greece, is presented; the investigation took place during the pandemic period of Covid-19. Measurements include thermal comfort parameters as well as Indoor Air Quality (IAQ) ones. As concern the ventilation of the buildings, the air exchange rates were determined according to the tracer gas decay and equilibrium analysis methods, using CO<sub>2</sub> as tracer gas; simulation analysis using appropriate computational approaches (CONTAM) was also applied. Different scenarios of ventilation, like natural ventilation with open or closed windows and mechanical ventilation, were applied; ventilation rates were assessed, as well as the concentration of chemical compounds like CO<sub>2</sub>. The elaboration of results leads to the formulation of a daily practice concerning the opening of the windows or the operation of the mechanical ventilation system, in order to optimize IAQ, while energy consumption would also be potentially decreased. The proposed approach, combining experimental and computational tools, can be further elaborated, towards the formulation of an integrated methodology, contributing to healthier and more comfortable indoor environment, while energy aspects can also be considered.

## KEYWORDS

IAQ; ventilation rate; office buildings; tracer gas method; CONTAM

## 1 INTRODUCTION

Covid-19 pandemic that we have been experiencing for the last years has led to the revision of the ventilation requirements for the residential buildings, especially as regards building units that show severe overcrowding like offices buildings (Sakellaris et., 2023) or educational facilities (Award et al., 2022). The ANSI/ASHRAE Standard 62.2 (ASHRAE, 2022), as well as the European CEN EN 16798-2 (CEN, 2018), are the most common standards which offer guidance on ventilation airflow rates. There are many factors that can affect indoor air quality (IAQ) like outdoor pollution sources, consumer products, building materials, human activities and ventilation (Baeza Romero et al., 2022). IAQ and generally the indoor environmental quality (IEQ) can influence health, comfort and productivity of the users. Building ventilation is an important parameter, in order to ensure adequate IAQ (WHO, 2010; Awbi, 1998). Ventilation can be provided by natural (passive) or mechanical supply and/or exhaust systems.

Air ventilation rate per hour is used to check the air renewal in a given place (ACH). The recommended minimum amount of fresh air at office buildings is about 8.5 l/s/person (ASHRAE, 2022) according to ASHRAE standard, while for the WHO is 10 l/s/person (WHO, 2010). The most common experimental methods to calculate ACH is the tracer gas and blower-door methods. The first method uses concentrations of gases like carbon dioxide (CO<sub>2</sub>) as tracers to predict the ACH, while the blower door method is a steady-state method, which can be implemented by fan pressurization in a range of pressure differences, usually in steps of 10–60 Pa (ASTM, 2018). On the other hand, the numerical simulation models include multi-zone airflow model, regional model and computational fluid dynamics (CFD) model. Multi-zone airflow model is believed to be the best choice for predicting ventilation performance on the building scale, while CFD model is most widely used to describe the airflow in a zone part with high accuracy (Chen et al., 2010).

In the present work, a theoretical and experimental investigation of ventilation rates at office buildings located in Western Macedonia at the city of Kozani, is presented. The experimental measurements carried out included, among others, the recording of carbon dioxide (CO<sub>2</sub>) concentrations of which can be used to calculate the ventilation rates of the spaces using tracer gas methods. At the same time, simulation of the ventilation was carried out in the multizone simulation program of CONTAM, investigating two natural ventilation scenarios, one with open windows at intervals and the other with closed ones. Then, CO<sub>2</sub> concentrations were calculated for the different simulated scenarios. The main objective of the work is to assess the effectiveness of the combination of experimental and theoretical methods, with an emphasis on naturally ventilated buildings, where the ventilation rate varies dynamically. The ability to accurately estimate indoor ventilation will contribute to formulating solutions to improve air quality, while avoiding uncontrolled energy consumption due to the consequent increase in heating and cooling loads brought by ventilation.

## **2 METHODOLOGY**

### **2.1 Description of the investigated buildings**

The buildings under investigation refer to three different natural ventilated office buildings, located at Kozani, Greece. The first is the building of the Research Committee of the University of Western Macedonia (Building I). The second one is the building of the Municipal Enterprise for Water Supply and Sewerage (Building II), while the third one is the building hosting the local tax authority (Building III). The climate of Kozani is characterized as the coldest one, regarding Greece (Kozani is ranked on D climate zone according to the Greek version of the EPBD (TEE, 2010)), because of its location and altitude (710m); rainfall is generally moderate, summers are mild and snowfall is frequent in the winter months. The occurring meteorological parameters during the campaign, have been obtained from a meteorological station installed for the scope of the research.

### **2.2 Experimental measurement set-up**

The monitoring period took place during winter period of 2022, when the Pandemic Period of Covid-19 still existed. The investigation per building lasted five days, from Monday morning to Friday afternoon. The measurement campaign was based on ISO 7726 (ISO, 2001) and ANSI/ASHRAE Standard 55 (ANSI/ASHRAE, 2023). Sensors that can record air temperature, relative humidity and CO<sub>2</sub> were used. The above parameters were measured at a height of 1.1 m, based on the recommendations of ISO 7726 (ISO, 2001). Special care was taken in order to

ensure that the instruments would not disturb any class activities. The time interval for all the environmental parameters are about 1-min (ISO, 2001). The characteristics of the installed instruments are presented in Table 1.

Table 1: Measuring quantity, instrument indication

Measuring Quantity	Instrument Type	Accuracy	Range
T-RH-C <sub>co2</sub>	Hobo Onset MX1102A	±0.21°C (T), ±2% (RH), ±50ppm (CO <sub>2</sub> )	0-50 °C (T), 1-95% (RH), 0-5000ppm (C <sub>co2</sub> )
T-RH-C <sub>co2</sub>	Hobo Onset U12-012	±0.5°C (T), ±5% (RH), ±50ppm (CO <sub>2</sub> )	-20 to 70 °C (T), 5-95% (RH), 0-2500ppm (C <sub>co2</sub> )
T-RH-C <sub>co2</sub>	Hobo Onset Talaire 7001	±0.5°C (T), ±5% (RH), ±50ppm (CO <sub>2</sub> )	-20 to 70 °C (T), 5-95% (RH), 0-5000ppm (C <sub>co2</sub> )
Wind Speed	Gill Instruments 3D Anemometer	±1.5% RMS	0-50m/s (u)
T-RH	DeltaOhm Hygrotransmitter HD9009TR	±0.5°C (T), ±5% (RH),	-40 to 80°C (T), 0-100% (RH)
Wind Speed	Thies CLIMA 4.3515.30.000	±0.5m/s (u)	0.5-40 m/s (u)
Wind Direction	Thies CLIMA 4.3127.40.000	±4°	0-360°

### 2.3 Tracer gas methods

For the estimation of the ventilation rate of the offices, the tracer gas approach is used (ASTM, 2018) as mentioned before. The steady-state or equilibrium method can be used when the concentration of the tracer gas becomes constant during the occupancy period. Since this method is a single zone method, it can only be used to estimate ventilation rate on a building with a uniform CO<sub>2</sub> concentration. On the other hand, decay or step-down methods can be used when a space is vacated after occupancy, or if there is a stepwise decrease in occupancy. The estimation of ventilation rate is made measuring the rate of the reduction of the tracer gas concentration over a certain period. Below are presented the equations of both models:

$$Q_S = \frac{10^6 G}{C_{in} - C_{out}} \quad (1)$$

where: Q<sub>S</sub>: Ventilation rate of the space [L/s], G: CO<sub>2</sub> generation rate [L/s], C<sub>in</sub>: Steady-state concentration CO<sub>2</sub> in the zone [ppm], C<sub>out</sub>: Outdoor CO<sub>2</sub> concentration [ppm]

$$Q_D = \frac{V}{\Delta t} \ln \left( \frac{C_1 - C_{out}}{C_0 - C_{out}} \right) \quad (2)$$

where: Q<sub>D</sub>: Ventilation rate of the space [L/s], V: Volume of the space [m<sup>3</sup>], C<sub>1</sub>: Maximum CO<sub>2</sub> concentration in decay period Δt [ppm], C<sub>0</sub>: Minimum CO<sub>2</sub> concentration in decay period Δt [ppm], C<sub>out</sub>: Outdoor CO<sub>2</sub> concentration [ppm], Δt: Time period [hours]

### 2.4 Simulation program

Contam is a multizone network software developed from the university of National Institute of Standards and Technology (Dolis and Polidoro, 2020). Contam can be used to calculate the ventilation rates of the building, taking advantage of the pressure differences observed between the zones of the building, as well as the external environment. In this way, it is possible to determine the air changes, but also the variation of the ventilation rate as a function of time. At the same time, the software can perform calculations regarding the concentration of pollutants inside the buildings, both due to external or internal sources. The steps of the simulation analysis are the following: firstly the design of the pseudo-geometry of the building with the inside zones is inserted; in figure 1 the case for Building I is presented. Then flow paths like



windows, doors or cracks that connect each zone together or with the outdoor environment are created. Weather data are also necessary for the simulations, as CONTAM calculates the airflows between rooms (and outdoor), by taking into account the wind pressure on the building envelope through the use of pressure coefficients with wind velocity and direction; these are the air pathways (Picard et al., 2022). The needed meteorological data were taken from the meteorological station used in the measurement campaign, while the pressure coefficients were taken from the Air Infiltration and Ventilation Center (AIVC) database (Orme et al., 1998).

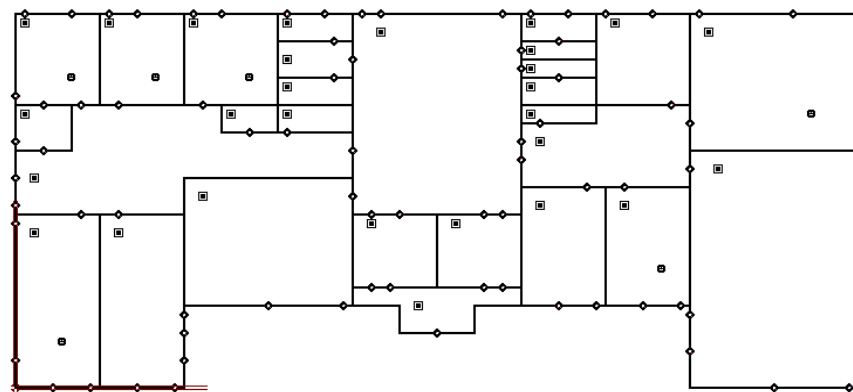


Figure 1: Pseudo-geometry of Building I

### 3 RESULTS/DISCUSSION

In this section, the ventilation rates determined using the experimental data with the tracer gas models, in comparison with the ventilation rates calculated by simulating them in the Contam computer program, for all three buildings, are presented. Following on, the CO<sub>2</sub> concentrations resulting from the experimental data, and from the CONTAM analysis, are presented.

#### 3.1 Ventilation rates

In the following table (table 2), the measurement days per building are presented, as well as the number of offices for which CO<sub>2</sub> concentration was analysed. It is important to note that the ventilation frequency of the offices differed not only from building to building, but also from office to office. The users in all the examined buildings did not follow a specific program of ventilation, both in terms of time and ventilation method, i.e. number of open windows/percentage of opening), noting that this creates difficulties in the exact calculation of the ventilation rate using the experimental data. At the same time, the experimental method using tracer gas method applied for the assessment of ventilation is presented.

Table 2: Measurement campaign information

Column Title	Time of /measurement campaign	Number of offices	Tracer gas method
Building I	31/01/2022-03/02/2022	4	Decay
Building II	12/04/2022-19/04/2022	3	Decay/Steady-state
Building III	24/01/2022-27/01/2022	4	Decay

Figure 2 presents the ventilation rate ( $\text{h}^{-1}$ ) for the first building (I), as it was determined according to the tracer gas methods (steady-state or decay), while also calculated on the basis of the simulation program (CONTAM). The decay method was implemented on a period when the users left from the offices. and  $\text{CO}_2$  generation equals zero; the calculation of ventilation rate with Contam for this case was performed for the same time period.

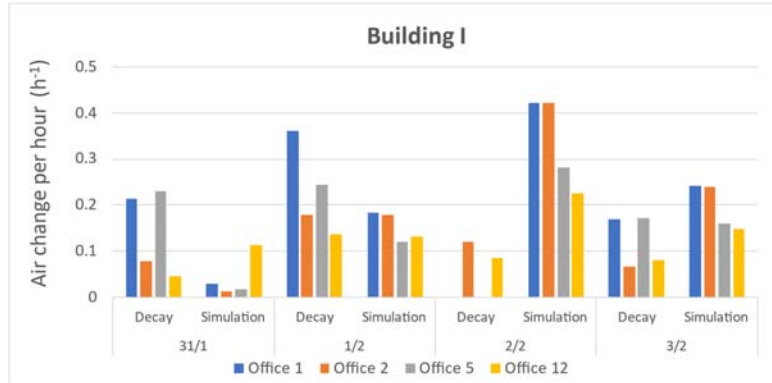


Figure 2: Ventilation rates of Building I

The absence of values at 2/2 for the decay method in Figure 2, is related to a problem in the measurement instrument. As it can be seen, in several cases the ventilation values of the decay method and the simulation present some deviation, , as for example on 1/31. This may be due to the meteorological data used to run the simulations or the selection of flowpaths and schedules entered into the software. From the results on 31/1 and 1/2, it is notable that the decay method gives higher ventilation rates compared to the simulation, in contrast to 2/2 & 3/2, where higher values of air changes per hour are observed according to Contam results. Nevertheless, on an overall assessment, the ventilation rate for each office is relatively small, i.e. less than  $0.5\text{h}^{-1}$ .

In the figures below (Figures 3 and 4), the ventilation rate calculated with the steady state model for the period 12/4 to 15/4 is presented, noting that conditions allowed the adoption of this model, while for the period 18/4 to 19/4, the decay method was implemented. Both results are compared with the simulation ones.

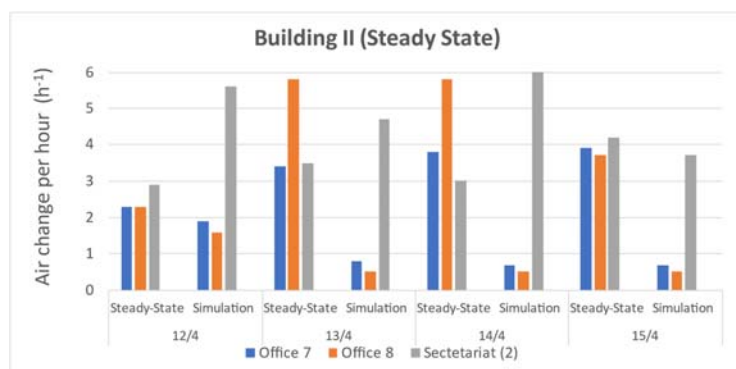


Figure 3: Ventilation rate for Building II (steady state method)

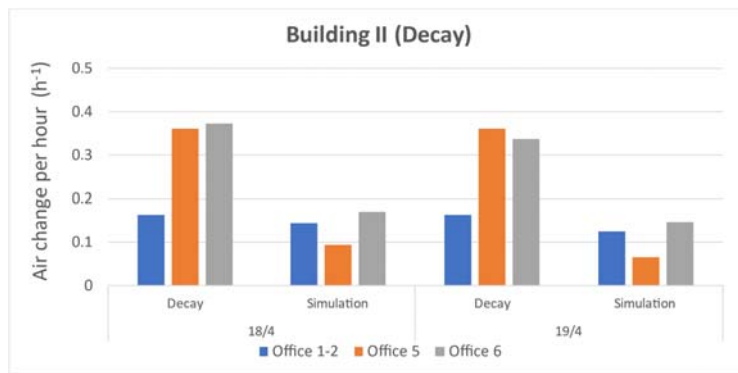


Figure 4: Ventilation rate for Building II (decay method)

The differences between the experimental and simulation results, regarding the ventilation rate estimation, are higher for the case of steady state, in comparison with the case of the decay method. This can be partly attributed to the fact that the time intervals selected for open windows, at the simulation runs, are different from the actual ones (referring to the steady-state method), as the good outdoor conditions give the opportunity to the users to open the windows for more time. On the other hand, during the measurement period of 18/4 and 19/4, the employees opened the windows of the offices for a shorter period of time as the external conditions were not very acceptable (low outside temperatures); this allowed the implementation of the decay method instead.

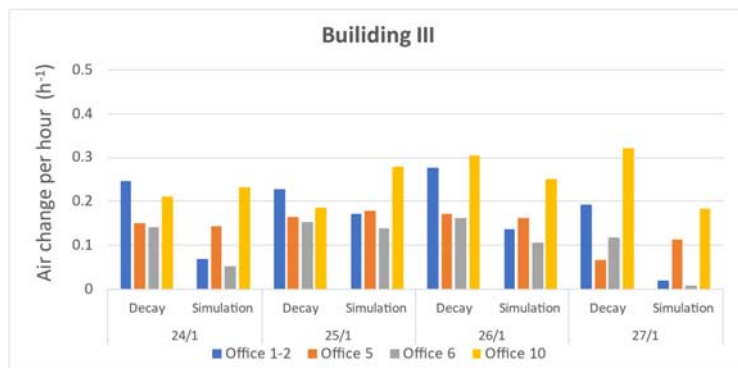


Figure 5: Ventilation rate for Building III (decay method)

Figure 5 presents the ventilation rates for Building III. The values are comparable between the simulation and experimental approach, with the main discrepancies to appear at offices 1&2, as well as office 6. On an overall assessment for all investigated buildings, the infiltration rates are similar and lower than  $0.5 \text{ h}^{-1}$ .

### 3.2 CO<sub>2</sub> concentration scenarios

Below are presented the CO<sub>2</sub> concentration diagrams for all buildings, as these are obtained from the experimental measurements, as well as from the simulation with the CONTAM software. The simulation scenarios included the business-as-usual scenario, referring to the conditions of the experimental analysis (scenario 1), an increased ventilation rate scenario, referring to the windows being opened at specific periods of the day (scenario 2), as well as a scenario with closed windows during the working hours (scenario 3); in table 3, specific characteristics of the experimental and simulation scenarios are summarized.

Table 3: Characteristics of experimental and simulation scenarios

<b>Scenario 1</b>	Experimental measurement of CO <sub>2</sub> using Hobo sensors (black color)
<b>Scenario 2</b>	Simulation results with open windows during some specific periods of working days: 9.00 – 9.15 a.m., 11.00 – 11.15 p.m. και 13.00 – 13.15 p.m. (green color)
<b>Scenario 3</b>	Simulation results with closed windows during working hours (yellow color)

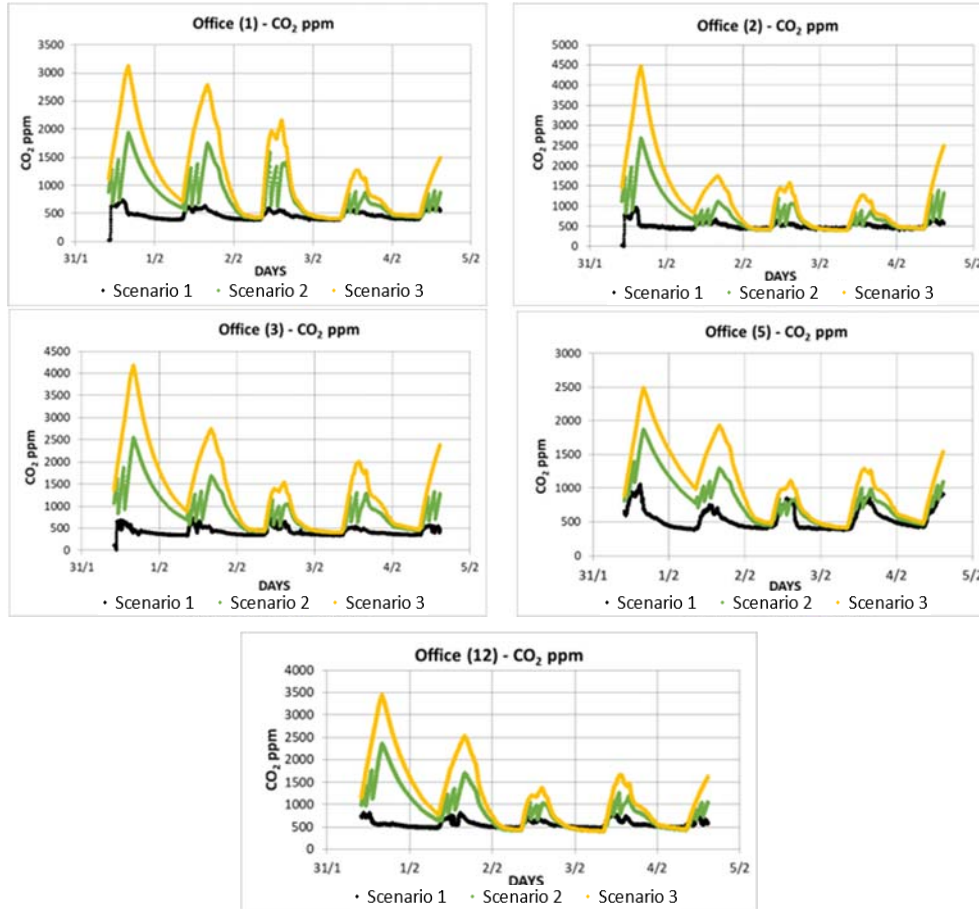


Figure 6: CO<sub>2</sub> concentration for experimental measurements and simulation scenarios for Building I

According to Figure 6, in all the offices of Building I it is notable that the actual CO<sub>2</sub> concentrations (scenario 1) are clearly lower than those obtained from the simulation (scenarios 2 & 3). The highest concentrations are shown in scenario 3, as the windows were closed, so CO<sub>2</sub> levels are expected to be considerably higher. Regarding scenario 2, the time program (schedule) for opening the windows that was selected was indicative, not representing the actual time that they were open. In general, the windows seem to open more hours for the actual case, as demonstrated by the results of scenario 1; this was also discussed above. In the time period 31/1 – 2/2 simulation included more people in the schedule of Contam, with regard to the actual case, leading to higher CO<sub>2</sub> concentration values for scenarios 2 and 3. Despite the discrepancies discussed above, one should note that for all scenarios the CO<sub>2</sub> concentration presets similar behavior; i.e. a gradual increase, after the users join their offices, accompanied by a decrease by the end of the working schedule.

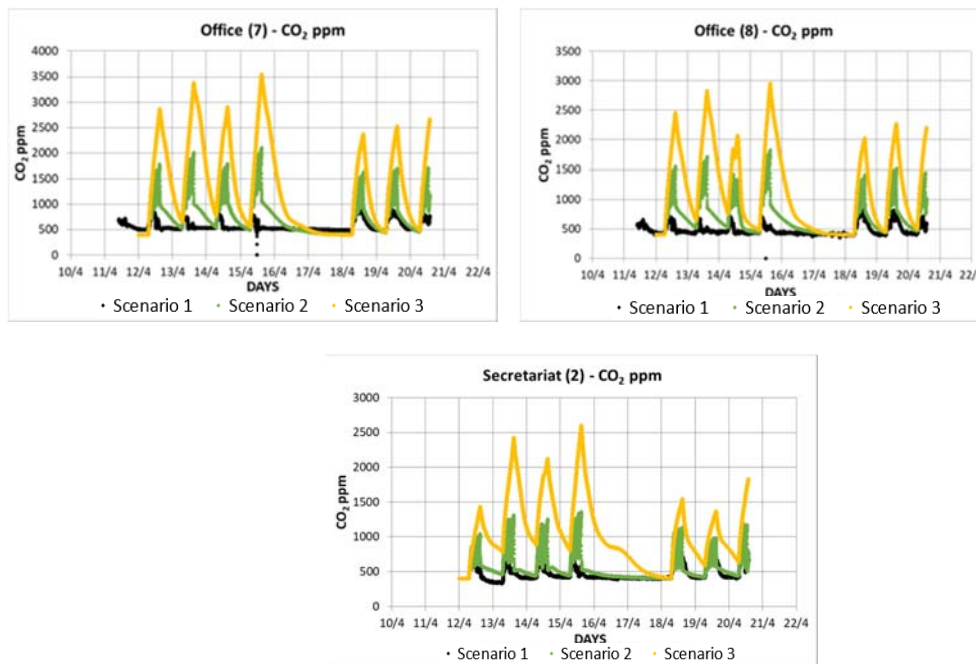


Figure 7: CO<sub>2</sub> concentration for experimental measurements and simulation scenarios for Building II

Similarly, in the case of Building II (figure 7), the CO<sub>2</sub> levels in scenario 1 are considerably lower than those in scenarios 2 and 3. The actual values of the experimental measurements are at low levels, as there was increased mobility of the employees during the day and many of them were absent from the workplaces. This mobility was difficult to be reflected at the schedule input of Contam, so the CO<sub>2</sub> concentration for scenarios 2 and 3 is higher. In addition, the open office spaces, as is the case of Building 2, lead to lower CO<sub>2</sub> concentrations (Sakellaris et al.,2023). Furthermore, the indicated differences in the CO<sub>2</sub> concentration, for scenarios 1 and 2, even on a qualitative basis, as indicated by the relevant curves in figure 7, can also be attributed to the meteorological data used in the simulation, since these were rather incomplete. Despite the indicated differences, the gradual increase in concentration from the arrival to the departure of the employees, is also observed for Building 2 for all scenarios. By the end of the working schedule, CO<sub>2</sub> concentration seems to exceed the indicated limits (ASHRAE, 2022) for scenarios 2 and 3.

Regarding Building III, and similar to the other buildings, the CO<sub>2</sub> concentration is higher for the scenario 3 since the windows are closed (figure 8). In offices 1-2, 5 and 6 it is notable that scenarios 1 and 2 are generally identical, as people remained in their desks for longer period, and the opening of the windows seems to have taken place according to the prescribed schedule. Finally, especially regarding Office 10, the CO<sub>2</sub> concentration is quite high, being in

considerable agreement with scenario 3, demonstrating that the windows at this office are mostly closed.

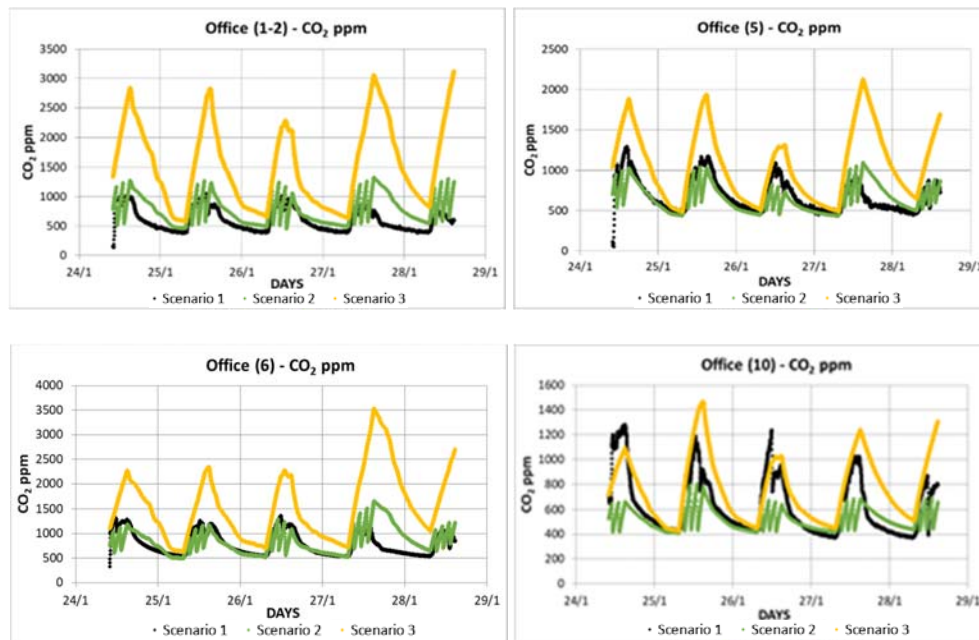


Figure 8: CO<sub>2</sub> concentration for experimental measurements and simulation scenarios for Building III

#### 4 CONCLUSIONS

The proposed work aims at presenting the potential of combined use of experimental and simulation approaches, towards the assessment of IAQ and ventilation rates for burdened indoor air cases, as the offices ones, during the Covid-19 pandemic.

The results demonstrated that the current situation is satisfactory for all buildings, while at the same time there is intention for reducing the ventilation rate, which will lead to a potential reduction in energy consumption to maintain thermal comfort conditions. The application of the experimental methods showed that ventilation rate lies within expected levels, as far as infiltration is concerned, while CO<sub>2</sub> concentration is in line with the relevant limits. The uncertainties of experimental analysis are related to the accuracy of the measuring instruments, the estimation of the actual number of people inside the spaces and, mainly, the varying ventilation program of the spaces.

The results of the simulation investigation showed that the air exchanges fluctuate at normal levels and similar to the experimental results, while the CO<sub>2</sub> levels are proportional to the ventilation scenarios. As mentioned, the simulation method can be used for the approximate evaluation of the existing conditions during measurement campaign, but also for the investigation of different ventilation scenarios, so that interventions can be made to improve it. The uncertainties of this method are significant and varied, especially when investigating naturally ventilated buildings. Characteristics of the openings of the building, the meteorological data used for the simulations, the number of people inside the offices are critical parameters of uncertainties. The proposed analysis aimed at the demonstration and evaluation of experimental and simulation methods, towards the integration of the selected solutions into a single approach, in order to overcome any uncertainties arising from each method separately. Future work will systematically address the development of an integrated methodology for the assessment of IAQ and ventilation rates in buildings of various uses, utilizing the experience

and results gained by this work, while also extending its applicability towards the consideration of energy aspects.

## 5 ACKNOWLEDGEMENTS

The authors of this work would like to thank the employees in all three buildings for their collaboration throughout the measuring campaign.

## 6 REFERENCES

ANSI/ASHRAE Standard 62.2-2022. Ventilation and Acceptable Indoor Air Quality in Residential Buildings, ASHRAE, Atlanta, Georgia.

ASTM D6245 (2018). Standard guide for using indoor carbon dioxide concentrations to evaluate indoor air quality and ventilation. United States: ASTM International

Awada, M., Becerik-Gerber, B., White, E., Hoque, S., O'Neill, Z., Pedrielli, G., Wen, J., Wu, T., (2022). Occupant health in buildings: Impact of the COVID-19 pandemic on the opinions of building professionals and implications on research. *Building and Environment* 207, 108440.

Baeza\_Romero, M.T., Dudzinska, M.R., Amouei Torkmahalleh, M., Barros, N., Coggins, A.M., Ruzgar, D.G., Kildsgaard, I., Naseri, M., Rong, L., Saffell, J., Scutaru, A.M., Staszowska, A., 2022. A review of critical residential buildings parameters and activities when investigating indoor air quality and pollutants. *Indoor Air* 32. <https://doi.org/10.1111/ina.13144>

Cheng, H., Norbäck, D., Zhang, H., Yang, L., Li, B., Zhang, Y., Zhao, Z., Deng, Q., Huang, C., Yang, X., Lu, C., Qian, H., Wang, T., Zhang, L., Yu, W., Wang, J., Zhang, X., (2024). Home environment exposure and sick building syndrome (SBS) symptoms among adults in southern China: Health associations in 2010 and 2019. *Building and Environment* 248, 111061.

ISO 7726. (2001). Ergonomics of the thermal environment—Instruments for measuring physical quantities, International Standardization Organization, Brussels.

Kumar, P., (2022). CO<sub>2</sub> exposure, ventilation, thermal comfort and health risks in low-income home kitchens of twelve global cities. *Journal of Building Engineering*.

Miranda, M.T., Romero, P., Valero-Amaro, V., Arranz, J.I., Montero, I., (2022). Ventilation conditions and their influence on thermal comfort in examination classrooms in times of COVID-19. A case study in a Spanish area with Mediterranean climate. *International Journal of Hygiene and Environmental Health* 240, 113910.

Sakellaris, I., Papadopoulos, G., Saraga, D., Xenofontos, T., Tolis, E., Panaras, G., Bartzis, J., 2023. Air Quality Versus Perceived Comfort and Health in Office Buildings at Western Macedonia Area, Greece during the Pandemic Period. *Applied Sciences* 13, 1137. <https://doi.org/10.3390/app13021137>

World Health Organization, (2010). WHO Guidelines for Indoor Air Quality: Selected Pollutants. Copenhagen Ø, Denmark.

# Assessing the level of adaptation to heat waves in Parisian housing

Letizia Roccamena<sup>\*1</sup>, Jean-Marie Alessandrini<sup>1</sup>, Pierrick Gervasi<sup>1</sup>, Julien Guilhot<sup>1</sup>, Georgios Kyriakodis<sup>1</sup>, Simon Molesin<sup>2</sup>, Maeva Sabre<sup>1</sup>, Wenjuan Wei<sup>1</sup>

*1 Centre Scientifique et Technique du Bâtiment (CSTB)  
84 Av. Jean Jaurès,  
77420, Champs-sur-Marne, France*

*2 Régie Immobilière de la Ville de Paris (RIVP)  
13, Av. de la Porte d'Italie,  
75621, Paris CEDEX 13, France*

*\*Corresponding author: letizia.roccamena@cstb.fr*

## ABSTRACT

The paper introduces an approach for assessing the resilience of buildings to both current heat waves and their recurrence in the future under the impact of climate change. The method, applied to the 60,000 dwellings of the RIVP (Régie Immobilière de la Ville de Paris), the second-largest social landlord in Paris, aims to provide reliable information to enable the buildings' owner to assess the heat-related health risk for the tenants and the actions to be taken to decrease it. To this end, it provides them with a quantifiable indicator, the probability of risk occurrence, to enable them to decide which adaptation pathways are suitable based on a cost-benefit balance.

Upon defining the study's scope, the method defines faultless performance criteria for dwellings, set here at operative temperatures below 27°C and 30°C at night-time and daytime respectively. Subsequently, it identifies the climatic sequences that make the dwellings faulty and finally quantifies their recurrence across present, near-future (2040), and distant-future (2080) scenarios.

By applying the method, dwellings are classified into three categories based on the number of times the climatic sequences that deteriorate the apartments' thermal performance are exceeded over a given period: those in which these boundary conditions are exceeded once every ten years or less, less than once a year, and more than once a year.

In addition to this classification, the study highlights the substantial benefits of thermal insulation and window solar protection and emphasizes the critical importance of opening windows at night to reduce indoor temperature. Despite the significant impact of employing passive solutions, the results indicate that maintaining nighttime temperature thresholds remains challenging due to difficulties in heat evacuation exacerbated by rising outdoor temperatures caused by global warming. Looking ahead, this method may find application in diverse contexts and urban settings.

## KEYWORDS

Social housing, Climate change, Resilience assessment, Refurbishment

## 1 INTRODUCTION

Under the altered oceanic climate characteristic of Paris, the presence of warm days and cool nights historically maintained a moderate indoor thermal environment in dwellings obviating the need for air conditioning systems. Over the last two decades, the combined effect of climate change and the urban heat island (UHI), has increasingly strained the efficacy of night ventilation to maintain indoor thermal comfort in Parisian dwellings (Daniel et al., 2018). While installing air conditioning systems within residential dwellings may be an effective solution amidst the escalating frequency of heatwaves, it is important to consider that this system is highly energy-consuming, emits greenhouse gases, contributing to the heating of the outside environment, particularly in densely populated areas (Tremeac et al., 2012).



In the context of social housing, landlords are faced with the challenge of wanting to protect the health of their dwellings' occupants in the face of climate change, without systematically resorting to the installation of air conditioning systems.

Recognizing the protective capacity of the building stock as a prerequisite, the challenge is to provide these owners with the necessary information to assess the effectiveness of climate change adaptation of their building stock. In cases where adaptation levels prove insufficient, refurbishment measures can be devised. Evaluating these actions under current and future climates enables building owners to establish adaptation pathways and minimize cooling requirements over time and space.

To address this objective, the reliability of dwellings is assessed based on three points:

1. Establishing the limits of the thermal environment that must not be exceeded to ensure fault-free operation.
2. Identifying the climatic conditions that must not be surpassed to comply with the operating limits.
3. Determining the probability of exceeding these climatic thresholds.

This paper presents the method developed as part of a study carried out in collaboration with the RIVP (Régie Immobilière de la Ville de Paris), the second-largest social landlord in Paris, and subsequently applies it to the RIVP building stock, both in its current state and post-refurbishment. This process involves calculating criteria and thresholds for fault-free operation (1), defining alert conditions for each dwelling (2), and determining their probability of occurrence (3) under the current climate, as well as projections for the 2040 and 2080 horizons.

## 2 METHOD

The risk is a danger whose occurrence is more or less predictable. Risk analysis involves defining the hazard and quantifying the probability of it occurring. To build an adaptation pathway for their dwellings, the building owners need to assess the risk using quantifiable criteria. The definition and method to calculate it were constructed in close collaboration between the stakeholders in a five-step method introduced afterward.

### 2.1 Description and quantification of comfort and health risk criteria

In an ideal indoor thermal environment, occupants' health and safety are preserved. To define the limits of this "flawless" thermal environment, we aim to identify the maximum indoor temperature and relative humidity (RH) values, known as "heat stress", that meet this requirement. Heat stress can be predicted by carefully selecting indicators and the related thresholds. Indicators must be understandable by stakeholders and easily measurable, while related threshold(s) must be set according to the action to be taken if it is exceeded and the time required to implement it. A margin for the threshold must therefore be provided to ensure that the risk does not become a danger.

Given the varying levels of sensitivity to heat among different population groups (such as disabled persons, the elderly, infants, pregnant women, athletes, etc.) (Alessandrini et al., 2018; Brücker, 2003), the selection of indicators and thresholds follows a structured approach:

1. Definition of the target population based on the priorities outlined by the building owner.
2. Identification of indicators and their thresholds in official literature (regulations or recommendation guides).
3. Calculation of the faultless thermal environment for the target population. A body thermo-physiological template is used to calculate the heat stress limits for the heat

strain indicator (the core temperature) at the threshold for which human health is not affected (Alessandrini et al., 2022).

4. Selection of the indicator to describe the heat stress aligning with the preferences of the building owner.
5. Realisation of a sensitivity analysis of the heat stress indicator to the thermo-physical characteristics of the environment to set its threshold (Alessandrini et al., 2023).

## 2.2 Buildings and dwellings sampling

The heat stress is assessed for a homogeneous indoor environment. Assuming its environment is homogeneous, the dwelling is the spatial scale chosen in this study. To streamline the study, a building typology is built. Then, for each typical building, the dwellings to be studied are sampled.

The typology is the result of a compromise between two objectives:

1. To retain the representative buildings according to the building owner,
2. To select the buildings most exposed to heat.

Once the representative buildings are selected, for each of them the flat sampling is realised according to the same logic:

- Selection of the most common flat in size, number of rooms, and floor (“typical” dwelling);
- Selection of the flat most exposed to heat (“vulnerable” dwelling).

The aim is to simulate their thermal behaviour with an hourly timestep and assessing their climate change adaptation level at different time horizons. In addition, a refurbishment program made of a combination of common passive technical solutions for the envelope is defined with the building owner for all dwellings.

## 2.3 Selection of climatic sequences

The process of identifying climatic conditions that must not be surpassed to comply with the dwellings’ operating limits, and determining the probability of exceeding these thresholds consists of three steps:

1. Selection of past heatwaves based on their correlation with estimated excess mortality during summertime.
2. Characterization of each sequence in terms of duration and intensity.
3. Selection of the hottest sequences based on the calculation of a criterion for each sequence (e.g. daily minimum temperature averaged over its duration).

## 2.4 Running required conditions

The required conditions are determined by the activity inside the building (internal conditions) and the climate (external conditions).

The occupancy scenario is established to maintain a good balance between:

- The most heat-protective conditions of use;
- Recommendations easily accessible to as many people as possible, so that the landlord can spread them to tenants to encourage them to adopt protective measures.

The required climate conditions are selected thanks to a sensitive study. The thermal behaviour of each flat modeled at §2.2 is simulated using the previously selected climatic sequences (see §2.3). For each flat, the climatic sequence defined as the outside limit required condition, is the one that leads to exceeding during more than a given time (defined based on the building

owner's requirements) the heat stress threshold. The outside limit required conditions are defined for each dwelling in its current state and after refurbishment.

Therefore, depending on whether or not a climate sequence leads to compliance with the previously established indoor exposure thresholds (outlined in §2.1), the functional or dysfunctional perimeter of the dwelling is defined.

### **2.5 Risk analysis (Calculation of occurrence probability)**

The following steps are followed to carry out the risk analysis:

1. The characteristic criterion (see §2.3) of each climatic sequence selected as the running required conditions for a given dwelling (as explained in §2.4), is calculated for current, near-future, and distant-future climates.
2. For a given period (present, near future, and distant future) the criterion values previously calculated are ranked in ascending order.
3. The probability of each climatic sequence being exceeded (according to the criterion previously defined) for the present, near future, and distant future is quantified.

As a result, the number of times the flat under study malfunctions is known for each given period. Based on this probability of occurrence, the building owner can assess the vulnerability to heat of each dwelling in the present, the near future, and the distant future. Depending on the results obtained with the renovation measures, they can identify the most suitable option for guaranteeing the health of the occupants.

## **3 RESULTS**

The method described hereinabove was applied to the 60000 dwellings of the RIVP. The results obtained for each phase of the method are illustrated in the following paragraphs.

### **3.1 Definition of the health risk thresholds**

In this study, the fault-free operating limit was defined by an operating temperature of 27°C at night (from 10 PM to 7 AM) and 30°C during the day.

This threshold was defined based on:

- World Health Organization (WHO) recommendations (not to exceed a thermometer temperature - equivalent to air temperature - of 24°C at night and 32°C during the day) (WHO, 2018)
- the use of a thermophysiological model (Kurazumi, 2008), which compares the thermal stress (characteristics of the indoor environment) and thermal strain (core temperature).

The daytime threshold of 32°C proposed by the WHO has been lowered to an operative temperature of 30°C to take account of the sensitivity of the elderly. Indeed, with an air temperature of 32°C, their body temperature exceeded 38°C, the maximum threshold tolerated for health reasons. Even with an air speed of 0.4 m/s, obtained using a fan, for example, the threshold is exceeded under the RH of 50%.

The nighttime threshold of 27°C for the operative temperature is the weighted average of wall and air temperatures. Considering that the 30°C daily threshold is not exceeded during the day, the wall temperature is supposed to be at the maximum of 30°C at 10 PM, while the air temperature is set at 24°C, the WHO night threshold.

The results of our thermophysiological study show that an operating temperature of 27°C causes a sharp rise in occupants' body temperature (close to 38°C) with an air velocity of 0,1 m/s and a RH of 60% (Alessandrini et al., 2023).

After several exchanges with the RIVP, the number of hours during each day/night that these health risk thresholds (30°C during the day and 27°C at night) are exceeded was chosen as the heat stress indicator. To avoid short breaks, it was decided to consider as indicative only the exceedances that last at least 5 hours during the heatwave.

### 3.2 Dwellings selection

Many buildings' characteristics depend on their periods of construction, such as the level of thermal insulation of the opaque and transparent envelope, the type of envelope and its geometric characteristics, the efficiency of the technological systems, etc. (Mutani et al. 2020). This is the information used to subdivide the RIVP building stock into five categories:

1. Buildings constructed between 1851 and 1917
2. Buildings constructed between 1918 and 1955
3. Buildings constructed between 1960 and 1974
4. Buildings constructed between 1975 and 1999
5. Buildings constructed after 2000

The choice of a representative building for each of these categories was made following two actions:

1. A satisfaction questionnaire was sent to all the buildings' caretakers, to understand which buildings had the worst behaviour in the summertime based on the percentage of dissatisfied occupants.
2. A discussion was held with RIVP to ask them which of the less-performing buildings was the most representative and the most deserving to be used as a 'type' building.

The chosen buildings are shown in Figure 1.



Figure 1 - Typology of RIVP buildings and selected buildings

It is important to note that the period 1955-1960 is a transition period for which it is difficult to give a clear "construction profile". Therefore a gap period does exist between 1955 and 1960, for which we are not proposing any standard buildings.

Once the buildings had been identified, two dwelling samples had to be selected for each building to be used for the modelling phase. The selection was based on two criteria: representativeness (criterion for choosing the "typical" dwelling) and exposure to heat in summer (criterion for choosing the "vulnerable" dwelling).

Typical dwellings were always those that were the most representative of the building in terms of size (two-bedroom flats), always at the intermediate level. The selection of vulnerable dwellings was more complex, but in general, the dwellings most exposed to heat are those on the top floor, small, with a single orientation, and that are not floor-through. The dwellings selected cannot cover all the dwellings in the stock; our objective was rather to cover three-quarters of the situations.

For each dwelling, several packages of passive solutions (different thicknesses and types of internal/external thermal insulation, installation of solar protection) were studied, based on their intrinsic characteristics. These packages of solutions were evaluated to find the optimum solution for each type of dwelling in terms of thermal performance (see §3.4).

### 3.3 Selection of climatic sequences

The climate data collected by the weather station located in the heart of Paris in a park called Montsouris in the summer period from 1981 to 2019 and the number of deaths caused by the heatwaves over the same period (reported by Santé Publique France, the French national public health agency) were analysed to select 8 summers that have had the most deadly impact (see table below).

For each of these summers, the daily minimal temperatures were ranked in descending order. Considering the number of consecutive hottest nights, 12 climatic sequences lasting from 3 to 12 successive days with a minimum temperature of 18.7°C to 21.2°C averaged over their duration, were selected as the hottest sequences. The minimum daily temperature averaged over the duration of each sequence represents the criterion used for characterizing it.

### 3.4 Implementation of required conditions

A realistic occupancy scenario was defined by determining repetitive behaviours that could be easily performed by the occupants (concerning the windows opening and the use of solar protection) and analysed the impact of this scenario on the thermal performance of all the dwellings by carrying out a numerical simulation campaign utilizing the COMETH simulation engine (Alessandrini et al., 2019; Mazza et al., 2017). In this model, the air change rate is calculated according to the EN 15242 airflow model through large openings (AFNOR, 2007). For each of them, the operative internal temperature was calculated during the 12 previously selected climatic sequences (see §3.3). The studied occupancy scenario considered all the windows of the dwelling to be open every night at 10 PM and keep them open all night until 7 AM (according to WHO recommendations), and the use of solar protection throughout the day, keeping 80% of glazed surfaces occluded. If this scenario is not applied, the dwellings' operating limits would be permanently exceeded, as the windows opening has a crucial role in heat evacuation.

To define the outside limit required conditions, a numerical simulation campaign was carried out, to check the thermal behaviour of each dwelling in the face of the 12 previously selected climatic sequences (see §3.3) in order to find which one would lead to the threshold for the previously selected indicator (see §3.1) being exceeded.

After carrying out many simulations of the dwellings' thermal behavior, it was noted that when the daytime thresholds are exceeded, the night-time thresholds are systematically exceeded, whereas the reverse is not true. Considering, moreover, that during the day people are less isolated and have more freedom of action (going out, looking for air-conditioned places, etc.), the criterion for defining fault-free operation has been set at a maximum of five hours above 27°C during the heatwave.

Each dwelling was tested in its current state and after applying different packages of refurbishment solutions. The impact of applying passive solution packages was assessed to find the 'optimal' refurbishment package for each type of dwelling, enabling the number of heatwave sequences in which it fails to perform to be reduced.

### 3.5 Risk analysis

Once the outside limit required conditions defined for each dwelling, these sequences were analyzed and ranked in ascending order according to their characteristic criterion defined in §3.3. In the second step, the number of times they appeared or were exceeded in the time series of data observed from 1981 to 2019 at the Paris Montsouris station was calculated. Since many of the outside limit required conditions were common to several dwellings, only five out of the twelve climatic sequences obtained in §3.3 were retained.

The results are summarized in the table below:

Table 1 - Analysis of climatic sequences and frequency of exceedances

Sequence	Initial occurrence	Duration (in days)	Mean minimum temperature (in °C)	Number of times the sequence has been equaled/exceeded between 1983 and 2019
1983 - 2	26/07 to 28/07/1983	3	19,6	23
2006 - 1	03/07 to 05/07/2006	3	18,7	44
2015 - 1	01/07 to 04/07/2015	4	20,6	4
2017 - 1	20/06 to 22/06/2017	3	19,9	13
2017 - 2	06/07 to 09/07/2017	4	18,8	30

For example, as can be noted, the sequence “2015-1”, characterised by a duration of 4 days and an average minimum temperature of 20.6°C, was equaled/exceeded 4 times during the 39 summers spanning from 1983 and 2019.

The same analysis applied to the observed data was carried out on the modeled data of the summers between 2020 and 2058 (near future horizon) and between 2059 and 2097 (distant future horizon). These climate models were obtained using the RCP8.5 scenario and 9 models of the Eurocordex database debiased using the CDF-t method (Michelangeli et al., 2009; Vrac et al., 2012). The near future climate results indicate that the number of times the 12 sequences are exceeded increases. For example, the above-mentioned sequence “2015-1” was equaled or even exceeded from 15 to 60 times (depending on which of the 9 models from the Eurocordex was used), during the 39 summers. The results for the distant future indicate an explosion in the number of excesses, whichever model is considered. In this horizon, the “2015-1” sequence was equaled or even exceeded from 37 to 172 times, during the 39 summers.

Based on this information, we were able to create a table (Table 2) that can inform the building owner of the probability that the occupants of each of the dwellings (in its current state and after applying the 'optimal' refurbishment package of solutions) enter into the health risk zone currently, in the near future, and in the distant future for each of the studied climatic sequence, by reporting the number of times this will happen.

Table 2 - Number of times each type of dwelling exceeds its outside limit required conditions in the present, near future, and distant future

	Outside limit required conditions				
	2006 - 1	2017 - 1	2015 - 1	1983 - 2	2017 - 2
<b>Type and period of construction of the dwellings becoming faulty</b>	“Vulnerable” dwellings before refurbishment: – before 1918 – 1918-1955 – 1960-1974 – 1975-1999 “Vulnerable” dwellings after refurbishment: – 1918-1955	“Typical” dwellings before refurbishment: – 1918-1955 – 1960-1974 “Vulnerable” dwellings after refurbishment: – 1960-1974 “Vulnerable” dwelling built after 2000	“Typical” dwellings after refurbishment: – before 1918 – 1918-1955 – 1960-1974 – 1975-1999 “Typical” dwelling built after 2000	“Typical” dwelling before refurbishment: – Before 1918	“Vulnerable” dwellings after refurbishment: – before 1918 – 1975-1999
<b>Number of times the climatic sequences are exceeded in the present</b>	More than once a year	Once every 3 years	Once every 10 years	Once every 2 years	More than once every 2 years
<b>Number of times the climatic sequences are exceeded in the near future</b>	More than twice a year	More than 4 times every 7 years	More than 4 times every 10 years	More than once a year	More than once a year
<b>Number of times the climatic sequences are exceeded in the distant future</b>	More than three times a year	Twice a year or more	Once a year or more	More than twice a year	More than twice a year

Using a color code, dwellings were classified into three categories based on the number of times their outside limit required conditions are exceeded in the present, near future, and distant future: those in which these boundary conditions are exceeded once every ten years or less are indicated in green, those in which it occurs less than once a year in yellow, and those in which it occurs once a year or more in red.

#### 4 DISCUSSION

In order to identify the dwellings' criteria with the greatest impact on the results, the characteristics of the dwellings constituting the 5 groups were analyzed. The results are summarised in the table below:

Table 3 - Characteristics of the 5 groups of dwellings sharing the same outside limit required conditions

Outside limit required conditions	2006 - 1	2017 - 1	2015 - 1	1983 - 2	2017 - 2
U value (in W/m <sup>2</sup> K) of the external walls	0,37 to 3,1	0,21 to 3,1	0,18 to 0,36	3,2	0,14 to 0,18
U value (in W/m <sup>2</sup> K) of the roof	0,3 to 3,6	0,16 to 0,22	-	-	0,13 to 0,16
Thermal capacity (in kJ/m <sup>2</sup> K) calculated according to ISO 13786 (AFNOR, 2017) for a period of 1 day and 14 days respectively	266 to 793; 348 to 864	383 to 849; 384 to 1212	434 to 662; 511 to 734	571; 656	419 to 434; 473 to 665
% of the glazed surface compared to the floor area	13 to 23	15 to 24	14 to 23	23	13 to 17

The risk analysis showed that not all the refurbished “vulnerable” dwellings share the same outside limit required condition (Table 2) even if they have similar heat gains (due to a similar U value obtained for the external walls/roof) and inertia. The differences in the results are essentially explained by the impact of the natural ventilation airflow, proportional to the size of their windows, which is a key factor in adaptation.

Concerning the refurbished “typical” dwellings, it was noted that at present, their limit climatic sequence is exceeded once every ten years. The validation of this adaptation score, the highest obtained in our study, is the responsibility of the building owner.

For non-renovated “vulnerable” dwellings, the outside limit required conditions were not found, as all the studied climatic sequences, starting from the less intense (2006-1), made them faulty throughout their duration. According to the more optimistic climatic model, the 2006-1 will be exceeded at least twice a year in the near future and three times a year in the distant one. A building should be usable during these episodes, especially given their frequency; this would require the use of an indicator capable of quantifying comfort, considering even lower operating thresholds, and not only health risk.

## 5 CONCLUSION

In this paper, an approach for assessing the resilience of buildings to both current heat waves and their recurrence in the future under the impact of climate change is described, as well as the results obtained applying it to the 60000 dwellings of the second-largest social landlord in Paris, the RIVP.

To succeed, the method developed requires close collaboration with the building owner, who must validate the key information that will be used to select reliable adaptation pathways and risk prevention plans:

- The thermal environment thresholds that must not be exceeded to ensure fault-free operation, adapted to the target population.
- The indicator that defines the outside limit required conditions that lead to exceeding during more than a given time the heat stress threshold.
- The level of adaptation required, set by the probability of occurrence or the return time of the hazard, in this case, the limiting climatic sequence.

For the housing stock studied, the size of the windows and the thermal insulation of the roofs are key elements in improving dwellings’ level of adaptation. For the dwellings located on an intermediate floor and floor-through (“typical” dwellings), thermal insulation of the walls, integration of solar protection, and instructions on opening windows at night provide sufficient protection from hazards with an occurrence factor of 1/10. In the future, the level of protection will deteriorate, with operating limits being exceeded every two years, or even every year by 2080; this implies that the level of adaptation of these dwellings must be improved, considering cooling solutions primarily for bedrooms at night to preserve sleep quality, an essential condition for the occupants’ health.

For the top-floor dwellings, in light of the results obtained in the present climate, the application of these solutions should already be taken into account.

To improve health risk prevention, the night-time threshold should be revisited in the future, with studies of the impact of heat on sleep and health. This work might be also complemented by an analysis of the urban ecosystem, where the urban heat island and nuisances, particularly noise pollution, associated with the density and diversity of activities, act as barriers to the dissipation of heat through ventilation.

To conclude, it is important to consider that the results of this work are based on simulations and would deserve to be corroborated by experimental work. Nevertheless, the major trends outlined here and the relative analysis, comparing one situation to another, make it possible to identify priority dwellings and the actions to be taken, and to open up new perspectives.

In future endeavors, this method holds promise for application across various contexts and urban environments.

## 6. ACKNOWLEDGEMENTS

The work described in this paper was supported by the French Agency for Environment and Energy Management (ADEME).



## 7. REFERENCES

- AFNOR (2007). EN 15242, NF EN Ventilation for buildings. Calculation methods for the determination of air flow rates in buildings including infiltration.
- AFNOR (2017). ISO 13786, NF EN Thermal performance of building components — Dynamic thermal characteristics — Calculation methods.
- Alessandrini, J.-M., Ribéron, J., Da Silva, D. (2019). Will naturally ventilated dwellings remain safe during heatwaves? *Energy & Buildings*, 183, 407-417.
- Alessandrini, J.-M., Wei, W., El Kadri, M., Molesin, S., Dominati, T., Ribéron, J., Pelé, C., Mandin, C. (2022). Evaluation of heat stress effect on health in dwellings using thermo-physiological model. *17th International Conference of the International Society of Indoor Air Quality & Climate*, Kuopio (Finland), 12-16/06/2022.
- Alessandrini, J.-M., Wei, W., Molesin, S., Dominati, T., Pelé, C., El Kadri, M., Sabre, M. (2023). Selection of thresholds to prevent heat-related health risks. *18th Healthy Buildings Europe Conference*, Aachen (Germany), 11-14/06/2023.
- Brücker, G. (2003). Impact sanitaire de la vague de chaleur d'août 2003 : premiers résultats et travaux à mener. *BEH – Bulletin épidémiologique hebdomadaire*, n°45-46.
- Daniel, M., Lemonsu, A., Vigié, V. (2017). Role of watering practices in large-scale urban planning strategies to face the heat-wave risk in future climate. *Urban Climate*, 23, 287-308.
- Kurazumi, Y., Tsuchikawa, T., Ishii, J., Fukagawa, K., Yamato, Y., Matsubara, N. (2008). Radiative and convective heat transfer coefficients of the human body in natural convection. *Building and Environment*, 43(12), 2142–2153.
- Mazza, D., El Asmi, E., Robert, S., Zreik, K., Hilaire, B. (2019). A versatile and extensible solution to the integration of BIM and energy simulation. *eWork and eBusiness in Architecture, Engineering and Construction - Proceedings of the 11th European Conference on Product and Process Modelling, ECPPM 2016, Limassol (Cyprus)*.
- Michelangeli, P.-A., Vrac, M., Loukos, H. (2009). Probabilistic downscaling approaches: Application to wind cumulative distribution functions. *Geophysical Research Letters*, 36, L11708.
- Mutani, G., Gabrielli, C., Nuvoli, G. (2020). Energy Performance Certificates Analysis in Piedmont Region (IT). A New Oil Field Never Exploited Has Been Discovered. *TECNICA ITALIANA-Italian Journal of Engineering Science*, 64, n°1, 71-82.
- Tremeac, B., Bousquet, P., de Munck, C., Pigeon, G., Masson, V., Marchadier, C., Merchat, M., Poeuf, P., Meunier, F. (2012). Influence of air conditioning management on heat island in Paris air street temperatures. *Applied Energy*, 95, 102-110.
- Vrac, M., Drobinski, P., Merlo, A., Herrmann, M., Lavaysse, C., Li, L., Somot, S. (2012). Dynamical and statistical downscaling of the French Mediterranean climate: uncertainty assessment. *Natural Hazards and Earth System Sciences*, 12, 2769-2784.

# Air Pressure Differences over the Building Envelope: Case Studies

Lara Deprez<sup>1</sup>, Kevin Verniers<sup>\*2</sup>, Ivan Pollet<sup>2</sup>, Niek-Jan Bink<sup>3</sup>, Jelle Laverge<sup>1</sup>

*1 Ghent University, Department of Architecture and  
Urban Planning  
Campus UFO T4, St-Pietersnieuwstraat 41  
Ghent, Belgium*

*2 Renson NV  
Maalbeekstraat 10  
Waregem, Belgium  
\*Corresponding author: kevin.verniers@renson.be*

*3 ACIN Instrumenten BV  
Handelskade 76  
Rijswijk, The Netherlands*

## ABSTRACT

Although the physics concerning air pressures in buildings don't differ between countries, often different reference values of the pressure difference over the envelope are used to determine air tightness and ventilation characteristics. The air transfer devices for natural ventilation, integrated in the façades or the internal building structure, are characterized at a pressure difference between 1 and 20 Pa depending on the country. For example, Belgium uses 2 or 10 Pa as a reference, the Netherlands adopts 1 Pa, whereas France applies 10 or 20 Pa. With respect to the building air tightness, the reference pressure used varies between 4 and 50 Pa over the countries.

To investigate this variability, differential air pressure measurements over the envelopes of two buildings were conducted within the context of a master's thesis. A Belgian single-family home and a high-rise student home were considered. The most elaborated case was the single-family home consisting of 2 floors and a flat roof where the following experiments took place. Firstly, the airtightness of the building envelope was determined based on three different test methods: a) the Blowerdoor test, b) the ACIN Air Tightness Tester or ATT, and c) the Pulse test. Secondly, simultaneous air pressure difference measurements were applied on all four walls of the home and at two different heights: floor and upper level. Lastly, wind speed sensors were attached in the middle of the exterior walls for measuring the wind speed near the wall surface. These measurements allowed (1) to compare the difference in measured building air tightness between the 3 test methods; (2) to analyse the variation of the pressure difference over the façades as a function of climate conditions; (3) to study the correlation between the local wind speed and the local pressure difference over the façade. For the high-rise building, only the measurements of air pressure difference and wind speed were conducted. These measurements were taken at the same façade at two different heights of the building. The results were compared with those found on the single-family house. An overview of the work done, used methodologies, and obtained results is presented in this paper.

## KEYWORDS

Air pressure difference, air tightness, single-family home, high-rise building

## 1 INTRODUCTION

The air pressure difference across the building envelope is affected by indoor and outdoor air conditions that vary over time. This complicates the design of ventilation systems consisting of natural air transfer devices. Therefore, a reference value for the air pressure difference is adopted. However, countries do not necessarily use the same value. For example, Belgium uses 2 or 10 Pa (NBN, 1991; VEKA, 2021), the Netherlands adopt 1 Pa (NEN, 2001), whereas France considers 10 or 20 Pa (AFNOR, 2017; Effinergie, 2010). Next to this, an

effective ventilation system requires a good building air tightness, which is characterized also at a certain reference pressure. Again, there is no agreement on the used value, some countries adopt 4 Pa while others go up to 50 Pa (Buildwise, 2015).

A master's thesis was conducted due to diverse reference values. The paper includes: Section 2 detailing the measurements and buildings; Section 3 discussing differential pressure measurements and air tightness methods; and Section 4 summarizing the findings.

## 2 METHODOLOGY

### 2.1 Examined building types

Figure 1 presents two buildings: a two-storey single-family home and a 14-storey high-rise student home. The entire single-family home was accessible for the measurements. In contrast, the student home had only two available rooms on the 1<sup>st</sup> and 10<sup>th</sup> floors, both located on the same north-east oriented façade of the building. The single-family home has mechanical extract ventilation, which was at its lowest setting (about 35 m<sup>3</sup>/h) during the measurements. For the student home, only natural ventilation is available.



Figure 1: The single-family home (left) and the high-rise student home (right) considered in this study.

### 2.2 Measurement setup: building air tightness

The air tightness of the single-family home was assessed using the three methods listed below. All vents and windows were closed, but interior doors were left open. The ventilation system was turned off, except for the second method.

1. Blowerdoor test (BlowerDoor, 2024): This common test measures air tightness in units of 50 Pa. The home is subjected to both underpressure and overpressure conditions using a fan in an external door opening. The measurements are averaged to estimate the air leakage through the building envelope.
2. ACIN Air Tightness Tester or ATT (ACIN Instruments, 2024): This test uses an indoor located vessel with a differential pressure sensor. After the vessel is acclimatized, the ventilation system is turned on and off, and pressure variations in the vessel are monitored. After several cycles, the result is calculated and presented at the desired reference pressure.
3. Pulse test (Build test solutions, 2024): This test uses a small container filled with compressed air. One or more pulses are discharged to pressurize the building to 4 Pa. The building's air tightness is determined from the pressure drop and airflow measurements over time. This test is recognized in the UK.

### 2.3 Measurement setup: air pressure difference and wind sensors

The SDP810-125Pa (Sensirion, 2024) differential pressure sensor based on a thermal sensing element was used and located indoors. A flexible tube connected this sensor to a perforated sphere catching the wind. In addition, wind speed near the wall was measured using Adafruit's Anemometer (Adafruit, 2024), which can record wind speeds up to 70 m/s. The sensor data was collected using the Espressif ESP32-DevKitC (Espressif, 2024), which has Wi-Fi and Bluetooth. The data was sent to the Cloud and simultaneously saved on an SD card. To synchronize timestamps, each ESP32 device used the Network Time Protocol. A one-second sampling period was targeted due to the rapid changes of the wind.

In the single-family home, wall pressure differences were measured at the floor and upper levels of the four façades. Flexible tubes connecting the sensors to the corresponding perforated spheres ran through the trickle vents where they were present. All window vents were fully open. For the sake of consistency, the same tube length of 10 meters with an outside diameter of 6 mm was used for all measurements, since the properties of the tube affect the output of the sensor. Wind speed close to the wall was measured only at the floor level. Figure 2 shows part of the setup. Roof sensors measured wind speed and direction.

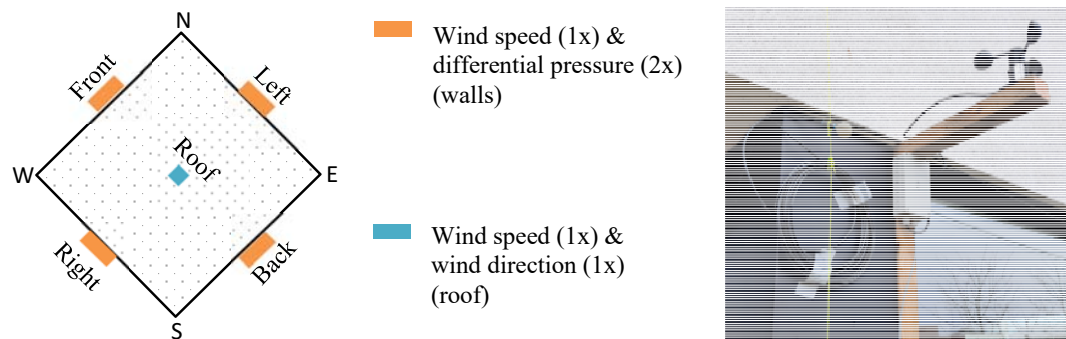


Figure 2: Left: sensor distribution in the single-family home (left). Right: illustration of the wind speed sensor and the perforated sphere (floor level) connected by a tube to a differential pressure sensor located indoors.

In the two rooms of the high-rise building, the same differential pressure sensor and wind speed sensor were mounted on a wooden plate in the window frame. The outer diameter of the tube remained unchanged, but the length was reduced to 0.5 meters. Figure 3 shows the setup on the 1<sup>st</sup> and 10<sup>th</sup> floors of the 14-story building.



Figure 3: Measurement setup on the 1<sup>st</sup> (left) and 10<sup>th</sup> (right) floors of the high-rise building.

In this paper, overpressure is the case where the pressure across the outer wall is greater on the outside than on the inside, while underpressure represents the opposite.

### 3 RESULTS AND DISCUSSION

#### 3.1 Air tightness measurements in the single-family home

Table 1 shows air leakage rates at both 50 and 4 Pa for the three air tightness methods under consideration, along with the corresponding  $n_{50}$  values. The converted air leakage rates, which are highlighted in italics, were derived using the Power Law for the Blowerdoor and ATT results. For the Pulse test, a specific formula was used to convert from 4 to 50 Pa (Build test solutions, 2021). Both the ATT and Pulse test were performed multiple times to check consistency between results.

The 2023 Blowerdoor test had a higher air leakage rate of about 35% compared to the 2019 test. The  $n_{50}$  value increased from 1.7 to 2.3  $\text{h}^{-1}$ , possibly due to changes in the façades over past four years affecting its air tightness, as was also observed in other studies. The decreased flow exponent also reveals an increase of envelope cracks over time. The measured  $n_{50}$  value is a common value for new Flemish dwellings.

The ATT was combined with the house's mechanical extract ventilation system that depressurized the house. Measurements at the same location were nearly identical. Compared to the 2023 Blowerdoor test, the results of the ATT were similar or up to 12% higher when using the standard flow exponent of 0.66 of the ATT. When this exponent is adjusted to that of the Blowerdoor test, the ATT results were close to or about 10% lower than the Blowerdoor results (second rows for ATT in Table 1).

The Pulse test results at 50 Pa were higher, with deviations up to 30% compared to the 2023 Blowerdoor result. This could be due to the extrapolation formula used and potential inaccuracies from the used Pulse device that had already undergone several repairs.

For the 4 Pa results, similar deviations were observed between the Pulse and Blowerdoor tests. These deviations also occur compared to the ATT results, except that the ATT results were now barely higher than those of the Blowerdoor test.

Table 1:  $n_{50}$  and air leakage rates at 50 and 4 Pa for three air tightness test methods. Converted values in italics.

Air tightness test method	Flow exponent $n$	Air leakage rate [ $\text{m}^3/\text{h}$ ]		$n_{50}$ [ $1/\text{h}$ ]
		50 Pa	4 Pa	
<b>Blowerdoor (under- &amp; overpressure)</b>				
2019: underpressure	0.690	965	<i>169</i>	1.6
2019: overpressure	0.780	978	<i>136</i>	1.7
2019: average	0.735	972	<i>153</i>	1.7
2023: underpressure	0.615	1314	<i>278</i>	2.2
2023: overpressure	0.671	1333	<i>245</i>	2.3
2023: average	0.643	1324	<i>262</i>	2.3
<b>ATT (underpressure): 2023</b>				
Test 1 downstairs: $q_{\text{extract}} = 326 \text{ m}^3/\text{h}$ ; $\Delta p = 5.1 \text{ Pa}$	0.660	<i>1471</i>	<i>278</i>	2.5
	0.615	<i>1327</i>	<i>281</i>	2.3
Test 2 downstairs: $q_{\text{extract}} = 326 \text{ m}^3/\text{h}$ ; $\Delta p = 5.2 \text{ Pa}$	0.660	<i>1452</i>	<i>274</i>	2.5
	0.615	<i>1311</i>	<i>277</i>	2.2
Test 3 upstairs: $q_{\text{extract}} = 326 \text{ m}^3/\text{h}$ ; $\Delta p = 6.1 \text{ Pa}$	0.660	<i>1307</i>	<i>247</i>	2.2
	0.615	<i>1189</i>	<i>252</i>	2.0
Test 4 upstairs: $q_{\text{extract}} = 326 \text{ m}^3/\text{h}$ ; $\Delta p = 6.0 \text{ Pa}$	0.660	<i>1321</i>	<i>249</i>	2.3
	0.615	<i>1201</i>	<i>254</i>	2.0
<b>Pulse (overpressure): 2024</b>				
Test 1: downstairs		<i>1450</i>	265	2.5
Test 2: downstairs		<i>1712</i>	317	2.9
Test 3: downstairs		<i>1676</i>	310	2.9

### 3.2 Differential pressure and wind speeds

The properties of the tube affect the readings of the differential pressure sensor (Sensirion, 2016). To calibrate, the output of the sensor was compared to a calibrated Setra Model 267, ranging from -100 to 100 Pa. Tube length in both cases was 0.5 or 10 meters, with a consistent outer diameter of 6 mm. Figure 4 shows a linear relationship in differential pressures between the sensors. The sensor used overestimates for 0.5 m and underestimates for 10 m. Regression line equations from Figure 4 are used to correct this. The 10 m equation is used for the single-family home, and the 0.5 m equation for the high-rise student home.

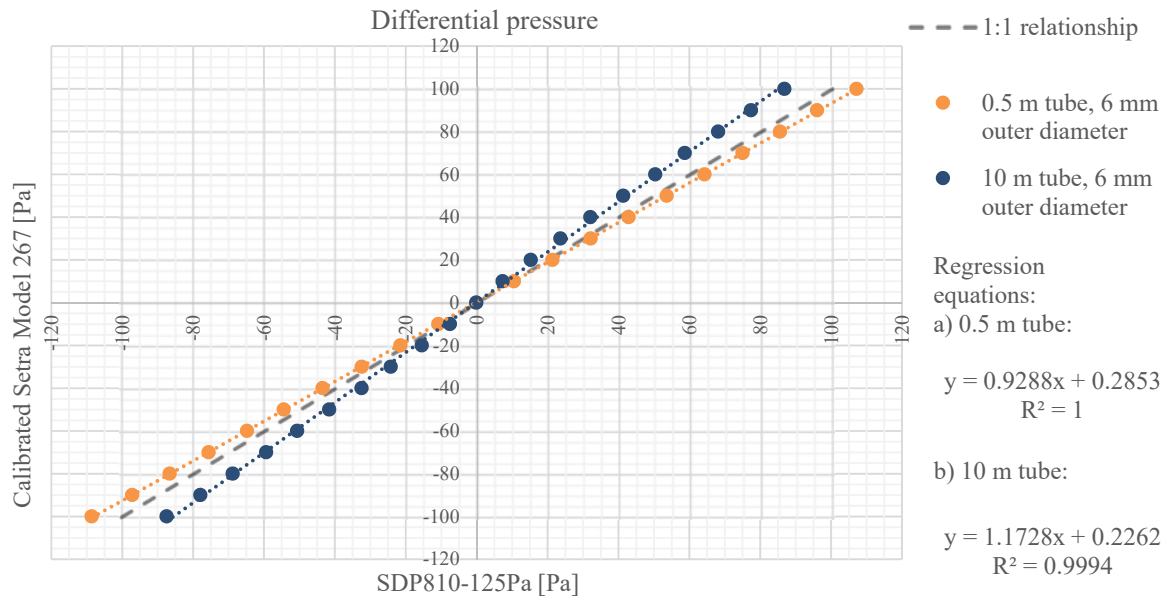


Figure 4: Relationship between a Setra Model 267 and a SDP810-125Pa with a 6 mm tube of 0.5 or 10 m length.

From January 17 to February 9, 2024, measurements were taken in the single-family home, and from March 7 to April 10, 2024, in the high-rise building. The time distribution between over- and underpressure conditions at each point is shown in Figure 5. In the high-rise building, the 1<sup>st</sup> floor façade experienced overpressure 90% of the time, dropping to nearly 50% on the 10<sup>th</sup> floor. The façade was mainly exposed to the leeward side, so the underpressure at the top was higher. Also the stack effect will slightly contribute. A similar trend was observed in the single-family home with the mechanical extract ventilation operating at 10% of its nominal rate (about 35 m<sup>3</sup>/h), with the upper level being in overpressure for less time than the floor level. Pressure varied between the façades due to wind effects. The south-west and south-east walls had predominantly positive pressure differences. In contrast, on the north-east and north-west upper levels, the pressure differences were mostly negative.

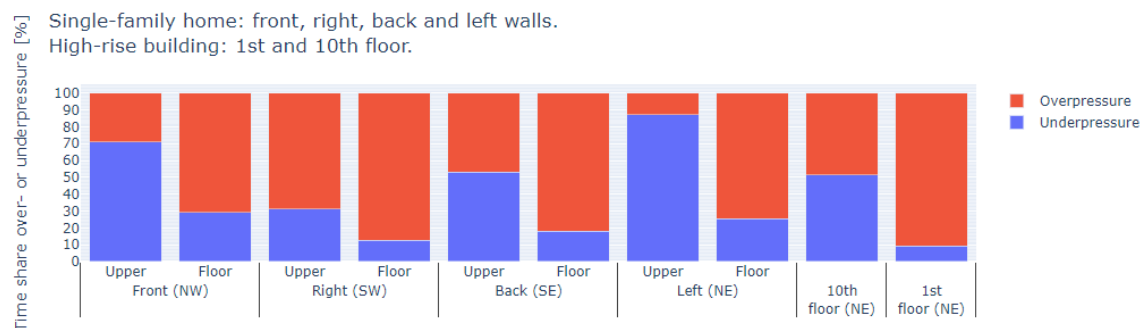


Figure 5: Time distribution between over- and underpressure conditions at each measurement point.

Figure 6 shows the Cumulative Distribution Functions (CDFs) of all pressure differences. The top graph illustrates the overpressure CDFs, while the bottom graph presents the absolute underpressure CDFs of both buildings.

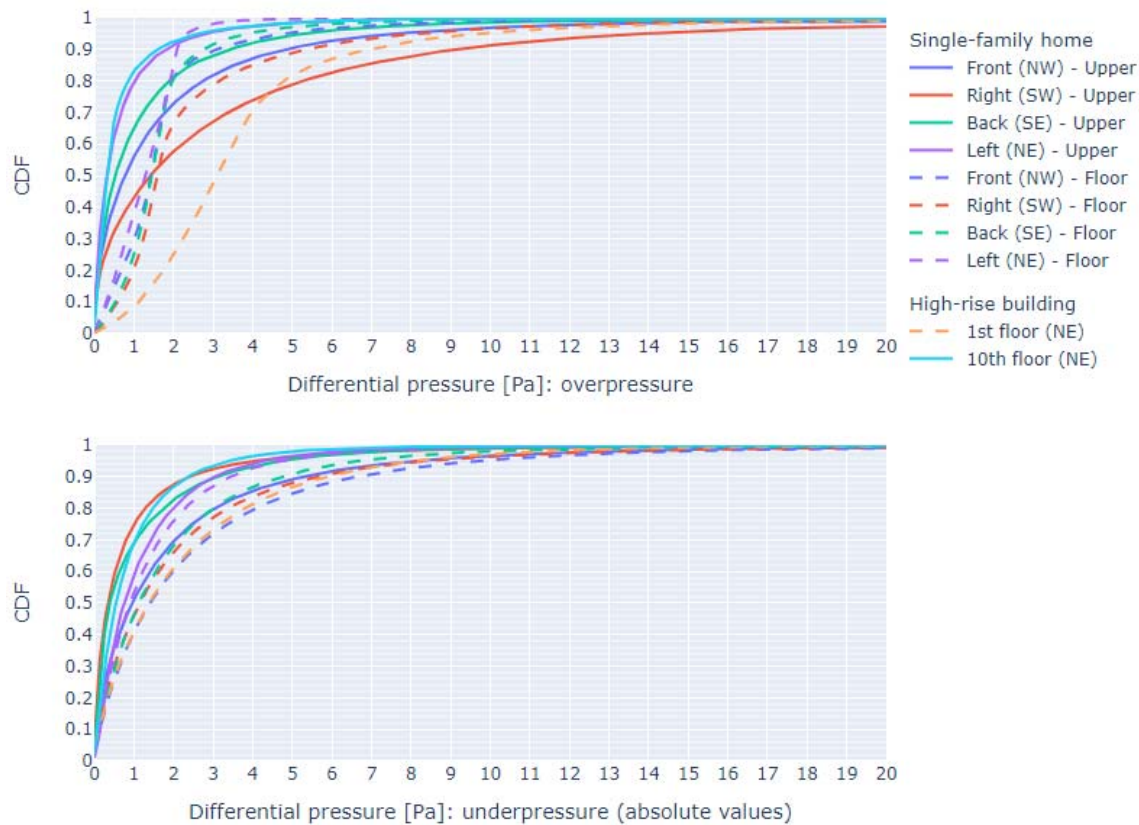


Figure 6: Cumulative distribution functions (CDFs) of the pressure differences across the façades of the single-family home and the high-rise building.

For the high-rise building, the overpressure CDF rises clearly faster at low pressure on the 10<sup>th</sup> floor than the 1<sup>st</sup>. Moreover, the 1<sup>st</sup> floor's CDF has an S-shape and is shifted to the right, illustrating the high positive pressure offset at the bottom of the façade, due to wind and stack effects. The P50 values are 0.3 and 3.1 Pa for the 10<sup>th</sup> and 1<sup>st</sup> floors, respectively. The underpressure CDF for 10<sup>th</sup> floor is again steeper than the 1<sup>st</sup>'s. Unlike overpressure CDFs, the 10<sup>th</sup> floors increase is less distinct, while the 1<sup>st</sup> floor's increase is more pronounced but without S-shape. The P50 values for underpressure are 0.5 and 1.4 Pa for the 10<sup>th</sup> and 1<sup>st</sup> floors, respectively.

For the single-family home, the overpressure CDFs at pressures below 1 Pa rise clearly slower at the floor level than the upper levels, likely due to the stack effect and wind effects. Between 1 and 2 Pa, the upper level's CDFs fall below the floor levels', possibly due to wind effects. At floor level, also an S-shape was observed in the overpressure CDF at all façades. The south-west wall shows the slowest increase in both levels, indicating higher overpressures. As a consequence, the opposite north-east façade experienced the lowest overpressures. The P50 values for the south-west wall are 1.4 and 1.6 Pa for the upper and floor levels, respectively, while its 0.3 and 1.3 Pa for the north-east wall.

The underpressure CDFs for the single-family home reveal that the floor level values surpass the upper levels. Examining the façades, the north-west has the least increase at both levels,

with P50 values of 1.4 and 1 Pa. The north-east wall shows a moderate and similar increase at the upper level and the floor level, with P50 values of 0.8 and 0.9 Pa. The south-east wall has the second-highest increase at both levels, with P50 values of 0.3 and 1.1 Pa. The south-west wall exhibits the highest increase at the upper level but a moderate rise at the floor level, with P50 values of 0.4 and 1.2 Pa. These variations could be due to wind effects.

Figure 7 shows the relationship between wind speeds near the walls and façade pressure differences, represented by boxplots for both over- and underpressure. The wind speeds are categorized according to the Beaufort scale.

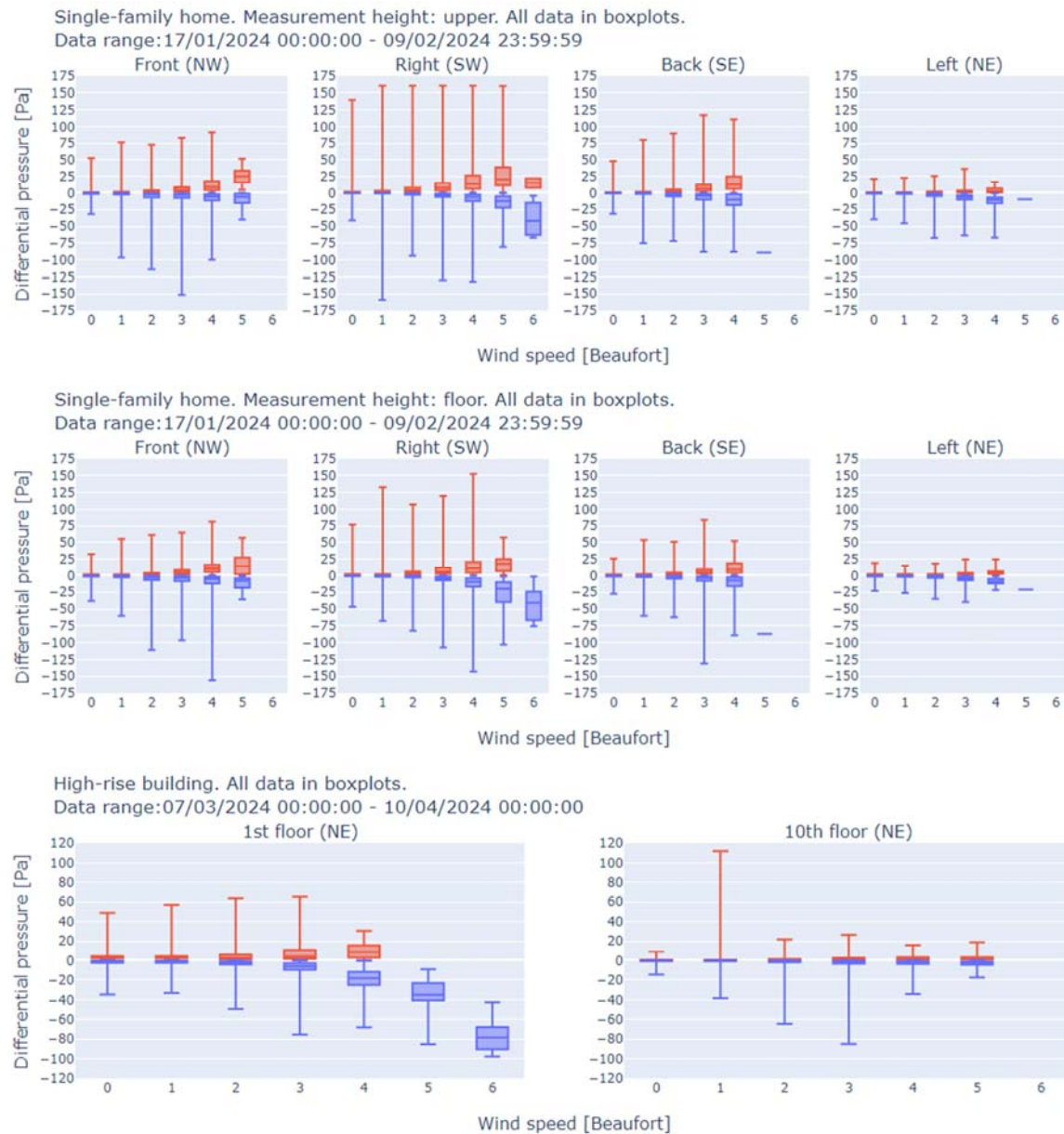


Figure 7: Boxplots of positive and negative median differential pressures as a function of median wind speed, classified by the Beaufort scale. All data points included in boxplots.

The boxplots reveal a substantial variation in differential pressure regardless of wind speed, especially on the south-west wall of the single-family home. As the wind speed escalates, the absolute value of the median increases. Theoretically, this increase should be according to the



square of the wind speed. This is demonstrated in Figure 8 where the median wind speed and median differential pressure for Beaufort classes 0 through 4 from Figure 7 were chosen and fitted using the formula  $ax^2+b$ . The coefficients of determination ( $R^2$ ) are generally above 0.9, with only 2 of 16 cases falling below  $R^2$  of 0.9 due to minor pressure differences between the Beaufort classes under consideration. The pressure difference seems to quite well predict the local wind speed, if the quadratic relation is known. Figure 7 shows that pressure differences across the wall, even when the vent is open, can sporadically escalate to substantial levels. This underscores the necessity of employing pressure-regulated vents. Generally speaking, the measured pressure differences are rather low: approximately 50% of the values are less than +1 Pa and 90% of the values range from 2 to 10 Pa, excluding any negative values.

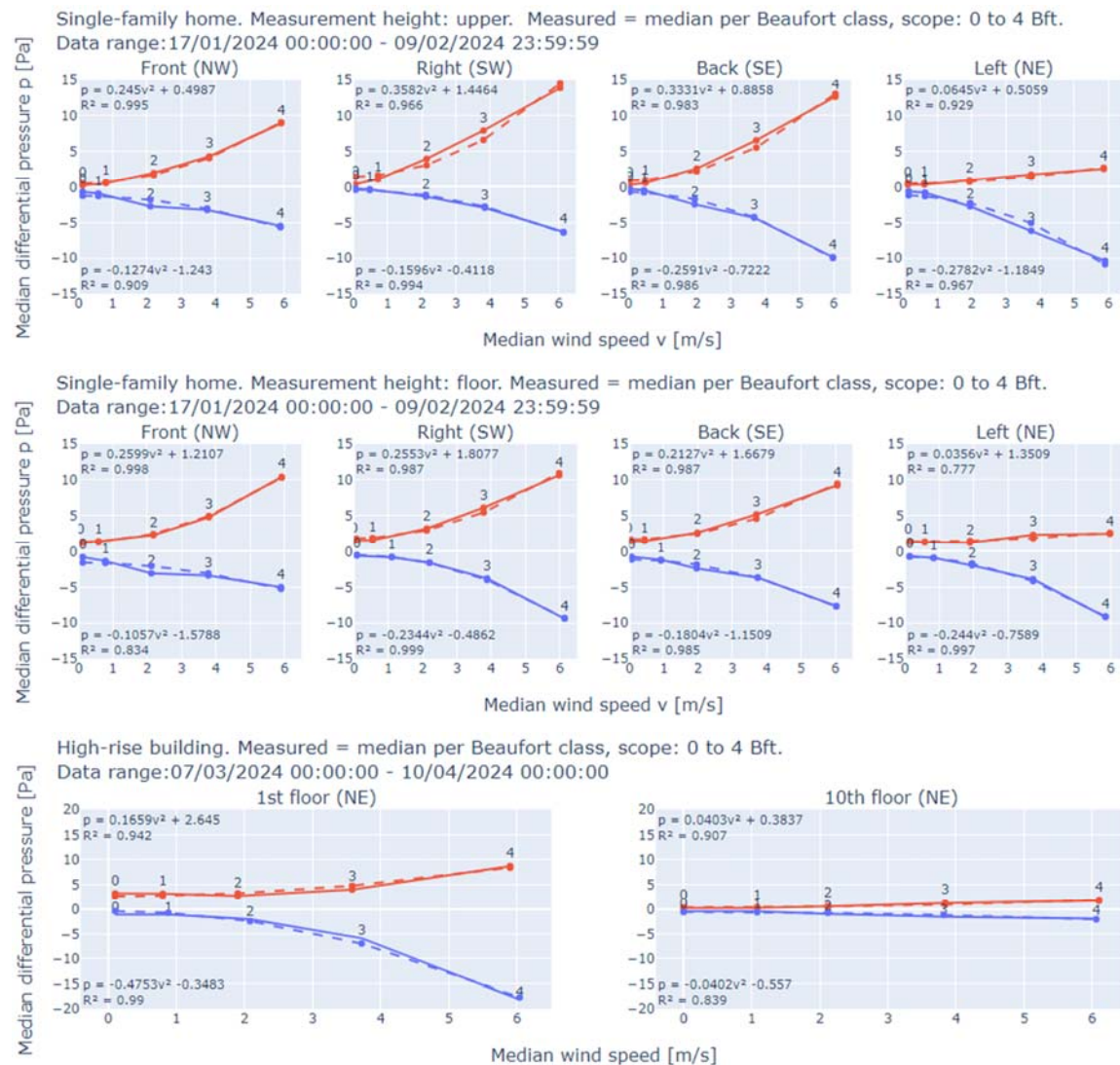


Figure 8: Median differential pressure as a function of median wind speed for Beaufort classes 0 through 4. Measured values derived from Figure 7. Curve fitting is employed to highlight quadratic correlation between wind speed and differential pressure.

Figure 9 shows the CDFs of the infiltration and exfiltration air leaks, where infiltration represents the case overpressure and exfiltration the case underpressure. The curves are obtained as follows. Each measured pressure difference is converted to its corresponding flow rate using the Power Law. The flow coefficient and exponent are derived from the Blowerdoor 2023 test. If the measured pressure is positive, the overpressure result from the

Blowerdoor test is used. For a negative pressure, the underpressure parameters are adopted. For conversion to flow, the flow coefficient is divided by eight because there are eight measurement locations around the house, while all walls have an equal area and it is assumed that the leaks are evenly distributed while an airtight roof is taken into account. Finally, for each time instant, the positive flow rates are added together and the same is done for the negative flow rates. This results in two time series representing overpressure and underpressure from which their CDFs are obtained.

The exfiltration CDF rises at lower flow rates compared to the infiltration CDF. This is due to the mechanical extract ventilation system operating at its minimum level, which is about 35 m<sup>3</sup>/h, during the measurements. At P50, the air leakage rates for exfiltration and infiltration are 36 and 71 m<sup>3</sup>/h, respectively. The difference between these two rates approximates the minimum airflow rate of the ventilation system. At P90, both infiltration and exfiltration increases to about 120 m<sup>3</sup>/h.

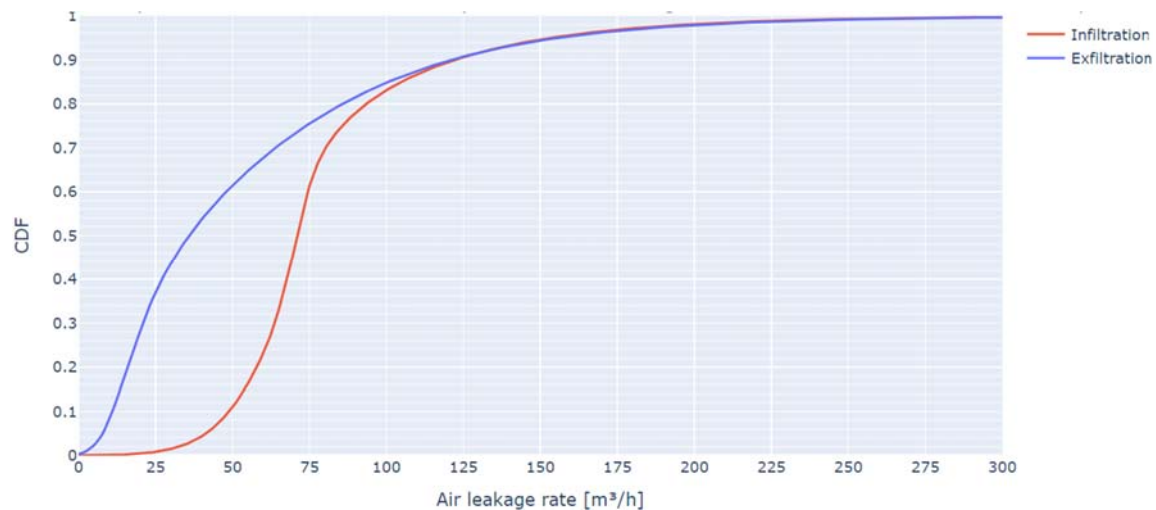


Figure 9: Single-family home: cumulative distribution functions of in- and exfiltration.

#### 4 CONCLUSIONS

The air tightness measurements in the single-family home show, for a reference pressure of 50 Pa, that the ATT results are comparable to, if not marginally higher than, the Blowerdoor test. When the reference pressure is changed to 4 Pa, the ATT gives similar or slightly lower values than the Blowerdoor test. When the flow exponent in the ATT's calculation is set equal to that of the Blowerdoor test, the results of the ATT are marginally lower for both 50 and 4 Pa. In contrast, the Pulse test gives persistently higher results than the Blowerdoor (up to 30%), regardless of the 50 or 4 Pa reference pressures.

The cumulative distribution functions of the pressure differences show that the wind effect is prominent for both types of buildings, highlighting the need for pressure-regulated vents. The contribution of the stack effect can also be observed between measurements at different heights. For the high-rise building, the median overpressures at P50 are 3.1 and 0.3 Pa for the 1<sup>st</sup> and 10<sup>th</sup> floors, respectively, while underpressure values are 1.4 and 0.5 Pa. For the single-family home, the wind effect is clearly noticeable, with the south-west façade frequently experiencing overpressure. The P50 values for all façades fall within the range of -1.5 to 1.5 Pa.

A high correlation ( $R^2 > 0.9$ ) between the square of the local wind speed and the differential pressure is found at most measuring points of both buildings, expressed as a quadratic

relationship between the median values. However, this relationship shows marked variability between façades, depending on the wind effect. At a Beaufort scale of 2, both buildings showed median pressure differences ranging from about 3 to -3 Pa. As the Beaufort scale increased to 4, the range broadened from 8 to -6 Pa. This effect is less visible on the 10<sup>th</sup> floor of the high-rise building because the both positive and negative median pressures remained low at 2 and -2 Pa, respectively.

The cumulative distribution functions of the infiltration and exfiltration leakage rates of the single-family home show the effect of the mechanical extract ventilation system. The exfiltration curve increases at lower leakage rates compared to the infiltration curve. At P50, the infiltration rate is 71 m<sup>3</sup>/h, while the exfiltration rate is 36 m<sup>3</sup>/h. The difference between these two rates is equal to the minimum airflow at which the mechanical extract ventilation system operated during the measurements.

## 5 REFERENCES

- ACIN Instruments. (2024). *Air Tightness Tester*. Retrieved from <https://acin.nl/en/air-tightness/air-tightness-tester/>
- Adafruit. (2024). *Anemometer wind speed sensor*. Retrieved from <https://www.adafruit.com/product/1733>
- AFNOR. (2017). NF DTU 68.3:2017. *Travaux de bâtiment - Installations de ventilation mécanique*. French Standardization Association.
- BlowerDoor. (2024). *BlowerDoor Measuring Principle*. Retrieved from <https://www.blowerdoor.com/measurement-systems/blowerdoor-standard/the-measuring-principle>
- Build test solutions. (2021). Retrieved from <https://www.buildtestsolutions.com/files/9705531c5d8042ce38699e0e934e51332879eb24.pdf>
- Build test solutions. (2024). *Measuring building air tightness with Pulse*. Retrieved from <https://www.buildtestsolutions.com/air-leakage-testing/pulse-air-permeability-testing/how-it-works>
- Buildwise. (2015). *TV255: Luchtdichtheid van gebouwen*. Buildwise. Retrieved from <https://www.buildwise.be/nl/publicaties/technische-voorlichtingen/255/>
- Effnergie. (2010). *Guide de la ventilation naturelle et hybride "VHNY"*.
- Espressif. (2024). *ESP32-DevKitC*. Retrieved from <https://www.espressif.com/en/products/devkits/esp32-devkitc/overview>
- NBN. (1991). NBN D50-001:1991. *Ventilation systems for housings*. Belgian Bureau for Standardization.
- NEN. (2001). NEN1087:2001. *Ventilation in buildings - Determination methods for new estate*. Netherlands Standardization Institute.
- Sensirion. (2016). *Compensation of pressure drop in a hose*. Retrieved from [https://sensirion.com/media/documents/E2B13D4F/6166C422/Sensirion\\_Differential\\_Pressure\\_Datasheet\\_SDP800\\_Pressure\\_drop\\_in\\_ho.pdf](https://sensirion.com/media/documents/E2B13D4F/6166C422/Sensirion_Differential_Pressure_Datasheet_SDP800_Pressure_drop_in_ho.pdf)
- Sensirion. (2024). *SDP810-125Pa*. Retrieved from <https://www.sensirion.com/products/catalog/SDP810-125Pa>
- VEKA. (2021). *Bijlage IX - ventilatievoorzieningen in woongebouwen: bepalingmethode en eisen*.

# Evaluating the IAQ and energy performance of two types of ventilation systems in multifamily buildings

Zohreh Kiani<sup>1,2,3</sup>, Ali Alexander Nour Eddine<sup>1\*</sup>, Kévin Taurines, Kátia Cordeiro Mendonça<sup>3,4</sup>, and Marc Abadie<sup>2</sup>

*1 Eurovent Certita Certification  
Paris, France*

*\*Corresponding author: aa.nour-  
eddine@eurovent-certification.com*

*3 RUPEE Lab  
Street address  
La Rochelle/Lagord, France*

*2 La Rochelle Université  
LaSIE UMR CNRS 7356  
La Rochelle, France*

*4 Tipee Plateforme Technologique  
du Bâtiment Durable  
Street address  
La Rochelle/Lagord, France*

## SUMMARY

This study evaluates the performance of Single-Flow and Dual-Flow ventilation systems in a residential building situated in Strasbourg, characterized by high PM<sub>2.5</sub> levels, permeable tightness, and strong wind conditions. The research examines indoor air quality by measuring CO<sub>2</sub> and PM<sub>2.5</sub> concentrations in bedrooms and compares the energy consumption of both systems across different cities. The findings indicate that the Dual-Flow system effectively maintains CO<sub>2</sub> levels between 500 and 1000 ppm, significantly reduces peak PM<sub>2.5</sub> levels, and demonstrates superior energy efficiency, particularly with heat recovery system. Conversely, the Single-Flow system shows limitations in controlling indoor air quality and higher energy consumption. Overall, the Dual-Flow ventilation system proves to be a more effective solution for enhancing indoor air quality and achieving energy savings in residential buildings under similar environmental conditions.

## KEYWORDS

Indoor Air Quality, energy efficiency, building simulation, balanced ventilation systems, multifamily residential buildings

## 1 INTRODUCTION

People spend most of their time indoors, exposing themselves to indoor pollutants that can cause health issues and affect productivity (WHO, 2010; Wargocki et al., 2006; Fisk, 2000). Residential buildings are critical as they account for 60 to 95% of lifetime airborne pollutant exposure (Borsboom et al., 2016). Indoor pollutants come from outdoor air and indoor activities. Improving air quality relies on increased ventilation, which is energy-intensive in temperate climates. Current standards use a prescriptive approach based on ventilation rates rather than pollutant concentrations (Chenari et al., 2016; Guyot et al., 2018). A performance-based approach, predicting pollutant concentrations through simulations, is more effective for assessing Indoor Air Quality (IAQ). This study compares the performance of Single-Flow and Dual-Flow ventilation systems installed in a two-storey residential building in terms of bedrooms' confinement, bedroom's PM<sub>2.5</sub> pollution level and energy consumption.

## 2 METHODOLOGY

The studied case is a residential two-storey building composed of 9 apartments of different sizes (Figure 1). The envelope airtightness of the building is low according to European standard EN 12831 (2017). Wind speeds imposed in this study can be considered as strong and are close to the conditions met in urban cities such as Helsinki, Athens or Strasbourg. The outdoor pollution (PM<sub>2.5</sub>) is set to a high pollution level i.e. with a mean annual PM<sub>2.5</sub> concentration higher than 20 µg/m<sup>3</sup> with peaks frequently reaching 50 µg/m<sup>3</sup> and even 100-300 µg/m<sup>3</sup> during winter. Simulations are performed with HEAVENLY (Holistic Evaluation tool for Air VENtiLation sYstems) based on a TRNSYS-CONTAM dynamic computations of heat, moisture, and pollutants (CO<sub>2</sub>, Formaldehyde and PM<sub>2.5</sub>) as described in Kiani et al. (2024).

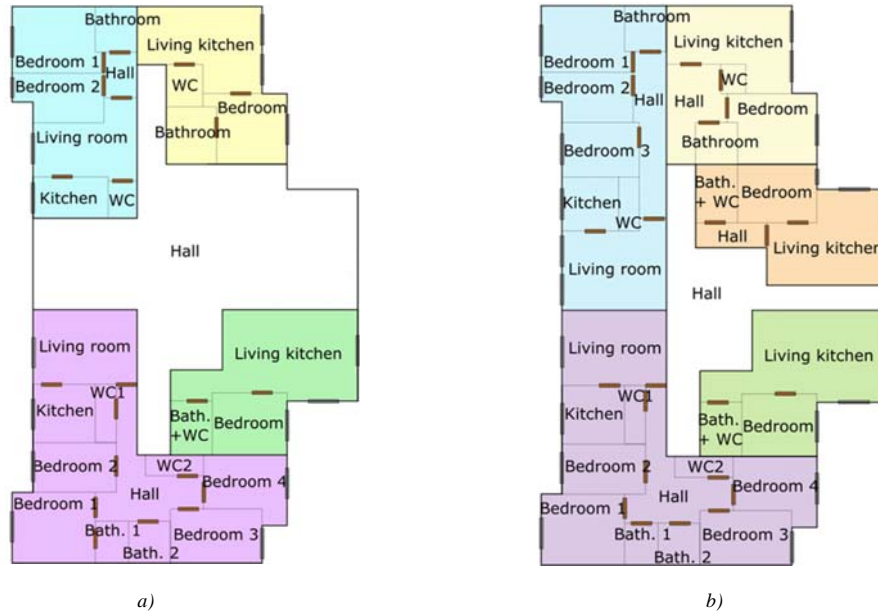


Figure 1: Representation of the 1<sup>st</sup> floor (a) and 2<sup>nd</sup> floor (b).

## 3 RESULTS AND ANALYSIS

### 3.1 CO<sub>2</sub> Concentration in bedrooms

Figure 1 illustrates the CO<sub>2</sub> concentration levels in the bedrooms for both Single-Flow and Dual-Flow ventilation systems. The Dual-Flow system effectively maintained CO<sub>2</sub> levels between 500 and 1000 ppm, demonstrating well-controlled ventilation. However, despite showing good control level CO<sub>2</sub>, the Single-Flow system revealed shortcomings in keeping indoor air quality at an optimal level.

### 3.2 PM<sub>2.5</sub> Concentration in bedrooms

Figure 2 depicts the PM<sub>2.5</sub> concentration levels in the bedrooms. High PM<sub>2.5</sub> values were mainly due to outdoor pollution. The figure also highlights the effectiveness of the filtration system (ePM<sub>2.5</sub> = 60%) in the Dual-Flow ventilation, significantly reducing peak levels and showing a clear improvement in overall air quality.

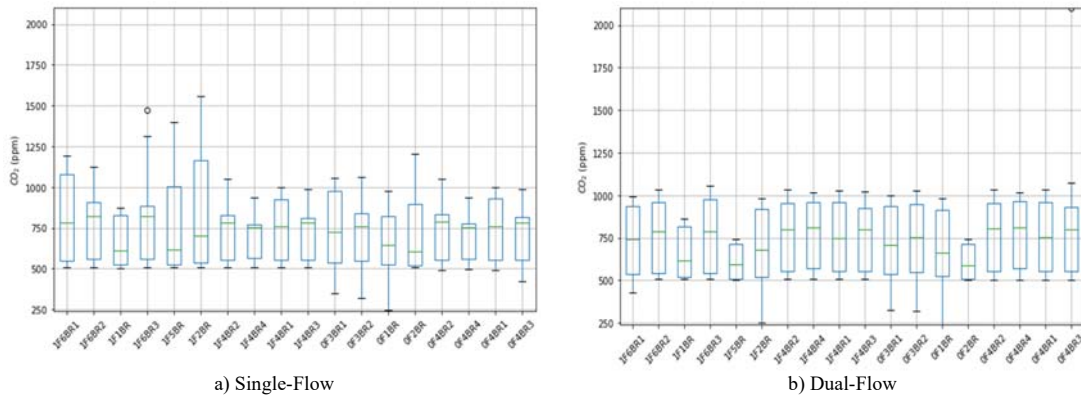


Figure 2: CO<sub>2</sub> concentration in bedrooms – Single-Flow (a) versus Dual-Flow (b).

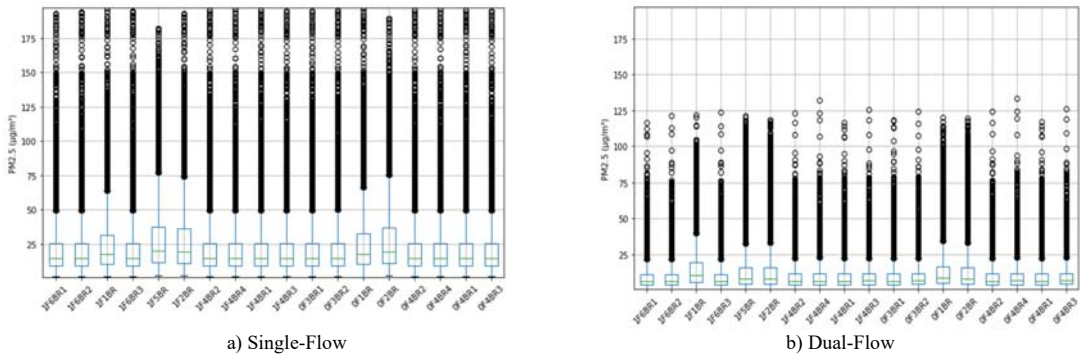


Figure 3: PM<sub>2.5</sub> concentration in bedrooms – Single-Flow (a) versus Dual-Flow (b).

**3.3 Energy Consumption for different geographical locations**

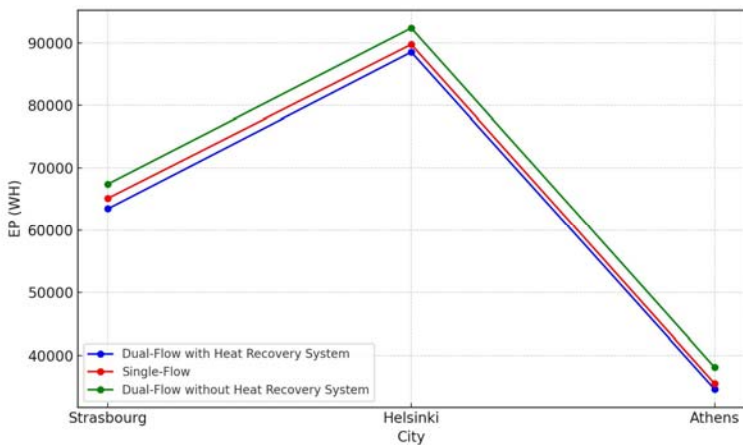


Figure 4. Comparison of energy consumption in different cities

Figure 3 compares the sum of the energy consumed by the fan(s) (electricity) and that due to thermal losses related to air renewing (gas). The resulting annual energy consumption (EP in Wh) is expressed here in terms of primary energy considering a final-to-primary energy conversion factors of 1 for gas and 2.5 for electricity. Calculations have been made to three cities presenting cold (Strasbourg and Helsinki) to mild (Athens) winters. The data shows that

the Dual-Flow with heat recovery system consistently consumes less energy than the Single-Flow system. This demonstrates the energy efficiency of the Dual-Flow system, particularly in reducing heating energy needs and highlighting its potential for significant energy savings. Note that the energy consumption for dual flow without HR is higher than the single flow one because of a slightly higher airflow rate used for Dual-Flow and because of the additional fan electricity consumption.

#### 4 CONCLUSION

The Dual-Flow ventilation system with Heat Recovery outperforms the Single-Flow system in both maintaining air quality and energy efficiency. It is a superior choice for residential buildings, especially under conditions like those of the present study, particularly the elevated outdoor pollution. However, the performance of mechanical ventilation systems in terms of IAQ and energy consumption depends on the outdoor pollution, wind intensity and building exposure, air tightness of the building envelope, urban/semi-urban site, climatic conditions... The HEAVENLY tool is designed to comprehensively assess mechanical ventilation systems by computing specific indicators for IAQ and energy consumption.

#### 5 REFERENCES

- Borsboom, W., De Gids, W., Logue, J., Sherman, M. H., Wargocki, P. (2016). *Technical note AIVC 68 residential ventilation and health*. Brussels: INIVE.
- Chenari, B., Carrilho, J. D., Da Silva, M. G. (2016). Towards sustainable, energy-efficient and healthy ventilation strategies in buildings: A review. *Renewable and Sustainable Energy Reviews*, 59, 1426-1447.
- EN 12831 (2017). *Energy performance of buildings - Method for calculation of the design heat load - Part 1: Space heating load, Module M3-3*.
- Fisk, W. J. (2000). Health and productivity gains from better indoor environments and their relationship with building energy efficiency. *Annual review of energy and the environment*, 25(1), 537-566.
- Guyot, G., Sherman, M. H., Walker, I. S. (2018). Smart ventilation energy and indoor air quality performance in residential buildings: A review. *Energy and Buildings*, 165, 416-430.
- Kiani, Z., Eddine, A. A. N., Taurines, K., Mendonça, K. C., Abadie, M. (2024). Evaluating the IAQ and energy performance of ventilation systems in multifamily buildings. In *E3S Web of Conferences* (Vol. 523, p. 01003). EDP Sciences.
- Wargocki, P., Seppanen, O., Andersson, J., Boestra, A., Clements-Croome, D., Fitzner, K., Hanssen, S. O. (2006). *Indoor climate and productivity in offices: How to integrate productivity in life cycle costs analysis of building services*. Rehva.
- World Health Organization. (2010). *WHO guidelines for indoor air quality: selected pollutants*.

# Comprehensive analysis of indoor air quality in a real home using low-cost sensors

Marc Olivier Abadie<sup>\*1,3</sup>, Kátia Cordeiro Mendonça<sup>2,3</sup>

*1 La Rochelle Université, LaSIE, UMR  
CNRS 7356  
Av. Michel Crépeau, 17042 La Rochelle,  
France*

*2 TIPEE Plateforme  
Technologique du Bâtiment  
Durable  
8 rue Isabelle Autissier, 17140  
Lagord, France*

*3 RUPEE Lab, a LaSIE-  
TIPEE common  
laboratory,  
La Rochelle/Lagord,  
France*

*\*Corresponding author: mabadie@univ-lr.fr*

## ABSTRACT

This study focuses on a comprehensive analysis of indoor air quality (IAQ) in a real dwelling by using data collected from six indoor and one outdoor low-cost sensors. The primary variables under scrutiny include temperature, relative humidity, indoor CO<sub>2</sub> and particles concentrations, and outdoor NO<sub>2</sub> concentration. The dataset, gathered at a high temporal resolution with a 10-second timestep over a one-month period encompassing both holidays and workdays, provides a good understanding of IAQ dynamics. To enhance the contextual understanding, a log file documenting key household activity such as cooking, showering, sleeping, and the open/close status of indoor doors has been maintained. This investigation aims to evaluate from these measurements parameters of interest to better understand the exposure of occupants such as outdoor pollution, room airflow rates, indoor particles sources and deposition to indoor surfaces. Results show that low-cost sensors can provide enough information to evaluate those parameters with accuracy if complementary information such as open/close door status and sleeping time are known.

## KEYWORDS

IAQ, in-situ measurements, low-cost sensors, dwelling.

## 1 INTRODUCTION

People spend most of their life in buildings. As a result, they are exposed in a daily basis to indoor pollutants that can produce adverse effects on their health such as headaches, allergies and respiratory diseases (WHO, 2010) and affect their productivity (Wargocki *et al.*, 2006; Fisk, Black and Brunner, 2011). Exposure to indoor pollutants in residential buildings is particularly important. Boorsboom *et al.* (2016) evoked that 60 to 95% of our total lifetime exposures to airborne pollutants occur in homes, with 30% of that being during sleeping time. Moreover, WHO data indicated that 180,000 deaths in Europe and Americas were attributable to household (indoor) air pollution (WHO, 2014). It is therefore important to understand indoor air quality (IAQ) dynamics in residential buildings to provide solutions to limit occupant's pollutants exposure and maintain a healthy indoor environment.

With the advent of low-cost air quality sensors, portable and with low-power consumption, monitoring air quality in real-time with high temporal and spatial coverage is nowadays an economic viable alternative to assess IAQ dynamics in residential buildings. Despite their limitations comparatively to scientific instruments, low-cost sensors can provide useful information for management and mitigation of IAQ issues and identification of possible emission sources (Garcia *et al.*, 2022).

The objective of this work is to contribute to the understanding of IAQ dynamics in residential buildings, by presenting a comprehensive evaluation of parameters of interest for IAQ analysis in a real dwelling based on data collected from low-cost sensors.



## 2 METHODOLOGY

The present analysis was based on the continuous monitoring of the air quality in a real dwelling and its neighbouring environment using low-cost sensors. The variables under scrutiny in the indoor environment were temperature (T), relative humidity (RH), CO<sub>2</sub> and PM<sub>1</sub>, PM<sub>2.5</sub> and PM<sub>10</sub> concentrations, while those concerning the outdoor environment were temperature, PM<sub>2.5</sub> and NO<sub>2</sub> concentrations. The monitoring campaign was conducted during one month in the winter season, from December 23<sup>rd</sup> 2023 to January 29<sup>th</sup> 2024, and included the documentation of the key house activities such as cooking, showering, sleeping, and the open/close status of indoor doors.

### 2.1 Case study

The measurements were carried out in a dwelling located in the city of La Rochelle on the French west coast. The 83.5 m<sup>2</sup> dwelling is constituted of a 1<sup>st</sup> floor composed of a living-room, a kitchen/dining room, a toilet and a stair/hall space and a 2<sup>nd</sup> floor made up of three bedrooms, a bathroom and a stair/corridor space, as illustrated in Figure 1.

Figure 1: Schematic representation of the dwelling's 1<sup>st</sup> floor (left) and 2<sup>nd</sup> floor (right)

Table 1: Geometric characteristics of the monitored rooms

Room	Floor surface (m <sup>2</sup> )	Room volume (m <sup>3</sup> )	Air volume (m <sup>3</sup> )*	Airflow rate (m <sup>3</sup> /h)	
				Fan speed 1	Fan speed 2
Bedroom 1	12	29	24.0		
Bedroom 2	9	22	21.0		-
Bedroom 3	9	22	20.6		
Kitchen/dining room	20	50	44.9	43-60	>131
Living-room	14	36	34.8		
Stair/Corridor	5	12	-	13-20	14.5-21.5
Toilet	-	-	-		
Bathroom	-	-	-		

\*Air volume = Room volume – Main furniture volume

The dwelling is equipped with a pressure-controlled extraction ventilation system, whose exhaust terminal vents are located in the kitchen, living-room, toilet, bathroom and corridor. Outside air enters the house by an air intake grille (8 cm in diameter) located on the north wall of the kitchen and through pressure-controlled inlets in the bedrooms (30 m<sup>3</sup>/h at 20 Pa). The kitchen is equipped with a mechanical extraction hood. The heating of both air and water is

provided by a gas boiler located in the basement. The gas boiler flue is located 2 meters away from the air intake grille, on the north wall of the kitchen. The house is inhabited by a non-smoking family composed of three people, two adults and a teenager.

Table 1 indicates the geometric characteristics of the rooms where the IAQ sensors were installed in (see Figure 1) and their corresponding volume of the breathable air. Table 1 also indicates the airflow rates of the ventilation system according to the manufacturer's specification.

## 2.2 Instrumentation

Two kinds of low-cost sensors were used for monitoring the air quality variables: one for the indoor measurements (Ellona POD2) and another for the outdoor measurements (Ellona WT1). The variables of interest measured by the sensors with their corresponding range, limit of detection (LOD), accuracy ( $R^2$ ) and precision are presented in Table 2.

Table 2: POD2 and WT1 – Measurement characteristics

Variable	Sensor	Range	LOD	Accuracy $R^2$	Precision
T	POD2	-40°C-+85°C	0.1°C	±1	0.1°C
	WT1	-40°C-+60°C			
RH	POD2/WT1	0-100 %	0.01 %	0.03	0.01 %
CO <sub>2</sub>	POD2	0-10,000 ppm	N/A	20 ppm +3%	1 ppm
PM (1/2.5/4/10)	POD2	0-1,000 µg/m <sup>3</sup>	N/A	10 µg/m <sup>3</sup>	0.1 µg/m <sup>3</sup>
TVOC	POD2	1-1,000 ppm	N/A	N/A	0.1 ppm
NO <sub>2</sub>	WT1	0-100 ppm	0.009 ppm	N/A	0.003 ppm
PM (1/2.5/10)	WT1	0-1,000 µg/m <sup>3</sup>	0.1 µg/m <sup>3</sup>	10 µg/m <sup>3</sup>	0.1 µg/m <sup>3</sup>

Laboratory tests have been conducted to compare the low-cost sensors measurements (T, RH, CO<sub>2</sub> and PM concentrations) with reference scientific equipment: calibrated DeltaOhm HD21 AB17 for CO<sub>2</sub> and MiniWRAS 1371 Portable wide-range aerosol spectrometer for PM<sub>2.5</sub> concentrations, both equipment also measuring T and RH.

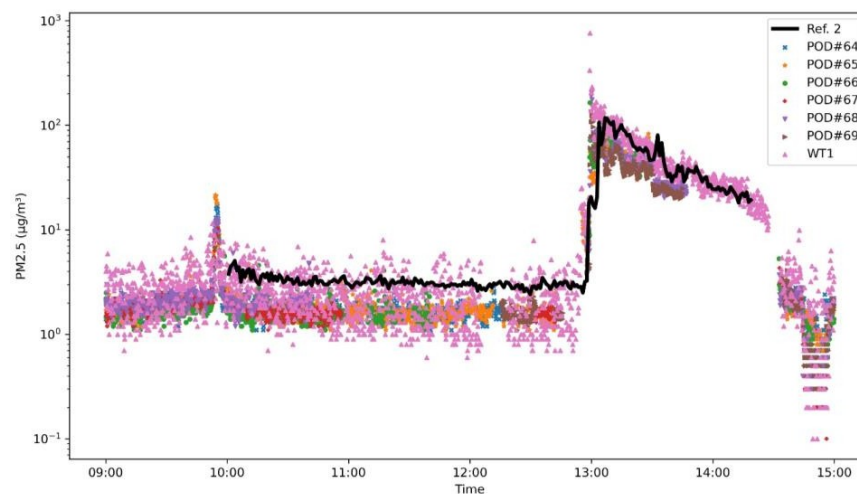


Figure 2: PM<sub>2.5</sub> concentration by MiniWRAS (Ref. 2) and low-cost sensors in the laboratory chamber

Responses to variations are similar for all equipment. Low-cost sensors' absolute values are within the expected error ranges except for PM concentration that shows higher divergence for the POD sensors when the WT1 agrees well with the MiniWRAS (Figure 2). As a result, post-calibration has been applied to POD PM<sub>2.5</sub> concentration based on a complementary period of one week before this study.

### 2.3 Airflow rate and particle source/sink assessment

Considering the control volume approach of a room with entering air coming only from outdoor, the mass balance of a pollutant under perfect mixing can be written:

$$V \frac{dC_{ind}}{dt} = Q_{air}C_{out} - Q_{air}C_{ind} + E_{ind} - S_{ind} \quad (1)$$

where  $V$  is the volume of the airspace that renews by outdoor air ( $m^3$ ),  $C_{ind}$  and  $C_{out}$  are the indoor and outdoor pollutant concentrations (ppm or  $\mu g/m^3$ ), respectively.  $Q_{air}$  is the airflow rate considering infiltration and ventilation ( $m^3/h$ ), respectively  $E_{ind}$  and  $S_{ind}$  are pollutant source and sink (ppm/h or  $\mu g/h$ ) and  $t$  is the time (h). The considered sources are the occupant for  $CO_2$  and the cooking activity for  $PM_{2.5}$ . Only  $PM_{2.5}$  deposition is considered as a sink.

In this study, the airflow rates by ventilation/infiltration are evaluated according to two methods. The first one is based on the  $CO_2$  concentration decay occurring when  $CO_2$  source (people) left a room, all other parameters remaining constant. The solution of equation (1) for this case is:

$$\Delta C = \Delta C(t = 0) \times \exp(-\lambda_v t) \quad (2)$$

where  $\Delta C = C_{ind} - C_{out}$  with the outdoor concentration considered constant to 400 ppm (or as the minimal value recorded during the campaign by the considered sensor) and  $\lambda = \frac{Q_{air}}{V}$  is the air change rate of ventilation/infiltration (/h).

The second method considers the  $CO_2$  concentration increase occurring during night in the bedroom with the presence of occupants. The solution of equation (1) for this case is:

$$\Delta C = \frac{E_{ind}}{Q_{air}} + [\Delta C(t = 0) - \frac{E_{ind}}{Q_{air}}] \times \exp(-\frac{Q_{air}}{V} t) \quad (3)$$

Note that equation (3) allows the evaluation of both  $Q_{air}$  and  $E_{ind}$  (i.e. the  $CO_2$  rate by occupants).

For the case of  $PM_{2.5}$  emissions by cooking activities, the source is so strong that airflow rates can be neglected in the mass balance and  $E_{ind}$  can be approximated by:

$$E_{ind} \sim V \frac{\Delta C_{ind}}{\Delta t} \quad (4)$$

$PM_{2.5}$  deposition velocity is also an important parameter to consider when modelling indoor particle concentration. Its definition is:

$$V_d = \frac{V}{A} \lambda_d \quad (5)$$

where  $V_d$  is the deposition velocity (m/h),  $\lambda_d$  is the deposition constant (/h) and  $A$  is the total surface area of particle deposition ( $m^2$ ).

The deposition constant can be evaluated when there are no more sources of particles or resuspension by occupants' activity considering the concentration decay induced by both the air renewal and particle deposition:

$$C_{ind} = C_{ind}(t = 0) \times \exp[-(\lambda_v + \lambda_d)t] \quad (6)$$

### 3 RESULTS AND DISCUSSIONS

Results presented here are focused on T, RH, CO<sub>2</sub> and PM<sub>2.5</sub> concentrations. Other measured parameters such as light intensity, noise, pressure or PM<sub>1</sub>, PM<sub>10</sub> and TVOC concentration are not presented in this paper.

#### 3.1 Local versus city station outdoor pollution

Figure 3 presents a comparison between the pollution (NO<sub>2</sub> and PM<sub>2.5</sub> concentrations) measured during the experimental campaign outside the house and the data from La Rochelle ATMO station. ATMO Nouvelle Aquitaine is the authorized observatory for monitoring air quality in La Rochelle. Realtime and historical data are available via the French LCSQA open data website (<https://files.data.gouv.fr/lcsqa>). The ATMO\_01 station is located downtown, 2 km west from the house.

The NO<sub>2</sub> concentration measured locally are usually much higher than that recorded downtown. The excess of NO<sub>2</sub> can be explained by the operation of the gas boiler during the space and water heating periods. This source of NO<sub>2</sub> clearly induced a local pollution for the house, at least for the northern façade, that is different from the ATMO station. Similar observation can be done for PM<sub>2.5</sub> concentration to a lower extent. It is important in this case to account for the source of pollutant to assess the penetration of outdoor pollutant in the house, and not rely only on data from distant station.

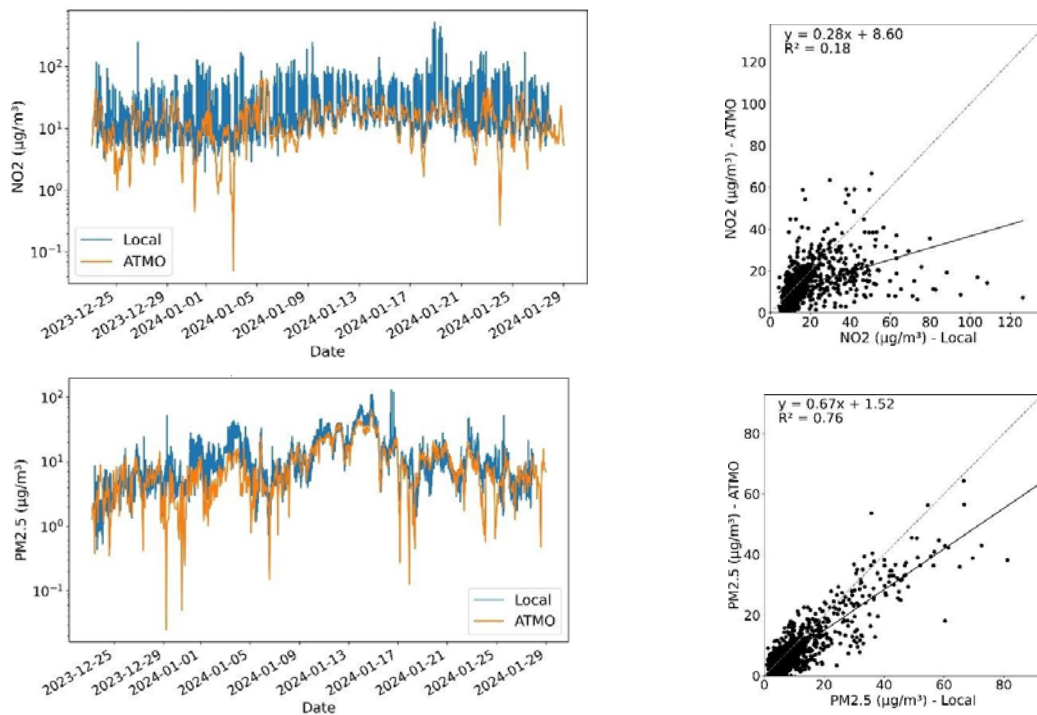


Figure 3: NO<sub>2</sub> and PM<sub>2.5</sub> concentration measured at local and city centre (ATMO) stations.

#### 3.2 Measurements

The statistics of the parameters measured during the monitoring campaign are presented in Table 2.

Independently on the other bedrooms' occupation, Bedroom 1 (1 or 2 occupants), Bedroom 3 (0 or 1 occupant), and their doors status (open/closed) during sleeping time, Bedroom 2 always presented a much higher level of CO<sub>2</sub> concentration than the others. Furthermore, as indicated

in Table 2, the average CO<sub>2</sub> concentration found in Bedroom 2 far exceed the limit concentration (950 ppm) requested by category II of the EN 16798-1:2019 indoor environment quality classification, which corresponds to a normal level of environment air quality expected by occupant. Regarding PM<sub>2.5</sub>, since there are no internal sources and the outdoor pollution remains relatively low (average =12.5 µg/m<sup>3</sup> for the whole campaign), the level of pollution in the bedrooms remains very low with an average lower than 10 µg/m<sup>3</sup>, the annual average limit given by EN 16798-1:2019 and remains close to the WHO value of 5 µg/m<sup>3</sup>.

As expected, because of their higher volume of breathable air, the pollution in the living-room and kitchen stays low in terms of CO<sub>2</sub> concentrations (whole campaign average under the limit value for occupants' exposure of 950 ppm for category I given by EN 16798-1:2019), as well as in terms of PM<sub>2.5</sub> (whole campaign average values < 10 µg/m<sup>3</sup>) despite the important internal sources.

Table 3: Indoor and outdoor parameters measured during each monitoring campaign in each investigated room (values presented as mean [min; max]).

Period	Room	T (°C)	RH (%)	CO <sub>2</sub> (ppm)	PM <sub>2.5</sub> (µg/m <sup>3</sup> )
Whole campaign	BD1	21.5 [17.4; 30.2]	52 [28; 75]	879 [385; 1962]	6.0 [0.4; 70.2]
	BD2	20.8 [16.3; 23.5]	60 [41; 87]	1411 [402; 4600]	5.9 [1.4; 48.4]
	BD3	20.8 [16.3; 23.0]	52 [34; 84]	829 [404; 2557]	6.4 [0.5; 47.0]
	LV	21.1 [14.6; 23.8]	53 [36; 86]	669 [389; 1783]	9.6 [0.3; 309.2]
	KT	21.0 [16.1; 24.8]	52 [34; 76]	649 [400; 1648]	8.3 [0.8; 436.1]
	Outdoor	9.0 [-0.3; 14.6]	72 [49; 89]	-	12.5 [0.4; 129.3]
<u>Period 1 (7 days)</u>	BD1	21.3 [17.4; 29.3]	58 [40; 75]	939 [414; 1911]	3.7 [0.4; 40.3]
Initial IAQ dynamics	BD2	20.9 [16.3; 23.0]	65 [52; 87]	1656 [402; 4600]	4.1 [1.4; 13.7]
	BD3	20.4 [16.8; 23.0]	59 [50; 76]	932 [404; 2557]	3.8 [0.5; 24.4]
	LV	21.6 [14.6; 23.8]	59 [45; 86]	786 [411; 1461]	8.1 [0.3; 309.2]
	KT	20.7 [16.1; 23.7]	60 [50; 76]	740 [427; 1433]	7.1 [0.8; 436.1]
	Outdoor	11.7 [7.2; 14.6]	77 [65; 84]	-	4.7 [0.4; 52.6]
	<u>Period 2 (3 days)</u>	BD1	21.8 [20.6; 27.4]	56 [43; 60]	946 [586; 1382]
IAQ dynamics after cleaning the air intakes in the bedrooms	BD2	21.1 [20.0; 23.1]	65 [53; 74]	1562 [565; 3387]	3.4 [1.6; 9.2]
	BD3	20.9 [20.0; 22.1]	57 [52; 62]	934 [593; 1402]	3.0 [0.9; 7.8]
	LV	21.8 [19.9; 23.6]	57 [49; 68]	817 [391; 1698]	3.7 [0.8; 24.9]
	KT	21.1 [17.8; 24.3]	58 [43; 69]	789 [430; 1468]	3.6 [1.3; 109.0]
	Outdoor	12.0 [10.7; 13.0]	73 [58; 83]	-	9.0 [2.2; 28.2]
	<u>Period 3 (12 days)</u>	BD1	21.5 [19.0; 29.5]	51 [30; 61]	891 [442; 1962]
IAQ dynamics after enlarging the air intakes in the bedrooms	BD2	20.6 [18.3; 22.5]	60 [43; 71]	1455 [434; 4049]	6.8 [1.5; 48.4]
	BD3	20.7 [16.3; 22.5]	52 [34; 84]	853 [437; 2073]	7.7 [0.8; 47.0]
	LV	21.0 [18.0; 23.0]	52 [39; 66]	654 [390; 1783]	11.2 [0.6; 231.4]
	KT	20.9 [17.9; 24.8]	50 [36; 64]	629 [400; 1648]	9.3 [1.0; 134.5]
	Outdoor	7.1 [0.9; 13.9]	66 [49; 82]	-	16.7 [0.7; 78.1]
	<u>Period 4 (14 days)</u>	BD1	21.6 [18.6; 30.2]	49 [28; 58]	825 [385; 1589]
IAQ dynamics after increasing the fan speed	BD2	20.9 [18.5; 23.5]	57 [41; 69]	1224 [430; 4371]	6.6 [1.4; 35.5]
	BD3	21.1 [18.3; 22.8]	48 [36; 57]	737 [429; 1492]	7.3 [0.6; 43.3]
	LV	20.9 [18.1; 23.7]	50 [36; 64]	602 [389; 1774]	10.2 [0.5; 100.5]
	KT	21.0 [17.9; 24.3]	47 [34; 63]	582 [402; 1564]	9.1 [1.0; 106.6]
	Outdoor	8.7 [-0.3; 14.3]	75 [51; 89]	-	13.4 [0.7; 129.3]

### 3.3 Ventilation airflow rates

#### *Airflow rates at the extraction vents*

Table 4 presents the measurements of the airflow rates at the extraction vents for period 1 (fan velocity 1) and period 4 (fan velocity 2). The actual airflows are lower than those from the manufacturer, especially for the kitchen. This is likely to be due to the solid/liquid particles that

have accumulated inside the ventilation ducts over time (15-year installation), as well as to the greater-than-recommended length of the kitchen duct (10 m instead of 6 m).

Table 4: Airflow rates at terminal vents – measurement ( $Q_{meas.}$ ) versus manufacturer ( $Q_{manu.}$ ).

Room	Fan velocity 1		Fan velocity 2	
	$Q_{meas.}$ (m <sup>3</sup> /h)	$Q_{manu.}$ (m <sup>3</sup> /h)	$Q_{meas.}$ (m <sup>3</sup> /h)	$Q_{manu.}$ (m <sup>3</sup> /h)
KT	22.2 ± 3.3	43 - 60	39.2 ± 5.9	131 - 145
LV	18.3 ± 2.7	13 - 20	18.7 ± 2.8	26 - 40
Toilet	17.2 ± 2.6	13 - 20	21.8 ± 3.3	26 - 40
Bathroom	17.6 ± 2.6	13 - 20	29.5 ± 4.4	26 - 40
Corridor	12.9 ± 1.9	13 - 20	14.5 ± 2.2	26 - 40
Total	88.1 ± 13.2	95 - 140	123.6 ± 18.5	235 - 305

#### Airflow rates in rooms

Figure 4 presents the airflow rates for all rooms and all considered periods of time calculated from all CO<sub>2</sub> concentration decays i.e. when the source of pollutant leaves the space. This method is simple to implement but is based on the pollutant mass balance of the room where air renewal is supposed to come only from outdoor (at constant concentration) and not connected to other rooms that may have different unknown concentration. This occurs for example when occupants leave their bedroom in the morning letting the door opened. That means that most of airflow rates calculated this way may be overestimated compared to the ones expected during nights (with closed door).

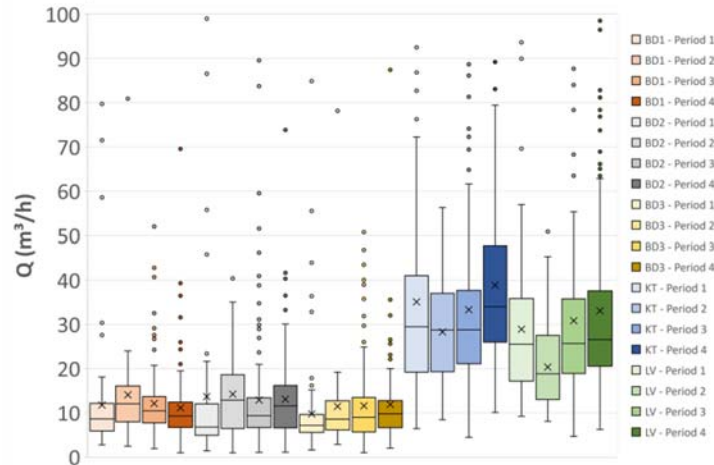


Figure 4: Airflow rates calculated from all CO<sub>2</sub> concentration decays

The second method is to evaluate the airflow rates when the source remains in the space. As an illustration, we consider bedroom 2 that remains always closed during night and with the door opened when the occupant leaves the room (Figure 5). Results clearly show that the calculated airflows with the second method are lower.

Table 5 presents the final airflow rates where those for bedrooms 1 and 3 have been calculated according to the log file to filter the case of only one occupant and the door closed during the night. Results for the kitchen and the living-room must be taken with care as the two spaces communicate to each other by two open doors.

The second method also allows the evaluation of the CO<sub>2</sub> emission by occupant during night. Figure 6 presents a comparison with the equations of Persily and de Jong (2017) that accounts for age, sex and basal metabolic rate of occupants. The evaluation from the sensors data gives

values close to those from the model with a slight underestimation for the two adults (occupant 1 and 3) whereas the result for the teenager (occupant 2) is quite accurate.

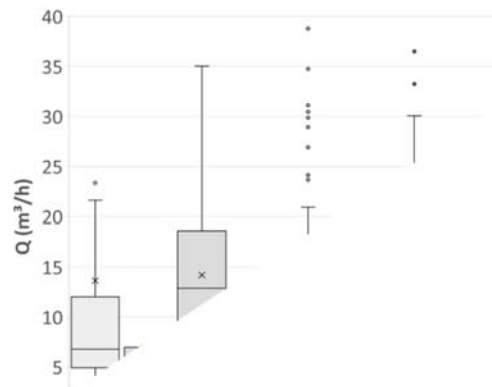


Figure 5: Airflow rates in BD2 calculated when the occupant leaves the bedroom (open door) and during night when sleeping (12PM-6AM, closed door)

Table 5: Airflow rates (m<sup>3</sup>/h) in rooms

Period	Room	min	Q1	median	mean	Q3	Max
Whole campaign	BD1	3.7	6.4	8.0	9.1	11.6	17.0
	BD2	2.2	4.2	5.4	5.6	6.5	9.7
	BD3	2.9	6.9	8.2	7.9	9.0	12.2
	LV	4.7	18.6	25.8	30.2	35.5	157.6
	KT	4.4	22.3	30.1	34.8	40.6	226.9

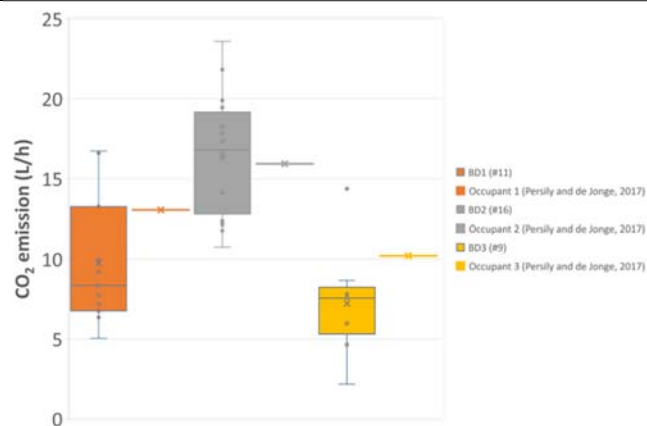


Figure 6: CO<sub>2</sub> emission rates from occupants

### 3.4 PM<sub>2.5</sub> emission from cooking

Figure 7 presents the emission rates (ER) of PM<sub>2.5</sub> from cooking events deduced from the high increase of PM<sub>2.5</sub> concentrations between 11AM-1PM and 6PM-8PM. Note that a kitchen hood has been used almost every time during cooking. ER are found very small for most of cooking events like boiling vegetables, using microwave or oven to reheat food... but high ER are observed for all frying events. Compared to PANDORA database (<https://db-pandora.univ-lr.fr/>), those ER are below the 75<sup>th</sup> percentile with a mean value for all cooking event during the experimental campaign (10 mg/h) very close to PANDORA's one (7 mg/h).

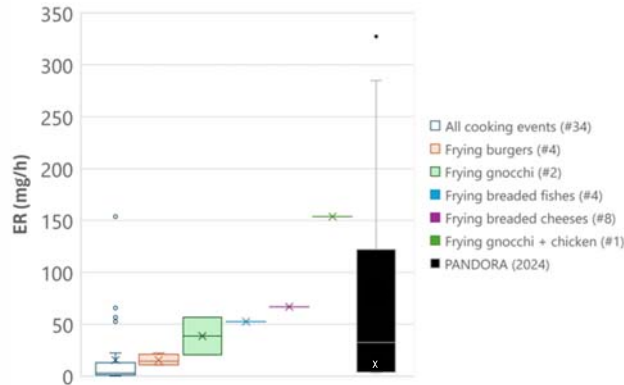


Figure 7: PM<sub>2.5</sub> emission rates from cooking events

### 3.5 Deposition velocity

Figure 8 presents the PM<sub>2.5</sub> deposition velocity in rooms calculated from the airflow rates and the evaluation of the deposition surfaces of the different rooms. These results must therefore be taken with caution regarding the possible cumulation of errors that may occur. Overall, the evaluated deposition velocities are within the extreme values from literature. However, one can observe that for all rooms but the kitchen, the mean values are two to three times higher than those of the literature so that this methodology may overestimate the deposition velocity. Results for kitchen are much more in line with the literature but, apart from the fact that the airflow rates are higher in the kitchen, no real cause for such different behaviour has been identified (about the same surface to volume ratio of 3, similar pollutant concentration levels...).

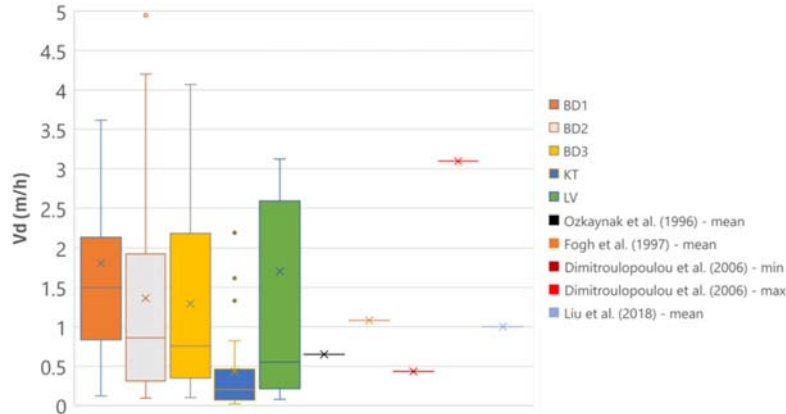


Figure 8: PM<sub>2.5</sub> deposition velocity in rooms

## 4 CONCLUSIONS

In this work, a monitoring campaign using low-cost air quality sensors was carried out in a real dwelling located in La Rochelle, France. CO<sub>2</sub> measurements have shown that one of the bedrooms (BD2) was under ventilated, even when the fan speed was increased. Indoor PM<sub>2.5</sub> concentration levels remained low in all rooms even in the kitchen and living-room, where the main internal sources were located. Local pollution was also identified mainly due to the gas boiler flue that emitted NO<sub>2</sub> and PM<sub>2.5</sub>.

Regarding the comparison between the two methods for calculating airflow rates, the second method, in which the source stays in the room (closed door), gives lower values than the first one where the source leaves the room (open door). In addition, the second method allows to



evaluate emission rates and particle deposition velocity in the rooms. CO<sub>2</sub> emission rates calculated for BD2 (always closed during sleeping time) and PM<sub>2.5</sub> emission rates calculated for cooking events, were found to be in line with values from the available literature. However, the method in question seems to overestimate the values calculated for particle deposition velocity.

To provide valuable insights in indoor pollutant behaviour, low-cost sensors must be completed with additional information such as room occupation and doors/windows status. In this study, the log file had this purpose, but it requires systematic recording of any changes and so it is not flawless. Occupation may be derived from the use of several signals from the sensors (CO<sub>2</sub> concentration, light intensity and noise level) but the knowledge of the doors/windows status needs additional connected sensors.

## 5 REFERENCES

- Borsboom, W., de Gids, W., Logue, J., Sherman, M.H., Wargocki, P. (2016). Technical note AIVC 68 - Residential ventilation and health, AIVC, Technical report.
- Dimitroulopoulou, C., Ashmore, M.R., Hill, M.T.R., Byrne, M.A., Kinnersley, R. (2006). INDAIR: A probabilistic model of indoor air pollution in UK homes. *Atm. Env.*, 40(33), 6362-6379.
- Fisk, W.J., Black, D., Brunner, G. (2011). Benefits and costs of improved IEQ in U.S. offices. *Indoor Air*, 21(5), 357-367.
- Fogh, C.L., Byrne, M.A., Roed, J., Goddard, A.J.H. (1997). Size specific indoor aerosol deposition measurements and derived I/O ratios. *Atm. Env.*, 31, 2193-2203.
- García, M.R., Spinazzé, A., Branco, P.T.B.S., Borghi, F., Villena, G., Cattaneo, A., Di Gilio, A., Mihucz, V.G., Álvarez, E.G., Lopes, S.I., Bergmans, B., Orłowski, C., Karatzas, K., Marques, G., Saffell, J., Sousa, S.I.V. (2022). Review of low-cost sensors for indoor air quality: Features and applications. *Applied Spectroscopy Reviews*, 57(9-10), 747-779.
- Liu, C., Yang, J., Ji, S., Lu, Y., Wu, P., Chen, C. (2018). Influence of natural ventilation rate on indoor PM<sub>2.5</sub> deposition. *Building and Environment*, 144, 357-364.
- NF EN 16798-1:2019. Energy performance of buildings - Ventilation for buildings - Part 2: interpretation of the requirements in EN 16798-1. Indoor environmental input parameters for design and assessment of energy performance of buildings addressing indoor air quality, thermal environment, lighting and acoustics (Module M1-6). 2019.
- Özkaynak, H., Xue, J., Spengler, J.D., Wallace, L.A., Pellizzari, E.D., Jenkins, P. (1996) Personal exposure to airborne particles and metals: results from the particle TEAM study in Riverside, California. *Journal of Exposure Analysis and Environmental Epidemiology*, 6, 57-78.
- Persily, A.K., de Jonge L. (2017). Carbon Dioxide Generation Rates of Building Occupants. *Indoor Air*, 27(5), 868-879.
- Wargocki, P., Seppänen, O., Andersson, J., Boerstra, A. (2006). Indoor climate and productivity in offices. How to integrate productivity in life-cycle cost analysis of building services, Brussels, *REHVA Guidebook n°6*.
- WHO (2010). WHO guidelines for indoor air quality: selected pollutants, World Health Organization, Regional office for Europe.
- WHO (2014), World Health Organization – Burden of Disease from the Joint Effects of Household and Ambient Air Pollution for 2012, Climate & Clean Air Coalition. <https://www.ccacoalition.org/en/resources/world-health-organization-%E2%80%93-burden-disease-joint-effects-household-and-ambient-air> (accessed June 26, 2024).

# Summertime Resilience in an L-Shaped Long-Term Care Facility with Mixed Natural Ventilation and Pressurized Corridors

Chang Shu<sup>\*1</sup>, Lili Ji<sup>1</sup>, Justin Berquist<sup>1</sup>, Liang Grace Zhou<sup>1</sup>

*1 Construction Research Center, National Research Council Canada  
1200 Montréal Road  
Ottawa, Ontario, Canada*

*\*Corresponding author: Chang.Shu2@nrc-cnrc.gc.ca*

## ABSTRACT

Climate change has exacerbated the summertime overheating in buildings, necessitating resilient adaptation strategies. Based on our previous work, which introduced a Thermal Resilience Index (TRI) ranging from Class F to Class A+ using a concept of resilient trapezoid framework, this study explores unit-level retrofit strategies for high-rise long-term care buildings. Utilizing a building simulation model validated by field data from a long-term care building located in Montreal, Canada, the thermal resilience of entire buildings and individual units is evaluated with mixed natural ventilation and pressurized corridors. The analysis highlights significant heterogeneity in units' resilience to extreme heat. The impact of different corridor ventilation configurations on room temperatures, thermal stratification across floors and unit-level thermal resilience are evaluated, following the ASHRAE standards 62.1, 62.2 and ventilation suggestions for the COVID pandemic. Results indicate that an enhanced ventilation rate in the corridor can mitigate the overheating conditions in the building, while it can yield diverse outcomes across units. These findings will inform our retrofit strategies in the field study and will be further evaluated with field-collected data.

## KEYWORDS

Thermal resilience, long-term care building, ventilation, pressurized corridor, overheating

## 1 INTRODUCTION

Increasing global temperatures pose significant challenges to indoor environmental quality, particularly in long-term care facilities where residents are especially vulnerable to heat-related stresses. Ensuring thermal comfort in these settings is not only a matter of energy efficiency but also of health and safety. Buildings with inner corridors, where rooms are distributed along both sides, can pose ventilation challenges. A CFD simulation study (Chen et al., 2024) of an L-shaped residence with such corridors shows poor natural ventilation, their results indicated a high age of air in both the corridor and the unit rooms. Studies show that opening doors between rooms and corridors significantly boosts interzonal air exchange volume, and larger temperature differences between areas can further amplify the air exchange (Lee et al., 2016). Furthermore, this approach can also improve the thermal environment within spaces. A case study in multi-zone buildings showed that overheating is significantly reduced when windows and room doors are fully opened to facilitate cross ventilation. (Schünemann et al., 2021).

During a site visit to several long-term care buildings in Montreal, Canada, in the summer of 2019, we observed that residents often leave room doors wide open to mitigate indoor overheating (Figure 1). This practice significantly enhances the exchange of airflow between

rooms and corridors. According to the ASHRAE handbook (2013), ventilation plans must address pollutants in rooms with contaminated air—such as chemistry laboratories, smoking rooms, bathrooms, hospitals, and medical facilities—because they can affect the air quality of adjacent areas. To solve this issue, a negative pressure difference between a contaminated room and its surrounding areas is required. The use of pressurized corridors (PC) has become a widespread solution for maintaining these pressure differences. However, the effectiveness of this system varies in high-rise buildings due to the stack effect, which can cause uneven ventilation, leading to under-ventilation in lower rooms, over-ventilation in upper rooms, and reduced corridor pressurization on lower floors. (Fine & Touchie, 2021).



Figure 1: Operation of room-to-corridor doors in long-term care buildings in Montreal, Canada (Photos taken during a site visit in July 2019)

Given the dual requirements for overheating relief and airflow control, it is essential to investigate mixed-mode ventilation that combines natural and mechanical pressurized corridor ventilation. The effects of this approach, involving pressurized corridors and window/door operations, on the building's thermal conditions across different floors and zone-level thermal resilience, are not yet well investigated.

This study investigated the thermal condition variations of a five-floor, L-shaped long-term care building in Montreal, Canada, through a parametric building simulation of various mixed-mode ventilation strategies. We explored how window and door openings, along with the distribution and flow rate of the pressurized corridor (PC) system, influence thermal conditions across different floors and rooms. The method for evaluating building and zonal thermal resilience developed in a previous study (Ji et al., 2023) has been applied to quantify and categorize the thermal resilience levels of rooms.

## 2 METHODOLOGY

### 2.1 Overview

Figure 1 outlines the workflow used in this paper to quantify the zonal thermal resilience with different ventilation strategies. In the first step, a multi-zone building model is created based on the actual building situations and the model is validated with field measurement data. Then, in the second step, the various ventilation scenarios with mechanical pressurized corridor ventilation and natural ventilation with different window/door operations are integrated into the model. The final step involves quantifying and comparing the zonal thermal resilience for each scenario. These steps are elaborated upon in Sections 2.2, 2.3, and 2.4, respectively.

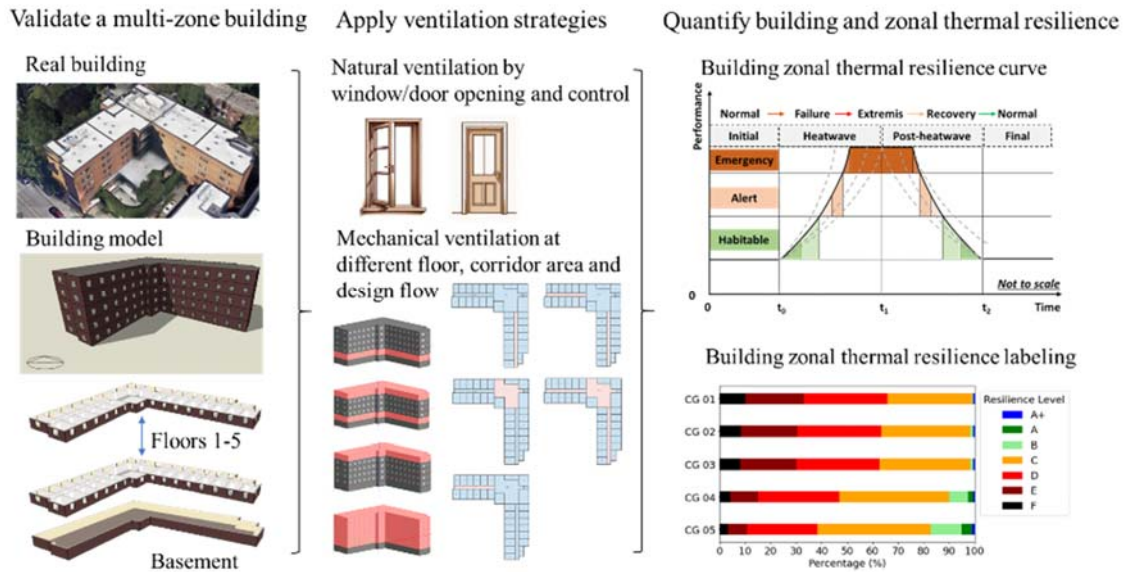


Figure 2: Workflow of quantifying the zonal thermal resilience with different ventilation strategies

## 2.2 Building model and validation

The building model was developed for a long-term care building constructed in the 1980s with a footage area of 817m<sup>2</sup>, which is one of the buildings in an overheating monitoring campaign conducted in Montreal, Canada since the summer of 2020 (Wang et al., 2020). The long-term care facility is an L-shaped building with five above-ground floors and a below-grade basement, facing south. Most of the patient rooms and offices in this building are naturally ventilated, with only a few rooms equipped with window air conditioners. The first column in Figure 1 shows the map view of the building.

The indoor temperature and relative humidity (RH) were continuously monitored in selected spaces on different floors and orientations, at a 15-minute interval. The sensor accuracy is  $\pm 0.21^{\circ}\text{C}$  for air temperature and  $\pm 2\%$  for relative humidity (RH) (Xie et al., 2021). Weather stations were placed on the roof of this building to gather local weather information, including air temperature ( $\pm 0.21^{\circ}\text{C}$ ), relative humidity ( $\pm 2\%$ ), solar radiation ( $\pm 10\text{ W/m}^2$ ), wind speed and direction, and precipitation. The measured indoor and outdoor environment data were used to calibrate and validate the building model (Ji et al., 2022a). The building parameters, architecture plan, operation schedules, and air conditioning information of the building were collected through a building survey and site visit (Wang & Shu, 2021). The unknown parameters, including envelope thermal properties, internal heat gains, and natural ventilation rate, were calibrated through a Monte Carlo method (Hoffman, 2014) based on the measured hourly indoor temperature (Ji et al., 2022a). At the room level, considering the  $\pm 0.21^{\circ}\text{C}$  sensor accuracy for indoor air temperature measurements, the root means square error (RMSE) between the simulated and measured temperatures during calibration and validation ranged from  $0.56^{\circ}\text{C}$  to  $1.13^{\circ}\text{C}$ . Both values are well within the acceptable limit of  $1.5^{\circ}\text{C}$  suggested by previous studies. (O' Donovan et al., 2019). More details on the calibration and validation of this building can be found in the studies by Ji et al. (2022, 2023). A total of 175 thermal zones, including naturally ventilated patient rooms, stairwells, and corridors, were investigated to analyse zone-level thermal resilience for this building.

## 2.3 Ventilation case design

Table 1: Designed cases of natural and mechanical ventilation strategies






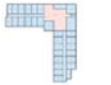
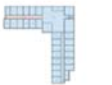
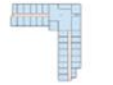

Natural ventilation (NV)	Window opening	5%		10%		15%					
	Window control	$(T_{in} > T_{setpoint26}) \& (T_{in} > T_{out})$									
	Door opening · time	2.5%		50%		100%					
	Door control	$(T_{in} > T_{setpoint26}) \& (T_{in} > T_{corridor})$			$(T_{in} > T_{setpoint26}) \& (T_{in} > T_{out})$						
Mechanical ventilation (MV)	MV floor	1 		5 		1+5 		1+2+3+4+5 			
	MV corridor	Right 		Center 		Left 		Right+Left 		Right+Center+Left 	
	MV design flow	0.3L/s/m <sup>2</sup> *		0.35ACH **		3ACH ***		6ACH ***			
	<small>* ASHRAE 62.1-2019: Ventilation for Acceptable Indoor Air Quality, 2019.  ** ASHRAE 62.2-2016: Ventilation and Acceptable Indoor Air Quality in Residential Buildings, 2016.  *** Salimifard P., Jones E., Allen J. "Portable Air Cleaners: Selection and Application Considerations for COVID-19 Risk Reduction." Harvard T.H. Chan School of Public Health Healthy Buildings Program, August, 2020.</small>										

Table 2: Cases grouped by MV design flow

Case group (CG)	Number of cases	Total number of zones	NV/MV	MV design flow
01	18	3150	NV	0
02	486	85050	NV+MV	0.3L/s/m <sup>2</sup>
03	486	85050	NV+MV	0.35ACH
04	486	85050	NV+MV	3ACH
05	486	85050	NV+MV	6ACH

To assess the impact of various ventilation strategies on zone-level thermal resilience, 1962 models were created. Of these, 18 were naturally ventilated (NV), while 1944 combined natural and mechanical ventilation (NV+MV). As detailed in Table 1, for the NV cases, the exterior windows and internal doors connecting each bedroom zone to the corridor in each zone are set with three possible opening percentages. The windows are opened when the indoor temperature ( $T_{in}$ ) is higher than the setpoint temperature of 26°C and at the same time higher than the outdoor temperature ( $T_{out}$ ). The doors are controlled by two possible strategies: a) they are opened when the indoor temperature is higher than both the setpoint temperature of 26°C and the corridor temperature ( $T_{corridor}$ ), b) they are opened when the indoor temperature higher than both the setpoint temperature of 26°C and the outdoor temperature ( $T_{out}$ ).

In NV+MV cases, alongside natural ventilation controls, mechanical ventilation from the corridors is distributed across different floors and various areas within each floor. Four potential mechanical ventilation (MV) design flows were considered, adhering to both standard ventilation requirements and enhanced protocols for COVID-19 risk reduction. (ASHRAE, 2022, 2022; Salimifard et al., 2020). The cases are organized into five groups (CG01 to CG05), categorized by different mechanical ventilation (MV) design flow rates as detailed in Table 2.

## 2.4 Thermal resilience quantification

The zone-level thermal resilience quantification method for multi-zone buildings was developed by the study of Ji et al. (2023). There are four main steps in the quantification of

building thermal resilience, 1) confirming of the thermal performance indicator, 2) constructing the thermal resilience curve, 3) calculating the thermal resilience quantification index, and 4) labelling the thermal resilience level.

In step one, the thermal performance indicator chosen should represent the thermal performance of each thermal zone. In this study, the Standard Effective Temperature (SET) was selected as the heat-stress index. SET is calculated using environmental parameters such as air temperature, relative humidity, mean radiant temperature, and airflow speed, as well as human parameters like activity and clothing levels, based on a two-node physiological model. In step two, the resilience trapezoid profile (Figure 2 a) is employed to construct the thermal resilience curve. This curve captures the timing and extent of system failure, duration of the extreme state, and recovery to a normal state. The building thermal resilience trapezoid consists of two periods—the heatwave period and the post-heatwave period—and includes three thresholds ( $SET_{\text{conf}} = 24.12\text{ }^{\circ}\text{C}$ ,  $SET_{\text{alert}} = 28.12\text{ }^{\circ}\text{C}$ ,  $SET_{\text{emer}} = 32.12\text{ }^{\circ}\text{C}$ ), and three hazard levels (habitable level, alert level, emergency level). In step three, the zone-level thermal resilience index ( $TRI_z$ ) is calculated by Equation (1)

$$TRI_z = WSETH_{z,0}/WSETH_z \quad (1)$$

where  $WSETH_{z,0}$  is the zone thermal resilience of a reference case. In this study, the reference case for other building settings is a natural ventilation scenario with 5 % window opening, 2.5 % door opening, and controlled by ( $T_{\text{in}} > 26\text{ }^{\circ}\text{C}$ ) & ( $T_{\text{in}} > T_{\text{corridor}}$ ).  $WSETH_z$  is the thermal resilience of a studied zone, which can be calculated by Equation (2)

$$WSETH_z = \sum_1^{12} WSETH_i = \sum_1^{12} SETH_i W_{1,i} W_{2,i} W_{3,i} \quad (2)$$

where  $i$  is the segment number of the 12 segments separated by the two periods, three hazard levels, and exposure time at each hazard level,  $SETH_i$  is the integration of SET above its hazard threshold over time,  $W_{1,i}$ ,  $W_{2,i}$ ,  $W_{3,i}$  are the penalty coefficients that the higher the penalty coefficient, the more difficult for the building to recover from exposure to heat.

In step four, according to the value of  $TRI_z$ , each zone can be labelled by their resilience class from Class F to Class A+ (Figure 2 b). More detailed explanations can be found in the study of Ji et al. (2023).

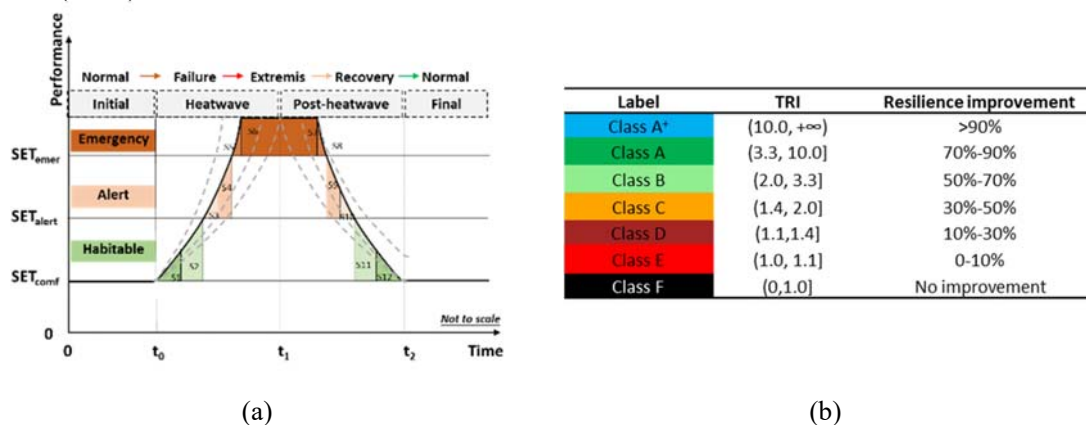


Figure 3: (a) Conceptual thermal resilience profile and (b) thermal resilience labelling system (Ji et al., 2023)

## 2.5 Study period and weather data

The simulation in this study focused on a heatwave event occurred in Montreal, Canada in the summer of 2018, from June 30 to July 05, which resulted in 66 heat-related deaths (Lamothe et al., 2019). The weather data was collected from hourly measurements from a weather station located in the urban area of Montreal (Shu et al., 2022). The air temperature, relative humidity, wind speed, wind direction, solar radiation, and precipitation were collected and converted to an EPW format for input to the Energyplus (DOE, 2022) building simulation model.

### 3 RESULTS

#### 3.1 Physical environment changes in buildings

Figure 3 shows the averaged physical parameters (temperature and relative humidity) of all cases in each case group. It can be noted that the indoor temperature (T) is reduced with the increase of mechanical ventilation design flow rate (Figure 3 a). The reduction in temperature is more notable in CG04 (PC ACH=3) and CG05 (PC ACH =6) than CG02 (PC flow rate =  $0.3\text{L/s/m}^2$ ) and CG03 (PC ACH = 0.35). The averaged RH in each case group is comparable while CG04 and CG05 present slightly higher RH due to the increased introduction of outdoor air.

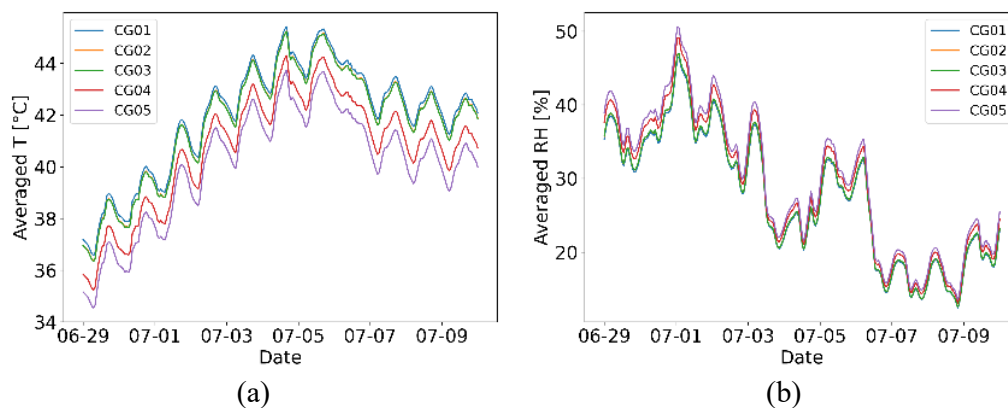


Figure 4: The averaged (a) zone means air temperature (T) (b) zone mean relative humidity (RH) of each case group

#### 3.2 Thermal stratification

Thermal index SET is calculated for each zone based on the calculated T, RH, mean radiant temperature ( $T_{mrt}$ ) and an assumed air flow of  $0.1\text{m/s}$ , an occupant metabolic rate of 1.2 met, a clothing level of 0.5clo, and a body surface area of  $1.8258\text{m}^2$ . The difference of SET in zones on Floors 2-5 with the SET in zones on Floor 1 is calculated to show the vertical thermal stratification in the building as presented in Figure 4. Notably, the SET difference is reduced from CG01 to CG05, as the increase of MV design flow rate suppressed the thermal stratification.

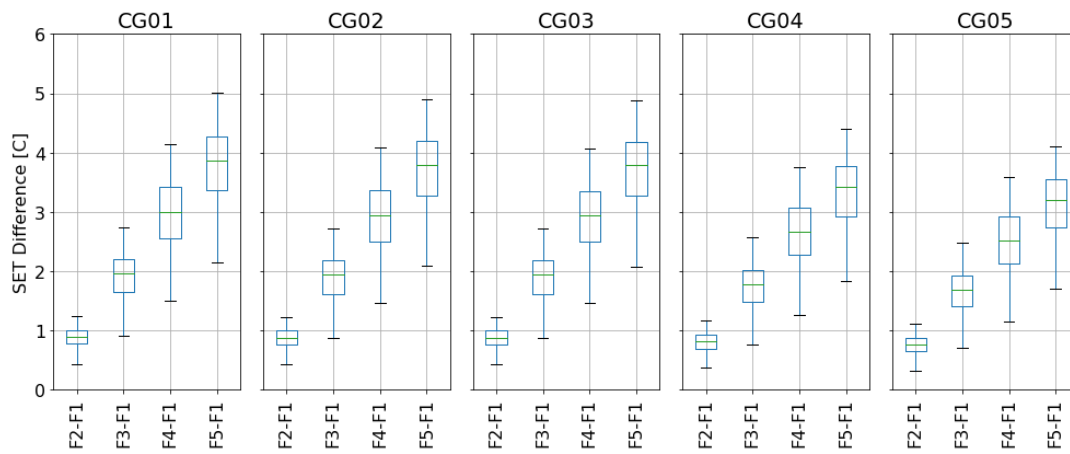


Figure 5: Distribution of the SET difference between floors 2-5 and floor 1 for each case group

### 3.3 Thermal zone resilience

Following the thermal resilience labelling method in Section 2.4, the TRIZ in each zone of each case is calculated for their resilience level labelling. Figure 5 shows the percentage of zones in different resilience levels for each case group. With an increased MV design flow rate, more zones achieve a higher resilience label. Compared to CG01 (the reference natural ventilation scenario), CG05 (PC ACH=6) can reduce the zones in Class F from 10% to less than 3% and increase the zones of Class A+, A, B and C from 34% to more than 60%. This means that compared to the reference natural ventilation case, the thermal resilience of more than half of zones are improved by at least 30%.

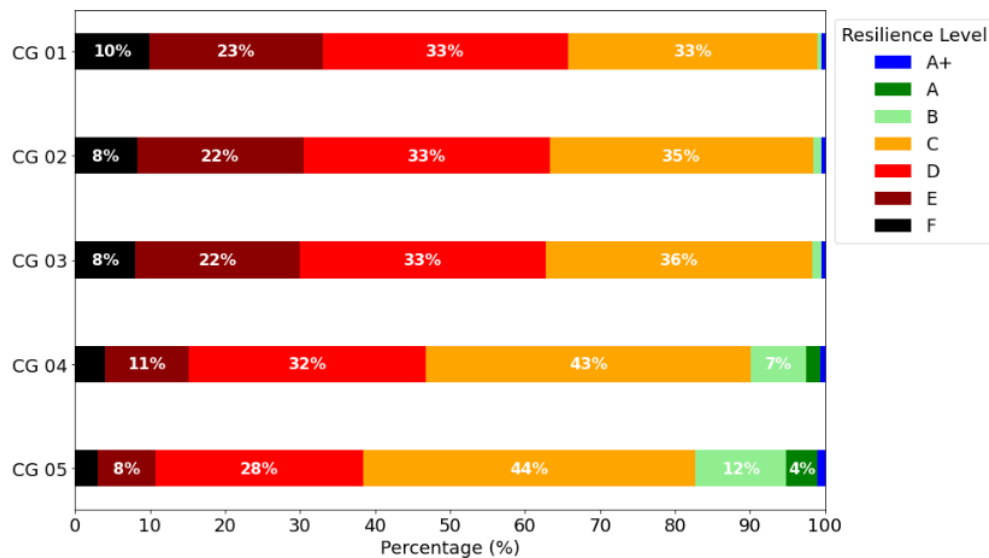


Figure 6: Percentage of zones in different classes of resilience levels in each case group

## 4 CONCLUSIONS

This study investigates how mixed-mode ventilation, combining pressurized corridors and natural ventilation, impacts thermal conditions and zone-level thermal resilience in an L-shaped, five-floor long-term care building. A parametric analysis of 1,962 scenarios, varying



corridor ventilation and window/door controls are simulated and analysed. Preliminary conclusions are as follows.

- The introduction of corridor ventilation reduces the overall indoor temperature and a higher air supply rate in the corridor can enhance the thermal resilience of the units.
- The thermal stratification in this building is suppressed by the increased corridor ventilation design flow rate.
- Compared to scenarios using only natural ventilation, mixed-mode ventilation with pressurized corridors enhances thermal resilience in over half of the zones by at least 30%.

The current study only focuses on the impact of corridor ventilation rates on the overheating conditions and thermal resilience in different units. The distribution of air supply vents and the operation of windows and doors will be further discussed in subsequent research.

## 5 ACKNOWLEDGEMENTS

This research was funded by the Resilient Residential Retrofit (R<sup>3</sup>) theme of the Climate Resilient Built Environment Initiative (CRBE) of the National Research Council Canada (NRCC) and received support from the seventh wave of Postdoctoral Fellowship (PDF) program of the NRCC.

## 6 REFERENCES

- ASHRAE. (2022). *ANSI/ASHRAE Standard 62.1: Ventilation and Acceptable Indoor Air Quality*. [www.ashrae.org/technology](http://www.ashrae.org/technology).
- ASHRAE. (2022). *ANSI/ASHRAE Standard 62.2: Ventilation and Acceptable Indoor Air Quality in Residential Buildings*. [www.ashrae.org](http://www.ashrae.org)
- ASHRAE handbook. (2013). *Health care facilities*. [www.healthdesign.com.au/haad.hfg/](http://www.healthdesign.com.au/haad.hfg/)
- Chen, S., Fan, Z., He, L., Ma, S., & Liu, J. (2024). Ventilation benefit assessment of space organization design for ‘L’ type inner corridor buildings. *Building and Environment*, 253. <https://doi.org/10.1016/j.buildenv.2024.111327>
- DOE. (2022). *EnergyPlus 22.1.0*. <https://energyplus.net/>
- Fine, J. P., & Touchie, M. F. (2021). Evaluating ventilation system retrofits for high-rise residential buildings using a CONTAM model. *Building and Environment*, 205. <https://doi.org/10.1016/j.buildenv.2021.108292>
- Hoffman. (2014). *The No-U-Turn Sampler: Adaptively Setting Path Lengths in Hamiltonian Monte Carlo*. 15, 1593–1623.
- Ji, L., Shu, C., Hou, D., Laouadi, A., Leon, L., & Lacasse, M. (2022a). Predicting indoor air temperatures by calibrating building thermal model with coupled airflow networks. 2022: *CLIMA 2022 The 14th REHVA HVAC World Congress*, 1–8. <https://doi.org/https://doi.org/10.34641/clima.2022.340>
- Ji, L., Shu, C., Hou, D., Laouadi, A., Leon, L., & Lacasse, M. (2022b). Predicting indoor air temperatures by calibrating building thermal model with coupled airflow networks. 2022: *CLIMA 2022 The 14th REHVA HVAC World Congress*, 1–8. <https://doi.org/https://doi.org/10.34641/clima.2022.340>
- Ji, L., Shu, C., Laouadi, A., Lacasse, M., & Wang, L. (Leon). (2023). Quantifying improvement of building and zone level thermal resilience by cooling retrofits against summertime heat events. *Building and Environment*, 229. <https://doi.org/10.1016/j.buildenv.2022.109914>

- Lamothe, F., Roy, M., & Racine-Hamel, S.-É. (2019). *Enquête épidémiologique - Vague de chaleur à l'été 2018 à Montréal*.  
[https://doi.org/https://santemontreal.qc.ca/fileadmin/user\\_upload/Uploads/tx\\_asssmpublications/pdf/publications/](https://doi.org/https://santemontreal.qc.ca/fileadmin/user_upload/Uploads/tx_asssmpublications/pdf/publications/)
- Lee, S., Park, B., & Kurabuchi, T. (2016). Numerical evaluation of influence of door opening on interzonal air exchange. *Building and Environment*, *102*, 230–242.  
<https://doi.org/10.1016/j.buildenv.2016.03.017>
- Leon, L., Shu, C., Ge, H., Zmeureanu, R., Lacasse, M., & Leroyer, S. (2020). Assessment of summertime overheating conditions in vulnerable buildings in Montréal. *2nd International Conference on New Horizons in Green Civil Engineering (NHICE-02)*, Victoria, BC, Canada, April 29 – May 01, 2020, November, 2–5.
- O' Donovan, A., O' Sullivan, P. D., & Murphy, M. D. (2019). Predicting air temperatures in a naturally ventilated nearly zero energy building: Calibration, validation, analysis and approaches. *Applied Energy*, *250*(May), 991–1010.  
<https://doi.org/10.1016/j.apenergy.2019.04.082>
- Salimifard, P., Jones E., & Allen J. (2020). *Portable Air Cleaners: Selection and Application Considerations for COVID-19 Risk Reduction*.
- Schünemann, C., Schiela, D., & Ortlepp, R. (2021). How window ventilation behaviour affects the heat resilience in multi-residential buildings. *Building and Environment*, *202*.  
<https://doi.org/10.1016/j.buildenv.2021.107987>
- Shu, C., Gaur, A., Wang, L. (Leon), Bartko, M., Laouadi, A., Ji, L., & Lacasse, M. (2022). Added value of convection permitting climate modelling in urban overheating assessments. *Building and Environment*, *207*(PA), 108415.  
<https://doi.org/10.1016/j.buildenv.2021.108415>
- Wang, L. (Leon), & Shu, C. (2021). Chapter 2: Assessment of the Effect of Urban Heat Island on Buildings. In N. Enteria, M. Santamouris, & U. Eicker (Eds.), *Urban Heat Island (UHI) Mitigation. Advances in 21st Century Human Settlements*. Springer.
- Xie, Z., Shu, C., Reich, B. Z., Wang, L., Baril, D., Ji, L., Yang, S., Bai, X., Zmeureanu, R., Lacasse, M., Wang, L., & Ge, H. (2021). A field study on summertime overheating of six schools in Montreal Canada. *Journal of Physics: Conference Series*, *2069*(1).  
<https://doi.org/10.1088/1742-6596/2069/1/012168>

# Assessment of SARS-CoV-2 and other IAQ parameters in 11 Belgian elderly care homes

Sarah L. Paralovo<sup>1\*</sup>, Annelies Asteur<sup>2</sup>, Borislav Lazarov<sup>1</sup>, Boudewijn Catry<sup>2</sup>, Koenraad Van Hoorde<sup>2</sup>, Maarten Spruyt<sup>1</sup>, Katrien Latour<sup>2</sup>, Marianne Stranger<sup>1</sup>

*1 VITO  
Boeretang 200  
Mol, Belgium*

*2 Sciensano  
Juliette Wytmanstraat 14  
Elsene, Belgium*

\*Corresponding author: sarah.paralovo@vito.be

## ABSTRACT

It is often difficult to implement prevention recommendations and plan targeted measures to limit the spread of airborne viruses in communal spaces. To effectively accomplish this goal, it is crucial to comprehensively characterize the indoor environmental quality in the space and, from these space-specific data, draw recommendations adapted to the setting. In this context, 11 elderly care homes in Belgium were selected for a comprehensive assessment of the indoor air quality (IAQ). IAQ and ventilation parameters were characterized by means of air sampling and questionnaire application. In each elderly care home, a survey on ventilation strategies and behaviour, building characteristics and COVID-19 prevention practices was applied, and 5 rooms were selected for IAQ measurements (2 resident bedrooms, at least one common room for residents, one staff room and one extra common room for residents or visitors). In each room, a set of IAQ parameters expected to be related to the indoor virus transmission (CO<sub>2</sub>, temperature and relative humidity in all rooms, plus PM<sub>2.5</sub> in selected rooms) were continuously monitored with an in-house developed and calibrated sensor box for 7 days. Biological samples were collected from the air (via liquid impingement) and surfaces (via swipe sampling), once per room, for in-lab detection of SARS-CoV-2 RNA copies via RT-qPCR. Particulate matter (PM<sub>2.5</sub>) concentrations in all facilities were most of the time low, not exceeding the applicable PM<sub>2.5</sub> indoor guideline value. CO<sub>2</sub> concentrations generally indicated acceptable levels of ventilation in all facilities, with the lowest CO<sub>2</sub>-concentrations measured in mechanically ventilated ones. Of all collected air samples, 28% contained traces of SARS-CoV-2 RNA, while 63% of the swab samples did. The number of positive SARS-CoV-2 samples collected in each elderly care centre did not follow the trend of Flemish COVID-19 incidence rate during each respective sampling week. In the care homes where there was an on-going COVID-19 outbreak during measurements, all air samples and most of the surface samples tested positive for SARS-CoV-2. In the absence of a reported on-going local outbreak, positive SARS-CoV-2 samples were found mainly on surfaces. These results indicate that more than one positive SARS-CoV-2 air sample in one building might work as an indicator of an on-going outbreak (or at least of the presence of SARS-CoV-2 RNA emitters), which in the context of asymptomatic persons in this setting occupied by a vulnerable population is of high value. Furthermore, even though an indoor CO<sub>2</sub> concentration below 900 ppm is often considered indication of lower risk of indoor virus transmission, the dominant variant at that time of the pandemic (delta) appeared in all SARS-CoV-2 positive air samples. Therefore it is recommended to initiate additional risk reduction strategies in case of a local outbreak, such as increasing ventilation rates, implementing effective air cleaning, using mouth masks and isolating infected persons (symptomatic or not), especially in sensitive settings like these.

## KEYWORDS

Indoor air quality, elderly care homes, airborne pathogens, SARS-CoV-2, COVID-19 prevention

## 1 INTRODUCTION

Respiratory viruses spread mostly through the air, both in short and long ranges, especially in crowded and/or poorly ventilated closed spaces (Morawska and Cao, 2020; Abdin and Mahmoud, 2024). Due to the lack of solid information about indoor air quality (IAQ) and ventilation/airing facilities and behaviour in communal spaces, especially those occupied by

vulnerable populations such as children and the elderly, it is often difficult to formulate targeted recommendations for infection prevention adapted to the setting and its actors. A comprehensive characterization of such indoor environments and their IAQ is crucial to generate appropriate preventive guidelines and recommendations adapted to the setting, based on space-specific data, relevant information and scientific evidence (Kakoulli et al., 2022).

In this context, different communal spaces in Belgium, including spaces for susceptible population groups, were selected for a comprehensive characterization of the indoor environment by means of IAQ measurements and a dedicated questionnaire on ventilation/disinfection behaviour of relevant actors. The data presented in this paper are part of a larger scale Belgian study during the COVID-19 pandemic in 2022, the “AIR-CO” project, which targeted IAQ assessments in elderly care centres, schools, indoor sports facilities and public transport. The primary aim of this study was to provide relevant, space-specific and up-to-date information on IAQ in a range of representative communal spaces to assist in the formulation of appropriate preventive recommendations and guidelines in the context of pandemic preparedness. The present paper focuses on part of this study, reporting the data collected in the elderly care homes in comparison to relevant IAQ Belgian guidelines (Flemish Indoor Environment Decree and Recognition Standard of Residential Care Centres).

The endpoint of this study was to identify priority risk environments and/or parameters to prioritize environments and to help formulate specific solutions or recommendations for a dedicated risk reduction in a specific setting. The ultimate goal was to contribute to the preventive approach to the spread of respiratory viruses in the future, particularly regarding COVID-19 and current/future variants. Finally, the findings can be extended to other sensitive settings in which people come together for relatively long periods of time, e.g. daycare centres, multi-purpose rooms, catering establishments, shopping centres.

## **2 MATERIAL AND METHODS**

### **2.1 Sampling locations**

In total, 11 elderly care homes (or WZCs, from the Dutch *woonzorgcentra*) across Belgium were selected. Indoor assessments took place during the first half of 2022. In each elderly care home (WZC), 5 rooms were selected for measurements: 2 resident bedrooms, at least one common dining room for residents, one staff room and one extra common room either for residents or for visitors, where available. In each selected room, indoor IAQ parameters (CO<sub>2</sub>, temperature and relative humidity in all rooms, plus PM<sub>2.5</sub> in selected rooms) were continuously monitored with an in-house developed sensor box for 7 consecutive days. During this period, air and surface biological samples were collected once per room to determine the presence of SARS-CoV-2 via qPCR analysis.

### **2.2 Measurement techniques**

Custom-made monitoring devices (sensor boxes) containing various low-cost electronic sensors were built for this study to continuously monitor indoor temperature (T), relative humidity (RH), CO<sub>2</sub> and particulate matter (PM<sub>2.5</sub>) in the selected rooms, at a 1-min time resolution. An integrated internal memory allowed secure storage of the measured data during the measurement periods. All sensors integrated into the sensor box were calibrated in lab prior to the assessments, against reference gases/mixtures under controlled conditions (test chamber) using standard measuring instruments as references. The installation of the sensor boxes and practical organisation of the IAQ assessment respected the ISO 16000-1 standard.

Biological samples for viral pathogen analysis were collected in each assessed room on the same day the sensor boxes were installed, in two different formats: surface samples via swabbing and air samples via liquid impingement. Swabs were collected using 3M™ hydrated sponges. Just before sampling, the liquid was poured onto the sponges, which were then rubbed on the desired surface for a few seconds. Ventilation grilles were the primary target surfaces in each room as they represent known points of particle accumulation. High-touch surfaces were the secondary targets (e.g. doorknobs, handles, tabletops, armrests of chairs). The entire target surfaces were scrubbed, thus the surface areas varied considerably between swab samples.

Airborne viral particles were sampled using a Coriolis  $\mu$  device manufactured by Bertin Technologies (St-Berthely, France), consisting of a cyclonic liquid impinger that captures aerosols with an aerodynamic diameter between 0.5 and 20  $\mu\text{m}$  at high air flow rates. Air sampling was performed according to Paralovo et al. (2024): 3 m<sup>3</sup> of air sampled in 3 ml of lysis buffer with one droplet of anti-foaming agent.

One air sample and three swab samples were collected in each assessed room of each selected WZC. The placement of the Coriolis  $\mu$  in the room also respected ISO 16000-1. After sampling, all biological samples were analysed in lab via RT-qPCR analysis, following the protocol described by Janssens et al. (2022). The test targeted three SARS-CoV-2 gene fragments: the nucleocapsid (N1 and N2) and the virus envelop.

Lastly, a survey was conducted to collect relevant information about the selected WZCs, focusing on ventilation characteristics and behaviour as well as disinfection practices. The responses were obtained from the person available to host the research team at the WZC (either a facility manager or a designated nurse).

### 3 RESULTS AND DISCUSSION

#### 3.1 Facilities characteristics and questionnaire responses

Table 1 summarizes the most relevant information collected in the responses to the questionnaires (3 of the 11 WZCs did not respond to the questionnaire). Out of the 11 WZCs, 7 had a balanced mechanical (type D) ventilation system, 3 had only natural ventilation (i.e. 'none' in Table 1), while WZC1 consisted of a newer block with mechanical ventilation (type C: natural air supply and mechanical exhaust) and an older block with only natural ventilation.

Table 1: Most relevant information collected in the responses to the questionnaires.

	WZC										
	1	2	3	4	5	6	7	8	9	10	11
<b>Number of rooms</b>	81	100	96	94	67	93	-	90	114	-	-
<b>Number of staff</b>	80	92	90	67	50	57	-	80	90	-	-
<b>COVID-19 vaxx staff</b>	≥90%	≥90%	≥90%	80-90%	≥90%	≥90%	-	≥90%	≥90%	-	-
<b>COVID-19 vaxx residents</b>	≥90%	≥90%	≥90%	≥90%	≥90%	≥90%	-	≥90%	≥90%	-	-
<b>COVID-19 booster residents</b>	≥90%	≥90%	≥90%	≥90%	≥90%	≥90%	-	≥90%	≥90%	-	-
<b>Number of residential units</b>	3	3	3	2	3	3	-	4	3	-	-
<b>Construction year</b>	<2000	<2000	>2000	<2000	>2000	>2000	-	>2000	>2000	-	-
<b>Infection prevention committee?</b>	Yes	Yes	Yes	No	No	No	-	Yes	No	-	-
<b>Cleaning surfaces: high-touch surf.</b>	Daily	Daily	Daily	Daily	Daily	Daily	-	Daily	Daily	-	-
<b>Cleaning surfaces: not touched often</b>	Weekly	Weekly	Weekly	GA	Daily	Weekly	-	Monthly	Weekly	-	-
<b>Isolation of COVID+ residents</b>	Ward/ Room	Room	Room	Room	Ward	Room	-	Room	Ward/ Room	-	-
<b>Type mech. vent. system*</b>	C/ None	None	D	None	D	D	D	D	D	D	None
<b>Ventilation altered since COVID-19</b>	No	No	Yes	No	No	No	-	Yes	No	-	-

\*Information collected by the research team regardless of survey response.

Overall, it was noticed that several facilities had difficulty answering questions regarding the ventilation systems and their practical operation in the facilities. This observation is in line with research projects on ventilation and IAQ performed by the research team in the last 15 years, e.g. in a study on the IAQ and ventilation characteristics of 15 Flemish WZCs (Flemish Government, 2024) and in several IAQ assessments in Flemish schools and daycare centres (De Jonge et al., 2023; Paralovo et al., 2023). This highlights the need for further sensibilization among WZC staff in general regarding the importance of ventilation.

### 3.2 CO<sub>2</sub> and PM<sub>2.5</sub>

During the COVID-19 pandemic a concentration of 900 ppm CO<sub>2</sub> (or 40 m<sup>3</sup> person<sup>-1</sup> hour<sup>-1</sup>) was recommended in Belgium as an indicator of sufficient ventilation in any indoor environment. This recommendation was exceeded at least once in at least one of the assessed rooms in all WZCs studied. Regarding PM<sub>2.5</sub>, all WZCs showed high isolated concentration peaks (most likely related to indoor activities such as cleaning), but during most of the sampling time concentrations were considerably low, complying with the Indoor Air Guideline's target value of 10 µg m<sup>-3</sup> as specified in the Flemish Indoor Air Decree (Flemish government, 2018), which applies to the public as well as private rooms in a WZC. Although low-cost sensors in general have lower accuracy than other IAQ monitors, their generated data are highly useful if they are properly calibrated.

Figure 1 summarizes the CO<sub>2</sub> and PM<sub>2.5</sub> data measured during the occupied hours in boxplots, in two different categorizations: by type of room (resident bedroom, common room, staff room and others) and by the presence of mechanical ventilation in each room. The occupied hours were defined per room type as:

- Common areas: 7h30 to 9h30 (breakfast), 11h to 13h (lunch), 16h30 to 18h30 (dinner)
- Resident rooms: 20h to 7h (sleeping hours)
- Staff rooms and others: 8h to 18h (working hours)

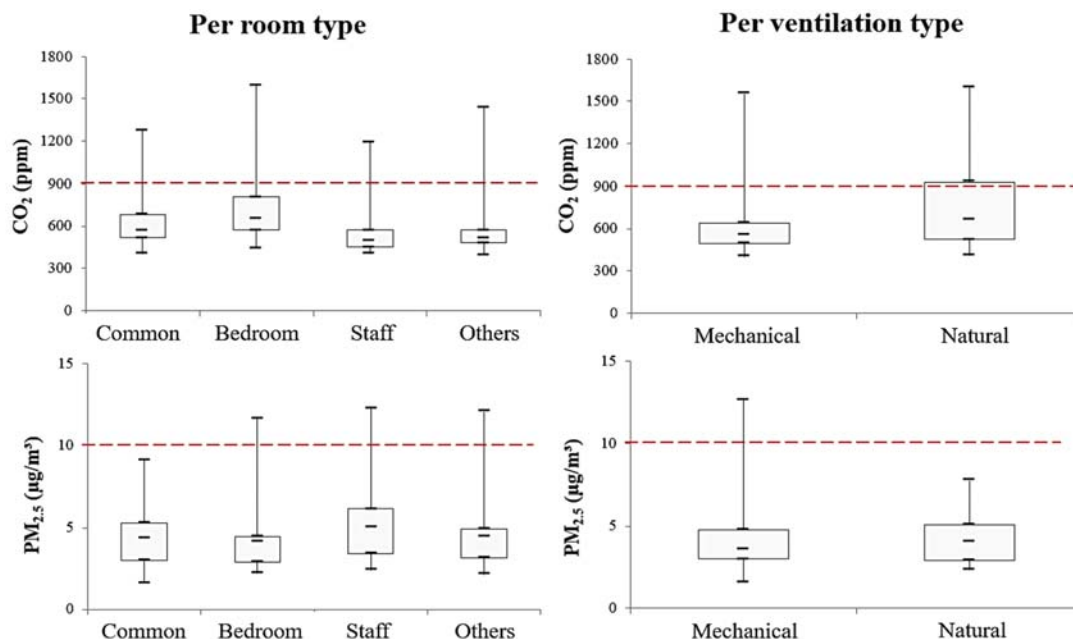


Figure 1: Concentrations of CO<sub>2</sub> (top) and PM<sub>2.5</sub> (bottom) classified by room type (left; 'others' include all assessed areas that have a different use: visitors cafeteria, entrance hall, hair salon, physiotherapy room) and type of ventilation in the room (right).

Analysing the box plots on the left side of Figure 1, no striking differences can be noted between the different room types in terms of CO<sub>2</sub> or PM<sub>2.5</sub> levels. It appears that resident bedrooms achieve slightly higher CO<sub>2</sub> concentrations, while staff rooms and others have the lowest overall concentrations on a daily basis (which is expected due to lower and more variable occupancy in the latter). The higher CO<sub>2</sub> concentrations in some resident rooms may indicate a less adequate ventilation during the night, which is commonly noticed in bedrooms as during the night, people tend to close windows and doors and ventilation systems often have a lower flow rate for energy saving reasons. The opposite was observed for PM<sub>2.5</sub>: the resident bedrooms had the lowest concentrations. This was expected because events that usually suspend the most particles to the air (e.g. dusting, cleaning, occupant's movement) usually occur during the working hours, which were excluded from the bedrooms' datasets for this analysis.

The box plots on the right side of Figure 1 indicate a clear difference between the CO<sub>2</sub> levels for the mechanically ventilated rooms versus the non-mechanically ventilated rooms. Although the maximum values were very similar, the mechanically ventilated rooms showed considerably lower P75 and average CO<sub>2</sub> concentrations, while in the naturally ventilated rooms the CO<sub>2</sub> concentration was above 932 ppm for 25% of the occupied period. Only in the 4 WZCs without mechanical ventilation (WZCs 1, 2, 4 and 11) did the P75 value exceed the 900-ppm guideline in at least one of the investigated areas. On the other hand, PM<sub>2.5</sub> concentrations were only moderately lower in the mechanically ventilated WZCs. A possible explanation is that most WZCs tend to be located in areas where outdoor PM is also considerably low (i.e. away from urban centers), and thus the absence of filtration of incoming air by mechanical ventilation systems might not be as relevant regarding the indoor PM.

### 3.3 Temperature and RH

According to the Flemish Indoor Environment Decree, indoor T must remain between 20-24°C and indoor RH between 40-60% during the cold season, and between 22-26°C and 30-70% during the warm season. Specifically for WZCs, the Decree of the Flemish Government regarding the Recognition Standard of Residential Care Centres (2019) stipulates that T in all living areas during the day is at least 22°C regardless of the season, and that all measures are taken to maintain T < 26°C in all accommodation spaces. Table 2 provides an overview of T and RH values measured in the 11 WZCs during occupied hours. Cells are coloured according to the Flemish recommendations: orange cells indicate T > 28°C or RH < 30%, yellow cells indicate 28°C > T > 26°C or 30% < RH < 40%, dark blue cells indicate T < 20°C or RH > 70%, and light blue cells indicate 20°C < T < 22 °C or 70% > RH > 60%.

In addition to its contribution to the thermal comfort of occupants, T can also strongly affect their behaviour, especially regarding ventilation (e.g. windows opening). Table 2 shows that in most WZCs there was a trend towards temperatures above the recommended value (26°C), even though the measurements were carried out during the cold season. WZC3 was particularly warm, as even the minimum temperatures in both resident bedrooms were above the maximum recommendation. This tendency towards overheating was less apparent in the rooms where residents are not expected to be present (staff rooms and others). On the other hand, in these rooms (and less often in the resident bedrooms and common areas) there were also some cases where T fell below the minimum recommended value for WZCs (22°C) or even the value stipulated by the Flemish decree (20°C).

Various of the interviewed employees reported that the residents often complain about feeling cold or chilly at temperatures that the staff themselves find pleasant, and that they therefore often increase heating in the resident rooms and common areas. Some employees also

mentioned that they often avoid opening windows, even if they feel that the air is "stuffy", for the sake of residents' thermal comfort.

Table 2: Overview of the temperature and RH measured during occupied periods in each studied room per WZC.

		T [°C]											RH [%]										
WZC		1	2	3	4	5	6	7	8	9	10	11	1	2	3	4	5	6	7	8	9	10	11
1 <sup>st</sup> Res. bedroom	Max.	24,2	25,2	29,3	27,4	27,7	27,4	26,5	26,1	27,7	27,0	26,2	44,8	30,5	29,8	30,4	38,5	39,1	36,2	34,1	30,6	39,7	49,4
	P75	22,5	24,7	29,0	26,7	25,3	26,0	26,1	24,9	26,9	26,3	23,9	36,2	26,6	27,3	21,9	31,5	32,7	31,3	31,8	25,7	37,1	46,1
	Mean	21,7	24,4	28,7	25,4	24,5	25,6	25,8	24,0	25,7	26,0	23,5	33,0	25,6	21,8	19,7	29,0	30,4	28,5	26,7	23,1	34,7	43,4
	Min.	19,1	22,9	27,4	22,9	22,6	24,2	25,0	19,0	23,4	25,1	22,4	22,6	22,2	13,6	15,4	22,0	20,0	24,3	16,3	16,2	26,9	29,8
	2 <sup>nd</sup> Res. bedroom	Max.	22,0	24,9	29,4	27,1	30,2	25,2	26,5	25,6	-	-	28,7	54,0	34,4	31,5	32,8	36,2	-	37,5	35,4	-	-
P75	21,2	23,9	28,5	26,3	27,8	24,4	26,0	24,6	-	-	25,9	49,3	32,7	28,0	31,2	28,1	-	30,5	32,4	-	-	42,9	
Mean	20,5	23,5	28,1	25,9	26,9	24,1	25,4	24,3	-	-	25,1	46,4	30,8	22,5	25,6	26,1	-	27,8	28,3	-	-	39,4	
Min.	19,3	22,2	26,5	24,7	24,4	23,0	24,1	23,2	-	-	23,2	38,0	25,9	14,9	16,0	19,0	-	21,4	22,5	-	-	27,2	
1 <sup>st</sup> Comm. room	Max.	27,9	25,2	27,8	32,0	26,4	26,2	25,8	25,8	25,6	32,3	-	43,1	31,4	36,7	43,6	61,9	42,2	42,5	43,5	38,2	49,1	-
	P75	26,2	24,3	26,3	24,5	24,4	25,5	25,1	24,8	24,8	28,6	-	34,2	27,2	30,0	31,9	32,3	33,5	33,0	31,8	27,8	35,4	-
	Mean	24,9	23,6	25,5	23,6	23,9	25,1	24,7	24,1	24,4	27,9	-	30,4	25,3	24,8	27,4	29,2	29,8	29,7	27,9	24,8	32,6	-
	Min.	20,4	20,4	17,8	19,3	21,3	23,3	23,0	21,7	19,8	23,2	-	20,1	19,1	14,5	13,1	19,2	14,9	22,6	18,9	15,5	22,6	-
	2 <sup>nd</sup> Comm. room	Max.	24,6	-	-	-	-	-	-	27,1	27,0	-	-	41,5	-	-	-	-	-	-	37,1	37,8	-
P75	23,7	-	-	-	-	-	-	25,9	26,2	-	-	34,2	-	-	-	-	-	-	28,2	26,8	-	-	
Mean	23,4	-	-	-	-	-	-	25,3	25,8	-	-	31,3	-	-	-	-	-	-	25,2	24,6	-	-	
Min.	21,9	-	-	-	-	-	-	22,6	24,1	-	-	20,7	-	-	-	-	-	-	17,1	16,6	-	-	
Staff room	Max.	24,0	22,9	25,0	27,0	26,2	27,5	25,1	22,3	25,6	23,8	28,0	52,8	58,4	43,7	32,3	44,1	39,6	58,6	44,9	41,4	57,0	49,4
	P75	22,9	19,1	23,7	26,7	25,5	26,0	24,1	21,3	24,3	23,2	26,8	41,3	30,4	32,7	27,8	32,5	32,1	34,2	32,8	31,3	46,9	41,1
	Mean	22,2	18,4	23,3	26,2	24,8	25,5	23,8	20,1	23,4	22,6	26,4	36,8	28,6	27,8	24,5	29,3	28,7	31,6	29,7	27,3	40,6	37,1
	Min.	18,5	15,5	18,5	24,8	21,4	21,8	22,6	18,2	19,6	20,7	24,7	18,9	21,4	17,0	16,1	16,3	16,4	25,7	20,7	18,6	23,0	28,1
	Others	Max.	-	21,9	25,2	25,2	33,7	24,5	26,7	-	25,1	25,9	27,6	-	34,9	34,8	39,0	43,7	50,5	36,0	-	43,6	53,9
P75	-	21,2	24,5	24,7	23,8	23,9	25,1	-	24,4	24,3	26,8	-	31,8	31,8	30,9	34,3	37,1	33,6	-	30,6	41,8	38,4	
Mean	-	20,8	24,2	24,6	23,2	23,7	24,4	-	23,9	24,0	26,3	-	29,4	26,4	27,5	30,2	32,7	31,4	-	27,1	37,1	33,3	
Min.	-	17,7	23,2	23,9	19,9	21,4	22,9	-	21,3	21,5	22,9	-	25,2	17,0	18,8	12,1	19,8	26,9	-	18,4	24,4	21,1	
Outdoor	Max.	13,0	13,0	16,0	16,0	18,0	19,0	17,0	17,0	18,0			100	88	87	87	93	100	93				
	P75	9,0	8,0	12,0	12,0	11,0	15,0	9,0	8,0	13,0			82	72	62	71	81	76	81				
	Mean	5,8	5,4	8,2	8,2	8,3	10,7	5,9	5,9	10,5			74	62	50	58	69	61	72				
	Min.	-1,0	-2,0	-4,0	-3,0	0,0	0,0	-2,0	-2,0	4,0			40	36	23	28	23	24	39				

RH was generally very low in most of the rooms examined in the 11 WZCs. It was particularly dry in the resident bedrooms, since in all but two WZCs (WZC1 and WZC11) even the maximum RH achieved in the resident bedrooms was below the recommended minimum for the cold season (40%). In many of the studied rooms, the P75 and average values were below the recommended minimum RH even for the warm season (30%). RH tends to decrease during the heating season, especially in buildings with mechanical ventilation where incoming air is heated. However, RH did not seem to be influenced by the presence of a mechanical ventilation system in this study.

Besides being an important comfort parameter, RH is also an important point of attention to limit the transmission of viruses indoors. Evidence from various international studies indicates that dry airways make people more susceptible to airway infections (Courtney and Bax, 2021). It has also been shown that humidity influences both evaporation kinematics and particle growth, meaning that in dry indoor spaces (< 40% RH) the risk of airborne transmission of SARS-CoV-2 is greater than that of humid spaces (Ahlawat et al., 2020). Recent research



indicates a strong negative relationship between RH and the transmission of both SARS-CoV-2 and influenza (Keetels et al., 2022), partly due to the greater sensitivity of respiratory tracts at lower humidity.

### 3.4 Viral particles

Table 3 presents the results collected after qPCR analysis of each biological sample (from the air and from the surfaces) collected in the 11 WZCs. It also indicates whether there was an active (A) or recent (R, i.e. active in the week prior to assessment) COVID-19 outbreak in the facility (N indicates neither active nor recent outbreaks reported). The facility with the highest percentage of positive samples was WZC10 (where only one of the samples collected, both in air and on surfaces, was negative), and the facility with the lowest percentage was WZC1. No clear correlation between positive viral samples and the other IAQ parameters measured was observed. The data shown in Table 3 clearly indicates a direct relation between an on-going COVID-19 outbreak and a high frequency of SARS-CoV-2 detection, in any room, both in air and on surfaces, which reflects the complexity of isolating infected persons to prevent virus transmission in a WZC during an outbreak; even when other IAQ parameters (i.e. CO<sub>2</sub> and PM<sub>2,5</sub> concentrations) indicate sufficient ventilation.

Table 3: Presence of SARS-CoV-2 in each biological sample taken in each room examined per WZC.

WZC		SARS-CoV-2 (Ct-value)										
		1	2	3	4	5	6	7	8	9	10	11
1 <sup>e</sup> Resident bedroom	Air	Neg	Neg	Neg	Neg	Neg	Neg	34,5	Neg	Neg	28,9	-
	Surf. 1	36,2	34,9	32,8	Neg	Neg	32,7	Neg	31,6	Neg	30,3	33,3
	Surf. 2	Neg	33,4	35,5	35,9	44,9	Neg	Neg	29,7	Neg	26,4	34,7
	Surf. 3	Neg	Neg	35,9	Neg	Neg	35,9	Neg	34,0	Neg	28,5	33,5
2 <sup>e</sup> Resident bedroom	Air	Neg	Neg	Neg	Neg	Neg	-	-	Neg	-	33,3	35,5
	Surf. 1	Neg	33,8	Neg	Neg	Neg	Neg	Neg	32,2	-	33,8	31,7
	Surf. 2	Neg	34,5	Neg	35,7	35,6	Neg	Neg	30,4	-	30,9	34,9
	Surf. 3	Neg	36,0	36,3	Neg	Neg	Neg	34,0	27,0	-	31,8	Neg
1 <sup>st</sup> Common room	Air	Neg	Neg	Neg	Neg	35,2	Neg	Neg	Neg	Neg	30,6	33,8
	Surf. 1	34,6	33,8	34,9	Neg	34,0	33,4	Neg	30,7	35,3	35,1	36,9
	Surf. 2	Neg	34,5	34,8	35,6	31,2	33,2	35,6	34,8	33,9	34,1	Neg
	Surf. 3	Neg	36,0	Neg	Neg	29,4	Neg	32,7	33,0	Neg	28,0	33,8
2 <sup>nd</sup> Common room	Air	Neg	-	-	-	-	-	-	Neg	34,2	-	-
	Surf. 1	32,6	-	-	-	-	-	-	37,9	27,7	-	-
	Surf. 2	35,6	-	-	-	-	-	-	33,4	27,9	-	-
	Surf. 3	Neg	-	-	-	-	-	-	32,0	31,8	-	-
Staff room	Air	Neg	Neg	Neg	Neg	32,7	Neg	Neg	Neg	-	31,1	33,4
	Surf. 1	37,2	Neg	35,8	36,2	Neg	Neg	Neg	38,2	Neg	37,0	33,2
	Surf. 2	35,0	34,8	Neg	Neg	35,1	Neg	33,2	34,7	Neg	Neg	Neg
	Surf. 3	38,8	35,6	35,8	36,7	34,6	Neg	35,0	32,0	Neg	36,9	Neg
Other	Air	-	Neg	Neg	35,1	Neg	Neg	Neg	-	Neg	36,0	36,6
	Surf. 1	35,9	33,8	Neg	Neg	35,2	38,2	34,2	-	Neg	34,4	34,7
	Surf. 2	Neg	36,9	34,6	32,8	Neg	33,4	32,9	-	30,5	36,4	Neg
	Surf. 3	-	36,0	33,8	33,1	Neg	38,0	35,7	-	Neg	36,2	Neg
Rate of positives (%)		36	65	50	40	53	37	47	75	37	95	68
Covid-19 outbreak?		N	R	N	N	N	N	N	R	N	A	A

Table 3 also presents the cycle threshold (Ct) values for each of the samples in which SARS-CoV-2 was detected. In a qPCR test, the Ct value is inversely proportional to the amount of viral RNA contained in the sample (Paralovo et al., 2024). The qPCR test stops after Ct = 45. The method's LoQ was determined as 20 gene copies/ml of liquid sample (Janssens et al., 2022), but Ct values are not converted to RNA copies/ml in this study because it was not possible to generate a standard calibration curve for SARS-CoV-2 in lysis buffer at that time.

Although the Ct value is not always a measure of infection risk, as the genetic target of both viable and non-viable microorganisms is measured indiscriminately, it might be considered as a proxy for infection risk, especially when applied to environmental samples (i.e. from the air and surfaces), as opposed to those taken from human body fluids (i.e. not yet distributed to the environment and thus not at immediate risk of contact with other individuals).

On the other hand, environmental samples will normally contain much smaller amounts of viral RNA compared to human samples, regardless of the concentration of virus-laden bioaerosols in the environment assessed, since the bioparticles emitted by infected individuals spread throughout the air volume in the room they are in, leading to high dilution factors. This means that the Ct value thresholds commonly considered to determine whether a sample is positive for e.g. nasal swabs (usually Ct value < 30) are not as adequate for environmental samples. Therefore, higher Ct values should still be considered indicative of a positive environmental sample. Paralovo et al. (2024) suggests that Ct values lower than 39.3 still offer a significant chance of being configured as positive air samples for SARS-CoV-2, while Ct values above 39.3 have greater uncertainty and therefore a smaller chance of configuring a true-positive.

In Table 3, the cells are coloured according to the Ct value of the sample: red for Ct < 30 (i.e. clearly positive, in the same range as nasal swabs), orange for 30 < Ct < 35 (i.e. smaller viral load but higher chance of configuring of true positive), yellow for 35 < Ct < 39.3 (i.e. a very small viral load, lower probability of configuring true positive) and green for Ct > 39.3 (samples considered negative for SARS-CoV-2). It is also important to note that identifying environmental samples as positive for SARS-CoV-2 RNA provides only a quick but superficial assessment of the potential infectivity in a given area (i.e. not a measure of viable virions).

Figure 2 shows the evolution of COVID-19 new cases per week among the Flemish population between February and April 2022, when the measurements were performed (Sciensano, 2024).



Figure 2: Weekly incidence of COVID-19 in the Flemish population during the entire sampling period.

An initial hypothesis in this study was that the incidence of COVID-19 in the WZCs (and therefore the number of positive biosamples) would (at least loosely) follow the regional or national incidence (both followed a very similar trend in the same period). If that were the case, WZC7 would have the highest number of positive samples, and the simultaneously sampled WZCs would have similar rates. Yet, analysing Table 3, this hypothesis is not confirmed: the highest percentage of positive samples was collected when the Flemish incidence was at relatively low level and pairs of simultaneously sampled WZCs differed considerably. The most likely explanation was that the WZC sample size was too small to observe such trend. The highest number of positive samples was taken in WZC10. The facilities with the 2<sup>nd</sup> and 3<sup>rd</sup> highest numbers of positive samples were WZC8 and WZC11. However, in WZC8 only swab samples were positive, while in WZC11 all four air samples collected were positive.

The measurements in WZC10 and WZC11 took place simultaneously in April 2022, while active COVID-19 outbreaks were occurring in both facilities. This is clearly reflected in the air sample results: WZC10 and WZC11 were the only facilities where all air samples collected were positive. An interesting situation occurred in WZC8, where the research team was informed by staff that a COVID-19 outbreak was ongoing during the measurement week. An outbreak had already occurred there a week before the measurements started, but some residents tested positive again and the staff therefore assumed that the outbreak was still ongoing. However, at the end of the measurement week, the staff informed the research team that it was indeed a 'false alarm', i.e. that on a second test all previously infected residents showed a negative result. This was also reflected in the WZC8 results: all air samples were negative, and all surface samples were positive, indicating a facility-wide outbreak in the past, but that was no longer active. A similar situation occurred in WZC2, where the staff reported that a COVID-19 outbreak had ended in the week prior to sampling. As shown in Table 3, all air samples in WZC2 were negative, while all but two surface samples were positive.

In fact, only 28% all air samples collected in WZCs were positive, while 63% of all swab samples were positive. Indeed, it was expected that more positive swab samples than air samples would be found due to the bioaerosol cycle itself: aerosols containing pathogenic material are emitted into the air by infected individuals remain suspended in the air for a period (depending on their particle size), and then settle by gravity on the inner surfaces. Deposition of such particles can also happen on high-touch surfaces by e.g. contaminated hands. In general, viral bioaerosols can remain airborne for a few hours, but once settled these particles can persist for 1 to 28 days (Suman et al., 2020; Marzoli et al., 2021), depending on the type of surface, the cleaning regime and the RNA degradation rate by RNAses present in the environment. It is therefore reasonable to consider the presence of airborne viral aerosols as a possible indication of an active emission source (e.g. during an ongoing COVID-19 outbreak or at least the presence of an infected person/emitter during sampling), while the presence of viral material on the surfaces could indicate a past emission source that may no longer be active (e.g. traces of SARS-CoV-2 remaining on surfaces several days or weeks after the end of a COVID-19 outbreak, depending on the 3 factors mentioned above). It is, however, important to keep in mind that the presence of an emitter of SARS-CoV-2 RNA does not necessarily implicate on active COVID-19 case(s), since it is possible to emit RNA but not viable virus (e.g. emitted RNA could consist of degraded products from an immune response).

#### 4 CONCLUSIONS

The CO<sub>2</sub> concentrations measured in this set of 11 WZCs generally seem to indicate an acceptable level of ventilation, especially for those with mechanical ventilation systems. Of all collected air samples, 28% contained genomic material, while 63% of swab samples did. The number of positive SARS-CoV-2 samples (from surfaces and air) did not follow the Flemish COVID-19 incidence during the measurement period, possibly due to the small sample size. On the other hand, positive air samples were found in all studied rooms of WZCs undergoing active COVID-19 outbreaks, while positive surface samples seemed to indicate (recent) previous outbreaks. This finding underlines the potential value of a combined assessment of the viral load in air and surface samples as an important tool to screen indoor spaces on the actual infection risk of occupants, without collecting human samples of each resident. Including more pathogens in similar studies would allow a wider assessment of the exposure and risk of susceptible populations, such as the elderly, and would enable a more targeted anticipation on initiated outbreaks. General recommendations for WZCs regarding airborne-spreading infections include more frequent testing of residents and staff (symptomatic or not), isolation

of positive-testing residents, use of mouth masks and increased ventilation/airing, especially in communal areas.

Additionally, an overall unawareness regarding ventilation systems was observed in the WZCs studied in this research. While management and staff did demonstrate understanding the importance of airing and ventilating the common spaces, it was very common that they did not know even if their respective facilities had a mechanical ventilation system installed. When they reported that they did have a ventilation system, they often did not know which type. In a few facilities, incorrect ventilation systems were reported, or had its presence/absence misreported. This indicates the importance of further increasing the sensibilization of the public regarding the importance of ventilation, especially when aimed at agents directly responsible for managing spaces where a more vulnerable population is present.

## 5 REFERENCES

- Abdin, T. A. R.; Mahmoud, A. H. A. (2024). Lessons from the coronavirus pandemic: a review of how the disease spreads in indoor spaces. *International Journal of Low-Carbon Technologies*, 19, 90–101.
- Ahlawat, A., Wiedensohler, A. Mishra, S.K. (2020). An Overview on the Role of Relative Humidity in Airborne Transmission of SARS-CoV-2 in Indoor Environments. *Aerosol Air Qual. Res.*, 20: 1856–1861.
- Courtney, J. M.; Bax, A. (2021). Hydrating the respiratory tract: An alternative explanation why masks lower severity of COVID-19. *Biophys J.*, 120(6): 994–1000.
- De Jonge, K.; Stranger, M.; Paralovo, S. L.; Spruyt, M.; Lazarov, B.; Geens, T., et al. (2023) Evaluating the impact of air cleaning and ventilation of airborne pathogens and human bio-effluents at two primary schools in Belgium. In: Proceedings of 43<sup>rd</sup> AIVC Conference, 11<sup>th</sup> TightVent Conference, 9<sup>th</sup> venticool Conference. INIVE. 43: 880–888.
- Flemish Government. (2018). *Besluit Van De Vlaamse Regering van 13 juli 2018 gepubliceerd op 07 september 2018*. 292p. [https://www.ejustice.just.fgov.be/mopdf/2018/09/07\\_1.pdf#page=203](https://www.ejustice.just.fgov.be/mopdf/2018/09/07_1.pdf#page=203)
- Flemish Government (2024). *Nota aan de Vlaamse Regering: Ontwerp van besluit van de Vlaamse Regering tot wijziging van bijlage 11 bij het besluit van de Vlaamse Regering van 28 juni 2019*.
- Janssens, R.; Hanoteaux, S.; Maloux, H.; Klamer, S.; Laisnez, V.; Verhaegen, B.; Linard, C.; Lahousse, L.; Delputte, P.; Terwagne, M.; et al. (2022) SARS-CoV-2 Surveillance in Belgian Wastewaters. *Viruses*, 14, 1950.
- Kakoulli, C.; Kyriacou, A.; Michaelides, M. P. (2022). A Review of Field Measurement Studies on Thermal Comfort, Indoor Air Quality and Virus Risk. *Atmosphere*, 13, 191.
- Keetels, G. H., Godderis, L., van de Wiel, B. J. H. (2022). Associative evidence for the potential of humidification as a non-pharmaceutical intervention for influenza and SARS-CoV-2 transmission. *Journal of Exposure Science & Environmental Epidemiology*, 32: 720 – 726.
- Marzoli, F.; Bortolami, A.; Pezzuto, A.; Mazzetto, E.; Piro, R; Terregino, C.; Bonfante, F.; Belluco, S. (2021). A systematic review of human coronaviruses survival on environmental surfaces. *Science of The Total Environment*, 778: 146191.
- Morawska, L.; Cao, J. (2020). Airborne transmission of SARSCoV- 2: the world should face the reality. *Environment International*, 139, 105730.
- Paralovo, S. L.; De Jonge, K.; Janssens, A.; Laverge, J.; Cartuyvels, R.; Van den Driessche, K.; Lazarov B.; Spruyt, M.; Stranger, M. (2023). Evaluating the impact of air cleaning on bioaerosols and other IAQ indicators in Belgian daycare facilities. In: *Proceedings of 43<sup>rd</sup> AIVC Conference, 11<sup>th</sup> TightVent Conference, 9<sup>th</sup> venticool Conference*. INIVE. Copenhagen, Denmark. 43: 795–804.
- Paralovo, S. L.; Driessche, K. V.; Cartuyvels, R.; Lazarov, B.; Vlieghe, E.; Vanstraelen, L.; Smets, R.; Spruyt, M.; Kreps, S.; Hufkens, N.; Stranger, M. (2024). Development of a Bioaerosol Sampling Method for Airborne Pathogen Detection with Focus on SARS-CoV-2. *Indoor Air*, 2024, Article ID 6638511, 14 p.
- Sciensano. Belgium COVID-19 epidemiological situation: dashboard. (2024). <https://lookerstudio.google.com/embed/reporting/c14a5cfc-cab7-4812-848c-0369173148ab/page/ZwmOB>.
- Suman, R.; Javaid, M.; Haleem, A.; Vaishya, R.; Bahl, S.; Nandan, D. (2020). Sustainability of Coronavirus on Different Surfaces. *J. of Clinical and Exp. Hepatology*, 10(4): 386-390.

# The Influence of Outdoor Conditions on Indoor Air Quality: Case Study of Norwegian Schools

Iselin Ørbek Eide<sup>1</sup>, Christer Eskedal<sup>2</sup>, Kai Gustavsen<sup>3</sup>, Kent Hart<sup>3</sup>, Azimil Gani Alam<sup>1</sup>, Guangyu Cao<sup>1</sup>

*1 Department of Energy and Process Engineering (EPT)  
Norwegian University of Science and Technology (NTNU),  
Kolbjørn Hejes v 1B  
7034 Trondheim, Norway*

*2 N3  
Rudssletta 60,  
1351 Rud, Norway*

*3 Norges Astma- og Allergiforbund  
Gnr 14 Bnr 4  
7039 Trondheim, Norway*

*corresponding email: Iselin.o.eide@ntnu.no*

## ABSTRACT

The project aims to investigate the degree of influence that outdoor conditions may have on the indoor environment in Norwegian schools. It also aims to ascertain whether it is possible to use outdoor parameters such as particulate matter, relative humidity, and air temperature, along with indoor parameters including CO<sub>2</sub>, relative humidity, and air temperature, to predict indoor particulate matter values. The outdoor data was gathered from various weather stations near the schools, while the indoor data was provided by N3, who collected it using sensors within the schools. To predict indoor particulate matter values, a machine learning algorithm, random forest regression, was employed. The project's findings highlight the significant impact of outdoor conditions on indoor environments. These encompass a wide spectrum, ranging from local weather effects, like cold temperatures leading to pollutant accumulation at lower altitudes, to remote occurrences, such as Sahara sands traveling thousands of kilometres by wind to Norway. Variations in the correlation between indoor and outdoor PM<sub>10</sub> values across different locations and classrooms suggest potential diverse sources of particulate matter, seasonal effects on indoor air quality, or disparities in ventilation systems and cleaning procedures. These initial findings were further investigated by a random forest regression algorithm in machine learning. This approach incorporated diverse outdoor and indoor parameters to assess feature importance and forecast indoor PM<sub>10</sub> levels, resulting in robust models with achieved R-squared values reaching 0.92. In January, outdoor temperature emerged as the primary influential factor, followed closely by outdoor PM<sub>2.5</sub> values and indoor relative humidity. In contrast, September emphasized indoor relative humidity as the most significant influence. Notably, indoor CO<sub>2</sub> demonstrated a consistent level of influence in both January and September, likely due to consistent student activity. The robustness of the random forest models and their close alignment with actual PM<sub>10</sub> values suggest a strong potential for establishing future cleaning procedures based on predictive models.

## KEYWORDS

Indoor Environment - Particulate Matter - Correlation Particulate Matter

## 1 INTRODUCTION

In recent years, the quality of Indoor Environmental Quality (IEQ) has emerged as a critical concern impacting health, well-being, and productivity on a global scale. The World Health Organization has highlighted the significance of IEQ, pointing out its direct correlation with public health outcomes across various settings (World Health Organization, 2010). Amidst this global context, the aspect of Indoor Air Quality in educational institutions, particularly elementary schools, demands special attention. Studies, including the 2019 National

Monitoring of Working Environment and Health (NOA) conducted by the National Institute of Occupational Health, reveal that 35 percent of elementary school teachers in Norway report poor IAQ due to inadequate ventilation, underscoring a widespread issue within educational settings.

The urgency to address IAQ is further magnified by the broader challenges posed by deteriorating outdoor air quality (Fenger, 2009). Pollution and environmental degradation exacerbate indoor air problems, creating a vicious cycle that impacts vulnerable populations, such as children in schools, the most. This interconnection between outdoor and indoor air quality underscores the necessity for comprehensive solutions that address both facets to ensure healthy living and learning environments.

Following the pandemic, there has been a global call from researchers for an indoor climate revolution, emphasizing the need for improved IEQ in schools to safeguard and enhance the learning experience (Eichholtz, 2024). The indoor environment plays a pivotal role in the health, well-being, and productivity of occupants, making it imperative to understand and optimize the factors influencing IAQ.

This study aims to investigate the feature importance of both indoor and outdoor parameters on indoor Particulate Matter (PM) values, uncovering the causes behind their significant impact on IAQ. Additionally, it seeks to develop a predictive model for indoor PM values using a random forest machine learning model, contributing to the body of knowledge on effective IEQ management and offering actionable insights for improving air quality in schools.

## **1.1 Scope and Delimitation**

Due to time constraints and the scope of the assignment, certain simplifications had to be made. The analysis was restricted to specific months instead of the entire year to save time, and the data solely pertains to the year 2023. While this renders the analysis more vulnerable to yearly fluctuations, it was deemed sufficiently robust to validate the results.

Various data discrepancies emerged throughout the project. Instances of missing data arose due to sensors being offline, damaged, or due to other unidentified reasons. Consequently, this led to less accurate results and some data sets remained uncalculated.

Notably, not all outdoor sensors were positioned on the school grounds, thereby introducing some inaccuracies in the results. The outdoor data slightly differs from the actual outdoor conditions on the school grounds. Nevertheless, the sensors were placed close, and the selected schools were chosen because of their proximity to the weather stations, aiming to mitigate significant impacts on the analysis.

## **2 METHODOLOGY**

### **2.1 Seasonal Investigation Parameters**

Due to the vast amount of data and the limited time and scope of the assignment, specific time periods of the year were selected for investigation rather than examining the entire year.

The objective was to explore time segments from various seasons to compare their respective impacts on the indoor environment. Additionally, it was crucial to choose months when the school was in full operation. Consequently, the summer months of June, July, and August were not feasible due to summer vacation. Similarly, April was affected by the Easter break, and May had various national holidays. As a result, the months chosen for further investigation were January, representing the winter season, March for spring, and September

for fall. Due to unforeseen issues with missing data from March in several schools, the machine learning model could not produce reliable predictions for this month.

## 2.2 Data Collection

The indoor data for the analysis were sourced from the N3smart sensors installed within the selected rooms, while the outdoor data originated from various weather stations located near the schools. Specifically, the outdoor PM10 and PM2.5 values were gathered from weather stations affiliated with NILU, an independent nonprofit research institution. The temperature and relative humidity data were obtained from the Norwegian Climate Service Centre (KSS), which serves as a hub for climate and hydrological data, facilitated through a collaboration between the Meteorological Institute, the Norwegian Water Resources and Energy Directorate, the Mapping Authority, NORCE, and the Bjerknes Centre.

Several different schools in Norway were chosen for the analysis, partly due to their proximity to weather stations. The schools are presented in Table 1.

Table 1: Selected schools and rooms

School Name	Location	Construction year	Room 1	Room 2
Stabekk	Bærum	2004	Ø203	V201
Åsveien	Trondheim	2015	Base 4	Locker room
Åsenhagen	Lillestrøm	2000	D-150	7D
Kjeller	Lillestrøm	2010	1020	1045
Høvik	Bærum	2013	3139	1007

The sensors that collected data inside the schools were provided by N3. These sensors gather data concerning CO<sub>2</sub>, air temperature, relative humidity, and PM10. The frequency at which new data is measured can be adjusted, but for this project, it was set to every 2 minutes. These sensors are positioned in the middle of the classrooms on the wall opposite the door.

Various weather stations were used to source data for the analysis, and different weather stations had to be used for the same school due to the particulate matter values and the temperature and relative humidity values not being recorded at the same stations. The weather stations used for PM<sub>10</sub>, PM<sub>2.5</sub>, relative humidity, and temperature can be seen in Table 2.

Table 2: Weather stations used for PM-values, relative humidity, and temperature. Distance from school in parentheses.

School	PM Weather station	Temp and RH Weather station
<b>Stabekk Primary School</b>	Bekkestua weather station (700 m)	Skriverberget weather station (2 km)
<b>Åsveien Primary School</b>	Åsveien skole weather station (50 m)	Saupstad weather station (3 km)
<b>Åsenhagen Primary School</b>	Vollaparken øst weather station (2 km)	Skedsmo-Hellerud weather station (700 m)
<b>Høvik Primary School</b>	E18 Høvik kirke weather station (500 m)	Skriverberget weather station (2,5 km)
<b>Kjeller Primary School</b>	Vigernes Weather station (3km)	Kjeller Weather station (300 m)

## 2.3 Machine Learning

Machine learning has become a proven method to be utilized in predicting indoor air quality (Wei, 2019). In this study, supervised ML with random forest algorithm was utilized to

predict indoor PM10 values based on eight parameters. These parameters were employed to train the model and determine which had the greatest impact on indoor PM10 values. Recorded indoor PM10 values were used as training data for the model. The input parameters are listed in Table 3. Additionally, decision tree and linear regression models were employed, but the random forest model consistently yielded more accurate results and were therefore used for the results.

Table 3: Input parameters

Indoor Values	Outdoor Values
Relative humidity	Relative humidity
Temperature	Temperature
PM <sub>10</sub>	PM <sub>10</sub>
CO <sub>2</sub>	PM <sub>2.5</sub>

### 3 RESULTS

#### 3.1 Outdoor Parameters

Figure 1 and Figure 2 display the outdoor PM10 values for all schools in January and September. The graph is divided into zones in compliance with TEK17s criteria for zoning in the planning of activities or construction. September exhibits lower values of PM10 than January. However, there is a noticeable increase for all schools between the 6th and 12th of September.

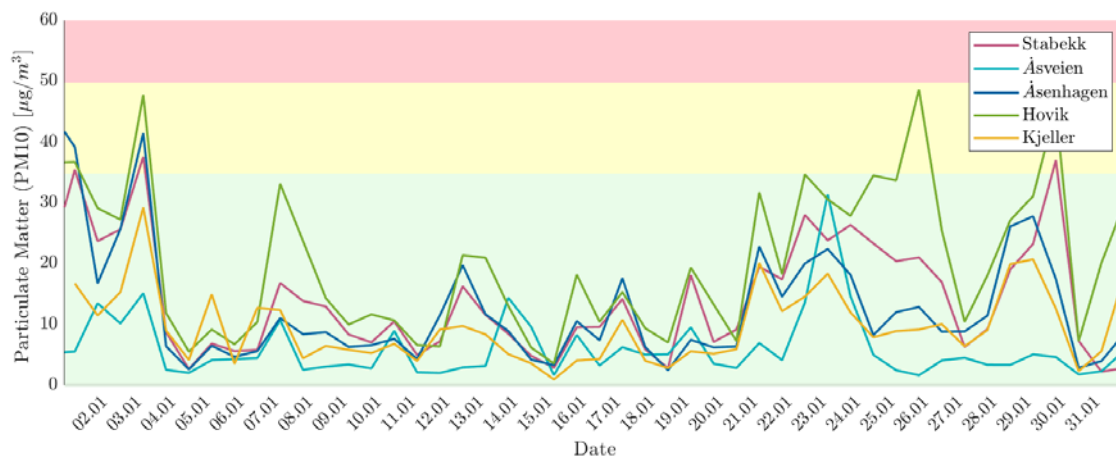


Figure 1: PM10 values outdoor for all schools, January.



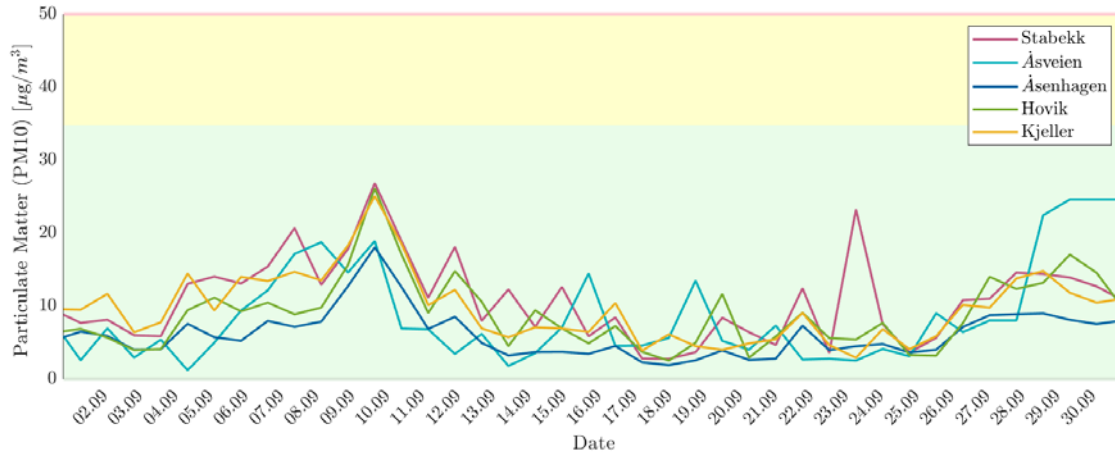


Figure 2: PM10 values outdoor for all schools, September.

Figure 3 and Figure 4 show the outdoor PM2.5 values for all schools. Both graphs follow the same trend as the PM10 graphs, albeit slightly smaller, which is natural since the PM10 values also include the values for PM2.5. The zones set by TEK17 contain information solely regarding PM10. However, since PM10 includes smaller particulate matter, it remains applicable to the PM2.5 graphs.

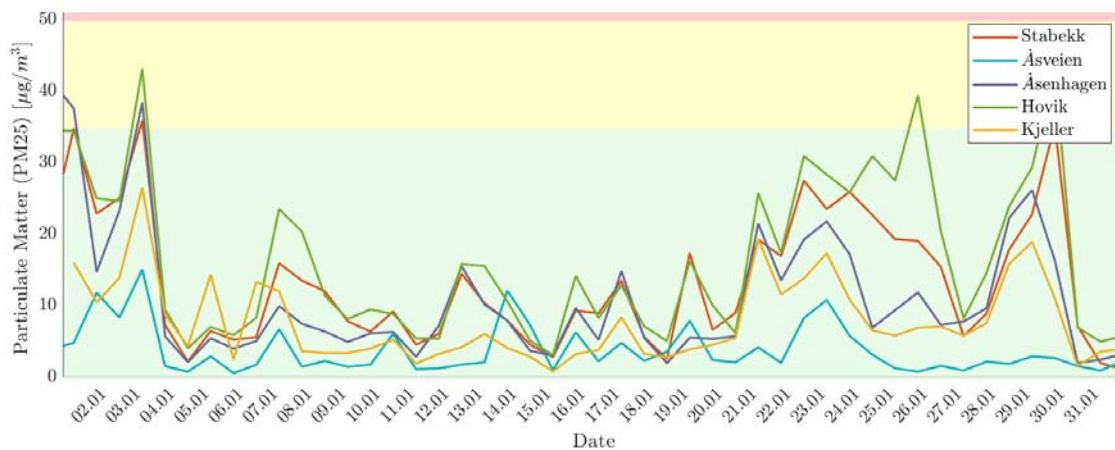


Figure 3: PM2.5 values outdoor for all schools, January.

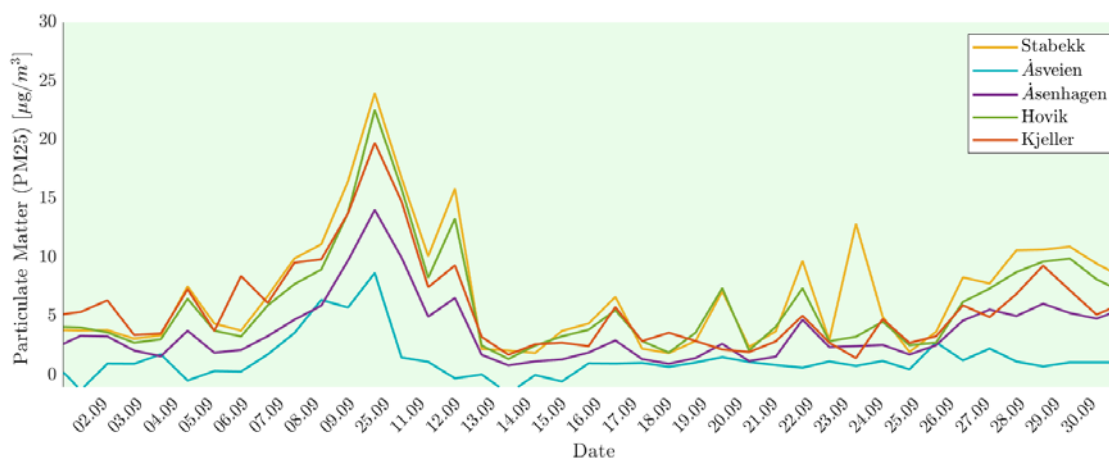


Figure 4: PM2.5 values outdoor for all schools, September.

Naturally, September was much warmer than January. Åsveien School exhibits the largest difference in temperature from the others, being situated much further north, in Trondheim. The relative humidity values from Stabekk and Høvik show unusually stable readings for a significant period in January, which might indicate sensor errors. Åsveien has some missing values for September. The relative humidity stays between 50 percent and 100 percent for both January and September, with Åsveien showing lower values than the other schools in January.

### 3.2 Correlation

The correlation between indoor and outdoor PM10 values is presented in Table 4. The correlation is calculated for the entire day and separately for workdays when ventilation is active. Some calculations involve incomplete outdoor or indoor data, leading to skewed results. Due to problems with several of the data sets for March, the month of March was removed from all the results.

Table 4: Correlation between indoor and outdoor PM10 values

School	Month	Sensor	Corr.	Corr. Daytime	Comment
Stabekk	January	Ø203	0.70	0.75	
		V201	0.71	0.79	
	September	Ø203	0.31	0.23	
		V201	0.36	0.29	
Åsveien	January	Sensor 4	0.35	0.40	
		Sensor 5	0.43	0.40	
	September	Sensor 4	0.49	0.44	
		Sensor 5	0.41	0.24	
Åsenhagen	January	D-150	0.59	0.52	Missing parts of outdoor data
		D7	-0.15	-0.13	Missing parts of outdoor data
	September	D-150	0.79	0.78	
		D7	0.75	0.69	
Kjeller	January	1020	0.29	0.42	Missing parts of indoor data
		1045	0.41	0.25	Missing parts of indoor data
	September	1020	0.52	0.47	
		1045	0.55	0.46	
Høvik	January	3139	0.52	0.50	
		1007	0.79	0.66	

September	3139	0.43	0.44
	1007	0.59	0.48

### 3.3 Predictive Patterns

Predictive patterns for the indoor PM10 values and what parameter that had the most significant impact were generated using a random forest model (regression). The Coefficient of variation (CV) and  $R^2$  values for the models can be seen in Table 5. Most of the models were strong or very strong, capturing a substantial amount of the variability. The model only uses data from when the ventilation was going during the day.

Table 5: CV and R2 values for the predictive model

School/Room	January		September	
	$R^2$	CV	$R^2$	CV
Stabekk Ø203	0.803	0.803	0.813	0.814
Stabekk V201	0.812	0.813	0.743	0.743
Åsveien base 4	0.802	0.802	0.730	0.730
Åsveien locker room	0.839	0.845	0.665	0.669
Åsenhagen D-150	X	X	0.890	0.890
Åsenhagen 7D	X	X	0.887	0.888
Kjeller 1020	X	X	0.796	0.800
Kjeller 1045	X	X	0.789	0.789
Høvik 3139	0.783	0.786	0.634	0.634
Høvik 1007	0.801	0.803	0.922	0.923

Figure 5 shows which feature had the largest impact on the indoor PM10 values for January 2023. The number of schools is reduced due to missing data from Åsenhagen and Kjeller. The most influential feature in January was the outdoor temperature, closely followed by outdoor PM2.5 values and indoor relative humidity.

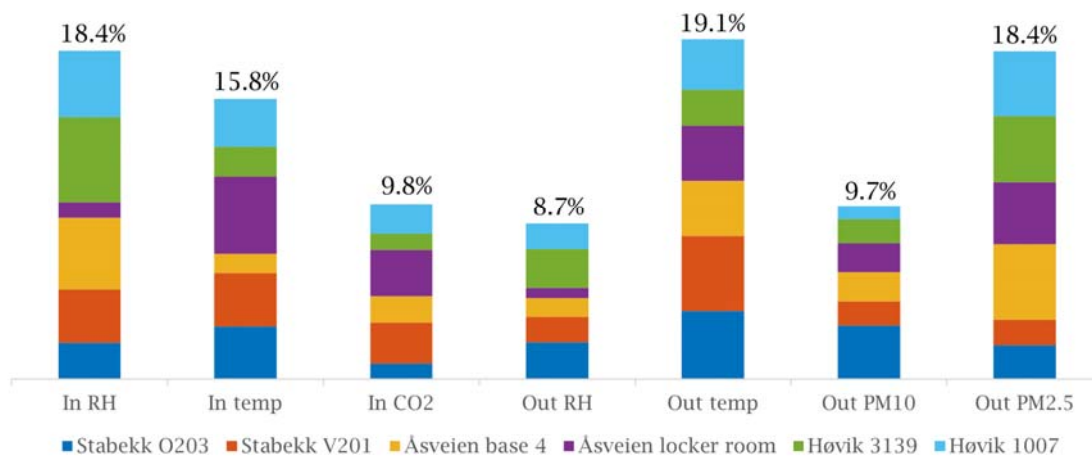


Figure 5: Feature importance, January

Figure 6 displays which feature had the most impact in each room, aiding in the distinction between room-specific differences.

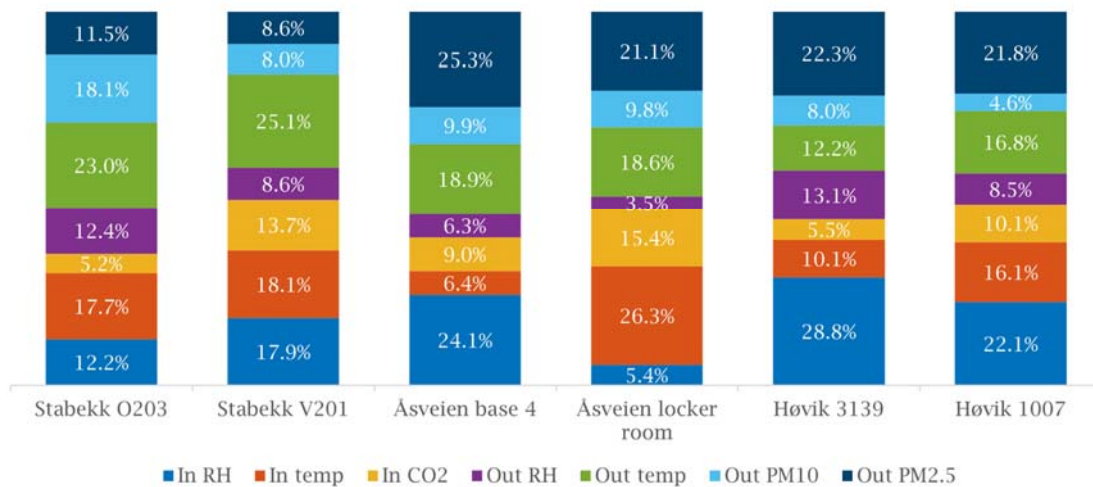


Figure 6: Feature importance for each room, January

Figure 7 shows which feature had the largest impact on the PM10 values for September 2023. It can be observed that indoor relative humidity had the most significant overall impact, albeit with some variations across different rooms.

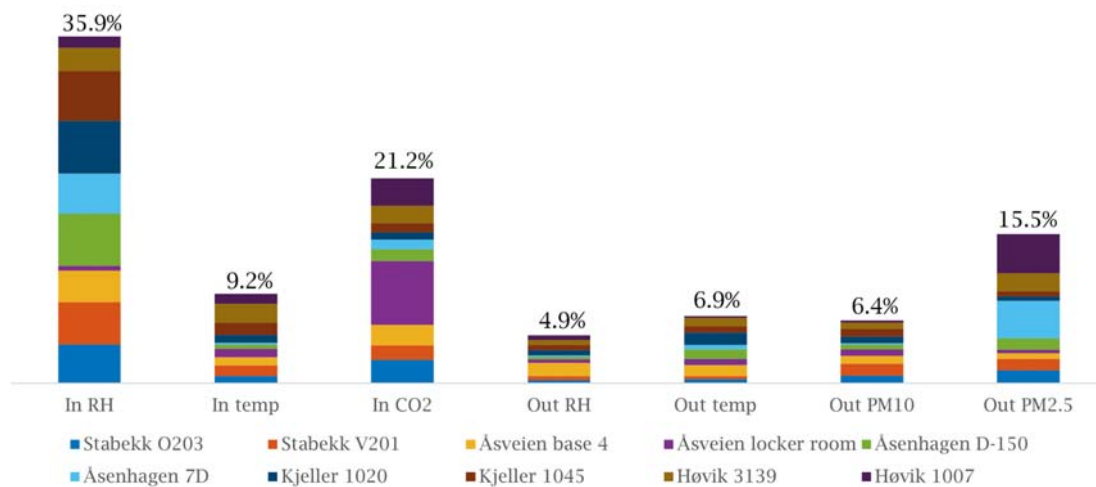


Figure 7: Feature importance, September

Figure 8 displays which feature had the most impact in each room, facilitating a clearer comparison between the rooms.

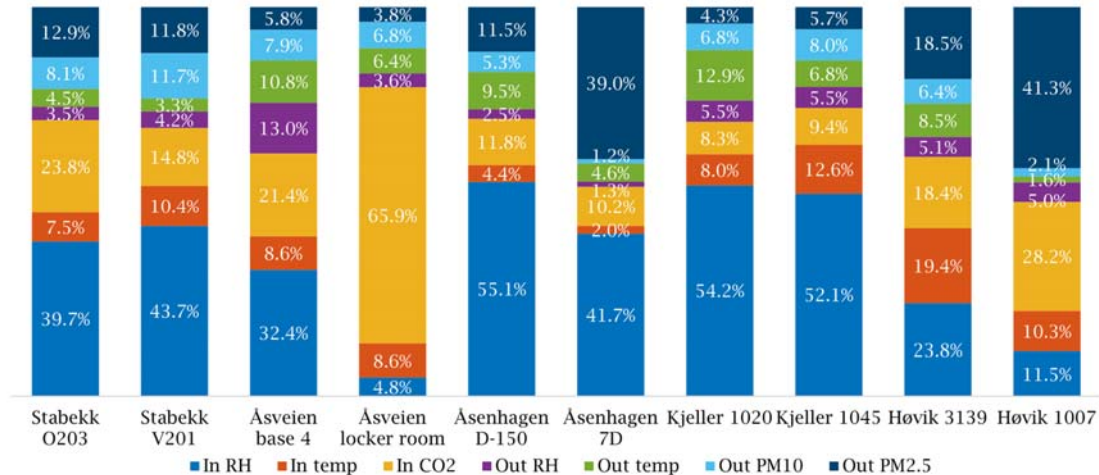


Figure 8: Feature importance for each room, September

## 4 DISCUSSION

### 4.1 Outdoor Parameters

The outdoor data for PM10 and PM2.5 indicates that Stabekk and Høvik primary schools have the highest values of PM overall. Both schools are situated near the European route E18, the main road leading into the capital, Oslo. It is reasonable to assume that the elevated values are due to road dust. The PM values are also generally higher for January than for September. This results from the concentration of outdoor pollutants in the lower atmosphere due to temperature inversions. Typically occurring in cold weather, the ascent of warm air to the upper atmosphere creates a layer that confines colder air below it. Consequently, pollutants accumulate at lower altitudes.

All schools experienced a distinct increase in particulate matter between the 6th and 12th of September. This increase was caused by a storm in the Sahara Desert. The dust was carried by the wind all the way from the Sahara Desert to Bærum, Lillestrøm, and even Trondheim, resulting in elevated dust levels for all the schools.

The outdoor temperature and relative humidity for Stabekk, Høvik, Åsenhagen, and Kjeller were quite similar for both January and September. All four schools are situated close to each other, with Høvik and Åsenhagen being the farthest apart at 35 km. Therefore, it is expected for them to have similar air temperatures and relative humidity. Åsveien, located in Trondheim, showed the largest difference from the others, especially regarding relative humidity, which was significantly lower in January.

### 4.2 Correlation

The outdoor and indoor PM10 values exhibit varying degrees of correlation, as displayed in Table 4. The lowest correlation, 0.23, was observed for Stabekk in September, while the highest, 0.79, was noted for Stabekk in January.

In September, Stabekk and Høvik have a lower correlation compared to January, whereas Åsenhagen and Kjeller exhibit a higher correlation in September than in January. Åsveien demonstrates the highest correlation in September for one room and in January for the other room.

These correlations suggest a notable discrepancy in the relationship between outdoor and indoor PM10 concentrations. To further investigate the matter regarding outdoor factors a predictive machine learning model was utilized.

### 4.3 Predictive Patterns

The analysis utilized a random forest regression algorithm in the machine learning model. Most models generated by this algorithm demonstrated strength, capturing a substantial amount of variability. The model exclusively utilized data collected during operational ventilation hours. The corresponding CV and  $R^2$  values for the model are presented in Table 5. Among these models, those for Åsenhagen and Høvik exhibited the highest strength, boasting  $R^2$  values as high as 0.89 and 0.92, respectively.

In January, the most influential feature was outdoor temperature, closely followed by outdoor PM2.5 values and indoor relative humidity. Indoor temperature also exhibited significance, while indoor CO<sub>2</sub> values, outdoor PM10, and relative humidity values played minor roles. In September, the most influential feature was indoor relative humidity. Indoor CO<sub>2</sub> exhibited a slightly larger level of influence compared to January. PM2.5 played a minor role, while indoor temperature, outdoor temperature, PM10, and relative humidity had minimal importance.

The CO<sub>2</sub> values exhibit a similar level of influence on indoor PM10 values for both January and September, slightly higher in September. This influence is likely due to consistent student activity, which remains constant regardless of the seasons.

For January, the outdoor temperature had the biggest impact on the indoor PM10 values followed by the PM2.5 values. These two parameters can be related. The low temperatures make the pollutants accumulate at lower altitudes. When there is a higher concentration of PM2.5 they will naturally have a higher impact on the indoor values.

The indoor relative humidity had a considerable importance for both January and September. There can be several reasons for this. In lower humidity the static electricity in the dust particles can increase, causing dust particles to repel each other and remain airborne longer. At the same time, higher humidity can reduce static charges, encouraging particles to clump and settle faster.

Higher humidity can also cause the dust particles to absorb moisture and clump together, making them heavier and settle on the floor or other surfaces.

## 5 CONCLUSIONS

The project aimed to determine the degree of influence that outdoor conditions have on the indoor environment in Norwegian schools. Additionally, it sought to ascertain whether using outdoor parameters would enable the prediction of indoor particulate matter values.

From the project findings, it is evident that the indoor environment is significantly impacted by outdoor conditions. These conditions vary widely, spanning local weather phenomena like cold temperatures that cause pollutants to accumulate at lower altitudes, to distant events such as Sahara sands being carried thousands of kilometres by the wind to Norway.

The correlation between indoor and outdoor PM10 values varies significantly across locations and classrooms. This variation may indicate diverse sources of particulate matter, seasonal influences on indoor air quality, or differences in ventilation systems and cleaning procedures. To delve deeper, machine learning was employed using a random forest regression algorithm. This algorithm utilized various outdoor and indoor parameters to determine feature importance

and predict indoor PM10 levels. The models demonstrated strength, with some achieving R<sup>2</sup> values as high as 0.92.

In January, outdoor temperature emerged as the most influential feature, closely followed by outdoor PM2.5 values and indoor relative humidity. Conversely, in September, indoor relative humidity held the most influence. Indoor CO<sub>2</sub> levels had influence in both January and September, likely attributed to consistent student activity.

Given the robustness of the random forest models and the close alignment between the predictive models and the actual PM10 values, there exists a high potential for future cleaning procedures to be founded upon predictive models. Embracing modern technology in cleaning processes could reduce redundant work and significantly enhance the indoor environment.

## 6 REFERENCES

- Berglund, B. a. (1992). Effects of indoor air pollution on human health. *Indoor air*, 2--25.
- Eichholtz, P. a. (2024). The effect of post-COVID-19 ventilation measures on indoor air quality in primary schools. *PNAS nexus*, pgad429.
- Fenger, J. (2009). Air pollution in the last 50 years--From local to global. *Atmospheric environment*, 13--22.
- Wei, W. a. (2019). Machine learning and statistical models for predicting indoor air quality. *Indoor Air*, 704--726.
- World Health Organization. (2010). *WHO guidelines for indoor air quality: selected pollutants*. World Health Organization Regional Office for Europe.: World Health Organization.

# Impact of filter class and airflow control on the indoor airborne particles in a nursery school

Mirela Robitu<sup>\*1</sup>, Alain Ginestet<sup>1</sup>, Dominique Pugnet<sup>1</sup> and Jean-Hugues Salazar<sup>1</sup>

*1 CETIAT*

*Domaine Scientifique de la Doua, 25 avenue des Arts  
69100 Villeurbanne, France*

*\*Corresponding author: mirela.robitu@cetiat.fr*

## ABSTRACT

This study focuses on the impact of filtration efficiency level and airflow control, based on CO<sub>2</sub>, on indoor air quality described by particle concentration in an urban low energy consumption nursery school during an autumn and a winter period. Measurements of indoor and outdoor particle concentrations have been carried out by using three different filter efficiency configurations in the school equipped with a balanced ventilation system with heat recovery. The tested filters are respectively classed G4, M5 and F7 according to NF EN 779 (2012). Some simulations were conducted to replicate the measurement configuration of the school equipped with G4+F7 filter configuration and to serve as a basis for the simulations with airflow control. The simulations were carried out using CONTAM multi-zone simulation tool. Measured particle concentration values have been used for the calculation of the filtration efficiency and the indoors to outdoors particle concentration ratio (I/O), the simulations boundary condition and simulations validations. The measurement results show that the efficiency on the finest particles (diameters lower than 1 µm) with G4 filter is very low, near zero, while with the G4+M5 and G4+F7 configurations the efficiency is slowly and considerably increased, at respectively about 20 to 50% and 82 to 90%, depending on the measurement day and particle diameters. For particles of diameter less than 1 µm, the I/O ratio decreases as the filtration efficiency increases. But for larger particles, the I/O ratio is higher and increases when the particle size considered increases and is higher when children are present in the classrooms.

The aim of the control of airflow based on CO<sub>2</sub> levels is to optimize indoor air quality and energy consumption by automatically adjusting airflow according to real-time needs in the classrooms. This can help to maintain acceptable CO<sub>2</sub> levels and reduce airborne particle concentrations, creating a healthier environment for kindergarten occupants. Simulations using CONTAM validated the model, showing that reducing airflow by 41% increased peak CO<sub>2</sub> by 25% and 0.4/2.5 µm particles by 19-35%, while demand-controlled ventilation based on CO<sub>2</sub> maintained CO<sub>2</sub> levels below threshold with only a 5.7% airflow increase, reducing 2.5 µm particles by 12.4%.

This research provides useful data for optimising indoor air quality in urban nursery schools using appropriate filters and intelligent control of airflow according to CO<sub>2</sub> levels.

## KEYWORDS

ventilation, air filtration, school, particles concentration, IAQ, CO<sub>2</sub>, control

## 1 INTRODUCTION

Children spend a significant part of their time in schools, and the quality of the indoor air in these environments can have a profound impact on their health, cognitive performance, and concentration levels. Studies have consistently shown that well-ventilated spaces contribute to the reduction of airborne pollutants, leading to improved concentration and enhanced learning outcomes (Wargocki & Wyon, 2007), (Wargocki & Wyon, 2017); (Sadrizadeh, et al., 2022); (Daisey, Angell, & Apte, 2003). Traditional ventilation systems, however, can introduce pollutants from outdoor and can be energy-intensive, affecting health, operational costs, and environmental sustainability.



To address the challenges of energy consumption and indoor air quality, integrating energy-efficient ventilation solutions has become crucial (Fisk, 2000), (Emmerich & Persily, 2001). These solutions, such as demand-controlled ventilation (DCV) and energy recovery ventilation, aim to regulate airflow according to real-time demand signals. DCV strategies involve adjusting ventilation airflows based on factors such as indoor air quality (IAQ) or energy efficiency (Guyot, Sherman, & Walker, 2018), thereby reducing energy consumption for fan operation and heating/cooling compared to traditional constant air volume (CAV) systems (Merema, Delwati, Sourbron, & Breesch, 2018). In certain European school buildings, DCV systems were deployed, utilizing control systems that respond to real-time signals such as CO<sub>2</sub> levels or temperature. Studies have shown significant energy savings achieved through DCV compared to CAV systems. For instance, research conducted across Norwegian school buildings reported a substantial decrease in energy demand, with reductions in heating energy demand and fan usage energy (Mysen, Berntsen, Nafstad, & Schild, 2005), (Wachenfeldt, Mysen, & Schild, 2007). Similarly, in Belgian educational buildings, DCV implementation resulted in significant reductions in fan energy consumption and ventilation heat loss while maintaining comparable CO<sub>2</sub> levels to CAV systems (Merema, Delwati, Sourbron, & Breesch, 2018).

Balanced ventilation systems with heat recovery can be used in buildings to reduce energy consumption. These systems typically incorporate air filters to protect the heat exchanger (on the fresh air and exhaust air sides) and to enhance the quality of the supplied air. The selection of these filters requires careful consideration to balance air quality benefits against energy consumption due to the pressure drop associated with filter use (Liu, et al., 2017). Several studies have investigated the impact of different filter types on indoor air quality and overall system performance. Some authors (Carlsson, 2008) show that achieving optimal filtration requires adjustments in airflow rate, building envelope airtightness, and filter cassette sealing. With the 2000 construction techniques, it was challenging to exceed F7 filtration efficiency. Considering infiltration and exfiltration, an F7/MERV13 filter class is deemed necessary, while M6/MERV12 is insufficient. Additionally, research has explored filter placement strategies to optimize both air quality and energy efficiency in buildings equipped with balanced ventilation systems. In study by Ginestet et al. (Ginestet, Pugnet, & Mouradin, 2013), the performance of various air filters in balanced ventilation systems was assessed. From an energy consumption perspective, the authors emphasized the advantage of employing an F7 filter, protected by a G4 pre-filter upstream, rather than using the F7 filter alone. This configuration results in a lower pressure drop increase over time while maintaining satisfactory filtration efficiency. Ginestet et al. (Ginestet, Pugnet, & Robitu, 2015) explored the impact of filtration efficiency on particle concentration in a rural school equipped with a balanced ventilation system. Three filters (G4, F7, F9) were tested, revealing lower efficiency for G4 on particles <1 µm, whereas F7 and F9 demonstrated superior efficiency, ranging from 47 to 55% and 82 to 87% at 0.4 µm, respectively. During school occupancy, the indoor-to-outdoor (I/O) ratio remained similar as when the school was unoccupied for particles <0.5 µm but increased as the particle size increased and as the filter class decreased, sometimes exceeding 1. Overall, the use of F7 or F9 filters in the school's ventilation system effectively protects occupants from harmful and abundant outdoor particles (<1 µm) with the I/O ratio consistently below 1.

Recently, Cabovská et al. (Cabovská, Bekö, Teli, Ekberg, & Dale, 2022) studied how different ventilation strategies impact IAQ in schools. The study involved measuring thermal conditions and IAQ over 5 days in 45 primary school classrooms in Gothenburg, Sweden. Classrooms were categorized into three ventilation systems: natural/exhaust ventilation or automated window opening (A), balanced mechanical ventilation with CAV (B), and VAV (C). Both category B and C were equipped with filters class F7. Regardless of ventilation system, classrooms maintained similar temperature and humidity levels. Lower levels of CO<sub>2</sub>,

formaldehyde, PM<sub>10</sub>, and PM<sub>2.5</sub> were obtained with categories B and C compared to A. The authors calculated the Indoor Air Pollution Index, IAPI (Sofuoglu & Moschandreas, 2003), which quantifies indoor air pollution levels from 0 (lowest) to 10 (highest) based on measured pollutant concentrations relative to minimum, maximum, and guideline limits. They found significantly higher IAPI values indicating poorer IAQ in category (A) classrooms. Despite periodic reductions in VAV system ventilation rates (category C classroom), pollutant concentrations did not substantially increase.

Alonso et al. (Alonso, Dols, & Mathisen, 2022) developed a co-simulation model, EnergyPlus-CONTAM, to assess ventilation strategies including DCV methods. The study focused on an office building in Trondheim, Norway, typically ventilated with 100% outdoor air. Results indicated that all simulated DCV strategies reduced energy consumption compared to a baseline schedule-based approach. However, CO<sub>2</sub>-based DCV led to increased indoor particulate levels, mitigated by PM<sub>2.5</sub> monitoring in ventilation control strategies. Overall, the study suggests that adjusting outdoor air fraction based on pollutant levels and local conditions can enhance both energy efficiency and indoor air quality.

Carbon dioxide (CO<sub>2</sub>) concentration is commonly used to evaluate ventilation adequacy (Persily, 2015), and many DCV systems rely solely on it to assess IAQ (Fisk & De Almeida, 1998), (Gram, 2019). While CO<sub>2</sub> can offer a general indication of IAQ, it does not account for other potential indoor pollutants (Apte, Fisk, & Daisey, 2000). Consequently, occupants may experience poor IAQ due to these other pollutants, even when CO<sub>2</sub> levels are within acceptable ranges (Chao & Hu, 2004).

This study focuses on the impact of filtration efficiency level and airflow control based on CO<sub>2</sub> levels on indoor air quality, specifically the particle concentration, in an urban low energy consumption nursery school during autumn and winter periods. The study aims to provide valuable data for optimizing indoor air quality in urban nursery schools using appropriate filters and intelligent control of airflow according to CO<sub>2</sub> levels.

## **2 MEASUREMENT AND SIMULATION METHODS**

### **2.1 Measurements**

Measurements with three filtration levels were performed in winter and autumn in a recent low energy consumption nursery school equipped with a mechanical ventilation system with heat recovery. The three types of filters are respectively classed G4, M5 and F7 according to NF EN 779 (2012).

The recent low energy consumption nursery school, built in 2012, is located in Villeurbanne, France, in an urban environment (see Figure 1a). It was designed to accommodate the staff and around 230 children from Monday to Friday, except Wednesday afternoons, in 8 classrooms, 2 sports rooms and 3 sleeping rooms, spread over two floors.

The school is ventilated by a balanced mechanical ventilation system with heat recovery between the incoming and outgoing air (see Figure 1b). To ensure good indoor air quality and prevent the entry of pollutants, particulates and pollen, the ventilation system is equipped with a multi-stage filtration system. Specifically, the system utilizes class G4 pleated filters and F7 V-bank filters (as per NF EN 779 (2012) standard) for the filtration of the incoming fresh air. Additionally, class G4 pleated filters are installed on the exhaust air flow to capture pollutants before the air enters in the heat recovery. The fresh air is diffused within the classrooms via

ceiling diffusers and is extracted via ceiling grilles. The airflow is dynamically adjusted based on CO<sub>2</sub> levels measured within the classrooms.

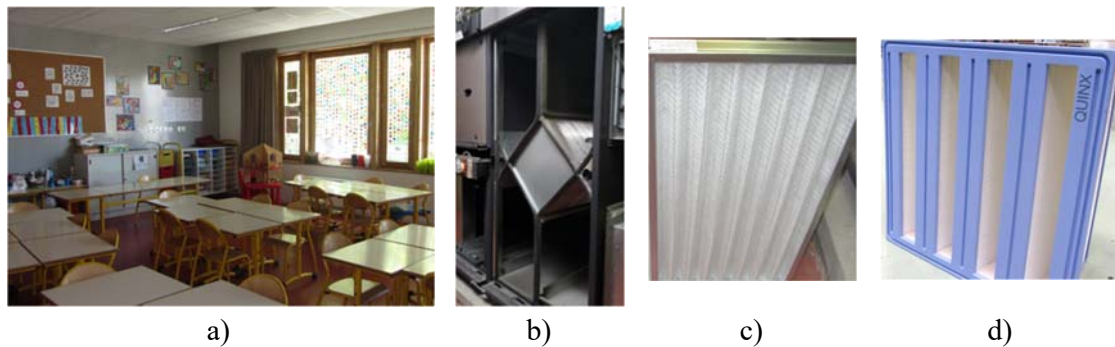


Figure 1: Photos of the school, AHU and filter. a) classroom, b) ventilation system, c) filter G4, b) filter F7

For this study, we conducted measurements using varying levels of filtration on the incoming air. Specifically, we tested three different filter configurations: G4, G4+M5, and G4+F7. Figure 1c and Figure 1d show the photos of the tested G4 and F7 class filters.

The measurements were carried out during autumn and winter using the same methodology as described by Ginestet et al. (Ginestet, Pugnet, & Robitu, 2015). This involved conducting measurements over a period of three consecutive days per week for three consecutive weeks in September and October 2015, as well as in January and February 2016. During these measurements, air flow was controlled and monitored periodically, with air velocity measured in straight sections of the ducts to maintain a constant air flow rate between 5000 and 5300 m<sup>3</sup>/h (corresponding to an air exchange rate (ACH) of 1.6 to 1.7 h<sup>-1</sup>). During the measurement periods, the air flow was kept constant and well balanced between supply and extract.

Particle concentrations ranging from 0.3 to 10 μm in size were measured using an optical particle counter. These measurements were conducted continuously and alternately at three key points within the ventilation system: at the inlet, representing outdoor air (O); at the outlet, within the delivered air duct, representing air being diffused indoors (S); and inside the exhaust air duct, representing air extracted from the indoor environment (I). These particle concentration values served two main purposes: first, for calculating in-situ filtration efficiency (E) by comparing particle concentrations measured in the fresh air duct (O) with those in the delivered air duct (S); and second, for determining the indoor-to-outdoor (I/O) particle concentration ratio. This ratio offers valuable insights into the extent of indoor particle pollution relative to outdoor conditions.

For each filtration level under investigation (G4, G4 + M5, and G4 + F7), measurements were taken once a week, with the day of measurement changing weekly. This resulted in three days of measurements for each filtration level studied. The filters were installed the day before the measurements, typically in the late afternoon. Normally, throughout the measurement period, the doors and windows of the school remained closed to maintain consistent testing conditions.

Additionally, prior to installation in-situ, the performance of the filters, including pressure drop and spectral efficiency in capturing DEHS (Di-Ethyl-Hexyl-Sebacat) particles, was measured in the laboratory. The test air flow rate in the laboratory was set at 3500 m<sup>3</sup>/h.

## 2.2 Simulations

Simulations of air and pollutant transfers, including particles and CO<sub>2</sub> from outside and CO<sub>2</sub> emitted by occupants were conducted using multizone CONTAM software developed by the U.S. National Institute of Standards and Technology (NIST) (Dols & Polidoro, 2020).

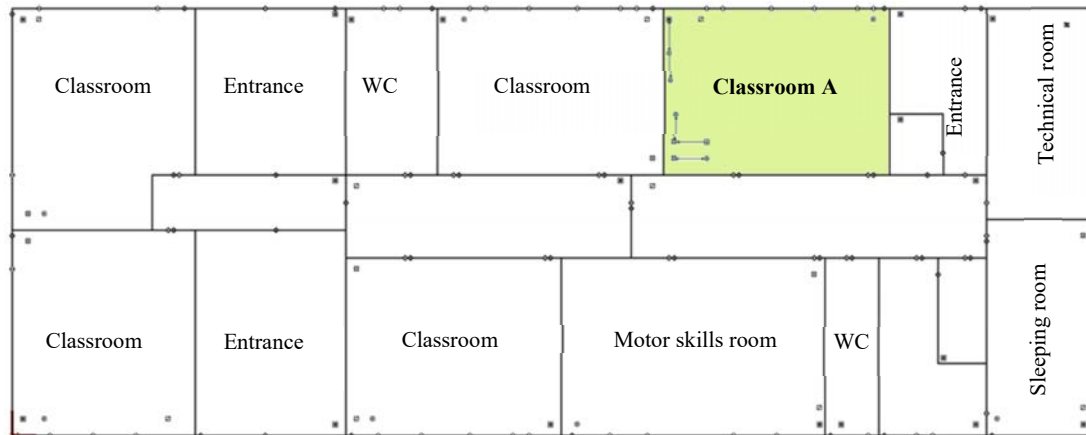


Figure 2: CONTAM model of the school floor

Modelling was conducted on one of the two floors of the school, and flow control was implemented only in classroom A, while the others are held constant. The results are presented solely for this classroom. The modelled floor (see Figure 1), covering an area of approximately 730 m<sup>2</sup> and a volume of around 2200 m<sup>3</sup>, comprises 5 classrooms, 1 motor skills room, 1 rest area, and accommodates approximately 150 children. The floor is ventilated by the balanced mechanical ventilation system, with a constant ventilation rate for classroom A set at 343 m<sup>3</sup>/h (corresponding to 5.96 L/s per person and an ACH of 1.91 h<sup>-1</sup>), determined via the decay method based on CO<sub>2</sub> reference measurements, Tuesday, September 22. The remaining airflow, up to 3167 m<sup>3</sup>/h, is distributed among the other rooms on the floor according to their volume. Initial simulations were based on particle and CO<sub>2</sub> concentration measurements conducted within the school premises. Outdoor air particle concentrations of 0.4 and 2.5 μm mean diameter, and the average filtration efficiency by particle size of the G4+F7 configuration determined from on-site measurements (80% (0.4 μm) and 90% (2.5 μm)), were used as input data. Indoor (I) and exhaust (E) air concentrations were utilized for result validation and calibration. Occupancy schedule and the number of occupants (maximum 12 children and the teacher) were retrieved from CO<sub>2</sub> measurements over a day. Students typically arrive in classroom at around 8:20 a.m., go out for recess twice in the morning, once at noon, and leave the classroom at around 4 p.m. Particle deposition was modelled for 0.4 and 2.5 μm particles with deposition rates of 2.50E-06 L/s and 6.00E-05 L/s respectively (Lai & Nazaroff, 2000). Resuspension was modelled using a model with a generation rate determined iteratively to match simulation results with measurement data. Significant resuspension of 0.4 μm particles was observed in the morning, potentially during cleaning and window opening before children's arrival. For 2.5 μm particles, a similar evolution with CO<sub>2</sub> was observed. Resuspension was modelled with a constant coefficient generation source of 0.193 μg/s weighted by presence and activity. The air temperature for both classroom A and the outdoors is considered at 20°C.

The internal and external openings include interior doors and undercutting, exterior windows, and external leakages. The doors of the classrooms are considered closed during the simulations. The external leakages simulate the infiltration between the zones and was modelled

with an envelope permeability of  $0.8 \text{ m}^3/(\text{h}\cdot\text{m}^2)\text{@}4\text{Pa}$ . The exterior window is always closed, while the interior doors are open 1 hour to simulate class break. The ventilation system includes AHU (1), air supply (2) and extract (3) to each zone. The air handling unit is set up considering filters. The simulations are done using 12 children plus one teacher, to recreate the actual conditions. Each occupant is assigned with a  $\text{CO}_2$  contaminant generation. The children are expected to be in medium activity (1.4 met), and between age 4-5. According to Batterman (Batterman, 2017), this group has a  $\text{CO}_2$  averaged emission rate of 0.147 L/min.

To assess the impact on  $\text{CO}_2$  and particle concentrations and to simulate the modulation of airflow based on  $\text{CO}_2$ , simulations were conducted with and without airflow regulation based on  $\text{CO}_2$  levels inside classroom, A, (with an area of  $60 \text{ m}^2$ ). Therefore, three simulations were performed with ventilation rates: 1) constant (cst 1) from measurements, 2) constant - minimum required and 3) modulated based on instantaneous  $\text{CO}_2$  levels. For the case 2, the airflow rate in classroom A was assumed to be approximately equal to the minimum regulatory airflow rate in France,  $200 \text{ m}^3/\text{h}$  ( $15 \text{ m}^3/\text{h}$  per occupant in kindergarten). For the case 3, the airflow rate is controlled by  $\text{CO}_2$  levels. If  $\text{CO}_2 < 800 \text{ ppm}$ , the airflow rate is  $200 \text{ m}^3/\text{h}$ , and if it exceeds this threshold, the rate is increased to  $400 \text{ m}^3/\text{h}$ .

### 3 RESULTS AND DISCUSSION

#### 3.1 Measurement results

Figure 3 shows the filter efficiency under both laboratory (lab) and in-situ conditions. Comparisons between these two sets of data are viable as the airflow rate per filter remains similar across both testing environments. The in-situ values, as shown in Figure 3, represent an average derived from the three days measurements for each filter. The results indicate that the in-situ filtration efficiency closely aligns with that observed in laboratory settings (refer to Figure 3), suggesting proper installation within the air handling unit with minimal leaks. As expected, G4 filters exhibit notably low efficiency for particles smaller than  $1 \mu\text{m}$ , nearly approaching zero. However, with the G4+M5 and G4+F7 configurations, efficiency gradually and significantly increases, reaching approximately 28 to 96% with the G4+M5 configuration and 82 to 99% with the G4+F7 configuration, depending on particle diameters.

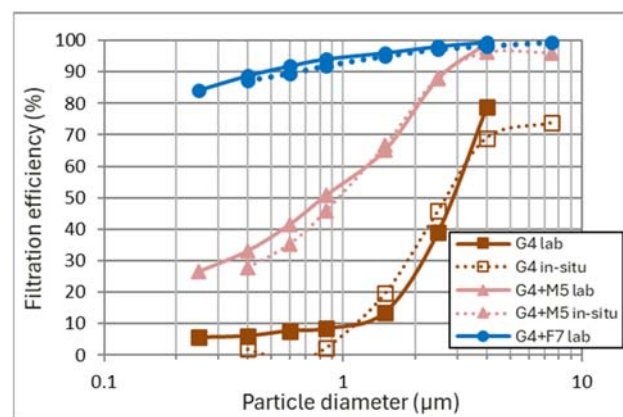


Figure 3: Filter efficiency determined in laboratory (lab) and in-situ

Figure 4 shows the results obtained throughout the 9-days measurement campaign, highlighting the ratio between indoor and outdoor particle concentration (I/O) as a function of inlet filter configurations (G4, G4+M5, G4+F7), the presence of children (with and without children), season (autumn and winter) and particle size ranging from  $0.3$  to  $10 \mu\text{m}$ . The results show that

the filter configuration significantly influences the I/O ratio. Typically, the I/O ratio decreases as filtration efficiency increases, particularly for particles smaller than 2  $\mu\text{m}$  in diameter. Specifically, with G4 filters, without children the mean ratio ranges from 0.7 to 0.8, while with G4 +M5 filters, it improves to 0.54 to 0.67, and with G4 +F7 filters, it further improves to 0.34 to 0.62 for particles smaller than 2  $\mu\text{m}$ . However, for larger particles where indoor and outdoor particle levels are low, no clear relationship is observed. For particles of 2-3  $\mu\text{m}$  and 5-10  $\mu\text{m}$ , the I/O ratio almost remains around 1 and increases at 4.8 respectively.

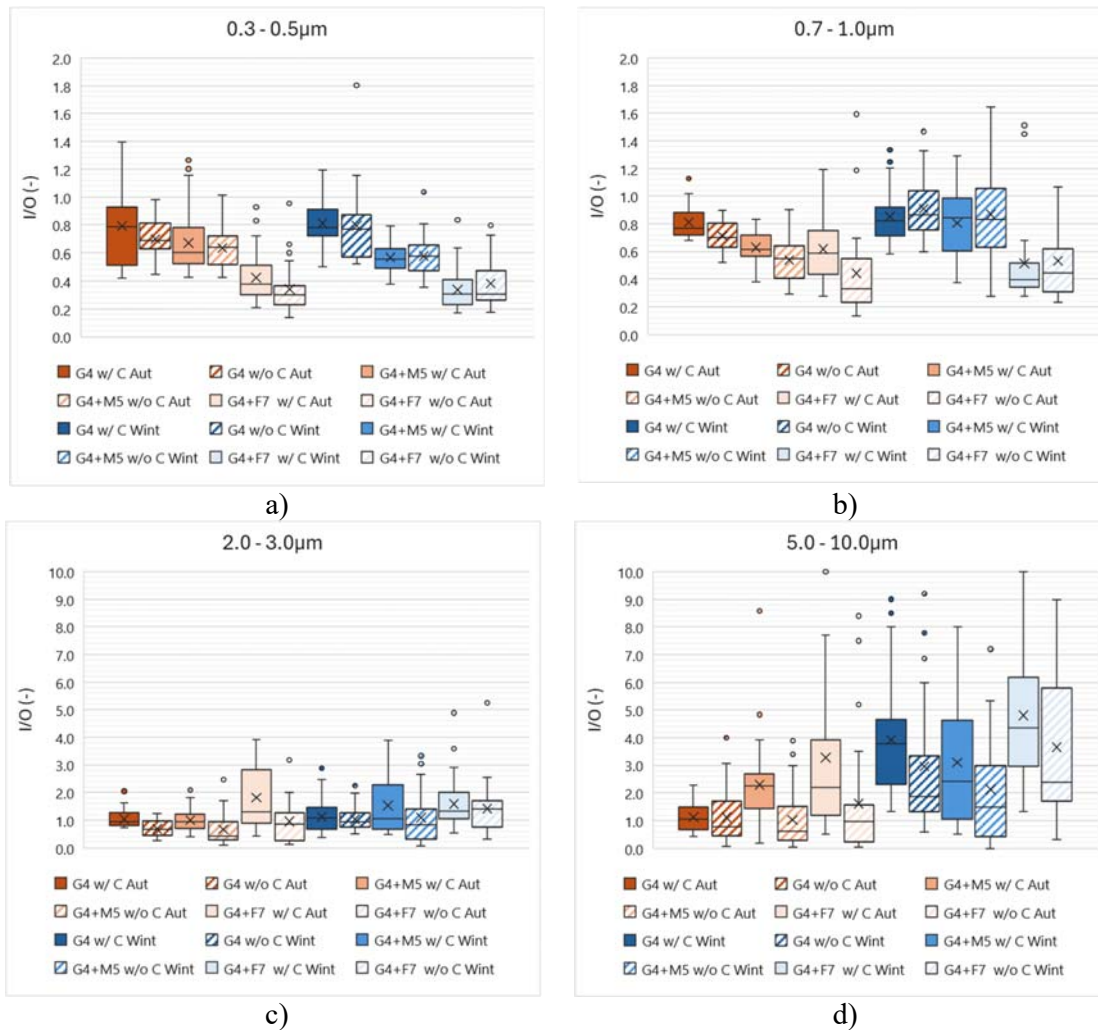


Figure 4: Indoor-to-outdoor (I/O) particle concentration ratio based on averages during occupied/unoccupied time (w/ C / w/o C) with different inlet filter configurations (G4, G4+M5 and G4+F7), seasons (autumn and winter) and particle size a) 0.3-0.5  $\mu\text{m}$ , b) 0.7-1.0  $\mu\text{m}$ , c) 2.0-3.0  $\mu\text{m}$ , d) 5.0-10  $\mu\text{m}$ .

Occupancy significantly influenced the indoor-to-outdoor (I/O) ratio especially for the largest particles. Scenarios with children (w/ C) generally displayed higher I/O ratios, ranging from 0.42 to 3.28, compared to scenarios without children (w/o C), which ranged from 0.34 to 1.61. This indicates that the presence of children intensifies indoor activity and pollutant generation, resulting in poorer indoor air quality.

The seasonal impact on the indoor-to-outdoor (I/O) particle ratio is moderate, with minor differences between autumn and winter. However, a consistent trend emerges: in winter, slightly higher mean I/O ratios (w/o C, ranging from 0.38 to 3.65) are typically observed across all filter configurations and particle size fractions compared to autumn (w/o C, ranging from

0.34 to 1.61). This suggests that during winter, increased indoor time for children may contribute to elevated indoor air pollution levels due to particle generation or resuspension. Interestingly, the trend is reversed for the G4+F7 filter configuration when considering particles smaller than  $5\ \mu\text{m}$ , with children present. This could be attributed to the potential opening of windows during the occupancy period.

### 3.2 Simulations results

Figure 5a and Figure 5b show the evolution of measured (mes) and simulated (sim) particle concentrations (PC) for  $0.4\ \mu\text{m}$  and  $2.7\ \mu\text{m}$  mean diameters respectively and  $\text{CO}_2$  using CONTAM for the three ventilation strategies (1-, 2-, 3-). The results demonstrate a good correlation between concentrations measured and simulated in the supplied air (AS) and indoor air (AI) with room (A). Figure 5b shows a strong correlation between measured AI values and  $\text{CO}_2$  levels, indicating that the finest particles (diameter less than  $0.7\ \mu\text{m}$ ) primarily originate from outdoors, while larger particles (diameter greater than  $0.7\ \mu\text{m}$ ) are generated indoors (due to the presence of people and activities).

The airborne particle concentration within the school (measured and simulated AI) is quite close to that of the supplied air (AS), with a positive deviation resulting from the influx of outdoor particles through envelope leakages and generated by the occupants and activities.

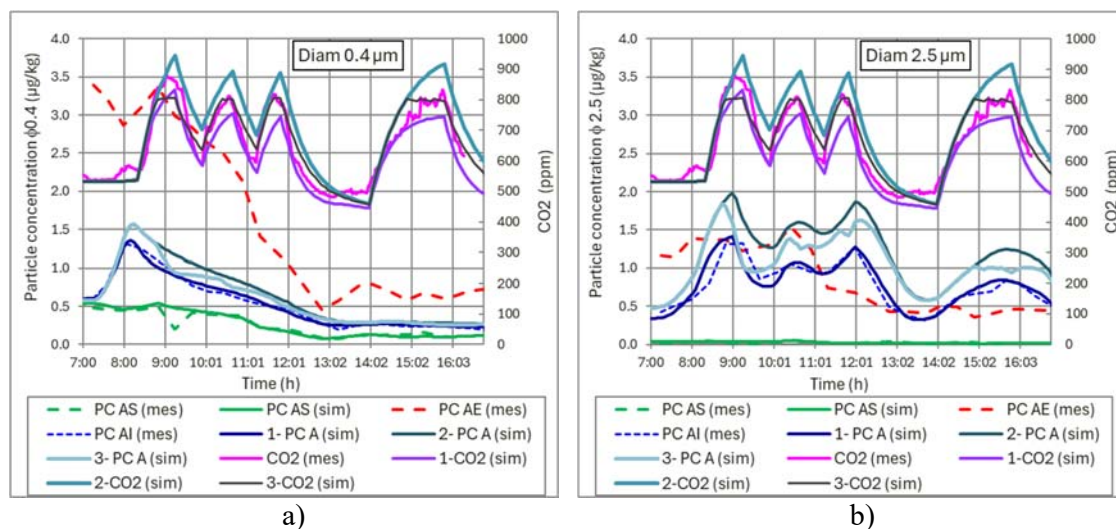


Figure 5: Measured (mes) and simulated (sim) particle concentrations (PC) for a)  $0.4\ \mu\text{m}$  and b)  $2.7\ \mu\text{m}$  mean diameters respectively and  $\text{CO}_2$  for the three ventilation strategies (1-, 2-, 3-)

The simulation results with the three ventilation strategies show that reducing the airflow rate by approximately 41% (strategy 1- to 2-) leads to an increase at peak times of around 25% for  $\text{CO}_2$ , 19% and 35% for  $0.4\ \mu\text{m}$  and  $2.5\ \mu\text{m}$  particles respectively. With demand-controlled ventilation based on  $\text{CO}_2$  levels (strategy 3-), the  $\text{CO}_2$  concentrations are maintained below the set threshold, while the airflow rate has been increased by approximately 5.7% above the minimum required (strategy 2-). Particle levels have decreased, particularly for  $2.5\ \mu\text{m}$  particles by 12.4%. For  $0.4\ \mu\text{m}$  particles, a slight decrease is noted.

## 4 CONCLUSIONS

This study provides valuable insights into optimizing indoor air quality in urban low energy consumption nursery school through appropriate filtration and intelligent airflow control based

on CO<sub>2</sub> levels. The results demonstrate that increasing filtration efficiency, particularly for particles smaller than 2 µm, significantly reduces the indoor-to-outdoor particle concentration ratio. Specifically, using G4+F7 filters improved the ratio from 0.7-0.8 with G4 filters to 0.34-0.62 for sub-2 µm particles. The presence of children and seasonal variations also impact indoor air quality, with higher particle levels observed during occupancy and winter months.

Simulations using CONTAM software accurately correlated measured and simulated particle and CO<sub>2</sub> concentrations, validating the model. Reducing airflow by 41% led to 25% higher peak CO<sub>2</sub> levels and 19-35% increases in 0.4 µm and 2.5 µm particle concentrations. In contrast, demand-controlled ventilation based on CO<sub>2</sub> maintained levels below the threshold while increasing airflow by only 5.7% above the minimum. This strategy reduced 2.5 µm particle levels by 12.4% and slightly decreased 0.4 µm particles. These findings highlight the importance of optimizing ventilation strategies and filtration to balance energy efficiency and indoor air quality in kindergartens. Demand-controlled ventilation based on CO<sub>2</sub> levels, combined with high-efficiency particulate filters, offers a promising approach to maintain healthy indoor environments while minimizing energy consumption.

Further research is needed to assess the long-term impacts and cost-effectiveness of these strategies in real-world settings.

## 5 ACKNOWLEDGEMENTS

This study has been sponsored by the French heating, air conditioning and air handling system manufacturers which are members of CETIAT. The authors are grateful to the city of Villeurbanne which has welcomed the study; many thanks to technical service of the city and to the teachers at the school who have facilitated the work of the people in charge of the measurements. The authors are also grateful to the manufacturer TITANAIR who facilitate the access to the school and have provided the filters used for the study.

## 6 REFERENCES

- Alonso, J., Dols, W., & Mathisen, H. (2022). Using Co-simulation between EnergyPlus and CONTAM to evaluate recirculation-based, demand-controlled ventilation strategies in an office building. *Building and Environment*, 211.
- Apte, M., Fisk, W., & Daisey, J. (2000). Associations between indoor CO<sub>2</sub> concentrations and sick building syndrome symptoms in U.S. office buildings: An analysis of the 1994-1996 BASE study data. *Indoor Air*, 10(2), 246–257.  
doi:<https://doi.org/10.1034/j.1600-0668.2000.010004246.x>
- Batterman, S. (2017). Review and Extension of CO<sub>2</sub>-Based Methods to Determine Ventilation Rates with Application to School Classrooms. *Int J Environ Res Public Health*, 14(2).
- Cabovská, B., Bekö, B., Teli, G., Ekberg, D., & Dale, L. (2022). Ventilation strategies and indoor air quality in Swedish primary school classrooms. *Building and Environment*, 226.
- Carlsson, T. (2008). Air filtration: Choosing the right filter class for HVAC systems. *Filtration & Separation*, 45(9), 36-38.
- Chao, C., & Hu, J. (2004). Development of a dual-mode demand control ventilation strategy for indoor air quality control and energy saving. *Building and Environment*, 39(4), 385–397. doi:<https://doi.org/10.1016/j.buildenv.2003.09.007>
- Daisey, J., Angell, W., & Apte, M. (2003). Indoor air quality, ventilation and health symptoms in schools: an analysis of existing information. *Indoor air*, 13(1), 53-64.



- Dols, W., & Polidoro, B. (2020). *CONTAM User Guide and Program Documentation Version 3.4*. Technical Note 1887, NIST.
- Emmerich, S., & Persily, A. (2001). *State-of-the-art review of CO2 demand controlled ventilation technology and application*. Internal Report, NIST Interagency.
- Fisk, W. (2000). Health and productivity gains from better indoor environments and their relationship with building energy efficiency. *Annual Review of Energy and the Environment*, 25(1), 537-566.
- Fisk, W., & De Almeida, A. (1998). Sensor-based demand-controlled ventilation: a review. *Energy and Buildings*, 21(1), 35-45.
- Ginestet, A., Pugnet, D., & Mouradin, L. (2013). Air filtration: Air filters for balanced ventilation systems. *Filtration and Separation*, 50(1), 30-33.
- Ginestet, A., Pugnet, D., & Robitu, M. (2015). How the filtration of the incoming air decreases the particle concentration within a school equipped with a balanced ventilation system. *36th AIVC Conference : Effective ventilation in high performance buildings*, (p. 8). Madrid, Spain.
- Gram, O. (2019). *Use of low cost pollutant sensors for developing healthy demand controlled ventilation strategies*. Master's thesis, Norwegian University of Science and Technology, Trondheim, Norway.
- Guyot, G., Sherman, M., & Walker, I. (2018). Smart ventilation energy and indoor air quality. *Energy and Buildings*, 165, 416-430.
- Lai, A., & Nazaroff, W. (2000). Modeling indoor particle deposition from turbulent flow onto smooth surfaces. *Journal of Aerosol Science*, 31(4), 463-476.
- Liu, X., Xiao, M., Zhang, X., Gal, C., Chen, X., Liu, L., . . . Clements-Croome, D. (2017). A review of air filtration technologies for sustainable and healthy building ventilation. *Sustainable Cities and Society*, 32, 375-396.
- Merema, B., Delwati, M., Sourbron, M., & Breesch, H. (2018). Demand controlled ventilation (DCV) in school and office buildings: Lessons learnt from case studies. *Energy and Buildings*, 172, 349-360.
- Mysen, M., Berntsen, S., Nafstad, P., & Schild, P. (2005). Occupancy density and benefits of demand-controlled ventilation in Norwegian primary schools. *Energy and Buildings*, 37(12), 1234-1240.
- Persily, A. (2015). Indoor Carbon Dioxide Concentrations in Ventilation and Indoor Air Quality Standards. *36th AIVC: Effective ventilation in high performance buildings*, (pp. 810-819). Madrid, Spain.
- Sadrizadeh, S., Yao, R., Yuan, F., Awbi, H., Bahnfleth, W., Bi, Y., . . . Li, B. (2022). Indoor air quality and health in schools: A critical review for developing the roadmap for the future school environment. *Building Engineering*, 57.
- Sofuoglu, S., & Moschandreas, D. (2003). The link between symptoms of office building occupants and in-office air pollution: the Indoor Air Pollution Index. *Indoor Air*, 13(4), 332-343.
- Wachenfeldt, B., Mysen, M., & Schild, P. (2007). Air flow rates and energy saving potential in schools with demand-controlled displacement ventilation. *Energy and Buildings*, 39(10), 1073-1079.
- Wargoeki, P., & Wyon, D. (2007). The effects of outdoor air supply rate and supply air filter condition in classrooms on the performance of schoolwork by children: ASHRAE 1257-RP. *HVAC&R Res.*, 13(2), 165-191.
- Wargoeki, P., & Wyon, D. (2017). Ten questions concerning thermal and indoor air quality effects on the performance of office work and schoolwork. *Building and Environment*, 112, 359-366.

# Data Analysis of Indoor Air Quality and Thermal Comfort in Dwellings in Santiago, Chile

Constanza Molina<sup>\*1</sup>, Benjamin Jones<sup>2</sup>, Ignacio Garrido<sup>1</sup>, Gioberti Morantes<sup>2</sup>

*1 Pontificia Universidad Católica de Chile  
Vicuña Mackenna 4860, Macul, Santiago  
Chile*

*2 Department of Architecture and Built Environment,  
University of Nottingham  
Nottingham, NG7 2UH, UK.*

*\*Corresponding author: cdmolina@uc.cl*

## ABSTRACT

Achieving better energy efficiency requires dwellings to face a delicate equilibrium, balancing thermal comfort and indoor air quality. This longitudinal study uses crowdsourced data collected over a year from 15 residences in Santiago, Chile, to examine the intricate relationship between these two parameters and the houses' typology.

Results highlight considerable variability in PM<sub>2.5</sub> and PM<sub>10</sub> concentrations and thermal comfort across the sample. PM concentrations are below the worldwide representative value, but the maximum values are above the representative maximum. Chronic harm from exposure to these concentrations is 1271 and 683 (DALYs/10<sup>5</sup> person/year) for PM<sub>2.5</sub> and PM<sub>10</sub>. Moreover, the annual WHO 2021 recommendations are not met during the measured time, and the daily mean is met by 25% and 72% of the measured days for PM<sub>2.5</sub> and PM<sub>10</sub>, respectively. Determinants of these variations may include geographical location and construction materials, which will be included in future research. The indoor environment does not provide the hygrothermal conditions to achieve acceptable thermal comfort, which is only reached during 56% of the measured time.

This research advocates for a comprehensive regulatory approach, ensuring that interventions are needed to optimize energy efficiency and prioritize occupant well-being. Insights from this study contribute to a better understanding of competing objectives in residential architecture, offering informed perspectives for strategic decision-making and impactful interventions.

## KEYWORDS

Indoor air quality; Thermal comfort; Particles; Longitudinal study; Residential

## 1 INTRODUCTION

Residential buildings play a crucial role in shaping human health and well-being by serving as the primary environments where individuals spend a significant proportion of their time. Comfortable and healthy homes contribute to physical health by providing optimal conditions that reduce the risk of respiratory illnesses and support mental well-being by creating spaces of shelter and relaxation, fostering emotional stability, and reducing stress. However, indoor environments and housing conditions vary from house to house due to a complex interplay of factors, such as household lifestyle, preferences and behavior, and socio-demographic and economic inequalities, all of which influence human health and well-being within residential settings. Furthermore, environmental factors such as climate, ambient pollution, and extreme weather events demand a more resilient housing design to mitigate these risks and safeguard occupants' safety and comfort.

Worldwide, diverse geographical, cultural, and socio-economic factors contribute to a wide range of housing conditions and lifestyles. From urban cities to rural villages along the country, housing types vary significantly, ranging from modern high-rise apartments to traditional single-family dwellings and informal settlements. Over the last two decades, Chile has begun to improve the efficiency and sustainability of its housing stock. The increasing demand for energy-efficient buildings has led to tighter envelopes with a corresponding reduction in ventilation and air infiltration. An unintended consequence of the drive for heating and cooling

demand reduction is a reduction in IAQ (Shrubsole et al., 2014; Molina et al., 2021). Therefore, if the Chilean housing stock aims to develop sustainably, it must simultaneously consider energy and IAQ targets, and the impacts of energy-demand reduction interventions on IAQ must be understood. Accordingly, it must promote occupant health and become people-centered.

This paper reports the beginning of a study that investigates particle concentrations and hygrothermal conditions in a sample of Santiago houses to inform public health interventions, urban planning, and sustainability in Chile. The study is currently measuring indoor environmental parameters in a sample of houses in Santiago. Section 2 describes the study and the methods of analysis carried out for this paper, and Section 3 shows and discusses the results.

## 2 METHODS

The research study measures IEQ parameters in a sample of 32 houses in Santiago using PurpleAir sensors, including relative humidity, air temperature, and particulate matter concentrations (PM<sub>2.5</sub> and PM<sub>10</sub>). Measurements are made every two minutes and recorded in the cloud. Sensors were installed in the living room or kitchen, away from direct solar radiation or sources of contamination, as these locations are where the concentration of the more harmful pollutants are expected to be. Data was collected over a year to represent the four seasons and then extracted from the platform at a ten-minute resolution (averaged). However, not all sensors recorded sufficient data to run the analyses, so a cleaning process was carried out, and only those sensors with adequate data (15) were retained for the study. The sample includes both houses and flats, all of which utilize natural ventilation exclusively. The climate in Santiago can be described as *Csb*, meaning *Temperate/DrySummer/Warm summer/ Rain in winter*, according to the Köppen classification (Peel *et al.*, 2007).

### 2.1 Data gathering

Web scraping techniques from publicly available sources included wildfires and treated them as *events*. These sources of information included CONAF, the Chilean National Forestry Corporation, and social media platforms. Monitored data was extracted using an automated code in Python and the "BeautifulSoup4" and "Requests" libraries, known for being effective at conducting clean Web-Scraping processes. Fifteen out of the 32 dwellings with complete data over a year were selected for this analysis to ensure coverage across different seasons. Parameters included the relative humidity, air temperature, atmospheric pressure, and particle concentrations.

### 2.2 Data processing and data analyses

Indoor thermal comfort and air quality analyses were carried out on two levels: i) inferential and descriptive statistics (Casella *et al.*, 2001) and ii) for thermal comfort, a hygrothermal analysis based on a psychrometric chart with standardized comfort zones and, for IAQ, the PM concentration exceeding the WHO recommendations for 24h mean averages (WHO, n.d.), and health impacts using Harm Intensities according to Morantes *et al.*, (2023). Morantes *et al.* developed an expression for quantifying chronic harm in DALYs based on harm intensities and contaminant concentrations. They combined toxicological and epidemiological data to calculate median harm intensities and uncertainties for the most common and reported indoor air contaminants.

A second analysis was carried out using the "k-means clustering" algorithm. This technique organizes the data into groups based on similarities. We used the "*scikit-learn*" library (Kramer *et al.*, 2016), which provides machine learning tools for data processing to create user-type profiles by identifying patterns in thermal comfort time-series data. This clustering considers the median relative humidity and air temperature in homes to provide a representative value for categorizing them.

After determining that the cleaned temperature data followed a normal distribution—minimizing errors and outliers—we used the *elbow method* to determine the number of clusters or subgroups (Shi *et al.*, 2021).

### 2.3 Data Visualization

A psychrometric chart visually represented thermal comfort, indicating whether the temperature and relative humidity fell within the acceptable comfort zones for the summer and winter seasons. A provisional dataset was also created with the dates of major extreme events (such as fires). This was generated using CONAF Chile data until July 2023 and the social network X (formerly known as Twitter) with data after July 2023. This information was used to find patterns in PM concentrations and increases in temperature in homes when these extreme events occurred.

## 3 RESULTS AND DISCUSSION

### 3.1 Data visualization

Data visualization and analysis tools are hosted online (GitHub repository link: <https://eccuc.github.io>), providing ongoing updates and interactive visualizations of the study's findings. Figure 1 shows the location of the 15 sensors in Santiago de Chile.

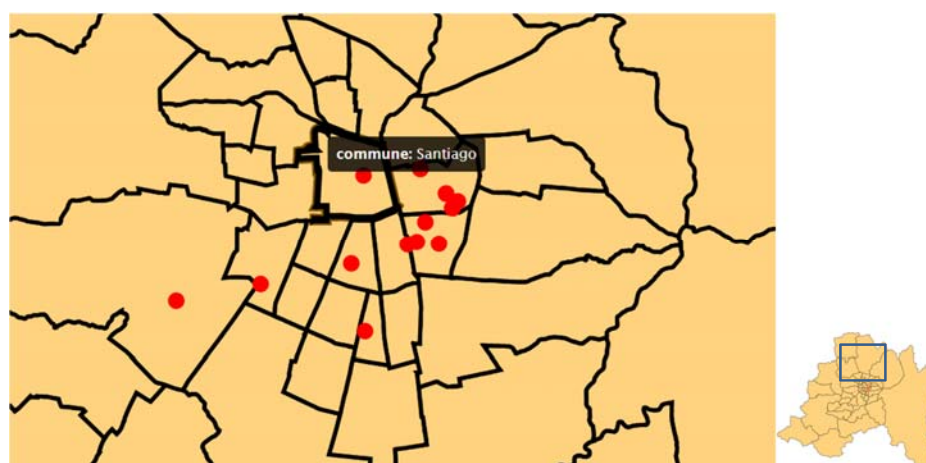


Figure 1: Location of the 15 sensors in the Metropolitan region. In the graph, only 13 sensors appear because two of them are very close to each other and thus appear overlapped.

### 3.2 Particle concentrations and harm

Table 1 shows the annual descriptive statistics of PM<sub>2.5</sub> and PM<sub>10</sub> concentrations with annual medians of 21.19 and 22.76  $\mu\text{g}/\text{m}^3$ , respectively. Harm Intensities for PM<sub>2.5</sub> and PM<sub>10</sub> are 30 and 60 DALY/ $\mu\text{g}/\text{m}^3/10^5$  person/year, giving 1271 and 683 DALYs/ $10^5$  person/year, respectively, and a total harm of 1954 DALYs/ $10^5$  person/year.

Table 1: Descriptive statistics and harm of particle concentrations (annual data). The worldwide statistics are in brackets. Arrows indicate whether the sample is below or above the world representative statistics from Morantes *et al.*.

Statistic		PM <sub>2.5</sub> ( $\mu\text{g}/\text{m}^3$ )		PM <sub>10</sub> ( $\mu\text{g}/\text{m}^3$ )
Max	↑	1688 (430)	↑	2082 (350)
P <sub>97.5</sub>	-	91.40	-	96.47
Median	↓	21.19 (26)	↓	22.76 (62)
Mean	↓	28.52 (52)	↓	32.31 (82)
P <sub>2.5</sub>	↓	3.85 (0.022 <sup>†</sup> )	↓	4.35 (17 <sup>†</sup> )
SD	↓	29.92 (67)	↓	33.69 (76)
Harm (DALYs/ $10^5$ person/year)	↓	1271.22 (1560)	↓	682.71 (1860)

<sup>†</sup>: Minimum concentration reported by Morantes *et al.*, 2024.

The PM<sub>2.5</sub> and PM<sub>10</sub> annual mean in 2023 were 28.52 and 32.31  $\mu\text{g}/\text{m}^3$ , surpassing the WHO guidelines of 5  $\mu\text{g}/\text{m}^3$  and 15  $\mu\text{g}/\text{m}^3$ . The 99<sup>th</sup> percentile of the daily 24-hour means were 94.10 and 102.11  $\mu\text{g}/\text{m}^3$  for PM<sub>2.5</sub> and PM<sub>10</sub>, respectively, above the recommended 15 and 45  $\mu\text{g}/\text{m}^3$ .

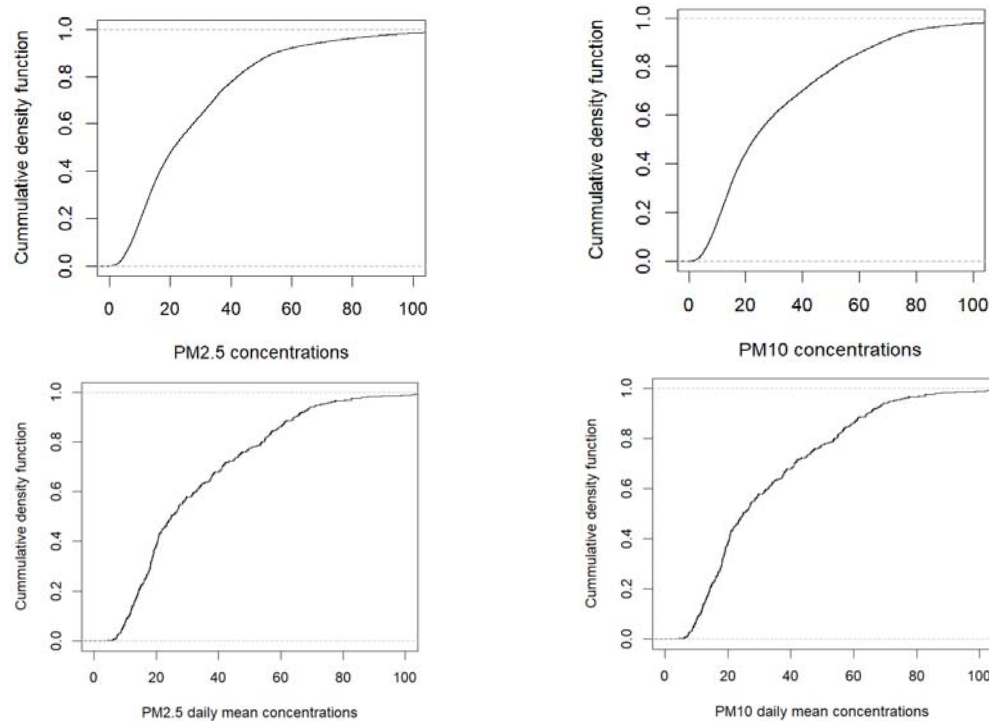


Figure 2: Cumulative density functions for PM concentrations during 2023 (above) and the daily means (below). Notice that the WHO 24-hour mean averages are met by 25% and 72% of the measured days for PM<sub>2.5</sub> and PM<sub>10</sub>, respectively.

### 3.3 Hygrothermal performance

A psychrometric chart with winter and summer comfort zones visually represented each house's thermal comfort; see Figure 3. Data indicate that households fell within acceptable comfort zones during 56% of the measured time. The indoor air temperatures ranged between 9.4 and 41°C, with a median of 26°C, whereas the relative humidity ranged between 9% and 73%, with a median of 34%. The charts are available for each house in both HTML web and Python versions. The charts display a heat map, where lighter to yellow areas indicate higher concentrations of absolute humidity and indoor temperature tuples.

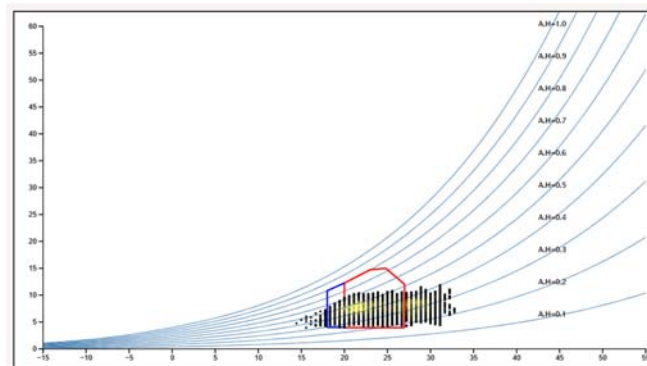


Figure 3: Psychrometric chart for one sensor, showing the data within the thermal comfort zone—red area for summer and blue and red area for winter. Gradients of yellow indicate data saturation.

For charts of other houses, visit the GitHub repository at <https://eccuc.github.io>.

According to the heat map shown in Figure 3, most dwellings tend to concentrate their hygrothermal conditions within the thermal comfort zone. These graphs can be viewed at <https://eccuc.github.io/fondecyt/higrometric/hygrometric.html>.

A rigorous future analysis might require incorporating construction materials (such as insulation materials and thermo panel windows) and conditioning elements (such as air conditioning and heating) into the equation, as they would allow for the development of a meta-statistical profile of thermal comfort in Chilean dwellings, creating more reliable profiles for developing public policies on hygrothermal conditioning.

### 3.4 Hygrothermal conditions during extreme or seasonal events

Overall, no statistical patterns regarding wildfires and hygrothermal conditions were found. This conclusion was reached through graphical visualization of the time-series data of temperature and relative humidity within the houses over the measured time while overlapping the extreme events and their dates. This first examination did not show a pattern worth exploring any deeper in Santiago, and the most visible pattern over time is the temperature and humidity variations, following a periodic function with high temperatures and low humidity in summer and the opposite in winter.

### 3.5 Comparative analysis and data clustering

The variation in indoor air quality and thermal comfort was influenced by factors such as the geographical location and the construction materials of the residences. *The k-means* clustering identifies distinct thermal comfort profiles, suggesting a need for tailored approaches in architectural design to enhance energy efficiency and thermal comfort. This is a subject of further investigation. Two primary clusters of dwellings were identified in the *Jupyter Notebook* based on the median relative humidity and temperature, with indoor relative humidity below and above 38% (Group 0 and Group 1, respectively), which showed different profiles of thermal comfort among the dwellings; see Figure 4a. A second iteration was applied using the elbow method to further sub-categorize the homes; see Figures 4a and 4b. Notice that two profiles, in red in Figure 4.a and green in 4.b, are overlapped.

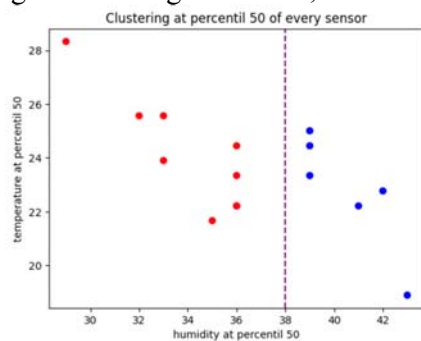


Figure 4.a: Sample clustering, groups 0 and 1.

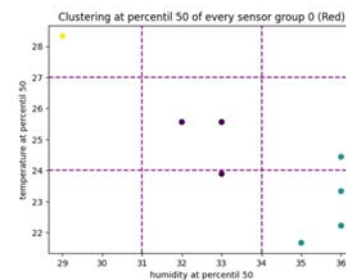


Figure 4.b: Clustering of Group 0, giving three user profiles.

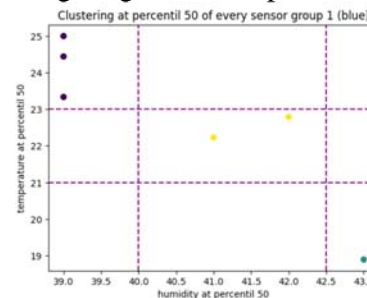


Figure 4.b: Clustering of Group 1, giving three user profiles.

In both cases, three subgroups were created within the quadrants. However, this subclassification is temporal because, given the restricted number of homes and the lack of

information about the presence of elements that might improve thermal comfort, such as HVAC equipment, it is impossible to state that these profiles represent the diverse Chilean realities.

#### 4 OTHER LIMITATIONS

Limitations of this study include the lack of verification for potential 'deviation' in the two sensors' response once they were deployed, as well as the absence of individual uncertainty analyses and consideration of seasonal variations.

#### 5 CONCLUSIONS

Data processing involved statistical and machine learning tools, both numerical and visual, including Python, R HTML, CSS, AND JavaScript. This study found great variability in PM<sub>2.5</sub> and PM<sub>10</sub> concentrations in the sampled houses, with average yearly levels of 21.19 µg/m<sup>3</sup> for PM<sub>2.5</sub> and 22.76 µg/m<sup>3</sup> for PM<sub>10</sub>. These concentrations are linked to health risks, contributing to harm quantified as 1271 DALYs/10<sup>5</sup> person/year for PM<sub>2.5</sub> and 683 DALYs/10<sup>5</sup> person/year for PM<sub>10</sub>. The analysis has also found that homes only achieved acceptable thermal comfort levels 56% of the measured time. Future research will focus on the variability within each house and its relation with the house and household characteristics.

These findings emphasize the need for an integrated approach in residential building design, incorporating both architectural and technological solutions to achieve optimal thermal comfort and air quality. The study advocates for robust regulatory frameworks to ensure these aspects are prioritized in future housing policies. Further research is recommended to include more diverse environmental conditions and housing typologies to generalize the findings more broadly across different climates and construction styles. Additionally, incorporating more advanced metrics for air quality and thermal comfort could refine the understanding of these interactions.

*For further details on quantifying the harm provided by exposure limit values (ELV) and their implications for public health, refer to the paper of this conference titled "The Protection from Harm to Populations of People Provided by Exposure Limit Values" by Jones et al..*

#### 6 ACKNOWLEDGEMENTS

Molina received funding from ANID Fondecyt Iniciación 11220965 and Garrido from IPRE-VRI 2023 from Pontificia Universidad Católica de Chile. Part of the data was gathered by André Vargas, whose work as a research assistant contributed to the quality of this research.

#### 7 REFERENCES

- Casella, George, and Berger, Roger L. (2001). Statistical Inference.
- Givoni B, A. (1969). Man, Climate, and Architecture.
- Kramer, O., & Kramer, O. (2016). Scikit-learn. *Machine learning for evolution strategies*, 45-53.
- Morantes, G., Jones, B., Molina, C., & Sherman, M. H. (2023). Harm from Residential Indoor Air Contaminants. *Environmental Science & Technology*, 58(1), 242-257.
- Peel, M. C., Finlayson, B. L., & McMahon, T. A. (2007). Updated world map of the Köppen-Geiger climate classification. *Hydrology and earth system sciences*, 11(5), 1633-1644.
- Shi, C., Wei, B., Wei, S., Wang, W., Liu, H., & Liu, J. (2021). A quantitative discriminant method of elbow point for the optimal number of clusters in clustering algorithm. *EURASIP journal on wireless communications and networking*, 2021, 1-16.
- WHO. (n.d.). *What are the WHO air quality guidelines?*. World Health Organization. <https://www.who.int/news-room/feature-stories/detail/what-are-the-who-air-quality-guidelines>

# The protection from harm to populations of people provided by Exposure Limit Values

Benjamin Jones<sup>\*1</sup>, Gioberti Morantes<sup>1</sup>, Constanza Molina<sup>2</sup>, Max Sherman<sup>1</sup>, James A. McGrath<sup>3</sup>

*1 Department of Architecture and Built Environment,  
University of Nottingham, NG7 2RD, United  
Kingdom*

*2 School of Civil Construction, Faculty of  
Engineering, Pontificia Universidad Católica de  
Chile*

*\*Corresponding author:  
benjamin.jones@nottingham.ac.uk*

*3 Department of Physics,  
Maynooth University, Maynooth,  
Co. Kildare, W23 F2H6, Ireland*

## ABSTRACT

The protection from chronic harm provided by exposure limit values (ELVs) is evaluated for indoor air contaminants set by regulatory bodies of member countries in the Air Infiltration and Ventilation Centre (AIVC). Significant variability was found in the regulated harm levels from ELVs for the same contaminants across different countries, highlighting inconsistencies in public health protection. The concept of a regulated harm budget (RHB) is introduced, representing the total allowed harm from regulated contaminants implicitly set by a regulatory body. Among AIVC countries, Spain is the only nation with an RHB of 2400 DALYs/10<sup>5</sup> person/year for the three key contaminants PM<sub>2.5</sub>, NO<sub>2</sub>, and formaldehyde. The RHBs for most AIVC countries exceeded harm values associated with smoking and alcoholism. This underscores the need for interventions to mitigate indoor air contaminant harm and reduce it to acceptable levels that are comparable to other regulated risks.

## KEYWORDS

DALY, IAQ, health, regulated harm budget, ELVs.

## 1 INTRODUCTION

A health-centred approach was recently used (Morantes et al. 2024) to quantify and compare the chronic harm caused by indoor air contaminants in dwellings of the Global North using the disability-adjusted life-year (DALY). Epidemiological and toxicological evidence of population morbidity and mortality was used to determine Harm Intensities (HI), a metric of chronic harm per unit of contaminant concentration. The HIs are specific to each contaminant and can be used for any environment. The chronic harm per year for each contaminant is the product of a long-term median exposure concentration and an HI. The harm for each contaminant can be summed to identify the harm caused by many contaminants.

The magnitude of harm for each contaminant can be used to rank them and identify Contaminants of Concern (CoC). The most harmful contaminants in dwellings are fine particulate matter (PM<sub>2.5</sub>), the coarse fraction of particulate matter (PM<sub>10-2.5</sub>), nitrogen dioxide (NO<sub>2</sub>), formaldehyde (HCHO), radon, and ozone (O<sub>3</sub>). They are CoCs because, together, they account for over 99% of total median harm in dwellings and so can then be used to regulate their IAQ. One way to do this is to set a harm budget, the distribution of harm that is expected in an acceptable reference scenario (Morantes et al. 2024).



National regulatory bodies, environmental agencies, and global health organizations regularly establish indoor and outdoor air quality standards and guidelines for various contaminants. These entities typically rely on exposure limit values (ELVs) to protect public health, defining the maximum permissible concentration experienced over a given exposure period. However, ELVs for the same contaminants may vary significantly across different organizations for identical exposure periods (Abdul-Wahab et al. 2015; Morantes et al. 2016; Salis et al. 2017). Such disparities in ELVs implicitly reflect varying assessments of contaminant harm influenced by policy considerations, policymaker judgments, and differences in available contaminant data, rather than representing consistent hazard levels. The derivation of guidelines and standards also varies, some as the consequence of practical experience, others from comprehensive reviews and expert consensus on the health effects of contaminants. Most standards are established through toxicological and epidemiological health impact assessments (Borsboom et al. 2016).

The concept of the harm budget (Morantes et al. 2024) can be refined further to incorporate the ELVs of contaminants along with their corresponding HIs. This refined approach, termed the Regulated Harm Budget (RHB), enables the determination of the magnitude of harm associated with each contaminant's ELV. Essentially, the RHB represents the total allowed harm from all regulated contaminants, implicitly established by a regulatory body. This approach also draws inspiration from the IAQ equivalence principle proposed by Sherman, Walker, and Logue (2012).

We assess the degree of protection from chronic harm by using exposure limit values (ELVs) of member countries of the Air Infiltration and Ventilation Centre (AIVC) for indoor environments. The method is described in Section 2. The results are presented in Section 3 and are discussed in Section 4.

## 2 METHOD

### 2.1 Estimating Chronic Harm

All-cause chronic population *harm* (DALY/person/year) from the inhalation of a specific airborne contaminant (indicated by the subscript  $i$ ) is a function of a harm intensity,  $HI_i$ , (DALY/ $\mu\text{g}/\text{m}^3$ /person/year) and a concentration,  $C_i$ .

$$Harm_i = HI_i \cdot C_i \quad (1)$$

Generally, the contaminant concentrations are reported in units of  $\mu\text{g}/\text{m}^3$ , but some have others, such as  $\text{Bq}/\text{m}^3$  for radon, and  $\text{CFU}/\text{m}^3$  for mold spores. The reported statistic should be an annual median given the expected log-normality of any distribution of contaminant measurements (Ott 1990). Harm intensities for a total of 110 contaminants are considered here: 45 indoor contaminants commonly found in dwellings are given in Morantes et al. (2024) and 65 other indoor contaminants (data not published).

The harm intensities are specific to individual contaminants and can be applied in any environment. However, a limitation persists: when the concentration surpasses a maximum median threshold, higher estimates of harm are obtained compared to a non-linear approach. In the case of epidemiology-based HIs, Table 1 gives appropriate concentration thresholds for a linear approach to HI, considering a 10% mean absolute percentage error overestimation as the limit (Morantes et al. 2024). Conversely, for toxicology-based HIs, no such limit is indicated, as this approach demonstrates applicability across a full range of concentrations (Fantke et al. 2017).

Table 1: Appropriate concentration thresholds for a linear HIi approach

Contaminant (i)	Concentration Regime ( $\mu\text{g}/\text{m}^3$ )	Mean Absolute Percentage Error (%)
Acrolein	(0 – 2.7)	10 (95% C.I. 9–20)
Benzene	(0 – 890)	10 (95% C.I. 8–10)
Formaldehyde	(0 – 33)	10 (95% C.I. 10–10)
Mold	(0 – 3750)	10 (95% C.I. 9–10)
Nitrogen dioxide	(0 – 225)	10 (95% C.I. 10–10)
Ozone	(0 – 495)	10 (95% C.I. 10–10)
PM <sub>10</sub>	(0 – 108)	10 (95% C.I. 10–10)
PM <sub>2.5</sub>	(0 – 50)	10 (95% C.I. 10–10)
Radon	(0 – 425)	9 (95% C.I. 8–10)
Sulphur dioxide	(0 – 66)	10 (95% C.I. 9–10)

## 2.2 Estimating Regulated Harm Budgets (RHB)

The total harm estimated using all contaminant ELVs specified by a regulatory body constitutes a Regulated Harm Budget (RHB). However, not all contaminants specified have a high HI and/or are only found at low concentrations, and so are not particularly harmful. The CoCs identified by Morantes et al. (2024) are harmful and so the analysis is restricted to these.

Accordingly, a RHB for any regulatory body is defined as

$$RHB = \sum_{i=1}^{N_{CoCs}} HI_i \cdot \hat{C}_i \quad (2)$$

Here,  $N_{CoCs}$  represents the total number of Contaminants of Concern for which ELVs are specified by a regulatory body, and  $\hat{C}$  denotes the long-term concentration threshold specified by a regulatory body in a relevant standard or guideline.

There is limited evidence of chronic synergistic effects at the concentrations expected in buildings and so the RHB in Equation (2) is calculated additively, following conventional risk assessment practice and the Concentration Addition principle (Morantes et al. 2024).

## 2.3 Sources of Data

We use the online guidelines database of the International Society of Indoor Air Quality and Climate (ISIAQ) STC34 Indoor Environmental Quality (IEQ), compiled by Dimitroulopoulou et al. (2023). It contains 844 entries, which we reduce to 746 by excluding non-contaminants, such as water,

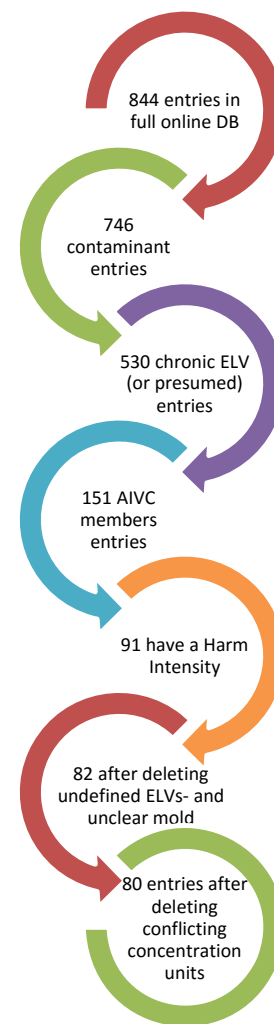


Figure 1. Data analysis workflow.

air temperature, relative humidity, and PM ratios. Entries are categorized based on averaging times, denoted as chronic (>24h, annual), acute (<24h), and no data. Entries without exposure periods were retained by assuming applicability across all timeframes. Removing acute entries left 530 entries. Restricting the dataset to member countries of the Air Infiltration and Ventilation Centre (AIVC) left 151 entries. Considering only contaminants with a harm intensity (including Total Volatile Organic Compounds, TVOCs) left 91 entries. Removing entries with undefined ELVs, indicated by statements such as "as low as possible", reduced the dataset to 85 entries. Two more entries for airborne mold were removed because some of the information was unclear, and to ensure consistency, entries with conflicting concentration units (pCi/L) were excluded, although they will be converted in future work. This gave a final dataset of 80 entries for assessment; see Figure 1.

### 3 RESULTS AND DISCUSSION

#### 3.1 Regulated Harm Budgets

To ensure a fair comparison between different RHBs, it is essential that they consider the same set of contaminants. So far, CoCs have only been identified in dwellings using a harm-based approach, but there is a need to extend the analysis to other common indoor environments, such as offices, schools, or shops, where the types and concentrations of contaminants may differ from dwellings.

Table 2 presents RHBs for countries where identical CoCs are regulated. It shows that Spain is the only country to have ELVs for all three CoCs, and so this RHB cannot be compared directly against the others. The magnitude of its RHB is a median of 2400 DALYs/10<sup>5</sup> person/year, and so if all buildings in Spain were compliant then the RHB indicates the maximum median population harm from exposure to HCHO, NO<sub>2</sub> and PM<sub>2.5</sub>.

China, Spain, and Norway have ELVs for the chronic exposure to both NO<sub>2</sub> and PM<sub>2.5</sub>. The USA and Spain are the only countries with ELVs for HCHO and PM<sub>2.5</sub>. ELVs for HCHO and NO<sub>2</sub> are specified by Sweden, Spain, France, and the UK. The ELVs for PM<sub>2.5</sub> typically result in a greater regulated harm when compared to other contaminants. This confirms the disparity in the allowable harm for different contaminant and highlights the need for consistent hazard levels.

Table 2: Regulated harm budgets for selected contaminants, by country.  
Highest to lowest median harm. DALYs/10<sup>5</sup> person/year.

Contaminants	Country	Regulated Harm Budget	Geometric Standard Deviation
HCHO, NO <sub>2</sub> , PM <sub>2.5</sub>	Spain	2400	1.3
NO <sub>2</sub> , PM <sub>2.5</sub>	China	3600	1.2
	Spain	2400	1.3
	Norway	1500	1.2
HCHO, PM <sub>2.5</sub>	USA	2200	1.2
	Spain	1200	1.2
HCHO, NO <sub>2</sub>	Sweden	7300	1.5
	Spain	1100	1.7
	France	570	1.8
	UK	280	1.6

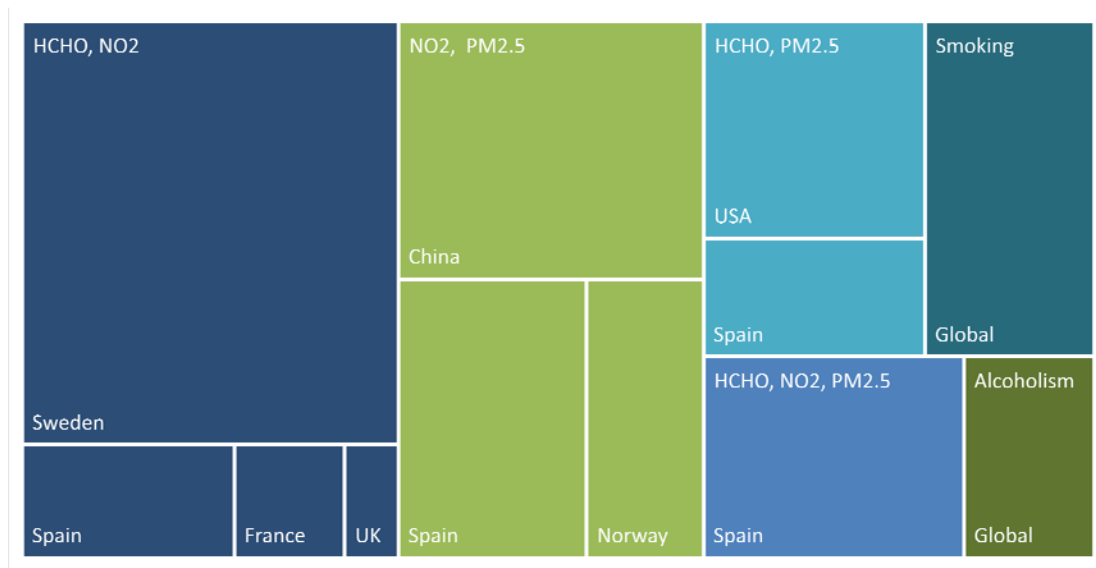


Figure 2. Median regulated harm budgets and other known risks treemap.

To contextualize the data in Table 2, the RHBs are compared against the harm caused by other daily hazards typically deemed unacceptable by the general population, such as the global burden attributed to alcoholism (1200 DALYs/10<sup>5</sup> person/year) and smoking (2600 DALYs/10<sup>5</sup> person/year) (IHME 2019). Figure 2 illustrates the median RHBs using a tree-map and shows that Spain's three-CoC RHB is equivalent to the burden of disease from smoking. The RHBs for most AIVC countries, however, exceed the harm values for smoking and alcoholism. There are already interventions in place in most countries to reduce population harm from them, and so these results suggest that appropriate interventions should be applied to mitigate against the harm from indoor air contaminants too and reduce it to an acceptable level.

### 3.2 Regulating IAQ

The results show the regulated harm budget (RHB) for the AIVC countries vary a lot, even when the same set of CoCs are considered. Those contaminants do not contribute equally to the budget. To ensure that they do, contaminants must be expected to be both present and at harmful concentrations. Conversely, it is inadvisable to include contaminants expected to cause little harm as the measurement, and control of those contaminants is not cost effective. CoCs for dwellings have been identified by Morantes et al. (2024); see Section 1. In that study, harm from 44 contaminants prevalent in dwellings was calculated at (median) 2,200 DALYs/10<sup>5</sup> person/year.

For typical occupancies, countries should determine a harm budget from those CoCs and allow trade-offs between them. ELVs can be used in special situations where other contaminants are expected at unusually high concentrations.

This work serves as an initial evaluation of RHBs using ELVs rather than a definitive benchmark. More research is needed on guideline development and resulting health impacts, as there is considerable uncertainty in this arena. Nonetheless, this approach provides a starting point for assessing the protectiveness of indoor air quality regulations.

Future work will evaluate RHBs for all countries in the ISIAQ database, for different regulatory bodies in the same country (ASHRAE and the Environmental Protection Agency), and for the World Health Organization. Additionally, an exploration of calculating harm intensities for contaminants not included in the current analysis will be conducted, effectively expanding the scope and depth of the study.

While our study provides insights into the assessment of regulated harm from indoor air contaminants, it is important to acknowledge certain limitations. Firstly, the ELVs for chronic exposures extracted from the database were assumed to be applicable without thorough validation. Therefore, future research should focus on ensuring the consistency and accuracy of these ELVs to enhance the reliability of our findings.

#### 4 CONCLUSIONS

There is significant variability in the regulated harm levels from exposure limit values set by different regulatory bodies for the same indoor air contaminants, highlighting inconsistencies in the level of public health protection provided.

We show a regulated harm budget, representing the total allowed harm from all regulated contaminants implicitly established by a regulatory body. Among the AIVC countries considered, Spain is the only nation with recommended chronic limit values for three key contaminants of concern (PM<sub>2.5</sub>, NO<sub>2</sub>, and formaldehyde), with an RHB of 2400 DALYs/10<sup>5</sup> person/year.

The regulated harm budgets for most AIVC countries exceed the harm values associated with smoking and alcoholism, suggesting that appropriate interventions should be applied to mitigate the harm from indoor air contaminants.

#### 5 ACKNOWLEDGEMENTS

Morantes was supported by a University of Nottingham Faculty of Engineering Research Excellence Scholarship and by the Chartered Institution of Building Services Engineers (CIBSE). Molina received funding from Agencia Nacional de Investigación y Desarrollo (ANID) of Chile, through the project ANID FONDECYT Iniciación 11220965.

#### 6 REFERENCES

- Abdul-Wahab, Sabah Ahmed, Stephen Chin Fah En, Ali Elkamel, Lena Ahmadi, and Kaan Yetilmmezsoy. 2015. 'A review of standards and guidelines set by international bodies for the parameters of indoor air quality', *Atmospheric Pollution Research*, 6: 751-67.
- Borsboom, Wouter, Willem De Gids, Jennifer Logue, Max Sherman, and Pawel Wargocki. 2016. 'TN 68: Residential ventilation and health'.
- Dimitroulopoulou, Sani, Marzenna R Dudzińska, Lars Gunnarsen, Linda Hägerhed, Henna Maula, Raja Singh Visualisation, Oluyemi Toyinbo Visualisation, and Ulla Haverinen-Shaughnessy. 2023. 'Indoor air quality guidelines from across the world: An appraisal considering energy saving, health, productivity, and comfort', *Environment International*: 108127.
- Fantke, Peter, Marian Bijster, Cécile Guignard, MZ Hauschild, MAJ Huijbregts, Olivier Jolliet, Anna Kounina, V Magaud, M Margni, and TE McKone. 2017. "USEtox 2.0: Documentation (Version 1)." In.: USEtox International Center.

- IHME. 2019. 'Institute for Health Metrics and Evaluation tool', Accessed Accessed on 2024-02-31. [www.vizhub.healthdata.org/gbd-results/](http://www.vizhub.healthdata.org/gbd-results/).
- Morantes, Gioberti, Benjamin Jones, Constanza Molina, and Max H Sherman. 2024. 'Harm from Residential Indoor Air Contaminants', *Environmental science & technology*, 58: 242-57.
- Morantes, Gioberti, Narciso Pérez, Rafael Santana, and Gladys Rincón. 2016. 'Revisión de instrumentos normativos de la calidad del aire y sistemas de monitoreo atmosférico: América Latina y el Caribe', *Interciencia*, 41: 235-42.
- Ott, Wayne R. 1990. 'A physical explanation of the lognormality of pollutant concentrations', *Journal of the Air & Waste Management Association*, 40: 1378-83.
- Salis, Louis Cony Renaud, Marc Abadie, Pawel Wargocki, and Carsten Rode. 2017. 'Towards the definition of indicators for assessment of indoor air quality and energy performance in low-energy residential buildings', *Energy and Buildings*, 152: 492-502.
- Sherman, Max H, Iain S Walker, and Jennifer M Logue. 2012. 'Equivalence in ventilation and indoor air quality', *HVAC&R Research*, 18: 760-73.

# Challenges in measurement for clean air in public indoor environment

Ralph Krause, Ralf Heidenreich\*

*Institut für Luft- und Kältetechnik gGmbH  
Main department of Ventilation and Air Conditioning  
Bertolt-Brecht-Allee 20  
D-01309 Dresden, Germany*

*\*Corresponding & Presenting author: ralf.heidenreich@ilkdresden.*

## SUMMARY

Recirculated air is critical from the perspective of transmitting pathogens to air conditioning systems. Usually, outside air is mainly free of pathogens, and contained particles/aerosols are separated in the first filter stage (at least ISO ePM1 50% @ ISO 16890). However, people in the supplied indoor spaces can release pathogens, particles, and smells into indoor air. These are captured via the exhaust air and fed back into the supply air and thus into the room via the circulating air. This case can enable the transmission of diseases and decrease indoor air quality. Recirculating air systems makes much sense for room air conditioning from an energy and economic point of view but should be rejected like conditions of the COVID-19 pandemic. Therefore, the carryover of aerosols from the exhaust air into the supply air has to be prevented, and it needs control by taking appropriate measures. Overall two topics are points of interest and done in the project: How much is the separation efficiency of a two stages HVAC filter unit against ultrafine particles and how is the transmission rate of gases from ETA air to SUP air via an rotary heat exchanger. Test were done at first in lab with filter tester for the material, second were carried out the measurement at airport HVAC sites with tracer gas SF<sub>6</sub> to measure gas transmission. In addition by using an aerosol spectrometer the separation efficiency at site were measured. At the site a combination of two F7- filter stages were used. The result was a transmission coefficient of 1:1369 and an average separation efficiency of around 84 % at relevant particle size range of 0.02 µm to 0.5 µm. So it meets not the result of separation efficiency according DIN EN 149 (FFP2). That means, leakages in filter units and other cases have huge influence. If real number are needed, measurement at site is necessary. Tracer gas and particle measurement together give a real good possibility for a safety background.

## KEYWORDS

IAQ, ventilation rate, tracer gas, infiltration, HVAC

## 1 SEPERATION EFFICIENCY OF FILTER MEDIA

Filters and filter media for HVAC application usually are tested according to ISO 16890. The standard describes two test aerosols – potassium chloride and DEHS. The particles size reaches from 0.2 µm to 10 µm. Main topic for protecting the health of room users was in times before COVID19 the separation of dust, bacteria and fungi. But, COVID19 brought a completely new view. Separation efficiency of HVAC filters for virus size was unknown. In this time a lot of testing was done, especially to improve face masks. So information of separation efficiency can be given for flat sheet material by using filter tester acc. to DIN EN 149. For example the Automated Filter Tester Model 8130A of TSI Inc. (see Figure 1) can be used to test filter media for use in respiratory protection devices or ventilators in accordance with a wide range of international standards. The test procedure is semi-automatic and complies with the relevant requirements of the individual test standards. NaCl cores (median particle diameter: 0.06 - 0.10 µm) and paraffin oil (median particle diameter: 0.29 - 0.45 µm) are used as test aerosols. In the case of salt aerosols, these are passed through a heating section after generation to evaporate the water, leaving the salt cores in the air. The test aerosol is then diluted with clean air in a mixing chamber to ensure optimal conditions for measuring the particle concentration and to meet the standard requirements. The diluted test aerosol is characterized with a raw gas photometer, passed through the test filter and the cleaned air is analysed again by another photometer. The test volume flow is 95 l/min in accordance with DIN EN 149 /1/. 10 filters were tested per test aerosol.

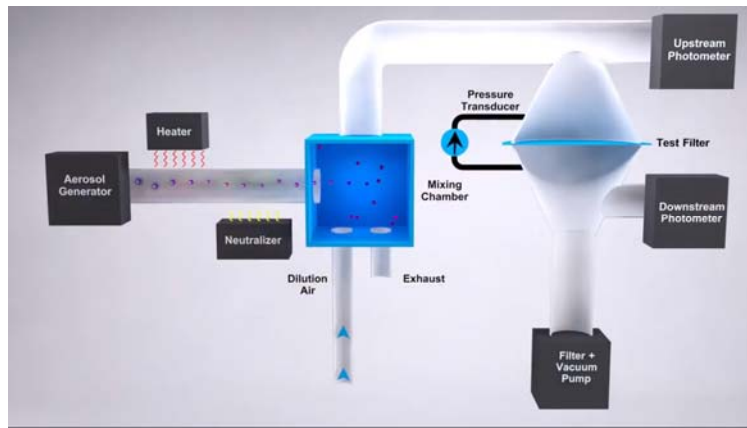


Figure 1: Filter tester for face mask material /2/

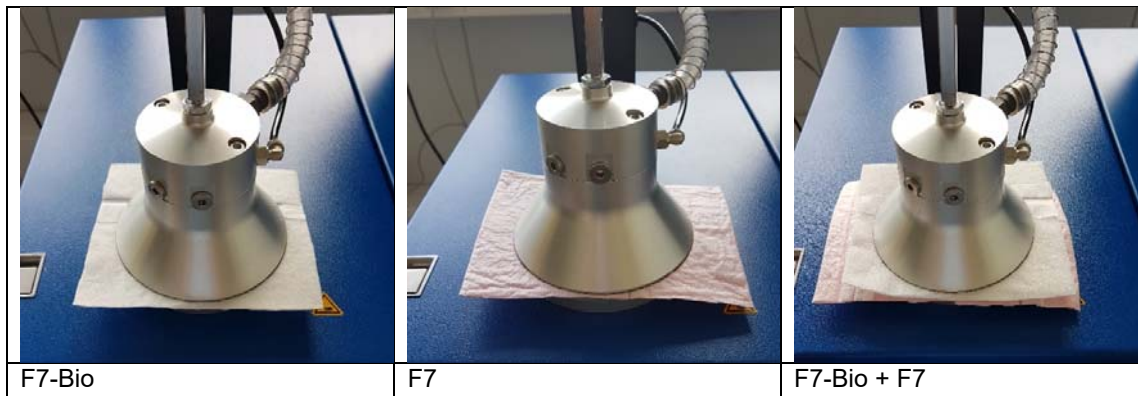


Figure 2: Filter materials in the test rig

The interesting point was to find out filtration efficiency of materials that are for years in the market and still used in HVAC application. A significant number are still labelled according to old and still not valid EN779. But filter classes “F7” and “F9” are common more known than new ePM1 – classes. Typical results, that we carried out are includes in Table 1.

Table 1: Filter classes acc. to DIN EN 149 /1/ @ 95 l/min

Protection class	sodium chloride penetration [%]	paraffin oil penetration [%]	Resistance [Pa ]
FFP1	20	20	210
FFP2	6	6	240
FFP3	1	1	300
Type 1 (F 7 biostatic)	9	17	94
Type 2 (F 7)	18	40	89
Type 3 (F 7 + biostatic)	2	7	201
Type 4 (F 7 + F 9)	3	3	292

In times of COVID19 it was pointed of, that FFP2 mask give a good safety level to protect yourself. Transferred to filtration of ETA air in HVAC application that means – separation efficiency of 94 % can give a protection. But, usual filter media don’t reach this level. Only combination of “F7” and “F9” reaches together a separation efficiency of 97 %.



## 2 MEASUREMENT AT SITE

### 2.1 Gas transmission

On the one hand, prevention can be a decisive second filter stage (e.g., ISO ePM1 80% @ ISO 16890 /4/) or the exclusion of recirculated air through heat recovery via closed circuit systems. In most of the present cases, heat recovery is realized by using rotary heat exchangers. Theoretically, a certain amount of slip in the rotor and leaks in conjunction with a false pressure gradient can cause aerosol transmission. This transmission can reach from the usual 1% up to 20% under unfavourable conditions and poor maintenance.

Direct measurements of aerosol transmission rates are complex and only possible under laboratory conditions. One possible variant is the use of tracer gases. It is assumed that very fine aerosols (less than 1 µm in diameter) behave like a gas. Therefore, the transmission rate is measured with a gas. The sulphur hexafluoride (SF<sub>6</sub>) used for this does not occur in regular atmospheric air, so an overlay of the measurement result with a background concentration can be ruled out. Based on this, deficient concentrations (down to the ppt range) can be detected using a gas chromatograph with an electron capture detector (ECD).

In order to determine the transfer factor from the exhaust air to the supply air, a known amount of tracer gas is measured into the exhaust air flow. The concentration can be determined on the exhaust air side. If transfer into the supply air occurs, a concentration that is above the detection limit must be detected on the supply air side. The difficulty of the procedure lies in choosing the correct concentration so that the exhaust air concentration can be measured without dilution and a concentration that is 1000 times lower can still be determined in the supply air. Alternatively, an approximation function can be determined by dosing different tracer concentrations and determining the associated concentrations. The accuracy of the measurement depends on the quality of the tracer injection concentration, the precision of the flow measurement of the injection gas, and the concentration analysis itself. Even with large volume flows in building technology, a diluted tracer gas/air mixture is usually sufficient for injection. The advantage is, on the one hand, that the diluted gas mixture of SF<sub>6</sub> and nitrogen has almost a specific gravity of air and, therefore, mixes more efficiently than pure SF<sub>6</sub>. Transmission rate of gas can be calculated acc. to equation (1).

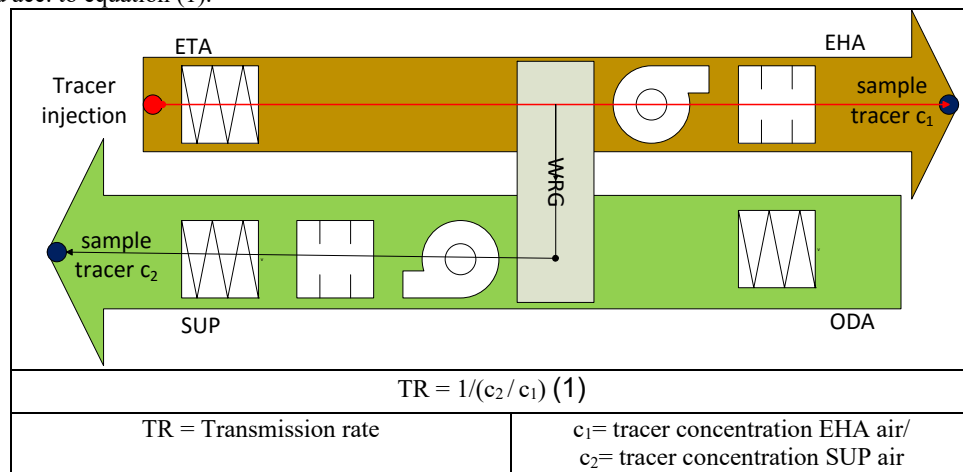


Figure 3: Injection and sample points @ rotary heat exchanger

In Figure 4 the measurement and the result can be seen. The dosing in the ETA air have to be very stable; also the tracer gas concentration have to be known. A calibration gas have to be used. As to be seen the tracer measurement includes some decades of concentration; that makes it possible to measure very low transmission rates too.

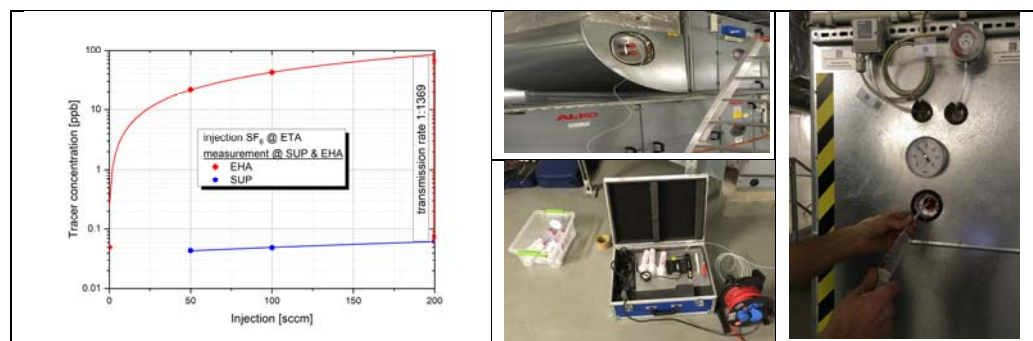


Figure 4: Result of measurement, sampling and injection of tracer gas at site

## 2.2 Aerosol measurement

A wide range aerosol spectrometer of the type Model 1371 from Grimm Aerosoltechnik /3/ was used for the tests. This measuring device can be used to determine both the number and size of the particles in the air. By combining scattered light measurement and mobility analysis, a measuring range of 10 nm to 35  $\mu\text{m}$  in 41 size classes can be recorded. Of particular interest in these measurements are particles in the size range of 20 nm to 500 nm, as this corresponds to the size of Covid19 viruses when they are in isolated form. In the HVAC system, a two-stage filtration is implemented on the supply air side, with both filter stages equipped with fine filters of filter class F 7 according to EN 779 (replaced by DIN EN ISO 16890 since 2017) (see Figure 5). The first filter stage is provided with biostatic equipment.



Figure 5: Measurement set up for particles at site

The concentration of PM<sub>2.5</sub> particles in the supply air is only about 1  $\mu\text{g}/\text{m}^3$  and fluctuates only slightly, while the outside air concentration varies in the range of 5 to 10  $\mu\text{g}/\text{m}^3$ . If the fractional separation efficiency is determined from the measured data, a curve as shown in Figure 6 results. Accordingly, the separation efficiency between outside and supply air is at least 78%. This means that the two filter stages together have a significantly lower separation efficiency than was determined under test conditions for the two materials. The separation minimum between 100 nm and 200 nm is also clearly shown.

In the relevant particle size range of 0.02  $\mu\text{m}$  to 0.5  $\mu\text{m}$ , the filter stage has an average separation efficiency of around 84%. This value is significantly lower than the value of > 90% determined in the filter test. In addition to leaks, this can also be due to the flow and the overall design of the filter (seams). From the point of view of the separation of aerosols with virus size, the second filter stage could be replaced by filters from the ePM1 80% group (formerly F9 according to EN 779). This can increase the protective effect even further and would then correspond to the level of protection of an FFP 2 mask.

By considering the entire system, excluding recirculation mode and the proven, very low transfer rate from the exhaust air to the supply air of only 0.1%, the filter effect can be considered sufficient.

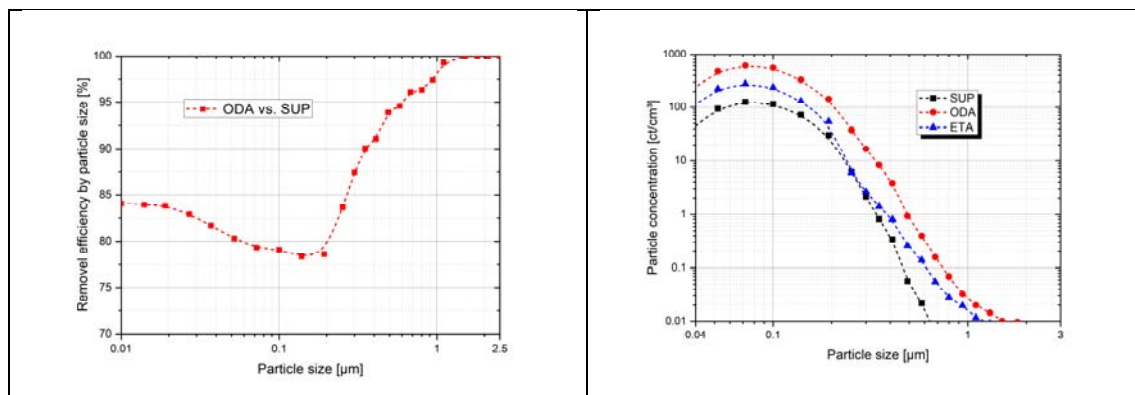


Figure 6: Particle size distribution and removal efficiency by particle size

### 3 REFERENCES

Click or tap here to enter text.

- [1] DIN EN 149: Respiratory protective devices - Filtering half masks to protect against particles - Requirements, testing, marking; German version EN 149:2001+A1:2009
- [2] <https://www.tsi.com/products/filter-testers/automated-filter-tester-8130a>
- [3] <https://www.grimm-aerosol.com/products-en/indoor-air-quality/the-wide-range-hybrid/1371/>
- [4] DIN EN ISO 16890-1:2017-08  
Air filters for general ventilation - Part 1: Technical specifications, requirements and classification system based upon particulate matter efficiency (ePM) (ISO 16890-1:2016); German version EN ISO 16890-1:2016

# The relationship between airtightness and summertime infiltration rates

Ben M. Roberts\*<sup>1</sup>, David Allinson<sup>1</sup>, and Kevin J. Lomas<sup>1</sup>

*1 Building Energy Research Group  
Loughborough University  
Loughborough, Leicestershire  
LE11 3TU, UK*

*\*Corresponding author: [b.m.roberts@lboro.ac.uk](mailto:b.m.roberts@lboro.ac.uk)*

*Presenting author: Ben M. Roberts*

## ABSTRACT

All new dwellings in England and Wales are required to undergo a model-based overheating risk assessment prior to construction. An important model input is the building infiltration rate, which is usually estimated using a conversion factor on the dwelling airtightness. There is a paucity of evidence regarding the reliability of these methods in summertime. The aim of this paper is to provide new evidence on the relationship between airtightness and infiltration during summertime. The airtightness of a single test house was repeatedly measured over a three-month period using a blower door. Following this, 15 whole house tracer gas tests were undertaken in the same test house over a summer season to measure infiltration rate. Eleven different infiltration estimation methods were used to calculate the infiltration rate and were compared to the measured infiltration rate. The summertime infiltration rates were predicted to be between 64 and 208% higher than measured. These findings have implications for the reliability of overheating risk assessment and suggest that these uncertainties must be accounted for when designing and modelling buildings to be resilient to summertime overheating.

## KEYWORDS

Airtightness; air permeability; infiltration; measurement; tracer gas

## 1 INTRODUCTION

Airtightness is commonly measured in dwellings in UK dwellings (Love et al., 2017). This is done using a blower door test or a low-pressure pulse test – both are relatively quick and easy methods compared to measuring infiltration rate, which is done using tracer gas techniques, and so infiltration rates are relatively rarely measured. Due to this, the relationship between airtightness and infiltration has long been used to estimate dwelling infiltration rates during the winter heating season (Jones et al., 2016). To allow for estimation of infiltration rates without a tracer gas test, several empirical and theoretical air infiltration models have been developed (ASHRAE, 2013; BRE, 2022; Jones et al., 2016; Shaw, 1981; Walker & Wilson, 1990, 1998; Warren & Webb, 1980). These methods were designed to estimate infiltration, primarily, during the winter heating season – usually using the measured airtightness. It is not yet known, however, whether airtightness can be reliably used to estimate infiltration rates outside of the weather conditions for which they were designed. This is problematic because with the introduction of mandatory overheating risk assessments in newly built homes in England and Wales (HMG, 2021), dwelling airtightness is increasingly being used to estimate infiltration rates in summer (Roberts, Allinson, Diamond, et al., 2019; Roberts et al., 2023). Pasos et al. (2020) have raised concerns about the reliability of the methods using a single test in multiple dwellings. There is a need for multiple tests to be conducted in a single dwelling during summer to quantify the variation in infiltration rates that may be observed under changing weather – which is the aim of this paper.

## 2 METHODS

### 2.1 The test house and weather

A single test house constructed in the 1930s with masonry cavity walls and uPVC double-glazed windows and doors was selected as the case study. Indoor dry-bulb temperatures were measured in every room at the volumetric centre at 1-minute intervals using shielded, calibrated sensors. Alongside this, the local weather was measured using a weather station mounted in the test house gardens and on the nearby University campus.

### 2.2 Measuring airtightness and infiltration rate

Airtightness was measured on 34 different occasions between January and March 2017 in a single test house using a blower door test via depressurisation, following ATTMA Method B (ATTMA, 2016). The same sealing scenario was maintained during the tracer gas tests. Infiltration rates were measured on 15 different occasions throughout the summer period using CO<sub>2</sub> gas as the tracer, detected by a photoacoustic infrared spectroscopy gas analyser which drew air from six monitoring points around the house. The decay method, in compliance with ASTM Standards, was used for all tracer gas tests (ASTM, 2000).

### 2.3 Infiltration estimation methods

Eleven different infiltration methods were selected for testing following a review of the literature. Each estimated infiltration rate was compared to a measured infiltration rate (of which there were 15 tests). Thus, where applicable, the weather measured during the tracer gas test was used in the infiltration method input. The different infiltration estimation methods required different inputs. These were sourced from publicly available data on the test house (Roberts, Allinson, & Lomas, 2019; Roberts et al., 2018).

The eleven infiltration estimation methods are as follows, with individual inputs listed in Roberts et al. (2023):

1. ASHRAE Basic (ASHRAE, 2013), called the Effective Leakage Area model in the EnergyPlus dynamic thermal model.
2. ASHRAE Enhanced (ASHRAE, 2013), called the Flow Coefficient model in EnergyPlus.
3. K-P (Kronvall-Persilly)<sup>1</sup> UK or the “divide-by-20” method. Uses a divisor of 20 to reduce the blower door AP<sub>50</sub> to infiltration. The method is applied differently in the UK and US – in the UK air permeability (AP<sub>50</sub>) is used (Poza-Casado et al., 2020).
4. K-P US or “divide-by-20”, dividing by N<sub>50</sub> following the US convention.
5. Lawrence Berkeley Laboratory (LBL) method (M. Sherman & Grimsrud, 1980; M. H. Sherman & Modera, 1986).
6. Modified divisor N<sub>50</sub>/30 – as suggested for low-rise buildings (Liddament, 1996).
7. SAP Algorithm (measured wind) (SAP, 2014).
8. SAP Algorithm (reference wind) (SAP, 2014).
9. SAP AP<sub>50</sub>/20 (SAP, 2014).
10. SAP AP<sub>50</sub>/20 (SAP, 2014).

---

<sup>1</sup> Frequently misattributed to Kronvall and Persily (Kronvall, 1978; Persily, 1983) as described by (Jones et al., 2016).

11. Sherman Simplified method (M. H. Sherman, 1987). This method usually requires annual average wind speed and indoor-outdoor temperature difference, but in this analysis the averages during each tracer gas test interval were used.

### 3 RESULTS

Comparing the measured infiltration to that predicted by the eleven infiltration estimation methods showed that the mean measured infiltration rates are overpredicted by the methods by between 64-208%. The ASHRAE Enhanced method was closest to the measured infiltration rate, but still significantly ( $p < 0.001$ ) higher than measured (Figure 1). The K-P US ( $N_{50}/20$ ) predicted furthest from the measured infiltration rate. A divisor of 58 would be required, in this example, to reliably predict infiltration in summer using  $AP_{50}$  alone.

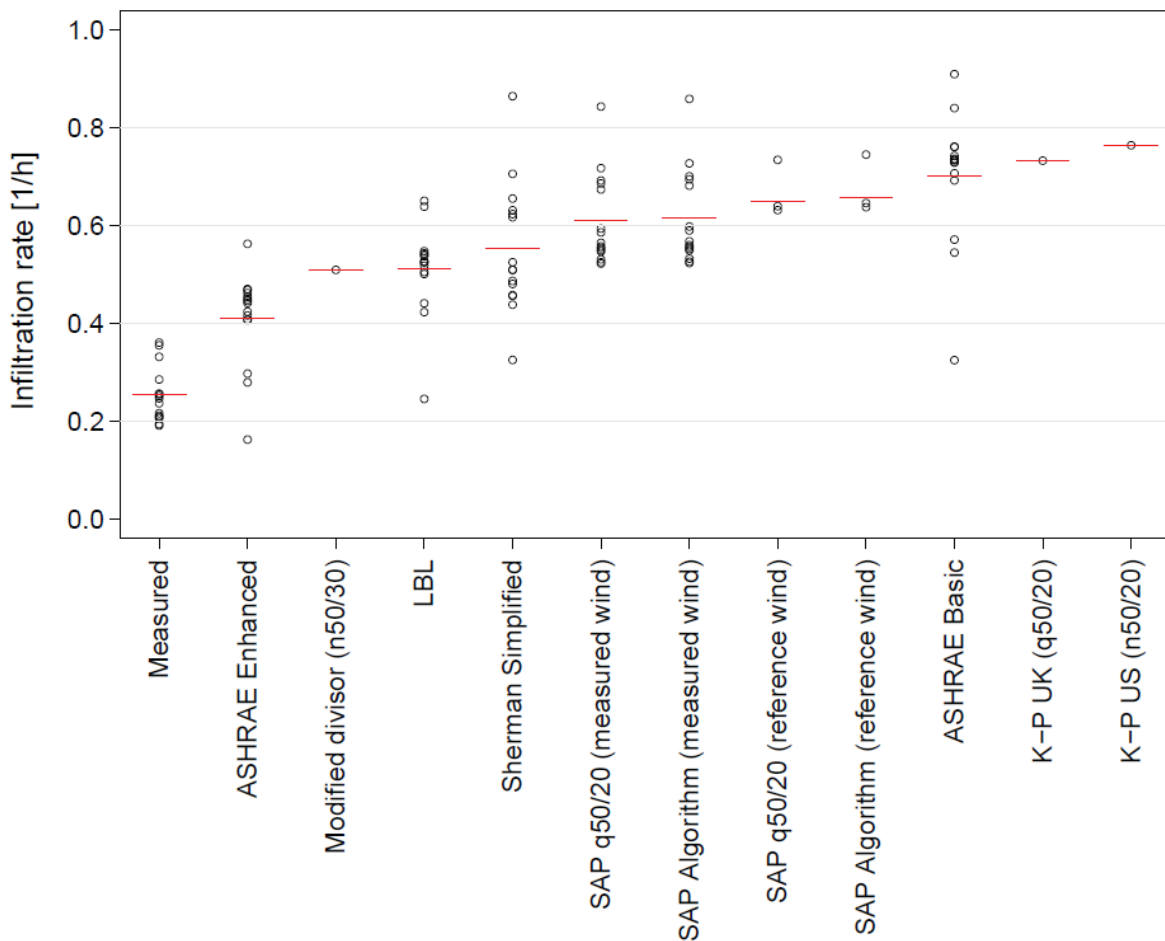


Figure 1: A comparison of the measured infiltration rates (tracer gas) and the estimated infiltration rates from each of the methods. Each data point represents one of the 15 measured or estimated infiltration rates. The mean value for each of the methods is indicated by the red horizontal bars. Arranged in ascending order from the lowest mean infiltration rate value

In some case, individual predictions of infiltration rate were close to the corresponding measured value (Figure 2). The ASHRAE Basic, ASHRAE Enhance, LBL model, and the Sherman Simplified method all had minimum errors of <math><0.10</math> ach (positive and negative, i.e., greater and lesser than measured). The infiltration estimation methods which accounted for the weather conditions (and indoor-outdoor temperature) were generally more reliable estimators of infiltration than those which did not. The use of a locally-available wind speed improved the predictions for the SAP methods. The slope of the regression line for each estimation method is indicative of each method's response to those weather conditions (Figure 2). The ASHRAE Enhanced, LBL and Sherman Simplified methods all appear to respond correctly to the change in weather conditions, with the slope angle of the lines close to 1, i.e. the line of quality, albeit significantly above (Figure 2).

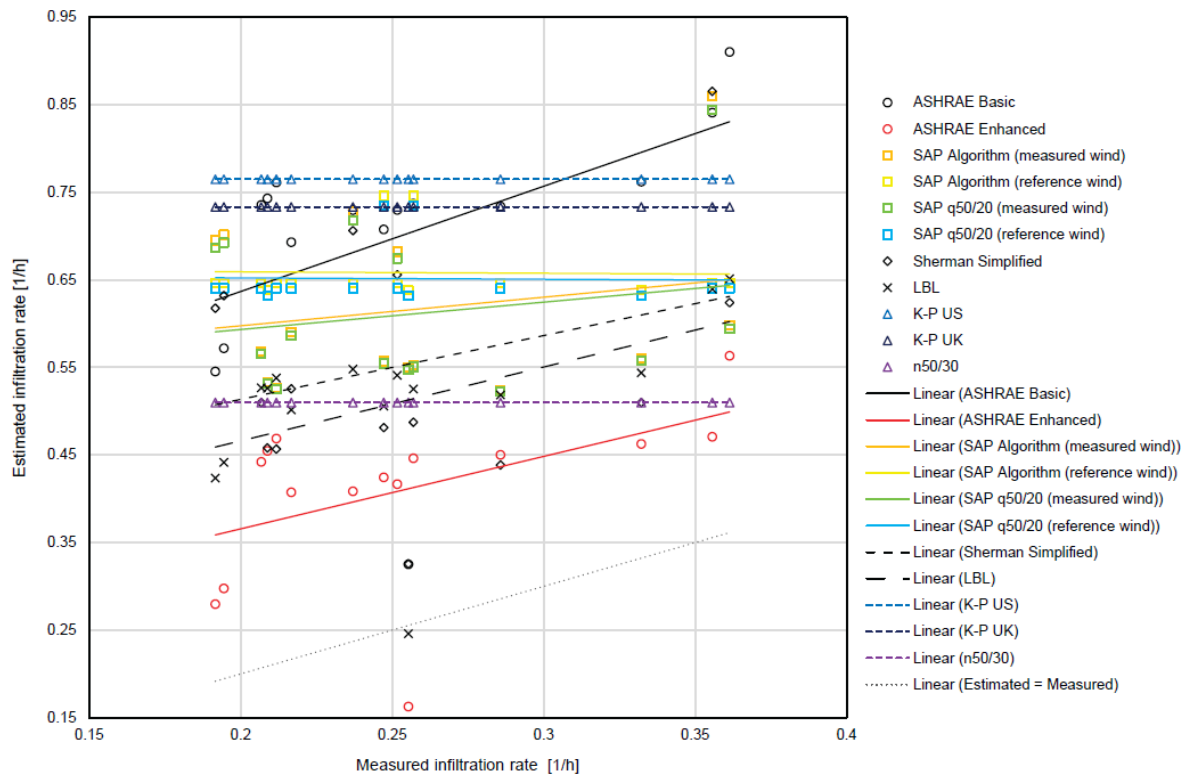


Figure 2: Measured infiltration rate plotted against estimated infiltration rate. Each data point represents one of the 15 tracer gas tests and the corresponding infiltration estimation method prediction.

## 4 DISCUSSION

Infiltration estimation methods were designed to predict infiltration rates in dwellings during the winter season. Due to their growing application to the summer season for overheating risk assessments in UK Building Regulations (HMG, 2021) this paper has found that their estimations of infiltration are unreliable and will add to modelling uncertainties in dynamic thermal models (Roberts, Allinson, Diamond, et al., 2019).

For the test house in question, a divisor of  $AP_{50}$  and  $N_{50}$  of 58 was suggested for, rather than the commonly used 20. Similarly, Pasos et al. (2020) has suggested a higher value, of 39. Seeking a single divisor for airtightness (or air permeability) may be a futile endeavour for anything other than low-resolution, low reliability estimation of annual infiltration rates. This is because there are complex geometrical considerations and infiltration is highly dynamic

and weather dependent (Jones et al., 2015). This paper has shown that the estimations are sensitive to weather during the summer season. The methods which accounted for the wind speed, indoor-outdoor temperature differences, and perhaps other information. Although it is not always possible or practical to obtain local weather data, there are clear benefits to doing so with respect to estimation reliability. These findings have implications for the reliable prediction of overheating risk and cooling demand. Overheating risk may be higher than models predict, as ventilative cooling is not as high as assumed by modellers. This could mean that appropriate and necessary passive overheating mitigation strategies are not implemented at the design stage. This could lead to overheating in new homes and the subsequent uptake of energy intensive air-conditioning. Further work should investigate the precise effect this has on overheating risk assessment. The ASHRAE Enhanced method estimated a mean infiltration rate that was both closest to the measured infiltration rate and the gradient of the regression line (Figure 2) was similar to the gradient of the line of equality. Thus, it appears that this method was reliably sensitive to the changes in infiltration rate. Therefore, the ASHRAE Enhanced method shows the greatest promise and further investigation and refinement of this approach for estimation of infiltration rate in summer is recommended.

#### **4.1 Limitations**

This study was conducted on a single test house. Whilst it benefits from multiple measurements of airtightness and infiltration under many different weather conditions, further investigation is needed to understand the reliability of infiltration estimation in different homes with different levels of airtightness and exposure to wind.

### **5 CONCLUSION**

The key conclusions are the following:

1. None of the eleven infiltration estimation methods trialled was a reliable estimator of the mean infiltration rate measured in the test house.
2. If the commonly used K–P “divide-by-20” rule of thumb is used to estimate infiltration in summertime, the divisor for  $AP_{50}$  and  $N_{50}$  should be replaced by 58 in the example of this single dwelling. However, attempts to define a single value to reduce blower door data ( $AP_{50}$  or  $N_{50}$ ) to infiltration rate is futile when considering the highly dynamic and weather-dependent nature of infiltration.
3. Infiltration estimation methods which account for wind speed (especially when locally measured), indoor-outdoor temperature differences, and perhaps other information about the building and wider site are recommended to achieve more reliable estimates of infiltration, but still differences between the measured and estimated infiltration remained.
4. The ASHRAE Enhanced infiltration estimation method was closest to the mean measured infiltration rate and demonstrated a similar rate of increase in estimated infiltration in line with the measured value. Thus, this method holds the greatest potential for adjustment and adaptation to be more suitable for estimating infiltration in typical UK homes during summer.
5. Incorrectly estimating infiltration could lead to incorrect assumptions regarding overheating risk.



## 6 ACKNOWLEDGEMENTS

This work was funded by the London-Loughborough Centre for Doctoral Research in Energy Demand (grant EP/L01517X/1).

## 7 REFERENCES

- ASHRAE. (2013). *ASHRAE Handbook Fundamentals SI Edition*. www.ashrae.org
- ASTM. (2000). *Standard Test Method for Determining Air Change in a Single Zone by Means of a Tracer Gas Dilution - E741-11*. <https://doi.org/10.1520/E0741-11>
- ATTMA. (2016). *Measuring air permeability in the envelopes of dwellings. Technical Standard L1*.
- BRE. (2022). *The Government's Standard Assessment Procedure for Energy Rating of Dwellings - SAP 10.2*. <https://doi.org/10.2>
- HMG. (2021). *The Building Regulations 2010 - Approved Document O: Overheating*. Her Majesty's Government.
- Jones, B., Das, P., Chalabi, Z., Davies, M., Hamilton, I., Lowe, R., Mavrogianni, A., Robinson, D., & Taylor, J. (2015). Assessing uncertainty in housing stock infiltration rates and associated heat loss: English and UK case studies. *Building and Environment*, 92, 644–656. <https://doi.org/10.1016/j.buildenv.2015.05.033>
- Jones, B., Persily, A., & Sherman, M. (2016). The origin and application of leakage-infiltration ratios. *AIVC Conference*.
- Kronvall, J. (1978). Testing of houses for air leakage using a pressure method. *ASHRAE Transactions*, 84(1), 72–79.
- Liddament, M. W. (1996). *A guide to energy efficient ventilation*. Air Infiltration and Ventilation Centre.
- Love, J., Wingfield, J., Smith, A. Z. P., Biddulph, P., Oreszczyk, T., Lowe, R., & Elwell, C. A. (2017). 'Hitting the target and missing the point': Analysis of air permeability data for new UK dwellings and what it reveals about the testing procedure. *Energy and Buildings*, 155, 88–97. <https://doi.org/10.1016/J.ENBUILD.2017.09.013>
- Pasos, A. V., Zheng, X., Smith, L., & Wood, C. (2020). Estimation of the infiltration rate of UK homes with the divide-by-20 rule and its comparison with site measurements. *Building and Environment*, 185. <https://doi.org/10.1016/j.buildenv.2020.107275>
- Persily, A. K. (1983). *Understanding air infiltration in homes*. Princeton University.
- Poza-Casado, I., Cardoso, V. E. M., Almeida, R. M. S. F., Meiss, A., Ramos, N. M. M., & Padilla-Marcos, M. Á. (2020). Residential buildings airtightness frameworks: A review on the main databases and setups in Europe and North America. In *Building and Environment* (Vol. 183). Elsevier Ltd. <https://doi.org/10.1016/j.buildenv.2020.107221>
- Roberts, B. M., Allinson, D., Diamond, S., Abel, B., Bhaumik, C. D., Khatami, N., & Lomas, K. J. (2019). Predictions of summertime overheating: Comparison of dynamic thermal models and measurements in synthetically occupied test houses. *Building Services Engineering Research and Technology*, 40(4), 512–552. <https://doi.org/10.1177/0143624419847349>
- Roberts, B. M., Allinson, D., & Lomas, K. (2019). Prediction of overheating in synthetically occupied UK homes: dataset for validating dynamic thermal models of buildings. In *Figshare Dataset*. <https://doi.org/10.17028/rd.lboro.8094575>
- Roberts, B. M., Allinson, D., & Lomas, K. J. (2018). A matched pair of test houses with synthetic occupants to investigate summertime overheating. *Journal of Sustainable Design & Applied Research*, 6(1), 29–38. <https://doi.org/10.21427/D70N8S>
- Roberts, B. M., Allinson, D., & Lomas, K. J. (2023). Evaluating methods for estimating whole house air infiltration rates in summer: implications for overheating and indoor air

- quality. *International Journal of Building Pathology and Adaptation*, 41(1), 45–72. <https://doi.org/10.1108/IJBPA-06-2021-0085>
- SAP. (2014). SAP 2012 The Government ' s Standard Assessment Procedure for Energy Rating of Dwellings. *Energy, March*, 174. <https://doi.org/10.1007/s13398-014-0173-7.2>
- Shaw, C. Y. (1981). Correlation between air infiltration and air tightness for houses in a developed residential area. *ASHRAE Trans.:(United States)*, 87(CONF-810657-).
- Sherman, M., & Grimsrud, D. (1980). Infiltration-pressurization correlation: simplified physical modeling. *ASHRAE Conference*.
- Sherman, M. H. (1987). Estimation of infiltration from leakage and climate indicators. *Energy and Buildings*, 10(1), 81–86. [https://doi.org/10.1016/0378-7788\(87\)90008-9](https://doi.org/10.1016/0378-7788(87)90008-9)
- Sherman, M. H., & Modera, M. P. (1986). Comparison of measured and predicted infiltration using the LBL infiltration model. In *Measured air leakage of buildings*. ASTM International.
- Walker, I. S., & Wilson, D. J. (1990). *AIM 2: The Alberta air infiltration model*.
- Walker, I. S., & Wilson, D. J. (1998). Field validation of algebraic equations for stack and wind driven air infiltration calculations. *HVAC&R Research*, 4(2), 119–139.
- Warren, P., & Webb, B. (1980). The relationship between tracer gas and pressurization techniques in dwellings. *Proceedings of First Air Infiltration Center Conference*, 245–276.

# Intervention study of climate correlation model predictions for occupant control of indoor environment

Maria Kolokotroni<sup>\*1</sup>, May Zune<sup>1</sup>, Thet Paing Tun<sup>1</sup>, Iliia Christantoni<sup>2</sup>, Dimitra Tsakanika<sup>2</sup>, Dorota Stawowczyk<sup>3</sup>, Tristan de Kerchove d'Exaerde<sup>4</sup>

*1 Brunel University London,  
Kingston Lane,  
Uxbridge, UK*

*\*Corresponding author:  
[maria.kolokotroni@brunel.ac.uk](mailto:maria.kolokotroni@brunel.ac.uk)*

*3 Blok Architekci Sp  
Krakowie przy ul.Szlak 65  
31-153 Kraków, Poland*

*2 DAEM SA,  
City of Athens IT Company,  
144 Peiraios,  
11854 Athens,  
Greece*

*4 Estia SA,  
EPFL Innovation Park –  
Bât. C, CH-1015  
Lausanne, Switzerland*

## ABSTRACT

Occupants in natural ventilated buildings usually control ventilation through window opening. As part of the PRELUDE H2020 project a framework of how to predict an indoor environment by correlating internal environmental variables and external climatic variables was developed; this was presented at the AIVC conference in 2022. The climate correlation model consists of equations correlating external and internal parameters, derived from predictions of a thermal model (EnergyPlus) of the target building. Using these equations, thermal comfort (operative temperature) and IAQ (CO<sub>2</sub> concentration) are calculated using short term (24hrs) forecasted external weather data (air temperature and wind speed) that informs for window opening actions by the occupants. The model was applied in three naturally ventilated buildings in Greece (hostel), Switzerland (apartment) and Poland (office). A climate correlation model was developed for each building and equations derived specifically for the building. Occupant actions for opening windows were then determined for two consequent days in each of the buildings. The actions were communicated to the building occupants using conventional method (email); this was done through the building manager for the hostel and directly to occupants for the office and apartment. Data of internal temperature and CO<sub>2</sub> concentration were measured, analysed and compared to the predictions of the climate correlation model. The tests were carried out successfully and the comparison of predictions (based on weather forecasts) and measurements in the building is quite good for IAQ (CO<sub>2</sub>) as the ventilation intervals are captured well. Thermal comfort was also captured well with some under prediction at night, because of differences in air flow rates due to different window opening areas and some divergence when windows were simulated open during cold days with heating off. This study demonstrates that for low technology buildings where actuators and sensors are not present, a single thermal study and associated correlation equations for the building can effectively inform the occupants on the best way to control their internal environment based on prevailing external conditions.

## KEYWORDS

Climate correlation; Thermal comfort; Indoor air quality; Natural ventilation.

## 1 INTRODUCTION

Within the PRELUDE H2020 project (PRELUDE project, 2024), a climate correlation model was developed to help occupants of low-technology buildings (i.e. no sensors and actuators) to get information on how to operate ventilation openings and shading devices to achieve the best internal environmental conditions in their space. The development of the climate correlation model was presented at the AIVC Conference in 2022 (Zune and Kolokotroni, 2022a) and a more detailed report can be found in (Zune and Kolokotroni, 2022b). In summary, for each building in which the model would be applied, a Dynamic Thermal (DTM)

and Daylighting Simulation model needs to be developed, simulations run for the whole year using appropriate weather files for the location, and linear correlations developed between external and internal conditions. Then, using the equations of the linear correlations, a prediction can be made for internal conditions in the space if we have a forecast of the external conditions for the days of interest. Considering the variability and uncertainty of weather forecasts, predictions should be made for one or two days ahead. Using the predictions, suggestions to the occupants can be made on how to operate their windows and shading devices so that they achieve the best environment in terms of thermal comfort, indoor air quality and daylighting.

The relatively simple linear correlation was used because the method should be able to be executed by working consulting engineers and building managers who might not be familiar with the use of more sophisticated data analysis techniques that could have been used; for example machine learning, a subset of artificial intelligence that has been used extensively in building data and energy analytics. The presented method requires only an engineer/architect familiar with DTM and Excel spreadsheets.

Therefore, although a simple method, this paper argues that it is successful as applied to three occupied buildings in Europe. This paper focuses on thermal comfort and indoor air quality.

## **2 METHOD OF INTERVENTION STUDY**

### **2.1 Case-study buildings and their climate**

Three operational buildings in Europe were used for the intervention study. Their external view and typical floor plans used for this study are shown in Figure 1 and Figure 2.

Athens: The Athens building is a municipal building in the centre of Athens, operating as a shelter for elderly/senior citizens and people in need. It has a total of 30 apartments over 5 floors, (Tsakanika and Christantoni, 2023). The intervention study carried over two days in April 2024 focussed on one of the apartments (bedroom) on the third floor occupied by a couple. Athens is located in the southernmost part of the Greek mainland and the city is known as one of the hottest cities in mainland Europe. Its Mediterranean climate (Köppen climate classification: Csa) represents a dominant alternation between prolonged hot and dry summers and mild, wet winters with moderate rainfall. July and August are the driest months with the highest outdoor dry bulb temperatures. The dominant southwest wind comes with higher wind speeds (WS) to Athens throughout the year. The heating degree days and cooling degree days of Athens indicate that the buildings in Athens need both heating and cooling for comfort.

Geneva: The Geneva building is located in Geneva's urban district. It is a multifamily housing with 56 apartments. The building was originally built in 1962 and its refurbishment was completed in 2021 with two additional floors added to the building. For the tests, one of the apartments on the 8<sup>th</sup> floor (new) was considered. This building has a ventilation system which is hygro-regulated. The inlets are in the window frames and autonomously open and close themselves in function of the difference of relative humidity between the room and outside. The outlets are placed in the wet rooms (bathrooms and kitchen) and are connected to the mechanical extraction that is installed on the roof. An air-water heat exchanger is installed in the extraction system (de Kerchove et al, 2023). Geneva is located in the east part of Switzerland and is characterised by a continental climate (Köppen climate classification: Cfb) with mild temperatures, fully humid and warm summer. July and August are the months with

the highest outdoor dry bulb temperatures. The dominant winds are from northeast and southwest with the southwest having higher speeds. The heating degree days are 2142 (base temperature 15.5 °C) and the cooling degree days are 61 (base temperature 24 °C) indicating the need for heating rather than cooling.

Krakow: The Krakow building is an office building located in a region in Poland with a marine west coast and warm summer; (Cfb in the Köppen climate classification). Krakow is heating-dominated with 2787 heating degree days (HDD) annually (base 15.5°C), and with only 13 annual cooling degree days (CDD) (base 26°C). Krakow experiences significant seasonal variation in the wind speed and the wind direction changes from the southeast direction in spring to the northeast direction for the other seasons. More information on the building can be found in (Marciniak et al, 2023).



Figure 1: External view of the three test buildings

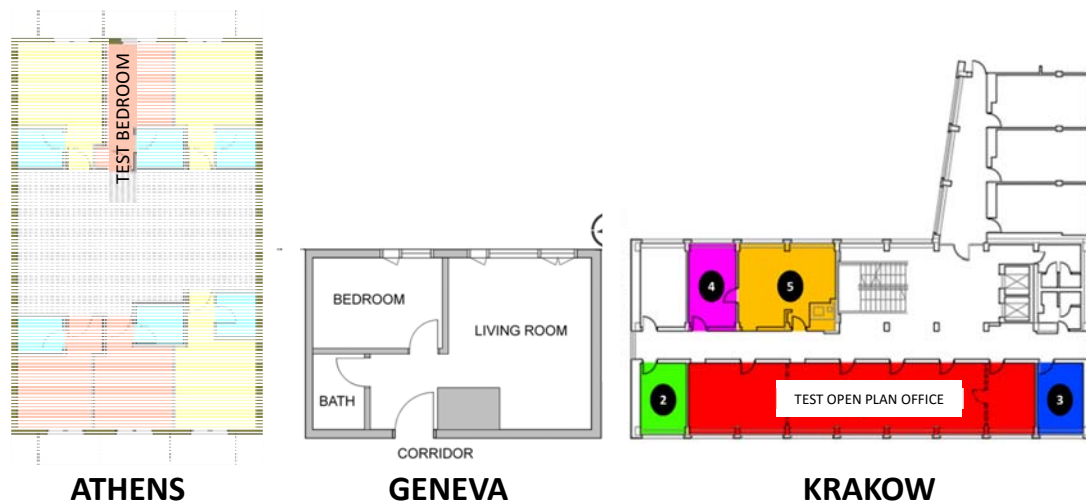


Figure 2: Floor plans of the three tested buildings (not in scale)

## 2.2 Development of climate correlation models

The DTM tool used was Energy Plus using the DesignBuilder interface (DesignBuilder, 2024). For each building a specific model was developed using its geometrical, construction

and operation characteristics, simulations run and correlations with its external weather parameters derived. The climate correlation model requires correlation equations to predict (a) internal operative temperature from external air temperature and (b) air flow rate from either wind speed or temperature gradient between inside and outside. Then internal contaminant concentrations can be calculated based on the air flow rate and using single-zone mass balance equations if the contaminant generation rate is known. These equations are embedded in the Excel spreadsheet which performs the calculations (Zune and Kolokotroni, 2022a). Simulations were carried out for each building and its weather under different operational scenarios and correlations were derived for each of them with the equations to be used for the Excel climate correlation model shown in Table 1. For the tests Scenario 3 was used for Athens (relatively hot period), scenario 2 was used for Geneva (cold period in spring) and scenario 2 was used for Krakow (cold spell in winter).

Table 1: Correlation Equations for Thermal Comfort and Ventilation

ATHENS							
Scenario	Correlation Parameters		Coefficient of determination (R <sup>2</sup> )		Correlation Equation for Thermal Comfort and Ventilation		
	x = Outdoor	y = indoor	Window Close	Window Open	Window Close	Window Open	
1	DBT	OT	0.8083	n/a	$y = 0.0049x^2 + 0.5684x + 13.13$	n/a	
	WS	ACH	0.3025		$y = 0.0009x^2 + 0.0003x + 0.0145$		
	IVT	ACH	0.0038		$y = 456006x^2 - 115.17x + 0.0296$		
2	DBT	OT	0.8058	0.9038	$y = 0.0062x^2 + 0.4961x + 13.302$	$y = 0.0054x^2 + 0.5891x + 10.573$	
	WS	ACH	0.2777	n/a	$y = 0.0006x^2 + 0.0028x + 0.0091$	n/a	
	IVT	ACH	0.0021	0.9239	$y = 443202x^2 - 88.192x + 0.0244$	$y = -1E+08x^2 + 46190x + 3.671$	
3	DBT	OT	0.6825	0.8371	$y = -0.0069x^2 + 0.991x + 7.1$	$y = -0.0119x^2 + 1.2893x + 4.6004$	
	WS	ACH	0.3241	n/a	$y = 0.0005x^2 + 0.0023x + 0.0044$	n/a	
	IVT	ACH	n/a	0.7947	n/a	$y = 5E+07x^2 + 29465x + 3.5756$	
1 = windows closed always							
2 = windows open (2 hours daily in winter)							
3 = windows open (2 hours daily plus summer: from 20:00 to 08:00)							
GENEVA							
Scenario	Correlation Parameters		Coefficient of determination (R <sup>2</sup> )		Correlation Equation for Thermal Comfort and Ventilation		
	x = Outdoor	y = indoor	Window Close	Window Open	Window Close	Window Open	
1	DBT	OT	0.7083	n/a	$y = -0.0011x^2 + 0.9102x + 19.007$	n/a	
	WS	ACH	0.6485		$y = 0.0013x^2 - 0.0008x + 0.0688$		
	IVT	ACH	n/a		n/a		
2	DBT	OT	0.6601	0.8832	$y = 0.0084x^2 + 0.2986x + 18.105$	$y = 0.0033x^2 + 0.4776x + 14.52$	
	WS	ACH	0.6225	n/a	$y = 0.0014x^2 + 3E-05x + 0.0529$	n/a	
	IVT	ACH	n/a	0.9774	n/a	$y = -8E+07x^2 + 37245x + 1.7477$	
3	DBT	OT	0.3047	0.704	$y = 0.0047x^2 + 0.0899x + 20.214$	$y = -0.0043x^2 + 0.7202x + 11.764$	
	WS	ACH	0.5978	n/a	$y = 0.0009x^2 + 0.0031x + 0.0277$	n/a	
	IVT	ACH	n/a	0.9272	n/a	$y = -1E+08x^2 + 41261x + 1.6779$	
Trickle Vents operating							
1: windows closed always							
2: Windows open 5 hours summer, 2 hours winter							
3: windows open (2 hours daily plus summer: from 20:00 to 08:00)							
KRAKOW							
Scenario	Correlation Parameters		Coefficient of determination (R <sup>2</sup> )		Correlation Equation for Thermal Comfort and Ventilation		
	x = Outdoor	y = indoor	Window Close	Window Open	Window Close	Window Open	
1	DBT	OT	0.7773	n/a	$y = 0.0063x^2 + 0.9309x + 20.318$	n/a	
	WS	ACH	0.0051		$y = 4E-05x^2 + 0.0001x + 0.0457$		
	IVT	ACH	0.2367		$y = -226398x^2 + 226.56x + 0.0057$		
2	DBT	OT	0.7990	0.9042	$y = 0.0047x^2 + 0.8807x + 17.15$	$y = 0.0027x^2 + 0.8927x + 12.622$	
	WS	ACH	0.0105	n/a	$y = 5E-05x^2 + 0.0002x + 0.0365$	n/a	
	IVT	ACH	0.1990	0.9155	$y = -137870x^2 + 166.84x + 0.0102$	$y = -6E+07x^2 + 43321x + 8.5437$	
3	DBT	OT	0.7494	0.9198	$y = -0.0025x^2 + 0.8661x + 13.007$	$y = -0.0018x^2 + 0.9828x + 8.0797$	
	WS	ACH	0.0293	n/a	$y = -5E-06x^2 + 0.0012x + 0.0291$	n/a	
	IVT	ACH	0.1130	0.9417	$y = -464366x^2 + 218.3x + 0.0104$	$y = -1E+08x^2 + 72146x + 5.1086$	
1 = windows closed always							
2 = windows open (2 hours daily in winter and occupied hours in summer)							
3 = windows open (2 hours daily during occupied hours plus summer: from 20:00 to 08:00)							
DBT: Dry bulb temperature (C) ; WS = Wind speed (m/s); IVT = Inverse of indoor and outdoor temperature differences							
OT = Indoor operative temperature (C); ACH = Air change per hour (ach)							

## 2.3 Tests

The climate correlation equations were implemented in an Excel spreadsheet in order to predict internal temperature and CO<sub>2</sub> as an indicator of IAQ in the apartment. CO<sub>2</sub> concentration was calculated within the spreadsheet from occupancy data for emission and predicted air flow rates using mass balance equations. The implementation in Athens is explained below as the example which was the most complicated. For the other two buildings, the same procedure was followed and the implementation instructions were sent directly to the occupant of the apartment and the supervisor of the office by email. It should be noted again that the climate correlation model is designed for low-tech buildings where occupants do not have easy access to the electronic platforms and the information should be communicated via SMS or email. Therefore, an Excel-based tool is appropriate for such buildings.

The test in the Athens building was carried out from 16 to 18 April 2024 during a relatively mild period. Forecast hourly data for external temperature, wind speed and global solar radiation was input into the Excel tool late in the evening of the day before; the hourly forecast data were obtained using Open Meteo (OpenMeteo, 2024). The Excel tool was run and the optimum operation for windows and blinds was derived and sent to Athens.

As this is a shelter for the homeless, the information was sent to the resident social worker via the PRELUDE partner DAEM. The occupants of the twin room were given the instructions by the social worker and were told not to compromise their comfort and if they felt they should not open windows as instructed to do so, just tell us what they did instead. A screenshot of the simulation results is shown in Figure 3.

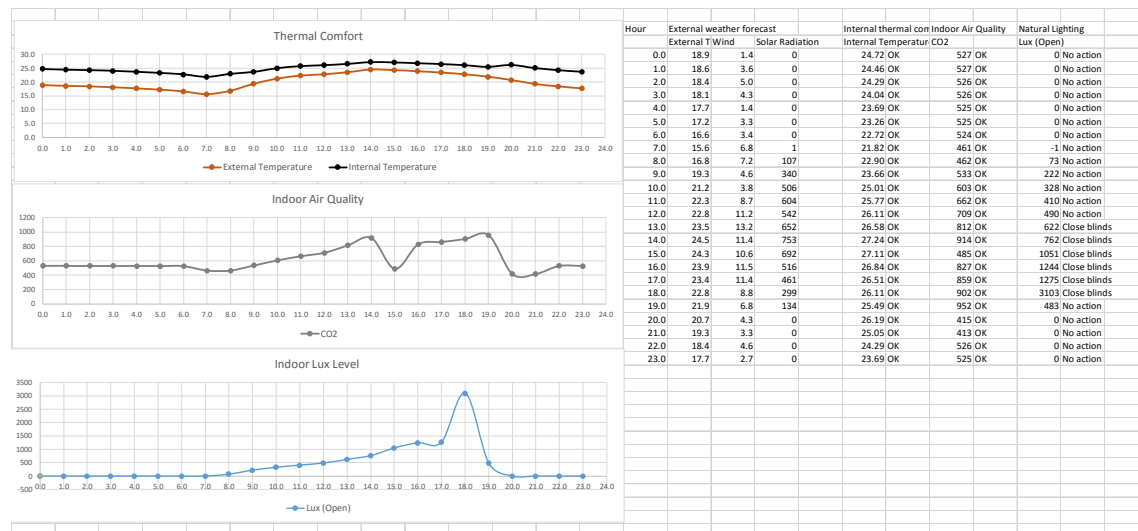


Figure 3: A screenshot of Excel tool predictions for 17 April 2024 in Athens

The recommended actions were:

Tuesday 16 April and Wednesday 17 April

*Close the window at 8 in the morning*

*Open the window at 3 for one hour*

*Open the window at 8 pm and leave it open during the night (and then close it at 8 in the morning).*

*The window does not need to be completely open, just ajar for example 10cm of opening (whatever is convenient – it does not matter how much it is open as long as it is open).  
If it is too cold at night, then they should close it and just tell us.  
Curtains should be closed between 3 pm and 6 pm.*

The occupants implemented the instructions very well and they told us some variations as follows: They started the test in the morning of 16 April at 8 am when they opened the window for 30mins and then they kept it closed as per instructions. They forgot to open the window at 15:00 but they did it the following day.

Similarly for the other two buildings, the instructions were simple and clear.

### **3 RESULTS OF TESTS AND DISCUSSION**

The predictions of the climate correlation module were compared with measured data in the three buildings. The buildings have air temperature and CO<sub>2</sub> sensors installed as part of the PRELUDE project and the data on the test days were retrieved successfully. In the Athens building sensors are placed in the common areas so an additional sensor Hobo MX CO<sub>2</sub> logger (HOBO, 2024) was installed in the target bedroom and data were successfully retrieved.

#### **3.1 Athens Building**

Figure 4 presents the measured data in the bedroom during the two days of the test and surrounding days. It can be seen clearly that the CO<sub>2</sub> level is much lower during the test days indicating improved IAQ through ventilation. The average CO<sub>2</sub> level was 853ppm during the test days in comparison to 1626ppm during the two surrounding days. The temperature trace also shows that internal thermal comfort is OK despite opening the window at night and the weather becoming a bit colder. The occupants seem to stay in their room during the afternoon and in hindsight opening the window in the afternoon for more than one hour should have been recommended. Nevertheless, the CO<sub>2</sub> levels are acceptable, especially the second afternoon when the window was opened for one hour as recommended (18 April).

A comparison of the predictions and measurements is presented in Figure 5 and Figure 6. Comparison with the illuminance predictions was not possible as there is no illuminance sensor in the room. Figure 5 presents the external temperature (forecasted and actual as measured on site) and internal temperature (predicted and as measured in the Athens pilot by the HOBO logger). Forecasted and actual external temperatures match quite well. Predicted and measured internal temperatures have some variation, with maximum temperatures predicted well but minimum temperatures under-predicted. In general, measured temperatures indicate a more stable profile during the 24 hours. This is probably due to the treatment of window opening in the simulation as a larger area is assumed open than what was implemented during the test. Also, the actual external temperature was higher than the forecasted one.

Figure 6 presents the CO<sub>2</sub> levels (predicted and as measured in the Athens pilot bedroom). The comparison is very satisfactory, especially during the night and it shows very clearly how the window opening has helped in improving IAQ. During the day larger differences can be observed but this is mainly on using the room during the afternoon more than what the simulations had assumed.



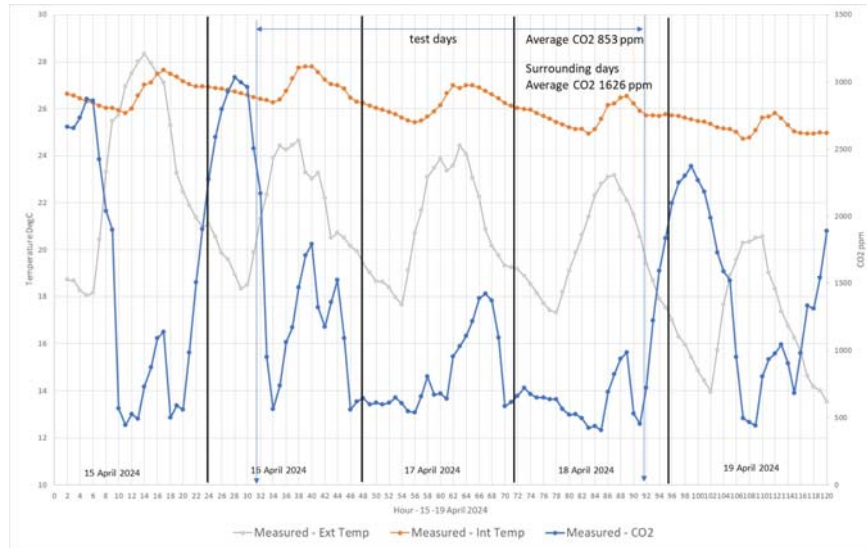


Figure 4: Athens: Environmental conditions in the bedroom for the two days of the test and surrounding days.

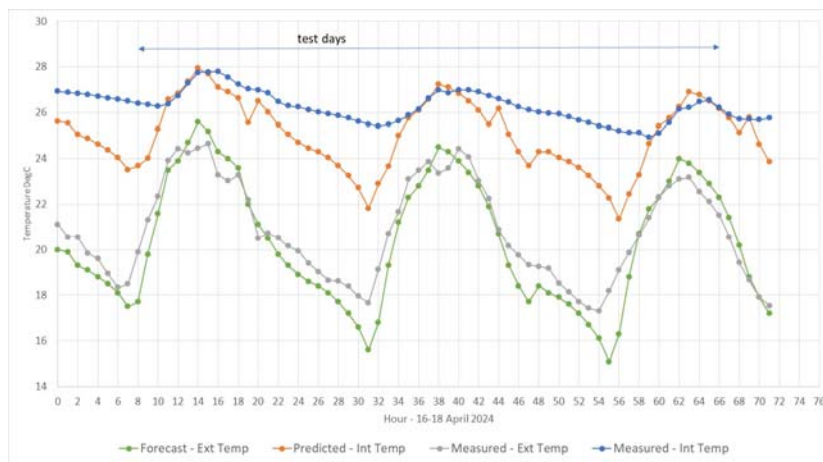


Figure 5: Athens: Thermal comfort predictions and measurements during the test period

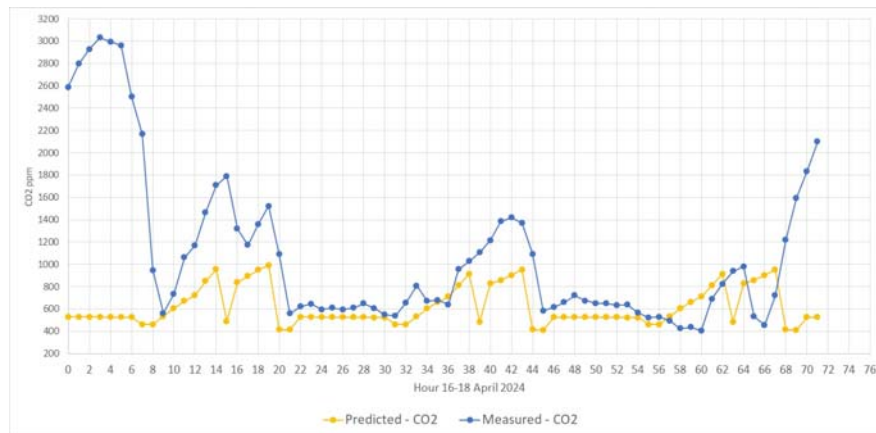


Figure 6: Athens: IAQ (CO<sub>2</sub>) predictions and measurements during the test period

### 3.2 Geneva and Krakow Building

Similar to the Athens building test, the tests were successful in the other two buildings. In Geneva, the test was during April while in Krakow during December with cold external temperatures.

Figure 7 presents the external temperature (forecasted and actual as measured on site) and internal temperature (predicted and as measured on site). Forecasted and actual external temperatures match quite well. Predicted and measured internal temperatures have some variation, with predictions showing an under-prediction tendency. The spikes in the predicted internal temperatures are because the simulations assume the opening of the windows at certain times which was not recommended on this occasion. This might have contributed to the under-prediction of internal temperatures in comparison with those measured.

In Krakow, for the first day (14 December) prediction and measurement match well; there are differences for the intervals that the windows are open and this is because in the model the heating is assumed off which has not been implemented in reality. Switching the heating off was not an option in this office and for such short periods. Also, it should be mentioned that the external temperatures were quite low so the windows were opened for shorter intervals (10-15mins) rather than the whole hour. On the second day (15 December) measured internal temperature was higher than predicted, possibly reflecting the lower forecasted external temperature. Thermal comfort is difficult to predict with a simplified model when a heating system is used; during winter the climate correlation module is more useful to indicate if window opening has helped with IAQ, which is shown in Figure 9, where CO<sub>2</sub> data are plotted.

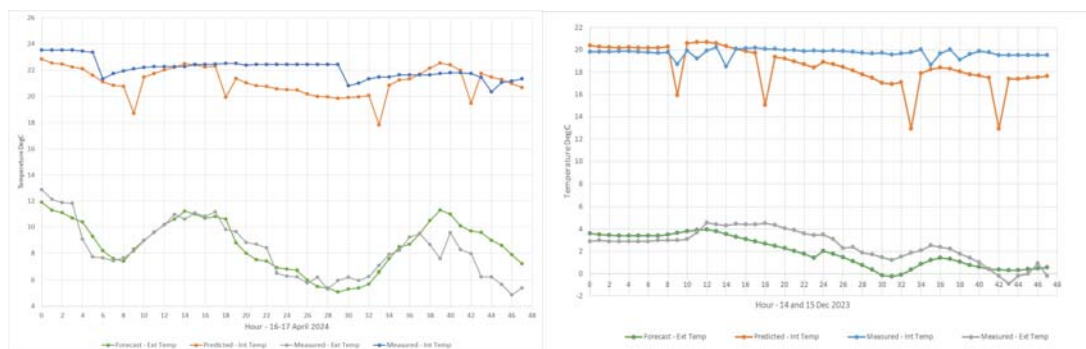


Figure 7: Thermal comfort predictions and measurements during the test period; Geneva left and Krakow right.

Figure 8 presents the CO<sub>2</sub> levels (predicted and as measured in the Geneva apartment). The comparison is very satisfactory as both night and day CO<sub>2</sub> levels are captured very well. There is an over prediction during the second night and this might be due to differences in forecasted and actual wind speeds which are used to calculate air flow rates and then the CO<sub>2</sub> concentration. It seems that the correlation module might be under predicting the air flow rate to the apartment maybe due to the simplified modelling of the trickle ventilators. Nevertheless, the agreement is good for a simplified approach and the thermal and IAQ conditions in the apartment are acceptable.

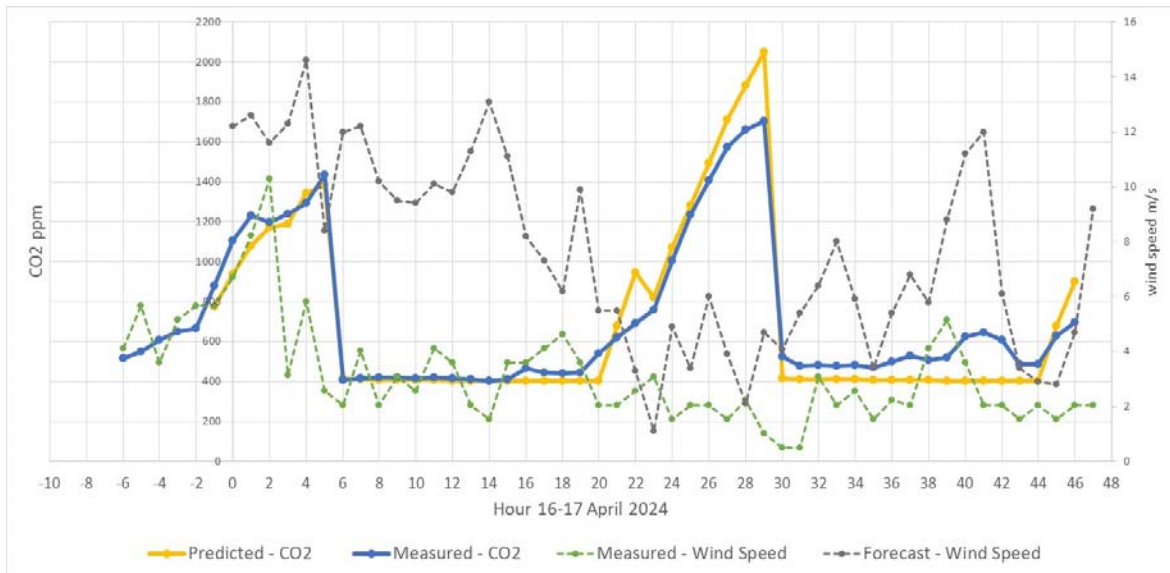


Figure 8: Geneva: IAQ (CO<sub>2</sub>) predictions and measurements during the test period

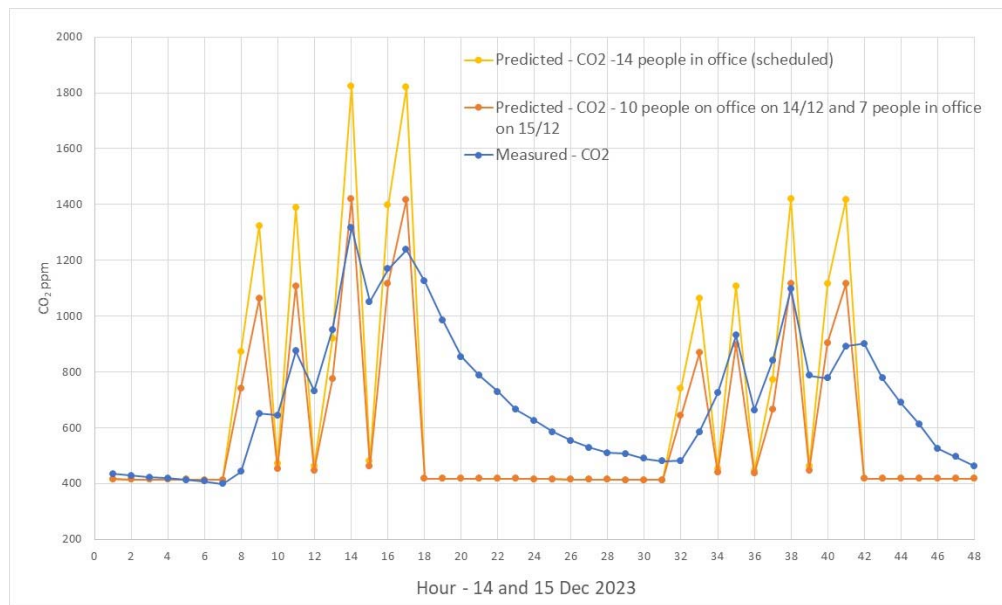


Figure 9: Krakow: IAQ (CO<sub>2</sub>) predictions and measurements during the test period

Figure 9 presents the CO<sub>2</sub> levels (predicted and as measured in the Krakow open plan office). The comparison is very satisfactory during the working time and it shows very clearly how the window opening has helped in improving IAQ. It appears that predicted CO<sub>2</sub> is higher than measured but the peaks are captured. It is worth noting that when the actual occupancy of 10 and 7 people was modelled the prediction matched the measurements much more closely. The decay of CO<sub>2</sub> after occupancy and after opening the windows is not captured well by the simple model but this does not affect the validity of the intervention in opening the windows are set intervals.

## 4 CONCLUSIONS

The implementation of the climate correlation model was carried out in three operational buildings, two residential and one office for short periods. The tests were carried out successfully with the occupants carrying out the instructions on how to use the windows and shading sent to them by text/email and based on forecast weather the previous day. Monitoring data were successfully retrieved and showed that IAQ can be improved in bedrooms using the results of the climate correlation model. Monitored data were also compared with the simple Excel simulations indicating that predictions (based on weather forecasts) and measurements in the building are quite good for IAQ (CO<sub>2</sub>) as the ventilation intervals are captured well. Thermal comfort was captured adequately and the difference might be due to the opening of window areas which would facilitate night cooling.

This study demonstrates that for low-technology buildings where actuators and sensors are not present, a single thermal study and associated correlation equations for the building can effectively inform the occupants on the best way to control their internal environment based on prevailing external conditions.

## 5 ACKNOWLEDGEMENTS

We gratefully acknowledge the collaboration of the occupants of the three buildings; this study would have not been possible without them. This study was funded by the European Union's Horizon 2020 research and innovation programme under Grant Agreement N° 958345 for the PRELUDE project (<https://prelude-project.eu>).

## 6 REFERENCES

- de Kerchove, T, Kolokotroni, M, and Siokas, G (2023). D7.2– Demo site #1 Switzerland. WP7 – Demonstrations in operational environment <https://prelude-project.eu/results/deliverables/>
- Design Builder, (2024). <https://designbuilder.co.uk/> (assessed 17 May 2024)
- HOBO (2024). MX CO2 Logger - <https://www.tempcon.co.uk/hobo-mx1102-bluetooth-co2-temp-rh-data-logger>
- Marciniak, P, Stawowczyk, D, Siokas G and Kolokotroni M (2023). D7.4 - Demo site report #3 Krakow. WP7 – Demonstrations in operational environment <https://prelude-project.eu/results/deliverables/>
- Open Meteo, Free Weather API, <https://open-meteo.com>
- PRELUDE project, (2024). Prescient building Operation utilizing Real-time data for Energy Dynamic Optimization, <https://prelude-project.eu> (assessed 17 May 2024)
- Tsakanika, D and Christantoni, I (2023). D7.5 - Demo site report #4 Athens. WP7 – Demonstrations in operational environment <https://prelude-project.eu/results/deliverables/>
- Zune, M. and Kolokotroni, M. (2022a). Climate correlation model to forecast thermal comfort and IAQ in naturally ventilated residential buildings. 42nd AIVC conference: Ventilation Challenges in a Changing World, 5th-6th October 2022, Rotterdam, Netherlands.
- Zune, M. and Kolokotroni, M. (2022b). D3.4: Indoor-outdoor correlation module. PRELUDE Project WP3: Interoperable dynamic module integration in multisimulation dataspace. <https://prelude-project.eu/results/deliverables/>

# IAQ-label for Belgian public spaces: Monitoring in 11 public spaces

Klaas De Jonge\*<sup>1</sup>, Arnold Janssens<sup>1</sup>

<sup>1</sup> Ghent University, Research group building physics

Sint-Pietersnieuwstraat 25

9000 Ghent, Belgium

\*Corresponding author: [klaas.dejonge@ugent.be](mailto:klaas.dejonge@ugent.be)

## ABSTRACT

In 2022, a new law was passed by the Belgian federal government with the purpose to enhance the indoor air quality in public spaces in the aftermath of the COVID-19 pandemic. This new law, among other things, requires publicly accessible spaces to apply a CO<sub>2</sub> meter and provides the option to have an IAQ label in place that informs the visitor about the indoor air quality of that space. Since then, the Belgian Federal Public Health Service has been developing the more detailed, practical implementation of this new law, in consultation with stakeholders and research institutes.

In support of the development of the IAQ label a measurement campaign was set up to obtain a better understanding of the IAQ achieved in public spaces. There is typically a lack of this data since public buildings such as restaurants, bars, sports infrastructure or theaters are studied less frequently in IAQ literature than e.g. offices or dwellings.

In this new monitoring campaign, measurements of CO<sub>2</sub>, Temperature, RH, PM<sub>2.5</sub> and PM<sub>10</sub> were carried out in 11 Belgian public spaces with a variety of functions for a duration of at least 7 days in March 2024. At the same time the spaces were inspected to obtain information about the use, potential sources of pollutants and possible ventilation systems in place.

The measurements show a broad range of IAQ-parameters depending on use, presence of specific sources and presence of a ventilation systems in the building. Specific sources of PM can dramatically change the indoor concentration to levels well above WHO Air Quality Guidelines for extended periods of time. Bars/restaurants have obtained the worst IAQ-parameters while most other locations, all equipped with mechanical ventilation systems, were able to achieve acceptable CO<sub>2</sub> and PM levels. The measurements highlight the complexity in the development of one consistent label applicable for all public spaces.

## KEYWORDS

IAQ in Public Spaces – Measurements - Particulate Matter – CO<sub>2</sub>

## 1 INTRODUCTION

Belgium has passed a law in 2022 aiming to enhance the indoor air quality in publicly accessible spaces in the aftermath of the COVID-19 pandemic (FOD Health, 2022). Part of this legislation focusses on raising awareness about indoor air quality in the general population as they are often not aware of the risks linked to high pollutant concentrations indoors. This law, among other things, will provide an official label and underlying certification procedure that allows publicly accessible spaces to quantifiably showcase the efforts done to maintain good Indoor Air Quality (IAQ).

Since then, the Belgian Federal Public Health Service has been developing the more detailed, practical implementation of this new law, in consultation with stakeholders and research institutes. The focus of the implementation first lied in locations that proved most challenging during the COVID-19 pandemic e.g. Bars, Restaurants, Theatres. In support of the development of the IAQ label a measurement campaign was set up to obtain a better understanding of the IAQ achieved in such public spaces. There is typically a lack of this data since public buildings such as restaurants, bars, sports infrastructure or shops are studied less frequently in IAQ literature than e.g. offices or dwellings. This paper reports on the measurement campaign and discusses results.

## 2 MONITORING CAMPAIGN

Measurements were originally planned and executed in 18 locations. Locations were randomly selected within the target functions based on availability and willingness of owners to participate. After checking the data quality and omitting cases that did not have a minimum duration of 7 days of effective acquired data, 11 locations were kept in the final dataset. The selected measurements took place between 7/03/2024 and 28/03/2024 with most spaces located near Ghent. Analysis of the outdoor temperature measurements gathered from open-access local weatherstation Vlinder 71 (VLINDER UGent, 2024) indicate a rather cold period with an average value of 9.6°C and a 95<sup>th</sup> percentile value of 14.2°C. Window opening is therefore expected to be limited.

All locations were measured with *NEMo diagnosis* loggers (Ethera Labs, 2024) with the following measured parameters: Temperature (T), Relative Humidity (RH), Carbon Dioxide (CO<sub>2</sub>) and two size ranges of Particulate Matter (PM<sub>2.5</sub> & PM<sub>10</sub>). Table 1 summarises the technical information of the NEMo logger.

Table 1 Summary of the data from the technical datasheet of the used NEMo Loggers (Ethera Labs, 2022)

<b>CO<sub>2</sub></b>	Detection method: Non Dispersive Infrared spectrometry (NDIR) Measuring range: 0 to 5000 ppm Resolution: 1 ppm Accuracy: ± 30 ppm ± 3 % of reading value Automatic Calibration algorithm (400ppm reference)
<b>PM<sub>2.5/10</sub></b> (10: calculated)	Detection method: Laser-based light scattering Measuring range: 0 - 1000 µg/m <sup>3</sup> Resolution: 1 µg/m <sup>3</sup> Accuracy: PM <sub>2.5</sub> : 10µg/m <sup>3</sup> (<100µg/m <sup>3</sup> ) or ± 10% of reading value (>100µg/m <sup>3</sup> ). PM <sub>10</sub> (calculated): 25 µg/m <sup>3</sup> (<100µg/m <sup>3</sup> ) or ± 25% of reading value (>100µg/m <sup>3</sup> )
<b>Temperature</b>	Measuring range: -55°C to +125°C Accuracy: ± 2°C from -25°C to 100°C (± 0.5°C after calibration)
<b>Relative Humidity</b>	Measuring range: 0 to 95 % Accuracy: ± 3 % from 11% to 89% (± 7 % for the rest of the range)

General descriptive data of each case was gathered with special attention to possible sources of particulate pollutants. For all cases information was gathered on opening hours and the possible presence of a mechanical ventilation system. Only in one case the technical specifications of the ventilation system were available, including design flow rates of outdoor air. In none of the locations air cleaning systems were in place.

## **2.1 Description of the spaces**

### **2.1.1 Bar KM**

Bar KM is a bar in a rural area of Flanders. It is a popular place for local organizations, small groups, to meet (e.g. Billiard, Card-games, Darts). Connected to the bar, there is a multi-purpose room which is used when additional seating is needed and where a *Boltra* course is present. According to the owner, you can expect 3 types of visitors: the regulars at the bar, the weekly visitors of local organisations and, during the day, ad-hoc bike-tourists. It does not have any means of mechanical ventilation.

### **2.1.2 Bar VO**

Bar VO is a relatively large bar and restaurant in the city center. It is part of a heritage building with high ceilings. They serve food and drinks which results in peak occupancy during lunch and dinner-time but will have customers all-day. The owners of this location have invested in a state-of-the-art variable airflow (CO<sub>2</sub> controlled) balanced mechanical ventilation system. The owners have also installed a CO<sub>2</sub>-sensor with public display near the counter.

### **2.1.3 Bar VM**

Bar VM is a bar situated next to two sport halls, a series of outdoor sport fields and a school. It serves as the place where groups go to have a drink after their sporting session but also as lunchroom for the school and space where kids can go play when the weather is bad. This makes for an intensively used location with a high number of unique customers that do not stay in the space very long. The bar has an air based heating system coupled to a mechanical balanced ventilation system. The system recirculates air to achieve the necessary airflow for heating. The mechanical airflow system was installed in 1990 and was never updated to newer airflow requirements.

### **2.1.4 Bar OW**

Bar OW is a bar in the city center. It is open from early noon to after midnight but as it is a popular bar for university students to have a seated drink, peak occupancy occurs in the evening and night hours. Candles are lit in the evening for lighting and atmosphere. The bar does not have a mechanical ventilation system and windows need to stay closed after 22u to limit noise disturbances of the neighbours.

### **2.1.5 Bar VL**

Bar VL is a bar linked to a soccer-field and soccer-club. It is only open in the evening when there is soccer practice and bi-weekly during the weekend when there is a soccer match. The building does not have a mechanical ventilation system but trickle-vents are placed above most of the windows to allow for naturally driven airflow even when windows are closed.

### **2.1.6 Gym WB**

Gym WB is a fitness room that is accessible 24/7. Although always accessible ,occupancy is highest during the evening hours. This gym is purpose built with a mechanical balanced ventilation system.

### **2.1.7 Gym SP**

Gym SP is a fitness room open during the day and evening. It is located in the underground level of a building in the city-center. Only the entrance is connected to outdoor air, accessible via a staircase from the street. Therefore the possibility of infiltration and natural airflow is limited. The building has a mechanical ventilation system.

### 2.1.8 Waiting room hospital

The hospital waiting room functions as a place for people in attendance of their scheduled appointments. The patients come and go, but the space is occupied continuously. There is a mechanical ventilation system present.

### 2.1.9 Store (sporting goods)

The store is a warehouse-type building, purpose built as store. It is only open during the day and is equipped with a mechanical ventilation system.

### 2.1.10 University restaurant

The university restaurant is open for lunch and evening meals. Peak occupancy is during lunch with a smaller peak in the evening. The hot dishes are served from a heated counter. Behind this counter there is a kitchen used to prepare fries with a separate local exhaust (industrial range hood). Both are situated in a space which is the same overall space as the measured lunchroom. A CO<sub>2</sub> controlled balanced mechanical ventilation system is present.

### 2.1.11 University Cafeteria

The university cafeteria is a place where sandwiches, soup and coffee can be bought. There is some space to sit and reside for some time but most people are only present for a short duration as they take-away lunch. The cafeteria is open during the day but with peak occupancy during lunch. The building is purpose-built with a state-of-the-art mechanical ventilation system.

## 3 RESULTS

Table 2 reports the key figures of the measured parameters during the opening hours of the different locations. The key figures are:

- 5% percentile (P5)
- 25% percentile (P25)
- Mean / 50% percentile (P50)
- 75% percentile (P75)
- 95% percentile (P95)
- Average (Avg.)
- Standard Deviation (St. dev.)

The key-figures for PM<sub>2.5</sub>, PM<sub>10</sub> and CO<sub>2</sub> are also visualised as box-plots where the min and max values are replaced by the P5 and P95 values in Figure 1 and Figure 2. It was necessary to plot the results of Bar KM separately as the PM<sub>2.5</sub> and PM<sub>10</sub> values were an order of magnitude higher. Locations without mechanical ventilation system are indicated in another colour.

On the same graph the WHO 1-day average (AQG Day) and yearly average Air Quality Guideline (AQG Year) values are shown as dotted lines for PM<sub>2.5</sub> and PM<sub>10</sub> (World Health Organisation, 2021). For CO<sub>2</sub>, the new IAQ legislation defines two reference levels A at 900 ppm and B at 1200 ppm, these reference levels are also shown as dotted lines.

With regards to CO<sub>2</sub>, only 5 out of 11 locations manages to have a P95-value below the upper reference level of 1200 ppm. The median value (P50) is above the lower reference level of 900 ppm for 4 out of 11 locations, this means that more than half of the time the occupants are exposed to air which is not meeting the legal reference A. For two of those, Bar OW and Bar KM, the median value is even above the 1200 ppm reference value.



Table 2 Key figures of measured parameters during opening hours

	<i>Bar KM</i>	<i>Bar VO</i>	<i>Bar VM</i>	<i>Bar OW</i>	<i>Bar VL</i>	<i>Gym WB</i>	<i>Gym SP</i>	<i>Waitin room</i>	<i>Store</i>	<i>Univ Rest.</i>	<i>Univ Lunch</i>	
<i>CO2</i>	<i>P5</i>	761	417	442	526	453	437	570	472	480	515	405
	<i>P25</i>	987	543	775	880	625	617	910	511	593	540	428
	<i>P50</i>	1358	691	1030	1559	792	768	1172	545	642	590	492
	<i>P75</i>	1848	786	1608	2477	1178	928	1551	611	741	841	597
	<i>P95</i>	3847	942	2732	3441	1694	1231	2190	815	908	978	730
	<i>Avg.</i>	1598	678	1277	1702	918	786	1279	581	669	686	523
	<i>St.dev</i>	873	165	750	957	407	228	531	110	123	177	107
<i>PM2.5</i>	<i>P5</i>	38	5	6	4	1	1	0	1	0	0	1
	<i>P25</i>	68	6	7	10	2	1	1	1	1	1	2
	<i>P50</i>	96	8	10	17	3	2	2	2	1	10	3
	<i>P75</i>	148	12	13	29	5	3	3	4	2	28	5
	<i>P95</i>	227	20	23	42	9	4	6	9	3	55	8
	<i>Avg.</i>	114.3	10.6	11.6	19.9	4.0	2.0	2.1	3.5	1.4	17.1	3.8
	<i>St.dev</i>	65.5	12.9	6.2	13.2	2.4	1.2	1.9	3.5	1.0	18.8	2.4
<i>PM10</i>	<i>P5</i>	45	6	7	5	2	1	0	1	0	0	2
	<i>P25</i>	80	7	8	11	3	1	1	1	1	2	3
	<i>P50</i>	107	9	11	18	4	2	2	3	2	12	4
	<i>P75</i>	169	13	14	31	6	4	5	6	5	35	6
	<i>P95</i>	246	21	24	44	10	8	9	12	10	72	9
	<i>Avg.</i>	129.0	11.6	12.6	21.3	5.0	3.1	3.2	4.4	3.1	22.1	4.8
	<i>St.dev</i>	70.8	13.1	6.3	13.6	2.4	2.5	3.0	4.2	3.2	25.1	2.4
<i>T</i>	<i>P5</i>	21.5	23.0	17.0	20.0	17.0	19.0	19.5	18.0	21.5	21.5	20.5
	<i>P25</i>	22.0	24.5	19.0	21.0	19.0	20.0	20.0	22.5	22.0	23.0	20.5
	<i>P50</i>	22.5	25.0	20.0	21.5	20.0	21.0	20.5	23.0	22.5	23.0	21.5
	<i>P75</i>	23.0	25.5	21.0	22.5	20.5	21.5	20.5	24.0	23.0	23.5	21.5
	<i>P95</i>	24.0	26.0	22.0	23.5	21.5	22.0	21.0	24.5	24.0	24.5	22.0
	<i>Avg.</i>	22.5	24.7	19.9	21.7	19.8	20.7	20.3	22.6	22.4	23.0	21.2
	<i>St.dev</i>	0.7	0.8	1.7	1.0	1.4	1.0	0.5	1.8	0.8	0.9	0.6
<i>RH</i>	<i>P5</i>	51	27	38	50	46	43	45	41	34	32	34
	<i>P25</i>	55	31	51	58	53	47	53	43	38	36	38
	<i>P50</i>	59	38	58	62	57	58	61	45	42	39	40
	<i>P75</i>	63	41	63	66	61	64	66	47	47	41	46
	<i>P95</i>	67	44	70	71	69	68	69	53	49	50	48
	<i>Avg.</i>	59	36	56	61	57	56	59	46	42	39	41
	<i>St.dev</i>	5	5	9	6	6	8	8	4	5	5	5

With regards to PM2.5 **Bar OW** and **Bar KM** have mean measured values (P50) during opening hours above the AQG Day which indicates unacceptable IAQ. The **University restaurant** has a lower value but still has a significant portion of its distribution above the AQG Day limit.

The trends in PM2.5 and CO<sub>2</sub> levels are similar which suggests that in most cases the PM2.5 sources are linked to the activities of occupants and a reverse correlation with the air change rate of the space. The **University restaurant** is an exception where CO<sub>2</sub> values are low compared to the measured PM values. This indicates that the people present and their activities are not the main source of PM. We suspect that the kitchen appliances (e.g. deep fryers) in the connected space act as a source of PM although local exhaust is provided (industrial range hood). **Gym SP** on the other hand shows relatively high CO<sub>2</sub> values compared to measured PM

values. However, also in **Gym WB** low PM values were measured indicating a lack of PM sources in these spaces but high CO<sub>2</sub> production rate because of the high intensity of the human activity levels. This trend is most outspoken in Gym SP because of smaller ventilation flow rates for the given occupancy and activity levels.

The conclusions for PM<sub>10</sub> are similar to the conclusions for PM<sub>2.5</sub> given the clear relation of both measured values which is due to the fact that PM<sub>10</sub> is an extrapolated value of the PM<sub>2.5</sub> data. Because of higher AQG values of PM<sub>10</sub> the results are less problematic with regards to healthy indoor air quality.

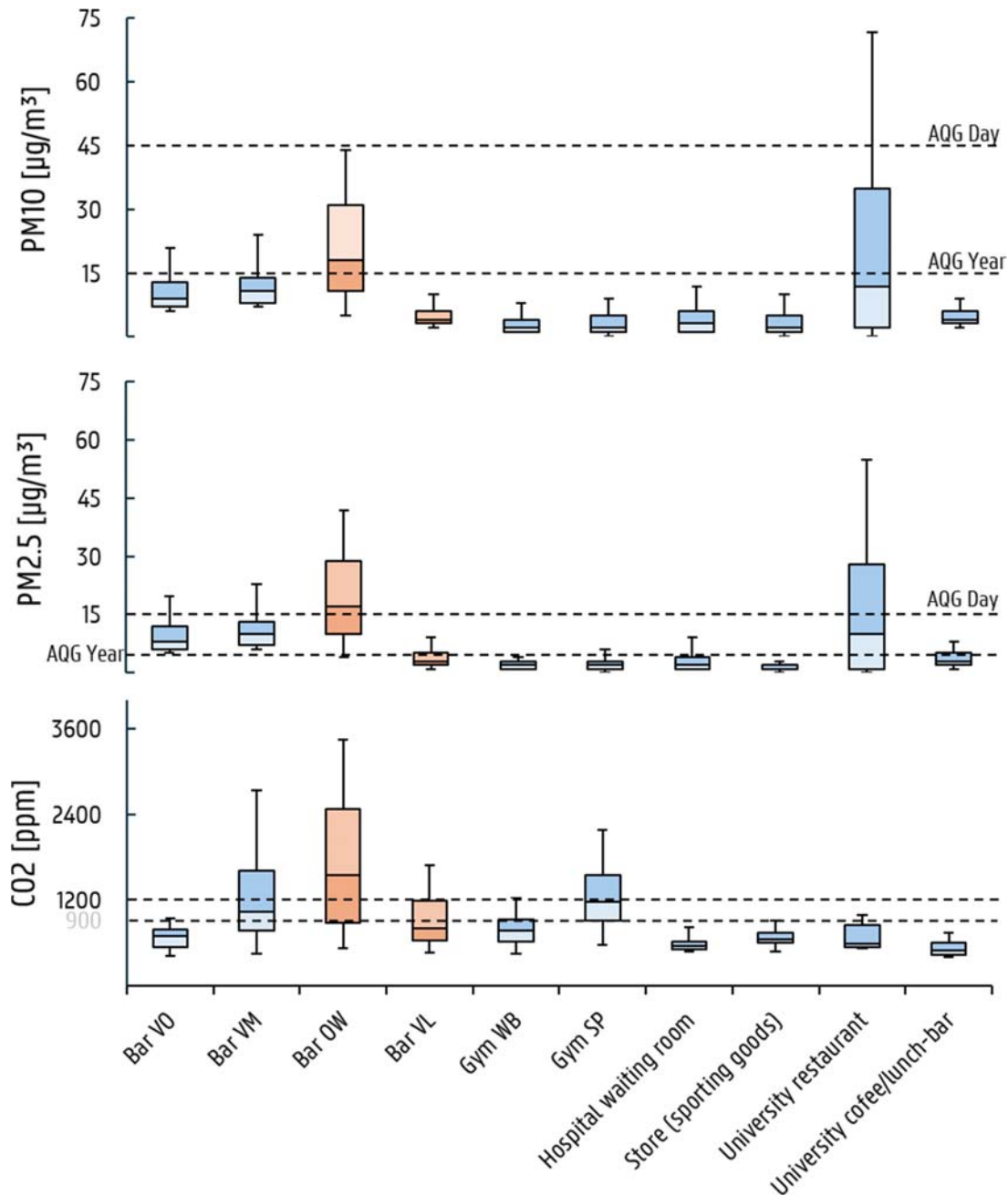


Figure 1 Boxplots of the CO<sub>2</sub>, PM<sub>2.5</sub> and PM<sub>10</sub> concentrations during the opening hours of all the measured locations except for BAR KM. The orange boxplots signify cases without mechanical ventilation system.

Finally, the measurements in **Bar KM** indicate a total disregard of IAQ in this place. PM2.5 and PM10 measurements are all above the limits for at least 95% of the time that the bar is open for the general population. Also the CO<sub>2</sub> levels are high with a P5-value of 761 and a mean measured value (P50) of 1358ppm. Although we have not observed it in place, we suspect that this bar does not obey the no-indoor-smoking policy which is in place in Belgium. The indoor air quality in this location is unacceptable on all accounts.

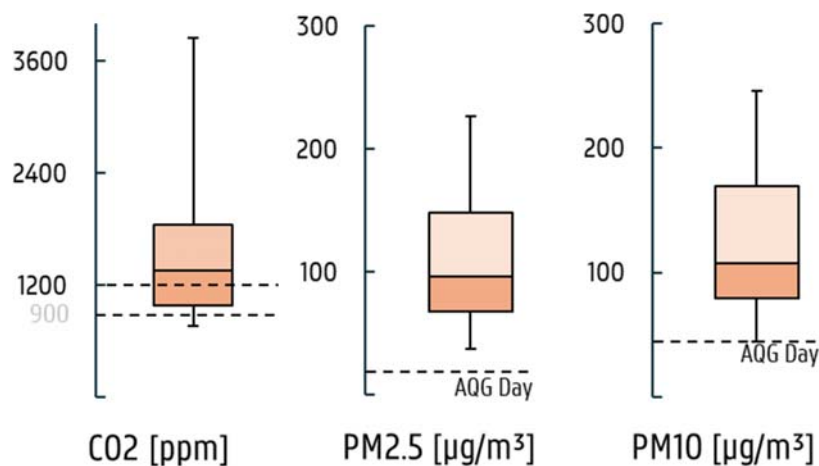


Figure 2 Results for BAR KM with high PM2.5 and PM10 values.

#### 4 CONCLUSIONS

Overall **Bar KM** and **Bar OW** perform worst with regards to CO<sub>2</sub>, PM25 and PM10 measurements. This is as expected since these are the cases without any dedicated provisions for ventilation. The measured **Bars** and **Gyms** have the tendency to perform worst with regards to IAQ even if a mechanical ventilation system is present but with low PM values in the Gyms due to the lack of sources. The presence of specific PM sources (e.g. fryers in student restaurant, suspected smoking in Bar KM, candles in Bar OW) can shift the measured PM values upwards dramatically, well above the WHO air quality guideline values. The other locations were all equipped with mechanical ventilation that managed the IAQ effectively for the occupation and activities present. This suggests a correct sizing and operation of the systems in these locations.

The measurement campaign confirms that the locations selected as priority locations by the Belgian Federal Public Health Service, namely bars and restaurants, are indeed more likely to have low IAQ and have a low airflow/person ratio. The development of an IAQ-label can prove challenging as giving an overall score or appreciation of the indoor air quality, especially the health aspect, purely based on CO<sub>2</sub> levels can underestimate the impact of PM when specific sources are present. A label based on a range of priority pollutants should be considered as alternative, possibly also including specific VOCs (e.g. Formaldehyde)

It should be noted that based on only three parameters and a relatively short measurement period clear differences in IAQ levels can be observed. Combined with observations and technical information general trends and results can be understood and explained. Technical information about the HVAC systems, e.g. ventilation airflow rates of the ventilation system were not often readily available to the tenants.

## 5 ACKNOWLEDGEMENTS

We would like to acknowledge the master students engineering: architecture at Ghent University who took part in the special topic *IAQ labelling* for gathering information and measurements at the different locations. We also acknowledge the company Airscan BV for helping with the logging equipment.

## 6 REFERENCES

Ethera Labs. (2022). *NEMo Classic Technical datasheet*.

Ethera Labs. (2024). Air quality monitoring station—NEMo. *Air Quality Monitoring Station - NEMo*. <https://www.etheralabs.com/en/air-quality-monitoring-station-nemo/>

VLINDER UGent. (2024). *VLINDER Station 71—Sterenwacht Armand Pien (Data downloaded from WOW.Meteo.be)*. <https://vlinder.ugent.be/>

Wet van 6 november 2022 betreffende de verbetering van de binnenluchtkwaliteit in gesloten plaatsen die publiek toegankelijk zijn, 2022034199, Federale Overheidsdienst Volksgezondheid, Veiligheid en Veiligheid van de Voedselketen, Belgisch Staatsblad—Moniteur Belgique 88761 (2022). [https://www.ejustice.just.fgov.be/cgi\\_loi/change\\_lg.pl?language=nl&la=N&cn=2022110604&table\\_name=wet](https://www.ejustice.just.fgov.be/cgi_loi/change_lg.pl?language=nl&la=N&cn=2022110604&table_name=wet)

World Health Organisation. (2021). *WHO global air quality guidelines. Particulate matter (PM2.5 and PM10), ozone, nitrogen dioxide, sulfur dioxide and carbon monoxide*.

# Test facility for building envelope leakage type analysis and improvement of acoustic and thermographic airtightness measurement methods

Markus Diel<sup>\*1</sup>, Björn Schiricke<sup>1</sup>, Johannes Pernpeintner<sup>1</sup>

*1 German Aerospace Center (DLR e.V.)*

*Institute of Solar Research*

*Linder Hoehe*

*51147 Cologne, Germany*

*\*Corresponding author: markus.diel@dlr.de*

## ABSTRACT

Ensuring the airtightness of building envelopes is crucial for enhancing the energy efficiency of buildings. The prompt detection of leaks is essential, particularly when undertaking building renovations. Consequently, efforts have been made in recent years to implement new measurement techniques that facilitate the rapid, straightforward, and wide-scale identification of leaks in building envelopes. Two notable methods are the use of acoustic and thermographic technologies. In the acoustic beamforming method, a microphone array technology is employed, whereby sound propagation is assumed to occur in a manner similar to that of airflow through the building envelope. The infrared camera, however, is capable of rapidly identifying problem areas through the use of intelligent experimental setups.

Although both methodologies have undergone preliminary evaluation on smaller façade elements and in field trials, this paper presents the initial findings of the first large-scale laboratory testing of these methodologies in the context of leak detection on building envelopes. To facilitate the investigation on such a comprehensive level, a new airtightness test facility was constructed. This test facility has a volume of approx. 11.4 m<sup>3</sup>, has an n50 value of 0.0088 and can hold test specimens of various sizes up to 3 m<sup>2</sup>.

Initial investigations utilising an acoustic camera revealed that a simple leakage in the form of a 3.3 mm hole could be precisely localised at different measurement distances. Furthermore, it was demonstrated that the spectra of different hole sizes exhibited a similar curve shape, and that there was a correlation between the maximum sound pressure level and the hole size.

Thermographic measurements with 6-7 K temperature difference, 50 Pa pressure were performed with camera distances between 1.5 m and 5.0 m at normal and 45° angle. Individual leaks of 3.3 mm diameter could be detected at all distances. With larger distance and shallower incidence angle, the signal reduced, but localization was possible with objects smaller than the pixel-resolution.

The outcomes of the tests conducted at the test facility confirmed the assumption that comprehensive laboratory testing is essential for a more accurate evaluation of both methods in the context of leak detection on building envelopes, and thus for subsequent field use. Further measurement campaigns are already underway and will continue to investigate the methods themselves, as well as more complex and therefore more realistic leakages.

## KEYWORDS

Airtightness, Acoustic Beam Forming, Thermography, Leak Localization, Test Facility

## 1 INTRODUCTION

It is estimated that approximately 30% of the energy consumed by a building for the purposes of heating and cooling can be attributed to unwanted air exchange through the building envelope (Jokisalo, Kurnitski, Korpi, Kalamees, & Vinha, 2009; Sawyer, 2014). The main method used

to measure the aggregated airtightness of buildings is the fan pressurisation method or “blower door test” (ISO 9972:2015, 2015). The fast and dependable detection of leaks is of critical importance, especially in the context of new constructions and the renovation of existing structures. Identifying and quantifying leaks using standard methods in conjunction with a blower door test, using tracer-gases (Ghazi & Marshall, 2014) for example, is a challenging, time-consuming process that is highly dependent on the experience of the respective energy consultant.

For this reason, various methods have been researched in recent years to overcome these weaknesses. Two prominent examples are the acoustic (Holstein, et al., 2020; Raman, Prakash, Ramachandran, Patel, & Chelliah, 2014) and thermographic (Mahmoodzadeh, Gretka, Wong, Froese, & Mukhopadhyaya, 2020) methods, both of which provide fast, simple and comprehensive detection and localisation of leaks in the building envelopes. While the acoustic beamforming method is based on a microphone array technology and assumes that sound primarily takes the same paths as air through the building envelope, the infrared camera can quickly identify problem areas through intelligent experimental setups such as lock-in thermography (Kölsch, Pernpeintner, Schiricke, & Lüpfer, 2023). Previous studies in both of these fields have demonstrated the potential of these technologies through measurements on existing buildings (Schiricke, Diel, & Kölsch, 2024) and on smaller façade elements (Feng, Shen, Shrestha, & Hun, 2024).

To the best of the authors' knowledge, no comprehensive laboratory studies have been conducted to date that employ either method in the context of leak detection in buildings. Such investigations have the advantage of further improving the reliability of leak detection by means of these measurement methods. Consequently, a laboratory test facility has been developed. The objective is to facilitate a comprehensive analysis of a multitude of leakages. A further area of interest is the variation and potential correlation in acoustic and thermal signatures according to the type and size of different leaks, as well as the conditions under which optimal localisation is possible.

## **2 METHODS**

### **2.1 Test facility**

The new test facility, designated ATLAS (Adaptable Testing Laboratory for Air Sealing), is located at the German Aerospace Center in Cologne, Germany. Figure 1 depicts the test facility, equipped with the essential measuring instruments.

The test facility is constructed on rollers, weighs approximately 500 kilograms and measures 2.0 meters in width, 2.5 meters in height and 3.0 meters in depth. An adapter plate is affixed to the posterior of the test facility, thereby enabling the attachment of a measuring fan. This fan is the Minneapolis DuctBlaster. The Minneapolis Micro Leakage Meter (MLM) system is connected to the adapter plate and the DuctBlaster via a hose system. The orifice within the MLM has a diameter of 4 mm, enabling the MLM to measure air volume flows in the range of 0.17 to 0.83 m<sup>3</sup>/h at a pressure difference of 80 Pa. However, experimental examinations have demonstrated that even lower volume flows of approximately 0.1 m<sup>3</sup>/h can be measured. The established blower door system characterizes the leaks by measuring the volume flow and will therefore help with the evaluation of the measurement results of the new measurement methods.

The test specimens can be attached to the front of the test facility using a quick-release mechanism. Two distinct sizes of test specimens can be clamped: the smaller specimens

measure 85 cm by 85 cm, while the larger specimens measure 170 cm by 170 cm. An acrylic glass plate (see Figure 1) serves as a reference plate for the measurement of the test facility's airtightness.



Figure 1: Test facility ATLAS equipped with its requisite measurement technology: Minneapolis DuctBlaster with Micro Leakage Meter (left), loudspeaker (inside), microphone array (right) and infrared camera (right)

In order to be able to measure the volume flow through emulated leakages of test specimens, the residual leakage of the test facility itself with an airtight reference plate as a specimen must first be measured. This value must then be subtracted from future measurements of other samples. The results of the residual leakage measurements are presented in Figure 2. In this experiment, the residual leakage was quantified three times for a chamber pressure of 50 Pa to 90 Pa in 10 Pa increments. Between each measurement series, the test specimen and door were removed and reinstalled to assess the reproducibility of the airtightness measurement. The average air flow of the linear regressions was 0.10 m<sup>3</sup>/h for a pressure of 50 Pa, which corresponds to an n50 value of 0.0088. The maximum deviation of the regressions from the mean was 4.4 % for an overpressure of 50 Pa.

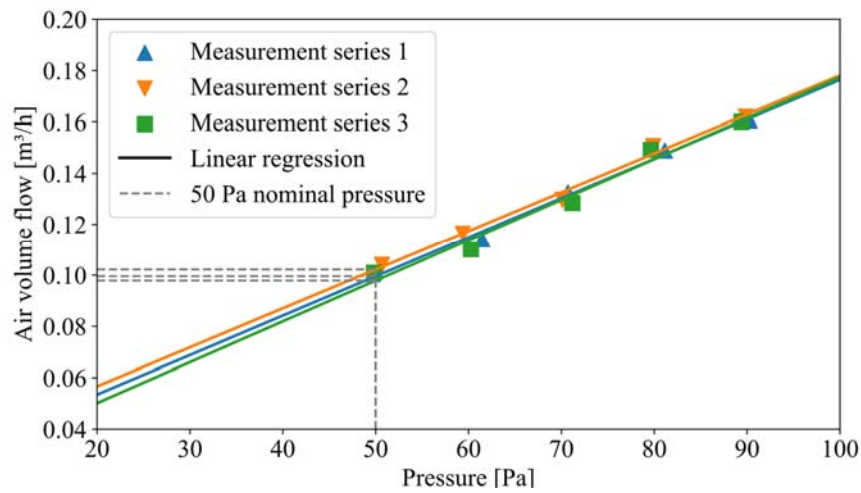


Figure 2: Reproducibility of residual leakage measurement at the ATLAS test facility using an acrylic reference plate as a test specimen

## 2.2 Acoustic leak detection

The localization of air leaks using an acoustic camera is based on the assumption that sound primarily follows the same path as air. In the measurements discussed here, the measurement setup for acoustic measurements consists of two components: the noise source, which is an omnidirectional transmitting loudspeaker and an amplifier connected to it, and the noise receiver, which is a microphone array (see Figure 1). Previous tests demonstrated that the positioning of the loudspeaker within the test facility had no impact on the measurement outcomes. For simplicity, the loudspeaker was therefore placed in the centre of the facility. The microphone array is situated at the height of the test specimen, at a distance of 1.5 meters. The camera utilized is the “Acoustic Camera Array Ring48 AC Pro” from gfai tech GmbH.

Acoustic camera measurement technology translates sound waves into a tangible representation by superimposing sound pressure level variations onto a visual image of the area of interest. Using beamforming, the camera accurately locates sound sources by considering the time it takes for the sound to reach each microphone. Advanced signal processing is essential for accurate measurement calculation and display. For a detailed description of this methodology, see the paper by Schiricke et al. (Schiricke, Diel, & Kölsch, 2024). In addition, the paper by Chiariotti et al. (Chiariotti, Martarelli, & Castellini, 2019) provides an in-depth explanation of beamforming.

## 2.3 Infrared leak detection

Leakages at building envelopes can be seen in infrared images, if there is airflow through the leak and the temperature of the leaking air and the surface surrounding the leak are not identical. Leaks can hence be emphasised by increasing the temperature difference, e.g. by blower heaters and by controlling pressure difference across the envelope using a blower door to increase the flowrate and control the direction of flow.

Leaks can be further separated from other structures in the image by active thermography. In that case, non-static blower operation is combined with image processing techniques. This can be as simple as taking differential images from before and after blower operation, as demonstrated by Kalamees (Kalamees, 2007). Time series analysis using physical models is performed in the BauTools Software distributed by BlowerDoor GmbH and described by Feng et al. (Feng, Shen, Shrestha, & Hun, 2024). An approach, that will be investigated further in this test facility is lock-in thermography. There, the blower is activated periodically enabling the time series of the pixels to be analysed by Fourier transform at the excitation frequency, as described by Kölsch et al. (Kölsch, Pernpeintner, Schiricke, & Lüpfer, 2023).

However, for the first measurements presented here classical thermography is chosen. The camera is a Workswell Wiris Pro with an uncooled 640x514 pixel microbolometer sensor and 13 mm lens. The spectral range of the camera is 7.5-13.5  $\mu\text{m}$ , the temperature sensitivity is specified to 30 mK. The time period for NUC-calibration was set to 3 minutes.

The camera is placed outside the test facility, compare Figure 1, and the test facility is operated at overpressure of 50 Pa creating airflow towards the camera. The camera is placed at distances of approximately 150 cm, 250 cm, and 500 cm from the test section, perpendicular to the test section, in one measurement at distance 150 cm, but at a 45° angle to the side. Fan heaters within the test facility heat the interior to 27°-28 °C, which is 6 K-7 K above the temperature of the laboratory at 21 °C. For the radiometric evaluation, emittance was set to 91% (Stephan,



et al., 2019), reflected temperature, temperature of atmosphere, and temperature of the lens to 21°C and relative humidity to 40%.

### 3 RESULTS

#### 3.1 Acoustic measurements

The results of three smaller measurement campaigns conducted with the acoustic setup on the ATLAS are presented below.

In the first series of measurements, the capacity of the acoustic system to identify the location of leaks at varying measuring distances was examined. To this end, a hole with a diameter of 3.3 mm was drilled into a 12 mm thick medium-density fibreboard. Four distinct measurement distances were examined, maintaining consistent noise source settings. The distances investigated were 0.5 m, 1.5 m (the standard configuration at the test facility), 2.5 m, and 5.0 m. Figure 3 depicts the acoustic images, which demonstrate that the hole could be localized at each distance. Nevertheless, the measured sound pressure level exhibited a decreasing trend with increasing distance of the array from the test specimen. In the 10 kHz third octave band, the sound pressure level at the hole was 16.6 dB for a measurement distance of 0.5 m and 5.9 dB at a distance of 5 m.

As part of the second series of measurements, the impact of varying hole sizes was examined. For this purpose, holes with diameters of 3.3 mm, 4.2 mm, 5.0 mm, 5.5 mm, and 6.0 mm were drilled into a particle. The experimental configuration, including the array spacing and output signal of the loudspeaker, remained constant throughout the experiments. Figure 4 illustrates the frequency spectra of the individual holes. Up to a frequency of 6 kHz, all holes display a highly similar acoustic signature. At higher frequencies, the sound pressure level curves continue to be similar in their monotonic behaviour, but there are noticeable differences in the maximum sound pressure level. The largest difference between the 3.3 mm and 6.0 mm holes is at a frequency of 9.84 kHz and is 7.64 dB. In addition, the sound pressure level for the largest hole is on average 5.37 dB higher in the range between 8 kHz and 16 kHz. All comparative data between each hole is shown in Table 1 below.

In the final series of measurements, the capacity of the acoustic measurement system to differentiate between holes in close proximity was examined. The identical configuration was utilized as in the preceding series. Three distinct distances were evaluated, comprising two 3.3 mm holes situated 30 mm, 40 mm, and 50 mm from the centre of the hole. The acoustic images are illustrated in Figure 5. In the case of the smallest hole spacing, the camera was unable to differentiate between the two holes at any frequency range. This was also the case for a hole spacing of 40 mm. However, the acoustic image displays a less punctual and more elongated local sound pressure level peak compared to the previous measurement. With the largest hole spacing, on the other hand, both sources could be easily differentiated. In this case, the ratio of measuring distance to hole spacing is 30.

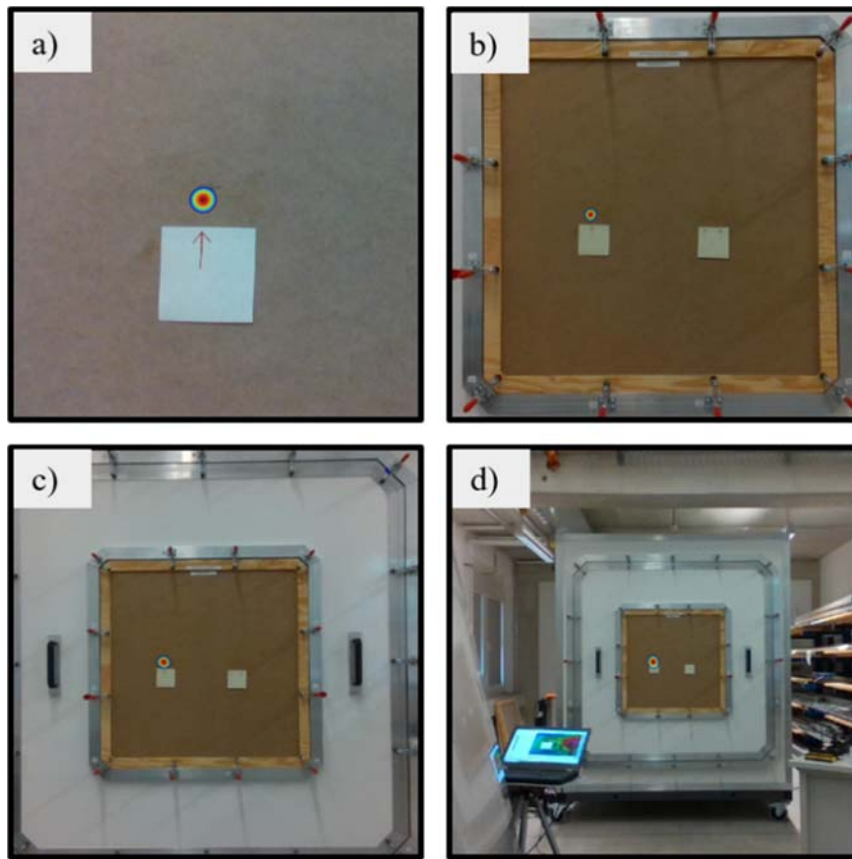


Figure 3: Recording of the acoustic camera of a 3.3 mm hole at a measuring distance of: a) 0.5 m, b) 1.5 m, c) 2.5 m, d) 5.0 m

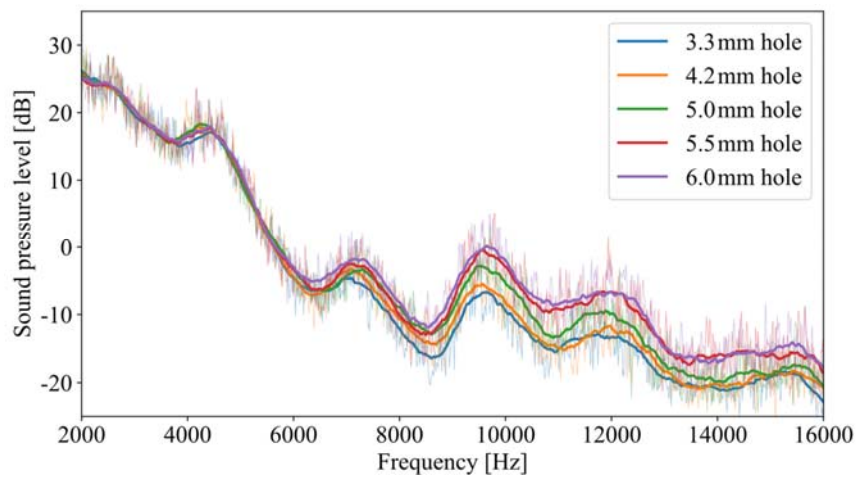


Figure 4: Moving average smoothed sound pressure level curve for five different hole sizes

Table 1: Comparison between measured sound pressure levels of different hole sizes

Hole size in mm	3.3	4.2	5.0	5.5	6.0
a = Hole area in $10^{-6} \times \text{m}^2$	8.55	13.85	19.63	23.76	28.27
$p_m$ = Mean sound pressure level between 8 kHz to 16 kHz in dB	-15.78	-14.95	-13.24	-11.04	-10.42
$p_m/a$ in $\text{dB}/\text{m}^2 \times 10^5$	-18.45	-10.79	-6.74	-4.65	-3.68

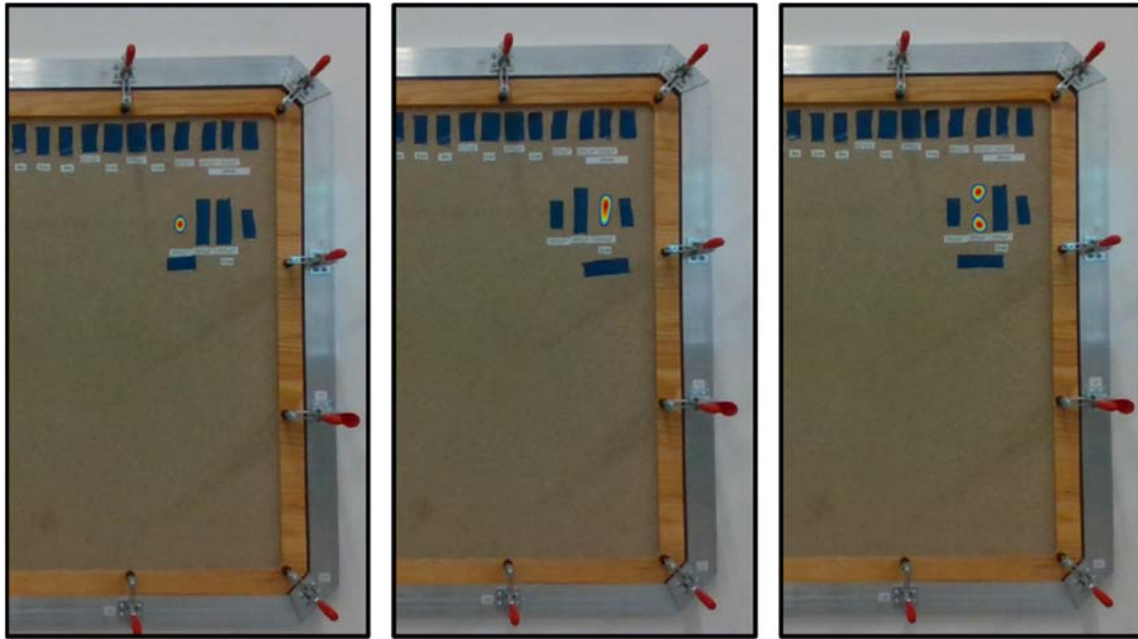


Figure 5: Acoustic camera recordings of two 3.3 mm holes at a distance of 30 mm (left), 40 mm (centre) and 50 mm (right) from each other

### 3.2 Infrared measurements

For the infrared measurements, a number of holes in the specimen (thickness 13 mm) were used ranging in diameter from 6 mm to 2 mm, compare Figure 6. This was the same test specimen used in the second and third series of acoustic tests. The distance of the holes (some covered by tape) is 40 mm. This compares to the pixel-resolution of the camera in the plane of the specimen of 2.0 mm at 150 cm, 3.3 mm at 250 cm and 6.5 mm at 500 cm camera distance.

Figure 8 b) to e) shows the result of four measurements at different distances and angles. In order to create comparable colour settings for all images in Figure 8 b) to e), the colour settings are adjusted to show identical range of 3 K, with the measured temperature of the specimen at a fixed colour, compare Figure 8 a). The images taken at 250 cm and 500 cm are cropped to show the same image section as the image taken at 150 cm camera distance.

First, images Figure 8 b) to e) are compared visually: The two small holes at the right cannot be separated in any image and appear in all images as a single leak. All other leaks can be separated. With larger camera distance, the temperature signal is reduced. A pixel increasingly images not only the hole but also the surrounding specimen. This is also visible in the profiles plotted in Figure 7. The larger the camera distance, the lower the measured peak value, and the wider the peak. For temperature measurements, it is typically recommended, that structures should be at least 3 pixels wide. As we are only interested in the location of the leak a reduction in signal is acceptable.

It is noteworthy, that in the measurement at 45° and 150 cm, compare Figure 8e), the signal is also significantly reduced - compared to the measurement at normal incidence and at identical distance, compare Figure 8b). At 45° the camera only visualises the internal walls close to the surface, where the temperature difference to the ambient is smaller than further inside.

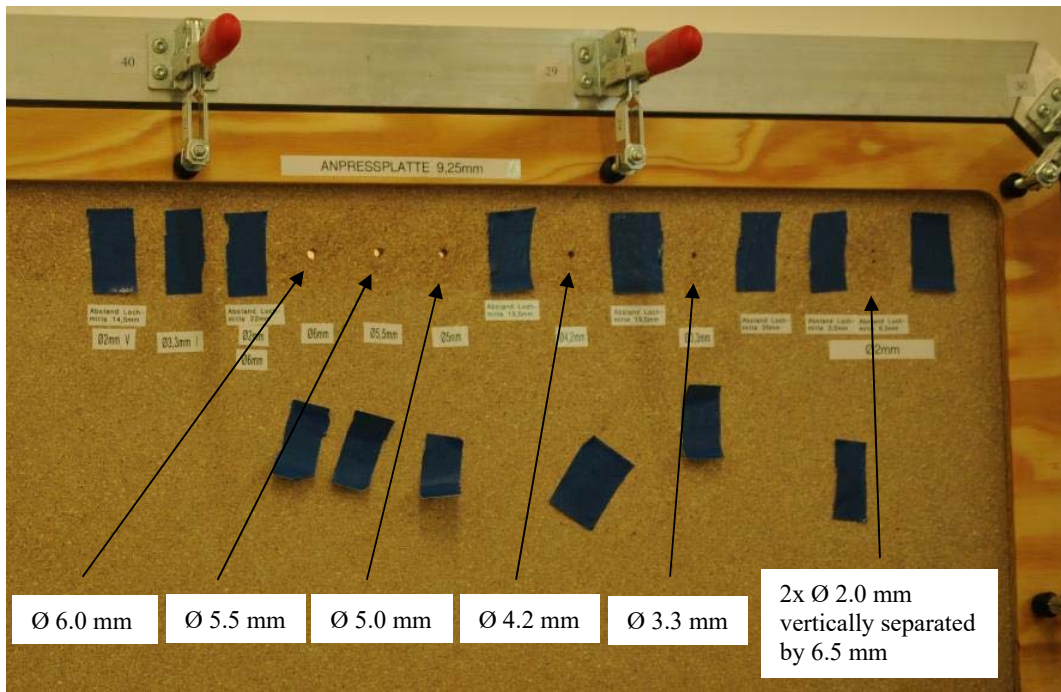


Figure 6: Specimen for infrared measurements, additional holes are covered by tape

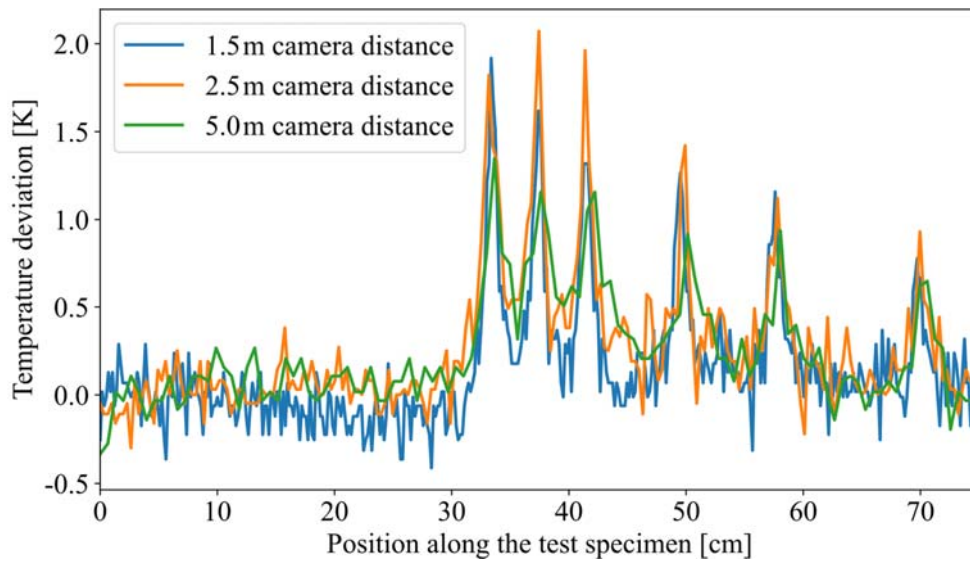


Figure 7: Temperature profile of specimen for three camera distances

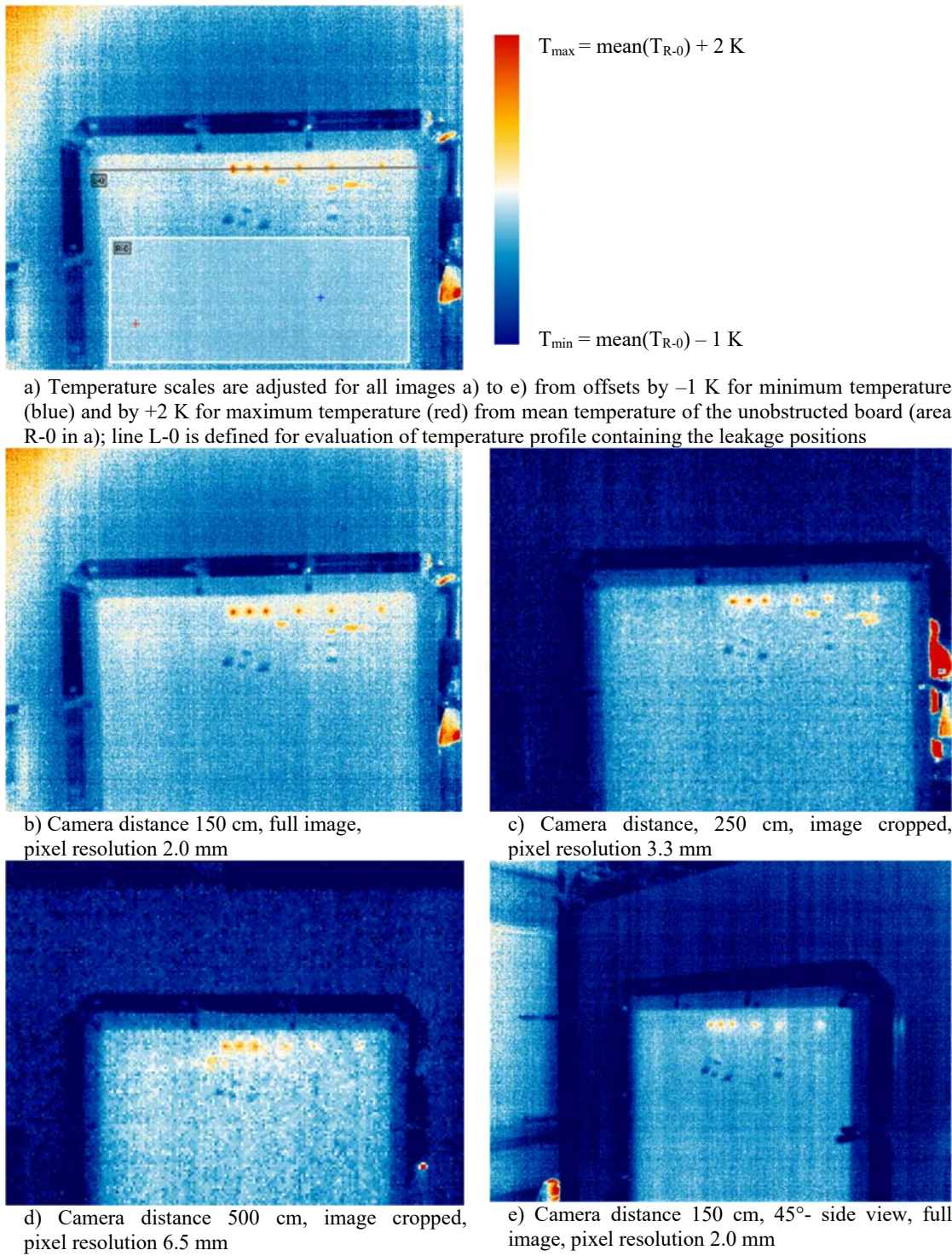


Figure 8: Infrared images of the test specimen at different distances and angles

## 4 CONCLUSIONS & OUTLOOK

The measurements demonstrate that the test facility offers a more controllable environment than field measurements, resulting in higher reproducibility and comparability of the measurements. Furthermore, the leakages can be measured individually, which significantly simplifies the characterisation of a single leakage. This can be observed in the air volume flow measured with the MLM, the acoustic signature and the thermographic image.

The acoustic measurements showed that small leaks can be localised at different measuring distances. Furthermore, a first correlation between measuring distance and hole spacing for the ability to distinguish holes from each other could be determined. Whether this is a constant or variable value needs to be clarified in further experiments. In addition, measurements on leaks of different sizes showed that the same leak types have similar spectral characteristics, and that the size of the sound pressure level peaks may allow conclusions to be drawn about the size of the leaks. In the context of future investigations, it will be of great relevance to ascertain whether this behaviour is also observed in other leakage types. In particular, it will be beneficial to determine the role of different spectral ranges on the ability of locating leaks, and whether an automated evaluation can be realised with a sufficiently large data basis.

The first IR-images were taken at various distances and angles showing that leaks smaller than the pixel resolution can be detected with reduced signal, as the traditional limits for temperature measurements do not apply. In addition, a reduction in signal was found at lower angles of incidence, reflecting the fact that the visible depth increases at angles closer to normal, where larger temperature differences can be observed.

In future experiments, more complex leakages will be investigated. Parameters such as the leakage path, the material through which the air passes as well as the entry and exit paths of air/sound (e.g. simple crack or socket) will be of special interest.

## 5 ACKNOWLEDGEMENTS

This work is part of the ongoing joint research project “Development of a combined method of acoustics and infrared thermography for quantitative evaluation of the airtightness of building envelopes and locating leaks (Q-Leak)”, conducted by the German Aerospace Center (DLR) with its project partners Gesellschaft zur Förderung angewandter Informatik e.V. (GFaI), SONOTEC GmbH, Ecoworks GmbH, BlowerDoor GmbH, alstria office REIT- AG. This project is funded by the German Federal Ministry for Economic Affairs and Climate Action (BMWK) under the grant number 03EN1079A. The authors would also like to thank Imke Grzempa and Karl Voitke from “R316 KontruktionsWerkstatt” for building the test facility.

## 6 REFERENCES

- Chiariotti, P., Martarelli, M., & Castellini, P. (2019). Acoustic beamforming for noise source localization--Reviews, methodology and applications. *Mechanical Systems and Signal Processing*(120), 422-448. doi:<https://doi.org/10.1016/j.ymsp.2018.09.019>
- Feng, T., Shen, Z., Shrestha, S. S., & Hun, D. E. (2024). A novel transient infrared imaging method for non-intrusive, low-cost, fast, and accurate air leakage detection in building envelopes. *Journal of Building Engineering*. doi:<https://doi.org/10.1016/j.jobbe.2024.109699>

- Ghazi, C., & Marshall, J. (2014). A CO<sub>2</sub> tracer-gas method for local air leakage detection and characterization. *Flow Measurement and Instrumentation*, 38, 72-81.  
doi:<https://doi.org/10.1016/j.flowmeasinst.2014.05.015>
- Holstein, P., Bader, N., Moeck, S., Münch, H.-J., Döbler, D., & Jahnke, A. (2020). Akustische Verfahren zur Ermittlung der Luftdichtheit von Bestandsgebäuden. *Denkmal und Energie 2020: Energieeffizienz, Nachhaltigkeit und Nutzerkomfort* (pp. 111-123). Springer. doi:[https://doi.org/10.1007/978-3-658-28753-5\\_8](https://doi.org/10.1007/978-3-658-28753-5_8)
- ISO 9972:2015. (2015). *Thermal Performance of Buildings—Determination of Air Permeability of Buildings—Fan Pressurization Method*. International Organization for Standardization: Geneva, Switzerland.
- Jokisalo, J., Kurnitski, J., Korpi, M., Kalamees, T., & Vinha, J. (2009). Building leakage, infiltration, and energy performance analyses for Finnish detached houses. *Building and Environment*, 44(2), 377-387. doi:<https://doi.org/10.1016/j.buildenv.2008.03.014>
- Kalamees, T. (2007). Air tightness and air leakages of new lightweight single-family detached houses in Estonia. *Building and environment*, 42(6), 2369-2377.  
doi:<https://doi.org/10.1016/j.buildenv.2006.06.001>
- Kölsch, B., Pernpeintner, J., Schiricke, B., & Lüpfer, E. (2023). Air leakage detection in building façades by combining lock-in thermography with blower excitation. *International Journal of Ventilation*, 22(4), 357-365.  
doi:<https://doi.org/10.1080/14733315.2023.2198791>
- Mahmoodzadeh, M., Gretka, V., Wong, S., Froese, T., & Mukhopadhyaya, P. (2020). Evaluating patterns of building envelope air leakage with infrared thermography. *Energies*, 13(14). doi:<https://doi.org/10.3390/en13143545>
- Raman, G., Prakash, M., Ramachandran, R. C., Patel, H., & Chelliah, K. (2014). Remote detection of building air infiltration using a compact microphone array and advanced beamforming methods. *Berlin Beamforming Conference*, (pp. 1-10).
- Sawyer, K. (2014). Windows and Building Envelope Research and Development: Roadmap for Emerging Technologies. *US Department of Energy: Washington, DC, USA*.
- Schiricke, B., Diel, M., & Kölsch, B. (2024). Field Testing of an Acoustic Method for Locating Air Leakages in Building Envelopes. *Buildings*, 14(4).  
doi:<https://doi.org/10.3390/buildings14041159>
- Stephan, P., Kabelac, S., Kind, M., Mewes, D., Schaber, K., & Wetzels, T. (2019). *VDI-Wärmeatlas: Fachlicher Träger VDI-Gesellschaft Verfahrenstechnik und Chemieingenieurwesen*. Springer-Verlag.

# **RENOVAIR: Study of the evolution of airtightness, ventilation, comfort and indoor air quality in 7 energy renovation operations of social housing in France**

**Andrés Litvak<sup>\*1</sup> Eddy Handtschoewercker<sup>1</sup>**

*1 Cerema Direction Territoriale Sud-Ouest, rue Pierre Ramond, 33165 Saint Médard en Jalles, FRANCE*

*\*Corresponding author: andres.litvak@cerema.fr*

## **ABSTRACT**

This article follows a first publication presented at the AIVC2022 conference (Handtschoewercker, 2022), with the preliminary results of the RENOVAIR project, that studies the impact of energy renovation works on social housing on the comfort and health of occupants when no requirements are given on IAQ, ventilation and airtightness performances.

In the frame of the eco-conditioned financial aid supported to the ERDF 2017-2022 operational program for the energy renovation of social housing building stocks, the eligibility conditions for financial aid concern requirements on energy consumption, thermal insulation performance and the energy efficiency of heating systems. Yet, the current specifications of this program do not condition any financial assistance on performance criteria relating to indoor air quality (IAQ), ventilation and airtightness of the building envelope. Thus, the RENOVAIR project studied the evolution of these performances, knowing that it is commonly admitted that these issues are essential for achieving comfortable low energy buildings.

RENOVAIR is based on 7 candidate operations for the ERDF program for the energy renovation of social housing in the Nouvelle-Aquitaine region (southwest of France). In this 3-year work, we sought to characterize the performances of IAQ, comfort, airtightness and ventilation, before and after the renovation work, through in situ measurement campaigns on 21 housing units, in order to assess the importance of such requirements in the implementation of public decarbonization policies.

This article presents the final results from the three measurement campaigns: before works, after works and one year after works. On each of the 7 pilot sites, measurements were carried out on 3 dwellings in order to characterize the evolution of performance following the energy renovation work:

- i. Through air flowrates and pressure measurements, we determined whether the ventilation systems allowed sufficient air renewal in the renovated housing for each campaign.
- ii. Airtightness measurements carried out according to the NF EN ISO 9972 standard highlighted the location of air leaks in homes during each of our visits and their evolution after each step.
- iii. Dynamic measurements of temperature, relative humidity and CO<sub>2</sub> and passive VOC measurements characterized the impact of the work on the IAQ in each dwelling.
- iv. The thermal comfort of the occupants was determined by commercial low-cost sensors in each accommodation for two weeks during the winter period

In light of the results of our work, which reveal in some cases a deterioration of performance, we discuss the need of explicit requirements regarding IAQ, ventilation and airtightness with the objective to reach low energy consumption renovated buildings. We also discuss the efficiency of the retrofits according to the associated cost, the energy gains and the discomfort problems that can arise.

## **KEYWORDS**

Airtightness – Ventilation – Indoor Air Quality – Comfort – Energy Renovation

## **1 INTRODUCTION**

For several decades, experts have admitted that efficient energy-efficient renovation of buildings requires extremely good management of air renewal, ventilation and airtightness. Moreover, the COVID-19 pandemic has accentuated the importance of indoor air quality (IAQ), becoming a major concern for building owners, in terms of occupant health and comfort. Studies show that poor IAQ can result in significant economic costs, including lost productivity and public health expenditure.



Public policies, notably through European programs such as the European Regional Development Fund Operational Program 2017-2022 (ERDF OP), offer financial aid for energy renovation, but these programs don't always take into account airtightness, ventilation or occupant comfort. Yet these elements are crucial to achieving low energy consumption.

From 2016 to 2023, Cerema assisted the Nouvelle-Aquitaine Region with the renovation of social housing, examining around 70 operations. The main objectives included verifying the quality of thermal studies, ensuring that works were consistent with energy diagnosis, and assisting with the analysis of environmental and social impacts of the ERDF OP. Cerema's assistance took place in three phases: the study of projects before construction, the verification during construction, and a final verification after construction. The main objectives of the assistance were:

- to ensure the quality of thermal studies and their consistency with actual implementation,
- to make sure that the planned work really does deliver sufficient energy savings to justify the financial assistance envisaged,
- to check the quality of the work and its consistency with diagnosis,
- to support the Nouvelle-Aquitaine region in analyzing the environmental and social impacts of the ERDF OP

## **2 OBJECTIVES AND METHODOLOGY**

### **2.1 Objectives**

The overall RENOVAIR project has three main objectives:

- To observe the effectiveness of the consideration given - or not given - to airtightness, ventilation and IAQ in the energy renovation of the 7 assisted projects monitored.
- Identify the conditions for improving the energy efficiency of renovations, in conjunction with the implementation of corrective solutions for airtightness, ventilation and IAQ, depending on the expected level of energy performance.
- Support public policies to define eco-conditionality criteria for airtightness of renovations, ventilation and IAQ, based on feedback from the field.

This article complements previous publications describing in detail the objectives and methodologies of our study (Handtschoewercker, 2022) (Handtschoewercker, 2023). We invite the reader to refer to it for more in-depth information.

### **2.2 General methodology**

For this work, the analysis of an operation was broken down into three phases:

- Phase 1: Pre-engineering study of renovation projects (BW). This phase consisted in checking that the theoretical energy gains presented in the project corresponded to reality. First, we checked that the building's actual initial state was consistent with that of the thermal study. Secondly, we verified that the planned work would actually generate the expected energy savings.
- Phase 2: Verification of execution and compliance of renovation work during construction. This stage involved monitoring the quality of the work and the effective implementation of the project's features.
- Phase 3: Final post-work verification (AW). During this stage, the conformity of the work carried out with that planned, and its quality, was verified. A certificate of conformity or non-conformity was issued, and this conditioned the payment of the grant.

The sample selected for our study consists of 7 social housing operations, applying for ERDF OP funding, located in the Aquitaine region, in the south-west of France.

This sample represents approximately 10% of the total number of refurbishment operations that Cerema inspected for the ERDF PO until now.

The detailed presentation of the energy renovation work for each operation is presented in a technical report (Handtschoewercker 2023). All the refurbishment works included heavy work on the thermal insulation of the envelope, changing the joineries and the heating and ventilation systems. The specific costs of energy renovation works for appraised operations are between 100 €/m<sup>2</sup> and 300 €/m<sup>2</sup>, which corresponds to the cost ratios observed at the national level for energy renovation for low-consumption buildings.

### **2.3 IAQ, comfort, ventilation and airtightness characterization**

The study consists of carrying out a series of measurements on airtightness, ventilation, comfort and IAQ during the three phases "before works" (BW), "after works" (AW) and "one year after the works" (1yAW), established as follows, for three dwellings on each operation :

- Carrying out on-site measurements of the airtightness of the envelope of the dwellings studied to determine the airtightness level and identifying the location of the infiltration leakage locations in three dwellings.
- Diagnosis of the ventilation system on three dwellings
- Installation of measurement sensors to characterize comfort and IAQ in three dwellings of the operation.

#### ▪ *Airtightness test*

The airtightness of the dwellings was tested in accordance with NF EN ISO 9972 (AFNOR, 2015) and its application guide FD P50-784 (AFNOR, 2016) using a "blower door" device. The indicator used is  $Q_{4PA-SURF}$  value (m<sup>3</sup>/h/m<sup>2</sup>), the air leakage rate related to the surface of envelope surfaces of the building under 4Pa expressed, as defined by the french Thermal Regulation RT2012 (MEEDDM, 2010). The corresponding regulatory requirements for new buildings are 0.60 m<sup>3</sup>/h/m<sup>2</sup> for single-family and 1.00 m<sup>3</sup>/h/m<sup>2</sup> for multi-family residential buildings. Test results were compared and trends in infiltration leakage were analyzed.

#### ▪ *Ventilation system diagnosis*

The diagnosis follows the PROMEVENT protocol (ADEME, 2016), applicable to new residential buildings, according to the new thermal regulation RE2020 (MTE, 2021). Measurements were carried out in three phases on three dwellings per renovated operation:

- 1) Visual diagnosis of the ventilation system before and after renovation,
- 2) User survey on the use of the ventilation system.
- 3) Pre- and post-retrofit ventilation measurements according to the PROMEVENT protocol for new residential buildings RE2020 (MTE, 2021).

#### ▪ *Comfort characterization*

Comfort is characterized by means of a questionnaire to occupants on their feelings, and by measurements with multisensory low cost commercial sensors (GreenMe®). These sensors, initially developed for office environments, measure eight parameters: i) Air temperature (°C); ii) Relative humidity (% RH); iii) Air quality (VOC and CO<sub>2</sub>); iv) Average noise level; v) Maximum noise level (dBA); vi) Lighting level (Lux); vii) Flicker (%); viii) Color temperature (K). Three sensors were installed in each home (living room, kitchen, bathroom) for 15 days. They allowed us to characterize the indoor environment through physical measurements and occupants' votes on their comfort.

#### ▪ *Indoor air quality characterization*

The assessment of IAQ was carried out using passive tubes to measure VOCs (Benzene / Formaldehyde / Toluene / Ethylbenzene / Xylenes), CO<sub>2</sub> and Temperature and Humidity.

Three rooms were instrumented per dwelling (preferably living room) for passive tubes and 2 rooms per dwelling were instrumented with temperature, relative humidity and CO<sub>2</sub> sensors (living room + bedroom). This instrumentation was carried out for a period of one week. Benzene, toluene, ethylbenzene, xylenes (BTEX) were measured by passive samplers set up for 7 days and then analyzed in the laboratory, according to the standard NF EN ISO 16017-2 (AFNOR, 2003). Formaldehyde was measured by passive samplers set up for 7 days and then analysed in the laboratory, according to the standard NF ISO 16000-4 (AFNOR, 2012). Air renewal efficiency was assessed continuously using an infrared radiation-based CO<sub>2</sub> sensor.

### 3 RESULTS

The first BW measurement campaign was carried out between January and June 2021, the second AW between April and July 2022, and the third 1yAW between January and March 2023. Due to the significant delay in the works, operation #07 could not be monitored by the project. Only BW measurements could be carried out for operation #07.

#### 3.1 Airtightness results

Comparing the results of the BW measurement campaign with the regulatory requirements for new residential buildings in France (MTE, 2021), we can see that airtightness levels were compliant with regulatory requirement in 6 out of 7 operations (see figure 3).

For these 6 residences equipped with self-regulating single-stream mechanical ventilation systems, Q<sub>4Pa-Surf</sub> measurements were below 1.0 m<sup>3</sup>/h/m<sup>2</sup> (requirement for new multi-family buildings). Only one operation (#05) showed results with mediocre performance: this natural ventilation operation on shunt ducts showed Q<sub>4Pa-Surf</sub> values exceeding 1.60 m<sup>3</sup>/h/m<sup>2</sup>.

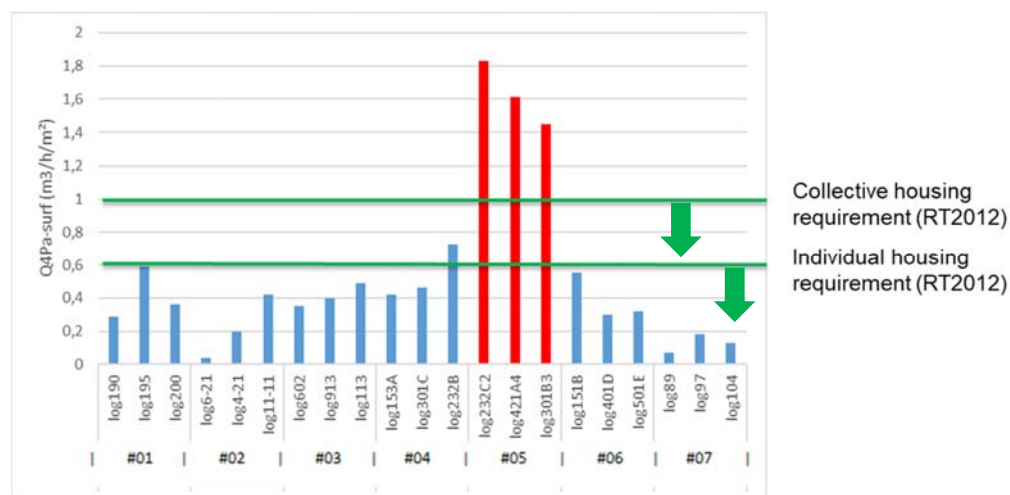


Figure 1 : Airtightness measurements prior to construction (BW)

We compared airtightness measurements from the BW, AW and 1yAW phases on 6 operations (see Figure 4). The results of the AW phase show a clear improvement in airtightness for 3 projects (#03, #05 and #06), particularly for the naturally ventilated residence which benefited from the installation of a single-flow mechanical ventilation system. On the other hand, one project (#01) suffered a significant deterioration in airtightness due to the installation of glass doors whose frames were warped on delivery. For the last 2 operations (#02 and #04), we found comparable levels of airtightness between the BW and AW phases.

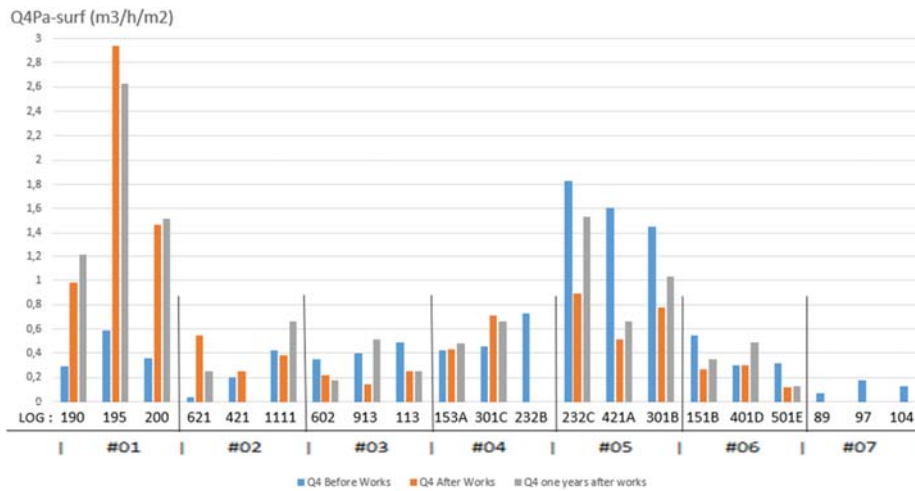


Figure 2 : Comparison of air leakage rates ( $\text{m}^3/\text{h}/\text{m}^2$ ) BW (blue), AW (orange) and 1yAW (grey)

Measurements 1yAW, taken 1 year after completion of the work, show both an improvement and a deterioration compared with the AW measurements, taken at the time of delivery. There is no significant trend to be noted in the comparison of AW and 1yAW measurements.

A qualitative analysis of each dwelling was carried out to identify the points of air infiltration for each measurement. Overall, it was found that the works improved the leak correction on the service doors and on the exterior joineries by replacing them.

On the other hand, it regularly appeared that new joineries also leaked, either between sash and frame due to adjustment problems, or between new and old frame due to their installation during renovation. These new leaks appear either as soon as they are installed (AW), or one year after installation (1yAW). Other new leaks often encountered concern roller shutter housings (boxes or manoeuvring bars) replacing old shutters, new air inlets on joinery, exhaust ducts from replaced gas boilers and wall penetrations due to plumbing work in WCs - bathrooms.

### 3.2 Ventilation results

Ventilation rates were measured during the BW campaign, see Figure 5. The majority of dwellings had systems with significant imbalances that did not achieve the extracted airflow rates compliant with regulations for new dwellings (French Government, 1982). We found a compliance rate of less than 25 % on total flow rates per dwelling for the 21 dwellings studied. This ratio is significantly lower than published statistics on compliance with ventilation regulations in new residential buildings in France, with a rate above 40% (ADEME, 2016).

Pressure measurements on extract units after renovation (AW) comply with regulatory requirements for new-build homes in 4 cases (see Figure 6 left). The 2 non-compliant operations show results below 50 Pa on each of the extract units in each dwelling (regulatory requirements range from 80 to 160 Pa  $\pm 10\%$ ). Pressure measurements on extract units one year after completion of work (Figure 6 right), still comply with regulatory requirements for 4 operations. It should be noted that the results are significantly better for operation #01, but are still mostly below the regulatory threshold for new buildings. After discussions with the building manager, he reportedly contacted the company in charge of the lot to request adjustments to the installation.

A functional check of the systems was carried out in accordance with the PROMEVENT protocol (ADEME, 2016). The observed non-compliances, apart from the impossibility of accessing the ventilation units, were air inlets in poor condition or deliberately blocked by the occupants of the dwellings, clogged extractions, and the absence or non-functioning of a manoeuvring system enabling the kitchen extraction to be switched to nominal timed flow.

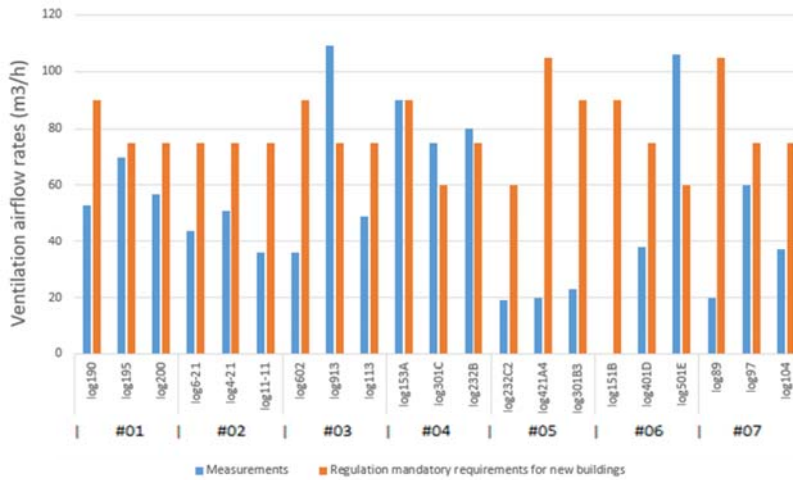


Figure 3 : Total ventilation airflow rates (m<sup>3</sup>/h) in the BW phase. Comparison between measurements (blue) and mandatory regulatory requirements for new buildings (orange)

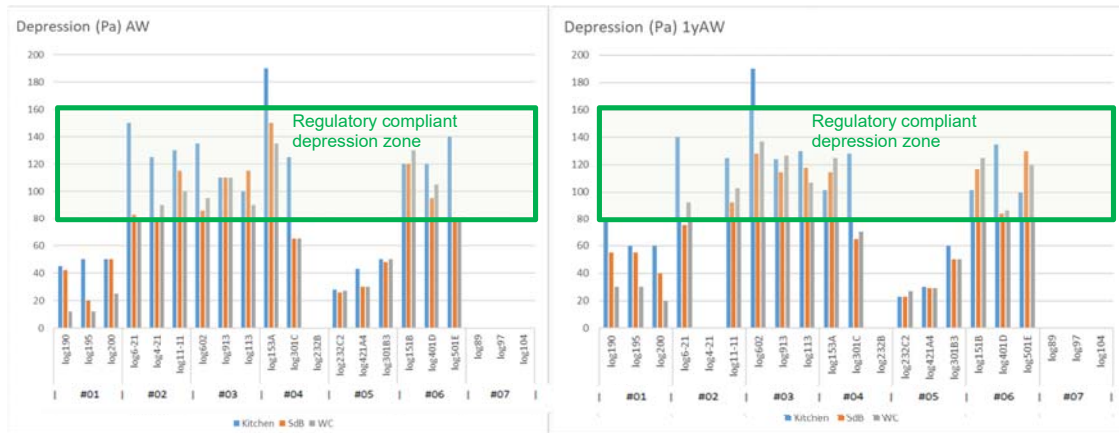


Figure 4 : Pressure measurements on extract units at AW Phase (left) and 1yAW Phase (right)

### 3.3 Comfort results

We assessed comfort in two different ways:

- Qualitative results: based on a questionnaire submitted to occupants,
- Quantitative results: based on an assessment of the percentage of time spent in comfort, deduced from temperature and relative humidity measurements.

With regard to comfort in the BW phase, the questionnaires given to occupants revealed a lack of thermal comfort in winter.

Comfort ratios derived from temperature and relative humidity measurements were evaluated for each operation according to the comfort ranges as defined in the standard EN 16798-1 (AFNOR, 2019) for category III (existing buildings), in three different locations in each of the three dwellings: living room, kitchen and bathroom. Due to the lack of seasonality for the post-work measurements (AW in spring), it was deemed more relevant to compare only the BW and 1yAW measurements in order to assess the impact of the work on the evolution of thermal comfort in the dwellings.

For the BW phase, the average comfort ratio per operation was calculated at between 25% and 86%, with an average for all operations of 56%. For operations with the lowest comfort levels,

our measurements essentially reveal discomfort due to temperatures below 20°C, which corroborates the results of the comfort questionnaires (qualitative results).

BW (2021)	#01			#02			#03			#04			#05			#06		
	log195	log200	log190	log6-21	log4-21	log11-11	log602	log913	log113	log153A	log301C	log232B	log232C2	log421A4	log301B3	log151B	log501E	log401D
LIVING ROOM	99%	98%	43%	58%	89%	67%	21%	0%	63%	85%	86%	5%	65%	100%	99%	2%	96%	
BATH ROOM	92%	99%	83%	1%	10%	71%	4%	0%	47%	99%	20%	46%	29%	97%	98%	0%	95%	
KITCHEN	99%	90%	68%	14%	78%	85%	6%	0%	83%	75%	1%	1%	27%	95%	96%	0%	93%	
Average per apartment	97%	96%	65%	24%	59%	74%	10%	0%	64%	86%	36%	17%	40%	97%	98%	1%	95%	
Average per operation	86%			53%			25%			46%			78%			48%		
13 - 27 January			1st - 12 March			8 - 22 March			15 - 29 March			26 Marchs - 9 April			31 March - 14 April			
1yAW (2023)	#01			#02			#03			#04			#05			#06		
	log195	log200	log190	log6-21	log4-21	log11-11	log602	log913	log113	log153A	log301C	log232B	log232C2	log421A4	log301B3	log211B	log501E	log401D
LIVING ROOM	83%	99%	78%	60%	9%	47%	0%	20%	99%	19%			9%	100%	96%	55%	0%	0%
BATH ROOM	100%	99%	90%	45%	76%	1%	0%	0%	99%	1%			85%	99%	97%	36%	0%	0%
KITCHEN	62%	27%	0%	15%	20%	9%	0%	52%	95%	0%			96%	100%	84%	78%	0%	9%
Average per apartment	82%	75%	56%	40%	35%	19%	0%	24%	98%	7%			63%	100%	92%	56%	0%	3%
Average per operation	71%			38%			14%			52%			85%			20%		
10 - 24 January			16 - 30 January			25 January - 8 February			1st - 15 February			21 February - 7 March			28 February - 14 March			

Figure 7 : Comfort ratios assessed at BW and 1yAW phases, as the rate of time in comfort zone for instrumented rooms in each dwelling of each site, according to standard EN 16798-1

A comparison of BW and 1yAW comfort ratios was carried out on 6 operations (Figure 7). Overall, we noted a deterioration in comfort levels, with average rates per operation ranging from 14% to 85%, with an average for all operations of 47%. Indeed, we note a decrease in the comfort rate for 4 out of 6 operations. The other 2 operations showed a slight improvement in their comfort levels, notably operation #05, which showed a clear improvement in its AW airtightness level.

Before linking comfort to the renovation work carried out, it's worth recalling the economic context at the time the 1yAW measurements were taken. In the midst of a global energy crisis following Russia's invasion of Ukraine in March 2022, the occupants of the homes we visited were often very concerned about their energy bills. They explained that they had changed their behavior regarding the use of their heating system. Their choice was to lower their usual set temperature in favor of warmer clothes.

### 3.4 IAQ results

During the BW phase, instrumentation revealed that the building in operation #05, the only one with natural ventilation, had higher concentrations of formaldehyde and CO<sub>2</sub> (see Figure 8), compared with the other buildings and with the median of the OQAI's measurement campaign CNL1 (OQAI, 2007). Concentrations of these two pollutants decreased after the works and the installation of mechanical ventilation systems.

In operation #01, CO<sub>2</sub> concentrations increased after the 1yAW phase. The value of 1 500 ppm defined by the HCSP (High Council of Public Health) as unacceptable air confinement was exceeded in several dwellings, during all three measurement phases. Also, operation #03 shows a slight increase in CO<sub>2</sub> concentrations, but the median value remains within the above-mentioned threshold (see Figure 8).

Comparing the concentrations obtained BW and 1yAW phases, it appears that formaldehyde concentrations in operation #01 have risen sharply, to the point of exceeding in several dwellings the values recorded during the CNL1 and the threshold concentrations of the French mandatory regulation for indoor air quality in establishment open to the public, limit value of 30 µg/m<sup>3</sup>. However, concentrations remain below the limit value (100 µg/m<sup>3</sup>) for which the local authorities are required to be informed.

Concentrations of toluene and ethylbenzene also increased slightly in operation #01, but remained well below the Guide Value for Indoor Air (GVIA) from the Ministry of Health and Prevention (22 000  $\mu\text{g}/\text{m}^3$  for toluene; 22 000  $\mu\text{g}/\text{m}^3$  short-term and 1 500  $\mu\text{g}/\text{m}^3$  long-term for ethylbenzene). In operations #02, #03, #05 and #06, benzene concentrations have increased over the past 1 year, exceeding the values recorded at the CNL1 and the GVIA (long-term exposure) of 2  $\mu\text{g}/\text{m}^3$ . Indeed, benzene concentrations are all below the limit value of 10  $\mu\text{g}/\text{m}^3$ . These increases are also visible in toluene (operations #03, #05 and #06) and ethylbenzene (operation #03) concentrations. However, toluene and ethylbenzene concentrations remain well below GVIA. Finally, operation #04 shows an increase in xylenes 1yAW concentrations, exceeding the values recorded at CNL1.

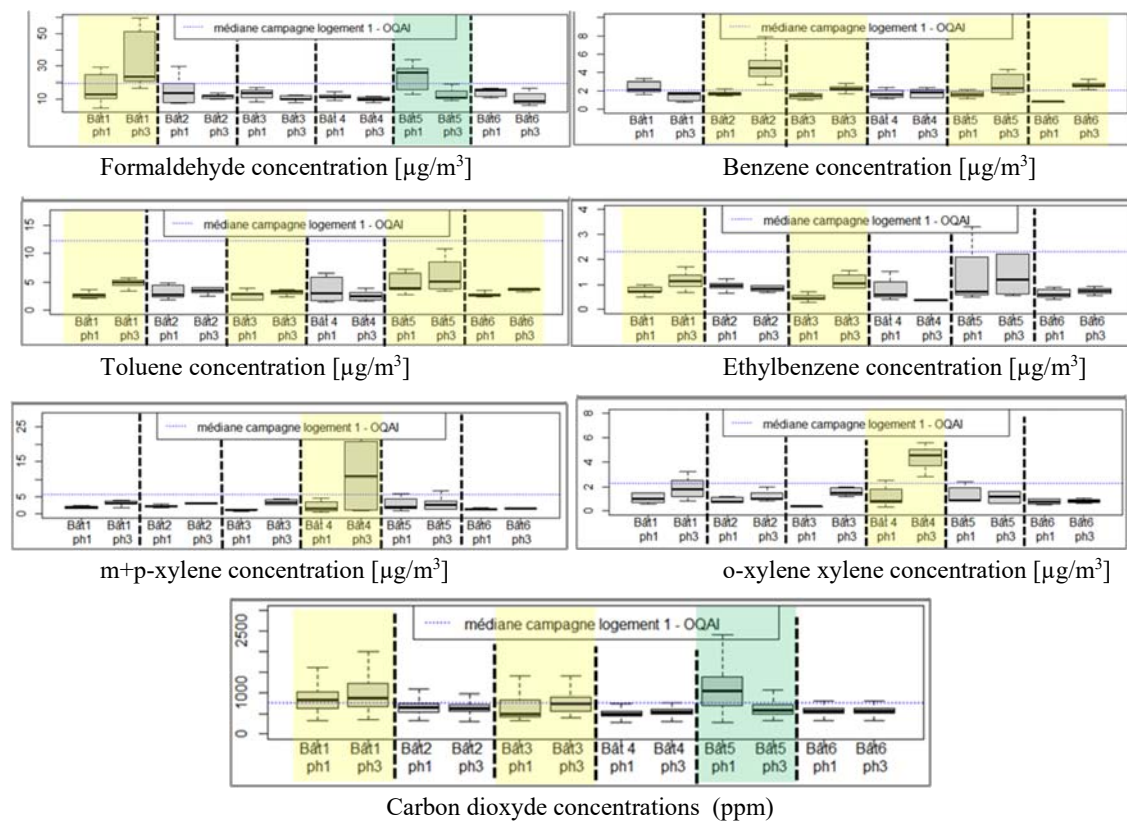


Figure 8: IAQ pollutants BW (ph1) and 1yAW (ph3), compared with the median of CNL1 (n=54)

As seasonality was not respected (higher temperatures and humidity) during the AW phase, compared with the BW and 1yAW phases, they are given for information only.

For several pollutants and buildings, higher concentrations are visible during the AW phase than during the BW and 1yAW phases. This may be explained by the fact that building materials installed just prior to the AW phase may have emitted a greater quantity of VOCs when they were new, then emissions decreased over time. It should be noted that temperatures were higher during the AW measurements, which may have resulted in greater VOC release. However, these warmer temperatures may also have resulted in better ventilation of the dwellings through more frequent opening of windows, and hence a reduction in actual VOC concentrations. The lower concentrations of AW carbon dioxide testify to better ventilation of dwellings during this period.

#### 4 DISCUSSIONS

The study analyses the impact of renovation work on the airtightness, ventilation, thermal comfort, and indoor air quality (IAQ) of residential buildings. Before the renovations, air-

permeability measurements indicated that most homes with mechanical ventilation were fairly airtight. The main air leaks were found in joinery, which were addressed by replacing them during the renovations, leading to significant improvements in airtightness post-renovation. Particularly notable improvements were seen in homes initially equipped with natural ventilation, which were upgraded to humidity-controlled mechanical ventilation (CMV). However, one project experienced a decline in airtightness due to the renovation activities.

Ventilation systems before the renovations were found to be inefficient across all monitored projects. AW measurements showed significant improvements due to the installation of humidity-controlled mechanical ventilation systems. Despite these improvements, two projects did not meet the regulatory requirements for new residential buildings. Efforts to obtain measurements from the responsible companies were largely unsuccessful, though one company did intervene to improve ventilation efficiency in one project, yet the results remained inadequate.

Regarding thermal comfort, the initial BW measurements showed varied results among the dwellings. The comparative analysis was complicated by the mismatch in seasonal conditions during the BW and AW measurements, with BW measurements taken during winter and AW measurements during spring. To address this, the 1yAW measurements were scheduled for the same time of year as the BW measurements to ensure a fair comparison. It was found that thermal comfort analysis should focus on living rooms rather than kitchens and bathrooms due to the specific and varied occupancy patterns of these spaces.

The energy crisis has significantly impacted household behavior towards heating systems, with many opting to reduce consumption at the expense of comfort, particularly in social housing where energy bills have a substantial impact.

In terms of IAQ, BW measurements indicated that natural ventilation was less effective compared to controlled mechanical ventilation, which provides more consistent air renewal and better pollutant extraction. Poor ventilation in one project led to higher-than-expected CO<sub>2</sub> concentrations, and renovation work introduced VOCs from new building materials, slightly degrading IAQ immediately post-renovation. However, VOC concentrations typically decreased over time, with 1yAW measurements generally showing lower levels than immediately post-renovation.

Despite these overall improvements, some dwellings showed an increase in VOC concentrations over the year, largely due to occupant behavior or the introduction of new furniture. Occupant activities such as smoking, using candles, and cleaning products contributed to this VOC pollution. The variability in occupant behavior between measurement periods complicates the assessment of renovation impacts on IAQ, suggesting that studies without occupants might better isolate building-related emissions.

## **5 CONCLUSIONS**

The RENOVAIR project, conducted from 2016 to 2023 in the Nouvelle-Aquitaine Region, examined the impact of renovations on airtightness, ventilation, thermal comfort, and indoor air quality (IAQ) in 70 social housing operations. The project's primary goals included ensuring thermal study quality, verifying energy savings consistency with diagnosis, and analysing environmental and social impacts of renovations funded by the ERDF Operational Program.

Key findings include:

- Airtightness: Pre-renovation measurements indicated fair airtightness in most buildings with mechanical ventilation. Post-renovation improvements were significant, particularly in homes upgraded from natural to humidity-controlled mechanical ventilation (CMV). However, one project experienced a decline due to renovation activities.



- Ventilation: Pre-renovation systems were inefficient. Post-renovation improvements were noted due to the installation of mechanical ventilation systems, yet two projects did not meet regulatory requirements. Efforts to obtain additional measurements were largely unsuccessful.
- Thermal Comfort: Initial measurements showed varied comfort levels. Seasonal mismatches in data collection complicated comparative analyses, but adjustments ensured better comparison. Thermal comfort analysis should focus on living rooms due to specific occupancy patterns in kitchens and bathrooms.
- IAQ: Initial measurements revealed inefficient natural ventilation in one project. Post-renovation, IAQ generally improved, but new building materials temporarily increased VOC emissions. Over time, IAQ levels mostly returned to pre-renovation levels, with occupant behavior and new furniture contributing to VOC pollution in some cases.

The study underscores the importance of explicitly integrating airtightness, ventilation, and IAQ considerations into energy-efficient renovations to ensure occupant health and comfort.

## 6 ACKNOWLEDGEMENTS

The authors would like to thank their colleagues Raphaël DEPRez (Cerema), Emilie PALKA (ATMO), Jérôme NICOLLE and Jordan LITAUD (TIPEE) for their valuable contributions to the onsite IAQ and comfort measurements. The authors would like to thank Nouvelle-Aquitaine Regional Council and the French Ministry of Ecological Transition for funding this study. The views and opinions of the authors do not necessarily reflect those of Nouvelle-Aquitaine Regional Council or the Ministry of Ecological Transition. The published material is distributed without warranty of any kind, either expressed or implied. The responsibility for the interpretation and use of the material lies with the reader. The authors should in no way be held responsible for damages resulting from its use. Any liability arising from the use of this report is the responsibility of the user.

## 7 REFERENCES

- ADEME (2016) *PROMEVENT "Improved measurement protocols for ventilation systems."* Cerema, CETIAT, ALLIE'AIR, CETII, PBC, EFFINERGIE, ICEE, PLEIAQ, 2016
- AFNOR (2015) *NF EN ISO 9972 "Thermal performance of buildings - Determination of air permeability of buildings - Fan pressurization method"* AFNOR, 2015
- AFNOR (2016) *FD P50-784 "Thermal performance of buildings - Application guide to NF EN ISO 9972"* AFNOR, 2016
- AFNOR (2019) *NF EN 16798-1 "Energy performance of buildings - Ventilation for buildings - Module M1-6"* AFNOR, 2019
- AFNOR (2003) *NF EN ISO 16017-2 "Indoor air, ambient air and workplace air. Sampling and analysis of volatile organic compounds by adsorption tube / thermal desorption / capillary gas chromatography"* AFNOR, 2003
- AFNOR (2012) *NF ISO 16000-4 "Indoor air. Determination of formaldehyde - Diffusive sampling method"* AFNOR, 2012
- French Government (1982) *Order of March 24, 1982 relating to the ventilation of housing,* <https://www.legifrance.gouv.fr/loda/id/JORFTEXT000000862344/>
- Handtschoewercker E., et al. (2022) *"RENOVAIR: a study of the evolution of airtightness, ventilation, comfort and indoor air quality in energy efficient refurbishment social housing operations in France"* 42nd AIVC Conference Proceedings, Rotterdam 2022 [https://www.aivc.org/sites/default/files/AIVCProceedings\\_015.pdf](https://www.aivc.org/sites/default/files/AIVCProceedings_015.pdf)
- Handtschoewercker E., et al. (2023) *"Rapport Final RENOVAIR"* Cerema Sud-Ouest, 2023
- MTE (2021) *RE2020 "Energy and environmental performance requirements for building constructions in metropolitan France"*, French Government 2021
- MEEDDM (2010) *RT2012 "Thermal characteristics and energy performance of buildings"* French Government 2010
- OQAI (2007) *Observatory on Indoor Air Quality National Survey : IAQ in French Dwellings*, CSTB, AFSSET - 2007

# Experimental study on the dehumidification performance of a window-type liquid desiccant ventilation system

Jabin Goo<sup>1</sup>, Woo Hyoung Lee<sup>2</sup>, Hyo Beom Jung<sup>1</sup>, Dong Hwa Kang<sup>1</sup>,  
Hyun Wook Park<sup>3</sup>, Dong Hee Choi<sup>\*4</sup>

*1 Department of Architectural Engineering,  
University of Seoul  
02504  
Seoul, Republic of Korea*

*2 Institution of Urban Science, University of Seoul  
02504  
Seoul, Republic of Korea*

*3 Kyungpook National University  
41566  
Daegu, Republic of Korea*

*4 Institute of Construction and Environment  
Engineering, Seoul National University  
08826  
Seoul, Republic of Korea*

*\* Corresponding author: mejoy1@snu.ac.kr*

## SUMMARY

This study proposes the feasibility of a window-type liquid desiccant ventilation system for residential buildings. Using a LiCl solution, the system was designed and experimentally evaluated under hot and humid conditions. The results indicated a 19% reduction in relative humidity and effective latent heat removal, showing significant dehumidification performance. The system maintained its dehumidification performance even with reduced humidity, suggesting improved thermal comfort. Future research will focus on optimizing dehumidification strategies under various conditions.

## KEYWORDS

Window-type ventilation, façade system, Liquid desiccant, Dehumidification performance, Experimental study

## 1 INTRODUCTION

As climate change causes the outdoor environment during the summer in Korea to transition into a hot and humid subtropical climate, maintaining a comfortable indoor thermal environment necessitates proper control of indoor temperature and humidity. Generally, the refrigerant dehumidification system used for humidity control has the advantage of easily adjustable dehumidification levels. In contrast, it suffers from energy efficiency drawbacks due to overcooling and reheating processes. In contrast, liquid desiccant systems utilizing liquid desiccants such as LiCl offer potential for energy savings through latent cooling for humidity control. Moreover, the alleviation of latent heat load during summer can reduce the possibility of condensation, thus potentially reducing peak summer loads and increasing thermal comfort time along with the possibility of using radiant cooling. However, existing studies primarily focus on the individual performance analysis of air conditioning systems installed in buildings or standalone dehumidification units, with experimental evaluations of dehumidification effects and applicability in residential spaces being rare. Therefore, this study proposes a window-type liquid desiccant ventilation system module applicable to residential buildings and presents its feasibility through an experiment.

## 2 MATERIALS AND METHOD

The dehumidification performance of a window-type liquid desiccant ventilation system was analysed by designing and fabricating the system module and conducting experiments under hot and humid conditions. Design conditions, such as the type of desiccant and airflow direction, were considered.

### 2.1 System design

The window-type liquid desiccant ventilation system module presented in this study is shown in Fig. 1. The LiCl solution was used, designed to be expelled in a thin film. The incoming air was directed from the bottom to the top of the window-type liquid desiccant ventilation system module, passing through the solution for dehumidification. Additionally, to prevent contamination of the indoor air by LiCl, a HEPA filter was added to the outlet part. The gap between the glasses was designed to be a minimum of 25 mm, to facilitate effective dehumidification.

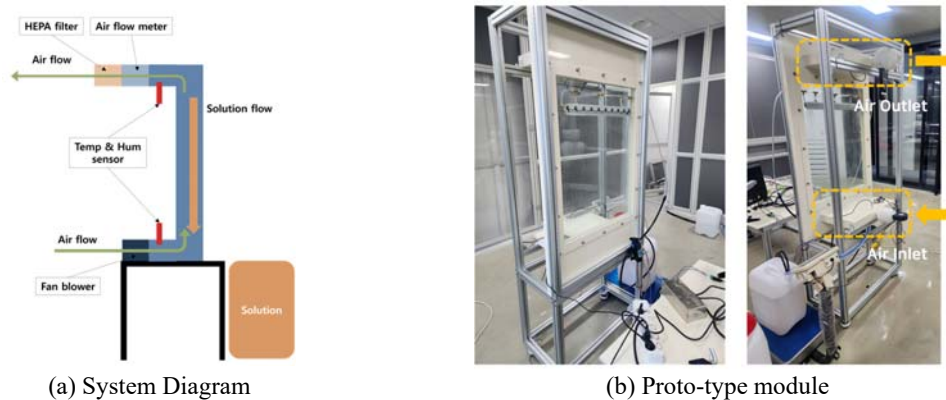


Figure 1: Window-type liquid desiccant ventilation system

### 2.2 Experimental condition

The experiment was conducted in an isolated space of 86.1 m<sup>3</sup> with minimal external influence under the conditions of 25 °C and 60% humidity for one hour. The humidity was consistently maintained by operating an ultrasonic and a mist humidifier throughout the experiment. Data was measured at one-minute intervals. As a result, the maximum wind speed, air volume flow rate, and LiCl flow rate were 2.24 m/s, 55.6 m<sup>3</sup>/h, and 5.5 L/min, respectively. The change in the concentration of the LiCl solution was shown by measuring the weight change.

## 3 RESULTS AND DISCUSSION

The dehumidification performance results of the window-type liquid desiccant ventilation system under hot and humid conditions are shown in Fig. 2. The average relative humidity was calculated as the mean of the relative humidity measured during each condition period. The dehumidification performance was assessed by evaluating the difference in relative humidity between the outlet and the inlet. Before the start of the experiment, in the initial conditions ((a) in Fig. 2, 0-6 min), the uniformity of the inlet and outlet air conditions was confirmed prior to the start of dehumidification. After the start of dehumidification ((b) in Fig. 2, 7-41 min), the humidity dropped rapidly within one minute. The average relative humidity at the inlet and outlet showed a significant dehumidification performance, with a 19% decrease from 62% to

43%. Additionally, the decrease in LiCl concentration from 40% to 38.45% confirmed the effective latent heat removal capability of LiCl. To verify the additional dehumidification effect under low humidity conditions, the humidifier was turned off ((c) in Fig. 2, 42-60 min). Despite the decrease in air relative humidity after stopping the humidifier, the system demonstrated an average relative humidity difference of 8%, indicating dehumidification performance even under low humidity conditions.

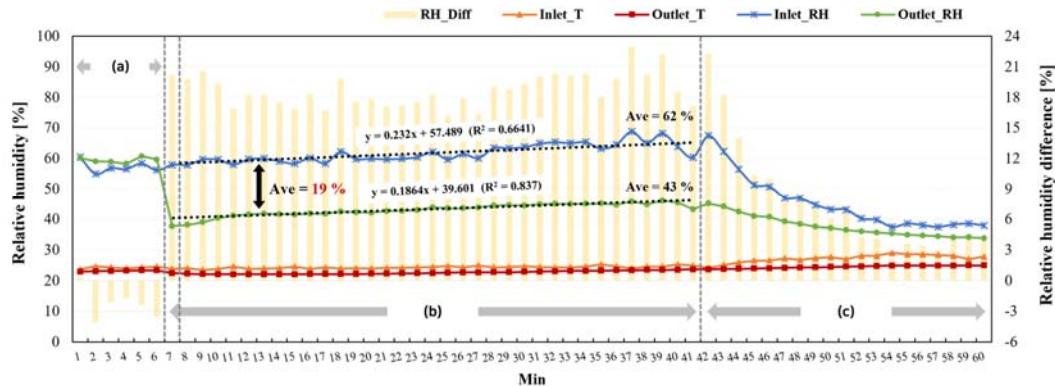


Figure 2: Evaluation results of dehumidification performance:

(a) Initial condition; (b) Dehumidification condition; (c) Humidifier off condition;

## 4 CONCLUSION

To address climate change and ensure comfortable humidity control, this study proposes the feasibility of a window-type liquid desiccant ventilation system for residential buildings. Using a LiCl solution, the system was designed and experimentally evaluated under hot and humid conditions. The results indicated a 19% reduction in relative humidity and effective latent heat removal, showing significant dehumidification performance. The system maintained its dehumidification performance even with reduced humidity, suggesting improved thermal comfort. Future research will aim to evaluate dehumidification capabilities under various experimental and control conditions to propose optimal dehumidification operation strategies.

## 5 ACKNOWLEDGEMENTS

This work was supported by the National Research Foundation of Korea (NRF) grant funded by Korean government (Ministry of Science and ICT) [NRF-2021R1A2C2014552].

## 6 REFERENCES

- Nicol, F. (2004). Adaptive thermal comfort standards in the hot-humid tropics. *Energy and buildings*, 36, 628-637.
- Qi, R., Lu, L., Qin, F. (2014). Model development for the wetted area of falling film liquid desiccant air-conditioning system. *International Journal of Heat and Mass Transfer*, 74, 206-209.
- Li, B., Tan, M., Liu, H., Ma, X., & Zhang, W. (2010). Occupant's perception and preference of thermal environment in free-running buildings in China. *Indoor and Built Environment*, 19, 405-412.
- Lee, W. (2023). Evaluation of dehumidification performance of window-type liquid desiccant ventilation system in residential buildings under different ventilation conditions. *Master's Thesis, University of Seoul*.

# Optimization of airflow rate in a displacement-ventilated room to minimize particle inhalation risk and control energy consumption

Alicia Murga\*<sup>1</sup>, Haruki Nakagawa<sup>\*2</sup>, Rahul Bale<sup>3</sup>, and Makoto Tsubokura<sup>4</sup>

*1 Kobe University  
1-1 Rokkodaicho, Nada Ward, Kobe  
Hyogo, Japan  
\*Corresponding author  
alicia.murga@harbor.kobe-u.ac.jp*

*2 Kobe University  
1-1 Rokkodaicho, Nada Ward, Kobe  
Hyogo, Japan*

*3 Kobe University  
1-1 Rokkodaicho, Nada Ward, Kobe  
Riken Centre for Computational Sciences  
7 Minatojima Minamimachi, Chuo Ward, Kobe  
Hyogo, Japan*

*4 Kobe University  
1-1 Rokkodaicho, Nada Ward, Kobe  
Riken Centre for Computational Sciences  
7 Minatojima Minamimachi, Chuo Ward, Kobe  
Hyogo, Japan  
Presenting author*

## SUMMARY

Indoor inhalation exposure can be minimized through mechanical ventilation. On the other hand, building and mechanical ventilation design remain as the main sources of energy consumption. The present study focuses on the optimization of a displacement-ventilated room by applying computational fluid dynamics, virtual manikins and a genetic algorithm in order to minimize airborne viral density while reducing the energy consumption level.

## KEYWORDS

Mechanical ventilation design; Genetic algorithm; Multi-objective optimization; Computational fluid dynamics

## 1 INTRODUCTION

In the built environment, ventilation systems are essential to maintain air quality but their performance is highly influenced by temperature, wind speed, supply-exhaust vents layout and size and airflow rate. Particles released by human activities greatly contribute to personal inhalation and must therefore be studied in conjunction with these building factors. Computational fluid dynamics (CFD) has been used to predict indoor airflow and distribution of pollutants, especially large eddy simulation, which precisely predicts particle movement (Murga et al., 2022). However, when considering ventilation design and its best outcome, study of multiple CFD-based cases can increase computational burden. This research applies a genetic algorithm to optimize the performance of a displacement system in a room with a speaking virtual manikin in terms of inhalation risk and energy consumption by adjusting the layout and size of the supply-exhaust vents and ventilation airflow rate. The objective was to enhance the built environment by integrating human-building flows and CFD-optimization algorithms.

## 2 METHODOLOGY

### 2.1 Built environment and virtual manikin

The target room had dimensions of  $3 \times 3 \times 3$  meters and the ventilation rate corresponded to the outdoor air requirement of 10 L/s per person. A displacement ventilation system was added,

where the air was supplied at a low height and exhausted at ceiling level, creating a stratified distribution to carry pollutants above occupant-level. Room design as well as supply-exhaust layout is shown in Figure 1 a) and b). A virtual manikin was standing in the middle of the room, constantly talking based on a 1-to-10 enumeration model, scaled 50% to simulate “loud” speaking [3]. Particles were released from its mouth at peak velocities during speech. The flow in the room was validated with previously reported simulation and experimental data of a similarly ventilated room by Yoo and Ito (2022) and Nielsen et al. (2003) (Figure 1 c)).

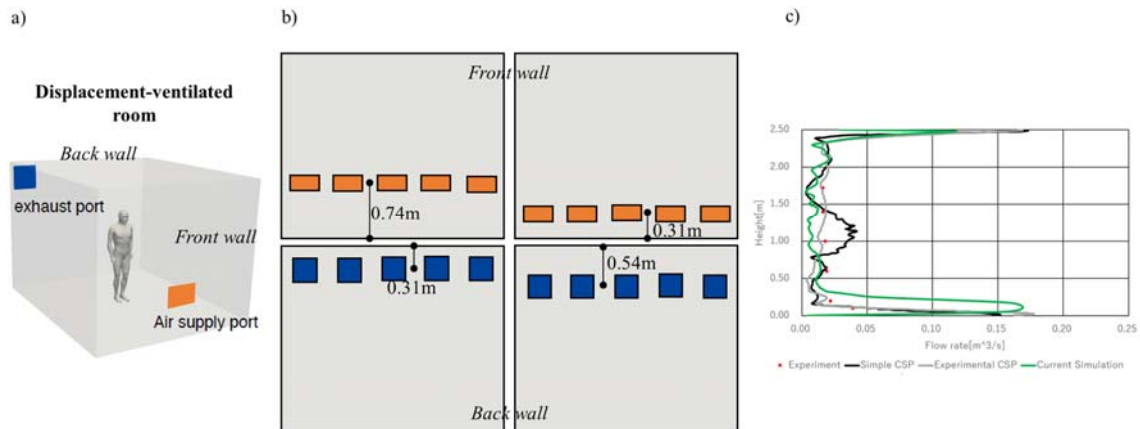


Figure 1: a) Room design, b) Layout of supply-exhaust vents and c) Indoor flow validation

## 2.2 Numerical methods

The current study uses a discrete particle model along with a fully compressible Navier-Stokes solver. The solver uses a Lagrangian-Eulerian method in which the carrier/background fluid equations of motion are resolved in an Eulerian reference frame. Concurrently, the particles are modelled as discrete Lagrangian particles. Governing equations and further details have already been published by Li et al. (2016).

## 2.3 Building optimization

Building parameters considered for optimization were: a) inlet size ( $0.2 \times 0.4$  m<sup>2</sup> or  $0.3 \times 0.5$  m<sup>2</sup>), b) outlet size ( $0.3 \times 0.3$  m<sup>2</sup> or  $0.45 \times 0.45$  m<sup>2</sup>), c) inlet/outlet location (Figure 1 b)) and d) airflow rate (0.01 to 0.06 m<sup>3</sup>/s). The first objective function of the genetic algorithm was the infection risk, measured through the time-averaged viral density in the inhalation zone (between 1.5 and 1.8 m). The second objective function was the energy consumption, measured through a normalized value obtained by dividing the airflow rate used by the minimum airflow rate in this study (0.01 m<sup>3</sup>/s). The Pareto solution was generated by advancing the calculation through six generations and was considered converged when the resulting hypervolume remained unchanged after two consecutive generations.

## 3 RESULTS

The dynamic interactions between indoor airflow and the flow around the human envelope were studied. results in terms of viral density and power are presented in Figure 2 a). Following the Pareto solution, particle number decreased by 50% when the worst case (P1) and the optimized solution that maintains the same power consumption (P2) are compared. On the other hand, power level can be lowered to 1 for energy reduction while slightly lowering virus density (P3) when compared to P1. Particle distribution inside the room for the worst- (P1) and best-case

(P3) scenarios in power level 6 are presented in Figure 2 b). Particles remained at breathing-level when building parameters were not optimized but were successfully removed after optimization. Then, optimization algorithms can be joined to virtual manikins to improve building design and minimize airborne transmission while managing energy consumption.

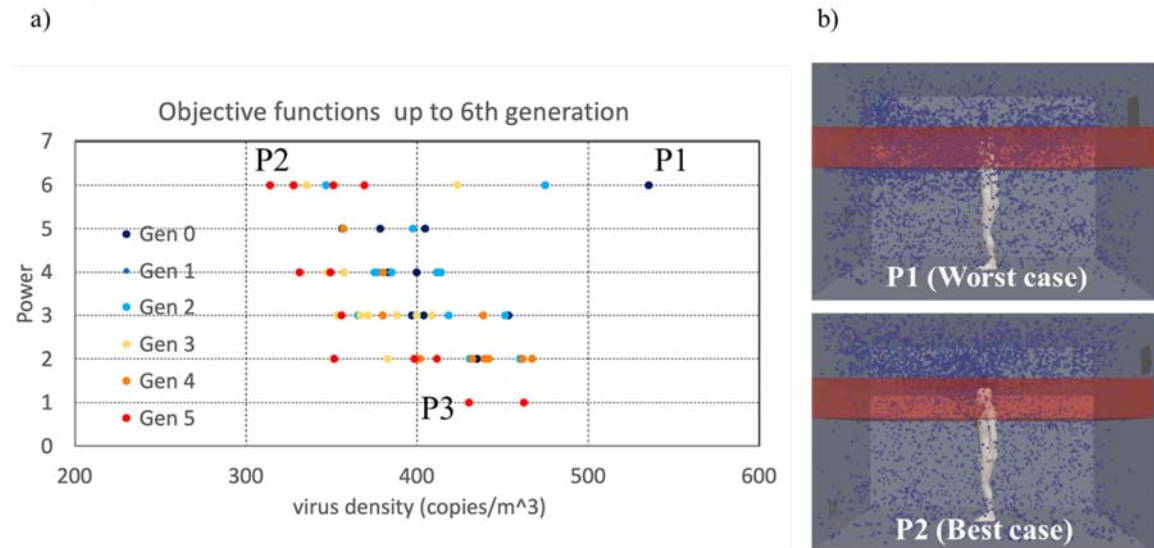


Figure 2: a) Pareto solution and b) Comparison of P1 and P2

## 4 CONCLUSIONS

This research introduced the application of virtual manikins and optimization algorithms to evaluate airborne transmission inside the indoor environment. The main objective of this study was to develop a framework for evaluation and design of a sustainable environment.

## 5 ACKNOWLEDGEMENTS

This work was supported by MEXT as “Program for Promoting Researches on the Supercomputer Fugaku” (JPMXP1020210316) and used computational resources of supercomputer Fugaku provided by the RIKEN Center for Computational Science (Project ID: hp220180, hp230193, hp240205).

## 6 REFERENCES

- Murga, A, Ohashi, S, Li CG, and Tsubokura M. (2022). Transient flow and particle deposition in the respiratory tract: RANS versus LES comparison. *In: Proceedings of Indoor Air 2022, Finland.*
- Yoo, SJ, and Ito K. (2022). Validation, verification, and quality control of computational fluid dynamics analysis for indoor environments using a computer-simulated person with respiratory tract. *Japan Architectural Review*, 5(4), 714-722.
- Nielsen, PV, Murakami, K, Topp, CN, and Yang, JH. (2003). Benchmark tests for a computer simulated person. *Aalborg University, Indoor Environmental Engineering.*
- Li, CG, Tsubokura, M, and Bale, R. (2016). Framework for simulation of natural convection in practical applications. *International Communications in Heat and Mass Transfer*, 75, 52-58.

# Adaptive comfort technology for temperature control in balanced ventilation systems

Bart Cremers

*Zehnder Group Zwolle  
Lingenstraat 2  
8028 PM Zwolle, The Netherlands  
bart.cremers@zehndergroup.com*

## ABSTRACT

Adaptive comfort technology is reflecting the fact that the human body adapts to changing temperatures. As such, the temperature level where people feel comfortable is not a constant value, but changes with the seasonal variations of indoor and outdoor temperatures.

In balanced ventilation systems, the desired indoor temperature can be changed by the occupant of a dwelling, to meet the personal demand on comfort. For balanced ventilation systems without postconditioning this indoor temperature setpoint regulates the use of the bypass, in order to temporarily reduce heat and moisture recovery partially or fully. For balanced ventilation systems with postconditioning, the desired indoor temperature does not only influence the bypass behaviour (passive cooling and heating) but also regulates the postheating and/or the postcooling of the supply air (active cooling and heating).

While occupants can set a fixed indoor temperature, adaptive temperature control is preferable. This method adjusts indoor temperature based on average outdoor temperatures, preventing excessive energy use for space cooling and consequently reducing costs. Moreover, the human body is still object to temperature changes during the year and therefore less sensitive to sudden temperature changes such as in heat waves.

This study describes the basic idea of the implementation of adaptive comfort technology in balanced ventilation units, with and without postconditioning. From monitored projects, examples are given how the indoor temperature setpoint of adaptive temperature control varies in time. Data is given how the bypass and the postconditioning react to changing indoor temperature setpoint. The combination of bypass and postconditioning influences the supply temperature of the fresh air, and ultimately influences the indoor temperature to comfortable levels.

## KEYWORDS

Balanced ventilation, smart ventilation, postconditioning, passive cooling, adaptive comfort technology

## 1 INTRODUCTION

Adaptive comfort is regarded as a way to express the comfort of residents in a building. It reflects the fact that the temperature where people feel comfortable is not fixed during the year, but it changes with the seasonal variation in outdoor temperature.

The adaptive comfort model is mostly used to assess the comfort range of people, given a range of indoor temperatures during the year. Yet, it is rarely used to set temperature setpoints in balanced ventilation systems.

Figure 1 is a simplified graphical representation how the temperature setpoint would vary during the year with a fixed temperature profile and an adaptive temperature profile. In case of the adaptive temperature profile, outside the heating season the temperature setpoint is gradually increased to higher levels when outdoor temperatures rise. During the heating season, however, the temperature setpoint remains constant.



The use of the adaptive temperature profile serves three goals:

1. It avoids discomfort in summer when indoor temperatures remain at winter levels. Indoor temperatures should ideally be no more than 5°C below outdoor levels.
2. Van Marken Lichtenbelt (2022) has indicated that an adaptive temperature profile prevents the body from ‘thermal boredom’ and increases the resistance of residents to heat waves.
3. An adaptive temperature profile reduces unnecessary cooling energy and costs.

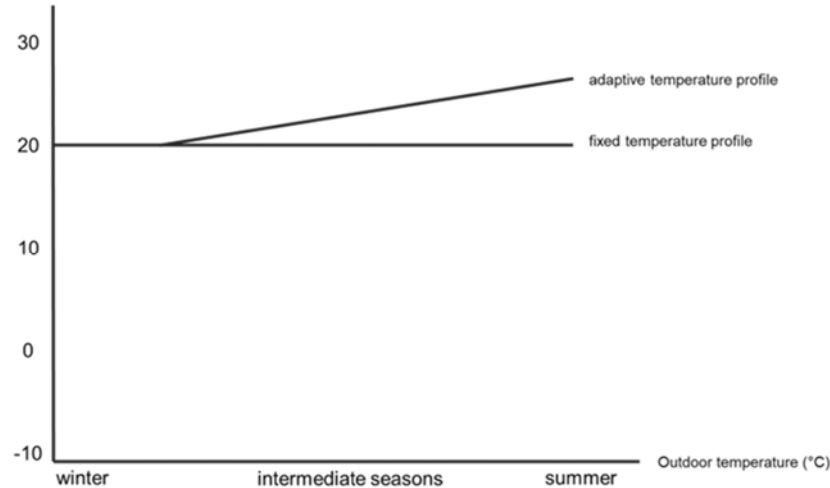


Figure 1: Schematic principle of fixed and adaptive temperature profile.

The theory and monitored results of the use of an adaptive temperature profile is explained in the next two paragraphs. Chapter 2 deals with balanced ventilation systems without postconditioning and chapter 3 describes balanced ventilation systems with postconditioning.

## 2 ADAPTIVE COMFORT TECHNOLOGY IN BALANCED VENTILATION SYSTEMS WITHOUT POSTCONDITIONING

### 2.1 Theory

Balanced ventilation systems bring filtered, fresh air into a building and extract stale air out of the building. The primary function is to refresh the indoor spaces for a healthy living and working environment. The secondary function of balanced ventilation systems is to bring in the fresh air in an energy efficient way and with comfortable supply air temperatures. Therefore, energy is transferred between the outgoing stale air and the incoming fresh air. When energy recovery is not needed, the recovery is temporarily reduced or switched off.

Figure 2 illustrates the basic principle of the control of a balanced ventilation system. The black sloping line is the indication of the indoor temperature setpoint, measured in the unit in the extract air. For warmer outdoor temperature, a warmer indoor (extract) temperature is accepted. A bypass for passive cooling is activated to reduce or switch off recovery when all of the following conditions are true:

1. Extract temperature is above the temperature setpoint (passive cooling is requested),
2. Outdoor temperature is below extract temperature (passive cooling is available),
3. Average outdoor temperature is above a threshold (no active heating in the house),
4. Supply temperature level does not lead to draughts and/or condensation on ducts.

In figure 2, this means that for low outdoor temperature heat recovery is used (supply temperature just below extract temperature). When outdoor temperatures are above a certain threshold, bypass can be activated to bring passive cooling to the house, but only when extract temperatures are higher than the temperature setpoint. When outdoor temperatures are above extract temperature, the bypass is deactivated again allowing cold recovery to supply fresh air while keeping most heat outside.

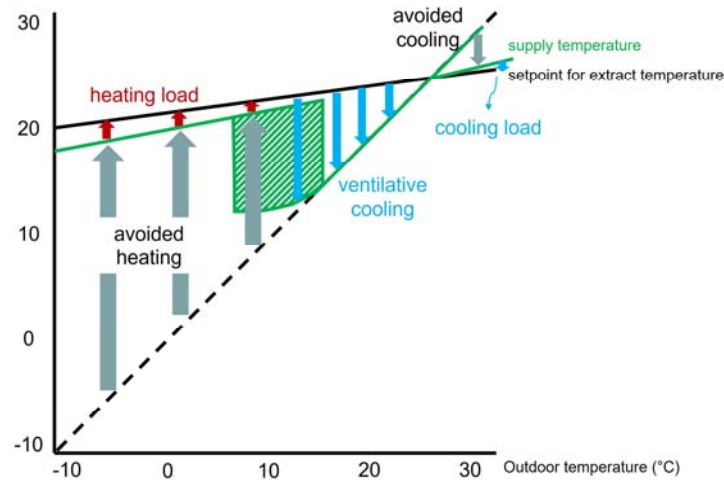


Figure 2: Schematic working principle of balanced ventilation system without postconditioning.

The extract temperature setpoint is the control parameter that decides how often the bypass is activated for passive cooling. For low setpoint, the bypass is activated more frequently than for a higher setpoint. The adaptive temperature control is implemented in balanced ventilation systems as indicated in figure 3. The default temperature profile NORMAL increases the extract temperature setpoint with running mean outdoor temperature. The end user has the possibility to change from the temperature profile NORMAL to temperature profiles COOL or WARM. This shifts the temperature setpoint below and above the default profile respectively. In all three profiles, the temperature setpoint changes with the average outdoor temperature, but the 'cooler' the profile, the more frequently the bypass will be used for passive cooling.

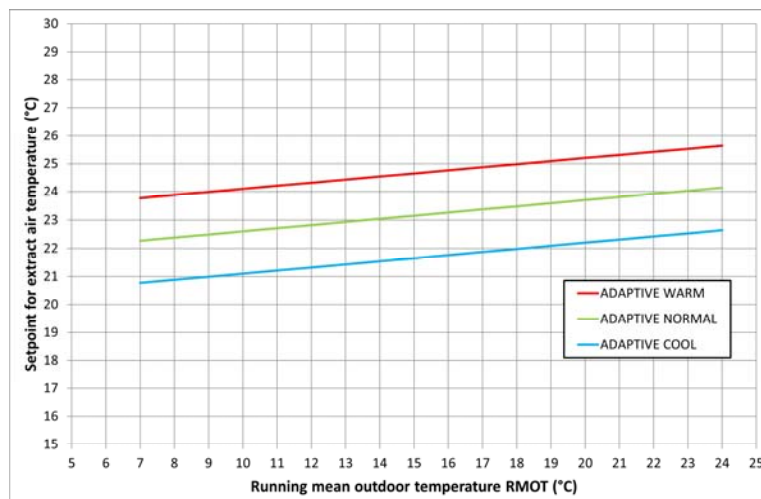


Figure 3: Adaptive temperature control as implemented in balanced ventilation system.

## 2.2 Monitored results

Figure 4 presents the result of the implemented adaptive temperature profile for a balanced ventilation system in a house in Switzerland. The graph shows the measured temperatures (measured in the unit) from January to July 2022. The outdoor temperature (light green) and the running mean outdoor temperature (dark green) are gradually rising from winter to summer. The running mean outdoor temperature rises in this period from 0 °C to 24 °C. The adaptive temperature setpoint (grey) in the normal temperature profile increases therefore in this period from 21.5 °C to 24 °C. The extract temperature (yellow) is also rising in this period from 22.5 °C to 25 °C. The supply temperature of the fresh air (red) shows that in January, February and March the heat recovery is maintaining a comfortable supply temperature which is just below the extract temperature. From April on, the bypass activation is allowed because the heating season has ended. Whenever the extract temperature is above the setpoint, and the outdoor temperature is below the extract temperature, the bypass is activated and the supply temperature will drop to levels close to the outdoor temperature, ensuring passive cooling. Please note that when the outdoor is warmer than the extract, the bypass does not activate, to keep the heat outside of the house.

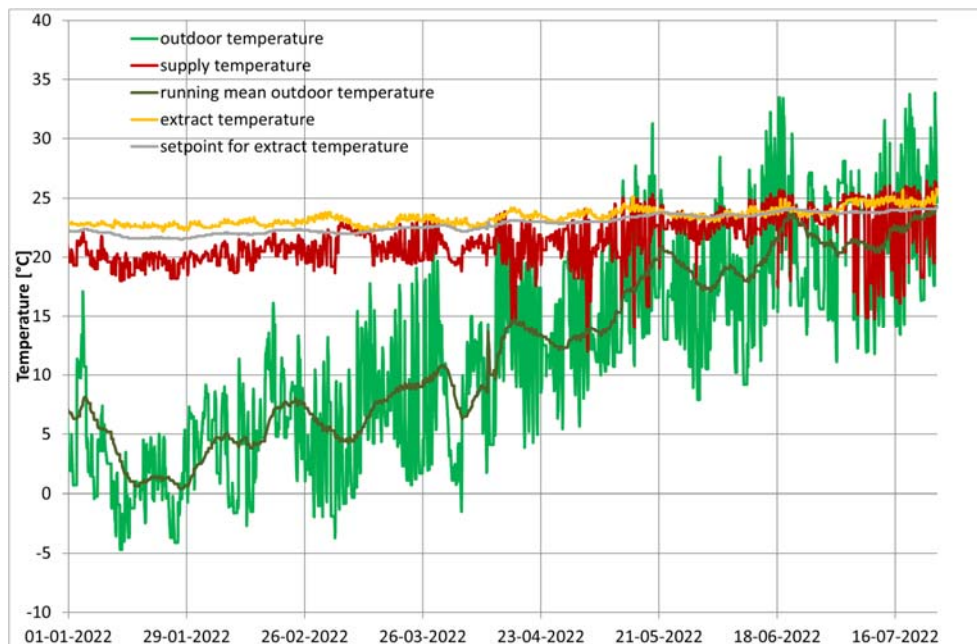


Figure 4: Monitored temperatures for a balanced ventilation system without postconditioning.

The measured extract temperatures rise when outdoor temperatures rise, because of transmission of heat through the construction, and solar gains through windows. For balanced ventilation without postconditioning, the bypass activation gives comfortably cool supply of fresh air, but mostly the amount of passive cooling is not enough to keep the house cool for a longer time.

Figure 5 shows another representation of the measured temperatures in the period January to July. As a function of the outdoor temperature, the extract temperatures (yellow) and the supply temperatures (red) are given for every hour in the relevant period. In this figure, the various modes of balanced ventilation can be observed: heat recovery, passive cooling with bypass and cold recovery. Note that the extract temperatures are slightly elevated in the warmer season with respect to the cooler season.

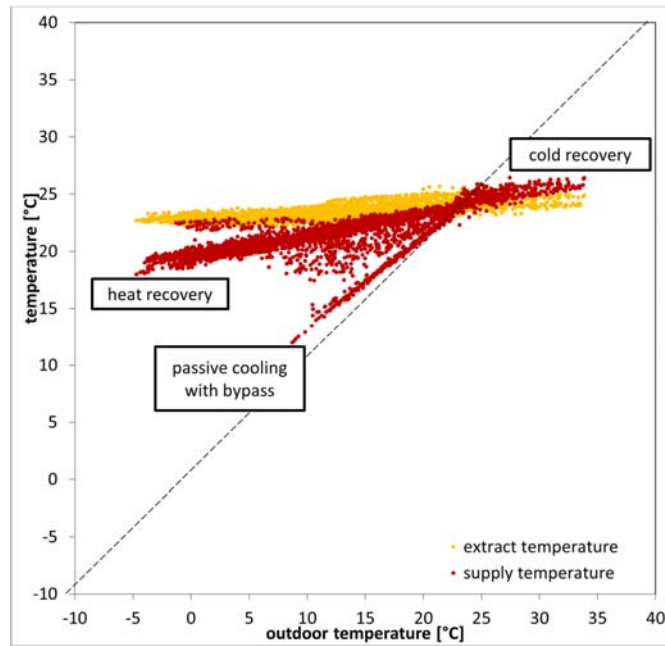


Figure 5: Correlation diagram of extract temperature (yellow) and supply temperature (red) as a function of outdoor air temperature for a balanced ventilation system without postconditioning.

### 3 ADAPTIVE COMFORT TECHNOLOGY IN BALANCED VENTILATION SYSTEMS WITH POSTCONDITIONING

#### 3.1 Theory

For balanced ventilation systems with postconditioning, figure 6 shows the basic principle of control. The ventilation system supplies fresh air in an energy efficient way by first attempting to use heat recovery (saving on central heating system) in the heating season and cold recovery (saving on central cooling system) in the cooling season. In the intermediate season and the cooling season, the fresh air supply is kept comfortably cool by possible activation of the bypass, as explained in the previous chapter.

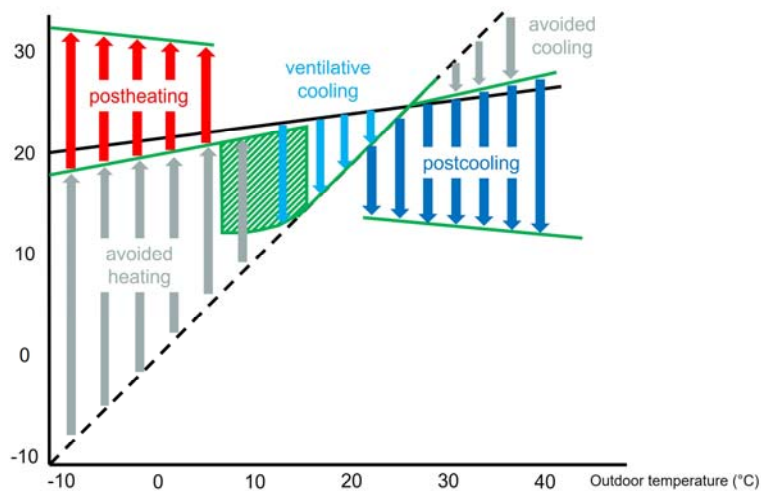


Figure 6: Schematic working principle of balanced ventilation system with postconditioning. Black line: extract temperature setpoint, green line: temperature of supply air.

Postconditioning is used to actively heat the ventilation air (in heating season) and actively cool the ventilation air (in cooling season) with the goal of maintaining a comfortable indoor temperature. The postheating and postcooling produces the energy needed to maintain the indoor temperature. Therefore, balanced ventilation systems with postcondition can really bring the indoor temperature to comfortable levels (as long as the specifications of the unit are sufficient for the thermal loads of the house). This technology is described in more detail by Cremers (2022).

### 3.2 Monitored results

Figure 7 shows the result of the implemented adaptive temperature profile for a balanced ventilation system with postconditioning in a house in Italy. The graph shows the measured temperatures (measured in the unit) from January to July 2022. The outdoor temperature (green) is gradually rising from  $-1^{\circ}\text{C}$  in winter to  $34^{\circ}\text{C}$  in summer. The adaptive temperature setpoint (black) therefore increases in this period from  $22^{\circ}\text{C}$  to  $26^{\circ}\text{C}$ . The extract temperature (yellow) is also rising in this period from  $23^{\circ}\text{C}$  to  $26^{\circ}\text{C}$  (diurnal variation originates from nighttime relaxation of setpoint).

The supply temperature of the fresh air (red) shows that in January, February and March postheating is used for maintaining a comfortable indoor climate. From the end of March, the bypass activation is allowed and it is sufficient to keep the extract temperature close to the adaptive temperature setpoint. From the end of May onwards, the heat transmission and solar gains are higher than the passive cooling with bypass can bring, so that the control switches to postcooling. Even in this period the extract temperature is close to the setpoint indicating that the postcooling output is sufficient in this low energy house.

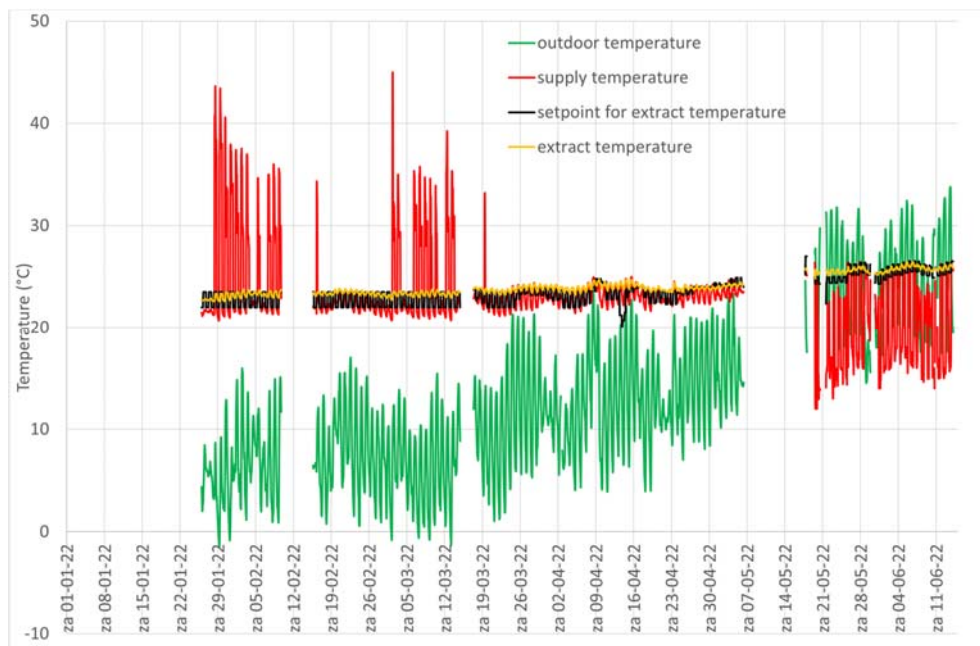


Figure 7: Monitored temperatures for a balanced ventilation system with postconditioning. Gaps in the chart are due to periods during which data transmission had failed.

Figure 8 shows another representation of the measured temperatures in the period January to July. As a function of the outdoor temperature, the extract temperatures (yellow) and the supply temperatures (red) are given for every hour in the relevant period. In this figure, the various modes of balanced ventilation can be observed: heat recovery (sometimes combined with postheating), passive cooling with bypass (sometimes combined with postcooling) and cold recovery (sometimes combined with postcooling).

Note that the extract temperatures are slightly elevated in the warmer season with respect to the cooler season.

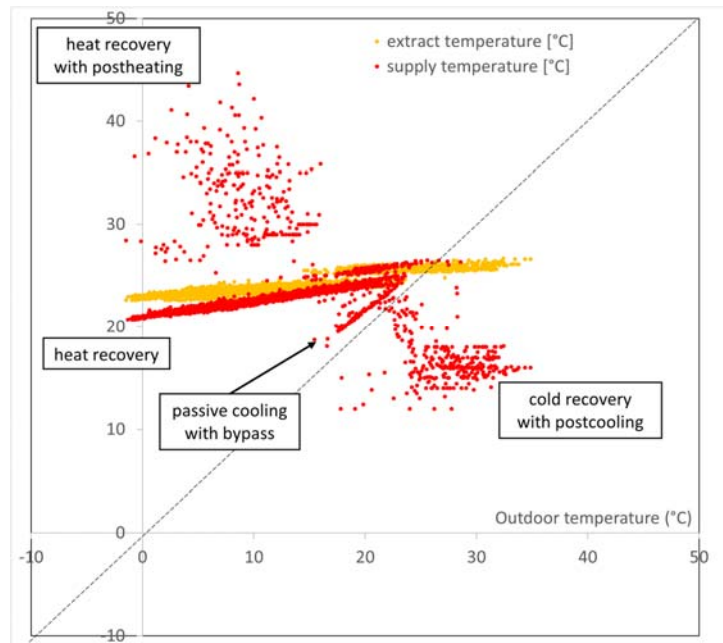


Figure 8: Correlation diagram of extract temperature (yellow) and supply temperature (red) as a function of outdoor air temperature for a balanced ventilation system with postconditioning.

#### 4 DISCUSSION AND CONCLUSIONS

The previous two chapters have shown how adaptive comfort theory can be used to determine the extract temperature setpoint for balanced ventilation systems.

For balanced ventilation systems without postconditioning, the setpoint is a parameter that is used to define whether a bypass will be activated. As the passive cooling with a bypass often cannot be fully sufficient as cooling output for the house (only in nearly zero-energy buildings), the term ‘setpoint’ can be argued. It’s not so much a temperature value that is attempted to be reached by the ventilation system, as there is no heating or cooling produced with a ventilation system, and the bypass activation cannot fulfil the cooling load. Rather than a setpoint it is a switch value for allowance of bypass activation. The term setpoint however, is maintained for similarity with the situation with postconditioning.

Even for a balanced ventilation without postconditioning, the adaptive temperature setpoint results in slightly lower comfort temperatures when outdoor temperatures are in the range of 10-17°C, and slightly higher comfort temperatures when outdoor temperatures are in the range of 17-23°C, when people are adapted to higher temperatures.

The result of adaptive temperature setpoint gets even more pronounced when postconditioning is used. In the algorithms of balanced ventilation systems with postconditioning, the temperature setpoint is kept fixed during the heating season. However, in the intermediate and cooling seasons, the setpoint is adaptive.

In this manner, the temperature setpoint during the warmer season is higher than during the intermediate season with mild outdoor temperatures. The resulting effect is that the comfort for residents is still good, but without too much (unnecessary) effort for the cooling system. Therefore, the cooling output stays within bounds which has benefits for a sustainable environment and for the costs for cooling for the residents. Moreover, the sound impact of the cooling system stays within bounds. In the long run, the variation in indoor temperatures also makes the human body more resistant to the impact of heat waves, as suggested by Van Marken Lichtenbelt (2022).

While the adaptive temperature setpoint generally offers advantages over a fixed setpoint, some occupants may prefer a fixed temperature. Therefore, the adaptive setpoint is the default option, but users can switch to a fixed setpoint if desired.

## 5 REFERENCES

- Cremers, B. E. (2022). The monitored performance of the combination of balanced ventilation with post-conditioning by an air-to-air heat pump. *Proceedings of the 42nd AIVC Conference*. Rotterdam, The Netherlands.
- Van Marken Lichtenbelt, W., Pallubinsky, H., & Kramer, R. (2022). Creating health and resilience by a dynamic indoor climate. *REHVA 14th HVAC World Congress*. Rotterdam, The Netherlands.

# Uncertainty of IAQ and energy performance schemes for residential smart ventilation

Baptiste Poirier<sup>1\*</sup>, Gaelle Guyot<sup>1</sup>, Monika Woloszyn<sup>2</sup>

*1 BPE Research Team—Cerema  
46, rue Saint-Théobald, 38080  
L'Isle d'Abeau, France*

*2 LOCIE UMR 5271  
Université Savoie Mont-Blanc, CNRS, 73376  
Le Bourget-du-Lac, France*

*\*Corresponding author: baptiste.poirier@cerema.fr*

Click or tap here to enter text.

## ABSTRACT

In high-efficient residential buildings, energy use due to ventilation can reach 60% of the total building. Smart-ventilation systems with variable airflows adapting to the need of buildings and occupants can increase the energy performance of the building and at the same time improve or maintain IAQ. They are also considered as a huge opportunity for new and existing residential buildings.

In some countries (like France and Belgium), smart ventilation has been widely used for dozen of years and has become reference strategies. In some other countries, smart ventilation strategies are quite recent or only partially implanted (only in some countries like Belgium, France, The Netherlands, Ireland, Spain...). Their IAQ and energy benefits need to be quantified through performance assessment schemes, still under development, notably in the framework of the IEA-EBC Annex 86. In this article, we propose to quantify the uncertainty of a new recent performance assessment method using RBD-FAST sensitivity analysis. We quantified the variations of impacts of input data such as: the pollutant emissions scenarios - moisture, formaldehyde and particle matter PM<sub>2.5</sub> -, model input parameters and ventilation strategies.

For this sensitivity analysis, five ventilation systems were studied on a French low energy house: 2 with constant airflows, 1 humidity-based exhaust-only smart ventilation and 2 humidity+CO<sub>2</sub> based smart ventilation. The sensitivity indices analysis shows that occupant bio-effluent, formaldehyde and PM<sub>2.5</sub> emissions rates are responsible for 11% to 87% of the uncertainty for the IAQ performance indicators. The PM<sub>2.5</sub> deposition velocity parameter is responsible of 50% of the uncertainty on the PM<sub>2.5</sub> indicator, which was an unknown impact until now and pushes toward more research in order to better characterize this parameter. In addition, the article highlights the energy benefits of this humidity-based ventilation, with heat losses on average 20% lower than those obtained with equivalent constant airflow ventilation. In addition, some smart ventilation strategies offer clear IAQ benefits without significantly increasing energy demand.

## KEYWORDS

Please provide a maximum of five keywords which reflect the content of the paper



## 1 INTRODUCTION

Indoor environments, where people spend 60 to 90% of their time (offices, schools, homes, etc.), generally have a lower indoor air quality (IAQ) than outdoor air. In buildings, once the sources of pollutants have been reduced, ventilation systems can help to dilute pollution by renewing the air and ensuring a good level of IAQ. On the other hand, ventilation systems are also a source of heat loss due to air renewal, representing in some cases a significant percentage of the building's total energy consumption.(30%, or more according to Jardinier et al., 2018). With the advent of smart ventilation systems with variable airflow strategies, there is a need for a robust method to evaluate their IAQ and energy performance. Evaluating ventilation performance is essential to understanding the benefits of these new variable airflow strategies over historical constant airflow strategies.

A recently developed performance-based method provides an initial opportunity to assess IAQ performance for different ventilation systems and strategies, such as exhaust ventilation, balanced ventilation and humidity demand controlled ventilation (Poirier et al., 2021b). This method proposes five IAQ performance indicators (CO<sub>2</sub>, PM<sub>2.5</sub>, HCHO, humidity, health and condensation risk) calculated using the CONTAM airflows model and input scenarios defined for occupant activities, pollutant scenarios, emissions, etc. (Poirier et al., 2021a).

However, the ventilation system performance results obtained may fluctuate depending on the input data used, and these fluctuations must be characterised. Indeed, the choice of input parameters in the building modelling process is a source of uncertainty. In the literature, several studies on building performance assessment have applied sensitivity analysis (SA) methods to test the impact of input data on output data. Such as the following non-exhaustive examples: type of architecture, air leakage, PM<sub>2.5</sub> deposition rate; emission rate; impact of meteorological conditions on PM<sub>2.5</sub> exposure, ventilation rate and heat loss. (Molina et al., 2021); the mass flow rate of domestic hot water, the air renewal rate and the occupancy schedule for the impact on hot water production with solar thermal system. (Burhenne et al., 2022); the position of shading devices controlled by the occupants, the thermal load of electrical equipment, the impact on thermal resistance and thermal stress in low-energy housing.(Gondian et al., 2019).

In this context and based on previous studies (Poirier et al., 2022a, 2022b, 2021a), we have identified several groups of input data likely to influence the proposed ventilation performance evaluation method. The main objective of this paper is to present the results of a study that quantifies the impact of input data variability on output data (performance indicators) by performing a sensitivity analysis.

## 2 METHODOLOGY

According to Tian's detailed review (Tian, 2013) on sensitivity analysis for building energy analysis, several methods exist and some are more relevant for building simulations. To explore the wide input space between pollutant emission scenarios, envelope air leakage, ventilation strategies and modelling assumptions, we have opted for a global method. Several methods exist, such as the mainly used Morris method, which gives a qualitative ranking of the most influential input data on the selected output, or variance-based methods, such as the ANOVA (analysis of variance) approach, which calculates the Sobol first-order sensitivity index, or ANOVA-FAST, which gives the variance of all input data on the output.(Mechri et al., 2010; Tian, 2013).

However a more recent method, EASI RBD-FAST (Goffart et al., 2015; Plischke, 2010) adapted from a combination of random balance design (RBD) (Tarantola et al., 2006) and Fourier amplitude sensitivity (FAST) (Saltelli and Bolado, 1998; Mara, 2009) seemed well

suited to our objectives. Goffart's (Goffart and Woloszyn, 2021) work on sensitivity analysis demonstrated that the RBD-FAST method was more appropriate for building simulation and performance evaluation than the Morris method. The EASI RBD-FAST method can be applied independently of the model and its complexity, and provides more information than the Morris method, such as quantified sensitivity indices and an analysis of the uncertainty in the inputs and outputs. It also has a lower computational cost than conventional variance-based methods and can easily be used to build simulations using SALib, a sensitivity analysis toolkit in Python (Herman and Usher, 2017; Iwanaga et al., 2022).

Based on the key steps for sensitivity analysis in building performance analysis presented in (Tian, 2013), we designed the methodology presented in Figure 1.

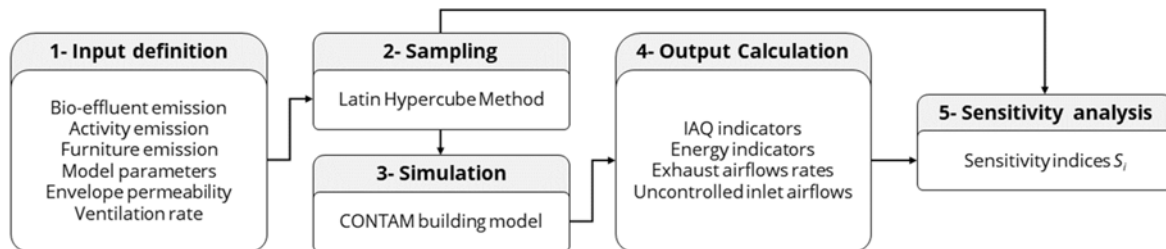


Figure 1: key steps for the sensitivity analysis

## 2.1 Case study

The case study, illustrated in Figure 2, is a low-energy, two-storey house fitted with balanced mechanical ventilation with heat recovery (MVHR) with constant airflows. The total occupied area of the building is 135 m<sup>2</sup>, with a ceiling height of 2.50 m. The house has 4 bedrooms (BR1, BR2, BR3, BR4), one bathroom per floor (BTH1, BTH2) and a kitchen opening onto the living room (LVR/KTC).

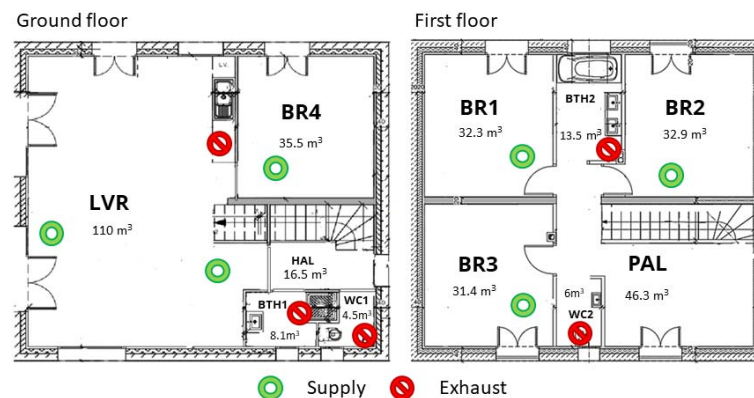


Figure 2 : Plan of the case study house; supply and exhaust location for MVHR; exhaust location only for MEV

According to the ventilation performance assessment method tested, the occupancy of the house was considered to be 5 people. The schedules associated with (Poirier et al., 2021a) for occupancy with the daily time spent by the occupants in the rooms were used, with, for example, 2h10 in the kitchen, 9h20 in the bedroom, and the occupancy state awake 14h40 per day.

Five ventilation systems were implemented in CONTAM model and implemented on French low energy house case study (Poirier et al., 2021b, 2022a) :

**MEV-CAV**, for mechanical exhaust-only ventilation with constant air volume

**MVHR-CAV**, for mechanical balanced ventilation with heat recovery and constant air volume

**MEV-RH**, for mechanical exhaust-only ventilation and humidity control,  
**MVHR-RB**, for mechanical balanced ventilation with heat recovery and CO<sub>2</sub> & humidity control at the room level  
**MEV-RB**, for mechanical exhaust-only ventilation and CO<sub>2</sub> & humidity control at the room as an adaptation of the MVHR-rb,,

## 2.2 Input définition

Based on lessons learnt from previous simulation work to assess ventilation performance (Poirier et al, 2022a, 2022b), twelve inputs were defined by category :

- Occupancy pollutant emissions,

**Bio-eff**, the considered bio-effluents are CO<sub>2</sub> and H<sub>2</sub>O, they are released into the room where the occupant is located. The resulting input is a float variable varying within the range of 0 (for a low emission occupant) to 1 (for a high emission occupant).

- Activity and furniture pollutant emissions

**Acti-H<sub>2</sub>O**, **Acti-PM<sub>2.5</sub>**, **Furn-HCHO** the activity and furniture emissions rates, we include emissions of H<sub>2</sub>O (cooking, shower, laundry, laundry drying), PM<sub>2.5</sub> from the occupants' activity (cooking) and HCHO from furniture and building materials. For H<sub>2</sub>O, the emissions rates of all activities are assumed to be correlated and to vary from -30% to + 30% of the reference scenario. Consequently, the resulting input for the H<sub>2</sub>O activity is a float variable, varying in the range 0.70 (for -30%) to 1.30 (for +30%). For the PM<sub>2.5</sub> activity the float variable named varying in the range 1.26 to 2.55 and referring to the PM<sub>2.5</sub> emission rate due to cooking activities (Poirier et al., 2022a, 2021a). For HCHO, the emission rates per m<sup>2</sup> of floor area will vary from the lowest scenario of 4.5 µg.h<sup>-1</sup>.m<sup>2</sup> to the highest scenario 23.6 µg.h<sup>-1</sup>.m<sup>2</sup>). Again, a float variable is introduced, and varies in the range 4.5 to 23.6, referring to the furniture emission rate.

- CONTAM model parameters

**Mbuff**, materials in buildings may influence the humidity in air depending on the composition of walls, furniture, floor, etc. This is because materials can absorb and release moisture over time that corresponds to the hygroscopic buffer effect. Here the hygroscopic buffer effect is described with the boundary layer diffusion model in CONTAM as a source/sink element. Two inputs are used: Mbuff-L (for Model buffer in Low adsorbing rooms) and Mbuff-H (for Model buffer in High adsorbing rooms), float variables varying respectively from 0 to 0.25 and 0.75 to 1.

**MPM<sub>2.5</sub>-vd**, **MP<sub>2.5</sub>-r** the CONTAM model parameters for deposition velocity and the resuspension rate. We have selected two MPM<sub>2.5</sub> inputs for the sensitivity analysis: the deposition velocity model MPM<sub>2.5</sub>-vd in the low and high range based on min (0.3 m.h<sup>-1</sup>) and max (1.8 m.h<sup>-1</sup>) values measured in houses with furniture in (Fogh et al., 1997; Thatcher and Layton, 1995), and the resuspension model MPM<sub>2.5</sub>-r varying within min (4.4 .10<sup>-7</sup> h<sup>-1</sup>) and max (1.8 .10<sup>-5</sup> h<sup>-1</sup>) values measured in (Thatcher and Layton, 1995). For both MPM<sub>2.5</sub> inputs we propose to use the median as the reference value.

**Perm**, the air leakage level through the envelope, we therefore propose an input varying in the range [0.05; 0.9] corresponding to the q<sub>4a</sub> airleakage level. According to data measured over 126,840 single family houses in France (116,847 with exhaust ventilation, 6,736 with balanced ventilation) the median q<sub>4a</sub> is around 0.4 h<sup>-1</sup> varying within the range 0.05 h<sup>-1</sup> to 0.9 h<sup>-1</sup> for extreme data (excluding outliers ±2.7 times the standard) (Mélois et al., 2019).

- Ventilation systems and strategies

**Q-exh, Q-max** two inputs varying in range [0.7; 1.3] focused on the exhaust airflows that could be adapted to the five ventilation systems modelled. The first one, Q-exh, is a constant multiplier coefficient to modify the total exhaust airflow and is applied to all exhaust paths in the CONTAM model (kitchen, bathrooms, toilet). The second input, Q-max, is a constant multiplier coefficient applied only to the maximum airflow Max/Qboost control value. For MVHR systems the supply airflows were adjusted to correspond to the Q-exh or Q-max edited exhaust airflows, in order to keep the balance between exhaust and supply.

### 2.3 Output calculation

To evaluate the most important inputs and the uncertainty of the ventilation performance assessment methods the first selected outputs were five IAQ performance indicators ( $I_{CO_2}$ ,  $I_{HCHO}$ ,  $I_{PM_{2.5}}$ ,  $I_{RH_{70}}$ ,  $I_{RH_{30-70}}$ ) of the method (Poirier et al., 2021b). These five indicators were then extended with two additional IAQ indicators for formaldehyde and PM<sub>2.5</sub> short-term exposure risks ( $I_{HCHO-s}$ ,  $I_{PM_{2.5-s}}$ ) and one energy indicator evaluating the thermal heat loss from supply airflows and uncontrolled infiltration ( $I_{E_{wh}}$ ) calculated with equation 1

$$I_{E_{wh}} = H_{th} = \frac{C_{pm}}{3600} \cdot (1 - \varepsilon_{heat_{ex}}) \int q_m(t) \cdot [T_{in}(t) - T_{ex}(t)] \cdot dt \quad (1)$$

with  $I_{E_{wh}}$  the energy indicator resulting directly from  $H_{th}$ , the heat losses from exhausted air [kWh],  $q_m$  the total exhaust mass airflows in [ $kg \cdot s^{-1}$ ],  $C_{pm}$  the heat capacity of air (we used  $1 \text{ kJ} \cdot \text{kg}^{-1} \cdot ^\circ\text{C}^{-1}$ ),  $\varepsilon_{heat_{ex}}$  the heat exchanger efficiency assumed to be ideal and constant. A constant theoretical efficiency of 0.8 can, for example, be used for MVHR and 0 with no heat recovery.  $T_{in}$  is the zone temperature where the air is exhausted, and  $T_{ex}$  the external temperature [ $^\circ\text{C}$ ].

In addition, a variant of  $I_{CO_2}$  was tested, with a variable exposure threshold based on a complementary input  $T_{CO_2}$ . This variant was referenced as  $I_{nCO_2-v}$  the maximum cumulative CO<sub>2</sub> exposure over  $T_{CO_2}$  ppm in the bedrooms, with  $T_{CO_2}$  included in the sampled variable input varying in the range [800; 1200].

All these IAQ and energy indicators are proposed with an associated acceptable threshold (AT) representing a reference limit of acceptable performance not to be exceeded. For results analysis the indicators were normalised by their AT and referenced with the notation [In -].

### 2.4 Summary of Inputs and Outputs

The selected 12 inputs and 9 outputs for the sensitivity analysis are summarised in Table 1-2, with their associated range of variation. The reference column, gathers reference or average values for all inputs.

Inputs	Description	Low	Reference	High
Bio-eff	occupant CO <sub>2</sub> and H <sub>2</sub> O emissions	0	0.333	1
Acti-H <sub>2</sub> O	moisture emissions from activities	0.7	1	1.3
Acti-PM <sub>2.5</sub>	emissions from cooking activities	1.26	1.91	2.55
Furn-	HCHO formaldehyde emissions from furniture	4.5	12	23.6
Mbuff-L	buffer effect for low adsorbing room	0	0	0.25
Mbuff-H	buffer effect for high adsorbing room	0.75	1	1
MPM <sub>2.5-vd</sub>	Deposition velocity	0,3	0,65	1,8
MPM <sub>2.5-r</sub>	Resuspension rate	$4.4 \cdot 10^{-7}$	$9.90 \cdot 10^{-7}$	$1.8 \cdot 10^{-5}$
Perm	Airleakage level based on a q4a	0.05	0.4	0.9
Q-exh	Total exhaust airflow multiplier	0.7	1	1.3
Q-max	Maximum airflow M/Qboost multiplier	0.7	1	1.3
TCO <sub>2</sub>	Variable CO <sub>2</sub> exposure AT for $I_{nCO_2-v}$ calculation	800	1000	1200

Table 1 : Summary of the proposed inputs for the sensitivity analysis

Outputs	Description	AT
I <sub>nCO2</sub>	Maximum cumulative CO <sub>2</sub> exposure over 1000 ppm	1000 .d (ppm.h)
I <sub>nCO2-v</sub>	Maximum cumulative CO <sub>2</sub> exposure over T <sub>CO2</sub> ppm	T <sub>CO2</sub> d (ppm.h)
I <sub>nHCHO</sub>	Maximum cumulative HCHO exposure among all the occupants	9.d (µg.m <sup>-3</sup> .h)
I <sub>nHCHO-s</sub>	Maximum occupant HCHO exposure over a one-hour average period	100 µg.m <sup>-3</sup>
I <sub>nPM25</sub>	Maximum cumulative PM <sub>2.5</sub> exposure among all the occupants	10.d (µg.m <sup>-3</sup> .h)
I <sub>nPM25-s</sub>	Maximum occupant PM <sub>2.5</sub> exposure over a 24-hour average period	25 µg.m <sup>-3</sup>
I <sub>nRH70</sub>	Maximum percentage of time with RH > 70% among all the rooms	18%; 10.8%;1.8%
I <sub>nRH30_70</sub>	Maximum percentage of occupant time spent with RH outside the range [30-70%]	14.4%
I <sub>Ewh</sub>	Heat losses from total exhaust airflows	-
Q-exh	Total exhaust airflow multiplier	0.7
Q-max	Maximum airflow M/Qboost multiplier	0.7
T <sub>CO2</sub>	Variable CO <sub>2</sub> exposure AT for I <sub>nCO2-v</sub> calculation	800

Table 2 : Summary of the proposed outputs for the sensitivity analysis

## 2.5 Simulation process :

The simulations were performed with CONTAM, a multi-zone modeling software developed by the National Institute of Standards and Technology (NIST). It is used in a wide range of applications, such as IAQ analysis, ventilation flow management and smoke propagation, and has been extensively validated (Walton and Emmerich, 1994). The whole process was then automated with Python scripts for sampling, running the simulations and output data saving. The inputs were sampled before the simulations using Latin Hypercube Sampling methods (Helton and Davis, 2003) following the sampling method recommended in the EASI RBD-FAST sensitivity analysis method (Goffart et al., 2015; Goffart and Woloszyn, 2021). This sampling was carried out with a Python function implemented in the SALib library.

The simulation included 500 simulations per ventilation system, for a total of 2,500 simulations carried out over the heating period from October 15, 00:00, to April 14, 12:00, i.e. 4466 hours, with time steps of 10 min depending on the heating period. Using CONTAM, which has reasonable computational costs, the simulation time was around 36h for the 2500 simulations, calculated with an Intel Core i5-7200U CPU @ 2.50GHz, 2712MHz, 2 cores and 8 GB RAM

In the EASI RBD-FAST method used, the sensitivity indices (**Error! Reference source not found.**) were the first-order indices from the popular Sobol method based on the variance decomposition of the model's output (Tarantola et al., 2006; Plischke, 2010; Tissot and Prieur, 2012; Goffart et al., 2015).

$$S_i = \frac{V[E[Y|X_i]]}{V[Y]} \quad (2)$$

with  $X_i$  the input random variable sampled with the LHS method for  $i = (1, \dots, k)$  the number of inputs;  $Y = f(X_1, \dots, X_k)$  output of the model;  $S_i$  the first-order sensitivity indices of input  $i$ ;  $E[Y|X_i]$  the conditional expectation of  $Y$  given  $X_i$ , and  $V[-]$  the variance of a random variable (Plischke, 2010).

The indices are between 0 and 1 and are the measure of sensitivity computed by the EASI RBD-FAST method. A high index indicates a strong relationship between the variation of  $X_i$  and the variation of the output  $Y$ . The total sum of  $S_i$  should be close to 1 and if it is significantly less than 1, this implies interactions between parameters (Goffart and Woloszyn, 2021). Finally, the  $S_i$  indices were calculated for all the tested outputs, to identify which outputs present the greatest uncertainty regarding the inputs variations.

### 3 RESULTS

#### 3.1 IAQ and Energy performance

Figure 3 with normalized indicators shows in the form of boxplots all the performance indicators calculated on the 500 simulations per strategy. In an overall analysis, the differences between strategies regarding IAQ performance appear relatively small and dependent on the pollutant. While the energy benefits present significant differences.

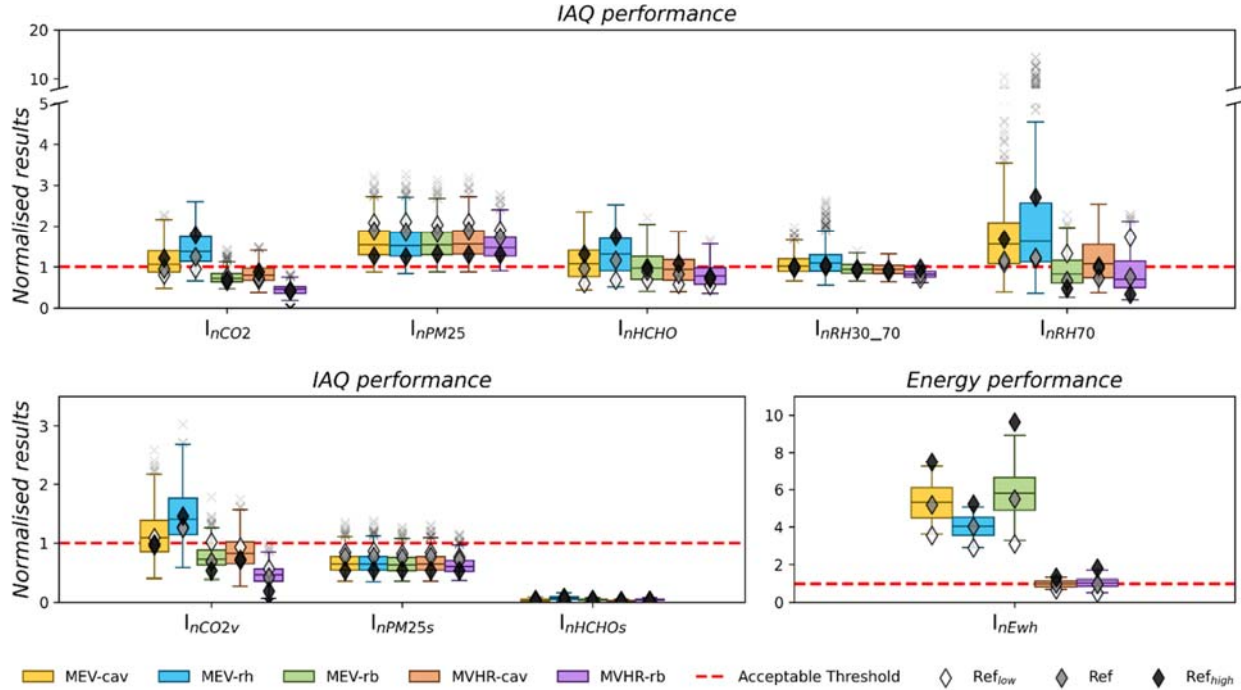


Figure 3 : Boxplot of normalized indicator performance results over the 500 simulations for the 5 ventilation strategies

The  $I_{nCO_2}$  indicator confirms the good performance of MEV-rb, MVHR-rb and MVHR-cav, while  $I_{nCO_2}$  remains mainly below the acceptable threshold. For MEV-cav and MEV-rh, the situation is different: in some simulations (e.g. for some inputs), the value of the indicator is lower than the threshold while in other cases it is higher. This position around the acceptable threshold depending on the input values is also observed for  $I_{nHCHO}$ ,  $I_{nRH30_70}$ ,  $I_{nRH70}$ . For  $PM_{2.5}$  performance, no strategy reaches the acceptable thresholds except in certain aberrant configurations. The outliers also show that the combination of specific inputs could generate a factor of 3 between the lowest and highest values in most cases. In some cases, this could even generate huge differences in performance ratings, up to 14 times the acceptable threshold for MEV-rh on the  $I_{nRH70}$ .

The additional QAI outputs for short-term exposures  $I_{nHCHO-s}$  and  $I_{nPM25-s}$ , for this case study and with the tested inputs, provide almost the same information as their long-term counterpart. For the short-term  $PM_{2.5}$  risk, with the exception of a few outliers, the q1, q3 and median values are below the acceptable thresholds; the chosen duration of the 24-hour average period for short-term exposure may not be appropriate to capture the maximum exposure risk. Using a variable threshold between 800 and 1200 ppm for calculating  $CO_2$  exposure  $I_{nCO_2-v}$  also gives the same information as  $I_{nCO_2}$ , with 1000 ppm. This means that in this configuration, a lower (or upper) limit of  $CO_2$  exposure does not significantly increase (nor reduce) the assessed exposure of occupants.

Finally, to normalize the energy indicator  $I_{Ewh}$  we decided to use the MVHR-cav strategy as a comparison reference and used the median performance result obtained over the 500 simulations, with the median  $I_{Ewh}$  of the MVHR-cav equal to 543 kWh (4.02 kWh.m<sup>-2</sup>). This normalization therefore shows that the energy requirements resulting from heat losses are for the 3 MEV strategies (MEV-cav, MEV-rh, MEV-rb) between 3 times and 10 times higher in comparison to the heat losses of the MVHR-cav strategy. But the comparison between MEV and MVHR is not particularly relevant: most of the energy savings come from the theoretical heat recovery efficiency of 0.8. However, this still highlights the fact that MEV-rh had lower energy losses than MEV-cav and MEV-rb, for IAQ performance equivalent to MEV-cav as noted above, but without the CO2 benefit provided by the MEV-rb. Finally, MVHR-rb, in some configurations, could be lower or higher than MVHR-cav, but had overall equivalent energy performance, with an additional advantage on all IAQ indicators compared to MVHR-cav and other MEV strategies.

### 3.2 Sensitivity Analysis

In this sensitivity analysis a total of 540 sensitivity indices (108 per ventilation strategy) were calculated across the 12 input variables and the 9 output indicators. Faced with the challenge of displaying the information from so many  $S_i$ , we built what we called a "flower graph" which groups all these 540 indices by ventilation strategy in Figure 3.

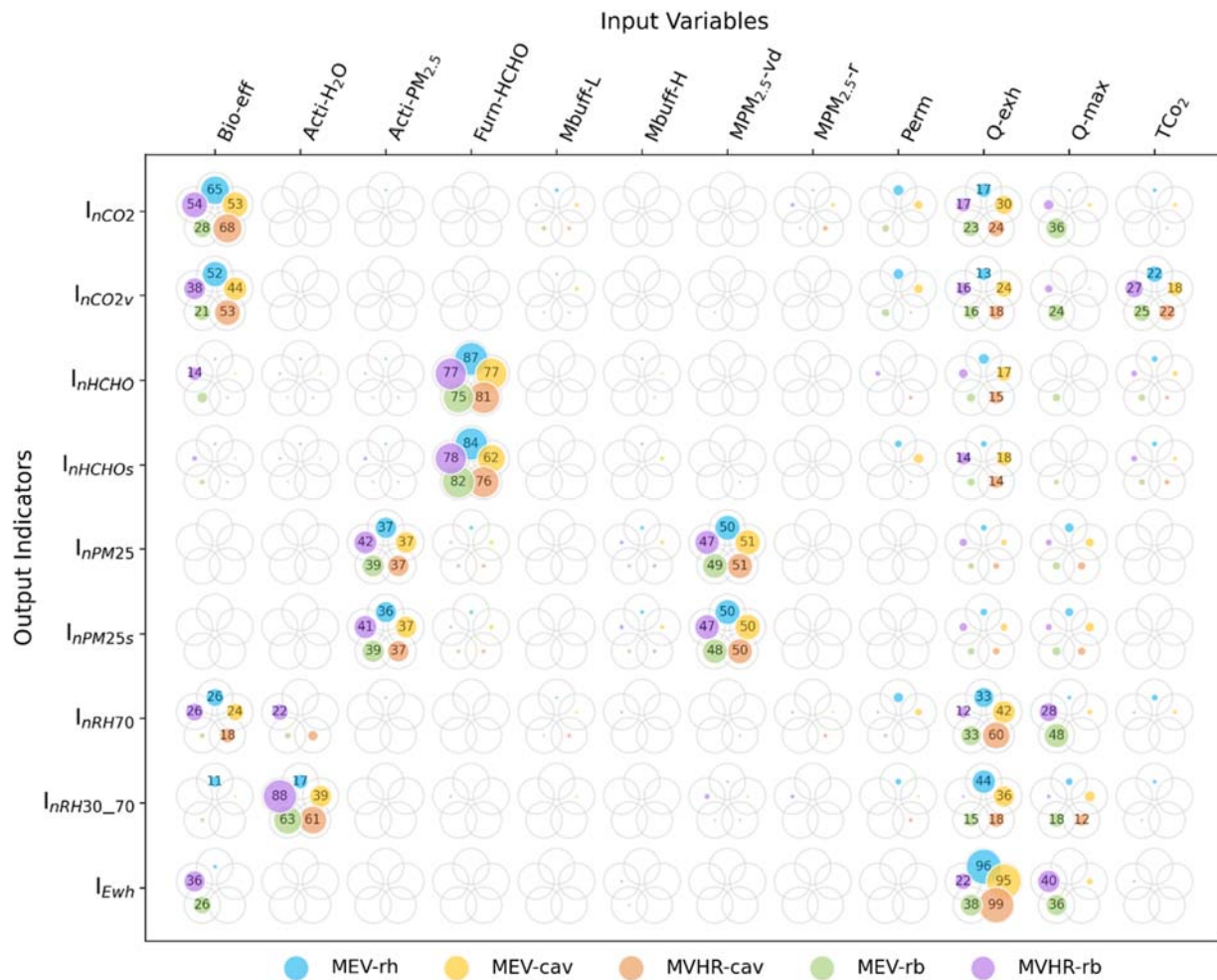


Figure 3 : Display of the sensitivity indices calculated for the 5 ventilation strategies

On this graph each row represents the output indicator and each column the input variable. Each of the 108 "flowers" has 5 circles, one for each ventilation strategy. The grey circle represents the maximum possible  $S_i$ , with a coloured circle sized proportionally to its real value. Each colour representing one system. In addition, the percentage value ( $S_i\%$ ) is added if the indices start to be significant ( $S_i > 0.1$ ) and the indices are not represented if  $S_i < 0.05$ . In other words, an empty flower means that for all ventilation systems the impact of the corresponding input variability on the output variability is insignificant, while coloured petals indicate important impact.

At first sight, the Mbuff-L, Mbuff-M, MPM<sub>2.5-r</sub> and Perm input variables present little or no influence on the outputs for all the strategies (empty flowers on corresponding columns). Acti-H<sub>2</sub>O, Acti-PM<sub>2.5</sub>, Furn-HCHO, MPM<sub>2.5-vd</sub> and TCO<sub>2</sub> influence one or two outputs, related to the pollutant associated with the specific input. The last inputs Bio-eff, Q-exh has a spread influence on several outputs. In the detailed of the sensitivity indices  $S_i$  values,  $I_{nCO_2}$  and  $I_{nCO_2v}$  are impacted mainly by the Bio-eff inputs; from 0.28 to 0.68 for  $I_{nCO_2}$  and from 0.21 to 0.53 for  $I_{nCO_2v}$  depending on the strategy. Additionally,  $I_{nCO_2}$  is also impacted by Q-exh with sensitivity indices from 0.17 to 0.3 depending on the strategy.  $I_{nCO_2v}$  is the only output influenced by TCO<sub>2</sub> with sensitivity indices between 0.18 - 0.27 depending on the strategy, but Bio-eff is still the most influential on the  $I_{nCO_2}$  indicator. This confirms that in our case the use of variable thresholds for CO<sub>2</sub> exposure is not necessarily useful and does not provide any additional information.

Regardless the ventilation strategy, the formaldehyde indicator  $I_{nHCHO}$  is not surprisingly influenced by Furn-HCHO as it is the only formaldehyde source input. The same could be true for Bio-eff impact on the CO<sub>2</sub> indicator, as Bio-eff is the only input varying the CO<sub>2</sub> emission source from the occupants. More unexpectedly, Bio-eff has also some impact on formaldehyde indicator  $I_{nHCHO}$  ( $S_i=0.14$ ), and this for MVHR-rb system only. This can be explained by the ventilation control strategy for MVHR-rb based on CO<sub>2</sub> which is related to the occupant but also impacts formaldehyde concentrations. For constant ventilation airflows (cav) the Q-exh value also has some influence on  $I_{nHCHO}$ , which can be explained by varying airflow rates. For the PM<sub>2.5</sub> indicators the 5 systems are almost equally impacted by the particle emission rates (Acti-PM<sub>2.5</sub>,  $S_i$  in [0.47-0.51]) and the deposition velocity (MPM<sub>2.5-vd</sub>,  $S_i$  in [0.37-0.42]) but not by the resuspension rate (MPM<sub>2.5-r</sub>,  $S_i < 0.05$ ). This result highlights the need to focus on the deposition velocity for the PM<sub>2.5</sub> model, as implemented in CONTAM, as its impact on the  $I_{nPM25}$  indicator is even higher than the impact of emission rates (sensitivity indices of 47 to 51 % for deposition velocity and 37 to 42% for emission rates). Regarding humidity-based indicators,  $I_{nRH70}$  is more impacted by occupants' emissions (Bio-eff), while  $I_{nRH30_70}$  is more impacted by activities emissions (Acti-H<sub>2</sub>O). This result is quite unexpected; indeed, moisture emissions from activities were expected to impact  $I_{nRH70}$ . Moisture emissions from activities are more intense and intermittent and, as peak emissions, should have an impact on high humidity levels (RH > 70%). But this has not been observed in the sensitivity results. In addition,  $I_{nRH70}$ , is strongly impacted by the exhaust airflows Q-exh and Q-max.

Lastly, for the heat loss indicator  $I_{nEwh}$ , its variability is influenced by Q-exh for MEV-cav, MEV-rh and MVHR-cav. While for the systems with the most complex control strategy (MEV-rb and MVHR-rb),  $I_{nEwh}$  are almost equally impacted by the Bio-eff, Q-exh and Q-max. The presence of Bio-eff for rb strategies could again be explained by the CO<sub>2</sub> control for the room-based systems. Surprisingly, inputs related to moisture sources (Bio-eff and Acti-H<sub>2</sub>O) have no impact on the energy performance for humidity-based control systems (MEV-rh and MVHR-rh).



## 4 CONCLUSION

These results allow the performance of IAQ and energy ventilation to be assessed over a wide range of tested scenarios, instead of the more usual reduced set of minimum, average and maximum scenarios.

The results of the sensitivity analysis showed that some identified inputs in CONTAM model could be set to default values, such as those used for humidity buffering and PM<sub>2.5</sub> resuspension. On the contrary, attention should be paid on the notable influence of inputs concerning bioeffluent emissions, PM<sub>2.5</sub> from cooking activity, humidity from activities, formaldehyde from furniture and construction materials and the speed of deposition of PM<sub>2.5</sub>, on the performance indicators. This confirms the need for further research to obtain robust input parameters and precise knowledge of pollutant emission scenarios.

To extend this sensitivity analysis, further simulations could focus on more detailed scenarios. For example, bioeffluent emission rates could vary independently for each occupant or different 'family types' could be tested. For PM<sub>2.5</sub> activity, the cooking emission scenario can be modified by differentiating the days or types of meals prepared throughout the week, in order to test 'cooking habits' and/or by adding PM<sub>2.5</sub> sources in other rooms. Moisture-generating activities can also be modified independently to achieve greater accuracy and identify specific actions that have an impact on relative humidity.

Finally, by including these lessons on uncertainty, the evaluated performance of the ventilation system could be more robust because the impact of the inputs on the performance indicator is better controlled. This paves the way for the use of IAQ and energy performance indicators in multiple building simulations to test and compare design parameters in a decision-making process and for the inclusion of these performance-based methods in new standards and regulations in Europe and beyond.

## 5 REFERENCES

- Burhenne, S., Jacob, D., Henze, G., 2022. UNCERTAINTY ANALYSIS IN BUILDING SIMULATION WITH MONTE CARLO TECHNIQUES.
- Fogh, C.L., Byrne, M.A., Roed, J., Goddard, A.J.H., 1997. Size specific indoor aerosol deposition measurements and derived I/O concentrations ratios. *Atmospheric Environment* 31, 2193–2203. [https://doi.org/10.1016/S1352-2310\(97\)00037-X](https://doi.org/10.1016/S1352-2310(97)00037-X)
- Goffart, J., Rabouille, M., Mendes, N., 2015. Uncertainty and sensitivity analysis applied to hygrothermal simulation of a brick building in a hot and humid climate. *Journal of Building Performance Simulation* 10, 1–21. <https://doi.org/10.1080/19401493.2015.1112430>
- Goffart, J., Woloszyn, M., 2021. EASI RBD-FAST: An efficient method of global sensitivity analysis for present and future challenges in building performance simulation. *Journal of Building Engineering* 43, 103129. <https://doi.org/10.1016/j.jobe.2021.103129>
- Gondian, L., Goffart, J., Woloszyn, M., Wurtz, E., Catherine, B., Maréchal, P., 2019. Towards Assessing Houses Robustness Against Thermal Stresses Using Temporal Sensitivity Analysis. <https://doi.org/10.26868/25222708.2019.210422>
- Helton, J.C., Davis, F.J., 2003. Latin hypercube sampling and the propagation of uncertainty in analyses of complex systems. *Reliability Engineering & System Safety* 81, 23–69. [https://doi.org/10.1016/S0951-8320\(03\)00058-9](https://doi.org/10.1016/S0951-8320(03)00058-9)
- Herman, J., Usher, W., 2017. SALib: An open-source Python library for Sensitivity Analysis. *The Journal of Open Source Software* 2. <https://doi.org/10.21105/joss.00097>
- Iwanaga, T., Usher, W., Herman, J., 2022. Toward SALib 2.0: Advancing the accessibility and interpretability of global sensitivity analyses. *Socio-Environmental Systems Modelling* 4, 18155–18155. <https://doi.org/10.18174/sesmo.18155>

- Jardinier, E., Parsy, F., Guyot, G., Berthin, S., Berthin, S., 2018. Durability of humidity-based demand-controlled ventilation performance: results of a 10 years monitoring in residential buildings, in: Proceedings of the 39th AIVC Conference “Smart Ventilation for Buildings.” Presented at the 39th AIVC conference “Smart ventilation for buildings,” Antibes Juan-Les-Pins, France.
- Mara, T.A., 2009. Extension of the RBD-FAST method to the computation of global sensitivity indices. *Reliability Engineering & System Safety* 94, 1274–1281. <https://doi.org/10.1016/j.ress.2009.01.012>
- Mechri, H.E., Capozzoli, A., Corrado, V., 2010. USE of the ANOVA approach for sensitive building energy design. *Applied Energy* 87, 3073–3083. <https://doi.org/10.1016/j.apenergy.2010.04.001>
- Mélois, A.B., Moujalled, B., Guyot, G., Leprince, V., 2019. Improving building envelope knowledge from analysis of 219,000 certified on-site air leakage measurements in France. *Building and Environment* 159, 106145. <https://doi.org/10.1016/j.buildenv.2019.05.023>
- Molina, C., Jones, B., Hall, I.P., Sherman, M.H., 2021. CHAARM: A model to predict uncertainties in indoor pollutant concentrations, ventilation and infiltration rates, and associated energy demand in Chilean houses. *Energy and Buildings* 230, 110539. <https://doi.org/10.1016/j.enbuild.2020.110539>
- Plischke, E., 2010. An effective algorithm for computing global sensitivity indices (EASI). *Reliability Engineering & System Safety* 95, 354–360. <https://doi.org/10.1016/j.ress.2009.11.005>
- Poirier, B., Guyot, G., Geoffroy, H., Woloszyn, M., Ondarts, M., Gonze, E., 2021a. Pollutants emission scenarios for residential ventilation performance assessment. A review. *Journal of Building Engineering* 42, 102488. <https://doi.org/10.1016/j.job.2021.102488>
- Poirier, B., Guyot, G., Woloszyn, M., Geoffroy, H., Ondarts, M., Gonze, E., 2021b. Development of an assessment methodology for IAQ ventilation performance in residential buildings: An investigation of relevant performance indicators. *Journal of Building Engineering* 43, 103140. <https://doi.org/10.1016/j.job.2021.103140>
- Poirier, B., Guyot, G., Woloszyn, M., 2022a. Development of Performance-Based Assessment Methods for Conventional and Smart Ventilation in Residential Buildings, in: *IAQ 2020: Indoor Environmental Quality Performance Approaches Transitioning from IAQ to IEQ*. AIVC-ASHRAE, Athens, Greece.
- Poirier, B., Kolarik, J., Guyot, G., Woloszyn, M., 2022b. Design of residential ventilation systems using performance-based evaluation of Indoor Air Quality: application to a Danish study case. Presented at the BuildSim Nordic 2022, IBPSA Nordic, Copenhagen, Denmark, p. 8.
- Tarantola, S., Gatelli, D., Mara, T.A., 2006. Random balance designs for the estimation of first order global sensitivity indices. *Reliability Engineering & System Safety* 91, 717–727. <https://doi.org/10.1016/j.ress.2005.06.003>
- Thatcher, T.L., Layton, D.W., 1995. Deposition, resuspension, and penetration of particles within a residence. *Atmospheric Environment* 29, 1487–1497. [https://doi.org/10.1016/1352-2310\(95\)00016-R](https://doi.org/10.1016/1352-2310(95)00016-R)
- Tian, W., 2013b. A review of sensitivity analysis methods in building energy analysis. *Renewable and Sustainable Energy Reviews* 20, 411–419. <https://doi.org/10.1016/j.rser.2012.12.014>
- Tissot, J.-Y., Prieur, C., 2012. Bias correction for the estimation of sensitivity indices based on random balance designs. *Reliability Engineering & System Safety* 107, 205–213. <https://doi.org/10.1016/j.ress.2012.06.010>
- Walton, G.N., Emmerich, S.J., 1994. CONTAM93: a multizone airflow and contaminant dispersal model with a graphic user interface. *Air Infiltration Review* 16, 6–8.

# Assessment of thermal environment and thermal comfort in air traffic control towers

Bassam Moujalled<sup>1\*</sup>, Fabrice Richieri<sup>2</sup>, Adeline Mollard<sup>3</sup>, Mathilde Hostein<sup>1,4</sup>

*1 BPE Research Team—Cerema  
46, rue Saint-Théobald, 38080  
L'Isle d'Abeau, France  
\*Corresponding author:  
bassam.moujalled@cerema.fr*

*2 DSNA,DTI  
12, avenue Martin Niel  
33688 Mérignac Cedex, France*

*3 SNIA  
82, rue des Pyrénées  
75 970 Paris Cedex, France*

*4 Univ. Lyon, ENTPE, Ecole Centrale de Lyon,  
CNRS, LTDS, UMR 5513 3 Rue Maurice Audin  
69518, Vaulx-en-Velin, France*

## ABSTRACT

Ensuring thermal comfort in air traffic control towers (ATCTs) is paramount, given the exacting demands of air traffic control, which require heightened levels of concentration and vigilance. ATCTs feature extensive glazed surfaces, leading to significant solar gains and heat loss within the indoor environment. To maintain thermally comfortable conditions throughout the year, air conditioning systems are employed to regulate the indoor climate, adjusting for varying thermal load. However, achieving uniform and stable thermal conditions poses a challenge due to the dynamic thermal loads inherent in the environment.

This paper aims to assess the thermal conditions and comfort levels within air traffic control towers across both winter and summer seasons. Furthermore, it seeks to evaluate the impact of glazing types and the air distribution systems on indoor thermal comfort.

Eight field measurement campaigns were conducted in four ATCTs from February 2019 to March 2020. The ATCTs are all located in France, with three single-glazed towers and one double-glazed tower. In each tower, indoor air temperature and relative humidity were monitored at different heights and locations over one-week periods during winter and summer. Supply and extract air temperatures were also monitored, alongside measurements of terminal velocities. The occupants' thermal comfort was assessed through targeted measurements of physical parameters related to thermal comfort and questionnaire surveys.

The results of the physical measurements generally indicate acceptable comfort conditions in all four towers during both winter and summer periods, with occasional issues of local discomfort related to draughts in some cases. The questionnaire results yielded a mixed response, with overall acceptable comfort conditions in winter, juxtaposed with some discomfort issues in summer. The discomforts were found to be associated with operational deficiencies in the conditioning systems that have been identified. As a result, improvement avenues have been proposed to reduce discomfort.

## KEYWORDS

Thermal comfort, air traffic tower control, field measurement, air distribution system

## 1 INTRODUCTION

Ensuring thermal comfort in air traffic control towers (ATCTs) is paramount, given the exacting demands of air traffic control, which require heightened levels of concentration and vigilance. ATCTs feature extensive glazed surfaces, leading to significant solar gains and heat loss within the indoor environment. To maintain thermally comfortable conditions throughout the year HVAC systems are employed to regulate the indoor climate, adjusting for varying thermal load. However, achieving uniform and stable thermal conditions poses a challenge due to the dynamic thermal loads inherent in the environment.

Different type of glazings are used in ATCTs: single or double glazing with or without solar control. The glazing has a significant impact on the energy performance of the ATCT, affecting both the energy loads and, consequently, the HVAC sizing and the annual energy consumption for heating and cooling (Richieri, et al., 2021).

This paper aims to assess the thermal conditions and comfort levels within air traffic control towers across both winter and summer seasons. Furthermore, it seeks to evaluate the impact of glazing types and the air distribution systems on indoor thermal comfort. The study is based on field measurement campaigns carried out in four ATCTs located in France, during winter and summer. The ATCTs include three single-glazed towers and one double-glazed tower.

## 2 METHOD

### 2.1 Description of the case studies

Four ATCTs were selected for the onsite measurement campaign (Figure 1): Bordeaux Airport, Roissy Airport (north and south towers), and Grenoble Airport. Table 1 presents the main characteristics the monitored ATCTs.



Figure 1. View of the ATCT of Bordeaux airport (a), north and south towers of Roissy airport (b and c respectively) and Grenoble airport (d)

Table 1. Main characteristics of the monitored ATCTs

	ATCT a	ATCT b	ATCT c	ATCT d
Shape	Circular	Circular	Circular	Square
Height	40 m	90 m	65 m	10 m
Floor area (podium area)	110 m <sup>2</sup> (65 m <sup>2</sup> )	80 m <sup>2</sup> (65 m <sup>2</sup> )	75 m <sup>2</sup> (50 m <sup>2</sup> )	34 m <sup>2</sup> (no podium)
Ceiling height	6 m	4.7 m	3.4 m	3 m
Volume	580 m <sup>3</sup>	375 m <sup>3</sup>	250 m <sup>3</sup>	102 m <sup>3</sup>
Glazing type	Single glazing	Single glazing	Single glazing	Double glazing
Glazing area	240 m <sup>2</sup>	170 m <sup>2</sup>	135 m <sup>2</sup>	45m <sup>2</sup>
Glazing slope	110°	110°	100°	107° (North at 90°)
Solar shading	Interior solar screen	Interior solar screen	Interior solar screen	Interior solar screen
# of controllers	6	9	8	5

Only the ATCT at Grenoble is double-glazed, while the other three are single-glazed, which is the majority of ATCTs in France. The ATCT at Bordeaux Airport is the largest with the highest glazing area. The north and south ATCTs at Roissy Airport are slightly smaller but have a high density of occupation, as Roissy Airport is a major European hub with intensive air traffic. Finally, the ATCT at Grenoble Airport is the smallest, with modest air traffic.

For the three ATCTs at Bordeaux and Roissy airport, the interior space is arranged with a central podium elevated by approximately 1.2 meters, which accommodates the controllers' activities, and a functional peripheral walkway for circulation and air distribution. Thus, workstations are located approximately 3 meters away from the glazing. For Grenoble airport, there is no podium and the workstations are close to the glazing.

Regarding HVAC equipment, AHUs (air handling units) are used in ATCT a, b and c, for heating, air conditioning, and ventilation, with an underfloor air distribution. Floor diffusers are located in the walkway near the glazing. For ATCT\_b, there are additional floor diffusers on the podium as shown in Figure 2. Return air grilles are also located in the walkway at the floor level near the floor diffusers for ATCT\_a, and in the staircase for the ATCT b and c. For the ATCT\_d, there is a central heating system with hot water radiator, two ceiling air conditioners with manual adjustment and single exhaust ventilation.



Figure 2. View of the supply air units in ATCT\_a, ATCT\_b and ATCT\_c

## 2.2 Measurement method

In order to assess the thermal comfort of the controllers in the ATCT, the thermal comfort indices PMV/PPD (ISO 7730, 2006) are used as recommended by (EN 16798-1, 2019) for heated and mechanically cooled buildings. As these indices characterises global thermal comfort, two additional local discomfort indices DR (draught rate) and PD (percentage dissatisfied) are used to assess the discomfort due to draught and vertical air temperature difference, respectively, that can result from the air distribution or stratification.

The PMV predicts the mean vote on the ASHRAE thermal sensation scale from cold (-3) to hot (+3) with a central neutral sensation (0) and the PPD predict the percentage of dissatisfied for a given PMV value. The indices DR and PD predict the percentage of dissatisfied due to draught and vertical air temperature difference respectively. Table 2 shows the recommended criteria for the thermal comfort indices in heated and air-conditioned spaces according to the level of expectation.

Table 2. Recommended criteria for the thermal comfort in heated and air-conditioned spaces (\* recommended value during winter; \*\* recommended value during summer)

Position	Global comfort		Draught		Vertical $t_a$ difference	
	PMV	PPD [%]	$v_a$ [m.s <sup>-1</sup> ]	DR [%]	$\Delta t_{a,v}$ [°C]	PD [%]
High level	-0.2 to +0.2	6%	0.10*/0.12** m.s <sup>-1</sup>	10%	2°C	3%
Normal level	-0.5 to +0.5	10%	0.16*/0.19** m.s <sup>-1</sup>	20%	3°C	5%

AHLBORN thermal comfort station (Figure 3) was used to measure the thermal parameters required to calculate the comfort indices: air temperature (accuracy  $\pm 0.2^\circ\text{C}$ ), globe temperature

(accuracy  $\pm 0.2^{\circ}\text{C}$ ), relative humidity (accuracy  $\pm 2.0\%$ ) and air velocity (accuracy  $\pm 0.04\text{ m}\cdot\text{s}^{-1} + 0.5\%$  of reading). These parameters were measured at the head, abdomen and ankle levels for a sitting and standing person (0.1/0.6/1.1 m and 0.1/1.1/1.7 m respectively) over a period of 20 minutes. The mean values were used to calculate the comfort indices as recommended by (ISO 7726, 2002). The measurements were carried out in each ATCT at two different positions over one day during winter and summer.

In order to assess the thermal environment and the operation of the AHUs, indoor air temperature and relative humidity (RH) were continuously monitored using Hobo dataloggers at different heights and two different locations on the podium over one-week periods during winter and summer (10 minutes timestep) (Figure 4). Supply and extract air temperatures were also monitored, alongside measurements of terminal velocities. Outdoor air temperature and RH were also monitored.

Finally, subjective questionnaires were used to assess the perceived comfort of the controllers as recommended by (ISO 10551, 2019).

The measurement campaigns also included measurements of heat transfer through glazing using a heat flow meter, but they are outside the scope of this paper and will not be presented here. They can be found in (Moujalled, et al., 2022).



Figure 3. Thermal comfort monitoring station at the head, abdomen and ankle levels for a standing person including an omnidirectional anemometer, globe temperature, and air temperature and RH sensor



Figure 4. T/RH dataloggers for the monitoring of the podium thermal environment, outdoor air, supply return air

### 3 RESULTS

#### 3.1 Analysis of AHU functioning: air supply and return

Figure 5 shows the boxplots of the supply and return air temperatures of the AHUs in the ATCT a, b and c during winter and summer. Figure 6 shows the evolution of the air temperatures for the ATCT\_a during the three hottest days of summer. Table 2 presents the main statistics of the measured air velocities of the floor diffusers.

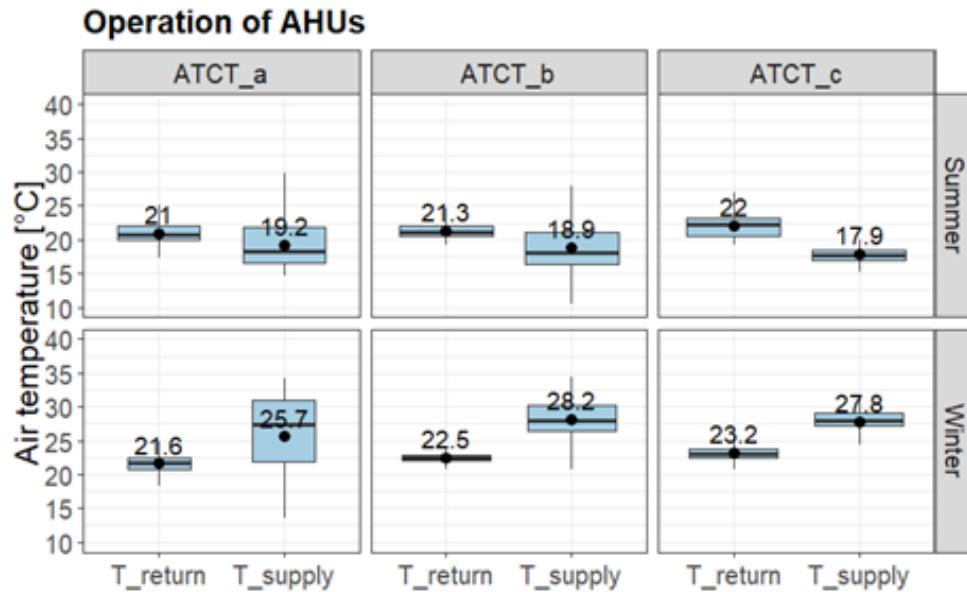


Figure 5. Boxplot with mean value of supply and return T in the ACTC a, b and c during summer and winter

The return air temperatures vary within a narrow range around an average value from 21°C to 23°C within the comfort range, depending on the heating and cooling setpoint temperatures in each ATCT. The supply air temperatures, especially in ATCT\_a, vary within a wide range from 13°C to 34°C. Indeed, the AHU alternates between heating and cooling modes in both seasons, depending on the outdoor temperature and solar radiation, as shown in Figure 6. Even during the hottest days in summer, we observe a heating mode for a few hours at night with supply temperatures around 24°C, and a cooling mode for the rest of the time with supply temperatures around 15°C. This overall shows good operation of the AHU, which maintains a return air temperature around the heating and cooling setpoints of 20°C and 22°C, respectively.

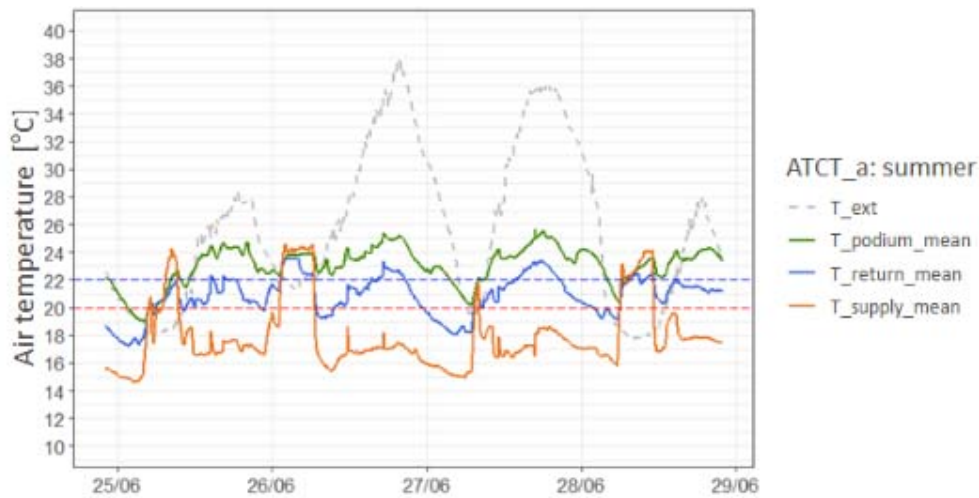


Figure 6. Evolution of air temperature in ATCT\_a during the hottest days of summer

However, we observe a significant discrepancy (2°C to 4°C) between the return air temperature and the average temperature on the podium when the AHU operates in cooling mode for ATCT\_a. The return air temperature varies slightly around its setpoint of 22°C, while the podium temperature rises to 26°C by the end of the day. This reveals a problem of recycling part of the cold supply air in cooling mode before reaching the podium, where the temperature remains 2°C to 4°C higher compared to the walkway. This recycling issue can be explained by the configuration of the supply diffusers and extraction grilles located face-to-face in the walkway and the low air velocity of the floor diffusers, as shown in Table 3. This introduces a bias in the cooling mode regulation of the AHU, which was based on the return air temperature significantly lower than that perceived by the controllers on the podium. Since then, the regulation has been renovated to operate according to the ambient sensors on the podium. For the North control tower at Roissy, the cold air supply on the podium (via floor diffusers) creates a cold draft at the controllers' ankles in summer, which is a source of discomfort as discussed in section 3.3.

Table 3. Descriptive statistics of the air diffuser velocities in ATCT\_a, ATCT\_b and ATCT\_d

		ATCT_a: walkway		ATCT_b: walkway		ATCT_b: podium		ATCT_c: walkway	
		Winter	Summer	Winter	Summer	Winter	Summer	Winter	Summer
Supply air velocity [m.s <sup>-1</sup> ]	Min	0.60	0.65	0.50	0.40	0.30	0.20	1.66	1.20
	Max	2.15	2.15	1.69	1.75	0.61	0.51	3.00	1.99
	Mean	1.28	1.37	1.12	1.05	0.46	0.41	2.16	1.55
	S.D.	0.39	0.37	0.28	0.30	0.11	0.11	0.36	0.22

### 3.2 Analysis of the indoor thermal environment

Figure 7 and Figure 8 show the boxplots of indoor air temperature ( $T_a$ ) and RH at different heights and positions in the ATCTs during winter and summer.

For ATCT\_a,  $T_a$  values vary little in winter and fall within the comfort range of 20°C to 24°C, with an average around 22°C. In summer, they vary within a wider range of 19°C to 26°C, with an average around 23°C. They never exceed the upper threshold of the thermal comfort range (26°C), and they are slightly below the lower threshold (23°C), especially at night when temperatures can drop to 19°C. This likely corresponds to periods when the control tower is



unoccupied. RH values are globally in the comfort ranges and slightly exceed 60% in the summer due to the air-conditioning.

For ATCT\_b, Ta values are homogeneous in winter with an average of around 23°C. They generally fall within the comfort range of 20°C to 24°C throughout the measurement period. In summer, the air temperatures on the podium are less homogeneous, with lower values at ankle level (around 21°C) than at head level (24°C). However, the differences remain within approximately 1°C of the average podium temperature, which is around 22.5°C. Overall, they vary within a wide range from 19°C to 28°C. They slightly exceed the upper threshold of the thermal comfort range in summer (26°C) on the hottest days (with more than 35°C outside), but are below the lower threshold of the comfort range (23°C) for nearly half the time, especially at night. RH values are globally in the comfort ranges.

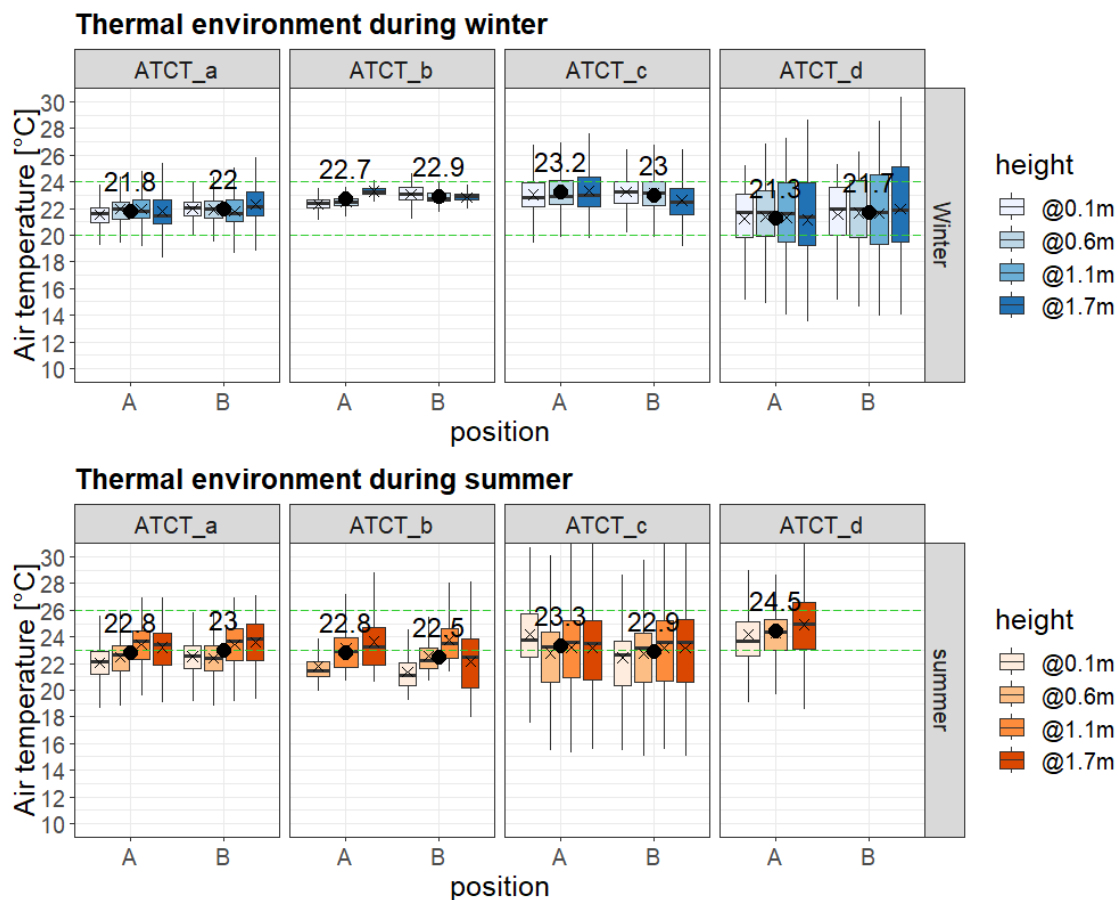


Figure 7. Boxplot with mean value (black point) of the indoor air temperatures in the ATCTs at different heights and positions

For ATCT\_c, Ta values vary within a wide range from 20°C to 28°C in winter, with an average of around 23°C. They never drop below the lower threshold of the comfort range of 20°C, but they often exceed the upper threshold of 24°C in the afternoon depending on the sun (up to 28°C). In summer, the air temperatures on the podium also average around 23°C. They vary within a wider range from 19°C to 30°C. They slightly exceed the upper threshold of the thermal comfort range in summer (26°C) on the hottest days (with more than 35°C outside). However, they are below the lower threshold (23°C) for nearly half the time. Indeed, they are generally between 23°C and 26°C during the day from 9 AM to 9 PM, but from 9 PM they drop more or

less quickly to 19°C before rising again in the early morning. RH values are globally in the comfort ranges.

For ATCT\_d, the situation is different with important variations during winter and summer. It is smallest ATCT with a moderate air traffic control activity and unoccupied periods. In winter, Ta values are generally homogeneous but vary significantly between 15°C (at night) and 28°C with an average of around 21°C. Ta drops below 20°C at night when the tower is unoccupied. During the day, it generally stays between 20°C and 24°C, frequently exceeding 24°C on sunny days and fluctuating more or less depending on the opening of the external door. In summer, Ta values also vary within a wide range from 19°C (at night) to 38°C (during the day, when unoccupied with 44°C outside) with an average of around 24°C. During the day and when occupied, the average Ta in the control tower generally stays within the comfort range of 23°C to 26°C, thanks to air conditioning with outdoor temperatures up to 35°C. When the outdoor temperature exceeds 35°C, Ta exceeds the 26°C threshold but remains below 28°C (with outdoor temperatures over 40°C). RH values are globally in the comfort ranges.

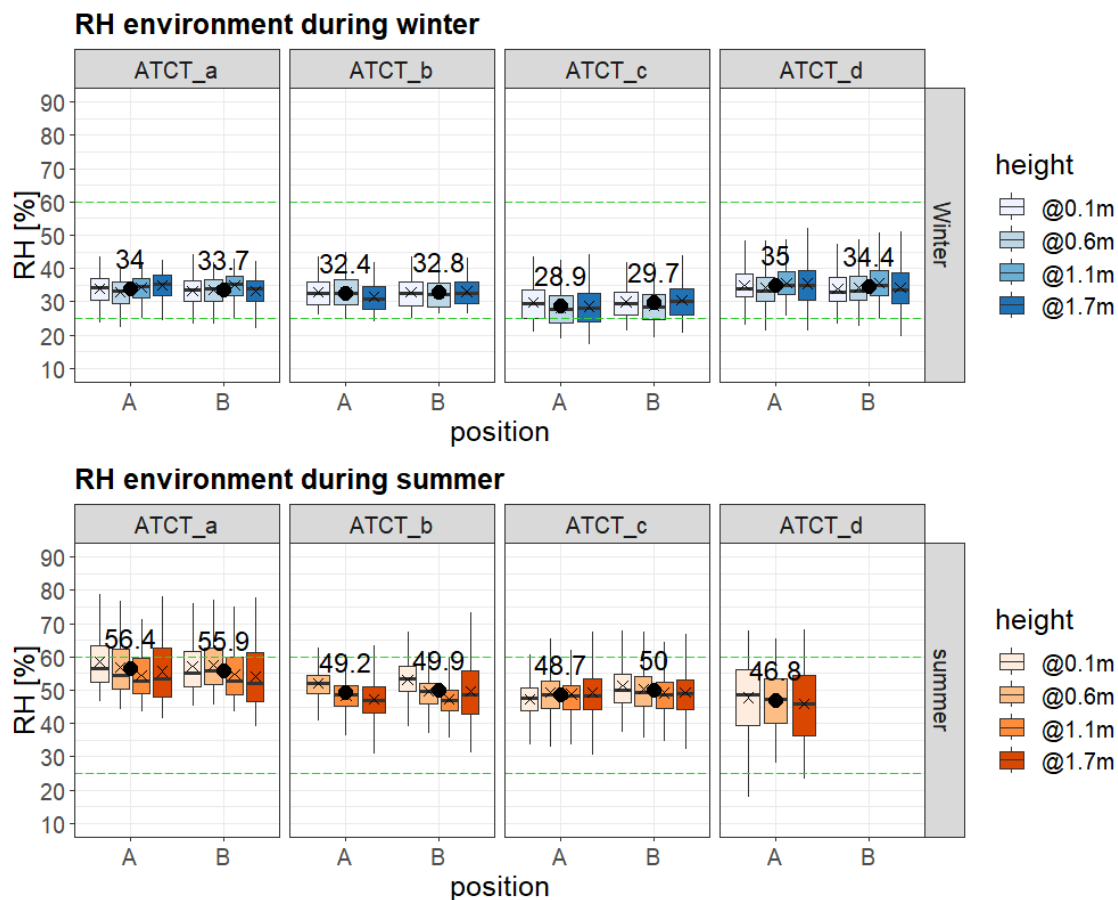


Figure 8. Boxplot with mean value of the indoor RH in the ATCTs at different heights and positions

### 3.3 Analysis of the thermal comfort

Table 4 presents the main results of the global comfort and local discomfort indices for a sitting person in the ATCTs during winter and summer.

In view of the global comfort and local discomfort indices, thermal comfort is generally satisfactory in the four control towers in winter and summer, with dissatisfaction rates always

below 10%, except for the ATCTs at Roissy in summer during the morning (ATCT b and c), and the ATCT\_d at Grenoble in winter.

For ATCT b and c in summer, this slight discomfort is due to the cool sensation in the morning (POS1) caused by the air-conditioning. Indeed, the floor diffusers on the podium blow cold air directly at the controllers' ankles, which also creates a higher draught risk. This problem is exacerbated when the controllers are performing static activities at their stations while wearing light summer clothing. However, this cool discomfort disappears in the afternoon (POS2).

For ATCTd in winter, the situation is different as the discomfort is due to warm sensation. The measurements were performed during a sunny day with outdoor air temperature around 15°C. The controllers opened the exterior door to avoid overheating.

The feedback from the controllers through questionnaires confirms the results observed by the measurements, with overall satisfactory perceived comfort, except for the Bordeaux control tower in summer. For the latter, unlike the results of the physical measurements, the feedback from the controllers is mixed, with issues of warm discomfort (5 controllers out of 9) and dry air (7 controllers out of 9), despite air temperatures below 26°C on the podium and relative humidity frequently exceeding 60%. This discrepancy between the thermal conditions on the podium and the controllers' perception is difficult to explain given the multisensory aspect of thermal comfort and the impact of psychological factors. Exposure to solar radiation or the difficulty in finely controlling the temperature on the podium (due to the recycling of cold blown air in the corridor as discussed in section 3.1) are constraints that could interfere with the controllers' perception of thermal comfort. Lastly, we note that for the ATCT\_d, the controllers mentioned the difficulty to manage the indoor temperature due to the multiplicity of HVAC systems, as well as the inertia of the central heating radiators.

Table 4. Results of the thermal comfort indices in the ATCTs during winter and summer

Tower	Period	Position	Global comfort		Draught		Vertical $t_a$ difference	
			PMV	PPD [%]	$v_a$ [ $m.s^{-1}$ ]	DR [%]	$\Delta t_{a,v}$ [°C]	PD [%]
ATCT_a	Winter	POS1	-0.1	5.1	0.07	5.8	1.9	1.6
		POS2	-0.2	5.7	0.15	21.9	2.2	2.1
	Summer	POS1	0.3	6.5	0.08	5.1	1.2	0.9
		POS2	0.0	5.0	0.10	7.8	0.9	0.7
ATCT_b	Winter	POS1	0.2	6.1	0.04	0.0	2.2	2.0
	Summer	POS1	<b>-0.7</b>	<b>14.9</b>	<b>0.19</b>	<b>22.3</b>	2.7	3.1
		POS2	-0.5	11.2	0.08	7.1	1.4	1.0
ATCT_c	Winter	POS1	0.3	7.1	0.01	0.0	0.1	0.3
	Summer	POS1	<b>-0.6</b>	<b>11.8</b>	<b>0.14</b>	<b>15.7</b>	0.5	0.5
		POS2	0.2	5.5	0.03	0.0	1.0	0.8
ATCT_d	Winter	POS1	0.6	12.7	0.12	9.7	1.5	1.1
		POS2	<b>0.7</b>	<b>14.3</b>	<b>0.20</b>	<b>17.6</b>	1.9	1.6
	Summer	POS1	0.3	7.4	0.04	0.0	1.0	0.7
		POS2	0.5	9.2	0.07	4.2	0.9	0.7

## 4 CONCLUSIONS

Eight field measurement campaigns were conducted in four ATCTs from February 2019 to March 2020. These ATCTs, all located in France, include three single-glazed towers and one double-glazed tower.

In each tower, indoor air temperature and relative humidity were monitored at different heights and locations over one-week periods during winter and summer. Supply and extract air temperatures were also monitored, alongside measurements of terminal velocities. The occupants' thermal comfort was assessed through targeted measurements of physical parameters related to thermal comfort and questionnaire surveys.

The results of the physical measurements generally indicate acceptable comfort conditions in all four towers during both winter and summer periods, with occasional issues of local discomfort related to draughts in some cases. The questionnaire results yielded a mixed response, with overall acceptable comfort conditions in winter, juxtaposed with some discomfort issues in summer.

Due to the small sample size, with only one double-glazed ATCT smaller than the other three, it was not possible to conclude on the impact of glazing type on thermal comfort. However, thanks to the HVAC systems, the indoor thermal conditions were generally within comfort ranges. The main observed discomfort issues were primarily related to operational deficiencies in the HVAC systems, particularly the air distribution of the AHUs, which caused issues with recycling supplied cool air and localized cold discomfort.

As a result, improvement avenues have been proposed to reduce discomfort, and some recommendations were integrated into a design specification guide for HVAC installations in control towers. These include air diffusion with minimum pressure for minimum velocity, a penalty coefficient for glazing losses, temperature setpoints for sizing, and consideration of temperature stratification in cooling.

## 5 ACKNOWLEDGEMENTS

The authors would like to thank the various departments of the French Directorate General of Civil Aviation (DGAC) for their collaboration on this study, particularly the National Airport Engineering Service (SNIA) and the Directorate of Air Navigation Services (DSNA).

## 6 REFERENCES

- EN 16798-1, 2019. *Energy performance of buildings - Ventilation for buildings - Part 1 : indoor environmental input parameters for design and assessment of energy performance of buildings addressing indoor air quality, thermal environment, lighting and acoustics - Module M*. France: AFNOR.
- ISO 10551, 2019. *Ergonomics of the physical environment - Subjective judgement scales for assessing physical environments*. France: AFNOR.
- ISO 7726, 2002. *Ergonomics of the Thermal Environment - Instruments for measuring physical quantities*. France: AFNOR.
- ISO 7730, 2006. *Ergonomics of the Thermal Environment - Analytical Determination and Interpretation of Thermal Comfort Using Calculation of the PMV and PPD indices and Local Thermal Comfort Criteria: International Organization for Standardization..* France: AFNOR.
- Moujalled, B., Moral, N., Cueille, R. & Chevallier, A., 2022. *Evaluation in situ du confort thermique: Suivi instrumenté de 4 vigies*, Bron, France: Cerema.
- Richieri, F., Moujalled, B. & Nicolle, E., 2021. Design of high-performance control towers: Importance and difficulty of achieving duct and envelope airtightness. *12th International BUILDAIR Symposium*.

# Assessment of in-situ aging and maintenance impact on Relative Humidity-Controlled Mechanical Extract Ventilation (RH-MEV) Systems: A Case study in multi-family social housing buildings

Juan Rios<sup>1\*</sup>, Marc Legree<sup>1</sup>, Adeline Mélois<sup>2</sup>, Ambre Marchand Moury<sup>3</sup>

*1 AERECO SA,  
Z.I de Lamirault, 62 Rue de Lamirault, 77090  
Collégien, France  
\*juan.rios@aereco.com*

*2 Cerema BPE Research Team,  
46 rue St Théobald, F-38080,  
L'Isle d'Abeau, France*

*3 Cerema Centre Est Groupe Bâtiments,  
Boulevard Bernard Giberstein, 71400  
Autun, France*

## ABSTRACT

This paper presents a comprehensive evaluation of Relative Humidity-Controlled Mechanical Extract Ventilation (RH-MEV) systems installed in multi-family social housing buildings, focusing on the assessment of in-situ aging and the impact of maintenance on the performance of the system. Building upon the Performance 2 project conducted from 2020 to 2024, which evaluated the durability and performance of RH-MEV systems over a 15-year period, this study delves deeper into the longevity and maintenance aspects of these systems. The research investigates the performance of provisory products, both inlet and extract units, after 1.25 years of operation under real conditions. Provisory units were installed and operate during the performance characterization in the lab after 13 years of in-situ operation of the real products between Performance 1 and Performance 2 projects. The performance of provisory products after 1.25 years of in-situ operation is compared to the manufacturer's specifications, highlighting the impact of factors such as aging and maintenance. Furthermore, the study examines the influence of maintenance on the performance of the system by comparing the results of the characterization of the provisory ventilation units as collected after 1.25 years of operation (dirty) and after cleaning (as could be done by the occupant), against the original manufacturer tolerances. The findings reveal significant variations in cleanliness among different types of ventilation units. Kitchen exhaust units were found to be the most heavily soiled, with oily residues, while some bathroom and shower room exhaust units appeared more encrusted with a mixture of dust and fibres. Despite these cleanliness challenges, the hygroscopic function of the units remains intact, allowing them to modulate ventilation rates based on humidity levels. However, airflow limitations were observed at low humidity levels in both kitchen and bathroom/shower room exhaust units. In contrast, air inlet units were generally cleaner and exhibited a positive response to changes in humidity levels, confirming their functionality in modulating airflow based on indoor conditions. Overall, most of the ventilation units met fabrication specifications, ensuring optimal operation despite the state of cleanliness, and guarantying the Indoor Air Quality (IAQ) in the housing buildings after 1.25 years. This analysis provides insights into the need of maintenance procedures in sustaining or enhancing the performance of RH-MEV systems over time. The paper discusses the implications of in-situ aging and maintenance on RH-MEV system performance, providing valuable insights for system designers, manufacturers, and building managers. By understanding how these factors affect long-term performance, stakeholders can make informed decisions regarding system design, maintenance schedules, and IAQ management strategies, ultimately enhancing IAQ and occupant comfort in multi-family social housing buildings.

## KEYWORDS

Smart ventilation, residential ventilation, IAQ, energy efficiency, durability

## 1 INTRODUCTION

In recent years, the focus on Indoor Air Quality (IAQ) in multi-family social housing buildings has intensified, driven by a growing understanding of its impact on occupants' health and well-being. In Europe, regulatory directives have underscored the importance of eco-design requirements and energy labelling for residential ventilation units, including the widespread adoption of low-pressure systems, demand-controlled ventilation (DCV) systems, and balanced heat recovery systems to ensure both energy efficiency and IAQ optimization [1]. Smart ventilation, particularly Relative Humidity-Controlled Mechanical Extract Ventilation (RH-MEV) systems, has emerged as a promising solution to address the dual challenges of energy consumption and IAQ management in residential buildings. These systems employ sophisticated controls to adjust ventilation rates based on real-time indicators such as humidity levels, ensuring optimal IAQ while minimizing energy usage. The adoption of such systems is increasingly supported by regulatory frameworks in various European countries, reflecting a broader recognition of their potential benefits [2], [3], [4].

Smart ventilation, using RH-MEV, was studied during the "Performance 1" project which included a large-scale monitoring on thirty-one new occupied apartments in two buildings extended from 2007 to 2009, respectively situated in Paris and Villeurbanne (near Lyon) and equipped with RH-MEV [5]. In each dwelling of both buildings of this study, the Air Terminal Devices – ATD (exhaust air ATDs and air inlet) were installed during the construction of the buildings more than 15 years ago. In Performance 2 project, and to evaluate the functioning of these ATDs after aging, these units were collected to characterize their current hygroscopic performances in the laboratory [6], [7]. During this period, non-instrumented new products temporarily replaced the collected ATDs to maintain building ventilation during the laboratory tests.

The research investigates provisory units, both inlet and extract units, installed for 1.25 years in Paris under real conditions during the characterization of actual products characterized in the laboratory after 13 years of in-situ operation (Figure 1).



Figure 1. Example of collected Kitchen extract units.

Comparisons are made between the performance of provisory products after 1.25 years of in-situ operation and the specifications of the manufacturer. Furthermore, the study compares the results of exhaust units and air inlets as collected (more or less dirty) and after cleaning (as it could be done by the occupant) to the original manufacturer tolerances. This analysis provides insights into the efficacy of maintenance procedures in sustaining or enhancing the performance of RH-MEV systems over time. The paper discusses the implications of in-situ aging and maintenance on RH-MEV system performance, providing valuable insights for system designers, manufacturers, and building managers. By understanding how these factors affect long-term performance, stakeholders can make informed decisions regarding system design, maintenance schedules, and IAQ management strategies, ultimately enhancing Indoor IAQ and occupant comfort in multi-family social housing buildings.

## 2 METHODOLOGY

Tests were conducted following the methodology used for the characterization of the instrumented ATDs [REF]. This characterization was made in two separate rooms for exhaust units and air inlets, each controlled for temperature and humidity by Air Handling Units (AHUs). Exhaust units were connected to a test bench comprising a fan, duct, and orifice flowmeter (Figure 2). Fan speed was regulated based on pressure measurements to maintain a constant pressure. Similarly, air inlets were positioned in test boxes connected to a fan and orifice flowmeter, with fan speed controlled based on pressure differentials. Airflow measurements were recorded for each humidity step (rise and decrease) to assess performance.



a. Air inlet.



b. Exhaust unit.

Figure 2. Example of the ATDs on the hygro-aeraulic test bench.

The characterization of air exhaust units was conducted under an operating pressure of 100 Pa. The airflow rate was continuously measured across various humidity levels, with the temperature maintained at a constant 21°C throughout the test. Similarly, the performance of air inlets was characterized using a comparable protocol. A pressure difference of 10 Pa was applied to the ATD terminal, and airflow rates were measured at different relative humidity

steps. The temperature was maintained at 21°C for the duration of the test. Each point on the hygro-aeraulic curve represents measurements taken at stable humidity and airflow rate values.

### 3 RESULTS AND ANALYSIS

Data collected from laboratory tests were analysed to characterize the performance of ATDs after 1.25 years of in-situ operation. Most of the collected ATDs, both air inlet and air exhaust units, have shown a low level of maintenance (regarding cleaning by the occupants and/or the maintenance company). Based on the state of the ventilation units observed, it was observed that the kitchen exhaust units were the most heavily soiled, exhibiting a layer of dirt that was predominantly oily in nature (Figure 3a). Some bathroom and shower room exhaust units appeared to be more encrusted than others, with a mixture of dust, hair, and other fibres. In contrast (Figure 3b), the air inlet units were generally found to be cleaner.



A. Kitchen

B. Bathroom

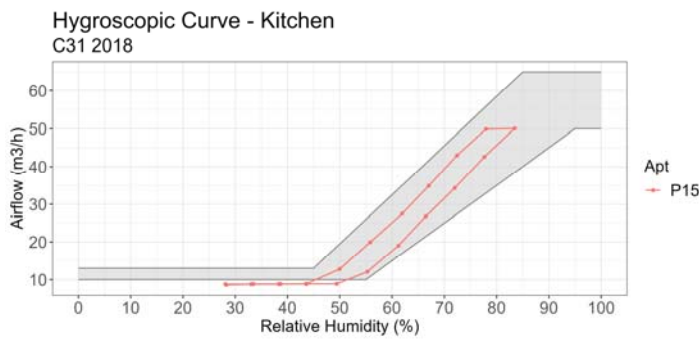
Figure 3. Example of the state of the collected units depending on the room.

Comparisons were made with the performance characterization against the fabrication specifications:

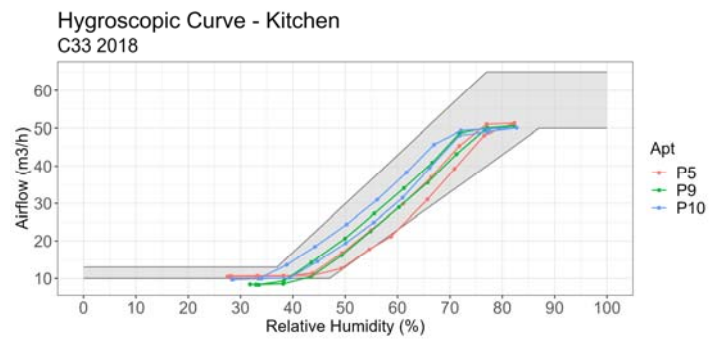
- Kitchen Exhaust Units:

Figure 4 displays the results for all the kitchen ATDs. As mentioned earlier, during the all the kitchen units were evaluated with an insufficient level of maintenance (Figure1).

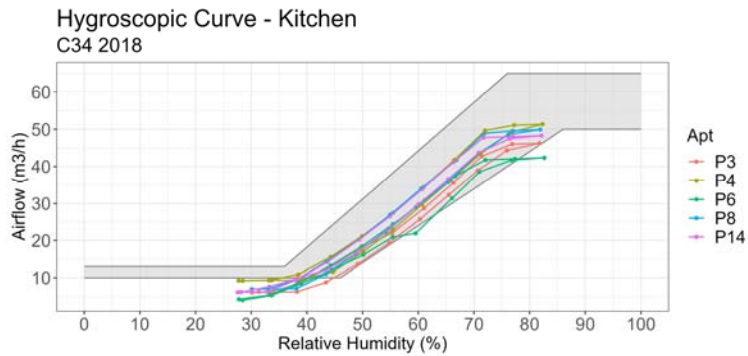




a. C31 2018



b. C33 2018



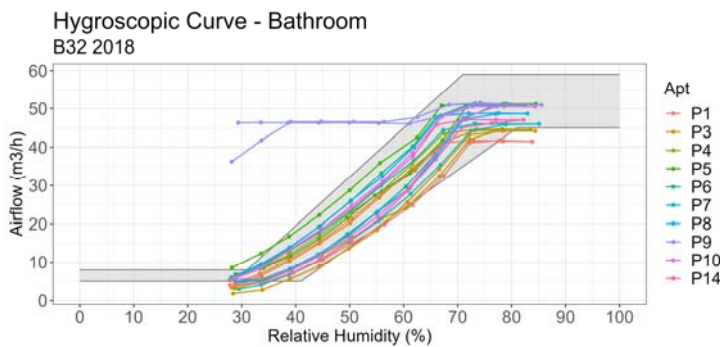
c. C34 2018

Figure 4. Results of the hygro-aeraulic curves – Kitchen.

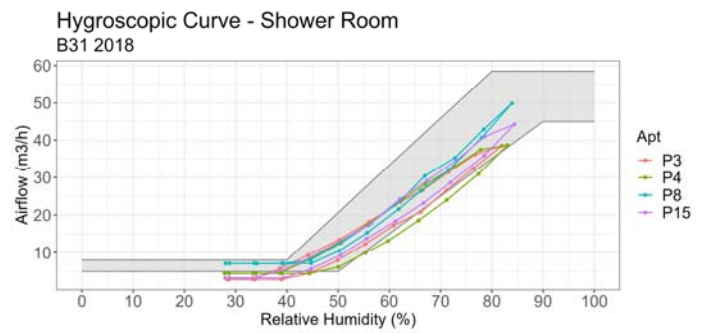
The results show that the curves generally fall within the expected envelopes, indicating a consistent response to changes in humidity levels. This responsiveness to humidity suggests that the hygroscopic functionality of the units remains intact, despite potential factors such as aging or environmental conditions. One interesting finding is the limitation of airflow at low humidity levels. This phenomenon raises questions regarding potential causes, with one possibility being the accumulation of debris or particulate matter on the shutter box over time. Such buildup could restrict airflow, resulting in reduced ventilation performance, particularly at lower humidity levels. However, it is noteworthy that despite the observed limitation in airflow at low humidity levels, the hygroscopic function of the units appears to remain effective. This suggests that while airflow may be restricted under certain conditions, the units continue to modulate ventilation rates based on humidity levels as intended. The robustness of the RH-MEV system (design and hygroscopic sensor) leads the exhaust units to deal well with obstruction or blocking over time.

- Bathroom Exhaust Units:

Bathroom exhaust units were characterized in the laboratory and their hygroscopic performance (airflow response to humidity) were compared to the tolerances of fabrication (Figure 5a). The curves depicting the performance of these units generally fall within the expected envelope, indicating a consistent response to changes in humidity levels. However, it is notable that all units except one exhibited a response to humidity, suggesting a high degree of functionality in modulating ventilation rates based on humidity levels.



a. Bathroom.



b. Shower Room

Figure 5. Results of the hygro-aeraulic curves.

A noteworthy trend observed in the bathroom exhaust units is the tendency towards a limitation of airflow at low humidity levels. This limitation could potentially be attributed to factors such as the accumulation of debris or particulate matter within the units, which may restrict airflow and impact overall ventilation performance, particularly in environments with lower humidity levels. This trend raises concerns regarding potential blockages and the need for periodic maintenance to address such issues. The one air exhaust unit that did not exhibit any response to changes in humidity levels presented a missing spring in the product.

- Shower Room Exhaust Units:

The laboratory characterization of exhaust units in the shower rooms yielded data from 4 tested units (Figure 5b). Similar to the bathroom units, the curves representing the performance of these units align well within the expected envelope. Additionally, all tested units exhibited a positive response to changes in humidity levels, confirming their functionality in modulating ventilation rates based on environmental conditions. However, a notable trend observed in the shower room exhaust units is the tendency towards a lower airflow at low humidity levels compared to the tolerances. This trend suggests a potential limitation in ventilation performance under specific humidity conditions. This could be indicative of factors such as blockages or obstructions within the units. While the units react well to humidity variations, the observed lower airflow at lower humidity levels warrants further investigation into potential causes.

While the units generally exhibit a consistent response to humidity and fall within expected performance envelopes, trends towards airflow limitation or suboptimal performance at low humidity levels raise concerns regarding potential maintenance issues. Addressing these concerns through regular maintenance protocols is crucial to ensure optimal performance and longevity of RH-MEV systems in multi-family social housing buildings.

- Bedroom and living room inlet units:

Hygroscopic performances of the air inlets were characterized in the laboratory and compared to the manufacturer specifications (Figure 6). The observations indicate that most of the characterized units exhibit performance within the expected envelope, with curves aligning well with the anticipated response to humidity variations.

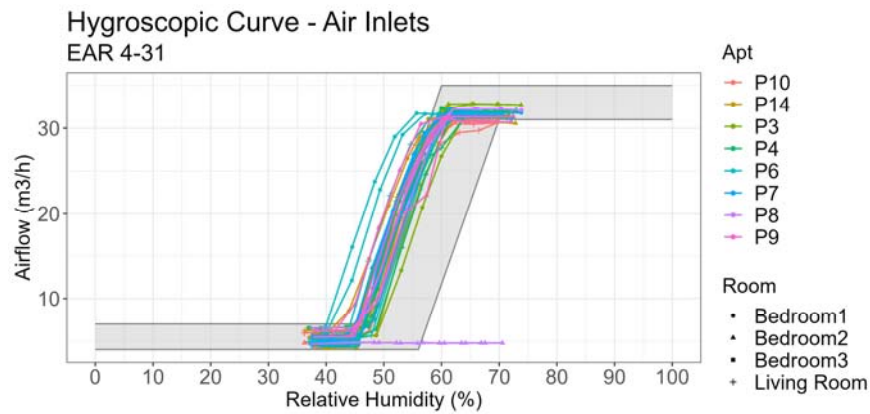


Figure 6. Results of the hygro-aeraulic curves – Bedrooms and living rooms.

One air inlet unit did not exhibit any response to changes in humidity levels. This anomaly is associated to a missing spring in the product. Another unit displayed a significant deviation from the expected performance specifications and only two others in the limit of this criteria, indicating potential irregularities or anomalies in its functionality. This deviation may warrant closer scrutiny to determine the root cause and assess the unit's overall effectiveness in modulating airflow based on humidity levels.

However, despite the particular case of the air inlet with a missing spring, all the air inlets units showed a positive response to changes in humidity levels, confirming their functionality in modulating airflow based on indoor conditions of the room. While this response aligns with the expected behaviour of hygroscopic air inlet units, most of the air inlets (16 out of 19) meet the specifications of fabrication to maintain optimal operation and therefore to ensure IAQ.

#### 4 CONCLUSIONS

The comprehensive analysis conducted in this study provides valuable insights into the performance and effectiveness of RH-MEV provisory units installed during 1.25 years in multi-family social housing buildings.

This variation in cleanliness among different types of ventilation units highlights the importance of more adequate maintenance strategies. For instance, the presence of oily residues in kitchen exhaust units may necessitate more frequent and thorough cleaning to prevent airflow obstruction and maintain optimal performance of the RH-MEV system. In addition, the discovery of two ATDs lacking a response to humidity levels, attributed to a missing spring in the product, raises concerns regarding potential discrepancies in maintenance practices. Specifically, this observation may be associated with the interchanging of three WC and bathroom facades during maintenance procedures. Such a deviation from standard configuration could indicate an oversight and underlines the importance of meticulous attention to detail and adherence to established maintenance guidelines to prevent similar issues from arising in the future.

Overall, these observations highlight the importance of proactive maintenance efforts adapted to the specific needs of each ventilation product. By addressing cleanliness issues and implementing appropriate maintenance measures, occupants can ensure the continued effectiveness and longevity of ventilation systems in multi-family social housing buildings.

The findings reveal several key observations:

- **Overall Performance:** Most air inlets and exhaust units meet the original specifications after 1.25 years of aging in real life conditions. Their correct response to humidity ensures a good balance between IAQ and energy consumption.
- **Maintenance Needs:** Proactive maintenance, including regular cleaning and inspection of ventilation units, may mitigate issues like airflow limitation or irregular performance, ensuring optimal system functionality over time.
- **Resilience:** Despite potential challenges such as airflow limitation or suboptimal performance under certain conditions, the hygroscopic functionality of RH-MEV systems remains largely intact, indicating their resilience and suitability for long-term use in multi-family social housing buildings.

In conclusion, the findings of this study underscore the importance of ongoing monitoring, maintenance, and optimization efforts to maximize the performance and longevity of RH-MEV systems in multi-family social housing buildings. By addressing maintenance needs and implementing quality assurance measures, stakeholders can enhance IAQ, improve energy efficiency, and promote healthier living environments for occupants. Moreover, moving forward, continued research and collaboration are essential to further advancing the effectiveness and sustainability of RH-MEV systems in addressing the complex challenges of IAQ management in residential buildings.

Further investigation includes the characterization of the remaining units, air inlet and exhaust units, to provide a comprehensive assessment of the lasting ATDs. In addition, the next step of this study will focus on the ATDs characterization after cleaning by comparing the results of the provisory ventilation units as collected after 1.25 years of operation (dirty) and cleaned (as could be done by the occupant), against the optimal fabrication tolerances. This will allow to assess the impact of the lack of maintenance on the ventilation unit performance.

## 5 ACKNOWLEDGEMENTS

The authors acknowledge the support of ADEME under the contract number 2004C0014.

## 6 REFERENCES

- [1] « COMMISSION REGULATION (EU) No 1253/2014 - of 7 July 2014 - implementing Directive 2009/125/EC of the European Parliament and of the Council with regard to ecodesign requirements for ventilation units - ».
- [2] D. Zukowska *et al.*, « Ventilation in low energy residences – a survey on code requirements, implementation barriers and operational challenges from seven European countries », *Int. J. Vent.*, vol. 20, n° 2, p. 83–102, avr. 2021, doi: 10.1080/14733315.2020.1732056.
- [3] G. Guyot, E. Jardinier, et F. Parsy, « Smart Ventilation Performance Durability Assessment: Preliminary Results from a Long-Term Residential Monitoring of Humidity-based Demand-Controlled Ventilation », 2021.
- [4] J.-L. S. and J. Laverge, « Demand-controlled ventilation: An outline of assessment methods and simulation tools », oct. 2011, Consulté le: 13 mars 2024. [En ligne]. Disponible

sur: <https://www.aivc.org/resource/demand-controlled-ventilation-outline-assessment-methods-and-simulation-tools>

[5] J.-L. Savin et A.-M. Bernard, « “Performance” project: Improvement of the ventilation and building air tightness performance in occupied dwellings in France », janv. 2009, Consulté le: 13 mars 2024. [En ligne]. Disponible sur:

<https://www.aivc.org/resource/performance-project-improvement-ventilation-and-building-air-tightness-performance-occupied>

[6] A. Mélois *et al.*, « Durability of humidity-based ventilation components after 13 years of operation in French residential buildings – Assessment of components performance in laboratory », *Energy Build.*, vol. 292, p. 113154, août 2023, doi: 10.1016/j.enbuild.2023.113154.

[7] B. Stéphane et P. François, « Feedback on installation, maintenance, and aging of mechanical humidity-controlled ventilation exhaust units ».

# Evaluation of the impact of window use on the heating energy use and IEQ in dwellings based on simulations

Silke Verbruggen, Arnold Janssens<sup>\*</sup>, Jelle Laverge

*Research Group Building Physics  
Ghent University  
Gent, Belgium*

*\*Corresponding author: [arnold.janssens@ugent.be](mailto:arnold.janssens@ugent.be)*

## ABSTRACT

Window opening behaviour can have an important impact on residential energy use, especially in energy efficient dwellings. A few studies indicated that the window use may be a habitual behaviour, meaning that the behaviour is performed without conscious thought as a consequence of frequently repeating this action. Verbruggen et al. (2021a) developed an event-based residential occupant behaviour model (EROB) based on habits as present in Belgian dwellings, including a window opening model. This habit-based approach has some advantages such as the prediction of inter-occupant diversity, easy implementation in Building Energy Simulation (BES) and the prediction of realistic actions that fit in the occupants' day-to-day life.

However, for application purposes it can be questioned if the inclusion of these habits makes a significant impact on the energy use and indoor climate. Therefore, this paper explores the impact of the habit-based occupant behaviour model on the energy use and indoor climate predictions in dwellings.

First, the modelling approach is introduced. One of the nearly zero energy houses (NZEB) in a case study neighbourhood has been modelled in the simulation environment Dymola-Ideas. In addition to the actual situation with NZEB performance, the house has also been modelled with a design reflecting a medium and poor energy performance. The library components and modelling assumptions are explained.

The simulations are carried out for 30 different household profiles, generated using the EROB-model. The evaluation of the impact of user behaviour is based on three criteria: the net energy use for space heating, the CO<sub>2</sub>-concentration as a measure for IAQ, and overheating as a measure for thermal discomfort. The simulations are carried out for both the overall model and for a base-model including only one type of occupant behaviour, to evaluate which has the largest influence. Additionally, the importance of predicting realistic window use actions, one of the intrinsic characteristics of the habit-based approach, is assessed.

The simulation results show a significant impact on the energy use and indoor climate predictions due to the inclusion of occupant behaviour, especially by the window use and especially in energy efficient buildings.

## KEYWORDS

Occupant behaviour, Window opening, Building energy simulation, IEQ, Heating energy use

## 1 INTRODUCTION

In residential buildings the energy use is defined by numerous aspects such as the building envelope, installed systems, climate, but as well the occupant behaviour. The building user can perform a wide set of actions that can have an effect on the energy use, such as opening or closing windows, using appliances, adapting the heating set-points. To predict the residential energy use more accurately, occupant behaviour models have been developed. The current approach towards occupant behaviour modelling is predominantly based on the assumption that occupant behaviour is deliberative, with many models relating the occupant behaviour to environmental and time-dependent variables. However, behavioural studies indicate that not all actions are deliberative, and that especially in a stable context such as a residential building, the actions are often performed without conscious thought, out of habit. By including habits in

occupant behaviour models the behavioural predictions and corresponding energy use and indoor environmental quality simulations can be improved.

Verbruggen et al. (2021a) developed a window use model based on data collected in an online survey in Belgium, an initial classification of households according to the habit-coherence across rooms in winter and a seasonality coherence. These predicted habits are coupled to an occupancy and activity model to predict window use profiles. Next, the window use habit model is combined with other types of occupant behaviour in an event-based residential occupant behaviour (EROB) model. This model based on time use data allows to predict the occupancy and activity profiles of households and linked to that the window use, heating set-points, domestic hot water use, electricity use, internal heat gains and CO<sub>2</sub>-production. This habit based model can be easily implemented in building energy simulations (BES) and allows for fast computation as it is not using (simulated) indoor environmental variables as inputs.

However, for application purposes it can be questioned if the inclusion of these habits makes a significant impact on the energy use and indoor climate. Therefore, this paper explores the impact of the habit-based occupant behaviour model on the energy use and indoor climate predictions in dwellings.

## 2 OCCUPANT BEHAVIOUR (OB) MODEL

Results of an online survey conducted with near 500 Belgian households revealed that almost all occupants habitually interact with at least one window. Some household and building characteristics were related to the presence of certain habits. However, this impact was rather small in comparison to the impact of the habits of other rooms. These insights were utilized for the creation of a window use habit model. The model starts by assigning a winter household-habit to each household. The different household winter window habits were generalised to five different categories:

- All windows closed (24.6%)
- All windows shortly opened (20.5%)
- Bedroom window opened more than the windows in other rooms (25.6%)
- Clear distinction between habits in the day-zone and night-zone (20.3%)
- Clear distinction between habits in the most occupied zones (living room, bedrooms) and in the less occupied zones (kitchen, bathroom) (9.0%)

The assignment of these habits is based on multinomial logistic regression with the following buildings and household characteristics as inputs: the type of ventilation system in the house, the year of built, the type of family, the presence of children and the employment types of the household members.

In the next step, the seasonality coherence is determined. The room-habits in summer are determined based on this seasonality coherence and the room habits in winter. The household-habits are for some households extended throughout the year, while others reveal other window opening behaviours in summer:

- Windows use is the same as in winter (18.0%)
- All windows opened more (46.6%)
- Windows in the dayzone opened more (25.3%)
- Windows in the nightzone opened more (10.0%)

Finally, these habits are coupled to stochastic occupancy and activity profiles, to predict the window use per time step. In this case the occupancy and activity model as present in the StROBe-model is applied (Stochastic Residential Occupant Behaviour Model, Aerts et al. 2014, Baetens and Saelens 2016). The StROBe-model generates three-state occupancy profiles (away, asleep, active) for the individuals of each household based on their employment type.

Activity probabilities are applied to determine the performance of specific energy consuming activities. The translation of the habits to discrete window use sequences is straightforward, since the habits relate the window use purely to changes in occupancy state and the performance of activities. Since the occupancy and activity profiles are stochastic, the resulting window use profiles are variable as well, and do not represent fixed schedules.

A comparison between this new window use habit model and four different window use models from literature indicated that the latter models underestimate the inter-individual diversity (Verbruggen et al. 2021b).

This window opening model was integrated in a new Event-based Residential Occupant Behaviour model (EROB) using the modelling approach of the StROBe-model. In first instance the occupancy and activity profiles of the household and its individual members are defined, based on some characteristics of the household. The other types of occupant behaviour (electricity use, heating behaviour, internal heat gains, domestic hot water use and window use) are subsequently linked to these profiles. The modelling of each of these steps and the adaptations compared to the StROBe-model is described in detail in the work of Verbruggen (2021).

### 3 MODELLING APPROACH

A mulizone building energy simulation model was created in the object-oriented modelling language Modelica, created based on components of the Modelica 3.2.3 and the IDEAS 2.1.0 library (Jorissen et al. 2018) within the simulation environment Dymola.

The model is based on one of the houses from a NZEB case-study neighbourhood (Janssens et al. 2017). It represents a 2-storey terraced house with 3 bedrooms, with a total floor area of 100 m<sup>2</sup>, north-south orientation, and operable windows in all rooms. In the model an ideal heating system is applied which directly compensates the heating demand to the given set-point profiles. The model is coupled to climate data from Uccle, Belgium. Figure 1 shows the floorplan of the house. The building structure components exist of 9 zones representing the different rooms. Three building designs with different energy performance levels were created:

- NZEB – Highly insulated and airtight building envelope ( $v_{50} = 1 \text{ m}^3/\text{h}/\text{m}^2$ ), balanced mechanical ventilation system with heat recovery (80% effectiveness), summer bypass and constant flow rate (122 m<sup>3</sup>/h dwelling flow rate).
- E100 - Medium energy performance: building envelope compatible to energy performance standards of 2006, at the start of the EPB regulations in Flanders, medium airtightness ( $v_{50} = 5 \text{ m}^3/\text{h}/\text{m}^2$ ), demand-controlled exhaust ventilation system (room flow rate is reduced from 100% of design flow rate to 20% when CO<sub>2</sub>-concentration in a room is lower than 800 ppm). Total dwelling design flow rate is 240 m<sup>3</sup>/h.
- Y70 - Poor energy performance: building envelope compatible to building practices in the 1970's. This means limited or no insulation, simple double glazing, a poor airtightness ( $v_{50} = 12 \text{ m}^3/\text{h}/\text{m}^2$ ), and no ventilation system.

The flow rate due to window airing is calculated with the equation of Phaff for single sided ventilation which is based on the temperature difference and wind speed (Dubrul 1988), assuming a tilted window as this was the most common window state according to the online survey. This approach was chosen over the use of the window/door-airflow component of IDEAS, since it results in faster simulations. The flow rate by infiltration is simulated per zone as a constant value based on the zone airtightness.

To assess the impact of occupant behaviour and window use on the energy use and IEQ, the outputs of the EROB-model are used as inputs in the Modelica model of the dwelling. Since



the EROB model is stochastic, 30 households were simulated to get a representative result sample. For each of the households, first the occupancy and activity-profiles are created. Based on the number of persons present in each zone, the metabolic heat gains and CO<sub>2</sub>-production are determined. Additionally, the heating set-points in each zone and the demand of domestic hot water is given to the heating system. Identical profiles are used for each of the three building designs, except for the window use as it is dependent on the installed ventilation system in the EROB model. A high diversity in window use is observed between the simulated households, as shown in Figure 2.



Figure 1: Ground and first floor of terraced house

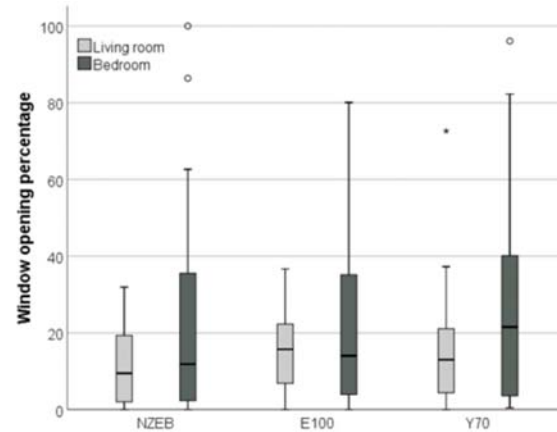


Figure 2: Window opening percentage for the different households in the living room and bedroom

## 4 IMPACT OF OCCUPANT BEHAVIOUR

To assess the influence of including the different types of OB, the simulations were carried out for each type of behaviour separately (occupancy/activity, heating behaviour, and window use) and for the combination of all OB types. The DHW and electricity use were not considered in this comparison as they do not have an influence on the energy use for space heating or indoor environmental quality. For the comparison only the behaviour under review was changed while the other types of behaviour remained fixed as in a base-model. The base-model represents a simple OB-model by assuming default settings:

- The heating set-point is always 20°C in all rooms.
- The windows are always closed.
- An average occupancy and activity profile is selected to account for the internal heat gains.

### 4.1 Impact on heating energy use

The results of the simulations for the energy use for space heating are given in Figure 3. The base-model predicts a yearly energy use for space heating of 1683 kWh/year, 5609 kWh/year and 13991 kWh/year, for respectively the NZEB-building, E100-building and Y70-building (surface area is 100 m<sup>2</sup>). The inclusion of different occupancy profiles and associated internal heat gains leads to a limited change and variation compared to the base profile. As can be expected, the introduction of heating behaviour (varying set-points) has a larger influence on the total heating energy demand. The average heating energy use is significantly lower compared to the base-model for all buildings. This can be attributed to the choice of a uniform heating set-point of 20°C in the base-model, while the EROB-model often predicts unheated bedrooms and bathrooms, and therefore a lower heating demand.

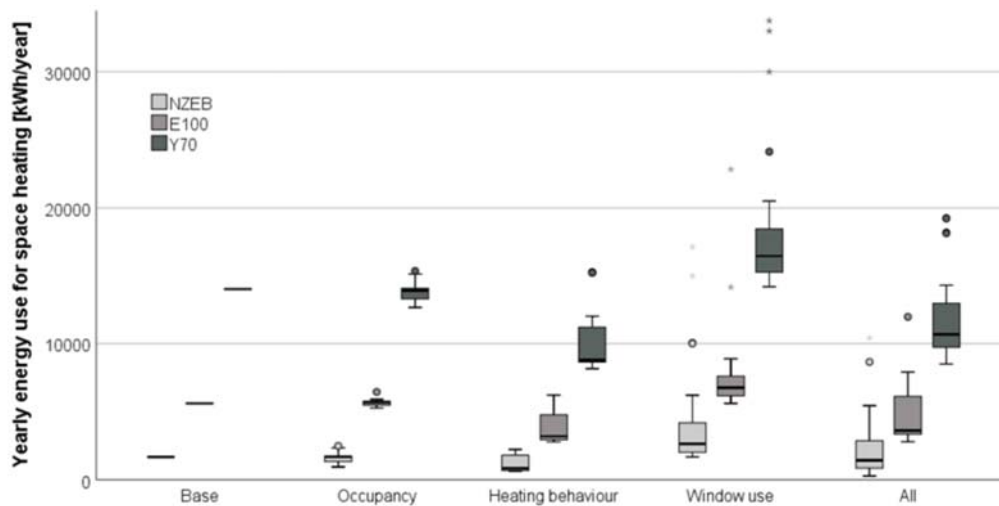


Figure 3: Variation of yearly energy use for space heating across 30 different households for three different dwelling performance levels and for the different types of occupant behaviour.

The inclusion of the window opening behaviour results in the highest variability in heating energy use. It is observed that the impact of including window use is proportionally smaller and leads to a smaller variation in the E100-building compared to the other buildings. Since the opening of windows reduces the CO<sub>2</sub>-concentration the demand controlled ventilation system operates less in boost-mode, reducing the ventilation flow rates of the ventilation system and with that the heating demand. The inclusion of the window use without including other types of OB leads to the highest average energy use for heating. This can be explained by the fact that in this case the heating set-point remains 20°C even when windows are opened.

The average heating energy use when all types of OB are jointly considered is respectively 2314 kWh/year, 4740 kWh/year and 11768 kWh/year for the different performance levels. This average energy use is higher than the base-model load for the NZEB-building, and lower for the E100 and Y70-building. This difference can be attributed to the combination of the heating behaviour and window use. While the inclusion of the window use increased the energy use compared to the base-model, the lower heating set-points reduced the energy use. Since the heating behaviour has a smaller impact in the NZEB-building the average energy use increased, while for the other buildings the average energy use decreased. As a consequence, the expected energy use reduction between E100 and NZEB is smaller when occupant behaviour diversity is considered compared to the base case.

In the previous simulations the different types of OB were simulated separately. While the connection between the occupancy and the other behaviours is taken into account, the heating set-point profiles are independent of window use profiles. In reality window use is possibly interrelated with the heating behaviour, as many occupants will close the window when turning on the heating or the other way around. To assess the impact of the combination of different types of behaviours, the complete model as discussed above is compared with a similar model but including the restriction that the heating is turned off in a room when the window is opened. The results of these simulations are shown in Figure 4. Obviously the heating energy use decreases when the heating is turned off with window opening. The average heating energy use is respectively 1977 kWh/year, 4583 kWh/year and 10272 kWh/year for the different performance levels. While the median energy use decreased only slightly, the households with very high energy use were reduced more significantly, with that reducing the range of the heating energy use. The difference with the base case is even more pronounced, specifically for the Y70 case. This also illustrates the importance of further research on OB relations.

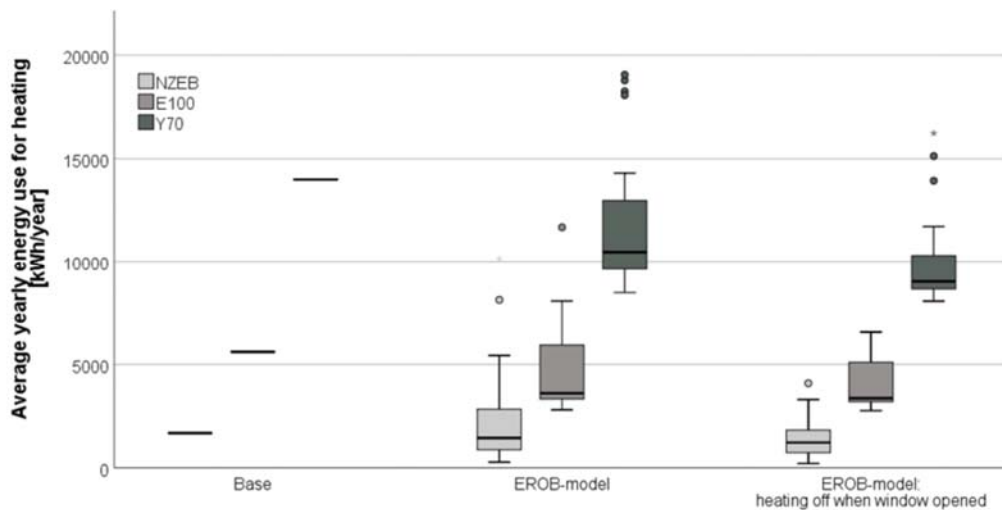


Figure 4: Variation of yearly energy use for space heating across 30 different households for three different dwelling performance levels for the combination of all OB and for the combination of all OB assuming the heating in a room is switched off when a window is open.

## 4.2 Impact on Indoor Air Quality (IAQ)

The impact of OB on IAQ is assessed using the CO<sub>2</sub>-concentrations as evaluation criteria. The average yearly CO<sub>2</sub>-concentrations as simulated for the master bedroom is shown in Figure 5 as an illustration of typical results.

The type of ventilation system and building envelope airtightness have an important influence on the average CO<sub>2</sub>-concentration in the rooms. The average yearly CO<sub>2</sub>-concentration is the highest for the Y70-building, followed by the NZEB-building and the E100-building. This finding applies both for the base case and for the cases with variations in OB. The constant flow rate of the balanced ventilation system in the NZEB-building (50% of the design flow rate to account for manual control settings) is not always sufficient leading to higher CO<sub>2</sub>-concentrations compared to the demand driven ventilation system (E100) for which the flow rate is increased to the design flow rate when the threshold of 800 ppm is exceeded. The Y70-building is the least airtight, but has no ventilation system, resulting in the highest CO<sub>2</sub>-concentrations.

The inclusion of different occupancy profiles results in wide variations in yearly average CO<sub>2</sub>-concentrations per household, especially in the NZEB and Y70-building. Due to the demand controlled ventilation system, the variation in CO<sub>2</sub>-concentration is more limited in the E100-building. The window use impacts the average CO<sub>2</sub>-concentration as well. While the maximum CO<sub>2</sub>-concentration is observed for the base-model (all windows closed), it was significantly reduced by the opening of windows. The effect is most pronounced in the seventies building, as the efficient use of the windows can reduce the CO<sub>2</sub>-concentrations to similar levels as in buildings where ventilation systems are installed.

## 4.3 Impact on overheating

Finally an assessment is made of the impact of OB modelling on the overheating predictions by including OB in the building simulations. The overheating is expressed in Kelvin hours above 26°C (operative temperature). Figure 6 shows the overheating for the living room.

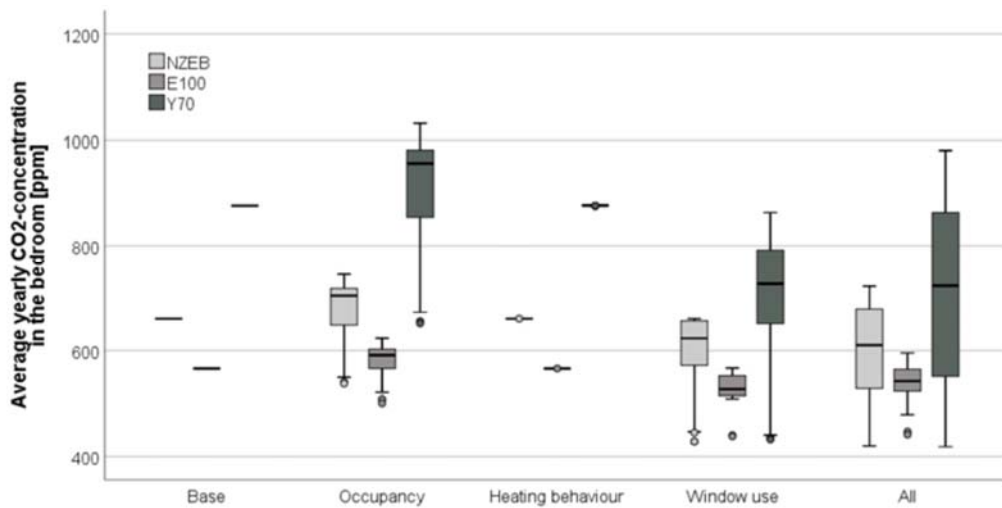


Figure 5: Variation of the yearly average CO<sub>2</sub>-concentration in the master bedroom, as a measure for the indoor air quality, across 30 different households, for three different dwelling performance levels and for the different types of occupant behaviour.

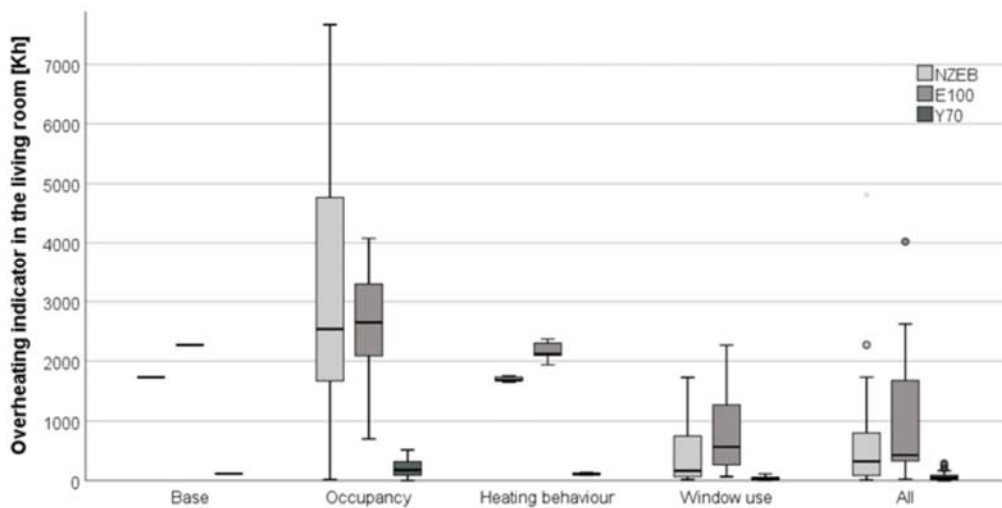


Figure 6: Variation of the overheating indicator in the living room across 30 different households, for three different dwelling performance levels and for the different types of occupant behaviour.

Overheating is more common in the NZEB and E100-buildings due to the well insulated building envelope, especially in the living rooms. In the E100-building overheating is even more prevailing than in the other two cases because of the lower ventilation rate as a result of demand control during times with low CO<sub>2</sub>-concentrations, when nobody is present in the room. The variation in occupancy profiles has a significant impact on the overheating prediction, especially in the energy efficient buildings. The internal heat gains due to persons and appliances lead to more overheating, but as well larger variations in the overheating indicator, with some households experiencing rarely any overheating. Again the window use has a significant impact on the overheating prediction, with the maximum overheating when the windows are always closed and no overheating at all when the windows are frequently used. The distribution of the overheating due to the varying window use is strongly skewed to the lower end, even though the window use itself is only slightly skewed for the NZEB-building and normally distributed for the other buildings. This indicates that even window use profiles with limited window opening are already sufficient to lower the overheating significantly.

## 5 CONCLUSIONS

The results revealed that occupant behaviour is important to take into consideration, not only for energy use predictions but as well for assessment of overheating and IAQ, especially in more energy efficient buildings. The use of the EROB-model does not only benefit the energy use predictions but as well the design and control of different systems such as for ventilation or cooling.

Of all OB-types window use had the most important influence on the three evaluated metrics, emphasising the importance of including window use in BES. While the inclusion of the window use led to an increase in the energy use, it led to a decrease in overheating and CO<sub>2</sub>-concentration, and thus in better assessed IEQ. The average energy use of the high performance NZEB-building increased when the OB-model was included compared to the base-model, while it decreased for the other two less energy efficient dwelling performance levels, revealing a similar trend as often observed in performance gap research. This indicates that occupant behaviour may be an important part of the explanation of the performance gap. To further improve the OB-models, research on the combination of different behaviours is necessary.

## 6 ACKNOWLEDGEMENTS

We gratefully acknowledge the financial support received for this work from the Fund for Scientific Research (FWO) in the frame of the strategic basic research (SBO) project “NEPBC: Next generation building energy assessment methods towards a carbon neutral building stock” (S009617N).

## 7 REFERENCES

- Aerts, D. et al. (2014). A method for the identification and modeling of realistic domestic occupancy sequences for building energy demand simulations and peer comparison. *Building and Environment*, 75, 67-78.
- Baetens, R. & D. Saelens. (2016). Modelling uncertainty in district energy simulations by stochastic residential occupant behaviour. *Journal of Building Performance Simulation*, 10(6), 653-671.
- Dubrul, C. (1988). *Inhabitant behaviour with respect to ventilation – a Summary Report of IEA Annex VIII*. TN23, AIVC. [www.aivc.org](http://www.aivc.org)
- Janssens, A., Vaillant Rebollar, J., Himpe, E., & Delghust, M. (2017). Transforming social housing neighbourhoods into sustainable carbon neutral districts. *11th Nordic Symposium on Building Physics (NSB2017)*, 132, 549-554. <https://doi.org/10.1016/j.egypro.2017.09.732>
- Jorissen, F. et al. (2018). Implementation and verification of the IDEAS building energy simulation library. *Journal of Building Performance Simulation*, 11, 669-688.
- Verbruggen, S. (2021). *Window use habits as an example of habitual occupant behaviour in residential buildings*. Doctoral dissertation, Ghent University, Faculty of Engineering and Architecture, Ghent, Belgium. <http://hdl.handle.net/1854/LU-8725674>
- Verbruggen, S., Delghust, M., Laverge, J., & Janssens, A. (2021a). Habitual window opening behaviour in residential buildings. *Energy and Buildings*, 252. <https://doi.org/10.1016/j.enbuild.2021.111454>
- Verbruggen, S., Delghust, M., Laverge, J., & Janssens, A. (2021b). Comparative window use study: habits versus deliberative actions in residential buildings. *Proceedings of Building Simulation 2021: 17th Conference of IBPSA* (17, 3639-3645). <https://doi.org/10.26868/25222708.2021.30847>

# Literature Review on Windows Airtightness Performances: Insights and Gaps

Martin Prignon<sup>1</sup>

<sup>1</sup> Buildwise  
Kleine Kloosterstraat, 23  
1932 Zaventem, Belgium

\*Corresponding author: [martin.prignon@buildwise.be](mailto:martin.prignon@buildwise.be)

## ABSTRACT

Old windows make a major contribution to the authentic look of a façade, and maintaining those elements whenever possible is essential for the conservation of our architectural heritage. However, those are often leaky and are consequently responsible for high energy losses, acoustical and thermal discomfort, and incorrect sizing of the ventilation systems. Having a better knowledge of windows airtightness performance is crucial in assessing need for an intervention based on the balance between costs and impact. In this paper, we review 43 studies published between 1930 and today reporting on window airtightness measurements. The results show that the lack of standardized way of expressing the results and the small number of reported results and the bad repartition among studies make it difficult to draw solid conclusions, especially for in-situ measurements. Despite those limitations, certain trends can be observed based on the reviewed studies: (1) in-situ testing provides worse results than laboratory tests, which is explained by the window-wall interface, the deterioration over time and the deterioration during installation; (2) since the arrival of weatherstripped windows, there is no clear improvement of the windows airtightness over time, for both laboratory and in-situ testing; (3) among the different opening mechanisms, sliding windows are found performing worse than others; (4) among different materials for window frames, steel and aluminium are found performing the worse and wood the best. However, those conclusions were strongly hindered by the identified limitations; (5) existing windows are notably leakier than newly installed windows and the performance seems to decrease over the years, but this was based on a very few numbers of windows tested. Further work should focus on acquiring data from in-situ measurements on existing windows. Those study should report the results in terms of leakage characteristics and minimum information should be the opening mechanism, window frame materials, the period of construction of windows and the year of testing. Additionally, those trends were observed by analysing considerable number of studies with different objectives. Each of the trends observed here should be confirmed and confronted through dedicated studies.

## KEYWORDS

Windows airtightness; Literature review; air infiltration; windows testing

## 1 INTRODUCTION

Windows play a crucial and significant role in our architecture thank to their capacity to admit natural light into interior spaces. Windows make a major contribution to the authentic look of a façade, and maintaining those elements whenever possible is essential for the conservation of our architectural heritage. However, old windows are often leaky, causing high energy and financial costs, as well as thermal and acoustic discomfort for the occupant. The level of leakiness is an important parameter for a building owner helping him to prioritise an intervention based on a balance between impact (e.g., energetic or comfort) and costs (e.g., financial or heritage value).

The first tests to assess the performance of windows regarding air infiltration were reported almost 100 years ago by (Larson et al., 1931). Over the years, multiple authors conducted studies on the quantification of window airtightness. Although each study draws its own conclusions, analyse the full range of studies conducted allows to answer some specific questions related to the evolution over time, the discrepancies between studies or the relevancy of testing more windows.

In this paper, we reviewed the scientific literature on windows airtightness, with a specific focus on the quantification of this component's performance. A total of 43 documents between 1930 and today were reviewed and analysed. Figure 1 shows the repartition of those references over time. Since 1930 the number of studies is constant over the year, except in the period 1940-1950 where no studies were reported and post-2010 where the subject provides a regain of interest. Note that the substantial increase post-2010 can be biased by the higher accessibility of the literature, and the impact of publication period in the research algorithms.

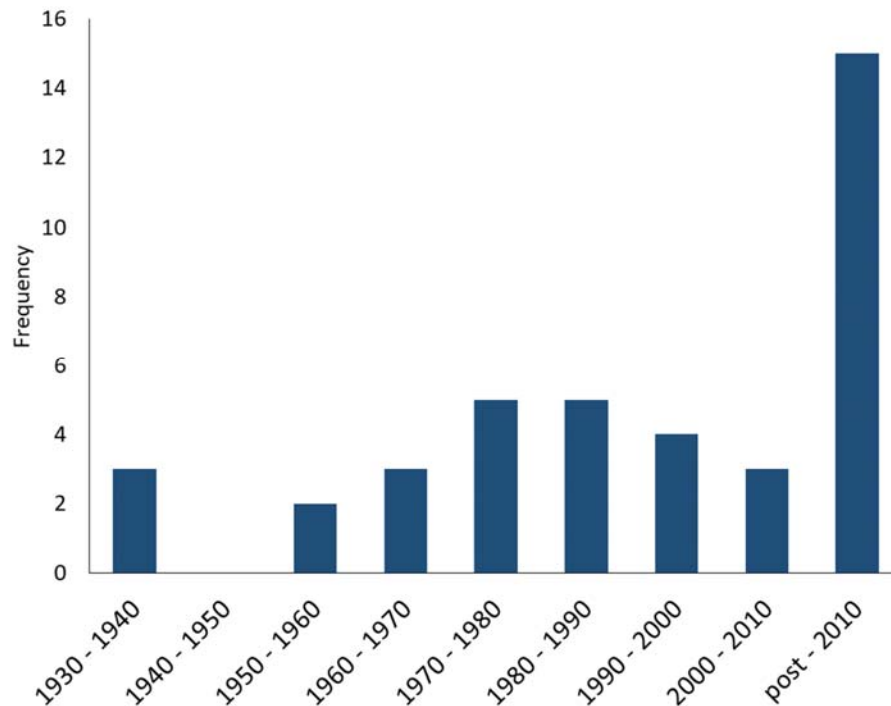


Figure 1: frequency of reported studies by period of publication.

This paper is structured as follows. Section 2 provides an overview of the studies integrated in the analysis as well as some key aspects of this analysis. Section 3 reports all the data coming from the studies and investigate some trends. Section 4 discusses the results with a specific focus on the limitations inherent to the available data. Lastly, section 5 concludes by summarizing the outcomes of this paper, the limitations, and the needed further research.

## 2 OVERVIEW OF THE STUDIES INCLUDED IN THE LITERATURE REVIEW

### 2.1 Methods for airtightness performance assessment

Among the 43 documents, eight were removed from the extended analysis for different reasons: one paper assesses the airtightness performance of windows through parametric approach and not measurements (Cheng and Li, 2018) ; one paper provides no information about the methodology for data acquisition (Jiu and Yu, 1983) ; six papers investigated the impact of an intervention on the airtightness performance by measuring the difference between pre- and post-intervention measurements, but the data provided could not be used to deduce the performance of the component itself (Catalina et al., 2020; Cuce, 2017; d'Ambrosio Alfano et al., 2016; Davies et al., 2005; Fernández-Agüera et al., 2012; Tombarević et al., 2023). In addition, two documents do not reported results of an experiment, but are databases: AIVC (Orme and Leksmono, 2002) and ASHRAE (ASHRAE, 2001). Note that the ASHRAE database is not provided anymore in the recent edition of the handbook of fundamentals. The 33 remaining

studies can be divided in three groups based on the methods for performance assessment: laboratory measurements, in-situ measurements using the direct method, and in-situ measurements using the indirect method.

Laboratory measurements consist in placing the tested window in an equipment that allows to pressurize and depressurize the window alone, then the air flow needed to maintain a pressure difference between both sides of the window is recorded. The test method is defined in different standards as such as (ISO 1026, 2016) or (ASTM E283, 2019). In-situ measurements can be divided into two types: the direct measurements where the tested window is isolated from the rest of the building and is directly pressurized and/or depressurized; and the indirect component where a whole zone is tested using traditional methods (e.g., the fan pressurization testing) two times consecutive, with the tested window sealed between both tests. The component performance is then given as the difference between both tests. It has been shown in (Prignon, 2020) that the indirect method provides higher uncertainties than the direct method. However, in some cases the ease of installation makes it a relevant alternative to the direct method. Table 1 shows the repartition of the methods of assessment used among different reported studies.

Table 1: repartition of 33 analysed references by assessment methods

Method used in the papers	N	References
Laboratory measurements	16	(Carruthers and Newman, 1977; Coleman and Heald, 1940; Fleury and Thomas, 1972; Konstantinov and Verkhovsky, 2020; Larson et al., 1931; Lund and Peterson, 1952; Mantle, 1958; Miškinis et al., 2019; Provan and Younger, 1986; Rousseau, 1991; Rusk et al., 1933; Sasaki and Wilson, 1965; Shoda et al., 1970; Van Den Bossche and Janssens, 2016; Villiere, 1962)
In-situ: direct measurement	11	(Daoud et al., 1991; Feng et al., 2020; Fournier et al., 2007; McGrath, 1982; Park and Kim, 2019; Persily and Grot, 1984; Prignon, 2020; Shapiro and James, 1997; Shaw, 1980; Ward and Sharples, 1982; Weidt, 1979)
In-situ: indirect measurement	6	(Almeida et al., 2017; Hall and Hauser, 2003; Kovanen and Sateri, 1997; Pereira et al., 2014; Pinto et al., 2011; Tamura, 1975)

## 2.2 Metrics for airtightness performance of windows and standardization

The performance of the window is defined by the air leakage rate of the window at different pressure differences. The relation between both is usually provided using following equation:

$$q = C_w(\Delta p)^{n_w} \quad (1)$$

Where  $q$  is the air leakage rate across the window for a pressure difference  $\Delta p$ ,  $C_w$  and  $n_w$  are the leakage characteristics of the characterised window. In the analysis of the 35 studies (33 quantification studies and two databases), four important aspects should be considered for a relevant comparison of the reported results:

- There are three different ways information are provided: 7 studies provide the full test result (table or graphic), 7 studies provide the leakage characteristics (leakage coefficient and exponent), and 21 studies provide the airflow at a reference value. Note that the leakage characteristics can be deduced from the full test results and the reference value can be deduced from the leakage characteristics.
- Units used for airflows are [m<sup>3</sup>/h] in 18 studies, [cfm] in 5 studies, [cfh] in 4 studies, ELA (effective leakage area) in 2 studies, [L/s] in 3 studies, [dm<sup>3</sup>/s] in 2 studies and [m<sup>3</sup>/s], in one study. For the pressure difference (only relevant when the reference value is used), units are [Pa] for 15 studies, [in] of water for 4 studies and [mph] for 2 studies. Although translating results from one unit system to another is not difficult, having them presented in different ways can be an obstacle when comparing results with existing literature.



- When a reference value is used, a reference pressure must be defined. Using Pascals as a common unit, the reference pressure is 4 Pa for 2 studies, 10 Pa for one study, 50 Pa for 8 studies, 75 Pa for 5 studies, 100 Pa for 4 studies, and 600 Pa for one study. If a reference value is used, one can assume a value for the flow exponent and use equation (1) to express the results at a different reference value. A typical value for the flow exponent for buildings is  $n = 0.65$  (ASHRAE, 2001), but a value of 0.6 is observed in this review, when looking at the 14 studies (Total sample size of 720) that provided enough information to deduce the flow exponent.
- The normalization of the results is usually done either considering  $L$ , the length of opening joint (18 studies); or  $A$ , the area of the window (7 studies). One study provides some results in terms of length of opening joint and others in terms of windows area, and 5 studies provide results normalized using both approaches. Three studies provide not-normalized results. When looking at the ratio  $L/A$  based on the 5 studies using both approaches, an average value of  $2.5 \text{ m/m}^2$  is found. This is an interesting observation since in the classification of EN 12207, a ratio of  $4 \text{ m/m}^2$  is assumed in the definition of class boundaries.

In this paper, the results are presented using a reference value of airflow in  $\text{m}^3/\text{h}$  at 50 Pa of reference pressure and normalized per meter of opening joint. When needed for conversion, an airflow exponent of 0.6 and a ratio  $L/A$  of  $2.5 \text{ m/m}^2$  were assumed. For 3 studies, the information was not sufficient to express the results in that way, and were consequently excluded in the following analysis.

### 2.3 Windows materials and typology

Different typologies and materials are analysed in the literature. However, the nomenclature used is different from one study to another. Here, we divide the results in four types of windows, based on opening mode:

- Horizontal sliding window,
- Pivot window, which includes vertical pivot, horizontal pivot, and awning,
- Single and double hung windows,
- Side-hung windows, which includes single side-hung, double side-hung, and tilt-and-turn.

Additionally, the window can be weather-stripped or not. Regarding the materials, four different frame materials are considered: wood, PVC, aluminium, and steel.

## 3 VALUES FOR WINDOWS AIRTIGHTNESS

### 3.1 Laboratory measurements

Among 16 studies reporting laboratory measurements, three of them were removed: (Rousseau, 1991) conducted test on whole assemblies and do not focus on the window itself, and both (Coleman and Heald, 1940) and (Villiere, 1962) provided results that could not be normalized. Table 2 provides the list of references that were analysed, including the number of windows tested, if information is provided about windows type and windows materials, and if non-weatherstripped windows are tested or not.

Table 2: List of reference analysed for the laboratory measurements conducted on windows

ID	Reference	N	Windows type	Windows materials	Non-WS
1	(Park et al., 2017)	2	Yes	Yes	No
2	(Larson et al., 1931)	18	No	Yes	Yes
3	(Rusk et al., 1933)	17	Yes	Yes	Yes
4	(Lund and Peterson, 1952)	?*	No	Yes	Yes
5	(Mantle, 1958)	1	No	Yes	No
6	(Sasaki and Wilson, 1965)	39	Yes	Yes	Yes
7	(Shoda et al., 1970)	8	Yes	Yes	Yes
8	(Fleury and Thomas, 1972)	3	Yes	Yes	No
9	(Carruthers and Newman, 1977)	131	Yes	Yes	Yes
10	(Provan and Younger, 1986)	772	Yes	Yes	Yes
11	(Van Den Bossche and Janssens, 2016)	305	Yes	Yes	No
12	(Miškinis et al., 2019)	33	No	Yes	No
13	(Konstantinov and Verkhovsky, 2020)	3	Yes	Yes	No

\* No information provided about the number of elements tested, a value of 1 is considered in the weighted averages

A first analysis of the results (Figure 2) shows for each study the average airflow at 50 Pa, in  $\text{m}^3/\text{h}$  per meter of opening joint. The error bars are given by the standard deviation of the reported results when it could be deduced. For weatherstripped windows the studies report values between 0.04 and  $7.83 \text{ m}^3/(\text{h.m})$ , with a weighted average of  $1.37 \text{ m}^3/(\text{h.m})$  (each study is weighted with the number of windows tested). For non-weatherstripped windows, the studies report values between 1.66 and  $8.71 \text{ m}^3/(\text{h.m})$ , except (Shoda et al., 1970) who reports one case at  $25.94 \text{ m}^3/(\text{h.m})$ , which seems an outlier compared to other results. The weighted average for non-weatherstripped windows is  $3.79 \text{ m}^3/(\text{h.m})$ . Note that (Provan and Younger, 1986) is the last study to report non-weatherstripped results. When looking at weatherstripped windows, no correlation is found between the year of testing (which is considered as the year of publication when no other information is provided) and the airtightness performance.

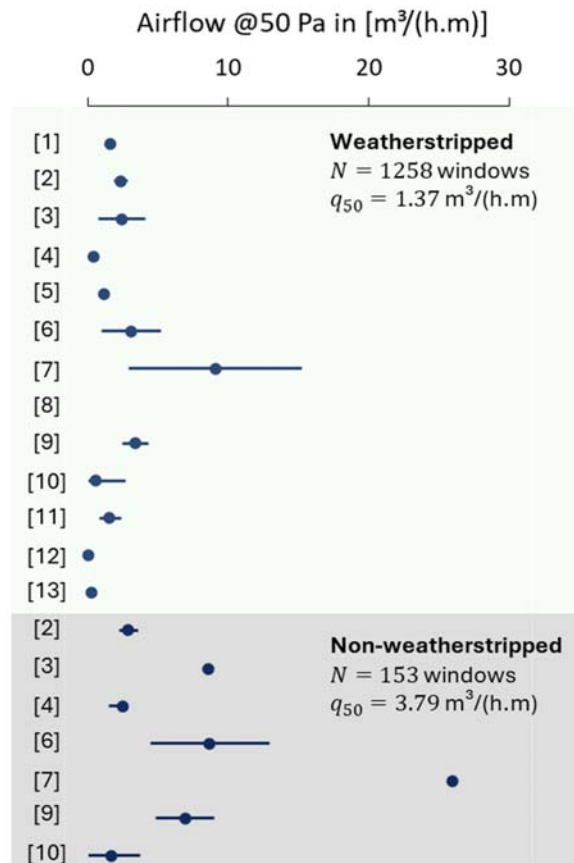


Figure 2. Average value for the airflow rate of each study, when windows are weatherstripped or not, for laboratory measurements.

Table 3 shows the weighted average performance of windows, depending on the opening mechanism. Sliding windows are found performing notably worse than other type of windows. Pivot windows seems to perform better, however only two studies reported those results: (Provan and Younger, 1986) and (Sasaki and Wilson, 1965) reporting respectively 392 and 4 tests on pivot windows.

Table 3: Airflow rate per windows type, for laboratory measurements

Windows type	N	$q_{50}$ [m/(h.m)]	References
Hung	233	0.93	[2; 3; 6; 7; 9; 10]
Pivot	396	0.40	[6; 10]
Side hung	343	1.00	[1; 3; 6; 8; 10; 11; 13]
Sliding	242	3.90	[6; 7; 9; 10; 11]
Unspecified	44	1.27	[4; 5; 7; 10; 12]
All	1258	1.37	-

Table 4 shows similar averages, but as a function of windows materials. Drawing conclusion about such a correlation is complicated because of the considerable number of studies labelled as “unspecified”. Indeed, both (Van Den Bossche and Janssens, 2016) and (Provan and Younger, 1986), combining together 85% of the tests, do not report results per materials. However, they suggest, in their work that no correlation was observed between the airtightness performance and the frame material. Note that steel windows represent less than 3% of the

tested windows for the combined 1062 tests of (Van Den Bossche and Janssens, 2016) and (Provan and Younger, 1986). When looking at the 196 remaining cases, steel seems to perform the least and wood the most.

Table 4: Airflow rate per windows materials, for laboratory measurements

Windows type	N	$q_{50}$ [m <sup>3</sup> /(h.m)]	References
Wood	72	1.32	[2; 3; 4; 6; 12]
Aluminium	99	3.36	[6; 9]
Steel	17	5.50	[3; 5; 6; 7]
PVC	8	3.37	[1; 8; 13]
Unspecified	1062	1.10	[10; 11]
All	1258	1.37	-

### 3.2 In-situ measurements

Among 17 studies reporting in-situ measurements four of them were removed from the analysis because the provided results could not be normalized: (Shapiro and James, 1997), (Pereira et al., 2014), (McGrath, 1982) and (Kovanen and Sateri, 1997). Table 5 provides the list of references that were analysed, including the number of windows tested, if information is provided about windows type and windows materials, and if the tested windows were newly installed or existing.

Table 5: List of reference analysed for the in-situ measurements conducted on windows

ID	Reference	N	Test method	Windows type	Windows materials	New
1	(Weidt, 1979)	192	Direct	Yes	Yes	Yes
2	(Shaw, 1980)	17	Direct	Yes	No	Yes & No
3	(Ward and Sharples, 1982)	10	Direct	Yes	No	No
4	(Persily and Grot, 1984)	18	Direct	Yes	No	No
5	(Daoud et al., 1991)	154	Direct	Yes	Yes	Yes & No
6	(Fournier et al., 2007)	10	Direct	No	No	Yes
7	(Park and Kim, 2019)	3	Direct	Yes	No	*
8	(Feng et al., 2020)	1	Direct	Yes	Yes	*
9	(Prignon, 2020)	13	Direct	Yes	Yes	Yes
10	(Pinto et al., 2011)	2	Indirect	Yes	No	Yes
11	(Tamura, 1975)	17	Indirect	Yes	Yes	No
12	(Hall and Hauser, 2003)	10	Indirect	Yes	No	Yes & No
13	(Almeida et al., 2017)	23	Indirect	Yes	Yes	Yes

\* Not enough information about year of testing and/or year of installation

Figure 3 (left) shows for each study the average airflow at 50 Pa, in m<sup>3</sup>/h per meter of opening joint. The error bars are given by the standard deviation of the reported results when it could be deduced. The results reported by (Fournier et al., 2007) of 57.56 m<sup>3</sup>/(h.m) seems an outlier compared to the other studies where the average lies between 1.66 m<sup>3</sup>/(h.m) and 12.47 m<sup>3</sup>/(h.m). Figure 3 (right) provides the results after removing the 10 cases from (Fournier et al., 2007). The weighted average is 7.43 m<sup>3</sup>/(h.m) considering all studies and 6.32 m<sup>3</sup>/(h.m) when the results reported by (Fournier et al., 2007) are removed. Note that the results from (Fournier et al., 2007) were removed from the rest of the analysis in order to avoid the large impact of this outlier in the global analysis.

The results are relatively similar when using direct and indirect methods (6.02 m<sup>3</sup>/(h.m) and 8.55 m<sup>3</sup>/(h.m) respectively), which is in line with what (Prignon, 2020) found: a difference in the random error is observed when comparing both methods, but no systematic difference. Those results are notably worse than the laboratory results. This was expected because of two major differences in the tested components: (1) laboratory measurements usually measure the

window frame alone, while in-situ measurements are used to quantify the total performance, including the window-wall interface, (2) laboratory measurements are conducted on new windows while in-situ measurements reports results from newly installed and existing windows. This means that a difference is also observed because of the deterioration during installation and the deterioration over time for the windows.

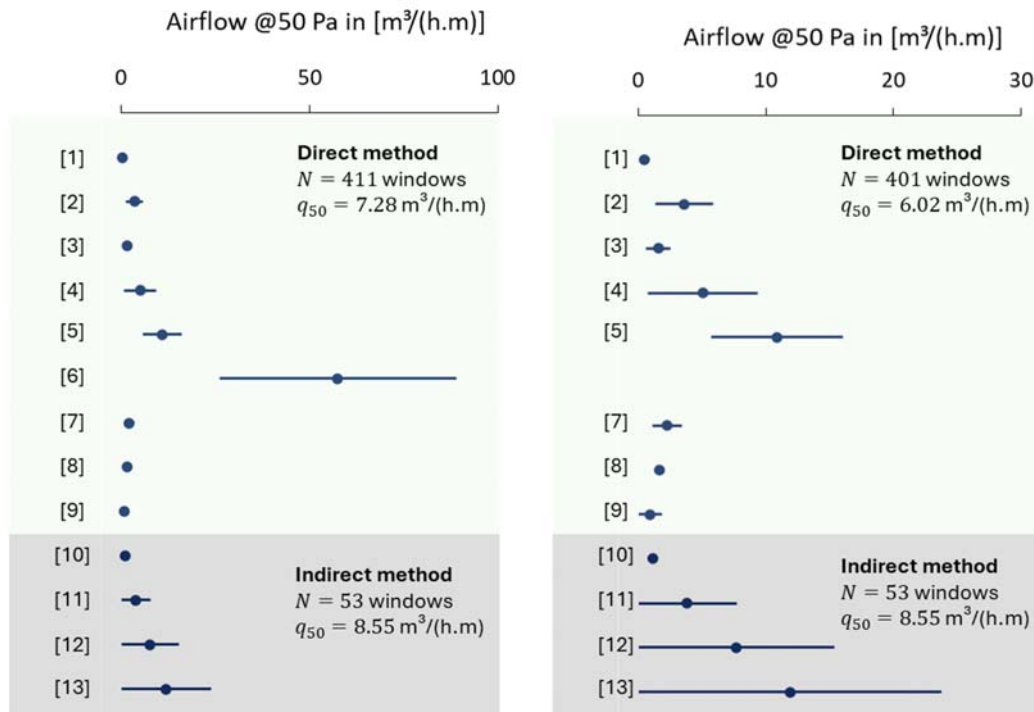


Figure 3. Average value for the airflow rate of each study, for indirect and direct in-situ measurements

Table 6 shows the impact of windows type on the airflow rate at 50 Pa for the in-situ measurements. Unfortunately, the small number of measurements and the large discrepancy between studies make difficult to draw solid conclusions from those results. This is especially true for the pivot windows, where 78% of the windows tested come from (Daoud et al., 1991). This means that the observed difference may also be related to the experimental designs of the study itself rather than the windows type. For the rest, the trends seem similar but less pronounced than the laboratory measurements: sliding windows perform worse than hung and side hung windows.

Table 6: Airflow rate per windows type, for laboratory measurements

Windows type	N	$q_{50}$ [m/(h.m)]	References
Hung	49	3.39	[1]
Pivot	32	17.01	[1; 2; 5; 12]
Side hung	172	5.17	[1; 5; 8; 9; 11; 12; 13]
Sliding	182	6.36	[1; 2; 3; 5; 7; 10; 11; 13]
Unspecified	19	5.85	[4; 13]
All	454	6.32	-

When investigating the correlation with windows materials, although the results are in line with the observations made for laboratory measurements (i.e., aluminium windows perform worse than wood windows), the same observation is made than for the windows type: the repartition

of tested windows among studies hinders the drawing of strong conclusions. Indeed, 67% of the results for aluminium windows come from (Daoud et al., 1991) and 87% of the results for wood windows come from (Weidt, 1979).

Table 7: Airflow rate per windows materials, for in-situ measurements

Windows materials	N	$q_{50}$ [m/(h.m)]	References
Wood	175	2.70	[1; 9; 11; 13]
Aluminium	219	9.26	[1; 5; 8; 9; 13]
Unspecified	70	6.17	[2; 3; 4; 7; 10; 12]
All	454	6.32	-

In-situ measurements are usually preferred over laboratory measurements in two cases: when there is a demand for measuring the difference between the manufacturer's datasheet and the real in-situ performance (including the impact of the window-wall interface and the damages during on site installation) or to assess the performances of existing windows and the potential impact of renovation. Table 8 provides the results obtained for newly installed windows compared to existing windows. Note that the studies of (Daoud et al., 1991) and (Hall and Hauser, 2003) were characterized as unspecified because they do not provide enough information to differentiate existing windows from newly installed windows. Nevertheless, (Daoud et al., 1991) state that when window age is < 10 years, age has no impact and that older windows had improved performances. Additionally, the standard deviation of newly installed windows was found larger than for older windows, suggesting that quality control has declined over time. Contrary to the observations made in (Daoud et al., 1991), here the newly installed windows are found performing better than existing windows (2.35 m<sup>3</sup>/(h.m) and 6.85 m<sup>3</sup>/(h.m) respectively). However, as for the opening mechanism and the materials, the repartition of number of windows tested was also a problem in this analysis since 87% of the newly installed windows were tested by (Weidt, 1979).

Table 8: Airflow rate for newly installed windows and existing windows, for in-situ measurements

Windows type	N	$q_{50}$ [m/(h.m)]	References
Newly installed	220	2.35	[1; 2; 9; 10]
Existing	73	6.85	[2; 3; 4; 11; 13]
Unspecified	161	11.51	[5; 7; 8; 12]
All	454	6.32	-

When looking at existing windows, an interesting information is the age of the window when the test is conducted. Since the data from (Ward and Sharples, 1982) were not enough detailed to include those windows to the analysis, 63 windows were divided in three categories: 0 – 10 years, 10 – 25 years and above 25 years. Results in Table 9 show that there seems to be degradation over time. However, the number of results reported in each category is low, as such as the number of different studies reporting it.

Table 9: Airflow rate as a function of windows age at the time of testing for existing windows, for in-situ measurements

Windows age	N	$q_{50}$ [m/(h.m)]	References
0 – 10 years	23	4.53	[2; 4; 13]
10 – 25 years	35	6.73	[2; 11; 13]
Above 25 years	5	17.02	[13]
All	63		-

#### 4 DISCUSSION

When a study reports testing results of windows airtightness, it usually provides enough information to meet its own objective. However, it misses sometimes basic information that could be relevant in the context of correlation assessment as it was done in this paper. Based on this literature review, we suggest for any study in that context to include at least:

- The method used for testing, which are laboratory measurement, in-situ direct measurement or in-situ indirect measurement.
- The number of windows tested, the type of opening mechanism, the materials of windows frame. In case of in-situ measurements, the age of the window and the installation period should also be provided.
- The airflow rate at 50 Pa per meter of opening joint should be the reference value. Ideally the windows characteristics (i.e.,  $C$  and  $n$ ) should be given so the airflow rate at any pressure difference could be deduced without any assumption on the leakage exponent. When possible, the area of the window should also be given.

Since standardized laboratory testing are now widespread practice for windows manufacturers, the number of test available is large (more than 1.400 vs. less than 500 for in-situ measurements). In addition, the number of variables in laboratory testing is lower, leading to a lower standard deviation of the results and, consequently, a lower number of measurements needed to draw relevant and significant conclusions. In this study, conclusions on in-situ measurements were complicated to draw because of the considerable number of variables and of the small number of data available. This is especially true when measuring the performance of existing windows with a specific focus on the performance deterioration over time. This question is of foremost importance given the ambitions of putting in place optimal renovation strategies. Indeed, that information is relevant in (1) choosing the more durable solution and (2) identifying the real potential of improvement when an intervention is done on a window.

#### 5 CONCLUSION

In this paper, we reviewed around 40 papers reporting measurements related to windows airtightness between 1930 and today. Among those, 33 could be used to directly deduce airtightness performance of windows, divided as follows: 16 laboratory measurements, 11 in-situ direct measurements and 6 in-situ indirect measurement. A series of interesting insights were deduced from the literature review:

- When needed for normalization of the results, following information could be used for windows: an airflow exponent of  $n = 0.6$  (average based on 720 cases from 14 studies) and an opening joint length to window area ratio of  $L/A = 2.5 \text{ m/m}^2$  (based on 429 cases from 5 studies).
- Based on laboratory measurements, (1) weatherstripped windows perform better than non-weatherstripped windows. However, those are not used anymore; (2) among weatherstripped windows, the year of test does not seem to impact window airtightness; (3) sliding windows are found performing the worse and pivot windows the best, but only two studies report results on pivot windows; (4) aluminium frames perform the worse and wood the best, but only 15% of the tested windows could be used to draw this conclusion because

of the lack of information. Those observations are not in line with the observations made by (Van Den Bossche and Janssens, 2016) and (Provan and Younger, 1986).

- Laboratory measurements provide better results than in-situ measurements, probably because the window-wall interface that is included in in-situ measurements, the deterioration during window installation and the deterioration over time.
- Based on in-situ measurements, almost no conclusion can be drawn because of the small number of reported studies and the bad repartition of them among different studies. Although trends are observed, those should not be considered as evidence because of those limitations.

In-situ measurements of windows airtightness provide high-quality information, especially on existing windows. Those could be helpful in defining durable choices based on the deterioration over time, and in predicting the real impact of a renovation on the global performance of the building. However, when looking at this review, testing on existing windows represents less than 5% of the total amount of windows tested. Further work should focus on acquiring high-quality data over airtightness performance of existing windows, depending on the year of installation. Additionally, those trends were observed by analysing considerable number of studies with different objectives. Those trends should now be confronted to dedicated studies, especially on the potential of improvement for leaky windows for different type of intervention (e.g., new joints or complete replacement).

## 6 ACKNOWLEDGEMENTS

This research is conducted in the context of the PERCHE project, funded by INNOVIRIS (Grant n° 2022-JRDIC-9a).

## 7 REFERENCES

- Almeida, R.M., Ramos, N.M., Pereira, P.F., 2017. A contribution for the quantification of the influence of windows on the airtightness of Southern European buildings. *Energy and Buildings* 139, 174–185. <https://doi.org/10.1016/j.enbuild.2017.01.012>
- ASHRAE, 2001. Handbook of fundamentals. American Society of Heating, Refrigerating and Air-Conditioning Engineers, Inc.
- ASTM E283, 2019. Standard Test Method for Determining Rate of Air Leakage Through Exterior Windows, Skylights, Curtain Walls, and Doors Under Specified Pressure Differences Across the Specimen.
- Carruthers, J.F.S., Newman, C., 1977. The repeatability and reproduceability of test results on windows and wall span elements and the expected results. Presented at the Paul Rousseau Symposium on the Testing of Wall Elements and Windows, Brussels, Belgium.
- Catalina, T., Iordache, V., Iordache, F., 2020. Correlation between air and sound propagation to determine air permeability of buildings for single/double wood pane windows. *Energy and Buildings* 224, 110253. <https://doi.org/10.1016/j.enbuild.2020.110253>
- Cheng, P.L., Li, X., 2018. Air infiltration rates in the bedrooms of 202 residences and estimated parametric infiltration rate distribution in Guangzhou, China. *Energy and Buildings* 164, 219–225. <https://doi.org/10.1016/j.enbuild.2017.12.062>
- Coleman, E.F., Heald, R.H., 1940. Air Infiltration Through Windows. National Bureau of Standards (U.S.).
- Cuce, E., 2017. Role of airtightness in energy loss from windows: Experimental results from in-situ tests. *Energy and Buildings* 139, 449–455. <https://doi.org/10.1016/j.enbuild.2017.01.027>
- d’Ambrosio Alfano, F.R., Dell’Isola, M., Ficco, G., Palella, B.I., Riccio, G., 2016. Experimental air-tightness analysis in mediterranean buildings after windows retrofit. *Sustainability* 8, 991. <https://doi.org/10.3390/su8100991>



- Daoud, O., Maheshwari, G., Al-Shami, H., 1991. Measured field performance of aluminium windows in Kuwait. *Energy and buildings* 17, 75–85. [https://doi.org/10.1016/0378-7788\(91\)90073-C](https://doi.org/10.1016/0378-7788(91)90073-C)
- Davies, M., Mumovic, D., Ridley, I., Oreszczyn, T., 2005. The reduction in air infiltration in dwellings due to window replacement. Presented at the 10th International Conference on Indoor Air Quality and Climate, Beijing, China.
- Feng, G., Wang, Y., Xu, X., Wang, K., 2020. Test and Analysis of Airtightness of External Windows for the Nearly Zero-Energy Building in Severe Cold Area. Presented at the 11th International Symposium on Heating, Ventilation and Air Conditioning (ISHVAC 2019), Harbing, China.
- Fernández-Agüera, J., Suárez, R., Heiselberg, P., 2012. Influence of improvement of air-tightness on energy retrofit of social housing, a case study in a mediterranean climate. Presented at the 12th AIVC Conference “Air Movement and Ventilation Control within Buildings,” Ottawa, Canada.
- Fleury, G., Thomas, M., 1972. Variation de la perméabilité à l’air des fenêtres en fonction de la température extérieure. Dispositif de mesure et exemples d’application. (No. 132), Cahier CSTB.
- Fournier, M., Berthault, S., Carrié, R., 2007. In situ measurement of window air tightness: stakes, feasibility, and first results. Presented at the 2nd PALENC Conference and 28th AIVC Conference, Crete Island, Greece.
- Hall, M., Hauser, G., 2003. In situ Quantifizierung von Leckagen bei Gebäuden in Holzbauart : Abschlussbericht (AIF-Forschungsvorhaben No. 12611 N). Universität Kassel.
- ISO 1026, 2016. Windows and doors - Air permeability - Test method.
- Jiu, G.X., Yu, T.H., 1983. The present situation of airtightness and thermal insulation of windows and the practical measures of energy saving. A brief report. Institute of Building Physics Chinese Academy of Building Research, Beijing, China.
- Konstantinov, A., Verkhovsky, A., 2020. Assessment of the negative temperatures influence on the PVC windows air permeability. IOP Conference Series: Materials Science and Engineering 753, 022092. <https://dx.doi.org/10.1088/1757-899X/753/2/022092>
- Kovanen, K., Sateri, J., 1997. Air tightness of apartments before and after renovation. Presented at the 18th AIVC conference, Athens, Greece.
- Larson, G., Nelson, D., Kubasta, R., 1931. Air Infiltration Through Double-Hung Wood Windows. *ASHVE Trans* 37, 571–600.
- Lund, C., Peterson, W., 1952. Air Infiltration through Weatherstripped and Non-Weatherstripped Windows, University of Minnesota (Bulletin No. 35). University of Minnesota.
- Mantle, K., 1958. The measurement of air infiltration through metal-framed windows. *The heating and Ventilating Engineer & Journal of Air Conditionning* 31, 529–531.
- McGrath, P., 1982. Prediction of air infiltration through building components; the assembly of a device to measure air infiltration through components with a suggested method of producing data which could be used to form the basis of a prediction model (Master Thesis). University of Manchester Institute of Science and Technology.
- Miškinis, K., Bliūdžius, R., Dikavičius, V., Burlingis, A., 2019. Assessment of acoustic and thermal properties of airtight wooden windows used in Baltic and Scandinavian countries. *Journal of environmental engineering and landscape management* 27, 135–143. <https://doi.org/10.3846/jeelm.2019.10793>
- Orme, M., Leksmono, N., 2002. GU 5: Ventilation modelling data guide (AIVC Guide No. 5).
- Park, J.J., Kim, Y.I., 2019. Study of infiltration through sliding windows with respect to closing mechanisms and their locations in a building during winter season.

- International Journal of Ventilation 18, 220–232.  
<https://doi.org/10.1080/14733315.2018.1462980>
- Park, S., Kim, M., Lim, J.-H., Song, S.-Y., 2017. Influence of Drainage Holes on Condensation Risk and Air-tightness of Windows. An Experimental Case Study of Triple Glazing PVC Windows. *Journal of Asian Architecture and Building Engineering* 16, 83–90. <https://doi.org/10.3130/jaabe.16.83>
- Pereira, P.F., Almeida, R.M., Ramos, N.M., Sousa, R., 2014. Testing for building components contribution to airtightness assessment. Presented at the 35th AIVC Conference “ Ventilation and airtightness in transforming the building stock to high performance,” Poznan, Poland.
- Persily, A.K., Grot, R.A., 1984. Pressurization testing of federal buildings. Presented at the Symposium on performance of building constructions, Philadelphia, United States.
- Pinto, M., Viegas, J., de Freitas, V., 2011. Air permeability measurements of dwellings and building components in Portugal. *Building and Environment* 46, 2480–2489. <https://doi.org/10.1016/j.buildenv.2011.06.009>
- Prignon, M., 2020. Airtightness of building components (Dissertation). UCLouvain, Belgium.
- Provan, T., Younger, J., 1986. Air infiltration characteristics of windows. *Energy and buildings* 9, 281–292. [https://doi.org/10.1016/0378-7788\(86\)90033-2](https://doi.org/10.1016/0378-7788(86)90033-2)
- Rousseau, J., 1991. CMHC research projects: testing of air barriers: construction details. Canada Mortgage and Housing Corporation.
- Rusk, D.O., Cherry, V., Boelter, L., 1933. Air infiltration through steel-framed windows. *ASHVE Trans* 39, 169–178.
- Sasaki, J., Wilson, A.G., 1965. Air leakage values for residential windows. *ASHRAE Transactions* 71, 81–88.
- Shapiro, A.M., James, B., 1997. Creating windows of energy saving opportunity. *Home Energy Magazine* 13–18.
- Shaw, C., 1980. Methods for conducting small-scale pressurization tests and air leakage data of multi-storey apartment buildings. *ASHRAE Transactions* 86, 241–250.
- Shoda, T., Terasawa, T., Katayama, T., 1970. Experimental study on air and water tightness of metal window sashes. Presented at the 5th International Congress for Heating, Ventilating and Air Conditioning, Copenhagen, Denmark.
- Tamura, C., 1975. Measurement of air leakage characteristics of house enclosures. *ASHRAE Transactions* 81.
- Tombarević, E., Vušanović, I., Šekularac, M., 2023. The Impact of Windows Replacement on Airtightness and Energy Consumption of a Single Apartment in a Multi-Family Residential Building in Montenegro: A Case Study. *Energies* 16, 2208. <https://doi.org/10.3390/en16052208>
- Van Den Bossche, N., Janssens, A., 2016. Airtightness and watertightness of window frames: Comparison of performance and requirements. *Building and Environment* 110, 129–139. <https://doi.org/10.1016/j.buildenv.2016.09.034>
- Villiere, M., 1962. Report on the air and water-tightness of wooden windows. Rapport sur l’étancheité à l’air et à l’eau des fenêtres en bois. Centre Technique du Bois.
- Ward, I., Sharples, S., 1982. An investigation of the infiltration characteristics of windows and doors in a tall building using pressurisation techniques (Report BS No. 68). Faculty of Architectural Studies, University of Sheffield.
- Weidt, J., 1979. Field air leakage of newly installed residential windows. Presented at the ASHRAE/DOE Conference, Florida, United States.

# Exploring the Effect of Post-Pandemic Behaviour of Occupants on Indoor Air Quality and Comfort Conditions in Existing Residential Buildings in Türkiye

Büşra Karadeniz Akkoç<sup>1</sup>, Gülsu Ulukavak Harputlugil<sup>2</sup>

*1 Çankaya University  
Mimar Sinan Street  
Ankara, Türkiye*

*\*Corresponding author:  
busrakaradeniz0000@gmail.com*

*2 Çankaya University  
Mimar Sinan Street  
Ankara, Türkiye  
gharputlugil@cankaya.edu.tr*

## SUMMARY

This study aims to investigate the impact of changing residential user behaviour after the Covid-19 pandemic in 2020-2021 on indoor health and comfort conditions. In this context, user behaviour-focused studies conducted before 2020, the year of the pandemic, and behavioural patterns that changed with the pandemic will be discussed comparatively. To determine the changing user behaviour in houses after the pandemic, we will first ascertain how the behaviour of today's users in the house changes based on the time spent at home, the number of people living in the household, and the evolving psychological expectations after the pandemic. The pandemic process has compelled many people to spend more time at home, leading to significant changes in housing usage habits. The impact of these changing behaviours on indoor air quality constitutes an important research area concerning health and life comfort. In this study, face-to-face interviews with residents will be complemented by measurements to determine indoor comfort conditions, which will be compared with previous data. Behavioural changes will be identified, and the effects of these changes on energy consumption, carbon emissions, and comfort will be discussed.

## KEYWORDS

Indoor Air Quality, Occupant Behaviour, Residential Buildings, Building Stock

## 1 PURPOSE AND SCOPE OF THE STUDY

The main objective of the study is to provide a comparison of the effects of user behaviours that change before and after the pandemic on indoor health and comfort conditions through statistical data. The main objectives can be listed as follows,

**Determination of User Behaviour:** Detailed determination of user behaviour changes that occur in residences after the pandemic. In this context, factors such as time spent at home, working habits, ventilation habits, and cleaning routines will be examined.

**Determination of Indoor Air Quality Parameters:** One of the focal points of the research is the identification of the factors affecting the indoor air quality of the dwelling. In this context, CO<sub>2</sub> level, relative humidity, temperature and atmospheric pressure will be measured and analysed.

**Examining the Relationship Between Two Variables:** Statistical examination of the relationship between user behaviour and indoor air quality parameters.

As a result of this study, the effect of user behaviour on indoor air quality will be analysed and the data obtained will be evaluated. In this way, the impact of changing user behaviour on

indoor air quality after the pandemic will be better understood and recommendations can be made when necessary. This study will contribute to the development of sustainable design and utilisation methods to improve indoor air quality in residential buildings.

## **2 RESEARCH METHODOLOGY**

The aim of the research is to determine the user behaviour profiles in the Turkish society after the pandemic and to reveal the effect of user behaviour on indoor air quality in residential buildings. The result of the study provides the development of a model that takes into account the actual behaviour of residential users and can be used as a decision tool when necessary.

The research is planned to be carried out in two phases, in winter and summer, since the user behaviour in the dwelling may show seasonal differences. In this context, the study is designed with a method based on the steps listed below:

### **2.1 Collecting information on housing users (Questionnaire Survey).**

Information on housing users will be collected through a questionnaire survey in a sample that will cover various housing typologies in Ankara.

2.1.1 Obtaining general information on housing users: The number of people living in the dwellings, as well as their age and gender, are important information for determining comfort perceptions. The planned method for making these determinations is to measure a dwelling for a total of three days, two days on weekdays and one day on weekends, and to fill out a diary that will allow users to track their behaviour in the dwelling during these three days. In addition, a survey will be conducted with each household member. Thus, it will be possible to evaluate their comfort-related behaviours during the hours of use.

2.1.2. Questioning the comfort-related behaviours of the users: In addition to the comfort-related statements of the users, it is also necessary to determine the extent to which the users perform the behaviours required to improve this comfort situation. These behaviours can be defined as opening and closing the windows, adjusting the heating system or thermostat settings, and using the air conditioner (if any). In the light of this information, the user behaviour patterns required for the study will be defined.

### **2.2 Collecting information on the physical characteristics of the dwellings (with the help of data recording systems)**

It is necessary to determine the physical characteristics of the houses together with the data on their users. Thus, as a result of the schemes of the sample groups to be formed according to their behavioural patterns, their relationship with indoor air quality will be clarified.

2.2.1. Determination of housing plans, materials and typologies: The plan diagrams of the houses forming the research sample will be prepared.

2.2.2. Measurement of dwellings with data recording systems: Measurements based on data logging systems will be carried out in order to define the physical characteristics of the dwellings and to compare the information given by the users about comfort in the dwellings, which may vary in the context of personal characteristics (age, gender, activity, etc.) with the average comfort values of the dwelling. During these measurements, the occupants will be asked to keep a record of their daily activities in the dwelling through an online form (such as the frequency of window opening during the day, whether they change the radiator settings, etc.). The occupants will be informed in advance that these measurements will be carried out and the measurements will be carried out with data loggers in the dwellings where permission for measurement is granted.

Measurements in Ankara, Turkey are planned to be conducted in a total of 12 households. These households will be determined to include flat, two storey apartment, detached house, adjacent detached house types. A total of 3 devices will be used for the measurements. For the cooling season measurements since the highest annual average temperature for Ankara occurs in July and August, the measurement dates were determined as July 15-August 10. Measurements will cover five weekdays and one weekend day from Monday to Saturday for each household. On Sundays, the measuring instruments will be collected from the households, the results will be taken and placed in new households.

Table 1: Timetable for measurements in households

Dates	Household A,B,C	Household D,E,F	Household G,H,J	Household K,L,M
15-20 July	x			
22-27 July		x		
29 July-3 August			x	
5-10 August				x

### 3 EXPECTED RESULTS

This study describes a framework for collecting and evaluating data on user behaviour towards indoor air quality in existing buildings. The evaluation of the cooling load, which is one of the expected results, constitutes the scope of this paper. Data collection and evaluation will continue for more than a year, including the heating season, and the results for the analysis of user behaviour can be interpreted after all data has been collected. The most important data source of the project is the measurements to be made in the dwellings and the interviews to be conducted with the users of the dwellings. In this context, housing choices may vary until there are dwellings where these measurements can be successfully collected and adequate interviews can be conducted with users in the same dwellings. Since access to the dwellings will be voluntary, it will be essential to access the dwelling-user groups that can be most easily worked with.

### 4 ACKNOWLEDGEMENTS

This paper forms a part of the study carried out within the scope of Çankaya University Scientific Research project (Project No: MF.24.002).

### 5 REFERENCES

- Darçın, P. (2008). Natural Ventilation Principles in Mitigating Indoor Air Pollution in Buildings (Master's thesis). Yıldız Technical University, Institute of Science, Istanbul.
- Ingeç, S. (2022). An Examination on the Adaptation Dependent on Spatial Perception of the Changing Housing Function After the Pandemic [Master's thesis, Beykent University, Department of Interior Architecture]. Beykent University.
- Sarica, S. N. (2022). Examination of Indoor Air Quality in Different Home Environments (Master's thesis). Eskişehir Technical University, Turkey.
- Yüksel, A., Arıcı, M., Krajčák, M., Civan, M. (2020). A review on thermal comfort, indoor air quality and energy consumption in temples. *Journal of Building Engineering*, 35, 102013.

# Assessment of PM<sub>2.5</sub> particulate matter exposure under different ventilation and air filtration strategies in a kindergarten

J.L. Sánchez-Jiménez<sup>\*1</sup>, M. Ruiz de Adana<sup>1</sup>

*1 Department of Chemistry, Physics and Applied Thermodynamics  
University of Cordoba, Spain*

*\*Corresponding author: p02sajij@uco.es*

## ABSTRACT

Many children between 1 and 3 years of age spend a fraction of their time in kindergartens. Poor indoor air quality, IAQ, could negatively affect children's health, particularly respiratory health, attendance, and academic achievement. Children are at greater risk of getting severe health consequences from indoor air since their bodies are still developing, and children are more susceptible to the effects of air contaminants because they play closer to the ground, engage in more hand-to-mouth activities, and have a decreased ability to identify and protect themselves from potential threats. IAQ and exposure of children to PM<sub>2.5</sub> particulate matter in kindergarten depends on the strategy of ventilation and filtration used. In this paper, an assessment of PM<sub>2.5</sub> particulate matter exposure under different ventilation and filtration systems strategies in a kindergarten was performed.

This study was carried out in a kindergarten for children aged 1-3 years located at Cordoba, Spain. A classroom of 114.87 m<sup>3</sup> with 12 children and one teacher was chosen. PM<sub>2.5</sub> particulate matter values were measured in the breathing zone of children (0.65 m) under three scenarios: a) no ventilation system; b) mechanical ventilation system; c) portable air cleaner and d), a combination of mechanical ventilation and portable air cleaner. The measured data were analysed according to the type of activity performed by the children during the school day (9:05-13:30). The results showed that the intake mass was reduced indoor the classroom with the ventilation system (11%) when concentration of PM<sub>2.5</sub> particles outdoor was low. However, if concentration of PM<sub>2.5</sub> particles outdoor was high the intake mass was worsened by using the ventilation system (353%), by using the portable air cleaner (50%) and by a combination of both systems (144%).

These results suggest that outdoor concentration has a high influence on indoor concentration. Therefore, to improve indoor air quality it is suggested the use of adequate air filters to avoid the ingress of outdoor contaminants to control the indoor PM<sub>2.5</sub> particles concentration.

## KEYWORDS

Air quality, particulate matter, kindergarten, ventilation system, portable air cleaner

## 1 INTRODUCTION

Respiratory diseases are one of the main conditions in the paediatric population, especially at an early age. These common illnesses include asthma, bronchitis, pneumonia, influenza and more recently covid19 (Cho, 2019), (Peláez, 2019). Indoor air quality is a critical factor that can significantly influence the incidence and severity of these diseases. Kindergartens, where children spend a large amount of time indoors (Daisey, 2003), are particularly sensitive

environments. Children have developing respiratory systems and are more vulnerable to air contaminants such as fine particulate matter (PM<sub>2.5</sub>). These particles can come from a variety of sources such as outdoor (Guo, 2010), from furniture or the children themselves depending on the daily activities indoor the classroom (Wang, 2015). Young children are more vulnerable to indoor air contaminants compared to adults (Cienciewicki, 2008). Long-term exposure to contaminated air can affect children's lung development, causing them to be less resistant to air contaminants (Hou, 2015). Therefore, ensuring good indoor air quality in these environments is crucial to protect children's respiratory health and promote healthy development.

Recent research has shown that the implementation of adequate ventilation strategies and the use of air cleaners can significantly reduce indoor air contaminant levels. In (Han, 2023) the evolution of the concentration of PM<sub>2.5</sub> in a kindergarten was studied. The increase in the flow rate of the ventilation system increased the concentration of PM<sub>2.5</sub> by 20%, as the system did not have a filter installed, thus supplying contaminated air indoors. In order to compensate for this, two portable air cleaners were used at their maximum air flow rate. With the installation of a MERV13 filter in the ventilation system, the concentration of PM<sub>2.5</sub> was reduced by 52%. In a similar study in a kindergarten in Shanghai (Gao, 2019), a mechanical ventilation system with a high efficiency filter (HEPA) significantly reduced the concentration of PM<sub>2.5</sub> (from 85.7 µg/m<sup>3</sup> to 29.1 µg/m<sup>3</sup>) by 66%.

Due to the limited experimental data available in the literature, the need for experimental studies emerged. The main objective of this work was to evaluate the indoor air quality in a kindergarten located in Cordoba (Spain) under different strategies using ventilation systems and/or portable air cleaners. In addition, the influence of the outdoor concentration on the indoor air quality of the kindergarten was analysed. The concentration of PM<sub>2.5</sub> inhaled by a child was also evaluated according to the activity performed during a school day.

## 2 METHODOLOGY

### 2.1 Experimental classroom

The experimental study was carried out in a classroom in a kindergarten located in the city of Cordoba, Spain. The classroom, 8.10 m length, 5.60 m width and 3.00 m height, has an area of 41 m<sup>2</sup> and a volume: 123 m<sup>3</sup>, see figure 1, is occupied by 11 children and one teacher. The experimental study was carried out on different days, always in the same period from 9:05 am to 1:30 pm. The classroom had no openings with the outdoor environment through windows or doors. Only a door leading to the kindergarten corridor, was opened temporarily with the movement of children or opened for a period when the children were outdoor the classroom.

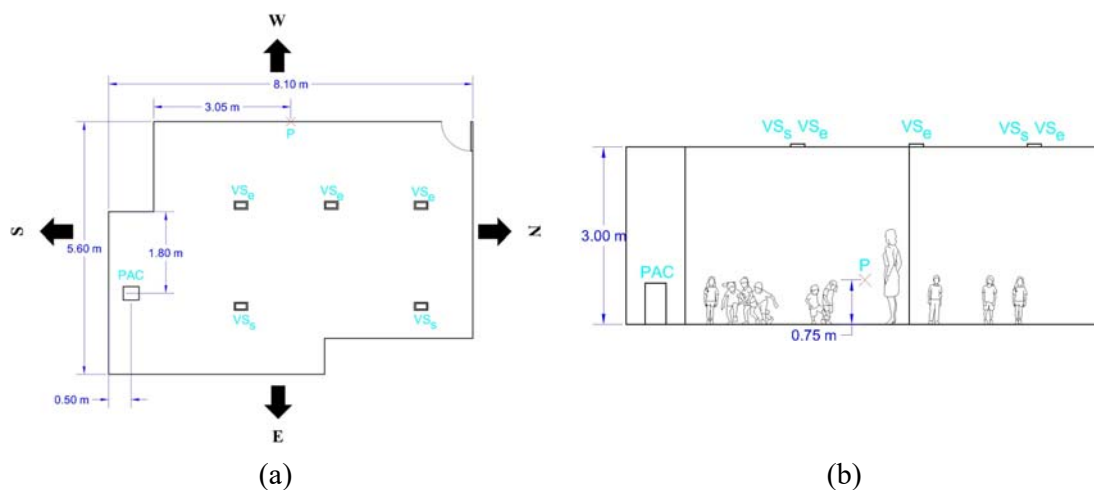


Figure 1. Experimental classroom setup: (a) Plan view (b) Elevation view.

## 2.2 Ventilation/filtration systems

The classroom had a ventilation system, VS, (CDA0707F145M41H, NINSUR, Spain) previously installed. VS supplied air from outdoor into the classroom through two grille diffusers, VSs, (0.24x0.12 m) and exhausted it to the street through three grilles with the same dimensions, VSe, see figure 1. VS supplied and exhausted an airflow rate of 175 m<sup>3</sup>/h (1.4 h<sup>-1</sup>). The VS did not incorporate any filters; therefore, the outdoor air was supplied unfiltered into the classroom. A portable air cleaner, PAC, (Pure Airbox Home, ZonAir 3D, Spain) was placed near the South wall of the classroom, see figure 1. PAC exhausted classroom air from the bottom and supplied filtered air through a rotational diffuser (DLQ, Trox, Germany) with an airflow rate of 235 m<sup>3</sup>/h (1.9 h<sup>-1</sup>). PAC incorporated a G4/Coarse 60% filter and an ePM1 95% filter.

## 2.3 Measurement equipment and experimental tests

For the measurement of the indoor concentration of PM2.5 particles, a sensor, P, (EcomZen2, DILUS, Spain) was placed on a wall of the classroom at the height of the children's breathing zone, 0.75 m, as can be seen in figure 1b. The sensor was placed on the West wall, see figure 1a, of the classroom. Outdoor particle concentration data were obtained from the Cordoba-Lepanto outdoor measuring air quality station (Junta de Andalucía, 2024). The air quality station is located 500 metres from the kindergarten studied and used a PM2.5 sensor (SPS30, Sensirion, Switzerland).

Five experimental cases were carried out: without ventilation (NV), using the ventilation system (VS1), using the portable air purifier (PAC), combining both systems (VS+PAC). Since the outdoor concentration was different in VS and VS+PAC, therefore, another experimental case was performed using the ventilation system (VS2), see table 1.

Table 1. Experimental tests.

Experimental case	Date	Timetable	Airflow rate		Equivalent airflow rate	
			m <sup>3</sup> /h	h <sup>-1</sup>	m <sup>3</sup> /h	h <sup>-1</sup>
NV	14/03/2023		49	0.4	0	0
VS1	09/03/2023	9:05	175	1.4	0	0
VS2	29/03/2023	to	175	1.4	0	0
PAC	28/03/2023	13:30	235	1.9	0	0
VS+PAC	21/03/2023		175	1.4	410	3.3

The classroom teacher had a fixed method of working: every 30 minutes she changed her activity (events). In order not to interfere with her working method, this study was adapted to this methodology. Depending on the activity performed by the children, the rate of inhaled airflow varied (Wang et al., 2015). All this can be seen in table 2.

Table 2. Working methodology.

Event	Time	Description	Inhaled airflow rate (m3/min)
1	9:05-9:30	Children's entrance	1.2·10 <sup>-2</sup>
2	9:30-10:00	Playing standing up	1.2·10 <sup>-2</sup>
3	10:00-10:30	Sitting talking	2.1·10 <sup>-2</sup>
4	10:30-11:00	Outdoor the classroom	0
5	11:00-11:30	Playing standing up	2.1·10 <sup>-2</sup>
6	11:30-12:00	Sitting watching TV	4.5·10 <sup>-3</sup>
7	12:00-12:30	Sitting at lunch	4.5·10 <sup>-3</sup>
8	12:30-13:00	Sitting watching TV	4.5·10 <sup>-3</sup>
9	13:00-13:30	Playing standing up	2.1·10 <sup>-2</sup>

## 2.4 Indoor/Outdoor (I/O) ratio

To assess the relationship between the indoor and outdoor PM2.5 concentration, the I/O index has been used (Chen & Zhao, 2011), (Abhijith, 2024), (Li, 2024):



$$I/O = \frac{\bar{C}_{in}}{\bar{C}_{out}} \quad (1)$$

Where  $\bar{C}_{in}$  is the average concentration of PM2.5 ( $\mu\text{g}/\text{m}^3$ ) in the indoor and  $\bar{C}_{out}$  is the average concentration of PM2.5 ( $\mu\text{g}/\text{m}^3$ ) in the outdoor in the same period of time.

## 2.5 Intake mass

To assess the exposure of children to PM2.5 particles under different ventilation strategies, an index indicating intake mass, IM, by a child (2) has been used (Nazaroff, 2008):

$$IM = \int_{t_0}^{t_f} C(t) \cdot \dot{Q}(t) \cdot dt \quad (2)$$

Where IM is the intake mass ( $\mu\text{g}$ ) by a child, C is the concentration of PM2.5 ( $\mu\text{g}/\text{m}^3$ ),  $\dot{Q}$  is the inhalation airflow rate of a child ( $\text{m}^3/\text{min}$ ),  $t_f$  and  $t_0$  are final time (min) and initial time (min) respectively.

## 3 RESULTS

### 3.1 PM2.5 concentration: indoor vs outdoor

The figure 2 shows the temporal evolution of indoor and outdoor PM2.5 particle concentration during the school day for all experimental (Martins & Carrilho da Graça, 2017).

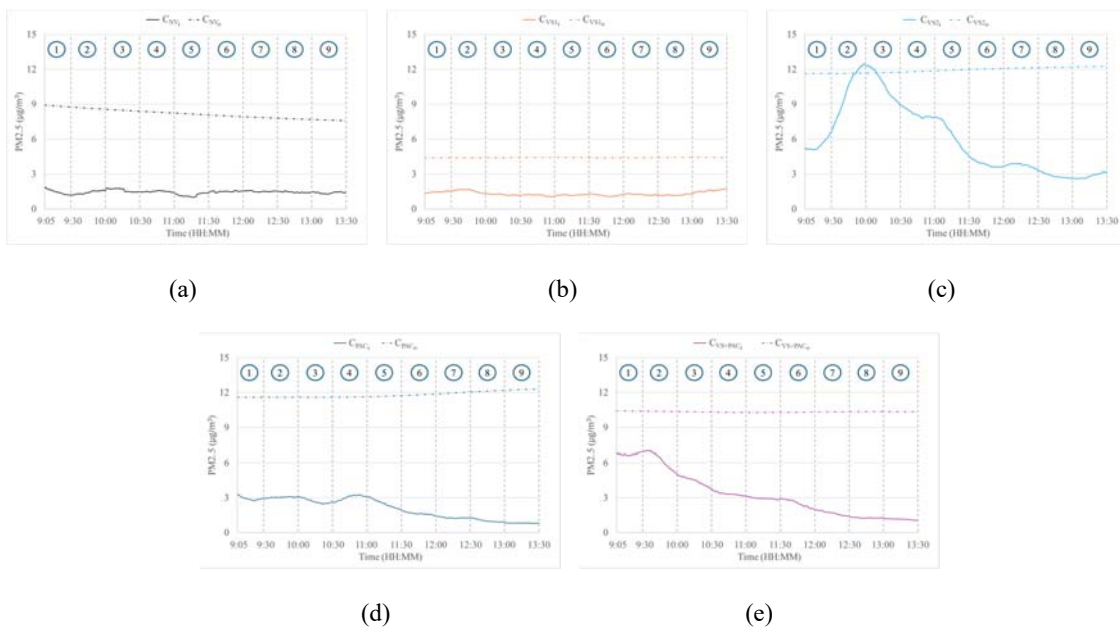


Figure 2. Temporal evolution of the concentration PM2.5 indoor and outdoor: (a) NV (b) VS1 (c) VS2 (d) PAC (e) VS+PAC

For the experimental case NV, it can be observed how the indoor concentration of PM2.5 particles, figure 2a, remained steady with the entry of children into the classroom (event 1). From 10:30 the concentration started to increase slightly when children started to play freely (event 2). Subsequently, concentration remained steady when the children sat on the floor to do an activity (event 3). On this day, the children left the classroom earlier, in the middle of event 3, and the corridor door was kept open. Therefore, concentration decreased in event 3 and remained steady until 11:00 (event 4). When children entered the classroom, they were playing freely (event 5). However, it can be observed that the concentration decreased, this was due to the fact that on this day the teacher kept the corridor door open until 11:15. At that time the

corridor door was closed, and concentration started to increase due to the children's activity. At 11:30, the children sat down to watch TV until 12:00 (event 6) which made the concentration steady. This concentration remained steady until 13:00 as the children remained seated. From 13:00 onwards, the children went back to playing freely around the classroom and concentration increased slightly. For this day, the outdoor particle concentration (average concentration of  $8.1 \mu\text{g}/\text{m}^3$ ) was not high, figure 2a. However, for this experimental case, as the ventilation was not turned on, there was no entry of particles from outdoor. Therefore, the only source of particles was from the children and the teacher.

For the experimental case VS1, it can be seen in the figure 2b how the concentration of PM2.5 increased exponentially in event 1. This increase occurred until the middle of event 2. From that moment on, the concentration decreased as the children started the activity corresponding to event 3. At the beginning of event 3, the concentration started to stabilise until the end of event 4. Therefore, there was no reduction in concentration, but it remained constant. When the children entered the classroom, the concentration increased slightly in event 5. Already in event 6 the concentration decreased again because the children were seated and therefore their exhalation rate decreased. Until 13:00 the concentration remained steady. However, at event 9, the concentration increased because the children's exhalation flow increased as they were playing freely in the classroom. In figure 2b it is shown that the outdoor concentration (average concentration of  $4.4 \mu\text{g}/\text{m}^3$ ) on this day remained steady. A low concentration was observed, so although it was constantly entering the indoor of the classroom, it did not have much effect on the indoor concentration.

Just the opposite happened for the experimental case VS2. In figure 2c it can be seen how the outdoor concentration was high (average concentration of  $12.0 \mu\text{g}/\text{m}^3$ ) and therefore influenced the indoor concentration, as the ventilation system did not filter the outdoor air. Figure 2c shows how the initial concentration was higher than in the previous experimental cases, possibly due to the outdoor concentration supplied through the ventilation system before the measurement started. During event 1 and 2 the concentration increased until it reached a peak of  $12.3 \mu\text{g}/\text{m}^3$ . Thereafter, the concentration decreased because the children's airflow decreased in event 3 and because they left the classroom in event 4. In the middle of this event, the concentration stabilised until the beginning of event 5. This led to a decrease in concentration until stability was reached in the middle of event 6. This stability was maintained until the middle of event 9, after which the concentration increased slightly due to the children's increased exhalation.

In the PAC experimental case, the concentration was different from the previous days, as can be seen in figure 2d. Although the exhalation flow rate of the children was high in event 1 and 2, the concentration did not increase due to the operation of the PAC. Furthermore, it should be noted that the children performed the activity corresponding to event 3 in the middle of event 2. Therefore, the children left the classroom in the middle of event 3 and re-entered the classroom in event 4. However, the concentration stabilised at levels similar to the beginning of the day, possibly due to the effect of the PAC. From event 5 onwards, the children were seated. This facilitated the task of the PAC, therefore the concentration decreased until the end of event 8. Already at event 9 the concentration stabilised because the children were playing freely, which led to an increase in the children's exhalation rate and meant that the concentration did not continue to decrease. During the school day, the outdoor concentration was high (average concentration of  $11.9 \mu\text{g}/\text{m}^3$ ), see figure 2d. However, as the ventilation system was not switched on, this concentration had no influence on the indoor concentration.

For the VS+PAC experimental case a high initial concentration was assumed, figure 2e, due to the fact that the ventilation system supplied a high external concentration (average concentration of  $10.3 \mu\text{g}/\text{m}^3$ ), see figure 2e. The ventilation system caused the high initial concentration; however, this concentration did not increase due to the PAC effect. As in the PAC experimental case, the activity corresponding to event 3 was carried out in the middle of event 2, which led to a decrease in the concentration, due to the decrease in the airflow of the

children and the operation of the PAC. This lead from event 3 to event 2 caused a lead in event 4, so the children left the classroom during the middle of event 3. The children returned to the classroom in the middle of event 4 and kept playing freely until the end of event 5. From event 6 onwards, the children sat down, and the concentration decreased again until it stabilised in event 9 due to the children playing freely in the classroom again.

### 3.2 Indoor/Outdoor (I/O) ratio

The relationship between the concentration of outdoor PM<sub>2.5</sub> and indoor PM<sub>2.5</sub> was obtained using the I/O index. The results obtained for each experimental case are shown in figure 3.

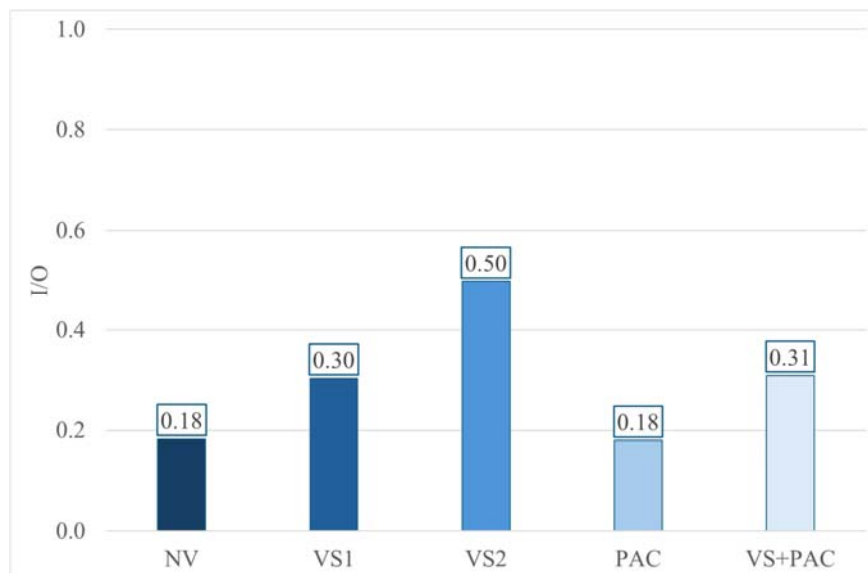


Figure 3. Indoor/Outdoor PM<sub>2.5</sub> concentration ratio under different ventilation strategies.

In NV, an I/O value of 0.18 was found as can see in figure 3. The non-ventilation case was very effective in controlling indoor PM<sub>2.5</sub> concentrations, thus suggesting that particles from outdoor were not entering significantly, which is to be expected when the environment is controlled. The low initial concentration, as shown in figure 2a, together with the non-existent ventilation, probably allowed the indoor concentration to stabilise close to the outdoor levels, resulting in a low I/O value. For VS1, the I/O value increased to 0.30, showing that although most of the outdoor PM<sub>2.5</sub> was not entering indoors, the unfiltered mechanical ventilation allowed a higher ingress of PM<sub>2.5</sub> compared to no ventilation. The low initial concentration (figure 2b) contributed to the value not being higher, but the non-filtered inlet air allowed more particles to enter indoors. At VS2, an even higher I/O value of 0.50 was reached, indicating that the indoor PM<sub>2.5</sub> concentration was half of the outdoor concentration. This higher value suggests a higher accumulation of PM<sub>2.5</sub> before the start of ventilation, as seen in figure 2c. Ventilation without a filter allowed the indoor and outdoor concentrations to equalise more quickly, resulting in a high I/O value. A similar value of I/O was found in (Evans, 2000) to that achieved in VS2. In PAC, an I/O value of 0.18 was again found, similar to NV. The use of a portable air cleaner was very effective in keeping indoor PM<sub>2.5</sub> concentrations low, thus proving its efficiency in removing particles from the air. At VS+PAC, an I/O value of 0.31 was achieved, similar to VS1. This indicates that approximately one third of the outdoor PM<sub>2.5</sub> was present indoor, resulting in moderate protection against outdoor PM<sub>2.5</sub>. Combining the ventilation system with the portable air cleaner improved the situation compared to ventilation alone (VS1 and VS2) but was not as effective as the air cleaner alone or no ventilation. The high initial concentration (figure 2e) required more time to achieve low indoor concentrations. The I/O value reflects a significant reduction, but not as low as with the air cleaner alone, due

to the high initial concentration. These results indicate the importance of filtration in ventilation systems to control indoor air quality and the effectiveness of filters air cleaner in reducing PM<sub>2.5</sub> concentrations. In addition, the initial PM<sub>2.5</sub> concentration had a significant impact on I/O values. Higher initial concentrations tended to result in higher I/O values, as the ventilation system required more time to remove the accumulated particles. Systems with effective filtering, such as the PAC, show a superior ability to keep I/O values low, even if the initial concentration was moderate. The combination of different ventilation strategies can significantly influence the indoor PM concentration and the resulting I/O values.

### 3.3 Daily intake mass

The daily intake mass, IM, by a child indoor the classroom at the end of the school day is shown in figure 4 for all experimental cases.

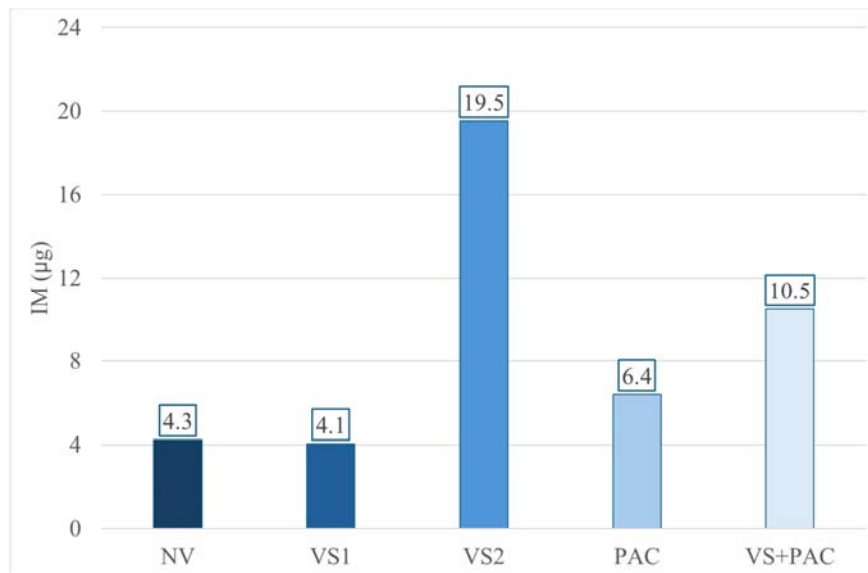


Figure 4. Daily intake mass, IM.

The maximum value of IM (19.5 µg) was found for VS2. However, for VS1 the minimum value of IM (4.1 µg) was achieved, as can be seen in figure 4. In figure 2 it can be observed clearly that the initial concentration influences the IM at the end of the school day. For the experimental cases NV and VS1, the initial concentration was low, as can be seen in figure 2a and 2b. For NV the outdoor concentration had no influence, as the ventilation system was turned off. For VS1 it also had no influence on the indoor concentration, as the outdoor concentration was low on that day. This caused that for NV and VS1, the IM was 4.3 µg and 4.1 µg respectively. However, for the experimental cases VS2, PAC and VS+PAC the initial concentration did influence the IM. Moreover, on these days the outdoor concentration was high in VS2 and VS+PAC, which caused the IM to be high, 19.5 µg and 10.5 µg respectively. On the other hand, although the ventilation system was not turned on for PAC, the high initial concentration caused the IM to be 6.4 µg.

### 3.4 Daily intake mass by events

The daily IM<sub>ev</sub> by a child indoor the classroom in each event during the school day is shown in figure 5 for all experimental cases. For each experimental case the IM<sub>ev</sub> value in µg and in % is shown. In % corresponds to the percentage of IM<sub>ev</sub> in each event with respect to the total (figure 4). Event 4 was not considered in this analysis, as the children were outdoor the classroom.

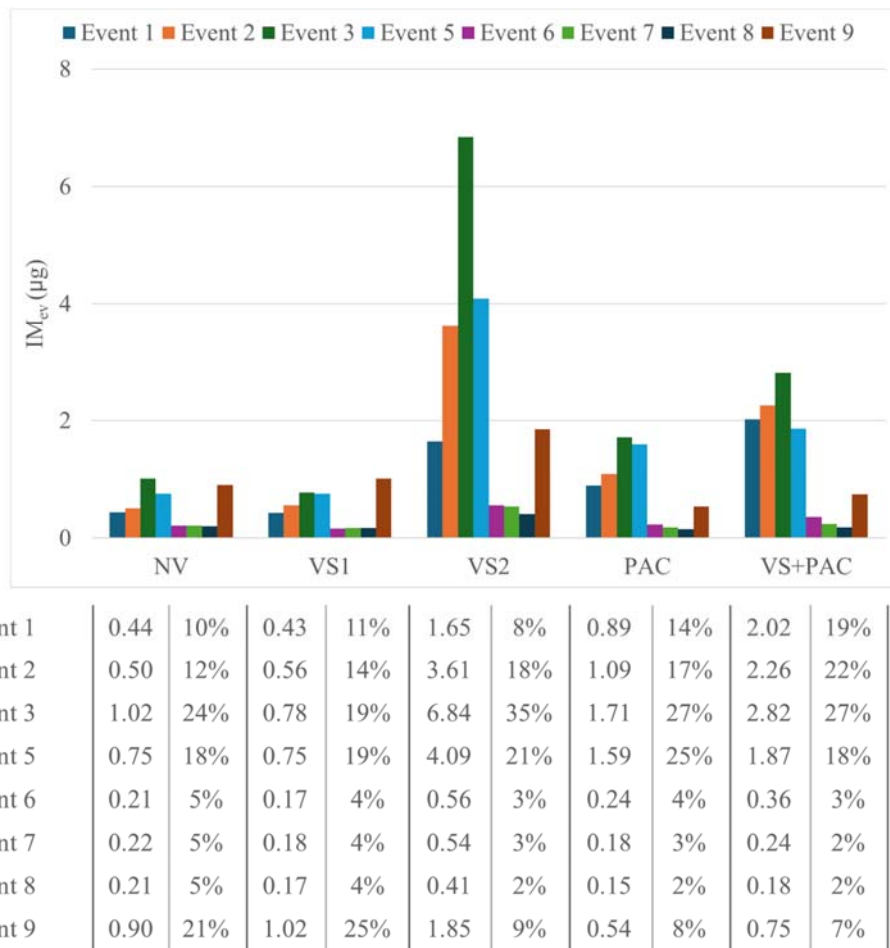


Figure 5. Daily intake mass by events,  $IM_{ev}$ .

Figure 5 shows that the event with the highest IM was event 3, 6.84  $\mu\text{g}$  (35%), 2.82  $\mu\text{g}$  (27%), 1.71  $\mu\text{g}$  (27%) and 1.02  $\mu\text{g}$  (24%), for the experimental cases VS2, VS+PAC, PAC and NV respectively. These measurements are in accordance with the fact that event 3 is the event that proceeds the initial events, which is when there was the most activity in the classroom. However, for VS1, although the IM in event 3 was high, 0.78  $\mu\text{g}$  (19%), the highest IM was obtained in event 9, 1.02  $\mu\text{g}$  (25%). For NV and VS1 the initial IM were similar, 0.44  $\mu\text{g}$  (10%) and 0.50  $\mu\text{g}$  (12%) (event 1 and 2) and 0.43  $\mu\text{g}$  (11%) and 0.56  $\mu\text{g}$  (14%) respectively. In contrast, for VS2, PAC and VS+PAC, the IM in event 1 was 1.65  $\mu\text{g}$  (8%), 0.89  $\mu\text{g}$  (14%) and 2.02  $\mu\text{g}$  (19%) respectively and 3.61  $\mu\text{g}$  (18%), 1.09  $\mu\text{g}$  (17%) and 2.26  $\mu\text{g}$  (22%) in event 2 respectively. This once again confirms that on these days the initial concentration played an important role, as it affected the measurements made during the school day. The lowest concentrations were found in events 6, 7 and 8 for all experimental cases. These events were the ones in which the children were least physically active. The IM increased in all experimental cases in event 9, as the children were playing around the classroom freely.

#### 4 CONCLUSIONS

This study assessed the PM<sub>2.5</sub> concentration in a kindergarten located in Córdoba (Spain) under different strategies: no ventilation (NV), only ventilation system (VS1-VS2), only portable air cleaner (PAC) and combination of both systems (VS+PAC). The main conclusions derived from the research are presented below:

- The indoor concentration of PM<sub>2.5</sub> behaved in relation to the activity carried out in the classroom by the children. However, the PM<sub>2.5</sub> indoor concentration in the classroom was also influenced by outdoor PM<sub>2.5</sub> concentrations.
- Intake mass (IM) and I/O ratio showed a significant correlation in different scenarios. In situations without outside air intake (NV and PAC), both IM and I/O ratio were low, indicating effective protection against external particles. However, in situations with outdoor concentration input (VS2 and VS+PAC), the correlation was also significant. However, in VS1, where ventilation without adequate filtration was used under low outdoor concentration conditions, no such a clear correlation was observed.
- Depending on the I/O ratio, an adequate ventilation strategy should be used with an adequate filtration system. If I/O ratio are high, ventilation system with inappropriate air filters increases the daily IM by a child. In these situations, a PAC with appropriate air filters are useful to reduce the daily IM by a child.

These results show the needs to understand the indoor-outdoor concentration of PM<sub>2.5</sub> in order to limit the exposure of children to PM<sub>2.5</sub> under different ventilation strategies.

## 5 ACKNOWLEDGEMENTS

The authors acknowledge the financial support received from the Spanish Ministry of Science, Innovation and Universities to the National R&D project BIORISK with reference RTI2018-094703-B-I00, entitled “Bioaerosols in hospital environments. Control and evaluation of the infection risk”. This project is financed by the European Regional Development Fund (ERDF).

## 6 REFERENCES

- Abhijith, K. V., Kumar, P., Omidvarborna, H., Emygdio, A. P. M., McCallan, B., & Carpenter-Lomax, D. (2024). Improving air pollution awareness of the general public through citizen science approach. *Sustainable Horizons*, 10(August 2023), 100086. <https://doi.org/10.1016/j.horiz.2023.100086>
- Chen, C., & Zhao, B. (2011). Review of relationship between indoor and outdoor particles: I/O ratio, infiltration factor and penetration factor. *Atmospheric Environment*, 45(2), 275–288. <https://doi.org/10.1016/j.atmosenv.2010.09.048>
- Cho, J., Woo, K., & Kim, B. S. (2019). Removal of airborne contamination in airborne infectious isolation rooms. *ASHRAE Journal*, 61(2), 8–21.
- Cienciewicki, J., Trivedi, S., & Kleeberger, S. R. (2008). Oxidants and the pathogenesis of lung diseases. *Journal of Allergy and Clinical Immunology*, 122(3), 456–468. <https://doi.org/10.1016/j.jaci.2008.08.004>
- Daisey, J. M., Angell, W. J., & Apte, M. G. (2003). Indoor air quality, ventilation and health symptoms in schools: An analysis of existing information. *Indoor Air*, 13(1), 53–64. <https://doi.org/10.1034/j.1600-0668.2003.00153.x>
- Evans, G. F., Highsmith, R. V., Sheldon, L. S., Suggs, J. C., Williams, R. W., Zweidinger, R. B., Creason, J. P., Walsh, D., Rodes, C. E., & Lawless, P. A. (2000). The 1999 fresno particulate matter exposure studies: Comparison of community, outdoor, and residential pm mass measurements. *Journal of the Air and Waste Management Association*, 50(11), 1887–3189656. <https://doi.org/10.1080/10473289.2000.10464224>
- Gao, X., Xu, Y., Cai, Y., Shi, J., Chen, F., Lin, Z., Chen, T., Xia, Y., Shi, W., & Zhao, Z. (2019). Effects of filtered fresh air ventilation on classroom indoor air and biomarkers in saliva and nasal samples: A randomized crossover intervention study in preschool children. *Environmental Research*, 179(July), 108749. <https://doi.org/10.1016/j.envres.2019.108749>

- Guo, H., Morawska, L., He, C., Zhang, Y. L., Ayoko, G., & Cao, M. (2010). Characterization of particle number concentrations and PM<sub>2.5</sub> in a school: Influence of outdoor air pollution on indoor air. *Environmental Science and Pollution Research*, 17(6), 1268–1278. <https://doi.org/10.1007/s11356-010-0306-2>
- Han, B. (2023). *Kindergarten : CO<sub>2</sub> and Fine Particulate Matter Concentrations*.
- Hou, Y., Liu, J., & Li, J. (2015). Investigation of Indoor Air Quality in Primary School Classrooms. *Procedia Engineering*, 121, 830–837. <https://doi.org/10.1016/j.proeng.2015.09.037>
- Junta de Andalucía. (2024). *Red de Vigilancia y Control de Calidad del Aire de Andalucía. Informe Horario de Calidad del Aire*. [https://ws041.juntadeandalucia.es/pentaho/api/repos/%3Apublic%3ACalidad\\_Aire%3ACalidad\\_Aire.wcdf/generatedContent](https://ws041.juntadeandalucia.es/pentaho/api/repos/%3Apublic%3ACalidad_Aire%3ACalidad_Aire.wcdf/generatedContent)
- Li, N., Chartier, R., Li, Y., Liu, Z., Li, N., Chang, J., Wang, Q., Xu, D., & Xu, C. (2024). Measuring and modeling of residential black carbon concentrations in two megacities, China. *Building and Environment*, 257(February), 1–10. <https://doi.org/10.1016/j.buildenv.2024.111558>
- Mainka, A., & Fantke, P. (2022). Preschool children health impacts from indoor exposure to PM<sub>2.5</sub> and metals. *Environment International*, 160, 107062. <https://doi.org/10.1016/j.envint.2021.107062>
- Martins, N. R., & Carrilho da Graça, G. (2017). Impact of outdoor PM<sub>2.5</sub> on natural ventilation usability in California’s nondomestic buildings. *Applied Energy*, 189, 711–724. <https://doi.org/10.1016/j.apenergy.2016.12.103>
- Nazaroff, W. W. (2008). Inhalation intake fraction of pollutants from episodic indoor emissions. *Building and Environment*, 43(3), 269–277. <https://doi.org/10.1016/j.buildenv.2006.03.021>
- Peláez, G., Giubergia, V., Lucero, B., Aguerre, V., Figueroa, J. M., & Claudio, C. (2019). *Childhood Severe Asthma: Relationship among asthma control scores, FeNO, spirometry and impulse oscilometry*. PA947. <https://doi.org/10.1183/13993003.congress-2019.pa947>
- Wang, B., Wang, Z., Wei, Y., Wang, F., & Duan, X. (2015). Inhalation Rates. *Highlights of the Chinese Exposure Factors Handbook, September*, 15–21. <https://doi.org/10.1016/B978-0-12-803125-4.00012-2>

# Proposal of a More Reliable Model and Procedures for Estimating Operational Leakage in Air Systems.

Federico Pedranzini\*<sup>1</sup>

<sup>1</sup> *Politecnico di Milano*  
*Energy Department*  
*Via Lambruschini, 4 - 20156 Milano, Italy*  
*\*Corresponding author:*  
*federico.pedranzini@polimi.it*

## ABSTRACT

The European Directive 2024/1275 issued in April 2024 reiterates the goal of having zero-emission buildings in 2050. The consequences in terms of lost energy and performance of poorly tight air ducting are among the biggest waste factors related to HVAC systems and have to be considered.

Nowadays, with the exception of a few specialist sectors, designers, installers and end users are not aware of the impact of leakage and are generally not in a position to measure or estimate it easily.

The current regulatory framework also refers to models that were formalized in the 1980s for classification purposes only, at a time when the technology available for testing was very different from what it is today; namely, the model that it was decided to apply and subsequently inherited is based on a power law that expresses the dependence of the exfiltrated flow rates on the difference in static pressure between the inside and outside of the channel raised to a constant exponent and equal to 0,65.

Both theory and experimental tests conducted and also reported by numerous authors in the scientific literature show that the exponent can vary in a range between 0.5 and 1, nevertheless the procedures reported by international standards and used to estimate operational leakage refer to that 0,65 model, introducing further ambiguities in the choice of pressure to be used in the evaluation under working conditions.

Modern measuring devices today allow for more complete automated tests than those required by the DALT standard for classification and would allow for a more refined characterization of leakage behavior with a little effort. The paper proposes a critical review of the original framework inherited from modern standards and makes an attempt to point out the issues that could allow a more reliable estimation today, proposing more effective measurement methods for the characterization of a reliable model, in analogy to what is done today in related fields such as the tightness of buildings.

The application of the advanced model shows, on the tests conducted for this study, a very high reliability, verifying, in one case tested, leakage exponents between 0.53 and 0.57 with values of the coefficient of determination  $R^2$  regularly exceeding 0,99.

## KEYWORDS

Air Systems Leakage, Air tightness, DALT, HVAC efficiency

## 1 INTRODUCTION

The European Economic Community Directive 2024/1275 issued on 24 April 2024 [1] sets 2050 as the target year to achieve zero-emission building stock within the union.

The goal is very ambitious and its pursuit cannot avoid considering all the so far neglected aspects that can lead to energy waste, and the subject of airtightness of both buildings and mechanical ventilation systems is explicitly mentioned. In particular, Article 4 requires all member states to have suitable methodologies for quantifying consumption and in Annex I - Common general framework for the calculation of the energy performance of buildings, the requirement for a calculation that takes into account the tightness of mechanical ventilation systems is explicitly mentioned.



Leakage faults in air systems have important consequences both in terms of performance and energy consumption; with regard to the latter, it is worth highlighting at least two aspects:

i) Increased fan consumption when leaks are compensated by an increase in the operating speed. This can occur e.g. as a result of an adjusting action required in the TAB operations of constant flow systems, or as compensation achieved by an automatic flow control in the case of variable flow systems; this type of increase is not easy to quantify because the calculation of fan power increases cannot be carried out by applying traditional fan laws, as the leakage phenomenon does not respect the quadratic relationship between pressure and flow rate that is generally assumed to be valid in HVAC systems [2].

ii) Increase in thermal energy consumption from thermal generators. This increase is primarily due to the increase in the flow of outside air passing through the treatment section of the air handling units but may also be linked to a deterioration in the performance of the heat recovery section due to the partial dilution of the expulsion air with potentially untreated air; In addition, in the case of recirculation, unconditioned air infiltration into the return ducts also constitutes an extra heat load.

Finally, although not strictly pertinent to the present discussion, it should be remembered that the infiltration of outside air into air-conditioned spaces due to tightness faults in the building envelope is often counteracted by creating overpressure conditions in the spaces through the imbalance between the flow rates of incoming and outgoing outside air. This imbalance has as a side effect the more or less significant reduction of the flow rate from which energy can be recovered.

Many studies and simulations have been conducted to quantify the energy cost of poorly sealed air systems, among others the 2022 work of N.Hurel et al. [3], 2018 and 2019 V. Leprince et [2,4] and the less recent ones by Soenens et al. from 2011 [5], by P. Stroo from 2011 [6] and by C.P. Wray et al. from 2010 [7] are significant.

These evaluations are based on the application of the models provided by the Standards in force or on the implementation of analytical models and lead to quantifications indicating that systems with good tightness can have lower consumption in the range of 30% to 46% when compared to systems with poor tightness.

### **1.1 Direct measurement of operational leakages according to the ASHRAE Standard 215:2018**

From a theoretical point of view, an effective methodology for determining operating leaks is to measure the difference between the flow rate measured at the fan and the sum of the flow rates measured at the terminals. This methodology is very simple in theory but presents significant metrological problems, as the uncertainty with which the two terms of the subtraction can be measured in practice is usually comparable or even greater than the magnitude of the expected result itself. The propagation of the measurement uncertainty on the leakage value obtained results in the uncertainty range of the measurement being greater in absolute value than the flow rate to be estimated.

This methodology is the subject of ASHRAE Standard 215 [8] which deals specifically with measurement uncertainty and instrument selection.

The main result is that, in the absence of efficient flow meters with very low uncertainty, direct measurement of leakage can lead to inconsistent measurements.

This criticality is amplified when the value of exfiltrations is low and consequently direct measurement may be easier (i.e. based on cheaper instrumentation) for the evaluation of low leakage systems, which, moreover, represent the majority of installations today [9].

Considering the future prospect of improved tightness systems, the above-mentioned complications make the method difficult to apply in the absence of expensive instrumentation. Furthermore, the main problem for the large-scale application of the Standard 215 could be in the fact that the proposed procedure cannot be carried out with the instrumentation already available to professionals in the field due to classification requirements.

## 2 MATERIAL AND METHODS

Faced with a need for calculation and assessment that is becoming increasingly explicit and the fact that direct measurement can be complicated, it is evident that little has been done to date to make the assessment of operational leakage as something feasible on a large scale, and almost all that has been done at the regulatory level is based on extending the application of the DALT models originally proposed for classification.

### 2.1 The DALT model.

As mentioned above, the trend is to use the reference models that were adopted in the 1980s and 1990s with the aim of implementing a method of classifying air components and systems that would be easy to apply with the technologies available at that time.

At the time, the idea was to prioritize the simplicity of measurement, and consequently a relationship was constructed that was able to provide the necessary elements for the classification of a system or (more often) a section of a system by means of a single measurement made at a reference pressure; nearly all the standards governing the characterization of the tightness of air systems for HVAC in both Europe and the United States (originally referring to SI and IP systems respectively) have adopted this strategy [10–26] and in the following we will refer to this relationship as the DALT model.

The DALT model is expressed in the form of a power law:

$$m_{exf} = f \times A \times \Delta P^n \quad (1)$$

Where  $m_{exf}$  [ $\text{l s}^{-1}$ ] (or [ $\text{m}^3 \text{s}^{-1}$ ]) is the leaked flow rate,

$f$  [ $\text{l s}^{-1} \text{m}^{-2}$ ] (or [ $\text{m}^3 \text{s}^{-1} \text{m}^{-2}$ ]) is the leakage coefficient that depends on the manufacturing characteristics of the air system,  $A$  [ $\text{m}^2$ ] the surface area of the duct,  $\Delta P$  [Pa] the static pressure difference across the duct surface,  $n$  leakage exponent currently assumed to be equal to 0,65.

Experimental evidence shows that indeed the power law form is correct, but that nevertheless the value of the leakage exponent  $n$  may vary, and this fact will be further explored later in this paper.

Using 1) in its form with  $n=0.65$ , it follows that by measuring the flow rate required to maintain at a certain pressure a section of plant whose leakage area is known, it is possible to determine the leakage coefficient  $f$ , this type of test is called Duct Air Leakage Test or DALT.

The DALT is carried out by closing the inlet section of the part of the ducting under test with a plate, capping all diffusers, and supplying compensation air via an external device equipped with a dedicated fan capable of modulating and measuring the flow necessary to reach and maintain the Test Pressure. This mode of operation allows, for systems with acceptable tightness, to consider the static pressure within the tested part of the system as constant, and consequently 1) can be applied by associating the flow rate dispersed across the entire surface of the part of the system under investigation with the test pressure value.

The calculation of  $f$  can be carried out downstream of the test as

$$f = \frac{m_{exf}}{A \times \Delta P^{0,65}} \quad (2)$$

With the sole exception of systems for which the value of  $n$  actually happens to be 0.65, this method of calculation leads to a different  $f$ -value for each pressure value, and it was therefore decided to consider for the classification of ducts and components the test conducted at a reference pressure indicated on tables in the Standards and referred to the expected tightness class and the pressure class of the system tested ( EN1507, EN 12237) [16,17].

Once the value of the leakage coefficient  $f$  has been determined, it is compared with threshold values that define the different air duct tightness classes.

The European standards dealing with the classification of air tightness of systems that have been published over time deal with systems characterized by certain construction specificities such as material, section geometry (circular or rectangular) of the type of component (ducts or line components) and provide for tests carried out on the individual component and also tests

carried out on the installed system, however they have practically in common the DALT model, the criterion of class assignment and the indications on the of test pressures.

The reference to the same relationship 1) offers the advantage of harmonizing the characterization of the components with the characterization of the installed systems, although a crucial role is played by the assembling operations, so it is not possible to state that a system composed of components belonging to a specific class belongs to that class without having carried out a field measurement.

As an indication, Table 1 conforming to EN 16798-3-2 (2017) [14] which is the most recent standard and contains cross-references to almost all previous standards, is given. The table shows the Class limits to consider for the leakage factor  $f$ .

Table 1. Classification of system air tightness according to EN 1698-3-2, with reference to the old Class nomenclature.

Air Tightness Class		$f_{\max}$ [ $\text{m}^3 \text{s}^{-1} \text{m}^{-2}$ ]
Old	New	
	ATC 7	$0,0675 \times P^{0,65} \times 10^{-3}$
A	ATC 5	$0,027 \times P^{0,65} \times 10^{-3}$
B	ATC 4	$0,009 \times P^{0,65} \times 10^{-3}$
C	ATC 3	$0,003 \times P^{0,65} \times 10^{-3}$
D	ATC2	$0,001 \times P^{0,65} \times 10^{-3}$
	ATC1	$0,00033 \times P^{0,65} \times 10^{-3}$

Table 2 shows the pressures at which the tightness test of ducts should be carried out with reference to the expected working pressure classes and tightness class according to EN 1507 (rectangular sheet metal ducts) and EN 12237 (circular sheet metal ducts) [16,17].

Table 2. Pressure reference values for leakage testing according to EN 1507:2006 and 12237:2003

Air Tightness Class	EN 1507 rectangular sheet metal ducts			EN 12237 circular sheet metal ducts		
	Negative at all pressure classes	Static pressure limits [Pa]			Static pressure limit [Pa]	
		Positive at pressure class			Negative	Positive
		1	2	3		
A	200	400			500	500
B	500	400	1000	2000	750	1000
C	750	400	1000	2000	750	2000
D	750	400	1000	2000	750	2000

It can be seen that Table 2 refers to the measurement of the ductwork only and that the values given in the table are values above or far above the pressures at which the systems are normally operated.

With regard to tests on the installed system complete with all components, EN 12599:2012 [27] (also referred to by EN 16798), indicates in its appendix D (point *D.8.1 Air Leakage - Measuring Method*) lower pressure levels by explicitly referring to the level as close as possible to the average operating pressure of the system, indicating as preferably the values of 200Pa, 400Pa or 1000Pa in the case of supply systems and 200Pa, 400Pa and 750Pa in the case of extract systems.

The same standard, however, admits that these pressure levels might be impossible to achieve during a DALT in the case of a poor seal and therefore considers the possibility of carrying out the test at lower pressures by applying the relationship 1) with  $n = 0,65$  to bring the values obtained in this way back to the reference pressure of the test. This in fact legitimises the application of 1) as a wide range model and is equivalent to assuming that the f-factor calculated at lower pressures is equal to that which would have been obtained by performing the test at the pressures indicated as preferable for the test. This assumption is incorrect because it implies

that 0,65 is the true value for all systems whereas the experimental evidence proves that this is not the case.

The definition of the value  $n=0.65$  adopted for the exponent  $n$  in the Dalt models comes from a collaborative study conducted in 1985 by SMACNA, ASHRAE and TIMA (Thermal Insulation Manufacturers Association) with the aim of identifying a unique value. This study was formalised in an ETL report No. 459507 *Investigation of Duct Leakage*, 1985 [28,29] and in the same year transposed into the SMACNA manuals [30]. The tests considered different geometries (rectangular, circular, flexible ducts), materials (metal or fibreglass ducts) and types of sealing, and the  $n = 0.65$  value identified for the characterization of leakage at the test conditions was established in terms of an average value within the range of  $0.5 \div 0.93$  found experimentally.

Ultimately, it can be concluded that the DALT model formalised by relation 1) can be used for classification, however, it requires that the test pressures are defined and are the same for all systems or components that are to be combined or compared with each other. Otherwise, if it is accepted to carry out tests even at lower pressures, relation 1) may lead to a mischaracterization. In the case of certain situations, it may also happen that the same system tested at different pressures may turn out to belong to different classes. These considerations lead to the conclusion that there is a need to review the model applied and adopt one that can make the measures more flexible and the results more consistent, also in terms of Classification.

## 2.2 Quantification of operational leakages according to EN 16798-5

Part 5-1 of the European Standard issued in 2017[13], deals with Calculation methods for energy requirements of ventilation and air conditioning systems, and proposes a simplified method for quantifying the lost flow rates in aeraulic systems. In Section 6.3.2.2 *duct leakage factors*, the amount of air leaked in the whole system is estimated by using the DALT model with  $n=0.65$  and applying the coefficients  $f$  associated with the leakage classes defined by EN 12237 and EN 1507 to the total area of the system estimated according to EN 14239 [31]. The pressure value considered for the calculation is “*the average between the pressure difference at the AHU outlet and the pressure difference right upstream of the air terminal device*”.

A discussion of the critical issues related to this methodology and the formulation of proposals that can be considered as an alternative is proceeded with.

## 3 DISCUSSION

The procedure for calculating operating losses proposed by EN16798, although simple and although based on an accepted model that has been in technical regulation for a long time, is weak for essentially three reasons:

- 1) The reliability of the model;
- 2) The consideration of prevalence calculated as an arithmetic mean;
- 3) The evaluation of the surface area using the procedures of EN 14239.

The three different aspects are developed below.

### 3.1 Model Reliability

The critical issues introduced by the constant exponent model already emerged when analysing how the model is also used for classification alone. In order to better address the issue of using the DALT model also for the assessment of operating leaks, it was decided to proceed with a quantitative approach. The first assessment that can be made relates to the potential error in the leakage assessment of three systems that when tested using DALT at a test pressure of 400Pa were found to have the same leakage consistent with Class A. The three systems, indistinguishable from each other at 400Pa, differ in the value of the leakage exponent which will be 0.5, 0.65 and 0.93 respectively with reference to the range identified by the 1985 collaborative study mentioned above.

Figure 1 shows the behaviour of the three systems in the pressure range between 50Pa and 500Pa.

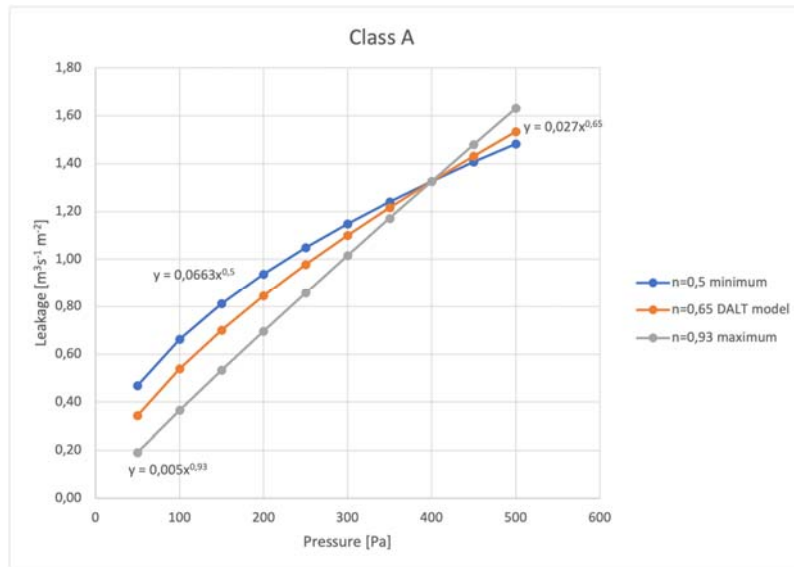


Figure 1: Comparison of systems with exponents other than  $n=0,65$

Assuming the Operating Leakage to be evaluated at an equivalent operating pressure of 100Pa, the calculation of the exfiltrated flow value shows that the system characterized by  $n = 0,65$  loses 47% more air than the system with  $n = 0,93$  and 19% less air than a system with  $n = 0,5$ . These differences are unacceptable and do not allow, for example, useful results to be obtained in an evaluation scenario of an investment to improve the tightness of an existing system.

Finally, in order to better highlight the criticalities of the constant exponent model, experimental tests were carried out on a real system. Figure 2 shows the leakage trend measured on a section of an existing system serving an office building located in Northern Italy. The tests were conducted by using a DALT native instruments (TSI - PAN341 model, Pressure probe accuracy  $1\% \pm 1\text{Pa}$  in the range  $\pm 2500\text{Pa}$ , Flowmeter accuracy  $\pm 2,5\%$  of reading or  $\pm 0,011/\text{s}$  in the range  $3,6 \div 720\text{m}^3/\text{h}$ , Barometric Pressure measurement accuracy  $\pm 2\%$ ) and were conducted at pressure steps increasing by 50Pa from within the range 50Pa to 500Pa. Table 3 shows the results of the test performed.

Table 3. Result of exfiltrated flow measurement conducted at different pressures..

Pressure (Pa)	$m_{\text{exf}} [\text{m}^3/\text{h}]$	$m_{\text{exf}} [1 \text{ s}^{-1} \text{ m}^{-2}]$
50	156	0,52
100	230	0,77
150	285	0,95
200	332	1,11
250	373	1,25
300	411	1,37
350	445	1,49
400	477	1,59
450	510	1,70
500	535	1,79
Instrument: TSI - PAN341 model		
Surface $83,1 \text{ m}^2$		

Standard 1507 provides for the possibility of testing at different pressures; Section 6.2 *Leakage Test Report* and Section 6.2.2 *Test Result* refer to the possibility of testing at different pressures, in which case, however, instead of considering the evaluation of a different exponent, it requires

plotting the different values of  $f$  obtained from the report at  $n = 0,65$  in relation to the different test pressures.

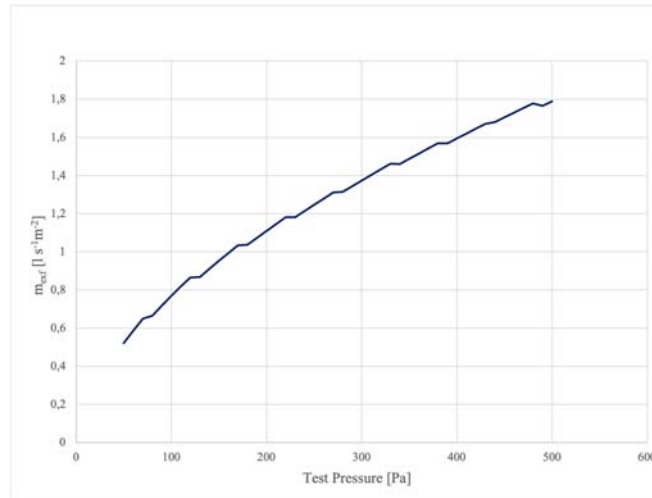


Figure 2: Trend of the model at  $n=0,65$  fitted to measurements at different test pressures

Figure 2 shows the reconstruction of the system's trend by associating a section of a curve at  $n=0.65$  around each pressure value tested, showing a step-like behaviour which is obviously far from any physical sense. Similarly, the required representation of the different values of  $f$  for each pressure value shows a discontinuous variation of the same (Figure 3) which is difficult to justify from the point of view of the fluid dynamics of leakage. The percentage variation from the mean value of  $f$  in the pressure range investigated goes from  $-9.8\%$  to  $+17.5\%$ .

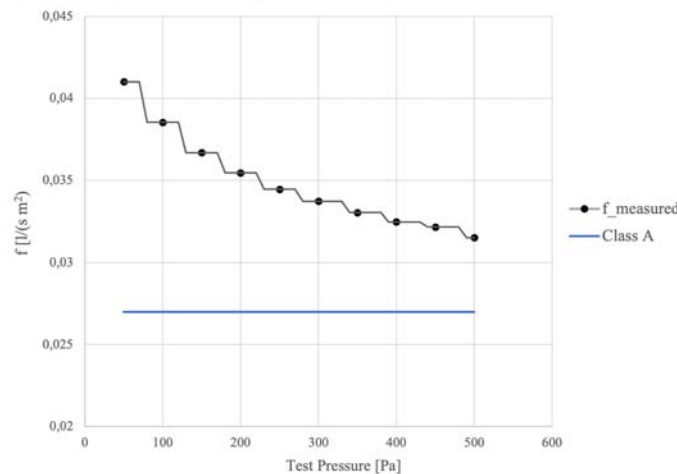


Figure 3: Trend in the value of the  $f$  coefficient calculated on the basis of the model forced at  $n=0.65$  obtained from tests at different pressure values, A Class limit is also represented.

Finally, the same measurements were analyzed by admitting the possibility of identifying an unblocked exponent trendline. The behavior of the resulting model is depicted in Figure 4.

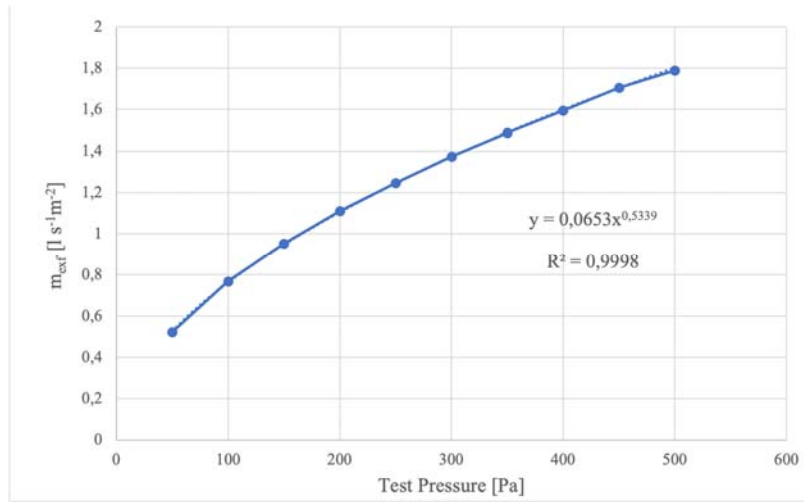


Figure 4: approximation curve obtained by calculating the value of n via logarithmic linear regression. n=0,5339

It can easily be seen that the obtained model proves, as was expected, a satisfactory consistency with the measurements and demonstrated through the evaluation of coefficient of determination  $R^2$ , whose value is very close to unity.

In terms of the usefulness of the application of the advanced model also for classification purposes, it can be seen that the leakage coefficient obtained from the regression process has a much smaller variation (-1.1% to +0.8% compared to the average value in the 50-500Pa range). Figure 5 shows the trend of  $f$  over the investigated pressure range.

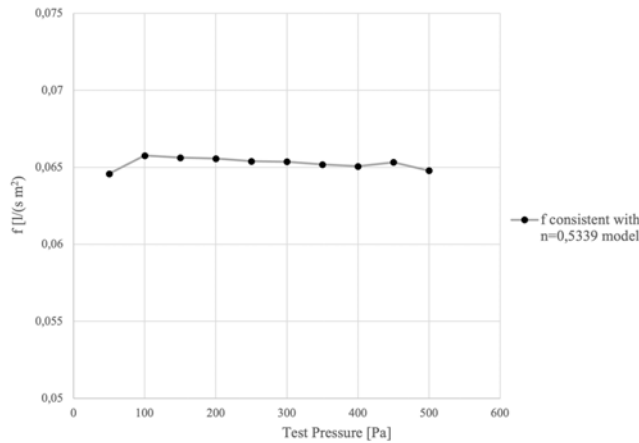


Figure 5: trend of  $f$  over the investigated pressure range 50÷500Pa and consistent with leakage exponent obtained by regression process.

Finally, it should be noted that the coefficient  $f$  calculated in the two modes incorporates the different contribution of the pressure term in the calculation, which is raised to different exponents and is consequently very different:

$$\frac{f_{n=0,5339} - f_{n=0,65}}{f_{n=0,5339}} \times 100 = \frac{0,065 - 0,032}{0,065} \times 100 = 50,1\% \quad 3)$$

This shows how the imposition of an incorrect value of the leakage exponent can also affect the parameter used for classification.

In assessing the suitability of the constant exponent model, it is useful to emphasise that the additional effort involved in performing a multiple test at different pressures to determine the correct exponent is relatively low.

Furthermore, the methodologies for calculating the exponent from multiple pressure tests are also well proven and reported in standards developed for related topics such as the tightness assessment of building envelopes.

These results and considerations are confirmed by the Literature, measurements performed by Aydin et al. 2006 [32] show how different construction types lead to  $n$  values in the range  $0,32 \div 0,66$ . In particular, it can be seen from the measurements carried out that the higher the construction quality, the higher the value of the exponent. Exponent values close to 0.5 can also be found in the literature in another work of 2012 by S. Moujaes, R. Gundavelli[33], where the exponents referring to different geometries in the leakages lie within the range  $0,46 \div 0,5$ . From a theoretical perspective, the range between 0.5 and 1 derives from the fact that the leakages can be composed of leakage phenomena that follow a behavior assimilable to turbulent-type flow characterized by the value 0.5 and phenomena assimilable to a laminar regime characterized by the value 1. However, this interpretation does not explain the presence of measured values of lower than 0,5, values that are characteristic of systems built without any care for tightness. It is considered that these aspects deserve further investigation but are also a further reason for abandoning the old model. The leakage model characterized by a variable leakage exponent and to be measured experimentally is already used in applications related to building leakage assessment, in which the tightness tests involve measurements using blower door instruments at different pressure values. Standards ASTM E779:2019 [34] and ASTM E1554/1554M:2018 [35] refers to the performance of a defined number of tests under increasing pressure/de-pressure to determine the value of the  $n$  exponent valid for the specific case. The same standards apply the unweighted log-linearized linear regression technique (E779 – Annex I) to calculate the leakage factor and exponent, which in this case are referred to as envelope leakage coefficient  $C$  and pressure exponent  $n$ , as well as to quantify the estimated precision error.

Furthermore, it is useful to point out that the instrumentation used for DALT testing is already functionally adequate for carrying out the necessary measurements.

### 3.2 Equivalent Operating Pressure

The second critical issue related to the evaluation of operating losses according to EN 16798-5, concerns the choice of average head as the value to which the model should be applied. The head to be considered cannot by definition be the average pressure.

If a reliable model is available, the first possibility for estimating operating leaks is the analytical calculation whereby the model is applied section by section, associating each pressure level with the relative share of the leaking surface.

Since this procedure can be cumbersome, an alternative is to find a way to identify the equivalent pressure level that takes into account the distribution of pressure values over all sections of the ductwork and allows the model to be applied only once and to the total area. A method for calculating the equivalent pressure for the purpose of estimating operating leakages was presented by the same author in a 2024 paper [36]. The name of the proposed method is 4-Bands Methods, the idea behind the method is to divide the range of pressure between the value at the fan  $P_{Sfan}$  and the value at the terminals (diffusers)  $P_{Sdiff}$  into four equal pressure bands and to calculate the percentage share of leaking surface associated with each pressure band. This calculation can be rather easily automated and implemented in the duct design procedure and provides the necessary indexes for an analytical calculation of the equivalent pressure in the form:

$$\Delta P_{Seq} = P_{Sfan} \times [\sum(\alpha_i \times C_i^n)]^{\frac{1}{n}} \quad (4)$$

Where  $\Delta P_{Seq}$  [Pa] is the equivalent operating pressure for leakage calculation purposes,  $P_{Sfan}$  [Pa] is the pressure at the fan,  $\alpha_{i=1,2,3,4}$   $[0 \div 1]$  are the shares of leaking area associated with each pressure band obtained from the preliminary analysis of the network,  $C_i$  are the calculation



constants that depend on the ratio between the pressure value at the fan and the pressure value at the terminals,  $n$  is the leakage exponent proper to the system and determined experimentally as indicated in the previous point.

It should be noted that the equivalent operating pressure value depends on the exponent and therefore the experimental determination of the correct value of the latter is also essential for this reason.

### 3.3 Evaluation of the Leaking Surface

EN 14239-2004 provides a calculation method for the leakage surface of both circular and rectangular ducts. The methodology is highly simplified so that comparable results can be guaranteed even when applied by different operators. In particular, fittings such as bends, tees, converging and diverging sections are not considered in their real geometry, but as virtual extensions of straight ducts whose extent is obtained through a simple geometric criterion. Area values are calculated as the multiplication of a perimeter by an increased length to account for the presence of fittings.

for the purposes of accurate leakage calculations this logic reveals two critical issues : the first is that special pieces are constructively more complex and normally have a significantly higher frequency of localized leakage failure situations than channels, and the second is that this calculation generally leads to significant underestimation of actual values and thus can significantly affect the results.

Actually, it should be emphasized that a precise quantification of the surface area is very important at the classification stage because the loss factor  $f$  is inversely proportional to the surface area value entered into the calculation, however, the really important parameter to be used when applying the model for the purpose of calculating operating leaks is the product  $A \times f$ , and if this value is obtained experimentally by means of a measurement applied to the entire system, it is not necessary to calculate the two factors  $f$  and  $A$  separately.

## 4 CONCLUSIONS

The research addresses some evaluations with reference to the existing regulatory framework for air leakage in HVAC air systems. The critical analysis of the methodologies currently adopted for leakage characterization highlights how measurement and modelling problems underlie an insufficient awareness of leakage and the consequent difficulty in quantifying lost energy. Experimental and literature evidence shows that the model historically adopted and used was created for classification purposes only, and that if used improperly, it can lead to errors (i.e. ranging from -19% to +47% in the case study). Considering the capabilities of modern DALT instruments and the existence of established calculation procedures in related fields such as building envelope tightness, it is believed that both technology and professionals are ready for a change in methodology and that the publication of local and international Standards adopting more reliable models is therefore desirable. Without this change, quantification cannot be considered satisfactory and the problem of leakage in aeraulic systems will not be addressed effectively.

## 5 ACKNOWLEDGEMENTS

The tests were conducted at the headquarters of Belimo Italia, which the authors wish to thank in the persons of Luca Pauletti and Michele Maestroni.

## 6 REFERENCES

- [1] The European Parliament And The Council Of The European Union, Directive (Eu) 2024/1275 Of The European Parliament And Of The Council Of 24 April 2024 on the energy performance of buildings, 2024.
- [2] V. Leprince, F.R. Carrié, Impact of ductwork airtightness on fan energy use: Calculation model and test case, Energy Build 176 (2018) 287–295.

- <https://doi.org/10.1016/j.enbuild.2018.07.029>.
- [3] N. Hurel, V. Leprince, Ductwork leakage: practical estimation of the impact on the energy overconsumption and IAQ, (2022). <https://www.aivc.org/resource/ductwork-leakage-practical-estimation-impact-energy-overconsumption-and-iaq>
  - [4] V. Leprince, PLEIAQ REPORT N°2019-01 Impact of ductwork leakage on the fan energy use of central mechanical ventilation units with heat recovery used in houses., 2019.
  - [5] J. Soenens, P. Pattijn, Feasibility study of ventilation system air-tightness, (2011). <https://www.aivc.org/resource/feasibility-study-ventilation-system-air-tightness>.
  - [6] P. Stroo, Class C air-tightness: Proven roi in black and white, (2011). <https://www.aivc.org/resource/class-c-air-tightness-proven-roi-black-and-white>.
  - [7] Craig P. Wray, Max H. Sherman, Duct Leakage Modeling in EnergyPlus and Analysis of Energy Savings from Implementing SAV with InCITe , 2010.
  - [8] ASHRAE, 215-2018 (RA 2021) Standard 215-2018 (RA 2021) -- Method of Test to Determine Leakage of Operative HVAC Air Distribution Systems (ANSI Approved), 2021.
  - [9] B. Moujalled, V. Leprince, A. Mélois, Statistical analysis of about 1,300 ductwork airtightness measurements in new French buildings: impacts of the type of ducts and ventilation systems, (2018). <https://www.aivc.org/resource/statistical-analysis-about-1300-ductwork-airtightness-measurements-new-french-buildings>.
  - [10] CEN/TC 156, EN 16798-3:2017 Energy performance of buildings - Ventilation for buildings. Part 3: For non-residential buildings - Performance requirements for ventilation and room-conditioning systems, 2017.
  - [11] CEN/TC 156, EN 16798-5-1:2017 Energy performance of buildings - Ventilation for buildings - Part 5-1: Calculation methods for energy requirements of ventilation and air conditioning systems , 2017.
  - [12] ASHRAE, Standard 90.1-2022—Energy Standard for Sites and Buildings Except Low-Rise Residential Buildings, n.d.
  - [13] CEN, EN 16798-5-1:2017 Energy performance of buildings - Ventilation for buildings, 2017.
  - [14] CEN, EN 16798-3:2017 Energy performance of buildings - Ventilation for buildings, 2017.
  - [15] EUROVENT, EUROVENT 2/2:1996 Air Leakage in Sheet Metal Air Distribution Systems, 1996.
  - [16] CEN, EN 12237:2003 Ventilation for buildings - Ductwork - Strength and leakage of circular sheet metal ducts., 2003.
  - [17] CEN, EN 1507:2006 Ventilation for buildings - Sheet metal air ducts with rectangular section - Requirements for strength and leakage, 2006.
  - [18] CEN, EN 17192:2018 Ventilation for buildings - Ductwork - Non-metallic ductwork - Requirements and test methods, 2018.
  - [19] CEN, EN 1751:2014 Ventilation for buildings - Air terminal devices - Aerodynamic testing of damper and valves, 2014.
  - [20] CEN, EN 15727:2010 Ventilation for buildings - Ducts and ductwork components, leakage classification and testing, 2010.
  - [21] CEN, EN 1886:2007 Ventilation for buildings - Air handling units - Mechanical performance, 2007.
  - [22] ANSI/ASHRAE/SMACNA, Standard 126-2016 Method of testing HVAC Air Ducts, 2016.
  - [23] ANSI/AMCA, 500-D-18 2018, Laboratory Methods of Testing Dampers for Rating, 2018.
  - [24] ANSI/AMCA, 511-13 Certified Ratings Program Product Rating Manual for Air Control Devices, 2013.
  - [25] ASHRAE, Standard 193-2010 (RA 2014) -- Method of Test for Determining the Airtightness of HVAC Equipment, 2014.
  - [26] CEN, EN 14239 2004 Ventilation for buildings - Ductwork - Measurement of ductwork surface area, 2004.
  - [27] CEN/CT156, EN 12599 Ventilation for buildings - Test procedures and measurement methods to hand over air conditioning and ventilation systems, 2012.
  - [28] L.A. Smith, The Current (2021) State of the Art for Air Leakage in Ductwork, 2021.
  - [29] SMACNA ASHRAE TIMA, ETL Report No. 459507 - Investigation of Duct Leakage, 1985.
  - [30] SMACNA, HVAC AIR DUCT LEAKAGE TEST MANUAL- 1985, 1985.
  - [31] CEN/TC 156, EN 14239:2004 Ventilation for buildings - Ductwork - Measurement of ductwork surface area, 2004.
  - [32] C. Aydin, B. Ozerdem, Air leakage measurement and analysis in duct systems, Energy Build 38 (2006) 207–213. <https://doi.org/10.1016/j.enbuild.2005.05.010>.
  - [33] S. Moujaes, R. Gundavelli, CFD simulation of leak in residential HVAC ducts, Energy Build 54 (2012) 534–539. <https://doi.org/10.1016/j.enbuild.2012.02.025>.

- [34] ASTM, E779:2019 Standard Test Method for Determining Air Leakage Rate by Fan Pressurization, 2019.
- [35] ASTM, 1554/E1554M:2018 Standard Test Methods for Determining Air Leakage of Air Distribution Systems by Fan Pressurization, 2018.
- [36] F. Pedranzini, E. Alloni, G. Ficco, A. Frattolillo, Proposal of a new method for the characterization and operational air leakages assessment in HVAC systems, Energy Build 305 (2024) 113881. <https://doi.org/10.1016/J.ENBUILD.2023.113881>.

# Experimental assessment of a resilient air-cooling system under extreme heat events in southern European climate conditions

María Jesús Romero-Lara\*<sup>1</sup>, Francisco Comino<sup>2</sup>, and Manuel Ruiz de Adana<sup>1</sup>

*1 Departamento de Química-Física y Termodinámica Aplicada, Escuela Politécnica Superior de Córdoba, Universidad de Córdoba*

*Campus de Rabanales, Antigua Carretera Nacional IV, km 396, 14071 Córdoba, España*

\*Corresponding author: [p42rolam@uco.es](mailto:p42rolam@uco.es)

*Presenting author*

*2 Departamento de Mecánica, Escuela Politécnica Superior de Córdoba, Universidad de Córdoba*

*Campus de Rabanales, Antigua Carretera Nacional IV, km 396, 14071 Córdoba, España*

## ABSTRACT

The global rise in average outdoor air temperatures has led to a significant increase in the demand for cooling energy in recent years. The development of resilient air-cooling systems capable of handling extreme heat events is essential to achieve the aim of Nearly Zero Energy Buildings. Ventilative cooling technologies based on indirect evaporative cooling systems are considered a sustainable solution in terms of indoor air quality and energy performance.

In this study, the daily energy performance of a renewable air-cooling unit (RACU) based on a dew-point indirect evaporative cooler (DIEC) and a desiccant wheel (DW) was experimentally evaluated under the real extreme heat events in southern Europe. The RACU prototype has been developed to be integrated into renewable District Heating and Cooling Networks. This air-cooling system allows controlling air humidity through the DW and air temperature and carbon dioxide emissions through the DIEC. The RACU system works with two inlet air streams: outdoor air (OA) and outdoor air for regeneration (ROA) to thermally activate DW. For the purposes of this work, both inlet air streams were 100% outdoor air. The RACU prototype does not use refrigerants.

The daily energy performance of the RACU was obtained in terms of Daily Energy Efficiency Ratio (DEER). The RACU system operated during four different days under the severe heat weather conditions in Cordoba, Spain, during office hours. Therefore, four different case studies were established to analyse the supply air conditions, sensible and latent capacities and DEER values for the RACU in this work.

Results indicated high DEER values for the RACU, ranged between 7.0 and 14.8. High values of daily sensible cooling energy, up to 177.0 MJ/day, and daily total latent capacity, up to 38.6 MJ/day, were also evident for the RACU. These results suggest that the use of resilient air-cooling systems as the RACU could be interesting under southern European climatic conditions of extreme heat, demonstrating high daily energy efficiency performance.

## KEYWORDS

Experimental results, evaporative cooling technology, Daily Energy Efficiency Ratio, severe weather conditions.

## 1 INTRODUCTION

Heating and cooling of buildings constitute 50% of the overall energy consumption in the European Union. Currently, 70% of this energy is generated from fossil fuels (Eurostat, 2023). In addition, one of the primary effects of climate change is the rise in outdoor temperatures worldwide, which directly increases the demand for cooling energy (IEA, 2023). Thus, designing and optimizing resilient air-cooling systems for extreme heat event scenarios is crucial to achieving the Nearly Zero Energy Buildings (NZEB) goal. Air-cooling systems based on the indirect evaporative cooling technology could be a potential solution in terms of thermal comfort, indoor air quality, reduction of carbon dioxide (CO<sub>2</sub>) emissions and higher energy efficiency (Romero-Lara, Comino, and Ruiz de Adana, 2021).

Thus, the main objective of the present work was to experimentally evaluate the daily energy performance of a renewable air-cooling unit (RACU) based on a dew-point indirect evaporative cooler (DIEC) and a desiccant wheel (DW), under real conditions of extreme heat in southern Europe. In this research work, the outdoor air conditions and supply air conditions for the RACU during four different days were also analysed to demonstrate the advantages of this prototype over traditional air-cooling systems, in terms of thermal comfort and energy savings.

## 2 MATERIAL AND METHODS

### 2.1 Description of the renewable air-cooling unit

The RACU prototype has been developed to be integrated into Renewable District Heating and Cooling Networks (RDHCN). This air-cooling system is mainly composed of a desiccant wheel (DW) for air humidity control and a dew-point indirect evaporative cooler (DIEC) for air temperature and indoor  $CO_2$  level control. The RACU works with two inlet air streams: outdoor air (OA) for the process side and outdoor air for regeneration (ROA), the latter being used to thermally activate the DW. The process side air is divided into supply air (SA), which supplies cool air to a building, and exhaust air (EA), which expels moist air after the indirect evaporative cooling process, as illustrated in Figure 1.

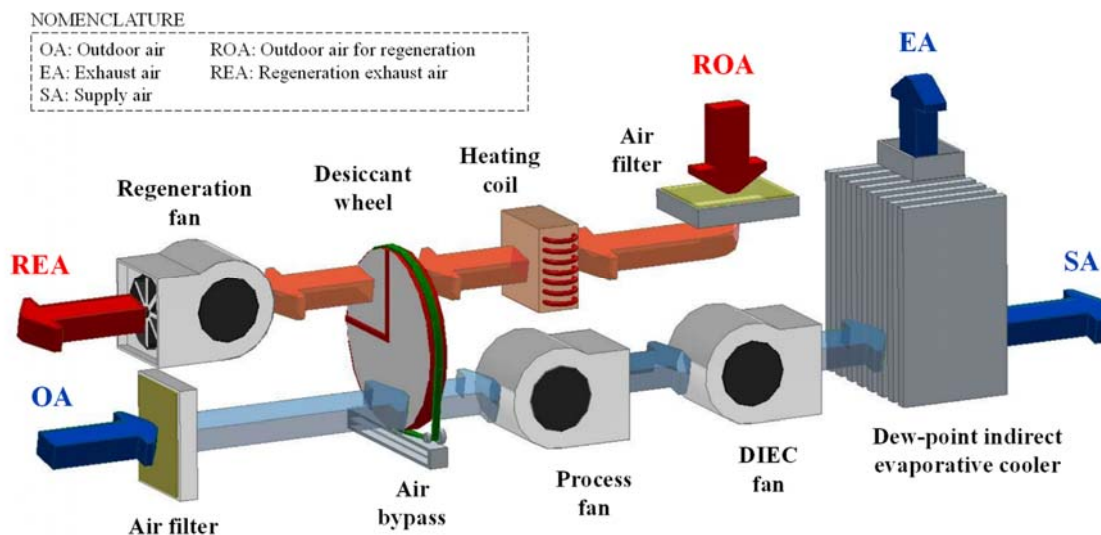


Figure 1: Main components of the renewable air-cooling unit (RACU).

The RACU operates without refrigerant gases and uses several elements to handle 100% outdoor air. The main technical characteristics of these components are described in a recent published work by the authors (Romero-Lara, Comino, and Ruiz de Adana, 2024). However, the main thermal characteristics of the RACU prototype are shown in Table 1.

Table 1: Thermal characteristics of the RACU.

Parameter	Value	Unit
Nominal process air flow rate	5236	m <sup>3</sup> /h
Nominal regeneration air flow rate	1745	m <sup>3</sup> /h
Nominal supply air flow rate	2880	m <sup>3</sup> /h
Nominal dehumidification capacity	16	kg/h

Nominal cooling capacity	18	kW
Process fan nominal power	2.65	kW
Regeneration fan nominal power	1.00	kW
DIEC fan nominal power	1.50	kW
Hydraulic pump nominal power	0.60	kW

## 2.2 Control system and operation modes

The RACU has been designed to independently control the indoor air temperature, indoor air humidity, and indoor air  $CO_2$  concentration in a building. In this work, an occupied room was not included since the main objective was to study the energy performance of the RACU. As can be observed from section 2.1.2 of the authors recent work (Romero-Lara, Comino, and Ruiz de Adana, 2024), three independent control loops were included to the RACU control system: temperature control (T), humidity control (H) and ventilation control (V). Seven different operation modes were established for the RACU according to these control loops. For this work, to analyse the energy performance of the RACU prototype under real severe outdoor air conditions in Cordoba, variable air flow rates were used, as illustrated in Figure 2.

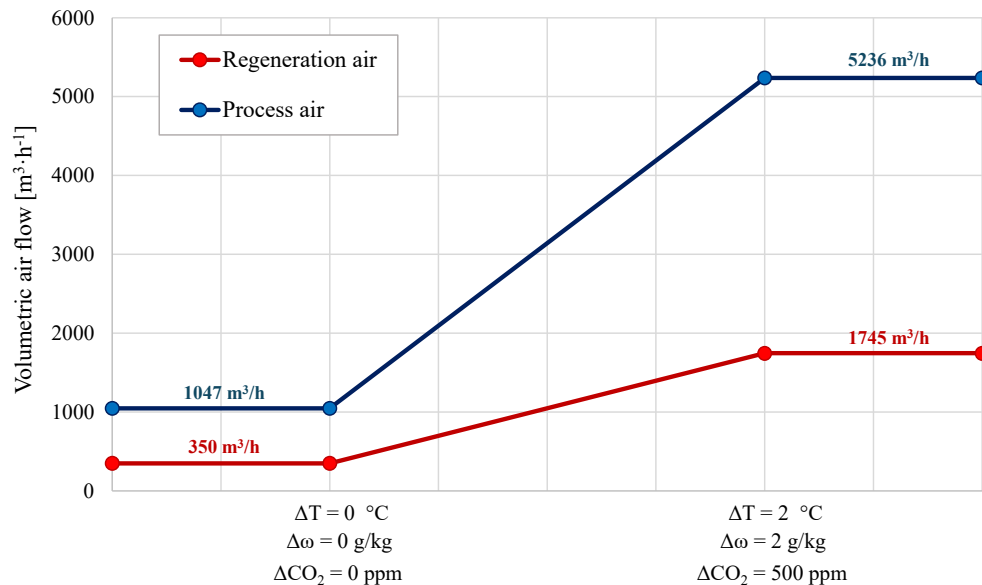


Figure 2: Variable volumetric air flow rates control for the RACU.

The process and regeneration volumetric air flows were adjusted from 20% to 100% of the respective nominal values, as shown in Figure 2. RACU worked at 100% of its nominal air flow rate when the increases of temperature ( $\Delta T$ ), humidity ratio ( $\Delta \omega$ ) and carbon dioxide ( $\Delta CO_2$ ) were equal to 2 °C, 2 g/kg and 500 ppm, respectively. When the set point (SP) conditions of temperature, humidity and  $CO_2$  were achieved, the percentage of these volumetric air flows was maintained at 20% to provide a minimum ventilation air flow rate, as observed in Figure 2.

## 2.3 Case studies under Cordoba weather conditions

For this work, the RACU operated under the severe summer weather conditions in Cordoba, Spain. According to the climate classification of the Basic Document HE Energy Savings – CTE (Ministerio de Fomento España, 2019), Cordoba has a “B4” classification, where “4” is the highest value of climate severity in summer, see Figure 3.

The RACU operated in four different days during office hours, that is, from 9:30 a.m. to 4:30 p.m. Therefore, four different case studies were generated for evaluating the SA conditions and the energy performance values for the RACU. Average value of OA temperature ( $T_{OA,avg}$ ) for study cases 1 and 2 was 25 °C. However,  $T_{OA,avg}$  value for study cases 3 and 4 was 33 °C. Average value of OA humidity ratio ( $\omega_{OA,avg}$ ) for study cases 1 and 3 was approximately 8 g/kg. However,  $\omega_{OA,avg}$  value for study cases 2 and 4 was approximately 9 g/kg. In addition, different values of set-point for temperature (16 or 18 °C) and humidity ratio (6 or 8 g/kg) were established to research the energy behaviour of the RACU under different working conditions.

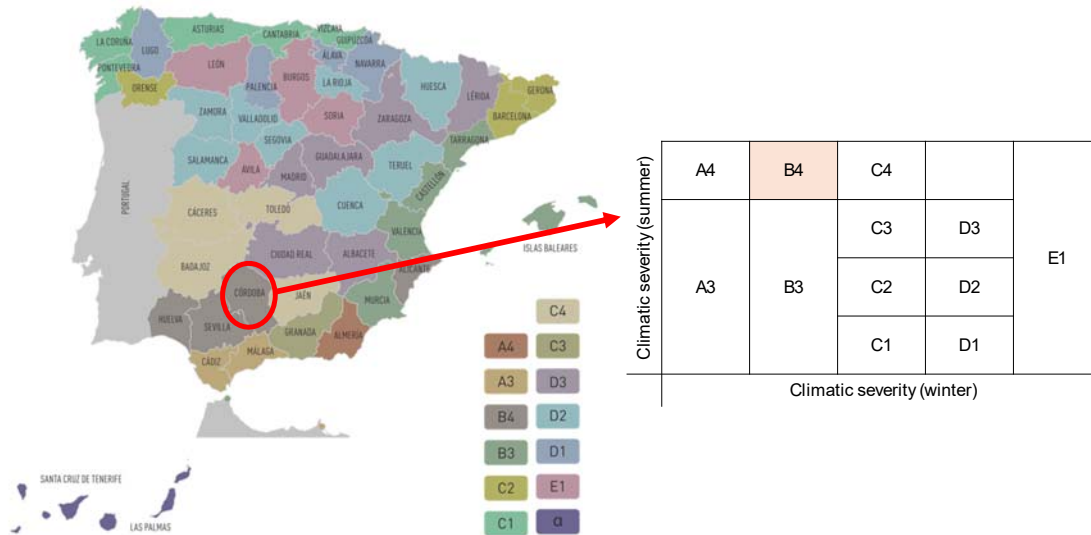


Figure 3: Climate classification for Cordoba, Spain.

## 2.4 Energy performance evaluation

In this work, the energy performance of the RACU was evaluated in terms of supply air conditions and Daily Energy Efficiency Ratio (DEER) for the four experimental cases studies. Sensible cooling capacity ( $\dot{Q}_S$ ), latent capacity ( $\dot{Q}_L$ ), and electrical power consumption ( $\dot{W}_{el}$ ) were calculated for the RACU according to Eq. 1, Eq. 2 and Eq.3, respectively.

$$\dot{Q}_S = \rho_{SA} \cdot \dot{V}_{SA} \cdot (h_{aux} - h_{SA}) \quad (1)$$

$$\dot{Q}_L = \rho_{SA} \cdot \dot{V}_{SA} \cdot (h_{OA} - h_{aux}) \quad (2)$$

$$\dot{W}_{el} = \dot{W}_{Process\ fan} + \dot{W}_{Regeneration\ fan} + \dot{W}_{DIEC\ fan} + \dot{W}_{motor,DW} + \dot{W}_{Hydraulic\ pump} \quad (3)$$

Where  $\rho_{SA}$  was the supply air density [ $\text{kg}/\text{m}^3$ ],  $\dot{V}_{SA}$  was the supply air volumetric air flow [ $\text{m}^3/\text{s}$ ] and  $h$  was the air specific enthalpy [ $\text{kJ}/\text{kg}$ ]. An auxiliary air state (aux) was defined as the combination of outdoor air temperature ( $T_{OA}$ ) and supply air humidity ratio ( $\omega_{SA}$ ). This auxiliary point was necessary to independently obtain the sensible capacity and latent capacity of the RACU. The  $\dot{W}_{elect}$  value for the RACU was obtained as the sum of the electrical power consumed by the three fans (process, regeneration and DIEC), the DW drive motor and the internal hydraulic pump in the DIEC, as shown in Eq. 3.

The  $\dot{Q}_S$ ,  $\dot{Q}_L$  and  $\dot{W}_{el}$  values for the RACU were obtained for each time interval (dt) of 30 seconds for each case study. Daily sensible cooling energy ( $Q_S$ ), daily latent capacity energy ( $Q_L$ ) and

daily electrical energy consumption ( $W_{el}$ ) were calculated for the RACU as the sum of sensible, latent and electrical energy shown for the RACU for one day operation (from 9:30 a.m. to 4:30 p.m). DEER values for the RACU were calculated as the ratio of daily sensible and latent energy to daily electrical consumption, as shown in Eq. 4.

$$DEER = \frac{Q_S + Q_L}{W_{el}} = \frac{\int (\dot{Q}_S + \dot{Q}_L) \cdot dt}{\int \dot{W}_{el} \cdot dt} \quad (4)$$

### 3 RESULTS AND ANALYSIS

Experimental results of four case studies are presented in this section. The values of supply air conditions of the RACU were analysed under real outdoor air conditions in Cordoba, Spain. The energy performance of the RACU in terms of daily sensible cooling capacity, daily latent capacity and DEER was also shown as main results of this work.

#### 3.1 Daily air conditions for Case study 1

Case study 1 consisted of the operation of the RACU during May 10, 2023, in Cordoba, Spain. The daily variation of  $T_{OA}$  and  $\omega_{OA}$  from 9:30 a.m. to 4:30 p.m. for this day can be observed in

Figure 4.  $T_{OA}$  values were between 17.2 °C and 29.8 °C and  $\omega_{OA}$  values were between 7.4 g/kg and 9.3 g/kg for this case study 1. According to these OA conditions values, the RACU came into operation 28.9% of period between 9:30 a.m. and 4:30 p.m. of that day. Since the values of  $T_{SP}$  and  $\Delta T$  were 18 °C and 2 °C, respectively, the DIEC of the RACU came into operation when  $T_{SA}$  value was higher than 20 °C and operated at the minimum air flow rate (20%) when  $T_{SA}$  of 18 °C was achieved, see Figure 4. According to the control system design for the RACU, the DW of the RACU came into operation if the DIEC was activated. A value of  $\omega_{SP}$  of 8 g/kg and a value of  $\Delta\omega$  of 1 g/kg were established for this case study 1. Thus, the DW worked when the DIEC was activated and  $\omega_{SA}$  value was higher than 9 g/kg, until  $\omega_{SP}$  of 8 g/kg was reached, see Figure 4. For this case study 1, the DIEC operated 85.6% of the RACU's daily operating time. However, the DW only operated 22.2% of that period due to the low outdoor air humidity values, as shown in Figure 4.

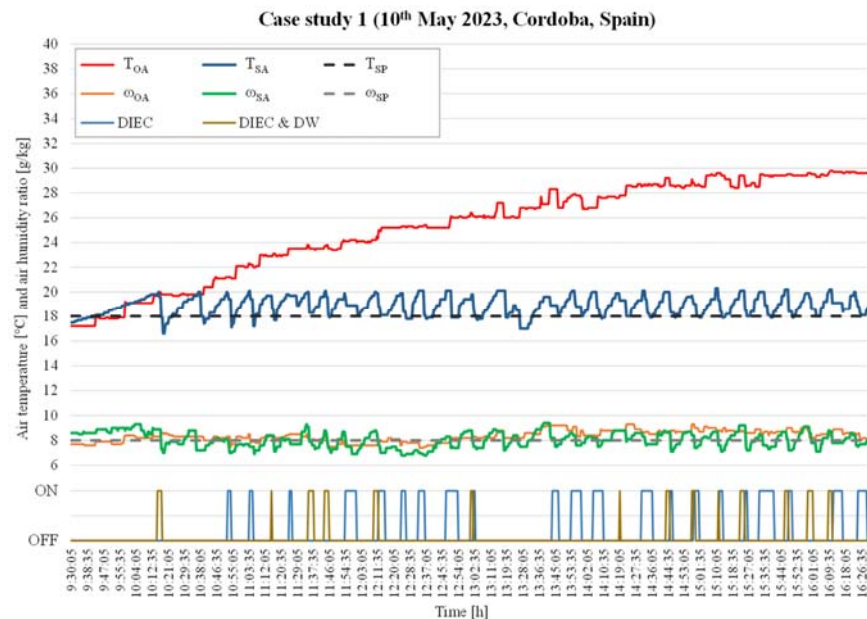


Figure 4: Air temperature and humidity values for Case study 1.



### 3.2 Daily air conditions for Case study 2

Case study 2 consisted of the operation of the RACU during October 4, 2023, in Cordoba, Spain. The daily variation of  $T_{OA}$  and  $\omega_{OA}$  from 9:30 a.m. to 4:30 p.m. for this day can be observed in Figure 5.  $T_{OA}$  values were between 17.7 °C and 29.9 °C and  $\omega_{OA}$  values were between 7.3 g/kg and 10.4 g/kg for this case study 2. According to these OA conditions values, the RACU came into operation 24.8% of period between 9:30 a.m. and 4:30 p.m of that day. Since the values of  $T_{SP}$  and  $\Delta T$  were 16 °C and 3 °C, respectively, the DIEC of the RACU came into operation when  $T_{SA}$  value was higher than 19 °C and operated at the minimum air flow rate (20%) when  $T_{SA}$  of 16 °C was achieved, see Figure 5. A value of  $\omega_{SP}$  of 6 g/kg and a value of  $\Delta\omega$  of 2 g/kg were established for this case study 2. Thus, the DW worked when the DIEC was activated and  $\omega_{SA}$  value was higher than 8 g/kg, until  $\omega_{SP}$  of 6 g/kg was reached, see Figure 5. For this case study 2, both the DIEC and the DW operated 98.1% of the RACU's daily operating time due to the higher outdoor air humidity values, as observed in Figure 5.

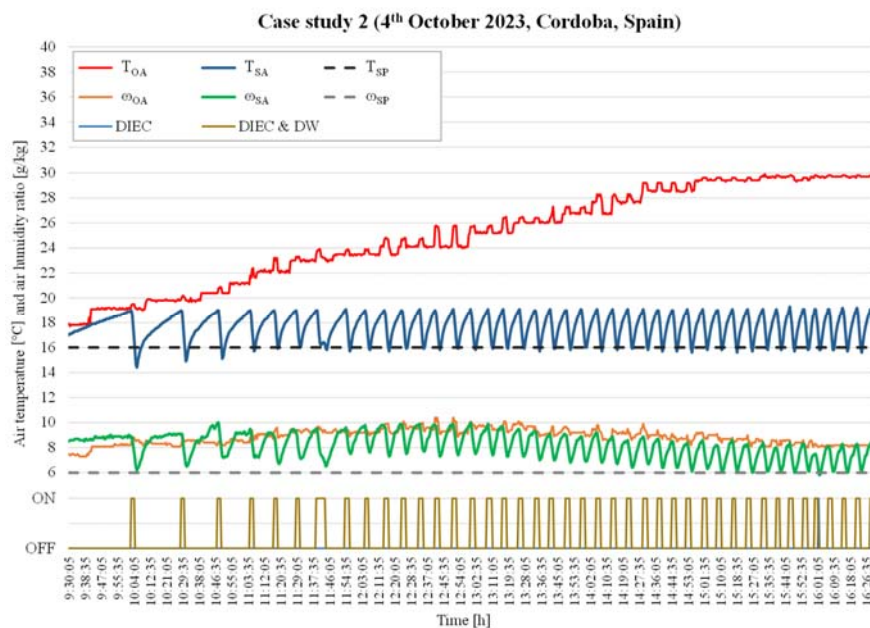


Figure 5: Air temperature and humidity values for Case study 2.

### 3.3 Daily air conditions for Case study 3

Case study 3 consisted of the operation of the RACU during June 14, 2023, in Cordoba, Spain. The daily variation of  $T_{OA}$  and  $\omega_{OA}$  from 9:30 a.m. to 4:30 p.m. for this day can be observed in Figure 6.  $T_{OA}$  values were between 25.2 °C and 38.4 °C and  $\omega_{OA}$  values were between 7.3 g/kg and 9.8 g/kg for this case study 3. According to these OA conditions values, RACU came into operation 52.0% of period between 9:30 a.m. and 4:30 p.m of that day. Since the values of  $T_{SP}$  and  $\Delta T$  were 18 °C and 3 °C, respectively, the DIEC of the RACU came into operation when  $T_{SA}$  value was higher than 21 °C and operated at the minimum air flow rate (20%) when  $T_{SA}$  of 18 °C was achieved, see Figure 6. A value of  $\omega_{SP}$  of 8 g/kg and a value of  $\Delta\omega$  of 1 g/kg were established for this case study 3. Thus, the DW worked when the DIEC was activated and  $\omega_{SA}$  value was higher than 9 g/kg, until  $\omega_{SP}$  of 8 g/kg was reached, see Figure 6. For this case study 3, the DIEC operated 97.04% of the RACU's daily operating time due to the high outdoor air

temperature values. However, the DW only operated 3.2% of that period due to the low outdoor air humidity values, see Figure 6.

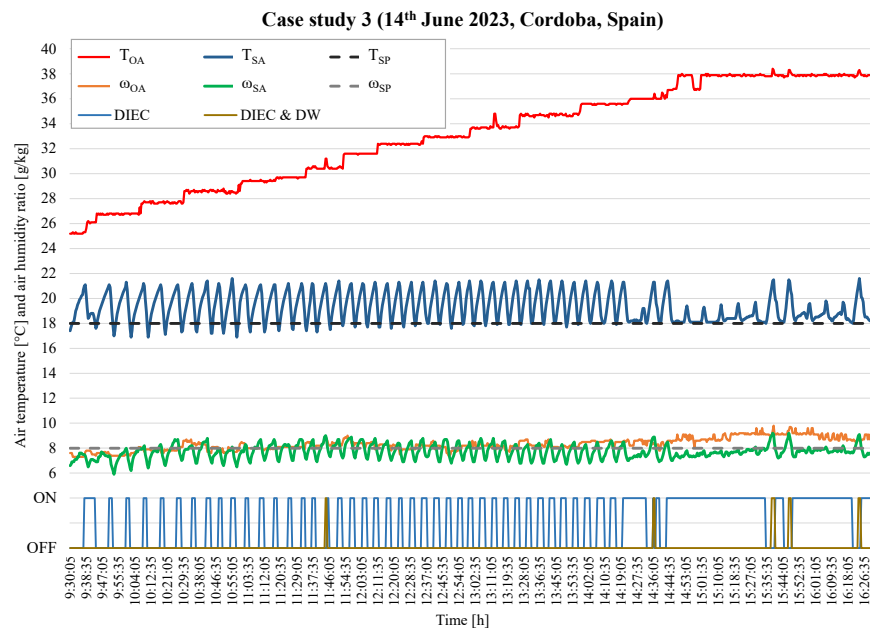


Figure 6: Air temperature and humidity values for Case study 3.

### 3.4 Daily air conditions for Case study 4

Case study 4 consisted of the operation of the RACU during July 27, 2023, in Cordoba, Spain. The daily variation of  $T_{OA}$  and  $\omega_{OA}$  from 9:30 a.m. to 4:30 p.m. for this day can be observed in Figure 7.  $T_{OA}$  values were between 26.0 °C and 38.3 °C and  $\omega_{OA}$  values were between 7.0 g/kg and 10.8 g/kg for this case study 4. According to these OA conditions values, RACU came into operation 70.7% of period between 9:30 a.m. and 4:30 p.m of that day. Since the values of  $T_{SP}$  and  $\Delta T$  were 16 °C and 3 °C, respectively, the DIEC of the RACU came into operation when  $T_{SA}$  value was higher than 19 °C and operated at the minimum air flow rate (20%) when  $T_{SA}$  of 16 °C was achieved, as shown in Figure 7. A value of  $\omega_{SP}$  of 6 g/kg and a value of  $\Delta\omega$  of 2 g/kg were established for this case study 4. Thus, the DW worked when the DIEC was activated and  $\omega_{SA}$  value was higher than 8 g/kg until  $\omega_{SP}$  of 6 g/kg was reached, as illustrated in Figure 7. For this case study 4, both the DIEC and the DW operated 96.8% of the RACU's daily operating time due to the high outdoor air temperature and humidity values, as observed in Figure 7.

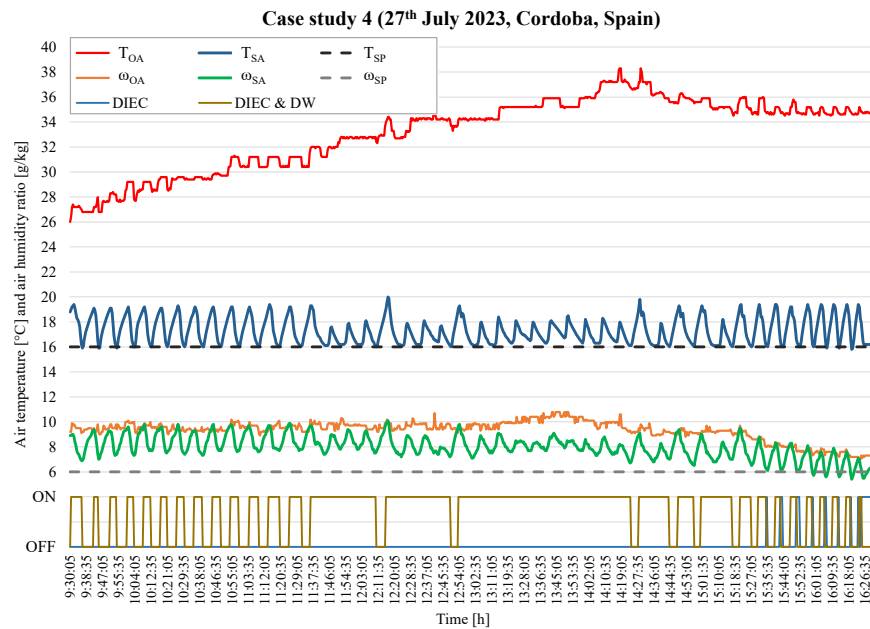


Figure 7: Air temperature and humidity values for Case study 4.

### 3.5 Comparative analysis of the RACU energy performance

Experimental results of the energy performance of the RACU are shown and analysed for the four case studies, as observed in Figure 8. The daily sensible cooling capacity, daily latent capacity, daily electrical-energy consumption and DEER values for RACU were calculated according to Eq. 1, Eq. 2, Eq. 3 and Eq. 4, respectively.

$Q_s$  values were between 28.1 MJ/day and 177.0 MJ/day for the RACU, as shown in Figure 8. Higher  $Q_s$  values were achieved for case study 3 (107.8 MJ/day) and case study 4 (177.0 MJ/day), the two days with the highest average  $T_{OA}$  values, around 33 °C. Regarding  $Q_L$  values, the RACU showed a lower range of values, between 4.6 MJ/day and 38.6 MJ/day, see Figure 8. The highest  $Q_L$  value was also achieved for case study 4 (38.6 MJ/day) due to the highest average  $\omega_{OA}$  value, around 9.3 g/kg. Therefore, the RACU achieved higher values of the total cooling capacity under more severe outdoor air conditions, that is, higher  $T_{OA}$  and  $\omega_{OA}$  values.

$W_{el}$  values for the RACU were between 2.7 MJ/day and 20.9 MJ/day, see Figure 8. The lowest  $W_{el}$  value (2.7 MJ/day) was shown for case study 1, for which  $T_{SP}$  and  $\omega_{SP}$  values were 18°C and 8 g/kg, respectively. In addition, low average  $T_{OA}$  and  $\omega_{OA}$  values were shown, 25 °C and 8 g/kg, respectively, for case study 1. However, the highest  $W_{el}$  value (20.9 MJ/day) was shown for case study 4, for which  $T_{SP}$  and  $\omega_{SP}$  values were 16°C and 6 g/kg, respectively. In addition, high average  $T_{OA}$  and  $\omega_{OA}$  values were shown, 33 °C and 9.3 g/kg, for case study 4, as illustrated in Figure 8. Therefore, higher  $W_{el}$  values were shown for higher OA conditions and lower SP conditions, due to the need for higher volumetric working airflow in RACU.

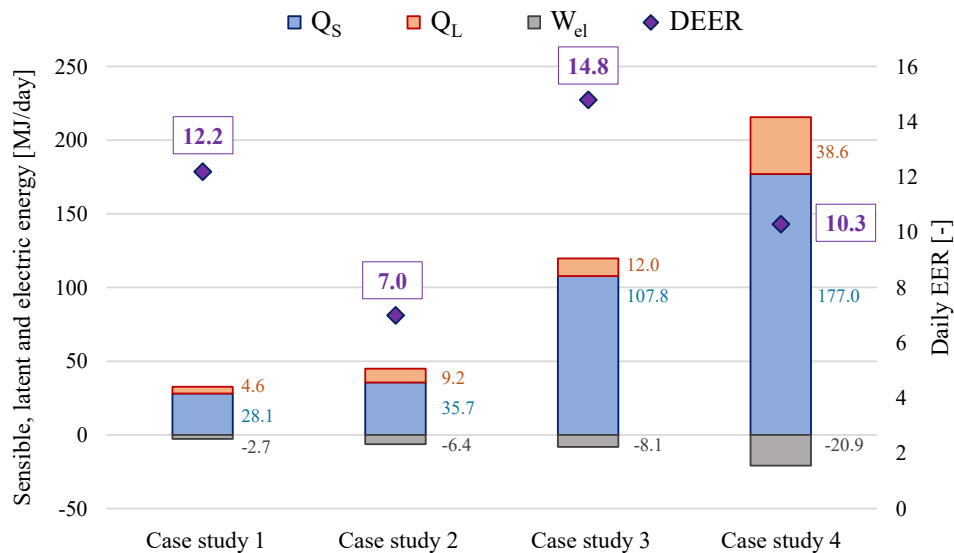


Figure 8: Energy performance values for the four case studies.

High DEER values were shown for the RACU in this work, between 7.0 and 14.8, see Figure 8. The lowest DEER value (7.0) was shown for case study 2, due to the low  $T_{OA}$  values range, as observed in Figure 5. Since the high  $\omega_{OA}$  values during that day, high operating percentage (98.1%) of the DW was shown, so, high value of working air flow in the RACU. However, the highest DEER value (14.8) was shown for case study 3, due to the high  $T_{OA}$  values range, see Figure 6. In addition, low  $\omega_{OA}$  values were shown for that day and, so, a low percentage of DW operation (3.2%). Therefore, higher DEER values were achieved for the RACU under lower values of outdoor air relative humidity and higher set-point conditions, due its higher  $Q_L$  and  $Q_S$  values and lower  $W_{el}$  values.

#### 4 CONCLUSIONS

The worldwide increase in average outdoor air temperatures has resulted in a higher demand for cooling energy in recent years. Developing resilient air-cooling systems for extreme heat event scenarios is essential to achieve high energy efficiency while improving thermal comfort and indoor air quality. In this work, the supply air conditions, and daily energy performance of a renewable air-cooling unit (RACU) are analysed for four different days under the severe heat weather conditions in Cordoba, Spain. The main findings obtained from this experimental evaluation were:

- Low supply air temperature values were reached, between 16°C and 18°C, despite high outdoor air temperatures, up to approximately 40°C. Supply air humidity was also reduced, showing values between 6 g/kg and 8 g/kg.
- High values of daily sensible cooling energy, up to 177.0 MJ/day, were achieved for the RACU, due to the high difference between outdoor air temperature and supply air temperature. High values of daily latent energy, up to 38.6 MJ/day, were also achieved for the RACU due to the DW operation. However, low consumed electrical energy values were shown for the RACU during the four different days, between 2.7 MJ/day and 20.9 MJ/day.
- The RACU achieved high values of daily energy efficiency ratio (DEER), between 7.0 and 14.8, despite using 100% outdoor air under severe heat weather conditions.

These results show that the use of resilient air-cooling systems as RACU could be a potential solution under southern European climatic conditions of extreme heat showing high daily energy efficiency performance.

## 5 ACKNOWLEDGEMENTS

The authors acknowledge the financial support received by European Union's Horizon 2020 research and innovation programme, through the research project WEDISTRICT Smart and local renewable Energy DISTRICT heating and cooling solutions for sustainable living, reference H2020-WIDESPREAD2018-03-857801.

## 6 REFERENCES

- Energy, Climate change, Environment. Heat pumps. Official website of the European Union. (2023). Available: [https://energy.ec.europa.eu/topics/energy-efficiency/heat-pumps\\_en](https://energy.ec.europa.eu/topics/energy-efficiency/heat-pumps_en).
- IEA - International Energy Agency's. (2023). Keeping cool in a hotter world is using more energy, making efficiency more important than ever. Available: <https://www.iea.org/commentaries/keeping-cool-in-a-hotter-world-is-using-more-energy-making-efficiency-more-important-than-ever>.
- Ministerio de Fomento, España. (2019). Documento Básico HE Ahorro de Energía 2019. *Código Técnico de La Edificación* 1–129.
- Romero-Lara, M.J.; Comino, F.; Ruiz de Adana, M. (2021). Seasonal analysis comparison of three air-cooling systems in terms of thermal comfort, air quality and energy consumption for school buildings in Mediterranean climates. *Energies* 14(4436).
- Romero-Lara, M.J., Comino F., Ruiz de Adana, M. (2024). Experimental assessment of the energy performance of a renewable air-cooling unit based on a dew-point indirect evaporative cooler and a desiccant wheel. *Energy Conversion and Management* 310(January):118486.

# Examining the Impact of Improving the Airtightness of the Building Envelopes on Differential Pressures and Contaminant Dispersion in Temporary Negative Pressure Isolation Rooms

Jooyeon Roh<sup>1</sup>, Shinye Lee<sup>1</sup>, Wonseok Lee<sup>1</sup>, Sejin Lee<sup>1</sup>, Myoung-souk Yeo<sup>\*2</sup>

*1 Department of Architecture and Architectural Engineering, Graduate School of Engineering, Seoul National University 08826 Seoul, Korea*

*2 Department of Architecture and Architectural Engineering / Institute of Construction and Environmental Engineering, Seoul National University 08826, Seoul, Korea*

*\*Corresponding author: msyeo@snu.ac.kr*

## SUMMARY

This study utilized a CONTAM simulation to assess the effects of airtightness improvements in TNPI rooms. Sobol sensitivity analysis was used to evaluate the impact of building envelope elements on pressure differentials and contaminant dispersion. Results showed that inter-room penetrations, ward doors, and ward ceilings significantly influenced differential pressure, while exterior walls and inter-room penetrations predominantly affected contaminant dispersion. These findings highlight the need for project-specific approaches in enhancing TNPI room airtightness, given that element impact varies by factors and does not correlate proportionally with their areas.

## KEYWORDS

Airtightness, Contaminant dispersion, Pressure differentials, Temporary negative pressure isolation room

## 1 INTRODUCTION

Airborne infection isolation room (AIIR) are used to isolate patients with respiratory pathogens and limit transmissions in health care facilities. When its capacity is met due to the surging number of patients, the general hospital wards are converted into temporary negative pressure isolation (TNPI) rooms. This adaptation involves installing portable high-efficiency particulate air (HEPA) exhaust fan units. Their volume flow rate is controlled to comply with the negative pressure criteria and was generally maintained high due to low airtightness as confirmed in prior studies (Lee et al., 2023; Shin et al., 2023). This high-volume flow rate has been raising concerns including increased noise and energy usage (Lee et al., 2023). To deal with these issues, checking for leakage and sealing areas in the room during the makeshift is necessary (Saravia et al., 2007) and related guidelines recommend enhancing the air tightness of the ward. Yet, the standardisation of sealing protocols or prioritization of sealing parts is vague and challenging due to several reasons. The conditions of the wards vary as confirmed in (Geeslin et al., 2008; Shin et al., 2023), which determine the initial pressure differentials. Changes in these leakage areas affect the subsequent variations in pressure differentials and potential contamination risks. Therefore, modifications to the airtightness performance and the extent of these improvements should first be considered in project-specific approaches. Thus, this study investigated the impact of enhancing the air tightness in wards on pressure differentials and contaminant dispersion.

## 2 METHODOLOGY

This study leveraged a CONTAM simulation model to assess the effects of enhancing the airtightness of the building envelopes in TNPI rooms, considering the practical challenges of

on-site experiments and comparative studies in real-world scenarios. As shown in Figure 1, the detailed methodology is outlined as follows:

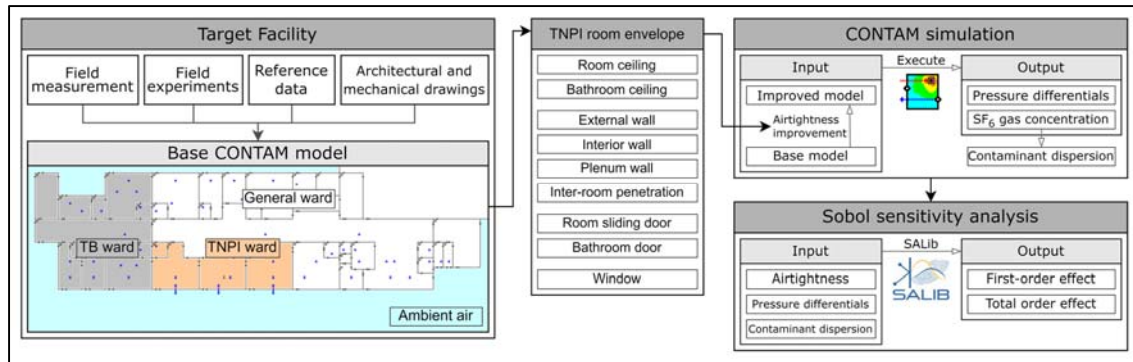


Figure 1: Schematic diagram depicting the methodology of the study

First, the target hospital ward was modeled using CONTAM. The initial airtightness was assumed based on reference datasets that can replicate the experimental data. Subsequently, it was hypothesized that the airtightness of the temporary negative pressure isolation (TNPI) rooms could be enhanced by up to 80%. These specific parameter ranges were employed in Sobol sensitivity analysis to quantitatively evaluate the impact of each building envelope on pressure differentials and contaminant dispersion. The elements considered for potential improvements included room ceilings, bathroom ceilings, windows, external walls, interior walls, inter-room penetrations, plenum walls, room sliding door, and bathroom doors.

### 3 RESULTS AND DISCUSSION

#### 3.1 Effects of improving the airtightness on pressure differentials

The analysis, which included both first-order and total-order effects, indicated that inter-room penetrations (0.44), ward doors (0.28), and ward ceilings (0.19) exert the most substantial influence on differential pressure, in that sequence. In contrast to the typical makeshift enhancements of existing facilities, where the exterior wall was previously identified as the major influencer on differential pressure magnitudes (Roh et al., 2024), the exterior wall exhibited a less significant effect in scenarios where airtightness was enhanced. This trend contrasts markedly with that observed for inter-room penetration. In the case of ward ceilings and doors, they significantly impact differential pressure as factors contributing to the overall facility's airtightness and leakage area during improvements.

#### 3.2 Effects of improving the airtightness on contaminant dispersion

Contaminant dispersion was evaluated based on the concentration of SF<sub>6</sub> gas detected in each zone, following its dispersion in the central room of three consecutive TNPI rooms. The analysis indicated negligible differences between the first-order and total-order effects on the potential infection risks by different elements. Contrary to the impact on differential pressure, the concentration of SF<sub>6</sub> gas within the TNPI rooms was significantly influenced by the exterior walls (0.33), followed by windows (0.13), ward ceilings (0.10), and bathroom ceilings (0.04). This pattern suggests that airflows expelled through the TNPI rooms' exterior walls and windows and re-entering through the windows of the general wards and corridors in the same row exert the most significant influence. For elements impacting the concentration in the general ward and corridor adjacent to TNPI rooms, the influence was ranked in order of exterior

wall, inter-room penetration, window, and ward door. However, it is notable that the absolute magnitudes of these effects were relatively small, approximately 0.3.

### **3.3 Overall results and discussion**

Considering both pressure differentials and contaminant dispersion, during the makeshift in the target facility, it is necessary to improve the airtightness performance in the following order: inter-room penetration, exterior wall, room sliding door, and room ceiling. Each element within the converted TNPI rooms affects the differential pressure and potential infection risks to varying degrees, regardless of its total area. Moreover, the magnitude of each impact does not correlate proportionally with the areas of the respective elements, underscoring the necessity for a project-specific approach. Yet, the simulations in this study were conducted with ambient air treated as a single zone for re-entry and diffusion, which may have resulted in underestimations of contaminant dispersion compared to real-world situations.

## **4 CONCLUSION**

This study responds to the urgent need to enhance airtightness in TNPI rooms, especially when general hospital wards are converted during high patient inflow. Utilizing CONTAM simulations, the improvements in airtightness by up to 80% and their effects on pressure differentials and potential infection risks were evaluated. Results indicate that inter-room penetrations and ward doors significantly influence differential pressures, while exterior walls and inter-room penetrations are the primary drivers of infection risks. Accordingly, enhancements in airtightness at inter-room penetrations, exterior walls, room sliding doors, and ward ceilings should be prioritized in such makeshift adaptations. The results underscore the necessity for tailored interventions, as the magnitude of impact is not proportional to the area of each modified element.

## **5 ACKNOWLEDGEMENTS**

This research was supported by a grant of the project for Infectious Disease Medical Safety, funded by the Ministry of Health & Welfare, Republic of Korea (grant number : RS-2022-KH124613(HG22C0017)).

## **6 REFERENCES**

- Geeslin, A., Streifel, A., & Nelson, G. (2008). Air Leakage Analysis of Special Ventilation Hospital Rooms. *ASHRAE Transactions*, 114(2), 447–452.
- Lee, S., Lee, W., Kim, E., & Yeo, M. (2023). Investigations on the emergency operation status of existing medical facilities to prepare for emerging infectious diseases in the post-COVID-19 era. *Journal of The Korea Institute of Healthcare Architecture*, 29(1), 43–51.
- Roh, J., Lee, W., Lee, S., & Yeo, M. (2024). Analysis of Airtightness Performance and Differential Pressure Relationships in Rapidly Converted Temporary Negative Pressure Isolation Rooms. *Korean Journal of Air-Conditioning and Refrigeration Engineering*, 36(7), 325–331.
- Saravia, S. A., Raynor, P. C., & Streifel, A. J. (2007). A performance assessment of airborne infection isolation rooms. *American Journal of Infection Control*, 35(5), 324–331.
- Shin, H. W., Kim, D. W., Kim, J. M., Jung, H. B., & Kang, D. H. (2023). Analysis of Minimum Airflow Differences between Supply and Exhaust Air according to Airtightness of Rapidly Converted Temporary Negative Pressure Isolation Rooms. *Journal of The Korea Institute of Healthcare Architecture*, 29(4), 69–77.



# Trends in Indoor Environmental Quality in Non-Domestic Energy-Efficient Buildings in Ireland: The BENEFIT Project

Jorge Fernandes<sup>1</sup>, Miriam Byrne<sup>1</sup>, Adam Collison<sup>1</sup>, and James A. McGrath<sup>2</sup>

*1 School of Natural Sciences  
University of Galway  
Galway, Ireland*

*2 Department of Experimental Physics  
Maynooth University  
Maynooth, Ireland*

*\*Corresponding author:  
jorge.fernandes@univeristyofgalway.ie*

## SUMMARY

The BENEFIT project seeks to assess indoor environmental quality and occupant comfort in energy efficient non-domestic Irish buildings with the aim of developing ventilation guidelines for future retrofits and new builds. The project, in collaboration with SEAI's Pathfinder programme, aims to conduct a comprehensive and scientifically robust assessment of the impacts of energy-efficient policies in non-domestic settings across Ireland, with a particular focus on newly constructed energy-efficient buildings. Multizone monitoring with an innovative hybrid methodology, via low-cost and high-grade sensors, is used to assess IEQ, capturing longer-term trends through precise measurements of indoor pollutants (PM<sub>2.5</sub>, Radon, TVOC, BTEX, Formaldehyde, Ozone, NO<sub>2</sub>, CO and CO<sub>2</sub>).

## KEYWORDS

Indoor Environmental Quality (IEQ), Energy Efficiency, Long-term monitoring, Schools, Offices

## 1 INTRODUCTION

The 2021 Glasgow Agreement (UNFCCC, 2021) underscores the continued global emphasis on reducing carbon emissions as a key political goal, and the International Energy Agency recognises the significance of energy efficiency advancements in their crucial role in achieving a low-carbon future. However, energy efficiency does not always equate to good indoor environmental quality (IEQ) as a consequence of compromises in ventilation rates and buildings' airtightness.

In recent years, significant research has concentrated on exploring the implications of energy improvements in the residential sector. Although much research has focused on residential energy enhancements, offices and schools have not received comparable attention. Addressing indoor air quality in such environments is critical for the health, well-being, and productivity of employees and students.

The maintenance of thermal comfort, in addition to indoor air quality, presents a further challenge when energy efficiency improvements are considered in public buildings. With expected increases in temperature due to future climate change, thermal comfort preservation requires not only the assurance of adequate warmth in buildings during the winter period, but also adequate cooling during summer, and this latter aspect has not been widely addressed in literature to date.

Vardoulakis et al. (Vardoulakis, et al., 2015) found that newly constructed, highly insulated buildings are at higher risk of overheating compared to older buildings. However,

Fosas et al. (Fosas, et al., 2018) argue that while increased insulation can cause overheating in poorly designed buildings, it reduces overheating in well-designed buildings. The current findings suggest that maintaining comfortable indoor conditions will become increasingly challenging as the climate warms, which is coupled at this stage with a deficit in studies, analysis, and data. The BENEFIT project aims to fill this research gap by assessing IEQ in energy-efficient offices and schools across Ireland. Utilising real-time monitoring, the project measures key pollutants such as PM<sub>2.5</sub>, TVOCs, formaldehyde, BTEX, ozone, radon, NO<sub>2</sub>, and CO<sub>2</sub>. The BENEFIT project aims to fill this research gap by conducting an assessment of IEQ in energy-efficient offices and schools across Ireland. Utilising real-time monitoring, the project measures key pollutants such as PM<sub>2.5</sub>, TVOCs, formaldehyde, BTEX, ozone, radon, NO<sub>2</sub>, and CO<sub>2</sub>.

## 2 METHODOLOGY

The research focuses on evaluating IEQ within newly constructed energy-efficient offices and schools. The methodology includes capturing data from various indoor environments, spanning different student age groups (5 to 18 years old) and multiple office settings. Newly constructed energy-efficient buildings across Ireland will be sampled using a combination of multizone real-time monitoring and hybrid methodologies. This involves deploying both high-grade and low-cost sensors, utilising real-time, active, and passive sampling approaches. (Table 1).

This approach enables a detailed assessment of IEQ by capturing longer-term trends and conducting precise measurements of critical indoor pollutants. The key pollutants monitored include PM<sub>2.5</sub>, Total Volatile Organic Compounds (TVOCs), formaldehyde, BTEX (benzene, toluene, ethylbenzene, and xylenes), ozone, radon, nitrogen dioxide (NO<sub>2</sub>), and carbon dioxide (CO<sub>2</sub>). Alongside monitoring pollutants, the study will collect data on thermal comfort (Temperature and Relative Humidity (RH)), occupant satisfaction, building and ventilation attributes, and activity and occupancy patterns through surveys.

Table 1: Sensor Specifications and Pollutant Detection in the BENEFIT Project

Sensor	Sampling	Level	Detectable Pollutants
Graywolf Direct Sense II	Real-time	High-Grade	TVOCs, CO, CO <sub>2</sub> , RH, Temp., NO <sub>2</sub> , O <sub>3</sub>
TSI SidePak AM520	Real-time	High-Grade	Particulate Matter (PM <sub>2.5</sub> )
Airthings Space Wave Plus	Real-time	Low-Cost	Radon, TVOCs, RH, Temp., CO <sub>2</sub>
GRADKO Sorbent tubes	Active	High-Grade	Individual VOCs (via GC-MS)
GRADKO Diffusion Tube NO	Passive	Low-cost	Nitrogen Oxides (NO <sub>x</sub> )
SKC UME <sub>x</sub> 100	Passive	Low-cost	Formaldehyde
SKC VOC Check 575	Passive	Low-cost	BTEX, Pinene, Limonene

## 3 RESULTS AND DISCUSSION

The results of this project include time series for PM<sub>2.5</sub>, Radon, TVOC, NO<sub>2</sub>, CO, CO<sub>2</sub>, Temperature and Relative Humidity from real-time measurements. Data analysis include identifying trends, assessing seasonality, and examining correlations between various pollutants. Air exchange rates, as well as statistical measures such as mean, median, and standard deviation, are estimated for all pollutants and will be contextualised and compared to guideline values for indoor environmental quality.

Furthermore, the quantification of individual VOCs, BTEX, and formaldehyde will be compared to guideline values, providing detailed information on exposure levels for workers and students in newly constructed buildings with energy-efficient mechanisms.

A system to visually evaluate each sampled room throughout all non-domestic buildings will be used for fast and qualitative evaluation of IEQ, identifying exceeding values, and concerning pollutants, thus contextualising building properties and ventilation effectiveness. This comprehensive analysis will offer valuable insights into the effectiveness of energy-efficient designs in maintaining healthy indoor air quality.

#### 4 CONCLUSIONS

The data collected during this project will provide unique insight into the increased energy performance standard in non-domestic buildings and provide a detailed assessment of the ventilation approach with accompanying indoor air pollution concentrations.

The analysis of all data will provide policymakers with insights into effective guidelines for energy-efficient buildings and integrate environmental standards into building regulations. Additionally, the extensive air quality and thermal comfort data will support the development of smarter ventilation controls, enhancing Ireland's capacity for energy research and fostering advancements in indoor environmental quality.

The study findings from indoor air quality monitoring will clarify if and how energy-efficient buildings maintain healthy indoor environments amidst changing climate conditions. This offers a comprehensive view of the effectiveness of current guidelines and regulations, addressing critical knowledge gaps and comparing outcomes between newly constructed and retrofitted buildings to inform future strategies and advancements.

#### 5 ACKNOWLEDGEMENTS

The BENEFIT project (668) is funded by the Government of Ireland through the Sustainable Energy Authority of Ireland's 2021 Research, Development and Demonstration Funding Programme.

#### 6 REFERENCES

- Fosas, D., Coley, D. A., Natarajan, S., Herrera, M., Fosas de Pando, M., & Ramallo-Gonzalez, A. (2018). Mitigation versus adaptation: Does insulating dwellings increase overheating risk? *Building and Environment*, 143:740-759.
- UNFCCC. (2021). *Glasgow Climate Pact*. Obtido de [https://unfccc.int/sites/default/files/resource/cop26\\_auv\\_2f\\_cover\\_decision.pdf](https://unfccc.int/sites/default/files/resource/cop26_auv_2f_cover_decision.pdf)
- Vardoulakis, S., Dimitroulopoulou, C., Thornes, J., Lai, K., Taylor, J., Myers, I., . . . Wilkinson, P. (2015). Impact of climate change on the domestic indoor environment and associated health risks in the UK. *Environ Int*, 85:299-313.

# Design and performance verification methods for naturally ventilated buildings from the experience of ABC 21 EU Project

Izabella Milto<sup>\*1,4</sup>, Silvia Erba<sup>1</sup>, Andrea Sangalli<sup>1</sup>, Guilherme Carrilho da Graça<sup>2</sup>, François Garde<sup>3</sup>, Lorenzo Pagliano<sup>1</sup>

*1 Polytechnic University of Milan  
Via Edoardo Bonardi 3  
Milan, Italy*

*2 University of Lisbon  
Campo Grande 1749-016  
Lisbon, Portugal*

*3 University of La Réunion  
40 Avenue de Soweto  
Saint Pierre, Réunion, France*

*4 IUSS School for Advanced Studies  
Piazza della Vittoria 15  
Pavia, Italy*

\*Corresponding author: [izabella.milto@iusspavia.it](mailto:izabella.milto@iusspavia.it)

Presenting author: underlined First & Last name

## ABSTRACT

The research exposes a critical feedback loop: the building sector's high energy consumption and emissions contribute significantly to climate change. Warming temperatures, in turn, lead to increased reliance on energy-intensive HVAC systems, further exacerbating the problem.

To investigate the potential of passive cooling systems for achieving energy-efficient buildings, the research proposes a methodology for building design and building performance evaluation. Focusing on the interplay between climate, building design, and urban planning, the research plans weather data analysis, measurement campaigns, and structures the design process into four phases favoring advanced natural ventilation.

The design methodology involves:

1. Identifying optimal cooling strategies based on local climate and building typology.
2. Developing a natural ventilation system, potentially supplemented with strategies to increase the ventilative cooling capacity.
3. Optimizing the ventilation solution.
4. Conducting detailed simulations for thermal comfort and energy use.

Additionally, a survey tool applicable to various case studies has been developed. The tool evaluates the feasibility and extent of natural ventilation use and determines the need for mechanical assistance (fans or passive methods) in driving the air flow.

Key findings reveal that while solely relying on natural ventilation might be challenging in hot and humid climates during rainy seasons, prioritizing passive cooling systems remains crucial. The study demonstrates that mechanically assisted natural ventilation can provide sufficient thermal comfort in many cases. Furthermore, strategies like Nocturnal Ventilative Cooling, coupled with a bioclimatic design approach during the planning phase, can significantly reduce the energy demand of HVAC systems.

By highlighting the potential of passive cooling systems for energy-efficient buildings, this research offers valuable insights for architects and urban planners seeking to create sustainable built environments. It underscores the importance of sustainable practices within building design and offers practical strategies for implementation.

## KEYWORDS

Natural ventilation, passive cooling systems, bioclimatic architecture, indoor thermal comfort, energy need for heating and cooling

## 1 INTRODUCTION

Global and regional climate change increases the temperature of cities and skyrockets the cooling energy use of buildings. The use of conventional compression cycle air conditioning increases the peak electricity demand and obliges utilities to build additional power plants that operate for a limited number of hours per year increasing the cost of the electricity supply [45].

Furthermore, air conditioning can be an important source of environmental and indoor air quality problems, like the ozone depletion and the potential warming of the ambient environment [47]. The considerable operational cost of air conditioning is a serious burden for low-income population that is living in non-thermally protected buildings, with the associated high energy needs for cooling [48].

Due to financial constraints, low-income population is exposed to extreme indoor temperatures highly exceeding the health and comfort thresholds [46]. Without strong and effective policies, the building sector's energy consumption is projected to rise significantly due to climate change combined with several technological, economic and social drivers [1]. During the recent years, several passive and active alternative cooling technologies and strategies for buildings and open spaces have been developed and successfully tested [16].

## 2 THERMAL COMFORT IN HOT CLIMATES

Thermal comfort is defined as: ‘that condition of mind which expresses satisfaction with the thermal environment and is assessed by subjective evaluation’ [58]. It is the parameter of indoor environmental quality (IEQ) which has been more widely investigated and extensive documentation is available in literature [11, 42, 44]. To evaluate the indoor thermal comfort conditions, many surveys about thermal sensations have been the base for the development of various comfort models aiming at predicting the average comfort perception of groups of people exposed to a certain environment.

The assessment of thermal comfort presented in the Standards EN 16798-1:2019 [56] and ASHRAE 55:2020 [58] indicates two main typologies of comfort model:

- the “Fanger (PMV/PPD) model” (EN ISO 7730 [27]), proposed for actively conditioned buildings,
- while the “Adaptive Model” is proposed for naturally conditioned spaces and when active systems, even if installed, are not in use (ASHRAE 55:2020).

In tropical climates and naturally conditioned spaces, field studies have found that the international standard for indoor climate, ISO 7730 [27] based on Fanger’s predicted mean vote equations, does not adequately describe comfortable conditions [9,14,37]. In warm climate conditions, PMV predicts that people will feel hotter than they actually do and therefore tends to encourage the use of more air conditioning than necessary. Fanger himself did recognize that “in non-air-conditioned buildings in warm climates, occupants may sense the warmth as being less severe than the PMV predicts“ [40].

In the last decades, several design activities and successful construction activities have taken place based on the Givoni’s comfort zone [16,21] or the Standard Effective Temperature (SET\*) model developed by Gagge [17,18,24] and growing evidence of comfort acceptance by occupants of those buildings has been found [30,31]. Studies and tools are available in literature to compare different thermal comfort models (e.g. Attia et al. [1] developed an analysis application for bioclimatic design strategies in hot humid climates and showed the comfort models comparison for the two major cities of Madagascar, situated off the southeast coast of Africa).

We include in this chapter a review of the recent updates and changes in the international standards. The summary is meant to facilitate practical application of the knowledge gathered in the last decade. The recent updates of the standard have relevant implications for the design and assessment of bioclimatic and passive strategies.

## 2.1 The Adaptive Comfort Model

The adaptive comfort theory has been developed from field studies and considers the building occupants as active agents interacting with their built environment [11]. This model relates indoor design temperatures or acceptable temperature ranges to outdoor meteorological or climatological parameters. There are currently two main standards related to indoor thermal comfort assessment which propose the adaptive model in buildings without mechanical cooling or heating systems in operation: the European EN 16798-1 [56] and the American ASHRAE 55 [58].

## 2.2 The Elevated Air Speed Comfort Zone Method

According to the standard ASHRAE 55:2020, the Elevated Air Speed Comfort Zone method uses the Analytical Comfort Zone Method combined with the Standard Effective Temperature (SET). It is permissible to apply the method to all spaces within the scope of the ASHRAE 55:2020 standard where the occupants have activity levels that result in average metabolic rates between 1.0 and 2.0 met, clothing insulation  $I_{cl}$  between 0.0 and 1.5 clo, and average air speeds  $V_a$  greater than 0.20 m/s.

Figure 1 represents two cases (0.5 and 1.0 clo) of the Elevated Air Speed Comfort Zone Method, and it is applicable as a method of compliance for the conditions specified in the figure. The figure also defines comfort zones for air movement with occupant control (darkly shaded) versus without occupant control (lightly shaded).

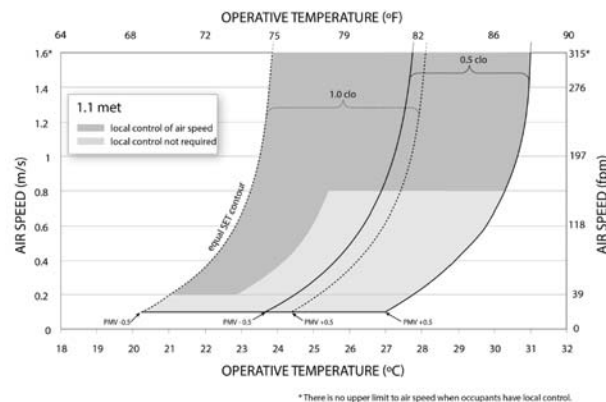


Figure 1: Acceptable ranges of operative temperature to and average air speed  $V_a$  for 1.0 and 0.5 clo comfort zones at humidity ratio 0.010, according to the ASHRAE Elevated Air Speed Comfort Zone Method [29]

Where there are fans (that can be controlled directly by occupants) or other means for personal air speed adjustment (e.g. personal ventilation systems, or personally operable windows) it is permitted to consider an increase of the upper acceptability temperature limits by the corresponding  $\Delta t_0$  reported in Table 1:

Table 1: Increases in acceptable operative temperature limits ( $\Delta t_0$ ) in occupant-controlled naturally conditioned spaces according to [58]

Average Air Speed $V_a$ [m/s]	$\Delta t_0$ [°C]
0.6	1.2
0.9	1.8
1.2	2.2

### 3 BIOCLIMATIC ARCHITECTURE AND PASSIVE SYSTEMS

The EU's buildings remain generally inefficient, accounting for 40% of final energy consumption and 36% of the EU's total CO<sub>2</sub> emissions [57]. The HVAC systems are one of the main contributors for the increase in energy consumption, being expected that in non-residential buildings, the energy use due to cooling will increase by 275% by 2050 [45].

The use of bioclimatic principles (geometry, orientation, shading...) and passive cooling systems should be strongly encouraged. As for the use of Natural Ventilation to this purpose, using the nomenclature of Givoni [22] we can distinguish (among the passive cooling systems):

**Comfort Ventilation:** When the indoor temperature, under still air conditions, seems to be too warm to occupants, it is possible to provide comfort through higher indoor air velocity. This strategy is useful when indoor comfort can be experienced at outdoor air temperature (up to about 30°C) with acceptable indoor air speed. If conditions are not favorable for opening windows, increase air velocity with well-designed and positioned ceiling fans, standing fans, and desk fans.

**Nocturnal Ventilative Cooling:** Night ventilation cools building masses by convective exchange with outdoor air. During the daytime, cooled masses can serve as a heat sink for solar and internal heat gains and ventilation should be minimized. Daytime comfort ventilation and nocturnal ventilative cooling are in many cases mutually exclusive. Figure 2, taken from [29] gives a qualitative idea of the type of climates where the two systems may be usefully adopted.

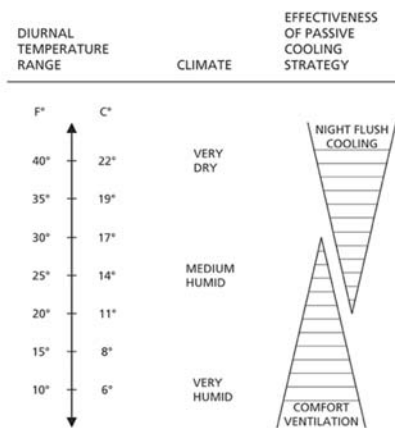


Figure 2: The performance of night-flush cooling and comfort ventilation is a function of diurnal temperature range (max – min outdoor temperature). Note that Lechner uses the term “night flush cooling” for the passive system which Givoni calls “Nocturnal ventilative cooling” [43]

Architectural design based on bioclimatic features has long been of interest to many designers. The literature review conducted by ABC21 [12] offers a non-exhaustive but rather complete view over the type of guidance available, particularly for the pre-design stage, where the most important and impactful decisions need to be taken, many details are still missing, and hence it is more important to apply well proven and understood physical knowledge, rather than performing complex numerical simulations.

The ABC21 Final Report highlights that several guidelines and studies have been developed in the last decades [10] targeting different areas and strategies. Most of these guidelines, also due to their date of publication, do not present in detail an up-to-date description of the comfort models and the comfort objectives to be used as a target for the design and for the assessment of the results achieved. The guidance that can be found is of the type offered in the examples below.

### 3.1 Guidelines

**Site:** Choose site with east-west building orientation. Main openings should face north or south (depending on hemisphere)

**Form:** Prioritize east-west elongated, compact layouts. Use atriums to centralize lighting and views. Use covered atriums for greater compactness. Adapt facade design based on solar orientation.

**Plan:** Use open designs in hot and humid climates. Compact layouts are favored in hot and arid regions for shading and cool spaces. Integrate plant and water features for cooling. Use buffer spaces on east and west sides. Discourage short elevator trips to promote physical activity. Implement open floor plans to maximize daylight and ventilation.

**Windows:** Design openings for ventilation and daylight based on climate. Larger openings for hot, humid climates. Smaller openings for hot, arid and semi-arid regions. Limit windows on east and west facades. Emphasize north or south orientations for more openings. Position windows to maximize daylight. Consider operable windows with cooling shut-off when open. Install low-transmittance windows or provide indoor night insulation in cold climates.

**Daylighting:** Utilize light shelves on east, west and south windows. Opt for high ceilings. Consider clerestories for top lighting. Avoid skylights. Use atriums with north or south-facing clerestories (depending on hemisphere). Explore light tubes, high R-value light-transmitting roof panels and prismatic daylighting glass. Use indoor blinds for glare control. Limit translucent walls. Maximize borrowed light with glass partitions and doors. Use light-colored paving outside first-floor windows for daylight enhancement.

**Shading:** Implement solar radiation protection for all openings. For east and west windows, use outdoor blinds, roller shades, horizontal louvers, avoid vertical fins. Use trees and plants for natural shading. Test shading designs to prevent solar outflanking. Extend shading to roofs, walls, and landscape. Prioritize vegetated walls on east and west sides in taller buildings. Prefer outdoor shading over indoor. Choose glazing to suit heating requirements and ensure shaded windows during overheated periods.

**Color:** Use light or reflective external surfaces to minimize sun energy collection and re-irradiation. Prioritize greenery and reduce paved areas. Enhance lighting efficiency with high-reflectance white ceilings, light-colored walls, furniture, and floor finishes. Aim for well-lit spaces with minimal lighting demands.

**Thermal mass:** Favor light-weight building envelopes in hot and humid climates. Opt for medium-weight structures in hot semi-arid/savannah regions. Ensure mass is exposed to airflow for nocturnal ventilative cooling, avoid covering it with insulating materials. Use sound absorption acoustic panels and partitions.

**Glazing:** Use various types on each facade and within windows for optimal daylighting. Use insulated translucent panels instead of glazing for clerestories and small skylights, avoid them on lower walls due to glare. Do not use reflective glazing if it causes glare or overheating, nor



single glazing for heated or cooled buildings. Use outdoor shading devices to block direct solar radiation and glazing with low solar heat-gain to block diffuse and reflected radiation.

**Air barrier:** Where heating is required implement air barrier to reduce infiltration. Use high-quality weatherstripping on windows and doors to reduce infiltration. Consider a vestibule or revolving door at the entrance. Opt for a heat exchanger ventilation system for indoor air quality.

**Natural ventilation:** Employ solar and stack-effect chimneys. Install cowl-type roof ventilators. Use exterior wing walls to divert wind and maximize airflow.

### 3.2 Advanced Natural Ventilation

Other approaches, like the design method described by certain authors as Advanced Natural Ventilation aim at creating zones protected from noise and pollution from where to draw the intake air [34]. One of the geometrical arrangements of the spaces relies on a one or more central lightwells or courtyards and stack chimneys at the outer border of the building to create a center in edge-out air flow (Figure 3). Intake air is drawn from these central protected spaces. The resulting air flow is “essentially wind neutral, that is, wind pressures will not hinder, or assist, the airflow; this gives added reliability to predictions of their likely, as-built, performance.” [34]

For certain nonresidential buildings, unoccupied at night, the night (only) ventilation strategy might allow to flush out energy at night when the absence of occupants removes the problem of disturbance by external noise. In some European cities the extension of pedestrian areas and the reduction of speed to 30 or 20 km/h as e.g. in Paris, might offer new spaces where the problems associated with noise and pollution are removed or significantly reduced. For new areas to be developed for the growing African population, a clear view of the need to co-design building and districts might help to create positive conditions for natural ventilation.

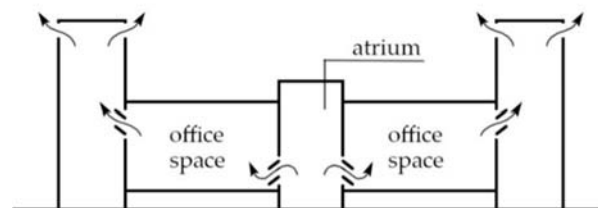


Figure 3: Schematic diagram of stack ventilation “center-in, edge-out”, drawing air from a space relatively protected from noise and pollution. Source: [43]

### 3.3 Bio-climatic charts

When designing bioclimatic buildings, it is common to use bioclimatic charts, which are simple tools that consider climate conditions to recommend appropriate design for different climates. Various types of bioclimatic charts have been developed such as the Olgay Bioclimatic chart, the Givoni–Milne Bioclimatic chart, the Szokolay Bioclimatic chart and the Mahoney Table [49]. For hot climates, it is recommended to use the Givoni bioclimatic chart. The originality of the work proposed by Givoni is to use the psychrometric chart as the base layer to characterize comfort zones [21,22].

Givoni has developed several comfort zones depending on:

- the level of air velocities on the users (0 to 2 m/s);
- the level of development of countries (developed countries and developing countries).

For developing countries, the upper limits of accepted temperature and humidity are higher than in developed countries, assuming that people are acclimatized to hot and humid conditions.

The Givoni bioclimatic chart is a useful tool to assess thermal comfort at the design stage or during the post occupancy evaluation process (Figure 4).

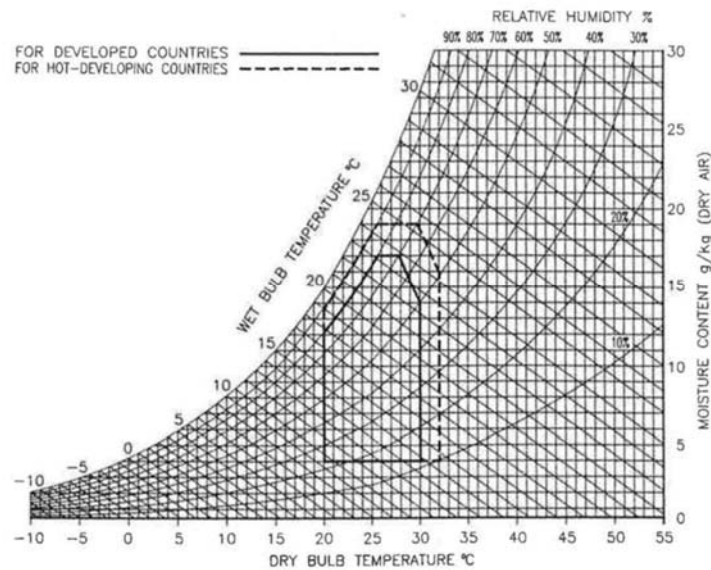


Figure 4: Comfort zones defined by Givoni [21,22] for an air speed of 2 m/s

### 3.4 The KPIs to support bioclimatic design

Key Performance Indicators (KPIs) are essential to quantify the building performance, detect malfunctioning or misuse of the building by the occupant or users, synthesize complex information. Several KPIs for thermal comfort assessment are available in literature and standards. Two main categories can be identified:

- indices that focus on comfort conditions at a certain time and position in space (e.g., the ASHRAE Likelihood of Dissatisfaction ALD [6], the overheating risk index NaOR [38])
- long-term comfort indices that aim at assessing thermal comfort quality of a building over a span of time and considering all the building zones [7].

Table 2 reports a selection of the reviewed indicators for assessing thermal comfort in bioclimatic buildings. They can be used to monitor and verify the conditions of the indoor thermal comfort in buildings, offer a comparison between the case studies and provide guidelines for bioclimatic design in warm climates.

Table 2: Long-term thermal comfort indicators

n	Thermal comfort index	UoM	Definition
1	Percentage of time outside an operative temperature range (Adaptive)	%	Calculate the number or percentage of hours, during the hours the building is occupied, the operative temperature is outside a specified range calculated according to the adaptive thermal comfort model.
2	Percentage of time outside an operative temperature range (Fanger)	%	Calculate the number or percentage of hours, during the hours the building is occupied, the operative temperature is outside a specified range defined according to the Fanger comfort model.

3	Degree-hours (Adaptive)	h	The time during which the actual operative temperature exceeds the specified range (calculated according to the adaptive thermal comfort model) during the occupied hours is multiplied with a weighting factor which is a function of how many degrees the range has been exceeded. The product of each hour for the corresponding weighting factor is then summed up over the period of interest, (e.g. summer)
4	Degree-hours (Fanger)	h	The time during which the actual operative temperature exceeds the specified range (defined according to the Fanger comfort model) during the occupied hours is multiplied with a weighting factor which is a function of how many degrees the range has been exceeded. The product of each hour for the corresponding weighting factor is then summed up over the period of interest, (e.g. summer)
5	Percentage of time inside the Givoni comfort zone for air velocity at 1 m/s	%	Calculate the number or percentage of hours during the hours the building is occupied, when the pair “operative temperature/relative humidity” is inside the specified comfort zone
6	Percentage of time inside the Givoni comfort zone for still air conditions, i.e. $v = 0$ m/s	%	Calculate the number or percentage of hours during the hours the building is occupied, when the pair “operative temperature/relative humidity” is inside the specified comfort zone
7	Number of hours during which the operative temperature is within a certain range	-	Calculate the number of hours during which the operative temperature is within a certain temperature range

#### 4 PROPOSED DESIGN METHODOLOGY

The design process must be carried out logically and sequentially since passive design requires to consider the features of the entire building, not just elements or machines in isolation. This is intended to minimize solar and heat gains and maximize the ability of a natural ventilation system to remove the cooling load. A Natural Ventilation design procedure consists of different phases, namely: conceptual design phase, basic design phase, detailed design phase and design evaluation. The Figure 2 illustrates the design procedure of a ventilative cooling system.

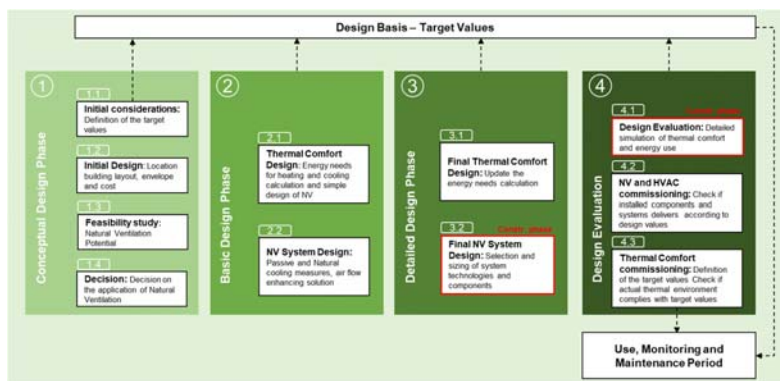


Figure 2: Design procedure for Ventilative Cooling

##### 4.1 Conceptual Design Phase

In the first step of this phase, the desired level of thermal comfort and energy performance objectives are defined, along with other requirements. Target values are set for metrics to assess thermal comfort and energy performance. Energy use targets and costs (preferred life cycle cost) are also defined. The potential for Ventilative Cooling (VC) of the local climate is

analyzed, considering factors like weather, opening type, building use, internal gains, and envelope characteristics.

Urban environments present challenges for natural ventilation due to wind disturbances, elevated air temperatures which decreases the stack effect [20], air pollution, and noise [8]. The ABC 21 case studies demonstrate strategies to reduce noise, pollution, and temperature using trees and limiting cars. Newer, quieter mobility solutions like e-bikes, electric public transport, and shared mobility are expected to improve urban environments.

Simplified models are used initially to assess VC potential based on internal loads, building characteristics, surrounding environment, and local climate. Supplementary natural or mechanical cooling systems may be needed to meet thermal comfort requirements during the hottest months.

A broad range of solutions are considered during the conceptual design phase. If a Natural Ventilation strategy is chosen, the potential benefits of a hybrid ventilation configuration (NV assisted in certain moments by fans) are analyzed. Table 3 and Table 4 provide a procedure for assessing if a hybrid strategy or additional cooling systems are needed. This procedure is iterative, and options involving "Yes" should be avoided to prevent additional costs and delays. Increased "Yes's" involve increased risks, to be evaluated in building contracts. Expert consultation and references to well-documented case studies are recommended.

Tables outline design concepts and boundary conditions for NV use, divided into categories (F1-F5 and C1-C4). Users select the relevant options for their case study, choosing only one option if multiple are available. Blank spaces in the tables represent available choices. First, users determine the need for additional mechanical/fan assistance or cooling systems based on building program data. The responses can be 'No', 'Maybe', or 'Yes'. Next, users define VC concepts for analysis or consider building modifications that reduce mechanical assistance need. The procedure in Table 3 and Table 4 is iterative. Avoid 'Yes' design concepts to implement certain ventilative cooling concepts without added costs and delays. Increased 'Yes' responses may raise risks, warranting consideration in construction contract discussions. Consulting expert guides and case studies on buildings with similar exterior conditions is advised.

Table 3: Survey of the need for supplementary natural or mechanical cooling solutions for CML kindergarten, Portugal.

Ventilative cooling system: is there a need for supplementary cooling?				
C1. Outdoor environment		N	M	Y
C1.1.2. Temperature (2-10°C from comfort zone)			O	
C1.2. Dense urban area with low wind speeds (low natural driving force)			O	
C1.3. Dense urban area with high night temperatures (heat island)			O	
C1.5. Noisy surroundings			O	
C2. Building heat load level		N	M	Y
C2.1.3. High internal loads > 30 W/m <sup>2</sup> during occupation	Temperate (2-10°C from comfort zone)		O	
C3. Thermal comfort		N	M	Y
C3.1.4. Normal requirements for 90% of occupancy hours			O	
C4. Building and system		N	M	Y
C4.1.3. High level of exposed building thermal mass		O		
C4.2. High space- and use-flexibility			O	

Table 4: Survey of the need for mechanical assistance (by fans or additional passive means) for CML kindergarten, Portugal.

Ventilative cooling: Is there a need for mechanical assistance (by fans or additional passive means)?						
F1. Outdoor environment		N		M		Y
F1.1.3. Hot and dry	Winter	O				
	Summer (low temp. difference)			O <sup>1</sup>		
F1.2. Dense urban area with low wind speeds (low natural driving force)					O	
F1.5. Noisy surroundings (high noise insulation needed)				O <sup>2</sup>		
F2. Building heat load level		N		M		Y
F2.1.3. High heat loads > 30 W/m <sup>2</sup> during occupation	Cold (> 10°C from comfort zone) (heat recovery needed)	O <sup>3</sup>				
	Temperate (2-10°C from comfort zone)	O <sup>3</sup>				
	Hot and dry (-2°C .... +2°C from comfort zone)				O <sup>1</sup>	
F3. Thermal comfort		N		M		Y
F3.1.4. Normal requirements for 90% of occupancy hours					O <sup>3</sup>	
F5. Building and system		N		M		Y
F5.1.3. High level of exposed building thermal mass		O <sup>4</sup>				

## 4.2 Basic Design Phase

During the conceptual design phase, VC availability is analyzed, and solutions are defined to achieve objectives. The basic design phase unfolds in three steps, beginning with orientation and layout designed to minimize internal heat loads and to create airflow paths to effectively remove the excess of heat loads. Poor decisions here significantly impact passive cooling and overall performance. Factors like window-to-wall ratio [15], shading devices, and thermal mass are vital [36]. Orientation also greatly influences NV system performance [19]. In climates and during season with a significant day-night temperature swing, high thermal mass buildings can utilize Nocturnal Ventilative Cooling to reduce operating temperature by 2 to 4 degrees [8]. Solar gains are the main factor that should be controlled in summer for optimal occupants' comfort and energy consumption.

The second step involves developing the NV system with supplementary strategies to increase the Ventilative Cooling capacity if necessary. Natural Cross Ventilation (NCV) and Single-Sided Ventilation (SSV) the most common approaches in naturally ventilated buildings. NCV's effectiveness depends on wind speed and direction, which can create discomfort due to intense drafts. The stack effect and wind effect increase the NV potential in SSV configurations. The same is not true for NCV configurations since the configuration of the openings can oppose the natural driving forces [8]. Thus, in NV systems with NCV configurations, the zones should have a geometry that allows an optimized exhaustion. The inlet airflow is made by a lower zone in the facade and extracted at the top of the opposite facade [8], and therefore avoiding the opposing forces. Still, the airflow in SSV is usually smaller than in NCV systems, so they have less cooling potential [4]. Buildings with narrow footprint or large spaces with high ceilings are design techniques that favor the performance of a NV system [8]. According to experimental data in areas with high-ceiling buildings, the stack effect is quite efficient [15]. In SSV

configurations the penetration depth of NV is usually equal to twice the zone's height; therefore, these configurations perform best in areas with low depth and high ceiling heights [8]. CIBSE recommends that the maximum zone depth for single-sided systems should be 2.5x the zone height. However, experimental studies have shown that these limits are very restrictive, and depths of 3H can be achieved [53]. On the other hand, for NCV, the depth of the space should not exceed five times the height of the space [54]. In buildings where there are areas with constant occupation and low height, it is necessary to implement chimneys or N systems to promote a fresh air intake [8].

High-rise buildings are less influenced by their surroundings than low buildings, which makes the wind an additional driving force to achieve the desired airflow rates [50]. Due to the decreasing of temperature with height, the upper half of these buildings can take advantage of the lower temperatures to exploit NV systems [8]. Tall buildings are subject to large pressure differences [41] since wind speed and pressure also increase with height [25]. Increasing wind speed results in increasing airflow, and a linear relationship has been found between wind speed and airflow for all wind directions independent of the number of openings [26]. Thus, in tall buildings, the NV system must operate differently in the first 4-6 floors due to the lack of wind-driven NV arising from the barrier effect caused by the surrounding buildings [8]. In high-rise buildings, this increase in pressure with height leads to some problems in the design of the opening area and type. In wind-driven ventilation, the airflow follows the pressure gradient and can be realized by other systems, such as wind catchers [54]. Wind catchers have demonstrated high performance in hot and dry climates [3,28].

The third step is the combination of different passive systems. The use of a single ventilation strategy may be insufficient. It has already been shown that combining earth-air heat exchangers (EAHE) with solar chimneys is a very effective strategy for maintaining thermal comfort in severe weather conditions [35]. According to [32], these systems achieve a temperature reduction of 10° to 13° with respect to the outdoor temperature. In the EAHE technique, the underground is used as a heat sink to supply air to the building at a constant temperature [35]. Another widely used strategy to improve the performance of natural ventilation systems is coupling passive storage systems such as Phase Change Materials (PCMs). According to the literature, coupling these passive storage systems with solar chimneys can increase the number of ventilation hours [33]. The coupling them with wind towers has also been shown to be quite effective, reducing the air temperature between 9°C and 12°C [5]. In areas where the wind is not predominant and, therefore, wind-driven ventilation is not efficient, the combination of solar chimneys with wind catchers can be a solution that increases the efficiency of the natural ventilation system. In this last step of the basic design phase, mechanical cooling systems are designed to supplement passive cooling systems in periods when they do not have the necessary capacity.

### **4.3 Detailed Design Phase**

The final design phase involves optimizing the developed solution. Key components like the ventilation system's openings are determined, including their type, size, and location. An effective simulation model is crucial to optimize the design, but it needs accurate input data and skilled handling to provide reliable results. Several issues must be considered, such as the correct specification of the relevant boundary conditions, evaluation and justification of the model simplifications, decision on the necessary time discretization, and evaluation of the risk associated with using detailed performance simulation model.

For passive cooling system design, understanding the parameters that affect performance is essential. Factors that affect solar and internal gains have a dominant influence on reducing the

cooling demand. In contrast, the discharge coefficient and the opening factor notably impact the number of hours of comfort. The required airflow rate is critical in determining the ventilation strategy, and the size and location of the openings must be optimized for different scenarios.

For Comfort Ventilation, ceiling or desk fans may be necessary when wind or stack driving forces are insufficient to achieve the desired air velocity. Modern fans come with aerodynamic design and efficient motors that can be remotely adjusted for speed. They also offer high stability against oscillations, low noise levels, and very high energy efficiency. The number of blades can vary, and a fan's efficiency increases with larger diameters. Tools like CFD analysis or simplified tools can assist in fan size selection and distribution.

#### **4.4 Design Evaluation**

Finally, detailed simulations of thermal comfort and energy use are made in the design evaluation phase to control whether the design meets the project objectives. The design tools and methods' wealth of detail and complexity increase as the design develops. The level of detail of the information and expectations about the accuracy of the predictions' results also increase.

### **5 CONCLUSIONS**

The paper based on *ABC21 Final Report on UPDATED technical guidelines and tools* offers an updated view of the future of bioclimatic architecture (which might be the architecture in a climate-compatible future of humanity) and passive systems under the new boundary conditions of XXI century, while taking advantage of accumulated wisdom and the work of the pioneers of XX century.

Bioclimatic architecture and passive systems are a key element of the future, with their evolution for considering the changes in climate, take profit of the improvements in local geo- and bio- based materials and the availability of totally new materials as the ones able to passively radiate more energy to the deep sky than they absorb from the sun. We aim at promoting to university and vocational training the use of the present guidelines and other training tools (reports, simplified pre-design tools, analysis of case studies, recording of webinars etc.) developed within the project. Those training activities should also be an occasion of breaking the harmful barriers between architects and engineers, with difficulties in quantitative analysis on one side and biases towards complex technologies and calculations, sometimes disconnected from user's needs and practical design, on the other side.

More work is needed, but we hope this collaboration between Africa and Europe offers suggestions for taking steps in the right direction.

### **6 ACKNOWLEDGEMENTS**

This paper is based entirely on the ABC21 Report, summarizing its key findings and recommendations on bioclimatic building design in warm climates. The ABC21 project's comprehensive analysis and insights have been instrumental in shaping this condensed overview. Further exploration of the project's resources is encouraged and can be found on the ABC21 website ([abc21.eu](http://abc21.eu)).

## 7 REFERENCES

- (1)  
Agency, I. The Future of Cooling: Opportunities for Energy-Efficient Air Conditioning, 2018.
- (2)  
Attia, S.; Lacombe, T.; Rakotondramiarana, H. T.; Garde, F.; Roshan, G. Analysis Tool for Bioclimatic Design Strategies in Hot Humid Climates. *Sustainable Cities and Society* **2019**, *45*, 8–24. <https://doi.org/10.1016/j.scs.2018.11.025>.
- (3)  
Bouchahm, Y.; Bourbia, F.; Belhamri, A. Performance Analysis and Improvement of the Use of Wind Tower in Hot Dry Climate. *Renewable Energy* **2011**, *36* (3), 898–906. <https://doi.org/10.1016/j.renene.2010.08.030>.
- (4)  
Breesch, H.; Janssens, A. Performance Evaluation of Passive Cooling in Office Buildings Based on Uncertainty and Sensitivity Analysis. *Solar Energy* **2010**, *84* (8), 1453–1467. <https://doi.org/10.1016/j.solener.2010.05.008>.
- (5)  
Calautit, J. K.; Hughes, B. R. Integration and Application of Passive Cooling within a Wind Tower for Hot Climates. *HVAC&R Research* **2014**, *20* (7), 722–730. <https://doi.org/10.1080/10789669.2014.936795>.
- (6)  
Carlucci, S.; Erba, S.; Pagliano, L.; de Dear, R. ASHRAE Likelihood of Dissatisfaction: A New Right-Here and Right-Now Thermal Comfort Index for Assessing the Likelihood of Dissatisfaction According to the ASHRAE Adaptive Comfort Model. *Energy and Buildings* **2021**, *250*, 111286. <https://doi.org/10.1016/j.enbuild.2021.111286>.
- (7)  
Carlucci, S.; Pagliano, L. A Review of Indices for the Long-Term Evaluation of the General Thermal Comfort Conditions in Buildings. *Energy and Buildings* **2012**, *53*, 194–205. <https://doi.org/10.1016/j.enbuild.2012.06.015>.
- (8)  
Carrilho da Graça, G.; Linden, P. Ten Questions about Natural Ventilation of Non-Domestic Buildings. *Building and Environment* **2016**, *107*, 263–273. <https://doi.org/10.1016/j.buildenv.2016.08.007>.
- (9)  
Cheung, T.; Schiavon, S.; Parkinson, T.; Li, P.; Brager, G. Analysis of the Accuracy on PMV – PPD Model Using the ASHRAE Global Thermal Comfort Database II. *Building and Environment* **2019**, *153*, 205–217. <https://doi.org/10.1016/j.buildenv.2019.01.055>.
- (10)  
Daemei, A. B.; Eghbali, S. R.; Khotbehsara, E. M. Bioclimatic Design Strategies: A Guideline to Enhance Human Thermal Comfort in Cfa Climate Zones. *Journal of Building Engineering* **2019**, *25*, 100758. <https://doi.org/10.1016/j.jobbe.2019.100758>.
- (11)



- de Dear, R.; Xiong, J.; Kim, J.; Cao, B. A Review of Adaptive Thermal Comfort Research since 1998. *Energy and Buildings* **2020**, *214*, 109893. <https://doi.org/10.1016/j.enbuild.2020.109893>. (12)
- Erba, S.; Pagliano, L.; Battistella, A.; Santamouris, M.; Khaldoun, A.; Del Pero, C.; Leonforte, F.; Fontana, C.; Rogora, A.; Delera, A. C.; Hassen, A. E.; Mughal, H.; Dione, E.; Simões, J.; da Graça, G. C. *ABC21 Final Report on UPDATED Technical Guidelines and Tools*; Africa-Europe BioClimatic buildings for XXI century; 2023; p 227. (13)
- European Committee for Standardization; ISO. *EN ISO 7726:2001 - Ergonomics of the thermal environment - Instruments for measuring physical quantities*; 2001; p 63. (14)
- Feriadi, H.; Wong, N. H. Thermal Comfort for Naturally Ventilated Houses in Indonesia. *Energy and Buildings* **2004**, *36* (7), 614–626. <https://doi.org/10.1016/j.enbuild.2004.01.011>. (15)
- Flourentzou, F. Ventilative Cooling in Tertiary Buildings: A School Demo-Case and Parametric Analyses Under Swiss Climate Conditions (Central Europe). In *Innovations in Ventilative Cooling*; Chiesa, G., Kolokotroni, M., Heiselberg, P., Eds.; Springer International Publishing: Cham, 2021; pp 269–328. [https://doi.org/10.1007/978-3-030-72385-9\\_12](https://doi.org/10.1007/978-3-030-72385-9_12). (16)
- François Garde PhD, P.; Mathieu David PhD, P.; Lenoir, A. Towards Net Zero Energy Buildings in Hot Climates: Part 1, New Tools and Methods. *ASHRAE transactions* **2011**, *117*, 450. (17)
- Gagge, A. P.; Fobelets, A.; Berglund, L. A Standard Predictive Index of Human Response to the Thermal Environment. **1986**. (18)
- Gagge, A. P. An Effective Temperature Scale Based on a Simple Model of Human Physiological Regulatory Response. *Ashrae Trans.* **1971**, *77*, 247–262. (19)
- Gao, C. F.; Lee, W. L. Evaluating the Influence of Openings Configuration on Natural Ventilation Performance of Residential Units in Hong Kong. *Building and Environment* **2011**, *46* (4), 961–969. <https://doi.org/10.1016/j.buildenv.2010.10.029>. (20)
- Ghiaus, C.; Allard, F.; Santamouris, M.; Georgakis, C.; Nicol, F. Urban Environment Influence on Natural Ventilation Potential. *Building and Environment* **2006**, *41* (4), 395–406. <https://doi.org/10.1016/j.buildenv.2005.02.003>. (21)
- Givoni, B. Comfort, Climate Analysis and Building Design Guidelines. *Energy and Buildings* **1992**, *18* (1), 11–23. [https://doi.org/10.1016/0378-7788\(92\)90047-K](https://doi.org/10.1016/0378-7788(92)90047-K). (22)

- Givoni, B. *Passive Low Energy Cooling of Buildings*; John Wiley & Sons, 1994. (23)
- Goetzler, W.; Guernsey, M.; Young, J.; Fujrman, J.; Abdelaziz, A. *The Future of Air Conditioning for Buildings*; Navigant Consulting, Burlington, MA (United States), 2016. (24)
- Gonzalez, R. R.; Nishi, Y.; Gagge, A. P. Experimental Evaluation of Standard Effective Temperature a New Biometeorological Index of Man's Thermal Discomfort. *Int J Biometeorol* **1974**, *18* (1), 1–15. <https://doi.org/10.1007/BF01450660>. (25)
- Gunel, M.; Ilgin, H. *Tall Buildings Structural Systems and Aerodynamic Form*; 2014. <https://doi.org/10.13140/2.1.2658.4002>. (26)
- Horan, J. M.; Finn, D. P. Sensitivity of Air Change Rates in a Naturally Ventilated Atrium Space Subject to Variations in External Wind Speed and Direction. *Energy and Buildings* **2008**, *40* (8), 1577–1585. <https://doi.org/10.1016/j.enbuild.2008.02.013>. (27)
- International Standard Organization. *ISO 7730:2005. Ergonomics of the Thermal Environment – Analytical Determination and Interpretation of Thermal Comfort Using Calculation of the PMV and PPD Indices and Local Thermal Comfort Criteria*; 2005. (28)
- Jomehzadeh, F.; Nejat, P.; Calautit, J. K.; Yusof, M. B. M.; Zaki, S. A.; Hughes, B. R.; Yazid, M. N. A. W. M. A Review on Windcatcher for Passive Cooling and Natural Ventilation in Buildings, Part 1: Indoor Air Quality and Thermal Comfort Assessment. *Renewable and Sustainable Energy Reviews* **2017**, *70*, 736–756. <https://doi.org/10.1016/j.rser.2016.11.254>. (29)
- Lechner, N.; Andrasik, P. *Heating, Cooling, Lighting: Sustainable Design Methods for Architects*, 5th ed.; John wiley & sons, 2021. (30)
- Lenoir, A.; Baird, G.; Garde, F. Post-Occupancy Evaluation and Experimental Feedback of a Net Zero-Energy Building in a Tropical Climate. *Architectural Science Review* **2012**, *55* (3), 156–168. <https://doi.org/10.1080/00038628.2012.702449>. (31)
- Lenoir, A.; Thellier, F.; Garde, F. Towards Net Zero Energy Buildings in Hot Climate, Part 2: Experimental Feedback. 8. (32)
- Li, H.; Yu, Y.; Niu, F.; Shafik, M.; Chen, B. Performance of a Coupled Cooling System with Earth-to-Air Heat Exchanger and Solar Chimney. *Renewable Energy* **2014**, *62*, 468–477. <https://doi.org/10.1016/j.renene.2013.08.008>. (33)

- Li, Y.; Liu, S. Experimental Study on Thermal Performance of a Solar Chimney Combined with PCM. *Applied Energy* **2014**, *114*, 172–178. <https://doi.org/10.1016/j.apenergy.2013.09.022>. (34)
- Lomas, K. J. Architectural Design of an Advanced Naturally Ventilated Building Form. *Energy and Buildings* **2007**, *39* (2), 166–181. <https://doi.org/10.1016/j.enbuild.2006.05.004>. (35)
- Maerefat, M.; Haghighi, A. P. Passive Cooling of Buildings by Using Integrated Earth to Air Heat Exchanger and Solar Chimney. *Renewable Energy* **2010**, *35* (10), 2316–2324. <https://doi.org/10.1016/j.renene.2010.03.003>. (36)
- Mirrahimi, S.; Mohamed, M. F.; Haw, L. C.; Ibrahim, N. L. N.; Yusoff, W. F. M.; Aflaki, A. The Effect of Building Envelope on the Thermal Comfort and Energy Saving for High-Rise Buildings in Hot–Humid Climate. *Renewable and Sustainable Energy Reviews* **2016**, *53*, 1508–1519. <https://doi.org/10.1016/j.rser.2015.09.055>. (37)
- Nicol, F. Adaptive Thermal Comfort Standards in the Hot–Humid Tropics. *Energy and Buildings* **2004**, *36* (7), 628–637. <https://doi.org/10.1016/j.enbuild.2004.01.016>. (38)
- Nicol, J. F.; Hacker, J.; Spires, B.; Davies, H. Suggestion for New Approach to Overheating Diagnostics. *Building Research & Information* **2009**, *37* (4), 348–357. <https://doi.org/10.1080/09613210902904981>. (39)
- Nomura, M.; Hiyama, K. A Review: Natural Ventilation Performance of Office Buildings in Japan. *Renewable and Sustainable Energy Reviews* **2017**, *74*, 746–754. <https://doi.org/10.1016/j.rser.2017.02.083>. (40)
- Ole Fanger, P.; Toftum, J. Extension of the PMV Model to Non-Air-Conditioned Buildings in Warm Climates. *Energy and Buildings* **2002**, *34* (6), 533–536. [https://doi.org/10.1016/S0378-7788\(02\)00003-8](https://doi.org/10.1016/S0378-7788(02)00003-8). (41)
- Omrani, S.; Garcia-Hansen, V.; Capra, B.; Drogemuller, R. Natural Ventilation in Multi-Storey Buildings: Design Process and Review of Evaluation Tools. *Building and Environment* **2017**, *116*, 182–194. <https://doi.org/10.1016/j.buildenv.2017.02.012>. (42)
- Pagliano, L.; Zangheri, P. Comfort Models and Cooling of Buildings in the Mediterranean Zone. *Advances in Building Energy Research* **2010**, *4* (1), 167–200. <https://doi.org/10.3763/aber.2009.0406>. (43)
- Pesic, N.; Roset Calzada, J.; Muros Alcojor, A. Assessment of Advanced Natural Ventilation Space Cooling Potential across Southern European Coastal Region. *Sustainability* **2018**, *10* (9), 3029. <https://doi.org/10.3390/su10093029>.

(44)

Rupp, R. F.; Vásquez, N. G.; Lamberts, R. A Review of Human Thermal Comfort in the Built Environment. *Energy and Buildings* **2015**, *105*, 178–205.  
<https://doi.org/10.1016/j.enbuild.2015.07.047>.

(45)

Santamouris, M.; Cartalis, C.; Synnefa, A.; Kolokotsa, D. On the Impact of Urban Heat Island and Global Warming on the Power Demand and Electricity Consumption of Buildings—A Review. *Energy and Buildings* **2015**, *98*, 119–124.  
<https://doi.org/10.1016/j.enbuild.2014.09.052>.

(46)

Santamouris, M.; Kapsis, K.; Korres, D.; Livada, I.; Pavlou, C.; Assimakopoulos, M. N. On the Relation between the Energy and Social Characteristics of the Residential Sector. *Energy and Buildings* **2007**, *39* (8), 893–905. <https://doi.org/10.1016/j.enbuild.2006.11.001>.

(47)

Santamouris, M. Innovating to Zero the Building Sector in Europe: Minimising the Energy Consumption, Eradication of the Energy Poverty and Mitigating the Local Climate Change. *Solar Energy* **2016**, *128*, 61–94. <https://doi.org/10.1016/j.solener.2016.01.021>.

(48)

Santamouris, M.; Kolokotsa, D. On the Impact of Urban Overheating and Extreme Climatic Conditions on Housing, Energy, Comfort and Environmental Quality of Vulnerable Population in Europe. *Energy and Buildings* **2015**, *98*, 125–133.  
<https://doi.org/10.1016/j.enbuild.2014.08.050>.

(49)

Santy; Matsumoto, H.; Tsuzuki, K.; Susanti, L. Bioclimatic Analysis in Pre-Design Stage of Passive House in Indonesia. *Buildings* **2017**, *7* (1), 24.

(50)

Tong, Z.; Chen, Y.; Malkawi, A. Defining the Influence Region in Neighborhood-Scale CFD Simulations for Natural Ventilation Design. *Applied Energy* **2016**, *182*, 625–633.  
<https://doi.org/10.1016/j.apenergy.2016.08.098>.

(51)

Walker, R. R.; White, M. K. Single-Sided Natural Ventilation—How Deep an Office?†. *Building Services Engineering Research and Technology* **1992**, *13* (4), 231–236.  
<https://doi.org/10.1177/014362449201300407>.

(52)

Wei, H.; Yang, D.; Guo, Y.; Chen, M. Coupling of Earth-to-Air Heat Exchangers and Buoyancy for Energy-Efficient Ventilation of Buildings Considering Dynamic Thermal Behavior and Cooling/Heating Capacity. *Energy* **2018**, *147*, 587–602.  
<https://doi.org/10.1016/j.energy.2018.01.067>.

(53)

White, M.; Walker, R. The Efficiency of Single-Sided and Cross Ventilation in Office Spaces.; 1996.

(54)

Zhang, H.; Yang, D.; Tam, V. W. Y.; Tao, Y.; Zhang, G.; Setunge, S.; Shi, L. A Critical Review of Combined Natural Ventilation Techniques in Sustainable Buildings. *Renewable and Sustainable Energy Reviews* **2021**, *141*, 110795. <https://doi.org/10.1016/j.rser.2021.110795>.

(55)

Goal 12 | Department of Economic and Social Affairs. <https://sdgs.un.org/goals/goal12> (accessed 2024-06-30).

(56)

*EN 16798-1:2019-Indoor Environmental Input Parameters for Design and Assessment of Energy Performance of Buildings Add*; 2019.

(57)

*Commission Recommendation (EU) 2019/1019 of 7 June 2019 on Building Modernisation (Text with EEA Relevance.)*; 2019; Vol. 165. <http://data.europa.eu/eli/reco/2019/1019/oj/eng> (accessed 2024-06-30).

(58)

*ANSI/ASHRAE Standard 55-2020. Thermal Environmental Conditions for Human Occupancy*; 2020; p 80. <https://www.ashrae.org/technical-resources/bookstore/standard-55-thermal-environmental-conditions-for-human-occupancy>.

# Estimation of Airborne Particle Removal Efficiency in Personal Isolation Room based on Full-scale Experiment

Shinhye Lee<sup>1</sup>, Hyunmin Kim<sup>1</sup>, Jooyeon Roh<sup>1</sup>, and Myoung-souk Yeo<sup>\*1,2</sup>

*1 Department of Architecture and Architectural  
Engineering, Seoul National University  
1, Gwanak-ro, Gwanak-gu  
Seoul, Republic of Korea  
Presenting author: underline First & Last name*

*2 Institute of Construction and Environmental  
Engineering, Seoul National University  
1, Gwanak-ro, Gwanak-gu  
Seoul, Republic of Korea  
\*Corresponding author: msyeo@snu.ac.kr*

## SUMMARY

This study investigates the performance of Temporary Isolation Rooms (TIRs) in controlling airborne transmission of aerosols. The study utilized a full-scale experimental chamber with various airflow rates of Fan Filter Units (FFUs) and Air Changes per Hour (ACH). Aerosol removal efficiency and penetration coefficients were evaluated using Di-Ethyl-Hexyl-Sebacate (DEHS) particles and optical particle counters. Results showed that TIR performance varies significantly with aerosol diameters and FFU airflow rates. Larger aerosol diameters and higher airflow rates improved removal efficiency, crucial for controlling smaller aerosols relevant to airborne transmission. However, aerosols with diameters from 0.3  $\mu\text{m}$  to 0.46  $\mu\text{m}$  consistently penetrated the TIR from the room, regardless of airflow rate. This study underscores the importance of optimizing airflow dynamics and understanding aerosol behavior for effective infection control in healthcare settings.

## KEYWORDS

Healthcare facility, infection control, temporary isolation room, parameter optimization, multi-zone airflow network, removal efficiency

## 1 INTRODUCTION

Temporary isolation room (TIR) is a small, lightweight structure designed to temporarily cover the patient bed area, preventing the transmission of infection throughout the healthcare facility. The need for effective infection control measures, such as isolation rooms, has significantly increased since the COVID-19 pandemic caused hospital operational paralysis. Temporary



Figure 1: Full-scale chamber experiment for evaluating efficiency of TIR

negative pressure isolation (TNPI) rooms, which share similar infection control principles with airborne infection isolation room (AIIR) using negative pressure, have been the focus of relatively active research on their effectiveness (Lee, 2020; Davis, 2008). In contrast, TIR does not employ negative pressure, leading to lower expectations for their infection control efficacy (Mitchell, 2017). However, due to their lower costs and faster turnover time, TIRs can serve as efficient alternatives to traditional isolation rooms (Mitchell, 2017). This study aims to assess the efficiency of the TIR in a full-scale chamber experiment and quantify the removal efficiency through parameter estimation.

## 2 METHODS AND MATERIALS

### 2.1 Full-scale experiment

As illustrated in Figure 1, a PIR is positioned at the third patient bed within the full-scale experimental chamber. The chamber measures 11m × 4.8m × 3m and contains four patient beds. The airflow rate of fan filter unit (FFU) within the PIR is adjustable, and the filter is rated as HEPA13. To evaluate the efficiency of the TIR, Di-Ethyl-Hexyl-Sebacate (DEHS) aerosols were generated inside the TIR using aerosol generator (3073, TSI). Real-time particle counts were monitored by optical particle counters (OPC-N3, Alphasense) deployed both inside and outside of the TIR.

### 2.2 Parameter optimization

The performance of the TIR can be quantitatively evaluated by estimating the aerosol removal efficiency using the equation below.

$$\frac{dC_{Room}}{dt} = (1 - \eta_r) \frac{Q_{TIR}}{V_{Room}} C_{TIR} - \left( \frac{Q_{TIR}}{V_{Room}} + \frac{Q_{Room}}{V_{Room}} + D_{Room} \right) C_{Room} \quad (1)$$

$$\frac{dC_{TIR}}{dt} = P \frac{Q_{TIR}}{V_{TIR}} C_{Room} - \left( \frac{Q_{TIR}}{V_{TIR}} + D_{TIR} \right) C_{TIR} \quad (2)$$

$C_{Room}, C_{TIR}$	concentration of experimental room and TIR [#/ $m^3$ ]
$Q_{Room}, Q_{TIR}$	airflow rate of experimental room and TIR [ $m^3/h$ ]
$V_{Room}, V_{TIR}$	Volume of experimental room and TIR [ $m^3$ ]
$D_{Room}, D_{TIR}$	Deposition rate in experimental room and TIR [ $m^3/h$ ]
$\eta_r$	removal efficiency of TIR [-]
$P$	penetration coefficient of TIR [-]

Equation (1) and equation (2) represents the derivative of aerosol concentration with respect to time in the experimental room and the TIR, respectively. These equations include unknown parameters such as the deposition rate, removal efficiency and penetration coefficient, which will be optimized.

## 3 RESULTS

Table 1 presents the average estimated removal efficiencies and penetration coefficients of TIR in various FFU airflow rates and air change rates (ACH). The penetration coefficient is a parameter related to aerosols that penetrate the TIR from the experimental room. Each experimental case with different airflow rates was repeated three times, except for two datasets of the experimental case with the lowest airflow rate (120  $m^3/h$ ), which were excluded from the analysis.

Table 1: Removal efficiency and penetration coefficient of the TIR

Airflow Rate	ACH	Removal efficiency			Penetration coefficient		
		0.3 – 0.46 $\mu$ m	0.46 - 1 $\mu$ m	1-5 $\mu$ m	0.3 – 0.46 $\mu$ m	0.46 - 1 $\mu$ m	1-5 $\mu$ m
120 m <sup>3</sup> /h	13 /h	0.48 (-)	0.71 (-)	0.43 (0.00)	1.00 (-)	1.00 (-)	1.00 (-)
200 m <sup>3</sup> /h	22 /h	0.76 (0.19)	0.97 (0.02)	0.98 (0.03)	1.00 (0.00)	0.95 (0.06)	0.85 (0.22)
290 m <sup>3</sup> /h	31 /h	0.88 (0.02)	0.96 (0.01)	0.98 (0.03)	1.00 (0.00)	0.67 (0.47)	0.33 (0.47)
500 m <sup>3</sup> /h	54 /h	0.96 (0.00)	1.00 (0.00)	1.00 (0.00)	1.00 (0.00)	0.50 (0.50)	1.00 (0.00)

The parentheses refer to sd (standard deviation)

The result implies that the performance of the TIR varies depending on the aerosol diameters and the airflow rates of the FFU. Larger aerosol diameters and higher airflow rates lead to higher removal efficiency; thus, a larger airflow rate is necessary for effectively removing smaller aerosols when controlling airborne transmission is the primary objective. The penetration coefficient also shows better performance with larger aerosol diameters and airflow rates. However, it was observed that aerosols with diameters ranging from 0.3  $\mu$ m – 0.46  $\mu$ m penetrate the TIR completely from the room, regardless of the airflow rate. Similarly, aerosols smaller than 5  $\mu$ m penetrate 100% into the TIR when the airflow rate is 120 m<sup>3</sup>/h.

#### 4 ACKNOWLEDGEMENTS

This research was supported by a grant of the project for Infectious Disease Medical Safety, funded by the Ministry of Health & Welfare, Republic of Korea (grant number: HG22C0020).

#### 5 REFERENCES

- Mitchell, B. G., Williams, A., & Wong, Z. (2017). Assessing the functionality of temporary isolation rooms. *American Journal of Infection Control*, 45(11), 1231-1237.
- Lee, S. Y., Choi, S. H., Park, J. E., Hwang, S., & Kwon, K. T. (2020). Crucial role of temporary airborne infection isolation rooms in an intensive care unit: containing the COVID-19 outbreak in South Korea. *Critical Care*, 24, 1-3.
- Mitchell, B. G., Williams, A., Wong, Z., & O'Connor, J. (2017). Assessing a temporary isolation room from an infection control perspective: A discussion paper. *Infection, Disease & Health*, 22(3), 129-135.
- Davis, M. A., Landesman, R., Tadmor, B., Hopmeier, M., Shenhar, G., Barker, T., ... & Walls, R. M. (2008). Initial test of emergency procedure performance in temporary negative pressure isolation by using simulation technologies. *Annals of emergency medicine*, 51(4), 420-425.



# Temperature, Relative humidity and Indoor Air Quality in office buildings and their subjective evaluation

Yoshinori Honma<sup>\*1</sup>, Kei Shimonosono<sup>2</sup>, Kenichi Azuma<sup>3</sup>, Dai Shimazaki<sup>2</sup>,  
Kenichi Kobayashi<sup>2</sup>, Michiko Bando<sup>2</sup> and Naoe Nishihara<sup>4</sup>

*1 National Institute of Public Health  
2-3-6, Minami, Wako city  
Saitama, 351-0197, JAPAN  
e-mail honma.y.aa@niph.go.jp*

*2 National Institute of Public Health  
2-3-6, Minami, Wako city  
Saitama, JAPAN*

*3 Kindai University  
3-4-1 Kowakae, Higashiosaka  
Osaka, JAPAN*

*4 Japan Women's University  
2-8-1, Mejirodai Bunkyo-ku  
Tokyo, JAPAN*

## ABSTRACT

Long-term continuous measurements of temperature, humidity and CO<sub>2</sub> concentrations were conducted in offices in three buildings of over 3,000 m<sup>2</sup> and three non-specified buildings of less than 3,000 m<sup>2</sup>. These measurements were carried out to investigate the effect of the hygrothermal environment in winter and summer, with a particular focus on the impact of humidity in winter and the hot and humid environment when air conditioning is turned off in summer, on microbial contamination. The impact of temperature and humidity conditions in winter and summer, particularly winter humidity and the high temperature and humidity environment in summer, on microbial contamination was examined.

Regarding relative humidity, the specified buildings A, B and C, which are humidified, are humidified to a sufficient degree to create an average absolute humidity difference of 2.75-6.10 g/kgDA with respect to the outdoor air. However, the percentage of time meeting the standard is not necessarily high: A: 58.9%, B: 9.3% and C: 3.9%. In contrast, non-specified building D exhibits a relative humidity below 40% (with an average of 15.7 ± 6.2%), while non-specified buildings E and F also meet the standard at a rate of 7.8% and 3.4%, respectively. In the subjective evaluation of the office workers, there was no statistically significant difference in the perceived relative humidity between those who reported feeling dry and those who did not. Conversely, the perception of dryness was found to be less pronounced in areas with higher absolute outdoor humidity.

Regarding microbiological contamination when air conditioning is turned off in the summer, in the specified building C, which has a high proportion of I/O ratios exceeding 1, there was no odour when arriving at work. In other buildings, 10-15% of office workers perceived some kind of odour. Buildings A, B and D also reported a mouldy odour. Furthermore, during normal office hours, 10-15% of employees reported an olfactory sensation, except for building B, which exhibited a mouldy odour. There were notable discrepancies between the specified buildings subject to the law and the non-specified buildings that were not obliged to comply, particularly regarding the humidification control. Additionally, significant differences were observed in the indoor relative humidity. Furthermore, differences were identified due to differences in building size, particularly regarding HVAC controls and the stability of non-steady-state temperature and humidity.

## KEYWORDS

*Office buildings, Relative humidity, Subjective evaluation, Act on Maintenance of Sanitation in Buildings*

## 1 INTRODUCTION

The temperature, humidity, and air quality of a building are affected by the type of air conditioning and ventilation unit and their operation. In addition, the thermal performance, airtightness, thermal capacity, and moisture capacity of a building play an important role. Humidification control is implemented by law regardless of building use. Dehumidification,

on the other hand, is performed simultaneously during cooling operation in conjunction with the cooling load.

The primary distinction between specified and non-specified buildings pertains to the regulation of humidity, which is subject to different stipulations depending on the applicability of legal obligations. In most cases, humidification units for packaged air conditioning systems are optional. However, the adoption rate remains relatively low due to the necessity for water supply pipes and the implementation of leakage prevention measures. The objective of this study is to elucidate the characteristics of office room temperature and humidity conditions in office buildings during winter and summer based on the results of long-term continuous measurements of temperature, humidity, and CO<sub>2</sub> concentration in office rooms of three specified buildings and three non-specified buildings.

## 2 METHODS

### 2.1 The Surveyed Buildings

Table 1 provides an overview of the surveyed buildings. Buildings A, B, and C are tenant buildings with a total floor area of 3000 m<sup>2</sup> or more and fall under the category of specified buildings as defined in the Act on Maintenance of Sanitation in Buildings. A building maintenance company provides comprehensive management, including air conditioning operation, building automation operation monitoring, and cleaning. Buildings D, E, and F, on the other hand, are equipped with a combination of packaged air conditioners and ventilation systems. The heating and cooling operations are controlled by switches and operation panels installed in each room. The buildings A to C operate on a Monday to Friday schedule, with the air conditioning system typically turned off on Saturdays and Sundays. Buildings D to F are off on Wednesdays, with another day off on Tuesdays, Saturdays, or Sundays.

Table 1: Discription of surveyed buildings

	Location	Total Floor Area (m <sup>2</sup> )	Tenant (m <sup>2</sup> )	Floor Level	AC	Ventilaition
A	Sapporo	25289	247	10F /16F	AHU(CAV)+FCU	AHU+HEX
B	Sendai	6800	142	7F /8F	PAC	OHU
C	Tokyo	93997	209	22F /35F	AHU(VAV)	AHU(VAV)
D	Sapporo	1373	325	2F /3F	PAC	HEX
E	Kumamoto	973	156	3F /3F	PAC	Exhaust Fan
F	Kanazawa	806	235	1F /1F	PAC	Exhaust Fan

### 2.2 Measurement

Temperature, humidity, and CO<sub>2</sub> measurements were logged at 10-minute intervals using a T&D TR-76Ui temperature/humidity/CO<sub>2</sub> logger. Continuous measurements commenced in October 2022 and are ongoing. The period from 1 October 2022 to 20 February 2023 was designated as the winter period, while the period from 26 June 2023 to 6 August 2023 was designated as the summer period. On one specific day during each season, suspended microorganisms (fungi and bacteria) were sampled. The suspended microorganisms were incubated with DG18 medium for fungi and SCD medium for bacteria at a specified temperature and time after the aspiration of 100 liters each was conducted using a bio sampler.

## 3 RESULTS

### 3.1 Results of Ventilation Rate Estimation During HVAC are not in Operation

The ventilation rate during the time that air conditioning was not in operation was estimated from the CO<sub>2</sub> concentration decay after working hours. In A to C, ventilation is also out of operation along with the air conditioning, while in D to F, the ventilation system is in continuous operation even when the air conditioning is off. The results for winter and summer are presented in Figure 1. The air change rate for A-F was 0.37, 0.11, 0.28, 0.45, and 0.4,

respectively. The respective values were 0.8 and 0.55 for winter, and 0.25, 0.12, 0.17, 0.4, 0.45, and 0.53 for summer. The estimated results for winter demonstrated greater variability, yet on average, no significant difference was observed between winter and summer. These findings suggest that the stack effect has a minimal impact. The amount of ventilation air during working hours was estimated based on the number of individuals in the room on specific days in winter and summer, the estimated amount of CO<sub>2</sub> exhalation for each, and the variation in CO<sub>2</sub> concentration. The results are presented in Table 2.

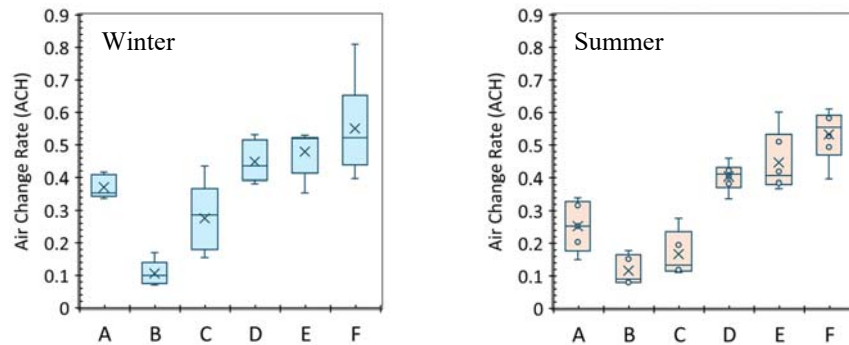


Figure 1: Estimation of ventilation rate during HVAC is out of service based on CO<sub>2</sub> concentration decay (Left figure is in winter, Right figure is in summer)

Table 2: Estimated ventilation rate during working hours

	Measured Ventilation Rate (Estimation)				Density (person/m <sup>2</sup> )	Floor Area (m <sup>2</sup> )
	Winter		Summer			
	m <sup>3</sup> /h/p	ACH	m <sup>3</sup> /h/p	ACH		
A	100.5	1.04	65.7	0.68	0.031	247.5
B	40.7	0.85	23.1	0.49	0.063	142.2
C	69.1	1.5	63.9	1.38	0.065	208.8
D	63	1.34	62.2	1.33	0.064	325.1
E	75.9	1.11	103.6	1.52	0.044	156
F	141.7	3.12	108	2.38	0.066	805.5

### 3.2 Temperature and humidity conditions in the office during winter

The mean values and standard deviations of CO<sub>2</sub> concentration, temperature, relative humidity, and absolute humidity from 10/01/2023 to 20/02/2023 are shown in Table 3. Office hours (9-17) and out of office hours (18-8) are calculated for each office. The temperature histograms for each office are presented in Table 4, the relative humidity histograms in Table 5, and the differences in absolute humidity between indoor and outdoor are illustrated in Figure 2. The specified buildings are maintained at a temperature range of approximately 24.7-25.0°C ± 1.0-1.8°C. In contrast, the temperatures in non-specified buildings A, B, and C range from 23.3 to 26.6°C ± 2.4 to 3.6°C, exhibiting a more pronounced variation compared to the specified buildings. Non-specified buildings D, E, and F display a notable decline in temperature during the winter months when the package air conditioning systems are deactivated. The continuous ventilation and thermal performance of the building play a role in this phenomenon. Regarding relative humidity, the specified buildings A, B, and C, which employ humidification, achieve an average absolute humidity difference of 2.75 to 6.10 g/kgDA relative to outdoor air. However, the percentages of relative humidity below 40% are relatively low: A: 41.1%, B: 90.7%, C: 96.1%. The percentage of non-specified buildings D is well below 40% relative humidity (15.7 ± 6.2%RH), and the percentage of buildings E and F which is less than 40% relative humidity is 7.8% and 3.4%, respectively. This is due to the lack of humidification in the facility and the lack of continuous ventilation.

		Working hours (9-17)				Out of Working hours (18-8)			
		CO <sub>2</sub> ppm	Temperature deg.C.	RH %	AH g/kgDA	CO <sub>2</sub> ppm	Temperature deg.C.	RH %	AH g/kgDA
A	average	691	25.0	41.0	8.10	530	21.5	41.4	6.66
	S.D.	60	0.7	3.4	0.56	75	1.3	3.8	0.97
B	average	819	24.7	29.4	5.70	601	20.2	38.0	5.64
	S.D.	111	0.9	6.2	1.24	158	1.9	3.1	0.93
C	average	904	24.8	35.0	6.81	614	21.2	36.8	5.75
	S.D.	73	0.5	2.1	0.42	140	1.8	2.5	0.72
D	average	797	26.6	15.7	3.40	496	21.3	15.6	2.51
	S.D.	119	1.8	3.1	0.74	131	3.1	4.2	0.91
E	average	634	25.8	27.7	5.74	453	22.9	30.8	5.47
	S.D.	84	1.2	6.8	1.50	87	2.8	7.7	1.83
F	average	610	23.3	28.2	5.01	451	16.9	34.3	4.11
	S.D.	60	1.3	4.7	0.91	79	5.0	8.2	1.22

Table 4: Temperature histograms for each office in winter  
(Left is in working hours:9-17, Right is out of working hours:18-8)

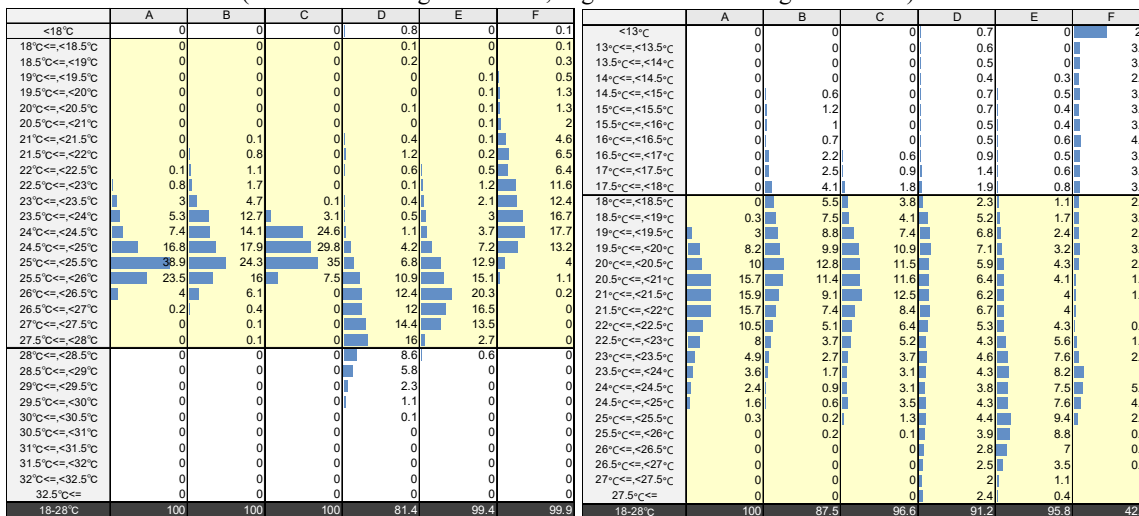


Table 5: Relative humidity histograms for each office in winter  
(Left is in working hours:9-17, Right is out of working hours:18-8)

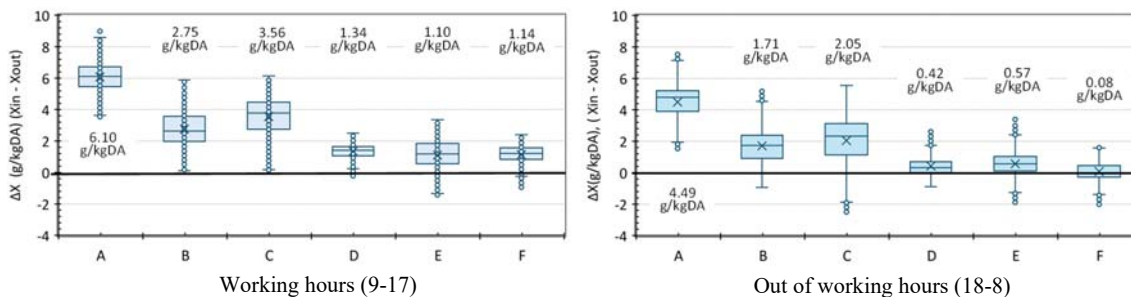
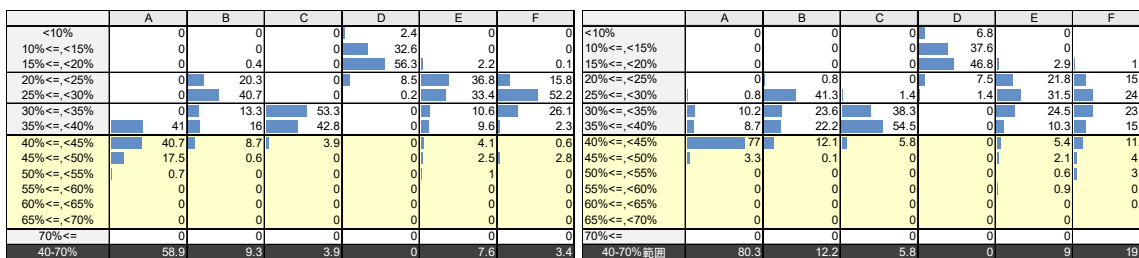


Figure 2: Boxplot of the differences in absolute humidity between indoor and outdoor in winter ((Left is in working hours:9-17, Right is out of working hours:18-8)

The reason for this is that in the specified buildings A, B, and C, ventilation is stopped when the air conditioning system is off, allowing the next operation of the air conditioning to commence from a relatively high indoor absolute humidity. In contrast, in the non-specified buildings D, E, and F, ventilation is continuous, resulting in the absolute humidity level dropping to the same level as the outdoor air during the night. However, in the subjective evaluation, many office workers report a sensation of dryness in the specified buildings A, B, and C, where a humidifier is used (Figure 3). The presence or absence of a feeling of dryness appears to be influenced by the absolute humidity of the outdoor air rather than the indoor relative humidity or absolute humidity.

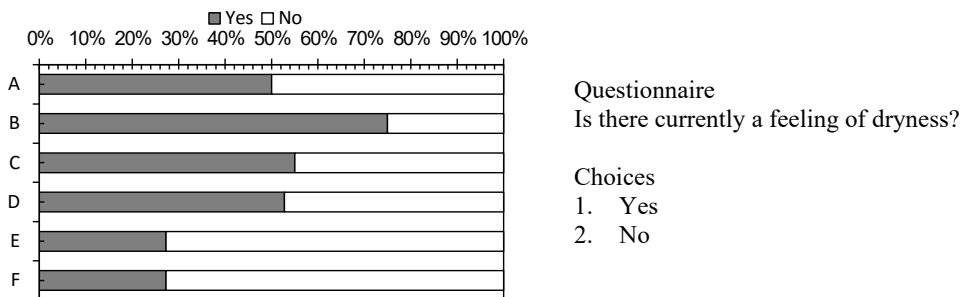


Figure 3: Subjective evaluation of dryness during working hours in winter

### 3.3 Self-reported winter relative humidity and dryness

The standard setting of 40% relative humidity in the Building Sanitation Law has not been changed since 1970. This value has not been changed as it is still effective as a countermeasure against influenza. Figure 4 shows the results of the subjective evaluation of dryness and the perceived relative humidity in each office. In many cases, the relative humidity experienced by those who indicated that they felt dry (respondent groups A1, B1, C1, D1, E1, and F1) was lower than that reported by those who did not feel dry (respondent groups A2, B2, C2, D2, E2, and F2). Furthermore, there was no significant discrepancy between the actual measured relative humidity and the reported perception. Nevertheless, no statistically significant difference was observed between the presence or absence of a feeling of dryness and the perceived relative humidity.

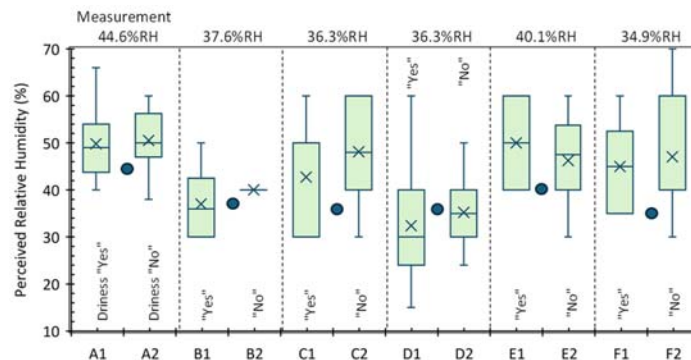


Figure 4: Subjective evaluation of dryness, perceived relative humidity and measured relative humidity during working hours in winter

### 3.4 Temperature and humidity conditions in the office during summer

The mean values and standard deviations of CO<sub>2</sub> concentration, temperature, relative humidity, and absolute humidity from 26/06/2023 to 06/08/2023 are shown in Table 6. The

temperature histograms for each office during the summer season are presented in Table 7, the relative humidity histograms in Table 8, and the differences in absolute humidity between the indoor and outdoor environments during the summer season are illustrated in Figure 5. It is notable that the average temperature in specific buildings A, B, and C is consistent with that observed during the winter season, ranging from 25.2 to 25.6 degrees Celsius. However, the variation is smaller than in winter, with a range of  $\pm 0.6$  to 1.0 deg.C. As the effect of solar radiation at the openings is minimal, the resulting cooling load fluctuation is also small and is more stable than in winter. Nevertheless, room temperature rises occur after the cooling operation has ceased. For building B, the temperature exceeds 28 deg.C. in 49% of periods. The mean temperatures of the non-specified buildings (D, E, and F) are also higher (25.9-26.6 deg.C.) due to their increased susceptibility to solar radiation at the openings. The variation is considerable, ranging from 1.2 to 2.8 deg.C. ( $2\sigma = 2.8$  deg.C. for F, which is largely attributable to window opening). Regarding relative humidity, both specified buildings A, B, and C are dehumidified (on average, minus 2.37 to 4.65 g/kgDA of outdoor air). Furthermore, the relative humidity exceeds 70% very infrequently, including when air conditioning is off. Conversely, for non-specified buildings D and E, the relative humidity is consistently below 70% RH during working hours. However, for all but non-specified building D, the relative humidity exceeds 70% at night (E: 5.3%, F: 66.9% of the time, the relative humidity is higher than 70%). In the case of E, the absolute humidity of the outdoor air is a determining factor since it is an exhaust-only mechanical ventilation system. Although packaged air conditioners only dehumidify according to the cooling load, the load factor is high due to the low thermal performance of the building, which results in a high air flow rate for the packaged air conditioners. Therefore, it is assumed that the amount of condensation water is also high.

### 3.5 Microbial contamination in summer

The Japanese climate is characterized by high humidity, and therefore, attention should be paid to microbial contamination when air conditioning is turned off. Furthermore, airborne fungi and bacteria were sampled in offices, common areas, and outside air on specific days in August and September 2023.

The maintenance and management standard (Architectural Institute of Japan) for the interior of office buildings is 50 CFU/m<sup>3</sup> or less for fungi and 500 CFU/m<sup>3</sup> or less for bacteria. These standards were exceeded in B, D, E, and F (Figure 6) for fungi and F for bacteria (Figure 7). In terms of both fungi and bacteria, many of the I/O ratios in the office did not exceed 1. However, only C exceeded 1 (bacteria 1.44). The concentrations of suspended microorganisms in common areas such as corridors were higher than those in the offices, with I/O ratios of E: fungi 1.04 and C: bacteria 3.56. Given that the relative humidity in the offices of buildings A, B, and C never exceeded 70% RH, including nights and holidays, there is a concern regarding bacterial proliferation in the air conditioning system or ducts in the common area of C. In contrast, among the non-specified buildings, the relative humidity in the offices of F exceeded 70% on many days (especially at night and on holidays), resulting in airborne microorganisms' concentration.

It can be reasonably assumed that the odours observed during the summer months are the result of microbial contamination. If the odour is present just after the start of the air conditioning operation, it is likely that it is growing inside the air handling unit or in the duct. However, C, with a high percentage of I/O ratio exceeding 1.0, reported no "bothersome odour" at the time of arrival at work. Ten to fifteen percent of the workers, aside from C, reported some kind of odour. A, B, and D reported a mouldy odour (Figure 8). Furthermore, during normal office hours, ten to fifteen percent of the office workers felt some odour, except for B, and mouldy odour was reported by A and F (Figure 9).

Table 6: The mean values and standard deviations of CO<sub>2</sub>, temperature, RH and AH in summer

		Working hours (9-17)				Out of Working hours (18-8)			
		CO <sub>2</sub>	Temperature	RH	AH	CO <sub>2</sub>	Temperature	RH	AH
		ppm	deg.C.	%	g/kgDA	ppm	deg.C.	%	g/kgDA
A	average	656	25.2	57.0	11.46	532	25.8	55.2	11.45
	S.D.	51	0.3	2.7	0.49	64	0.5	3.0	0.72
B	average	859	25.4	51.4	10.43	617	27.6	51.8	11.98
	S.D.	139	0.5	3.8	0.89	162	0.7	3.0	0.97
C	average	849	25.6	61.2	12.56	641	26.6	60.1	13.13
	S.D.	45	0.3	1.8	0.47	109	0.6	2.1	0.66
D	average	775	26.2	51.0	10.86	479	26.1	53.4	11.30
	S.D.	128	0.6	3.8	0.85	104	0.7	4.8	1.21
E	average	659	25.9	52.2	10.87	489	27.3	63.7	14.61
	S.D.	88	0.7	5.4	1.09	105	1.3	5.2	2.07
F	average	553	26.6	68.0	14.86	456	25.4	73.9	15.11
	S.D.	75	1.4	6.2	1.29	61	0.8	5.7	1.31

Table 7: Temperature histograms for each office in summer (Left is in working hours:9-17, Right is out of working hours:18-8)

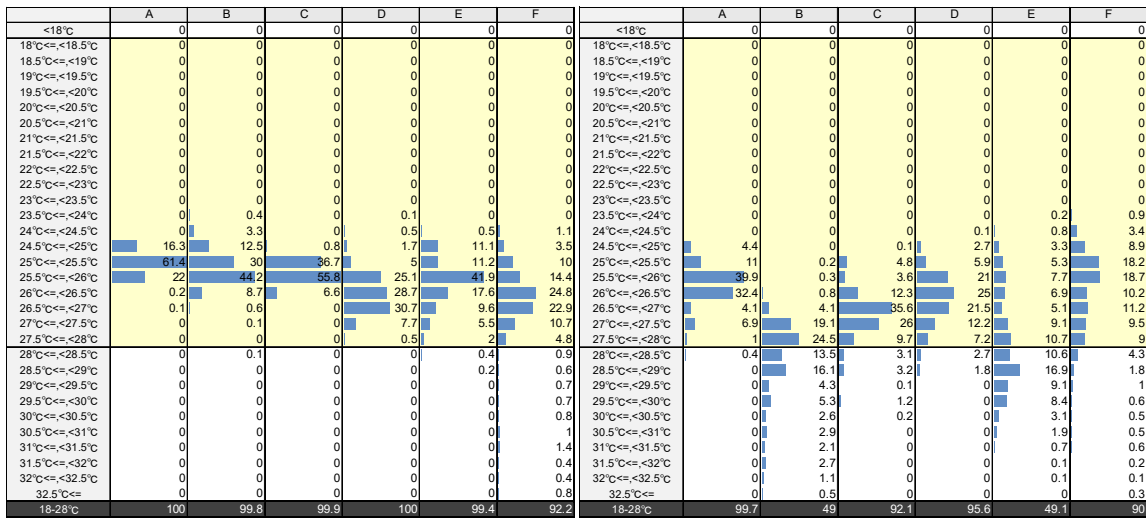


Table 8: Relative humidity histograms for each office in summer (Left is in working hours:9-17, Right is out of working hours:18-8)

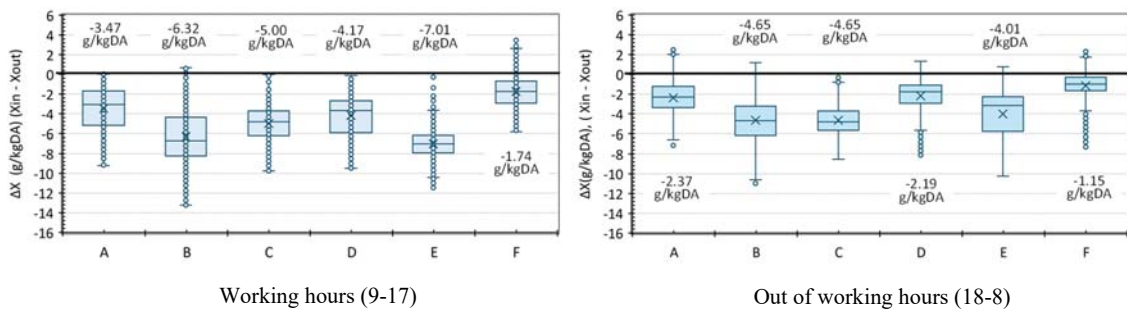
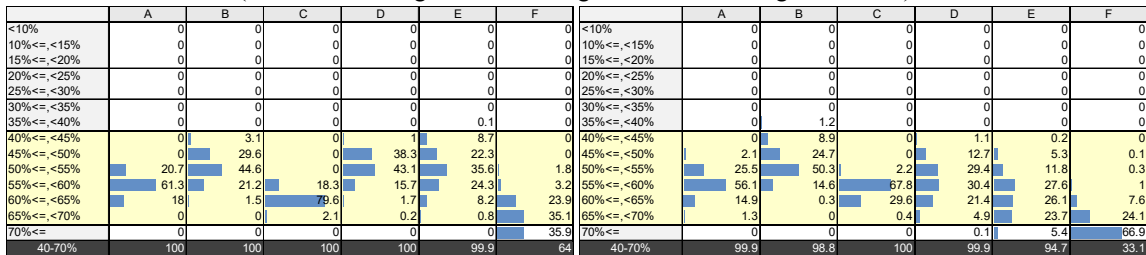


Figure 5: Boxplot of the differences in absolute humidity between indoor and outdoor in summer ((Left is in working hours:9-17, Right is out of working hours:18-8)

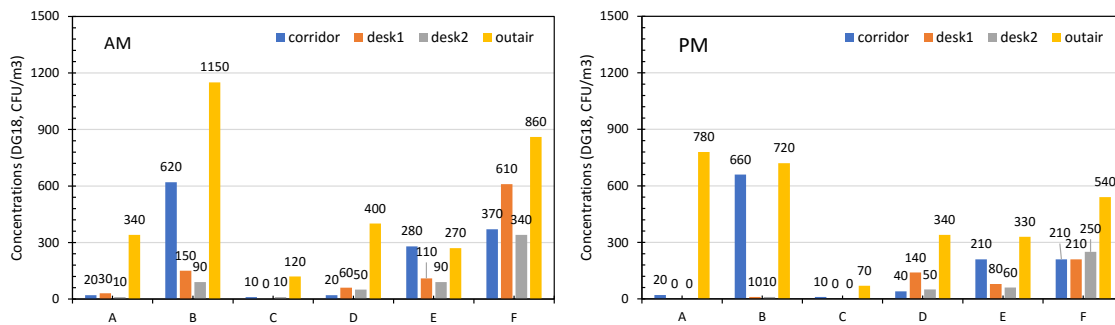


Figure 6: Concentration of airborne fungi in summer (Left is in AM, Right is in PM)

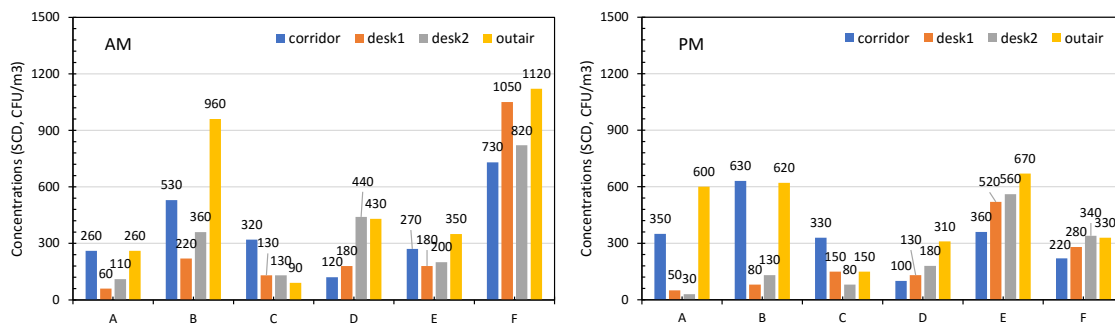
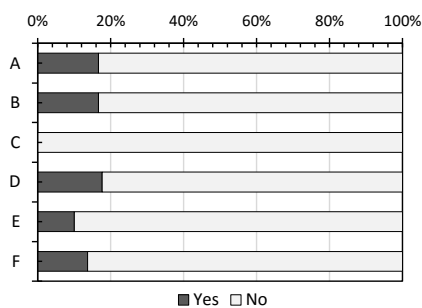


Figure 7: Concentration of airborne bacteria in summer (Left is in AM, Right is in PM)



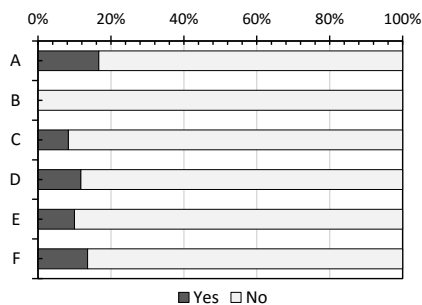
Questionnaire

Is there an odour in the office when you arrive? This odour is noticeable when you arrive, but it becomes less noticeable over time.

Choices

1. Yes
2. No

Figure 8: Subjective evaluation of odour problems in the office on arrival at work in summer



Questionnaire

Are there any odours of concern in the space you are currently in?

Choices

1. Yes
2. No

Figure 9: Subjective evaluation of current odour problems in the office in summer



#### **4 DISCUSSION**

A, B, and C are specific buildings of more than 3000 m<sup>2</sup> and are designed in accordance with the standards of air management. In case B, where air conditioning is intermittently operated to reduce energy costs by stopping air conditioning during lunch break and ending operation at 15:00, the percentage of temperature and relative humidity exceeding the standard values increased compared to A and C. Furthermore, there were complaints from workers about the heat and cold. Regarding the perception of winter dryness, the sense of dryness was higher in buildings A, B, and C, where humidification was employed, while there was no statistically significant difference in the relative humidity experienced by office workers who complained of dryness and those who did not. Furthermore, buildings A and D (both located in Sapporo), although there was a significant difference in the measured indoor relative humidity, there was no significant difference in the perception of dryness.

#### **5 CONCLUSIONS**

A comparative analysis of buildings A, B, and C, which have a central HVAC unit, and buildings D, E, and F, which are not obliged to meet the requirements of the Act on Maintenance of Sanitation in Buildings, revealed that the temperature and humidity environments formed are completely different due to differences in building performance and operating methods. A summary is given below.

- It was found that buildings with a larger area scale exhibited greater stability in terms of temperature. Furthermore, it was verified that the air conditioning system maintains relatively stable conditions throughout the year, as there is no outside air introduced when the air conditioning unit is turned off.
- It was found that non-specified buildings were significantly affected by outside air due to separate control of air conditioning systems and ventilation systems, as well as continuous ventilation during the night. The colder the weather, the lower the absolute outdoor humidity, and thus the more humidification is required. However, the office workers do not experience the benefits of this humidification.

#### **6 ACKNOWLEDGEMENTS**

- The authors would like to express their gratitude to all the stakeholders for their cooperation in the conduct of this study and to those who filled in the questionnaire.
- In conducting the subjective evaluation survey, approval was obtained from the Ethical Review Committee of the National Institute of Public Health (approval number NIPH-IBRA#12425).
- This study was funded by the Ministry of Health, Labour and Welfare's Grant-in-Aid for Scientific Research (Comprehensive Research Project on Health, Safety and Crisis Management Measures, 22LA1011, PI: Yoshinori Honma).

## 7 REFERENCES

- Amar Aganovic (2021). Estimating the impact of indoor relative humidity on SARS CoV-2 airborne transmission risk using a new modification of the Wells-Riley model, *Building and Environment*, 205 108278
- Anthony K.Y Law (2001). Characteristics of bioaerosol profile in office buildings in Hong Kong. *Building and Environment*, Volume 36, Issue 4, 527-541
- Architectural Institute of JAPAN (2013), Standards for Design and Maintenance on Indoor Air Pollution by Microbe (AIJES-A 0002-2013) in Japanese
- EN 16798-1:2019 Energy performance of buildings - Part 1: Indoor environmental input parameters for design and assessment of energy performance of buildings addressing indoor air quality, thermal environment, lighting, and acoustics CEN (2019).
- Schuit M (2020). Airborne SARS-CoV-2 Is Rapidly Inactivated by Simulated Sunlight, *The Journal of Infectious Diseases*, Volume 222, Issue 4, 15 Pages 564–571
- Wolkoff, Peder (2018). Indoor air humidity, air quality, and health. *International Journal of Hygiene and Environmental Health*, vol. 221, issue3, 376-390

# Measurements in Greece of installed windows and comparison between the given air permeability classification and the classification applied to the building envelope

Theodoros Sotirios Tountas<sup>1</sup>

*1 FUV  
39 Ipirou Str.  
11146 Galatsi Athens, Greece*

## ABSTRACT

According to the European regulation EN 12207:2017-03, the air permeability of windows and doors is categorized in four different classes and when they are installed on the building envelope, the declared air permeability class should remain unchanged.

The approach is to perform on-site measurements and to confront 40 different cases of windows and doors installed on new and retrofit projects in Athens, Greece.

The purpose is to discover and highlight the most common errors to the correct installation and suggest easy tactics to prevent them.

At the same time, beside the correct installation testing, the measurements registered and confirmed separately on-site each frames air permeability class and compared to the declared one by the manufacturer. The results are that in some cases, the declared classification was different than the classification measured on-site, which means that the product was faulty without any visual confirmation.

The conclusion is that at 95% of the cases, the installed classification was minor of he declared one. This conclusion confirms that the installation methods are not evolved technically as the frame industry has and the given quality of the window manufacturer is not applied on the building envelope. This situation leads to energy losses because of the bad technical instructions, even though the owner of the building has invested on a better-quality product.

This reality urges the need to evolve the legislation and impose mandatory air-tightness checks during every application of window and doors on the building envelope.

## KEYWORDS

Air Permeability, Window Measurement, Window Installation, EN 12207

## 1 INTRODUCTION

Having a large, recorded experience in the energy design of new constructions as well as in the renovation of existing buildings, a large gap has been identified in the field of frames and the airtightness of the building envelope. There is a big difference between the purchase of a certified product and its final application on the wall. This study investigates 40 different cases of airtightness tests on isolated frames, in new constructions and in renovations.

## 2 METHODOLOGY

Using BlowerDoor GmbH's A-Wert test method, each frame was individually isolated and measured. Two different installations were applied in each frame. First, a strong nylon was placed around the perimeter of the frame, on which a special ring of a certain diameter was applied. With pressure rubbers, the external pressure and the pressure between the nylon and

the frame were measured. An average of 7 measurements were taken for each frame at different pressures, starting at 10 Pa and reaching about 60Pa. After recording the air permeability through the frame at the different pressures, the results were used to calculate the total leakages, given the surface of each frame. A final report was given for the air flow per 1 meter of frame opening length and the total air flow. With the above results, the comparison was made with the data of EN 12207:2017-03 in order to make a classification according to the corresponding category (1 to 4).

The nylon was then removed and placed on the wall, around the frame where the same process followed. In this way we arrived at new data, comparable to the previous measurement according to EN 12207:2017-03.

The measurement tables of the 40 different frames are as follows. In table 1 are described: the surface area, the length of each opening, the air flow per 1 meter of opening length with the frame isolated and the air flow per 1 meter with the frame applied to the wall.

In table 2 and for the same frames, we can find: the total air flow from each frame, first isolated and then applied to the wall.

In table 3 we find the average measurements of all the 40 frames, compared to the specifications of EN12207:2017-03, in both cases, frame first isolated and then measured including the wall.

Table 1: Airflow through 1m joint

Area	Joint Length	Frame Number	Frame only m <sup>3</sup> /(h*m)	On the wall m <sup>3</sup> /(h*m)
3,27	5,17	Frame_01	2,51	3,77
5,99	7,62	Frame_02	2,56	5,32
4,50	6,24	Frame_03	3,12	6,06
4,62	6,40	Frame_04	3,52	5,63
2,64	5,16	Frame_05	3,07	6,04
1,20	3,24	Frame_06	5,40	9,50
1,28	3,38	Frame_07	3,94	6,50
4,03	5,70	Frame_08	3,07	6,81
4,00	5,68	Frame_09	3,05	6,76
7,54	8,40	Frame_10	5,74	12,74
6,51	8,30	Frame_11	4,96	11,00
4,20	6,10	Frame_12	3,20	7,09
3,90	5,60	Frame_13	2,97	6,59
2,75	4,86	Frame_14	2,10	4,65
1,89	4,20	Frame_15	1,44	3,18
3,91	5,62	Frame_16	2,98	6,60

2,60	4,60	Frame_17	1,98	4,39
3,90	5,60	Frame_18	2,97	6,59
1,32	3,26	Frame_19	1,01	4,53
2,07	4,07	Frame_20	1,57	3,49
3,50	5,30	Frame_21	2,67	5,91
2,00	4,10	Frame_22	1,52	3,38
1,09	2,95	Frame_23	0,83	1,83
3,50	5,30	Frame_24	2,67	5,91
0,53	2,14	Frame_25	0,40	0,52
0,63	2,25	Frame_26	0,48	0,65
3,50	5,30	Frame_27	2,67	5,91
2,56	4,80	Frame_28	1,95	4,32
0,95	3,00	Frame_29	0,72	1,60
3,00	4,90	Frame_30	2,29	5,07
2,24	4,60	Frame_31	1,71	3,78
3,50	5,30	Frame_32	2,67	5,91
0,82	2,57	Frame_33	0,63	1,39
3,00	4,90	Frame_34	2,29	5,07
6,25	7,50	Frame_35	4,76	10,56
4,00	6,60	Frame_36	3,05	6,76
1,72	3,74	Frame_37	1,31	2,91
4,32	6,00	Frame_38	3,29	7,30
0,82	2,57	Frame_39	0,63	1,39
1,72	3,74	Frame_40	1,31	2,91

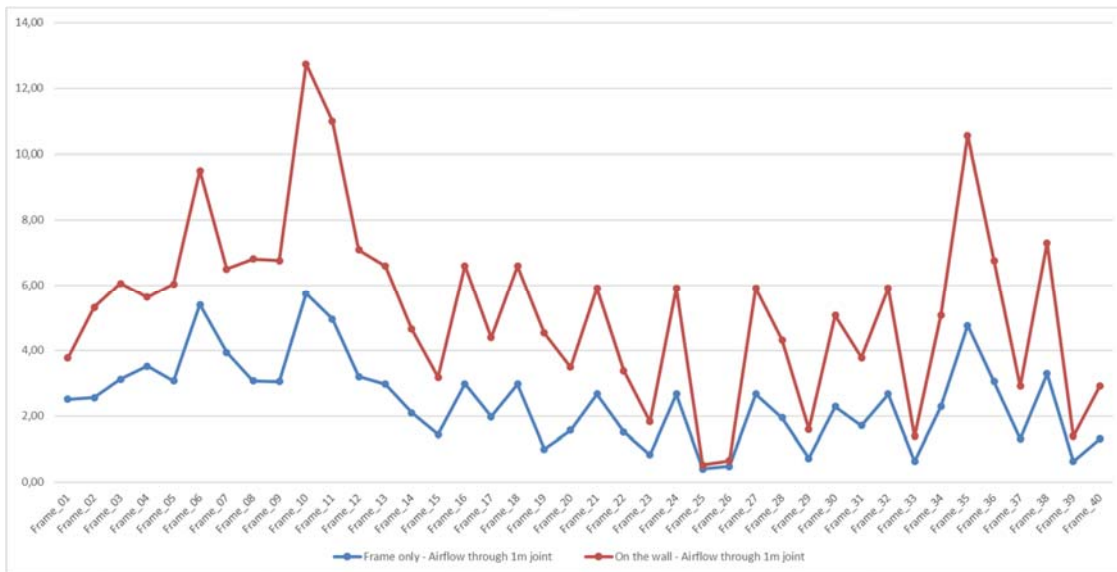


Figure 1: Airflow through 1m joint

Table 2: Total airflow through the window

Area	Joint Length	Frame Number	Frame only m³/h	On the wall m³/h
3,27	5,17	Frame_01	13,00	21,62
5,99	7,62	Frame_02	19,48	40,56
4,50	6,24	Frame_03	19,48	37,81
4,62	6,40	Frame_04	22,51	36,04
2,64	5,16	Frame_05	19,63	38,66
1,20	3,24	Frame_06	17,48	38,66
1,28	3,38	Frame_07	15,83	35,60
4,03	5,70	Frame_08	23,68	31,92
4,00	5,68	Frame_09	23,50	31,81
7,54	8,40	Frame_10	44,26	47,04
6,51	8,30	Frame_11	38,21	46,48
4,20	6,10	Frame_12	24,65	34,16
3,90	5,60	Frame_13	22,89	31,36
2,75	4,86	Frame_14	16,17	27,22

1,89	4,20	Frame_15	11,06	23,52
3,91	5,62	Frame_16	22,93	31,47
2,60	4,60	Frame_17	15,26	25,76
3,90	5,60	Frame_18	22,89	31,36
1,32	3,26	Frame_19	7,75	18,26
2,07	4,07	Frame_20	12,13	22,79
3,50	5,30	Frame_21	20,55	29,68
2,00	4,10	Frame_22	11,74	22,96
1,09	2,95	Frame_23	6,37	16,52
3,50	5,30	Frame_24	20,55	29,68
0,53	2,14	Frame_25	3,11	11,98
0,63	2,25	Frame_26	3,67	12,60
3,50	5,30	Frame_27	20,55	29,68
2,56	4,80	Frame_28	15,03	26,88
0,95	3,00	Frame_29	5,55	16,80
3,00	4,90	Frame_30	17,61	27,44
2,24	4,60	Frame_31	13,15	25,76
3,50	5,30	Frame_32	20,55	29,68
0,82	2,57	Frame_33	4,83	14,39
3,00	4,90	Frame_34	17,61	27,44
6,25	7,50	Frame_35	36,69	42,00
4,00	6,60	Frame_36	23,48	36,96
1,72	3,74	Frame_37	10,11	20,94
4,32	6,00	Frame_38	25,36	33,60
0,82	2,57	Frame_39	4,83	14,39
1,72	3,74	Frame_40	10,11	20,94

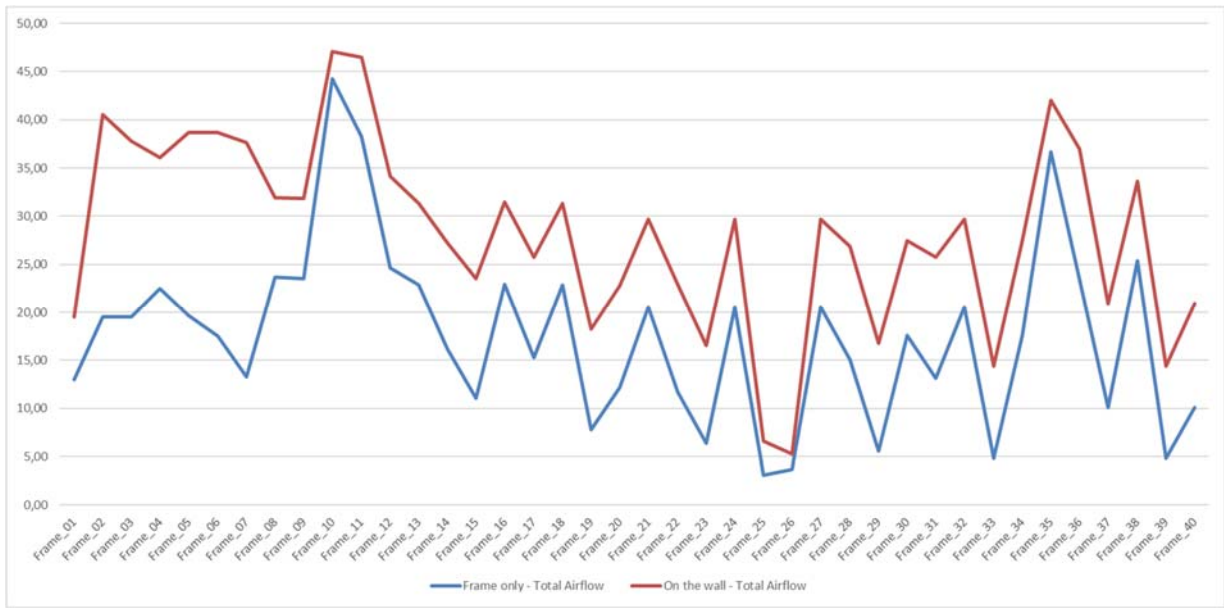


Figure 2: Total airflow through the window

Table 3: Obtained air permeability compared to class 4 requirements

	<b>Requirement Class4 @ 100Pa</b>	<b>Frame only</b>	<b>On the wall</b>
Total Airflow	3,00	17,61	28,56
Airflow through 1m joint	0,75	2,47	5,26

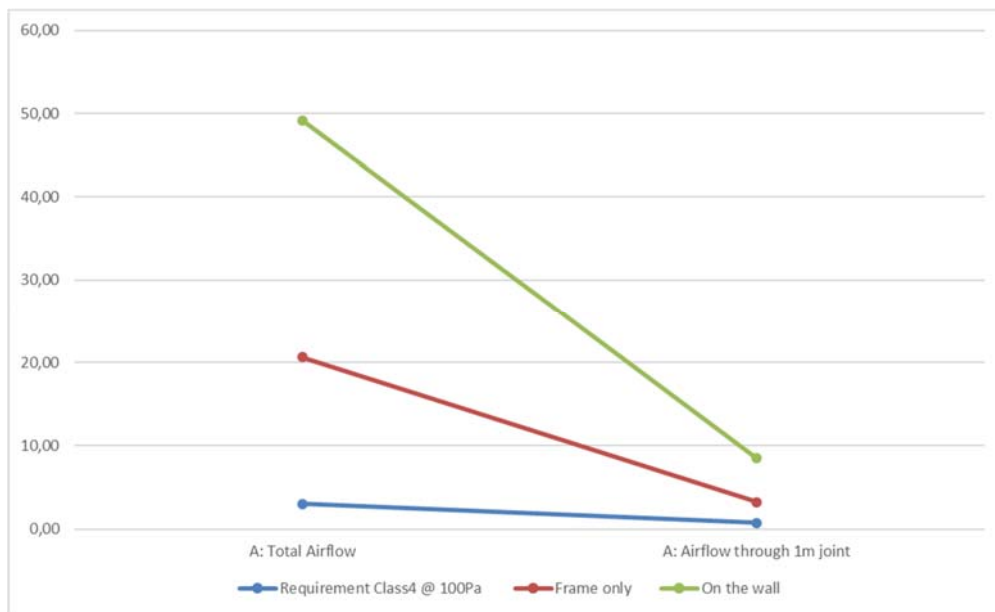


Figure 3: Obtained air permeability compared to class 4 requirements



### 3 CONCLUSIONS

The main conclusion of the research is that the air tightness quality of a frame, from the factory to the application, loses more than 50% of its value, in almost all cases. This results in the end consumer receiving a lower quality product compared to what was agreed upon, while the worst consequence is overall as energy savings deviate from their target by at least 50%.

More specifically, while a category 4 frame must have  $0.75 \text{ m}^3/(\text{hm})$ , in all the tested frames an average value of  $2.47 \text{ m}^3/(\text{hm})$  was measured, while applied to the wall  $5.26 \text{ m}^3$  was measured  $/(\text{hm})$ .

In this way investments are not redeemed while huge resources are wasted in an idle and ineffective way. There is a great and immediate need to educate both the construction industry and the public on the importance of detail in achieving the goal of reducing the CO<sub>2</sub> energy footprint.

### 4 ACKNOWLEDGEMENTS

Credits to the architect Giuseppe Cabini, the engineer Matteo Rondoni and the Italian Agenzia CasaClima for the training sessions and the education they provided.

### 5 REFERENCES

Giuseppe Cabini, (2020). *Sostenibilmente riqualificata Abitazione*, Offanengo (CR).  
*EdicomEdizioni*, 76-81.

# Numerical simulation guided design of novel experimental chamber used to assess the effectiveness of ventilation strategies with hygro-regulated air terminals

Jean Paul Harrouz<sup>1\*</sup>, Bassam Moujalled<sup>1</sup>, Michel Ondarts<sup>2</sup>, Benjamin Golly<sup>2</sup>,  
Adeline Mélois<sup>1</sup>, Gaelle Guyot<sup>1</sup>, Jérémy Depoorter<sup>3</sup>

*1 BPE Research Team—Cerema  
46, rue Saint-Théobald, 38080  
L'Isle d'Abeau, France*

*\*Corresponding author: jean-  
paul.harrouz@cerema.fr*

*2 LOCIE UMR 5271  
Université Savoie Mont-  
Blanc, CNRS, 73376  
Le Bourget-du-Lac, France*

*3 ANJOS VENTILATION  
Lot. Roche Blanche, 01230  
Torcieu, France*

## ABSTRACT

Ensuring acceptable indoor air quality (IAQ) is critical for managing built environments. This is done by ventilating spaces with outdoor air to keep indoor pollutants like CO<sub>2</sub>, humidity, particulate matter, and VOCs within healthy levels. The effectiveness of ventilation strategies depends on factors like occupancy, pollutant types, and air terminal devices, which can be influenced by outdoor air quality, especially in urban areas with particulate matter and NO<sub>x</sub>. Ventilation devices can operate with constant airflow or adjust based on occupancy. Demand-controlled ventilation, using indoor CO<sub>2</sub> levels as an indicator, is more energy-efficient than constant-flow methods. For over 40 years, humidity-sensitive terminals (HST) have been used in French homes, mainly characterized by their flowrate and humidity control, but rarely in terms of IAQ. To optimize IAQ at minimal energy cost, it's essential to understand how HSTs transfer indoor and outdoor pollutants. This study aims to design an experimental chamber to test ventilation strategies using HST. First, a literature review of the existing experimental chamber highlighted the limitations to be overcome by the current developed testing facility. Second, numerical models were developed on CONTAM and computational fluid dynamics (CFD) to guide the chamber design. On one hand, CONTAM model was used to determine the emission rates of pollutants and the corresponding sizing of the generators and the proper selection of the control equipment (sensors, mass flow controllers). On the other, the CFD model assisted in determining the appropriate location of these various instruments for better control as well as proper functioning of the experimental chamber.

## KEYWORDS

Ventilation strategy, indoor air quality, environmental chamber, pollutant transfer, computational fluid dynamics

## 1 INTRODUCTION

Humans are spending more than 90 % of their times in enclosed indoor spaces, whose envelope have been constructed with increasing airtightness, especially residential buildings, to limit air leakage and reduce energy losses (Paukštys *et al.*, 2021). However, indoor air quality (IAQ) of these buildings is deteriorated due to reduced outdoor air intake, which dilutes and evacuates the indoor contaminants. The latter have adverse health effects on occupants if left untreated, and they consist of a wide range of gaseous and solid pollutants originating from various sources. Outdoor generated contaminants englobe combustion products such as NO<sub>x</sub> and particulate matter (PM), whereas indoor generated contaminants come from building materials such as volatile organic compounds (VOCs) or from occupants themselves such as moisture and CO<sub>2</sub>. Although these two species are not typical pollutants, their presence at inadequate concentrations have indirect implication on human health. Low relative humidity (RH) levels cause eye dryness and skin irritation, while high RH cause mould formation in building structure, leading to fungus growth and asthma reactions as well as affecting the perceived

thermal comfort (Du *et al.*, 2021). Moreover, high CO<sub>2</sub> levels reduce attention span and cognitive performance while increasing absenteeism and air staleness.

Accordingly, ventilation systems have been used to regulate the outdoor air flowrate introduced indoors to maintain these species concentrations within acceptable thresholds. Typical ventilation strategies adopted a constant outdoor air flowrate that is supplied to the space throughout the day. Such systems resulted in elevated energy consumption, which gave rise to demand-controlled ventilation (DCV) where the outdoor air is supplied based on occupants needs. This led to more energy saving by limiting the use ventilation system during unoccupied periods of the houses (Nielsen & Drivsholm, 2010). Such smart ventilation systems rely conventionally on indoor CO<sub>2</sub> levels as occupancy indicator, due to its association with human activities through breathing (Lu *et al.*, 2022). Nonetheless, residential houses may be subject to pollution episodes not related to human metabolic emissions such as cooking and laundry, but that emits high loads of moisture and increasing indoor RH. Therefore, adopted humidity-based demand-controlled ventilation (HDCV) becomes a more suitable smart ventilation system for residential buildings. In fact, HDCV has been considered the reference ventilation system in most European countries (Sowa & Mijakowski, 2020), especially in France where it has been used for more than 40 years (Mélois *et al.*, 2023). HDCV systems operate based on the sweeping mechanisms where mechanical exhaust fans creates negative pressure in the house, causing outdoor air to enter through trickle vents placed on main living quarters (living and bedrooms) and pass to utility rooms (kitchen, toilets and bathrooms) through undercuts in the partition doors. For effective operation, these systems employ humidity-sensitive terminals (HST) for air inlets and outlets placed in the main and utility rooms, respectively. Using humidity-responsive material, the area of HST passively increases with the indoor RH levels, allowing higher outdoor air to sweep the residential building.

These HDCV systems show promising potential in energy saving in reaching up to 60 % in various climate conditions through numerical simulations (Guyot *et al.*, 2017). However, their IAQ performance have not been totally characterized, and is conducted with respect to a limited number of pollutants. Sowa and Mijakowski (Sowa & Mijakowski, 2020) studied, using multizone model, the indoor CO<sub>2</sub> and humidity variations in dwellings using HDCV with HST, and showed the system ability to meet required RH levels at the expense of a slight increase in CO<sub>2</sub> levels to 1200 ppm. Afshari and Bergsøe (Afshari & Bergsoee, 2009) constructed a real-life scale dwelling to experimentally study the evolution of indoor generated gaseous contaminants (humidity, CO<sub>2</sub> and VOCs) only using a HDCV system controlled using RH sensors placed in the chambers instead of HST. Therefore, it is of interest to have a holistic understanding of the HDCV, especially using HST due to their practicality by eliminating the need for sensor placement, and complex ventilation control systems. In this regard, experimental investigations prove a crucial tool for the study of such terminals due to the complex physics involving pollutants transfer, especially PM subject to effect of deposition and resuspension along with the indoor air aerodynamics.

The objective of this work is thus to develop a novel real-life scale experimental chamber that replicates a typical French dwelling in the aim of evaluating the ventilation effectiveness of exhaust HDCV using HST with respect to outdoor- and indoor-sourced contaminants of gaseous and particulate nature. To better guide the chamber design, this work first presents a literature review of the existing experimental chamber in literature. Second, numerical simulations are used with both CONTAM multizone and detailed computational fluid dynamics (CFD) models. The numerical simulation helps in making preliminary decisions regarding the placement of the different species generation and measurement ports. CONTAM serves in assessing the chamber dynamic performance across various ventilation flowrates. This aids in calculating pollutant emission rates required to attain pre-defined levels and dimensioning diverse pollutant generators. CFD simulations enable the knowledge of the pollutants spatial distribution to ensure homogeneity of conditions in the buffer zone and determine the correct

sensors placement. This ensures reliable readings, reflecting the pollutant dispersion needed to evaluate the ventilation strategies effectiveness under various HST types and locations, building airtightness levels and interior zones connection types.

## 2 REVIEW OF EXPERIMENTAL CHAMBERS

In literature, many experimental chambers have been developed to study various facets of IAQ and/or various ventilation systems. Mahyuddin and Awbi (Mahyuddin & Awbi, 2010) used a 17.75 m<sup>3</sup> testing chamber representing a classroom to study various recirculation air fraction in a mixing ventilation arrangement. Heiselberg and Perino (Heiselberg & Perino, 2010) and Najafi Ziarani *et al.* (Najafi Ziarani *et al.*, 2023) developed experimental chambers with volumes of 35.4 m<sup>3</sup> and 15.4 m<sup>3</sup>, respectively, to study indoor room airing by natural ventilation and its implication on IAQ. Metabolic CO<sub>2</sub> concentration was used to calculate local ventilation effectiveness, mean age of air and air change rates, without considering the other pollutants, especially the adverse effects of natural ventilation in polluted outdoor environment.

Harb *et al.* (Harb *et al.*, 2016) developed an innovative 40 m<sup>3</sup> experimental chamber (IRINA) containing a CO<sub>2</sub> source and a heated pressurized injection of vaporized VOCs. The chamber is equipped with gaseous analyzers to conduct various IAQ studies such as testing the reliability of electronic gas sensors (Caron *et al.*, 2016), characterizing gaseous emissions from typical household and construction material (Harb *et al.*, 2018; Thevenet *et al.*, 2018) and evaluating localized air treatment and purification systems (Harb *et al.*, 2020). It can be noted that the majority of these studies focuses on gaseous indoor pollutants, especially VOCs even though it is equipped with a particulate analyzer. Moreover, no ventilation system/strategy has been studied so far using the developed IRINA chamber.

Jurelionis *et al.* (Jurelionis *et al.*, 2015) developed an experimental office space of 35.8 m<sup>3</sup> to test evacuation effectiveness of PM emitted from two different sources using various outdoor air flowrates and ventilation configurations (mixing, displacement). Li *et al.* (Li *et al.*, 2023) tested, in a 50 m<sup>3</sup> chamber, the effectiveness of stratum ventilation in reducing the cross-contamination between infected and healthy occupants with PM emissions to represent bioaerosols emitted from coughing or sneezing. Although the findings of the study were insightful, the study was limited to singular and short PM injection that simulate instantaneous indoor PM source (bioaerosols), and did not consider the effect of varying ventilation flowrates on other contaminants. Ciuzas *et al.* (Ciuzas *et al.*, 2015) developed a 35.8 m<sup>3</sup> test chamber representing a standard living room to study the dynamics of PM evolution from other indoor pollution episodes such as cooking, smoldering cigarettes, burning candles and household/beauty product sprays. They noticed that PM build-up depends on the source type, whereas PM decay is affected by the emission duration. However, the effect of the ventilation system was not evaluated with respect to different flowrates or air terminal configurations.

From the above literature review, it can be clearly outlined that the need for the current developed experimental chamber that overcomes the limitations in the existing chambers as summarized below:

- No exhaust-based ventilation system has been considered, only supply ventilation with different configurations (mixing, displacement, stratum),
- Studies were conducted at specific constant ventilation rates with absence to variable demand-controlled ventilation, especially based on indoor humidity,
- Indoor moisture transfer was neglected as the studies are conducted at constant RH levels,
- A single type of pollutants is considered at a time with the ventilation effectiveness calculated relative to the adopted pollutant instead of using more comprehensive IAQ indicators,
- Only indoor generated pollutants are studied and outdoor contaminants transfer is disregarded (use of filtered clean outdoor air).

### 3 CHAMBER DESCRIPTION

The experimental chamber is built inside an insulated and thermally conditioned hangar, acting as a thermostatic holding area with relatively controlled air conditions. The experimental chamber comprises three main zones, illustrated in Figure 1. Zone 1 acts as a buffer simulating the building exterior, where pollutants are generated and maintained at constant target levels. Air from the thermostatic holding area is filtered and introduced via a large air grill at the floor, ensures clean air entering the chamber through a high-efficiency filter. Zones 2 and 3 represent a typical French residence, with zone 2 as the main living area and zone 3 as the utility room. The experimental chamber is equipped with an HDCV system designed to extract simulated outdoor air from zone 1 into zone 2 via the inlet HST. To increase the modularity of the chamber design, three air inlets with individual opening and closing controls are installed at the interface between these zones. This setup allows for studying the effects of the number and placement of air inlets. Additionally, three modular leakage defects are installed in this interface to assess the impact of different building airtightness levels and shapes on the H-DCV system's effectiveness. These defects can adjust the opening area to provide zone 2 with an airtightness ranging from 0 to  $1.2 \text{ m}^3/\text{h}\cdot\text{m}^2$  (air flowrate at 4 Pa per envelope area excluding lower floor), with a specific focus on achieving  $0.6 \text{ m}^3/\text{h}\cdot\text{m}^2$ , which aligns with the French EP regulation for single-family buildings (Moujalled & Mélois, 2023). The defects, which are rectangular and circular, are installed at 0.9 m and 0.2 m above the floor, respectively, to represent common air leakage sources such as windowsills and electrical outlets (Desmarais *et al.*, 1998). The main chamber zones (zones 2 and 3) are separated by a demountable wall that includes a standard door ( $0.84 \times 2.04 \text{ m}^2$ ) with a 2-cm undercut, allowing the sweeping air to pass to zone 3 when the door is closed. This setup simulates the air passage in actual residences equipped with HDCV systems. Furthermore, the interface between these zones is demountable, transforming the main chamber into a single-room residence, another common configuration in France. This flexibility is crucial for simulating the effectiveness of HDCV systems when living quarters and utility rooms, particularly kitchens, are connected. Finally, an exhaust HST is installed in zone 3 to drive filtered air from the thermostatic holding area through the previous two zones. Zone 3 also accommodates transient pollutant emissions associated with human activities, such as cooking or showering.

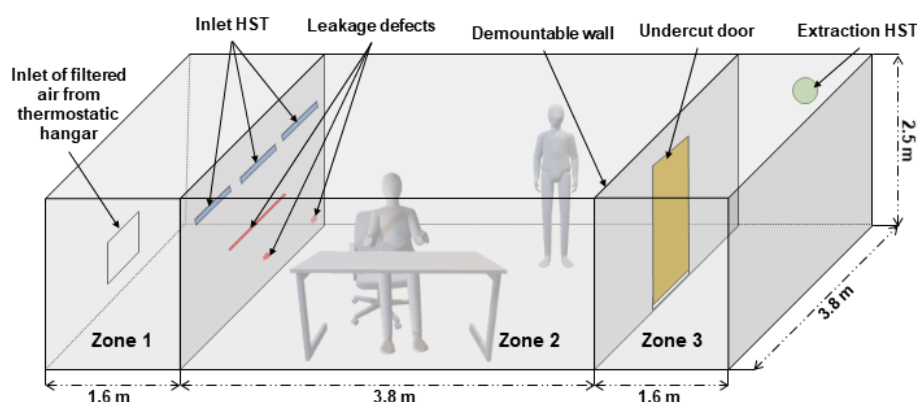


Figure 1: Schematic drawing of the current developed experimental chamber located in a thermostatic hangar

### 4 DESIGN REQUIREMENTS

Several requirements must be met to ensure the environmental chamber operates effectively and accurately represents actual H-DCV performance in homes. These requirements include

both physical aspects, such as geometry and envelope materials, and operational aspects, such as airtightness and pollutant generation.

The chamber volume affects airflow patterns and, consequently, the ventilation system's performance. In existing literature, chamber volumes range from a few litres to over 90 m<sup>3</sup> (Harb et al., 2016). While small volume chambers facilitate easier control of operating conditions like temperature and humidity and faster pollutant homogenization, larger chambers (exceeding 30 m<sup>3</sup>) offer significant advantages despite technical and experimental challenges. Larger volumes allow for the study of commercial treatment systems, human exposure to air pollutants, and provide accurate surface-to-volume ratios and compliant air volumes to test ventilation systems. Therefore, the main chamber zones are designed with volumes of 36.1 m<sup>3</sup> and 15.2 m<sup>3</sup> for zones 2 and 3, respectively, with the dimensions presented in Figure 1, which indicates the smallest chamber volume possible while adhering the French codes of construction for minimal inhabitable areas (*Code de La Construction et de l'habitation - Légifrance*, n.d.) and ensuring a sensible chamber volume suitable for testing. Finally, the volume of zone 1 needs to be large enough to generate the simulated polluted outdoor air without requiring excessive preparation time to reach and homogenize contaminants at the desired concentration. Therefore, its volume was set to 15.2 m<sup>3</sup>, similar to zone 3. The filtered outdoor air inlet to zone 1 is positioned near the floor level and sized to maintain a supply air velocity of 0.1 – 0.2 m/s, akin to a displacement ventilation system, known to have minimal particle deposition due to its upward airflow pattern (Habchi et al., 2015). Axial fans are strategically placed near the floor level within the zone to aid mixing without disrupting the airflow pattern near the ceiling-level inlet HST. The direction of air blowing out of these fans is determined based on numerical simulations to ensure the highest homogeneous PM distribution.

Regarding the chamber inner surface material, stainless steel is used due to its non-adsorbing and chemically passive characteristics, eliminating any source/sink of undesired and unaccounted VOCs. Moreover, the chamber inner surfaces are electrically grounded to eliminate electrostatic forces that might affect PM deposition on the walls. The experimental chamber walls are also insulated with 8-cm of polystyrene to minimise the influence of surrounding air conditions on the inner zones. To better control indoor temperature and RH levels, separate air conditioning units are used: i) sensible cooling coil for air temperature control, ii) humidification wheel for moisture generation, and iii) dry airstream for indoor moisture reduction. The dry air is generated using a rotating desiccant wheel based on silica gel.

To assess the ventilation effectiveness of the HDVC system, various indoor pollutants are generated in the chamber. Outdoor-sourced species, such as NO<sub>x</sub> and PM from combustion products, are chosen as they represent both gaseous and solid contaminants, enabling the study of different transport mechanisms. For indoor-sourced pollutants, moisture and CO<sub>2</sub> sources simulate occupant-related contaminants, including heat source to create thermal plumes affecting the airflow patterns. Additionally, VOCs like formaldehyde and toluene simulate emissions from materials, however, for this work, toluene has been selected due to the commercial availability of the chemical. Since VOCs are emitted from surfaces instead of punctual sources, the VOCs is released from a perforated tube placed along the zone wall to ensure a uniform injection of the gaseous product. Furthermore, PM is generated in zone 3 to replicate transient pollution episodes to mimic diverse human activities such as cooking, laundry, or showering and their associated contaminant emissions, as detailed in studies by Poirier *et al.* (Poirier *et al.*, 2021). The emission of PM is ensured by using an atomizer with saline solution. On one hand, atomization ensures the generation of electrically neutral particles compared to the use of dust generators, even though the latter offer easier control of emission rates. On the other hand, saline solutions are relative cheap (such as NaCl), which is crucial when the chamber is to be operated for prolonged durations, even though they provide a

polydisperse PM profile as opposed to the use of latex-based granules with more known monodisperse size distribution.

Moreover, the chamber maintains very low air permeability to minimize contaminant infiltration or exfiltration between zones and from its surroundings. This ensures accurate quantification of pollutant transport from desired sources without interference from unaccounted envelope leakage (Afshari & Bergsoee, 2009).

## 5 NUMERICAL METHODOLOGY

Numerical modelling and experiments complement each other: simulations help design experiments, while experimental data validates and calibrate the developed models. In this work, both CONTAM and Ansys Fluent are used to develop models for the new experimental chamber.

### 5.1 CONTAM model

CONTAM is a multizone airflow model that is commonly used to study pollutant transfer in indoor spaces due to its accuracy, ease of development, and low computational cost. It calculates airflows between zones and their surroundings, then determines pollutant concentrations based on these airflows. Each zone is treated as a homogeneous volume, connected to others through airflow paths like doors, windows, air terminals and leakage defects as shown in Figure 2. Additionally, pollutant emission for both gaseous and PM species are included in the model along with various sources/sinks types such as adsorption/desorption and chemical reactions for gases, and deposition/resuspension for particles (see Figure 2) (Szczepanik-Scislo & Scislo, 2021). The model uses mass balance to determine pollutant concentrations after calculating the interzonal airflows induced by their pressure differences using the Bernoulli's momentum balance and the orifice/power law for openings while also considering other factors such as thermal draft and wind pressure.

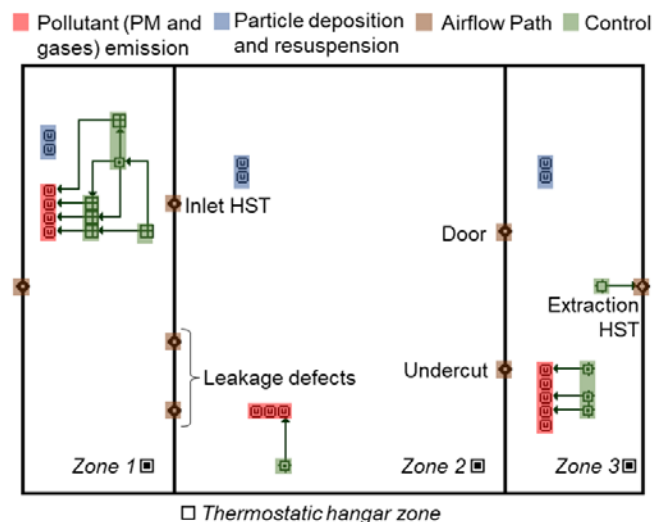


Figure 2: Layout of the environmental chamber used in the developed CONTAM model

### 5.2 CFD model

While CONTAM simulations provide reliable results for zonal pollutants concentrations, their assumption of well-mixed zones has limitations, particularly for PM, whose distribution is

affected by airflow patterns, gravitational settling, thermal stratification, and HST locations. CFD modelling using Ansys Fluent is thus adopted to better capture these different phenomena. The developed CFD model for the environmental chamber is depicted in Figure 3, along with the domain meshing at critical cross-sections, including the zones 1-2 interface, occupant manikin, and symmetry plane. In this study, two axial ventilators are used in zone 1 to ensure pollutant dispersion and mixing. These ventilators are placed near the floor at an elevation of 0.2 m to avoid disrupting the pressure distribution at the interface openings. The study explores two fan supply air directions to determine which provides the fastest and most uniform mixing. Pollutant generation locations are tested at two points: the centre of the room and the lateral walls perpendicular to the zone 1-2 interface, with injection points at a height of 0.5 m from the floor, as used by (Harb et al., 2016). To simulate occupants, two cylinders with a total area of 1.8 m<sup>2</sup> each are placed in zone 2, 0.5 m from the wall. Each cylinder has a circular opening of 192 mm<sup>2</sup> at a height of 1.2 m, representing a seated person's mouth, oriented to simulate two seated occupants facing away from the wall in a living room setting. Finally, an air-conditioning unit is modelled as a rectangular box with inlet and outlet openings at the top and bottom faces. This unit is added to zone 2, positioned 2.3 m above the floor on the wall behind the occupants and is operated to keep a constant temperature of 21 °C, similar to all inlet temperatures. This is adopted to reduce the effect of thermal stratification on PM transport and focus on that of the airflow pattern created by the HDCV system.

The domain is meshed using unstructured tetrahedral elements with varying face sizes for openings (1 mm) and walls (1 – 10 cm) along with inflation layers to ensure high mesh quality resulting with 2,187,559 elements and a  $y^+$  below 1. Due to the high turbulence of the indoor airflow patterns, the CFD numerical model uses the two-equation RNG  $k-\varepsilon$  model due to its robustness, accuracy, and low computational cost (Karam *et al.*, 2024). The model is used with enhanced wall treatment functions and full buoyancy effect consideration to better capture the boundary layer for reliable particle transport modelling (Katramiz *et al.*, 2022) along with the Boussinesq approximation. Discrete phase is simulated with the discrete random walk model to track the PM transport through a Lagrangian frame while accounting for local eddies. Only gravitational settling and drag forces are considered for the studied particle size ( $> 0.1 \mu\text{m}$ ), which is assumed constant. The equations are discretized using the second-order upwind scheme, while the “PRESTO!” scheme is employed for pressure discretization. The coupling of the continuity and momentum equations is achieved using the SIMPLE algorithm. Convergence of the solution is reached when the residuals are less than  $10^{-7}$ .

Although transient emissions can be simulated in the chamber, especially for humidity emissions that affect the HST openings, steady-state simulations are adopted in the CFD model at discrete points reflecting the transitional conditions of typical HST as function of RH levels. Finally, for the boundary conditions, all walls are considered adiabatic with reflect option for the PM, while a heat load of 39 W/m<sup>2</sup> and trap conditions are used for the cylinders. Pollutants emissions are simulated as velocity inlets with a unity mass fraction. Exhaust HST is also treated as inlet with negative velocity while the hangar air inlet is considered as a pressure inlet. Escape and reflect options are considered for the PM modelling, respectively. Inlet HST, leakage defects and door are considered as walls when they are closed and as interior otherwise.



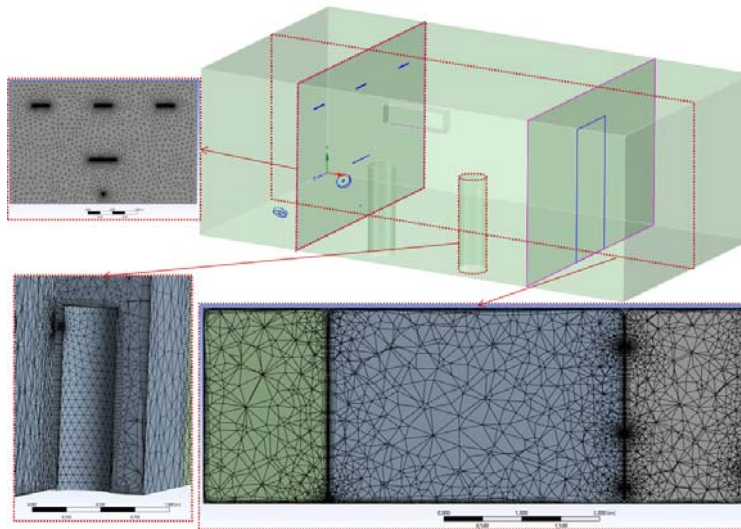


Figure 3: Illustration of the CFD computational domain with meshing at different cross-sections

## 6 PRELIMINARY RESULTS AND DISCUSSION

The developed models have been used to make preliminary decision regarding the chamber design, calculate the pollutants emission rates at different operating conditions needed to create simulated polluted air in zone 1. For this work, the “simulated outdoor air” of zone 1 is considered polluted with combustion products  $\text{NO}_x$  simulated with  $\text{NO}$  emission due to the lack of  $\text{NO}_2$  tanks, as well as  $\text{PM}$ , with special focus on  $\text{PM}_{2.5}$  and  $\text{PM}_{10}$  as they are the fractions of  $\text{PM}$  covered by IAQ regulations. The needed concentrations of these pollutants are  $500 \mu\text{g}/\text{m}^3$ ,  $300 \mu\text{g}/\text{m}^3$  and  $150 \mu\text{g}/\text{m}^3$ , respectively, in addition to a  $\text{CO}_2$  concentration of 500 ppm. Another assumption that was adopted is to limit the preparation time of zone 1 to 15 minutes only while all openings are closed in the interface with zone 2. However, the axial fans are operated and an extraction flowrate is operated with exhaust to the outside near actual inlet at the ceiling levels. With these assumptions, the resulting emission rates of the pollutants in zone 1 are presented in Table 1, for three extraction flowrates typical for HST used in French dwellings (10, 45 and  $135 \text{ m}^3/\text{h}$ ). Note that deposition and resuspension of  $\text{PM}$  are considered with velocities presented by (Thatcher & Layton, 1995). These parameters are to be calibrated in later work with the experimental results. The corresponding temporal variation of the pollutant concentrations in all zones are presented in Figure 4 for an operation of the chamber for one day, showcasing the stability of the established conditions, especially in zone 1. No emission scenario is included in the remaining zones at this stage.

As it can be seen, the emission rate of  $\text{PM}$  is expressed in terms of mass flowrate, however, the selection of the proper atomizer requires the knowledge of the particle count rate. For the conversion between the two rates, the particle volume and density are needed, and for this reason, the  $\text{PM}$  are assumed to have spherical shape with a density of  $2 \text{ g}/\text{cm}^3$  (average density of typical salts used in such applications), which gives a combined particle flowrate between  $9 \times 10^4$  and  $5 \times 10^5$  particle/s, which falls within the range of the atomizer generation rates. Moreover, using the same logic for the conversion, the total particle count in the zone corresponding to the required target concentrations is around  $1 \times 10^7$  particle/ $\text{m}^3$ , which is used to select the appropriate particle analyzer for the experimental chamber.

For the other pollutants, gas tanks are used with mass flowmeters to control the emission rates. Commercially, gas tanks for  $\text{CO}_2$  and  $\text{NO}$  are available with high purity ( $>99.99\%$ ), resulting in gas flowrates of 17 – 225 mLPM and 0.07 – 5.4 mLPM, respectively.

Table 1: Emission rates (mg/h) of pollutants into zone 1 to reach required concentrations of polluted outdoor air

Flowrate (m <sup>3</sup> /h)	CO <sub>2</sub>	NO	PM <sub>10</sub>	PM <sub>2.5</sub>
10	1830	4.85	47.30	4.73
45	8235	21.83	58.00	10.00
135	24705	65.43	84.80	23.50

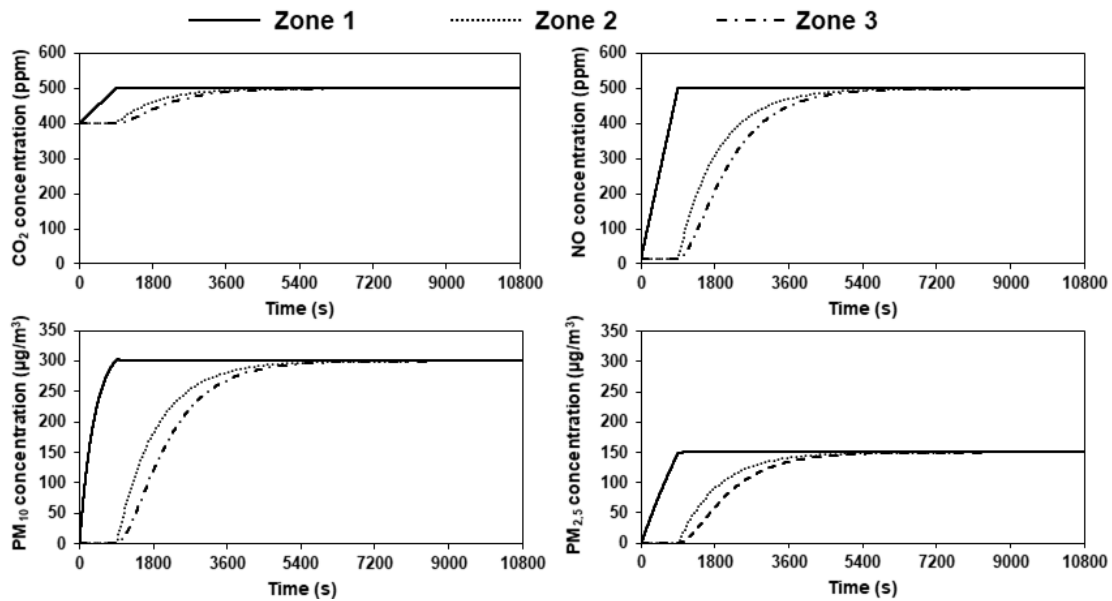


Figure 4: Pollutants concentration obtained in the experimental chamber zones using CONTAM

The obtained pollutants emission rates from CONTAM have been used as boundary conditions for the CFD model in two different configurations, center room and center wall emissions, along with two directions of the axial fans supply. The results of the simulations are presented in Figure 5 for the highest extraction flowrate of 135 m<sup>3</sup>/h, with an airtightness level of 0.6 m<sup>3</sup>/h·m<sup>2</sup> for the leakage defects. These conditions are selected to ensure uniform conditions at the different openings of the interface of zones 1 and 2. As it can be seen from Figure 5(a), the axial ventilators, with upward supply direction, creates additional turbulence in the zone with maximum velocities of 1 m/s along the fans axis, while maintaining low velocities below 0.15 m/s elsewhere. This was important to reduce their effect on the pressure field surrounding inlets while still ensuring enough mixing. Using this supply direction, it can be seen that emissions from the center of the wall provided higher homogeneity level compared to that in the center of the room, especially at the level of the inlet HST. In fact, a clear pollutant bypass can be clearly seen in Figure 5(b) when the emissions are room-centered caused by short-circuiting the air from the outdoor air inlet to the HST. Similar results have been obtained for PM concentrations where better mixed conditions is obtained in the case of wall-centered emissions. This can be attributed to the extraction of pollutants from the injection port near the wall directly into the stream of the fans before they are distributed. Hence, adopting wall emissions of the pollutants in zone 1 would be more suitable choice. Nonetheless, it should be noted that perfectly mixed and fully uniform PM distribution was not attained in either configuration, especially near the walls. This indicates that the sensors placement for the chamber control has a high influence on its behavior. For this reason, the control PM sensor were advised to be placed at the inlet HST, at midplane between the wall and the room center.

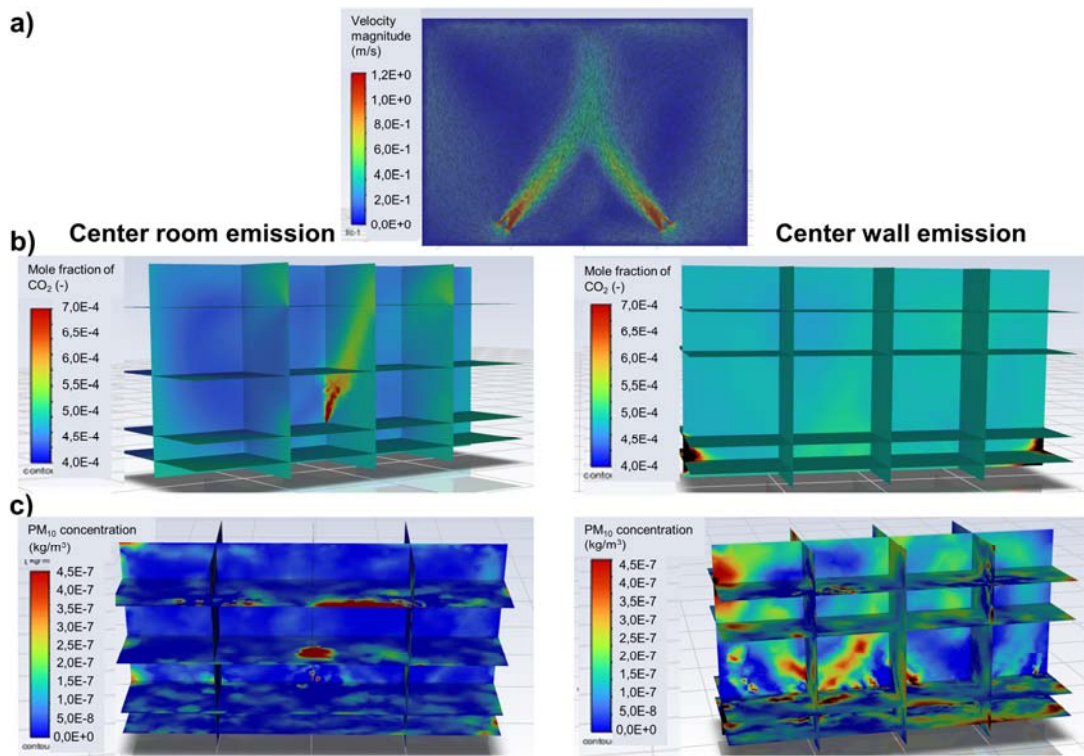


Figure 5: Results obtained using CFD simulations for upward supplying fans showing a) velocity profile, and the concentrations of b) CO<sub>2</sub> and c) PM<sub>10</sub> obtained from room and wall emissions

Using the pollutant emission scenario previously selected, the direction of the axial fans was reversed to provide downward supply of air, and the results are presented in Figure 6. As it can be seen, air velocities in the room center were below 0.15 m/s similar to the previous case. However, with the supply oriented to the floor, the Coandă effect is more pronounced, attaching thus the emitted pollutant jet to the adjacent wall, resulting in a higher local concentration. This can also be seen for PM concentrations were higher near the wall, along with a higher discrepancy between the PM concentration at the level of the different inlets. This was expected as supplying the air upwards, the fans extract the room air from the floor level and near wall and corners and supplied towards the room center; making thus this configuration more appropriate for the zone homogenization. Finally, compared between the two models, similar steady state conditions have been reached for gaseous components, while relatively larger differences ( $< 400 \mu\text{g}/\text{m}^3$  combined concentration of PM<sub>2.5-10</sub>), which highlights the need for models' calibration with experimental data from the chamber.

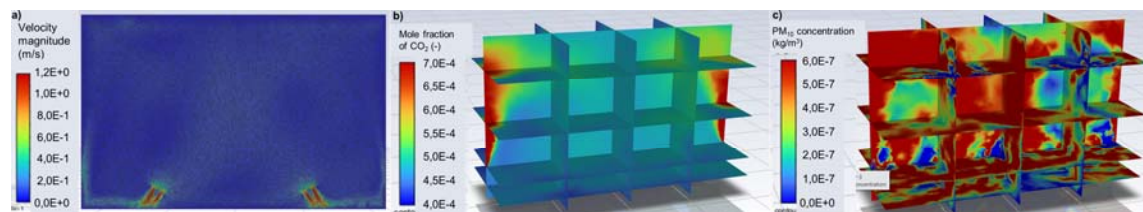


Figure 6: Results obtained using CFD simulations for downward supplying fans showing a) velocity profile, and the concentrations of b) CO<sub>2</sub> and c) PM<sub>10</sub> obtained from wall emissions

## 7 CONCLUSIONS

Maintaining acceptable IAQ is crucial for managing built environments, which is achieved by ventilating spaces with outdoor. In this regard, many ventilation systems have been developed

and tested. However, a literature review showed that there is a lack of experimental as well as numerical investigation concerning HDCV using HST that is considered as reference system in most European countries, especially France. For this reason, this work proposed the construction of a new experimental chamber, equipped with variety of equipment and with a high modularity. The chamber allows studying various HDCV strategies under typical operating conditions with respect to both outdoor- and indoor-generated pollutants, which has been shown lacking in the existing IAQ chambers. Numerical models were developed using CONTAM and CFD to guide the chamber design. The CONTAM model was used to determine pollutant emission rates, size the generators, and select the appropriate control equipment. Meanwhile, the CFD model helped determine the optimal placement of these instruments for better control and proper functioning of the experimental chamber.

## 8 REFERENCES

- Afshari, A., & Bergsoe, N. C. (2009). Humidity as a control parameter for ventilation. Phase 2: Development and testing of ventilation strategies in the laboratory. *Danish Building Research Institute*. <https://www.osti.gov/etdeweb/biblio/966475>
- Caron, A., Redon, N., Thevenet, F., Hanoune, B., & Coddeville, P. (2016). Performances and limitations of electronic gas sensors to investigate an indoor air quality event. *Building and Environment*, *107*, 19–28. <https://doi.org/10.1016/j.buildenv.2016.07.006>
- Ciuzas, D., Prasauskas, T., Krugly, E., Sidaraviciute, R., Jurelionis, A., Seduikyte, L., Kauneliene, V., Wierzbicka, A., & Martuzevicius, D. (2015). Characterization of indoor aerosol temporal variations for the real-time management of indoor air quality. *Atmospheric Environment*, *118*, 107–117. <https://doi.org/10.1016/j.atmosenv.2015.07.044>
- Code de la construction et de l'habitation—Légifrance*. (n.d.). Retrieved 3 June 2024, from [https://www.legifrance.gouv.fr/codes/texte\\_lc/LEGITEXT000006074096](https://www.legifrance.gouv.fr/codes/texte_lc/LEGITEXT000006074096)
- Desmarais, G., Derome, D., & Fazio, P. (1998). *Experimental Setup for the Study of Air Leakage Patterns*.
- Du, C., Li, B., & Yu, W. (2021). Indoor mould exposure: Characteristics, influences and corresponding associations with built environment—A review. *Journal of Building Engineering*, *35*, 101983. <https://doi.org/10.1016/j.job.2020.101983>
- Guyot, G., Sherman, M., Walker, I., & Clark, J. D. (2017). *Residential smart ventilation: A review* (Research Report LBNL-2001056). LAWRENCE BERKELEY NATIONAL LABORATORY. <https://hal.science/hal-01670527>
- Habchi, C., Ghali, K., & Ghaddar, N. (2015). Displacement ventilation zonal model for particle distribution resulting from high momentum respiratory activities. *Building and Environment*, *90*, 1–14.
- Harb, P., Locoge, N., & Thevenet, F. (2018). Emissions and treatment of VOCs emitted from wood-based construction materials: Impact on indoor air quality. *Chemical Engineering Journal*, *354*, 641–652. <https://doi.org/10.1016/j.cej.2018.08.085>
- Harb, P., Locoge, N., & Thevenet, F. (2020). Treatment of household product emissions in indoor air: Real scale assessment of the removal processes. *Chemical Engineering Journal*, *380*, 122525. <https://doi.org/10.1016/j.cej.2019.122525>
- Harb, P., Sivachandiran, L., Gaudion, V., Thevenet, F., & Locoge, N. (2016). The 40 m<sup>3</sup> Innovative experimental Room for INdoor Air studies (IRINA): Development and validations. *Chemical Engineering Journal*, *306*, 568–578. <https://doi.org/10.1016/j.cej.2016.07.102>
- Heiselberg, P., & Perino, M. (2010). Short-term airing by natural ventilation – implication on IAQ and thermal comfort. *Indoor Air*, *20*(2), 126–140. <https://doi.org/10.1111/j.1600-0668.2009.00630.x>
- Jurelionis, A., Gagytė, L., Prasauskas, T., Čiuzas, D., Krugly, E., Šeduikytė, L., & Martuzevičius, D. (2015). The impact of the air distribution method in ventilated rooms on the aerosol particle

- dispersion and removal: The experimental approach. *Energy and Buildings*, 86, 305–313. <https://doi.org/10.1016/j.enbuild.2014.10.014>
- Karam, J., Ghali, K., & Ghaddar, N. (2024). Resilience of Personalized Ventilation in Maintaining Acceptable Breathable Air Quality When Combined with Mixing Ventilation Subject to External Shocks. *Buildings*, 14(3), Article 3. <https://doi.org/10.3390/buildings14030654>
- Katramiz, E., Ghaddar, N., & Ghali, K. (2022). Novel personalized chair-ventilation design integrated with displacement ventilation for cross-contamination mitigation in classrooms. *Building and Environment*, 213, 108885. <https://doi.org/10.1016/j.buildenv.2022.108885>
- Li, H., Lan, Y., Liu, M., Kong, X., & Fan, M. (2023). Experimental research on the cross-infection control performance of different ventilation strategies. *Building and Environment*, 243, 110683. <https://doi.org/10.1016/j.buildenv.2023.110683>
- Lu, X., Pang, Z., Fu, Y., & O'Neill, Z. (2022). The nexus of the indoor CO<sub>2</sub> concentration and ventilation demands underlying CO<sub>2</sub>-based demand-controlled ventilation in commercial buildings: A critical review. *Building and Environment*, 218, 109116. <https://doi.org/10.1016/j.buildenv.2022.109116>
- Mahyuddin, N., & Awbi, H. (2010). The spatial distribution of carbon dioxide in an environmental test chamber. *Building and Environment*, 45(9), 1993–2001. <https://doi.org/10.1016/j.buildenv.2010.02.001>
- Mélois, A., Legree, M., Sebastian Rios Mora, J., Depoorter, J., Jardinier, E., Berthin, S., Parsy, F., & Guyot, G. (2023). Durability of humidity-based ventilation components after 13 years of operation in French residential buildings – Assessment of components performance in laboratory. *Energy and Buildings*, 292, 113154. <https://doi.org/10.1016/j.enbuild.2023.113154>
- Moujalled, B., & Mélois, A. (2023). *Trends in building and ductwork airtightness in France*.
- Najafi Ziarani, N., Cook, M. J., & O'Sullivan, P. D. (2023). Experimental evaluation of airflow guiding components for wind-driven single-sided natural ventilation: A comparative study in a test chamber. *Energy and Buildings*, 300, 113627. <https://doi.org/10.1016/j.enbuild.2023.113627>
- Nielsen, T. R., & Drivsholm, C. (2010). Energy efficient demand controlled ventilation in single family houses. *Energy and Buildings*, 42(11), 1995–1998. <https://doi.org/10.1016/j.enbuild.2010.06.006>
- Paukštys, V., Cinelis, G., Mockienė, J., & Daukšys, M. (2021). Airtightness and Heat Energy Loss of Mid-Size Terraced Houses Built of Different Construction Materials. *Energies*, 14(19), Article 19. <https://doi.org/10.3390/en14196367>
- Poirier, B., Guyot, G., Geoffroy, H., Woloszyn, M., Ondarts, M., & Gonze, E. (2021). Pollutants emission scenarios for residential ventilation performance assessment. A review. *Journal of Building Engineering*, 42, 102488. <https://doi.org/10.1016/j.jobbe.2021.102488>
- Sowa, J., & Mijakowski, M. (2020). Humidity-Sensitive, Demand-Controlled Ventilation Applied to Multiunit Residential Building—Performance and Energy Consumption in Dfb Continental Climate. *Energies*, 13(24), Article 24. <https://doi.org/10.3390/en13246669>
- Szczepanik-Scislo, N., & Scislo, L. (2021). Comparison of CFD and Multizone Modeling from Contaminant Migration from a Household Gas Furnace. *Atmosphere*, 12(1), Article 1. <https://doi.org/10.3390/atmos12010079>
- Thatcher, T. L., & Layton, D. W. (1995). Deposition, resuspension, and penetration of particles within a residence. *Atmospheric Environment*, 29(13), 1487–1497. [https://doi.org/10.1016/1352-2310\(95\)00016-R](https://doi.org/10.1016/1352-2310(95)00016-R)
- Thevenet, F., Debono, O., Rizk, M., Caron, F., Verrièle, M., & Locoge, N. (2018). VOC uptakes on gypsum boards: Sorption performances and impact on indoor air quality. *Building and Environment*, 137, 138–146. <https://doi.org/10.1016/j.buildenv.2018.04.011>

# Assessment of Airborne Cross-infection Risk Across Various Body Orientations in Indoor Airflow Environments

Hee Won Shin<sup>1</sup>, Hyun Wook Park<sup>2</sup>, Jae Hyun Park<sup>\*3</sup>, and Dong Hwa Kang<sup>\*4</sup>

*1 University of Seoul  
163 Seoulsiripdae-ro, Dongdaemun-gu  
Seoul, Republic of Korea*

*2 Kyungpook National University  
80 Daehak-ro, Buk-gu,  
Daegu, Republic of Korea*

*3 Sungkyunkwan University School of Medicine  
2066 Seobu-ro, Jangan-gu  
Suwon, Republic of Korea*

*4 University of Seoul  
163 Seoulsiripdae-ro, Dongdaemun-gu  
Seoul, Republic of Korea*

*\*Corresponding author: pjaehyun@skku.edu*

*\*Corresponding author: dhkang@uos.ac.kr*

## SUMMARY

This study aims to evaluate airborne cross-infection risk under different discharge angle ( $-20^\circ$ ,  $0^\circ$ , and  $+20^\circ$ ) and supply temperatures (18, 25, and  $30^\circ\text{C}$ ) of an air-conditioner, with various body orientations (face-to-face, side-by-side, and back-to-back). Field experiments on particle dispersion were conducted within a full-scale test chamber using a manikin-shaped particle generator and detector with simulated particles (NaCl). Initial trends in particle transmission varied with body orientations. Meanwhile, the cross-infection risk was lower at  $-20^\circ$  and higher at  $+20^\circ$  under a supply temperature of  $25^\circ\text{C}$  for all body orientations. However, discharge angles associated with lower or higher cross-infection risk varied with changes in supply temperatures. The findings indicated that body orientation is a crucial factor influencing cross-infection risk, and careful adjustment of discharge angles and supply temperatures is essential to prevent airborne cross-infection in such airflow environments.

## KEYWORDS

Airborne infection; Cross-infection risk; Particle transmission; Air-conditioners; Body orientations

## 1 INTRODUCTION

Global attention has turned to pandemic planning and preparedness due to frequent infectious disease outbreaks. Recent transmissions have been associated with indoor airflow environments, especially air-conditioned room (Kwon et al., 2020). The particle dispersion can also be influenced by system settings such as supply temperatures (Kang et al., 2011), however; previous studies have mainly evaluated on ventilation strategies to prevent airborne cross-infection. Additionally, the diverse seating arrangements in indoor spaces such as restaurants necessitate evaluation with consideration of various body orientations. Therefore, this study evaluated airborne cross-infection risk under different settings of an air-conditioner considering different body orientations.

## 2 METHODS

The field experiments of particle dispersion were conducted within a full-scale test chamber, employing two seated manikins to simulate both the source and target individuals in the center of the chamber with a distance of 2 m between them. The source and target manikins continuously emitted and counted simulated particles of NaCl from their circular opening mouths, with a volumetric breathing

rate of 2.83 L/min considering speaking activities. The stand-type air conditioner used in this study was installed facing the center of the chamber, with evaluation conditions set for air discharge angles ranging from  $-20^{\circ}$ ~ $+20^{\circ}$  vertically and temperatures ranging from 18°C to 30°C. We evaluated intake fraction to assess airborne cross-infection risk based on different body orientations (face-to-face, side-by-side, and back-to-back). Each experiment case consisted of a 5-minute pre-measurement of background concentration with the target manikin, followed by 20 min continuous particle emission.

Table 1: Evaluation cases of particle dispersion experiments

Condition	Air-conditioner		Body orientation
	Supply temperature	Discharge angle	
Base	Na.	Na.	FTF, SBS, BTB
Heating	30°C	$-20^{\circ}$ , $0^{\circ}$ , $+20^{\circ}$	FTF, SBS, BTB
Moderate heating	25°C	$-20^{\circ}$ , $0^{\circ}$ , $+20^{\circ}$	FTF, SBS, BTB
Cooling	18°C	$-20^{\circ}$ , $0^{\circ}$ , $+20^{\circ}$	FTF, SBS, BTB



Figure 1: Experiment settings in the test chamber

### 3 RESULTS AND DISCUSSION

The Initial trends in particle transmission varied with body orientations, showing not only the highest levels in face-to-face but also in side-by-side and back-to-back in certain cases. Meanwhile, the intake fraction remained consistently low at a downward discharge angle ( $-20^{\circ}$ ) over time under a supply temperature of 25°C for all body orientations. However, the lowest intake fraction showed at an upward ( $+20^{\circ}$ ) discharge angle under a supply temperature of 30°C, and at a straight ( $0^{\circ}$ ) discharge angle under 18°C. This suggests that cross-infection risk related to body orientation varies with indoor airflow, which is influenced by the operational settings of the air conditioner.

### 4 CONCLUSIONS

Experimental results showed that body orientations significantly affected cross-infection risk, even with the same distance between individuals. Additionally, careful adjustment of discharge angles and supply temperatures is essential to prevent airborne cross-infection in such airflow environments.

### 5 ACKNOWLEDGEMENTS

This research was supported by the National IT Industry Promotion Agency (NIPA) under the ‘AI-integrated New Infectious Disease Response System’ project and the National Research Foundation of Korea (NRF) grant funded by the Ministry of Science and ICT [No.2022R1A2C2011296]

### 6 REFERENCES

- Kwon, K. S., Park, J. I., Park, Y. J., Jung, D. M., Ryu, K. W., Lee, J. H. (2020). Evidence of long-distance droplet transmission of SARS-CoV-2 by direct air flow in a restaurant in Korea. *Journal of Korean Medical Science*, 35(46).
- Kang, Y., Wang, Y., Zhong, K. (2011). Effects of supply air temperature and inlet location on particle dispersion in displacement ventilation rooms. *Particuology*, 9(6), 619-625.

# Proposal for improving the linear regression method and uncertainty calculation in building airtightness tests

Benedikt Kölsch<sup>1</sup>, Valérie Leprince<sup>\*2</sup>

*1 German Aerospace Center (DLR)  
Institute of Solar Research  
Linder Höhe  
51147 Cologne, Germany*

*2 Cerema  
2 rue Antoine Charial  
69003 Lyon, France  
\*Corresponding author: valerie.leprince@cerema.fr*

## ABSTRACT

Improving the energy efficiency of buildings and the quality of indoor air requires accurate assessments of airtightness. The conventional regression method, Ordinary Least Squares (OLS) regression—as shown in ISO 9972—encounters challenges in the occurrence of fluctuating wind conditions, affecting the reliability of air permeability measurements. This study explores the potential of alternative regression techniques, specifically Weighted Least Squares (WLS) and Weighted Line of Organic Correlation (WLOC), to enhance the precision and reliability of building airtightness tests across varied environmental settings. Through the analysis of a comprehensive dataset derived from over 6,000 on-site blower door tests conducted on a multitude of house configurations, this research assesses the relative accuracy of these methods. Additionally, it introduces a new approach to global uncertainty calculation for the WLOC method.

Findings indicate that while all methods exhibit similar in predicting the airflow at 50 Pa, WLS and WLOC\_2 reduce prediction error by up to 6 percentage points at 4 Pa under wind speeds exceeding 4 m/s compared to other methods. At 50 Pa, the OLS 95% confidence interval covers the reference airtightness value for only 25% of the data, compared to WLOC\_2 with 42% and WLS with 91%. At 4 Pa, while OLS interval covers only 21% of measurements, WLS overestimates uncertainty with 100% coverage, and WLOC\_2 achieves 82% coverage. These results support incorporating weighted regression methods in airtightness testing standards.

## KEYWORDS

Airtightness test, regression method, ISO 9972, WLOC

## 1 INTRODUCTION

ISO 9972 (ISO 9972:2015, 2015) employs a regression analysis to interpret measured pressure and airflow data, Recommending the Ordinary Least Squares (OLS) regression to the logarithms of the measured values in its Annex C . However, recent studies (Delmotte, 2017; Delmotte & Laverge, 2011; M. Sherman & Palmiter, 1995; Walker et al., 1998) have highlighted OLS's limitation in accurately representing pressure/flow data at data extremes (Prignon et al., 2020) or extrapolating to low pressures, leading to significant biases and large uncertainties at higher windspeeds (Kölsch & Walker, 2020, 2022). This is critical because envelope pressures associated with natural infiltration in buildings are often at low pressures below 5 Pa (Etheridge, 2015; M. H. Sherman & Chan, 2006), which is essential in energy performance codes in places like France (AFNOR, 2016; Moujalled & Mélois, 2023) and California (California Energy Commission, 2022). Moreover, OLS fails to propagate the uncertainty of pressure measurements accurately (Prignon et al., 2020).

The objectives of this paper are:

1. Propose a simple uncertainty calculation to be included in the weighting scheme for the WLOC method.
2. Conduct a comprehensive comparison of uncertainty calculations for regression methods as proposed in two existing standards (OLS\_1 and WLS) and in line with the



- “Guide to the expression of uncertainty in measurements” (GUM) (Joint & Committee for Guides in Metrology, 2008) for the OLS and WLOC regression methods.
3. Utilize an extensive dataset of over 6,000 blower door tests to assess each method's ability to accurately predict airflow values and estimate 95% confidence intervals.

## 2 METHOD

### 2.1 Description and limitations of existing alternatives for linear regression

The OLS regression method in Annex C of ISO 9972 minimizes the sum of squared residuals, which are the vertical distances between the measured values and the regression line. For this regression procedure, the pressure difference is defined as the independent variable and the air flow as the dependent variable assuming negligible error in pressure difference. However, fluctuations of wind speed and direction affect building pressure difference, causing higher relative uncertainty at lower pressures. Smaller measurement points, logarithmized before calculating the least squares fit, influence results more significantly.

To mitigate this effect, the German National Annex to ISO 9972 (*DIN EN ISO 9972:2018-12*, 2018) and the Canadian CAN/CGSB-149.10 standard (*CAN/CGSB-149.10-2019*, 2019) proposed the Weighted Least Square (WLS) regression, which weights pressure measurement data by the square of the volume flow, limiting the impact of measurements at lower pressures.

Okuyama et al. (Okuyama & Onishi, 2012) worked on an Iterative Weighted Least Squares (IWLS) approach, while Delmotte proposed the Weighted Line of Organic Correlation (WLOC) (Delmotte, 2017), which minimizes the sum of products of the weighted horizontal and vertical differences between the measured values and the predicted line, considering both pressure and airflow uncertainties are non-negligible and unequal in reality. In addition, WLOC includes a ponderation of each point according to their uncertainty: giving less weight to points with higher uncertainty.

WLOC would provide more reliable measurements at low pressure differences and better uncertainty estimation, which was supported by Prignon et al. (Prignon et al., 2018, 2020) and Kim et al. (Kim et al., 2022) in small-scale studies conducted in Belgium and Korea. However, these studies were limited by their dataset size.

### 2.2 New WLOC method

A new “WLOC\_2” method introduced in this study calculates the uncertainties of pressure difference  $u(\Delta p_i)$  and airflow  $u(q_{env,i})$  using data available during a “normal ISO 9972” test without additional measurement requirement.

To account for pressure fluctuations during the test, we included the standard deviation of the measurement as the first term of Eq. (1). The second term incorporated the measurement device uncertainty specified by ISO 9972. The third term addresses the impact of pressure variation along the building façade, which we assume to be in the order of magnitude of the zero-flow pressure difference measured before and after the test.

Thus, the uncertainty of the pressure difference  $u(\Delta p_i)$  is expressed as:

$$u(\Delta p_i) = \sqrt{\sigma^2(\Delta p_{m,i}) + u^2(\Delta p_{m,i}) + \left(\frac{\Delta p_{0,1} + \Delta p_{0,2}}{2}\right)^2} \quad (1)$$

where  $\sigma(\Delta p_{m,i})$  represents the standard deviation of the pressure measurement at each station. In this context, “station” means the series of measuring points at one pressure difference target. The maximum permissible measurement error (MPME) for the pressure measurement device is specified as 0.5 Pa with a resolution of 0.25 Pa.

The WLOC\_2 uncertainties of airflow  $u(q_{env,i})$  for pressurization (p) and depressurization (d) are defined as:

$$u(q_{env,p,i}) = u_c(q_{m,p,i}) \cdot \frac{T_{int}}{T_e} = \sqrt{\sigma^2(q_{m,i}) + \left(u(q_{r,i}) \cdot \sqrt{\frac{T_e}{T_0}}\right)^2} \cdot \frac{T_{int}}{T_e} \quad (2)$$

$$u(q_{env,d,i}) = u_c(q_{m,d,i}) \cdot \frac{T_e}{T_{int}} = \sqrt{\sigma^2(q_{m,i}) + \left(u(q_{r,i}) \cdot \sqrt{\frac{T_{int}}{T_0}}\right)^2} \cdot \frac{T_e}{T_{int}} \quad (3)$$

where  $\sigma(q_{m,i})$  represents the standard deviation for each flow measurement station, and  $u(q_{r,i})$  is the uncertainty of the flow measurement device (3% of the airflow reading).

Note that this methodology does not consider the systematic error due to the mathematical model error.

The general calculation procedure standard uncertainties  $u_c(n_{WLOC})$  and  $u_c(\ln(C_{env,WLOC}))$  for WLOC\_1 and WLOC\_2 is similar to what is proposed in (Delmotte, 2013).

Since the procedure for calculating the 95% confidence interval (CI) in ISO 9972 does not align with the GUM, the uncertainty calculation was adapted according to (Delmotte, 2013; Joint & Committee for Guides in Metrology, 2008), resulting in the OLS\_2 method. Consequently, the CI of  $q_{ref}$  is computed using the expanded uncertainty  $U$ , which is derived by multiplying the combined standard uncertainty  $u_c(q_{ref})$  with a coverage factor  $k$ :

$$CI(q_{ref})_{GUM} = q_{ref} \pm U(q_{ref}) = q_{ref} \pm k \cdot u_c(q_{ref}) \quad (4)$$

It is a good choice to take  $k = 2$  to define a CI of 95%. The combined standard uncertainty,  $u_c(q_{ref})$ , is calculated using the propagation of uncertainty principle (Joint & Committee for Guides in Metrology, 2008):

$$u_c(q_{ref}) = \sqrt{\left(\frac{\partial q_{ref}}{\partial n} \cdot u_c(n)\right)^2 + \left(\frac{\partial q_{ref}}{\partial \ln(C_{env})} \cdot u_c(\ln(C_{env}))\right)^2 + 2 \cdot \frac{\partial q_{ref}}{\partial n} \cdot \frac{\partial q_{ref}}{\partial \ln(C_{env})} \cdot u_c(n) \cdot u_c(\ln(C_{env})) \cdot r(n, \ln(C_{env}))} \quad (5)$$

Unlike the equations outlined by Delmotte (Delmotte, 2013), we neglected uncertainties due to temperature measurements for simplification, assuming they have a minor influence on the final results. The third term in the equation represents the “correlation coefficient”, reflecting the high correlation between the uncertainties on  $n$  and  $C_{env}$ .

### 2.3 Synthesis of regression techniques methodology

Figure 1 provides a schematic representation of the minimization criteria for each regression techniques (OLS, WLS, and WLOC). Table 1 details the procedure for calculating the confidence interval for these techniques.

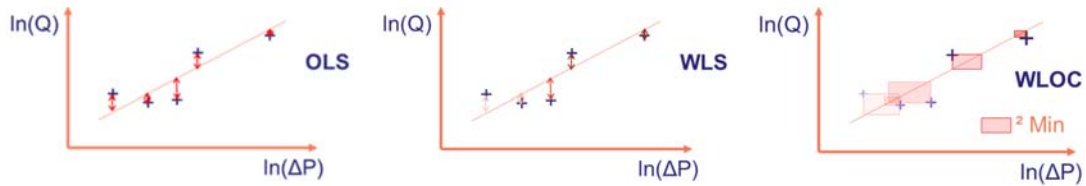


Figure 1: Schematic representation of regression techniques methodology for OLS, WLS, and WLOC

Table 2: Regression techniques and confidence interval calculation procedures

Procedures	OLS_1	OLS_2	WLS	WLOC_1	WLOC_2
Calculation of uncertainty on pressure difference and air flow rate measuring point	not considered	not considered	not considered	According to Delmotte and Prignon et al.	As proposed in this paper
Regression Technique	OLS	OLS	WLS	WLOC	WLOC
Calculation of uncertainty / confidence interval on the results	ISO 9972	In line with the GUM	Based on DIN EN ISO 9972	In line with the GUM	In line with the GUM

### 2.4 Dataset used for comparison

The data for this study was collected at the Alberta Home Heating Research Facility (AHHRF) in Edmonton, Alberta, Canada. This facility features six unoccupied test houses, each with unique construction. Detailed information about the facility and the dataset is available in Refs. (Walker et al., 2013; Wilson & Walker, 1993).

Each house underwent multiple measurements in various configurations, resulting in nearly 7,500 tests. These configurations varied due to different construction features like flue openings, sliding window states, or passive vent adjustments, leading to 127 distinct test scenarios. Each configuration involved between 5 and 140 tests, with 39% conducted in pressurization mode and 61% in depressurization mode.

This dataset underwent rigorous filtering to remove any missing or erroneous data. Additionally, the filtering process adhered to the following criteria set by ISO 9972:

- The absolute value of zero-flow pressure difference at the start and end of each test should not exceed 5 Pa.
- Each test must contain at least five data points, with the lowest data point being at least 10 Pa or five times the zero-flow pressure difference measured at the start. Some data points might be removed from a test to comply with this requirement.
- The highest pressure point in each test should be at least 50 Pa.

After this filtering process, the dataset was narrowed down to 6197 tests. Pressure and airflow readings were collected at 15-second intervals. A key aspect of our study was accounting for external environmental factors, such as varying wind conditions, on airtightness measurement results. Repeated measurements under diverse environmental settings provided a nuanced understanding of how such factors impact on building airtightness metrics. Meteorological, including outside temperatures ranging from -32 °C to +34 °C and wind speeds from close to 0 m/s to more than 10 m/s, were recorded in parallel with each pressure/airflow reading. Figure 2 demonstrated that the dataset includes tests conducted under challenging conditions (high wind), while the zero-flow pressure remains below 5Pa despite these conditions.

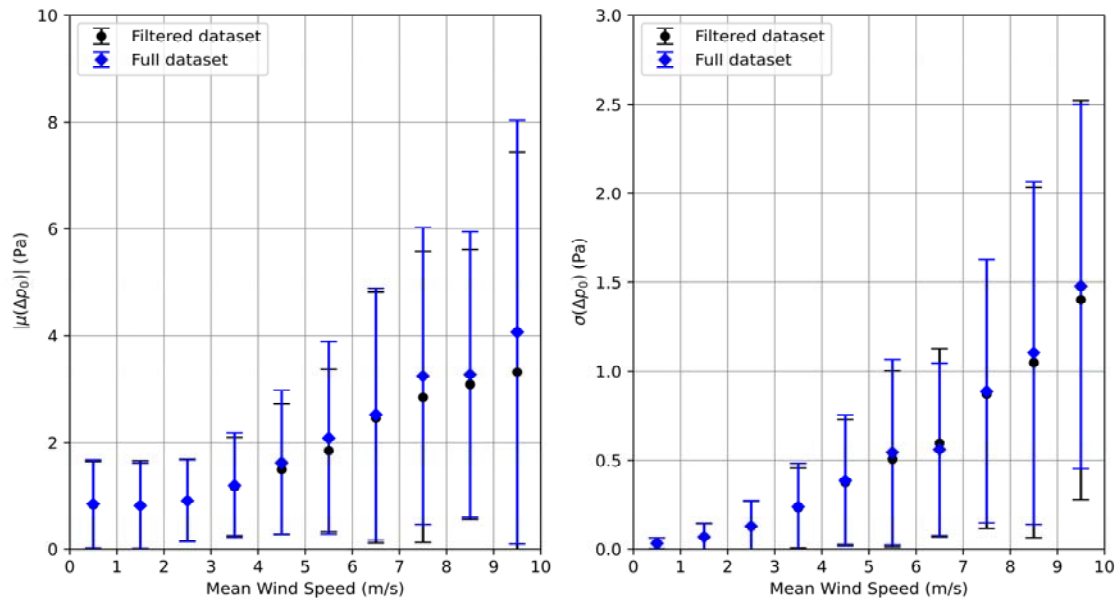


Figure 2: Distribution of mean absolute zero-flow pressure differences (left) and their respective fluctuations represented by the standard deviation (right) at increasing wind speeds in this dataset (black) and the full dataset (blue)

### 3 RESULTS AND DISCUSSION

#### 3.1 Predictive capability

Figure 3 evaluates the efficacy of the five regression methods in predicting airflow at two distinct pressure differences: 50 Pa ( $q_{50}$ ) on the left and 4 Pa ( $q_4$ ) on the right side. The horizontal axis represents wind speed, ranging from 0 m/s to 10 m/s, while the vertical axis shows the Percentage Difference (PD) between the measured and the reference airflow values. Data points indicate the average PDs for measurements within each 1 m/s increment of wind speed.

Since OLS\_2 employs the same regression method as OLS\_1, their results overlap in the graphs. At 50 Pa, all regression methods demonstrate a similar ability to predict the reference airflow, with mean PDs not exceeding -6%, even at higher wind speeds. This consistency suggests that the choice of regression method minimally impacts the accuracy of airflow predictions at 50 Pa. Additionally, the error bars are similar across all regression method.

For both pressure differences, the mean PD remains around zero up to approximately 3 m/s, indicating that wind-induced errors do not introduce any bias at these lower wind speeds. Errors appear randomly distributed around zero, suggesting that other sources of random error are dominant. However, as wind speed increases beyond 3 m/s, a clear trend towards higher negative PDs emerges, particularly for  $q_4$ , highlighting wind as a dominant source of error. The

negative bias indicates an underestimation of the leakage flow rate due to the systematic error caused by the model that all leaks are considered as a single leak. At high wind speeds, the error is approximately 4 percentage points higher for OLS and WLOC\_1 compared to WLS and WLOC\_2 for  $q_4$ .

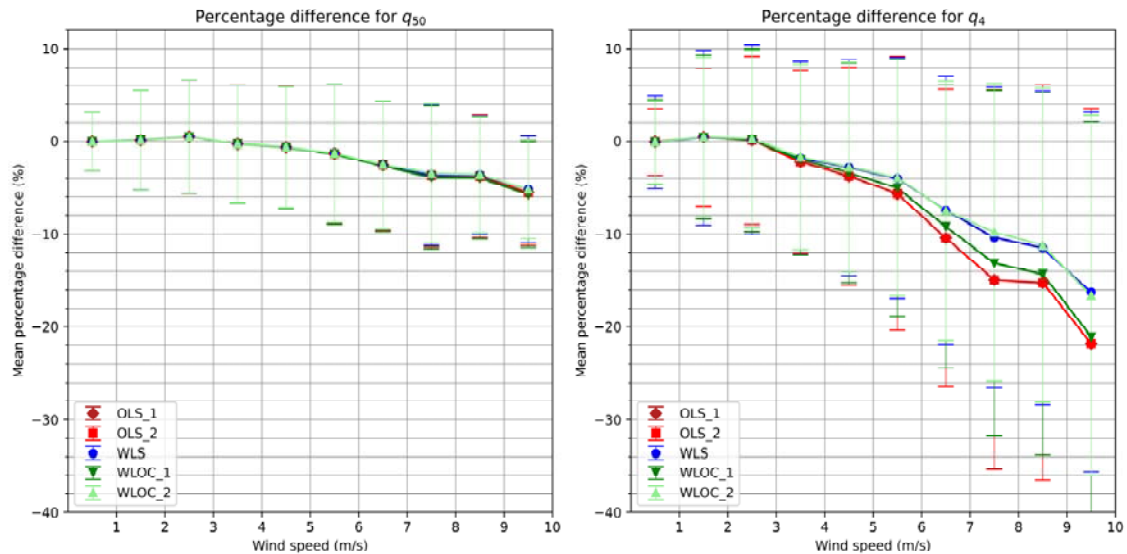


Figure 3: Mean values for increasing wind speeds of the percentage difference (PD) for calculated airflows at pressure differences of 50 Pa (left) and 4 Pa (right) and a reference value at these pressures with error bars representing the standard deviation

### 3.2 Uncertainty calculation relevance

Figure 4 illustrates the overall percentage of data points where the mean values of the calculated airflows at both 50 Pa and 4 Pa fall within the designated 95% confidence intervals, showing the relative performance of each regression method across the entire dataset.

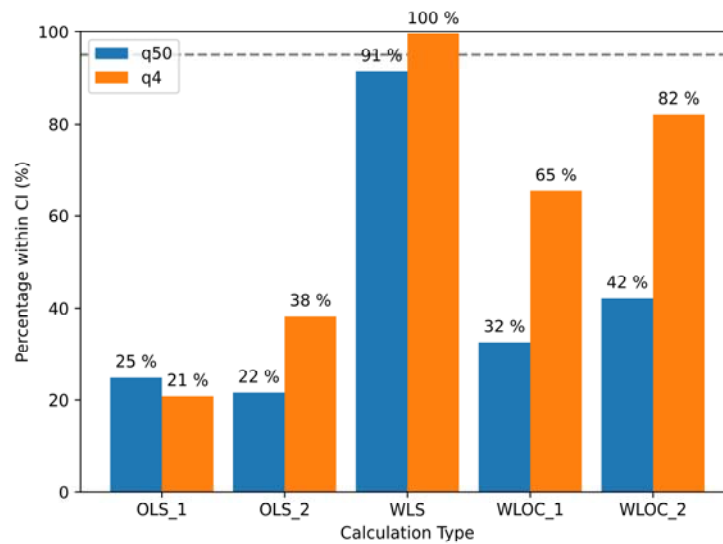


Figure 4: Total percentage per type of regression where mean values of calculated airflows at 50 Pa and 4 Pa fall into the 95% confidence interval

The WLS method demonstrates high overall coverage, achieving 91% for airflows at 50 Pa and full coverage at 4 Pa. Among the other regression techniques, WLOC\_2 shows the best performance, maintaining coverage above 80% when extrapolating the flowrate at low pressure.

However, its effectiveness decreases when the calculating airflow at 50Pa, where coverage remains below 50%. This variation suggests that the method underestimate the actual uncertainty.

One reason the uncertainty calculation might fail to cover the 95% confidence interval is that not all sources of uncertainty are accounted for, and there is a systematic error that increases with wind speed, as shown in Figure 3. This error arises from the model itself. When correcting the data of this database for the average systematic error according to wind speed (Figure 3), the coverage changes only negligibly, not enough to alter the conclusion of this study. This systematic error depends on the distribution of leaks, which is unknown and cannot be corrected a priori. Although this error is systematic for a given building, it is effectively random because the exact leakage distribution in a given building cannot be known or controlled. An alternative approach could be to incorporate this model-induced error into the uncertainty calculation, which could be based on previous research (Carrié & Leprince, 2016; Delmotte, 2021).

#### 4 CONCLUSIONS

This study presents a comprehensive evaluation of over 6,000 test series spanning 127 testing scenarios to assess the reliability and accuracy of three different regression analysis methods and different approaches for estimating measurement uncertainties in building airtightness measurements under varying climatic conditions. Our analysis particularly focuses on the influence of wind speeds on the results.

The findings reveal that the OLS and WLOC\_1 regression methods seem slightly less effective in providing reliable airflow rates compared to WLS and WLOC\_2, especially when the reference pressure is at 4 Pa and wind speeds exceed 4 m/s. A key observation is the systematic variation in measured air flow rates under different wind conditions. Data indicate that higher wind speeds consistently yield lower airflow rates than those measured under calmer conditions, highlighting the significant impact of wind on air leakage measurements.

Regarding error estimation, our analysis suggests that all methods, except WLS, tend to underestimate the actual uncertainty involved, which is consistent with expectations given that none of them can consider all sources of error. In contrast, the WLS method appears overly pessimistic at higher wind speeds and especially for lower pressures extrapolation, suggesting that in practice, pressure fluctuations may be less severe than predicted by this method. Wind speed variations are generally not as extreme, and the wind pressure coefficient on most building envelopes is significantly lower than 1. However, the procedure described in DIN EN ISO 9972 is not designed for calculating confidence intervals, and the method chosen in this paper is an attempt to approximate these intervals.

The WLOC\_2 method seems to provide a notable improvement in error estimates over the OLS\_1, as currently prescribed by ISO 9972, in particular at low pressure differences. However, there is still room for enhancement, particularly in integrating additional sources of error.

A limitation of this study lies in its relevance on real building configurations, where the 'true' values of airtightness are inherently unknown and can only be estimated under optimal conditions. Additionally, the study utilizes only a single building topology in the dataset. Future research could benefit from validating these findings under controlled laboratory settings, as suggested in (Mélois et al., 2024), to strengthen their applicability.

This study underscores significant implications for the standardization of building airtightness testing. We evaluated the performance of two standardized methods, OLS\_1 and WLS, against three other methods that incorporate an improved uncertainty calculation procedure, including a simplified weighting scheme in the WLOC\_2 method. Although the weighting procedure of WLOC could benefit from further refinement, the performances of the WLS and WLOC\_2 regression methods suggest they should be considered for future inclusion in standards such as ISO 9972, given their respective advantages. However, the uncertainty estimation according to

wind should be adapted for WLS. WLOC<sub>2</sub>, with its valid uncertainty calculation procedure, and WLS both provide flexibility and enhanced reliability in testing procedures. Further investigation into the potential inclusion of the model-induced systematic error in the uncertainty calculation would be beneficial.

As we conclude, this study not only challenges existing methodologies but also paves the way developing more accurate and reliable airtightness testing standards. Adopting these advanced regression techniques and integrating comprehensive uncertainty calculations will be important for enhancing the predictive accuracy of airtightness tests.

## 5 ACKNOWLEDGEMENT

We would like to express our gratitude to Iain S. Walker from Lawrence Berkeley National Laboratory for his provision of the data set and his scientific expertise to this research. Additionally, we extend our thanks to Joachim Zeller for his insightful discussions and constructive feedback. Both have contributed to an extended version of this paper that is currently under review.

## 6 REFERENCES

- AFNOR. (2016). *FD P50-784. Thermal performance of buildings—Implementation guide for NF EN ISO 9972.*
- California Energy Commission. (2022). *2022 Single-Family Residential Compliance Manual: For the 2022 Building Energy Efficiency Standards (CEC-400-2022-006).*
- CAN/CGSB-149.10-2019—*Determination of the airtightness of building envelopes by the fan depressurization method.* (2019).
- Carrié, F. R., & Leprince, V. (2016). Uncertainties in building pressurisation tests due to steady wind. *Energy and Buildings, 116*, 656–665. <https://doi.org/10.1016/j.enbuild.2016.01.029>
- Delmotte, C. (2013). Airtightness of buildings—Calculation of combined standard uncertainty. *Proceedings of the 34th AIVC Conference.*
- Delmotte, C. (2017). Airtightness of Buildings – Considerations regarding the Zero-Flow Pressure and the Weighted Line of Organic Correlation. *Proceedings of the 38th AIVC Conference.*
- Delmotte, C. (2021). Airtightness of buildings – Assessment of leakage-infiltration ratio and systematic measurement error due to steady wind and stack effect. *Energy and Buildings, 241*, 110969. <https://doi.org/10.1016/j.enbuild.2021.110969>
- Delmotte, C., & Laverge, J. (2011). Interlaboratory tests for the determination of repeatability and reproducibility of buildings airtightness measurements. *Proceedings of the 32nd AIVC Conference.*
- DIN EN ISO 9972:2018-12—*Thermal performance of buildings - Determination of air permeability of buildings - Fan pressurization method (9972:2018-12).* (2018). Beuth Verlag.
- Etheridge, D. (2015). A perspective on fifty years of natural ventilation research. *Building and Environment, 91*, 51–60. <https://doi.org/10.1016/j.buildenv.2015.02.033>
- ISO 9972:2015—*Thermal performance of buildings - Determination of air permeability of buildings - Fan pressurization method.* (2015).

- Joint & Committee for Guides in Metrology. (2008). *JCGM 100:2008—Evaluation of measurement data—Guide to the expression of uncertainty in measurements*.
- Kim, J.-H., Hwang, I.-T., & Park, J.-H. (2022). Comparison Building Airtightness based on the Regression Techniques (Ordinary Least Square vs. Weighted Line of Organic Correlation). *Journal of Korean Institute of Architectural Sustainable Environment and Building Systems*, 16(5), 333–345. <https://doi.org/10.22696/JKIAEBS.20220029>
- Kölsch, B., & Walker, I. S. (2020). Improving air leakage prediction of buildings using the fan pressurization method with the Weighted Line of Organic Correlation. *Building and Environment*, 181, 107157. <https://doi.org/10.1016/j.buildenv.2020.107157>
- Kölsch, B., & Walker, I. S. (2022). Reducing Wind Sensitivity for Blower Door Testing. *Proceedings of the 41st AIVC - ASHRAE IAQ Joint Conference*.
- Mélois, A., Tran, A. D., Moujalled, B., El Mankibi, M., Guyot, G., Kölsch, B., & Leprince, V. (2024). Model-Scale Reproduction of Fan Pressurization Measurements in a Wind Tunnel: Design and Characterization of a New Experimental Facility. *Buildings*, 14(2), 400. <https://doi.org/10.3390/buildings14020400>
- Moujalled, B., & Mélois, A. (2023). Trends in building and ductwork airtightness in France. *AIVC Ventilation Information Paper 45.6*.
- Okuyama, H., & Onishi, Y. (2012). Reconsideration of parameter estimation and reliability evaluation methods for building airtightness measurement using fan pressurization. *Building and Environment*, 47, 373–384. <https://doi.org/10.1016/j.buildenv.2011.06.027>
- Prignon, M., Dawans, A., & Van Moeseke, G. (2018). Uncertainties in airtightness measurements: Regression methods and pressure sequences. *Proceedings of the 39th AIVC Conference*.
- Prignon, M., Delmotte, C., Dawans, A., Altomonte, S., & Van Moeseke, G. (2020). On the impact of regression technique to airtightness measurements uncertainties. *Energy and Buildings*, 215, 109919. <https://doi.org/10.1016/j.enbuild.2020.109919>
- Sherman, M. H., & Chan, W. R. (2006). Building air tightness: Research and practice. In *Building Ventilation: The state of the art* (pp. 137–162). Earthscan.
- Sherman, M., & Palmiter, L. (1995). Uncertainties in Fan Pressurization Measurements. In M. P. Modera & A. K. Persily (Eds.), *Airflow Performance of Building Envelopes, Components, and Systems* (pp. 266–283). ASTM International.
- Walker, I. S., Sherman, M. H., Joh, J., & Chan, W. R. (2013). Applying Large Datasets to Developing a Better Understanding of Air Leakage Measurement in Homes. *International Journal of Ventilation*, 11(4), 323–338. <https://doi.org/10.1080/14733315.2013.11683991>
- Walker, I. S., Wilson, D. J., & Sherman, M. H. (1998). A comparison of the power law to quadratic formulations for air infiltration calculations. *Energy and Buildings*, 27(3), 293–299. [https://doi.org/10.1016/S0378-7788\(97\)00047-9](https://doi.org/10.1016/S0378-7788(97)00047-9)
- Wilson, D. J., & Walker, I. S. (1993). Infiltration Data from the Alberta Home Heating Research Facility. *AIVC Technical Note No. 41*.



# Optimizing the design of retirement homes concerning the indoor environment, energy efficiency, and climate change resiliency

Julie Lindgaard Hald<sup>1</sup>, Daria Zukowska-Tejsen<sup>1</sup>, Jakub Kolarik<sup>\*1</sup>

<sup>1</sup> *Department of Civil and Mechanical Engineering  
Technical University of Denmark  
Brovej 118  
Kgs. Lyngby, Denmark  
\*Corresponding author: jakol@dtu.dk*

## SUMMARY

This study explored the design optimization possibilities for Danish retirement homes while considering an increased risk of overheating due to elevated temperatures imposed by climate change. The focus was on combinations of design features and technical components ensuring thermal comfort and daylight. The study used a dynamic simulation tool to consider the current Danish design reference year and future climate predictions. The results indicate that using predicted climate data for 2050 could reduce overheating degree hours by 80% due to predicted direct solar radiation discrepancies. The study suggests using heatwave data to assess occupants' heat exposure. Design measures such as solar control coating on glazing reduced overheating by up to 53% while reducing daylight and increasing heating energy consumption. Ventilation hatches provided increased airflow and mitigated overheating without increasing energy consumption. A combination of static shading, solar control coating, and natural ventilation was sufficient for south-facing windows, but dynamic shading was necessary for east and west-facing windows.

## KEYWORDS

Thermal comfort, daylight autonomy, elderly home, design optimization, climate change

## 1 INTRODUCTION AND OBJECTIVES

Climate change is one of the biggest challenges facing modern society. One expected consequence in Northern Europe is longer-lasting summers with more frequent and intense heat waves (Meehl, Tebaldi 2004). Denmark and other northern European countries have ambitious goals regarding reducing CO<sub>2</sub> emissions and energy efficiency. At the same time, they require high indoor environmental quality (IEQ), including daylight. The consequence is highly airtight and insulated buildings with pronounced glazed areas that tend to overheat (Simone et al. 2014). The climate change with heat waves and prolonged warm periods, together with buildings that have a tendency to overheat, mean a significant danger for the most sensitive members of the society- young children and the elderly Bundle et al. (2018).

Our objective was to investigate how future weather conditions can be considered during design of retirement homes. We explored combinations of building design and design of building services (e.g. ventilation, heating, solar shading) that would be able to ensure high IEQ.

## 2 METHODS

The study design and investigated technological solutions were based on interviews with construction professionals working on retirement home projects. We conducted a typology study of 57 buildings to identify representative typical geometry and other characteristics of Danish elderly homes. Based on that, we modelled a two-bedroom nursing home apartment using a dynamic building simulation tool (Figure 1). The constructions were following current Danish building regulations (BR18 2024).

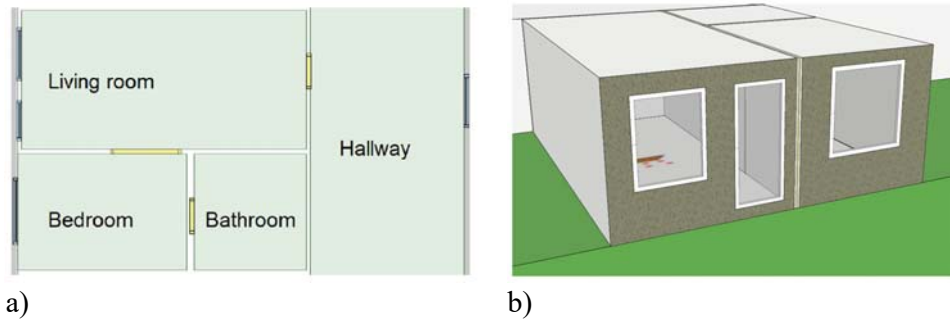


Figure 1: a) Floorplan of a simulated apartment in the retirement home, b) 3D representation of the model

For yearly simulations, we used the current Danish design reference year (DRY2013) and Typical Meteorological Year data for years 2050 and 2090 (RCP 8.5), according to Witchen et al. (2021). We added an extra heat wave scenario using historical weather data to ensure that the overheating risk was not underestimated. We used weather files for extremely high temperatures and extremely high solar radiation levels by (Witchen et al. 2021) but simulated only two weeks in August. Table 1 summarizes the modelled technical solutions.

Table 1: Modelled technical solutions

Component	Description
Ventilation hatches	$C_d = 0.3$ , effective opening area 74%, $U = 0.3 \text{ W/m}^2\text{K}$
Low energy glazing	$g = 0.54$ , $U = 0.61 \text{ W/m}^2\text{K}$ , $T_{vis} = 73\%$
Solar control glazing	$g = 0.31$ and $0.28$ , $U = 0.58 \text{ W/m}^2\text{K}$ , $T_{vis} = 63\%$ and $53\%$
Static solar shading	Overhang (0.25-2.5 m), vertical fins (0.25-1.6 m), loggia (2 m deep)
Active solar shading	External blinds: $T_{vis} = 0\%$ , $R = 0.67$ and external screen: $T_{vis} = 3\%$ , $R = 0.09$ , controlled by the solar radiation on the façade (threshold range 100-250 $\text{W/m}^2$ )
Mechanical ventilation	CAV at 15 L/, 20 L/s and 30 L/s, VAV 11.6 (0.3 $\text{L/s}\cdot\text{m}^2$ )-30 L/s, controlled by $\text{CO}_2$ and temperature

### 3 RESULTS AND DISCUSSION

First, we evaluated all technical solutions separately. Consequently, we evaluated their combination. Figure 2 shows an example of the results evaluation design scenarios using dynamic shading and VAV ventilation.

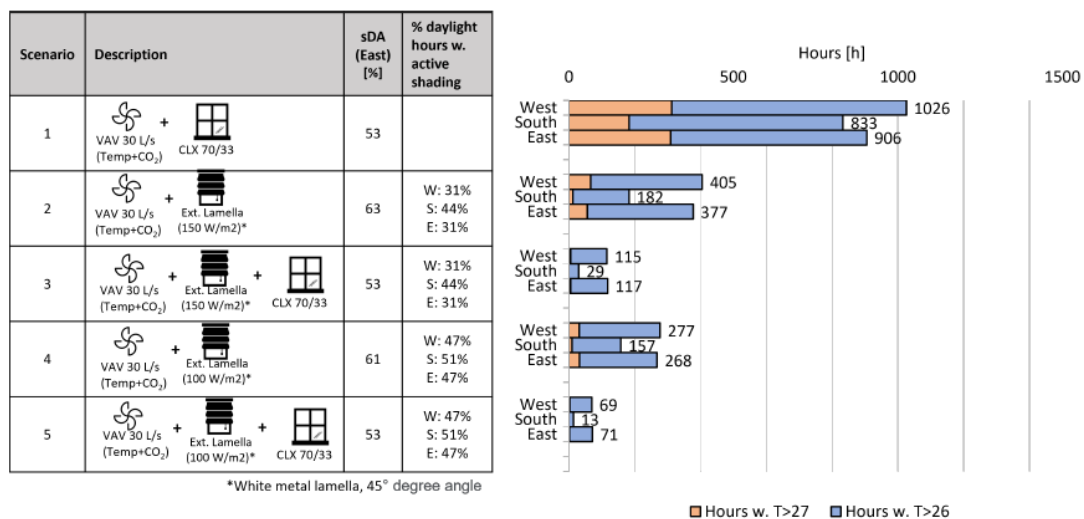


Figure 2: Example of results evaluating combinations of technical solutions. CLX is solar control glazing, T is operative temperature; sDA is spatial daylight autonomy.

Figure 3 shows the optimum set of design scenarios towards the south evaluated according to DR2013 and heat wave weather data.











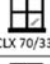



Scenario	Description	[°C h] DRY2013	[°C h] Extreme heat	Δ[°C h]	HWP
S1	 +  +  H: 1.15m + CLX 70/33 + Temp. Ctl. + Summer open at $T_{\text{ext}} > 16^{\circ}\text{C}$	3	19	15	0.4
S2	 +  +  H: 1.15m + CLX 70/33 + CAV 20 L/s	9	54	46	1.3
S3	 +  +  2m Int. balcony + Temp. Ctl. + Summer open at $T_{\text{ext}} > 16^{\circ}\text{C}$	8	35	27	0.8
S4	 +  MS-F 60/14 + CLX 70/33	9	91	82	2.3
S5	 +  +  Ext. Lamella (150 W/m <sup>2</sup> )* + CLX 70/33 + VAV 20 L/s (Temp+CO <sub>2</sub> )	4	14	11	0.3

Figure 3: Example of results evaluating combinations of technical solutions. °C·h - degree hours according to EN 16798; HPW is heat wave performance index – lower number indicates better performance during heat waves.

#### 4 CONCLUSIONS

- Future weather conditions could be considered by assessing the heat exposure of building occupants during a heatwave instead of using projected future weather data.
- The solar control glazing was an effective solution to reduce overheating by up to 53%. However, it also reduced spatial daylight autonomy by up to 13% and increased heating demand by up to 6%.
- Natural ventilation through ventilation hatches could increase airflow by up to 10 L/s, averaged over a month during summer, helping to mitigate overheating without increasing ventilation energy consumption.
- A combination of static horizontal shading, solar control coating, and natural ventilation was sufficient for South-facing windows. However, dynamic shading was necessary for East and West-facing windows to reach the thermal comfort target.

#### 5 REFERENCES

Meehl, G.A., Tebaldi, C. (2004) More intense, more frequent, and longer lasting heat waves in the 21st century. *Science* 305(5686), pp. 994-997.

Simone, A. et al. (2014) Analyses of passive cooling strategies' effect on overheating in low-energy residential buildings in Danish climate. In proc. of Indoor Air 2014, pp. 220-222.

Bundle, N. et al. (2017) A public health needs assessment for domestic indoor overheating. *Public Health* 161, pp. 147-153.

BR18 (2021) Danish Building Regulations. Available online <https://byggningsreglementet.dk/> (visited June 2021).

Wittchen, K. B., Trangbæk Jønsson, K. (2021) Vejrdata til fremtidens byggeri (in Danish). Institut for Byggeri, By og Miljø (BUILD), Aalborg Universitet, Danmark.

# **Room integrity tests and registration of the actual situation regarding the fire protection and holding times in fire compartments in Greece**

Theodoros Sotirios Tountas<sup>1</sup>

*1 FUV  
39 Ipirou Str.  
11146 Galatsi Athens, Greece*

## **ABSTRACT**

The need of maximum airtightness is essential in order to ensure that the fire compartment can maintain the required concentration of suppression gas for a specified duration and effectively suppress or extinguish a fire. In Greece there are many facilities with requirements for a high-level protection, but until today, most (if not all) of them have not any integrity test certification. They are complacent by the certifications of the materials applied and the only way to confirm the effectiveness of the room's integrity is when a fire will take place. A number of integrity tests have been made since 2022 and the registration of the results still takes place in various companies and institutions in Greece by the FUV research team. The main purpose of this registration is to complete a list of results regarding the holding time in each room and public the findings. The secondary purpose is to expand the knowledge regarding the existence of this kind of testing. The conclusion is that in most cases the holding time is minor than the ISO 14520 defines and there is a need for annual integrity tests is to confirm the reaction of each room.

## **KEYWORDS**

Air Permeability, Data Center, Fire protection, EN 15004:2019

## **1 INTRODUCTION**

In companies and public services with installed Data Centers, air tightness tests were performed to confirm their adequacy and to determine the Hold time according to the EN 15004:2019 standard. During the audits, it was found that in most cases, the spaces used as Data Centers are small storage rooms, without proper planning and paying attention to the selection of materials and their application.

## **2 MEASUREMENTS**

In all measurements, the EN 15004:2019 standard was applied, and a second measurement was made for the field check calibration. Beside the insufficient envelope, the presence of flammable materials was observed in the spaces inside the premises, such as polystyrene encased in the ceilings.

Table 1: Measuring Hold Time

	Measured hold time (min.)	Requested hold time (min.)
Room 1	2,30	10,00
Room 2	7,90	10,00
Room 3	3,40	10,00
Room 4	9,80	10,00
Room 5	15,60	10,00
Room 6	24,30	10,00
Room 7	4,80	10,00
Room 8	3,90	10,00
Room 9	12,50	10,00
Room 10	1,90	10,00
Room 11	8,90	10,00

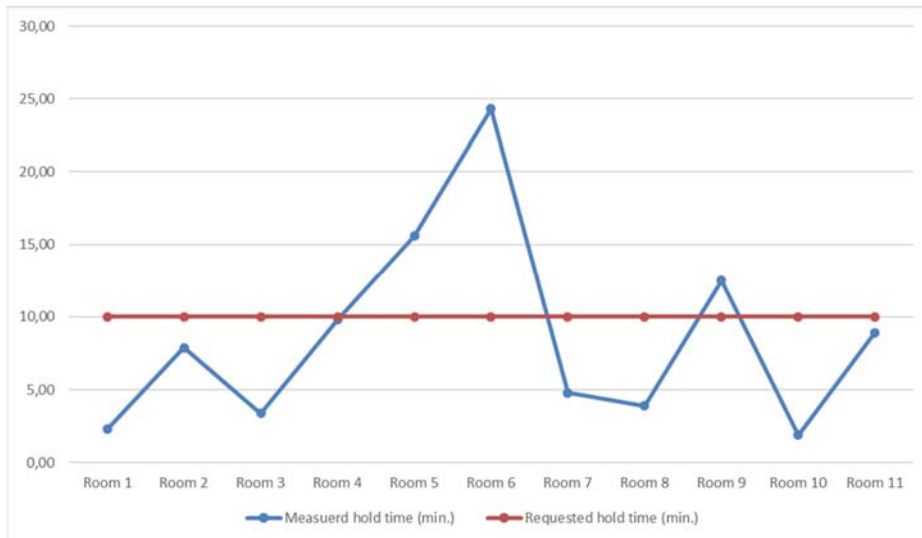


Figure 1: Hold Time comparing to the standard

Table 2: Room area comparing to Leakage Area

	Volume (m <sup>3</sup> )	Leakage area (cm <sup>2</sup> )
Room 1	185	344
Room 2	263	533
Room 3	185	378
Room 4	491	506
Room 5	203	136
Room 6	154	192
Room 7	492	982
Room 8	492	475
Room 9	239	371
Room 10	64	298
Room 11	100	510

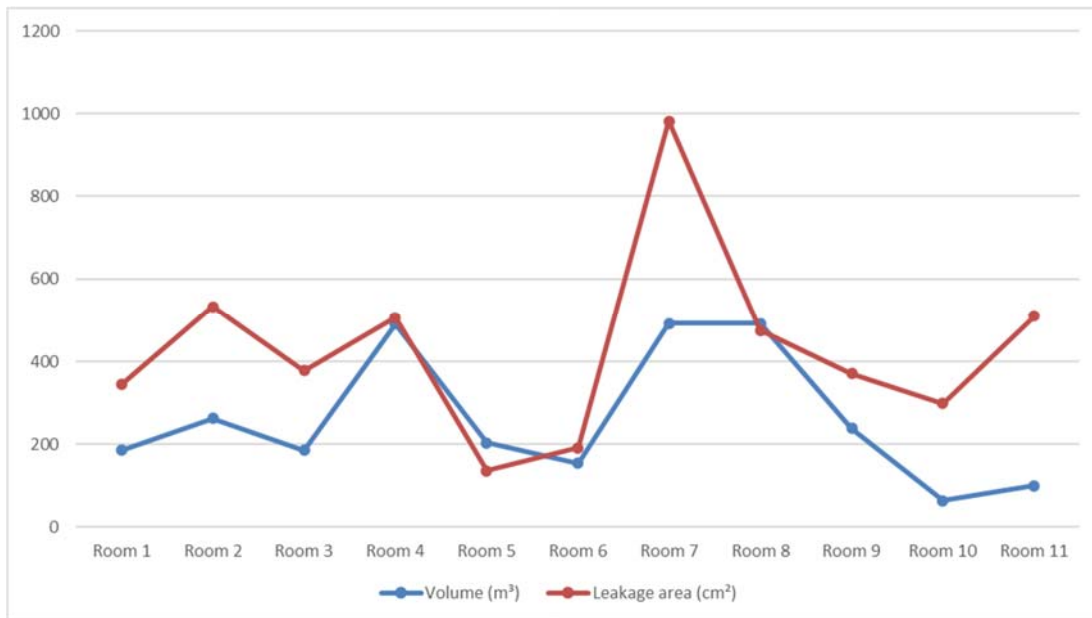


Figure 2: Room area comparing to leakage area

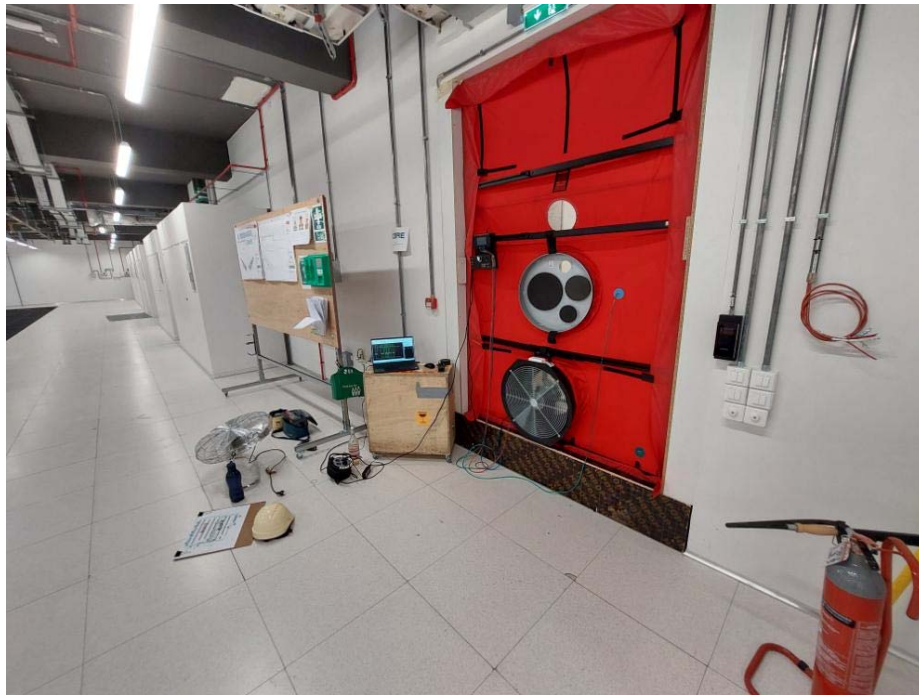


Figure 3: Example of a large data center testing

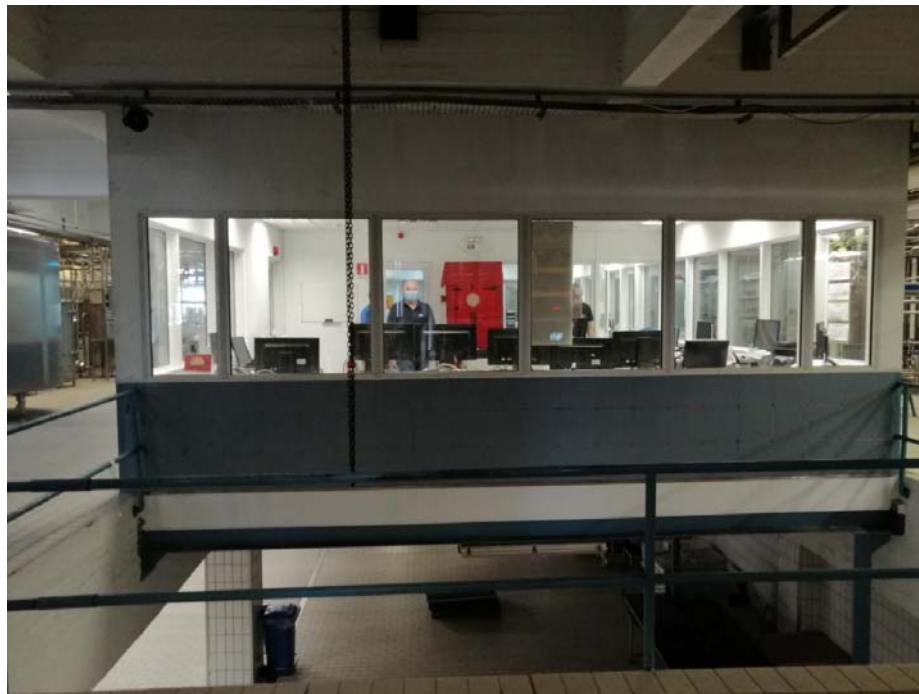


Figure 4: Example of a small data center inside a large food factory

### **3 CONCLUSIONS**

The conclusion is that investors aim for the best results, but construction are not familiar with good manufacturing and quality control techniques. Although large sums of money are invested in technologies and the requirements are high, only three out of eleven Data Centers meet the requirements of the standard.

### **4 REFERENCES**

EN 15004:2019

ISO 14520



# Performance 2 project - Analysis of the interactions between the Humidity-based DCV systems and IAQ in homes 15 years after their construction

Adeline Mélois<sup>1\*</sup>, Ambre Marchand Moury<sup>2</sup>, Juan Rios<sup>3</sup>, Marc Legrée<sup>3</sup>, Jérémy Depoorter<sup>4</sup>, Sylvain Rebières<sup>2</sup>, Gaëlle Guyot<sup>1</sup>

*1 Cerema BPE research team, 46 rue St Théobald, F-38080, L'Isle d'Abeau, France*

*3 AERECO SA, Z.I de Lamirault, 62 Rue de Lamirault, 77090 Collégien, France*

*\*Corresponding author: adeline.melois@cerema.fr*

*2 Cerema Centre Est – Agence d'Autun – Groupe Bâtiments, Boulevard Bernard Giberstein, 71400 Autun, France*

*4 ANJOS VENTILATION, Lot. Roche Blanche, 01230 Torcieu, France*

## ABSTRACT

The Performance 2 project (2020-2024) is a French national research project that aims to evaluate the long-term performance and durability of Humidity-based Demand Controlled Ventilation (DCV) systems installed in two multi-family social housing buildings, located in Paris and Villeurbanne, France. This study investigates the interaction between the ventilation systems and the Indoor Air Quality (IAQ) 15 years after construction.

Continuous measurements over a two-year period were conducted on the Air Terminal Devices (ATDs) of the ventilation system functioning and the IAQ (CO<sub>2</sub>, Relative Humidity, and for Paris, Particulate Matters – PM<sub>2.5</sub>, Volatile Organic Compounds - VOC); with the sensors located close to the ATDs. Additional monitors measuring all the IAQ parameters plus Formaldehyde were placed in dry rooms for two separate winter IAQ campaigns. Occupants interviews were used to assess occupants' behaviour over that two separate two weekly periods. This study has been carried out on 18 existing dwellings (13 in Paris and 5 in Villeurbanne, France) using data collected from November 2021 to December 2023 in Paris and from June 2022 to May 2023 in Villeurbanne.

This analysis provides insights into the dynamics of pollutant concentrations, considering both standard reference values and temporal trends (dynamics). Focus was given to PM<sub>2.5</sub>, with findings revealing significant PM<sub>2.5</sub> concentrations primarily in dwellings occupied by smokers. VOC concentrations varied among dwellings, with one particular case due to an under-ventilation situation (no source of humidity detected therefore the ventilation system provides always low airflow) leading to elevated levels, however most of the cases show consistent levels due to a daily use of perfumed candles, air freshener and incense. CO<sub>2</sub> levels were generally low, however certain rooms exhibited higher concentrations attributed to under-ventilation in Villeurbanne and high occupancy in Paris.

## KEYWORDS

Smart ventilation, residential ventilation, IAQ, energy efficiency, durability, humidity

## 1 INTRODUCTION

Relative humidity-controlled mechanical extract ventilation (RH-MEV) systems have been widely used in France for 40 years [1]. Most of the new residential buildings complying with RT 2012 and now RE 2020 energy performance regulations, are equipped with such systems [2] and currently they are considered as a reference system. In 2019, “Performance 2” project was launched in three phases to:

1. conduct a full winter analysis of the system after 13 years of in-situ operation using the installed sensors (non-recalibrated) and without major intervention;
2. collect the air terminal devices – ATDs (inlet and exhaust units) and sensors for laboratory testing before and after cleaning and maintenance and finally,
3. re-install the cleaned and maintained ATDs (where the hygroscopic component reminds intact) with calibrated and new (in Paris) sensors.

The phase (1) has been described in [3] and phase (2) in [1]. This paper presents the methodology and the results of the data analysis of the measurements collected over 2 years after these phases regarding the Indoor Air Quality in the dwellings studied in this project. The objectives of this study are to identify the interactions between the performance of the RH-MEV systems and the concentrations of different other pollutants, including VOC, Formaldehyde, and PM<sub>2.5</sub>, and CO<sub>2</sub>.

The evaluation of the durability of the RH-MEV systems in these two buildings after 15 years has been carried out by comparing the current energy performance and IAQ (RH and CO<sub>2</sub> only) with the results obtained at the commissioning, as well as the theoretical performances evaluated 15 years ago, and presented in previous papers [4–6].

## 2 METHOD

### 2.1 Case studies, campaigns and previous diagnosis

The two French social housing buildings studied are:

- a building of Paris Habitat where 19 dwellings were instrumented by Aereco in 2007 (from the 4<sup>th</sup> to the 8<sup>th</sup> floor), in Paris,
- a building of Lyon Métropole Habitat where 12 dwellings were instrumented by Anjos in 2007 (from the 1<sup>st</sup> to the 5<sup>th</sup> floor), in Villeurbanne (near Lyon).

At the beginning of the project, an inspection of the ventilation installations was carried out, partly applying the French Promevent protocol [8].

The Performance 2 campaigns include:

- Continuous measurements close to the ventilation terminals, which already had CO<sub>2</sub>, Temperature and RH sensors in place since the Performance 1 project 15 years ago. For Performance 2 and only for the building located in Paris, VOC and PM measurements were added to the previous ones. Additionally, two outdoor weather stations have been installed on the Paris building;
- Two IAQ winter campaigns (one in winter 2021-2022 and another in winter 2022-2023) during which two NEMOs IAQ monitors were installed in each voluntary dwelling (one in the living room and one in the parental bedroom). These monitors measured CO<sub>2</sub>, Temperature, RH, light VOCs, Formaldehyde and PM<sub>2.5</sub>. Additionally, an outdoor NEMOs was installed during each winter campaign. Quality data have been collected regarding the dwelling and the occupant's behaviour using a technical questionnaire, a weekly log filled by the occupants during the winter IAQ campaign and answers of the occupants during an interview conducted at the end of the winter IAQ campaigns [7];
- Laboratory campaigns to assess the current hygro-regulated performance of the ventilation terminals, verify the operation and reliability of the on-board sensors after 13 to 15 years in the dwellings [1], and to characterize the uncertainty of the sensors (embedded and NEMOs).

### 2.2 Characterisation of collected data

During the different on-site campaigns (2-years monitoring at ATDs and the 2 winter IAQ campaigns) and the laboratory campaigns (ATDs and sensors characterization), we have collected the following data for each dwelling:

- information about the dwelling;
- information on the "life of the occupants" during the winter IAQ campaigns;
- information on occupants' habits, their use and knowledge of their ventilation system, and their perception of IAQ;
- results of measurements of indoor parameters and pollutants, using NEMOs sensors for 2 weeks;

- results of measurements of indoor parameters and pollutants, from embedded sensors;
- ventilation system operating measurement results.

We have identified limits for each of this type of data by analysis of the characteristics of each sensor, the results of the inter-comparison of the sensors (during laboratory campaign), the campaign protocols and the disruptive events noted during the project (Table 1). This preliminary analysis of the data is essential to assess the quality of the data and to identify analyses that cannot be carried out, in particular the use of the “absolute values” for some measured parameters. This stage, often overlooked, has raised awareness of the importance of questioning the reliability of each measurement and each data, in order to propose scientifically acceptable analyses.

Table 1: Main limitations associated with the various data collected in Performance 2 project

Parameter	Sensor	Main limits	What to do?
CO <sub>2</sub>	NEMos	Weekly autocalibration to lowest value cannot be deactivated and cannot be traced	Paris first IAQ Campaign no useful (2 autocalibrations non traced)
	Board Sensors	Saturation ≤ 2000 ppm In Villeurbanne: weekly on lowest value which cannot be deactivated	No mean calculation
Formaldehyde	NEMos	Average over 2 hours Dispersion of values	
Total VOC	Board Sensors - Paris	“Human nose” mimicry	Vigilance on results and dynamics
Ligh VOC	NEMos	Dispersion of values	No threshold value
PM2.5	Board Sensors - Paris	High uncertainty Artifact: one-time peak	Vigilance on descriptive statistics
	NEMos	High uncertainty Dispersion of values	Vigilance on descriptive statistics
PM10	For certain NEMos	Extrapolated measurements with PM2.5	No useful
PM1	NEMos	High uncertainty	Vigilance on descriptive statistics
Emission Sources	Declarative (logbook / interview)	Cognitive biases + Social desirability	
Aeration	Declarative (logbook / interview)	Cognitive biases + Social desirability	Correlation with drop in temperature/RH/CO <sub>2</sub>

### 3 RESULTS

#### 3.1 CO<sub>2</sub> levels

CO<sub>2</sub> is not toxic in the proportions found in dwellings. It is nonetheless an excellent indicator of the occupancy/air renewal balance. To evaluate the durability of the ventilation systems, we had conducted previous analysis of the CO<sub>2</sub> levels in the dwellings according to an indicator used 15 years ago during the Performance 2 project [5]. This indicator used a threshold at 2000 ppm. Two dwellings in Paris were identified with high CO<sub>2</sub> concentrations, mainly due over-occupation in bedrooms. In a deeper analysis, we studied three new thresholds:

- 800 ppm: threshold accepted as protective against airborne transmission by both the French “Haut Conseil de Santé Publique” and the World Health Organisation (re-evaluated since the Covid crisis), and the first threshold in the ICONE index;
- 1000 ppm: defined in the French Standard Departmental Health Regulations;
- 1500 ppm: second ICONE index threshold.

### 3.1.1 Focus on probable occupancy periods without airing

The distribution of the CO<sub>2</sub> values measured was analysed first over the entire monitoring period, then we focused on the difference between heating season/outside the heating season, day/night (midnight to 6 am), and finally, for the bedrooms, a focus on the night during the heating season (conditions assumed to be the most penalising). When we separated data from heating and non-heating periods, we identified a clear increase in values during the heating period, as might be expected in a period when the use of airing by windows opening is largely reduced. Then, we focused on the most critical period in terms of CO<sub>2</sub>, which is at night, during the heating period, since this is the longest recurring period of occupancy in a room, during which only ventilation system provides air renewal. The data collected cannot be used to estimate occupant exposure, as it is too difficult (and unreliable) to judge the exact period during which they are present in a room. The advantage of successive focuses is that we can obtain information on air renewal during periods when occupancy is almost certain (at night in the bedroom), and when the risk of confinement is highest (during the heating period), without drowning out these values in the middle of periods when occupancy is much less certain. A synthesis of these night-time distributions over the heating period is given for all the main bedrooms in Villeurbanne (left) and Paris (right) in Figure 1. For six apartments in Paris, the CO<sub>2</sub> concentrations are above 1000 ppm around 90% of the time at night during the heating period, and for one apartment (P10) CO<sub>2</sub> concentrations are higher than 1000 ppm for 75% of the studied period, which illustrate an insufficient air renewable in these rooms.

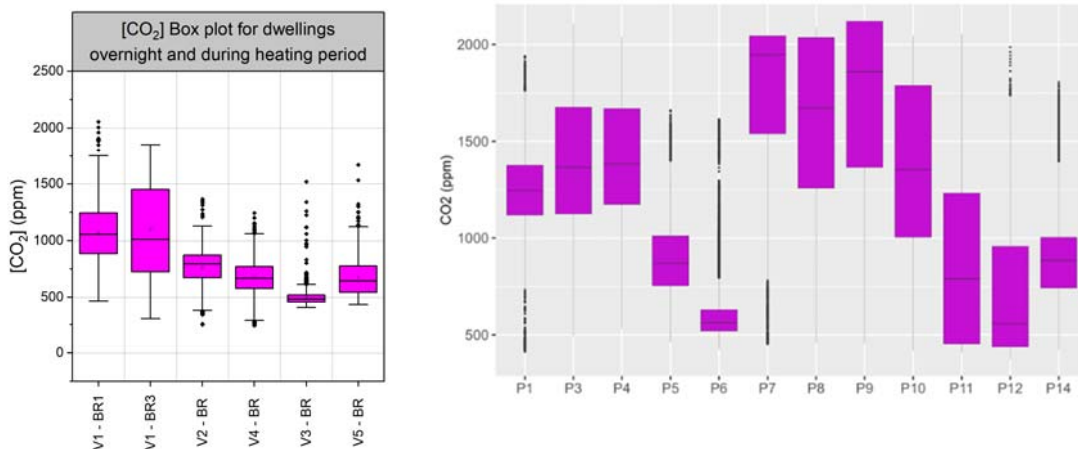


Figure 1: Distribution of CO<sub>2</sub> concentrations at night during the heating period in 2022 in the main bedrooms in Villeurbanne (left) and Paris (right)

Here the explanations we have been able to identify for the apartments with the higher levels of CO<sub>2</sub>:

- P1: limitation in maximum airflow of extract ATDs and insufficient pression evidenced. So, even if the appartement presents high relative humidity production and total extracted airflow seems to be not lower than the other dwellings for the same typology, airflow is not enough to extract the production of CO<sub>2</sub>.
- P3 and P4: no dysfunction of the ventilation system. No data collected from the occupants. Analysis of the CO<sub>2</sub> concentrations distribution shows that the main part of the time, the CO<sub>2</sub> concentration are below 1500 ppm.
- P7: extracted flows are almost at a minimum and not sufficient to evacuate the CO<sub>2</sub>. We identify no production of humidity, shower or cooking in this apartment, explaining the very low total airflow (no explanation has been identified to explain the CO<sub>2</sub> level during night).

- P8: 64% of the time above 1500 ppm. No dysfunction of the ventilation system. The bedroom is occupied by two persons, who have declared that they sleep with the door closed. The occupants stated that they had identified leaks around the windows in some rooms: an unequal distribution of leaks on the envelope could induce an under-ventilation of some rooms, which could explain the CO<sub>2</sub> values measured in the bedroom. A detailed diagnosis of the apartment airtightness and airflow modelling would be needed to confirm this hypothesis.
- P9: over-occupation of the bedroom. Used to be the “kids bedroom” but now the two kids are adults and have two big dogs with them in the small bedroom, and sleep with the door closed.
- P10: no dysfunction of the ventilation system. No data collected from the occupants.
- In Villeurbanne, both for the bedroom in V1 and V2, the air inlets showed during the laboratory campaign dysfunction with limited airflow rates. Nevertheless, the CO<sub>2</sub> concentrations do not exceed 1500 ppm.

### 3.1.2 ICONÉ index

In France, the "ICONÉ" index has been developed by the CSTB to assess the air stuffiness of a room by giving it a score from 0 to 5, particularly for schools (0 corresponds to absence of air stuffiness and 5 corresponds to an extreme air stuffiness). By extension to other types of buildings, the ICONÉ index can be used to assess the quality and efficiency of ventilation and air renewal systems in an enclosed, occupied space. It is calculated exclusively for the periods during which the room is occupied and incorporates both a notion of thresholds with two levels (800 ppm et 1500 ppm) and a notion of time, considering the length of time during which they are exceeded in the presence of the occupants. In Performance 2, we considered only the night periods (midnight to 6 am) in the bedrooms during which the occupants are *a priori* present (Figure 2). In Paris, the ICONÉ index shows three cases of "very high" stuffiness: the bedrooms in apartments P7, P8 and P9. Apartments P1, P3, P4 and P10 also show "high" stuffiness. These results are consistent with the previous analysis with the threshold at 1000 ppm. Like any index, the ICONÉ is not free from threshold effects. To consider the variability of realities within each category of the ICONÉ index, we calculated the percentage of time the 1500 ppm threshold is exceeded at night for each apartment in Paris (Figure 3). In P7, the threshold is exceeded more than three-quarters of the time at night, which distinguishes it from P8 and P9 by around 10 points. The difference between P1 and P3, P4 and P10 is also particularly visible on this graph. Only 10% of the night, i.e. relatively marginally, did P1 exceed the 1500 ppm threshold. In Villeurbanne, calculation of the ICONÉ index shows a favourable situation for all dwellings.

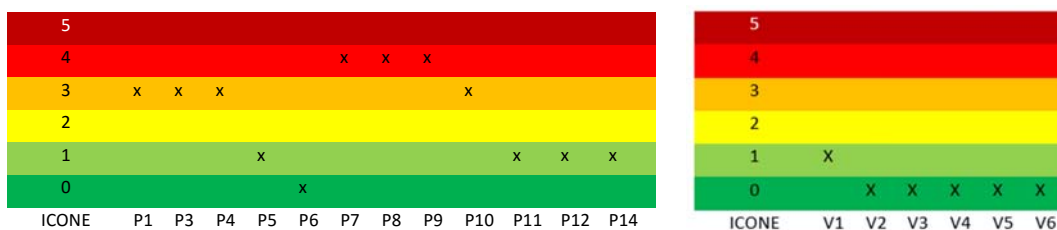


Figure 2: ICONÉ index calculated during night (0h – 6h) for each bedroom - Paris (left) and Villeurbanne (right)

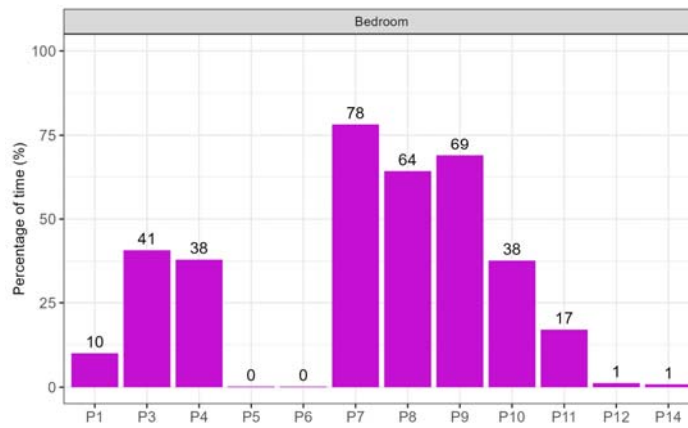


Figure 3 : Percentage of time CO<sub>2</sub> exceeds 1500 ppm at night during the heating season in Paris

Lastly, although some apartments are over-occupied and have occupants who sleep with the door closed, only ¼ of the bedrooms have 50% of the nighttime spent over 1500 ppm of CO<sub>2</sub>.

### 3.2 PM 2.5

#### 3.2.1 High PM<sub>2.5</sub> concentrations in several apartments

Even if the uncertainty of the PM<sub>2.5</sub> sensors is quite high in relation to the thresholds, we decided to analyse the measurements results in regards the two following thresholds:

- 5 µg/m<sup>3</sup>: threshold value proposed by the WHO for the long term;
- 15 µg/m<sup>3</sup>: threshold value proposed by the WHO for the short term.

The value of 5 µg/m<sup>3</sup> makes sense in terms of an annual average. Occasional exceedances during the year are therefore "normal", or at least not alarming. In fact, most apartments regularly exceed it. We focused more on the 15 µg/m<sup>3</sup> value over a one-hour period, which can lead to short-term health problems. Figure 4 represents the percentage of time above this value for the year 2022 in Paris (no data available in Villeurbanne). This indicator clearly brings P6 and P9 out, with PM<sub>2.5</sub> concentration higher than 15 µg/m<sup>3</sup> more than 30% of the time. The occupants' questionnaires indicate that these are smoking apartments. The kitchen in P11 also has high values. In the absence of a questionnaire conducted in this apartment, a possible explanation would be the frequent use of a frying pan, but this cannot be verified here.



Figure 4: Percentage of time (in dark) PM<sub>2.5</sub> concentrations are above 5 µg/m<sup>3</sup> and mean value (in red) of PM<sub>2.5</sub> for each room in Paris in 2022

To eliminate the small variations of the measurement that do not have health significance in relation to a long-term value, we decided to consider the sliding average value over one hour for each apartment (**Error! Reference source not found.**). P6 and P9 still present bad results without surprise. Apartment P8 also obtained relatively high values, which can be linked to the "very regular" use of scented candles and even incense mentioned in the questionnaire. As P10 was not included in winter IAQ campaign, we no dot have information regarding PM<sub>2.5</sub> emission in the dwelling.

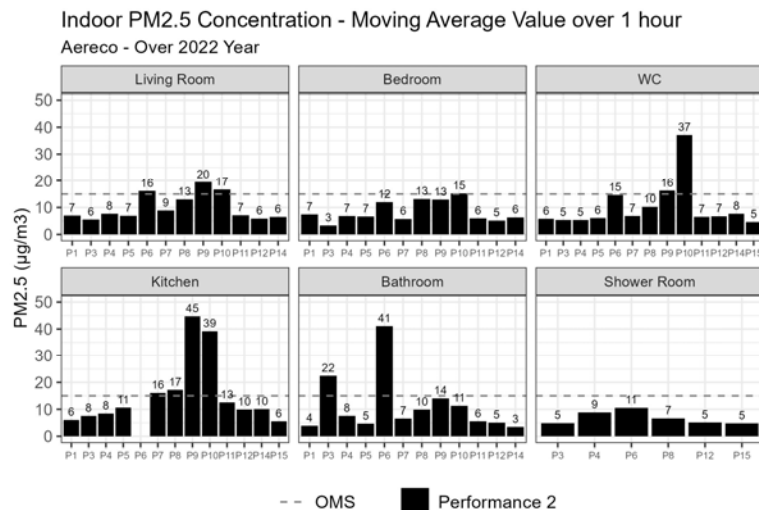


Figure 5: 1-hour moving average PM<sub>2.5</sub> concentration per room in Paris in 2022

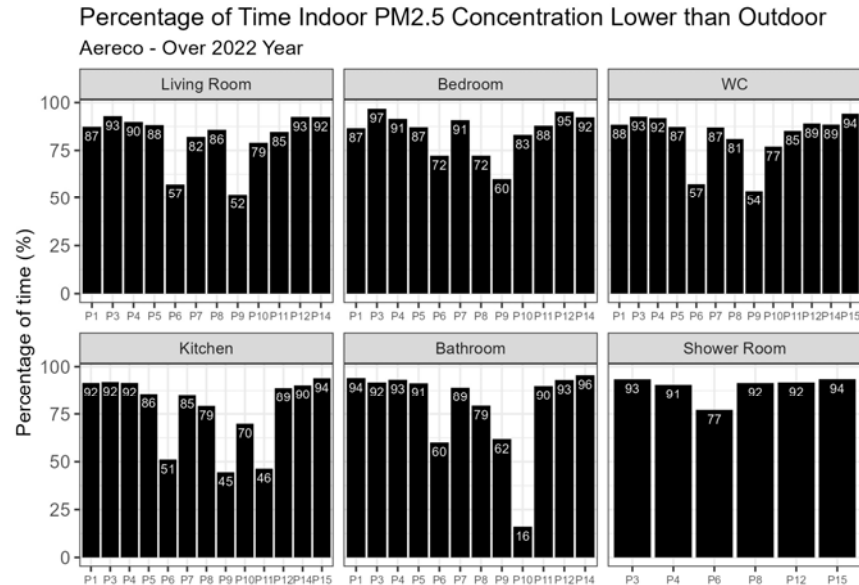


Figure 6: Percentage of time when the indoor PM<sub>2.5</sub> concentration is lower than the outdoor concentration for each room in Paris in 2022

### 3.2.2 Comparison PM<sub>2.5</sub> concentration inside and outside

As the main source of PM<sub>2.5</sub> is usually from outdoor, we evaluated the time when indoor concentrations are lower than those from outdoors (**Error! Reference source not found.**). Excepted for smoking apartments P6 and P9, PM<sub>2.5</sub> concentrations are lower in living rooms

than outdoors 80% to 97% of the time. This is also generally the case in the utility rooms, but with greater variation between apartments.

### 3.3 VOC

#### 3.3.1 Total VOC

Due to the high uncertainty of the sensors used during the campaign, the analysis of the measurements data needs to be considered with a lot of precaution. Thus, our approach consists mainly in identifying the more polluted apartments in terms of VOCs and identifying the probable sources. Figure 7 represents the measured value of VOC for which the concentration are above 70% of the time. We identify that the rooms with the highest values of VOC are toilets, bathrooms and shower rooms. These are the rooms where the use of scented products, particularly in spray form, is most widespread. P6 has particularly high concentrations in its toilets (massive use of air fresheners), and to a lesser extent in the bathroom (use of cosmetics). On the contrary, in living rooms, we measured relatively low values, despite the use of scented candles, which can be compared with the very good performance of the ventilation in this dwelling. Indeed, in addition to important air flow rates, the direction of circulation generated by the ventilation is particularly favorable in the case of pollutants emitted mainly in utility rooms. P8 has the second highest values in the living room, which can be linked to the daily use of essential oils and scented candles. The bathroom also has high values, which can be linked to the systematic use of eau de Cologne.

In dwellings where ventilation malfunctions, we identified that even relatively low emissions in utility rooms can lead to relatively high concentrations in living rooms. This is particularly noticeable in P7, which was identified during the CO<sub>2</sub> analysis, where concentrations in the toilets are rather low compared with the other dwellings, but which have the highest value in the living rooms. We also observed that the apartments with high CO<sub>2</sub> values are also those with the highest VOC concentration in the living rooms, that illustrate interaction between exposure to VOCs and air renewal.

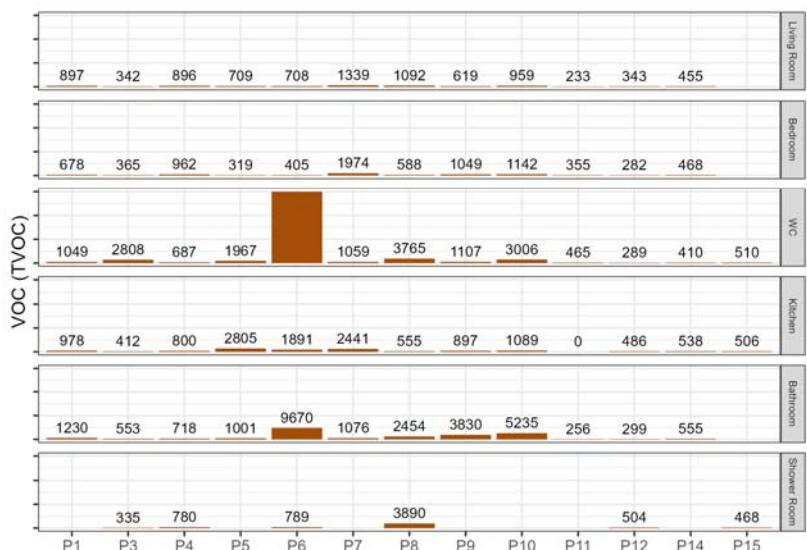


Figure 7: Measured value of VOC for which the concentration are above 70% of the time in Paris

### 3.4 Formaldehyde

Two threshold values are considered:



- 30 µg/m<sup>3</sup>: French regulation for monitoring IAQ in establishments open to the public buildings (i.e. schools);
- 100 µg/m<sup>3</sup>: Indoor Air Guide Value (VGAI) - Anses.

As only the NEMOs measured the formaldehyde, we have data only for apartments included in the winter IAQ campaigns (Figure 8).

Two apartments in Villeurbanne significantly exceeded the 30 µg/m<sup>3</sup> threshold during the first campaign, and much less so during the second. In one case, the occupants changed their habits between the two campaigns thanks to a personal inscription to a training on indoor air quality. For the second, the renovation of the floor and wall paintings before the 1<sup>st</sup> campaign could be responsible for the levels we measured. In Paris, an apartment exceeded the 30 µg/m<sup>3</sup> threshold almost 20% of the time during the first campaign, whereas this no longer occurred at all during the second. The information gathered from the occupants does not allow us to put forward any hypothesis to explain the difference between the 1<sup>st</sup> and 2nd campaigns. Regarding the second threshold, no apartment have reached 100 µg/m<sup>3</sup>.

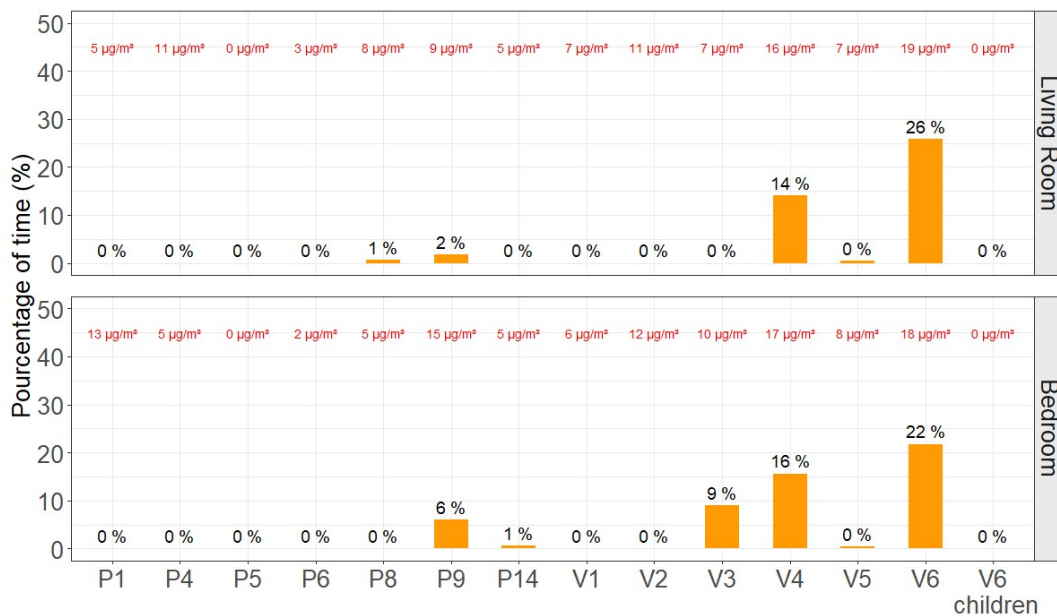


Figure 8: Percentage of time the 30 µg/m<sup>3</sup> value is exceeded in the instrumented rooms of each dwelling during the 1<sup>st</sup> winter IAQ campaign

#### 4 CONCLUSIONS

The Performance 2 project focused on the ventilation system performance in two multi-family social housing buildings, located in Paris and Villeurbanne (France), built 15 years ago and equipped with Humidity-based Demand Controlled Ventilation. It included the analyses of data collected during 2 years from monitoring at ATDs, winter IAQ campaign with IAQ sensors and interviews of occupants, and laboratory campaigns on the ATDs and the IAQ sensors. This paper presented the main results of the analysis dedicated to the IAQ in the dwellings studied in the project.

Overall, the CO<sub>2</sub> concentrations are quite acceptable within the limits considered (800 ppm, 1000 ppm and 1500 ppm). The high CO<sub>2</sub> concentration measured in some bedrooms are mostly due to over-occupation with closed door during the night.

The measurements of PM<sub>2.5</sub> carried out showed that:

- The values are around the long-term guide value 5 µg/m<sup>3</sup> recommended by the WHO as an annual average (but the uncertainty of the sensor is high) ;

- Indoor particle levels are generally lower than outdoor levels, almost systematically in dwellings, except for the smoking apartments;
- The values measured in smoking dwellings recurrently exceed the short-term guide value  $15 \mu\text{g}/\text{m}^3$ , regardless of the effectiveness of the ventilation system;
- To a lesser extent, the use of scented candles or incense significantly increases indoor PM levels.

The measurements of VOC, even with very high uncertainty of the sensors, show that:

- The rooms most affected by high VOC concentrations are utility rooms, due to the use of scented products in spray form;
- Living rooms are, on average, more polluted with VOCs than bedrooms;
- Changing household products has a direct impact in terms of lowering formaldehyde concentrations, which is much less obvious for light VOCs;
- Even high emissions in utility rooms are diluted by ventilation without generating pollution in the living areas when there is no dysfunction of the ventilation system.

## 5 ACKNOWLEDGEMENTS

The authors acknowledge the support of ADEME under the contract number 2004C0014.

The studies of the Performance 2 project have been carried out by Cerema, AERECO, ANJOS and LOCIE.

## 6 REFERENCES

- [1] A. Mélois, M. Legree, J. Sebastian Rios Mora, J. Depoorter, E. Jardinier, S. Berthin, F. Parsy, G. Guyot, Durability of humidity-based ventilation components after 13 years of operation in French residential buildings – Assessment of components performance in laboratory, *Energy and Buildings* 292 (2023) 113154. <https://doi.org/10.1016/j.enbuild.2023.113154>.
- [2] A.B. Mélois, B. Moujalled, G. Guyot, V. Leprince, Improving building envelope knowledge from analysis of 219,000 certified on-site air leakage measurements in France, *Building and Environment* (2019). <https://doi.org/10.1016/j.buildenv.2019.05.023>.
- [3] G. Guyot, E. Jardinier, F. Parsy, S. Berthin, E. roux, S. Charrier, Smart Ventilation Performance Durability Assessment: Preliminary Results from a Long-Term Residential Monitoring of Humidity-Based Demand-Controlled Ventilation, in: *IAQ 2020: Indoor Environmental Quality Performance Approaches Transitioning from IAQ to IEQ*, AIVC-ASHRAE, Athens, Greece, 2022.
- [4] G. Guyot, A. Mélois, M. Legree, R. Juan, Durability of humidity-based ventilation components after 15 years of operation in French residential buildings – Lab tests, in: *Rotterdam, The Netherlands*, 2022.
- [5] A. Melois, A. MArchand-Moury, M. Legree, J. Rios, J. Depoorter, N. Dufour, S. Rebières, G. Guyot, Performance 2 project - Winter IAQ campaigns in 13 dwellings equipped with Humidity-based DCV systems: analysis of the ventilation performance after 15 years of use, in: *Copenhagen, Denmark*, 2023.
- [6] A. Mélois, J. Sebastian Rios Mora, A. Marchand-Moury, M. Legree, J. Depoorter, N. Dufour, S. Rebières, G. Guyot, Performance 2 project - Winter IAQ campaigns in 13 dwellings equipped with Humidity-based DCV systems: analysis of the ventilation performance after 15 years of use, in: *Stockholm*, 2024.
- [7] A. Mélois, N. Vala, A. MArchand-Moury, C. Nauleau, R. Jobert, How to collect reliable information regarding occupants' behavior during IAQ campaigns? Performance 2 project first feedbacks, in: *Rotterdam, The Netherlands*, 2022.
- [8] A. Bailly Melois, L. Mouradian, Applications of the Promevent protocol for ventilation systems inspection in French regulation and certification programs, in: *Proceedings of the 39th AIVC Conference "Smart Ventilation for Buildings," Antibes Juan-Les-Pins, France*, 2018.

# Review and analysis of existing diagnostic methods for characterizing air transfers in existing homes

Imane Mannan<sup>1</sup>, Adeline Mélois<sup>1</sup>, Bassam Moujalled<sup>1</sup>, Luke Smith<sup>2</sup>, Christopher Wood<sup>3</sup>, Xiaofeng Zheng<sup>3</sup>

*1 Cerema, BPE Research Team 46 rue Saint Théobald F-38081, L'Isle d'Abeau, France*

*2 Build Test Solutions Ltd., Building 8, The Royal Ordnance Depot NN7 4PS, UK*

*\*Corresponding author: e-mail address imane.mannan@cerema.fr*

*3 Architecture, Climate and Environment Research Group, Faculty of Engineering, University of Nottingham, Nottingham, University Park, Nottingham NG7 2RD, UK*

## ABSTRACT

Buildings energy renovation is a major priority in most European countries in order to achieve a fully decarbonized building stock by 2050. In France, 7 million homes are poorly insulated and 14% of French people feel cold in their homes. The government has thus implemented an ambitious plan to scale up energy-efficient renovations of buildings to achieve carbon neutrality by 2050 while also pursuing a social objective of combating energy precarity.

More and more energy audits are being carried out, and the diagnostic method will be overhauled in 2024. These audits are often the only diagnostic work carried out prior to energy renovation, which must be done on a massive scale and quickly if the government's targets are to be met. Yet, existing homes feature a wide range of ventilation systems (non-existent, natural, mechanical) and levels of envelope air permeability. Overlooking these essential parameters in the energy renovation process, which are vital for ensuring good indoor air quality, could result in a proliferation of under-ventilated dwellings.

Air change rate in dwellings have an impact on both their energy performance and indoor air quality, particularly through the air infiltration of dwellings and the ventilation airflow. Methods currently exist for characterizing and assessing these factors using in situ measurements. However, these methods are often time-consuming to perform, and there are constraints on their widespread use during housing renovations. The most commonly used methods to characterize building air permeability and natural airflow rate are the blower door and tracer gas, respectively.

Recently, alternative methods for measuring building airtightness such as the Pulse method have been developed. This paper aims to investigate the existing measurement methods and devices for in-situ diagnostic of air change rate (air permeability of the envelope and natural ventilation airflow) in existing French and English dwellings.

This paper presents a review of the various existing methods for measuring building air permeability and natural airflow rate, and analyses the advantages and disadvantages of their use in existing occupied dwellings based on the reliability of the measured parameters and practical constraints.

## KEYWORDS

Airtightness, blower door, pulse, tracer gas

## 1 INTRODUCTION

Buildings energy renovation is a major priority in most European countries in order to achieve a fully decarbonized building stock by 2050. In France, 7 million homes are poorly insulated and 14% of French people are cold in their homes. The government has thus implemented an ambitious plan to scale up energy-efficient renovations of buildings to achieve carbon neutrality by 2050 while also pursuing a social objective of combating energy precarity. In 2017, the UK government set out a target to improve the rating of all fuel-poor homes to band C by 2030, and an aspiration for as many homes as possible to band C by 2035.

Thus, more and more energy audits are being carried out, but they are often the only diagnostic work carried out prior to energy renovation, which must be done on a massive scale and quickly. Yet, existing homes exhibit a wide range of ventilation systems (non-existent, natural, mechanical, hybrid, etc.) and envelope air permeability levels. Overlooking these essential parameters in the energy renovation process, which are vital for ensuring good indoor air quality, could result in a proliferation of under-ventilated dwellings. Indeed, air transfers in dwellings have an impact on both their energy performance and indoor air quality, particularly through the air permeability of dwellings and the air change rate. Methods currently exist for characterizing and assessing these factors using in situ measurements. However, these methods are often time-consuming, and there are constraints on their widespread use during housing renovations. The most commonly used methods to characterize building air permeability and natural airflow rate are the blower door and tracer gas, respectively. Recently, alternative methods such as the Pulse method have been developed and is authorized in regulatory context in the UK. This paper aims to investigate the existing measurement methods and devices for in-situ diagnostic of air transfers (air permeability of the envelope and air change rate) in existing French and UK dwellings. In this paper, we first describe the current context regarding ventilation in existing dwellings in France and the UK. Then, we present the different tools we are studying for the development of a new protocol adapted to these dwellings, and the first results of comparison between the three tools we have used in laboratory conditions and in an office building.

### 1.1 French context

Since the late 60s, France has seen a huge growth in the energy efficiency of the new residential buildings after implementing successive thermal regulations. In the meantime, with the coming into force of the ventilation regulations, with the decree of 1969 (JO 1969) and then the decree of 1982 (JO 1982), the use of controlled mechanical ventilation systems has become mandatory in housing and has led to a progressive abandonment of natural ventilation (Moujalled et al. 2022). On January 2022, France had replaced the last thermal regulation, RT2012, with the new energy and environmental regulation for all new construction RE2020, which is more ambitious and more demanding for the construction sector. This regulatory framework has been made in order to ensure good indoor air quality by allowing occupants to have reliable and efficient mechanical ventilation systems, with the introduction of the mandatory inspection of the ventilation systems for dwellings. Nevertheless, all these regulations only apply for new buildings.

In French old dwellings, air change rate is most of the time ensured by the leaks located on the envelope, with sometimes also natural ventilation and rarely mechanical ventilation. Yet, when

it comes to energy renovation that often leads to more airtight buildings, ventilation rates and air permeability levels are always neglected, which raises many questions about indoor air quality levels post the renovation process. This is why we are studying the use of existing diagnostic tools dedicated to airflow measurements in order to propose a method to evaluate the need for new mechanical ventilation systems in these dwellings that are being retrofitted. Since 1982, all new dwellings have to comply with the same regulation regarding ventilation. This regulation requires that the air must be able to circulate freely from the air inlets located in the main rooms, all the way to the air outlets in the service rooms, at least in kitchens, bathrooms or showers and toilets, made by vertical ducts or natural exhaust with natural draft or mechanical devices. The airflow rate extracted by the ventilation system in each room depends on the number of the main rooms in dwellings. These exhaust airflow are defined in Table 1 (JO 1982).

Table 1: Airflow rates to be extracted which can be achieved simultaneously or not (JO 1982)

Number of main rooms	Minimum Exhaust Airflow rate (m <sup>3</sup> /h)						
	Global minimum	Kitchen (basic)	Kitchen (peak)	Bathroom with or without toilet	Other bathrooms	Toilet	
						First one	Others
1	35	20	75	15	15	15	15
2	60	30	90	15	15	15	15
3	75	45	105	30	15	15	15
4	90	45	120	30	15	30	15
5	105	45	135	30	15	30	15
6	120	45	135	30	15	30	15
7	135	45	135	30	15	30	15

## 1.2 British context

In England, properties are required to comply with the Part F Regulation (UK Government 2022), which guides ventilation within buildings. The minimum whole dwelling ventilation rates in the habitable rooms should respect the values presented in Table 2.

Table 2: Minimum whole dwelling ventilation rates determined by the number of bedrooms

Number of bedrooms	Minimum ventilation rate by number of bedrooms (m <sup>3</sup> /h)
1	68.4
2	90
3	111.6
4	133.2
5	154.8

Exhaust outlets should be located properly, in places where the re-entry of exhaust air into the building, or into nearby ones would be minimized. For each additional bedroom, 6l/s must be added to the values of the table 2 (UK Government 2022).

In contrast to France, when a building is being assessed for retrofit, property owners in England are provided with a guide (IAA 2021), to help them determine whether their existing ventilation is adequate, if it requires modest intervention or more advanced and extensive ventilation work. The guide includes a methodology to identify the need to improve the ventilation strategy in case of renovation (Figure 1). This methodology includes air permeability measurements.

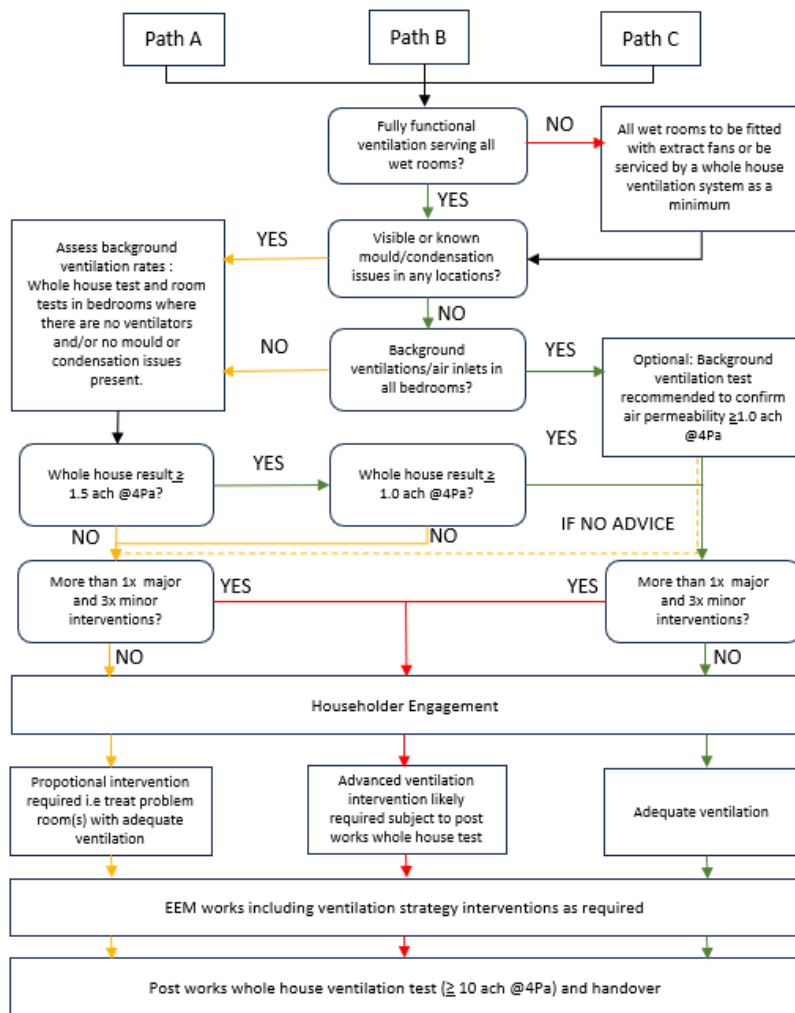


Figure 1: Ventilation assessment matrix (IAA 2021)

## 2 MEASUREMENT METHODS

We investigate in this paper the use of existing measurement methods and devices for in-situ diagnostic of air transfers (air permeability of the envelope and air change rate) in order to develop a new protocol adapted to existing dwellings before retrofitting. Thus, we present in this section the methods and tools we have considered.

### 2.1 Measurement of envelope airtightness

Building airtightness is mostly characterized by two indicators; air permeability, which is described as the amount of air per hour per square meter that moves through the building's envelope, and air changes per hour (ACH) which is how many times per hour the volume of air is replaced within a building.

The fan pressurization test is the most commonly used method to measure air permeability; by creating a range of high-pressure differences (10-100 Pa) between the inside and the outside of the building and the corresponding airflow through the measurement device is simultaneously determined. The main shortcoming of this method is how it is affected by outdoor conditions, ISO 9972 (ISO 2015) claims that the overall uncertainty for tests in accordance with this standard can be calculated and is estimated to be under 10% for calm conditions and to reach 20% in windy conditions. An additional source of uncertainties is the extrapolation of air

permeability to 4 Pa; which is a more suitable pressure for infiltration under normal operating conditions.

Alternatively, the novel Pulse method is attracting considerable interest due to the testing that is being conducted under low pressure levels. By rapidly releasing bursts of air (pulses) into the tested building, thereby creating an instant pressure rise that quickly reaches “quasi-steady” condition, Pulse determines the building air leakage in the range of 1-10 Pa and reports it at 4 Pa without extrapolation (Hsu 2021). Another strength of Pulse lies in how quick it is, which drives the uncertainties generated by the wind to become less significant.

## 2.2 Measurement of natural airflow rate

When characterizing natural airflow rate, tracer gas is widely used and it is considered to be the most reliable method that allows testing in natural conditions. In this context, the tracer gas method will be used as a reference when using both the Blower door and Pulse to determine whether the ventilation rates are sufficient in buildings with natural ventilation systems post energy renovation or not.

Tracer gas methods that derive benefit from metabolic CO<sub>2</sub> are generating considerable interest, since they do not require any gas injection, and are consequently less expensive and less harmful to the environment. The decay method consists of using the observed decays of metabolic CO<sub>2</sub> concentration, when the occupants leave the building, and using it as an indicator of indoor air quality within the tested area. In order to use this method effectively, we focused on the maximum recorded CO<sub>2</sub> concentration at 6pm, so that we can have the most important decay, which in our case corresponds to 26/03/2024.

In order to determine the air change rate with this approach, two methods were used. The first method can be modeled by the equation 1 (Asadi, Costa, and Gameiro da Silva 2011).

$$C(t) - C_{\text{equi}} = (C_0 - C_{\text{equi}}) * e^{-\lambda t} \quad (1)$$

where:

- C(t) is the concentration of the pollutant at time t [ppm];
- C<sub>equi</sub> is the asymptotic value of the concentration when equilibrium is reached [ppm];
- C<sub>0</sub> is the initial concentration value [ppm];
- λ is the infiltration rate of the indoor compartment [vol.h-1].

The second method uses multiple points, making the results more accurate (Remion 2020)

$$N_n = \frac{\sum t_i * \sum \ln(C_i - C_{\text{ext}}) - n * \sum t_i * \ln(C_i - C_{\text{ext}})}{n * \sum t_i^2 - (\sum t_i)^2} \quad (2)$$

- N is the ventilation rate [vol.h-1];
- C<sub>i</sub> is the concentration at t<sub>i</sub> [ppm];
- C<sub>ext</sub> is the external concentration [ppm];
- t<sub>i</sub> is the time [h].

In Table 3, we give a first evaluation of advantages and disadvantages for the different methods we consider.

Table 3: First comparison of different considered methods

	Blower door	Pulse	Metabolic CO <sub>2</sub> decay	Injected CO <sub>2</sub> decay
Time of installation	+++	+	+	++
Time of measurement	++	+	++++	+++
Possible with occupancy	Yes	Yes	Yes	Not in all rooms

Direct result of air change rate	No	No	Yes	Yes
Accuracy	?	?	+	+++

### 3 METHOD

#### 3.1 Tests in laboratory

It is of interest to investigate the ability of Pulse to generate similar results for multiple tests, especially when it comes to how accurate this measuring device can be when it is used to test naturally ventilated buildings. With a total surface area of 37.2 m<sup>2</sup> and a volume of 14.5 m<sup>3</sup>, a sheltered chamber at Build test solutions (Pulse supplier) was tested using Pulse with 3 different leakage profiles and n exponents (Figure 2):

- Moderately airtight dwelling (Configuration 1);
- Average building (Configuration 2);
- Leaky building (Configuration 3).

When testing the chamber, two types of Pulse were used; the default production Pulse MK2 (Figure 3) and another version of Pulse; MK3 (Figure 4) which is not yet commercialized.

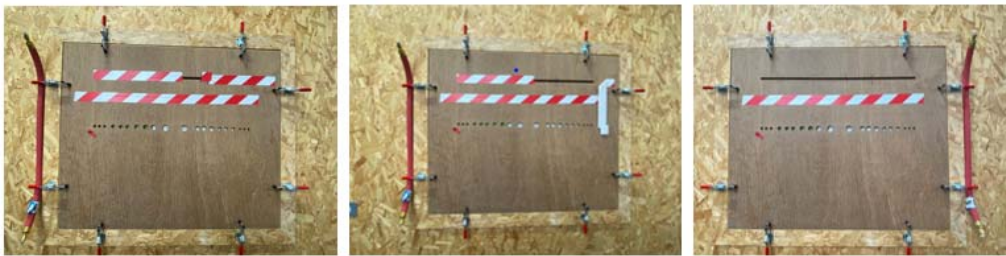


Figure 2: Configuration 1, 2 and 3



Figure 3 : Default Production pulse (MK2)



Figure 4 : Pulse MK2 controller, MK3 Air receiver

5 combinations of parameters for each device have been tested, including different durations of valve opening, different pressure inside the tank and different number of steps (Table 4).

Table 4: Parameters combinations for Pulse tests in laboratory

	Default Production pulse (MK2)			Pulse MK2 controller, MK3 Air receiver		
	Valve opening duration (s)	Number of steps	Tank pressure (bar)	Valve opening duration (s)	Number of steps	Tank pressure (bar)
C1	1.5	2	1	1.5	1	0.5



	1.5	1	0.5	1.5	2	0.8
	1.5	3	1, 1.5	1.5	3	0.8
	3	1	0.8	3	1	0.8
	3	2	1	3	2	1.5
C2	1.5	2	2	1.5	1	0.6
	1.5	3	0.8	1.5	2	2
	1.5	1	0.6	1.5	3	0.8
	3	1	0.9	3	1	0.9
	3	2	1	3	2	1
C3	1.5			1.5	1	1.4
	3			1.5	2	3, 2.5
				1.5	3	3.5
				3	1	1.7
				3	2	3.5

The same chamber at BTS was tested using the blower door with the same 3 configurations. During our Blower door tests, one of the challenges that we faced was the door frame from the blower door not getting adjusted to the actual door frame of the test chamber. The gaps were sealed with tape, but even after that, it was obvious that many openings were left uncovered.

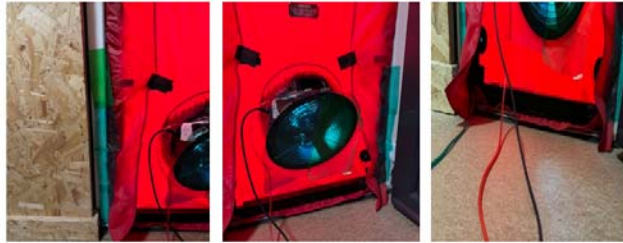


Figure 5: Sealed gaps while using the blower door

### 3.2 Tests in office space

To get a better understanding of how occupants metabolic CO<sub>2</sub> is used as a tracer gas, the office area at Build test solutions was tested and both infiltration rate and air change rate were determined using both Pulse, and the decay method. Figure 5 shows the tested area, our focus is only on places that are mostly occupied, i.e. the office/kitchen area. Regarding the decay method, the used CO<sub>2</sub> data collected from the CO<sub>2</sub> sensors covered the period from 7:30pm to 4:30am on the 26<sup>th</sup> of March 2024. 3 Pulse tests were conducted, with the fan of the ventilation system on, covered, and then off.



Figure 5: Office/kitchen area at BTS

## 4 RESULTS

### 4.1 Laboratory results

Figure 6, Figure 7 and Figure 8 present the results for the different combinations of parameters for each of the three configurations of the laboratory with Pulse. First, we consider the distribution of the values we have measured. For all three configurations, the median and mean values of Air Permeability at 4 Pa given by Pulse are quite similar, the distribution can thus be

considered symmetric. When the mean values of the standard deviation of each test type are compared, it is clear how the results given by the MK2 and the ones given by the MK3 do not differ much, the MK2 mean standard deviation value only exceeds the MK3 one by approximately 5.5%.

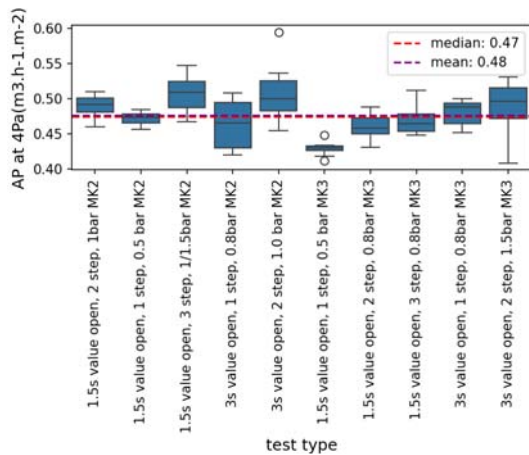


Figure 6: Air permeability at 4Pa using Pulse (Configuration 1)

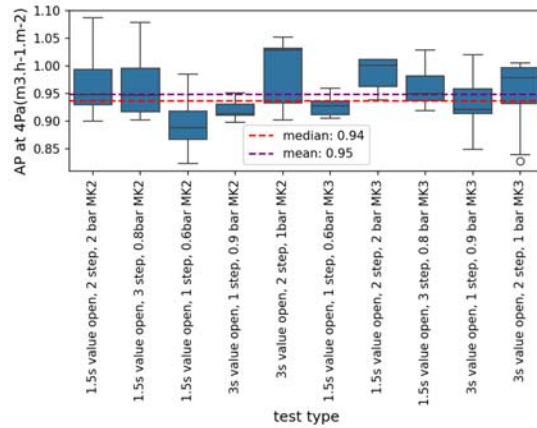


Figure 7: Air permeability at 4Pa using Pulse (Configuration 2)

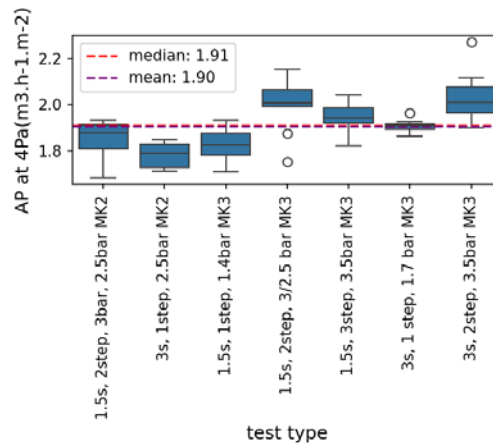


Figure 8: Air permeability at 4Pa using Pulse (Configuration 3)

Then we compared these results with the ones we have obtained with the blower door tests: Table 3 compares the results of air permeability at 4 Pa using the blower door and Pulse. The air permeability appears to be higher when measured by the Blower door. The contrast between our results can be explained by the gaps we failed to completely seal, and the windy conditions that day.

Table 3: Values of Air permeability at 4Pa using the Blower door and Pulse for the 3 configurations

Test type	Air permeability at 4Pa (m3/h/m2)		
	Config 1	Config 2	Config 3
Blower door (Pressurization)	0.87	1.82	2.52
Blower door (Depressurization)	1	1.50	2.84
Pulse test	0.48	0.95	1.90

## 4.2 Office space results

Figure 9 shows the result of the application of the CO<sub>2</sub> decay method to evaluate the infiltration rate in the office space. In the office/kitchen area we get 3.22 air changes per day which makes it 0.13 air changes per hour when applying the 2 points decay method. The same result was obtained when using the multi-points method.

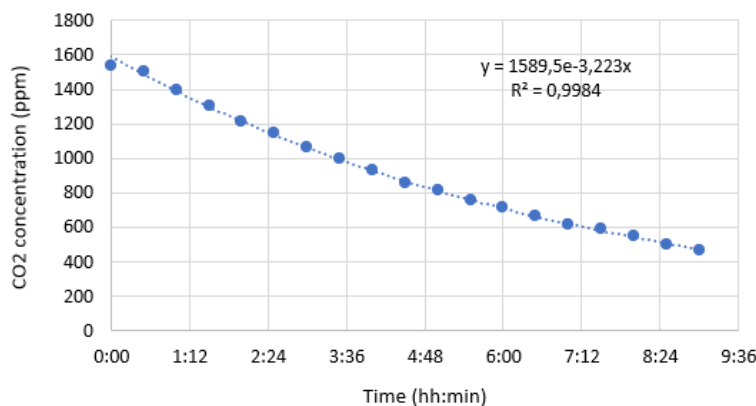


Figure 9: Infiltration rate using the 2 points method

In the UK, for high pressure airtightness testing at 50Pa, the divide by 20 rule is applied to get the infiltration rate by directly dividing the air permeability by 20. The proposed value for N if the ratio uses low-pressure airtightness measurements (4 Pa) is 7.9, The standard error is approximately  $\pm 0.5$  (Vega Pasos 2020).

Tests using Pulse were conducted in the office space, with the mechanical ventilation system on (Fan On), with it off (Fan Off) and with the ventilation duct covered (Fan covered).

The results of air permeability given by Pulse were divided by 7.9 to get the infiltration-air leakage rate (Table 4).

Table 4: Evaluation of infiltration-air leakage rate with Pulse and the CO<sub>2</sub> decay method

	AP @4Pa	Infiltration rate or air change rate (/h)
Pulse Fan On	1.83	0.23
Pulse Fan covered	1.74	0.22
Pulse Fan Off	1.81	0.23
Decay 2 points	-	0.13
Decay multipoints	-	0.13

As expected, the highest value of air permeability given by Pulse is the one with the fan on, followed by the one given when the fan was off, and then the one when the fan was covered. Although our results differ slightly, it is worth noting that the divide by 7.9 rule is not yet widely used. Therefore, in the upcoming study, we will also be investigating its accuracy. Another limitation of this study is that the tested building is not a typical domestic building, with no controlled CO<sub>2</sub> conditions (only metabolic CO<sub>2</sub> with a starting concentration level around 1600ppm with a drop of 1000ppm, in addition to only 2 CO<sub>2</sub> sensors being used).

## 5 CONCLUSION AND PERSPECTIVES

In this paper, we presented the very first result of our investigation of existing measurement methods and devices for in-situ diagnostic of air transfers (air permeability of the envelope and air change rate) in order to develop a new protocol to evaluate the airflow through natural ventilation system in existing dwellings. We presented two approaches: one included tests in a laboratory and one in an office space. From laboratory results and office space tests, we have seen significant differences between the results from the methods we have tested. Thus, we identified the need to complete the study with new tests in order to better define the link between Blower door results, Pulse results and CO<sub>2</sub> decay method results.

A follow-up study will be carried out in 3 old dwellings with natural ventilation systems, in the city of Lyon, France. Our main target will be to verify if the ventilation ensured by the natural ventilation ducts is enough after the building's renovation or not, using the fan pressurization method, Pulse and tracer gas. Airflow measurements will be conducted with the ducts sealed in order to determine the airflow that is passing through the leaks on the envelope and then with the ducts uncovered, which will enable us to get the airflow rate through the natural ventilation ducts and determine how effective they are. Other laboratory tests will be performed in a new facility near Lyon, with a perfectly known envelope airtightness and different openings that have been perfectly characterized.

## 6 REFERENCES

- Asadi, Ehsan, J. J. Costa, and Manuel Gameiro da Silva. 2011. "Indoor Air Quality Audit Implementation in a Hotel Building in Portugal." *Building and Environment* 46 (8): 1617–23. <https://doi.org/10.1016/j.buildenv.2011.01.027>.
- Cooper, Edward, Xiaofeng Zheng, Christopher Wood, Mark Gillot, David Tetlow, Saffa Riffat, and Lia De Simon. 2016. "Field Trialling of a Pulse Airtightness Tester in a Range of UK Homes." *International Journal of Ventilation* 18 (1): 1–18. <https://doi.org/10.1080/14733315.2016.1252155>.
- Hsu, Yun-Sheng. 2021. "The Impact of Wind on the Building Airtightness Measurement Using the Pulse Technique." Thesis, University of Nottingham.
- IAA. 2021. "Best Practice Guide - Background Ventilation Assessment of Existing Buildings." Insulation Assurance Authority.
- ISO. 2015. "EN ISO 9972: Thermal Performance of Buildings - Determination of Air Permeability of Buildings - Fan Pressurization Method." ISO.
- JO. 1969. "Arrêté Du 22 Octobre 1969 Relatif à l'aération Des Logements."
- . 1982. "Arrêté du 24 mars 1982 consolidée relatif à l'aération des logements : aération générale ou permanente."
- Moujalled, Bassam, Adeline Mélois, Valérie Leprince, and Gaëlle Guyot. 2022. "French Building Airtightness Database after 10 Years of Operation: Statistical Analyses of about 500,000 Measurements." In . Rotterdam, The Netherlands.
- Remion, Gabriel. 2020. "Mesure in Situ Des Performances Aérauliques d'un Système de Ventilation Naturelle Par Conduit." Thèse de Doctorat, Vaulx-en-Velin, France: Université de Lyon.
- UK Government. 2022. "Ventilation: Approved Document F."
- Vega Pasos, Alan Emmanuel. 2020. "Air Infiltration Modelling Based on Low-Pressure Airtightness Measurements." Thesis, University of Nottingham.

# Evaluation of Indoor Environmental Quality and Thermal Environment in Airtight Energy-Efficient Naturally Ventilated Dwellings

Ibrahim Alhindawi<sup>\*1</sup>, James McGrath<sup>2</sup>, Divyanshu Sood<sup>3</sup>, James O'Donnell<sup>3</sup>,  
and Miriam Byrne<sup>1</sup>

*1 Physics Unit, School of Natural Sciences and the Ryan Institute's Centre for Climate and Air Pollution Studies, University of Galway, Galway, Ireland*

*3 School of Mechanical & Materials Engineering and UCD Energy Institute, University College Dublin, Dublin, Ireland*

*\*Corresponding author:*

*i.alhindawi1@universityofgalway.ie*

*2 Department of Physics, Maynooth University, Maynooth, County Kildare, Ireland*

## SUMMARY

Noticeably higher concentrations of gaseous pollutants were measured in bedrooms than living rooms, and in winter than summer, where p-values were found to be of a stringent significance (average  $p = 0.008$ ).  $PM_{2.5}$  concentrations were found to be exceeding the WHO 24-h average threshold of  $15 \mu\text{g}/\text{m}^3$  in kitchens for the week-long monitoring time (92% in winter, 51% in summer). High percentages of carbon dioxide concentrations exceeded the WHO guideline in bedrooms during the winter week (mean: 1251 ppm) and summer week (mean: 1028 ppm), with lower percentages in living rooms in comparison (mean in winter: 893 ppm, mean in summer: 735 ppm). TVOC week-long mean values across the bedrooms was 463 ppb in winter and 293 ppb in summer. Temperature and humidity were within limits in general. Air change rate mean values ranged from 0.08 to  $0.37 \text{ h}^{-1}$  in summer, and from 0.09 to  $0.27 \text{ h}^{-1}$  in winter, across the monitored bedrooms.

## INTRODUCTION

Enhancing building energy efficiency is a global priority that necessitates reducing carbon emissions from the building sector. Since approximately 60-80% of primary energy use is used on space and water heating (SEAI, 2022), energy performance improvements are often achieved by enhancing the thermal and insulation properties of a building to minimise heat loss. However, these strategies may inadvertently lead to a higher risk of overheating, necessitating active cooling systems during warmer months, and thereby increasing energy usage (International Energy Agency (IEA), 2015). In contrast, natural ventilation presents distinct advantages during summer by providing passive cooling opportunities (Schulze & Eicker, 2013), thereby reducing reliance on mechanically driven cooling systems and promoting energy conservation.

Despite the recognised benefits in energy performance associated with increased airtightness, there is a knowledge gap surrounding the ability of natural ventilation to maintain adequate ventilation rates across different seasons. This may result in the accumulation of indoor air pollutants and moisture beyond recommended levels, a concern only further amplified by the impacts of climate change, thereby posing risks to occupants' health and comfort. This study addresses this knowledge gap by evaluating indoor environmental quality and thermal comfort across nine airtight, energy-efficient naturally-ventilated dwellings in both summer and winter periods.

## KEYWORDS

Natural ventilation; Airtightness; Energy Efficiency; IEQ; Sensors

## METHODS

The house selection criteria focused on a cohort of semi-detached dwellings ( $n = 9$ ), which represent 40.7% of the total naturally-ventilated energy-efficient houses in Ireland, with an 'A' Building Energy Rating (BER), denoting a maximum primary energy consumption of up to  $75 \text{ kWh}/\text{m}^2$  per year, indicative of highly insulated airtight

structures; air permeability of 3 to 5 m<sup>3</sup>/h.m<sup>2</sup> (*Part F: Technical Guidance Document F-Ventilation*, 2019). For a week-long monitoring period, the SidePak AM520 (TSI, Minnesota, USA) was used to measure PM<sub>2.5</sub> at 1-min interval, while the and the GrayWolf DirectSense II (GrayWolf Sensing Solutions, Ireland) was used to collect measurements of carbon dioxide (CO<sub>2</sub>), total volatile organic compounds (TVOC), nitrogen dioxide (NO<sub>2</sub>), and carbon monoxide (CO), alongside complementary measurements of temperature and relative humidity levels at 5-min interval. All parameters were analysed based on standardised guidelines. The instrumentations were placed in the main rooms of each house; bedroom, living room, kitchen, collecting over 435,000 datapoints across the monitored houses. Measurements of PM<sub>2.5</sub> were not taken in the bedrooms due to the absence of direct sources and the low tolerance of occupants for active pumps noise. Apart from PM<sub>2.5</sub>, the parameters of CO<sub>2</sub>, Temp, and RH were not measured in the kitchen due to the high variation caused by the cooking activities affecting the levels of these parameters, as the study focuses on the rooms of higher and more consistent occupancy rates.

## RESULTS

Generally, the results in Table 1 show higher levels of the monitored parameters in the bedrooms and kitchens than the living rooms. CO<sub>2</sub> concentrations in the bedrooms were higher in the than the living rooms during occupancy times, due to the sleeping time CO<sub>2</sub> accumulation through longer times of occupancy. Same applied to TVOC concentrations, while there are more sources of TVOC in the bedrooms than the living rooms, as the occupants reported. Moreover, the PM<sub>2.5</sub> concentrations in the kitchens were observed to be consistently higher than the living rooms, while the direct sources of particles were present in the kitchens.

Table 1 – Data Analysis Summary of the Monitored Parameters – Winter and Summer

Parameter	Bedrooms (Kitchen for PM <sub>2.5</sub> )-Winter		Living Rooms-Winter	
	Mean (s.d. *)	Median (25th %ile, 75th %ile)	Mean (s.d.)	Median (25th %ile, 75th %ile)
PM <sub>2.5</sub> (µg/m <sup>3</sup> )	88 (137)	46 (29, 96)	72 (158)	25 (9, 70)
CO <sub>2</sub> (ppm)	1251 (538)	1079 (800, 1620)	839 (260)	782 (658, 961)
TVOC (ppb)	463 (279)	378 (296, 540)	348 (212)	296 (209, 418)
NO <sub>2</sub> (µg/m <sup>3</sup> )	32 (16)	32 (14, 43)	54 (4.2)	56 (50, 58)
CO (mg/m <sup>3</sup> )	1.4 (0.7)	1.4 (0.7, 1.9)	1.3 (1.6)	1.0 (0.4, 1.6)
Temp (°C)	20.0 (0.97)	19.99 (19.39, 20.65)	19.7 (1.04)	19.7 (19.0, 20.5)
RH (%)	55.3 (5)	55.1 (52, 58)	51.6 (3)	51.4 (48, 53)

Parameter	Bedrooms (Kitchens for PM <sub>2.5</sub> )-Summer		Living Rooms-Summer	
	Mean (s.d.)	Median (25th %ile, 75th %ile)	Mean (s.d.)	Median (25th %ile, 75th %ile)
PM <sub>2.5</sub> (µg/m <sup>3</sup> )	21 (95)	10 (6, 17)	18 (36)	10 (4, 17)
CO <sub>2</sub> (ppm)	1028 (535)	791 (608, 1436)	735 (175)	701 (605, 823)
TVOC (ppb)	293 (152)	280 (226, 330)	208 (69)	194 (162, 252)
NO <sub>2</sub> (µg/m <sup>3</sup> )	33 (36)	12 (1.9, 80)	101 (53)	106 (44, 138)
CO (mg/m <sup>3</sup> )	0.7 (0.4)	0.6 (0.4, 0.9)	0.8 (0.3)	0.9 (0.6, 1.0)
Temp (°C)	23.6 (0.8)	23.6 (23.2, 24.1)	23.0 (0.7)	22.9 (22.5, 23.5)
RH (%)	60.2 (3.2)	60.1 (58.2, 62.1)	58.4 (2.9)	58.2 (56.7, 60.2)

## CONCLUSIONS

The natural ventilation's design and operation was concluded to be inefficient to maintain the CO<sub>2</sub> concentrations within acceptable levels during the occupancy time in the bedrooms, and at some points in the living rooms over the monitoring period. Improved ventilation strategies in the bedrooms may participate in bridging the gap between the emission rates of CO<sub>2</sub> and the dilution rates of the existing purpose-provided natural ventilation elements. The design of the monitored energy-efficient dwellings aimed to supply sufficient airflow rates in order to maintain acceptable IEQ levels, nevertheless, this research identified a performance gap between the design aims and the operational performance regarding the effectiveness of natural ventilation.

## ACKNOWLEDGEMENTS

The ALIVE project (19/RDD/537) is funded by the Government of Ireland through the Sustainable Energy Authority of Ireland's Research, Development and Demonstration Funding Programme 2019.

## REFERENCES

- International Energy Agency (IEA). (2015). *Capturing the Multiple Benefits of Energy Efficiency*. <https://www.iea.org/reports/capturing-the-multiple-benefits-of-energy-efficiency>
- Part F: Technical Guidance Document F-Ventilation*. (2019). Dublin, Ireland: Minister for Housing, Planning and Local Government under article 7 of the Building Regulations 1997
- Schulze, T., & Eicker, U. (2013). Controlled natural ventilation for energy efficient buildings. *Energy and Buildings*, 56, 221–232. <https://doi.org/10.1016/j.enbuild.2012.07.044>
- SEAI. (2022). *National Heat Study: Heating and Cooling in Ireland Today*.

# A Longitudinal Study to Assess Indoor Environmental Quality in Airtight Energy-Efficient Naturally Ventilated Dwellings

Ibrahim Alhindawi<sup>\*1</sup>, James McGrath<sup>2</sup>, Divyanshu Sood<sup>3</sup>, James O'Donnell<sup>3</sup>,  
and Miriam Byrne<sup>1</sup>

*1 Physics Unit, School of Natural Sciences and the Ryan Institute's Centre for Climate and Air Pollution Studies, University of Galway, Galway, Ireland*

*2 Department of Physics, Maynooth University, Maynooth, County Kildare, Ireland*

*\*Corresponding author:  
i.alhindawi1@universityofgalway.ie*

*3 School of Mechanical & Materials Engineering and UCD Energy Institute, University College Dublin, Dublin, Ireland*

## SUMMARY

The global demand to improve the energy performance of buildings has led to greater air tightness and uncertainty in the ability of natural ventilation to maintain adequate indoor environmental quality. A monitoring campaign was carried out to evaluate the long-term indoor environmental quality across a year-long period in energy-efficient Irish dwellings. During the winter months (December, January, February), the mean PM<sub>2.5</sub> concentration in kitchens was 19 µg/m<sup>3</sup>, which is 38% higher compared to the summer months (June, July, August), where the mean concentration was 13 µg/m<sup>3</sup>. The mean PM<sub>2.5</sub> increased 58% in winter (19 µg/m<sup>3</sup>) than in summer (12 µg/m<sup>3</sup>). In bedrooms, the mean CO<sub>2</sub> concentration during winter was 1116 ppm, reflecting a 19% increase over the summer concentration of 919 ppm. In the living room, CO<sub>2</sub> increased 29% in winter from summer. Additionally, radon levels in the dwellings were 52% higher in winter than in summer; however, they remained well below the Irish EPA threshold of 200 Bq/m<sup>3</sup>. VOC mean values in winter and summer showed similar ranges across the monitored dwellings, referring to the greater impact of occupancy activities than ventilation.

## KEYWORDS

Natural ventilation; Airtightness; Energy Efficiency; IEQ; Sensors

## INTRODUCTION

While it is globally imperative to conserve energy in buildings and reduce greenhouse gas emissions from the building sector. Poor application of some energy-efficient measures, such as increased airtightness, may induce elevated levels of indoor air pollutants and thermal parameters; this may lead to non-compliant levels of indoor environmental quality (International Energy Agency (IEA), 2015). While ventilation is the main mechanism to dilute pollutants and provide the required air change rates, it does not always operate optimally, and natural ventilation, in particular, is dependent on multiple factors. Although natural ventilation may save energy and provide higher air change rates (Schulze & Eicker, 2013), the main drawback is lower ventilation rates and compromise thermal comfort in winter. While it is challenging to conduct long-term indoor environmental quality monitoring using high-grade instruments, low-cost sensors, with the capability for remotely-transmitting information for several parameters, allow a unique opportunity to gather large-scale monitoring data without the traditional constraints (Omidvarborna et al., 2021). This research aims to evaluate indoor environmental quality in semi-detached energy-efficient dwellings for a full year, by deploying remotely-operated low-cost sensors in the main rooms of each dwelling.

## METHODS



The criteria for house selection concentrated on a group of nine semi-detached naturally-ventilated, energy-efficient houses in Ireland with an 'A' Building Energy Rating (BER). This rating signifies a maximum primary energy consumption of up to 75 kWh/m<sup>2</sup> per year, reflecting highly insulated, airtight structures with an air permeability of 3 to 5 m<sup>3</sup>/h.m<sup>2</sup> (*Technical Guidance Document F-Ventilation*, 2019). Consumer-grade sensors (Space Pro, Space Plus-Airthings, Oslo, Norway, and Foobot SAT-Airboxlab SA, Luxembourg) were used to map the year-long trends for particulate matter (PM<sub>2.5</sub>, PM<sub>1</sub>), carbon dioxide (CO<sub>2</sub>), total volatile organic compounds (TVOC), temperature (temp), relative humidity (RH), and radon (Rn). These devices are installed in the living room, kitchen, and bedroom within each dwelling. Over 20 million datapoints were collected at a 5-min interval for the monitored parameters.

## RESULTS

The results in Table 1 show a selection of the data summary for the measurements across the monitored dwellings. In general, the rooms with indoor-generated emission sources showed higher mean values of air pollution concentration across the year. The annual average CO<sub>2</sub> concentrations were higher in the bedrooms than in the living rooms and kitchens, surpassing the World Health Organisation (WHO) guidelines. However, the mean PM concentrations were within similar ranges in all the rooms, surpassing the annual WHO guideline level of 5 µg/m<sup>3</sup>. The mean TVOC concentrations were observed to be surpassing 130 ppb ("I.S. EN 16798-1," 2019) in all the monitored rooms. The mean values for temp and RH were within the recommended levels of WHO. The mean PM<sub>2.5</sub> winter concentration (19 µg/m<sup>3</sup>) was 38% higher than in the summer period (13 µg/m<sup>3</sup>) across the kitchens. The mean CO<sub>2</sub> winter concentration (1116 ppm) was 19% higher than the summer concentration (919 ppm) across the bedrooms. Radon was observed to be 52% higher in winter than summer yet, it was well below 200 Bq/m<sup>3</sup> (Irish EPA threshold) across the dwellings.

Figure 1, illustrates the long-term variations in one of the monitored dwellings' bedrooms, demonstrating the wider data distribution in the colder months than the warmer months. The latter observation suggests higher ventilation rates in summer than in winter, caused at least by a higher frequency of window opening in warmer months.

Table 1 – Annual Data Summary of the Monitored Parameters

Parameter	Mean	Median	Min	Max	25 <sup>th</sup> ile	50 <sup>th</sup> ile	75 <sup>th</sup> ile
<b>Bedrooms</b>							
PM <sub>2.5</sub>	14	7	1	783	3	7	15
PM <sub>1</sub>	13	7	1	422	3	7	14
CO <sub>2</sub>	1037	856	397	3879	585	856	1343
VOC	311	147	24	4715	68	147	385
Temp	21.81	21.77	16.42	27.62	20.80	21.77	22.77
RH	58.3	58.6	32.7	81.6	53.8	58.6	63.3
<b>Living Rooms</b>							
PM <sub>2.5</sub>	15	7	1	627	3	7	18
PM <sub>1</sub>	14	7	1	451	3	7	18
CO <sub>2</sub>	731	669	400	2723	542	669	850
VOC	210	132	42	3311	74	132	258
Temp	21.87	21.85	16.68	27.65	20.76	21.85	22.86
RH	54.2	54.3	30.4	77.3	49.3	54.3	59.2
<b>Kitchens</b>							
PM <sub>2.5</sub>	16	7	1	895	3	7	19
PM <sub>1</sub>	15	7	1	637	3	7	18
CO <sub>2</sub>	666	619	400	2350	519	619	762
VOC	201	133	34	3916	76	133	249
Temp	21.60	21.53	16.08	27.38	20.54	21.53	22.71
RH	56.0	56.1	31.0	84.8	51.2	56.1	60.9

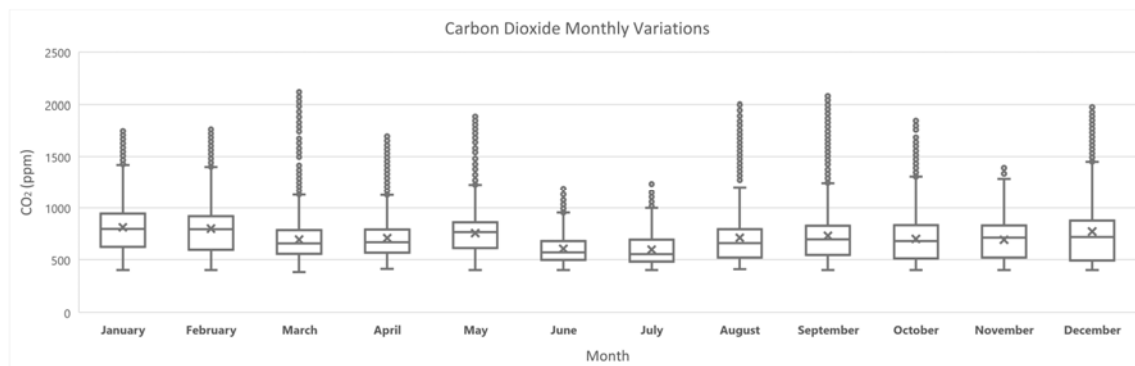


Figure 1: Monthly CO<sub>2</sub> Data Distribution

## CONCLUSIONS

This study seeks to assess the indoor environmental quality across a sample of energy-efficient dwellings over the course of an entire year, utilising remotely-operated, low-cost sensors placed in the primary rooms of each dwelling. The use of consumer-grade sensors showed practicality and resilience in terms of measurements and data collection of the long-term data. The longitudinal study provides a large-scale description of the data trends on an annual and a seasonal basis. The levels of the monitored parameters indicated the deficiency of natural ventilation, at least within the current operation strategy, in maintaining acceptable levels of indoor environmental quality. Additionally, seasonal variations suggest an adaptive ventilation strategy in the monitored airtight houses to maintain pace with the deviations of the impacting factors on indoor environmental quality.

## ACKNOWLEDGEMENTS

The ALIVE project (19/RDD/537) is funded by the Government of Ireland through the Sustainable Energy Authority of Ireland's Research, Development and Demonstration Funding Programme 2019.

## REFERENCES

- I.S. EN 16798-1. (2019). In *Method 2 - method using limit values of substance concentration*: The National Standards Authority of Ireland (NSAI).
- International Energy Agency (IEA). (2015). *Capturing the Multiple Benefits of Energy Efficiency*. <https://www.iea.org/reports/capturing-the-multiple-benefits-of-energy-efficiency>
- Omidvarborna, H., Kumar, P., Hayward, J., Gupta, M., & Sperandio Nascimento, E. G. (2021). Low-Cost Air Quality Sensing towards Smart Homes. *Atmosphere*, 12, 453. <https://doi.org/10.3390/atmos12040453>
- Schulze, T., & Eicker, U. (2013). Controlled natural ventilation for energy efficient buildings. *Energy and Buildings*, 56, 221–232. <https://doi.org/10.1016/j.enbuild.2012.07.044>
- Technical Guidance Document F-Ventilation*. (2019). Dublin, Ireland: Minister for Housing, Planning and Local Government under article 7 of the Building Regulations 1997

# Are Irish Low Energy School Designs Resilient Against Overheating?

Elahe Tavakoli\*, Adam O' Donovan, Paul D. O'Sullivan

*Department of Process, Energy and Transport Engineering, Munster Technological University (Cork Campus), Rossa Avenue, Bishopstown, Cork, Ireland*

*MaREI, the SFI Research Centre for Energy, Climate and Marine, Beaufort Building, Environmental Research Institute, Ringaskiddy, Cork, Ireland*

*\*Corresponding author: [elahe.tavakoli@mycit.ie](mailto:elahe.tavakoli@mycit.ie)*

## ABSTRACT

The challenges posed by climate change and related thermal discomfort in school classrooms are a worldwide challenge. Recent research indicates that numerous low energy school buildings do not comply with comfort criteria and suffer from overheating. This study aimed to determine when indoor air temperature conditions in classrooms were vulnerable to overheating risk. Secondly, quantify the contribution and correlation of outdoor air temperature and individual building features on the indoor air temperature in Irish low energy naturally ventilated schools.

To achieve these objectives, this research analysed 45 classrooms in five low energy naturally ventilated schools in Ireland. Advanced sensors were employed to gather precise and extensive air temperature readings across various classrooms and schoolyards. The investigation utilised an extensive database detailing the school buildings' features as well as indoor and outdoor air temperatures. The study applied advanced statistical methods to analyse and understand temperature dynamics in school buildings. A descriptive statistical analysis was used to uncover patterns and fluctuations in temperature within the school buildings. The analysis of variance for hypothesis testing was employed to reveal significant temperature differences between various school classrooms and levels. Cohen's d statistic was also used to quantify the effect sizes, providing insight into how specific building features impact indoor air temperatures.

The findings show that the classrooms are able to meet overheating thresholds in the present, so they scored high on their indoor thermal resilience under future climate scenarios. They have sufficient natural ventilation potential to ensure thermal building resilience in current weather conditions. The field study-based approach adopted in the study offered a useful method to evaluate indoor thermal resilience in the existing building when the opportunity to avoid vulnerability "lock-in" is greatest. This study also comprehensively explains the relationship between school building features and indoor air temperature. The analysis using Cohen's d effect sizes prioritised certain building features when designing or retrofitting school buildings to improve the thermal comfort performance of classrooms against overheating. This study recommends utilising natural ventilation, developing robustness and recoverability plans for passive cooling systems, and occupant performance in overheating situations.

## KEYWORDS

Resilient cooling, Schools, Natural ventilation, Low energy building, Overheating risk

## 1 INTRODUCTION

Most non-residential buildings in Ireland are educational, with primary schools making up the largest portion [1]. School buildings have some of the most demanding requirements for occupant comfort due to the large number of people spending a significant amount of time inside and the importance of students' learning performance [2]. As climate change progresses, rising temperatures may significantly impact the indoor thermal environment, especially during the non-heating and summer seasons [3][4]. This could increase the risk of overheating, particularly in newly constructed schools designed to meet Zero Energy Building (ZEB)

standards, which focus on optimising heating season performance through airtightness and insulation [5].

Climate change presents significant challenges worldwide, particularly in the educational sector, where extreme classroom temperatures can affect students' and staff's learning and well-being [6]. Recent research has indicated that many low energy school buildings, designed with sustainability in mind, fail to meet comfort criteria, particularly during extreme temperatures, leading to overheating and associated risks [7][8].

Overheating not only results from climatic conditions but also from factors intrinsic to school buildings, such as solar heat gains through large windows, high internal heat gains and inadequate ventilation [5][9], posing significant health risks, including heat-related mortality [10][11]. Compounding this issue is the physiological vulnerability of students, especially those under the age of 12, whose developing thermoregulatory systems make them more susceptible to heat [12]. Despite limited epidemiological studies specifically addressing heat mortality among students, there is a well-documented impact of overheating on cognitive functions and learning performance [12][7][13][14], highlighting the urgency of addressing thermal comfort in schools to safeguard the health and academic success of students in the face of escalating overheating.

In light of these considerations, this paper explores the thermal resilience of classrooms in five low energy, naturally ventilated (NV) schools in Ireland, investigating their ability to maintain comfortable indoor temperatures. The study collected detailed indoor and outdoor air temperature data and building information from 45 classrooms in the schools, using advanced sensors to provide a robust dataset of indoor and outdoor environmental conditions.

The research aims to accomplish two objectives:

- 1. To determine the specific conditions under which indoor temperatures in these classrooms are at risk of overheating.
- 2. To quantify how outdoor air temperature and specific building characteristics correlate with and influence indoor air temperatures, using descriptive statistics, ANOVA analysis, and the calculation of effect sizes using Cohen's d statistic.

This analysis aims to understand the effectiveness of current design features and the potential need for additional strategies to enhance thermal comfort.

## **2 METHODOLOGY**

This methodology section elaborates on the systematic process of creating a detailed database for studying five naturally ventilated, low energy schools across Ireland. The comprehensive database, depicted in Figure 1, from 45 different zones within these schools, integrates meticulous indoor and outdoor air temperature measurements and essential school building information. The process thoroughly analysed the varied building parameters and their respective impacts on indoor air temperatures.

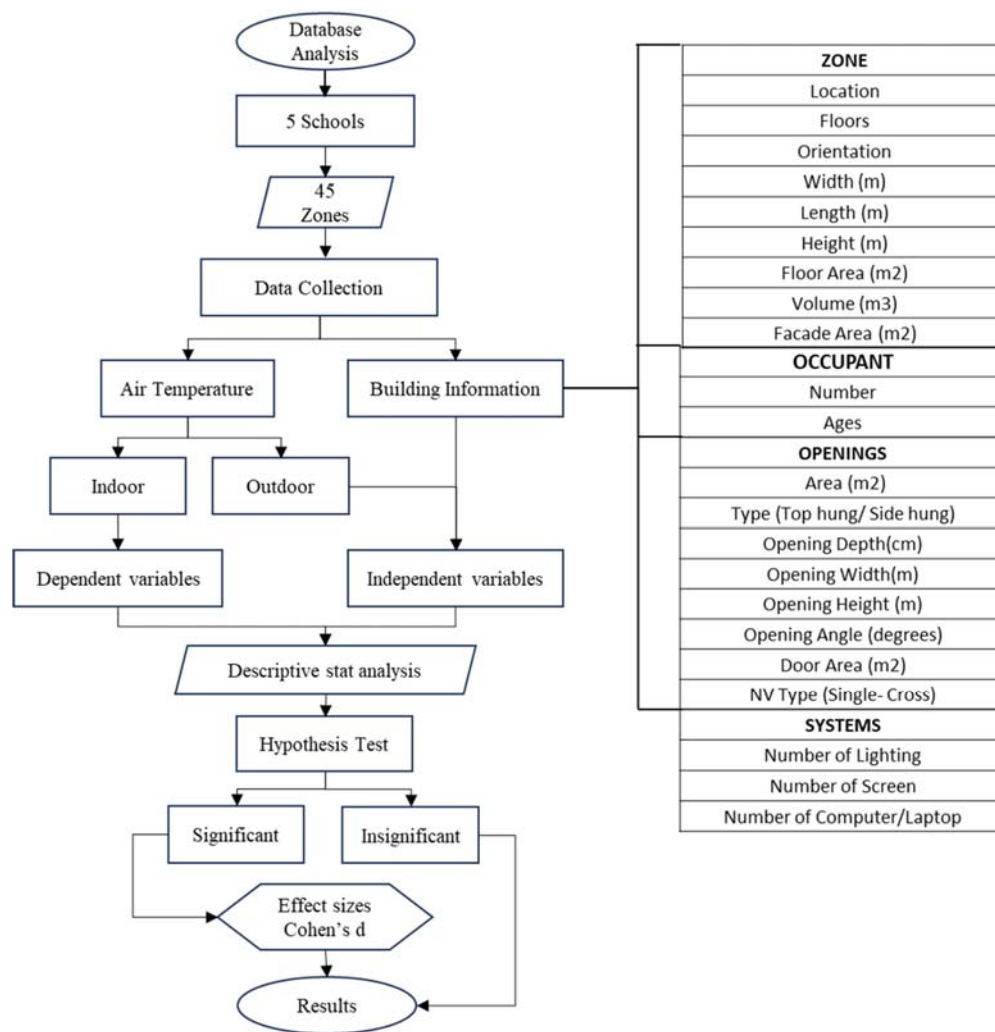


Figure 1: Methodology Process

## 2.1 Data Collection

A detailed and strategic data collection process was implemented using advanced sensor technology to comprehensively assess the thermal environment within the classrooms. The sensor types used and their specifications are presented in Table 1. These sensors were positioned within each classroom at the height of 1.5m, ensuring that data collection encompassed diverse environmental conditions across different parts of the schools.

Table 1: The sensors model and their specifications

Sensor Model	Temperature Accuracy	Humidity Accuracy	CO2 Accuracy	Ref
LASCAR EL-SIE	±0.3°C	±2% RH	N/A	[15]
TESTO 440	±0.3°C to ±0.4°C (NTC)	±(0.6% RH + 0.7 % of m.v.) (0 to 90% RH)	N/A	[16]
Airthings	±0.5°C at 25°C, ±1.0°C in 0-65°C range	±1.8% RH (10 to 90%RH @ +25°C)	Optimum accuracy of ±30ppm ±3% after initial calibration	[17]
LASCAR WIFI-TH	±0.2°C (0 to +60°C)	±1.8% RH (10 to 90%RH @ +25°C)	N/A	[18]

## 2.2 Data Analysis Techniques

The study uses several data analytic techniques to analyse indoor and outdoor air temperature trends and building specifications. The comprehensive descriptive statistical analysis was conducted to calculate key descriptive statistics, such as the number of observations (N), the mean temperature, standard deviation (SD), minimum and maximum temperatures, quartiles (Q1 and Q3), median temperature, and the interquartile range (IQR) for each classroom zone which helped in understanding the central tendencies and variability within the data.

Additionally, a comprehensive correlation and regression analysis was conducted to find the relationship between indoor and outdoor air temperatures. This method sought to determine how closely aligned the fluctuations in outdoor air temperatures are with those of indoor temperatures and provided critical insights into how indoor conditions might be predicted based on outdoor environmental changes. This statistical approach involved calculating the Pearson correlation coefficient, which quantifies the degree to which two variables are related linearly. It is calculated using the formula (1).

$$r = \frac{\sum(X_i - \bar{X})(Y_i - \bar{Y})}{\sqrt{\sum(X_i - \bar{X})^2 \sum(Y_i - \bar{Y})^2}} \quad (1)$$

Where  $X_i$  and  $Y_i$  are the individual sample points indexed with  $i$ ,  $\bar{X}$  and  $\bar{Y}$  are the means of the X and Y variables, respectively. This formula results in a value between -1 and 1. A value of 1 indicates a perfect positive linear relationship, -1 indicates a perfect negative linear relationship, and 0 indicates no linear relationship between the variables.

This study employed hypothesis testing, where the null hypothesis ( $H_0$ ) assumes no significant disparity in indoor air temperature across the various zones of the selected Irish schools. On the other hand, the alternative hypothesis ( $H_1$ ) proposes a significant difference in temperature readings between these distinct areas. To navigate through these hypotheses, an Analysis of Variance (ANOVA) was employed to compare the means of air temperatures across multiple classrooms, zones, and floor levels.

Lastly, the study utilised Cohen's d to determine the effect size and quantify the tangible magnitude of differences observed. This measure offers a quantitative interpretation of the magnitude of differences observed, shedding light on the practical significance that each building characteristic might have on the temperature dynamics. Cohen's d statistic is specifically calculated as the difference between two group means, normalised by the pooled standard deviation, with thresholds established for small (0.2), medium (0.5), and large (0.8) effects. Cohen's d statistic was meticulously computed for each parameter, reflecting how different building characteristics within classroom zones influence indoor air temperature. The formula (2) used is as follows:

$$d = \frac{M_1 - M_2}{SD_{pooled}} \quad (2)$$

Where  $M_1$  and  $M_2$  are the means of two groups, and  $SD_{pooled}$  is the pooled standard deviation, calculated as formula (3):

$$SD_{pooled} = \sqrt{\frac{(n_1 - 1)SD_1^2 + (n_2 - 1)SD_2^2}{n_1 + n_2 - 2}} \quad (3)$$

Where  $n_1$  and  $n_2$  are sample sizes of two groups.  $SD_1$  and  $SD_2$  are the standard variations of two groups.

This study assessed the vulnerability of classrooms, identifying and addressing risks based on overheating criteria in CIBSE TM52 [19] and BB101 [20] standards, refer to Table 2. Based on

adaptive thermal comfort descriptions used in the mentioned standards, as shown in formula (4), the indoor comfort temperatures are influenced by the outdoor running mean temperature.

$$T_c = 0.33 \times MAX(10, T_{rm}) + 18.8 \pm T_{lim} \quad (4)$$

Where  $T_c$  is comfort temperature,  $T_{rm}$  is running mean temperature and  $T_{lim}$  is category range limit of comfort. In this study  $T_{lim}$  is defined as a high level of expectation ( $\pm 2$ , Category I) recommended for young children [21][22].

Table 2: Overheating Assessment Criteria

Criteria	Name	Formula	CIBSE TM52 2013	BB101 2018
<b>Criterion 1</b>	Hours of Exceedance	$He = \sum_{i=1}^n (T_{int,i} - T_{comf})$ $T_{int,i} > T_{comf} + 1^\circ\text{C}$	$\leq 3\%$ of occupied hours	$\leq 40$ occupied hours
<b>Criterion 2</b>	Daily Weighted Exceedance	$We = \sum_{i=1}^{24} (T_{int,i} - T_{comf})$	$\leq 6$ occupied days	$\leq 6$ occupied days
<b>Criterion 3</b>	Upper Limit Temperature	$T_{upp} = T_{comf} + 4^\circ\text{C}$	$T_{int} \leq T_{upp}$	$T_{int} \leq T_{upp}$

$T_{int}$  : Indoor air temperature  
 $T_{comf}$  : Threshold comfort temperature  
 $T_{upp}$  : Upper limit temperature

### 3 RESULT

The descriptive statistical analysis conducted within this study has illuminated significant variances in the indoor air temperatures of the studied classrooms. The boxplots in Figure 2 illustrate the distribution of temperature readings inside classrooms and in the outdoor environments of GGA, CBS, BRC, GMC, and LIN schools. The comparison of boxplots showed that each school exhibits its own unique thermal characteristics, both indoors and outdoors, with specific trends. The indoor median temperatures across the classrooms in all schools are consistent, suggesting a stable thermal environment likely maintained by the schools' heating and NV systems. However, BRC displays a wider range of classroom temperatures, indicated by longer whiskers and larger interquartile ranges, hinting at more significant temperature fluctuations or diverse classroom conditions.

Outdoor temperatures, marked in orange, for all schools, show greater variability than indoor temperatures, as evidenced by broader interquartile ranges and longer whiskers in the outdoor boxplots. Outliers in schools like CBS and LIN suggest occasional deviations from typical temperatures, which could be due to specific weather events or irregularities in indoor climate management. Despite these anomalies, the overall temperature distribution in the schools' points to generally effective regulation of indoor climates, contrasting with the natural variability experienced outdoors.

Table 3: Comparative Pearson correlation coefficient of indoor and outdoor temperature across four studied schools

<b>GGA</b>	<b>C3</b>	<b>C7</b>	<b>C11</b>	<b>C14</b>	<b>C16</b>	
	0.80	0.80	0.77	0.80	0.81	
<b>CBS</b>	<b>C6</b>	<b>C9</b>	<b>C13</b>	<b>C19</b>	<b>C22</b>	
	0.80	0.83	0.82	0.79	0.77	
<b>GMC</b>	<b>C2</b>	<b>C10</b>	<b>C11</b>	<b>C13</b>	<b>C21</b>	<b>C22</b>
	0.75	0.75	0.74	0.75	0.76	0.75
<b>LIN</b>	<b>C2</b>	<b>C5</b>	<b>C6</b>	<b>C10</b>	<b>C11</b>	
	0.30	0.46	0.49	0.41	0.32	

Table 3 presents the Pearson correlation coefficient reflecting the relationship between indoor and outdoor temperatures for various classrooms within the studied schools. The classrooms of GGA and CBS schools show high correlation coefficients (around 0.80), suggesting a strong and consistent positive relationship between indoor and outdoor temperatures across these classrooms. This implies that the indoor temperatures in these schools are closely aligned with the variations in outdoor temperatures.

GMC classrooms have slightly lower coefficients, with values mostly around 0.75, which still indicates a strong positive correlation but slightly less so than GGA and CBS. The indoor temperatures in GMC classrooms follow outdoor temperatures closely, but factors such as insulation or ventilation might affect the tightness of this relationship.

In contrast, classrooms in LIN schools show a lower correlation between indoor and outdoor temperatures, with coefficients ranging from 0.30 to 0.49. This significant drop suggests that indoor temperatures in LIN classrooms are much less influenced by outdoor temperatures, which could be due to various factors like better insulation, more effective thermal control systems, or differing building orientations and designs that minimise the impact of outdoor temperature fluctuations. Overall, the table indicates that while some schools may have indoor climates that are remarkably influenced by outdoor conditions, others manage to maintain a more controlled indoor environment regardless of external temperature changes.

All the studied classrooms successfully met the overheating assessment criteria as defined by the standards explained in Table 2. According to Criterion 1, the classrooms remained within the permissible limits for hours of exceedance, where the indoor air temperature did not exceed the comfort temperature by more than 1 °C for over 3% of occupied hours based on CIBSE TM52 or 40 hours based on BB101. Additionally, Criterion 2, daily weighted exceedance, was within the acceptable range of no more than six occupied days with temperature exceedances. Finally, the indoor temperatures stayed below the upper limit temperature by more than 4°C based on Criterion 3.



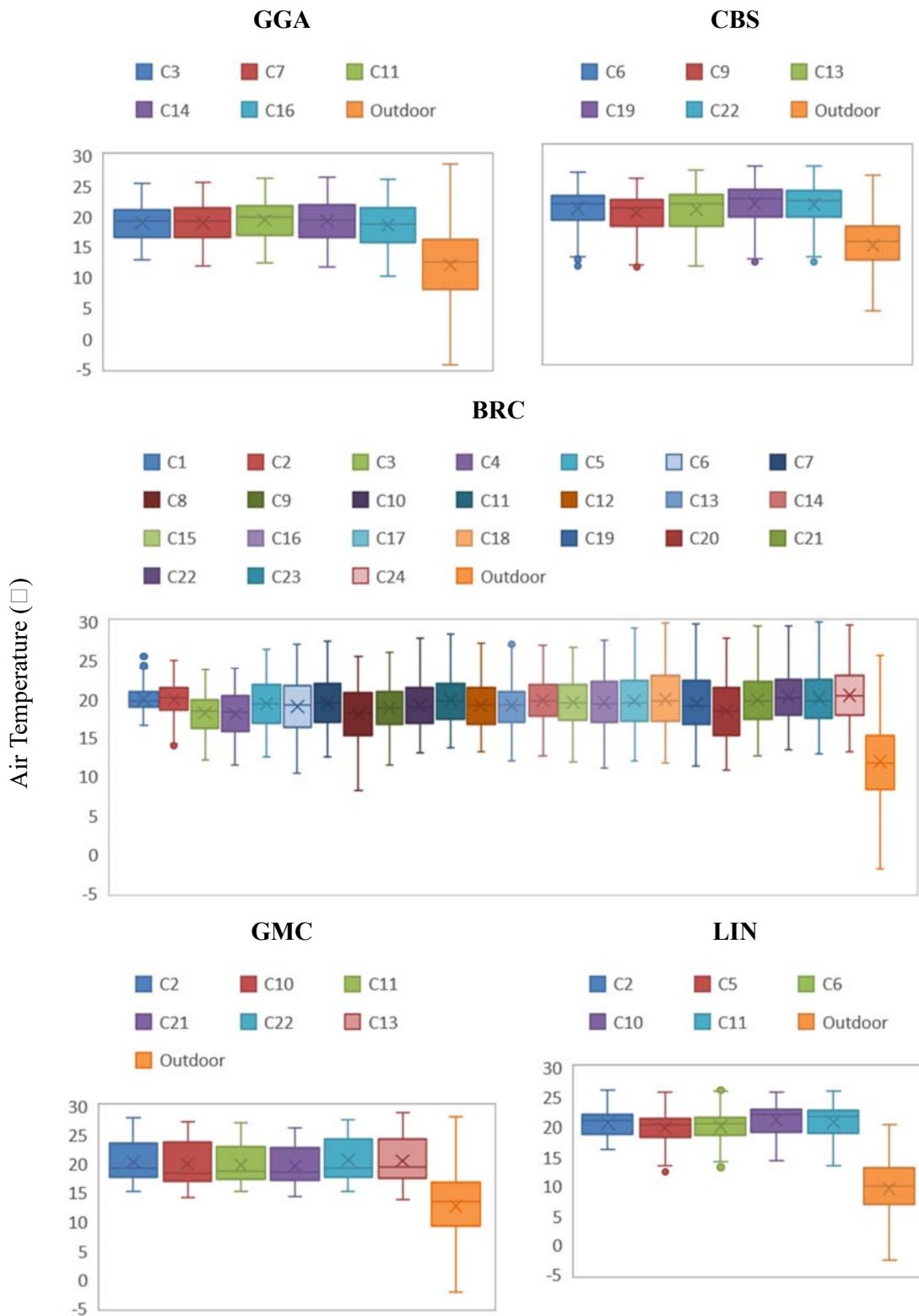


Figure 2: Comparative box and whisker plots of measured indoor and outdoor temperature readings across different studied schools and classrooms

Figure 3 illustrates Cohen's d effect sizes for various factors impacting indoor air temperature in classrooms. These effect sizes vary in magnitude, reflecting the relative influence each factor has on indoor temperature. Remarkably, all studied parameters exhibit effect sizes greater than 0.8, signifying a large effect. Among these, factors such as floor level, NV type (Single/Cross NV), openable window type (top/side/bottom hung), average height of opening, orientation, and the height and colour of internal walls show particularly high effect sizes. This indicates that they have a significant influence on indoor air temperature. The factors such as outdoor temperature, number of occupants, facade area, and opening depth, while they have a large effect size of greater than 0.8, have relatively smaller effect sizes compared to other studied parameters. This implies that these factors have a lesser impact on indoor temperature. This analysis provides valuable insights into the critical parameters affecting indoor air temperature, which can be effective in devising strategies to optimise thermal comfort in classrooms.

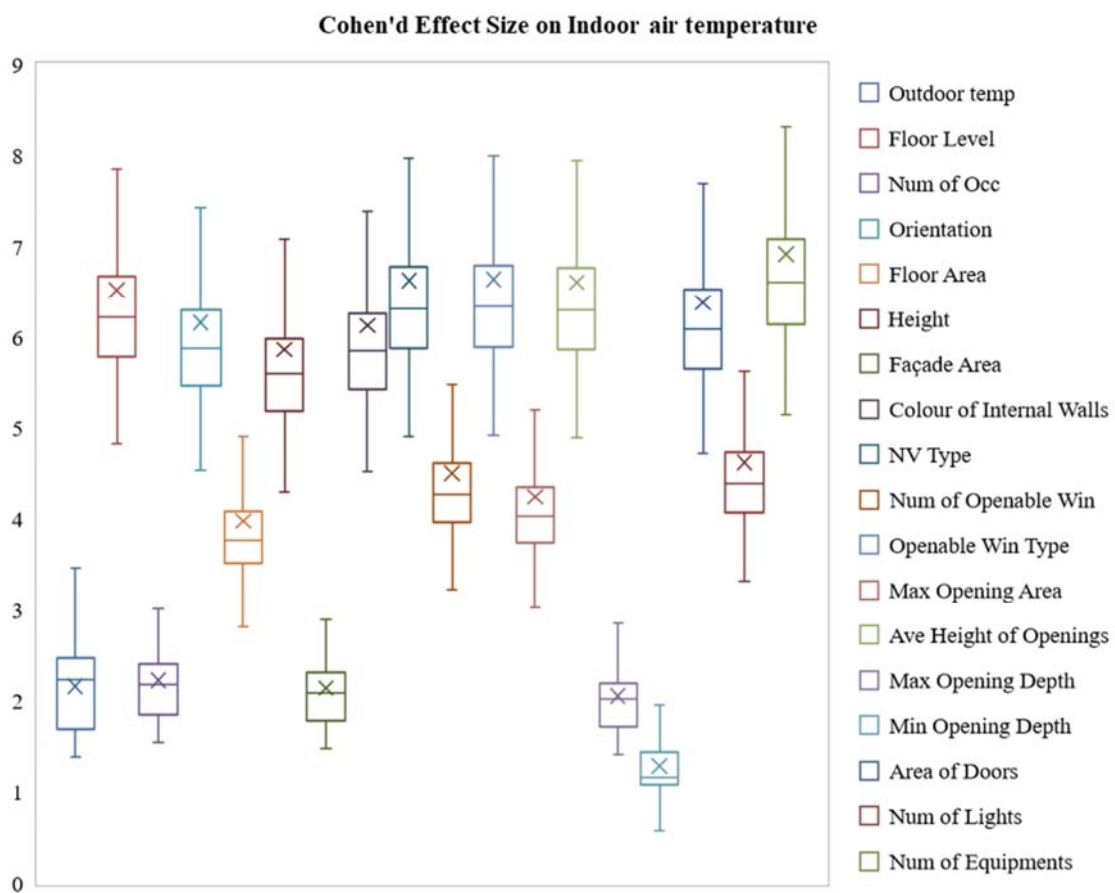


Figure 3: Comparative box and whisker plots of Cohen's d effect size for outdoor air temperature and studied building information parameters on indoor air temperature

## 4 CONCLUSIONS

This study provides a comprehensive assessment of the resilience of Irish low energy school buildings against overheating, with a focus on NV classrooms. The findings indicate that the classrooms currently exhibit high thermal resilience. Key conclusions drawn from the research are as follows:

- The schools generally maintain a stable indoor air temperature relative to the more variable outdoor temperatures. In addition, the classrooms met the overheating assessment criteria defined by CIBSE TM52 and BB101 standards, with current designs able to adequately ensure thermal comfort during warmer periods. This suggests that the existing NV systems contribute positively to indoor climate regulation.
- The Pearson correlation coefficients indicate a strong relationship between indoor and outdoor temperatures in most schools.
- The analysis using Cohen's d effect sizes revealed that certain building features such as floor level, NV type (single/cross NV), openable window type (top/side/bottom hung), average height of opening, orientation, and the height and colour of internal walls, have a substantial impact on indoor air temperature. These factors should be prioritised when designing or retrofitting school buildings to improve thermal comfort.

To address these findings, the following recommendations are proposed:

- Improvements in the design and implementation of NV systems are critical. This includes optimising the types and positions of openable windows and enhancing the height and orientation of openings.
- Educating occupants about effective NV practices and encouraging behaviours that support thermal comfort can further improve indoor conditions.

The insights from this study are expected to guide future strategies for designing resilient, low energy school buildings that can better withstand the challenges of climate change, which can influence both comfort and cognitive performance within the learning spaces.

## 5 ACKNOWLEDGEMENTS

This research has been funded by the Sustainable Energy Authority of Ireland (SEAI) RD&D fund 2019, grant number RDD/00496

## REFERENCES

- [1] European Commission, "Better Buildings A National Renovation Strategy for Ireland," *Dep. Commun. Energy, Nat. Resour.*, pp. 1–77, 2014.
- [2] C. Heraclous *et al.*, "Climate change resilience of school premises in Cyprus: An examination of retrofit approaches and their implications on thermal and energy performance," 2021.
- [3] S. E. Perkins, L. V. Alexander, and J. R. Nairn, "Increasing frequency, intensity and duration of observed global heatwaves and warm spells," *Geophys. Res. Lett.*, vol. 39, no. 20, pp. 1–5, 2012, doi: 10.1029/2012GL053361.
- [4] Ö. Duran and K. J. Lomas, "Retrofitting post-war office buildings: Interventions for energy efficiency, improved comfort, productivity and cost reduction," *J. Build. Eng.*, vol. 42, no. February, p. 102746, 2021, doi: 10.1016/j.job.2021.102746.
- [5] S. Mohamed, L. Rodrigues, S. Omer, and J. Calautit, "Overheating and indoor air

- quality in primary schools in the UK," *Energy Build.*, vol. 250, p. 111291, 2021, doi: 10.1016/j.enbuild.2021.111291.
- [6] S. Mohamed, L. Rodrigues, S. Omer, and J. Calautit, "Overheating and indoor air quality in primary schools in the UK," *Energy Build.*, vol. 250, p. 111291, 2021, doi: 10.1016/j.enbuild.2021.111291.
- [7] K. Tsuzuki, "Effects of heat exposure on the thermoregulatory responses of young children," *J. Therm. Biol.*, vol. 113, no. October 2022, p. 103507, 2023, doi: 10.1016/j.jtherbio.2023.103507.
- [8] J. Kim and R. De Dear, "Thermal comfort expectations and adaptive behavioural characteristics of primary and secondary school students," *Build. Environ.*, vol. 127, no. September 2017, pp. 13–22, 2018, doi: 10.1016/j.buildenv.2017.10.031.
- [9] A. Montazami and F. Nicol, "Overheating in schools: Comparing existing and new guidelines," *Build. Res. Inf.*, vol. 41, no. 3, pp. 317–329, 2013, doi: 10.1080/09613218.2013.770716.
- [10] B. C. C. Service, "Extreme Heat and Human Mortality : A Review of Heat-Related Deaths in B . C . in Summer 2021 Report to the Chief Coroner of British Columbia," 2022.
- [11] R. Bustinza, G. Lebel, P. Gosselin, D. Bélanger, and F. Chebana, "Health impacts of the July 2010 heat wave in Québec, Canada," *BMC Public Health*, vol. 13, no. 1, 2013, doi: 10.1186/1471-2458-13-56.
- [12] C. J. Smith, "Pediatric Thermoregulation : Considerations in the Face of Global Climate Change," pp. 15–18, 2019.
- [13] Y. Chen, M. Tao, and W. Liu, "High temperature impairs cognitive performance during a moderate intensity activity," *Build. Environ.*, vol. 186, no. October, p. 107372, 2020, doi: 10.1016/j.buildenv.2020.107372.
- [14] X. Li *et al.*, "Schooling of migrant children in china: Perspectives of school teachers," *Vulnerable Child. Youth Stud.*, vol. 5, no. 1, pp. 79–87, 2010, doi: 10.1080/17450120903193931.
- [15] "LASCAR EL-SIE." <https://uk.rs-online.com/web/p/data-loggers/1993851>.
- [16] "TESTO 174." <https://ie.farnell.com/testo/testo-174-t/mini-data-logger-temp-30-to-70/dp/2678069>.
- [17] "Airthings View Plus." <https://www.airthings.com/en/view-plus>.
- [18] "LASCAR WIFI-TH." <https://lascarelectronics.com/data-loggers/temperature-humidity/el-wifi-th/>.
- [19] C. TM52, "CIBSE TM52: The limits of thermal comfort," pp. 1–25, 2013.
- [20] BB101, "Guidelines on ventilation thermal comfort and indoor air quality in schools - BB101," no. August, 2018.
- [21] A. O. Donovan, M. D. Murphy, and P. D. O. Sullivan, "Passive control strategies for cooling a non-residential nearly zero energy office : Simulated comfort resilience now and in the future Energy & Buildings Passive control strategies for cooling a non-residential nearly zero energy office : Simulated comfo," *Energy Build.*, no. November, p. 110607, 2020, doi: 10.1016/j.enbuild.2020.110607.
- [22] BS EN 16798, *Energy performance of buildings. Ventilation for buildings - Indoor environmental input parameters for design and assessment of energy performance of buildings addressing indoor air quality, thermal environment, lighting and acoustics*. 2019.

# Experimental evaluation of the bidirectional filtration efficiency of respirators and face masks against airborne particles during cyclic breathing

Dennis Derwein<sup>1</sup>, Tobias Maria Burgholz<sup>2</sup>, Kai Rewitz<sup>1</sup>, Dirk Müller<sup>1,2</sup>

*1 RWTH Aachen University,  
E.ON Energy Research Center  
Institute for Energy Efficient Buildings and Indoor  
Climate  
Mathieustraße 10  
52074 Aachen, Germany*

*2 Heinz Trox Wissenschafts gGmbH  
Mathieustraße 18  
52074 Aachen*

## ABSTRACT

In this work we investigate the bidirectional filtration efficiencies of respirators, such as FFP2 masks and medical masks, under cyclic breathing and different fits. We developed a test bench, which consists of a test chamber with an artificial head, and which is connected to a specially developed artificial breathing function. The exhalation filtration performance of masks can be evaluated by exhaling particle-laden air into the test chamber. Similarly, the inhalation filtration performance can be evaluated by inhalation of particle-laden air from the test chamber. We compare four different types of masks (medical mask and three types of FFP2 masks). In addition, we investigate the influence of different mask fits (e.g., nose clip fitting) on the filtration efficiency of the masks, as a perfect mask fit cannot always be guaranteed in realistic scenarios and filtration efficiency may therefore be reduced. The results show that different maximum filtration efficiencies are achieved depending on the mask type. Only one of the three FFP2 masks can achieve filtration efficiencies above 89% while one only achieves a maximum of 59%. Depending on the fit, the medical mask can achieve up to 55% for self-protection. The fit of the mask has a major influence on the filtration efficiencies. If the mask is used without putting on the nose clip, a value of only 10 to 45% can be achieved, depending on the mask type and direction of protection. With two of the FFP2 masks, simply putting on the nose clip is enough to achieve filtration efficiencies of at least 75%. It was also shown that a medical mask with the best fit protects at least as well in both directions as the three FFP2 masks with the worst fit level. In addition, the fit of the mask and the filtration efficiency correlate very well with the measured pressure difference across the mask.

## KEYWORDS

face mask, mask fit, filtration efficiency, airborne particles, infection risk

## 1 INTRODUCTION

Respirators, such as FFP2 masks and medical masks, are a widely used measure to reduce the airborne transmission of potentially viral particles between individuals. FFP2 masks promise a high level of self-protection. DIN 149 specifies that the total inward leakage of FFP2 masks must not exceed 11%, which corresponds to a total filtration rate of 89% (DIN EN 149). If a high level of protection must be guaranteed, so-called fit tests can be carried out. Qualitative fit tests according to DIN ISO 16975-3 even specify fit factors of at least 100, which corresponds to a filtration rate of around 99% (ISO 16975-3).

Such tests are only common in work areas where a high level of protection must be guaranteed, for example in medical facilities (Regli et al. 2021). During pandemic situations, common people need to be protected by FFP2 masks, who are not trained in the correct use of FFP2 masks and do not have access to fit tests in everyday situations. It can therefore be assumed that in everyday situations, FFP2 masks are more likely to be worn imperfectly, so that the protective effect is reduced (Knobloch et al. 2023). To evaluate the effectiveness of

masks in containing infectious diseases, such as during the COVID-19 pandemic, it is therefore essential to consider reduced filtration efficiency due to imperfect use.

One method of determining the filtration efficiency of masks is to use test benches that evaluate the filtration efficiency of masks by measuring particles using an artificial head and inhaled or ambient air contaminated with artificial particles (Tcharkhtchi et al. 2021). Previous studies have shown with these kind of test benches that the masks should be accurately evaluated under cyclic breathing (Mahdavi et al. 2014) and that the filtration efficiency varies depending on the direction of filtration (self and external protection) (Berger et al. 2023). While several studies have evaluated filtration efficiency for self-protection under cyclic breathing (Balazy et al. 2006; Mahdavi et al. 2014), there are few studies on the evaluation of filtration efficiency during cyclic breathing for external protection (Lindsley et al. 2023) or in both directions (Koh et al. 2022). A bidirectional evaluation should be carried out in a comparable setting, as both directions of filtration are relevant to the overall assessment of the effectiveness of masks in reducing the transmission of particles between individuals. In addition, there are no studies yet that have dealt with reduced fit. In those studies mentioned above, the fit of the mask is not further specified or, in some cases, an optimized fit is simulated by gluing the mask seal to the manikin (Berger et al. 2023; Mahdavi et al. 2014).

The aim of this study is to determine the bidirectional filtration efficiencies of different shapes of FFP2 mask types and medical masks and the reduction of these efficiencies due to imperfect mask fit. To achieve this, we have developed a test stand in which the masks can be measured on an artificial head under cyclical breathing.

Firstly, the design and functionality of the test bench is presented. Then the analysed masks and boundary conditions of the test plan are explained. The resulting filtration efficiencies are then presented and subsequently discussed. Finally, an outlook and conclusion are given.

## 2 TEST BENCH DESCRIPTION

A sketch of the mask test bench is given in Figure 1. The mask test bench consists of two main components: the test chamber (as seen on the left of Figure 1) and the artificial lung (as seen on the right of Figure 1). These two components are described below.

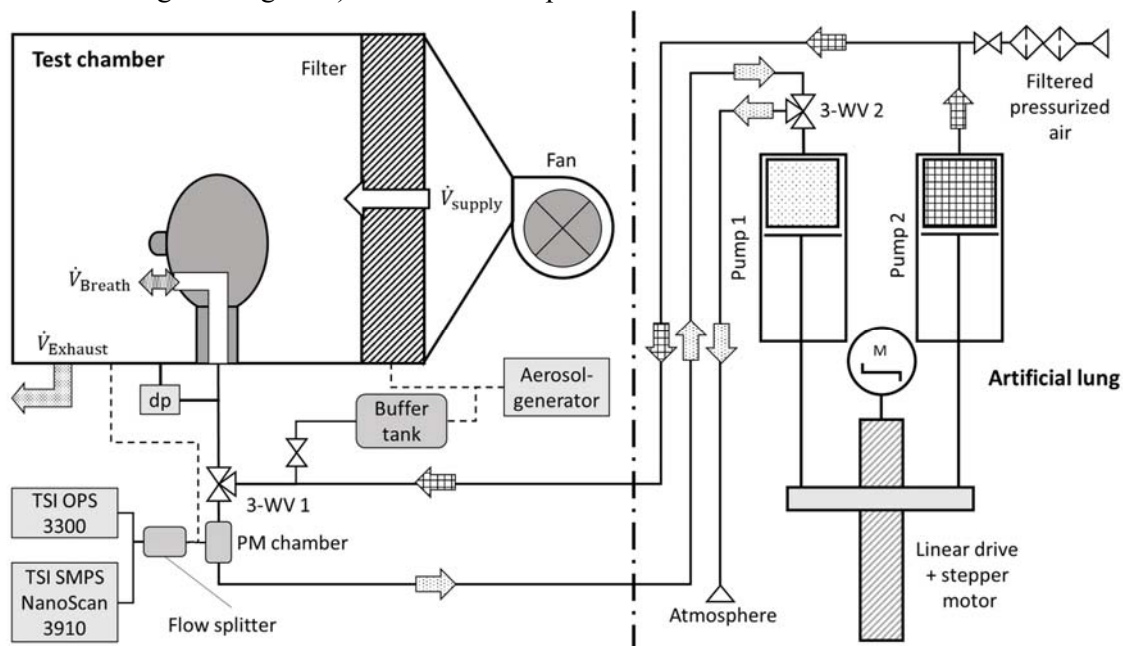


Figure 1: Layout of the test chamber and the artificial lung

## 2.1 Test chamber

The test chamber consists of a rectangular chamber with the dimensions of 1000 x 700 x 700 cm<sup>3</sup>, thus amounting to a volume of roughly 490 litres. The side walls and the top wall are made of glass to ensure transparency and the front consists of a glass door to allow access into the test chamber. The base plate, which is made of a plastic plate, holds the artificial head and is used for power, data and hose connections. An F9/ePM1 and HEPA/H14 two-stage filter installed at the rear enables particle-free supply of air into the chamber through the entire cross-section. The supply air is delivered into the test chamber by a centrifugal scroll housing fan of the type “RadiCal G3G133-RO15-11” manufactured by “ebm-pabst” with an integrated constant air flow controller. The exhaust air is routed via a hose connection on the front side of the base plate, thus creating a mean flow from rear to the front of the chamber. In addition, five computer cooling fans are installed in the chamber to ensure well mixing and thus an equal distribution of particles in the chamber.

An artificial head is installed in the centre of the base plate. This artificial head is part of an "Airway Management Trainer" from "Laerdal Medical GmbH" and is connected to the artificial lung via tubes. We measure the pressure drop over the masks with an “SDP810-500Pa” differential pressure sensor by the company “Sensirion AG”, which is marked as “dp” in Figure 1.

Two particle analysers from “TSI Inc.” are used to measure the particle concentrations: an “SMPS NanoScan 3910” scanning mobility particle sizer measures the particles in the range from 10 nm to 420 nm while the optical particle sizer “OPS 3300” covers particle sizes from 300 nm to 10 µm. The two particle analysers are connected via a flow splitter (“FS” in Figure 1) of the type “3708” by the same manufacturer to the test chamber. The particles are generated by a portable test aerosol generator of the type “3073”, also from “TSI Inc.”, by atomisation of “Di-Ethyl-Hexyl-Sebacate (DEHS)” as the particle generator liquid. This enables the evaluation of a wide range of particle sizes between 87 nm and 2 µm, thus covering the "most penetrating particle sizes" of FFP2 masks (approx. 50–100 nm) and medical masks (approx. 300 nm) (Tcharkhtchi et al. 2021).

In the mode in which the particle filtration efficiency for the external protection is evaluated, the particle generator is connected to the exhalation pipe through the buffer tank and the exhaled air is loaded with particles. In these cases, the particle concentration is measured in the test chamber. In the mode in which particle filtration is assessed for the self-protection, the particle generator is connected to the test chamber and the test chamber air is loaded with particles. In these cases, the particle concentration is measured in the measurement chamber in the neck area.

## 2.2 Artificial lung

We use an artificial lung to mimic a cyclic breathing process through the artificial head. The artificial lung was firstly used for investigating exhaled air distributions in car cabin environments (Nabilou et al. 2023). The main part of the test stand consists of two spirometer calibration piston pumps from the manufacturer "Vitalograph GmbH", which are moved in parallel by a linear drive. The pumps each have a volume of 3 litres. During the breathing cycles, their volume can be adjusted using the stroke pathway of the pump. The volume flow profile of the breathing cycle can be controlled by applying a velocity profile of the stepper motor. The linear drive is driven by a stepper motor of type “AS2041-1H10” by the company “Beckhoff Automation GmbH & Co. KG”. The stepper motor and the valves are controlled by a programmable logic controller (PLC) from the same manufacturer. The use of two piston pumps allows the inhalation and exhalation process to be separated so that an air exchange can be guaranteed. The process works as follows. During the inhalation, the pumps are moved

downwards by the linear drive. 3-way valve 1 (“3-WV 1”) and 3-way valve 2 (“3-WV 2”) open the path between “Pump 1” and the artificial head. “Pump 1” draws in the air from the test chamber through the artificial head and the two 3-way valves, thus creating an inhalation flow. Pump 2 draws in filtered compressed air. In the application where filtration efficiency for external protection is to be analysed, aerosol is also injected from the buffer tank during the inhalation phase into the pipe between “3WV-1” and “Pump1”. When exhaling, the two 3-way valves are switched, so that the pathway between “Pump 2” and the artificial head as well as the pathway between “Pump 1” and the exhaust opening to the atmosphere are opened. The linear drive moves upwards so that the inhaled air in “Pump 1” is released into the atmosphere and “Pump 2” pushes air through “3WV-1” and the artificial head into the chamber, thus creating the exhalation flow.

### 3 EXPERIMENTAL DESIGN

The experimental investigations are carried out according to a fully factorial test plan, whereby 3 factors are analysed: Mask type, mask fit, and filtration direction. There are various forms of FFP2 masks. The designations of the forms in this paper are based on the designations of Knobloch et al. (Knobloch et al. 2023). We analyse three different forms of FFP2 masks in this work. FFP2\_1 corresponds to a so-called "coffee filter" shaped mask, FFP2\_2 corresponds to a so-called "three-folded" mask, and FFP2\_3 to a “rigid dome” shaped model. FFP2\_1 is fixed to the head by ear loops, while FFP2\_2 and FFP2\_3 are fixed to the head by loops around the head. A medical mask is also analysed as a comparison, which is also fixed to the head by ear loops.

Table 1: Overview over the investigated masks

Mask	Manufacturer	Name	Type	Shape	Fixation
med. Mask	Unknown	OP-Mundschutz “SOFT PROTECT GERMANY” blau- BASIC	EN 14683 Typ II R	Medical mask	Ear loop
FFP2_1	Unknown	Atenschutz - Faltmaske FFP2 NR “Komfort20“	FFP2 NR	Coffee filter	Ear loop
FFP2_2	3M	Aura 9320D+	FFP2 NR D	Three-folded	Head band
FFP2_3	3M	8810	FFP2 NR D	Rigid dome	Head band

The mask fit is varied in 3 stages. In the first stage (Fit1), the mask is placed on the face and fixed in place by the loops, but no further measures are taken to optimise the fit. Furthermore, the nose clip is not fitted, so that the overall aim is to imitate a very careless wearing of the mask. In the second stage (Fit2), the mask is also put on without optimisation measures, but the nose clip is fitted around the nose. In the third stage (Fit3), a careful mask fit is imitated by applying the nose clip and optimising the mask fit so that possible leakage via the face seal is avoided as far as possible, thus attempting to imitate a "fit-tested mask". As a medical mask cannot be fitted anyway, only Fit1 and Fit2 are used when analysing the medical mask. Based on the three factors and considering that the medical mask is not examined in Fit3, this results in a fully factorial test plan of 22 tests, where each test point is carried out three times. A sinusoidal breathing profile is used as the breathing profile, which corresponds to the sinusoidal breathing profile A from EN 13274-3 with a breathing frequency of 10/min, a respiratory volume of 1 litre and a peak air flow of 34,2 litres/minute (DIN EN 13274-7). As pressure equalisation must still take place when switching between the inhalation and exhalation process and between the exhalation and inhalation process, pauses of 250 milliseconds are set in each case. The test procedure for each test point is as follows: First, a reference point without a mask is determined. After stable constant particle concentrations have been established, the particle concentrations are measured for 20 minutes, so that a total



of 20 samples with a sample duration of 1 minute each are recorded for the two particle measuring devices. The three repetitions of the measuring point are then carried out by putting on the mask and measuring for 30 minutes. Experience has shown that a constant concentration is then established after about 10 minutes, so that 20 samples are also recorded for each repetition. The particle size-dependent filtration efficiency  $\eta_{i,j}(d_{\text{Particle}})$  for test point  $i$  and repetition  $j$  is calculated using Formula (1). Here,  $c_{\text{mean},i,j}(d_{\text{Particle}})$  corresponds to the particle concentration averaged over the 20 samples for test point  $i$  and repetition  $j$  and  $c_{\text{mean},\text{ref}}(d_{\text{Particle}})$  corresponds to the particle concentration of the reference measurement averaged for the test point  $i$  over the 20 samples, both measured in the measuring chamber in the neck area:

$$\eta_{\text{in},i,j}(d_{\text{Particle}}) = \left( 1 - \frac{c_{\text{mean},i,j}(d_{\text{Particle}})}{c_{\text{mean},i,\text{ref}}(d_{\text{Particle}})} \right) * 100 \% \quad (1)$$

The differential pressure over the artificial head is measured in a frequency of 5 Hz, so that the differential pressure curve over time during the breathing cycle can be clearly recorded. The peak-values of the differential pressures for both inhalation and exhalation are averaged for the reference points and the test points. The mean mask differential pressures for inhalation and exhalation are then determined by subtracting the mean differential pressures of the test points and mean differential pressures of the reference points without a mask.

#### 4 RESULTS

Figure 2 shows the particle size averaged filtration efficiencies for the 22 test points in the form of a grouped bar chart, whereby the particle size-dependent filtration efficiencies have been averaged over the particle sizes from 86 nm to 1023 nm. The bars are sorted into four groups, each representing the six test points for each mask type. For the medical mask, the external filtration efficiencies for the external protection are 10% to 41% for Fit1 and Fit2. For self-protection, the filtration efficiencies are at 21% and 53%. For the FFP2\_1 mask, the filtration efficiencies for the external protection are at 15%, 40% and 56% and for the self-protection at 35%, 43% and 50%. For the FFP2\_2 mask, the external filtration efficiencies are at 24%, 89% and 96% and for the self-protection at 35%, 86% and 98%. For the FFP2\_3 mask, the external filtration efficiencies are at 41%, 75% and 91% and for the self-protection at 46%, 77% and 88%. The medical mask provides a higher self-protection than external protection. We also see that fitting the nose clip has a large impact and leads to a large increase in filtration efficiencies. FFP2\_2 shows similar values for external protection for Fit1 and Fit2 as for the medical mask. Furthermore, the differences between Fit1, Fit2 and Fit3 in terms of self-protection are only very slight. It should also be noted that in this study, FFP2\_1 can only achieve a level of self-protection that is way below the minimum filtration efficiency of 89% as specified in the DIN EN 149 standard (DIN EN 149) in this case, even performs worse than the medical mask. For the FFP2\_2 mask, Fit2 already achieved comparatively high filtration efficiencies of over 80% for both directions, which are further increased by Fit3. FFP2\_3 already achieves comparably high values for both directions in Fit1, but for Fit2 and Fit3 lower filtration efficiencies compared to FFP2\_2 are achieved and furthermore for Fit3 only an average value slightly below the required minimum value of 89% could be achieved.

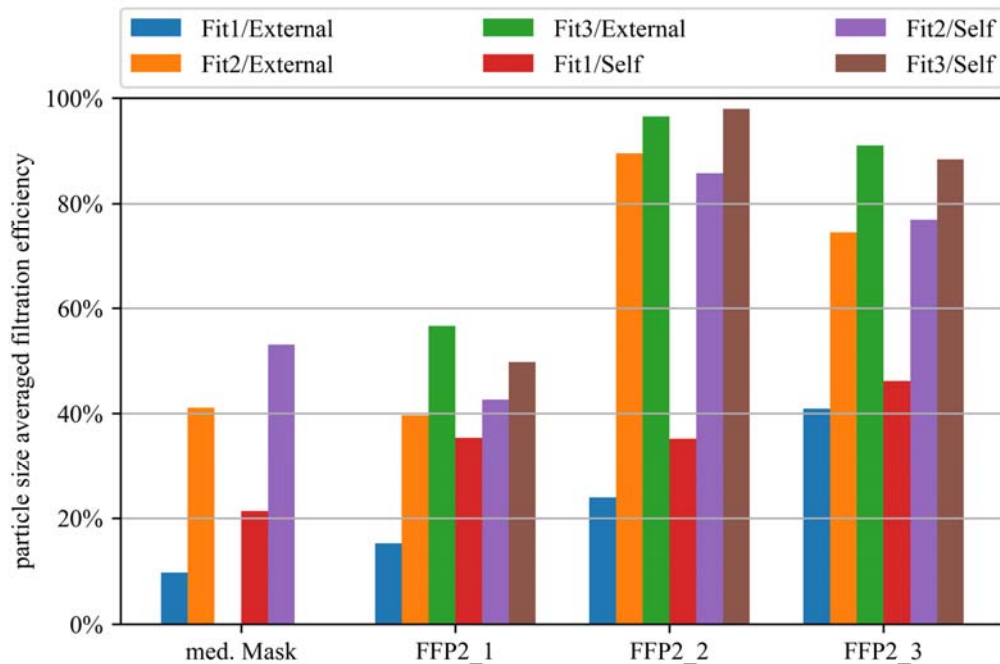


Figure 2: Overview over the particle size averaged filtration efficiencies for the investigated test points.

Furthermore, the differences between Fit1, Fit2, and Fit3 in terms of self-protection are only marginal. With this mask, we have found that the nose clip cannot be completely fitted to the nose, so that leakage still occurs in the nostril area. This may be due to the mechanical properties of the nose clip, as it is not very rigid compared to those of FFP2\_2 and FFP2\_3, and always springs back a little after fitting. With FFP2\_2, very high filtration efficiencies of over 80% could already be achieved with Fit2, which shows that the design in this case also achieves a good fit without great effort. With Fit3 filtration efficiencies for self-protection are achieved that are clearly above the minimum requirements specified in DIN EN 149. FFP2\_3 shows slightly lower filtration efficiencies for Fit2 and Fit3 than FFP2\_2 and here, too, the minimum requirement from DIN EN 149 is slightly undershot. However, this mask shows the highest filtration efficiencies for Fit1 compared to the other three masks. Quite comparable filtration efficiencies for self- and external protection are achieved for all test points. To gain further insights into the fit of the masks, the pressure differences over the tests are analysed. In Figure 3, the particle size averaged filtration efficiencies are plotted over the mean mask differential pressures. In this case, we analyse the repetitions of each test point instead of the mean values for each test point. The fit levels are marked with the shapes and the masks with the colours. A clear correlation between the filtration efficiency and differential pressure can be derived from this diagram. It is notable that the points for the medical mask, FFP2\_2 and FFP2\_3 for external protection and the self-protection cases are each in very similar ranges. It should be noted that the points for the medical mask are in similar ranges to those of FFP2\_2 and FFP2\_3, despite the much thinner mask material. The points for FFP2\_1 are substantially lower and achieve much higher differential pressures with similar filtration efficiencies. Based on this observation, a further hypothesis can be put forward for the lower filtration efficiencies of FFP2\_1. It can be assumed that the mask material of FFP2\_1 generates a far higher flow resistance than that of the other three masks. In combination with the poor fit of the nose clip, far more air flows through the leaks in the nose wing area, which is not filtered.

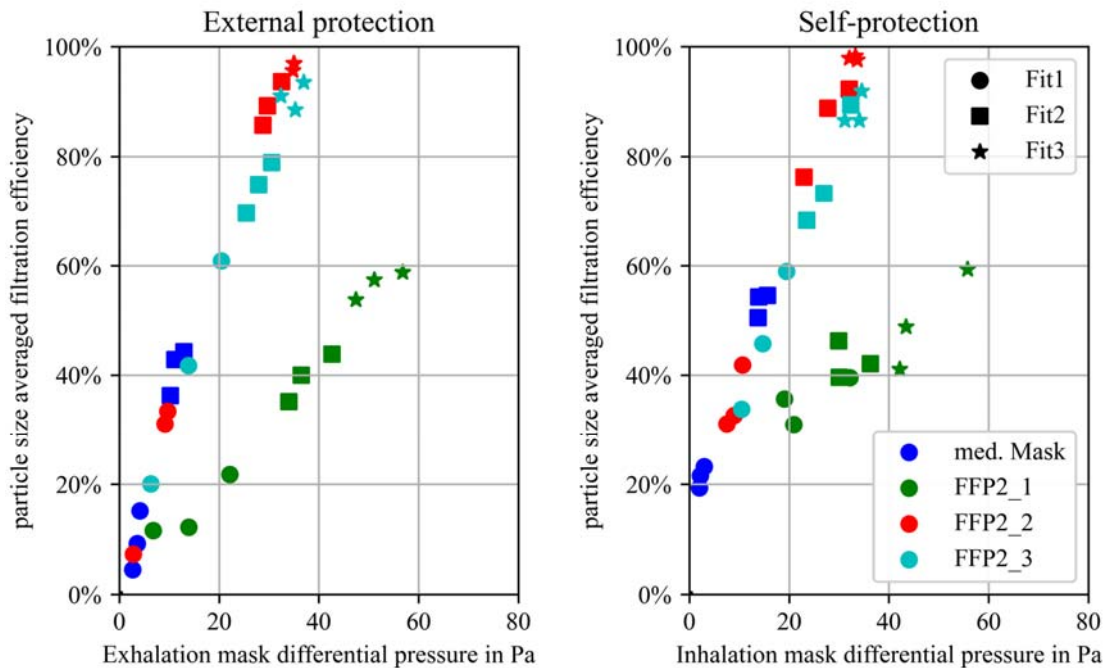


Figure 3: Filtration efficiencies for each test point repetition over the mask differential pressures

## 5 CONCLUSIONS

The results show that, both the mask type and the mask fit have clear influence on the filtration efficiencies. For instance, the fitting of the nose clip already has a big impact on filtration efficiency. The minimum filtration efficiency for self-protection of FFP2 masks specified in the standard DIN EN 149 could only be achieved with the "three-folded" FFP2 mask. Furthermore, the "coffee filter" shaped FFP2 mask only achieves a filtration efficiency that is way below the minimum requirements. This result is consistent with the findings of a literature review, in which a poor performance of such FFP2 mask types was determined in quantitative fit tests (Knobloch et al. 2023). Furthermore, the results show that a correctly worn medical mask performs at least as well as a poorly fitted FFP2 mask in this investigation. In addition, all masks show similar results depending on the direction of protection (external and self-protection). It was also shown that the fit-dependent filtration efficiencies correlate very well with the measured pressure difference. Far higher pressure differences were determined for the "coffee filter" shaped mask than for the other masks, from which can be concluded that the material may be responsible for the low filtration efficiency, among other things.

In future studies, the influence of the respiratory volume flow can additionally be investigated, and other mask types or different models of the same mask shape can be analysed. In this way, it can also be determined whether the "coffee filter" shaped mask also has similar problems for other models. The results can, for example, be used in model-based infection risk calculations in the future to determine the influence of imperfect fit on the risk of infection (Müller et al. 2021).

## 6 ACKNOWLEDGEMENTS

This work was financially supported by the Heinz Trox Wissenschafts gGmbH (research grant HTx0022).

## 7 REFERENCES

- Balazy, Anna; Toivola, Mika; Reponen, Tiina; Podgórski, Albert; Zimmer, Anthony; Grinshpun, Sergey A. (2006): Manikin-based performance evaluation of N95 filtering-facepiece respirators challenged with nanoparticles. In *The Annals of occupational hygiene* 50 (3), pp. 259–269. DOI: 10.1093/annhyg/mei058.
- Berger, Simon; Mattern, Marvin; Niessner, Jennifer (2023): Face mask performance related to potentially infectious aerosol particles, breathing mode and facial leakage. In *International journal of hygiene and environmental health* 248, p. 114103. DOI: 10.1016/j.ijheh.2022.114103.
- Knobloch, J. K.; Franke, G.; Knobloch, M. J.; Knobling, B.; Kampf, G. (2023): Overview of tight fit and infection prevention benefits of respirators (filtering face pieces). In *The Journal of hospital infection* 134, pp. 89–96. DOI: 10.1016/j.jhin.2023.01.009.
- Koh, Xue Qi; Sng, Anqi; Chee, Jing Yee; Sadovoy, Anton; Luo, Ping; Daniel, Dan (2022): Outward and inward protection efficiencies of different mask designs for different respiratory activities. In *Journal of Aerosol Science* 160, p. 105905. DOI: 10.1016/j.jaerosci.2021.105905.
- Lindsley, William G.; Blachere, Francoise M.; Derk, Raymond C.; Boots, Theresa; Duling, Matthew G.; Boutin, Brenda et al. (2023): Constant vs. cyclic flow when testing face masks and respirators as source control devices for simulated respiratory aerosols. In *Aerosol Science and Technology* 57 (3), pp. 215–232. DOI: 10.1080/02786826.2023.2165898.
- Mahdavi, Alireza; Bahloul, Ali; Haghghat, Fariborz; Ostiguy, Claude (2014): Contribution of breathing frequency and inhalation flow rate on performance of N95 filtering facepiece respirators. In *The Annals of occupational hygiene* 58 (2), pp. 195–205. DOI: 10.1093/annhyg/met051.
- Müller, Dirk; Rewitz, Kai; Derwein, Dennis; Burgholz, Tobias Maria; Schweiker, Marcel; Bardey, Janine; Tappler, Peter (2021): Estimation of the risk of infection by aerosol-borne viruses in ventilated rooms. Aachen.
- Nabilou, Fatemeh; Derwein, Dennis; Rewitz, Kai; Müller, Dirk (2023): Experimental assessment of CO<sub>2</sub> tracer gas and aerosol particles during breathing, coughing, and sneezing. In M. Schweiker, C. van Treeck, D. Müller, J. Fels, T. Kraus, H. Pallubinsky (Eds.): *Proceedings of Healthy Buildings 2023 Europe*. Aachen, Germany.
- Regli, A.; Sommerfield, A.; Ungern-Sternberg, B. S. von (2021): The role of fit testing N95/FFP2/FFP3 masks: a narrative review. In *Anaesthesia* 76 (1), pp. 91–100. DOI: 10.1111/anae.15261.
- DIN EN 149, 2009: Respiratory protective devices - Filtering half masks to protect against particles - Requirements, testing, marking.
- DIN EN 13274-7, 2019: Respiratory protective devices - Methods of test - Part 7: Determination of particle filter penetration.
- ISO 16975-3, 2022: Respiratory protective devices - Selection, use and maintenance - Part 3: Fit-testing procedures.
- Tcharkhtchi, A.; Abbasnezhad, N.; Zarbini Seydani, M.; Zirak, N.; Farzaneh, S.; Shirinbayan, M. (2021): An overview of filtration efficiency through the masks: Mechanisms of the aerosols penetration. In *Bioactive materials* 6 (1), pp. 106–122. DOI: 10.1016/j.bioactmat.2020.08.002.

# Assessment of the indoor/outdoor dynamic of some air pollutants in three buildings located in the valley city of Chambéry, France

Diana Decilap<sup>\*1,2</sup>, Gaëlle Guyot<sup>2</sup>, Jean-Luc Besombes<sup>3</sup>, and Benjamin Golly<sup>1</sup>

*1 Univ. Savoie Mont Blanc, CNRS, LOCIE  
73000 Chambéry, France*

*\*Corresponding author:  
diana.decilap@developpement-durable.gouv.fr  
Presenting author*

*2 Cerema, BPE research team  
46 rue St Théobald  
38081 L'Isle d'Abeau, France*

*3 Univ. Savoie Mont Blanc, CNRS, EDYTEM  
73000 Chambéry, France*

## KEYWORDS

Air pollution, I/O ratio, PM<sub>2.5</sub>, NO<sub>2</sub>, building ventilation system

## 1 INTRODUCTION

In recent years, population exposure to air pollution has been a major concern. Indoor air quality (IAQ) is mainly monitored with CO<sub>2</sub>-concentration-based indicators. High levels of CO<sub>2</sub>-concentration are avoided in buildings when airing by the windows is done and/or when air exchange rate of the existing ventilation is regulated, based on a CO<sub>2</sub>-level-information. However, as contributing to maintain low CO<sub>2</sub>-concentration-levels indoors, the increase of outdoor air intake is associated with a more or less important introduction of outdoor air pollutants in the building. Among these pollutants, there are particulate pollutants as PM<sub>2.5</sub> and there is NO<sub>2</sub> that is a gaseous pollutant mainly emitted by the road-traffic. Many previous papers dealt with the indoor/outdoor dynamics. However, only rare studies, like Bucur et Danet (2019), Bi et al. (2021) or Nezis et al. (2022), were based on outdoor air measurements up to 500 m away from the studied buildings.

The aim of this study is to evaluate such dynamics for PM<sub>2.5</sub> and NO<sub>2</sub>. It was based on a two-months measurements campaign in three buildings presenting different ventilation types. In addition to the reference data of the local air quality monitoring station, an optical particles measurement was introduced on the façade of the buildings.

## 2 METHODS AND MATERIAL

### 2.1 Site description

For this study, three public buildings with different ventilation conditions were chosen within a 300 m of an ambient air quality monitoring station. The environment is an urban busy traffic. A short description of the characteristics of these buildings is given in *Table 1* **Error! Reference source not found.**

### 2.2 Sampling methods

Different sensors were used for the campaign to measure the concentrations of particulate matter with an equivalent diameter less than 2.5 µg.m<sup>-3</sup> (PM<sub>2.5</sub>), black carbon (BC), nitrogen oxides (NO<sub>x</sub>, NO<sub>2</sub>, NO). Indoors, there was at least one monitor or sensor for each kind of measurement. And there was one PM<sub>2.5</sub> sensor on the air intake façade of each building, that also provides air pressure. The technology to measure the particle matter is optical particle

counter. A low-cost monitor is used here, that also delivers measurements of CO<sub>2</sub>, temperature and relative humidity inside. NO<sub>x</sub> measurement has been possible in one of the buildings only, using a chemiluminescence-based analyser. The technology used to measure the black carbon is an aethalometer. And Atmo AuRA, the air pollution surveillance actor for the region, delivered data from the nearby station. *Table 2* gives details on the used material in the buildings and on their façades. Prior to the campaign, the eight AirVisual sensors were put under inter-comparison for three months in the laboratory. The installation of PM<sub>2.5</sub> measurements devices for each building of the campaign was then based on the AirVisual technology version and on the determination coefficient results, as shown in *Table 3*.

Table 1 : Main characteristics of the buildings included in the measurements campaign

Building	Floors number	Façade measurement (campaign)	Year of construction	Refurbishment	Ventilation type
School	4	West	1960's	Upcoming	No system, manual airing (windows)
Event center	2	West	1990's	Upcoming	Balanced ventilation (activated when an event is scheduled)
Library	6	East	1990's	No	HVAC system with filters. Turned off at night and on Sundays

Table 2 : Main characteristics of the sampling material for the measurements campaign

Building	Floor (Nb of rooms)	Nb of monitors	Brand of monitor/sensor/analyser			Building facade
			PM <sub>2.5</sub> , CO <sub>2</sub> , Temp, RH	BC	NO <sub>x</sub>	PM <sub>2.5</sub>
School	3 <sup>rd</sup> floor (2)	2	AirVisual NODE (IQAir)	AE31 (Magee Scientific)	ENVEA analyser (Atmo AuRA)	AirVisual Outdoor (IQAir)
Event center	Staircase (1)	1	AirVisual PRO (IQAir)	MA300 (Aethlabs)	-	AirVisual Outdoor (IQAir)
Library	2 <sup>d</sup> and 3 <sup>rd</sup> floors (2)	2	AirVisual PRO (IQAir)	MA300 (Aethlabs)	-	AirVisual Outdoor (IQAir)

Table 3 : AirVisual Indoor and Outdoor inter-comparison results (R<sup>2</sup>)

AirVisual Indoor device(s)	Indoor/Indoor R <sup>2</sup>	Indoor /Outdoor R <sup>2</sup>	Building destination into the campaign
Pair of NODE	0.984	0.983 <sup>a</sup>	School
Pair of PRO	0.986	0.981 <sup>a</sup>	Library
Remaining PRO	-	0.966	Event Center

*a: This determination coefficient is the average of the determination coefficients of the Outdoor device with each Indoor monitor of the Indoor pair.*

### 2.3 Data Analysis method

The campaign was carried out from January 11<sup>th</sup> to March 7<sup>th</sup>, 2024. After collecting the data from the monitors and analysers, a cleaning step was performed, mainly to keep out the

temporal discrepancies from the outputs of the AirVisual devices. The cleaned data were then averaged into different time-step levels with the R package *openair* (Carslaw et al., 2011), i) to match the time step of the data provided by the ambient air quality monitoring station (15 minutes), ii) to determine the European Air Quality Index, EAQI, of the concentrations from the station (respectively 1 hour and 1-day-time steps for NO<sub>2</sub> and PM<sub>2.5</sub>). As the black carbon data treatment is not yet finished, the present summary only covers the PM<sub>2.5</sub> and NO<sub>x</sub> analysis.

The data were analysed to get a knowledge of the outdoor-indoor air pollution dynamics: i) at the campaign' scale, and ii) at specific high pollution periods within the campaign. The global study involves several approaches and parameters such as a statistical approach of the distribution of the measurements, the occupation' definition through surveys, etc. Here, the summary presents the results on a daily profile approach, with the 15-minutes I/O ratio of PM<sub>2.5</sub> and NO<sub>2</sub> concentrations.

### 3 RESULTS

#### 3.1 Indoor/outdoor dynamics of NO<sub>2</sub>

During the campaign, the outdoor NO<sub>2</sub> concentration never exceeded 90 µg.m<sup>-3</sup> per hour, the EAQI upper limit for the Fair class. Indeed, the NO<sub>2</sub> 1-hour-step outdoor concentration stayed within the interval of 0.7 to 73.5 µg.m<sup>-3</sup>. In the daily-profiled concentrations presented in *Figure 1.a*), we can observe two peaks in the outdoor concentration, one in the morning and the other at the end of the day, corresponding to the peaks of traffic in urban areas. The indoor concentration curve is rather flat, and the maximum I/O ratio of 0.70 was found at mid-day.

#### 3.2 Indoor/outdoor dynamics of PM<sub>2.5</sub>

We plotted the PM<sub>2.5</sub> concentration indoors and outdoors and the I/O ratios for the school, the event center and the library within a daily profile, on a 15-minutes time-step level (*Figure 1.b to d*). Two days in January and two in February, we observed at the station that the outdoor PM<sub>2.5</sub> concentration did go beyond the value of 25 µg.m<sup>-3</sup> per day, the upper limit of the Moderate class of the European Air Quality Index. In *Table 4* are presented the minimum and maximum I/O ratios representing the indoor averaged concentrations over the station outdoor concentrations during the campaign period. It also gives the detail of the median I/O ratio values in and out of the four dates where the daily concentration is above 25 µg.m<sup>-3</sup>. It is noteworthy that, according to the occupation's survey, a window was opened in one of the two monitored rooms of the school at 1.00 PM UTC, on date no. 3, and that no event was mentioned on any of these dates in the monitored room of the event center. There, the ventilation was then off. In the school, the maximum I/O ratio of 5.49 corresponded to a reported combustion activity in one of the classroom, in the beginning of March.

Table 4 : 15-minutes-averaged concentration I/O ratio of PM<sub>2.5</sub> during the campaign period (µg.m<sup>-3</sup>)

Building	Days where daily concentration is under 25 µg.m <sup>-3</sup>			Dates where daily concentration is above 25 µg.m <sup>-3</sup>		
	Min.	Max.	Median	Min.	Max.	Median
School <sup>a</sup>	0.00	5.49	0.34	0.12	0.59	0.29
Event center <sup>b</sup>	0.00	5.35	0.54	0.39	0.85	0.59
Library <sup>a</sup>	0.00	2.05	0.12	0.04	0.33	0.13

a: Indoor concentration as the average of the values of two sensors.

b: Indoor concentration as the value of one sensor.

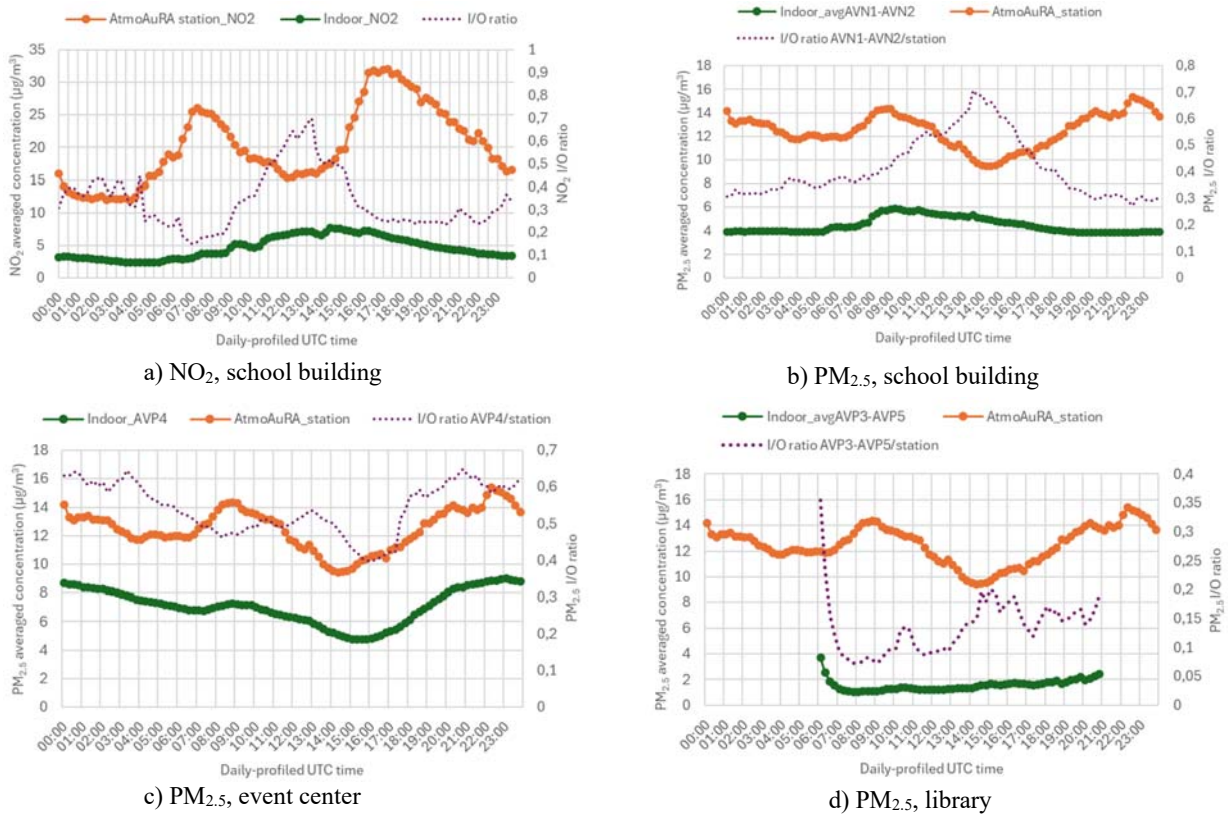


Figure 1 : 15-minutes-averaged concentration in a daily profile of the campaign period

#### 4 DISCUSSION

Considering the daily profile of I/O ratios, having the inside measured concentration above the outside measured concentration never happens for both pollutants. In the case of PM<sub>2.5</sub>, early morning corresponds to the library's highest I/O ratio, when the ventilation is turned on back for the day. Otherwise, the indoor concentration of the library stays far below the outside one during the day. That can be due to the performance of filters. For both pollutants, the peak of I/O ratio for the school is at mid-day, and a weaker one occurs after midnight in the case of NO<sub>2</sub>. No clear pattern comes out of the daily profile of the event center, which could be due to an activation of ventilation only when a meeting takes place in the monitored room (seven events reported on seven different dates, four during the day and three at the end of the day or at night). The same can be said of the library, and in this case, it might be due to a random presence of visitors and rooms with a larger volume, but there are two peaks, one in the morning and a wider one in the afternoon. Except for the library, the daily profiles let us guess a transfer of the pollution from the outside to the inside, especially in the case of the event center. Time series give a better indication of potential delays of the transfer, and further analysis will allow an accurate determination. To enhance the knowledge of the air pollution transfer in the building, the impact of different parameters should be further investigated. For example, measurements *in situ*, including air flows of the ventilation systems will be used to characterize the ventilation parameters. The CO<sub>2</sub> concentration decay method could be implemented, like Persily did (Persily, 1997), to determine Air Change Rate (ACR) in the rooms, specifically for the school and its manual airing.



## 5 CONCLUSION & PERSPECTIVES

The monitored rooms in these three different buildings present specific indoor air pollution temporal evolution, and we observe that the less polluted building is the library (mechanically ventilated with filters), followed by the event center (mechanically ventilated when occupied only) and at last, by the school (manual ventilation). On a daily profile point of view, both NO<sub>2</sub> and PM<sub>2.5</sub> I/O ratios never exceed the value of 1, but they can be close to it, when considering the school. Looking specifically at the median I/O ratio, higher outdoor pollution seems to rise the PM<sub>2.5</sub> transfer to the buildings, except for the school, which shows in this study the limit of that indicator and/or which indicates that the data quality step needs to be strengthened if working with I/O ratios. As for NO<sub>2</sub>, we found out a daily-profiled I/O ratio under the value of 1 and an hourly-concentration below the EAQI' Fair class upper limit.

As for the experiment method, a configuration where PM<sub>2.5</sub> sensors are installed on the façade, as near as possible of the air intake, led to similar measurements between the three buildings, that are in the same neighbourhood. Nonetheless, an even greater remarkable point is that the three measurements seem to be well correlated with the ambient air quality monitoring station in their surroundings, excepting when the outside PM<sub>2.5</sub> pollution rises in a peak.

Thus, this study brings important information for a global comprehensive understanding of the dynamics of outdoor/façade/ indoor concentrations of particulate matter (PM<sub>2.5</sub>) and gaseous pollution (NO<sub>2</sub>), because data were produced from different monitored buildings/ventilation systems. A second step in this work will be to characterize the transfer into the buildings, comparing the following results from both points of view of the façades and the station: amount of concentration, time delay. And if possible, the health impact of this transfer will be determined. We will analyse an additional pollutant, measured in each building, that is black carbon, particularly specific to outdoor emissions. A third step will be to conduct a second measurements campaign, in three other public buildings and in the same region. Finally, the results of the experimental phasis will be used in air pollution and aeraulic modelling programs to further investigate the question of the transfer control and its parameters.

## 6 ACKNOWLEDGEMENTS

This work was founded by the French Agency For Ecological Transition (ADEME) within the AQACIA program (project no.: 2204D0048). All of the authors would like to thank Atmo Auvergne Rhône-Alpes, the local air pollution surveillance actor, for providing data, material and support. The Grand Chambéry and the Département of Savoie, local territorial actors, for support and making public buildings available.

## 7 REFERENCES

- Bi et al. (2021). Characterizing Outdoor Infiltration and Indoor Contribution of PM<sub>2.5</sub> with Citizen-Based Low-Cost Monitoring Data. *Environmental Pollution* 276 (May 2021): 116763. <https://doi.org/10.1016/j.envpol.2021.116763>.
- Bucur et Danet (2019). Indoor/outdoor correlations regarding indoor air pollution with particulate matter. *Environmental Engineering and Management Journal* 18, no. 2 (February 2019): 425-32.
- Carslaw, David C., and Karl Ropkins. (2012). Openair An R Package for Air Quality Data Analysis. *Environmental Modelling & Software* 27–28: 52–61. <https://doi.org/10.1016/j.envsoft.2011.09.008>.

European Environment Agency, *About the European Air Quality Index*

<https://www.eea.europa.eu/themes/air/air-quality-index>

Nezis et al. (2022). Linking Indoor Particulate Matter and Black Carbon with Sick Building Syndrome Symptoms in a Public Office Building. *Atmospheric Pollution Research* 13, no. 1 (January 2022): 101292. <https://doi.org/10.1016/j.apr.2021.101292>.

Persily. (1997). Evaluating Building IAQ and Ventilation with Indoor Carbon Dioxide.

<https://www.aivc.org/resource/evaluating-building-iaq-and-ventilation-indoor-carbon-dioxide>

# Leakage in Large-Building Duct Systems: Modelling the Savings for Various Applications

Mark Modera<sup>\*1,2</sup>, Mahmood Farzaneh Gord<sup>2</sup>

*1 University of California, Davis  
215 Sage St Suite 100  
Davis CA 95616, USA  
mpmodera@ucdavis.edu*

*2 Aero seal Inc.  
225 Byers Road  
Miamisburg, OH 45342, USA*

## ABSTRACT

Decisions about whether it is worthwhile to seal duct leakage in large buildings are based upon different needs in different applications, ranging from the need to meet diffuser/exhaust-grille flow requirements for ventilation regulations, to meeting fire-safety specifications, to maintaining zone pressurization/depressurization requirements in hospitals. However, many decisions about whether to seal duct leaks are based upon the energy and peak-electricity-demand implications of sealing that leakage. This paper discusses the varying energy and peak-demand savings mechanisms for different types of duct systems, starting with simple exhaust ventilation systems, and including Constant Air Volume systems as well as Variable Air Volume systems with different means for controlling Outdoor Air. The magnitudes of different savings mechanisms (fan power, Outdoor Air conditioning, terminal reheat, peak power reduction) will be compared for different system types, and the functional dependence on leakage level will be presented for each energy implication for each type of HVAC system.

## KEYWORDS

Ducts, Leakage, Commercial Buildings, Energy Modelling, Energy Saving

## 1 INTRODUCTION

Duct leakage has often been an unseen culprit relative to the performance of air distribution systems in buildings. Unlike water leakage, which makes its presence undeniably obvious, duct leakage is often not obvious. Decisions about whether there is enough duct leakage to justify sealing that leakage in an existing large building depend upon understanding the magnitude of that leakage, as well as the implications of that leakage in different applications. These implications range from the need to meet diffuser/exhaust-grille flow requirements for ventilation regulations, to meeting fire-safety specifications, to maintaining zone pressurization/depressurization requirements in hospitals. However, many decisions about whether to seal duct leaks are based upon the energy and peak-electricity-demand implications of sealing that leakage.

The prevalence of duct leakage in non-residential buildings, as well as some of the energy savings mechanisms associated with reducing that duct leakage have been presented in various papers over the years. This includes work on European duct systems by Carrie et al. (Carrie, 2000), as well as work on US duct systems by Modera et al. (Modera, 2014). Other

work includes modelling of energy savings from duct sealing for Variable Air Volume (VAV) systems by Franconi et al. (Franconi, 1998), as well as by Wray and Matson (Wray, 2003), and even an analysis of the specific impacts of duct sealing on Outdoor Air (OA) conditioning by Krishnamoorthy and Modera (Krishnamoorthy, 2016).

This paper builds upon earlier work, focusing on the implications of system type and building controls on the value of duct sealing, including the impacts on duct-sealing energy savings associated with different fractional outdoor-air and relief-air rates. The implications of sealing duct leakage are explored numerically using a hypothetical comparison of the impacts of sealing 20% leakage in three different types of exhaust systems, and two types of Constant Air Volume (CAV) supply systems. The implications of Outdoor Air (OA) and building pressure control for Variable Air Volume (VAV) systems are also explored.

## **2 MECHANISMS BEHIND ENERGY SAVINGS**

There are several mechanisms by which duct leakage impacts energy use, however all these mechanisms result in changes in either fan power or thermal-conditioning energy use. The basic mechanism for duct leakage increasing fan power is that the fan must move more air to satisfy building needs when the ducts leak. This generally translates to either: a) providing specified flows at grilles or diffusers, or b) meeting the thermal conditioning needs of building zones, or both. The major input variables for determining the fan power impacts of duct sealing are the operating schedule of the fan system, and the relationship between flow and power. Concerning the latter, the fan power for exhaust systems typically scales with the flow cubed, whereas for supply systems it is generally assumed to scale with the flow raised to the power 2.4. The cube law stems from the fact that turbulent-flow duct pressure loss scales with the flow rate squared, however the 2.4 power is an empirical observation that likely stems from some pressure losses scaling with the flow raised to a power less than 2. Thus, the 2.4 power likely varies between buildings and systems, however that variation will not be addressed in this paper.

Thermal conditioning implications of duct leakage are far more complex, stemming from different mechanisms for different systems. For both fan power and thermal energy implications of leakage, the implicit assumptions behind the analyses in this paper are that the zone air flow and thermal conditioning needs of the building will be met to the same extent before and after sealing duct leakage. That said, other building needs might be met to differing extents before and after sealing. For example, depending on the control mechanisms for ventilation and building pressurization, those operating parameters may change after sealing. Specifically, if building pressurization and Outdoor Air flow rates are not actively controlled, both are likely to be reduced after sealing.

### **2.1 Thermal Conditioning Impacts**

There are four categories of duct leakage impacts on thermal conditioning: 1) cooling required to remove the heat generated by excess fan power, 2) cooling or heating required to condition any changes in outdoor air flow associated with duct leakage, 3) changes in the amount of terminal reheat required due to duct leakage, and 4) changes in the enthalpy of air being exhausted from the building due to duct leakage. The first two categories have been analysed in several of the papers referenced above, however the latter two categories have received much less attention.

Concerning the cooling required to remove fan heat, the basic idea is that all fan power ultimately turns into heat, which then must be removed by the cooling system. However, for

exhaust systems this is not the case, and for supply systems the analysis can be complicated by the changes in Sensible Heat Ratio seen by the cooling coil associated with fan heat (which is all sensible). In addition, as will be seen below, some of that fan heat is exhausted from the building in relief air flows, in particular fan heat associated with fans. All these complications for supply systems will not be addressed in this paper, instead we will use the following simple approximations: 1) all supply fan heat shows up as a load, 2) half of the fan power is in the return fan, and 3) the fractional relief air times the return fan heat represents the fan heat that does not show up as a load.

The second mechanism, increased outdoor air conditioning due to duct leakage, was discussed in detail by Krishnamoorthy and Modera (Krishnamoorthy, 2016), however that paper assumed that the Outdoor Air (OA) flow into the building was a fixed fraction of the supply air flow, which implies that the increased fan flow associated with duct leakage results in increased outdoor air flow. Another implicit assumption in that paper is that the OA flow is all exhausted through the building envelope at the zone-air enthalpy. Examining building operations more carefully, this latter assumption is not appropriate in many buildings, namely any buildings that have relief air flows. The first assumption is also not valid for buildings that control the absolute OA flow and/or the pressure differential across the building shell through some combination of damper controls and supply/return/relief fan controls. The problems with these assumptions are most obvious for hospitals, which generally operate at high OA fractions (50-100% of supply flow), and which therefore must have relief flows to avoid over-pressurization of the building envelope. Moreover, because the outdoor air flows are so large for hospitals, they are very likely to have active building pressurization control. The impact of assuming that all exhausted air is at zone-air conditions can be quite dramatic for hospitals, which exhaust a large fraction of the building air rather than recirculating that air. What this means is that a significant fraction of supply duct leakage into the return plenum (i.e. ceiling-plenum return) is exhausted from the building through the relief damper, thereby changing the enthalpy of the air leaving the building. This is the third category of thermal conditioning impacts due to duct leakage listed above. It should be noted that hospitals are also more likely to have ducted return systems, but that such installations are not analysed in this paper, as such an analysis depends upon the ratio of supply to return leakage levels.

Finally, the fourth category of thermal conditioning impact, changes in reheat due to duct leakage, has not seen much attention. Moreover, it is important to note that this impact only arises for leakage downstream of terminal boxes (i.e. downstream of the terminal reheat coils), and the impact has opposite signs for CAV and VAV systems. For this analysis, the implicit assumptions are that zone loads are the same with and without duct leakage, and therefore, assuming that the supply air temperature is unchanged by duct leakage, that the supply air flows into those zones are the same with and without duct leakage. This assumption could be questioned, as higher velocities in trunk sections when there is duct leakage could result in lower thermal losses to the return plenum.

In the case of CAV systems, the assumption of constant zone air flow means that the fan flow needs to be adjusted manually after sealing to maintain the same zone air flow. For VAV systems it is assumed that the zone thermostats automatically adjust the zone flows, and that the supply fan automatically adjusts its flow based upon the flow through the VAV boxes (i.e. it is controlled to maintain a specific pressure at some point in the supply trunk, which automatically responds to the openings of the VAV dampers, and to any leakage from the supply trunk).

Returning to the location of the leakage, it should be clear that leakage upstream of the terminal reheat coils will not impact the amount of reheat, based upon the assumption that the air temperature arriving at the terminal boxes is not impacted by duct leakage. On the other hand, leakage downstream of the reheat coil does impact reheat. In the case of CAV systems this impact can be quite dramatic, as the amount of reheat scales with the air flow passing through the terminal box, which is higher when there is duct leakage downstream of the terminal box. This stems from the assumption that the zone air flow remains unchanged after sealing, and that the thermostat is therefore producing the same temperature of that air after sealing. Thus, the extra reheated air is leaked into the return plenum, and the extra heat in that return air must be removed by the cooling coil to produce the desired supply air temperature, resulting in a two-fold impact. For a VAV system, when reheat is being used to actually heat zones (versus to avoid over-cooling zones), the effect of downstream duct leakage is the same as for CAV systems. On the other hand, when reheat is being used to increase the temperature of the minimum ventilation air flow to the zone to avoid over-cooling a zone, sealing duct leakage has the opposite effect on reheat. This is because leakage downstream of the VAV box reduces the amount of cold air being delivered to the zone, thereby reducing the over-cooling, and thereby reducing the need for reheat. Due to these complexities, and the complexity of coming up with a simple estimate of the amount reheat required in a given building in a given climate, the reheat impacts of duct leakage are only addressed in a cursory manner in the discussion section of this paper.

### 3 LEAKAGE IMPACT COMPARISON

To illustrate the variability in savings associated with sealing duct leakage in different applications, a comparison of the impacts of sealing the same amount of duct leakage in two exhaust-system applications and two CAV supply-system applications. The analyses are performed assuming that 100% of the leakage is sealed. Although that is not generally achievable, the math becomes much simpler, and the savings magnitudes will roughly scale when the more typical 80-90% sealing is achieved. The basic assumptions for systems being sealed are presented in Table 1, which shows that all applications are assumed to have the same zone flows, duct leakage, and total pressure differential seen by the fan. In addition, all applications are assumed to be in New York City for climate purposes, and the zone flow is assumed to be the same before and after sealing, implying that the fan speed is adjusted to make that the case. Also, for all cases initial duct leakage is assumed to be 20%, initial total fan pressure is assumed to be 500 Pa, fan efficiency is assumed to be constant at 50%, and fan motor efficiency is assumed to be constant at 80%. Finally, for all thermal conditioning calculations, it is assumed that the conditioning is done with a heat pump, with a constant COP of 3 for both heating and cooling.

Table 1: Assumptions for Comparison of Duct Sealing Impacts

Application	Zone Flow [l/s]	Initial OA Fraction	Initial Relief Air Fraction	Operating Hours
CAV Office Supply	23,600	20%	10%	Weekdays 07-18
CAV Hospital Supply	23,600	70%	60%	8760 h/year
Office Exhaust	23,600	N/A	N/A	Weekdays 07-18
Multifamily Exhaust	23,600	N/A	N/A	8760 h/year

### 3.1 Exhaust System Savings

Starting with the exhaust systems, the fan power savings is calculated as follows:

$$\text{Initial Fan Flow} = \text{Zone Flow} / (1 - \% \text{Leakage}) = 23,600 / (1 - 20\%) = 29,500 \text{ [l/s]} \quad (1)$$

$$\text{Initial Fan Power} = 29,500 \text{ [l/s]} / 1000 \text{ [l/m}^3\text{]} \times 500 \text{ [Nt/m}^2\text{]} / 50\% / 80\% = 36.9 \text{ kW} \quad (2)$$

$$\text{Final Total Fan Pressure} = 500 * (23,600 / 29,500)^2 = 320 \text{ [Pa]} \quad (3)$$

$$\text{Final Fan Power} = 23,600 \text{ [l/s]} / 1000 \text{ [l/m}^3\text{]} \times 320 \text{ [Nt/m}^2\text{]} / 50\% / 80\% = 18.9 \text{ kW} \quad (4)$$

To determine annual savings, the difference between these two power levels needs to be integrated over all operating hours in the year.

For exhaust systems, the only thermal conditioning savings is associated with having to condition less outdoor air after sealing, however the outdoor air conditioning savings is application dependent. For an exhaust-ventilated apartment building, any excess exhaust air shows up as an increased infiltration load, assuming that the leakage is within the conditioned envelope of the building. To calculate the savings over an entire year, the integrated indoor to outdoor enthalpy differential needs to be calculated for the climate in which the system is located using appropriate conditions for the indoors during each season. For this we define:

$$\text{ECDH} = \sum (\square_{OA} - h_{zone}) \quad \text{if } (\square_{OA} - h_{zone}) > 0, \text{ else } 0 \quad (5a)$$

$$\text{EHDH} = \sum (\square_{zone} - h_{OA}) \quad \text{if } (\square_{zone} - h_{OA}) > 0, \text{ else } 0 \quad (5b)$$

$$Q_{cool} = 1.2 \text{ [kg/m}^3\text{]} \times \text{Flow [l/s]} / 1000 \text{ [l/m}^3\text{]} \times \text{ECDH [kJ h/kg]} \quad (6a)$$

$$Q_{heat} = 1.2 \text{ [kg/m}^3\text{]} \times \text{Flow [l/s]} / 1000 \text{ [l/m}^3\text{]} \times \text{EHDH [kJ h/kg]} \quad (6b)$$

where:

$\square_{OA}$  is the enthalpy of the incoming outdoor air [kJ/kg], and

$\square_{zone}$  is the enthalpy of the air leaving the zones [kJ/kg]

For an exhaust system in a commercial building, the impact is different, as excess exhaust air shows up as potential changes in flow through the OA intake of the supply air system. Assuming that the pressure across the envelope of the building is being controlled, the amount of outdoor air decreases after sealing, assuming further that there is always more air needed for pressurization than for ventilation. In this case, the cooling sum in Equations 5a and 6a remain the same, however the heating sum in Equations 5b and 6b changes, as the supply system is producing cold air, which means that the penalty for bringing in excess outdoor air is based upon the enthalpy difference between the mixed air (combination of outdoor air and zone air) and the supply air, i.e., substituting  $(\square_{sup} - h_{mixed})$  into Equation 5b. Note that  $\square_{OA}$  comes into this calculation, as  $\square_{mixed} = \square_{zone} \times (1 - \%OA) + \square_{OA} \times \%OA$ .

The savings described above were turned into a breakdown of annual savings in Table 2, using 2200 hours of operation for the office application (200 days x 11 h/day), and ECDH and EHDH values for apartment building and office applications, calculated using TMY3 data for New York City.

Table 2: Duct Sealing Impacts for Sealing 20% Exhaust Leakage for 23,600 l/s, 500 Pa system in NYC

Application	Fan Power [kWh]	ECDH [kJ h/kg]	EHDH [kJ h/kg]	Cooling [kWh]	Heating [kWh]	Total Savings [kWh]
Office Exhaust	39,600	3606	99	8509	234	48,300
Multifamily Exhaust	157,600	6387	22,550	15,073	53,217	225,900

### 3.2 Supply System Savings

Turning to the CAV supply systems, the fan power savings is calculated using Equations 1-4, except that the Final Total Fan Pressure =  $500 \cdot (23,600/29,500)^{1.4} = 366$  [Pa] is used in Equations 3 and 4, yielding a Final Fan Power of 21.6 kW.

For supply systems, the thermal conditioning impact of duct sealing includes fan power, which is calculated as follows:

$$\text{Fan Heat Cooling Electricity Savings} = (36,900 - 21,600) [W] / 3 [-] \cdot (1 - 0.5 \cdot \% \text{relief}) \quad (7)$$

This translates to  $5100W \cdot (1 - 0.5 \cdot 10\%) = 4845W$  for the office building, and  $5100W \cdot (1 - 0.5 \cdot 60\%) = 3570W$  for the hospital, based on parameters in Table 1.

To better understand the analysis of outdoor air conditioning savings, the air flow pathways for the CAV supply system are illustrated in Figure 1. In this Figure the red arrows represent hot outdoor air being pulled into the building, the light green arrows represent air at zone conditions, and the blue arrows represent air at supply conditions. The red dotted line represents the envelope of the building. Note that some of the zone air leaves the building as “Pressurization Air”, some is returned to the supply fan, and some is exhausted as relief air. As for the supply air, some is leaked out into the ceiling-plenum return through supply duct leakage, some of which is returned to the supply fan, and some of which is exhausted as relief air. Another important distinction for the CAV system analysis is that they are assumed to be non-changeover, meaning that the air handler provides cold air all year round, rather than switching to warm air in the winter. This makes sense for any system that is serving both core and perimeter zones, as core zones need cooling year-round.



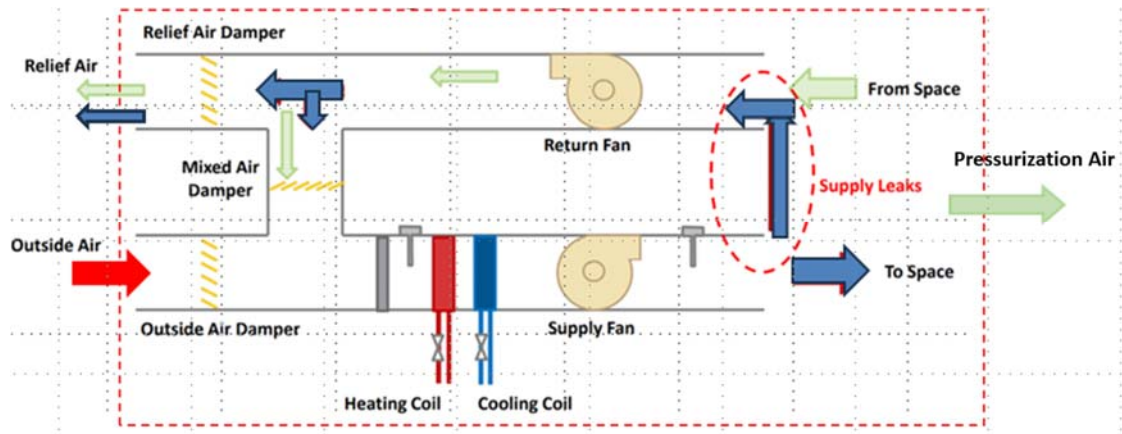


Figure 1: Schematic of Air Flow Pathways for CAV Supply System

Focusing on Figure 1, the savings associated with conditioning OA depends upon how the building is adjusted after duct sealing. It is assumed that the fan is slowed down after sealing to produce the air flow into the zones, but in addition to slowing down the fan, the dampers controlling the OA flow and the relief flow must be adjusted to keep the same ventilation air flow rate and building pressure as before sealing. Thus, savings analyses are performed assuming that this damper adjustment occurs, and assuming that it does not happen. Although this adjustment might or might not happen in an office building setting, it is assumed to always occur in a hospital setting. For any application where the damper adjustment occurs, the effect of exhausting supply leakage through the relief damper is captured by equations 8 to 10:

$$Q_{cool,0\%} = \rho \times \dot{V}_{OA} \times (\square_{OA-h \text{ zone}}) \quad (8)$$

$$Q_{cool,leaky} = \rho \times \dot{V}_{OA} \times (\square_{OA-h \text{ zone}}) + \rho \times \dot{V}_{leak} \times \dot{V}_{relief} / (\dot{V}_{leak} + \dot{V}_{zone} - \dot{V}_{env}) \times (\square_{zone-h \text{ sup}}) \quad (9)$$

$$Q_{cool,savings} = \rho \times \dot{V}_{leak} \times \dot{V}_{relief} / (\dot{V}_{leak} + \dot{V}_{zone} - \dot{V}_{env}) \times (\square_{zone-h \text{ sup}}) \quad (10)$$

where:

$\dot{V}_{OA}$  is the incoming outdoor air flowrate [l/s],

$\dot{V}_{leak}$  is the supply duct leakage flowrate [l/s],

$\dot{V}_{relief}$  is the outgoing relief air flowrate [l/s],

$\dot{V}_{zone}$  is the supply air flowrate to the conditioned zones [l/s],

$\dot{V}_{env}$  is the outgoing air flowrate through the building envelope [l/s], and

$\square_{sup}$  is the enthalpy of the supply air [kJ/kg].

It is worth noting that this savings is independent of outdoor air conditions, which is not the case if the dampers are not adjusted. In that case there is an additional savings associated with reduction in outdoor air flow when the fan is slowed down. The change in outdoor air flow is the product of the OA fraction, the fractional leakage, and the fan flow. The annual implications of that flow change can then be calculated using Equation 6a, while the annual implications of Equation 10 are calculated by simply multiplying Equation 10 by the number of operating hours in a year. For heating of outdoor air, the only savings occur when the dampers are not adjusted, in which case the savings are calculated by using the OA flow change in Equation 6b, along with EHDH calculated using Equation 11, which only indicates

heating savings when the OA is so cold as to make the mixed air enthalpy lower than the supply air enthalpy, which is the same value used for office exhaust systems:

$$EHDH = \sum (\square_{\text{sup}} - h_{\text{mixed}}) \quad \text{if } (\square_{\text{sup}} - h_{\text{mixed}}) > 0, \text{ else } 0 \quad (11)$$

The annual implications of fan power reduction are calculated from the instantaneous 36.9 kW-21.6 kW, and the fan-power cooling savings in Equation 7. These values need to be multiplied by operating hours, which in the office-building example are 2200 h, and for the hospital example are 8760 hours.

The results of these calculations are summarized in Table 3.

Table 3: Duct Sealing Impacts for Sealing 20% Supply Leakage for 23,600 l/s, 500 Pa system in NYC

Application	Fan Power [kWh]	Fan-Heat Cooling [kWh]	Extra OA Cooling [kWh]	Total OA Cooling [kWh]	OA Heating [kWh]	Total Savings [kWh]
Office CAV Supply (fixed %OA)	33,638	10,659	1,702	3,938	47	49,984
Office CAV Supply (fixed OA, $\Delta P_{\text{building}}$ )	33,638	10,659	0	2,236	0	46,533
Hospital CAV Supply (fixed OA, $\Delta P_{\text{building}}$ )	133,942	31,273	0	53,426	0	218,641

The larger savings for hospitals in Table 2 is not surprising, considering that they operate roughly four times as many hours in a year, however some of the results in Table 2 merit some explanation. For example, the fan power savings for hospitals is 4 times higher than for offices, but the fan heat savings is only three times higher. This is because much of the excess fan heat is exhausted through the higher relief air flows in hospitals. The flip side of this is that the relief flows dramatically increase the outdoor air conditioning savings, by a factor of 24, due to a large fraction of supply duct leakage being simply exhausted to the outdoors. The results for all the different exhaust and CAV systems can be normalized by expressing the savings in annual kWh saved per cfm sealed, which are summarized in Figure 1.

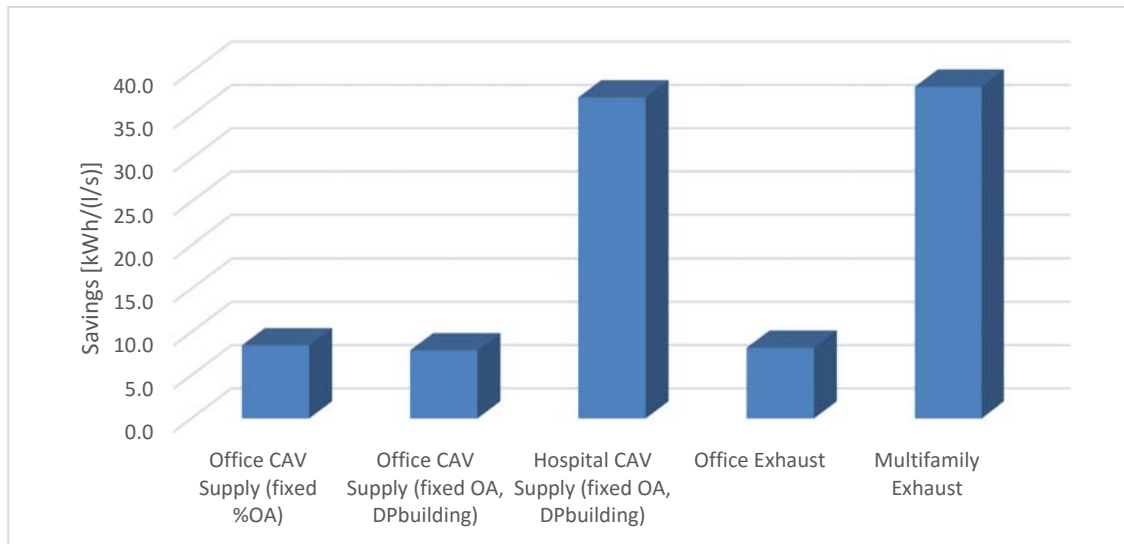


Figure 2: Normalized energy savings from duct sealing

#### 4 DISCUSSION

Although this paper provides fairly comprehensive analyses of duct-sealing savings for CAV and exhaust systems, three key issues were not addressed, namely: 1) the impact of duct leakage on terminal reheat energy use, 2) the magnitude of duct leakage savings for VAV Systems, and 3) the impact of energy recovery on exhaust or relief air.

Starting with the issue of terminal reheat, although the mechanisms for reheat savings were discussed above, the magnitude of the savings was not calculated. This magnitude can however be roughly estimated by assuming that fan power is roughly 40% of HVAC energy use, that reheat is 20% of HVAC energy use for a CAV system, and that 50% of the system leakage is downstream of the terminal boxes. Based upon these assumptions, sealing the 10% leakage downstream of the terminal boxes (50% of 20% leakage) means that the reheat would be reduced by 10%, and that the cooling required to recondition the reheated air being recirculated would be roughly twice the reheat energy (cooling it down to zone-air enthalpy, then down to supply air enthalpy). Thus, for the CAV example above, the annual fan power for the office building is  $36.9 \text{ kW} \times 2200 \text{ hours} = 81,180 \text{ kWh}$ , which means the total reheat energy use would be  $40,590 \text{ kWh}$ , 10% of which is  $4,059 \text{ kWh}$ , followed by  $7306 \text{ kWh}$  ( $2 \times 4059 \times (1 - 10\% \text{ relief})$ ) of cooling, which represents a 23% increase in savings. The fractional increase in savings turns out to be lower for the hospital example, namely 13%, because of the larger relief fraction in that example.

Turning to VAV systems, the savings mechanisms are similar to those for CAV systems, however for the same design flow and pressure there should always be lower absolute savings for VAV systems, as they always have lower fan power due to the fan ramping down at part load, and lower absolute leakage downstream of VAV boxes due to reduced flows at low loads and constant fractional leakage downstream of VAV boxes. Also, VAV systems will not experience the reheat savings associated with sealing leakage downstream of terminal boxes in CAV systems. In fact, there should be a small absolute increase in terminal reheat due to sealing of downstream leakage in VAV systems, as described above.

As for the impact of energy recovery on exhaust or relief air, it should be clear that these systems will have lower savings with respect to outdoor air conditioning, as the overall magnitude of these energy flows will be considerably lower. That said, executing energy recovery could be fairly straightforward for relief air, but not so much for exhaust systems. The issue for exhaust systems is that an additional fan plus supply ductwork would be needed to execute that recovery, unless the exhaust is all located close to supply-air air handling unit.

Finally, it should be noted that for simplicity the pressure difference seen by the fan was assumed to be the same in all example applications, however this is generally not realistic. Supply systems typically have significantly larger fan pressure differentials due to filters, coils, and pressure drops in terminal boxes, all told approximately 2 to 3 times larger than exhaust systems for the same flows. This significantly increases the savings for supply systems relative to exhaust systems.

## 5 CONCLUSIONS

The key conclusion to be drawn from this paper is that the savings associated with sealing a given amount of duct leakage varies dramatically between applications, with the largest factors being the operating hours of the system, the relief air fraction, and the impact of sealing on OA conditioning needs. Specifically, the savings per l/s of leakage sealed ranges from 8 kWh per l/s to 38 kWh per l/s, a factor of 4.

Another important conclusion is that there can be significant thermal conditioning savings that are independent of climate, which are tied to the relief air fraction, making this an important savings mechanism in hospitals. Moreover, this savings occurs even if the outdoor air and relief air flows remain constant before and after sealing.

## 6 REFERENCES

- Aydin, C., Ozerdem, B., (2006) Air leakage measurement and analysis in duct systems, *Energy and Buildings*, 38 (3) 207–213.
- Carrie, F. R., Bossaer, A., Andersson, J.V., Wouters, P., Liddament, M.W., (2000) Duct leakage in European buildings: status and perspectives, *Energy and Buildings*, 32 (3) 235–243.
- Franconi, E., Delp, W., Modera, M.P., (1998) Impact of Duct Air-Leakage on VAV System Energy Use. *Lawrence Berkeley National Laboratory Draft Report*, LBNL-42417.
- Krishnamoorthy, S., Modera, M., (2016) Impacts of duct leakage on central outdoor-air conditioning for commercial-building VAV systems, *Energy and Buildings* 119, pages 340–351.
- Modera, M., Wray, C., Dickerhoff, D., (2014) Low Pressure Air-Handling System Leakage in Large Commercial Buildings, *HVAC&R Journal* Volume 20, Issue 5, pages 559-569.
- Wray, C., Matson, N., (2003) Duct leakage impacts on VAV System Performance in California Large Commercial Buildings. *Lawrence Berkeley National Laboratory Report*, LBNL-53605.

# Performance of smart ventilation in residential buildings: a literature review

Yu Wang<sup>1</sup>, Daniela Mortari<sup>\*2</sup>, Manfred Plagmann<sup>1</sup>, Nathan Mendes<sup>3</sup>,  
Gaëlle Guyot<sup>2</sup>

*1 BRANZ  
1222 Moonshine Road, RD1,  
Porirua 5381, New Zealand*

*2 CEREMA Centre-Est  
46 Rue Saint-Théobald, 38080  
L'Isle D'Abeau, France*

*\*Corresponding author: daniela.mortari@cerema.fr*

*3 Pontifical Catholic University of Paraná,  
1155 Imaculada. Conceição Street, 80215-901  
Curitiba, Brazil*

## ABSTRACT

Smart ventilation in residential buildings has gained rising attention recently for the benefits of reducing energy consumption and improving indoor environmental quality. This paper presents a review of the smart ventilation in residential buildings papers published from January 2017 to August 2023, as a continuation of (Guyot, Sherman, and Walker 2018) who reviewed the publications in this area up to 2016. A systematic approach was used following the PRISMA protocol. Smart ventilation in residential buildings has been rapidly developed over the past seven years, compared to being an emerging technology prior to 2016. In total, 44 papers were analysed, which consisted of 22 journal articles and 22 conference papers. Belgium appears as the country with the most research activity in this field, followed by France, the United States, and Denmark. Most of these smart ventilation studies have been conducted via the simulation approach. Single-family dwellings and a unit in apartment buildings are the settings for most of the reviewed studies. The findings show the evolution of trends in smart ventilation over the years, in which health has emerged as an indicator for evaluating ventilation system performance. Furthermore, the new developments include performance-based assessment, decentralised ventilation, using data-driven methods to form control strategy, and the Internet of Things. Regarding indoor air quality, in addition to CO<sub>2</sub> and relative humidity, new indicators have been applied, such as formaldehyde, PM<sub>2.5</sub> and volatile organic compounds. The challenge related to the diversity of simulation model input data and the performance indicators was highlighted. Though the research in this area has rapidly grown, international collaborations are lacking, as is the field testing of the proposed strategies.

## KEYWORDS

Demand-controlled ventilation, indoor air quality, energy consumption, occupant behaviour, performance indicators

## 1 INTRODUCTION

With the goal of reducing ventilation energy consumption and improving the level of thermal comfort and indoor air quality (IAQ), the concept of smart ventilation was introduced in 1980. A working group of Air Infiltration and Ventilation Centre (AIVC) experts has defined smart ventilation as ‘a process to continually adjust the ventilation system in time, and optionally by location, to provide the desired IAQ benefits while minimizing energy consumption, utility bills, and other non-IAQ costs, such as thermal discomfort or noise (Durier, Carrié, and Sherman 2018). The key concept of smart ventilation is to use controls to ventilate more where and when it provides either an energy or IAQ advantage or other non-IAQ cost, and less where and when it provides a disadvantage (Guyot et al., 2018). The parameters to which smart ventilation systems can respond include occupancy, indoor temperature and/or contaminants, outdoor temperature and humidity, outdoor air quality, electricity grid needs, and the operation of other air moving or cleaning systems (Durier et al. 2018). Smart ventilation, which responds

to the direct sensing of indoor contaminants, is a form of demand-controlled ventilation (DCV). Thus, smart ventilation includes DCV.

The goal of this paper is to provide an update on developments in the smart ventilation field from 2017 to 2023 as a continuation of the literature review conducted by (Guyot et al. 2018). This previous review showed that up to 60% of ventilation energy savings can be obtained without compromising IAQ. Since 2016, there have been many new developments in residential smart ventilation. Energy savings in the building sector are highly demanded, as is the need to provide an acceptable IAQ, which makes ventilation play a more crucial role. Since residential buildings are often unoccupied or occupied at a lower level, the smart ventilation strategy is extremely important to achieve the high potential of energy savings and assure a good IAQ. In this context, a review is conducted with the aim of summarizing the evidence of the benefits of implementing smart ventilation in residential homes, focusing on the ventilation strategies related to energy consumption, IAQ, comfort, health, and other advantages. This paper mainly shows the review results of the occupant's pattern (behaviour), pollutants and contaminants generation scenarios, and ventilation system performance indicators.

## **2 METHODOLOGY**

A systematic review was performed according to the PRISMA (Preferred Reporting Items for Systematic Reviews and Meta-Analyses Statement) recommendations (Liberati et al. 2009). The search process aimed to answer the questions: How much is the indoor environment quality (IEQ) improved, and how much energy savings are obtained with the use of smart ventilation in residential buildings compared to a reference system? The electronic databases used to perform the search were the Web of Science, Scopus, and AIVC collections. The AIVC is the International Energy Agency's information centre on energy-efficient ventilation. This review included articles published from January 2017 to August 2023.

The string used in searching the database combined three groups of keywords related to ventilation, IEQ, and energy efficiency, as presented as follows: {"advanced control" OR "airflow control" OR "algorithm" OR "building ventilation" OR "demand-controlled ventilation" OR "demand ventilation" OR "emission control" OR "performance based" OR "smart ventilation" OR "ventilation control" OR "ventilation system" OR "window open"} AND {"cost" OR "energy" OR "consumption" OR "efficiency" OR "power demand"} AND {"indoor air quality" OR "IAQ" OR "air quality" OR "home" OR "residential" OR "indoor environment" OR "humidity" OR "thermal comfort"}. The search string was permuted in both the Web of Science and Scopus databases, with an integrated search in the article title, abstract, and keywords. Our search was limited to publications written in English. The AIVC bibliographic database AIRBASE was searched using the 'Title contains (1 word)' option with the words 'demand' or 'control' or 'smart' in the publication title from 2017 to 2023. After the databases were searched, the duplicated papers were excluded, and inclusion and exclusion criteria were generated to guide the selection process of the articles. This process was carried out by using the platform Rayyan, which is a free tool that enables authors to classify articles in a blinded mode, reducing the risk of bias.

## **3 RESULTS**

### **3.1 Papers context**

Out of 754 papers (after removing the duplicates) obtained from the search, 681 papers were excluded based on manually reviewing their titles and abstracts, and 29 papers were excluded

after fully reviewing the paper. In total, 44 papers were included in this review, which consisted of 22 journal articles and 22 conference papers. Belgium, France, and the United States appear as the countries with the majority of publications in this research topic, where 61% of the included papers originated from these three countries. Considering the climatic conditions, many studies on residential smart ventilation were carried out in Northwest Europe, where winters are mild and summers are cool.

When analysing the co-occurrence of keywords reported in the included papers, the evolving trends in smart ventilation publications reveal a shift. Publications from 2017 to 2021 focused on themes such as CO<sub>2</sub> and humidity-based control ventilation, energy savings, and building-generated pollution, while publications after 2022 emphasize themes such as health, pollutant-based approaches such as volatile organic compounds (VOCs) and PM<sub>2.5</sub>, performance-based assessment, decentralised ventilation, data-driven methods, and the Internet of Things (IoT).

From the total included papers, 75% (33 studies) used the simulation approach, 20% (nine studies) were experimental studies that measured the performance of the ventilation system, and 5% (two studies) combined both the simulation and experimental approaches. Regarding the study subjects, 80% used either single-family detached houses, typical apartment units, or both. This review paper focuses on results of the simulation studies.

### **3.2 Occupant's pattern, and pollutants and contaminants generation scenarios**

The occupant's pattern has a significant impact on ventilation performance because their behaviour dictates the pollutant emission scenarios, whether bio-effluents or pollutants from indoor activities such as cooking, showering, and cleaning, among others. In addition, the knowledge of occupancy behaviour enables the prediction of occupant exposure to pollutants. Many efforts have been devoted to addressing occupant behaviour in residential buildings, including monitoring occupancy, developing occupant behaviour models, and applying those models in building performance simulation (Balvedi, Ghisi, and Lamberts 2018; Franceschini and Neves 2022). When analysing the schedule pattern used by the authors in this review, we observed wide differences related to the occupants' number (ranging from 1 to 4), time spent at home, school, and work, the schedule of weekdays and weekends, and the occupant's activities. The occupant's pattern data used by authors were often defined according to standards (Carbonare et al. 2019, 2020) or derived from time-use survey data, as presented by (De Jonge and Laverge 2022; Poirier et al. 2021).

The pollutants and contaminants generation scenarios used in the simulation studies, including occupant's bio-effluents and occupant's main activities, are summarised in Table 1. In this review paper, humidity is considered as a contaminant. The generation scenario of these pollutants and contaminants is either from a standard or from an in-situ measurement. In Table 1, the emission rate column shows the values or ranges used by different authors. As it can be observed, the variations are not only the values or ranges but also the units from one study to another. This variation in pollutant generation scenarios results in distinct outcomes in ventilation system performance, making it impractical to compare ventilation strategies.

Table 1: Pollutant and contaminant emission generation scenarios used in simulation studies.

Pollutants and contaminants		Emission rate	Reference
CO <sub>2</sub> (bio-effluent)	Adult awake	12 L.h <sup>-1</sup> , 14.4 L.h <sup>-1</sup> , 16 L.h <sup>-1</sup> , 18 L.h <sup>-1</sup> , 19 L.h <sup>-1</sup> , 10 mg.s <sup>-1</sup> , 8.5 mg.s <sup>-1</sup> , 0.25 L.min <sup>-1</sup> varying from 1.86 e-4 m <sup>3</sup> .s <sup>-1</sup> to 9.69e-4 m <sup>3</sup> .s <sup>-1</sup> depending on the activity level, varying from 15 dm <sup>3</sup> .h <sup>-1</sup> to 35 dm <sup>3</sup> .h <sup>-1</sup> depending on the activity level	(Van Gaever, Laverge, and Caillou 2017) (Pecceu, Caillou, and Gaever 2018) (Poirier et al. 2021) (Walker et al. 2021)
	Adult asleep	10 L.h <sup>-1</sup> , 15 L.h <sup>-1</sup> , 6.5 mg.s <sup>-1</sup> , 1.65e-4 m <sup>3</sup> .s <sup>-1</sup> , 10 dm <sup>3</sup> .h <sup>-1</sup> , 0.20 L.min <sup>-1</sup>	(Ghijssels, Jonge, and Laverge 2022)
	Child awake	6.5 mg.s <sup>-1</sup> , 12 L.h <sup>-1</sup> , 12.6 L.h <sup>-1</sup> , 9 L.h <sup>-1</sup>	(De Jonge, Ghijssels, and Laverge 2022)
	Child asleep	4 mg.s <sup>-1</sup> , 8 L.h <sup>-1</sup>	(Carbonare et al. 2020)
H <sub>2</sub> O (bio-effluent)	Adult awake	55 g.h <sup>-1</sup> , 15 mg.s <sup>-1</sup> , 45 g.h <sup>-1</sup> , 40 – 45 g.h <sup>-1</sup>	(Belmans et al. 2019)
	Adult asleep	40 g.h <sup>-1</sup> , 9 mg.s <sup>-1</sup>	(Filis et al. 2023)
	child awake	10 mg.s <sup>-1</sup> , 41.3 g.h <sup>-1</sup> , 35 g.h <sup>-1</sup>	(Kim, Kim, and Moon 2022)
	child asleep	6 mg.s <sup>-1</sup>	(Müller and Dębowski 2020) (Rojas 2022) (Shin et al. 2018)
H <sub>2</sub> O (human activities)	cooking	1. morning and noon 0.5 L.s <sup>-1</sup> (10min); evening 0.6 L.s <sup>-1</sup> (10min) + 1 L.s <sup>-1</sup> (10 min) + 1.5 L.s <sup>-1</sup> (10min), 2. Breakfast 1512 g.h <sup>-1</sup> , lunch 2268 g.h <sup>-1</sup> , dinner 2844 g.h <sup>-1</sup> , 3. 140 mg.s <sup>-1</sup> , 4. 500 g.h <sup>-1</sup> , 5. Breakfast 50 g/person, lunch 150 g/person, dinner 300 g/person, 6. 1.33·10 <sup>-4</sup> kg.s <sup>-1</sup>	(Van Gaever et al. 2017) (Poirier et al. 2021) (Ghijssels et al. 2022) (De Jonge et al. 2022) (Carbonare et al. 2020) (Belmans et al. 2019)
	dishwashing	130 mg.s <sup>-1</sup> , 200 g.h <sup>-1</sup>	(Filis et al. 2023)
	shower	0.5 L.s <sup>-1</sup> per shower (10min), 1440 g.h <sup>-1</sup> , 330 mg.s <sup>-1</sup> , 500 g.h <sup>-1</sup> , 300 g/shower/person, 7.22·10 <sup>-4</sup> kg.s <sup>-1</sup>	(Johnston et al. 2020) (Kim et al. 2022)
	Laundry room	0.06 L.s <sup>-1</sup> (12h), 252 g.h <sup>-1</sup> , 250 g.h <sup>-1</sup> , Laundry + dry 136.8g/h, 200 g/laundry, 1000 g/drying	
H <sub>2</sub> O plants		30 g.h <sup>-1</sup>	
VOCs Proportional to the floor area		From 4.5 µg.h <sup>-1</sup> .m <sup>-2</sup> to 23.6 µg.h <sup>-1</sup> .m <sup>-2</sup>	
PM <sub>2.5</sub> from cooking		1). 0.0208 mg.s <sup>-1</sup> , 2). From 1.26 mg.min <sup>-1</sup> to 2.55 mg.min <sup>-1</sup> , 3). Per activitie: 70 µg.min <sup>-1</sup> – vacuuming 10 µg.min <sup>-1</sup> - oven 283 µg.min <sup>-1</sup> – grilled, 1483 µg.min <sup>-1</sup> - fried	
Generic contaminant		18 µg/m <sup>2</sup> /h	(Walker et al. 2021)
Formaldehyde		3.06 µg.h <sup>-1</sup> .m <sup>-2</sup> for furniture (wood), 4.50 µg.h <sup>-1</sup> .m <sup>-2</sup> for doors (wood), 3.00 µg.h <sup>-1</sup> .m <sup>-2</sup> for cushion, 4.27 µg.h <sup>-1</sup> .m <sup>-2</sup> for carpet	(De Jonge and Laverge 2022)
Benzene		1.40 µg.h <sup>-1</sup> .m <sup>-2</sup> for furniture (wood), 2.00 µg.h <sup>-1</sup> .m <sup>-2</sup> for cushion, 0.21 µg.h <sup>-1</sup> .m <sup>-2</sup> for carpet	
Naphthalene		5.68 µg.h <sup>-1</sup> .m <sup>-2</sup> for furniture (wood) and 0.47 µg.h <sup>-1</sup> .m <sup>-2</sup> for carpet	
Toluene		11.00 µg.h <sup>-1</sup> .m <sup>-2</sup> for Cushions, 0.20 µg.h <sup>-1</sup> .m <sup>-2</sup> for carpet, 0.5 µg.h <sup>-1</sup> .m <sup>-2</sup> for gypsum	
Limonene		1912 µg.h <sup>-1</sup> .m <sup>-2</sup> for cleaning, 24.8 µg.h <sup>-1</sup> for dishes 1200 µg.h <sup>-1</sup> for shower (soap/shampoo), 2000 µg/event for deodorant	
Naphthalene		3.76 µg.h <sup>-1</sup> Shower (soap/shampoo)	



### 3.3 Ventilation system performance indicators

The most employed indicators to evaluate ventilation performance can be categorised into five groups: IAQ, energy savings, building air exchange rate, comfort, and health impacts. CO<sub>2</sub> and RH are the parameters frequently employed to evaluate smart ventilation performance. This is consistent with the findings previously presented by (Guyot et al. 2018). The indicators applied to evaluate IAQ included CO<sub>2</sub> concentration, CO<sub>2</sub> unmet hours for a specific threshold, CO<sub>2</sub> cumulative exposure exceeding the reference value, percentage of time that CO<sub>2</sub> was above a threshold, PM<sub>2.5</sub> exposure exceeding the reference value, formaldehyde exposure exceeding the reference value, TVOC and VOCs cumulative exposure, and generic pollutant cumulative exposure and concentration. The reference threshold value for CO<sub>2</sub> ranges from 600 ppm to 2000 ppm (Carbonare et al. 2020; Faure et al. 2018; Müller and Dębowski 2020; Van Gaever et al. 2017).

The indicators applied to evaluate energy savings included annual ventilation energy consumption, total energy consumption (by all appliances and the ventilation system), space heating and ventilation system, fan energy savings, energy consumption for cooling, and primary energy consumption. The air exchange rate and air flow rates are related to ventilation indicators, and they have a great effect on energy savings since higher values ventilation demand higher energy consumption for space cooling or heating. On the other hand, higher values indicate higher levels of pollutants dilution, improving IAQ.

The indicators used to evaluate comfort included the percentage of time that temperature is outside the reference range, the unmet hour in which temperature is outside the reference range, the unmet hour in which RH is outside the reference range, and the overheating risk. The air temperature reference ranges from 15 °C to 27 °C (Belmans et al. 2019; De Maré et al. 2019; Johnston et al. 2020). For RH, the setpoint for ventilation control varies, such as 35% < RH < 70% (De Jonge et al. 2022), 30% < RH < 70% (Carbonare et al. 2020; De Maré et al. 2019), 25% < RH < 70% (Belmans et al. 2019), 25% < RH < 60% (De Maré et al. 2019), and 20% < RH < 80% (Johnston et al. 2020). Some authors specify indoor comfort ranges according to standards such as EN16798-1 (2019) (De Maré et al. 2019) and NBN EN 15251 (Belmans et al. 2019). Comfort analysis in these studies adopts various definitions, including thermal comfort based solely to air temperature (Cakyova et al. 2021; Grygierek and Ferdyn-Grygierek 2022; Johnston et al. 2020; Laffeter et al. 2019), both air temperature and RH, and indoor comfort encompassing temperature, RH, and CO<sub>2</sub> (Carbonare et al. 2019; De Jonge et al. 2022; De Maré et al. 2019).

Regarding health impact, some studies employed indicators such as pollutant relative exposure and DALYS (Disability-Adjusted Life Years). Additionally, some authors investigated indicators related to building performance, such as condensation risk on building materials (RH > 70%), mould growth risk, financial payback time of the ventilation system, and peak power demand reduction.

### 3.4 Smart ventilation control strategies and performance

To evaluate smart ventilation performances, authors have used different calculation methods and parameters based on a wide range of ventilation systems and controls. The ventilation control strategies described include (1) occupancy-based control, (2) outdoor conditions-based control, (3) CO<sub>2</sub>, PM<sub>2.5</sub>, wind speed, and temperature-based control applied for hybrid ventilation and ventilation for cooling, (4) temperature, humidity and/or CO<sub>2</sub> based control

ventilation for decentralized systems, and (5) others using DCV based on CO<sub>2</sub>, humidity, and TVOCs. The main findings are summarised as follows.

Due to the occupant's generation of pollutants in the indoor environment, many studies have developed occupancy-based ventilation control strategies. (Clark et al. 2019) used the relative exposure approach to assess the IAQ and energy savings of three occupancy-based ventilation strategies for residential buildings located in the four California climate zones. Results showed that when ventilation is completely turned off during the unoccupied period, in addition to the occupants experiencing a peak of exposure to pollutants when re-entering the environment due to the increase in the pollutant's concentration during the off period, the energy consumption on ventilation to recover the air quality indices makes this strategy not viable. The addition of a pre-occupancy flush period by turning on the ventilation 1 hour or 2 hours prior to the occupants returning home proved to be the best strategy in terms of energy savings and exposure to peak pollutants, which can result in up to 60% energy savings for the 2-story buildings with an ACH<sub>50</sub> of 5.

Regarding the outdoor conditions-based approach, simulation results showed that outdoor temperature-based strategies can save ventilation energy up to 33% while maintaining the equivalent IAQ compared to the constant ventilation system. Ambient temperature-based controlled ventilation is less effective in cold climate regions due to its lack of the cooling season and low diurnal temperature swings. More energy savings are obtained from buildings located in regions with higher cooling demands, and from buildings with less-tight envelopes, as observed across simulation cases with 1, 3, and 5 ACH<sub>50</sub> (Less et al. 2019). Another outdoor conditions-based simulation study performed by (De Jonge et al. 2022) conducted in a typical Belgian apartment unit, assumed that the outdoor air quality is not always better than the IAQ and consequently sometimes not be suitable for diluting indoor pollutants (De Jonge et al. 2022). The authors investigated two ventilation control strategies: one considering both the outdoor air quality and the IAQ, and another strategy only considering the IAQ, evaluating health, comfort, and energy use performance indicators. Simulation results showed that, compared with the control algorithm only based on IAQ, the control algorithm taking into account both IAQ and outdoor air quality achieved 44% of the energy savings and reduced about 10% of the total DALYs count. However, the trade-off was less comfort due to increased exposure to high levels of indoor CO<sub>2</sub> (De Jonge et al. 2022).

Regarding hybrid ventilation systems, the studies performed by (Belmans et al. 2019) showed that mixed-mode ventilation performed equally well as DCV systems in winter in terms of energy consumption and IAQ achieved. However, hybrid ventilation can minimize energy consumption in summer to achieve good thermal comfort as less mechanical ventilation is needed and more free cooling natural ventilation can be supplied (Belmans et al. 2019). Hybrid ventilation was also applied for cooling by (Cakyova et al. 2021) and they found that for energy demand, night ventilation through window openings (turning off the CAV system at night) provided 28% of the reduction compared to constant mechanical ventilation.

For decentralised ventilation systems, (Carbonare et al. 2019) proposed two comfort-oriented control strategies based on the façade integrated room-based ventilation unit and compared these two strategies with the commonly used linear and step control strategies. On average, 10% energy savings were achieved from these two proposed strategies, compared to the linear and step control strategies. In another simulation study on façade integrated room-based ventilation units, (Carbonare et al. 2020) evaluated four control strategies, namely linear, steps, comfort-oriented, and fuzzy control. The fuzzy controlled strategy is defined by a mathematical model based on the interpretation of indoor RH and CO<sub>2</sub> concentration. Then, the fan speed is

controlled based on real-time measurements of these two parameters. The proposed fuzzy controlled strategy achieved about 25% energy savings compared to a constant airflow strategy and about 12% energy savings compared to a step-controlled DCV system (Carbonare et al. 2020). (Smith and Kolarik 2019) also simulated and assessed a manifold of fans that connects to an apartment level air-handling unit to control the supply of airflow to each room in an apartment. The results showed that this system was effective in saving energy and maintaining IAQ targets related to CO<sub>2</sub>, RH, and temperature, where 74% savings in fan energy consumption relative to the reference constant air volume system were achieved. CO<sub>2</sub> only exceeded the limit in the bathroom, where it did not have CO<sub>2</sub>-based control.

For centralised systems, (Baptiste Poirier, Guyot, Woloszyn, et al. 2021) employed five indicators to effectively demonstrate the IAQ achieved through DCV systems. These are CO<sub>2</sub> cumulative exposure (thresholds of 1000 *d* ppm.h), humidity from the health perspective (percentage of time spent by an occupant with RH outside of the range between 30% and 70%), humidity from the condensation risk perspective (percentage of time with RH above 70%), cumulative formaldehyde exposure (threshold of 9 *d* µg m<sup>-3</sup>.h), and cumulative PM<sub>2.5</sub> exposure (threshold of 10 *d* µg m<sup>-3</sup>.h), in which *d* is the simulation duration in hours (h). Simulation studies during the heating season in Lyon, France, showed that among the constant-MEV, constant balanced mechanical ventilation, and humidity-based DCV systems, none of them can achieve all five proposed IAQ targets. The PM<sub>2.5</sub> targets are not reached under any of the ventilation strategies (Baptiste Poirier, Guyot, Woloszyn, et al. 2021; B. Poirier, Guyot, and Woloszyn 2021). Another study conducted by (Poirier et al. 2022) applied the proposed five IAQ indicators to assess the performance of five DCV systems in a newly renovated Danish apartment building and found a similar result: none of the investigated ventilation systems were able to achieve the targeted PM<sub>2.5</sub> exposure. The MVHR resulted in a better IAQ in terms of CO<sub>2</sub> and formaldehyde exposure. However, none of the investigated DCV and non DCV systems resulted in acceptable formaldehyde exposure when the emission rates were in the medium and high scenarios.

(Sowa and Mijakowski 2020) analysed a humidity-based DCV system that was installed in an eight-floor multiunit residential building in Poland. They discovered minimal variation in ventilation performance among units on the same floor level when different ventilation options were implemented. The efficiency of passive stack ventilation is influenced by outdoor temperature and wind conditions, leading to increased instances of unwanted backflows and significant airflow discrepancies between units situated on lower and higher floors of the building, such as between the second and eighth floors. Humidity-controlled stack ventilation systems resulted in fewer backflows but less air flow into the building compared to passive stack ventilation systems and were unable to achieve the required ventilation rate. However, the difference in the air flows on different levels of the building is lower, and the air flow is not dependent on the ambient temperature. Compared with the humidity-controlled stack ventilation system, the performance of the ventilation system was better when this system had exhaust fans mounted on the roof above the individual exhaust ducts to support airflows induced by natural forces when needed, and no unwanted backflows occurred under this ventilation option. The average CO<sub>2</sub> concentrations under these three ventilation options were, respectively, 1146 ppm (passive stack ventilation), 1289 ppm (humidity-controlled stack ventilation), and 1053 ppm (humidity-controlled ventilation with a roof-mounted exhaust fan). Using humidity-controlled ventilation with a roof-mounted exhaust fan ventilation, the energy needed to heat the ventilation air is 21% lower than passive stack ventilation.

## 4 CONCLUSION

This study evaluated 44 papers published from 2017 to 2023, on smart ventilation in residential buildings and showed that new developments have been emerged. The new developments include performance-based assessment, decentralised ventilation units, data-driven approach to form the optimal strategy, and the IoT-enabled devices and sensors. Belgium, France, and the US are the top three countries where smart ventilation studies have been conducted. Single-family houses and apartment units are the most investigated building types. Over the past seven years, smart ventilation concepts have been applied to some new areas, for example, ventilation for cooling and hybrid ventilation. The use of DALYs to estimate the health impacts of operating DCV is also a new development, as includes the financial analysis of the system. Decentralized DCV is an emerging area, as it is beneficial to apartment unit renovation where the building may not have the space to install the central unit and to meet the individual needs of occupants in every zone within a building. However, the energy consumption by multiple fans in the decentralized DCV system might be a shortcoming of this system.

Most studies consider that outdoor air is always cleaner than indoor air and that it is suitable to dilute indoor pollutants, but only a few studies point out that this is not always the case. The analysis of IAQ indicators has revealed that in addition to the most widely used parameters of RH and CO<sub>2</sub>, other IAQ parameters have been used to indicate the air quality, for example, HCHO, PM<sub>2.5</sub>, and TVOC. The DALYs approach to estimating the health impacts shines a light on the importance of balancing energy savings and the IAQ. The challenge related to the diversity of input data and the performance indicators was highlighted. Though the research in this area has rapidly grown, international collaborations are lacking, as is the field testing of the proposed strategies.

## 5 ACKNOWLEDGEMENTS

The authors would like to acknowledge the New Zealand Building Research Levy (Grant number MR15537) for funding the contribution of BRANZ, the Coordenação de Aperfeiçoamento de Pessoal de Nível Superior – Brazil (CAPES – Process number: 88887.700599/2022-00) of the Ministry of Education for the financial support, the International Cooperation Program CAPES/COFECUB (Grant # 898/18), in collaboration with the laboratory LOCIE at the Université Savoie Mont-Blanc, France.

## 6 REFERENCES

- Balvedi, Bruna Faitão, Enedir Ghisi, and Roberto Lamberts. 2018. ‘A Review of Occupant Behaviour in Residential Buildings’. *Energy and Buildings* 174:495–505. doi: 10.1016/j.enbuild.2018.06.049.
- Belmans, B., D. Aerts, S. Verbeke, A. Audenaert, and F. Descamps. 2019. ‘Set-up and Evaluation of a Virtual Test Bed for Simulating and Comparing Single- and Mixed-Mode Ventilation Strategies’. *Building and Environment* 151. doi: 10.1016/j.buildenv.2019.01.027.
- Cakyova, K., A. Figueiredo, R. Oliveira, F. Rebelo, R. Vicente, and P. Fokaides. 2021. ‘Simulation of Passive Ventilation Strategies towards Indoor CO<sub>2</sub> Concentration Reduction for Passive Houses’. *Journal of Building Engineering* 43. doi: 10.1016/j.job.2021.103108.

- Carbonare, N., T. Pflug, C. Bongs, and A. Wagner. 2019. 'Comfort-Oriented Control Strategies for Decentralized Ventilation Using Co-Simulation'. P. 032018 in *IOP Conference Series: Materials Science and Engineering*. Vol. 609.
- Carbonare, N., T. Pflug, C. Bongs, and A. Wagner. 2020. 'Simulative Study of a Novel Fuzzy Demand Controlled Ventilation for Façade-Integrated Decentralized Systems in Renovated Residential Buildings'. *Science and Technology for the Built Environment* 26(10):1412–26. doi: 10.1080/23744731.2020.1797442.
- Clark, Jordan D., Brennan D. Less, Spencer M. Dutton, Iain S. Walker, and Max H. Sherman. 2019. 'Efficacy of Occupancy-Based Smart Ventilation Control Strategies in Energy-Efficient Homes in the United States'. *Building and Environment* 156:253–67. doi: 10.1016/j.buildenv.2019.03.002.
- De Jonge, Klaas, Janneke Ghijsels, and Jelle Laverge. 2022. 'Energy Savings and Exposure to VOCs of Different Household Sizes with a Smart Ventilation System'. in *Proceedings of the 42th AIVC Conference*. Rotterdam, the Netherlands.
- De Jonge, Klaas, and Jelle Laverge. 2022. 'Time-resolved Dynamic Disability Adjusted Life-years Estimation'. *Indoor Air* 32(11). doi: 10.1111/ina.13149.
- De Maré, Bavo, Stijn Germonpré, Jelle Laverge, Frederik Losfeld, Ivan Pollet, and Steven Vandekerckhove. 2019. 'Large-Scale Performance Analysis of a Smart Residential MEV System Based on Cloud Data'. in *Proceedings of the 40th AIVC Conference*. Ghent, Belgium.
- Durier, F., R. Carrié, and M. Sherman. 2018. 'VIP 38: What Is Smart Ventilation?'
- Faure, Xavier, Frederik Losfeld, Ivan Pollet, Etienne Wurtz, and Ophélie Ouvrier Bonnaz. 2018. 'Resilient Demand Control Ventilation System for Dwellings'. in *Proceedings of the 39th AIVC Conference*. Antibes Juan-Les-Pins, France.
- Filis, Vasileios, Kevin Michael Smith, Jakub Kolarik, Frédéric Kuznik, and Lucie Merlier. 2023. 'The Indoor Environmental Quality and Energy Savings Potential of Room Ventilation Units Compared to Exhaust-Only Ventilation Systems in France'. *International Journal of Ventilation* 22(4):346–56. doi: 10.1080/14733315.2023.2198804.
- Franceschini, Paula Brumer, and Leticia Oliveira Neves. 2022. 'A Critical Review on Occupant Behaviour Modelling for Building Performance Simulation of Naturally Ventilated School Buildings and Potential Changes Due to the COVID-19 Pandemic'. *Energy and Buildings* 258:111831. doi: 10.1016/j.enbuild.2022.111831.
- Ghijsels, Janneke, Klaas De Jonge, and Jelle Laverge. 2022. 'Health and Energy Assessment of a Demand Controlled Mechanical Extraction Ventilation System'. *CLIMA 2022 Conference*. doi: 10.34641/clima.2022.155.
- Grygierek, K., and J. Ferdyn-Grygierek. 2022. 'Design of Ventilation Systems in a Single-Family House in Terms of Heating Demand and Indoor Environment Quality'. *Energies* 15(22). doi: 10.3390/en15228456.

- Guyot, Gaëlle, Max H. Sherman, and Iain S. Walker. 2018. 'Smart Ventilation Energy and Indoor Air Quality Performance in Residential Buildings: A Review'. *Energy and Buildings* 165:416–30. doi: 10.1016/j.enbuild.2017.12.051.
- Johnston, Christopher Just, Rune Korsholm Andersen, Jørn Toftum, and Toke Rammer Nielsen. 2020. 'Effect of Formaldehyde on Ventilation Rate and Energy Demand in Danish Homes: Development of Emission Models and Building Performance Simulation'. *Building Simulation* 13(1):197–212. doi: 10.1007/s12273-019-0553-1.
- Kim, Sun Ho, Jeong Won Kim, and Hyeun Jun Moon. 2022. 'Advanced Optimal Control of Indoor Environmental Devices for Indoor Air Quality Using Reinforcement Learning'. in *Proceedings of the 42th AIVC Conference*. Rotterdam, the Netherlands.
- Laffeter, Clement, Xavier Faure, Michele Potard, Claude Bardoul, Julien Escaich, Ophelie Ouvrier Bonnaz, and Etienne Wurtz. 2019. 'Performances of a Demand-Controlled Mechanical Supply Ventilation System under Real Conditions: Indoor Air Quality and Power Distribution for Thermal Comfort'. in *Proceedings of the 40th AIVC Conference*. Ghent, Belgium.
- Less, Brennan D., Spencer M. Dutton, Iain S. Walker, Max H. Sherman, and Jordan D. Clark. 2019. 'Energy Savings with Outdoor Temperature-Based Smart Ventilation Control Strategies in Advanced California Homes'. *Energy and Buildings* 194:317–27. doi: 10.1016/j.enbuild.2019.04.028.
- Liberati, Alessandro, Douglas G. Altman, Jennifer Tetzlaff, Cynthia Mulrow, Peter C. Gøtzsche, John P. A. Ioannidis, Mike Clarke, P. J. Devereaux, Jos Kleijnen, and David Moher. 2009. 'The PRISMA Statement for Reporting Systematic Reviews and Meta-Analyses of Studies That Evaluate Healthcare Interventions: Explanation and Elaboration'. *BMJ* 339:b2700. doi: 10.1136/bmj.b2700.
- Müller, Jarosław, and Maciej Dębowski. 2020. 'Indoor Air Quality Assessment in a Single-Family House Equipped with Demand Controlled Mechanical Ventilation'. *Ecological Chemistry and Engineering S* 27(3):387–402. doi: 10.2478/eces-2020-0025.
- Pecceu, Sébastien, Samuel Caillou, and Romy Van Gaever. 2018. 'Demand Controlled Ventilation: Relevance of Humidity Based Detection Systems for the Control of Ventilation in the Spaces Occupied by Persons'. in *Proceedings of the 39th AIVC Conference*. Antibes Juan-Les-Pins, France.
- Poirier, B., G. Guyot, and M. Woloszyn. 2021. 'Development of Performance-Based Assessment Methods for Conventional and Smart Ventilation in Residential Buildings'. Athens, Greece.
- Poirier, Baptiste, Gaëlle Guyot, Hugo Geoffroy, Monika Woloszyn, Michel Ondarts, and Evelyne Gonze. 2021. 'Pollutants Emission Scenarios for Residential Ventilation Performance Assessment. A Review'. *Journal of Building Engineering* 42:102488. doi: 10.1016/j.job.2021.102488.
- Poirier, Baptiste, Gaëlle Guyot, Monika Woloszyn, Hugo Geoffroy, Michel Ondarts, and Evelyne Gonze. 2021. 'Development of an Assessment Methodology for IAQ Ventilation Performance in Residential Buildings: An Investigation of Relevant

- Performance Indicators'. *Journal of Building Engineering* 43:103140. doi: 10.1016/j.jobe.2021.103140.
- Poirier, Baptiste, Jakub Kolarik, Gaëlle Guyot, and Woloszyn Monika. 2022. 'Design of Residential Ventilation Systems Using Performance-Based Evaluation of Indoor Air Quality: Application to a Danish Study Case'.
- Rojas, Gabriel. 2022. 'Assessing Demand-Controlled Ventilation Strategies Based on One CO2 Sensor'. in *Proceedings of the 42th AIVC Conference*. Rotterdam, the Netherlands.
- Shin, Mi-Su, Kyu-Nam Rhee, Eun-Tack Lee, and Gun-Joo Jung. 2018. 'Performance Evaluation of CO2-Based Ventilation Control to Reduce CO2 Concentration and Condensation Risk in Residential Buildings'. *Building and Environment* 142:451–63. doi: 10.1016/j.buildenv.2018.06.042.
- Smith, K. M., and J. Kolarik. 2019. 'Simulations of a Novel Demand-Controlled Room-Based Ventilation System for Renovated Apartments'. P. 032041 in *IOP Conf. Series: Materials Science and Engineering*. Vol. 609.
- Sowa, Jerzy, and Maciej Mijakowski. 2020. 'Humidity-Sensitive, Demand-Controlled Ventilation Applied to Multiunit Residential Building—Performance and Energy Consumption in Dfb Continental Climate'. *Energies* 13(24):6669. doi: 10.3390/en13246669.
- Van Gaever, Romy, Jelle Laverge, and Samuel Caillou. 2017. 'The Influence of Different Ventilation Strategies and Airflow Control on the Indoor Air Quality in Dwellings.' in *Proceedings of the 38th AIVC Conference*. Nottingham, UK.
- Walker, I., B. Less, D. Lorenzetti, and M. Sohn. 2021. 'Development of Advanced Smart Ventilation Controls for Residential Applications'. *Energies* 14(17). doi: 10.3390/en14175257.

# IEQ and energy performance of residential smart ventilation strategies in France

Raïssa Andrade<sup>1</sup>, Gaëlle Guyot<sup>\*1</sup>

*1 Cerema  
46, Rue Saint-Théobald  
L'Isle-d'Abeau, France*

*\*Corresponding author: gaelle.guyot@cerema.fr*

## SUMMARY

Smart-ventilation with airflows adapting to the need of buildings reduces energy consumptions and can improve IAQ. In some countries, smart ventilation strategies have been widely used for a long term (like Belgium, France,...). We still need to quantify IAQ and energy benefits of smart ventilation through a common internationally validated performance assessment scheme, still under development, notably in the framework of the IEA-EBC Annex 86. The SmartAIR French project focuses on the adaptation of the tools developed in the framework of the Annex 86 project and test their relevance in the context of the generalization of humidify-based ventilation and the innovation towards new ventilation systems.

## KEYWORDS

Smart ventilation; Pollutant; Ventilation strategies; Dwellings.

## 1 INTRODUCTION

Several pollutant emissions have been identified in dwellings due to building materials and household furniture, human activities and occupancy. In addition to metabolic activities, which produce CO<sub>2</sub> and humidity, human emit pollutants due to their activities, such as cooking (PM<sub>2.5</sub> and humidity), laundry, laundry dry and shower (humidity). Therefore, the level of indoor pollutant concentrations combined with the amount of time humans spends indoors are the cause of respiratory and cardiovascular diseases, that can evolve and lead to death due to chronic or acute exposures (Clark et al., 2019).

In this context, the implementation of a ventilation system in dwellings is crucial for human health, since it improves the indoor air quality by diluting the pollutants concentrations. However, it can increase energy consumption depending on the specifications of the fans and the control system applied (De Jonge et al., 2023). The smart ventilation is as an alternative solution, as it provides continuous adjustment of the ventilation system in real-time and by location, thereby achieving the desired indoor air quality (IAQ) while minimizing energy consumption (Durier et al., 2018; Guyot et al., 2018b).

Various ventilation systems and strategies can be employed within the scope of smart ventilation, directly impacting system performance and indoor air quality (IAQ). These systems have been used for a long time in European countries such as France and Belgium, focused on a humidity or CO<sub>2</sub> controls (Poirier et al., 2021a; Guyot et al., 2018a), but their widespread implementation and further innovation remain challenging. One challenge is that we still need to quantify IAQ and energy benefits of smart ventilation through a common internationally validated performance assessment scheme, still under development, notably in the framework of the IEA-EBC Annex 86. This is a pre-condition to make possible to identify energy and IAQ benefits of such systems, at an international level and to open the markets to this innovation. Therefore, the present work aims to evaluate several smart ventilation systems and the influence



of the country, dwelling geometry, occupancy scenario, pollutant emissions on dwelling ventilation.

## 2 METHODOLOGY

The development of the present work was based on the results of the 1<sup>st</sup> common exercise of the IEA-EBC Annex 86, that evaluated different ventilation systems, each one adapted to a participating country. Most cases selected the same input values, such as CO<sub>2</sub> and humidity emissions, while the occupancy schedules, cooking and showering times and duration varied to better represent the country's habits.

The ventilation systems developed by the research groups of Cerema (France), DTU (Denmark), KU Leuven (Belgium), PUCPR (Brazil) and UIBK (Austria) were selected for further studying in the 2<sup>nd</sup> common exercise and the SmartAIR French project, that aims to improve the energy efficiency of the IAQ management strategies in operation and focuses on the adaptation of the tools developed on the Annex 86. Since each research group worked with different modelling softwares, geometries and other input conditions, it is difficult to compare the performances of the different ventilation systems tested. Therefore, it was created a modelling plan, validated by the participating research groups, to better compare these cases.

First, all simulations are going to be performed in the software CONTAM, for the same geometry, a single-family house with 5 occupants (2 parents and 3 children), the same occupancy scenarios, emissions rates, meteorological data and simulated period, from 1<sup>st</sup> October to 1<sup>st</sup> April (heating period in France), to each ventilation system selected. Then, the next step is to evaluate the influence of the country, performing the simulations with different meteorological and external pollution data, occupancy scenarios, cooking and emissions times and duration. After that, it will be evaluated the ventilation in an apartment geometry, for the conditions that presented the better results in the previous steps. Finally, a sensibility analysis will be performed to determine the influence of these parameters on the ventilation strategies performances.

Detailed information about the parameters studied is given in the following subtopics.

### 2.1 Geometry and occupancy scenarios

The floor plant of the single-family house simulated in the first part of the project is represented in Figure 1 (Poirier et al., 2021a) and has two floors and eleven rooms, each one represented by a zone in CONTAM. On the first floor there is a hall, a living room with an integrated kitchen, a children's bedroom, a bathroom and a toilet, while on the second floor there is a mezzanine, a parent's bedroom, 2 other children's bedroom, a second bathroom and toilet. Besides that, the occupancy schedule used was the same as Poirier (2019), showed in Table 1.

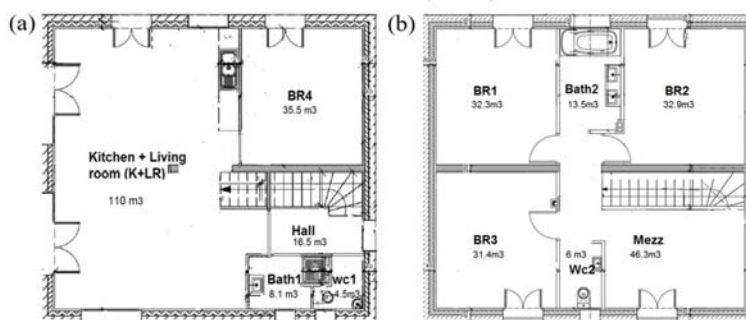


Figure 1: Single-family's house floor plant (a) first floor and (b) second floor, from Poirier et al. (2021)

Table 1: Single-family house occupancy scenario

Room   Occupant	Mother/Father	Child 1	Child 2	Child 3
Living room +	07h00-08h30	06h20-08h30	06h20-08h30	06h20-08h30
Kitchen	12h00-14h00	12h00-14h00	12h00-14h00	12h00-14h00
	19h00-21h00	19h00-20h20	19h00-19h40	19h00-20h20
			20h20-21h00	
Bathroom	06h20-07h00 (BATH2)	20h20-21h00 (BATH2)	19h40-20h20 (BATH1)	20h20-21h00 (BATH1)
Bedroom	21h00-06h20 (BR1)	21h00-06h20 (BR2)	21h00-06h20 (BR3)	21h00-06h20 (BR4)

## 2.2 Pollutant emissions

Poirier et al. (2021b) did an extensive research about the inputs used in ventilation systems and most were selected to be used in this work. However, the values of formaldehyde emissions were obtained using the Pandora Database developed by the laboratory LaSIE at University of La Rochelle (Abadie and Blondeau, 2011). This database gathers the emission rates of different pollutants and allows the user to select the room dimensions and sources.

Table 2: Pollutant emissions

Pollutant	Source	Emission
CO <sub>2</sub>	Breathing	Awake/Asleep: 18/15 L.h <sup>-1</sup>
Humidity	Breathing	Awake/Asleep: 55/40 g.h <sup>-1</sup>
	Cooking	Breakfast/Lunch /Dinner: 1512/2268/2844 g.h <sup>-1</sup> (15/30/40 min)
	Shower	1440 g.h <sup>-1</sup> (10 min/day/person)
	Laundry	252 g.h <sup>-1</sup> (2h/week/person)
	Laundry dry	136.8 g.h <sup>-1</sup> (11h/week/person)
Formaldehyde (HCHO)	Furniture	Low/Medium/High: 5.6/14.8/29.1 µg.h <sup>-1</sup> .m <sup>-2</sup>
PM <sub>2.5</sub>	Cooking	Low/Medium/High: 1.26/1.91/2.55 mg.min <sup>-1</sup>
Fictive	-	10 µg.h <sup>-1</sup> .m <sup>-2</sup>

## 2.3 Ventilation systems

Five main ventilation systems were selected to the simulations, 2 are exhaust-only ventilation and 3 are balanced ventilation. These systems are briefly described below and further details regarding the constant air volume and the humidity control systems can be found in Poirier et al. (2022b), and the room-based systems are detailed in Poirier et al. (2022a).

- Mechanical exhaust-only ventilation (MEV):
  - Constant air volume (MEV-cav): presents air exhausts in the kitchen, the toilets and bathroom<sup>1</sup> and 1-hour boost of 135 m<sup>3</sup>.h<sup>-1</sup> in the kitchen during cooking activities. As a result, the total extract airflow in the whole house is 135 m<sup>3</sup>.h<sup>-1</sup> during basic mode and 225 m<sup>3</sup>.h<sup>-1</sup> during peak mode. Air enters the building through trickle vents located on windows of bedrooms and living room.
  - Humidity control (MEV-rh): the inlets (trickle vents on windows) and outlets airflows are located at the same place than in the MEV-cav system, but are regulated by adjusting the cross-section through its hygroscopic fabric, also with 1-hour boost.
- Mechanical balanced ventilation (MVHR):
  - Heat recovery and constant air volume (MVHR-cav): The exhausted airflows are the same than with MEV-cav but the trickle vents are replaced by suppliers in the living room and bedroom.

<sup>1</sup> Exhausts are 30 m<sup>3</sup>.h<sup>-1</sup> in each bathroom, 15 m<sup>3</sup>.h<sup>-1</sup> in each toilet, and 45 m<sup>3</sup>.h<sup>-1</sup> in the kitchen

- Heat recovery and humidity control at the apartment level (MVHR-rh): this system has a relative humidity sensor in the exhaust duct that regulates the airflows to operate in a low, nominal or high level, this last one is activated during the 1-hour boost in the kitchen.
- Heat recovery, CO<sub>2</sub> and humidity control at the room level (MVHR-room): in this system, a sensor can be placed into each room to provide an individual airflow control, based on CO<sub>2</sub> for the living room and bedrooms, while in the kitchen is based on CO<sub>2</sub> and humidity (with 1-hour boost).

## 2.4 Output data and performance indicators

To each ventilation system simulated, CO<sub>2</sub> and relative humidity concentrations profiles will be collected in all rooms, as well as the exposure concentrations profiles to all contaminants. Moreover, these systems will be evaluated by the performance indicators described in Table 3.

Table 3: Description of the performance indicators selected

Performance Indicator	Unit	Description
DALY	[years.10 <sup>5</sup> ]	The total health impact is the sum of all DALYs (Dynamic Disability-Adjusted Life Years).
E <sub>CO2</sub>	[ppm.h]	Normalized cumulative exposure when concentrations are higher than 1000 ppm in a room.
P <sub>CO2</sub>	[ppm]	95 <sup>th</sup> percentile of the CO <sub>2</sub> exposure concentrations.
T <sub>RH</sub>	[%]	Percentage of time spent out of the humidity range of 25-60%.
E <sub>HCHO</sub>	[μg m <sup>-3</sup> . h]	Cumulative formaldehyde occupant exposure.
E <sub>fictive</sub>	[μg m <sup>-3</sup> . h]	Cumulative fictive occupant exposure.
E <sub>PM2.5</sub>	[μg m <sup>-3</sup> . h]	Cumulative PM <sub>2.5</sub> occupant exposure.
E <sub>HCHO_acute</sub>	[μg m <sup>-3</sup> . h]	Maximum of the formaldehyde cumulative occupant exposure over 1h.
E <sub>fictive_acute</sub>	[μg m <sup>-3</sup> . h]	Maximum of the fictive cumulative occupant exposure over 1h.
E <sub>PM2.5_acute</sub>	[μg m <sup>-3</sup> . h]	Maximum of the PM <sub>2.5</sub> cumulative occupant exposure over 1h.
ACH	h <sup>-1</sup>	Average building air changes per hour due to ventilation.
E <sub>losses</sub>	[kJ]	Energy losses due to ACH ventilation
E <sub>elec</sub>	[kJ]	Energy due to the fan(s) electric consumption

## 3 ACKNOWLEDGEMENTS

The French Agency for ecological transition ADEME – (Grant number 2262D0108) for funding the contribution of Cerema.

The IEA-EBC Annex 86 experts group, and especially the ST4-Smart ventilation group: Jelle Laverge, Jakub Kolarik, Douaa Al Assad, Quiten Carton, Marcos Batistella, Markus Wirnsberger, Daniela Mortari and Klaas de Jonge.

## 4 REFERENCES

- Abadie, M. O., Blondeau, P. (2011). PANDORA database: A compilation of indoor air pollutant emissions. *HVAC&R Research*, 17(4), 602–613.
- Clark, J. D., Less, B. D., Dutton, S. M., Walker, I. S., Sherman, M. H. (2018). Efficacy of occupancy-based smart ventilation control strategies in energy efficient homes in the United States. *Building and Environment*, (156), 253-267.
- De Jonge, K., Ghijssels, J., Laverge, J. (2023). Energy savings and exposure to VOCs of different household sizes for three residential smart ventilation systems with heat recovery. *Energy & Buildings*, (290).

- Durier, F., Carrié, F.R., Sherman, M. (2018). What is smart ventilation? *AIVC VIP 38*.
- Guyot, G., Walker, I. S., Sherman, M. H. (2018a). Performance based approaches in standards and regulations for smart ventilation in residential buildings: a summary review. *International Journal of Ventilation*, 18(2), 96–112.
- Guyot, G., Sherman, M.H., Walker, I. S. (2018b). Smart ventilation energy and indoor air quality performance in residential buildings: A review. *Energy & Buildings*, (165), 416-430.
- Poirier, B. (2019). Étude numérique de la performance de la ventilation intelligente. *Master's Thesis, L'école nationale des travaux publics de l'État (ENTPE)*.
- Poirier, B., Guyot, G., Woloszyn, M., Geoffroy, H., Ondarts, M., Gonze, E. (2021a). Development of an assessment methodology for IAQ ventilation performance in residential buildings: An investigation of relevant performance indicators. *Journal of Building Engineering*, (43).
- Poirier, B., Guyot, G., Geoffroy, H., Woloszyn, M., Ondarts, M., Gonze, E. (2021b). Pollutants emission scenarios for residential ventilation performance assessment. A review. *Journal of Building Engineering*, (42).
- Poirier, B., Jakub, K., Guyot, G., Woloszyn, M. (2022a). Design of residential ventilation systems using performance-based evaluation of Indoor Air Quality: application to a Danish study case. *E3S Web of Conferences*, (362).
- Poirier, B., Guyot, G., Woloszyn, M. (2022b). Development of Performance-Based Assessment Methods for Conventional and Smart Ventilation in Residential Buildings, in: *IAQ 2020: Indoor Environmental Quality Performance Approaches Transitioning from IAQ to IEQ*. AIVC-ASHRAE, Athens, Greece.

# Particulate matter in UK school classrooms – building an evidence base for improving classroom air quality

Alice Handy\*<sup>1</sup>, Henry Burridge<sup>1</sup>, the SAMHE consortium<sup>2</sup>

*1 Imperial College London,  
Department of Civil and Environmental Engineering,  
London,  
SW7 2AZ*

*2 The SAMHE consortium, see †*

*\*Corresponding author: a.handy23@imperial.ac.uk*

## SUMMARY

Identifying factors that affect classroom concentrations of particulate matter is important for enabling effective mitigation of the associated negative health and cognitive effects, of which children can be especially susceptible. This study examines particulate matter concentrations in school classrooms from across the UK which have participated in the Schools' Air quality Monitoring for Health and Education (SAMHE) project. Data from the 2023/2024 academic year is analysed and outdoor sources of particulate matter (PM) are shown to be a key source of PM in classrooms. Outdoor particulate matter events, taken to be short periods of elevated outdoor PM concentrations, are evidenced within classroom measurement and result in the likely classroom exposures during these events being significantly over-weighted within the longer-term exposure to PM over the academic year.

## KEYWORDS

Indoor Air Quality, Particulate matter, Schools, Exposure

## 1 INTRODUCTION

The air quality of school classrooms can be a modifier to the health of students and teachers due to the durations spent indoors as school, predominately in classrooms. Negative health effects of poor air quality can be more pronounced in children than in adults and, due to its effects on cognitive performance, air quality has also been linked to attainment in schools (Sadrizadeh et al. 2022). Understanding and monitoring the air quality in schools is essential for evidencing strategies to reduce exposure to indoor air pollutants. The Schools' indoor Air quality Monitoring for Health and Education (SAMHE) project has set out to produce an unparalleled data set of UK classroom indoor air quality across a range of metrics.

This study investigates the particulate matter PM<sub>2.5</sub> in UK classrooms, which is of particular interest as childhood exposure to PM<sub>2.5</sub> is associated with the onset of asthma, and the UK has one of the highest rates of childhood asthma globally (Bloom et al 2019). Central to the goal of the SAMHE project is to better enable students and teachers to manage their indoor air quality.

## 2 METHODS

Schools that participate in the SAMHE project receive a low-cost air quality monitor and access to an interactive Web App. Once connected to the school WiFi, data is stored by cloud-services for analysis and, data feeds to the Web App enable, schools to view readings of CO<sub>2</sub>, relative humidity, total volatile organic compounds, temperature and particulate matter. A citizen science approach was adopted to recruit and engage schools and tailor educational materials to the needs of pupils and teachers, this method highly scalable deployment

(Chatzidiakou et al 2023). As of July 2024, over 1,300 schools have been recruited to the project and each has received a monitor, over 880 of these monitors within schools have recorded IAQ data. Recruited schools are broadly representative of the UK school population in terms of the balance of constituent countries, fee-paying status, and Index of Multiple Deprivation. This study reports on the three terms of the academic year of 2023/2024. In this study a selection of schools was considered that met data completeness criteria. The SAMHE data set is compared to outdoor concentrations of PM<sub>2.5</sub> as reported from Defra AURN background stations that are the nearest to the selected schools.

### **3 RESULTS**

By comparing the concentration of PM<sub>2.5</sub> averaged across the study SAMHE school monitors and outdoor concentration of PM<sub>2.5</sub> averaged across the AURN stations, we find that school PM concentrations are largely determined by outdoor concentrations. Whilst the outdoor concentrations are generally larger than school concentrations, the peaks in indoor occur simultaneously with peaks in outdoor levels. Given the many possible sources of PM<sub>2.5</sub> within schools it is perhaps surprising that such a close correlation between schools' and outdoor concentrations are seen at a national scale. These peaks in outdoor concentration occur over the period of a day to a week and can be caused by metrological events or arise due to anthropogenic sources. We investigate how outdoor 'events', periods of elevated outdoor PM<sub>2.5</sub>, affect the classroom concentrations. Some of the short events occur during evenings when school buildings are typically closed. Despite this, the events are detected in the readings of PM<sub>2.5</sub> from classroom monitors. This indicates that UK school buildings are relatively permeable to PM pollution even when closed. When the classroom concentrations are considered only during occupied school hours, some of these short events do not significantly increase concentrations in classrooms.

However, larger events, those that last up to six days and have higher outdoor concentrations, are shown to affect classroom concentrations during occupied school hours. Estimates of potential exposure to classroom PM<sub>2.5</sub> during school hours over the academic year shows that days of low concentration contribute to more than half of students' exposures. However, the contribution to in-school exposure on days of outdoor PM pollution events is significant, with exposure on these PM event days being 2-3 times overweight within the total exposure.

### **4 CONCLUSIONS**

Trends in classroom particulate matter concentrations are significantly influenced by outdoor concentration trends. Periods of elevated outdoor PM<sub>2.5</sub> concentration 'events' were routinely detected by SAMHE school monitors, exposures on these days might contribute significantly to the long-term exposure to PM<sub>2.5</sub> over the academic year.

The findings of this study demonstrate the need for data driven evidence to develop guidance to improve indoor air quality and inform future building, and retrofitting, of school buildings. Ventilation is the key means by which indoor pollutants can be flushed from classrooms. However, in the context of particulate matter, care must be taken as outdoor air can be a major source of PM pollution in classrooms.

### **5 ACKNOWLEDGEMENTS**

The authors would like to thank all of the schools, teachers and pupils who have participated in the SAMHE project and acknowledge the contribution of everyone involved from the SAMHE consortium. In particular, thanks to Sam Wood and Kat Roberts for their assistance in the development of this research, as well as Ben Barret, Ian Chen and Chris Malley who have

provided invaluable guidance in understanding and contextualising outdoor particulate matter concentrations and behaviour.

† The SAMHE project consortium members consist of the following, Imperial College London: Ben Barratt, Henry Burridge, Alice Handy, Christopher Pain, Kat Roberts, Samuel Wood; Stockholm Environment Institute, University of York: Rhys Archer, Victoria Beale, Sam Bland, Douglas Wang, Lucy Way, Sarah West; UK Health Security Agency (UKHSA): Holly Carter, Dale Weston, Natalie Williams; University of Cambridge: Hannah Edwards, Paul Linden, Mark Winterbottom; University of Sheffield: Carolanne Vouriot; University of Leeds: Chris Brown, Marco-Felipe King, Mark Mon-Williams; University of Surrey: Sarkawt Hama, Prashant Kumar.

## 6 REFERENCES

Sadrizadeh S, Yao R, Yuan F, Awbi H, Bahnfleth W, Bi Y, Cao G, Croitoru C, de Dear R, Haghighat F, Kumar P. Indoor air quality and health in schools: A critical review for developing the roadmap for the future school environment. *Journal of Building Engineering*. 2022 Oct 1;57:104908.

Bloom CI, Saglani S, Feary J, Jarvis D, Quint JK. Changing prevalence of current asthma and inhaled corticosteroid treatment in the UK: population-based cohort 2006–2016. *European Respiratory Journal*. 2019 Apr 1;53(4).

Chatzidiakou, L., Archer, R., Beale, V., Bland, S., Carter, H., Castro-Faccetti, C., Edwards, H., Finneran, J., Hama, S., Jones, R.L. and Kumar, P., 2023. Schools' air quality monitoring for health and education: Methods and protocols of the SAMHE initiative and project. *Developments in the Built Environment*, 16, p.100266.

# Utilization of ventilation systems to maintain selected environmental comfort parameters at the required level

Małgorzata Basińska<sup>1\*</sup>, Joanna Kubiak<sup>1,2</sup>, and Michał Michałkiewicz<sup>1</sup>

*1 Poznan University of Technology, Faculty of Environmental Engineering and Energy, Institute of Environmental Engineering and Building Installations, Berdychowo 4 Str., 61-131 Poznań, Poland*

*2 Doctoral School of the Poznan University of Technology, 60-965 Poznan, Poland,*

*\*Corresponding author: malgorzata.basinska@put.poznan.pl*

## SUMMARY

In recent times, society has become increasingly aware of potential health problems associated with indoor environments. This is particularly important when considering young children, whose immune systems are not fully developed. Additionally, indoor air quality is influenced by outdoor air quality, which is often poor in many areas, especially in urbanized areas. This article presents the results of research on selected environmental comfort parameters conducted in preschool classrooms located near busy roads. Each preschool classroom has an independent ventilation system managed by childcare providers. The article focuses on microbiological indicators of air quality (the general count of mesophilic bacteria, the general count of psychrophilic bacteria, the count of *Staphylococcus* (*Staphylococcus*) mannitol positive (type  $\alpha$ ) and mannitol negative (type  $\beta$ ), the count of *Pseudomonas fluorescens* bacteria, actinomycetes (*Actinobacteria*), physical parameters (temperature, relative humidity, suspended particles), and chemical parameters (carbon dioxide and radon concentrations). Our analysis indicates that when the ventilation system in the building is consciously operated, it ensures the maintenance of the analysed parameters at an acceptable level. The main sources of microbial air pollutants in indoor environments are the buildings themselves, including the people inside them. The use of the ventilation system has led to an improvement in the physical property of the air, but did not significantly improve its microbiological quality.

## KEYWORDS

preschool, air quality, microbiological contamination, ventilation installation

## 1 INTRODUCTION

According to studies on environmental air quality (IEQ), both microbiological contaminations and physical and chemical conditions (temperature, humidity, dust and gases) can have a significant negative impact on human health, comfort and productivity (Bragoszewska et al., 2018; Al Horr et al., 2016; Asadi et al., 2017; Niu et al., 2022). The quality of environment air depends on, in addition to the building technical state, the quality of the air outside the building, indoor contaminant sources, and a way to control the air flow in the room. Well-designed ventilation systems can improve the quality of the indoor environment, but if they are used without adequate knowledge, we may experience a periodic deterioration of IAQ.

## 2 METHODOLOGY

Air samples were collected in the selected rooms of the preschool and outdoor in the vicinity of the buildings. We present results of measurements of microbiological and chemical parameters that were conducted in one day in March 2024. The measurements were carried out in a room with a volume of 168 m<sup>3</sup>, where on the day of the measurements there were 11 children and two caretakers.



The measurement devices for the physical and chemical parameters were placed at a height of approximately 150 cm above the floor. The microbiological parameters of the measurement devices were placed 1.5 m above floor level in the middle of each room and 1.5 m above the ground level for outdoor air samples. We analysed the air samples for the following microorganisms: mesophilic bacteria on nutrient agar, psychrophilic bacteria on nutrient agar, mannitol-positive (M+) and mannitol-negative (M-) *Staphylococcus* on Chapman medium, *Actinobacteria* on Pochon medium, *Pseudomonas fluorescens* on King B medium and identification of colonies in UV rays, as well as the total number of microscopic fungi on Czapek-Dox and Waksman medium (Basińska et al., 2019).

### 3 RESULTS

The purpose of the study was to check whether the design air stream supplied to a preschool room from a centralised supply and exhaust system could improve air quality. Along with the measurement of CO<sub>2</sub>, a microbiological assessment was carried out, the concentrations of which were related to the parameters of the outdoor air. Figure 1 shows the change in CO<sub>2</sub> concentration over time on Friday 8 March 2024, which shows that after the supply and exhaust system is turned off and the children leave the room, the CO<sub>2</sub> concentration decreases to the value close to the outdoor air - stable condition.

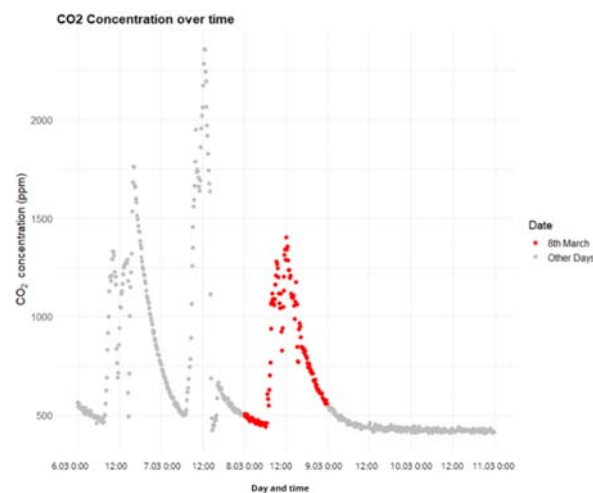


Figure 1: Change in CO<sub>2</sub> concentration over time

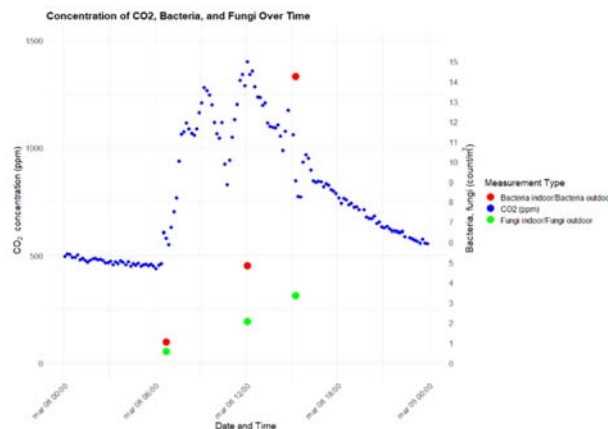


Figure 2: Change in CO<sub>2</sub> concentration and bacteria and fungi on march 8

Figure 2 shows the sum of bacteria and the average value of fungi from colonies grown on two media in relation to a given number of colonies in the outdoor air.

During the entire day of operation of the ventilation system, the CO<sub>2</sub> concentration is maintained at a satisfactory level. Microbiological measurements performed at 6:00 a.m., 12:00 p.m. and 5:00 p.m. indicate a significant increase in the concentration of microorganisms in the preschool room. The recorded maximum value for fungi is 1540 CFU/m<sup>3</sup> or for bacteria is 8560 CFU/m<sup>3</sup>, both recorded for 3 pm. These values are significant compared to the measurements of other researchers in public buildings (Hayleeyesus et al., 2014) and close to the value of lecture rooms at the University of Poznań, however, these researchers did not record such large increases as we do (more than 10 times) in the number of bacteria in relation to the morning hour (Stryjakowska-Sekulska et al., 2007).

#### 4 CONCLUSION

The use of the ventilation system has led to an improvement in the physical property of the air, but did not significantly improve its microbiological quality.

The high number of people per unit area of the room contributes to poor air quality in terms of microbiology, but reducing the number of children per unit area is not possible. It is possible that supplementing children's activity and play schedules with longer periods of time outdoors even in lower temperatures could have a positive impact on air quality. In our opinion, the most popular indicator of carbon dioxide concentration should be supplemented by the microbiological indicators i.e. the number of bacteria and fungi.

#### 5 REFERENCES

Braęoszewska E, Biedroń I, Kozielska B, Pastuszka JS. (2018). Microbiological indoor air quality in an office building in Gliwice, Poland: Analysis of the case study. *Air Qual. Atmos. Health*. <https://doi.org/10.1007/s11869-018-0579-z>

Al Horr Y, Arif M, Kaushik A, Mazroei A, Katafygiotou M, Elsarrag E. (2016). Occupant productivity and office indoor environment quality: A review of the literature. *Build and Environ*. <https://doi.org/10.1016/j.buildenv.2016.06.001>

Asadi I, Mahyuddin N, Shafigh P. (2017). A review on Indoor Environmental Quality (IEQ) and energy consumption in buildings based on occupant behaviour. *Facilities*. 66: 684–95.

Basińska M, Michałkiewicz M, Ratajczak K. (2019). Impact of physical and microbiological parameters on proper indoor air quality in nursery. *Environ Inter*. <https://doi.org/10.1016/j.envint.2019.105098>

Hayleeyesus, S. F., & Manaye, A. M. (2014). Microbiological quality of indoor air in university libraries. *Asian Pacific journal of tropical biomedicine*, 4, S312-S317.

Niu R, Chen X, Liu H. (2022). Analysis of the impact of a fresh air system on the indoor environment in office buildings. *Sustainable Cities and Society*. <https://doi.org/10.1016/j.scs.2022.103934>

Stryjakowska-Sekulska, M., Piotraszewska-Pajak, A., Szyszka, A., Nowicki, M., Filipiak, M. (2007). Microbiological quality of indoor air in university rooms. *Polish Journal of Environmental Studies*, 16(4), 623.

# Quantifying ventilation rates in heterogeneous rooms based on point measurements of carbon dioxide

Joshua Finneran<sup>\*1</sup>, Henry C Burridge<sup>2</sup>,

*1 Wolfson School of Mechanical, Electrical and Manufacturing Engineering,  
Loughborough University,  
Loughborough, UK*

*2 Department of Civil and Environmental Engineering,  
Imperial College London,  
London, UK*

\*Corresponding author: [j.finneran2@lboro.ac.uk](mailto:j.finneran2@lboro.ac.uk)

## KEYWORDS

Ventilation, Indoor air quality, Carbon dioxide, Schools

## SUMMARY

**Introduction:** Indoor air quality (IAQ) is increasingly accepted as a leading factor in human health, and the ventilation of our indoor spaces is a key modifier of IAQ as the principal means by which indoor pollutants are diluted. Knowledge of the ventilation rate is essential for understanding and modelling our indoor environment, yet quantifying the ventilation rate for regular operational spaces remains a challenge. Measurements of carbon dioxide (CO<sub>2</sub>) concentrations indoors are established as a reasonable general indicator of IAQ in occupied spaces and are the basis of many regulations and standards, e.g. ASHRAE (2022). We present a robust method to better exploit point CO<sub>2</sub> measurements to estimate the daily mean per-person ventilation rate  $\bar{Q}_{pp}$ , requiring very limited other contextual information.

Current widely applied methods rely on special-case solutions to the CO<sub>2</sub> mass balance equation (Sherman, 1990; Batterman, 2017). These methods include: the decay rate, for which the space must be unoccupied, and the ventilation rate is assumed constant during the decay; and the steady-state method, for which the balance between the source and ventilation must remain constant for a sufficiently long time so concentration becomes constant. Both methods further assume the room to be well-mixed. The present method overcomes some limitations of these methods since it makes no assumptions regarding the ventilation provision throughout the day, nor requires the room to be in a steady state, nor the air within to be well-mixed. Importantly, the method facilitates ventilation estimates in operational spaces during normal use, not requiring the room to be unoccupied. This is significant since ventilation provision can significantly differ during occupied and unoccupied periods (Godwin, 2007).

**Theory & Methodology:** Beginning with the general CO<sub>2</sub> mass balance equation for a room, it can be shown that the daily average per-person ventilation rate  $\bar{Q}_{pp}$  can be expressed precisely as

$$\bar{Q}_{pp} = K \frac{F_{occ} \overline{\langle G \rangle}_N}{\bar{C}_X}, \quad (1)$$

where  $F_{occ}$  is the fraction of time which the given room is occupied during the day (from first occupancy until CO<sub>2</sub> decays to background at the end of the day),  $\overline{\langle G \rangle}_N$  is the time average of the per-person average CO<sub>2</sub> generation rate, and  $\bar{C}_X$  is the time averaged excess CO<sub>2</sub> concentration at the sensor location, which is measured. Details of the dimensionless coefficient  $K$  and the full derivation of Eq. (1) are given in Finneran & Burridge (2024). The coefficient  $K$  captures effects of ventilation rate variability during the day, and the effects of heterogeneity of CO<sub>2</sub> in the room. Heterogeneity causes a discrepancy between the room averaged excess CO<sub>2</sub>  $\langle C \rangle_V$  and that measured by the sensor  $C_X$ . Importantly,  $K = 1$  if the ventilation rates (total and per-person) are constant, and if the room is well-mixed, but we make no such assumptions. The challenge is that for a given scenario, the coefficient  $K$  and the average per-person generation rate  $\overline{\langle G \rangle}_N$  are unknown, but we show that the uncertainty in these parameters is sufficiently low, enabling meaningful estimates of  $\bar{Q}_{pp}$  with very little contextual information.

Taking UK secondary school classrooms as a case study, simulations of CO<sub>2</sub> levels in classrooms with a high degree of variability were conducted using Monte Carlo methods. Reasonable probability distributions (informed by available data) were assigned to all relevant parameters, including: the classroom volume, the ventilation rate profile, the occupancy levels and duration, the CO<sub>2</sub> generation rate of occupants, and the CO<sub>2</sub> heterogeneity in the

room. From these randomly generated inputs, the excess CO<sub>2</sub> at the sensor location  $C_X$  (that would be measured) can be calculated. Approximately  $10^7$  classroom days were simulated and results of one illustrative example simulation are shown in Figure 1.

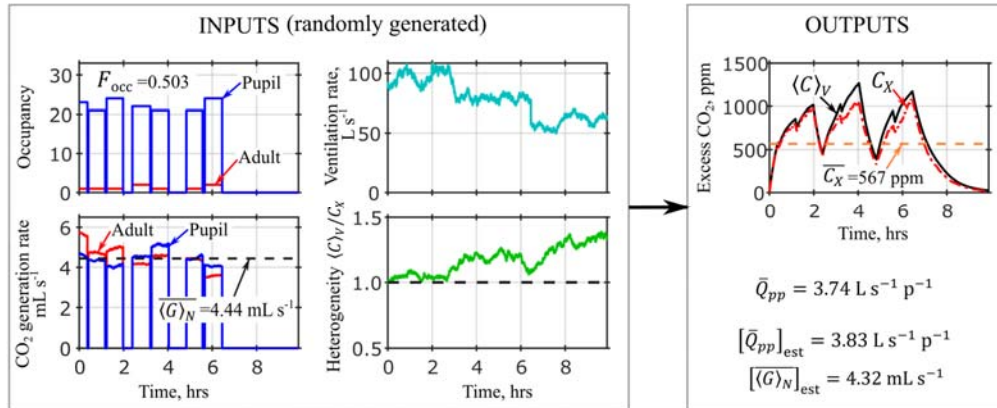


Figure 1: Illustrative example of classroom day simulation. The inputs are randomly generated with data-informed stochastic models. The precise value of  $\bar{Q}_{pp} = 3.74 \text{ L s}^{-1} \text{ p}^{-1}$  is known within the simulation and can be estimated accurately using Eq. (2) as  $[\bar{Q}_{pp}]_{\text{est}} = 3.83 \text{ L s}^{-1} \text{ p}^{-1}$ . Room volume =  $190 \text{ m}^3$ .

**Results & concluding discussion:** It was found that the coefficient  $K$  is remarkably constrained and close to a value of unity, despite the large variability of input parameters. Uncertainty in  $K$  can be reduced with knowledge of spatial CO<sub>2</sub> distributions (e.g. using multiple sensors), and/or knowledge that the ventilation rate is reasonably constant (e.g. mechanical ventilation). Also, since classrooms typically contain large numbers of occupants of a similar age, uncertainty in  $\langle G \rangle_N$  is relatively constrained. These findings provide justification for the estimate of  $\bar{Q}_{pp}$  via

$$[\bar{Q}_{pp}]_{\text{est}} = \frac{F_{\text{occ}} [\langle G \rangle_N]_{\text{est}}}{\bar{C}_X}, \quad (2)$$

requiring only the measured CO<sub>2</sub> levels to calculate  $\bar{C}_X$ , the occupied time fraction  $F_{\text{occ}}$ , and an estimate for the average per-person generation rate  $[\langle G \rangle_N]_{\text{est}}$ . An estimate  $[\langle G \rangle_N]_{\text{est}}$  can be informed by knowledge of the age of occupants and classroom activities. The accuracy of this calculation tool, Eq. (2), is shown in Figure 2. For the worst-case scenario of no contextual information (hence  $[\langle G \rangle_N]_{\text{est}} = 4.32 \text{ mL s}^{-1}$  is used as the average over all occupants and activities) uncertainty is approximately  $\pm 22\%$ . However, for the high-information scenario (e.g. gathering information of occupants age and room activities, and using multiple CO<sub>2</sub> sensors), uncertainty is reduced to approximately  $\pm 12\%$ , with 95% confidence.

This calculation tool, Eq. (2), can be applied to CO<sub>2</sub> data to calculate the average per-person ventilation rate. Uncertainty has been rigorously quantified for the case study of UK secondary school classrooms. It is expected that this method can be extended to many other building types, and it is a challenge for future work to explore uncertainties in other applications.

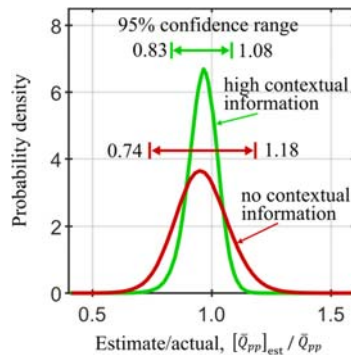


Figure 2: Probability density function for estimated  $\bar{Q}_{pp}$  from Eq. (2) compared to the true value, for no and detailed contextual information scenarios

## ACKNOWLEDGEMENTS

The authors would like to acknowledge all members of the ‘School Air quality Monitoring for Health and Education’ (SAMHE) project consortium. Funding was provided from the SAMHE project — an extension of the CO-TRACE project, which was funded by the EPSRC, United Kingdom under grant number EP/W001411/1, and additional funding was received from the UK’s Department for Education.

## REFERENCES

ASHRAE. (2022). ANSI/ASHRAE Standard 62.2-2022: Ventilation and Acceptable Indoor Air Quality in Residential Buildings. American Society of Heating, Refrigerating and Air-Conditioning Engineers.

Batterman, S. (2017). Review and extension of CO<sub>2</sub>-based methods to determine ventilation rates with application to school classrooms. *International Journal of Environmental Research and Public Health*, 14(2), 1–22. <https://doi.org/10.3390/ijerph14020145>

Finneran, J., & Burrige, H. C. (2024). Inferring ventilation rates with quantified uncertainty in operational rooms using point measurements of carbon dioxide: Classrooms as a case study. *Building and Environment*, 254(January), 111309. <https://doi.org/10.1016/j.buildenv.2024.111309>

Godwin, C., & Batterman, S. (2007). Indoor air quality in Michigan schools. *Indoor Air*, 17(2), 109-121. <http://dx.doi.org/10.1111/j.1600-0668.2006.00459.x>.

Sherman, M. H. (1990). Tracer-gas techniques for measuring ventilation in a single zone. *Building and Environment*, 25(4), 365–374. [https://doi.org/10.1016/0360-1323\(90\)90010-O](https://doi.org/10.1016/0360-1323(90)90010-O)

# Incomplete resistance; ventilation, mould growth and built in furniture in a 1930's Dublin clinker concrete apartment building

Gearóid Carvilla<sup>1\*</sup>, Joseph Little<sup>a</sup>, Andrew Lundberg<sup>a</sup>

<sup>a</sup>Dublin School of Architecture, TU Dublin, Ireland

[\\*D17126585@mytudublin.ie](mailto:*D17126585@mytudublin.ie)

## Summary

Steady state and dynamic simulations tools based on current ISO standards play a crucial role in designing thermal envelopes that are robust and minimise risks of interstitial and surface condensation. These tools can also be used in a forensic way when supplemented by environmental and material data from site to analyse building failure. In this case study issues of mould and surface condensation observed in social housing apartments in a 1930's building was investigated using ISO standards to show the impact of IWI, changes to ventilation and role of cabinetry in exasperating critical levels of surface temperature in a 1990's service and fabric upgrade.

**Keywords:** Ventilation, Solidwall building; Internal Wall Insulation; Condensation, Surface Resistivity, Temperature factor

## Nomenclature

ISO	International Organisation for Standardisation	fRsi	Temperature Factor
IWI	Internal Wall Insulation	Rsi/Rse	Interior/Exterior Surface resistivity
CRA	Condensation Risk Analysis	$\Delta P$	Vapour pressure difference, inside to outside (Pa)
WUFI	Wärme Und Feuchte Instationär		

1.



Figure 1. (a) photo of external access and external stair tower; (b) Thermal model through deck access, pre-refurb, showing ceiling temperature of 13.67C

83% of respondents in a recent (2021) resident survey from Dublin's Oliver Bond social housing scheme reported having issues with damp and mould and 57.8% reported having been told that conditions were their fault and responsibility. These 396 apartments spread over 16 blocks in the city centre were constructed in 1938 of in situ cast 'Clinker' concrete, with external staircase and gantry access to each level. In the 1990's the apartments were partially dry lined with 38mm mineral wool and

service alterations which reduced room ventilation. Two case study apartments were selected each a 2 bed, east orientated, mid floor unit with 2 working adult occupants.

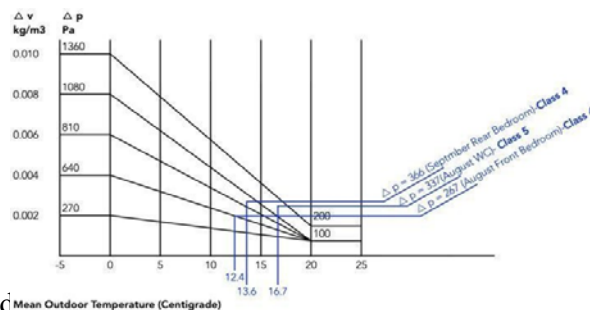
This study aimed to investigate the impact changes to ventilation and the discontinuously applied IWI. The study found that bespoke calculations for surface resistance (Rsi) were limited due to the linearisation of convective and radiative co-efficient values but found elevated values for Rsi in Austrian and German building codes [1] which better reflected the impact of furniture and built-in units on surface temperature than those offered by EN 6946[2] or EN 13788[3].

## 2. Methodology

Site investigation, material and environmental data was applied to three standards, EN 13788, EN 10211[4] (using Psitherm) and EN 15026[5] (using WUFI). Internal Temperature and humidity data was used to calculate the fRsi.min and max values and also the Humidity Class of the internal spaces[6]. These Classifications were subsequently modelled in WUFI where the impact of differing levels of surface resistivity was also simulated. Thermal modelling software was used to compare the impact on fRsi of the of the original and refurbished construction, surface resistivity as well as the impact of modelling with measured versus calculated values.

## 3. Results

Figure 2. (a) Impact of reduced ventilation; Humidity classification based on Delta P values in Apartment 205;



The fRsi.max results based on measured temperature and humidity for July-December showed different results for each apartment but the humidity class results for both apartments having class 4 (e.g canteen/sports hall) & 5 spaces (e.g. brewery/laundry) illustrating the impact of changes to the ventilation. These classes were incorporated into WUFI simulations but did not lead to critical levels of surface humidity. The thermal models revealed that in many locations the addition of IWI lowered the critical surface temperature as well as highlighting the impact of missing insulation and not returning IWI into reveals etc. Both WUFI and Psitherm modelling indicated the significant impact Rsi has on surface temperature. A mould risk was clearly identified in WUFI when combining both the humidity class and elevated surface resistance and risk was confirmed in WUFI Bio for the internal surface of the IWI. Further site inspection confirmed the lowest internal surface temperatures found at the back of wardrobes and around cabinetry and greater correlation between the measured/observed temperatures and thermal models was found where the 0.5 & 1.0 m<sup>2</sup>K/W values were used.

Table 1. Thermal model results showing impact of interior surface resistance on surface temperature, fRsi and u-value.

Rsi	Rse	Rsi	Surface	fRsi	U-value for wall
Interior surface	Exterior surface	Data Source	Temperature at junction		

e resista nce m <sup>2</sup> K/ W	e resista nce m <sup>2</sup> K/ W		ofext. wall & ceiling		W/m <sup>2</sup> K
0.13	0.04	EN 6946	13.31	0.77	0.682
0.25	0.04	EN 13788	13.64	0.68	0.630
0.50	0.04	DIN 4108-8	11.92	0.60	0.544
1.00	0.04	DIN 4108-8	9.98	0.50	0.428

#### 4. Conclusions

The installation of IWI lead to a lowering of critical surface temperatures and increased the risk of condensation and mould. Changes made by landlord (to services/fireplace/boilers) and by tenant (installing cabinets) have increased the internal moisture loads to critical levels. Rsi values offered by EN 13788 and EN 6946 did not properly account for the impact on built-in cabinetry on surface temperatures (and fRsi) as recorded and observed on site. Surface resistivity has greatest impact where thermal transmittance is high, in poorly insulated buildings so the impact of cabinetry should be considered more by designers in the areas of refurbishment and conservation whereas fit out is not currently seen as impacting on fabric and being solely ‘decoration’. This research also highlights the issue of giving advice on u-value targets or limits as apart from Rsi all the calculations in figure 2 use the same wall build up with significantly different results.

#### Reference

- [1] DIN-Fachbericht 4108-8:2020-09 Thermal insulation and energy economy in buildings - Part 8: Avoidance of mould growth in residential buildings
- [2] BS EN ISO 6946:2017 Building components and building elements - thermal resistance and thermal transmittance - calculation method
- [3] BS EN ISO 13788:2012 Hygrothermal performance of building components and building elements - Internal surface temperature to avoid critical surface humidity and interstitial condensation - Calculation methods (ISO 13788:2012)
- [4] BS EN ISO 10211:2017 Thermal bridges in building construction - heat flows and surface temperatures - detailed calculations
- [5] BS EN 15026:2007 Hygrothermal performance of building components and building elements - assessment of moisture transfer by numerical simulation.
- [6] BS 5250:2021 Management of moisture in buildings, Code of practice



# Log-normal distribution for radon measurements in one room

J. Kubiak<sup>12\*</sup>, M. Basińska<sup>2</sup>

*1 Doctoral School of the Poznan University of  
Technology, 60-965 Poznan, Poland,*

*\*Corresponding author:*

*joanna.kubiak@doctorate.put.poznan.pl*

*2 Poznan University of Technology, Faculty of  
Environmental Engineering and Energy, Institute of  
Environmental Engineering and Building  
Installations, Berdychowo 4 Str., 61-131 Poznań,  
Poland*

## ABSTRACT

Increasing attention is being paid to radon concentrations in the assessment of indoor climatic comfort. Radon is a naturally occurring radioactive element that, under unfavourable circumstances, accumulates in excess in a building. Elevated concentrations of it can adversely affect the health of building occupants, resulting in increased interest in this element. The purpose of this study is to carry out a pilot study analysing the distribution and statistics of radon measurements as a preliminary to the analysis of how long radon measurements should be carried out in a given room in order to obtain results that can be regarded as reliable information on annual average radon concentrations. To this end, studies of radon concentrations in a selected room of a building located in central Poland were carried out over a year. Active meters were used for the measurements. Log-normal distributions were fitted to the long-term measurements and statistical measures were generated. As a result of the analyses, two periods of radon concentration were distinguished - summer and winter. It was noted that the distribution for the whole year is a composite of two log-normal distributions. In the situation where the room was used in a typical manner and the comparative level studied was appropriate for the selected measurement period for the winter months, shorter than monthly measurement periods generated meaningful information on radon concentrations. The expected value of the distribution can then be approximated by the median, the geometric mean or the arithmetic mean. Median is probably the best statistical measure for radon measurements.

## KEYWORDS

radon, distribution, statistics, measurements, IAQ

## 1 INTRODUCTION

Radon is a radioactive chemical element that is produced by the decay of radium. Radium, which is one of the elements of the uranium-radium chain, is found in rock minerals. As a result of leaks in the foundations and building materials, radon gets from the soil into the rooms. An indoor radon concentration limit has been set by the World Health Organisation (WHO) at 100 Bq/m<sup>3</sup> level (WHO, 2009). Researchers note that radon concentration measurements show a log-normal distribution (Aladeniyi et al., 2020; Antignani et al., 2019; Daraktchieva et al., 2014; Vukotic et al., 2019). However, researchers note that this distribution may be a composite of several log-normal distributions (Bossew, 2010). The aim of the work is to determine on a pilot basis how long radon concentration measurements should be made so that the results obtained can be considered reliable information on the average annual radon concentrations. For this purpose, radon concentration tests were conducted for over a year in a selected room of a building located in central Poland. Active meters were used for measurements. Pilot studies involve fitting statistics and distributions to measurements.

## 2 METHODOLOGY

Radon measurements were taken using Ethern meters, an active radon meter with an interval of 10 minutes. Parametrics of the device are given in an earlier article by the authors (Kubiak and Basińska, 2023). Measurements were taken between 3.12.2022 and 22.01.2024 - non-physical measurements (coarse errors) were removed and data were split. The building is a single-family house on the outskirts of the city with natural ventilation. The room where the measurements were taken is used almost daily as an office and during the day it is used as a bedroom. R software was used to calculate basic statistical measures from the weeks. A Cullen and Frey chart was drawn to fit the distribution to the measurement data. Based on the graphs and knowledge from the literature, a log-normal distribution (density function - equation 1) was fitted to the entire measurement period. The MATLAB environment was used to fit the log-normal distribution.

$$f(x) = \frac{1}{\sqrt{2 \cdot \pi} \cdot b \cdot x} \cdot e^{-\frac{(\log(x)-a)^2}{2 \cdot b^2}} \quad (1)$$

where:

a, b - distribution parameters,  $\mu, \sigma$

x - random variable

Using the Matlab environment, the log-normal distribution density function was fitted to the probability density function graphs in a way that made it possible to read the values of the parameters a and b (equation 1). Given the values of a and b, the expected value, median and modal were calculated from equations 2-4.

$$E(x) = e^{a + \frac{b^2}{2}} \quad (2)$$

where:

E(x) - expected value

$$M(x) = e^a \quad (3)$$

where:

M(x) - median

$$D(x) = e^{a - b^2} \quad (4)$$

where:

D(x) - dominant

The Cullen and Frey chart will be used to analyze the evaluation of the data distribution feature (Tsapalov and Kovler, 2022).

## 3 RESULTS

Histogram with an interval of 5 Bq/m<sup>3</sup> has been prepared (Fig. 1). Observing the graph, you can see two distinctive peaks, which indicates that the distribution of measurements may probably be a composite of two or more distributions. After seeing the histogram, it was decided to divide the measurement period into two periods - summer and heating season. When the division took place and histograms were generated for individual periods, not two peaks were observed, but one.

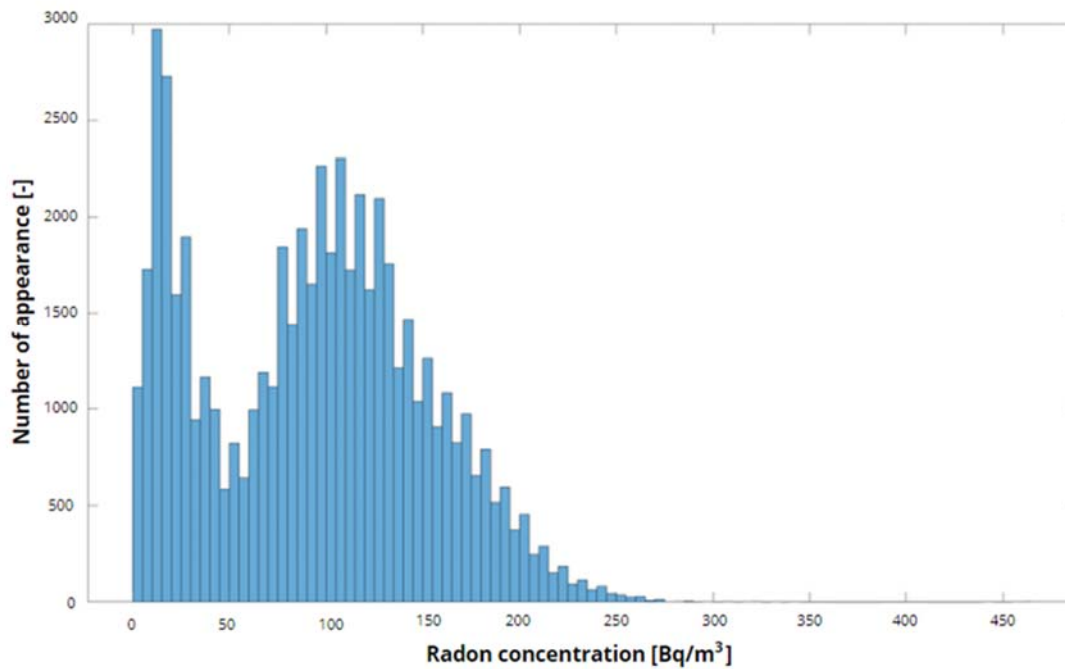
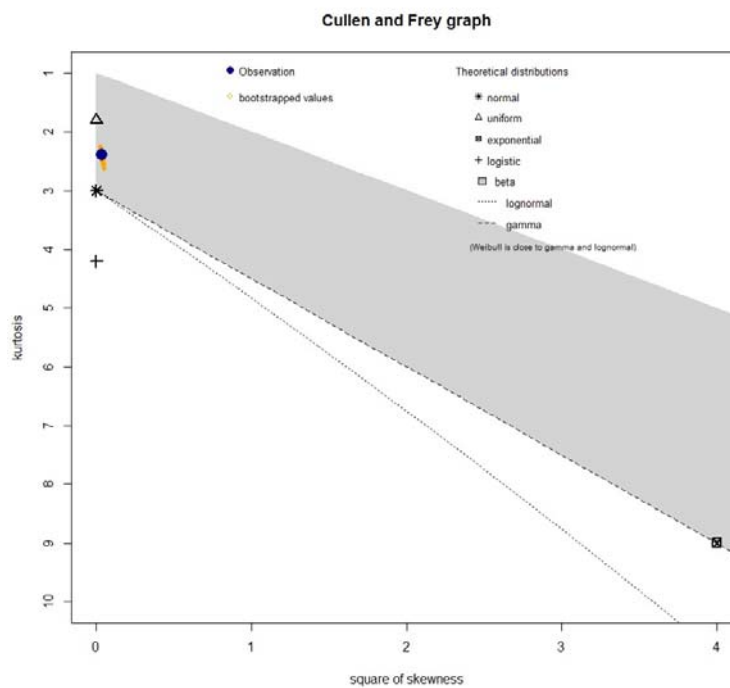


Figure 1 Histogram showing the frequency of occurrence of given measurement values during the year

### 3.1 Fit distribution

A Cullen and Frey Graph was generated for the entire measurement period and for the heating season (Fig. 1).

a)



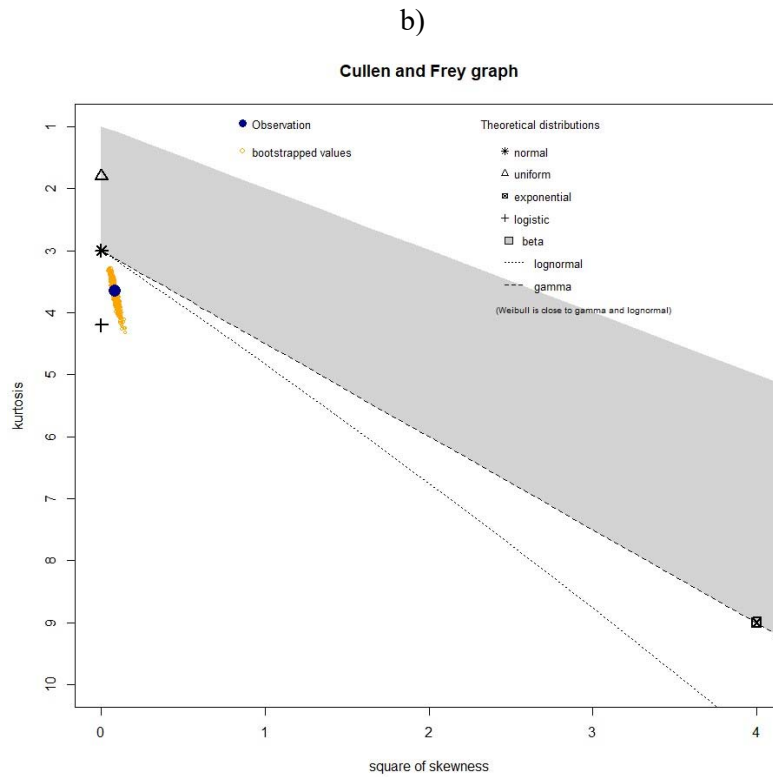


Figure 2 Cullen and Frey Graph a) the entire measurement period b) for the heating season (October to April)

A fit of the log-normal distribution was performed (Fig 2). It is noted that for year-round measurements, there is an overlap between the two log-normal distributions on one chart. When the entire measurement year is included in the Cullen and Frey diagram, the measurement data show a beta distribution, whereas if the measurement data from the summer period are removed from the period, the distribution tends towards a log-normal distribution (Fig. 2b). When the measurement period is divided into the heating period from October to April and the summer period, there is a significantly better fit to the measurement data (Fig. 2).

### 3.2 Distribution and statistical parameters

After considering the type of distribution, a lognormal distribution was fitted to the measurements. The probability density distribution function of the log-normal distribution was fitted for the whole year and the separated heating months, for which the following distribution parameters were obtained (Tab 1).

Tab. 1 Distribution parameters

Parameters of the log-normal distribution	a	b	R <sup>2</sup>	E(x) [Bq/m <sup>3</sup> ]	M(x) [Bq/m <sup>3</sup> ]	D(x) [Bq/m <sup>3</sup> ]
Entire period	4.641	1.169	0.6030	205.1	103.6	26.4
Heating season	4.773	0.351	0.9897	125.8	118.2	104.5

Then basic statistics were generated for the measured data (Tab 2.).

Tab. 2 Basic statistics

Parameters	arithmetic mean [Bq/m <sup>3</sup> ]	geometric mean [Bq/m <sup>3</sup> ]	standard deviation [Bq/m <sup>3</sup> ]	median [Bq/m <sup>3</sup> ]	harmonic mean [Bq/m <sup>3</sup> ]	coefficient of variation [Bq/m <sup>3</sup> ]	asymmetry [Bq/m <sup>3</sup> ]
Whole year	93.8	67.1	57.6	97.4	26.6	0.614	0.189
Heating season	118.7	107.6	43.6	115.0	70.4	0.368	0.241

From the statistics generated, it can be seen that the fitted distributions differ, with a much better fit of  $R^2 = 0.99$  being obtained for the heating season fit. A poor  $R^2 = 0.60$  compared to the heating season fit of the distribution generates significant deviations in the values calculated from the distribution (for example  $E(x)$ ) compared to the statistics calculated from the data (arithmetic and geometric mean). In the case of the heating season, all parameters such as geometric mean and median differ slightly, while in the case of the annual period, the geometric mean deviates from the median and arithmetic mean. There is right-handed asymmetry in both measurement periods. The coefficient of variation for the entire measurement period shows a strong correlation for the heating season, being 50% lower. For the entire period, lower average radon concentrations are observed compared to the heating season.

#### 4 DISCUSSION

The way the room is used by people has a strong influence on the radon concentration profile in the room (Yarmoshenko et al., 2021). When analysing the results obtained, the season in which the survey took place must be taken into account. The statistics as well as the distributions in the summer and heating seasons differ significantly from each other. In the heating season, the differences between statistical measures (minimum - maximum) do not exceed 10%, so meticulous consideration of the selection of the appropriate statistic for analysis - median, geometric mean, arithmetic mean - does not seem very necessary. For the entire measurement period, the difference between the maximum and minimum statistical value is more than 45%. The proposed statistical measure proposed by the authors to estimate the annual radon concentration is the median, which reflects well the expected value of the distribution of radon measurements, taking into account the asymmetry of the distribution. The geometric mean, although it seems appropriate, considering the coefficient of variation, underestimates the measurements which was also evident in the results from other researchers (Ptíček Siročić et al., 2020). The question of how long radon measurements have to be recorded with active meters in order to give a meaningful result on an annual basis and how to take into account the correction for a given measurement month is still under discussion. Studies by other researchers indicate that it is possible to estimate annual variability from short-term measurements, however, seasonal variability is important (Li et al., 2023), which is probably strongly influenced by the user (Kubiak and Basińska, 2022), and meteorological conditions (Rey et al., 2023), building-related parameters such as air tightness also have a significant influence (McGrath et al., 2021). Some researchers claim that estimation of long-term measurements is not possible (Nunes and Curado, 2023). However, such conclusions may be the result of an inaccurate choice of measurement location and measurement period. Undoubtedly, determining how long short-term measurements must be in order to estimate the indoor situation will contribute to reducing the costs of measurement campaigns, which currently amount to millions of euro (Gruber et al., 2021). However, pilot studies have shown that it is potentially possible to assess long-term measurement statistics on the basis of short-term measurements, but this requires a strategy to take appropriate corrections into account, which is already being considered by researchers (Tsapalov and Kovler, 2022).

## 5 CONCLUSIONS

Radon measurements are characterised by a log-normal distribution. However, the measurement period should be divided between the heating season and the summer season to obtain a good fit. For the heating season, the expected value of the distribution can be approximated by the median, the geometric mean, the arithmetic mean, for the whole year the statistical parameters differ - the geometric mean is then recommended due to the large coefficient of variation for all measurements, while the median also appears to be a good fit due to its closeness to the value calculated from the distribution. The geometric mean underestimates the expected value of the distribution and the median for the entire measurement period better reflects the expected value of the heating season. For the heating season, the distribution of radon measurements is characterised by right-handed asymmetry with mean variation.

Further analyses need to be carried out in order to determine the periods of radon measurements that clearly resonate in the analysis carried out. The above analyses should also be checked in other building types.

## 6 REFERENCES

- Aladeniyi, K., Arogunjo, A.M., Pereira, A.J., Ajayi, O.S. and Fuwape, I.A. 2020. Radiometric evaluation of indoor radon levels with influence of building characteristics in residential homes from southwestern Nigeria. *Environmental Monitoring and Assessment* 192, 1-15.
- Antignani, S., Venoso, G., Carpentieri, C. and Bochicchio, F. 2019. Analytical method for evaluating (and correcting) the impact of outdoor radon concentration on the estimates of percentage of dwellings exceeding reference levels. *Journal of environmental radioactivity* 196, 264-267.
- Bossey, P. 2010. Radon: exploring the log-normal mystery. *Journal of environmental radioactivity* 101(10), 826-834.
- Daraktchieva, Z., Miles, J. and McColl, N. 2014. Radon, the lognormal distribution and deviation from it. *Journal of Radiological Protection* 34(1), 183.
- Gruber, V., Baumann, S., Wurm, G., Ringer, W. and Alber, O. 2021. The new Austrian indoor radon survey (ÖNRAP 2, 2013–2019): design, implementation, results. *Journal of Environmental Radioactivity* 233, 106618.
- Kubiak, J. and Basińska, M. 2023. Assessment of annual effective dose and health risk due to radon exposure in nurseries in the city of Poznań, Poland. *Building and Environment*, 110782.
- Kubiak, J.A. and Basińska, M. 2022. Analysis of the Radon Concentration in Selected Rooms of Buildings in Poznan County. *Atmosphere* 13(10), 1664.

- Li, L., Coull, B.A. and Koutrakis, P. 2023. A national comparison between the collocated short-and long-term radon measurements in the United States. *Journal of exposure science & environmental epidemiology* 33(3), 455-464.
- Nunes, L.J. and Curado, A. 2023. Long-term vs. short-term measurements in indoor Rn concentration monitoring: Establishing a procedure for assessing exposure potential (RnEP). *Results in Engineering* 17, 100966.
- McGrath, J. A., Aghamolaei, R., O'Donnell, J., & Byrne, M. A. (2021). Factors influencing radon concentration during energy retrofitting in domestic buildings: A computational evaluation. *Building and Environment*, 194, 107712.
- Ptiček Siročić, A., Stanko, D., Sakač, N., Dogančić, D. and Trojko, T. 2020. Short-term measurement of indoor radon concentration in Northern Croatia. *Applied Sciences* 10(7), 2341.
- Rey, J.F., Goyette, S. and Goyette Pernot, J. 2023. Weather Impacts on Indoor Radon Short-Term Measurements in Switzerland. *Atmosphere* 14(7), 1163.
- Tsapalov, A. and Kovler, K. 2022. Temporal uncertainty versus coefficient of variation for rational regulation of indoor radon. *Indoor air* 32(9), e13098.
- Vukotic, P., Antovic, N., Djurovic, A., Zekic, R., Svrkota, N., Andjelic, T., Svrkota, R., Mrdak, R., Bjelica, N. and Djurovic, T. 2019. Radon survey in Montenegro—A base to set national radon reference and “urgent action” level. *Journal of environmental radioactivity* 196, 232-239.
- WHO (2009) WHO handbook on indoor radon: a public health perspective, World Health Organization.
- Yarmoshenko, I., Zhukovsky, M., Onishchenko, A., Vasilyev, A. and Malinovsky, G. 2021. Factors influencing temporal variations of radon concentration in high-rise buildings. *Journal of Environmental Radioactivity* 232, 106575.

# On the estimate and reduction of the zero-flow pressure estimation uncertainty in fan pressurization measurement

Martin Prignon<sup>1</sup>, Christophe Delmotte<sup>1</sup>, Benedikt Kölsch<sup>2</sup>

<sup>1</sup> Buildwise  
Kleine Kloosterstraat 23  
1932 ZAVENTEM,  
Belgium

<sup>2</sup> German Aerospace Center (DLR),  
Institute of Solar Research,  
Linder Höhe, 51147 Cologne,  
Germany

\*Corresponding author: [martin.prignon@buildwise.be](mailto:martin.prignon@buildwise.be)

## ABSTRACT

Building airtightness is of foremost importance because of its impact on global energy consumption, but also on occupant's comfort, dimensioning of ventilation systems, hygrothermal behaviour, fire safety, etc. This building characteristic is usually measured with the fan pressurization method, following ISO 9972:2015 standard. This method requires to assume that the pressure difference due to wind and stack effect, called the zero-flow pressure difference, is constant during the test and that its value is the average of pre- and post-test measurements. This bold hypothesis leads to some uncertainty, referred in the literature as  $u(\Delta p_{0,a})$ . In this paper, we use two different datasets in order to (1) assess the validity of the formula proposed in literature to quantify this uncertainty term, (2) investigate some variations in the measurement protocol to reduce this source of uncertainty, and (3) evaluate the impact of this uncertainty source on the final result of the fan pressurization test. Results show that, specifically for this data set, this estimation represents a large uncertainty of 1.27 Pa in pressure measurements that could be slightly reduced by increasing the number of measurement or using a multiple-estimator procedure. This uncertainty source could represent a 1% uncertainty in the airflow rate at 50 Pa (the final result of the fan pressurization test). Further research should focus on using other datasets to remove some limitations of this study, and on the development of alternative procedures in order to reduce this consequent source of uncertainty.

## KEYWORDS

Fan pressurization measurement; zero-flow pressure difference; uncertainty calculation.

## 1 INTRODUCTION

In practice, during a fan pressurization test, the pressure difference between the indoor and outdoor probes at a time  $t$  is the combination of the fan-induced pressure difference ( $\Delta p_{ind,t}$ ) and the zero-flow pressure difference ( $\Delta p_{0,t}$ ), which is the pressure difference induced by climatic conditions (Eq. 1).

$$\Delta p_t = \Delta p_{ind,t} + \Delta p_{0,t} \quad (1)$$

The value of interest ( $\Delta p_{ind,t}$ ) cannot be measured directly, while the zero-flow pressure difference can only be measured when the fan is not operating (i.e.,  $\Delta p_{ind,t} = 0$ ). Consequently, the value of  $\Delta p_{0,t}$  when the fan is operating has to be assumed. The (ISO 9972, 2015) standard suggests that the zero-flow pressure should be considered as a constant value during the test, based on a series of measurements taken before ( $\Delta p_{0,pre,j}$ ) and after ( $\Delta p_{0,post,j}$ ) the test. In this study, we assume that the same number  $N_0$  of measurements are taken for both periods, leading to Eq. 2:

$$\Delta p_{0,t} = \Delta p_0 = 0.5 * \left( \frac{\sum_{j=1}^{N_0} \Delta p_{0,pre,j}}{N_0} + \frac{\sum_{j=1}^{N_0} \Delta p_{0,post,j}}{N_0} \right) \quad (2)$$



When there is wind or temperature variations during the test, the zero-flow pressure difference varies, and the constant assumption is not valid anymore. Mathematically, this is considered by defining an additional uncertainty term in the calculation,  $u(\Delta p_{0,a})$ . In the literature, different approaches to quantify this uncertainty source have been suggested by (Delmotte, 2017) (Eq. 3) and (Prignon et al., 2021) (Eq. 4):

$$u(\Delta p_{0,a})|_1 = \frac{\max(|\Delta p_{0,max} - \Delta p_{0,av}|; |\Delta p_{0,min} - \Delta p_{0,av}|)}{\sqrt{6}} = \frac{\delta}{\sqrt{6}} \approx \frac{\delta}{2.45} \quad (3)$$

$$u(\Delta p_{0,a})|_2 = \frac{(0.11 + 0.98 * \sigma(\Delta p_{0,m}))}{1.35} \quad (4)$$

This paper is a continuation of previous work and aims to (1) assess the validity of the formula proposed in the literature, (2) investigate some variations in the measurement protocol to reduce this source of uncertainty, and (3) evaluate the impact of this uncertainty source on the final result of the fan pressurization test. This paper is structured as follows. In the methodology section, the different datasets are described, and the methods for data analysis are illustrated. The outcome of this analysis is provided in the result section, including the quantification of the uncertainty source, comparison with values suggested in the literature, potential improvements through adaptations of the procedure, and assessment of its impact on the final results. Finally, in the conclusion, we summarize the outcomes of this work, highlight the limitations of the study, and describe the further work needed in this field of research.

## 2 METHODOLOGY

In this paper, two different datasets are used and manipulated in order to draw conclusions about the studied uncertainty source: 30 zero-flow pressure profiles and a dataset of 127 repeatability studies. Those datasets and how the analysis is performed is outlined in this section of the paper.

### 2.1 Zero-flow pressure profiles

The zero-flow pressure dataset includes 30 zero-flow pressure profiles obtained from measurements made on the same apartment in Brussels, without changing the location of the pressure probes. More details about the building geometry and orientation are provided in (Prignon et al., 2019). A zero-flow pressure profile is the measurement of zero-flow pressure difference for 15 minutes, which corresponds approximately to the duration of a fan pressurization test. As depicted in Figure 1, those profiles are divided into two parts: the estimation parts (in orange) used for zero-flow pressure estimation, and the estimated part (in green) used for assessing the estimation “quality” by comparing it with the measured value. Note that during a real fan pressurization test, the data recorded in the central part is not available since the fan is operating.

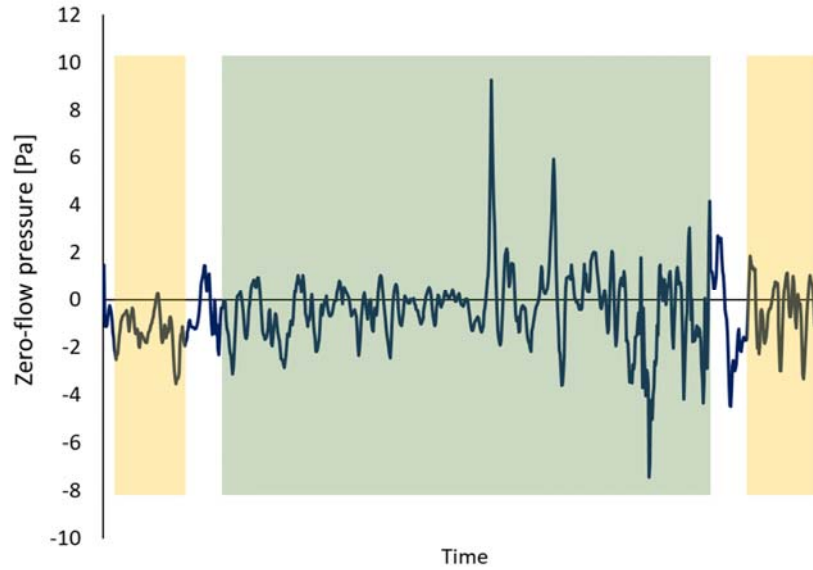


Figure 1. Typical zero-flow pressure profiles with the estimation (orange) and estimated (green) zones.

Those profiles are used to quantify  $u(\Delta p_{0,a})$  by comparing the estimated zero-flow pressure for a given estimation procedure ( $\Delta p_{0,est}$ ) with 10 equally-spaced averages of  $N$  measurements made in the estimated zone (green) of the profiles ( $\Delta p_{0,real,i}$ ,  $i = 1, \dots, 10$ ). The error is then defined for each average as the difference between the estimation and the average (Eq. 5).

$$e_i = \Delta p_{0,est} - \Delta p_{0,real,i} \quad (5)$$

We assume in this paper that the standard deviation of the 300 calculated values (10 for each test) provides a good approximation of the uncertainty source:  $\sigma(e_i) \approx u(\Delta p_{0,a})$ . Indeed, (JCGM, 2008) states that if  $e_i$  is normally distributed, then the uncertainty on the standard deviation estimate (i.e., the risk that the standard deviation of the estimate is different from the standard deviation of the data) is 4.1%, which seems acceptable to us.

Then, the same methodology is used in order to compare another estimation procedure called the multiple-estimators procedure. Instead of considering a constant zero-flow pressure during the whole test as suggested by ISO 9972:2015, the zero-flow pressure is measured before and after each pressure station, and an approximation is made for each. Figure 2 shows how the estimation and estimated zones from Figure 1 are adapted in that situation.

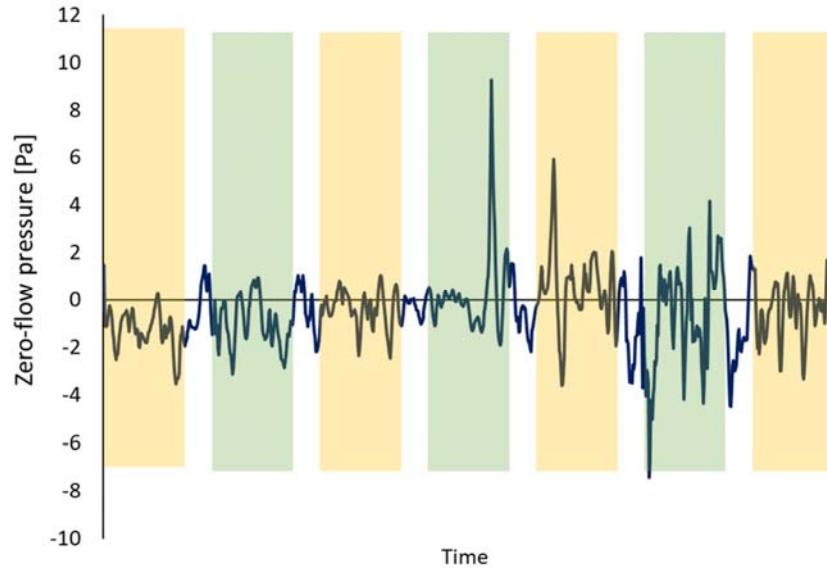


Figure 2. Typical zero-flow pressure profiles with the estimation (orange) and estimated (green) zones for the multiple-estimators procedure.

Under this estimation procedure, the zero-flow pressure estimate at pressure station  $i$  is the average of  $N_0$  zero-flow pressure measurements made before and after that pressure station (Eq. 6). Except for the first and last, each estimation zone is used for two pressure stations. Note that the change of the estimation procedure also affects the total duration of the test, which is not an aspect further considered in this paper.

$$\Delta p_{0,i} = 0.5 * \left( \frac{\sum_{j=1}^{N_0} \Delta p_{0,i,pre,j}}{N_0} + \frac{\sum_{j=1}^{N_0} \Delta p_{0,i,post,j}}{N_0} \right) \quad (6)$$

The same dataset is also used to validate the uncertainty estimation suggested in the literature (Eq. 3 and Eq. 4). In that context, two criteria were observed:

1. The relevance of the variables used. This is done by calculating the Pearson's correlation coefficient between the absolute error,  $|e_i|$ , and the relevant variables:  $\delta$  and  $\sigma(\Delta p_{0,m})$ .
2. The order of magnitude of the estimation. This is done by comparing the standard deviation of the observed error with the average of the calculated uncertainty of each dataset using one or another formula.

## 2.2 Semi-theoretical tests

Those zero-flow profiles were then combined with theoretical “perfect” fan-induced pressure profiles in order to estimate the impact of this uncertainty source on the uncertainty in the final results. These “perfect” profiles were obtained with 10 successive pressure stations of  $N$  measurements. For the ISO 9972 estimation procedure, 10 seconds were used for the transition from one station to another. For the multiple-estimators procedure, 20 seconds were needed to go from 0 to each station, while 10 seconds were needed to go from high-pressure measurements to 0. The combination is illustrated in Figure 3 for both estimation procedures.

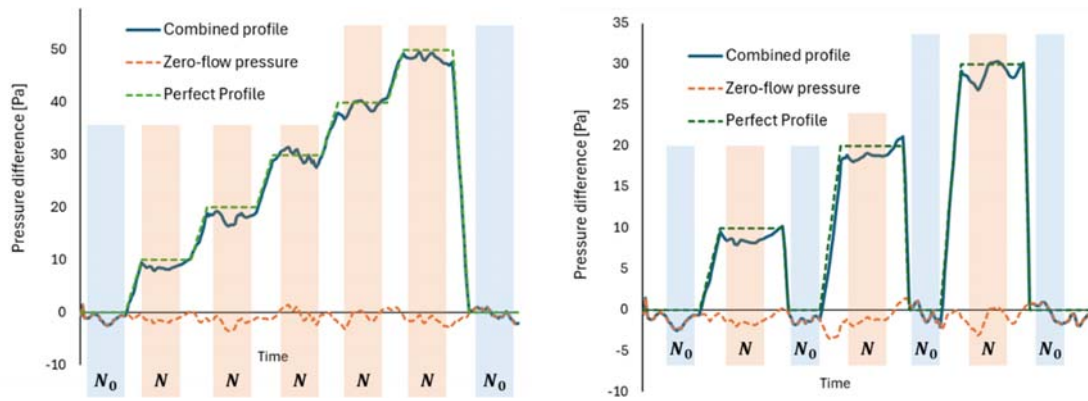


Figure 3. Example of semi-theoretical profiles obtained by combining zero-flow pressure profiles with “perfect” fan-induced pressure profiles created for the estimation procedure in line with ISO 9972:2015 (left) and the multiple-estimators procedure (right).

In parallel, the 30 “perfect” fan-induced pressure profiles were then used to create 30 “perfect” airflow profiles, by assuming a power-law relation with  $C = 55$  and  $n = 0.67$  (Eq. 7).

$$q_t = 55 * (\Delta p_{ind,t})^{0.67} \quad (7)$$

Note that the total pressure is not “perfect” since it is the sum of the induced pressure and the zero-flow pressure. However, since the induced pressure is used to determine the airflow profile, this one is “perfect” (i.e., the airflow rate through the fan is constant at each station). Those profiles produce 30 semi-theoretical tests that are then used as a set of repeatability tests where only the zero-flow pressure varies. The rest of the ISO 9972:2015 procedure was applied without considering any other source of error than the zero-flow pressure estimation. In such conditions, the standard deviation of the 30 final air leakage rates is assumed being the uncertainty in the final result caused by the zero-flow pressure variation during a fan pressurization test.

### 2.3 Large dataset

A dataset of 127 repeatability studies, including more than 6.000 fan pressurization tests conducted on 6 different houses was also used in order to evaluate how different estimation procedures impact the variation in the final result. This dataset is described in detail in (Walker et al., 2013). In that dataset, the zero-flow pressure was measured before and after each pressure station, allowing the computation of the ISO 9972:2015 estimation procedure by considering only the first and the last zero-flow pressure measurements and the multiple-estimators procedure by considering all averages. Two important aspects are worth noticing when drawing conclusions based on this dataset:

1. The estimation procedure suggested in ISO 9972:2015 is expected to take less time than the multiple-estimator procedure. This is not investigated in this dataset because regardless of the measurements effectively used in the procedure, all were measured in practice.
2. All the pressure differences were determined by averaging measurements made on four different facades of the building, which does not follow the ISO 9972:2015 procedure. This has an important impact on the results and, consequently, conclusions drawn from this dataset should not be compared to the conclusion drawn from the other dataset and should be used in the context of 4-point averages only.

The comparison of both estimation procedures is made by averaging the 127 standards deviations observed.

### 3 RESULTS

#### 3.1 Quantification of $u(\Delta p_{0,a})$

Figure 4 (left) shows the distribution profile of the errors due to zero-flow pressure difference estimation ( $e_i$ ) using ISO 9972:2015 procedure, with  $N_0 = N = 30$ . The average is  $\mu(e_i) = -0.06$  Pa and the standard deviation is  $\sigma(e_i) = 1.27$  Pa. Figure 4 (right) shows the equivalent distribution when using the multiple-estimator procedure with  $N_0 = N = 25$ . For this second procedure,  $\mu(e_i) = 0.09$  Pa and  $\sigma(e_i) = 1.09$  Pa. Note that different  $N_0$  and  $N$  were compared in both procedures because the dataset was not large enough to compare the second procedure with the same values for  $N$  and  $N_0$ .

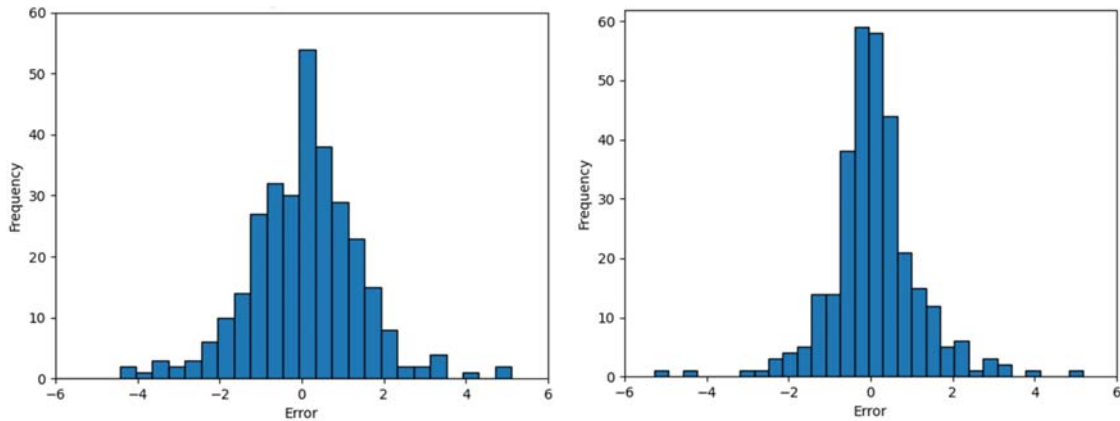


Figure 4. Distribution of the  $e_i$  values obtained with Eq. 5 when using the ISO 9972:2015 estimation procedure with  $N_0 = N = 30$  measurements (left) and the multiple-estimators procedure with  $N_0 = N = 25$ .

The standard deviation of the error is influenced by the number of zero-flow pressure measurements used for the estimation ( $N_0$ ) and the number of pressure measurements made at each pressure station ( $N$ ). However, this influence is expected to vary depending on climatic conditions. The zero-flow pressure profile used in this study were obtained on a single-story apartment, which means that the stack effect is expected to be relatively small, and under wind conditions varying from 0.4 m/s to 4.0 m/s (15 min average during the tests).

Figure 5 shows how  $u(\Delta p_{0,a})$  is impacted by a variation in  $N$  and  $N_0$  values, where the ISO 9972:2015 estimation procedure is used. It shows that increasing the number of zero-flow pressure measurements ( $N_0$ ) and the number of pressure measurements ( $N$ ) provides a lower uncertainty. However, the large scattering of the results suggests that those observation should be considered with some caution and that a larger dataset should be used to generalize them, especially regarding the impact of  $N_0$ .

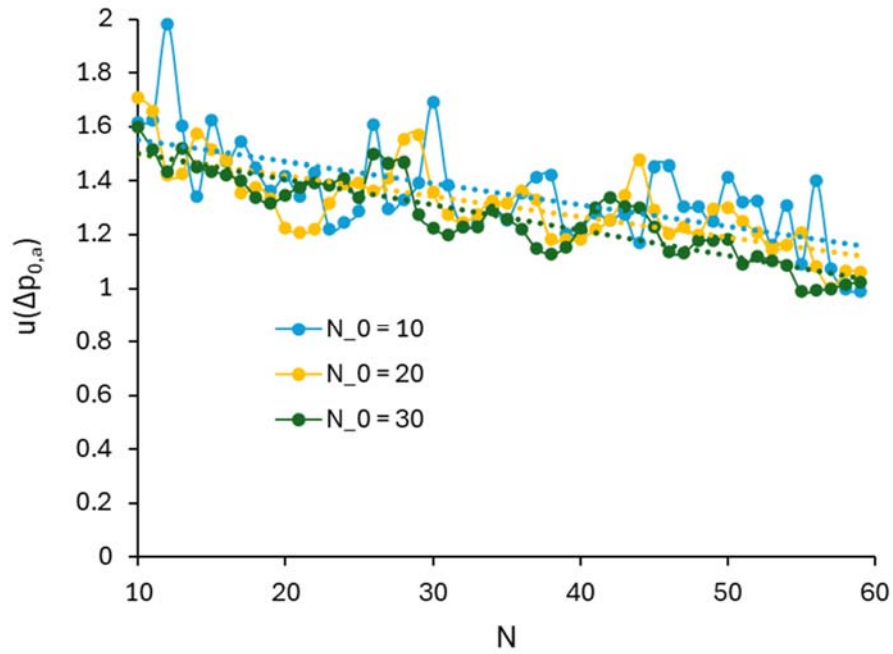


Figure 5. Impact of  $N_0$  and  $N$  on the uncertainty estimation, calculated with Eq. 5, for the estimation procedure following ISO 9972:2015

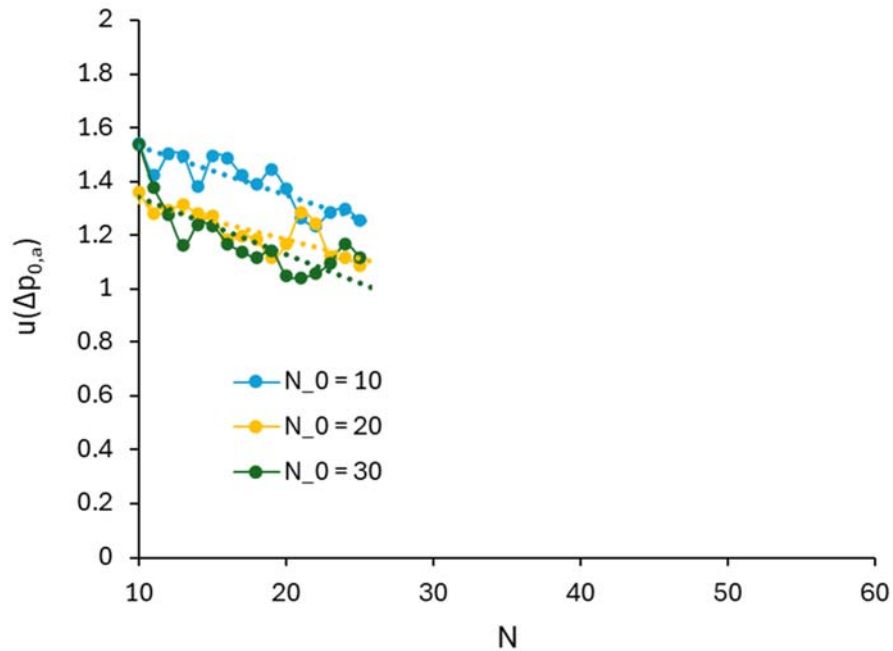


Figure 6 Figure 6 shows a similar graph for the multiple-estimator procedure. In this case, the impact of having  $N_0 > 10$  is more pronounced, while  $N_0 = 20$  and  $N_0 = 30$  seems to perform similarly. Whatever the  $N_0$  value, increasing the number of pressure measurements at pressure station ( $N$ ) also reduces the uncertainty. Note that due to the longer duration of this second procedure, it was not possible to check cases with  $N > 30$  with the dataset.

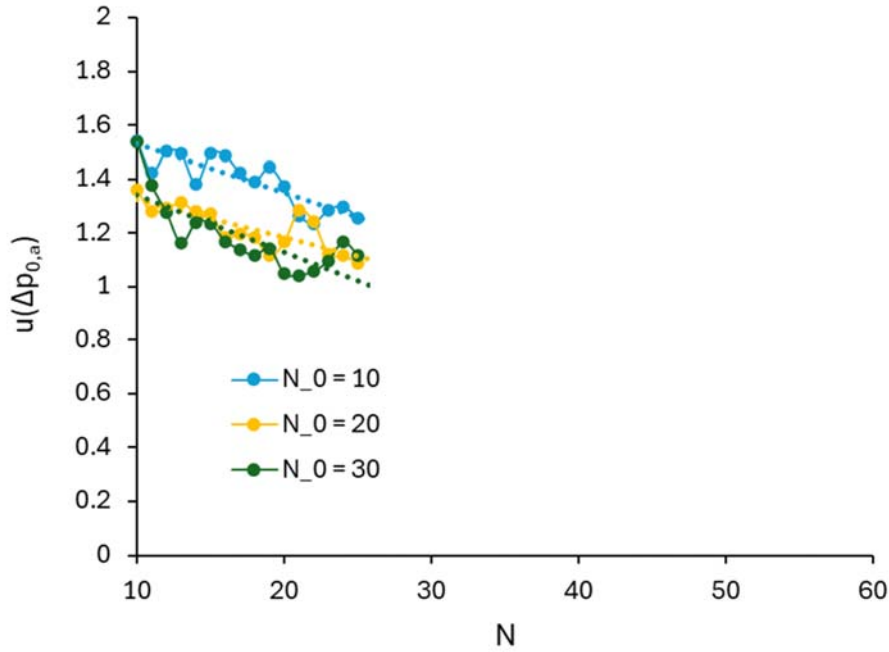


Figure 6. Impact of  $N_0$  and  $N$  on the uncertainty estimation, calculated with Eq. 5, for the multiple estimator procedure.

### 3.2 Comparison with the uncertainty terms suggested in literature

When applying ISO 9972:2015, medium correlations (Pearson's correlation coefficient  $0.5 > r > 0.3$ ; (Ellis, 2010)) were found between the absolute error and the variables used in the literature for quantification of the approximation uncertainty. Additionally, the averages of the calculated uncertainties are in the same order of magnitude as the standard deviation of error ( $u(\Delta p_{0,a}) \approx \sigma(e_i) = 1.27$  Pa, for  $N_0 = N = 30$ ):

- $\overline{u(\Delta p_{0,a})}|_1 = 1.53$  Pa ; and  $r(\delta ; |e|) = 0.35$
- $\overline{u(\Delta p_{0,a})}|_2 = 0.94$  Pa ; and  $r(\sigma(\Delta p_0) ; |e|) = 0.35$

Those results suggest that the choices made in the literature were relevant, but they do not perfectly grasp the real error caused by this approximation. However, based on the dataset used in this study, Eq. 4 could be adapted to provide a better estimate of the uncertainty:

$$\begin{aligned}
 u(\Delta p_{0,a})|_{2,new} &= 1.1 * \sigma(\Delta p_{0,m}) \\
 \rightarrow \overline{u(\Delta p_{0,a})}|_{2,new} &= 1.28 \text{ Pa}
 \end{aligned}
 \tag{9}$$

Note that although Eq. 3 seems to overestimate the uncertainty, it is based on a mathematical background (triangular distribution) and adapting the proposed equation would not be relevant since it would have no physical meaning. This is not the case for Eq. 4, which is empirically derived. Note that regardless of the equation used, it should always be zero in case of constant wind and constant temperature differences, which is the case for both suggestions here.

### 3.3 Impact on final result uncertainty

Table 1 shows the evolution of  $\sigma(q_{50})$  and  $\sigma(q_4)$  (in % of measured airflow) using both estimation procedures and for both datasets. The post-processing of the data uses WLOC

regression method and Eq. 4 for  $u(\Delta p_{0,a})$ . Note, however, that using another regression method or another equation for  $u(\Delta p_{0,a})$  is not expected to provide much different results for those observed variables.

Table 1. Standard deviation of the repeatability studies using the semi-theoretical profiles and the large dataset, for the ISO 9972:2015 estimation procedure and the multiple-estimator procedure, at 4 and 50 Pa of pressure difference.

	Semi-theoretical profiles (1 repeatability study)		Large dataset (109 repeatability studies)	
	$\sigma(q_4)$	$\sigma(q_{50})$	$\overline{\sigma(q_4)}$	$\overline{\sigma(q_{50})}$
ISO 9972:2015 procedure	4.35	1.06	8.35	4.27
Multiple-estimator procedure	3.23	0.42	7.94	4.21

For the semi-theoretical profiles (i.e., constant airflows and induced pressure at each pressure station), the results from the 30 tests are not normally distributed (checked with Shapiro-Wilk test for both procedures at 4 and 50 Pa). Consequently, non-parametric tools should be used to check the statistical significance of the differences observed between the procedures (Wilcoxon signed-rank test for the mean comparison, and Fligner-Killeen Test for the variance comparison):

- At  $q_{50}$ , using different estimation procedures shows no significant differences in averages but a significant difference in their variances. This suggests that using a multiple-estimator procedure reduces the uncertainty without creating any bias compared to the ISO 9972:2015 procedure.
- At  $q_4$ , however, there is neither a significant difference in averages nor in their variances. This suggests that the multiple-estimator procedure has no added value.

When examining the large dataset, the repeatability tests with  $N < 10$  were removed, resulting in the analysis of 109 of the 127 repeatability tests. This arbitrary choice was made to avoid cases with strong risks of having a standard deviation that is not a good estimate of the uncertainty. Since most of the tests are not normally distributed, the same non-parametric tests were used to assess the statistical significance of the observed difference:

- At  $q_{50}$ , using different estimation procedures shows a significant difference in averages for 20 of the 109 repeatability studies, and a significance difference in the standard deviation for none of them.
- At  $q_4$ , results show a significant difference in averages for 45 of the 109 repeatability studies, while a significance difference in standard deviation is found for only one of them. Those results suggest that the multiple-estimator procedure has no added value in this context.

Note that because of the variations observed in the methodology for data acquisition (e.g., averaging the pressure difference using four different manometers placed on different facades, as mentioned in section 2.3), the results using semi-theoretical profiles and those using the large dataset cannot be directly compared.

An additional interesting observation is that the values found in Table 1 for applying the ISO 9972:2015 procedure on semi-theoretical profiles ( $\sigma(q_{50}) = 1.06\%$ ) are close to the values found on other repeatability studies where  $\sigma(q_{50})$  is in the range [1.1% ; 2.3%] (Bracke et al.,



2016; Delmotte and Laverge, 2011; Kim and Shaw, 1986; Novak, 2015; Persily, 1982; Prignon et al., 2018). This suggests that this source of uncertainty could represent a large part of the final random error.

#### 4 CONCLUSION

In this study, we analysed the impact of the zero-flow pressure estimation on the uncertainty of the fan pressurization test and investigated two ways to reduce this uncertainty source: increasing the number of measurements ( $N$  and  $N_0$ ) or using another estimation procedure. This was done by analysing two different datasets: one is a dataset of zero-flow pressure profiles while the other is a dataset of 127 repeatability test. The main findings can be summarized as follows:

- There is a large uncertainty on the pressure measurements due to the zero-flow pressure estimation ( $u(\Delta p_{0,a}) = 1.27$  Pa in this dataset). This uncertainty also affects the final result of the fan pressurization test (a random error of 1.06% of the measured airflow rate in this study).
- While using a multiple-estimators procedure to replace the ISO 9972:2015 seems to lower the final uncertainty (as shown in Table 1), those trends were not statistically confirmed except at 50 Pa for the zero-flow pressure dataset.
- This source of uncertainty can be reduced by increasing the number of measurements for the zero-flow pressure ( $N_0$ ) and at each pressure station ( $N$ ). No clear threshold value was found, and larger datasets should be used to draw relevant guidelines.

Those results provide a better knowledge of the uncertainty of the fan pressurization measurement, which is relevant in order to suggest improvement of the measurement protocol. Additionally, quantifying uncertainty terms is needed when applying weighted regression techniques, such as WLOC described by (Delmotte, 2017), which have been shown to provide a better estimate of the real uncertainty by (Delmotte, 2017; Prignon et al., 2020).

This work contains some limitations, including but not limited to the small size of the first dataset, which does not allow for a comprehensive analysis of the impact of  $N$  and  $N_0$  on the uncertainty calculation. Additionally, the conclusion drawn from both datasets could not be compared to each other due to the variations in the measurement procedure.

Given that this important source of uncertainty seems to be responsible for a large part of the final uncertainty of the test, further research should investigate adaptations of the fan pressurization protocol that could reduce this source of uncertainty. Moreover, the results obtained in this study should be confirmed by applying the same methodology to other datasets of zero-flow pressure measurements, including different building typologies and different locations of pressure probes within the building.

#### 5 ACKNOWLEDGEMENTS

The authors would like to gratefully thank Iain Walker for access to the large database of repeatability studies that were used to derive part of the conclusions drawn in this paper.

#### 6 NOMENCLATURE

##### Variables

$\Delta p$	Total pressure difference
$\Delta p_{ind}$	Fan-induced pressure difference
$\Delta p_0$	Zero-flow pressure difference
$u(\Delta p_{0,a})$	Uncertainty due to the zero-flow pressure approximation
$N$	Number of measurements made for the pressure averages at each stations
$N_0$	Number of measurements made for the average of zero-flow pressure
$\delta$	Term used to simplify Eq. 3, with no physical meaning

### Subscripts

$i, j$	refer to an element in a series
$t$	refers to a moment in time
$m$	refers to a measured quantity
<i>new</i>	refers to a new version of the model
<i>pre, post</i>	refer to measurements period before and after the period with the fan operating
<i>est</i>	refers to an estimated value
<i>real</i>	refers to a real value
1, 2	refer to two different uncertainty estimation formula provided in the literature
4, 50	refer to two typical pressure difference used in standards

## 7 REFERENCES

- Bracke, W., Laverge, J., Bossche, N.V.D., Janssens, A., 2016. Durability and measurement uncertainty of airtightness in extremely airtight dwellings. *International Journal of Ventilation* 14, 383–394.
- Delmotte, C., 2017. Airtightness of buildings-considerations regarding the zero-flow pressure and the weighted line of organic correlation. Presented at the 38th AIVC Conference.
- Delmotte, C., Laverge, J., 2011. Interlaboratory tests for the determination of repeatability and reproducibility of buildings airtightness measurements. Presented at the 32nd AIVC conference and 1st TightVent Conference.
- Ellis, P.D., 2010. *The essential guide to effect sizes: Statistical power, meta-analysis, and the interpretation of research results*. Cambridge university press.
- ISO 9972, 2015. *Thermal performance of buildings - Determination of air permeability of buildings - Fan pressurization method*.
- JCGM, 2008. *Evaluation of measurement data - Guide to the Expression of Uncertainty in Measurement*. Joint Committee for Guides in Metrology.
- Kim, A.K., Shaw, C.Y., 1986. Seasonal variation in airtightness of two detached houses, in: *Measured Air Leakage of Buildings*. ASTM International.
- Novak, J., 2015. Repeatability and reproducibility of blower door tests—five years’ experience of round-robin tests in the Czech Republic. Presented at the 9th Buildair Symposium, Germany.
- Persily, A., 1982. Repeatability and accuracy of pressurization testing. Presented at the DOE/ASHRAE Conference “Thermal Performance of the Exterior Envelopes of Buildings II”, Las Vegas.
- Prignon, M., Dawans, A., Altomonte, S., Van Moeseke, G., 2019. A method to quantify uncertainties in airtightness measurements: Zero-flow and envelope pressure. *Energy and Buildings* 188, 12–24.
- Prignon, M., Dawans, A., van Moeseke, G., 2021. Quantification of uncertainty in zero-flow pressure approximation. *International Journal of Ventilation* 20, 248–257.
- Prignon, M., Dawans, A., Van Moeseke, G., 2018. Uncertainties in airtightness measurements: regression methods and pressure sequences. Presented at the 39th AIVC conference, France.

- Prignon, M., Delmotte, C., Dawans, A., Altomonte, S., van Moeseke, G., 2020. On the impact of regression technique to airtightness measurements uncertainties. *Energy and Buildings* 215, 109919.
- Walker, I., Sherman, M.H., Joh, J., Chan, W., 2013. Applying Large Datasets to Developing a Better Understanding of Air Leakage Measurement in Homes. *International Journal of Ventilation* 11, 323–338.

# A Pre-Post Retrofit Evaluation on Indoor Air Quality and Comfort in Classrooms and Offices: Pre-Retrofit Findings

Adam Collison<sup>1\*</sup>, Miriam Byrne<sup>1</sup>, James A. McGrath<sup>2</sup>

*1 School of Natural Sciences  
University of Galway  
Galway, Ireland*

*2 Department of Experimental Physics  
Maynooth University  
Maynooth, Ireland*

*\*Corresponding author:  
a.collison1@universityofgalway.ie*

## SUMMARY

The BENEFIT project evaluates the indoor environmental quality in non-domestic buildings where energy efficiency upgrades will be implemented; a baseline for indoor air quality has been established across 50+ environments prior to the commencement of retrofit activities. Initial findings in pre-retrofit environments reveal widespread underventilation and the significant influence of outdoor PM<sub>2.5</sub> levels indoors in existing classroom and office environments. Detailed pre-retrofit results will be presented at an upcoming conference.

## KEYWORDS

Low-cost sensors; Long-term monitoring; PM<sub>2.5</sub>; Natural Ventilation

## 1 INTRODUCTION

Retrofitting existing buildings to improve energy efficiency is crucial for reducing greenhouse gas emissions, particularly since a large portion of the existing buildings will remain in use beyond 2050. In Ireland, 37% of CO<sub>2</sub> emissions stem from the built environment [1], the public sector plays a pivotal role in leading climate action, exemplified by initiatives like the Public Sector Climate Action Mandate [2]. While previous studies focussed on IAQ measurements in pre-post retrofits, these studies focussed on residential dwellings [3, 4]. There remains a significant knowledge gap regarding the impacts of energy retrofits on IEQ, namely, classrooms and offices. While reducing emissions is essential, it's equally important to ensure adequate IEQ for occupants' health and well-being through proper ventilation and retrofit strategies.

## 2 METHODOLOGY

The study employs a dual-monitoring approach using research-grade and consumer-grade ('low-cost') sensors to measure a large suite of environmental parameters. Research-grade monitors capture precise week-long data on key indoor air quality metrics pre- and post-retrofit (including PM<sub>2.5</sub>, NO<sub>2</sub>, CO, O<sub>3</sub>, formaldehyde, limonene, BTEX, temperature, humidity, CO<sub>2</sub>, TVOCs), while low-cost sensors provide long-term data for up to a year pre- and post-retrofit (including CO<sub>2</sub>, temperature, humidity, radon, TVOCs).

Complementing monitoring data, surveys on thermal comfort, occupant satisfaction, building/ventilation characteristics, and activity/occupancy profiles contribute additional insights into indoor air pollution sources. Meteorological conditions and outdoor pollutant concentrations are sourced from nearby monitoring stations and historical forecasts, facilitating the identification of indoor and outdoor pollution contributions.

The study encompasses 17 buildings with multi-zone monitoring, typically three rooms per building. The monitoring campaign commenced in May 2023 and concluded in June 2024.

### 3 RESULTS

Figure 1 illustrates CO<sub>2</sub> levels during school hours from a sample of 14 classrooms, revealing prolonged periods where concentrations exceed 1000 ppm, a threshold often associated with inadequate ventilation. The interquartile ranges for temperature and humidity during occupied hours were 18-21°C and 41-53%, respectively. However, there were instances where temperature levels dropped as low as 13°C, and humidity levels rose as high as 76% during opening hours. These deviations from the typical ranges warrant further investigation to understand their causes and implications. Additionally, frequent exceedances of WHO daily mean guideline values for PM<sub>2.5</sub> have been observed (Figure 2), in instances exceeding the guideline value sixfold. Preliminary analysis indicates considerable spatial variability in PM<sub>2.5</sub> concentrations, potentially influenced by factors such as building orientation, flooring materials, occupant activities, and window orientation and usage patterns.

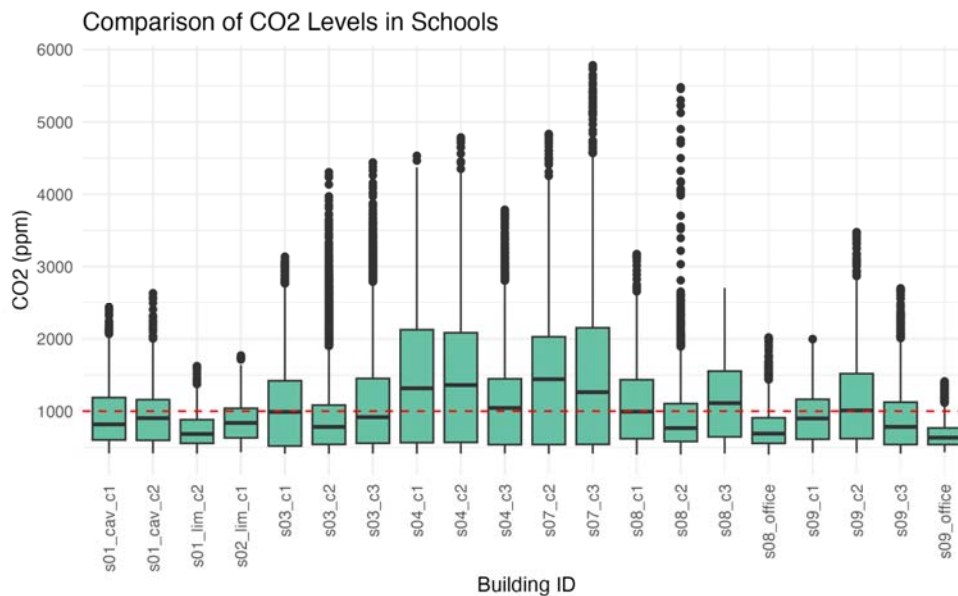


Figure 1, CO<sub>2</sub> concentration (ppm) during occupied hours across 20 school environments. The dashed line at 1000ppm, for reference, is frequently used as a marker of poor ventilation.

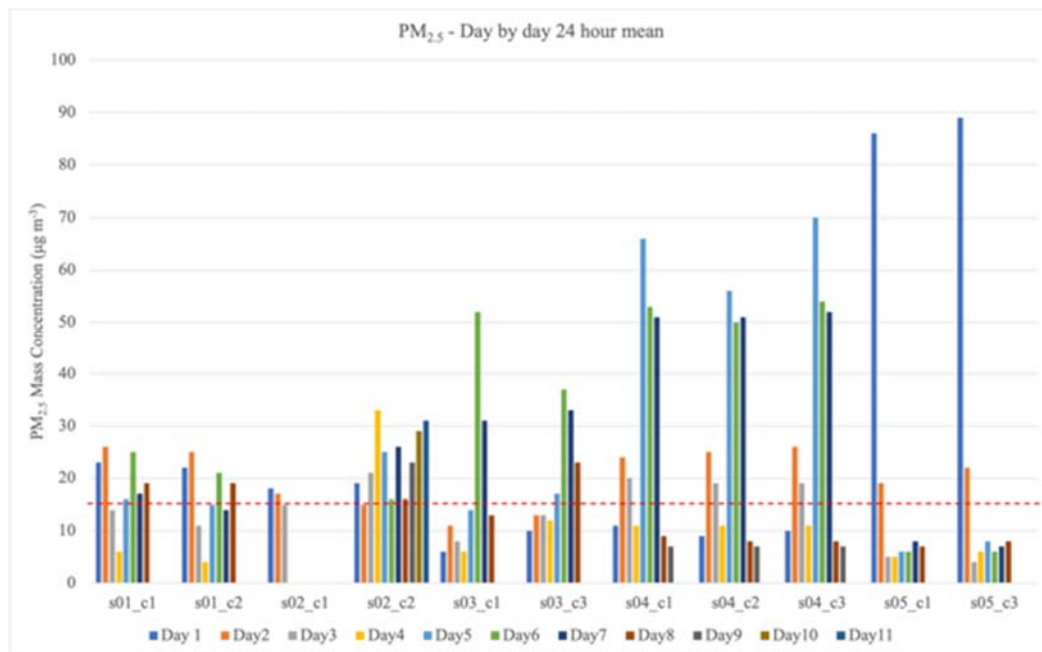


Figure 2. Daily mean PM<sub>2.5</sub> concentration highlighting exceedance of WHO guideline value (red line) and temporal variation across 7 days of monitoring.

#### 4 CONCLUSIONS & DISCUSSION

The preliminary findings reveal significant indoor environmental quality challenges in Irish offices and schools, including suboptimal temperature, humidity, ventilation, and particulate matter concentrations. To address these issues, a thorough statistical analysis is planned to better understand pollutant behaviours and building performance. Additionally, the effectiveness of current ventilation strategies and key determinants of indoor air pollution will be assessed to inform targeted interventions. Future work includes a post-retrofit monitoring campaign starting in Autumn 2024 across 50+ environments to evaluate the impact of energy efficiency and thermal retrofits on indoor environmental quality, providing comparative insights into pre- and post-retrofit conditions.

#### 5 ACKNOWLEDGEMENTS

The BENEFIT project is funded by the Government of Ireland through the Sustainable Energy Authority of Ireland's 2021 Research, Development and Demonstration Funding Programme.

#### 6 REFERENCES

1. *Embodied Carbon in the Built Environment*. 2022, House of the Oireachtas.
2. *Climate Action Plan 2023*. 2023, Government of Ireland.
3. Broderick, Á., et al., *A pre and post evaluation of indoor air quality, ventilation, and thermal comfort in retrofitted co-operative social housing*. *Building and Environment*, 2017. **122**: p. 126-133.
4. Coggins, M., et al., *Indoor air quality, thermal comfort and ventilation in deep energy retrofitted Irish dwellings*. *Building and Environment*, 2022. **219**: p. 109236.

# Assessing the Prediction of Human CO<sub>2</sub> Emissions for IAQ Applications

Oluwatobi Oke<sup>\*</sup>, Andrew Persily

*National Institute of Standards and Technology  
100 Bureau Drive, MS8600  
Gaithersburg, Maryland 20899 USA*

## ABSTRACT

The field of building ventilation and indoor air quality (IAQ) often employs indoor CO<sub>2</sub> concentrations as an indicator of outdoor air ventilation rates and, in some cases, as a contaminant impacting human health and comfort. Many of these applications require CO<sub>2</sub> emission rates from building occupants (VCO<sub>2</sub>), which can be predicted based on occupant characteristics (e.g., body mass, sex, age) and activity level (e.g., sleeping, exercise, resting). In some applications, this information is fairly well known. However, in many other cases, the occupant characteristics and activity levels that impact the values of VCO<sub>2</sub> are difficult to know with much precision, thereby requiring assumptions about the occupants and their activity levels. The ability to use literature-based values for the required input is particularly important during the building design phase when there are no actual occupants to characterize or when considering occupied spaces where it is not practical to characterize the occupants. Whether these inputs are known or not, it is important to characterize the predictive accuracy of calculated VCO<sub>2</sub> values to aid in interpreting indoor CO<sub>2</sub> concentrations.

This study leverages data from whole-room indirect calorimeter chamber measurements of VCO<sub>2</sub> to evaluate the accuracy of two VCO<sub>2</sub> estimation approaches—ASHRAE Fundamentals Handbook (2021) and Persily and De Jonge (2017). The chamber experiments involved 50 healthy, non-smoking individuals aged 20 to 64 years, engaged in activities such as sleeping, stationary cycling, and sitting (performing sedentary tasks like reading or watching television). Metabolic parameters such as VCO<sub>2</sub>, rate of oxygen consumption (VO<sub>2</sub>), basal metabolic rate (BMR), respiratory quotient (RQ), and energy expenditure (EE) were collected during these activities. The validation exercise is performed using two types of input values to estimate VCO<sub>2</sub>—measured data from the chamber experiments and data from the literature. The results indicate that whether using either type of input values, the Persily and de Jonge (PdJ) predictive values are closer to the measured VCO<sub>2</sub> than the values calculated using the ASHRAE approach. PdJ predictions exhibit an absolute mean error of 6 % when using measured inputs, smaller than the ASHRAE predictive error of 28 %. When utilizing literature inputs, the mean predictive error of PdJ is 19 %, comparable to 28 % for the ASHRAE approach.

## KEYWORDS

human CO<sub>2</sub> emissions; indoor air quality; indoor CO<sub>2</sub>; prediction; ventilation VCO<sub>2</sub>?

## 1 INTRODUCTION

IAQ and ventilation assessments have long involved indoor CO<sub>2</sub> concentrations (Persily, 1997; ASTM 2024), although, in practice, many of these applications are implemented without a sound understanding of the underlying technical concepts and the assumptions involved (ASHRAE, 2022). More specifically, many applications require the CO<sub>2</sub> emission rates of building occupants (VCO<sub>2</sub>), which are calculated using the expression in the ASHRAE Handbook - Fundamentals (ASHRAE, 2021) given by Equation 1,

$$VCO_2 = VO_2 \cdot RQ = \frac{0.00276A_DMRQ}{(0.23RQ+0.77)} \quad (1)$$

where:

$V_{CO_2}$  = rate of  $CO_2$  generation (L/s),

$VO_2$  = rate of  $O_2$  consumption (L/s),

RQ = respiratory quotient (dimensionless)

M = metabolic rate (met), or level of physical activity,

$A_D$  = DuBois surface area ( $m^2$ ), calculated from height H in m and body mass W in kg as follows:

$$A_D = 0.202H^{0.725}W^{0.425} \quad (2)$$

The respiratory quotient RQ in Equation 1 is equal to the ratio of  $V_{CO_2}$  to  $VO_2$ . This equation, which first appeared in the Thermal Comfort chapter of the ASHRAE Handbook in 1989, does not discuss the basis of the equation nor provide references and does not directly account for key occupant characteristics that affect  $CO_2$  generation, e.g., age and sex. The ASHRAE presentation of these  $V_{CO_2}$  calculations also provides met rates (a metric of the level of physical activity) for various activities, which are based on references predominantly from the 1960s.

Recognizing these limitations, Persily and de Jonge (2017) proposed an alternative approach (herein referred to as PdJ) for predicting  $V_{CO_2}$  based on concepts from the fields of human metabolism and exercise physiology, which is given by Equation 3,

$$V_{CO_2} = RQ \cdot BMR \cdot M \left( \frac{T}{P} \right) 0.000211 \quad (3)$$

where BMR is the basal metabolic rate (MJ/day), and T and P are the air temperature (K) and pressure (kPa) in the occupied space, respectively. This approach incorporates occupant characteristics, specifically age, sex, and body mass, which are used to calculate BMR. However, both the ASHRAE and PdJ approaches require detailed occupant information that can be challenging to obtain in real-world settings, for example, in actual occupied spaces as opposed to test chambers where the test participants can be well characterized. Also, some applications of indoor  $CO_2$  involve spaces that are still in the design phase or otherwise for which the input data are not available; in these cases, assumptions need to be made about the occupants and their activities.

This study evaluates the predictive accuracy of the ASHRAE and PdJ approaches to estimating  $V_{CO_2}$  using two types of input data: first, when input values are not available and must be based on literature values. In the second case, measured values of the inputs from chamber experiments are used. Sample calculations are presented for one chamber study dataset, but similar analyses are currently underway with other datasets. By understanding the uncertainties or predictive errors of these estimating approaches, we can make more informed decisions about their application in IAQ assessments and building ventilation design.

## 2 METHODS

In collaboration with researchers at the National Institute for Health and Care Research (NIHR) Cambridge Clinical Research Facility, we obtained experimental data from indirect whole-body calorimetry chamber studies. These studies focused on energy expenditure, substrate oxidation, and macronutrient intake from food consumption, with the experimental methods documented in Murgatroyd et al. (1999). The chamber study was ethically reviewed by a local ethics committee, and all participants provided written informed consent.

The study involved fifty (50) healthy non-smokers aged between 20 and 64 years. Participants were provided with balanced meals designed to meet their energy requirements, consisting of 50 % to 55 % carbohydrates, 30 % to 35 % fat, and 12 % to 15 % protein by energy content. Each participant stayed in the calorimetry chamber for three days, following a strict schedule



that included sleeping, cycling at 50 W with a cadence of 40 to 60 RPM, and engaging in sedentary activities such as reading, sitting, or watching television. During their stay, the following parameters were collected at 30-minute intervals:  $VO_2$ ,  $VCO_2$ , BMR, RQ, and total energy expenditure (EE). Additionally, anonymized anthropometric data were gathered, including sex, age, body mass, height, and body mass index (BMI). The collected data enabled a comparison between measured  $VCO_2$  values and predictions made using the ASHRAE and PdJ approaches. The predicted  $VCO_2$  values using chamber data are then compared with predicted  $VCO_2$  values using literature data.

## 2.1 Data Analysis

*Predicted  $VCO_2$  using input parameters from experimental measurements:* First, the Schofield equations are used to estimate BMR based on an individual's age, sex, and body weight as described in Persily and de Jonge (2017). The general form of the Schofield equations is:

$$\text{Males: BMR} = [a \times \text{weight (kg)}] + b;$$

$$\text{Females: BMR} = [c \times \text{weight (kg)}] + d \quad (4)$$

where a, b, c, and d, are constants that vary depending on the age of the individual. Once the BMR is calculated using these equations, the EE value is divided by BMR to estimate the metabolic rate (met). Then, the value of RQ is estimated by dividing the measured  $VCO_2$  by the measured  $VO_2$ . These parameters are subsequently input into the ASHRAE and PdJ expressions using Equations 1 and 2.

*Predicted  $VCO_2$  using input parameters from literature values:* The  $VCO_2$  prediction based on literature values utilized several established sources. The value of BMR was estimated using the Schofield equations (Equation 4). RQ values were derived from energy requirement values reported by the Food and Agricultural Organization of the United Nations (FAO, 2001). Additionally, metabolic rates were obtained from an online compendium of physical activities (Ainsworth et al., 2011).

The comparison between the predicted  $VCO_2$  using input parameters from direct experimental measurements and literature values aims to provide a basis for evaluating the applicability of the ASHRAE and PdJ equations in scenarios where direct measurements of the inputs are unavailable.

## 3 RESULTS AND DISCUSSION

Table 1 presents the mean and absolute percentage differences between predicted and measured  $VCO_2$  values using literature and measured inputs using the ASHRAE and PdJ approaches. These percentage differences are calculated relative to the mean of the measured and predicted values. For the chamber data used in this study, the absolute percentage mean  $VCO_2$  prediction error using the ASHRAE approach with literature inputs is 28 %, which is identical to the error using measured inputs. In contrast, the prediction error using literature inputs with the PdJ approach is 19 % and 7 % when using measured input values. In both scenarios, the PdJ approach exhibits smaller prediction errors than the ASHRAE approach. Notably, the ASHRAE approach consistently underestimates the  $VCO_2$  measurements, regardless of whether literature-based or measured inputs are used.

Table 1. Percentage differences between measured and predicted VCO<sub>2</sub> values

	ASHRAE		PdJ	
	Mean difference	Mean absolute difference	Mean difference	Mean absolute difference
Literature inputs	-28 %	28 %	-19 %	19 %
Measured inputs	-28 %	28 %	-7 %	7 %

Bland-Altman plots were generated to evaluate the bias between measured and predicted VCO<sub>2</sub> values (Bland and Altman, 1986 and 1999) for the ASHRAE and PdJ approaches, as shown in Figures 1 through 4. The X-axis is the mean of the measured and predicted VCO<sub>2</sub> values, while the Y-axis is the percentage difference between these values. The black horizontal solid line at zero percent on the vertical axis is the reference line for “no difference” between the measured and predicted VCO<sub>2</sub> values. The red line represents the mean of the differences for all the data points. The further this line deviates from the zero-reference line, the greater the bias. The red dashed lines are the 95 % confidence intervals for the mean of the differences, based on normality assumptions. If the red solid line falls within this confidence interval, it indicates that the mean difference between the measured and predicted values is not statistically significant from zero, i.e., no statistically significant bias. The blue dashed lines represent the 95 % lower and upper limits of agreement, showing the range within which most differences between the measured and predicted values lie.

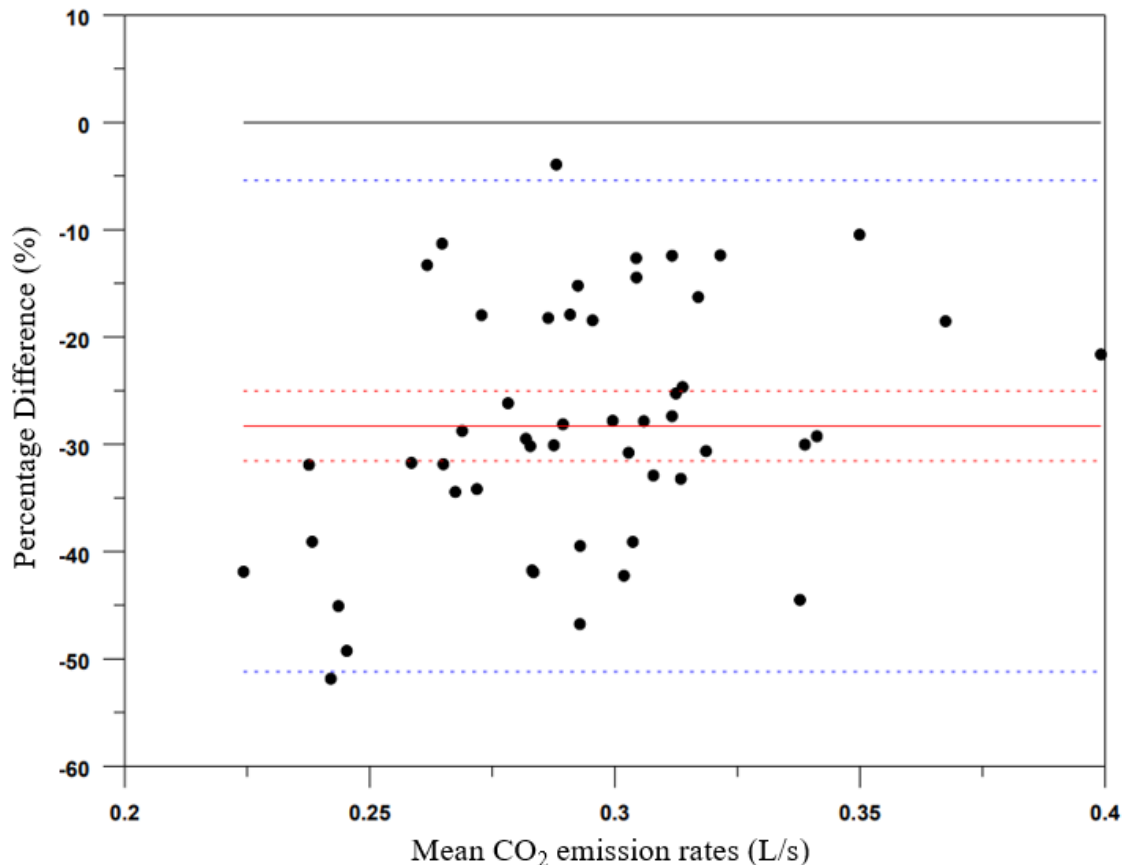


Figure 1: Bland-Altman plot comparing measured VCO<sub>2</sub> to ASHRAE predictions using chamber inputs. The black line at zero represents no difference, the red line shows the mean difference, and the red dashed lines indicate the 95 % confidence intervals. The blue dashed lines are the 95 % limits of agreement.

The Bland-Altman plots for predicted VCO<sub>2</sub> values using the ASHRAE equation for both chamber inputs (Figure 1) and literature inputs (Figure 2) demonstrate that the mean difference line is significantly below the zero-reference line, and the confidence limits for the mean

difference do not contain the zero-reference line. This result indicates evidence of a significant systematic bias. In addition, both predictions indicate a consistent underestimation of the measured CO<sub>2</sub> emission rates, with the degree of underestimation varying across the emission rate range. Specifically, when using chamber input values, the predicted average VCO<sub>2</sub> was 28 % ( $\pm 9$  %) lower than the measured VCO<sub>2</sub> (Figure 1). Similarly, predictions using literature input values were 28 % ( $\pm 11$  %) lower than the measured VCO<sub>2</sub> (Figure 2). The blue dashed lines in Figures 1 and 2 show that the majority of the values lie within the upper and lower limits of agreement (mean bias  $\pm 1.96$  SD).

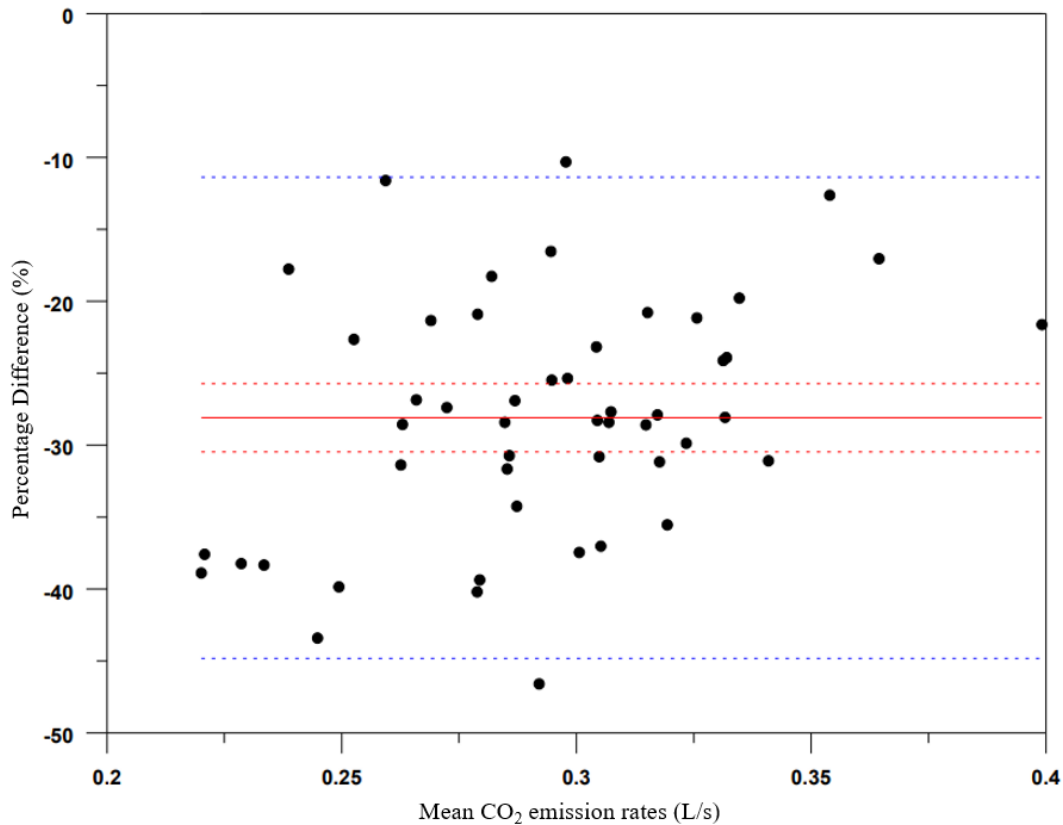


Figure 2: Bland-Altman plot comparing measured VCO<sub>2</sub> to ASHRAE predictions using literature inputs. The black line at zero represents no difference, the red line shows the mean difference, and the red dashed lines indicate the 95 % confidence intervals. The blue dashed lines are the 95 % limits of agreement.

Figure 3 shows the comparison between measured VCO<sub>2</sub> and predicted VCO<sub>2</sub> using chamber-measured input values with the PdJ approach. There is also significant bias in this case, but the data points exhibit a relatively narrow spread around the mean difference line, suggesting consistent agreement between the measured and predicted values with low variability. For this dataset, the plot reveals a percentage mean difference of -7 % ( $\pm 2$  %). Most data points fall within the limits of agreement, indicating that the predicted VCO<sub>2</sub> values generally align well with the measured values. Figure 4 compares the measured VCO<sub>2</sub> with predicted VCO<sub>2</sub> using the literature input values with the PdJ approach. The plot shows evidence of a significant systematic bias, and the predicted VCO<sub>2</sub> values are 19 % ( $\pm 2$  %) lower than the measured values, with most data points within the limits of agreement.

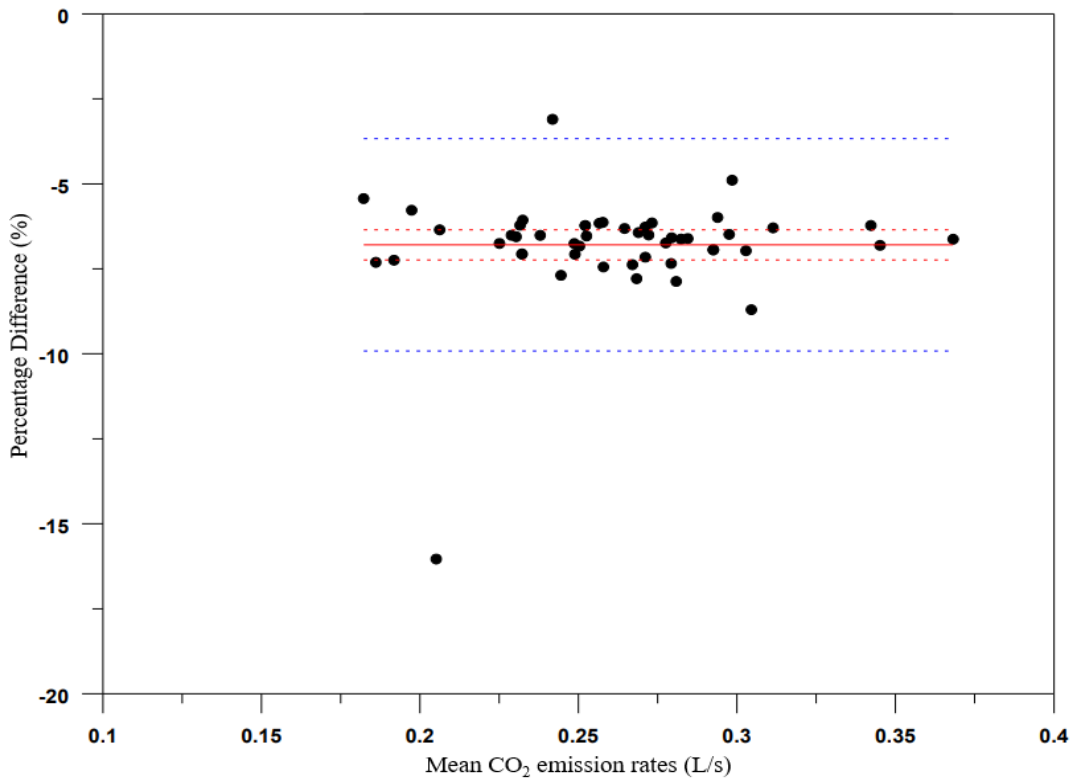


Figure 3: Bland-Altman plot comparing measured  $\text{VCO}_2$  to PdJ predictions using chamber inputs. The black line at zero represents no difference, the red line shows the mean difference, and the red dashed lines indicate the 95 % confidence intervals. The blue dashed lines are the 95 % limits of agreement.

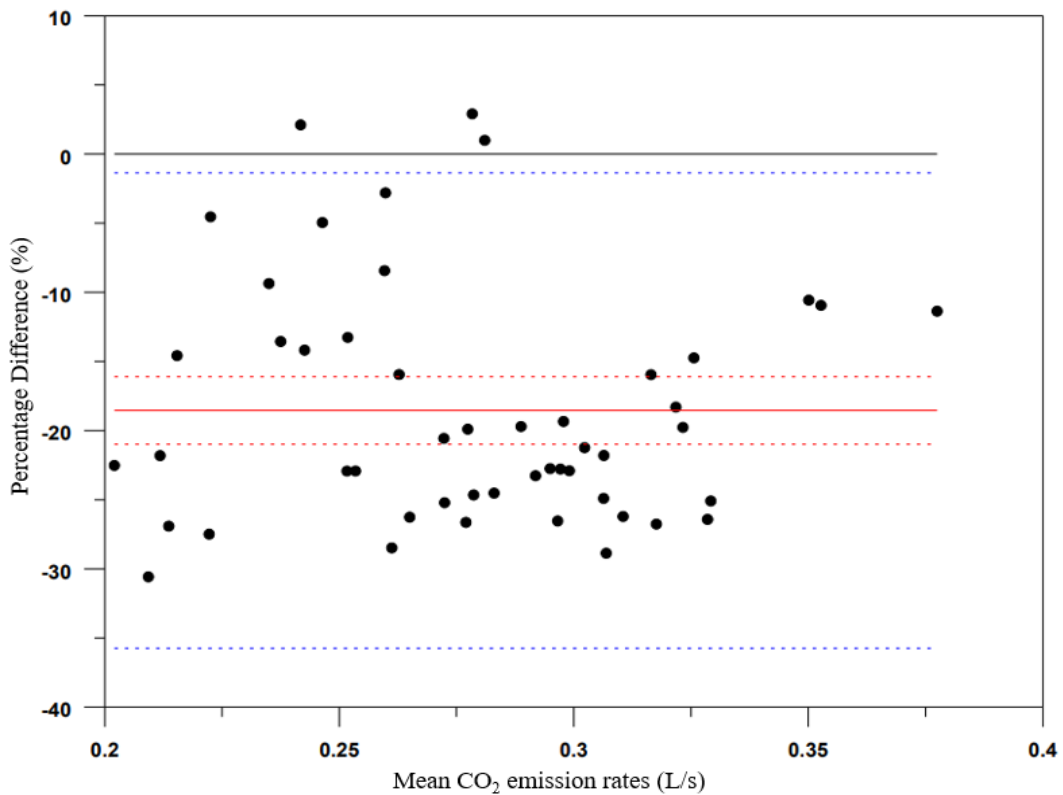


Figure 4: Bland-Altman plot comparing measured  $\text{VCO}_2$  to PdJ predictions using literature inputs. The black line at zero represents no difference, the red line shows the mean difference, and the red dashed lines indicate the 95 % confidence intervals. The blue dashed lines are the 95 % limits of agreement.

## 4 CONCLUSIONS

For the dataset considered here, the PdJ and ASHRAE approaches underestimate the VCO<sub>2</sub> measurements, regardless of whether literature-based or measured inputs are used. However, the predicted VCO<sub>2</sub> values using the PdJ approach are, on average, within 20 % or less of the measured data, exhibiting smaller prediction errors than the ASHRAE approach. While other datasets are being studied for presentation in future publications, these results are encouraging given that BMR values, RQ, and met rates are not generally available except in chamber studies. These additional datasets sometimes include measured quantities other than those considered here (e.g., BMR), different activities, and different test durations. The ability to use literature-based values for BMR, RQ, and met rate is particularly important during the building design phase when there are no actual occupants to characterize or when considering occupied spaces where it is not practical to characterize the occupants. Also, there are applications in which expected CO<sub>2</sub> concentrations are calculated as a function of ventilation rate, occupancy, and other factors to understand various aspects of IAQ, and these efforts require reliable values of VCO<sub>2</sub>. Addressing these challenges in predicting VCO<sub>2</sub> is critical to interpreting indoor CO<sub>2</sub> concentrations and will be the focus of future work.

## 5 ACKNOWLEDGEMENTS

The National Institute of Standards and Technology Institutional Review Board reviewed and approved the protocol for this project and all subjects provided informed consent in accordance with 15CFR27, the Common Rule for the Protection of Human Subjects.

The authors would like to thank Dr. Laura Watson, PhD., at the NIHR Cambridge Clinical Research Facility, Cambridge University, for providing and discussing the experimental data used in this study.

## 6 REFERENCES

- ASTM. (2024). ASTM D6245-24. Standard Guide on the Relationship of Indoor Carbon Dioxide Concentrations to Indoor Air Quality and Ventilation. West Conshohocken, PA.
- ASHRAE. (2021). *Handbook - Fundamentals*. Peachtree Corners, GA: ASHRAE, Inc.
- ASHRAE. (2022). *Position Document on Indoor CO<sub>2</sub>*. Peachtree Corners, GA: ASHRAE, Inc.
- Bland JM, Altman DG (1986). Statistical method for assessing agreement between two methods of clinical measurement. *The Lancet i*:307-310.
- Bland JM, Altman DG (1999) Measuring agreement in method comparison studies. *Statistical Methods in Medical Research 8*:135-160
- Buskirk ER. (1960) Problems related to the caloric cost of living. *Bull N Y Acad Med*. 1960; 36:365-388.
- Murgatroyd, P. R., Goldberg, G. R., Leahy, F. E., Gilsenan, M. B., & Prentice, A. M. (1999). Effects of inactivity and diet composition on human energy balance. *International journal of obesity and related metabolic disorders: journal of the International Association for the Study of Obesity*, 23(12), 1269–1275.
- Passmore R, Durnin JVGA. (1967). *Energy, Work and Leisure*, London: Heinemann Educational Books Ltd.
- Persily, A.K. (1997). Evaluating Building IAQ and Ventilation with Indoor Carbon Dioxide. *ASHRAE Transactions*, 103 (2), 193-204.
- Persily A, de Jonge L. (2017). Carbon dioxide generation rates for building occupants. *Indoor Air*. 27:868–879.

# Applying a composite indoor environmental quality indicator to Danish office spaces: The TAIL rating scheme

Asit K Mishra\*<sup>1,2</sup>, Dania T Pharaon<sup>2</sup>, Ida B Feldskou<sup>2</sup>, Lina F Præstegaard<sup>2</sup>  
and Pawel Wargocki<sup>2</sup>

*1 School of Public Health  
University College Cork  
Cork, Ireland*

*2 DTU Sustain  
Technical University of Denmark  
Lyngby, Denmark*

*\*Corresponding author: akumarmishra@ucc.ie*

## SUMMARY

A composite rating scheme for indoor environmental quality (IEQ) can help provide a summary picture of buildings for occupants, inform the building managers regarding IEQ performance that need attention, and raise awareness on regarding the importance of IEQ parameters. The TAIL IEQ rating scheme has been designed to communicate such aspects in a simple, easy to use manner.

## KEYWORDS

indoor environmental quality; IEQ rating scheme; composite index; multidomain effects; office space

## 1 INTRODUCTION

Indoor environmental quality (IEQ) impacts occupant wellbeing and work performance. A considerable amount of research effort has been devoted to IEQ rating schemes, encompassing the different domains, viz., Thermal, Acoustic, Indoor Air, and Lighting. Building rating schemes like LEED, BREEAM have a scoring system that includes certain IEQ aspects. To create IEQ rating schemes, researchers have used subjective feedback from occupants, objective measurements of IEQ, and combinations of these two approaches. They have used methods such as regression analysis, multi-criteria decision analysis, and analytical hierarchical processing to analyse the data (Roumi et al. 2022). There currently exists little concurrence regarding relative importance of different domain and the parameters to use.

Apart from accuracy and repeatability of an IEQ rating scheme, there are practical considerations. Ease of communication, cost of the measurements/surveys involved, and how informative it can be for the stake holders are important. This is particularly important for buildings where there are stake holders with different perspectives and levels of understanding of IEQ. To address some of these challenges, as part of the EU ALDREN project, the TAIL (Temperature, Acoustic, Indoor air, and Lighting) rating scheme was developed (Wargocki et al. 2021). TAIL was created in form of a framework linking existing regulations related to occupant comfort and health – EN16798, WHO Air Quality Guidelines, Level(s) – so that they could be used together to rate IEQ. Initial applications of TAIL focused on building energy retrofits. However, it is suitable for a wide range of use cases and building types.

The twelve components of TAIL are – **Thermal environment**: Air temperature; **Acoustic environment**: Sound pressure level; **Indoor air environment**: Ventilation rate, CO<sub>2</sub> concentration, Formaldehyde concentration, Benzene concentration, PM<sub>2.5</sub> concentration, Radon concentration, Air relative humidity, & Visible mould area; **Luminous environment**: Illuminance, & Daylight factor. The TAIL rating is shown as a roman numeral (I-IV), with the component exhibiting the poorest performance being used to determine the overall rating. This motivates action by building management and operations, indicating which renovation strategies should be prioritized. In this work we report the application of TAIL to office buildings in the campus of the Technical University of Denmark (DTU).

## 2 STUDY METHOD

The study was undertaken in five buildings of DTU, in the Lyngby campus. These primarily house single occupancy offices (~60%). To ensure representation, 60-70% of the available monitors were deployed in single-person offices. Offices from all floors were selected, with approximately 10% of the total office floor area in each building being covered. Measurements typically spanned a full working week (Monday morning through Friday afternoon).

We used 15 AtmoCube monitors (AtmoCube 2024). The monitors were placed on the desks of the occupants, about 0.8-1m from ground, at least one meter from window, walls, radiators or ventilation grilles. They were positioned about 0.5 m from the occupants so as not to be affected by their body heat or the exhaled air. The AtmoCubes measured temperature, sound pressure level, illuminance, humidity, formaldehyde, CO<sub>2</sub>, and PM<sub>2.5</sub> concentration. One-year dynamic daylight simulations were conducted in IDA Indoor Climate and Energy, with an overcast sky. The building classification was through a two-step process. First, a classification is given for I and L, based on the simulated or logged values for the parameters within the domain. Then, the classification of the worst performing domain is given to the building.

During the months when the physical environment was being monitored, a comprehensive survey was also conducted in the buildings to gauge occupant perception of their workplace IEQ. Occupants were queried regarding their overall perception and sensation on all four domains along with an overall rating of IEQ. The survey also included the questionnaire associated with the Flourishing measure. Developed by the Human Flourishing Program at Harvard University's Institute for Quantitative Social Science, the Flourishing measure examines human flourishing around five central domains: happiness and life satisfaction, physical and mental health, meaning and purpose, character and virtue, and close social relationships (VanderWeele 2017).

## 3 RESULTS AND DISCUSSION

Figure 1 provides the TAIL ratings of all five buildings monitored during this campaign. As the monitoring period was during a shoulder season when winter heating had not been discontinued but the outdoors was also getting warmer, the buildings had warmer thermal conditions than the winter limits for air temperature in TAIL I and II. Thermal and light sensation votes from the subjective survey showed relatively high correlations with median temperature ( $r = 0.75$ ) and median illuminance ( $r = 0.83$ ), respectively, in the buildings. The correlations of odor and noise sensations with physically measured parameters were not as remarkable.



Figure 1: Tail rating schemas for the five monitored buildings.

We observed that the objective measurements and subjective surveys can serve to suitably complement each other, presenting a holistic picture of the IEQ. There are parameters, e.g., local discomfort from radiant asymmetry or drafts, that cannot be easily or economically measured but were easily ascertained from the subjective feedback. Similarly, measured parameters like PM, formaldehyde, daylight factor are not easy for occupants to discern. Our results also suggest that monitoring needs to be carried out in different seasons, different rooms, and for a long enough period to get a picture of the typical use of the building. The AtmoCubes had a logging frequency of one minute. Using one-minute logged data and 10-minute averaged data did not change the ratings to any considerable degree.

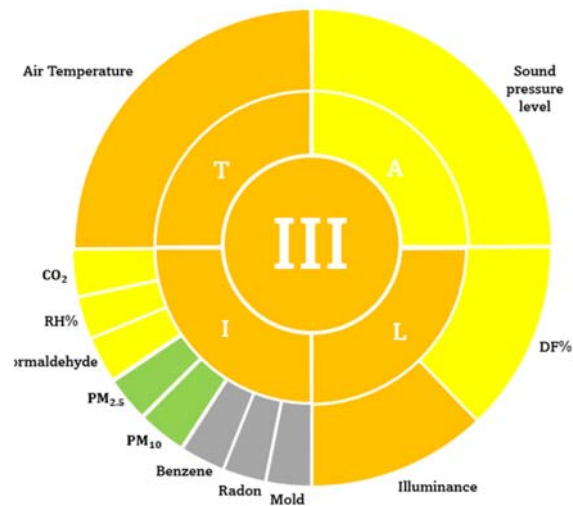


Figure 2: A more detailed representation for TAIL in Building 1. Grey sections indicate parameters that were not evaluated in the current campaign.

Figure 2 provides a more detailed view of the evaluated TAIL for Building 1. As can be seen from this illustration, the quadrants can be expanded or contracted depending on what level of details need to be communicated to a particular audience. At the same time, further parameters can be added to each quadrant without impacting the overall structure of the scheme.

#### 4 CONCLUSION

The TAIL rating scheme provides a good basis for IEQ evaluation. It is easy to communicate to lay occupants yet comprehensive enough to include information relevant for designers and building managers. More studies like the current one, exploring the application of TAIL in different building types and contexts, can help build the utility of TAIL. Our results indicate that specific components defining IEQ can be supplemented with subjective ratings to improve the quality of evaluation and achieve a complete rating scheme.

#### 5 ACKNOWLEDGEMENTS

AKM is funded by the European Union’s Horizon 2020 research and innovation programme under the Marie Skłodowska-Curie grant agreement No 101034345.

#### 6 REFERENCES

- AtmoCube. 2024. “Atmocube – Indoor Air Quality Monitor for Businesses and Enterprises.” 2024. <https://atmotube.com/atmocube>.
- Roumi, Soheil, Fan Zhang, Rodney A. Stewart, and Mattheos Santamouris. 2022. “Commercial Building Indoor Environmental Quality Models: A Critical Review.” *Energy and Buildings* 263:112033.
- VanderWeele, Tyler J. 2017. “On the Promotion of Human Flourishing.” *Proceedings of the National Academy of Sciences* 114 (31): 8148–56. <https://doi.org/10.1073/pnas.1702996114>.
- Wargocki, Pawel, Wenjuan Wei, Jana Bendžalová, Carlos Espigares-Correa, Christophe Gerard, Olivier Greslou, Mathieu Rivallain, et al. 2021. “TAIL, a New Scheme for Rating Indoor Environmental Quality in Offices and Hotels Undergoing Deep Energy Renovation (EU ALDREN Project).” *Energy and Buildings* 244 (August):111029. <https://doi.org/10.1016/j.enbuild.2021.111029>.



# Thermal comfort of adolescent children in classrooms: Some reflections on the state-of-the-art

Asit K Mishra\*<sup>1,2</sup>, Pawel Wargocki<sup>2</sup>, and Eilis J O'Reilly<sup>1</sup>

*1 School of Public Health  
University College Cork  
Cork, Ireland*

*2 DTU Sustain  
Technical University of Denmark  
Lyngby, Denmark*

\*Corresponding author: [akumarmishra@ucc.ie](mailto:akumarmishra@ucc.ie)

## SUMMARY

Thermal comfort of adolescents (10-17 year olds) in school classrooms is an important but less explored topic. The classroom thermal environment impacts students comfort, learning, and health. Due to differences related to physiology and ability to influence their environments, children's thermal comfort needs and even their interpretation of thermal comfort differs from adults. Based on an overview of the current thermal comfort databases, we advocate that there is an urgent need for studies, spread across different climatic regions, examining classroom comfort for young children. The impact of climate change further drives this urgency.

## KEYWORDS

thermal comfort; classrooms; adolescent children; thermal comfort zone; healthy classrooms

## 1 INTRODUCTION

Children are likely to spend 10-15% of the first 18 years of life in schools, primarily indoors, inside classrooms (Arya *et al.*, 2024). The indoor thermal environment of school classrooms has a crucial bearing on student's thermal comfort as well as their learning and task performance (Wargocki, Porras-Salazar and Contreras-Espinoza, 2019). Current thermal comfort standards are based on studies which examined the thermal comfort and behaviours of adults, primarily in office settings. There are several reasons why children would perceive the same thermal environment differently than adults. Due to their developmental stage, their breathing rates are higher than adults, their metabolic rates are also higher, their clothing patterns are different, a school day is generally more active than an office day, and classrooms have limited adaptive opportunities that young children can freely undertake.

There is a dearth of thermal comfort studies with adolescents as the participants. For example, in the ASHRAE Thermal Comfort Database II (Ličina *et al.*, 2018), nearly 5000 records correspond to studies conducted in classrooms, with age of respondents available. Only 356 of these correspond to the age group 10-17. In the current scenario, this becomes an even bigger concern as periods of unusual weather, leading to thermal discomfort, are on the rise due to climate change. Children are also more prone to adverse effects from exposure to extreme thermal environments due to their developmental stage.

## 2 ANALYSIS OF THE ASHRAE THERMAL COMFORT DATABASE II

For this work, we used the largest available thermal comfort surveys database, the ASHRAE Thermal Comfort Database II (ATCD2), to examine briefly the available data on thermal comfort in school classrooms. We compared the information available for the 10 to under 18 age group with the 18 to 22 age group. A summary of the thermal sensation data available in the database has been provided in Table 1. In the age group 10-17, most of the data available are for students 16-years-old or over. The 18-22 category has almost 10 times more responses than the younger ages. The linear fits in Figure 1, for the 10-17 vs the 18-22 age group from the ATCD2 provides a neutral temperature of 23.1 °C for the younger age group vs 24.5 °C for the 18-22-year-olds, which can lead to over 10% difference in air conditioning energy use.

Table 1: Summary of thermal sensation votes from ATCD2 for two age groups

Age group	Mean (s.d.)	Median (10 <sup>th</sup> ,90 <sup>th</sup> %ile)
10–17-year-olds (356 responses)		
Age	16.3 (1.2)	17 (14,17)
Air temperature	26.6 (2.6)	26.3 (23.6, 31.1)
18–22-year-olds (3592 responses)		
Age	19.8 (1.3)	20 (18,22)
Air temperature	26.4 (2.0)	25.9 (24.1,29.5)
Thermal sensation votes distribution (%)		
10–17-year-olds	Cold (0.6), Cool (4.5), Slightly cool (12.1), Neutral (43), Slightly warm (25.6), Warm (11.8), Hot (2.2)	
18–22-year-olds	Cold (0.3), Cool (1.9), Slightly cool (12.9), Neutral (50.7), Slightly warm (23.1), Warm (9.4), Hot (1.6)	

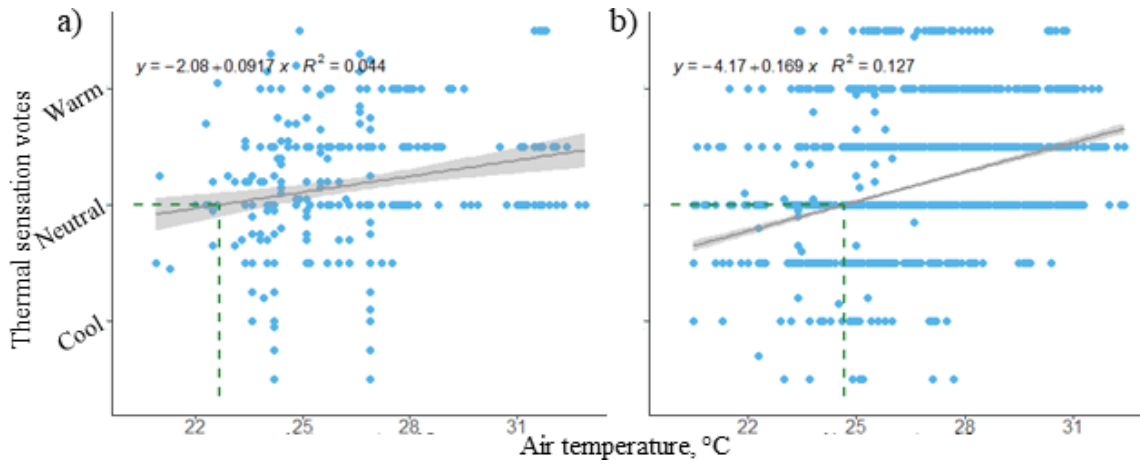


Figure 1: Thermal sensation votes and indoor air temperature in classrooms – linear regression fits for a) 10–17-year-olds and b) 18–22-year-olds

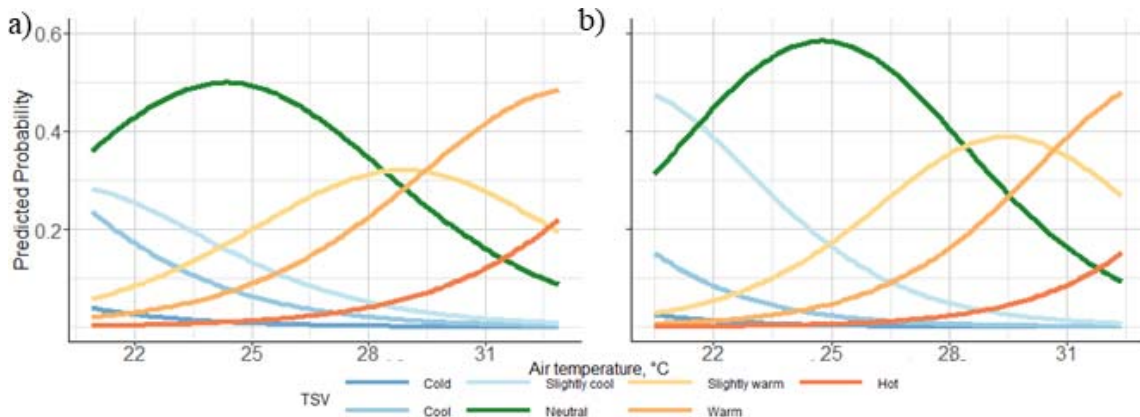


Figure 2: Ordinal regression model for thermal sensation votes and indoor air temperature in classrooms a) 10–17-year-olds and b) 18–22-year-olds

Similarly, an ordinal model (Figure 2) estimating the probability of votes under the different thermal categories are different for the two age groups. This highlights the need for more widespread studies in school classrooms, covering different stages of schooling, focusing on narrower age groups. The 10-17 vs 18-22 presents two very broad groupings, unsuitable for nuanced comparisons.

From a teaching-learning point of view, since different stages of education have different curriculum and learning objectives, the suitable thermal conditions for a learning environment would also depend on the stage of school. As has been observed, the thermal comfort needs for

primary, middle, and high school students tend to be different, with a linear relationship between age and neutral temperature (Torriani *et al.*, 2023).

### 3 MOVING FORWARD

The available evidence clearly demonstrates the distinct nature of children's thermal comfort. The relative dearth of studies also suggests the need for urgent and focused action, in different climatic and cultural contexts. The urgency is driven by the changing climate where warming classroom conditions will have a significant impact on learning, disproportionately impacting minorities and economically disadvantaged groups (Park *et al.*, 2020).

Chamber-based studies with children can be especially difficult with the issues related to transporting them to an unfamiliar thermal environment and the impact this may have on their responses. Also, as has been observed, thermal comfort questionnaire scales can be interpreted differently based on a number of factors (Schweiker *et al.*, 2020). For children to interpret the questionnaires, a more descriptive approach, involving suitable imagery, is desired (Aparicio-Ruiz *et al.*, 2021; Zapata-Lancaster *et al.*, 2023; Caporale *et al.*, 2024).

Additionally, ongoing and future studies of classroom thermal comfort need to pay due attention to its impact on children's health. While so far the focus has been on comfort and cognitive performance, this is a domain where architects and building engineers need to work in synchronization with public health experts. Due to the long duration children spend in classrooms, a healthy classroom thermal environment can be an important part of public health strategies, especially during acute situations, like a heatwave.

### 4 ACKNOWLEDGEMENTS

AKM is funded by the European Union's Horizon 2020 research and innovation programme under the Marie Skłodowska-Curie grant agreement No 101034345.

### 5 REFERENCES

Aparicio-Ruiz, P. *et al.* (2021) 'A field study on adaptive thermal comfort in Spanish primary classrooms during summer season', *Building and Environment*, 203, p. 108089. Available at: <https://doi.org/10.1016/j.buildenv.2021.108089>.

Arya, V.K. *et al.* (2024) 'Comparative Analysis of Indoor Air Quality and Thermal Comfort Standards in School Buildings across New Zealand with Other OECD Countries', *Buildings*, 14(6), p. 1556.

Caporale, A. *et al.* (2024) 'An experimental study investigating school-age children's thermal environment perception', in. *Indoor Air 2024*, Honolulu.

Ličina, V.F. *et al.* (2018) 'Development of the ASHRAE global thermal comfort database II', *Building and Environment*, 142, pp. 502–512.

Park, R.J. *et al.* (2020) 'Heat and Learning', *American Economic Journal: Economic Policy*, 12(2), pp. 306–339. Available at: <https://doi.org/10.1257/pol.20180612>.

Schweiker, M. *et al.* (2020) 'Evaluating assumptions of scales for subjective assessment of thermal environments—Do laypersons perceive them the way, we researchers believe?', *Energy and Buildings*, 211, p. 109761.

Torriani, G. *et al.* (2023) 'Thermal comfort and adaptive capacities: Differences among students at various school stages', *Building and Environment*, 237, p. 110340.

Wargocki, P., Pórras-Salazar, J.A. and Contreras-Espinoza, S. (2019) 'The relationship between classroom temperature and children's performance in school', *Building and Environment*, 157, pp. 197–204. Available at: <https://doi.org/10.1016/j.buildenv.2019.04.046>.

Zapata-Lancaster, M.G. *et al.* (2023) 'Carbon Dioxide Concentration Levels and Thermal Comfort in Primary School Classrooms: What Pupils and Teachers Do', *Sustainability*, 15(6), p. 4803. Available at: <https://doi.org/10.3390/su15064803>.

# Estimating the health impact of exposure to indoor PM<sub>2.5</sub> concentrations in Irish deep energy retrofitted residential dwellings – ARDEN

Hala Hassan<sup>\*1</sup>, Asit Kumar Mishra<sup>2</sup>, Hilary Cowie<sup>3</sup>, and Marie Coggins<sup>1</sup>

*1 School of Natural Sciences & Ryan Institute, University of Galway, Galway, H91TK33, Ireland  
\*hala.hassan@universityofgalway.ie*

*2 School of Public Health, University College Cork, College Road, Cork, Ireland*

*3 Institute of Occupational Medicine (IOM), Edinburgh, EH14 4AP, UK*

## SUMMARY

Maintaining good indoor air quality (IAQ) post energy retrofit is essential to ensure the health and wellbeing of building occupants. In this study, a number of indoor air pollutants were measured in a sample of Irish homes pre and post deep energy retrofit (DER). Airborne concentrations of PM<sub>2.5</sub> and formaldehyde showed significant increases ( $p < 0.0001$ ) post-retrofit. A health impact assessment was conducted and the results suggest that the greatest health burden (for lung cancer and all-cause mortality) was associated with exposure to PM<sub>2.5</sub>.

## KEYWORDS

Energy Retrofit, Indoor air quality, Particulate Matter (PM<sub>2.5</sub>), Health Impact Assessment

## 1 METHODOLOGY

PM<sub>2.5</sub>, CO<sub>2</sub>, CO, TVOC, formaldehyde, temperature and relative humidity were measured over a period of 24-72 hours in the bedrooms and living rooms of 11 homes (pre-post retrofit) and 14 homes (post retrofit only). Radon was also measured in the same rooms post retrofit for a period of 3-9 months. All homes had participated in the SEAI DER pilot programme and were upgraded to a minimum building energy rating (BER) of A3 following retrofit. A summary of building characteristics and details on the measurement campaigns and equipment used have been published [1, 2].

The homeowners completed an activity diary during the measurement period to inform possible pollution sources, and a questionnaire survey to collect information about the dwelling, occupant behaviour, thermal comfort and overall satisfaction with the retrofit. Pre retrofit, all homes were naturally ventilated and mechanical ventilation was installed in all homes as part of the retrofit. Survey data was collated using a spreadsheet application (Microsoft Excel) and further data analysis was carried out using R statistical software. In our analysis we assumed that the living rooms are likely to be occupied during the daytime (7:00 – 22:00) while bedrooms are occupied during the night-time (22:00 – 7:00). We used linear mixed-effects models (LMEs) and performed t-test calculations to determine the impact of the retrofit.

A health impact assessment was conducted to estimate the change in health burden due to retrofit from exposure to PM<sub>2.5</sub>, formaldehyde, and radon. The health impact analysis was performed using baseline data from 2019 to exclude the impact of the Covid19 pandemic. Concentration-response functions (CRFs) [3], linking the change in the incidence of disease in a population with the change in exposure in pollutant level, were used to calculate the health burden of certain health end-points (Table 1) known to be associated with the selected pollutants. For time-series data, such as the case with PM<sub>2.5</sub>, we used the 24-hr time weighted average (TWA) based on daytime concentrations for the living rooms and night-time concentrations for the bedrooms. For formaldehyde, we used the 72-hr averages for bedrooms and living rooms, and for radon we used the overall average over the measurement period. Population data and background rates of disease for Ireland were taken from the Central Statistics Office Ireland and the National Cancer Registry Ireland [4, 5].

Table 1: A summary of the measured pollutants and the selected health endpoints and relevant concentration-response functions

Health endpoint	Pollutant	Risk function
All-Cause Mortality	PM <sub>2.5</sub>	8.0 % per 10 µg m <sup>-3</sup> PM <sub>2.5</sub> [3]
Lung Cancer	PM <sub>2.5</sub>	9.0 % per 10 µg m <sup>-3</sup> PM <sub>2.5</sub> [3]
	radon	8.4% per 100 Bq m <sup>-3</sup> [6]
Leukaemia	radon	12.0% per 100 Bq m <sup>-3</sup> [7]

## 2 RESULTS & DISCUSSION

The LME model showed that PM<sub>2.5</sub> increased significantly ( $p < 0.0001$ ) post retrofit (in the homes with pre-post data). PM<sub>2.5</sub> 24-hr average concentrations post retrofit in the bedrooms ranged from 4.8 µg m<sup>-3</sup> to 310.6 µg m<sup>-3</sup> and in the living rooms from 7.4 µg m<sup>-3</sup> to 238.0 µg m<sup>-3</sup>, and they exceeded the WHO daily guideline (15 µg m<sup>-3</sup>) in 72% and 77% of the measured bedrooms and living rooms, respectively. For the 11 homes examined pre retrofit, formaldehyde showed a significant increase post retrofit ( $p < 0.05$ ) in both bedrooms and living rooms. The average formaldehyde concentrations post retrofit ranged between 12.0 µg/m<sup>3</sup> and 128.0 µg/m<sup>3</sup> (Figure 1). Figure 2 shows the average radon concentrations measured post retrofit in 18 homes. The overall average concentration across all homes (107.6 Bq m<sup>-3</sup>) exceeded the Irish indoor average for residential buildings (77.0 Bq m<sup>-3</sup>) and the pre-1998 average (89.0 Bq m<sup>-3</sup>) [8].

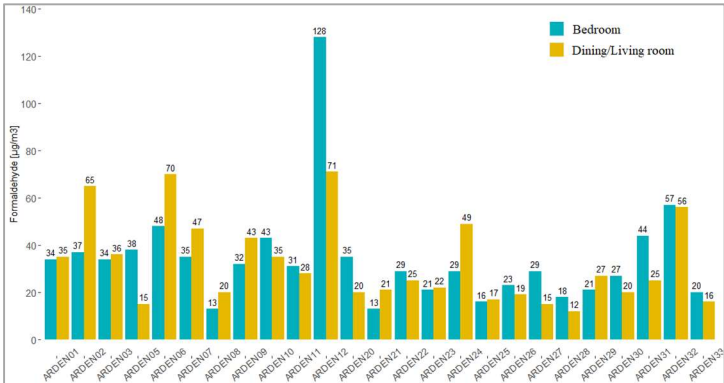


Figure 1: Formaldehyde concentration post retrofit in bedrooms and living rooms

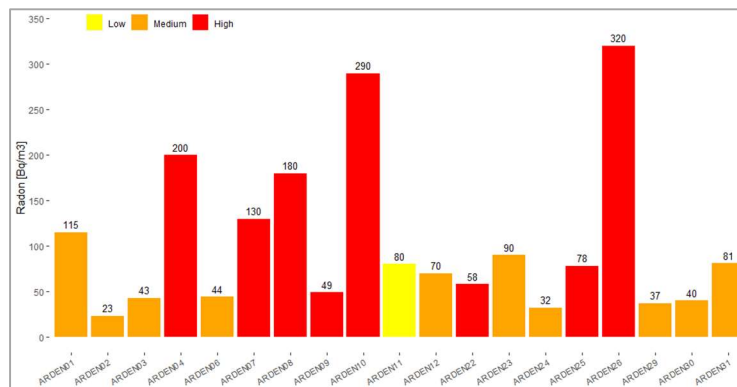


Figure 2: Radon average concentrations post-retrofit. Colours indicate low, medium, and high radon areas [9]

Preliminary results from the health impact assessment suggest that the greatest health burden is due to exposure to increased PM<sub>2.5</sub>, followed by radon. For formaldehyde, we were not able to quantify any carcinogenic health effects as the measured post retrofit levels were below the concentrations at which health effects have been shown in other studies, which are typically based on highly exposed occupational cohorts [10]. The PM<sub>2.5</sub> data post retrofit was highly variable and increases should not be attributed to the retrofit alone, but are more likely due to a combination of sources including: ingress of outdoor PM<sub>2.5</sub> from residential combustion or traffic sources, indoor sources (e.g. cooking, wood burning stoves or burning scented candles) sometimes in the absence of good ventilation [11].

### 3 ACKNOWLEDGEMENTS

The ARDEN study was funded by the Sustainable Energy Authority of Ireland under the SEAI Research, Development & Demonstration Funding Programme 2018, Grant number 18/RDD/204. Radon monitoring was funded by the Irish Environmental Protection Agency (EPA). The project team would like to thank the homes who participated in this study.

### 4 REFERENCES

- [1] Hassan, H., Mishra, A.K., Wemken, N., O'Dea, P., Cowie, H., McIntyre, B., and Coggins, A.M., *Deep energy renovations' impact on indoor air quality and thermal comfort of residential dwellings in Ireland – ARDEN project*. Building and Environment, 2024. **259**: p. 111637 DOI: <https://doi.org/10.1016/j.buildenv.2024.111637>.
- [2] Coggins, A.M., Wemken, N., Mishra, A.K., Sharkey, M., Horgan, L., Cowie, H., Bourdin, E., and McIntyre, B., *Indoor air quality, thermal comfort and ventilation in deep energy retrofitted Irish dwellings*. Building and Environment, 2022. **219**: p. 109236 DOI: <https://doi.org/10.1016/j.buildenv.2022.109236>.
- [3] Birchby, D., Sendall, J., and Stedman, J., *Report for Defra (ECM\_61369). Air Quality damage cost update 2023 – FINAL Report*, U.D.f.E.F.R. Affairs. 2023: <https://www.gov.uk/government/organisations/department-for-environment-food-rural-affairs> (accessed April 2024).
- [4] Ireland, C.S.O. 2019: <https://www.cso.ie/en/index.html> [accessed April 2024].
- [5] NCRI, *National Cancer Registry Ireland. Incidence statistics*. . <https://www.ncri.ie/data/incidence-statistics> (accessed April 2024).
- [6] Darby, S., Hill, D., Auvinen, A., Barros-Dios, J.M., Baysson, H., Bochicchio, F., Deo, H., Falk, R., Forastiere, F., Hakama, M., Heid, I., Kreienbrock, L., Kreuzer, M., Lagarde, F., Mäkeläinen, I., Muirhead, C., Oberaigner, W., Pershagen, G., Ruano-

- Ravina, A., Ruosteenoja, E., Rosario, A.S., Tirmarche, M., Tomáscaron, ek, L., Whitley, E., Wichmann, H.-E., and Doll, R., *Radon in homes and risk of lung cancer: collaborative analysis of individual data from 13 European case-control studies*. *BMJ*, 2005. **330**(7485): p. 223 DOI: 10.1136/bmj.38308.477650.63.
- [7] Moon, J. and Yoo, H., *Residential radon exposure and leukemia: A meta-analysis and dose-response meta-analyses for ecological, case-control, and cohort studies*. *Environmental Research*, 2021. **202**: p. 111714 DOI: <https://doi.org/10.1016/j.envres.2021.111714>.
- [8] Environmental Protection Agency, *National Radon Control Strategy. Phase Two: 2019-2024. Report of the National Radon Control Strategy Coordination Group*. 2019: <https://www.epa.ie/publications/monitoring--assessment/radon/The-National-Radon-Control-Strategy-Phase-2.pdf>
- [9] Environmental Protection Agency, *Environmental Protection Agency, Radon risk map: . 2023: <https://gis.epa.ie/EPAMaps/Radon?&lid=EPA:RadonRiskMapofIreland>* (accessed July 2023).
- [10] WHO, *WHO Guidelines for indoor air quality: selected Pollutants*. 2010, [www.euro.who.int/\\_data/assets/pdf\\_file/0009/128169/e94535.pdf](http://www.euro.who.int/_data/assets/pdf_file/0009/128169/e94535.pdf) (accessed February 2023).
- [11] Morawska, L., Ayoko, G.A., Bae, G.N., Buonanno, G., Chao, C.Y.H., Clifford, S., Fu, S.C., Hänninen, O., He, C., Isaxon, C., Mazaheri, M., Salthammer, T., Waring, M.S., and Wierzbicka, A., *Airborne particles in indoor environment of homes, schools, offices and aged care facilities: The main routes of exposure*. *Environment International*, 2017. **108**: p. 75-83 DOI: <https://doi.org/10.1016/j.envint.2017.07.025>.

# Filling the Indoor Air Quality Data Gap: Research Challenges and Opportunities

Gráinne McGill<sup>1\*</sup>, Marco-Felipe King<sup>2</sup>, James McGrath<sup>3</sup>, and Douglas Booker<sup>4</sup>

*1 University of Strathclyde  
Richmond Street  
Glasgow, UK*

*2 University of Leeds  
Woodhouse,  
Leeds, UK*

*\*Corresponding author: grainne.mcgill@strath.ac.uk*

*3 Maynooth University  
Maynooth,  
Ireland*

*4 University of Leeds  
Woodhouse,  
Leeds, UK*

## SUMMARY

The rapid growth in the use of low-cost sensors for indoor air quality (IAQ) measurement campaigns, following the COVID-19 pandemic, has significantly improved public awareness of ventilation and IAQ in buildings. Yet, we still know very little about the level of pollutants in our indoor environments. Unlike outdoor air, IAQ is not routinely actively monitored and there are currently no widely accepted, standardised methodologies, procedures or regulations for doing so.

No systematic long-term monitoring of IAQ in the UK or Ireland exists, despite recent calls to establish a large-scale programme akin to those already present in France and the US. The standard practice of short-term, sporadic measurements is not sufficient to determine total exposure or to quantify current levels of ventilation in the existing building stock. This information is vital to determine the effectiveness of current policy and to provide the basis for future decision making, such as pandemic preparation or building standards.

Such a systematic, long-term UK monitoring programme or *observatory* would offer an unprecedented opportunity to quantify current ventilation and indoor pollution exposure, while providing data to establish the impact of changes to behaviour and policy over time, such as improved energy standards, higher internal temperatures and increasing levels of airtightness. However, before this can be achieved, key challenges must be addressed. A standardised, validated method of measuring and recording IAQ and building data is now essential to support the collation of large-scale datasets. An integrated approach to remote low-cost sensor-based monitoring would help maximise any future monitoring campaigns and ensure data is captured in the most effective way. Moreover, there is a real opportunity to capitalise on the significant increase in IAQ monitoring through the growth of consumer-oriented air pollution sensors and sensor-based ventilation control systems, to help fill the IAQ data gap.

This paper presents a review of existing monitoring standards/guidance and available datasets to propose a roadmap to standardise the collection, storage and analysis of IAQ data for the purpose of evidencing the impact on health. This information will provide a useful resource for researchers and practitioners interested in measuring building performance and IAQ. Future research directions and opportunities are also discussed, with strategies presented on how to fill the IAQ data gap.

## KEYWORDS

Monitoring protocols, data connectivity, standardisation, roadmap

## 1 BACKGROUND

Capturing high-quality indoor air quality (IAQ) and ventilation data in housing at a national level is critical to inform future building standards and ultimately improve public health. Measurement is key to management; without comprehensive, regular monitoring of indoor pollutant exposure and ventilation in a representative sample of the housing stock it is impossible to quantify the impact of strategies to reduce exposure and associated health effects.



Moreover, measurement without sufficient contextual information can result in significant gaps in overall knowledge; in other words, *data without context is just noise*. Whilst the overall number of monitoring studies have been gradually increasing, the lack of internationally accepted measurement protocols and lack of contextual information mean comparisons between studies are difficult. Given the variability and complexity of the indoor environment, monitoring studies are often small in scale and can vary significantly in nature.

At present, there is no nationally representative data on ventilation levels in UK or Irish homes. A recent survey of ventilation provision in Great Britain found 71% of homes did not have minimum ventilation provision in adherence with long-standing building regulations (Van Rooyen & Sharpe, 2024). Airflow rate measurements taken in 52 homes as part of the UK Building Performance Evaluation Programme found 44% of systems did not meet the designed airflow rate (Sharpe et al. 2016). Similarly, a study by MHCLG (2019) found only 3 out of 80 monitored homes met minimum ventilation regulations.

The House Condition Survey is conducted annually in England and Scotland, providing valuable information on the quality and energy performance of a representative sample of housing stock, however, data for the rest of the UK is significantly limited. In Ireland, the last Irish National Survey of Housing Quality was conducted in 2002.

Likewise, there is no national monitoring programme for the UK or Ireland to routinely measure indoor pollutant exposure in a statistically valid sample of buildings (like existing observatories in France or the US). The last representative survey of IAQ in 876 English homes was conducted by BRE in 2001 (Coward et al. 2001). As such, very limited UK/Ireland specific evidence exists to examine historical trends in indoor pollution exposure or its significance relative to outdoor air (Lewis, 2022; Holgate et al. 2020). As highlighted by Lewis et al. (2022, p.13), ‘*There is an urgent need to establish a national baseline assessment of indoor air quality across the UK in both heating and non-heating seasons.*’

## **2 MONITORING STANDARDS AND GUIDANCE**

Key questions need to be addressed to establish a long-term national monitoring programme to inform policy, for instance: i) Which pollutants should be monitored and for how long, ii) Where do we place sensors, iii) Which validation and calibration methods should be applied, iv) What contextual data is required, v) What format should data be stored in, vi) How should the data be processed and managed? There is a particular need to identify the types of behavioural data required and to evaluate the most effective (and acceptable) means to capture this.

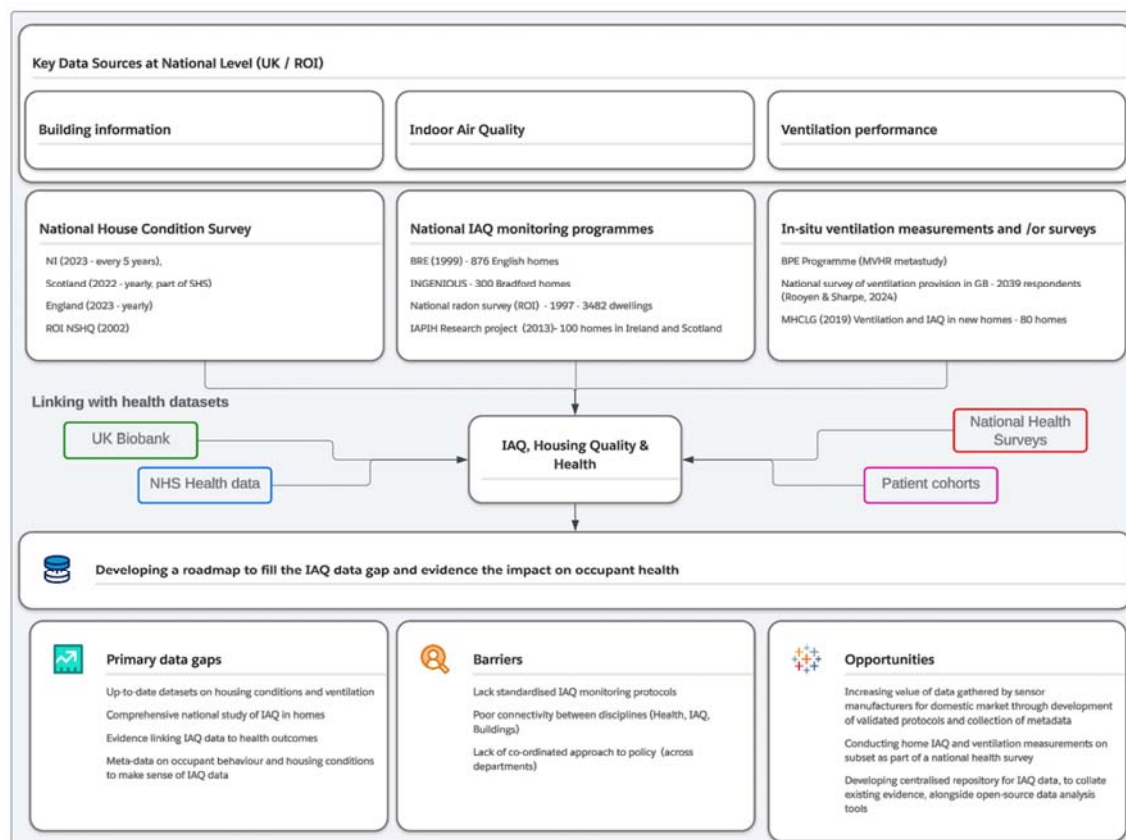
BS 40101:2022 provides limited guidance on sensor placement (e.g. min distances from radiators, windows, ventilation terminals etc.) and recommends calibration in accordance with manufacturer’s recommendations. EPA (2022) provides key considerations when placing IAQ sensors, including i) security, ii) power, iii) access, iv) take photos, v) documentation, vi) communications and vii) placement. Whilst these guidance documents are useful, there is a need for standardized protocols for large-scale, nationally representative monitoring programmes. In 2002, BRE proposed a draft protocol for assessing IAQ in homes and offices, however updated guidance is considerably lacking.

## **3 CONNECTING DATASETS: A ROADMAP TO FILLING THE IAQ DATA GAP**

Greater support for multidisciplinary research is essential to gather high-quality evidence that tracks building ventilation, IAQ and health, which will require a coordinated approach to monitoring and management at a national level. This should include activity-based emissions inventories, which are fundamental to underpin modelling of indoor pollution levels (Lewis et al. 2022). Moreover, new strategies and tools are needed for research-led measurements to

develop better process-level understanding of IAQ, including further research to ensure data quality from low-cost sensors (Lewis et al. 2022).

Figure 1: A roadmap to filling the IAQ data gap



#### 4 FUTURE RESEARCH DIRECTIONS AND OPPORTUNITIES

The significant increase in measurement and availability of IAQ data through low-cost sensor development and SMART building systems represents a significant opportunity for data sharing, however validated measurement strategies and detailed metadata is essential to derive value from this data. A centralised repository for research-led IAQ monitoring campaigns would support collation of existing evidence. Moreover, the development of open-source tools for the analysis and visualisation of IAQ data, including tools to support validation and calibration of the data would significantly enhance research in this field.

#### 5 REFERENCES

Van Rooyen, C., Sharpe, T. (2024) [Ventilation provision and use in homes in Great Britain](#)  
 Sharpe et al. (2016), [Characteristics and performance of MVHR systems](#)  
 MHCLG, (2019), [Ventilation and IAQ in new homes](#)  
 Coward et al. (2001). Indoor air quality in homes in England, Technical Report/CRC (BR433)  
 Lewis, A. et al. (2022), [Air quality expert group: Indoor Air Quality](#)  
 Holgate et al. (2022), [The Inside Story: Health Effects of IAQ on children and young people](#)  
 BS 40101 (2022), [Building performance evaluation of occupied and operational buildings](#)  
 EPA (2022), [The enhanced air sensor guidebook](#)  
 BRE (2002), A protocol for the assessment of indoor air quality in homes and offices

# Balanced ventilation - energy efficient and healthy

Piet Jacobs<sup>\*1</sup>, Wim Kornaat<sup>1</sup>, Wouter Borsboom<sup>1</sup>

*1 TNO  
Molengraaffsingel 8  
2629 JD Delft, the Netherlands  
\*piet.jacobs@tno.nl*

## ABSTRACT

When making homes more sustainable, the emphasis is on scaling up to achieve the climate and energy objectives. Little attention is paid to air quality in homes, despite the fact that an estimated 98% of the Dutch homes do not meet the WHO's 2021 annual guideline value for PM<sub>2.5</sub>. Tackling sustainability and the indoor environment hand in hand is therefore important. Airtight homes with balanced ventilation and effective range hoods offer the opportunity to significantly improve the air quality for residents in the homes, by reducing both particulate matter from indoor and outdoor sources. This possibility is currently not fully utilized. Most systems use coarse filters, while better indoor air quality can be achieved with a better filter class. The research question in this article is: What influence do ventilation systems, airtightness and effective range hoods and users have on the particulate matter concentration in the indoor air and, in particular, what is the effect of improved filtering? To answer this question, simulations were carried out with a ventilation model that included the effect of the type of ventilation system, cooking extraction, air tightness and window use. The effect of open windows was modelled with wind pressure coefficients and turbulent exchange.

The simulations show that good cooking extraction in combination with better filtering of the ventilation air in the mechanical supply can significantly reduce exposure to particulate matter in homes, even when windows are open in the bedrooms for a large part of the year. This is mainly due to the much lower exposure in the living room.

The simulated PM<sub>2.5</sub> exposure in for both homes with supply via grilles and for homes with balanced ventilation with standard filters did not meet the WHO annual guideline value. Balanced ventilation with F7 particulate matter filters (ePM1 55%) resulted in a exposure below the WHO annual guideline value. Because the simulations assume that windows are open for cooling during part of the year, the use of even better filters only has a limited effect. In homes with active cooling, there is clear added value to using better filters than F7 quality, because then windows can remain closed.

## KEYWORDS

PM<sub>2.5</sub>, simulation, window use, ventilation system, cooking exhaust

## 1 INTRODUCTION

When renovating homes, the emphasis is on energy savings in order to achieve the climate and energy objectives. Energy savings, necessary to meet the obliged energy efficiency requirements, are usually also the reason for using balanced ventilation in new-build homes. In other sectors such as offices and schools near busy roads, balanced ventilation in combination with good filters is also used to protect users against particulate matter from the

outside air (PvE Healthy offices 2021; PvE fresh schools, 2021). The fact that balanced ventilation, in addition to meeting energetic requirements, can also be used to improve air quality and thus the health of residents, receives little attention in homes.

In any case, little attention is paid to air quality in homes, despite the fact that an estimated 98% of homes do not meet the WHO's 2021 recommended value for PM<sub>2.5</sub>. A large-scale and long-term monitoring study (TKI Be Aware, 2020) established that 15 of the 100 homes examined did not meet the 'old' WHO PM<sub>2.5</sub> recommended value of 10 µg/m<sup>3</sup> annual average. The annual average concentration in the kitchen/living room was on average 8.2 µg/m<sup>3</sup>. In September 2021, this recommended value was adjusted by the WHO to 5 µg/m<sup>3</sup> annual average. Using this new recommended value, 98% of the homes examined no longer met (TVVL 2021).

Based on the Be Aware monitoring study, simulations were carried out in 2020 with the TRNSYS building model linked to the ventilation calculation model TRNFlow (COMIS). Two important simplifications were made when carrying out these simulations. Firstly, a ventilation model was used in which only the living room/kitchen was considered. In addition, the windows were assumed to be closed. This is certainly not a good assumption outside the heating season. The research question in this article is therefore: What influence do ventilation systems and users have on the particulate matter concentration in homes and, in particular, what is the effect of improved filtering? To answer this question, simulations were carried out with a ventilation model that included the effect of the type of ventilation system, cooking extraction, air tightness and window use.

## 2 SIMULATION SETUP

### 2.1 Multizone ventilation model

With a multi-zone ventilation model the annual average particulate matter concentration in a single-family home has been determined. The model consists of 4 zones, see figure 1. The zones are all connected to the stairwell via a gap of 120 cm<sup>2</sup> under the interior doors. To prevent drafts from occurring straight through the house from facade to facade at higher wind speeds when windows are open, it is assumed that the interior doors are closed.

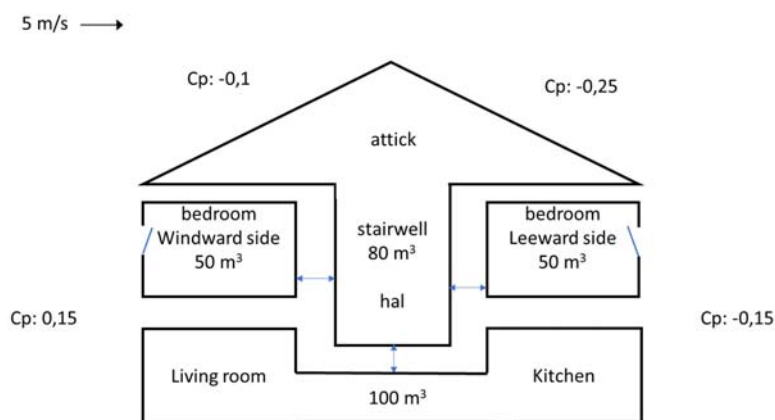


Figure 1: schematic representation of ventilation model with connections between the zones

The ventilation model calculates the air flows between the zones based on wind effects, thermal effects and the type of ventilation system. A constant air speed of 5 m/s perpendicular to the facade has been assumed for the wind. This speed is the average wind speed in the Netherlands. Two air leakages have been assumed, 20 and 80 dm<sup>3</sup>/s at 10 Pa. The air leaks

through seams and cracks are distributed over the home envelope in accordance with the BKN equivalence methodology (2018) and are mainly present in the attic. The wind pressure coefficients for the facade and roof surface have also been adopted in accordance with this methodology. Thermal effects are modelled depending on the season. The daily average indoor and outdoor temperatures used for this are shown in table 1.

Table 1: Simulated indoor and outdoor temperatures per season

	<b>Outside temperature</b>	<b>Living room temperature</b>	<b>Bedroom temperature</b>
Winter	6	20	18
Spring and autumn	14	20	20
Summer	20	20	20

## 2.2 Turbulent exchange through open windows

Many residents of new-build homes, even in the heating season, experience the temperature of the bedrooms as too high and open the windows to cool (Jacobs, 2012). This can cause so-called turbulent exchange, in which warm air simultaneously flows out at the top and cold air flows in at the bottom. This turbulent exchange can be calculated from the temperature difference between inside and outside, the open surface and the height over which the exchange occurs (AIVC, 1988). Here a tilting window has been simulated for each bedroom, which is opened 10 cm at the top in the tilt position. The height of the window is 1.3 m and the width is 0.57 m.

Window use over the seasons has been simplified as follows: in winter all windows are assumed to be closed, in spring and autumn the bedroom windows are in the tilt position while sleeping and in the summer these windows are in the tilt position throughout the day.

## 2.3 Particulate matter sources and deposition

The annual average PM<sub>2.5</sub> particulate matter concentration in the outdoor air in urban areas has decreased in recent years due to cleaner techniques and COVID-19 lockdown measures to approximately 9 µg/m<sup>3</sup> (range 7-11 µg/m<sup>3</sup>). In this simulation study, an average outdoor concentration of 11 µg/m<sup>3</sup> was used to compare the results with the outdoor conditions during the TKI Be Aware measurement study that was carried out from September 2017 to September 2018.

In the home, the PM<sub>2.5</sub> particulate matter emissions due to cooking have been simulated according to the 50 percentile emission pattern from TKI Be Aware. This emission pattern includes emissions resulting from the preparation of breakfast, lunch and dinner. Some of the particulate matter in the indoor environment settles on surfaces, this is called deposition. For the simulation study, it was assumed that the effect of this deposition is equivalent to an additional ventilation flow with clean air of 40 m<sup>3</sup>/hour in a room of 100 m<sup>3</sup> (TKI Be Aware, 2020).

## 2.4 Cooking extractor

Simulations with and without cooking extraction were carried out. A capture efficiency of 95% has been assumed for the capture of PM<sub>2.5</sub> present in the cooking fumes when the extractor hood is switched on (100% extraction capacity). This is a typical value for a chimney extractor hood at 300 m<sup>3</sup>/hour. The size of this extraction flow is comparable to the maximum extraction flow of a ventilation unit for a single-family home.

## 2.5 Ventilation system and filtering

Two ventilation systems have been simulated in the house. A system C ventilation system, which consists of supply grilles in the facade in every living room and a mechanical exhaust in the kitchen, bathroom and toilet. And a balanced ventilation system (system D) with mechanical supply in every living room and mechanical exhaust in the kitchen, bathroom and toilet. The nominal ventilation capacities are in accordance with the Dutch Building Decree. Situations with low setting (30% of the nominal ventilation capacity) and medium setting (70% of the nominal ventilation capacity) when there is presence are simulated. In the absence, it is assumed that the system is always in low mode. It is assumed that the ventilation grilles in the living room are closed and that they are continuously open in the bedroom. This is a common practical situation that arises after experiencing drafts in the winter and forgetting to open the grilles in the spring. In system C it is assumed that only very coarse parts such as insects are captured from the grilles and that no capture of  $PM_{2.5}$  takes place. The balanced ventilation system is equipped with G3 filters as standard. For a balanced ventilation unit equipped with such a coarse filter, a  $PM_{2.5}$  capture efficiency of 15% is expected based on ongoing practical measurements. Equipped with an F7 filter (e $PM_{1}$  55%), see figure 2, the capture efficiency of the balance ventilation unit increases to approximately 75%. These two values were used in the simulations. In addition, simulations have also been carried out with a  $PM_{2.5}$  capture percentage of 99%. This performance can be achieved when using an electrostatic filter that is placed downstream of the balanced ventilation unit (Khoury et al. 2017).



Figure 2: energy-efficient and healthy, in the balanced ventilation unit an F7 (e $PM_{1}$  55%) fine dust filter has been placed in the air intake instead of the standard G3 coarse filter, such a filter is still in the exhaust.

## 2.6 Particulate matter concentration and exposure

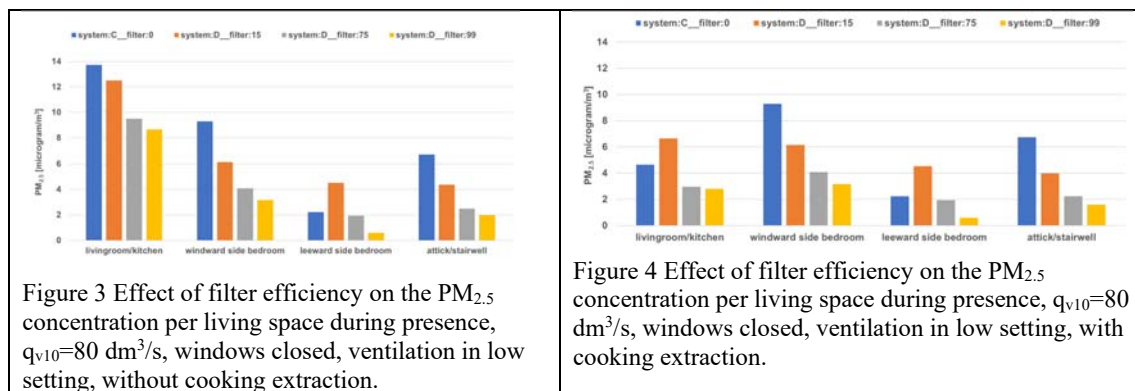
The COMIS ventilation model was used to calculate the concentrations in the various rooms in the house over time. The concentration when present in the various living areas was then determined. For this purpose, the following stay has been adopted: 9 hours per day in the bedroom, 5 hours in the living room/kitchen during the week and 10 hours per day in the living room/kitchen at the weekend. The average exposure to particulate matter in the home has been determined based on these times.

### 3 SIMULATION RESULTS

#### 3.1 Effect of filtering and cooking extraction on concentrations with closed windows

Without using a cooking extractor, see figure 3, the highest particulate matter concentrations occur in the living room/kitchen. The simulated concentrations correspond well with the measured concentrations in the Be Aware study during presence. Figure 4 shows that better filtering of the ventilation air only results in a limited reduction in concentration in the living room/kitchen. In the bedroom on the windward side, relatively high concentrations occur, especially in system C, because a lot of unfiltered outside air flows in through the grille and the seams and cracks. In the leeward room, system C scores better in terms of particulate matter than system D with a standard filter (15% capture efficiency), because exfiltration occurs via the grilles and therefore supply via the inner door from the relatively clean stairwell (as a result of deposition in the home).

With a cooking extractor, see figure 4, the particulate matter concentrations in the bedroom remain unchanged. However, the concentrations in the living room/kitchen decrease sharply. It is striking to see that there is almost no concentration difference between the F7 filter with 75% capture efficiency and a filter with 99% capture efficiency. This is caused by the fact that ventilation is set to low during the rest of the day, except during cooking, and the contribution of infiltration is then relatively large. With ventilation in the middle position (figure not shown), the concentration in the living room with the standard G4 filter (15% capture efficiency) remains virtually the same, but with a filter with 99% capture efficiency it decreases to  $2 \mu\text{g}/\text{m}^3$ .



#### 3.2 Effect of airtightness and window use with two filter classes

Figures 5 and 6 show the particulate matter concentration for the different rooms with different assumptions for air tightness and outside temperature for 15% and 75% filter efficiency respectively. A limited influence of the airtightness ( $q_{v10}$  value) is visible in winter ( $T_{\text{outside}} [\text{C}]:6$ ) when the windows are closed. In spring and autumn ( $T_{\text{outside}} [\text{C}]:14$ ) and summer ( $T_{\text{outside}} [\text{C}]:20$ ), opening windows in particular determines the exposure to particulate matter in the bedrooms. The filter class has the greatest effect in the living room. In the bedroom, an effect is visible in winter and the effect is limited during the rest of the year due to the assumed window use.

It is striking to see that in the leeward bedroom the particulate matter concentration decreases in summer compared to spring and autumn. This is because the simulations in summer assume that the indoor temperature is the same as the outdoor temperature and therefore no turbulent exchange occurs across the open windows. Turbulent exchange is the phenomenon in which warm indoor air flows out at the top of the window and the same amount of cold outside air flows in at the bottom. Due to the higher particulate matter concentration outside compared to inside, turbulent exchange results in an additional particulate matter load for the

bedrooms. It is noted that in reality temperature differences can also be expected in summer and therefore turbulent exchange will also take place (albeit to a lesser extent than in spring and autumn). To study this effect further, simulations with, for example, hourly values will be carried out at a later stage.

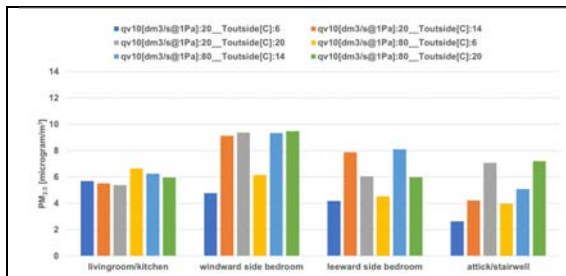


Figure 5 System D with 15% filter efficiency, effect of air tightness ( $q_{v10}$ ) and outside temperature on the  $PM_{2.5}$  concentration in the presence of each living room, ventilation in low mode, with cooking extraction, windows open or closed depending on the temperature.

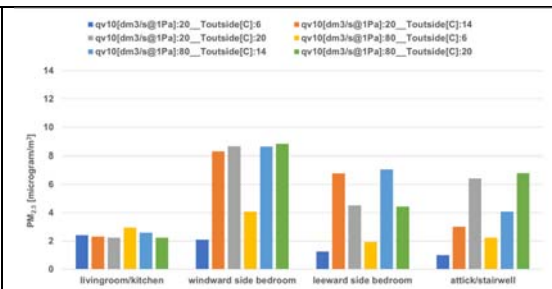


Figure 6 System D with 75% filter efficiency, effect of air tightness ( $q_{v10}$ ) and outside temperature on the  $PM_{2.5}$  concentration when present per living room, ventilation in low setting, with cooking extraction, windows open or closed depending on the temperature.

### 3.3 Effect on exposure

The average annual particulate matter exposure in the home has been determined by averaging the particulate matter concentrations present in the various rooms during the four seasons. It follows from Figure 7 that in both a home equipped with system C and system D with a standard filter (15% capture efficiency), the exposure is higher than the WHO annual average  $PM_{2.5}$  recommended value of  $5 \mu\text{g}/\text{m}^3$ . Increasing the ventilation flow rate when present to the medium setting even results in an increase in exposure in this situation. This is because when the amount of ventilation is increased, the effect of deposition decreases relatively speaking. Replacing the G3 supply filter in system D with an F7 particulate filter leads to exposure below the WHO recommended value. Installing an electrostatic filter with a 99% capture efficiency only results in a limited reduction in exposure, because the bedroom windows are open during part of the year. Figure 8 shows the potential of filtering in combination with mechanical cooling (bedroom windows are no longer opened). This reduces exposure by more than half compared to a F7 filter. And with an electrostatic filter, exposure in the home can even be reduced to below  $1 \mu\text{g}/\text{m}^3$ .

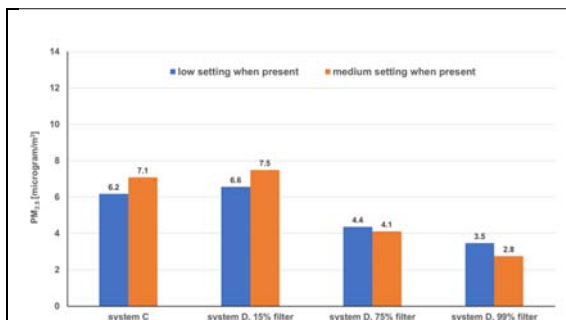


Figure 7 Exposure to  $PM_{2.5}$  particulate matter for different ventilation systems and filter efficiencies . Bedroom windows tilted in spring, autumn and summer, airtightness  $q_{v10}=20 \text{ dm}^3/\text{s}$  and with cooking extractor.

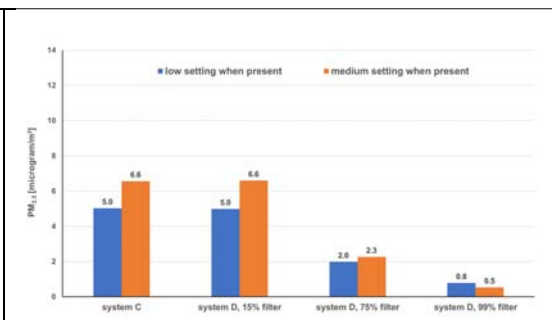


Figure 8 Exposure to  $PM_{2.5}$  particulate matter for different ventilation systems and filter efficiencies . Bedroom windows closed (mechanical cooling), air tightness  $q_{v10}=20 \text{ dm}^3/\text{s}$  and with cooking extractor.



## 4 CONCLUSIONS

This simulation study shows that good cooking extraction in combination with better filtering of the ventilation air in the mechanical supply can significantly reduce exposure to particulate matter in homes, even when windows are open in the bedrooms for a large part of the year. With balanced ventilation with F7 particulate matter filters (ePM<sub>1</sub> 55%), the new WHO recommended value is met. Because the simulations assume that windows are open for cooling during part of the year, the use of even better filters only has a limited effect. In homes with active cooling, there is clear added value to using better filters than F7 quality, because then windows can remain closed.

This study is a simulation study with a large number of other assumptions in addition to the previous simplification. Practical measurements are required to validate the results. For this purpose, detailed measurements are planned in homes in 2024, in which particulate matter is measured in multiple zones and information is collected about, among other things, open windows, ventilation flow rates and meteorological data. In addition, the effect of better filtering will be measured in homes with balanced ventilation to validate the model described here.

## 5 REFERENCES

AIVC, Inhabitant Behavior with Respect to Ventilation – a Summary Report of IEA Annex VIII, Technical Note AIVC 23, Air Infiltration and Ventilation Centre, March 1988.

Indoor climate technology, PvE Healthy offices 2021 (<https://www.binnenklimaattechniek.nl/document/pve-gezonde-kantoor-2021/>)

Interview, Almost no home meets the new WHO particulate matter standard, TVVL magazine 06, December 2021 (in Dutch).

Jacobs P., Ventilation in new-build homes with balanced ventilation, TVVL magazine, December 2012 (in Dutch).

Khoury E., Wijsman S, Vons V., Combating wood smoke nuisance in homes, TVVL magazine 2017 (in Dutch).

Public final report TKI Be Aware - Awareness of indoor air quality in homes: sources and effective energy efficient intervention strategies, TNO report 2020 R10627, April 2020 (in Dutch).

RIVM, Compendium for the living environment, [Finer fraction of particulate matter \(PM<sub>2.5</sub>\) in air, 2009-2022 | Compendium for the Living Environment \(clo.nl\)](#), accessed on 6/12/2023.

Program of Requirements Frisse schools 2021 (<https://www.arbocatalogue-vo.nl/media/1149/programma-van-eisen-frisse-scholen-2021.pdf>)

VLA methodology equivalence for energy-saving ventilation solutions in homes, version 1.3, 2018

# Indoor air quality post deep energy retrofit in social homes in Ireland (HAVEN)

Marie Coggins\*<sup>1</sup>, Daniel Norton<sup>1</sup>, Asit Kumar Mishra<sup>3</sup>, Victoria Hogan<sup>2</sup>, Nina Wemken<sup>1</sup>, Hala Hassan<sup>1</sup>, and Medeina Macenaite<sup>1</sup>

*1 School of Natural Sciences & Ryan Institute, University of Galway, Galway, H91TK33, Ireland*

*2 School of Health Sciences, University of Galway, Galway, H91TK33, Ireland*

*\*marie.coggins@universityofgalway.ie*

*3 School of Public Health, University College Cork, College Road, Cork, Ireland*

## SUMMARY

Improving the energy performance of a building has been shown to improve health outcomes in fuel poor homes (Wang et al., 2022). However, increasing building air tightness through provision of increased insulation, without due regard to building ventilation, can result in poorer air quality and impaired health for residents, in particular impaired respiratory health (Wimalasena et al., 2021; McGill et al., 2015; Ferguson et al., 2020). The Health Impact Assessment of Energy Renovations on Irish Domestic Dwellings (HAVEN) research project aimed to study the health impact and associated benefits of energy renovation among Irish social housing. This paper summarises the indoor air quality measurements collected in a sample of Irish social housing properties pre and post-energy retrofit. Our research suggests that occupant behaviour such as blocking wall vents and smoking have the potential to negatively impact on indoor air quality. In order to optimise the co-benefits of energy retrofit to IEQ in social housing, renovation needs to include an effective communication strategy, with targeted messaging to tenants on indoor air quality and its relationship with health.

## KEYWORDS

Indoor air quality, ventilation, social housing, PM<sub>2.5</sub>, formaldehyde

## 1.0 METHODOLOGIES

A total of 14 homes participated at pre- and post-retrofit stage, including 11 social housing properties and 3 private dwellings. Within the main living area and main bedroom of each home the following indoor environmental parameters were monitored; temperature (°C), relative humidity (%), carbon monoxide (ppm) (measured at 5-min intervals for 48-72 hours using GrayWolf IAQ-610 sensing probes), PM<sub>2.5</sub> (µg.m<sup>3</sup>) (measured at one-minute intervals for 48 hours using a TSI SidePak AM520), formaldehyde (µg.m<sup>3</sup>) (UMEX passive sampler for 3 days) and radon (Bq.m<sup>3</sup>) (Radtrak closed alpha-track detector for 3 months). If mechanical ventilation systems were installed, they were also assessed. During the survey participants were asked to complete a short questionnaire to record information such as occupant demographics, typical household activities, space heating and ventilation methods. Participants were also asked to complete an activity diary to document household activities that may have influenced indoor air quality e.g., cooking activities, burning incense. Ventilation rates were calculated using bedroom night-time (10 pm-7 am) CO<sub>2</sub> data using the steady-state method (Persily & de Jonge, 2017). Project data was collated using Microsoft Excel and analysed using R statistical software. The impact of the retrofit on air quality was analysed using t-tests and linear mixed effects models in R.

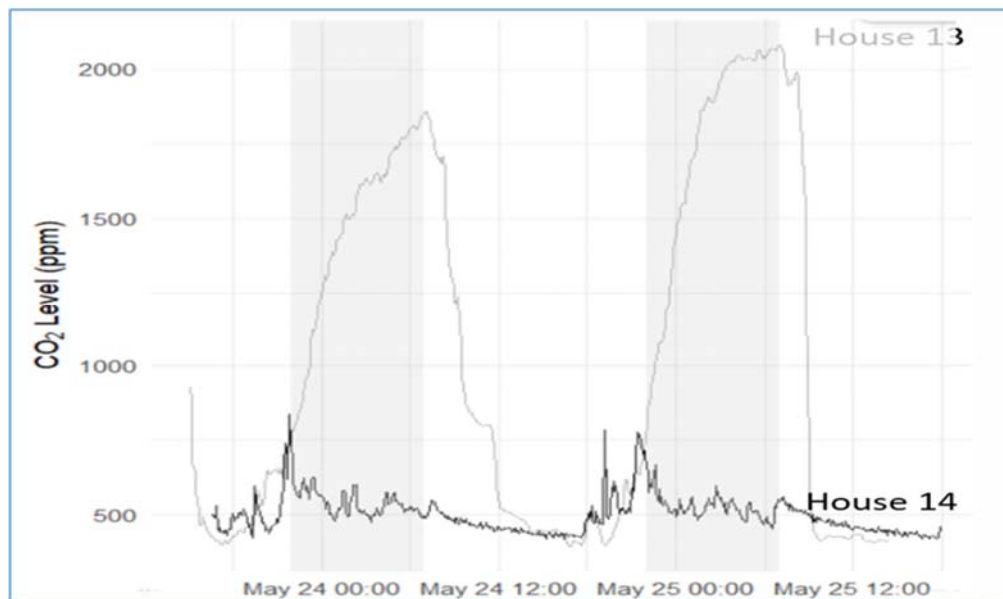


Figure 1. Time series plot of carbon dioxide concentrations during the nighttime period in a home with blocked wall vents (House 13) and unblocked wall vents (House 14).

## 2.0 RESULTS AND DISCUSSION

All homes had a significant energy uplift post-retrofit. Fossil fuel-based heating systems were replaced with a heat pump, some homes received extra wall and/or attic insulation, and new energy efficient windows or doors. The three private homes, and two of the social housing properties had demand control ventilation systems installed. Post-retrofit median air temperatures were within EN16798 Category I limits, and respondents reported less thermal discomfort due to draughts. Post-retrofit median CO<sub>2</sub> concentrations were lower in mechanically ventilated homes in comparison with the naturally ventilated homes and bedroom ventilation rates were higher in mechanically ventilated dwellings (up to 5.0 L.s<sup>-1</sup>.p in naturally ventilated homes compared to up to 12.0 L.s<sup>-1</sup>.p in mechanically ventilated dwellings). Analysis of the indoor concentrations of carbon dioxide and PM<sub>2.5</sub> highlighted the impact of occupant behaviour on indoor air quality. Blocked wall vents were observed in 45% of the social housing properties, which resulted in higher CO<sub>2</sub> concentrations particularly in bedrooms (median value of 1425 ppm versus 859 ppm in bedrooms with and without blocked wall vents respectively). Figure 1 compares the nighttime bedroom CO<sub>2</sub> concentration in the main bedroom (occupied by two persons) of two identical homes, surveyed during the same period. The concentration profile for Home 13 shows the impact of blocked wall vents on CO<sub>2</sub> concentration compared to Home 14 which had unblocked wall vents. Smoking and or vaping was observed in four social housing properties, and levels of PM<sub>2.5</sub> in such homes were higher than the WHO 24-hour guideline value of 15 µg/m<sup>3</sup> (WHO, 2021) both pre and post- retrofit. PM<sub>2.5</sub> concentrations in smoker homes (median value of between 56–58 µg/m<sup>3</sup>) are within the range of those reported previously for smoking residences (Semple et al., 2015), and in the presence of lower ventilation post retrofit, presents an increased risk of PM<sub>2.5</sub> exposure post retrofit. Formaldehyde concentrations increased post retrofit, similar to observations from previous studies on indoor air quality in energy retrofits (Hassan et al., 2024).

### 3.0 CONCLUSION

Our research suggests that occupant activities such as blocking wall vents and smoking indoors have the potential to negatively impact on indoor air quality in social housing retrofits. As part of the ventilation strategy for social housing efforts are required to consult with tenants to determine factors contributing to occupant behaviours leading to poor indoor environmental quality. Considering the vulnerability of the residents of many social housing properties, it is imperative that retrofit does not negatively impact on indoor air quality.

### 4.0 ACKNOWLEDGEMENTS

The Government of Ireland through the Sustainable Energy Authority of Ireland's Research, Development and Demonstration Funding Programme 2018 funds this project (RDD435).

### 5.0 REFERENCES

Ferguson, L., et al., (2020). Exposure to indoor air pollution across socio-economic groups in high-income countries: A scoping review of the literature and a modelling methodology. *Environ Int*, 143, 105748. doi:10.1016/j.envint.2020.105748.

Hassan, H., et al., (2024). Deep Energy Renovations' impact on indoor air quality and thermal comfort of residential dwellings in Ireland –Arden project. *Build and Environ*, 259, 111637. doi:10.1016/j.buildenv.2024.111637

McGill, G., et al., (2015). Case study investigation of indoor air quality in mechanically ventilated and naturally ventilated UK social housing. *Int. J. Sustain. Built Environ*, 4(1), 58–77. doi:10.1016/j.ijbsbe.2015.03.002

Persily, A., & de Jonge, L. (2017). Carbon dioxide generation rates for building occupants. *Indoor Air*, 27(5), 868–879. doi:10.1111/ina.12383

Semple, S., et al., (2015). Fine particulate matter concentrations in smoking households: Just how much secondhand smoke do you breathe in if you live with a smoker who smokes indoors? *Tobacco Control*, 24(e3). doi:10.1136/tobaccocontrol-2014-051635

Wang, Y., et al., (2022). Exploring the relationship between window operation behavior and thermal and air quality factors: A case study of UK residential buildings. *Build. Eng.*, 48, 103997. doi:10.1016/j.job.2022.103997

WHO. (2021). Global Air Quality Guidelines: Particulate matter (PM2.5 and PM10), ozone, nitrogen dioxide, sulfur dioxide and carbon monoxide. Retrieved from <https://www.who.int/publications/i/item/9789240034228>

Wimalasena, N. N., et al., (2021). Housing risk factors associated with respiratory disease: A systematic review. *Int J Environ Res Public Health*, 18(6), 2815. doi:10.3390/ijerph18062815

# Calibration methodology for combined heating and ventilation models

Wouter Borsboom<sup>1</sup>, Ruud van der Linden<sup>1</sup>

*1 TNO, Molengraaffsingel 8  
2629JD Delft, Netherlands*

## ABSTRACT

By 2050, Europe aims for energy-neutral buildings, necessitating effective integration of renewable energy sources and smart grid management. To address peak energy demands and prevent grid congestion, building-level energy management is crucial. This paper presents a stepwise calibration methodology for hybrid building models, enhancing flexibility in HVAC systems and thermal buffers.

The methodology involves: (1) utilizing known building and installation data to reduce calibration parameters, (2) independently calibrating subsystems like floor heating and cooling, (3) selecting optimal time periods for parameter estimation based on different physical mechanisms, and (4) validating the model with actual measurements.

The SirinE hybrid model combines physical and data-driven components, leveraging known building data to minimize the need for detailed measurements. Successfully applied in various projects, SirinE improves PV energy self-utilization and electrical energy demand.

Future work will focus on automating calibration, enhancing model robustness against user behaviour and sensor failures, and refining the hybrid model for evaluating residential renovations in an open source version. This methodology supports efficient energy management and integration of renewable sources in the built environment.

## KEYWORDS

Heat-network, ventilation-model, calibration, control, congestion

## 1 INTRODUCTION

By 2050, the entire built environment in Europe must be energy-neutral. A major challenge in this energy transition is integrating energy-producing neighbourhoods into the existing energy infrastructure. The exponential increase in photovoltaic (PV) systems, electric vehicle charging, batteries, electric cooking, and heat pumps will lead to higher peaks in electricity demand and supply (Bunn 2016). The intermittent availability of various renewable energy sources, along with associated trade platforms, will require energy systems to switch between energy sources smoothly and on short notice.

The maximum demand and supply are limited by the capacity of the grid connection, which can be a fixed value or time-limited by the district service operator (DSO). Energy systems must be capable of smartly balancing supply and demand at the district level to avoid network congestion. To ensure stability and security of supply, the energy network will need to incorporate a mix of different commodities (electricity, heat, and possibly hydrogen networks).

Building-level energy management (in houses, offices, hotels, etc.) can play an important role in reducing peak demands by distributing energy demand over time and across different commodities. Control based on building models can assist in load balancing by accurately predicting how much energy can be shifted in time for ventilation, heating, cooling, and domestic hot water at specific moments. Currently, other commodities like batteries, PV, and

EV charging are often used to enable flexibility due to the time required to calibrate these models.

For the market uptake of HVAC flexibility, it is important to have a model that can be initiated very rapidly. The challenge is to develop a building model controller that includes an automated calibration procedure that can be initiated by an installer within a few hours. To balance energy production within the capacity constraints of the local grid, reliable predictions of both decentralized renewable energy production and building energy use are needed. Choosing the right control scenario requires short-term predictions based on different scenarios, ideally providing a one-day-ahead forecast of both energy demand and decentralized renewable energy production.

Occupant behavior significantly influences a building's energy demand, making it essential to predict the impact of behavior on energy use. Involving occupants in the process may lead to behavioral changes, requiring the prediction model to continuously adapt.

Current research in this field follows two main directions. The first focuses on smart district-level control using Artificial Neural Networks, agent technology, or Model Predictive Control (Canizares 2014) (Mynhoff, 2018) (Mocanu 2018). These models often represent individual building energy requirements simplistically and statistically, using fixed demand/supply curves. The second research direction involves single-building scheduling and control studies using physical models simulated in specific tools, such as TRNSYS or Energy-Plus (Ascione 2016) (Schirrer 2016), or RC networks (Deconinck, 2017).

Recent academic focus has shifted from black-box models to hybrid models, which offer better predictions and higher robustness (Bourdeau 2019). Hybrid models use known physical relations, such as the cooling down of a building, and therefore require less informative data than black-box approaches. Unknown aspects, like user behaviour, are modelled using black-box techniques or profiles. The current generation of hybrid building models primarily focuses on a single type of building and often uses fixed user profiles for heating demand. Both research directions require calibration time, but this paper focuses on the calibration method of hybrid building models. TNO has developed and successfully tested this hybrid model for model predictive control (Borsboom, 2022) and is currently working on an open-source version for the Dutch government to evaluate building renovation measures. The described stepwise calibration methodology can be applied to both these models and other physical based models

## **2 METHODOLOGY TO QUANTIFY FLEXIBILITY ON A BUILDING LEVEL**

At the district level, there is a need to balance the supply and demand of energy as well as to manage congestion to stay within the grid's maximum capacities. The District Service Operator (DSO), responsible for the proper functioning of the grid, will manage buildings to control congestion and therefore available consumption or delivery capacity. Energy markets provide price incentives at various timescales for the prices of energy for both supply and demand within a given time horizon. These controls will translate into signals for a controller located behind the energy meter, at the building or building campus level. This controller can manage one or more active components in such a way that the demand or supply of energy changes over time. For this, it is important that the controller receives an accurate prediction of the available flexibility. For example, it is important to know how much cooling demand is predicted and how much this can be increased or decreased at a certain point in the time horizon used by the DSO or Energy Market.

The first step is to identify which components can be actively controlled. Key components for managing the electricity grid include the HVAC system, PV panels, EV charging stations, local

heat buffers, and batteries. Additionally, smart appliances, such as household appliances, offer further control possibilities. This paper focuses specifically on shifting heating demand within the building model.

The second step involves predicting the flexibility potential of these active components, described through active demand response (ADR) events (EIA Annex 6, 2019). An ADR event specifies how a component's flexibility can be adjusted, such as changing a temperature setpoint by a fixed amount within a set time frame. Shifting energy use at specific times impacts consumption either upward or downward and can lead to a rebound effect later. The building model calculates these shifts and rebound effects based on control signals and other input parameters, such as outside temperature and occupant behaviour. Currently, various standards have been developed to describe ADR events, including PAS 1878/1879, EEBUS, and S2 of EN 50491-12-2.

The third step is to select the most effective control strategy based on ADR predictions. ADR describes how a component responds to fixed control strategies. In Model Predictive Control, multiple control strategies can be simulated within a single time step using the building model. These ADR scenarios are evaluated using a cost function derived from price signals from the Distribution System Operator (DSO) or the energy market, leading to the selection of the optimal control signal for the active component.

Currently, various standards have been developed to describe ADR events, including PAS 1878/1879, EEBUS, and S2 of EN 50491-12-2.

### **3 HYBRID BUILDING MODEL SIRINE**

An important issue in determining the ADR of a building to changes in the active control inputs is that the ADR is dependent on dynamically varying external conditions, such as ambient temperature, solar radiation, wind, the current thermal energy stored in the building structure, user behaviour and constraints in the operation of the HVAC installation. This makes the ADR a complex multi-variable function that is hard to determine, requiring informative data over the whole operational range.

To avoid the need for large and high-information content datasets of historical data of buildings in a district, a hybrid modelling approach is taken. The basic idea is that limiting the number of unknown parameters, that must be estimated from the data, will reduce parameter identifiability problems.

SirinE is a hybrid predictive digital twin model for buildings (Borsboom, 2022). It comprises a physical building model that solves heat flow balance equations and a data-driven occupant model that simulates occupant interactions with building components (e.g., thermostats, windows, electric appliances), incorporating these actions into the heat flow balance equations.

The main idea behind SirinE is to leverage available building data and known physical relationships to minimize the need for high quality data. There is usually plenty of time-series data available from energy meters, temperature sensors, and smart building systems (e.g., heat pumps, building and control systems (BACS), smart home systems, smart thermostats, electric vehicle systems). However, this data is often not detailed enough to calibrate a model for reliable energy predictions. By using known building and installation data, SirinE reduces the requirement for highly detailed data. An additional advantage is that the relations between

measured variables are governed by physical laws and that parameters have physical interpretation and allowable ranges.

The building model of SirinE includes a heat balance and ventilation network (Kornaat 2020) that is automatically derived from the Building Information Model (BIM), which describes the geometric configuration and construction properties of the building (including all spaces, walls, windows, doors, roofs, etc.), and the Building Energy Model (BEM), which describes the building's heating, cooling, and ventilation equipment and controllers. With the automatic generation of the heat network, the simulation model can be easily adapted to different building types, such as apartment buildings, row houses, and office buildings. Furthermore, the data used to calibrate the model utilizes standardized ontologies like Haystack, making the simulation model easily scalable for different building typologies.

This heat network needs calibration for two reasons: firstly, not all necessary information is always available, such as the masses of the floors and walls. Secondly, the provided information may not be accurate, such as thermal bridges or airtightness being less than specified due to construction quality. This paper describes a strategy to calibrate the heat and ventilation networks.

SirinE includes a generic occupant module (framework) that reproduces the interactions of occupants with the building. The occupant module contains distinct submodules, each associated with specific occupant behaviour, such as occupancy, window interactions, or thermostat setpoint adjustments. The implementation is flexible, allowing each submodule to connect to various predictive models, ranging from simplistic approaches (e.g., fixed hourly profiles) to complex AI algorithms. Receiving the building's state at each timestep from the building simulator, along with weather information, the occupant module predicts occupant behaviour for the next timestep and sends it back to the building simulator. The AI-based occupant module, combined with the physics-based building simulator, makes SirinE a hybrid digital twin.

The building heat balance model dynamically interacts with the occupant model, implemented in an agent-based framework. All individual users (or groups of users defined as a user role) are agents that interact with the heat balance model in a dynamic simulation over the prediction horizon. The occupant models that have been implemented (simple hourly schedules, models for thermostat and appliances based on sliding averages, Markov chain models for window-opening behaviour) highlight the hybrid nature of SirinE. However, it is important to note that this is a general framework that can be coupled with any occupant model. We have developed different strategies to calibrate user behaviour, and this paper focuses on the calibration of the ventilation and heat networks.

## **4 CALIBRATION STRATEGY**

### **4.1 Introduction of the calibration strategy**

The calibration strategy developed can be described in a number of steps, ranging from zero up to 4.



Table 1: Calibration steps

<b>Step</b>	<b>Description of the calibration step</b>
0	Collect information from the building BIM and HVAC installation data sheets. Eliminate from estimation all parameters that are known with sufficient confidence
1	Identify subsystems which can be calibrated independently
2	Identify special time periods in which part of the parameters can be discarded, limiting the number of parameters to be identified.
3	Perform overall parameter estimation
4	Perform validation over a time series not used in parameter estimation

The idea behind this methodology is to start in step 0 with as many known properties of the building and installation, and known physical relationships, using the heat and ventilation network. This approach addresses the issue that time series data available for calibration is often insufficiently informative, leading to large parameter uncertainty and inaccurate model predictions.

In step 1, we identify subsystems with parameters that can be calibrated independently, such as a floor heating system. In step 2, We identify special time periods in which part of the parameters can be discarded. Limiting the number of parameters to be identified. We also utilize the fact that different physical transfer mechanisms have different dynamics. For example, ventilation can heat a space faster than solar radiation and heat conduction. By choosing time periods where the effect of a transfer mechanism is large compared to others the parameters involved can be estimated neglecting correlation with other parameters. For instance, ventilation can be calibrated when there is a large difference between indoor and outdoor temperatures, while solar radiation can be calibrated best during the transitional seasons.

The complete set of parameters will be estimated in step 3 using the already determined parameters in steps 0,1 and 2 as initial estimates and uncertainty ranges.

Step 4 involves validating the simulation against actual measurements.

The different steps are detailed in the section below. To illustrate the calibration steps, data and estimation results for a 4-room apartment in an apartment building, with data recorded over a 1-2 year period, will be shown. The well-insulated apartment has a ground source water-to-water heat pump for domestic hot water and floor heating and is equipped with individual PV panels.

## **4.2 Step 0 BIM/HVAC information collection**

To reduce the number of parameters that need calibration, we incorporate as much known building information as possible into the physics-based ventilation and heat network. By utilizing known physical relationships, such as heat conduction and radiative heat transfer, less informative data is required for calibration. This process begins with collecting Building Information Modeling (BIM) data and HVAC installation data sheets.

For the SirenE model, the required building geometry information includes details on the façade, roof, floor, windows, doors, inner construction areas, and orientation, as well as the

material properties of each layer of these elements. The BIM information is then used to automatically configure a 50 nodes RC-network of the building.

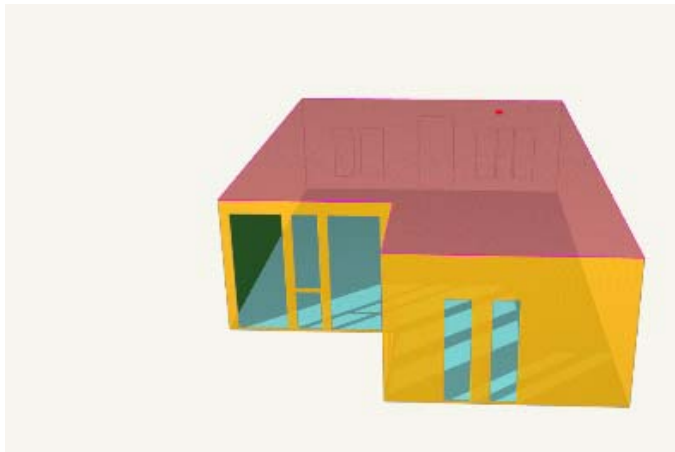


Figure 1: Apartment geometry derived from the BIM

Information on the heat pump, floor heating, floor cooling, boiler dimensions, and PV installation is retrieved from manufacturer data sheets or EPBD calculation inputs. User behaviour must be calibrated, which can be done through questionnaires or derived from real data if available, including room temperature setpoints, CO<sub>2</sub> levels, and electricity consumption. Alternatively, standardized user profiles can be used.

#### **4.3 Step 1 Identify subsystems which can be calibrated independently**

Depending on the standard available equipment sensors, subsystems can be calibrated independently.

In the example case, the heat pump (HP) control system is typically equipped with temperature sensors at the inlet and outlet of the evaporator and condenser loops, boiler temperature sensors, switches for floor heating, floor cooling, domestic water heating modes, and power consumption of the HP. A simple physical HP energy balance model is sufficient to describe the HP's dynamic response. A relative efficiency factor (compared to the data sheet) and a COP correction factor are calibrated based on the measured data. The floor heating power calculated from the measured data may suffer from discretization noise due to the low accuracy of the temperature sensors, but this effect averages out. The maximum difference in cumulative floor heating power at any time is less than 1%.

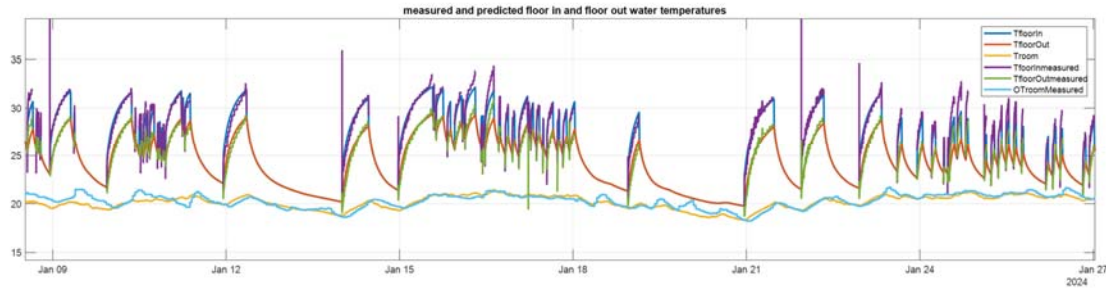


Figure 2: Model predicted floor input/output temperatures and measured temperatures.

The PV-system power output is accurately described as a function of the measured solar influx and needs no further calibration

#### 4.4 step 2 Identify special time series in which a subset of parameters can be discarded

We identify specific time periods during which some parameters can be excluded, thereby reducing the number of parameters to be identified. For instance, in the spring and autumn, there are extended intervals when the heating system is off, so the floor heating system has no impact. We also leverage the fact that different physical transfer mechanisms have distinct dynamics. For example, ventilation and solar radiation have a faster dynamical effect on space temperature than heat conduction. By selecting time periods when the effect of a particular transfer mechanism is greatest, these mechanisms can be calibrated independently. For instance, ventilation can be calibrated when there is a large difference between indoor and outdoor temperatures, preferably when there is no heating or cooling. Meanwhile, solar radiation can be calibrated more effectively during transitional seasons when there is less

difference between indoor and outdoor temperatures. The effect of solar influx through windows on room temperature heavily depends on internal and external shading. The dynamics of solar influx through windows differ significantly from those of thermal conduction or ventilation, which is correlated with wind speed.

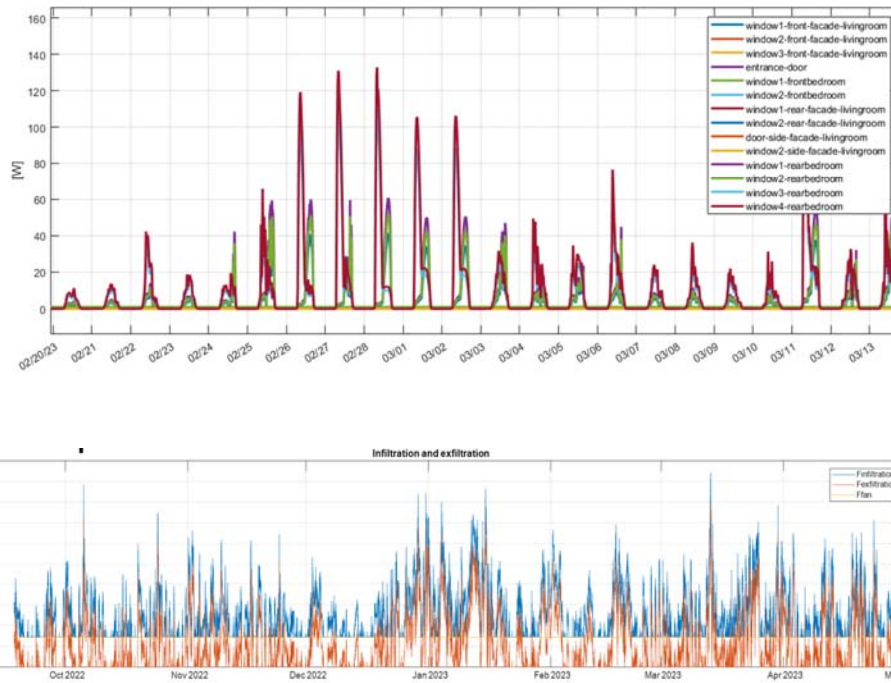


Figure 3: (top) simulated effect of solar radiation through each window and (bottom) simulated effect of infiltration and exfiltration

#### 4.5 step 3 Overall parameter estimation

After fixing parameters independently identified in the previous steps the parameters are not yet fixed are calibrated, using a non-linear output error minimization solver.

For the example case the result is shown below.

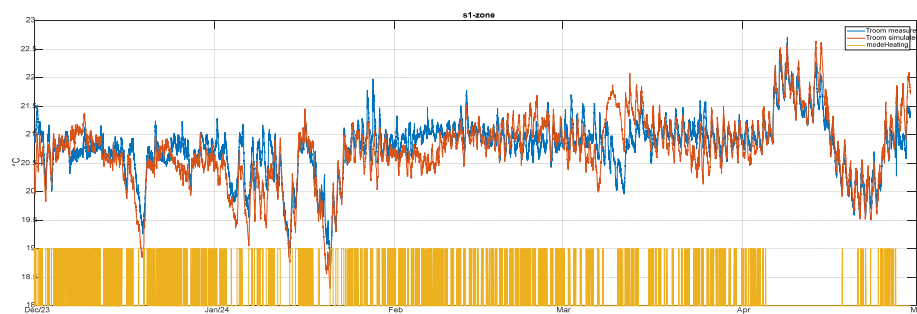


Figure 4: Measured and model predicted living room temperatures and floor heating mode

Although the dynamics is described sufficiently accurate over the total time series, there are periods with high mismatch that need further analysis. For example, in March sensor values of the heat pump mode and of solar influx were frozen for 5 days. In the parameter minimization problem such periods are neglected in calculation of the output error.

#### **4.6 Future directions for the advancement of the methods**

This method has been applied in various office buildings for monitoring and calibration in the Mooi Brains for Building project and in several apartments as part of the Horizon2020 Syn.ikia project for a model predictive controller. This controller has been successfully implemented in various apartments, doubling the self-utilization of solar power. Important future directions for development include making the method more robust against deviations in building, installation, and user behavior. This includes dealing with failed sensors, incorrect weather data, and neighboring apartments that are either very warm or hardly heated at all.

Another important direction is the development of automatic procedure for the calibration process to minimize the time required to configure the controller with an adequate prediction model for the MPC. For example, maintenance parties have suggested a configuration time of only several hours for a typical office building.

Main items in achieving fast calibration are automatic configuration of the heat and ventilation network from standard BIM/BEM formats and robust parameter estimation from BMS history datasets with medium or even low informative data quality.

## **5 CONCLUSIONS**

In the future, it will become increasingly important for buildings, including residential and commercial campuses, to align energy demand with the irregular availability of sustainable energy. At the same time, it is crucial to stay within the existing capacity of the energy grid to prevent congestion. Effective control is necessary to respond properly to signals from the Distribution System Operator (DSO) and the energy market. Currently, managing active components like climate installations and thermal buffers is often too time-consuming and costly, leading to the preference for battery solutions or controlling electric vehicle charging stations instead. Automatic methods for calibrating model-based controllers can significantly contribute to reducing the initialization time and costs of these controllers. The calibration methodology described here can provide a solution and has been useful, for example, in applying a controller in Syn.ikia to enhance the self-utilization of PV energy. In the coming period, various projects will focus on developing an automatic calibration method. It is also important that this method is robust against different deviations in user behaviour and failures in sensors and installations. Additionally, further work will be done on the hybrid building model, including an open-source model for evaluating renovation measures of residential properties, with calibration based on the energy usage of the building's initial configuration (Kornaat 2023).

## **6 ACKNOWLEDGEMENTS**

This project has received funding from the internal Applied AI program of TNO and the European Union's Horizon 2020 research and innovation program under grant agreement No 869918. Authors wishing to acknowledge the assistance and encouragement from the other team members contributing to the SirinE model: Behrouz Eslami Mossallam, Wim Kornaat, Andries van Wijhe, Olav Vijlbrief. A special thanks to Arjen Adriaanse, our science director,

and our management of supporting this development. The Brains for Buildings project received funding from the Dutch Ministry of Economic Affairs and Climate Policy and the Ministry of the Interior and Kingdom Relations under the MOOI program (MOOI32004).

## 7 REFERENCES

Ascione F, Bianco N, De Stasio C, Mauro G M and Vanoli G P 2016 Simulation-based model predictive control by the multi-objective optimization of building energy performance and thermal comfort *Energy and Buildings* **111** 131-144

Borsboom W, et al(2022), *A novel model based approach of an integrated ventilation and heating model for monitoring and control*, AIVC 2022

Borsboom W, et all. (2022) *Reducing peak load of renewable energy at district level with predictive twins* SBE, conference

Bunn D W and Muñoz J I 2016 Supporting the externality of intermittency in policies for renewable energy *Energy Policy* **88** 594-602

Canizares C 2014 Trends in microgrid control *IEEE Transactions on Smart Grid* **5** 1905-19

Deconinck A, Roels S 2017 Is stochastic grey-box modelling suited for physical properties estimation of building components from on-site measurements? *Journal of Building Physics* **40** 444-471

Bourdeau M 2019 Modeling and forecasting building energy consumption: A review of data-driven techniques *Sustainable Cities and Society* **48** 101533

EIA Annex 67 2019, Characterization of Energy Flexibility in Buildings, Energy in Buildings and Communities Programme Energy flexible buildings

Kornaat W et all. 2020 KIP2020-Energieprestatie en binnenmilieukwaliteit, WP2: Uitbreiding digital twin met eigen ventilatiemodel (AirMAPs), TNO internal report

Kornaat W et. All, 2023, Calculation of the effect of ventilation measures in existing dwellings to reduce the carbon footprint, 43rd AIVC conference.

Leguijt C et al. 2019 Rapportage systeemstudie energie-infrastructuur Noord-Holland 2020-2050 *CE Delft* 19.180084.084

Mocanu E, Mocanu D C, Nguyen P H, Liotta A, Webber M E, Gibescu M and Slootweg J G 2018 On-line building energy optimization using deep reinforcement learning, *IEEE transactions on smart grid* **10** 3698-3708

Mynhoff P A, Mocanu E and Gibescu M 2018 Statistical learning versus deep learning: performance comparison for building energy prediction methods *IEEE PES innovative smart grid technologies conference Europe (ISGT-Europe)* 1-6

Schirrer A, Brandstetter M, Leobner I, Hauer S and Kozek M 2016 Nonlinear model predictive control for a heating and cooling system of a low-energy office building *Energy and Buildings* **125** 86-98

# Perceptions of thermal comfort following deep energy retrofit in social homes in Ireland (HAVEN)

Victoria Hogan\*<sup>1</sup>, Daniel Norton<sup>2</sup>, Asit Kumar Mishra<sup>3</sup>, Nina Wemken<sup>2</sup>, Hilary Cowie<sup>4</sup>, and Marie Coggins<sup>2</sup>

*1 School of Health Sciences,  
University of Galway  
Galway, H91TK33, Ireland*

*\*victoria.hogan@universityofgalway.ie*

*2 School of Natural  
Sciences & Ryan Institute  
University of Galway  
Galway, H91TK33, Ireland*

*3 School of Public Health  
University College Cork  
College Road, Cork,  
Ireland*

*4 Institute of Occupational Medicine (IOM)  
Edinburgh EH14 4AP, UK*

## SUMMARY

Research suggests that energy retrofit measures can have a positive impact on temperature, relative humidity, and can reduce the occurrence of damp and mould (Wang et al., 2022, Fisk et al., 2020). Furthermore, energy renovation offers an opportunity to improve living conditions and the health of occupants of social housing by reducing exposure to indoor air pollution and by improving thermal comfort (Wang et al., 2022, Patino and Siegel, 2018). However, within the extant literature, studies examining occupant-reported thermal comfort post-retrofit are limited and findings vary. The Health Impact Assessment of Energy Renovations on Irish Domestic Dwellings (HAVEN), research project aimed to examine both objectively measured indoor thermal conditions (n=14) and the perceived thermal comfort pre and post retrofit in a sample (n=56) of Irish dwellings. In this paper, we outline the changes in energy usage, carbon emissions and perceived thermal comfort, temperature satisfaction and sources of thermal discomfort. This study demonstrates some of the potential co-benefits and challenges associated with energy efficient retrofit to indoor environmental quality.

## KEYWORDS

Thermal comfort, retrofit, questionnaire, indoor air quality

## 1. METHODOLOGY

The study employed a mixed methods approach, combining environmental monitoring of homes and a questionnaire survey. Recruitment for the study was facilitated by Local Authorities, approved housing bodies (AHBs) and private retrofit companies who aided in the identification of suitable homes and the distribution of study materials to potential participants. The inclusion criteria for the study were (1) homes due to receive a retrofit to a minimum of BER B2 standard (2) participants were aged over 18 years (3) informed consent was secured.

Ethical approval for this project was granted by the University of Galway Research Ethics Committee (Ref:2020.03.009).

### **1.1 Environmental Monitoring**

At the pre-retrofit stage, 38 out of 300 homes contacted, agreed to participate. In total, 14 homes participated in both the pre- and post-retrofit environmental monitoring. Within each home, temperature and relative humidity measurements were collected at five-minute intervals. For the majority of homes 40 - 50 hours of data was collected in the main living room and master bedroom, pre- and post-retrofit. Measurements of the thermal environment were collected using a Graywolf TG-502 or Graywolf IQ-610, using a Pt100 sensor (temperature accuracy/uncertainty of  $\pm 0.3^{\circ}\text{C}$ ) and a capacitive detector (RH, accuracy/uncertainty of  $\pm 2.0\%$ ), supplemented with measurements made using an ARANET4 Sensor (SHT3x-DIS CMOSens® Sensor Chip, resolution – temp.  $0.1^{\circ}\text{C}$ , RH 1%, accuracy-temperature,  $0.3^{\circ}\text{C}$  RH 3%).

### **1.2 Questionnaire Survey**

A quantitative, multivariate questionnaire survey was designed with reference to the extant literature. The questionnaire included measures of thermal comfort and temperature satisfaction, sources of thermal discomfort, perceived indoor air quality, odour perception and response, observance of mould and/or condensation and noise disturbance. The questionnaire was piloted and feedback was incorporated to improve the questionnaire. At the pre-retrofit stage, 112 out of the 700 homes contacted, agreed to participate in the survey. At the post-retrofit survey stage, 56 (50%) questionnaires were returned, of which 79% of the participating homes were from Local Authorities or AHBs. Pre/post comparisons of survey measures were conducted, employing Chi square, McNemar and Wilcoxon signed rank tests.

## **2. RESULTS & DISCUSSION**

All homes participating in the questionnaire survey had their legacy heating system replaced with a heating pump and most homes received an upgrade to their building envelope (better fenestration, insulation, etc.). The majority of the houses pre-retrofit had a BER C (51%) while post-retrofit most houses (98%) had a BER rating of B2 or higher. Post-retrofit, several improvements related to thermal comfort were observed. Specifically, participants reported improved thermal comfort ( $p < 0.01$ ) increased satisfaction with temperature ( $p < 0.01$ ), improved thermal sensation perceptions during hot/warm weather ( $p < 0.05$ ) and in cool/cold weather ( $p < 0.01$ ) and a reduction in sources of thermal discomfort such as draughts ( $p < 0.05$ ), temperature changes between rooms ( $p < 0.01$ ) and hot/cold surrounding surfaces ( $p < 0.05$ ) and significantly reduced levels of condensation ( $p < 0.01$ ). The median reduction in predicted energy use across the 56 dwellings was  $184 \text{ kWhm}^{-2}\text{yr}^{-1}$  (sd  $144 \text{ kWhm}^{-2}\text{yr}^{-1}$ ), corresponding to median change of 68% and the a median reduction of predicted carbon emissions of  $48 \text{ kg CO}_2 \text{ m}^{-2} \text{ yr}^{-1}$  (s.d.  $43 \text{ kg CO}_2 \text{ m}^{-2} \text{ yr}^{-1}$ ), or 76%. Around a quarter of the homes (26%) experienced mould and condensation issues post-retrofit.

In the homes where environmental monitoring was conducted, a slight decrease in room temperature was observed in both room types, post-retrofit. However, median air temperatures in the bedrooms and living rooms at both pre and post-retrofit were within EN16798 Category



I limits of between 21 and 25.5 °C. Median relative humidity values ranged from 52-62%, both pre- and post-retrofit. Most participants in the environmental monitoring component (85%) expressed satisfaction with the heating in their home post-retrofit, however a minority reported issues with draughts and blocking of air vents was observed during fieldwork (n=5).

### **3. CONCLUSIONS**

Use of questionnaire survey data in conjunction with objective measurement of temperature and humidity pre/post retrofit, offers a more nuanced overview of issues related to thermal comfort that cannot be assessed solely based on monitoring air temperature. This study contributes to the evidence base by demonstrating the additional benefits of energy retrofits to homeowners over and above those related to energy efficiency and also providing valuable insights into occupant concerns and sources of satisfaction.

### **4. ACKNOWLEDGEMENTS**

The Government of Ireland through the Sustainable Energy Authority of Ireland's Research, Development and Demonstration Funding Programme 2018 funds this project (RDD435).

### **5. REFERENCES**

- Fisk, W.J., Singer, B.C. & Chan, W.R. (2020). Association of residential energy retrofits with indoor environmental quality, comfort and health: A review of empirical data. *Building and Environment*, 180, 107067.
- Patino, E.S.L. & Siegal, J.A. (2018). Indoor environmental quality in social housing: A Literature review. *Building and Environment*, 131, 231-241.
- Wang, C., Wang, J. & Norback, D. (2022). A systematic review of associations between energy use, fuel poverty, energy efficiency improvements and health. *International Journal of Environmental Research and Public Health*, 19, 7393.

# Investigating the Impacts of New Energy Renovation Strategies on Indoor Environmental Quality

Buddila Wijeyesekera<sup>\*1</sup>, Miriam Byrne<sup>1</sup>, James O'Donnell<sup>2</sup>, Reihaneh Aghamolaei<sup>3</sup>, James A. McGrath<sup>4</sup>

*1. Physics Unit, School of Natural Sciences and the Ryan Institute's Centre for Climate and Air Pollution Studies, University of Galway, University Road, Galway, H91 CF50, Ireland.*

*\*Corresponding author:*

[W.Wijeyesekera1@universityofgalway.ie](mailto:W.Wijeyesekera1@universityofgalway.ie)

*2. School of Mechanical and Materials Engineering, University College Dublin Belfield Dublin 4 Ireland*

*3 School of Mechanical & Manufacturing Engineering, Dublin City University DCU Glasnevin Campus, Dublin 9, D09 V209 Ireland*

*4 Department of Physics Maynooth University Maynooth, Co. Kildare, Ireland*

## SUMMARY

There is a pressing need for large-scale energy retrofits in domestic dwellings to reduce carbon emissions. However, these retrofit strategies must be carefully balanced against the embodied carbon, operational energy, and indoor environmental quality in dwellings. This research aims to analyse the implications of indoor environmental quality arising from energy retrofit scenarios in the Irish context. Building physics simulations will determine a range of pre and post-energy retrofit scenarios and address the implications under various scenarios. The data collected will contribute to a larger project investigating the life cycle assessment of these building cohorts.

## KEYWORDS

Climate Change, Built Environment, Indoor environmental quality, economic, renovation strategy

## 1 INTRODUCTION

Climate change is a major concern that is being addressed across various sectors and geographies. The built environment sector consumes considerable energy and is responsible for a large share of total greenhouse gas emissions. As concerns grow towards sustaining the planet, it is imperative that greener and more sustainable strategies are adopted so as to minimise the impacts towards the environment and the human population. The aim of this research as a part of the ENABLE Project is to investigate the impacts that may be caused by new energy interventions on the indoor environmental quality of residential buildings. A life-cycle-based renovation approach is of the utmost importance as energy efficiency and renovation measures that only target the operation phase of buildings (e.g., heating, cooling and lighting) may lead to the selection of inappropriate and more carbon-emitting solutions, which may also impact the indoor environmental quality parameters. Inappropriate retrofit actions can incorrectly consider energy consumption, thermal discomfort, and IEQ in dwellings, highlighting the need for a deeper understanding and better strategies to address these multifaceted issues.

A previous study of 15 Irish dwellings reported that CO<sub>2</sub>, VOCs, and PM<sub>2.5</sub> concentrations significantly increased post-retrofit and were correlated with lower building air

exchange rates (Broderick et al., (2017)). These dwellings, constructed according to the 1990 Irish Building Regulations, featured a combination of cavity walls (built-in 2000) and hollow blocks (built in 1994). In another Irish study (Hassan et al., (2024)), a similar increase in PM<sub>2.5</sub> and formaldehyde concentrations was observed for deep energy-retrofitted dwellings that ranged in age from 15 to 60 years. Therefore, there is a need for an in-depth analysis of the broad range of factors influencing IEQ during energy retrofit and, in particular, in the context of ventilation.

This research aims to achieve a sturdy balance between improved energy efficiency and maintaining the appropriate levels of indoor environmental quality parameters within domestic dwellings as defined by the respective international and national level organisations. The existing literature indicates that there is no user-friendly decision support tool that can aid residential portfolio owners and policy in choosing the most appropriate renovation strategy complying with the indoor environmental quality parameter standards for different geographical scales and building types. An economical solution that will reduce energy consumption whilst maintaining the relevant indoor environmental quality parameters of a variety of Irish dwellings will be the overarching goal of this study.

## **2 METHODOLOGY**

A number of different types of Irish dwellings will be considered in this study and will analyse the impact of various energy retrofit interventions on indoor environmental quality. BIM-based archetype simulations will be carried out using CONTAM software to perform the indoor environmental quality (IEQ) analysis. The environmental parameters that will be considered will include temperature, relative humidity and the behaviour and distribution of air pollutants such as PM<sub>2.5</sub><sup>1</sup>, Radon, Formaldehyde, Total Volatile Compounds (TVOCs) and Carbon Monoxide. The simulations will be carried out for both pre and post-energy retrofits to ensure a comparison between the two scenarios for different building archetypes under different ventilation systems and a variety of emission profiles in relation to IEQ and will also consider the utilisation of renewable energy with different occupancy case scenarios. Comparisons will be made for different types of ventilation systems, including, but not limited to, natural, demand control and mechanical systems.

## **3 EXPECTED RESULTS**

The simulations' results will be validated against data collected from previous projects carried out by members of the same research collaborations. The simulations will include a variety of rooms with different dimensions, additional emissions and pollutant cases, various meteorological conditions, occupancy profiles, ventilation, and air-tightness characteristics. Changes in pollutant changes will be mapped against the outputs of Annex86 Subtask 1, and change in DALYs will be determined. Therefore, a sensitivity analysis will be performed to determine the impact of the aforesaid energy interventions and thereby identify any possible high-risk renovation strategies. This will ensure that the proposed renovation strategy will not adversely impact the human population.

## **4 CONCLUSION**

The outputs from the indoor environmental quality assessment will form part of wider a decision-support tool that will enable the relevant stakeholders to select the most appropriate renovation strategy without compromising the indoor environmental quality of domestic

---

<sup>1</sup> PM 2.5 – Refers to Fine particulate matter with particle diameter size less than or equal to 2.5 micrometres

dwellings. This will support long-term efforts to decarbonise residential buildings with the appropriate indoor environmental quality metrics.

## **5 ACKNOWLEDGEMENTS**

The ENABLE project (RD& 822) is funded by the Government of Ireland through the Sustainable Energy Authority of Ireland's 2022 Research, Development and Demonstration Funding Programme.

## **6 REFERENCES**

- Broderick, Á., et al., *A pre and post evaluation of indoor air quality, ventilation, and thermal comfort in retrofitted co-operative social housing*. Building and Environment, 2017. **122**: p. 126-133.
- Hassan, H., et al., *Deep energy renovations' impact on indoor air quality and thermal comfort of residential dwellings in Ireland – ARDEN project*. Building and Environment, 2024. **259**: p. 111637.

# Decarbonization Within the Path of Sustainable Development Goals

Constanza Molina<sup>1</sup>

*1 Escuela de Construcción Civil,  
Pontificia Universidad Católica de Chile  
Santiago, Chile*

*\*Corresponding author: cdmolina@uc.cl*

## ABSTRACT

Building ventilation and retrofitting strategies for homes can bring multiple benefits in the context of achieving Sustainable Development Goals (SDGs) by reducing carbon emissions in the building sector. However, current SDG approaches are fragmented, narrowly focusing on specific areas related to each goal, which now requires an integrated approach. Analyzing the relationships discovered in the literature, we can visually map these connections to understand the complexity of interactions and the diverse positive and negative effects of retrofitting strategies, ventilation standards, and the broader sustainability agenda. This mapping allows us to identify how our discipline and efforts can positively, negatively, or neutrally affect the achievement of SDGs.

## KEYWORDS

Energy retrofit, ventilation, residential buildings

## 1 INTRODUCTION

In this presentation, we will explore the effects of thermal retrofitting of homes on the Sustainable Development Goals (SDGs). Thermal retrofitting is a key strategy for reducing carbon emissions in the residential sector, aligning with the broader goals of sustainability and human well-being. The information was gathered by a systematic review, focusing on identifying both positive and negative impacts of thermal retrofitting on various SDGs.

## 2. RESULTS AND DISCUSSION

The studies reviewed indicate that thermal retrofitting significantly reduces energy demand and greenhouse gas emissions through improved insulation and energy efficiency measures, which, in turn, lead to lower energy consumption, contributing directly to SDG 7 (Affordable and Clean Energy) and SDG 13 (Climate Action). This reduction in energy demand also positively impacts SDG 11 (Sustainable Cities and Communities) by lowering urban energy consumption and emissions. The economic benefits of retrofitting homes are substantial, as it reduces basic utility costs, particularly benefiting low-income households and addressing SDG 1 (No Poverty) and SDG 10 (Reduced Inequality). Lower energy bills reduce energy poverty and provide economic relief to vulnerable populations. Additionally, the economic benefits extend to job creation and business opportunities in the construction and energy sectors, promoting SDG 8 (Decent Work and Economic Growth).

Improved indoor environmental quality (IEQ) is another significant benefit of thermal retrofitting. Enhanced thermal comfort, better air quality, and reduced dampness and mold improve health outcomes, aligning with SDG 3 (Good Health and Well-being). However, there are potential negative effects, such as the risk of poor indoor air quality if ventilation is not adequately addressed. Some studies highlighted issues like over-tightening of buildings and inadequate ventilation, which can cause health problems related to indoor air pollutants, negatively impacting SDG 3. Retrofitting may also enhance the aesthetic value of

neighborhoods, contributing to community pride and social cohesion (SDG 11). It can reduce social tensions and promote social equity by improving living conditions across different socio-economic groups. Reducing environmental noise through better insulation also contributes to improved community well-being.

Environmentally, there is a clear reduction in waste production due to a less frequent need for building maintenance and repairs, positively affecting SDG 12 (Responsible Consumption and Production). The lifecycle extension of buildings through retrofitting reduces the need for new construction, conserving natural resources and reducing environmental impact. The review identifies a crucial challenge in implementing effective ventilation systems to avoid negative health impacts. Integrated strategies that combine thermal retrofitting with proper ventilation are essential to maximize benefits and minimize risks.

### **3. CONCLUSIONS**

Thermal retrofitting underlines the multifaceted benefits in achieving SDGs, emphasizing the need for an integrated approach that considers energy efficiency, ventilation standards, and broader sustainability goals. It provides a comprehensive understanding of the positive, negative, and neutral influences of thermal retrofitting on SDGs, advocating for strategic planning and implementation to maximize overall benefits and contribute to a sustainable and resilient built environment.

The search highlights a gap in quantitative analysis of the impacts, suggesting that future research should focus on the magnitude of effects to better inform policy and decision-making. Future studies should then focus on quantifying the impacts of thermal retrofitting to provide more data for policymakers. Additionally, exploring the long-term effects of retrofitting on health, social equity, and environmental sustainability will be needed to develop holistic and effective sustainable development strategies.

# Retrofitting and Ventilation: Challenges, Benefits and Lessons Learnt

James A. McGrath<sup>1</sup>

*1 Department of Physics  
Maynooth University  
County Kildare, Ireland*

*\*Corresponding author: james.mcgrath@mu.ie*

## ABSTRACT

A significant challenge lies in decarbonising existing residential stock to meet higher energy performance standards, necessitating increased energy retrofit activity. Despite the importance of energy retrofits, challenges arise in maintaining indoor environmental quality. While positive air quality and health benefits have been reported through targeted energy-retrofit activities, there are also numerous cases where indoor pollutant concentrations increase post-retrofit. Ventilation is often directly or indirectly impacted by changes in airtightness and/or ventilation systems, and the introduction of new building materials/products. Addressing these challenges ensures energy retrofits contribute to reduced environmental impact while maintaining a healthy indoor environment. Highlighting several examples of case studies is anticipated to promote discussion on informing priorities regarding retrofit strategies.

## KEYWORDS

Energy retrofit, radon, ventilation, IEQ

## 1 INTRODUCTION

The 2021 Glasgow Agreement highlighted the urgent need for global carbon emission reductions to avert a climate catastrophe. In response, various countries have established climate-neutral greenhouse gas emission targets for 2030 and 2050, including the European Climate Directive (Regulation 2021/1119/EU).

In Europe, buildings are reported as the single largest energy consumer sector, accounting for 40% of energy consumption and 36% of CO<sub>2</sub> emissions. A major challenge is decarbonising the existing residential stock by meeting higher energy performance standards and increasing renovation activity. The issue is further complicated due to the consequences of the renovation process on the health and well-being of residents, such as thermal comfort and indoor environmental quality (IEQ). The EU Energy Performance of Buildings Directive (EPBD) (Directive (EU) 2018/844) also states that "Measures to further improve the energy performance of buildings should take into account climatic and local conditions as well as indoor climate environment and cost-effectiveness".

Changes in a building's airtightness due to energy retrofit strategies can adversely impact IEQ. Ventilation is a critical aspect that affects IEQ and thermal comfort in buildings. However, while improving thermal efficiency reduces energy consumption, indoor environmental quality may become compromised if adequate ventilation is not maintained. Several studies have reported the challenges associated with increased pollutant concentrations following energy retrofits (Underhill et al., 2020, Földvary et al., 2017). For example, Du et al. (2019) investigated 37 Finish buildings in Finland and 15 Lithuanian buildings that underwent energy retrofits and observed a significant increase in BTEX concentrations post-energy retrofit. A study of 15 Irish dwellings reported that CO<sub>2</sub>, VOCs, and PM<sub>2.5</sub> concentrations significantly increased post-retrofit and were correlated with lower building air exchange rates (Broderick et al., 2017), underperforming ventilation, and new building materials played a role in the increased pollution concentrations.

In addition to indoor-generated air pollutants, radon poses unique challenges in certain countries due to its geogenic radon potential. One French study reported that thermally retrofitted homes had a median radon concentration of 180 Bq/m<sup>3</sup> compared to 114 Bq/m<sup>3</sup> in non-retrofitted dwellings (Collignan et al., 2016). Computer simulations reported that radon concentrations could increase up to 107% in Irish dwellings post-renovation based on modest changes to the building's airtightness. While it was acknowledged that ventilation strategies could address increases in radon concentrations (McGrath et al., 2021).

Similarly, Tieskens et al. (2021) simulated the impact on indoor air quality resulting from energy renovations in multi-family housing complexes in Boston. They reported that incorporating increased ventilation into the renovation strategy offers opportunities to provide cost-effective interventions to address health disparities.

## 2 CONCLUSION

Despite the importance of energy retrofits, maintaining indoor environmental quality presents challenges. While targeted energy-retrofit activities have reported positive IEQ and health benefits, numerous cases show increased indoor pollutant concentrations post-retrofit. The scale of retrofit projects varies due to national considerations, building types, occupants' needs, and local conditions. Addressing these challenges is crucial to ensure that energy retrofits reduce environmental impact while maintaining a healthy indoor environment. The presentation will summarise case studies from the literature on the challenges, benefits, and lessons learnt from retrofitting and ventilation. Highlighting several case studies will promote discussion and inform priorities regarding effective retrofit strategies.

## 3 REFERENCES

- BRODERICK, Á., BYRNE, M., ARMSTRONG, S., SHEAHAN, J. & COGGINS, A. M. 2017. A pre and post evaluation of indoor air quality, ventilation, and thermal comfort in retrofitted co-operative social housing. *Building and Environment*, 122, 126-133.
- COLLIGNAN, B., LE PONNER, E. & MANDIN, C. 2016. Relationships between indoor radon concentrations, thermal retrofit and dwelling characteristics. *Journal of environmental radioactivity*, 165, 124-130.
- DU, L., LEIVO, V., PRASAUSKAS, T., TÄUBEL, M., MARTUZEVICIUS, D., & HAVERINEN-SHAUGHNESSY, U. 2019. Effects of energy retrofits on Indoor Air Quality in multifamily buildings. *Indoor Air*, 29(4), 686-697.
- FÖLDVÁRY, V., BEKÖ, G., LANGER, S., ARRHENIUS, K. & PETRÁŠ, D. 2017. Effect of energy renovation on indoor air quality in multifamily residential buildings in Slovakia. *Building and Environment*, 122, 363-372.
- MCGRATH, J. A., AGHAMOLAEI, R., O'DONNELL, J. & BYRNE, M. A. 2021. Factors influencing radon concentration during energy retrofitting in domestic buildings: A computational evaluation. *Building and Environment*, 194, 107712.
- TIESKENS, K. F., MILANDO, C. W., UNDERHILL, L. J., VERMEER, K., LEVY, J. I. & FABIAN, M. P. 2021. The impact of energy retrofits on pediatric asthma exacerbation in a Boston multi-family housing complex: a systems science approach. *Environmental Health*, 20, 1-9.
- UNDERHILL, L. J., MILANDO, C. W., LEVY, J. I., DOLS, W. S., LEE, S. K. & FABIAN, M. P. 2020. Simulation of indoor and outdoor air quality and health impacts following installation of energy-efficient retrofits in a multifamily housing unit. *Building and Environment*, 170, 106507.



# Impact of dust build-up on building airtightness durability: preliminary results of the Durabilitair2 project

Andrés Litvak<sup>\*1</sup>, Eddy Handschoewercker<sup>1</sup>  
Sylvain Berthault<sup>2</sup> and Romain Mathieu<sup>3</sup>

*1 Cerema - Cerema Sud-Ouest, Sustainable Building Group, F-33160 Saint-Médard-en-Jalles, France*

*2 Cerema - Cerema Centre-Est Boulevard Giberstein BP 141 F-71405, Autun, France*

*\*Corresponding author: andres.litvak@cerema.fr*

*3 IUT Bordeaux – BUT Mesures Physiques 15, rue Naudet 33175 Gradignan Cedex France*

## CONTEXT:

The DURABILITAIR project, conducted from 2016 to 2019, aimed to assess the durability of air sealing products used in building envelopes. Key findings were presented at the AIVC conferences in 2017 (Nottingham, UK) and 2019 (Ghent, Belgium). This research enhanced understanding of the in-situ characterization of air tightness evolution in homes over time and contributed to developing accelerated aging test protocols under controlled laboratory conditions.

Built on the previous project, DURABILITAIR2 seeks to deepen knowledge of air tightness evolution, particularly focusing on the implementation and early use of air sealing in newly built single-family homes. This project addresses the French Ministry of Construction's request to further investigate the energy performance of buildings over time.

## OBJECTIVES AND PROTOCOL:

The DURABILITAIR2 research and development project has the following major objectives:

- To identify factors that degrade the air tightness of building envelopes during the first year of occupancy.
- To provide concrete recommendations to mitigate or eliminate these factors, especially those related to the implementation conditions of air sealing products.
- To quantify the impact of poor implementation conditions on the durability of airtightness.

Various bibliographic and metrological studies are currently being conducted both on-site and in laboratories in order to:

- 1) characterize the factors degrading airtightness within the first year of occupancy through a field measurement campaign on construction sites of individual houses
- 2) establish a protocol for accelerated aging of air sealing product assemblies under controlled laboratory conditions in an environmental chamber.

International standards require surfaces to be clean, stable, dry, and free of grease and dust to guarantee optimal performance. It appears to us that no company is ready to guarantee the adhesion of its products on dusty surfaces. In fact, we have identified as the limit of guaranteed adhesion the criteria of temperature, humidity and dust. This study investigates the physical-chemical cleanliness, specifically dust, which may impair adhesion surfaces and degrade the performance of air sealing over time. Hence, this article focuses on assessing the feasibility of an experimental method to quantify dust contamination on surfaces where air sealing products are applied.

Different methods of dust quantification have been examined, among them:

- Light Diffraction: Using laser granulometry to measure particles on a transparent surface.
- Visual Contrast: Assessing dust on a standardized color surface, as per NF X 50-792.
- Weight Measurement: Measuring dust mass collected between adhesive tapes, the method chosen for this study.

We defined an operational procedure for on-site sampling based on weight measurement but also visually using an evaluation grid. Dust samples were collected using adhesive tapes before air sealing application, at the dustiest stages of construction. Samples were weighed using a high-precision balance to quantify dust from various construction sites.

## RESULTS AND INTERPRETATION:

Seventeen dust samples from different sites were weighed. The weight difference between dusted and reference samples was used to calculate dust mass. Uncertainty calculations confirmed the reliability of the measurements.

Differences were observed between floor and vertical surface samples. Floor samples had significantly higher dust masses, while uncertainties in vertical surface samples often exceeded the measured values, indicating insufficient dust quantity for significant evaluation.

## CONCLUSION AND FUTURE PERSPECTIVES:

The weight measurement method appears to be suitable for quantifying floor dust but less effective for vertical surfaces due to higher uncertainties. To improve reliability, increasing the adhesive tape area or reducing sample size might help. Consideration of various uncertainties, such as adhesive characteristics and environmental factors, appears to be essential.

In summary, while the weighing method effectively quantifies floor dust, further refinement and exploration of alternative methods are necessary to improve the overall reliability of dust quantification in construction sites. Such a method may help to better understand the mechanism of degradation of airtightness performance over time due to dusty surfaces.

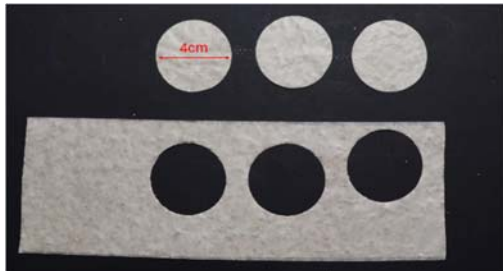


Figure 1: Preparation of samples taken on site

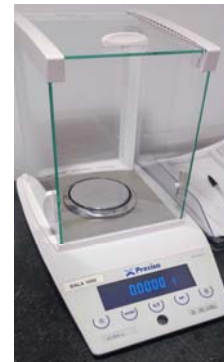


Figure 2: Balance Precisa BALA1055

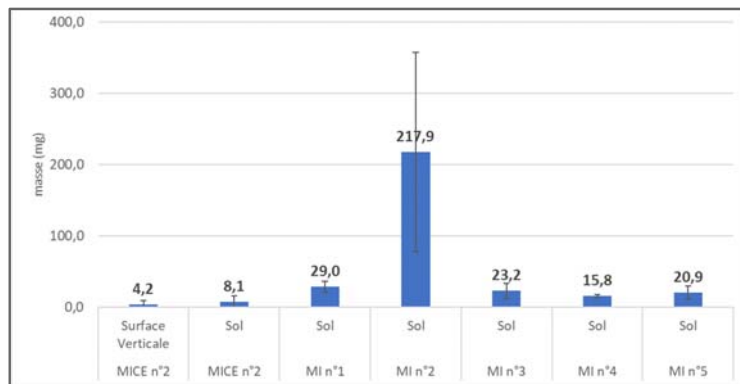


Figure 3: Average mass and associated uncertainties of samples per site

# On the potential of HAMSTER's bi-climatic chamber for testing building component airtightness durability

Martin Prignon\*<sup>1</sup>

*1 Buildwise  
Kleine Kloosterstraat, 23  
1932 Zaventem, Belgium*

\*Corresponding author: [martin.prignon@buildwise.be](mailto:martin.prignon@buildwise.be)

## SUMMARY

Durability of airtightness – and more generally of thermal performances – is an important question at both building and component levels. Its assessment is complicated in practice mainly due to the logistical aspects of those long duration studies and experiments. One can conduct laboratory tests with artificial ageing or deduce information from repeated in-situ tests or data analysis of existing components. In this paper, we describe two projects relevant in this context. On one hand, HAMSTER is a new bi-climatic chamber installed in 2022 in Brussels. It has great potential to assess the airtightness of building components in various conditions including, but not limited to, its durability. Two main applications are identified: (1) measuring airtightness performances in specific climatic conditions and (2) assessing the durability of building components through accelerated ageing. On the other hand, PERCHE is a research project where airtightness of existing old wood windows with heritage value is assessed through in-situ measurements using the direct technique. Additionally, the potential of improvement of different interventions is also quantified in that research.

## KEYWORDS

Bi-climatic chamber; HAMSTER; airtightness durability of building components; old wood windows; PERCHE

## 1 LABORATORY TESTING

### 1.1 HAMSTER testing facility

HAMSTER is a new hot box – cold box testing facility installed in 2022 in Brussels, Belgium. This equipment is used to conduct HAM-test of 3 m x 3 m walls, or flat or inclined roofs. The equipment is made of two climatic chambers: a cold box to reproduce exterior climate and a hot box to simulate interior conditions. It also includes numerous features to reproduce rain, pressure difference or infrared radiations. The accessible ranges of temperatures and relative humidities in both chambers are shown in Figure 1. Using this bi-climatic chamber in the context of building component airtightness is interesting in two specific contexts: (1) testing a component performance in specific climatic conditions; and (3) testing a component after an accelerated ageing process.

Although the assessment of airtightness performance is generally conducted in standardized and reproducible conditions, the elements responsible for airtightness are not performing equally under any conditions. For example, (Fleury and Thomas, 1972) and (Konstantinov and Verkhovsky, 2020) studied the air permeability of windows under different temperature conditions, and (Kysela et al., 2023) use a bi-climatic chamber to investigate the impact of seasonal variation changes on the airtightness performance of joint in timber-frame structures. Note that contrary to the traditional climatic chambers, bi-climatic chambers allow to control the climatic conditions on both sides of the tested element. This can be useful for testing elements of the building envelope, subjected to difference of temperature and relative humidity rather than homogeneous climatic conditions.

In real conditions, building components are subjected to different climate exposures during their lifetime, which creates some deterioration and affects their characteristics, including airtightness. However, studying these characteristics in real conditions (i.e., natural ageing) is often too long. Artificial ageing is then used to reproduce the impact of natural ageing

in laboratory conditions in shorter duration. In the literature, different methods are used for artificial ageing, the most common being (NORDTEST, 2000). However, the method should always be designed to meet the specific objective of the study, which explain why many different methods exists. As far as possible, the component should not be exposed to climatic stresses to which it is not exposed during natural ageing, in order to avoid any unrealistic chemical or physical reactions. However, extreme conditions allow to increase the acceleration factor, i.e., the ratio between durations of natural ageing and artificial ageing. Table 1 provides a series of studies assessing the durability of components' airtightness through accelerated ageing, the type of cycles done and the potential of reproducibility with HAMSTER.

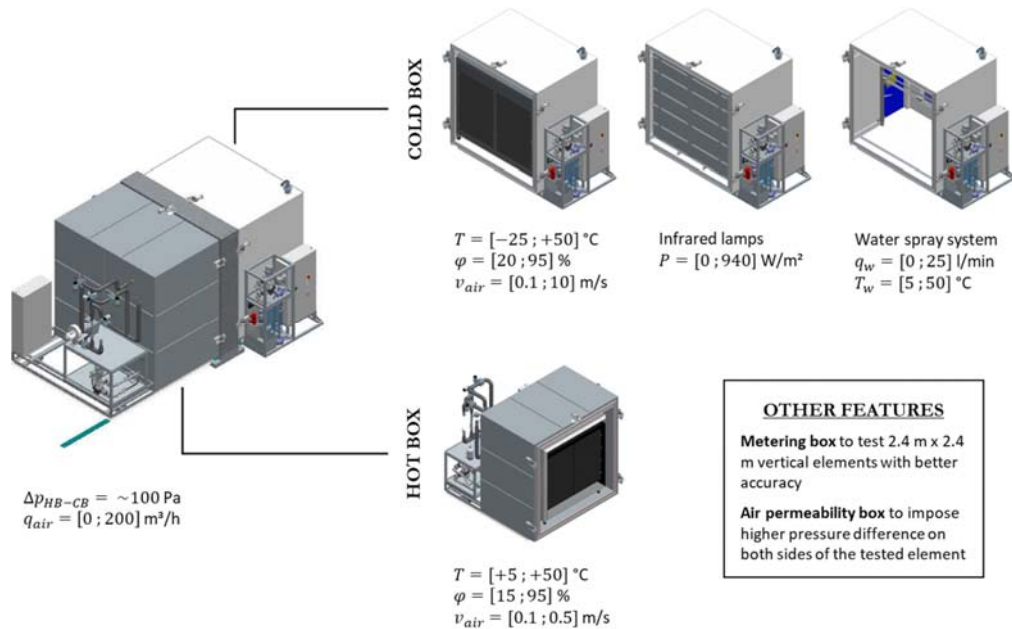


Figure 1. Features for HAMSTER equipment.

Table 1: studies assessing the durability of components' airtightness through accelerated ageing

Reference	Tested components	Type of cycles	Reproducible with HAMSTER?
(Van Linden and Van Den Bossche, 2020)	Different sealing materials for building joints	Wetting and drying; Mechanical ageing; Mechanical deformation;	Yes Yes Yes
(Gullbrekken et al., 2019)	Clamped joints in the vapour barrier	Wetting and drying	No (70°C)
(Langmans et al., 2015)	Taped joints for exterior air barrier	Thermal loads; hygrothermal loads; UV and vapour loads	No (70°C) No (70°C) No (UV and 60°C)
(Litvak et al., 2019)	Window-wall interface	Thermal creep; Weathering; Wind exposure; Break test	No (60°C) Yes Yes No (180°C)
(Michaux et al., 2014)	Walls where airtightness is ensured by coatings, wood panels, membrane, and industrialized systems	Wind and storm; Moisture; temperature	Yes Yes No (70°C)

## 2 IN-SITU MEASUREMENTS

Another way of looking at the durability of building components' airtightness is by empirical observations of in-situ testing conducted on existing elements. In this context, the project PERCHE aims to measure airtightness of existing wood windows having a heritage value, and to quantify the impact of typical solutions implemented to improve their airtightness without replacing them. Measurements are done using the direct method as described in (Prignon, 2020) on different relevant typologies for Brussels' Region.

## 3 ACKNOWLEDGEMENTS

This paper was written and is presented in the context of the PERCHE project, funded by INNOVIRIS (Grant n° 2022-JRDIC-9a).

## 4 REFERENCES

- Fleury, G., Thomas, M., 1972. Variation de la perméabilité à l'air des fenêtres en fonction de la température extérieure. Dispositif de mesure et exemples d'application. (No. 132), Cahier CSTB.
- Gullbrekken, L., Gradeci, K., Norvik, Ø., Rütther, P., Geving, S., 2019. Durability of traditional clamped joints in the vapour barrier layer: experimental and numerical analysis. *Can. J. Civ. Eng.* 46, 996–1000. <https://doi.org/10.1139/cjce-2018-0593>
- Konstantinov, A., Verkhovsky, A., 2020. Assessment of the negative temperatures influence on the PVC windows air permeability. *IOP Conference Series: Materials Science and Engineering* 753, 022092. <https://dx.doi.org/10.1088/1757-899X/753/2/022092>
- Kysela, P., Ponechal, R., Micháľková, D., 2023. Airtightness of a Critical Joint in a Timber-Based Building Affected by the Seasonal Climate Change. *Buildings* 13. <https://doi.org/10.3390/buildings13030698>
- Langmans, J., Desta, T., Alderweireldt, L., Roels, S., 2015. Laboratory investigation on the durability of taped joints in exterior air barrier applications. Presented at the 36th AIVC Conference "Effective ventilation in high performance buildings," Madrid, Spain.
- Litvak, A., Allègre, F., Moujalled, B., Leprince, V., 2019. Assessment of the durability of airtightness products in laboratory controlled conditions: development and presentation of the experimental protocol. Presented at the 40th AIVC-8th TightVent & 6th venticool Conference-From energy crisis to sustainable indoor climate.
- Michaux, B., Mees, C., Nguyen, E., Loncour, X., 2014. Assessment of the durability of the airtightness of building elements via laboratory tests. Presented at the 35th AIVC Conference "Ventilation and airtightness in transforming the building stock to high performance", Poznań, Poland, pp. 738–746.
- NORDTEST, 2000. Building materials and components in the vertical position: Exposure to accelerated climatic strains. (No. NT BUILD 495). Finland.
- Prignon, M., 2020. Airtightness of building components (Dissertation). UCLouvain, Belgium.
- Van Linden, S., Van Den Bossche, N., 2020. Airtightness of sealed building joints: Comparison of performance before and after artificial ageing. *Building and Environment* 180, 107010. <https://doi.org/10.1016/j.buildenv.2020.107010>

# Research on airtightness durability in Norway

Tore Kolstad Linløkken<sup>1</sup> and Bozena Dorota Hrynyszyn\*<sup>1</sup>

<sup>1</sup>Department of Civil and Environmental Engineering, NTNU, NO-7491 Trondheim, Norway

\*Corresponding author: [bozena.d.hrynyszyn@ntnu.no](mailto:bozena.d.hrynyszyn@ntnu.no)

## SUMMARY

Achieving adequate airtightness of a building envelope is crucial for preventing moisture-related damages in cold and humid climate zones, such as in Norway. Leaky joints and perforations in air and vapor barriers are often critical points where damaging air leakages arise. Thus, the durability of products, such as adhesive tapes, is crucial to ensure a proper airtightness and performance of critical building details and overall constructions. Having in mind that deterioration of airtightness due to failure of the adhesive systems leads usually to increased heat losses and in turn an increased heat demand, the energy efficiency can be significantly weakened as well. The TightEN competence project carried out in the years 2019-2022 and led by one of Europe's largest research institutes, SINTEF, in cooperation with industry and university partners, among others the Norwegian University of Science and Technology (NTNU) in Trondheim, aimed to highlight and strengthen the research on adhesive tapes and develop test methods adequate in the cold climate conditions to ensure a proper durability of sealing solutions over time so that energy efficiency is maintained throughout buildings' lifetime.

## KEYWORDS

Airtightness durability, Building envelope, Experimental test method, Durability of joints, Adhesive tapes.

## 1 INTRODUCTION

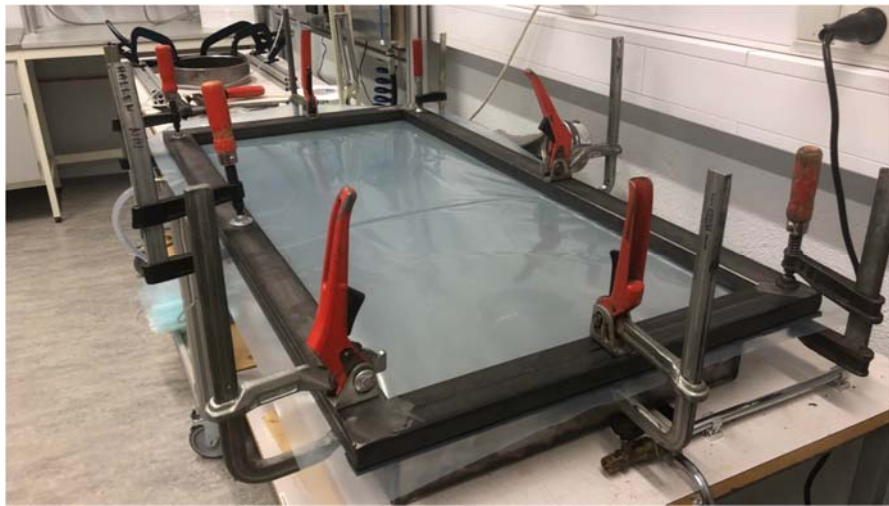
In recent years, adhesive tapes have gained popularity as a mean of air-sealing joints and perforations in the building envelope. Early on, these tapes had a reputation for having poor adhesive properties and durability. More recently, along with further product development, adhesive tapes have been recognized for their ability to provide adequate air tightness [1]. The use of tape also allows for innovative solutions, along with a simple and quick application, making it a highly convenient option for air-sealing details.

However, as adhesive tapes represent a relatively recent way of air-sealing buildings, there are concerns and uncertainty regarding the long-term durability of the products and solutions. Current evaluation methods used in the certification of products and systems are primarily based on assessing the mechanical and adhesive properties of products, rather than addressing the airtightness directly.

## 2 METHOD

In connection to the TightEN competence project, sub-projects were established in cooperation with MSc-students at NTNU to contribute to the development of a new test method to be used for certification and application of adhesive tapes in building skins regarding the Norwegian technical requirements, TEK17 [2]. Based on relevant theoretical background and including

knowledge and experience from established methods for evaluation of tape joints durability, currently being used [3-9], a new testing methodology addressing local, Norwegian, conditions was proposed to evaluate tape products and systems for air-sealing application in buildings with sufficient accuracy, reproducibility, and repeatability regarding their performance in the long-term. The new test method proposed, based on air permeability measurements using a Test Stand (see Figure) made from welded-together steel plates, was further developed, and presented in the MSc thesis, *Development of a Test Method for Evaluating Durability of Adhesive Tapes in Construction*, from 2023 by Tore Kolstad Linløkken [10]. The durability of products is assessed by measuring and comparing permeability rates before and after artificial ageing. The aptness of the method is assessed through a measurement program involving six different material samples, each made by combining an adhesive tape with a substrate material. Two substrate materials were involved, a vapor barrier and a roofing membrane, along with three different adhesive tapes. Parallely to the air permeability tests, the material samples were tested for peel resistance according to the Norwegian standard NS-EN 12316-2:2013, before and after the same artificial ageing procedures to examine how the two methods compare with regard to durability assessment.



**Figure:** Test Stand leakage evaluation setup.

### 3 RESULTS

The artificial ageing procedures led to significant degradation of air permeability across all material samples. Changes in peel resistance were comparatively small, and three out of six material samples even exhibited increased peel resistance after ageing. Fluctuating system leakage contributed to uncertainty in the permeability measurements and made it difficult to determine what share of air leakage could be attributed to the tape joints themselves. Additionally, as permeability rates seemingly depended on the implementation quality of individual specimens, the method in its current form is not perceived as reliable enough to precisely determine the airtightness inherent to distinctive tape products. However, the method is considered applicable for verifying that permeability rates remain below relevant threshold values after ageing.

The system leakage constitutes a systematic uncertainty when evaluating the air permeability of the test samples. A series of tests have thus been performed in an effort to evaluate the magnitude and variations of the system leakages. Results from these tests are used to assess whether the system leakages vary along with the installation technique, and in turn how the system leakage can be minimized. The Test Stand is considered highly configurable, as it allows

for the specimen layout to be altered, for instance by utilizing solid boards as substrates and including additional components, such as adhesive pipe collars. This versatility makes it possible to perform permeability tests on the same standard substrates already used in the Technical Approval of air and vapor barrier tapes. Furthermore, specimens can be inverted, enabling exposure to both positive and negative pressure differences. The permeability of a specimen as a whole expressed as leakage per unit area, can then be used for comparison against predefined threshold values. In terms of durability evaluation criteria, it is considered more suitable to establish absolute threshold values for permeability before and after ageing, in contrast to current guidelines for peel and shear resistance evaluation, in which durability is evaluated based on the relative change in material properties after artificial ageing.

## 4 CONCLUSIONS

Although the method in development displays limitations in its current form, it is regarded as a promising concept. Through further development, the method is believed to be suitable for potential integration into wider evaluation programs addressing adhesive tape durability, supplementary to existing methods such as defined in NS-EN 12316-2:2013 [11].

## 5 ACKNOWLEDGEMENTS

The Research Council of Norway financially supported this research. The authors would like to thank our colleagues from SINTEF, within the research project TightEN (project no. 102020444-2), who provided expertise that assisted the research.

## 6 REFERENCES

- [1] Skogstad, H. B., Kvalvik, M. and Jelle, B. P. (2010), 'Bruk tape med varig heft', <https://www.sintef.no/globalassets/upload/artikkel-10-byggaktuelt.pdf>.
- [2] Direktoratet for Byggkvalitet (2017), 'Byggteknisk forskrift TEK17', <https://dibk.no/regelverk/byggteknisk-forskrift-tek17/>.
- [3] Fufa, S. M. et al. (2017), 'Durability evaluation of adhesive tapes for building applications', *Construction and Building Materials* .
- [4] Møller, E. and Rasmussen, T. (2020), 'Testing Joints of Air and Vapour Barriers, Do We Use Relevant Testing Methods?'
- [5] NORDTEST (2000), 'NT BUILD 495: Building materials and components in the vertical positions: Exposure to accelerated climatic strains'.
- [6] Sletnes, M. and Frank, S. (2020), 'Performance and durability of adhesive tapes for building applications. from product documentation to scientific knowledge (and back again)', XV International Conference on Durability of Building Materials and Components .
- [7] Van den Bossche, N. et al. (2012), 'Airtightness of the window–wall interface in cavity brick walls', *Energy and Buildings* .
- [8] Van Linden, S. and Van den Bossche, N. (2017), 'Airtightness of sealed building joints: Comparison of performance before and after artificial ageing', *Building and Environment*.
- [9] Ylmén, P., Hansén, M. and Romild, J. (2012), 'Beständighet hos lufttäthetslösningar'.
- [10] Linløkken T.K., Development of a Test Method for Evaluating Durability of Adhesive Tapes in Construction, NTNU Open, 2023. [NTNU Open: Development of a Test Method for Evaluating Durability of Adhesive Tapes in Construction](#)
- [11] Standard Norge (2013c), 'NS-EN 12316-2 Flexible sheets for waterproofing Determination of peel resistance of joints Part 2: Plastic and rubber sheets for roof waterproofing'.



# The Recast Energy Performance of Buildings Directive: a green light for clean air?

Ciarán CUFFE

*Green Party  
16/17 Suffolk Street, D02 AT85  
Dublin2, Ireland  
ciarancuffeoffice@gmail.com*

## SUMMARY

Ciarán Cuffe served as a member of the European Parliament from 2019 -2024. He was the European Parliament's Rapporteur on the Recast Energy Performance of Buildings Directive. He is a qualified architect and planner. He will discuss the political and economic challenges of renovating our building stock, as well as the opportunity that the Recast Energy Performance of Buildings Directive offers to building owners and occupiers as well as to industry.

## KEYWORDS

#RenovationWave, #Decarbonisation, #EuropeanGreenDeal, #EnergyEfficiencyFirst

## 1 REFERENCES

European Commission, (2019) *The European Green Deal* Retrieved from [https://commission.europa.eu/strategy-and-policy/priorities-2019-2024/european-green-deal\\_en](https://commission.europa.eu/strategy-and-policy/priorities-2019-2024/european-green-deal_en)

European Commission (2020) Maximising the energy efficiency potential of the EU building stock Report. Retrieved from [https://www.europarl.europa.eu/doceo/document/TA-9-2020-0227\\_EN.html](https://www.europarl.europa.eu/doceo/document/TA-9-2020-0227_EN.html)

European Commission, (2024) Recast Energy Performance of Buildings Directive Retrieved from [https://energy.ec.europa.eu/topics/energy-efficiency/energy-efficient-buildings/energy-performance-buildings-directive\\_en](https://energy.ec.europa.eu/topics/energy-efficiency/energy-efficient-buildings/energy-performance-buildings-directive_en)

# What do we know about the current state of indoor air in buildings and associated human health effects?

Corinne Mandin

*Institute for Radiation Protection and Nuclear Safety (IRSN)  
31, avenue de la Division Leclerc  
92260, Fontenay-aux-Roses, France*

## SUMMARY

This keynote aims to review the state of knowledge on indoor air quality in our main living spaces, including homes, daycare centers, schools, and offices, emphasizing the differences according to building types and occupancy. The health effects associated with exposure to various indoor pollutants will be examined. Recent evolutions and future trends will be presented.

## KEYWORDS

Indoor air quality; IAQ; human exposure; health effects

## 1 INDOOR AIR QUALITY IN VARIOUS BUILDINGS

Dwellings are the buildings with the greatest heterogeneity of indoor air pollution: there are numerous sources, the buildings vary widely in construction, and occupants all have different lifestyles, consumer product use habits, and window-opening practices (Halios et al., 2022).

Schools have a high occupancy density and specific sources of indoor pollution, such as school supplies. The high density of furniture leads to emissions of volatile organic compounds. Moreover, each school is located close to traffic, making outdoor air pollution a significant factor affecting indoor air quality in classrooms (Sadrizadeh et al., 2022). Daycare centres have also their own characteristics, including frequent cleaning and disinfection of surfaces (Zhang et al., 2022).

Offices also have their own characteristics, such as a high density of office equipment and daily cleaning. Additionally, in some high-rise buildings, windows cannot be opened; indoor air quality depends entirely on the mechanical ventilation system (Mandin et al., 2017).

## 2 HEALTH EFFECTS ASSOCIATED WITH INDOOR AIR EXPOSURE: LESSONS FROM EPIDEMIOLOGICAL STUDIES

Although epidemiological studies on the effects of indoor pollution are much rarer than those on outdoor air pollution, epidemiological evidence has expanded in recent years. The health effects associated with indoor exposure to mold, radon, nitrogen dioxide, and formaldehyde are well-documented. These effects are as varied as the pollutants themselves, ranging from eye irritation, asthma and respiratory disorders to lung cancer. Other health effects related to indoor pollution are also being explored, e.g., cardiovascular effects, reproductive toxicity, attention disorders, and impacts on mental health.

### 3 EVOLUTION OF IAQ OVER TIME AND FUTURE TRENDS

The presentation will conclude with an overview of changes observed in recent years regarding air quality in living spaces, including reduction in some volatile organic compounds and increase in indoor concentrations of others. Future trends will be discussed, focusing on emerging pollutants (Salthammer, 2020), the development of new measurement methods, and the influence of climate change (Mansouri et al., 2022).

### 4 REFERENCES

Halios, C.H., Landeg-Cox, C., Lowther, S.D., *et al.* (2022). Chemicals in European residences - Part I: A review of emissions, concentrations and health effects of volatile organic compounds (VOCs). *Sci Total Environ*, 839, 156201. <https://doi.org/10.1016/j.scitotenv.2022.156201>

Mandin, C., Trantallidi, M., Cattaneo, A., *et al.* (2017). Assessment of indoor air quality in office buildings across Europe - The OFFICAIR study. *Sci Total Environ*, 579, 169-178. <https://doi.org/10.1016/j.scitotenv.2016.10.238>

Mansouri, A., Wei, W., Alessandrini, J.M., *et al.* (2022). Impact of climate change on indoor air quality: review. *Int J Environ Res Public Health*, 19(23), 15616. <https://www.mdpi.com/1660-4601/19/23/15616>

Sadrizadeh, S., Yao, R., Yuan, F., *et al.* (2022). Indoor air quality and health in schools: A critical review for developing the roadmap for the future school environment. *J of Build Engin*, 57, 104908. <https://doi.org/10.1016/j.jobe.2022.104908>.

Salthammer, T. (2020). Emerging indoor pollutants. *Int J Hyg Environ Health*, 224, 113423. <https://doi.org/10.1016/j.ijheh.2019.113423>

Zhang, S., Cooper, E., Stamp, S., *et al.* (2022). Indoor air quality in day-care centers. In: Zhang, Y., Hopke, P.K., Mandin, C. (eds) *Handbook of Indoor Air Quality*. Springer, Singapore. [https://doi.org/10.1007/978-981-16-7680-2\\_68](https://doi.org/10.1007/978-981-16-7680-2_68)

# Perfect Mixing or Imperfect Terminology

Andrew Persily

*NIST  
Gaithersburg  
United States of America*

## ABSTRACT

Air and airborne contaminant mixing in building spaces is important to ventilation system design and performance, tracer gas measurements of ventilation rates, and occupant exposure to indoor pollutants. The physics of air and contaminant mixing have been studied for decades and are fairly well understood. Nevertheless, many discussions of building ventilation, air movement and indoor air quality use the term “perfect mixing” without a clear discussion of what it means or how it applies to the situation being considered. In most cases, the term refers to an idealized situation in which supply air from ventilation systems, entering outdoor air (e.g., via infiltration), air from adjoining space, and indoor-generated contaminants are instantaneously and uniformly mixed with the room or building air volume of interest. This idealized situation is just that, an idealization, which is not achievable in practice, though it is a useful concept for considering metrics and measurements of air distribution and contaminant uniformity. While the existence of perfect mixing within a space is difficult to define and therefore verify; air distribution within a building air volume and the uniformity of contaminant concentrations can be defined and verified through measurement or analysis of modeling (e.g., computational fluid dynamics) results.

The degree of uniformity of indoor air contaminant or tracer gas concentrations in a space are critically important for characterizing indoor air quality and occupant exposure to contaminants, contaminant transport modeling, the application of tracer gas measurement methods, ventilation system design (e.g., air terminal location and discharge velocity), and compliance with ventilation standards (e.g., ASHRAE Standard 62.1). Too often the uniformity issue is dismissed by stating that a space is perfectly mixed, again without a clear discussion of what this means and how this idealization actually applies. In practice, the uniformity of contaminant and tracer gas concentrations depend on the air movement patterns in the space and on the nature of the contaminant (or tracer gas) source including the temperature of the source, air movement associated with the source, and the distribution of the source in the space (i.e., highly localized or distributed throughout the space). For the same air distribution patterns, different sources can in general result in quite different contaminant distributions. Therefore, instead of using the term perfect mixing to describe a space, contaminant or tracer gas concentration uniformity should be used, which is more straightforward to define and quantify.

This presentation will review the history of how air and contaminant mixing has been characterized over the decades and clarify how the important concepts of air distribution and contaminant uniformity can be quantified.

# Guidance on damp and mould: understanding and addressing the health risks in the home

Sani Dimitroulopoulou

*Air Quality and Public Health  
UK Health Security Agency  
Harwell Campus, Didcot, Oxford, OX11 0RQ, UK*

## SUMMARY

This keynote will present the new government guidance on the health risks of damp and mould for the housing sector in England. This guidance highlights the serious risks that damp and mould can pose to tenants' health, the legal responsibilities of social and private rented housing providers, the imperative to respond quickly, and the practical steps that should be taken both to address damp and mould and prevent them. Research led by UKHSA found that there was a considerable burden of respiratory illness in England from residential damp and mould. This work has fed into the new consolidated guidance.

## KEYWORDS

Damp, mould, guidance, housing, burden of disease assessment

## 1 INTRODUCTION

In September 2023, the government in England issued new guidance on mould and damp in rented homes, following the Coroner's report into the death of two year-old boy, Awaab Ishak, who died from prolonged exposure to damp and mould in the home. The Coroner's 'prevention of future deaths' report included the concern (matter of concern 3) that: "There was no evidence that up-to-date relevant health information pertinent to the risk of damp and mould was easily accessible to the housing sector." The guidance is published jointly by the Office for Health Improvement and Disparities, the UK Health Security Agency, and the Ministry of Housing, Communities and Local Government (DHSC/UKHSA/DLUHC, 2023), following extensive engagement with the housing and health sectors, including tenant representative groups.

## 2 BURDEN OF DISEASE ASSESSMENT

An estimated 962,000 to 6.5 million (4% to 27%) households in England live with damp and mould. While living in a damp and/or mouldy home is associated with the development or exacerbation of several respiratory diseases, conditions and symptoms, little is known about the burden of disease at a national scale in England. UKHSA research assessed the burden of asthma, lower respiratory infections, and allergic rhinitis from exposure to damp and/or mould in England in 2019 (Clark et al., 2023). For this purpose, epidemiological evidence was combined with health and exposure data from nation-wide annual surveys and modelled estimates.

In 2019, the presence of damp and/or mould in English residences (4% of homes) was estimated to be associated with approximately 5,000 cases of asthma; 8,500 cases of lower respiratory infections among children and adults and contributed to: 1 to 2% of new cases of allergic rhinitis in that year. Alternative data sources, primarily from self-reporting, suggest

that the percentage of dwellings affected by damp and/or mould may be even higher than the estimates used for this study, in which case the total number of cases could be 3 to 8 times greater. They also found that ethnic and minority and disadvantaged groups were disproportionately impacted by damp and mould, reflecting a persistent environmental health inequity. This research contributed to the development of the new consolidated guidance on damp and mould.

### **3 THE GUIDANCE**

The consolidated guidance (DHSC/UKHSA/DLUHC, 2023) primarily aims at social and private rented housing providers and their workforce (managing agents, and temporary accommodation providers). It may also be of interest to health and social care professionals, owner-occupiers and tenants. The guidance highlights the health effects to damp and mould, the people who are at increased risk from exposure to damp and mould as well as the relevant regulation on damp and mould in social and private rented properties. It provides details to help landlords understand the overall process of how to deal with reports of damp and mould and highlights the need for expediency, particularly in severe cases or when involving vulnerable households. Finally, it provides advice how the landlords can take a proactive approach to addressing damp and mould.

### **4 REFERENCES**

Clark, S.N.; Lam, H.C.Y.; Goode, E.-J.; Marczylo, E.L.; Exley, K.S.; Dimitroulopoulou, S (2023). The Burden of Respiratory Disease from Formaldehyde, Damp and Mould in English Housing. *Environments*, 10(8), 136.

<https://doi.org/10.3390/environments10080136>

DHSC/UKHSA/DLUHC (2023) Guidance on Damp and mould: understanding and addressing the health risks for rented housing providers

<https://www.gov.uk/government/publications/damp-and-mould-understanding-and-addressing-the-health-risks-for-rented-housing-providers>

# **Risk mitigation for indoor air quality on example of construction products**

Ana Maria Scutaru

*German Environment Agency  
Corrensplatz 1  
14195 Berlin, Germany*

## **SUMMARY**

Most people in Central Europe spend the majority of the day indoors. The quality of indoor air is therefore very important for health and well-being. Construction products can be an important source of indoor pollution through their emissions. The implementation of health requirements to assess emissions of volatile organic compounds (VOC) from construction products into indoor air under the Construction Products Regulation has been under discussion since 2010. The necessary tools are now ready for use: The test method EN 16516 and the EU-LCI list (LCI: lowest concentration of interest) with harmonised reference values for the health impacts of VOC. This talk highlights challenges and chances of a harmonised European health evaluation for construction products emissions.

## **KEYWORDS**

Indoor air quality, construction products emissions, EU-LCI, European harmonisation

## **1 INTRODUCTION**

People in Central Europe spend the majority of the day indoors. A good indoor air quality is therefore crucial for a healthy life. Unfortunately, good indoor air quality cannot be taken for granted. It depends on many factors: Construction products and furnishings present in the building, indoor climate conditions (temperature, relative humidity), how and how often occupants ventilate, what they do in the rooms, and what household chemicals they use. Construction products can be an important source of indoor pollution through their emissions of volatile organic compounds (VOC).

The European Green Deal (EGD) launched by the European Commission in 2019 aims at solving the big environmental and social challenges of our time. Two major actions and initiatives of the EGD are the new renovation initiative and the zero-pollution ambition for a toxic-free environment. This ambitious policy framework set by the European Commission flags the importance of indoor air quality in buildings. In the future also the effects of the climate change on indoor air quality will become more drastic e.g. due to temperature increase indoors (Zhao, 2024).

## **2 CALL FOR HARMONISED CRITERIA FOR A RELIABLE EMISSION DECLARATION OF CONSTRUCTION PRODUCTS**

The use of low emission construction products is a prerequisite for a good indoor air quality. This has become more important in modern construction and especially in energy-efficient buildings, where the rate of air exchange with fresh ambient air may be limited (Müller, 2017).

In the last years many efforts have been made to provide instruments for the enforcement of the Construction Products Regulation (CPR) Basic Work Requirement “Hygiene, health and the environment” for construction works. The goal is to provide information on the emission performance of the construction products in a harmonised format. The necessary tools are now ready for use: The test method EN 16516 Construction products: Assessment of release of dangerous substances - Determination of emissions into indoor air is available, fully validated and suitable for all construction products emitting VOC (EN 16516, 2020). The second tool, a first list with harmonised reference values for the health impacts of VOC, EU-LCI (LCI: lowest concentration of interest), was published in November 2023 (European Commission, 2023).

In the past years also many proposals were brought to the table on how to best declare the emission performance of construction products and how to define VOC classes for communication of test results. However, until today, no consensus could be reached between the European Commission and the EU Member States on this topic.

### **3 PROPOSAL TO ASSIGN AND COMMUNICATE VOC EMISSION CLASSES**

To revitalize the discussions on a harmonised communication of VOC emissions from construction products the German Environment Agency (UBA) organised the international online conference ‘Limiting health impacts of construction products regarding VOC’ in April 2021 (<https://www.umweltbundesamt.de/en/international-conference-limiting-health-impacts-of>). The core of the conference was the discussion of a specific proposal for VOC classes and ways of application and implementation towards a future VOC declaration (Reihlen, 2021).

Four essential performance characteristics are suggested:

- Sum of EU-LCI ratios (R-value): For the health evaluation of emissions, reference values (EU-LCI) are set for individual VOCs. By dividing the reference room concentration of a compound by its corresponding EU-LCI value the EU-LCI ratio is established. Additive effects of VOCs are accounted for by summing up the individual EU-LCI ratios to a hazard index (R value).
- CMR<sub>VOC</sub>: VOCs with carcinogenic, mutagenic or reprotoxic properties are assessed separately.
- Formaldehyde: This substance is evaluated individually because it is frequently measured in indoor air and included in many assessment schemes.
- TVOC: The sum of all emitted VOCs from a product according to the EN 16516 is determined. Measurement of TVOC is included in most assessment schemes and also as parameter in building certification systems.

### **4 CONCLUSIONS**

A consensus for a quick and simple solution regarding information on VOC emissions of construction products is imperative (figure 1). The European Commission presented a new proposal for the communication of VOC emissions in June 2024 which will be discussed with the EU Member States in the next months. If health criteria for marketing of construction products in Europe cannot be implemented within the current CPR, other initiatives need to be tackled: Environmental Product Declarations provide important information on products and their application. So far, this means only declaration and no evaluation of data and VOC emissions were often not included to date. Digitalisation of the release of dangerous substances (Smart CE marking) in the context of the Building Information Modelling could also offer a possibility to quicker progress on this topic.





Figure 1: Example for a possible “translation” of information into VOC emission classes

## 5 REFERENCES

- EN 16516. (2020). Construction products: Assessment of release of dangerous substances - Determination of emissions into indoor air. EN 16516:2017+A1:2020.
- European Commission. (2023). *List of "Lowest Concentration of interest" (LCI) values 2023*. Retrieved from Publications Office of the European Union: <https://data.europa.eu/doi/10.2873/88989>
- Müller, B. M. (2017). *Indoor air quality after installation of building products in energy-efficient buildings*. Berlin: UBA Texte 73/2017, Umweltbundesamt.
- Reihlen, A. J. (2021). *Harmonised VOC emission classes for construction products - A tool to achieve healthy buildings*. Berlin: Dokumentation 05/2021. Umweltbundesamt.
- Zhao, J. U. (2024). Long-term prediction of the effects of climate change on indoor climate and air quality. *Environmental Research*, 243, S. 117804.

# How a harm budget can be used to regulate Indoor Air Quality in Dwellings

Benjamin Jones<sup>\*1</sup>, Gioberttti Morantes<sup>1</sup>, Constanza Molina<sup>2</sup>, Max Sherman<sup>1</sup>

*1 Department of Architecture and Built Environment,  
University of Nottingham, NG7 2RD, United  
Kingdom*

*2 School of Civil Construction, Faculty of  
Engineering, Pontificia Universidad Católica de  
Chile*

*\*Corresponding author:  
benjamin.jones@nottingham.ac.uk*

## ABSTRACT

This work quantifies the chronic harm caused by long-term exposure to common indoor air contaminants in dwellings located in the global north. Two methods are used to compute DALYs. The first uses incidence data and the second considers toxicological evidence. They are synthesised to produce Harm Intensities, the number of DALYs per person per unit of annual-average concentration the person is exposed to. Then, uncertainty in annual mean concentrations for 45 contaminants commonly found in dwellings in the global north is determined from a systematic literature review.

PM<sub>2.5</sub>, PM<sub>10-2.5</sub>, NO<sub>2</sub>, O<sub>3</sub>, and HCHO are estimated to be the most harmful contaminants by an order of magnitude. Together they account for >99% of the estimated harm from typical indoor exposures and should be designated *contaminants of concern* in dwellings in the global north. A harm budget approach is used to show that complying with ASHRAE standard 62.2 could see the total population harm drop by ~70%.

## KEYWORDS

DALY, dwelling, harm intensity, harm budget, ranking, *acceptable* indoor air quality

## 1 INTRODUCTION

Common metrics for assessing air quality in buildings are based on guidelines and standards that regulate concentrations by stating threshold concentrations that should not be exceeded over a period of time. There is disagreement on the magnitude of these thresholds, perhaps because methods for determining them do not relate the magnitude of any exceedance to specific health outcomes. Accordingly, there is a need to develop health-centred IAQ metrics that can quantify the burden of disease using current epidemiological and toxicological evidence of population morbidity and mortality. The Disability Adjusted Life Year (DALY) is used as an air quality metric because it can be used to quantify and rank the burden of household air contaminants.

## 2 METHODS

Two methods are used to compute DALYs. The first uses incidence data and the second considers toxicological evidence. They are synthesised to produce Harm Intensities, the number of DALYs per person per unit of annual-average concentration the person is exposed to. Then, uncertainty in annual mean concentrations for 45 contaminants commonly found in dwellings in the global north is determined from a systematic literature review.

Uncertainty in the median DALYs for the 45 contaminants is estimated by combining the harm intensities and concentrations for the epidemiological and toxicological models and pooling results. The contaminants are then ranked by the magnitudes of predicted harm.

Preliminary results are contained in Morantes et al. (2023). Finally, an acceptable limit of population harm is set using a *harm budget* where any combination of exposures is permissible as long the total harm stays below a limit. This limit is determined using a *reference scenario*, a sample of 70 houses that all comply with the California energy code, and thus ASHRAE Standard 62.2, for mechanical ventilation. HIs and measurements of some CoCs (PM<sub>2.5</sub>, HCHO, NO<sub>2</sub>) and guideline values (Rn, O<sub>3</sub>) are used to set the budget.

### 3 RESULTS

Coarse and fine particulate matter, NO<sub>2</sub>, O<sub>3</sub>, and formaldehyde are estimated to be the most harmful contaminants by an order of magnitude. Accordingly, these should be designated contaminants of concern in dwellings, prioritised for removal, and regulated. The total median harm from these contaminants is 2,200 DALYs/10<sup>5</sup> people /year. The total median harm for the 70 houses of the reference scenario is 610 DALYs/10<sup>5</sup> people /year, showing a reduction of around 70%.

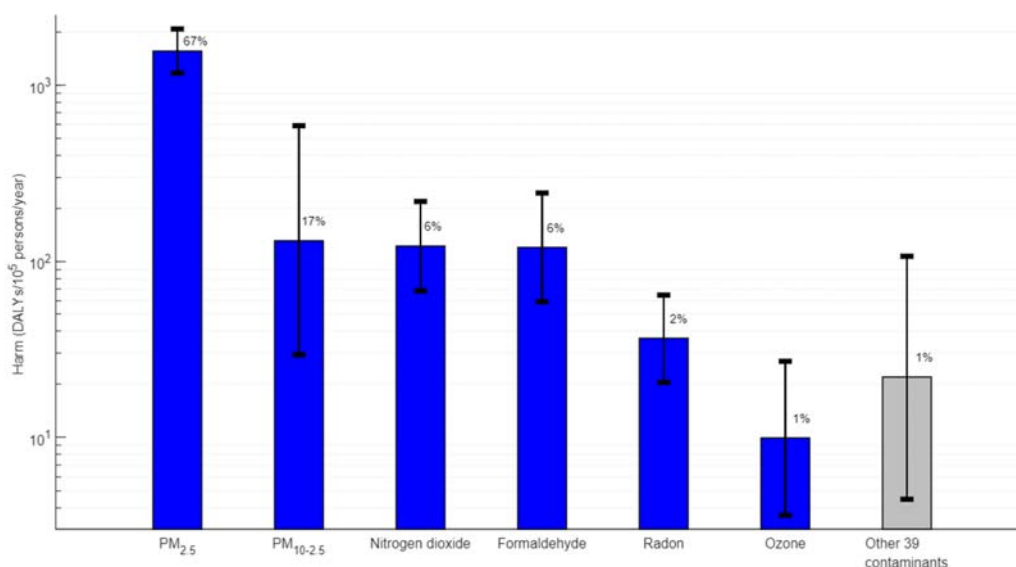


Figure 1: Harm caused by contaminants of concern. Median (bar) & GSD (error bar). Percentage contribution for total harm.

### 4 DISCUSSION

A new method is required to regulate contaminants and a harm budget is proposed as a way to quantitatively determine *acceptable* IAQ in dwellings. It sets a maximum acceptable limit of population harm and then permits any combination of exposures to CoC so long as the harm stays below the limit. The methods we propose can be used to re-evaluate the harm the contaminants cause, or to consider other contaminants, as new evidence emerges. Harm is shown to be a way of prioritising the contaminants that cause the greatest chronic harm to populations of people, and the harm budget is used to quantitatively set *acceptable* IAQ based on exposure to airborne contaminants in buildings. Generalizing to dwellings is not possible, but the approach used here is a starting point for harm budget evaluation rather than a definitive solution. Changes in the budget's magnitude will occur when comparing the magnitude against other non-IAQ hazards and when considering additional houses.

### 5 CONCLUSIONS

The most harmful contaminants in dwellings are PM<sub>2.5</sub>, PM<sub>10-2.5</sub>, NO<sub>2</sub>, formaldehyde, radon, and O<sub>3</sub>, accounting for over 99% of total median harm of 2,200 DALYs/10<sup>5</sup> person/year. The

chronic harm caused by all airborne contaminants in dwellings accounts for 7% of the total global burden from all diseases.

An acceptable harm budget of 610 DALYs/10<sup>5</sup> person/year is set using a reference scenario, and is as a way to quantitatively determine acceptable IAQ based on exposure to airborne contaminants in buildings.

## **6 ACKNOWLEDGEMENTS**

This work was supported by a University of Nottingham Faculty of Engineering Research Excellence Scholarship and by the Chartered Institution of Building Services Engineers (CIBSE).

## **7 REFERENCES**

Morantes G, Jones B, Sherman M, Molina C. A preliminary assessment of the health impacts of indoor air contaminants determined using the DALY metric. *International Journal of Ventilation*. 2023:1-10.

# Methodology to define new performance indicator for ventilation regulation in France

Valérie Leprince<sup>1</sup>, Baptiste Poirier

*Cerema  
2 rue Antoine Charial  
69003 Lyon, France  
Valerie.leprince@cerema.fr*

## KEYWORDS

Ventilation, performance based regulation, France

## INTRODUCTION

In France, the regulation context for ventilation is based on the decree « Arrêté de 1982 » which is a prescriptive regulation, requiring extracted flowrate in every utility room. These extracted airflow should respond to several principles:

1. The air renewal in dwelling is general and permanent at least during the heating season.
2. The air renewal system shall include natural or mechanical inlet in main rooms and outlet in utility rooms. The air shall circulate between main and utility rooms
3. The ventilation system shall be able to reach, simultaneously or not a set of prescribed flowrates by room with exhaust, function of the type of the room and the size of the dwelling
4. The total extract flowrate can be reduced with a minimal flowrate to be respected (function of the number of main rooms)
5. The air inlet shall be designed to reach the prescribed flowrates in utility rooms.

These principles were strong basis to generalise mechanical ventilations in residential building to avoid humidity issues and mould growth thanks to these minimal flowrates to be respected. However, it is quite restrictive for other ventilation systems with variable flowrate that could be temporarily lower. Moreover, this decree has no requirement on supply flowrate. As result, lots of existing systems are not compatible with the actual regulation such as supply only system, ventilation per room, system without higher flowrate in the kitchen, and generally more advanced control strategies.

The new building code « code de la construction » propose an alternative to the prescriptive approach, based on the following statement:

*« Air renewal, shall be such as, in normal condition of use, the indoor air pollution does not endanger health and security of occupants and that condensation is avoided, except temporarily »*

These new principles in building code for air renewal open the possibility for a range of systems to be compatible with the regulation. But this switch from a prescriptive approach to

a performance-based approach need to be adapted in the regulation with a robust methodology to assess the effective performance of ventilation systems. In addition, the requirements for performance should be such as most of system that comply with 1982 requirements fulfil performance requirements.

The objectives of this work is to define a set of key performance indicator (KPI) for ventilation that are equivalent to the existing prescriptive regulation. Which is ambitious because defining KPI for ventilation is still a matter of research, this is worked on in IEA-EBC Annex 86.

## 1 APPROACH

To define performance-based requirement, the aim of the regulation needs to be clearly identified with its objectives. Including principles which describe the essential elements of the area covered by the code. To assess whether objectives are meet or not, measurable (or calculable) indicators should defined. Lastly verifiers demonstrate that the assessed performance met the required state based on observation and information.

### 1.1 Objectives and principles

In general, the performance indicators for IAQ measures should rate their impact on the Indoor Air Quality according to:

- **Health** aspect to prevent risk from long term exposure, acute effect and disease transmission.
- **Well-being** with the aim to improve quality of sleep, productivity and perceived air quality.
- **Building durability** to avoid mould growth and damage from condensation

In the French context, the regulation deals only with “ventilation” and no other IAQ measures (such as source reduction or air cleaning), so it will only evaluate performance that can be improved by an increase of the ventilation rate.

Objectives, and therefore requirements, are on the removal capacity of pollutant produced indoor (inc. humidity and CO<sub>2</sub>) but they are no requirement on air treatment (increase humidity level, temperature, quality of supply air, etc.).

In IAQ regulation several principles have to be wisely choose to meet these objectives on health, well-being and building durability for ventilation performance assessment. These principles give orientations for the definition of the performance indicator and their ability to be relevant regarding the objectives.

The selected principles for the French IAQ are:

- Performance indicator should be suitable for validation through preliminary simulations not through on-site measurements.
  - o Nevertheless, their ability to be compared to on-site measurement is a criterion to define them.
- The threshold values for those indicators should be consistent with performance of systems that respect the current prescriptive regulation « Arrêté de 82 ».
  - o In addition, some prescriptive requirement can be kept as safe-guards to guarantee a minimal air renewal and performance level.

### 1.2 Define performance Parameters & indicators

Regarding the objectives of the French IAQ regulation, five parameters are selected and declined across nine performance indicators:

**CO<sub>2</sub>**, a well-known reference, to evaluate the adequacy between the ventilation air flow rate and the occupation, it is both measurable and suitable for simulation

- For each room, the CO<sub>2</sub> concentration (in ppm) below which it remains 67% of occupied time
  - o An indicator in ppm is more easily readable than a cumulative exposure in ppm.h
- For each room, the CO<sub>2</sub> concentration (in ppm) below which it remains 95% of the occupied time

**Humidity**, relevant for the risk of condensation, measurable and suitable for simulation

- For every room, a maximum percentage of time over 75% of relative humidity during the heating period. The maximum value will depend on the type of room (as surface finishing standards depend on it)

**Proxy pollutant P1**, permanently emitted, cover all pollutants emitted by material and passive equipment, suitable only for simulation,

- The mean exposure (for the most exposed person)
- The maximum exposure over one hour (moving average, for the most exposed person).

**Proxy pollutant P2**, emitted during cooking periods, representative of episodic emissions linked with human activities, suitable only for simulation

- The maximum exposure over one hour (moving average, in the kitchen).
- The concentration below which it remains 95% time in bedroom

This selection of two proxy have the objective to cover all pollutants and not a specific one to avoid air cleaning systems that would remove only this one without taking care of others. Moreover, for performance assessment based on simulation there is a need for relevant data of emission for each project and that depends on occupant, construction behaviour, external condition and complex physic phenomena. This could be difficult to generalise with multitude pollutant declination. Lastly depending on the pollutant, the target values could be difficult to define with possible opposition between health guidelines and the assessed performance of existing systems

**Air renewal**, relevant to control sage-guard on minimum air renewal and easy solution for the toilet. It is suitable for simulation and measurable

- Minimum and reachable air renewal flow rate in the toilet
- Air renewal rate above which the dwelling is 95% of the time

### 1.3 Verification with simulated existing systems on reference cases

Associated with this performance indicators, acceptable thresholds are necessary to assess the performance of ventilation. However, performance validation through simulations could largely be influenced by input parameters such as the building configuration or weather. Sensitivity analysis experiment was made with the objectives to define the threshold values and to check the impact of the various input parameters.

Two typical French mechanical ventilations were simulated; an extract only mechanical ventilation with constant airflow and an extract only with relative humidity-based demand

control. The performance was assessed over 2000 simulations with variables parameters statistically consistent with the French housing stock (ventilation airflows, architecture, kind of dwelling, number of rooms, building airtightness). 8 climatic zones with various wind exposure were implemented. The only fixed parameters were the occupancy and the pollutant emissions scenario. The simulations were performed with a software called « MATHIS » which is a multi-zone airflow model equivalent to CONTAM. Threshold values were suggested such as around 75% of simulations would comply with them.

#### 1.4 Define Target values

Table 1: Target value for indicators

Parameter	Indicator	Location	Suggested values
CO <sub>2</sub>	The CO <sub>2</sub> concentration (in ppm) below which it remains 67% of occupied time	Maximum of occupied rooms	~1900 ppm [1800-2000]
	The CO <sub>2</sub> concentration (in ppm) below which it remains 95% of occupied time	Maximum of occupied rooms	~2700 ppm [2500-2900]
Relative Humidity	Percentage of time over 75% of relative humidity during the heating period	Bathroom	~14% [12-16]
		Kitchen	~6% [5-8]
		Other rooms	~1% [1-3]
P1	The mean exposure	Most exposed person	~2300 P1/m <sup>3</sup> [2100-2500]
	Maximum exposure over one hour	Most exposed person	~7000 P1/m <sup>3</sup> [7000-9000]
P2	Maximum exposure over one hour	Kitchen	~1800 P2/m <sup>3</sup> [1700-2000]
	The concentration below which it remains 95% time	Maximum of main rooms	~100 P2/m <sup>3</sup> [50-200]
Air renewal	Extracted Air Flow rate above which it is 95% of time	Toilets	~5m <sup>3</sup> /h
	E.A.F.R. above which it is 95% of occupied time	Toilets	~15m <sup>3</sup> /h
	Air replacement above which it is 95% of time	Full dwelling	0,38 m <sup>3</sup> /h/m <sup>2</sup> [0,36-0,54]

#### 1.5 Define Validation process

To be validated a project must:

- Include a system inspection and maintenance protocol
- Respect the minimum safeguards
- Prove through simulation (pre-project) that it meets the minimum IAQ criteria

Two alternatives are foreseen for the validation:

- Alternative 1 for industrial system that is meant to be installed in multiple projects
  - 2 steps validation
- Alternative 2 for ventilation system fitted for one given project
  - 1 step validation

For the first alternative

- First a commission will validate (once):
  - The modeling of the system in Mathis (and interface for end-user)
    - This will include input parameters
  - The relevance of inspection and maintenance protocol
- Then, for each project, a qualified design office will
  - Design the ventilation system
  - Check through simulations that KPI are met



- At commissioning of each project, a qualified ventilation inspector will
  - Apply the inspection protocol
  - Conclude on the conformity (or not) of the system.

For the second alternative, everything should be done for each project by a specifically qualified design office.

## **2 CONCLUSION**

France will soon have a performance-based regulation for ventilation in dwellings has an alternative to the prescriptive one. Performance criteria defined are not ambitious but they are in line with actual systems performances.

Nevertheless, having establishing performance criteria is now a formidable opportunity for better performing systems to demonstrate so.

It also allows to developpe label of performance that go farther than the regulation.

# Assessing IAQ in existing residential buildings within a performance-based regulatory framework through a predictive model

Sonia García-Ortega<sup>\*1,2</sup>, Pilar Linares-Alemparte<sup>1</sup>

*1 Quality in Construction Department,  
Instituto de ciencias de la construcción Eduardo  
Torroja - CSIC  
4, Serrano Galvache St.  
Madrid, Spain*

*Escuela Técnica Superior de Arquitectura,  
Universidad Politécnica de Madrid  
Spain*

*\*Corresponding author: plinares@ietcc.csic.es*

## SUMMARY

In many countries, the traditional method of ventilating dwellings involved natural ventilation, based on the operation of windows and high levels of infiltration through the building envelope, particularly through windows and window-wall joints. In Spain, in the middle of the last century, the use of vertical ventilation shafts in the wet rooms of dwellings became widespread, and it is currently the most common ventilation system in existing dwellings. It is a dedicated ventilation system with exhaust of stale air from wet rooms, circulation of air from dry to wet rooms and intake of fresh outdoor air to dry rooms by infiltration [1]. This passive stack ventilation employs the principles of thermal buoyancy and the Venturi effect to remove stale air from wet rooms.

Despite its widespread use, this system has four principal limitations. Firstly, there is a lack of ventilation in the absence of thermal buoyancy and even thermal inversion during periods of high temperatures, which can result in the circulation of stale air back into dwellings. Secondly, there is no ventilation when there is a lack of Venturi effect during periods of low wind speed. Thirdly, there are thermal losses due to involuntary infiltrations and uncontrolled aeration. Finally, there is uncertainty associated with natural ventilation systems. As a result, the actual IAQ in the majority of the current housing stock is unknown.

It can be reasonably assumed that the implementation of this ventilation system would result in a superior IAQ during the winter months in comparison to the summer season. However, field studies [2] indicate that this is not the case. In monitored dwellings, IAQ is generally superior in summer than in winter. This discrepancy may be attributed to the influence of occupants and their varying responses to factors affecting ventilation, such as the opening and closing of windows or the compartmentalisation of dwellings through the use of interior doors. If the season or weather exerts a significant influence on occupant behaviour, can this be statistically linked? Can IAQ be predicted by taking into account occupant behaviour at the macroscopic level?

A plethora of studies have been conducted on the determination of IAQ when the ventilation flow rate is known, the calculation of the ventilation flow rate, and the impact of specific actions of occupant behaviour. Nevertheless, the proposal is to analyse the relationship between influencing factors and final IAQ without calculating the specific ventilation rate or the behaviour of occupants.

At the Eduardo Torroja Institute for Construction Sciences (IETcc), which is a research institution belonging to the Spanish National Research Council (CSIC), studies are being conducted to correlate the outcomes of real CO<sub>2</sub> measurements in rooms where the occupants have been able to behave freely with factors such as the season of the year, the surface area of the dwelling, the permeability, or the number of occupants. The a priori intention is not to ascertain how occupants behave, but rather to ascertain the final effect and other factors may have on IAQ. These relationships are proving to be significant enough to develop predictive statistical models with high predictive capability. The current approach is to use parameters that are easily obtainable on a large scale, such as floor area, year of construction, etc., in order to avoid factors that require field measurements such as permeability.

The objective of these models is to provide useful insights that could inform the development of IAQ regulations, guidelines or building renovation plans. These insights could be used to:

- assess the potential IAQ in a given neighbourhood based on its building typology and construction characteristics;
- identify building typologies that are more prone to IAQ problems;
- evaluate the differences in occupant behaviour according to geographical location, climate, socio-economic level, etc.

In the case of Europe, based on the European directives on energy efficiency, until now renovation policies have been directed almost exclusively towards energy renovation rates. This has meant that IAQ aspects have been relegated to second place or ignored. Furthermore, the increased airtightness of buildings in pursuit of enhanced thermal insulation has resulted in a deterioration of IAQ.

However, the recent Directive (EU) 2024/1275 on the energy performance of buildings [3] appears to take action by stating in its Article 1 that indoor environmental quality requirements must be taken into account, including factors such as ventilation rate and presence of contaminants. This will necessitate the utilisation of analytical tools such as the aforementioned predictive models.

## **KEYWORDS**

Natural ventilation; Occupant behaviour; Dwellings; Indoor air quality; Predictive model; CO<sub>2</sub>

## **ACKNOWLEDGEMENTS**

This project is supported by the Spanish National Research Council and the Ministry of Housing and Urban Agenda of Spain.

## **REFERENCES**

- [1] Government of Spain, 'Normativa Tecnológica de la Edificación - Instalaciones de salubridad - Ventilación'. 1975.
- [2] Garcia-Ortega, S., & Linares-Alemparte, P. (2023). Indoor air quality in naturally ventilated dwellings in Spain. *Informes De La Construcción*, 75(572), e519. <https://doi.org/10.3989/ic.6447>

[3] Directive (EU) 2024/1275 of the European Parliament and of the Council of 24 April 2024 on the energy performance of buildings ELI:  
<http://data.europa.eu/eli/dir/2024/1275/oj>

# The importance of performance-based regulations for residential ventilation. State of the art.

Gaëlle Guyot<sup>1\*</sup>, Valérie Leprince

*1 Cerema  
25 Av. François Mitterrand,  
69500 Bron , France.*

*\*Corresponding author: gaelle.guyot@cerema.fr*

## KEYWORDS

Ventilation, indoor air quality, energy, performance, residential buildings, smart ventilation

## 1 INTRODUCTION

The context of climate change and the need of saving energy has required rethinking the ventilation and the air change rates in buildings, because of their increased impact on thermal losses. Indeed, ventilation plays a crucial role estimated around 30-50% of the energy delivered to buildings, becoming an even higher part in high-efficient buildings (Liddament and Orme, 1998, AIVC FAQ).

Indoor air quality is another major area of concern in buildings which is influenced by ventilation. Because people spend most of the time in residential buildings (Klepeis et al., 2001) and 60-90% of their life in indoor environments (homes, offices, schools, etc.) (Klepeis et al., 2001; European Commission, 2003; Brasche and Bischof, 2005; Zeghnoun et al., 2010; Jantunen et al., 2011), indoor air quality is a major factor affecting public health. Logue et al. (2011b) estimated that the current damage to public health from all sources attributable to IAQ, excluding second-hand smoke (SHS) and radon, was in the range of 4,000–11,000  $\mu$ DALYs (disability-adjusted life years) per person per year. By way of comparison, this means the damage attributable to indoor air is somewhere between the health effects of road traffic accidents (4,000  $\mu$ DALYs/p/yr) and heart disease from all causes (11,000  $\mu$ DALYs/p/yr). According to the World Health Organization (WHO, 2014), 99,000 deaths in Europe and 81,000 in the Americas were attributable to household (indoor) air pollution in 2012.

Thus, by optimizing airflows where and when needs are higher, a smart ventilation system can truly improve IEQ while significantly minimizing energy consumption (Durier et al., 2018; Guyot et al., 2018a).

## 2 A MAJORITY OF VENTILATION REGULATIONS ARE PRESCRIPTIVE

IAQ performance-based approaches for ventilation at the design stage of a building are rarely used. Instead, prescribed ventilation rates have been used. As a result, standards and regulations, such as ASHRAE 62.2-2016 and others in Europe (Dimitroulopoulou, 2012), often prescribe ventilation strategies requiring three constraints on airflow rates:

1. A constant airflow based on a rough estimation of the emissions of the buildings, for instance one that considers size of the home, the number and type of occupants, or combinations thereof;
2. Minimum airflows (for instance during unoccupied periods);

3. Sometimes also provisions for short-term forced airflows to dilute and remove a source pollutant generated by activities as cooking, showering, house cleaning, etc.

### **3 PERFORMANCE-BASED APPROACHES FOR SMART VENTILATION**

In order to conciliate energy saving and indoor air quality issues, interest for smart ventilation systems has been growing thanks to performance-based approaches. Such systems must often be compared either to constant-airflow systems (“equivalence approaches”) or to fixed IAQ metrics thresholds.

A paper published in 2016 proposed a review of performance-based approaches used in 5 countries around the world for the assessment of smart ventilation strategies (Guyot et al., 2019, 2018b).

### **4 WHAT IS NEW IN 2024 ?**

In our international context in 2024, IAQ and energy are still issues of interest. Nevertheless, other aspects should be included in the performance indicators. An efficient ventilation system should ensure the exchange of stale indoor air with fresh outdoor air, thus improving indoor environmental quality (IEQ), preventing the build-up of pollutants and excessive moisture or viruses, without needlessly wasting energy heating or cooling incoming air, taking into account environmental and climate changes (heatwaves, pollution peaks, pandemics, ...).

Since 2016, new research has been published and collected, notably in the context of the IEA-EBC Annex 86 Energy Efficient Indoor Air Quality Management in Residential Buildings (2022-2025).

This new presentation gives an updated overview of how the performance-based concept has been used and developed in research projects since 2016, and how it has been transposed in standards and some regulations since.

### **5 REFERENCES**

- Brasche, S., Bischof, W., 2005. Daily time spent indoors in German homes--baseline data for the assessment of indoor exposure of German occupants. *Int. J. Hyg. Environ. Health* 208, 247–253. <https://doi.org/10.1016/j.ijheh.2005.03.003>
- Dimitroulopoulou, C., 2012. Ventilation in European dwellings: A review. *Build. Environ.* 47, 109–125. <https://doi.org/10.1016/j.buildenv.2011.07.016>
- Durier, F., Carrié, F.R., Sherman, M., 2018. VIP 38: What is smart ventilation? AIVC.
- European Commission, 2003. Communiqué de presse - Indoor air pollution: new EU research reveals higher risks than previously thought.
- Guyot, G., Sherman, M.H., Walker, I.S., 2018a. Smart ventilation energy and indoor air quality performance in residential buildings: A review. *Energy Build.* 165, 416–430. <https://doi.org/10.1016/j.enbuild.2017.12.051>
- Guyot, G., Walker, I.S., Sherman, M., Linares, P., Garcia Ortega, S., Caillou, S., 2019. VIP 39: A review of performance-based approaches to residential smart ventilation. AIVC.
- Guyot, G., Walker, I.S., Sherman, M.H., 2018b. Performance based approaches in standards and regulations for smart ventilation in residential buildings: a summary review. *Int. J. Vent.* 0, 1–17. <https://doi.org/10.1080/14733315.2018.1435025>

- Jantunen, M., Oliveira Fernandes, E., Carrer, P., Kephelopoulos, S., European Commission, Directorate General for Health & Consumers, 2011. Promoting actions for healthy indoor air (IAIAQ). European Commission, Luxembourg.
- Klepeis, N.E., Nelson, W.C., Ott, W.R., Robinson, J.P., Tsang, A.M., Switzer, P., Behar, J.V., Hern, S.C., Engelmann, W.H., 2001. The National Human Activity Pattern Survey (NHAPS): a resource for assessing exposure to environmental pollutants. *J. Expo. Anal. Environ. Epidemiol.* 11, 231–252. <https://doi.org/10.1038/sj.jea.7500165>
- Liddament, M.W., Orme, M., 1998. Energy and ventilation. *Appl. Therm. Eng.* 18, 1101–1109. [https://doi.org/10.1016/S1359-4311\(98\)00040-4](https://doi.org/10.1016/S1359-4311(98)00040-4)
- WHO, 2014. Burden of disease from Household Air Pollution for 2012. World Health Organization.
- Zeghnoun, A., Dor, F., Grégoire, A., 2010. Description du budget espace-temps et estimation de l'exposition de la population française dans son logement. *Inst. Veille Sanit. Qual. L'air Intér.* Dispon. Sur [Www Air-Interieur Org](http://www.Air-Interieur.Org).

# The IAQ performance-based regulation in Spain: description, identified problems for its application, and foreseen changes

Pilar Linares-Alemparte<sup>1\*</sup>, Sonia García-Ortega<sup>1</sup>

*1 Instituto de las ciencias de la construcción Eduardo Torroja - CSIC  
4, Serrano Galvache St.  
Madrid, Spain*

*\*Corresponding author: plinares@ietcc.csic.es*

## ABSTRACT

Efforts must be made to promote the use of efficient ventilation systems in buildings with the aim of reducing energy demand, as ventilation is a major source of energy loss. Nevertheless, the implementation of efficient ventilation systems is frequently constrained by regulations. It is therefore essential that governments and regulatory bodies facilitate and even encourage the use of appropriate solutions through the introduction of performance-based regulations.

Prescriptive regulations establish particular conditions or specifications for deemed-to-satisfy solutions or systems, thereby limiting the utilization of any alternative solution or system. In general, indoor air quality (IAQ) regulatory frameworks worldwide are still mainly based on prescriptive approaches that set fixed requirements for airflows or air change rates (Dimitroulopoulou, C., 2012). This can hinder the implementation of innovative and more efficient ventilation systems.

In contrast, performance-based regulations provide a flexible regulatory framework that can accommodate any solution that meets the specified performance requirements, regardless of whether it is explicitly outlined in the regulations. This approach allows for innovation, promoting the utilisation of novel techniques and building practices that result in enhanced efficiency (IRCC, 1998). Therefore, to promote the use of efficient ventilation systems, it is imperative to develop and implement performance-based IAQ regulations that require IAQ performance indicators during the building design stage. A number of countries have already implemented performance-based IAQ regulations (Guyot, G. et al., 2019) with the intention of encouraging the use of efficient ventilation strategies.

This paper presents a description of the IAQ performance-based regulation in Spain, along with an analysis of the main identified problems for its application and the anticipated changes that are likely to occur in the near future.

## KEYWORDS

Ventilation, IAQ, regulations, performance-based, building code, CO<sub>2</sub>

## 1 REGULATORY FRAMEWORK

The primary regulatory framework in Spain for ensuring the quality of buildings is the *Código Técnico de la Edificación* (CTE, 2006). It encompasses a comprehensive range of requirements pertaining to matters including energy efficiency and IAQ. The provisions for regulating IAQ within dwellings are included in Section DB HS3 *Calidad del aire interior*



(Indoor air quality) (Fig. 1). The DB HS3 was originally based on the establishment of minimum constant ventilation flow rates for supply and exhaust air in habitable rooms, which were formulated as deem-to-satisfy solutions. Efficient ventilation systems, such as smart ventilation systems, were not included among the deemed-to-satisfy solutions. Instead, compliance was to be demonstrated through the assessment of a *Documento de Idoneidad Técnica* (Technical Approval Document, DIT).

In response to the growing demand for sustainable policies and regulations that promote the use of more efficient ventilation systems, section DB HS3 was reviewed (Linares, P. et al., 2014) and subsequently enforced in 2017 (DB HS3, 2017). The revised regulations currently adopt a fully performance-based approach, which allows the use of systems that can adjust ventilation rates to meet actual needs. The current requirement is to limit the concentration of CO<sub>2</sub> as an indicator of pollutants related to human activity and to establish a minimum ventilation rate to reduce other pollutants related to the building and its furnishings. These performance-based regulations facilitate the implementation of efficient ventilation systems avoiding the inherent regulatory obstacles associated with prescriptive regulations. Additionally, the 2017 revision retained the constant flow rates as deemed-to-satisfy solutions but optimised them to meet the set performance-based requirements.

This approach enables designers to utilise optimised constant ventilation flow rates, utilising ventilation systems that have already been certified with DIT or assessing the compliance of other systems in real dwellings according to the performance-based requirements. Consequently, it is more straightforward to optimise energy demand by utilising either variable or constant flow ventilation systems.



Figure 1. Left: web page of the *Código Técnico de la Edificación*. Right: Cover of DB HS3 *Calidad del aire interior*

## 2 IAQ INDICATOR AND METRICS

The IAQ level is typically determined by the concentration of pollutants generated in buildings that can affect people's health and comfort. A number of common pollutants are found in buildings including fine and coarse particulate matter, NO<sub>2</sub>, second-hand smoke, radon, formaldehyde and ozone (Morantes et al., 2023; Logue et al., 2011). Pollutants may be generated by human activity or exhaled from furniture and finishes. It is a challenging task to establish a relationship between pollutant concentration and its effect on the health of occupants. Furthermore, the majority of common pollutants are challenging to quantify or assess without the use of sophisticated instrumentation.

In this context, the Spanish regulations (DB HS3, 2017) opted to select an easily measurable indicator as a performance-based requirement to represent the state of the IAQ. Although there is no general consensus on the health risks posed by CO<sub>2</sub> at typical indoor concentrations, and the relationship between CO<sub>2</sub> and other important pollutants remains uncertain (Persily, A., 2022), CO<sub>2</sub> concentration can still be considered a reliable indicator of ventilation rate, it is easy to measure and closely related to human activity and bioeffluent emissions. For these reasons, it has traditionally been used as an IAQ indicator and was chosen in DB HS3 as the indicator for pollutants directly related to human activity.

In order to quantify the performance-based requirement two thresholds for CO<sub>2</sub> concentration were established:

- the maximum annual average concentration of CO<sub>2</sub> should not exceed 900 ppm;
- the maximum annual accumulated concentration of CO<sub>2</sub> above 1,600 ppm should not exceed 500,000 ppm per hour. This parameter indicates the relationship between the duration of CO<sub>2</sub> concentrations above a specified limit value over a year. It can be calculated as the sum of the areas (ppm·h) within the limit value of 1,600 ppm and the representation of the CO<sub>2</sub> concentration as a time function (Fig. 2).

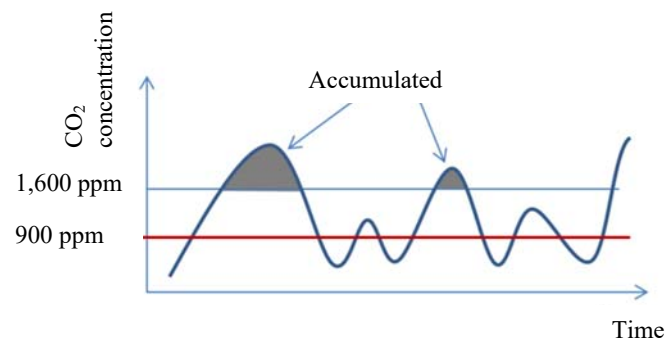


Figure 2. Annual accumulated concentration of CO<sub>2</sub> above 1,600 ppm

These thresholds must not be exceeded under the design conditions established in DB HS3, which include occupancy scenarios and CO<sub>2</sub> production rates. These thresholds are considered 'design performance' as it is not possible to measure them on-site under precisely these conditions; they can only be assessed during the design stage.

In addition to the aforementioned performance-based requirement, a minimum constant flow rate of 1.5 l/s was established in order to regulate the concentration of pollutants that are not directly related to human activity, such as those originating from furniture and finishes (for instance formaldehyde).

### 3 DEEMED-TO-SATISFY SOLUTIONS AND VERIFICATION METHOD

Compliance with performance-based requirements can be achieved either through a deemed-to-satisfy solution or a specialised verification method.

Deemed-to-satisfy solutions are designed with the intention of being user-friendly for non-specialist practitioners, and their use serves as a guarantee of compliance with the performance-based requirements. On the other hand, specialist practitioners may elect to utilise alternative solutions that demonstrate their compliance with the specified verification method.

### 3.1 Deemed-to-satisfy solutions

The deemed-to-satisfy solutions consist of minimum constant ventilation flow rates, as indicated in Table 1, for the supply and exhaust of air in habitable rooms. The required flow rates depend on the type of dwelling according to the number of bedrooms.

Table 1. Constant ventilation flow rates (l/s)

Number of bedrooms in the dwelling	Dry rooms			Wet rooms	
	Master bedroom	Other bedrooms	Dining and living rooms	Global	Each room <sup>(1)</sup>
0 or 1	8	-	6	12	6
2	8	4	8	24	7
≥ 3	8	4	10	33	8

(1) Kitchen and bathrooms.

Fresh air must be supplied to dry rooms and stale air must be extracted from wet rooms. Table 1 illustrates the supply and exhaust flow rates for each room.

The total supply flow rate is calculated by adding together the individual supply flow rates for each dry room. In parallel, the total exhaust flow rate is determined by taking the greater of the global flow rate for wet rooms and the sum of the individual exhaust flow rates for each wet room. It is necessary that the total supply and exhaust flows for the entire dwelling are balanced, so that the total ventilation flow rate for the design of the system is equal to the largest of the exhaust and supply flows. Therefore, it may eventually be necessary to increase the flow rate in some rooms (wet or dry) in order to achieve equilibrium within the system. The decision regarding which room(s) to increase the flow rate will be made by the designer.

### 2.2 Verification method

The verification method involves specialised software to assess the CO<sub>2</sub> concentration in each room. While no specific software is designated, the values of the fundamental parameters to be considered are explicitly outlined. The simulation should incorporate these influencing parameters, including the number of occupants, occupancy scenarios, weather conditions, the CO<sub>2</sub> production rate, the annual average outdoor CO<sub>2</sub> concentration, and closed doors.

The aim of the verification method is to verify compliance with performance-based requirements at the design stage. On-site CO<sub>2</sub> monitoring is not required to demonstrate compliance. Performance-based requirements are considered 'design performance' as they cannot be measured in situ under precisely the very same conditions as those used to set the thresholds; they can only be assessed at the design stage.

It is possible to assess any ventilation system for compliance with the performance-based requirements.

## 4 ENERGY SAVING WITH THE CURRENT APPROACH

The principal advantage of the performance-based approach is that any ventilation system can demonstrate compliance with the performance-based requirements. This allows the utilisation of energy-efficient systems such as demand controlled ventilation (DCV) systems.

Figure 3 illustrates the reduction in demand achieved in 20 case studies when DCV systems that fulfil the performance-based current regulations are employed instead of the constant airflows derived from the application of the old regulations (Linares, P. et al., 2015). A total of five dwellings were studied in two climate zones (D3 and A3) with two orientations (north and south). In all cases, both heating and cooling demands were found to be reduced. Nevertheless, the reduction in heating demand was considerably more pronounced, with figures ranging from 21% to 100%.

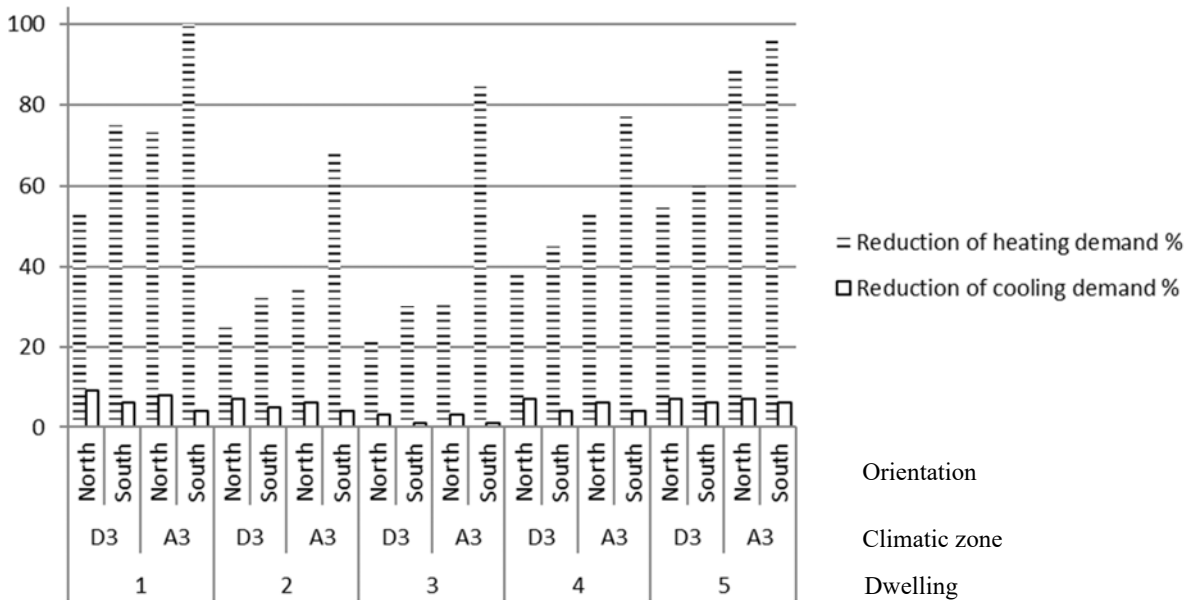


Figure 3. Reduction of demand

## 5 PROBLEMS IDENTIFIED IN ITS APPLICATION

Following the initial implementation of DB HS3 approximately twenty years ago and the subsequent introduction of the current performance-based version seven years ago, a number of issues have been identified in its application (AIVC VIP 48.1, 2024). These issues primarily relate to the consideration of smart ventilation systems in energy assessment tools and the rise of condensation risk in renovations. Although only the first one is directly related to the new performance-based approach, the other one is also described below because of its relevance.

### 5.1 Lack of consideration of smart ventilation systems in energy assessment tools

The use of efficient ventilation systems can result in significant energy savings. However, the most commonly used building energy assessment tools do not fully account for these benefits due to inaccurate ventilation flow rates used in the energy assessment and suboptimal integration of demand-controlled ventilation systems.

In Spain, the most commonly used tool for assessing the energy performance of buildings is the *Herramienta Unificada Lider-Calener* (HULC). HULC is a whole building energy simulation software that is used to assess energy demand and consumption. It comprises the earlier software tools LIDER and CALENER, allowing both assessment of energy qualification and fulfilment of the energy saving requirements. The software is offered by the *Ministerio de Fomento* and the *Ministerio de Industria, Energía y Turismo - Instituto para la diversificación y ahorro de la energía* (IDAE), having been developed by *Grupo de Termotecnia de la Asociación de Investigación y Cooperación Industrial de Andalucía* (AICIA) from the *Escuela Técnica Superior de Ingenieros* from *Universidad de Sevilla*, in collaboration with the *Unidad de Calidad en la Construcción* from *Instituto Eduardo Torroja de Ciencias de la Construcción* (IETCC-CSIC).

HULC takes into account the constant ventilation flow rate of the entire building and the electrical energy consumption based on the specifications of the ventilation system (ErP technical data, data from fan curves (flow rates and power) or data for heat recovery systems). However, these ventilation flow rates and energy consumption are not optimised to match real needs and are assumed to be constant at all times. The only viable option is to calculate the equivalent average flow over the year under design conditions.

## **5.2 Rise of condensation risk in renovations**

It is probable that surface condensation will occur on the inner side of façade walls during a renovation of a dwelling in which existing windows are replaced by other airtight windows without the provision of additional means of intake of fresh air.

Historically, the ventilation system most commonly employed in Spanish dwellings was based on the occupants' habits of opening windows, high infiltration rates through the building envelope, primarily window frames (Hoek, T., et al., 2022), and the extraction of stale air through thermal buoyancy-based vertical stacks located in wet rooms, mainly bathrooms and toilets, and sometimes kitchens (Linares-Alemparte, P. et al., 2024).

In order to enhance the energy efficiency in renovations, it is frequently the case that existing permeable windows are replaced with airtight ones, which are sometimes equipped with microventilation. The microventilation system is a device integrated into the window frame, usually a tilt-and-turn design, that opens a 4-5mm gap around the perimeter of the active window sash when activated by the window handle. This results in a small but permanent airflow. However, occupants are typically unaware of this possibility.

In the event that microventilation or other means of fresh air intake are not provided, in addition to opening windows, there is a risk of insufficient ventilation, leading to the accumulation of humidity and surface condensation. Despite the current DB HS3 already emphasizes the importance of not compromising performance during renovations, instances of this occurring are still common. A preliminary study has revealed that 50% of existing buildings fail to meet the current CO<sub>2</sub> values established in the IAQ regulations.

## **6 FORESEEN CHANGES**

The plan to revise HULC already includes targets to more accurately account for the energy saving benefits of utilising efficient ventilation systems, including:

- adjusting the ventilation flow rates used in the energy performance assessment to make them more accurate and reflective of actual rates;
- optimising the integration of demand-controlled ventilation systems into the energy performance assessment methodology and simulation tools.

Efforts must be made to ensure that regulations emphasise the need to maintain or improve IAQ performance when replacing existing windows with airtight ones, including the provision of fresh air supplies. There is a need to raise awareness of the issue among designers and to guarantee the implementation of suitable building controls for monitoring compliance.

In the near future, regulations are expected to further embrace a performance-based approach. This may involve a move away from CO<sub>2</sub> as the sole indicator of IAQ and the setting of thresholds levels for other pollutants. A major challenge in implementing this change is to establish the correlation between pollutant concentration and its impact on occupant health. Research is currently underway to investigate the generation of the most common pollutants in dwellings, their concentration and their impact on occupant health in terms of Disability-Adjusted Life Years (DALYs). Other challenges include the lack of accuracy of readily available pollutant detectors for controlling ventilation systems.

## 7 ACKNOWLEDGEMENTS

This work was supported by the *Consejo Superior de Investigaciones Científicas* and the *Ministerio de Transportes, movilidad y agenda urbana* of Spain.

## 8 REFERENCES

Dimitroulopoulou, C. (2012). Ventilation in European dwellings: A review. *Building and Environment*. 47, 109–125.

García-Ortega, S., & Linares-Alemparte, P. (2023). Indoor air quality in naturally ventilated dwellings in Spain. *Informes De La Construcción*, 75(572), e519.  
<https://doi.org/10.3989/ic.6447>

Guyot, G., Walker, I., Sherman, M., Linares, P., García-Ortega, S. and Caillou, S. (2019). *AIVCVIP 39: A review of performance-based approaches to residential smart ventilation*. AIVC.

Hoek, T., Poza-Casado, I. and Melgosa, S. (2022). *AIVC VIP 45.2. Trends in building and ductwork airtightness in Spain*. AIVC.

Inter-Jurisdictional Regulatory Collaboration Committee, 1998. *Guidelines for the Introduction of Performance-Based Building Regulations*. On line.

[https://ircc.info/Doc/Guidelines%20for%20the%20Introduction%20of%20Performance-Based%20Building%20Regulations%20%5BDiscussion%20Paper%5D%20\(1998\).pdf](https://ircc.info/Doc/Guidelines%20for%20the%20Introduction%20of%20Performance-Based%20Building%20Regulations%20%5BDiscussion%20Paper%5D%20(1998).pdf)  
[Consulted 14/02/2024].

Linares, P., García, S., Sotorrió, G. and Tenorio, J.A. (2014). Proposed change in Spanish regulations relating to indoor air quality with the aim of reducing energy consumption of ventilation systems. *Proceedings of 35th AIVC Conference, 4th TightVent Conference and 2nd venticool Conference: Ventilation and airtightness in transforming the building stock to high performance*. Poznań (Poland).

- Linares, P., García, S., Larrumbide, E. and Tenorio, J.A. (2015). Energy saving as a consequence of the proposed change in Spanish regulations relating to indoor air quality. *Proceedings of 36th AIVC Conference, 5th TightVent Conference and 3rd venticool Conference: Effective ventilation in high performance buildings*. Madrid (Spain).
- Linares-Alemparte, P., García-Ortega, S., Feldman, F., Romero-Fernández, A., Sorribes-Gil, M. and Villar-Burke, R. (2024). *AIVC VIP 48.1 Trends in building ventilation requirements and inspection in Spain*. AIVC.
- Logue, J.M., Price, P.N., Sherman, M.H. and Singer, B.C. (2011) A Method to estimate the chronic health impact of air pollutants in U.S. residences. *Environmental Health Perspectives*. 120 (2), 216-222.
- Ministerio de Fomento (2006) *CTE Código Técnico de la Edificación (Building Regulations)*. On line.  
<https://www.codigotecnico.org/> [Consulted 14/02/2024].
- Ministerio de Fomento (2016). *Guía de aplicación del DB HR (Guidebook for the application of the DB HR)*. On line.  
<https://www.codigotecnico.org/Guias/GuiaHR.html> [Consulted 20/06/2024].
- Ministerio de Fomento (2017). *DB HS3 Calidad del aire interior (Indoor Air Quality)*. On line.  
<https://www.codigotecnico.org/pdf/Documentos/HS/DBHS.pdf>. [Consulted 14/02/2024].
- Ministerio de Fomento (2019). *DB HR Protección frente al ruido (Protection against noise)*. On line.  
<https://www.codigotecnico.org/pdf/Documentos/HR/DBHR.pdf>. [Consulted 20/06/2024].
- Morantes, G., Jones, B., Sherman, M. and Molina, C. (2023). A preliminary assessment of the health impacts of indoor air contaminants determined using the DALY metric: International Journal of Ventilation. *International Journal of Ventilation*. 22:4, 307-316.
- Persily, A. (2022) Development and application of an indoor carbon dioxide metric. *Indoor Air*. 32 (7).

# Challenges and opportunities arising from different ventilation approaches: controlled experiments conducted at the Canadian Centre for Housing Technology

Liang Grace Zhou<sup>1</sup>, Yunyi Ethan Li<sup>1</sup>, Janet Gaskin<sup>\*1</sup>, Patrique Tardif<sup>1</sup>

*1 National Research Council Canada  
1200 Montreal Road  
Ottawa, Canada, K1A 0R6*

*Presenting author: Liang Grace Zhou  
\*Corresponding author: Janet Gaskin*

## SUMMARY

## KEYWORDS

Indoor radon, depressurization, built environment, ventilation

## 1 BACKGROUND

The ingress of naturally occurring radioactive radon gas from the soil into buildings can occur both by convection through any openings in the foundations as a result of pressure differentials and by diffusion across an airtight barrier (World Health Organization 2009). Residential ventilation systems and exhaust devices can affect indoor radon concentrations if they result in depressurization of the conditioned space relative to the outdoors or to the soil below the foundations or if they supply outdoor air directly. Balanced mechanical supply and exhaust ventilation (MSEV) systems tend to dilute the indoor radon concentration; however, some depressurization of the lower level can result from the air distribution if air is primarily supplied to upper level rooms and exhausted from lower level rooms. Mechanical exhaust only ventilation (MEV) systems depressurize the conditioned space and rely on the resulting infiltration of air across the building envelope that can be above and below grade. Higher indoor radon concentrations have been reported for the larger depressurization of 5-9 Pa in MEV houses relative to 2-3 Pa in MSEV houses (Arvela et al. 2014). In this study, indoor radon concentrations were measured in the National Research Council (NRC) Canadian Centre for Housing Technology (CCHT) semi-detached net-zero energy-ready smart house during depressurization testing using a duct blaster, and the depressurization resulting from typical exhaust devices was evaluated. Indoor radon concentrations were also measured during depressurization testing in a smaller NRC test house.

## 2 METHODS

The Canadian Centre for Housing Technology (CCHT) research facility is located in Ottawa, Canada, and enables testing and monitoring of building technologies in full sized Canadian housing. The depressurization testing was conducted in the full-size two storey semi-detached twin houses (mirrored about the party wall) constructed to the Canadian 2012 R-2000 standard that have an airtightness of about 1.5 air change per hour at 50 Pa (Figure 1). Both houses had a natural gas furnace, a central air conditioner, and energy recovery ventilator (ERV). A duct system distributed conditioned outdoor air and re-circulated throughout the houses. A 20-mil polyethylene radon barrier was installed during the construction of the basement and foundation. Depressurization testing was also conducted in an older, smaller NRC test house with a main floor and basement that had a 6-mil polyethylene membrane installed beneath concrete slab foundation as a vapour barrier. This test house had electrical



baseboard heaters, a split air conditioning unit, a ducted heat recovery ventilator (HRV), and no exhaust device.

Prior to the depressurization testing, the mechanical supply and exhaust ventilation (MSEV) system and exhaust devices were turned off and sealed in all the test houses. The furnace and the recirculation fan were turned off in the semi-detached house in the first round of testing and running in the semi-detached houses during the second round of testing. The indoor radon concentration and differential pressures were measured during a 48 hour period on each floor of the semi-detached house at three levels of depressurization, achieved using a duct blaster installed on the first (ground) floor through a slot in the garage door in M24E: -5 Pa, -10 Pa, and -20 Pa relative to the outdoors. The differential pressure between the basement and the subslab area was also measured. Representing MEV conditions, the relative depressurization on each floor was measured in M24F during a 30 minute operation period for each exhaust device that vented directly outdoors, individually and in combination: a range hood, two bathroom fans, and a clothes dryer. The smaller experimental house had electric heating only and no recirculation while the HRV (MSEV) was turned off and sealed. Indoor radon concentrations were measured using continuous radon monitors every 10 minutes in the semi-detached houses (AlphaGuard) and every hour in the smaller test house (CorentiumPro).



Figure 1: CCHT semi-detached twin houses

### 3 RESULTS AND DISCUSSION

The indoor radon concentrations and differential pressures measured in the depressurization testing conducted in M24E using the duct blaster were plotted in Figure 2. The highest radon concentrations were measured in the basement during each test, and were highest for the most modest depressurization scenario at -5 Pa relative to outdoors. Stratification of indoor radon was evident when the furnace and the recirculation fan were turned off, as shown in Figure 2A, with the lowest radon concentration on the second floor. Building depressurization would have resulted in infiltration of outdoor air on the upper floor diluting the radon concentration and soil gas infiltration across the foundations in the basement increasing the radon concentration. Nearly uniform indoor radon concentration was observed across all floors when the furnace and the recirculation fan were turned on, as shown in Figure 2B. The indoor radon concentrations on all floors were higher under a building depressurization of -5 Pa when the recirculation fan was turned on than the baseline average indoor radon concentration of 174 Bq/m<sup>3</sup> measured over a two-week period for M24E with the ERV turned off, suggesting that more infiltration occurred across the foundations at -5 Pa. At higher building depressurizations, the indoor radon concentrations were lower than the baseline average indoor radon concentration, suggesting that higher infiltration of outdoor air occurred across the above ground building envelope at

depressurizations of -10 Pa and -20 Pa. The average indoor radon concentration in M24E with the ERV operated continuously over the two-week period was 94 Bq/m<sup>3</sup>, confirming the effectiveness of balanced MSEV ventilating the house at 0.27 air changes per hour.

By contrast, in the smaller CCHT test house, the indoor radon concentration in the basement rooms increased with increasing depressurization. This pattern was consistent with the increasing indoor radon concentrations reported for increasing house depressurization conducted using a blower door testing in France (Collignan, Lorkowski, and Améon 2012).

During the MEV testing, depressurization of close to -5 Pa on each floor of M24F was measured during the operation each bathroom fan and the clothes dryer, while the range hood and combinations of exhaust devices resulted in depressurizations that ranged from -15 to -40 Pa. This research suggests that radon infiltration at depressurization of about -5 Pa may be an issue of concern, despite being considered low enough to prevent spillage of combustion products from combustion appliances that do not have direct supply and exhaust vents. Basements tend to be occupied spaces in Canada that include bedrooms and family rooms.

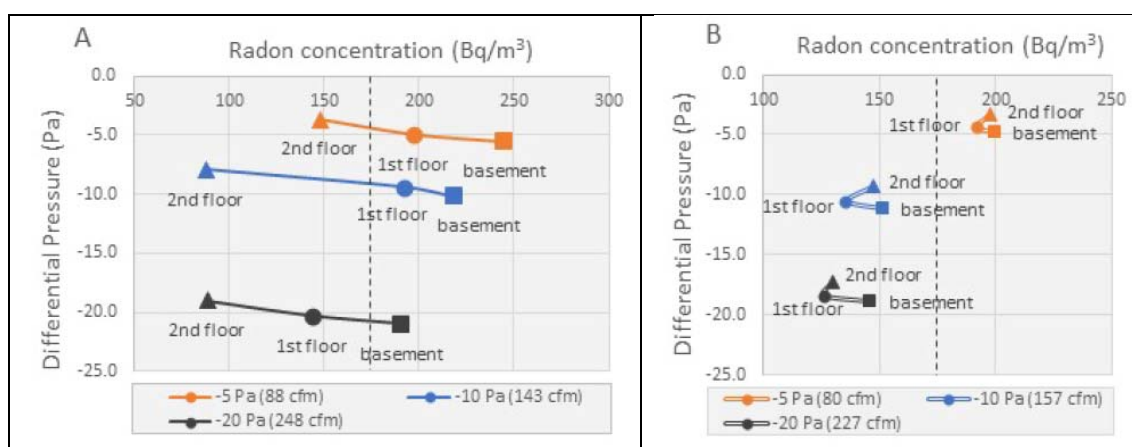


Figure 2: Radon concentration and differential pressure measured in M24E in the basement, first (ground) floor and second floor during depressurization in CCHT using a duct blaster located on the first (ground) floor with: A) furnace and recirculation fan off, and B) furnace and recirculation fan on. The dotted line shows the average indoor radon of 174 Bq/m<sup>3</sup> measured during a two-week period in M24E when ERV was turned off.

#### 4 CONCLUSIONS

Increased indoor radon concentrations were measured during the depressurization testing conducted in the CCHT semi-detached net-zero energy-ready twin houses and in the smaller test house. The highest indoor radon concentrations occurred for the lower depressurizations resulting from single exhaust devices (bathroom fan, clothes dryer) operating under a typical MEV condition. Balanced MSEV was an effective strategy for radon control in the twin houses.

#### 5 REFERENCES

- Arvela, H., O. Holmgren, H. Reisbacka, and J. Vinha. 2014. "Review of Low-Energy Construction, Air Tightness, Ventilation Strategies and Indoor Radon: Results from Finnish Houses and Apartments." *Radiation Protection Dosimetry* 162 (3): 351–63. <https://doi.org/10.1093/rpd/nct278>.
- Collignan, Bernard, Christophe Lorkowski, and Roselyne Améon. 2012. "Development of a Methodology to Characterize Radon Entry in Dwellings." *Building and Environment* 57 (November):176–83. <https://doi.org/10.1016/j.buildenv.2012.05.002>.
- World Health Organization. 2009. "Who Handbook on Indoor Radon."

# Field study measurements evaluating radon concentrations under different ventilation scenarios

Janet Gaskin\*<sup>1</sup>, Yunyi Ethan Li<sup>1</sup>, Marcel Brascoupe<sup>2</sup>, Liang Grace Zhou<sup>1</sup>

*1 National Research Council Canada  
1200 Montreal Road  
Ottawa, Canada*

*2 MB Radon Solutions  
75 Pitobig Mikan  
Maniwaki, Canada*

*Presenting author: Janet Gaskin*

*\*Corresponding author: Janet.Gaskin@nrc-cnrc.gc.ca*

## ABSTRACT

**Background:** Increasing indoor ventilation has the potential to dilute indoor radon and may be an appropriate first step when measured indoor radon concentrations are close to the mitigation threshold for an existing low-rise house that lacks balanced mechanical ventilation. A ventilation system that includes a heat exchange core is recommended in cold climates to reduce the energy loss associated with replacing stale indoor air with outdoor air that must be either cooled or heated to maintain thermal comfort. A field study of the effectiveness of heat recovery ventilation systems (HRVs) at reducing moderate indoor radon concentration was conducted in 16 houses between 2020 and 2023 in the National Capital Region in Canada.

**Methods:** The average indoor radon concentration for different HRV settings within a season were compared to estimate the effectiveness of radon reduction. Hourly measurements on lower and upper floors were made using continuous radon monitors and averaged over a one-month period for each HRV setting evaluated: off, running continuously or periodically (typically 20 minutes per hour), and with a fan speed of high or low when running. The effect of the HRV system on indoor radon concentrations was evaluated for sixteen houses, while a comparison of the effect of operating both the passive depressurization system (PSD) for radon mitigation and the HRV was also evaluated for four of the study houses.

**Results and Conclusions:** The initial radon concentrations measured on the lower floor in the 16 study houses with the HRV off were moderate, ranging from 91 to 312 Bq/m<sup>3</sup>, and were roughly lognormally distributed with a geometric mean of 166 Bq/m<sup>3</sup>. The arithmetic mean indoor radon was reduced by 40% for continuous HRV operation in the 13 houses with forced air furnace heating systems, with the reduction effectiveness characterized by a normal distribution with a standard deviation of 12%, a minimum reduction of 20% and a maximum of 56%. A higher reduction effectiveness of 80% was observed in the occupied house that had electric baseboard heating and in which an independently ducted HRV was installed. There was an overall trend of higher reduction effectiveness for continuous than periodic fan operation for houses in which more than two HRV settings were assessed. Well designed and installed HRV systems were effective at reducing the moderate indoor radon concentrations measured in these houses that lacked a balanced mechanical ventilation system. In one house, both a passive radon depressurization system and an HRV were required to reduce the indoor radon concentration below the recommended mitigation threshold of 200 Bq/m<sup>3</sup> for existing housing in Canada.

## KEYWORDS

Indoor radon, heat recovery ventilation, housing, mitigation,

## 1 INTRODUCTION

Radon is a naturally occurring radioactive gas that is formed as uranium in the soil decays and that can concentrate indoors as a result of infiltration through the foundations of buildings. The World Health Organization recommends that national radon programs reduce both the population exposure to radon and the exposure of individuals at highest risk (World Health Organization, 2009). Long-term exposure to radon is the second leading cause of lung cancer after smoking in Canada, to which about 3,000 deaths are attributable annually in Canada (Chen et al., 2012; Gaskin et al., 2018). The Health Canada guideline recommends

mitigating average annual indoor radon concentrations above 200 Bq/m<sup>3</sup> in existing housing and suggests residents may choose to mitigate lower radon exposures because any reduction in indoor radon will decrease the associated lung cancer risk (Health Canada, 2017).

A balanced mechanical ventilation system that both supplies and exhausts air draws less radon gas through the foundations than a system that has a mechanical exhaust system and relies on the resulting depressurization to draw replacement air through cracks and gaps in the foundation, floors and walls (Arvela et al., 2014). A heat or energy recovery ventilation system includes a heat exchange core to reduce the energy loss associated with replacing stale indoor air with outdoor air that must be either cooled or heated to maintain thermal comfort. Lower indoor radon concentration was reported for low-rise housing that included balanced mechanical ventilation systems compared to those with exhaust only ventilation in Finland, Norway and Sweden (Arvela et al., 2014; Finne et al., 2019; Haanes et al., 2022; Khan et al., 2021; Valmari et al., 2011). Significantly reduced indoor radon was reported for houses built after 2003 in Japan, when a balanced mechanical ventilation system was required by the building code to keep formaldehyde concentrations below the guidelines value and prevent “sick building” syndrome (Suzuki et al., 2010). Improved ventilation in older housing was also associated with decreased indoor radon in two municipalities in Sweden (Tondel et al., 2009). A field study of the effectiveness of heat/energy recovery ventilation systems (HRVs) at reducing moderate indoor radon concentration was conducted in 16 existing houses between 2020 and 2023 in the National Capital Region in Canada.

## 2 METHODS

The recruitment of study houses was restricted to those in which moderate initial radon concentrations were measured. HRV systems were retrofitted in 13 occupied houses in the community that lacked balanced supply and exhaust mechanical ventilation systems. The field study testing also included three National Research Council (NRC) experimental houses in which HRV systems were already installed. Two of the NRC experimental houses were full size, side-by-side, energy efficient duplexes, designed to the R-2000 standard (Natural Resources Canada, 2012), in which typical occupant behaviours such as opening doors were mechanically simulated. The third NRC house was a smaller experimental house. The characteristics of the study houses are described in Table 1, including house type, number of floors (excluding the basement), the presence/absence of a basement, the type of heating system, and whether the house has a passive soil depressurization (PSD) system installed for radon mitigation. All of the houses have a basement, and most have a forced air furnace for heating while two had electric heating. The study houses include one and two-storey detached houses, and two-storey semi-detached and townhouses. Half of the houses have a PSD system installed for radon mitigation.

Table 1: Study house characteristics

House ID	House Type	# floors	Basement	Heating Type	Passive soil depressurization
1	town	2	✓	Forced-air furnace	✗
2	town	2	✓	Forced-air furnace	✗
3	det	2	✓	Forced-air furnace	✓
4	det	1	✓	Forced-air furnace	✓
5	det	1	✓	Forced-air furnace	✗
6	det	2	✓	Forced-air furnace	✓
7	det	2	✓	Forced-air furnace	✗
8	det	2	✓	Forced-air furnace	✓

9	det	1	✓	Electric heater	✓
10	semi-det	2	✓	Forced-air furnace	✓
11	semi-det	2	✓	Forced-air furnace	✓
12	det	1	✓	Electric baseboard	✗
13	det	2	✓	Forced-air furnace	✓
14	det	2	✓	Forced-air furnace	✗
15	det	2	✓	Forced-air furnace	✗
16	det	2	✓	Forced-air furnace	✗

Note: # floors excluding basement

The indoor radon concentration was measured every hour on both the lower and upper floors using a continuous radon monitor. The average indoor radon concentration was measured over roughly a one-month period for each HRV setting evaluated in the occupied houses, with testing conducted sequentially within a single season for each scenario. The HRV settings evaluated included the following: off, running continuously or periodically (typically 20 minutes per hour), and with a higher or lower fan speed when running. Shorter two-week periods of radon measurement were conducted in the highly controlled NRC experimental houses for each HRV setting. In four occupied houses in the community, the indoor radon concentrations for different HRV settings were measured both in combination with the operation of the PSD system installed, and without the PSD system operating (stack closed position). The residents were asked to maintain closed house conditions during the testing.

### 3 RESULTS AND DISCUSSION

The indoor radon concentrations measured in the 16 study houses are presented in Table 2. The initial radon concentrations measured on the lower floor in the 16 study houses with the HRV off were moderate, ranging from 91 to 312 Bq/m<sup>3</sup>, and were lognormally distributed with a geometric mean of 166 Bq/m<sup>3</sup>. The indoor radon concentrations included in this table were measured with the fan at the design (higher) speed for continuous HRV operation to represent the upper limit for radon reduction under normal occupancy conditions.

Table 2: radon concentrations measured on upper and lower floors with HRV off compared to operated continuously

House #	Season	Time period	PSD installed & operating	Radon (Bq/m <sup>3</sup> ) L floor HRV off	Radon (Bq/m <sup>3</sup> ) L floor HRV cont.	Radon (Bq/m <sup>3</sup> ) U floor HRV off	Radon (Bq/m <sup>3</sup> ) U floor HRV cont.
1	winter	2020-12-23/ 2021-03-03	✗	125 ± 8	77 ± 6	125 ± 8	70 ± 6
2	winter	2020-12-23/ 2021-03-13	✗	91 ± 7	73 ± 6	75 ± 6	57 ± 5
3	winter	2021-01-16/ 2021-03-15	✗	127 ± 8	97 ± 7	123 ± 8	99 ± 7
3	spring	2021-04-19/ 2021-06-15	✓	26 ± 3	17 ± 3	-	-
4	spring	2021-01-29/ 2021-04-07	✗	208 ± 12	101 ± 7	156 ± 10	77 ± 6
4	fall	2021-11-06/ 2022-01-01	✓	110 ± 8	61 ± 5	78 ± 6	49 ± 4
5	spring	2021-01-28/ 2021-04-02	✗	104 ± 7	57 ± 5	98 ± 7	52 ± 5
6	spring	2021-02-17/ 2021-04-19	✗	309 ± 17	162 ± 10	174 ± 11	140 ± 9
6	summer	2021-05-19/	✓	119 ± 8	43 ± 4	80 ± 6	34 ± 4

7	spring	2021-07-26 2021-03-19/ 2021-05-26	✗	109 ± 7	58 ± 5	54 ± 5	24 ± 3
8	summer	2021-05-17/ 2021-07-16	✓	134 ± 9	57 ± 5	108 ± 7	50 ± 5
9	winter	2021-02-10/ 2021-04-07	✗	312 ± 18	171 ± 7	299 ± 17	160 ± 7
10	winter	2021-01-08/ 2021-02-19	✗	166 ± 10	95 ± 7	181 ± 11	92 ± 7
11	winter	2021-01-08/ 2021-02-19	✗	184 ± 11	65 ± 5	-	-
12	spring	2021-03-26/ 2021-05-27	✗	259 ± 15	68 ± 5	150 ± 10	14 ± 3
13	fall	2021-10-29/ 2021-12-24	✓	217 ± 13	164 ± 10	174 ± 11	150 ± 10
14	winter	2022-11-04/ 2023-01-06	✗	220 ± 13	108 ± 7	217 ± 13	91 ± 7
15	winter	2022-11-21/ 2023-01-16	✗	241 ± 14	177 ± 11	183 ± 11	94 ± 7
16	winter	2022-11-29/ 2023-02-11	✗	104 ± 7	61 ± 5	50 ± 5	37 ± 4

The effectiveness of the radon reduction was calculated from the indoor radon concentration with the HRV operating compared to the HRV turned off as described in Equation 1:

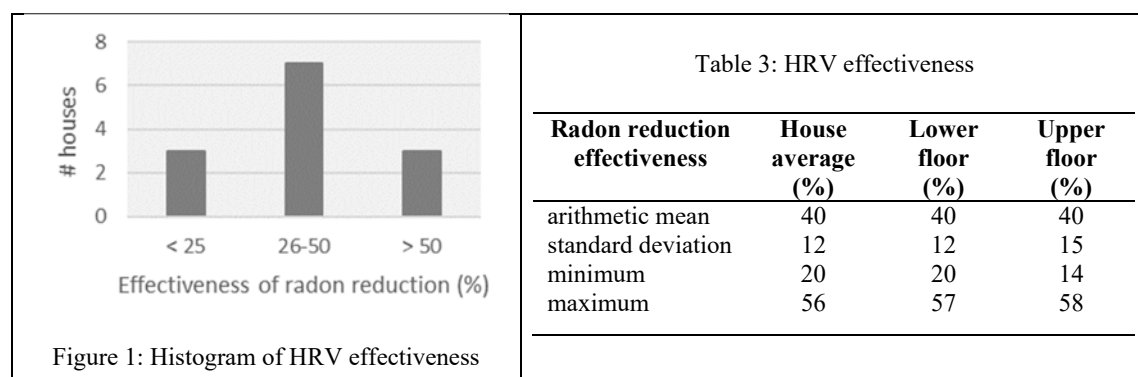
$$\text{effectiveness} = 100 (1 - C_{\text{HRV\_on}} / C_{\text{HRV\_off}}) \quad (1)$$

where:

$C_{\text{HRV\_on}}$  – average indoor radon concentration with HRV in operation

$C_{\text{HRV\_off}}$  – average indoor radon concentration with HRV off

The indoor radon concentration was reduced by the continuous operation of the HRV system in every study house. The average effectiveness of the HRV at reducing indoor radon when operated continuously, for the 13 study houses that had forced air furnace heating and measurements on both lower and upper floors, was normally distributed (see Figure 1) with an arithmetic mean of 40% and a standard deviation of 12% (see Table 3). The highest effectiveness at reducing radon was for the occupied house with electric baseboard heating, at 80%, where the independently ducted HRV supplied outdoor air to the main living area and exhausted basement air. While the arithmetic mean radon reduction was the same on the lower and upper floors measured in the 14 houses that had a forced air furnace when an HRV was operated continuously at the higher design fan speed, there was wider distribution for the upper than the lower floor.



The average radon reduction of 40% measured in this study is consistent with the results of a Finnish study, which reported that indoor radon concentrations were 20 to 47% lower in houses with mechanical supply and exhaust ventilation systems with heat recovery than in houses with mechanical exhaust only (Arvela et al., 2014). The average effectiveness of radon reduction may be a little higher for houses in this study because it was determined from indoor radon concentrations measured before and after the recent installation and balancing in each study house of an HRV system operated continuously at the design fan speed.

The trends in indoor radon reduction by HRV setting was plotted in Figure 2 for the 8 study houses in which more than two HRV settings were assessed. An overall trend of higher reduction effectiveness for continuous than periodic fan operation and for higher than lower fan speed was evident, although in some houses there was little difference in indoor radon concentration between lower or higher fan speed for continuous HRV operation.

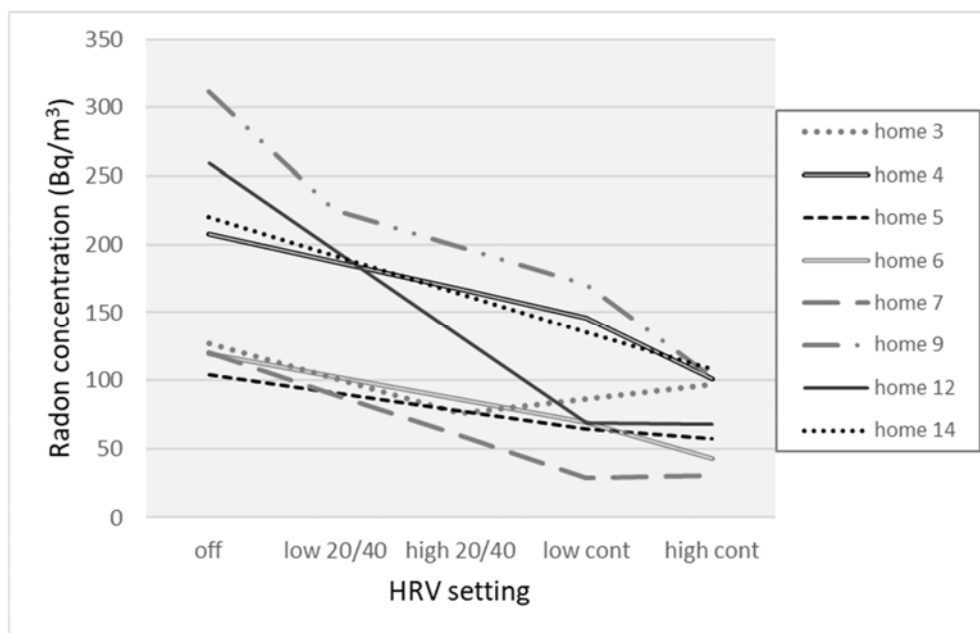


Figure 2: Trends in lower floor radon concentration with HRV setting

The indoor radon concentrations in houses when the HRV was operated in combination with the PSD radon mitigation system are presented in Table 4. The indoor radon concentration was much lower in each floor in every study house when the passive radon depressurization mitigation system was operating. As before, the operation of the HRV system always reduced the indoor radon concentration, both used with and without a PSD radon mitigation system. In three houses, a somewhat higher effectiveness in radon reduction was observed on each floor from the continuous operation of the HRV system when the PSD system was operating also, but in the fourth house the opposite was observed. A similar average radon reduction was observed for continuous HRV operation with and without the PSD radon mitigation system, at 42% and 40% on the lower floor, respectively, and 36% and 27% on the upper floor, respectively. This observation of similar effectiveness of radon reduction for HRV operation with and without a PSD system operating is consistent with the independent operation of the two systems, where the sub-slab depressurization system reduces the ingress of radon indoors from the soil and the HRV system subsequently reduces indoor radon concentration by dilution. The indoor radon concentrations measured in study house 13 during both shoulder seasons for

different HRV settings (fall and spring) were included in this table due to the relatively small number of homes used to compare the effectiveness of radon reduction using HRV with and without the PSD system operating. In study house #13, both a passive radon depressurization system and an HRV were required to reduce the indoor radon concentration below the recommended mitigation threshold of 200 Bq/m<sup>3</sup> for existing housing in Canada. This result was consistent with Norwegian studies that reported significantly lower indoor radon and separate effects identified in multivariate regression for balanced mechanical supply and exhaust ventilation with heat recovery and for a passive radon depressurization system in houses built after the 2010 building code change in Norway (Finne et al., 2019; Haanes et al., 2022).

Table 4: initial radon concentrations and effectiveness of radon reduction on upper and lower floors from HRV operated continuously, with and without passive radon mitigation system operating

House #	Season	Time period	PSD operating	Initial radon (Bq/m <sup>3</sup> )	Reduction effectiveness (%)	Initial radon (Bq/m <sup>3</sup> )	Reduction effectiveness (%)
				L floor HRV off	L floor HRV cont.	U floor HRV off	U floor HRV cont.
3	winter	2021-01-16/ 2021-03-15	✗	127 ± 8	24%	123 ± 8	20%
3	spring	2021-04-19/ 2021-06-15	✓	26 ± 3	35%	-	-
4	spring	2021-03-07/ 2021-05-07	✗	146 ± 9	31%	128 ± 8	40%
4	fall	2021-11-06/ 2022-01-01	✓	110 ± 8	45%	78 ± 6	37%
6	spring	2021-02-17/ 2021-04-19	✗	309 ± 17	48%	174 ± 11	20%
6	summer	2021-05-19/ 2021-07-26	✓	119 ± 8	64%	80 ± 6	58%
13	heating	2021-09-28/ 2022-03-01	✗	593 ± 32	56%	348 ± 19	29%
13	fall	2021-10-29/ 2021-12-24	✓	217 ± 13	24%	174 ± 11	14%

Note: the HRV was operated continuously at low speed for House #4 but at the higher design speed for the other houses, for house #6 the heating season measurements were of one month duration each but not measured consecutively.

This study estimated the upper limit of the effectiveness of HRV systems to reduce indoor radon concentrations. The residential HRV systems were recently installed and balanced by a certified individual, and therefore did not incorporate any changes over time due to differences in maintenance activities, such as the frequency of filter and duct cleaning. The HRV settings evaluated were measured during consecutive periods within a season to reduce confounding from other factors that can influence indoor radon concentration. The design, installation, commissioning, operation and maintenance lower have all been reported to affect ventilation effectiveness by the Canadian Mortgage and Housing Corporation, and can result in problems ranging from poor ventilation to complete system failure (CMHC, 2017). Residents may also choose to operate their HRV systems intermittently and at lower fan speeds to reduce energy consumption, and this should be considered before extrapolating the results of this study to the general population. The impact of residential HRV operation modes on energy consumption and effectiveness of indoor radon reduction have recently been evaluated (Jiránek and Kačmaříková, 2020).



Improving the energy efficiency of housing is an important part of Canada's plan to address climate change and to meet its 2030 and 2050 commitments to reduce emissions (Environment and Climate Change Canada, 2020). New energy efficient housing designs that incorporated adequate balanced mechanical ventilation systems have been reported to have lower indoor radon than conventional housing having mechanical exhaust only ventilation (Arvela et al., 2014; McCarron et al., 2020; Ringer, 2014). The presence of balanced mechanical ventilation systems with heat recovery may be sufficient to prevent an increase in indoor radon in housing undergoing energy efficiency retrofits (Du et al., 2019; Jiránek and Kačmaříková, 2020). Future studies will be conducted to evaluate the effectiveness as a radon control measure of HRV systems incorporated into housing undergoing energy efficiency retrofits and HRV systems included in new energy efficient housing designs in Canada.

#### 4 CONCLUSIONS

The arithmetic mean average indoor radon was reduced by 40% with a standard deviation of 12% for continuous HRV operation in the 13 study houses with forced air furnace heating systems, ranging from a minimum reduction of 20% to a maximum of 56%. An overall trend of more effective reduction was observed for continuous than periodic fan operation for houses in which more than two HRV settings were assessed. In the eight study houses with a passive radon depressurization mitigation system, a similar average radon reduction was observed for continuous HRV operation with and without the passive radon depressurization system operating. Well designed and installed HRV systems were effective at reducing the moderate initial indoor radon concentrations measured in these houses that lacked a balanced mechanical supply and exhaust ventilation system. In one house, both a passive radon depressurization system and an HRV were required to reduce the indoor radon concentration below the recommended mitigation threshold of 200 Bq/m<sup>3</sup> for existing housing in Canada.

#### 5 REFERENCES

- Arvela, H., Holmgren, O., Reisbacka, H., Vinha, J., 2014. Review of low-energy construction, air tightness, ventilation strategies and indoor radon: Results from Finnish houses and apartments. *Radiat Prot Dosimetry* 162, 351–363. <https://doi.org/10.1093/rpd/nct278>
- Chen, J., Moir, D., Whyte, J., 2012. Canadian population risk of radon induced lung cancer: A re-assessment based on the recent cross-Canada radon survey. *Radiat Prot Dosimetry* 152, 9–13. <https://doi.org/10.1093/rpd/ncs147>
- CMHC, 2017. Survey of HRV/ERV Performance Issues in Canada's Near North and Far North: Final Report.
- Du, L., Leivo, V., Prasauskas, T., Täubel, M., Martuzevicius, D., Haverinen-Shaughnessy, U., 2019. Effects of energy retrofits on Indoor Air Quality in multifamily buildings. *Indoor Air* 29, 686–697. <https://doi.org/10.1111/ina.12555>
- Environment and Climate Change Canada, 2020. A healthy environment and a healthy economy [WWW Document]. URL <https://www.canada.ca/en/services/environment/weather/climatechange/climate-plan/climate-plan-overview/healthy-environment-healthy-economy.html>
- Finne, I.E., Kolstad, T., Larsson, M., Olsen, B., Prendergast, J., Rudjord, A.L., 2019. Significant reduction in indoor radon in newly built houses. *J Environ Radioact* 196, 259–263. <https://doi.org/10.1016/j.jenvrad.2018.01.013>

- Gaskin, J., Coyle, D., Whyte, J., Krewski, D., 2018. Global Estimate of Lung Cancer Mortality Attributable to Residential Radon. *Environ Health Perspect* 126, 057009. <https://doi.org/10.1289/EHP2503>
- Haanes, H., Kolstad, T., Finne, I.E., Olsen, B., 2022. The effect of new building regulations on indoor radon in radonprone municipalities. *Journal of the European Radon Association*. <https://doi.org/10.35815/radon.v3.7886>
- Health Canada, 2017. *Guide for Radon Measurements in Residential Dwellings (Homes)*. Ottawa, Canada.
- Jiránek, M., Kačmaříková, V., 2020. Applicability of ventilation systems for reducing the indoor radon concentration. *Radiat Prot Dosimetry* 191, 202–208. <https://doi.org/10.1093/rpd/naa148>
- Khan, S.M., Pearson, D.D., Rönnqvist, T., Nielsen, M.E., Taron, J.M., Goodarzi, A.A., 2021. Rising Canadian and falling Swedish radon gas exposure as a consequence of 20th to 21st century residential build practices. *Sci Rep* 11, 1–15. <https://doi.org/10.1038/s41598-021-96928-x>
- McCarron, B., Meng, X., Colclough, S., 2020. An investigation into indoor radon concentrations in certified passive house homes. *Int J Environ Res Public Health* 17, 1–13. <https://doi.org/10.3390/ijerph17114149>
- Natural Resources Canada, 2012. 2012 R-2000 standard. Office of Energy Efficiency.
- Ringer, W., 2014. Monitoring trends in civil engineering and their effect on indoor radon. *Radiat Prot Dosimetry* 160, 38–42. <https://doi.org/10.1093/rpd/ncu107>
- Suzuki, G., Yamaguchi, I., Ogata, H., Sugiyama, H., Yonehara, H., Kasagi, F., Fujiwara, S., Tatsukawa, Y., Mori, I., Kimura, S., 2010. A nation-wide survey on indoor radon from 2007 to 2010 in Japan. *J Radiat Res* 51, 683–689. <https://doi.org/10.1269/jrr.10083>
- Tondel, M., Andersson, E.M., Barregard, L., 2009. Time Trends in Indoor Radon Concentrations in Sweden. *Epidemiology* 20, S146. <https://doi.org/10.1097/01.ede.0000362499.63328.36>
- Valmari, T., Mäkeläinen, I., Reisbacka, H., Arvela, H., 2011. Finnish radon situation analysed using national measurement database. *Radiat Prot Dosimetry* 145, 101–106. <https://doi.org/10.1093/rpd/ncr075>
- World Health Organization, 2009. *Who Handbook on Indoor Radon*.

# Passive sumps as a method of reducing radon levels in Irish dwellings

Alison Dowdall<sup>1</sup>

*1 Environmental Protection Agency, Dublin.  
McCumiskey House  
Richview  
Clonskeagh Road  
Dublin 14  
D14 YR62*

*\*Corresponding author: A.Dowdall@epa.ie*

## KEYWORDS

Radon Remediation, mitigation, radon, Passive sumps

## 1 INTRODUCTION

Radon gas is the second biggest cause of lung cancer after smoking and is directly linked to approximately 350 lung cancer cases in Ireland each year. It is a serious public health hazard, and the Government has published a National Radon Control Strategy to tackle the problem. The most cost-effective way of protecting the population from radon is to ensure that new dwellings are built to prevent the entry of this gas from below the building.

The two methods most commonly used to protect new buildings from radon are the installation of a radon membrane and a mechanism to depressurize the building. Since 1998, Irish Building Regulations have required that all new dwellings are fitted with a capped standby sump which can be activated if high radon levels are measured. Dwellings built in areas that are more at risk from radon (High Radon Areas) are also required to have a radon membrane installed. EPA data has shown a decrease of 13% in the average indoor radon level in Irish dwellings since the introduction of these requirements.

The protection of new buildings through depressurisation has been successfully achieved in other countries through the installation of a passive radon sump. The application of this simple, effective and inexpensive measure in Irish dwellings was researched by University of Galway in laboratory studies. This research showed that passive radon sumps have significant potential to reduce indoor radon levels and that the fitting of a static cowl to the passive sump increased its effectiveness. A limitation of the University of Galway study was that the system was not tested with natural wind conditions in dwellings.

## 2 METHODOLOGY

To address this limitation, a field trial of passive radon sumps and static cowls was carried out in a sample of Irish houses built to the requirements of the Building Regulations. The study focused on six adjacent, south-east facing houses of identical construction to reduce the factors that cause variations. This meant that the study was carried out under highly controlled conditions.

The radon levels in each of the houses were measured using digital radon monitors over a 6-week period under three test conditions:

1. Passive sump closed (test condition A)
2. Passive sump open (test condition B)
3. Passive sump open with a static cowl installed (test condition C)

### **3 RESULTS AND DISCUSSION**

The results show an average reduction of 65% in radon levels due to the installation of a wind-driven passive sump (test condition B). The number of observations that exceed the Government's Reference Level for dwellings of 200 Bq/m<sup>3</sup> was reduced from 38% to 9% when the passive radon sump was in operation. This result has been confirmed as statistically significant. The cumulative effect of the installation of a passive sump plus a static cowl was an average reduction in radon levels of 75% (test condition C). The number of observations that exceed the Reference Level of 200 Bq/m<sup>3</sup> was reduced from 38% to 0% when a passive radon sump and static cowl were installed. The study concludes that the installation of a passive sump fitted with a static cowl in new houses is a low cost, effective method of reducing radon exposure in new Irish houses.

# Quantify Factors Influencing Radon Flux in Dwellings

Mohsen Pourkiaei<sup>1\*</sup>, Miriam Byrne<sup>2</sup>, Patrick Murphy<sup>3</sup>, James A. McGrath<sup>1</sup>

*1 Maynooth University  
Department of Physics  
County Kildare, Ireland*

*2 School of Natural Sciences,  
University of Galway  
County Galway, Ireland*

*\*Corresponding author: mohsen.pourkiaei@mu.ie*

*3 University College Dublin,  
School of Mathematical Sciences  
County Dublin, Ireland*

## SUMMARY

Radon, a naturally occurring radioactive gas, is a leading cause of lung cancer and has the potential to increase significantly due to current renovation strategies. Understanding the factors influencing radon infiltration into buildings is vital. Radon flux into buildings is a highly dynamic process influenced by various factors. The current study analyses a historical time-series dataset to determine radon entry rates into buildings and identify statistical factors driving the radon flux based on meteorological, environmental, and building characteristics. Through this research and analysis, this project seeks to enhance our understanding of radon factors in dwellings and improve the predictive ability regarding radon within dwellings.

## KEYWORDS

Radon, Indoor Air, Energy Retrofits, Radon Entry Rates, Model Parameterisation.

## INTRODUCTION

Radon ( $^{222}_{86}\text{Rn}$ ) is a naturally occurring radioactive gas and is the leading source of radiation exposure, contributing to 350 cases of lung cancer in Ireland each year [1] and further concerns caused by energy retrofits have already been identified [2]. Radon typically enters buildings from the ground through minuscule gaps in the floor or foundation of the building. However, the rate at which radon enters the building is highly dynamic, even within the same dwelling, and is influenced by several variables, including soil permeability, meteorological conditions, and building ventilation rates [3].

Fluctuations in these variables can cause significant variations in indoor radon levels over short-time period. In order to evaluate radon as part of energy strategies, radon within dwellings needs to be reliably predicted. However, to date, detailed model parameterisation values that account for this dynamic process are lacking. The INFORM project seeks to enhance the understanding of factors that influence radon flux into dwellings, determine model parameterisation values, and ultimately improve indoor radon modelling capabilities.

## MATERIALS

During a previously completed project, real-time monitors (Wave Plus, Airthings, Oslo, Norway) measured radon, temperature, pressure, relative humidity, carbon dioxide, and volatile organic compounds [4]. Long-term measurements were conducted from October 2019 to December 2021 across 87 Irish homes. Sampling was conducted in four zones within each house: the living room, bedroom, kitchen, and bathroom. Radon concentrations were collected hourly, resulting in an extensive dataset of approximately 55 million hourly data points, including additional outdoor meteorological data.

## METHODOLOGY

The radon entry rates (E) are derived using a mass-balance equation (1). E is the dynamic radon entry rate (Bq/h),  $C_{in}$  is the indoor radon concentration (Bq/m<sup>3</sup>) at this time step t,  $C_{out}$  is the

outdoor radon concentration ( $Bq/m^3$ ),  $\lambda_v$  is the air exchange rate ( $h^{-1}$ ),  $\lambda_{Rn}$  is the radon decay constant ( $h^{-1}$ ),  $\lambda_l$  is the building area leakage rate ( $h^{-1}$ ), and  $V$  is the zonal volume.

$$E = \frac{\int [C_{in(t)} - C_{in(t-1)}] e^{-(\lambda_v + \lambda_l + \lambda_{Rn})t} dt}{(1 - e^{-(\lambda_v + \lambda_l + \lambda_{Rn})t})} [V(\lambda_v + \lambda_l + \lambda_{Rn})] - V(\lambda_v)C_{out} \quad (1)$$

## RESULTS

Radon entry fluxes (entry rates per area) were determined based on Equation 1 and preliminary data is presented in Figure 1. Figure 1 shows a box plot of radon entry flux distributions among 84 case studies over 18 months for the living room in each dwelling. As expected, there is considerable variability across the dwellings and within each dwelling, which is reflected by the wide distribution, highlighting the dynamic process. Ongoing analysis is investigating the correlation between the radon entry rates to seasonal and metrological factors to account for this distribution.

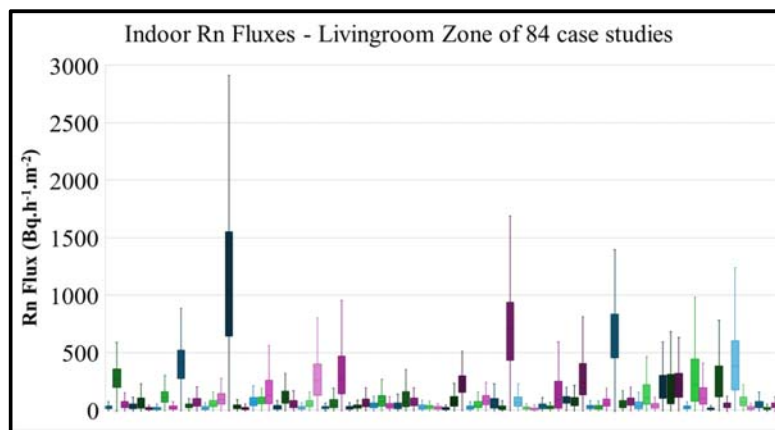


Figure 1. Box plots of radon fluxes distributions of 84 case studies over 18 months.

## CONCLUSION

The initial analysis supports the temporal variation in radon concentrations by accounting for the wide distribution of radon flux rates in dwellings. The following stages will focus on refining the radon fluxes, providing a more detailed understanding of radon dynamics. The study outcomes will enhance modelling capabilities and inform radon mitigation strategies.

## ACKNOWLEDGEMENTS

This research project (Ref: 2022-HE-1120) is funded by the Irish Environmental Protection Agency (EPA) under the Irish EPA Research Programme 2021-2030.

## REFERENCES

1. Murphy, P., Dowdall, A., Long, S., Curtin, B. and Fenton, D., 2021. Estimating population lung cancer risk from radon using a resource efficient stratified population weighted sample survey protocol—Lessons and results from Ireland. *Journal of Environmental Radioactivity*, 233, p.106582.
2. McGrath, J.A., Aghamolaei, R., O'Donnell, J. and Byrne, M.A., 2021. *Factors influencing radon concentration during energy retrofitting in domestic buildings: A computational evaluation*. Building and Environment, 194, p.107712.
3. McGrath, J.A. and Byrne, M.A., 2021. An approach to predicting indoor radon concentration based on depressurisation measurements. *Indoor and Built Environment*, 30(8), pp.1042-1050.
4. McGrath, J. A., & Byrne, M. A., <https://www.universityofgalway.ie/validate/>

# A novel indicator to assess thermal resilience of buildings to overheating

Abantika Sengupta<sup>\*1</sup>, Douaa Al Assaad<sup>1</sup>, Hilde Breesch<sup>1</sup>, and Marijke Steeman<sup>2</sup>

*1 KU Leuven  
Gebroeders de Smetstraat 1  
9000, Gent, Belgium*

*\*Corresponding author :  
abantika.sengupta@kuleuven.be  
Presenting author: Abantika Sengupta*

*2 Ghent University  
Campus Boekentoren - Plateau  
Jozef Plateaustraat 22  
9000 Gent, Belgium*

## ABSTRACT

The increasing frequency and intensity of heatwaves highlight the necessity for resilient building design to reduce heat-stress-related discomfort and mortality among occupants. "Thermal resilience" refers to a building's capacity to endure thermal disruptions, maintain habitable conditions, and return to its intended state. This study aims to develop a thermal resilience indicator to make resilience an actionable concept for architects and HVAC engineers to assess and improve thermal resilience of buildings to overheating. To do this, different building types such as mid-sized offices, schools and apartments were evaluated during 3 different type of heatwaves (severe, intense and long) conducting building energy simulations. Building and system design parameters such as building orientation, envelope and glazing properties, occupancy pattern, airtightness, operation of solar shading and natural night ventilation, cooling capacity and cooling set-points were varied within standard design ranges. This study utilised global sensitivity analysis to identify the most influential design parameters affecting shock impact on heat stress of occupants i.e. degree hours above Standard Effective Temperature (SET-Dh) of 28°C. Sensitivity analysis revealed that for all three increasing shocks, and two cooling systems (convective and radiant), parameters such as window-to-wall ratio (WWR), cooling capacity, and the operation of passive strategies like natural night ventilation (NNV) and solar shading had twice the influence compared to building orientation, envelope and glazing properties, occupancy pattern, airtightness, and cooling set-point. Based on the results of the sensitivity analysis, regression models/thermal resilience indicators were developed to predict SET-Dh for each type of buildings- office, apartments and classrooms during 3 increasing shocks. The indicator is based on the most influential design parameters and the impact of overheating on the occupants health during increasing degree of shock (in this case, different types of heatwaves). The performance of the developed indicators are tested on two case study building type-(a) office and (b) residential buildings during 2 heatwaves. This research aims to guide architects, engineers, and policymakers in assessing and enhancing buildings' ability to withstand and recover from overheating risk.

## KEYWORDS

Heatwaves, Thermal resilience to overheating, Resilient design, Standard Effective Temperature, Thermal resilience indicator

## 1. INTRODUCTION

Overheating in buildings during heatwaves elevates core-body temperatures, disrupting essential bodily functions and causing heat-related illnesses like sleep deprivation, heat stroke, and even death [2]. Historical data shows increased mortality during heatwaves in Europe [3]. By 2050, such heatwaves are expected to become more frequent, potentially increasing heat-related mortality by 257% [4]. This underscores the urgent need to enhance buildings' thermal

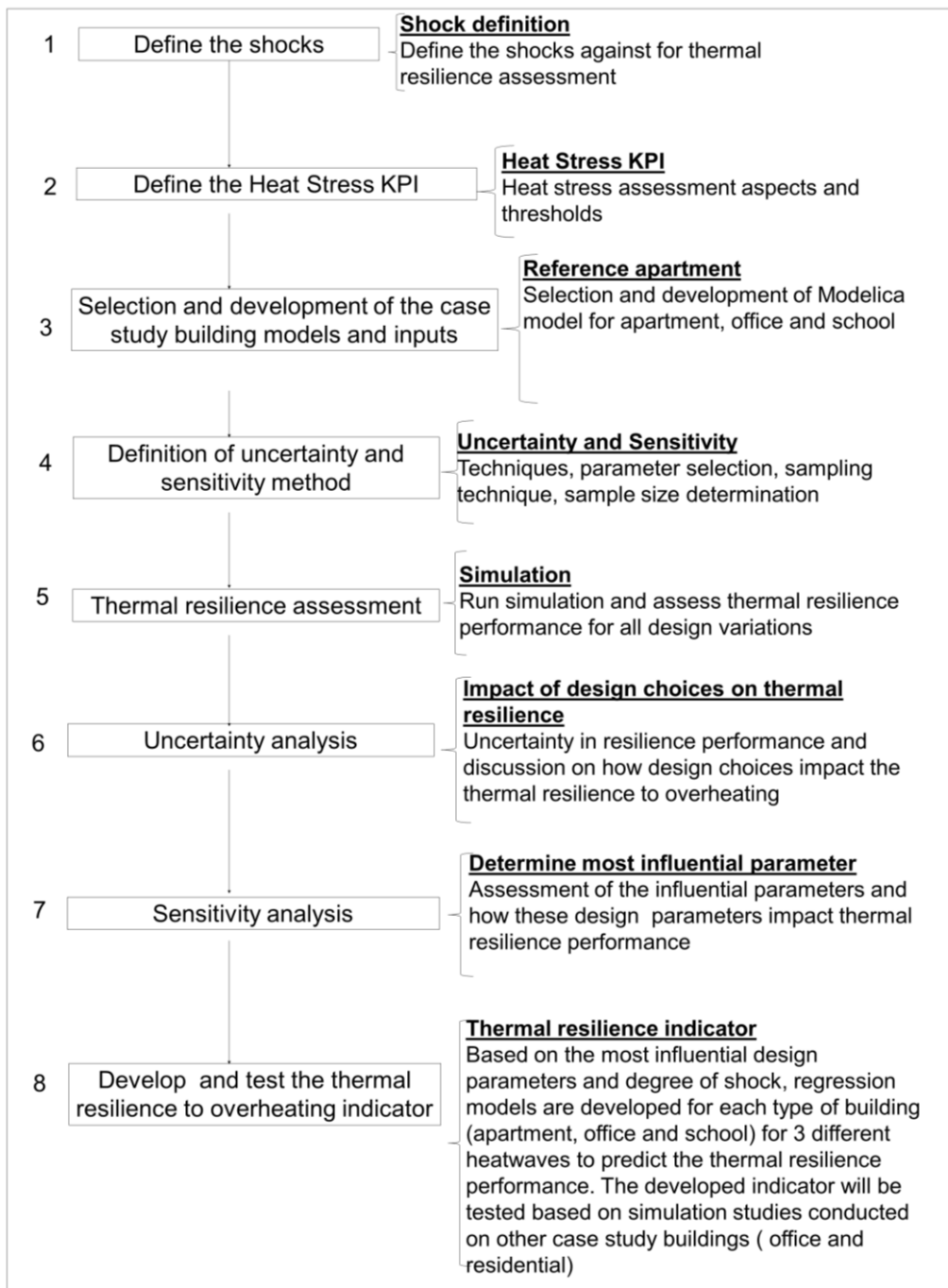
resilience. The IEA EBC Annex 80 defines thermal resilience as a building's ability to withstand disruptive thermal events, maintain habitable conditions, and recover to its designed state [5]. Studies have both qualitatively and quantitatively evaluated building thermal resilience [6] [7]. Research has also focused on developing resilience assessment frameworks, such as, Zhang et al. [8] outlined criteria such as absorptive, adaptive, and restorative capacities, while Ji et al. [9] created a Thermal Resilience Index linking performance with occupants' predicted heat strain. Despite these advancements, existing methods often fail to compare resilience across varying shocks and overlook the influence of building parameters.

To address this, Sengupta et al. [10] introduced the degree of shock (*doS*) metric to compare varying thermal shocks and test buildings and systems' thermal resilience performance and identify the most influential design parameters affecting thermal resilience. This study focuses on developing a thermal resilience indicator to assess and improve thermal resilience to overheating in buildings.

## 2. METHODOLOGY

The methodology for this study involves a structured, eight-step process (see **Figure 1**) to develop and test the novel thermal resilience indicator. Initially, shocks such as heatwaves are defined in step 1 to establish the context for resilience assessment. Key Performance Indicators (KPIs) are then determined in step 2, focusing on critical aspects and thresholds of thermal resilience. Subsequently, reference buildings, including apartments, offices, and schools, are selected, and detailed Modelica models are developed for these structures in step 3. Uncertainty and sensitivity methods are defined in step 4, encompassing parameter selection, sampling techniques, and sample size determination. Simulations are conducted in step 5 to assess the thermal resilience performance of the models under various design variations. An uncertainty analysis is performed in step 6 to understand the impact of design choices on resilience, followed by a sensitivity analysis in step 7 to identify the most influential design parameters. Finally, regression models are developed in step 8 to predict thermal resilience performance, resulting in the creation of a thermal resilience to overheating indicator for different building types and heatwave scenarios. Furthermore, the developed thermal resilience indicator is evaluated based on the simulation studies conducted by the project partners of the project 'ReCOVer++: Improving resilience of buildings to overheating' [11] in their case study buildings- mainly offices and residential buildings. The research process involves first defining the shocks relevant to thermal resilience assessment, followed by establishing key performance indicators (KPI) for heat stress, including assessment aspects and thresholds. Next, case study building models (such as apartments, offices, and schools) are selected and developed, with Modelica. The research then defines the methods for uncertainty and sensitivity analysis, determining the appropriate techniques, parameters, and sampling methods. Simulations are run to assess thermal resilience performance across different design variations. Following this, an uncertainty analysis is conducted to evaluate how design choices impact thermal resilience, and a sensitivity analysis identifies the most influential parameters. Finally, regression models are developed to predict thermal resilience based on these parameters, and these models are tested on other case study buildings to refine and validate the thermal resilience indicator.





**Figure 1.** Methodology to develop the thermal resilience indicator

## 2.1. Shock definition

A shock is defined as a sudden disturbance that causes the building to deviate partially or completely from its designed conditions for a certain period. This disruption tests the resilience performance of buildings. Shocks are characterized by both severity and duration which triggers different thermal response from the building. To evaluate and compare the impact of different shocks and determine most influential design parameter affecting building's thermal resilience it is essential to define, classify, and quantify these disturbances. In a prior study, Sengupta et al. [10] classified and quantified normalized degree of shock (*doS*) to compare different shock types. The study demonstrated that heatwaves notably affect buildings more than system shocks, emerging as the most severe shocks due to their effects on temperature and passive cooling strategies. Highlighting the growing frequency and severity of

heatwaves in current and future climate scenario, this study focused on different heatwaves. Normalized  $doS$  for heatwaves is expressed as:

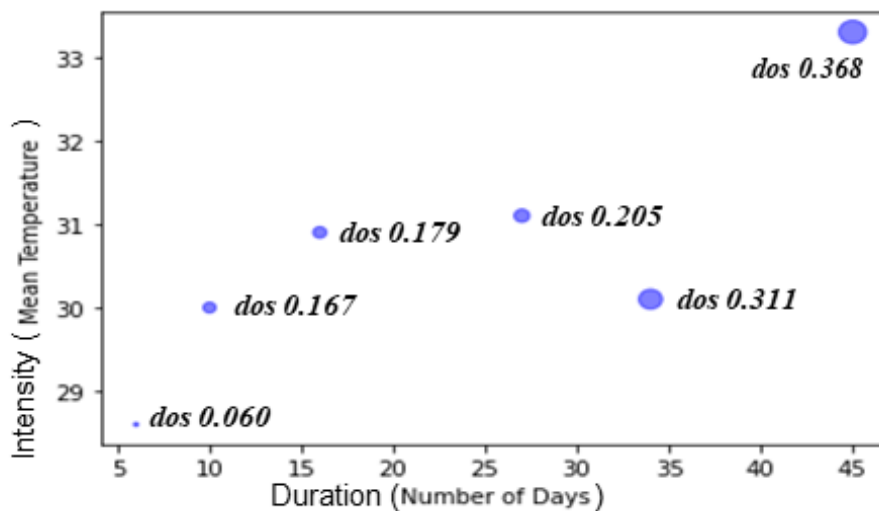
$$doS = \underbrace{\frac{T_{shock} - T_{ref}}{T_{ref}}}_{Severity} \times \underbrace{\frac{t_{shock}}{t_{ref}}}_{Duration} \quad (1)$$

For this study, three heatwaves with increasing  $doS$  (low, medium and high) were selected from six different extreme heatwaves predicted for Ghent for a period between 2001-2100 (see **Table.1** and **Fig.2**). The extreme weather datasets were developed using the methodology developed by the IEA EBC Annex 80 [12].

**Table 1.**  $doS$  of the 6 extreme (severe, intense and longest ) heatwaves for Ghent (Belgium) between 2001-2100

Heatwave period and ID	$T_{shock}$ ( average temperature during heatwave)	$T_{ref}$ (average outdoor temperature during corresponding TMY period)	$t_{shock}$ ( Duration of heatwave in days)	$t_{ref}$ (duration of the longest heatwave in days)	$doS$
Contemporary 1A	26.8	15	10	45	0.167
Contemporary 1B	25	18.6	27	45	0.205
Mid-term 2A ( <b>doS<sub>low</sub></b> )*	24.9	17.1	6	45	<b>0.060</b>
Mid-term 2B ( <b>doS<sub>medium</sub></b> )*	26.3	17.5	16	45	<b>0.179</b>
Long-term 3A	25.3	17.9	34	45	0.311
Long-term 3B ( <b>doS<sub>high</sub></b> )*	25.7	18.8	45	45	<b>0.368</b>

\*Selected  $doS$  for this study



**Figure 2.**  $doS$  (diameter of each circle) with duration in days (x -axis) and the mean temperature during HWs (y-axis left)

## 2.2. Heat stress Index

To evaluate shock impact, it is crucial to select a rational heat-stress index that considers multiple indoor environmental parameters (temperature, RH, air velocity, etc.) and occupants' physiological responses (sweat rate, core temperature, heart rate, etc.). The Standard Effective Temperature (SET), based on the two-node physiological model by Gagge et al. [13] and recommended by ASHRAE Standard 55 [14], is a widely accepted metric. Hourly SET was calculated based on [15]. Previous studies have linked SET to human-predicted thermal sensation according to the ASHRAE 7-point scale [16], establishing three SET thresholds: SET-comfortable (24.1°C), SET-alert (28.1°C), and SET-emergency (32.1°C)[9]. These thresholds define habitable, heat alert, and emergency levels, impacting occupants' health based on exposure time. Set-Dh [17] was adopted to assess shock impact. SET-Dh was defined as :

$$SET - Dh = \sum_{t=1}^N (SET(t) - 28) * \Delta t \quad (2)$$

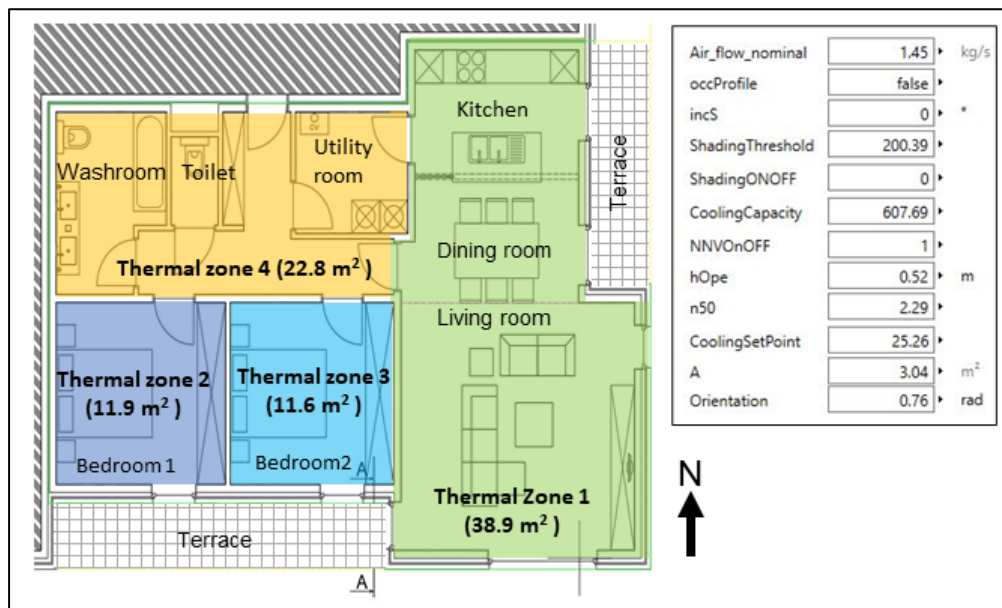
Where, SET-Dh represents the total degree-hours above 28°C,  $SET(t)$  is the Standard Effective Temperature at time  $t$ , 28 the SET-alert threshold and  $\Delta t$  is the duration of each time interval (typically one hour). Dynamic metabolism (met) and clothing resistance (clo) for day and night were utilized in the calculations. Overheating is declared when SET-Dh exceeds  $230 \pm 42$  °C\*h for young healthy adults and  $117 \pm 30$  °C\*h for older adults [18]. Higher shock impact indicates lower thermal resilience to overheating. The buildings and system have higher thermal resilience if SET 28°C threshold is not violated.

## 2.3. Case study buildings

### 2.3.1. Reference apartment-case study for the development of thermal resilience indicator

Unique floor plans for a reference apartment in Belgium were developed, while maintaining some degree of freedom (floor area, number of bedrooms, open/closed kitchen, number of surfaces exposed to external conditions, level of apartment-ground, middle or upper floor), in order to perform parametric study. The floor plans are based on information of Flemish Energy and Climate Agency (VEKA) [19] data from 2016 to 2020 (new buildings).

**Figure 3** illustrates the plan of the selected reference apartment showing the four thermal zones (TZs). The default apartment has a brick wall with external insulation resulting in a U-value of 0.24 W/m<sup>2</sup>K and has heavy thermal mass according to the EN ISO 13790 [20]. The separating floors and common walls connecting the apartment to common space were modelled as adiabatic. Since the apartment is situated between upper and lower floors, the floors and ceilings are considered airtight. The sensible and latent heat generation from occupants are 75 W and 45 W respectively during sedentary activities [21]. For lighting, 300 lux of illuminance in each bedroom, 400 lux in kitchen and living room, 70 lux in corridor and 500 lux in washroom and toilet [22]. The lights turned on when occupants are present and are considered off during night time (10.00 p.m. to 7.00 a.m.). More details of the reference apartment can be found in **Table 2**.



**Figure 3.** Plan of the reference apartment

**Table 2.** Characteristics of the reference apartment and ranges of the parameters tested

Parameters	Default value for the reference apartment	Ranges to be varied for the uncertainty and sensitivity analysis
Number of occupants Internal gains (people, and equipment) calculated according to EN 16798-1 [23].	3	-
Net floor are (m <sup>2</sup> )	85.2	-
Floor Height (m)	2.55	-
Orientation of living room and bedroom	0° (South)	0°-360°
Airtightness n50 (h <sup>-1</sup> )	1.47	0.6-3
Thermal mass (according to EN ISO 13790 [20])	Heavy	Heavy-Medium-Light
External envelope U-value (W/m <sup>2</sup> K) Brick wall with external insulation	0.24	0.1-0.3
U-value of the window (double glazed windows)	U-value = 1.00 W/m <sup>2</sup> K g-value = 0.56	0.6-1.0
Window-to-wall ratio (WWR)	25%	25-75%
Solar shading operation	ON	ON-OFF

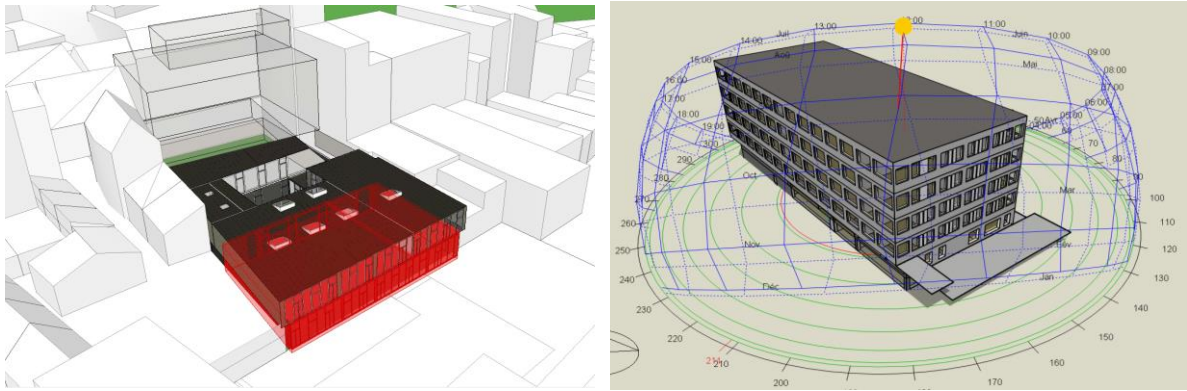
Solar shading threshold (W/m <sup>2</sup> )	250	100-300
Cooling setpoint	25°C	24°C-26°C
Cooling capacity(W/m <sup>2</sup> )	21	0-40
Natural Night Ventilation (NNV) Operation	ON	ON-OFF
Effective opening area of windows for NNV expressed as % of floor area	4%	1-8%

### 2.3.2. Case study buildings for testing thermal resilience indicator

To test the developed thermal resilience indicator 3 case study buildings are selected. **Table 3** shows the details of each of the demonstration case study details. The details of Office 01 (case study -Archipelago) and residential ( Renson concept home) can be found in [1].

**Table 3.** Details of the case study office and residential building to test the developed Thermal Resilience Indicator

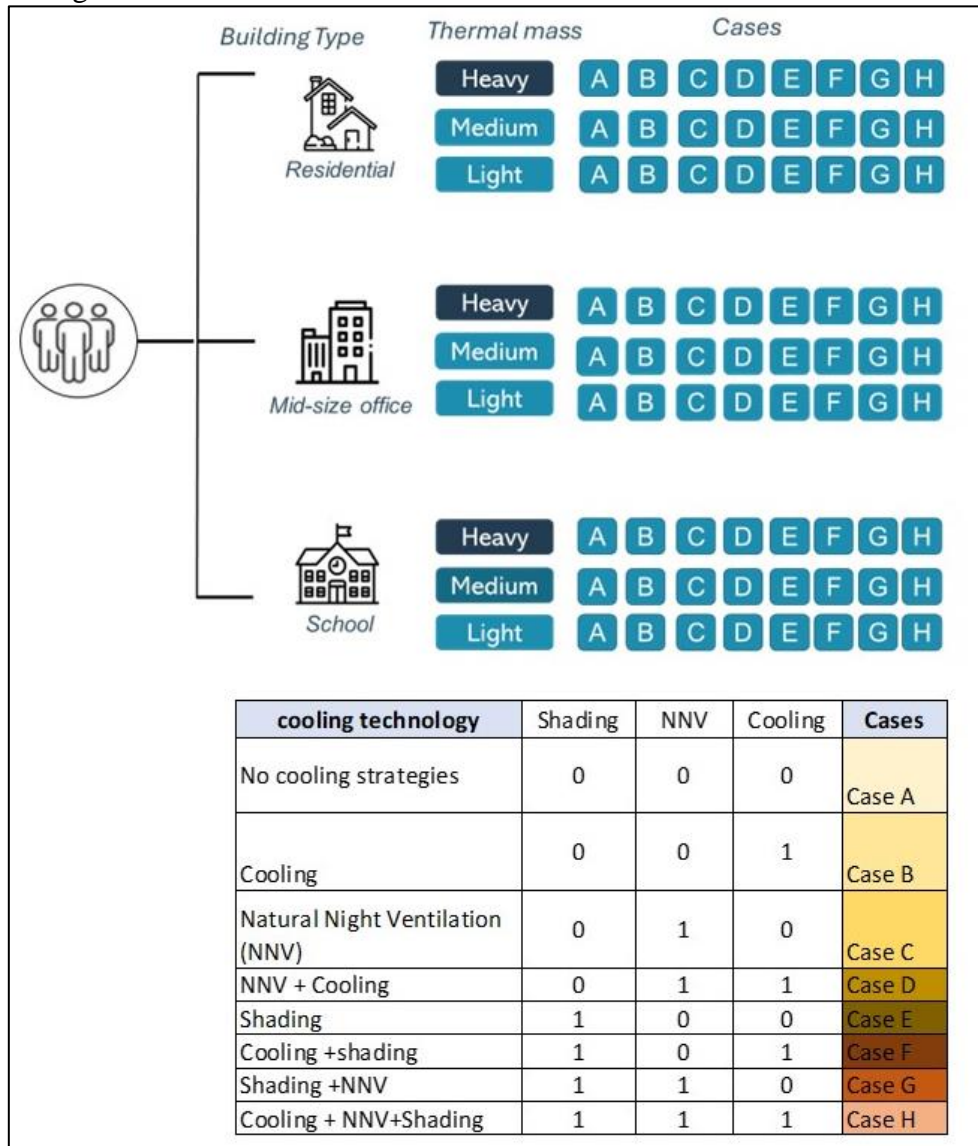
Building Type	Residential	Office 01	Office 02
Thermal zones	4	3	2
u-value of external wall (W/m <sup>2</sup> K)	0.15	0.16	0.14
u-value of glazing (W/m <sup>2</sup> K)	1	1.06	1
Occupant density (m <sup>2</sup> /per person)	28.5	10	10
Occupied hours	Always present at least 1 occupant	From 8h to 17h	From 8h to 17h
Ventilation rates (m <sup>3</sup> /h per person)	30 for bedrooms (it varies depending on the zone type)	42	40
Thermal mass	Medium	Medium	Medium
Building orientation	South-east	North-east	South-east
WWR (%)	49.1	41.3	33
Air tightness (n50)	3	0.5	1
Solar shading threshold (external blinds)	300	100	250
Effective window opening area for natural night ventilation (represented as % of floor area)	-	4.1	5.3
Cooling set-point (°C)	26	25	26
Cooling capacity (W/m <sup>2</sup> )	30	29.3	38



**Figure 4.** Demonstration case study office buildings (office 01-left, office 02-right)

## 2.4. Development of the thermal resilience indicator

Uncertainty and sensitivity analysis was conducted on 3 building types- (a) office (b) apartment and (c) classrooms during 3 increasing *doS*. Building and system design parameters were varied within the ranges as mentioned in table 2.



**Figure 5.** Decision tree for the development of thermal resilience indicators for different building types, thermal mass and operation of resilient cooling strategies

Uncertainty analysis demonstrated the uncertainty in thermal resilience performance of buildings due to varying design choices. Sensitivity analysis evaluated the most influential design parameters that impact thermal resilience performance. Based on the sensitivity analysis, linear regression models are developed for each type of buildings and each type of *doS*. The validity of the developed regression models are assessed on the simulation study of the case study buildings ( in this paper, the focus is on the office 01). **Figure 5** shows the decision tree of the thermal resilience indicator developed for different building types, thermal mass and operation of systems.

### 3 ACKNOWLEDGEMENTS

This study is performed under the framework of International Energy Agency’s Energy in Buildings and Communities (IEA EBC) Annex 80 - Resilient Cooling of Buildings. This work has been supported by the Flanders Innovation and Entrepreneurship (VLAIO) in the Flux 50 Project ‘ReCOVer++: Improving resilience of buildings to overheating.’

### 4. REFERENCES

- [1] Resilient Cooling Design Guidelines, (n.d.). <https://www.rehva.eu/eshop/detail/resilient-cooling-design-guidelines> (accessed August 12, 2024).
- [2] B.G. Armstrong, Z. Chalabi, B. Fenn, S. Hajat, S. Kovats, A. Milojevic, P. Wilkinson, Association of mortality with high temperatures in a temperate climate: England and Wales, *J. Epidemiol. Community Health*. 65 (2011) 340–345. <https://doi.org/10.1136/jech.2009.093161>.
- [3] P. Pirard, S. Vandentorren, M. Pascal, K. Laaidi, A. Le Tertre, S. Cassadou, M. Ledrans, Summary of the mortality impact assessment of the 2003 heat wave in France., *Euro Surveill*. 10 (2005) 153–156. <https://doi.org/10.2807/ESM.10.07.00554-EN/CITE/REFWORKS>.
- [4] C. Hughes, S. Natarajan, Summer thermal comfort and overheating in the elderly, *Build. Serv. Eng. Res. Technol*. 40 (2019) 426–445. <https://doi.org/10.1177/0143624419844518>.
- [5] IEA EBC || Annex 80 || Resilient Cooling, (n.d.). <http://annex80.iea-ebc.org/> (accessed February 28, 2020).
- [6] A. Sengupta, M. Steeman, H. Breesch, Analysis of Resilience of Ventilative Cooling Technologies in a Case Study Building, *ICRBE Procedia*. (2020). <https://doi.org/10.32438/iCRBE.202041>.
- [7] K. Sun, W. Zhang, Z. Zeng, R. Levinson, M. Wei, T. Hong, Passive cooling designs to improve heat resilience of homes in underserved and vulnerable communities, *Energy Build*. 252 (2021) 111383. <https://doi.org/10.1016/J.ENBUILD.2021.111383>.
- [8] C. Zhang, O.B. Kazanci, R. Levinson, P. Heiselberg, B.W. Olesen, G. Chiesa, B. Sodagar, Z. Ai, S. Selkowitz, M. Zinzi, A. Mahdavi, H. Teufl, M. Kolokotroni, A. Salvati, E. Bozonnet, F. Chtioui, P. Salagnac, R. Rahif, S. Attia, V. Lemort, E. Elnagar, H. Breesch, A. Sengupta, L.L. Wang, D. Qi, P. Stern, N. Yoon, D.I. Bogatu, R.F. Rupp, T. Arghand, S. Javed, J. Akander, A. Hayati, M. Cehlin, S. Sayadi, S. Forghani, H. Zhang, E. Arens, G. Zhang, Resilient cooling strategies – A critical review and qualitative assessment, *Energy Build*. 251 (2021) 111312. <https://doi.org/10.1016/J.ENBUILD.2021.111312>.
- [9] L. Ji, C. Shu, A. Laouadi, M. Lacasse, L. (Leon) Wang, Quantifying improvement of building and zone level thermal resilience by cooling retrofits against summertime heat events, *Build. Environ*. 229 (2023) 109914. <https://doi.org/10.1016/j.buildenv.2022.109914>.
- [10] A. Sengupta, D. Al Assaad, J.B. Bastero, M. Steeman, H. Breesch, Impact of heatwaves and system shocks on a nearly zero energy educational building: Is it resilient to overheating?, *Build. Environ*. 234 (2023). <https://doi.org/10.1016/j.buildenv.2023.110152>.
- [11] ReCOVer++: Improving resilience of buildings to overheating — Department of Architecture and Urban Planning — Ghent University, (n.d.). <https://www.ugent.be/ea/architectuur/en/research/research-projects/all-research-projects/recover-improving-resilience-of-buildings-to-overheating> (accessed November 27, 2023).
- [12] A. Machard, A. Salvati, M.P. Tootkaboni, A. Gaur, J. Zou, Typical and extreme weather datasets for studying the resilience of buildings to climate change and heatwaves, (2024) 1–21. <https://doi.org/10.1038/s41597-024-03319-8>.
- [13] L. Ji, A. Laouadi, C. Shu, L. Wang, M.A. Lacasse, Evaluation and improvement of the thermoregulatory system for the two-node bioheat model, *Energy Build*. 249 (2021) 111235.

- <https://doi.org/10.1016/j.enbuild.2021.111235>.
- [14] Standard 55 – Thermal Environmental Conditions for Human Occupancy, (n.d.). <https://www.ashrae.org/technical-resources/bookstore/standard-55-thermal-environmental-conditions-for-human-occupancy> (accessed April 12, 2023).
- [15] F. Tartarini, S. Schiavon, pythermalcomfort: A Python package for thermal comfort research, *SoftwareX*. 12 (2020) 100578. <https://doi.org/10.1016/j.softx.2020.100578>.
- [16] J. Gao, Y. Wang, P. Wargocki, Comparative analysis of modified PMV models and SET models to predict human thermal sensation in naturally ventilated buildings, *Build. Environ.* 92 (2015) 200–208. <https://doi.org/10.1016/j.buildenv.2015.04.030>.
- [17] L. Ji, C. Shu, A. Laouadi, M. Lacasse, L. (Leon) Wang, Quantifying improvement of building and zone level thermal resilience by cooling retrofits against summertime heat events, *Build. Environ.* 229 (2023) 109914. <https://doi.org/10.1016/j.buildenv.2022.109914>.
- [18] A. Laouadi, M. Bartko, M.A. Lacasse, A new methodology of evaluation of overheating in buildings, *Energy Build.* 226 (2020) 110360. <https://doi.org/10.1016/j.enbuild.2020.110360>.
- [19] Over het Vlaams Energie- en Klimaatagentschap (VEKA) | Vlaanderen.be, (n.d.). <https://www.vlaanderen.be/veka/over-het-vlaams-energie-en-klimaatagentschap-veka> (accessed April 11, 2023).
- [20] C. Sigauke, M.M. Nemukula, Modelling extreme peak electricity demand during a heatwave period: a case study, *Energy Syst.* 11 (2020) 139–161. <https://doi.org/10.1007/s12667-018-0311-y>.
- [21] K. Ahmed, J. Kurnitski, B. Olesen, Data for occupancy internal heat gain calculation in main building categories, *Data Br.* 15 (2017) 1030–1034. <https://doi.org/10.1016/j.dib.2017.10.036>.
- [22] NEN-EN 12464-1:2021 en, (n.d.). <https://www.nen.nl/nen-en-12464-1-2021-en-286866> (accessed March 6, 2024).
- [23] Norm NBN EN 16798-1:2019 | NBN Shop, (n.d.). [https://www.nbn.be/shop/nl/norm/nbn-en-16798-1-2019\\_8687/](https://www.nbn.be/shop/nl/norm/nbn-en-16798-1-2019_8687/) (accessed November 29, 2022).



# Exploring the effect of different measures on thermal resilience: implications for design of HVAC systems and energy use

Debora Resta<sup>\*1</sup>, Bert Lemmens<sup>1</sup>, Hilde Breesch<sup>2</sup>, Abantika Sengupta<sup>2</sup>, Douaa Al-assaad<sup>2</sup>, Steven Delrue<sup>3</sup>, Joost Declercq<sup>4</sup>, and Marijke Steeman<sup>5</sup>

*1 Arcadis  
Markiesstraat 1 Rue du Marquis  
B-1000 Brussels, Belgium  
\*Debora.Resta@arcadis.com  
Presenting author*

*2 KU Leuven  
Faculty of Engineering Technology  
Campus Ghent,  
Gebroeders De Smetstraat 1  
B-9000 Ghent, Belgium*

*3 Renson  
Industriezone 2 Vijverdam -  
Maalbeekstraat 10  
B-8790 Waregem, Belgium*

*4 Archipelago  
Woluwe Gate – 4<sup>th</sup> floor  
Boulevard de la Woluwe 2  
B-1150 Brussels, Belgium*

*5 UGent  
Onderzoeksgroep Bouwfysica  
Campus UFO  
Sint-Pietersnieuwstraat 41  
B-9000 Ghent, Belgium*

## SUMMARY

The commitment to improving the energy efficiency of buildings by 2030, with the goal of achieving carbon neutrality by 2050, has been triggered by environmental challenges and the increasing scarcity of energy resources. To this end, European countries are adopting stricter regulations on building energy consumption, as illustrated by the EPB system in Belgium.

Considering the increase in extreme weather events, the intensity and frequency of heatwaves in many regions of the world, it is essential that buildings are able to adapt to extreme events.

This study evaluates the energy and comfort thermal performance of an office building through energy simulations. The goal is to compare the effectiveness and impact of mechanical air conditioning systems with the implementation of passives strategies. This analysis aims to verify thermal comfort and energy consumption during expected future heatwaves.

## KEYWORDS

Thermal resilience, Energy consumption, Heating and Cooling power, Future Heatwaves

## INTRODUCTION

Over the past decade, there has been a growing emphasis on the thermal resilience of buildings and cooling strategies in various studies. For instance, Attia et al. [1] defines cooling resilience as the ability of the building system to maintain the initial design conditions when faced with disruptions such as heatwaves or power outages.

This study is part of a collaborative project with the objective of identifying a thermal resilience metric that can assess and enhance the resilience of buildings against overheating risks resulting

from climate change-related events (e.g., heatwaves) and operational failures (e.g., blackouts, cooling system malfunctions).

Within this report, we focus specifically on HVAC systems and their impact on building resilience. The analysis delves into how passive and active cooling techniques can assist an office building in mitigating the increasing internal overheating risks posed by mounting external thermal challenges in future climate scenarios.

Amid the backdrop of climate change, cooling strategies play a pivotal role in mitigating the surging impacts of overheating, contributing not only to human comfort but also to environmental sustainability.

In the following section, the methodology employed, and the demonstrative case are described. Section 2 presents the results. Section 3 wraps up the document.

This work has been supported by the Flanders Innovation and Entrepreneurship (VLAIO) in the flux 50 ICON-Project ‘ReCOVer++: Improving resilience of buildings to overheating.’

## 1 METHODOLOGY

The following table shows the research methodology of this article.

Table 1: Methodology

Methodology
<u>Weather data:</u> HW weather data based on CORDEX (RCP 8.5 scenario) for midterm 2043 and 2051
<u>Building typology:</u> Office building
<u>Cooling strategies:</u> <ul style="list-style-type: none"><li>- Solar shading</li><li>- Natural Night cooling</li><li>- Mechanical cooling</li><li>- Free mechanical cooling</li></ul>
<u>Performance evaluation:</u> <ul style="list-style-type: none"><li>- CD and HD : Cooling demand and heating demand [kWh/m<sup>2</sup>]</li><li>- HP and CP : Heating and Cooling power [W/m<sup>2</sup>]</li><li>- CEP : Primary energy consumption [kWh<sub>ep</sub>/m<sup>2</sup>]</li><li>- GES : gas emission CO<sub>2</sub> [tCO<sub>2</sub>]</li><li>- Tair : Indoor air temperature</li><li>- Top : Indoor operative temperature</li><li>- EH28A : Annual Exceedance Hours when the Top ≥ 28°C</li><li>- EH28HW : Exceedance Hours during Heatwaves Period when the Top ≥ 28°C</li></ul>

### 1.1 Simulation Program

In this document, to conduct the simulations, the software DesignBuilder 7.0.2.006 based on the simulation engine EnergyPlus Version 9.4.0.002 is used.

EnergyPlus is developed by the US Department of Energy (US DOE) as one of the twenty main building energy simulation programs to run the simulations. EnergyPlus contains an integrated thermal and mass balance module and a building system module. The simulation results are then post-processed to calculate the results values.

## 1.2 Demonstration Case

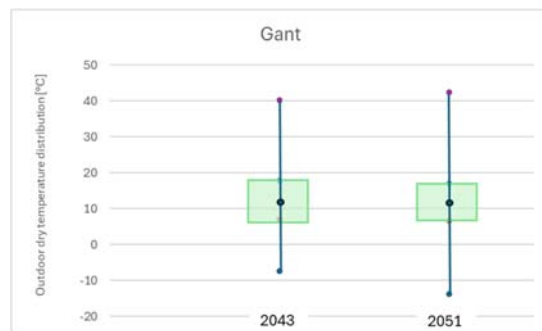
This section describes a demonstration case to compare the thermal performance to overheating due to climate change by simulating various passive and active cooling strategies and assessing the HVAC's impact on the building.

### 1.2.1 Weather data

The project, as described in the "case study" chapter, is located in Ghent. Ghent University has provided two future meteorological scenarios for 2043 and 2051, corresponding to medium-term heatwaves with the highest intensity and severity, respectively. The table and figure below show the annual distribution of hourly outdoor air temperature for Scenario 2043 and 2051.

Table 2: Weather data

Outside temperature	HW 2043	HW 2051
Min	-7.4	-13.7
Percentile 25%	7.0	6.7
Median	11.8	11.5
Percentile 75%	17.8	17.1
Max	40.2	42.4
AWD <sup>1</sup>	11.33	13.29
CDH 18°	9.289	8.401



The two climates under consideration show a substantial increase in the maximum outdoor temperature of 6/8°C compared to current standardized climates and a doubling of cooling hours compared to 2024, and a decrease in heating hours by approximately 15%.

### 1.2.2 Case study

The case study is an office and laboratory building located in Ghent. It is a new project currently being studied by ARCADIS.

Here is an image of the 3D model and solar curve.

<sup>1</sup> The Ambient Warmness Degree AWD [°C] metric is used to quantify the severity of outdoor thermal conditions by averaging the Cooling Degree hours

(CDh) calculated for a base temperature (T<sub>b</sub>) of 18 °C over the total number of building occupied hours.

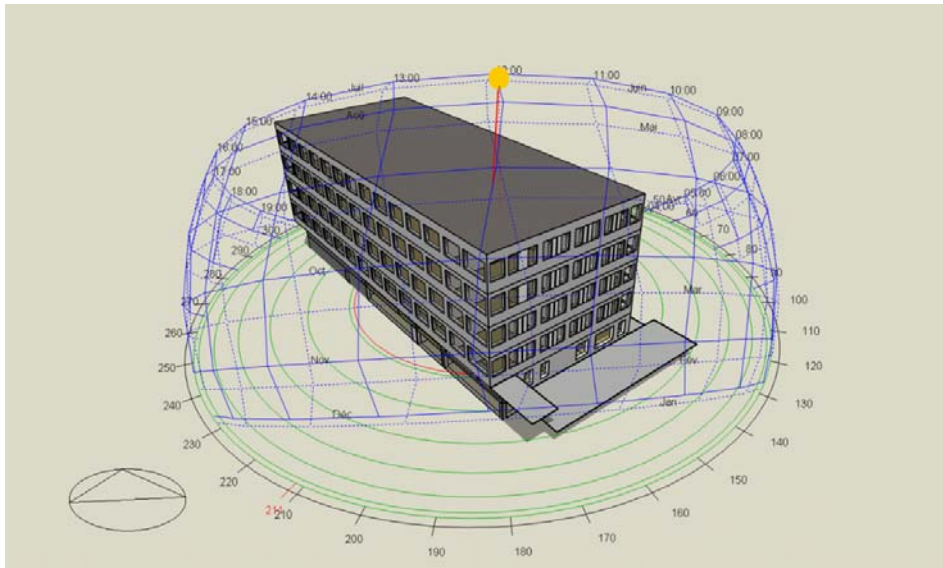


Figure 2: case study 3D model in Design Builder

The building envelope characteristics represent the values of new passive constructions (complying with EPB regulatory standards) and are summarized in Table 3. The building envelope, geometry, as well as the orientation are the same as the building. For joint analysis with different partners, the occupancy densities and planning follow those of the EN 16798-1:2019 standard for an office environment. It is also assumed that occupants wear generic winter clothes rated at 1 clo and summer clothes rated at 0.5 clo, with a sedentary metabolic activity rate of 123 W/person and an air speed of 0.1 m/s. For this analysis, we focused on studying the two office rooms (4.1.6 and 4.7) that represent the worst scenario. They are positioned facing southwest and located under the roof.

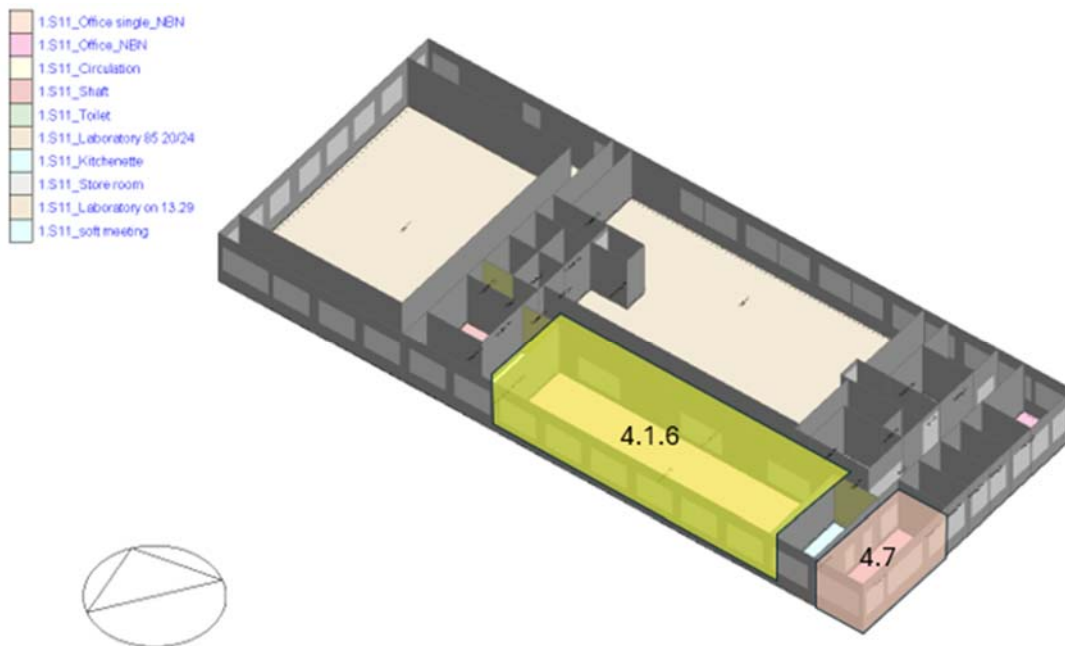


Figure 3: Last floor plan

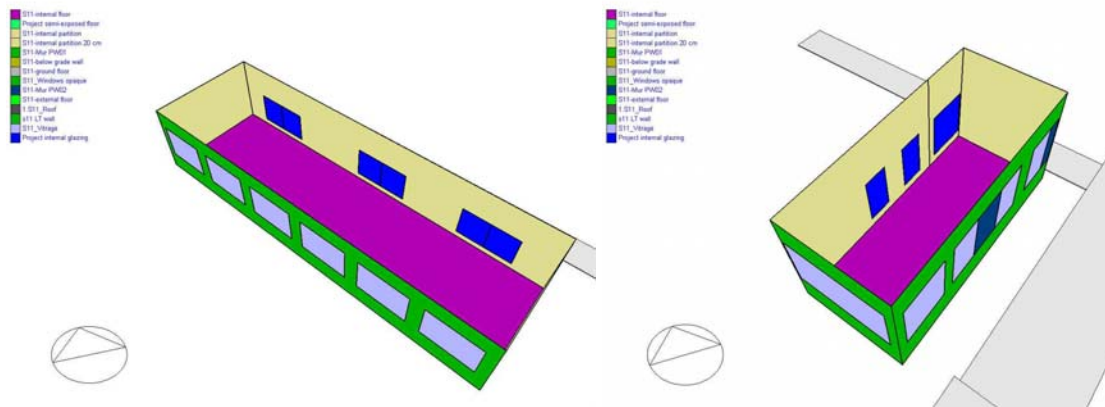


Figure 4: office's room 4.1.6 (left) and 4.7 (right)

Table 4: Orientation

Rooms	Orientation	WWR (windows to wall ratio)
4.7	227	37%
4.1.6	182	33%

### 1.2.3 Energy performance of walls assumption

#### 1.2.3.1 Insulation

The table below shows all U-Value considered in the simulation:

Table 3: U-value

Code	Envelop	Description	U-value [W/m <sup>2</sup> K] Including bridges
<b>R1</b>	<b>Roof</b>	300 mm Concrete slabs with 50 mm of screed PUR insulation 230 mm Roofing bitumen sheet	0.12
<b>S1</b>	<b>Slab intermediate floor</b>	300 mm Concrete slabs with 50 mm of screed Finishing: Carpet	1.46
<b>W1</b>	<b>Walls above grade</b>	Fibrocement tiles Air gap Mineral wool 240 mm Concrete 200mm Mortar gypsum	0.15
<b>W2</b>	<b>Walls above grade</b>	Aluminium Air gap PUR 100mm Concrete 200mm Mortar gypsum	0.24
<b>P1</b>	<b>Partition</b>	Standard metal C stud partitions Acoustic Roll Plasterboard	0.4
<b>EG</b>	<b>Vertical Windows</b>	Aluminum frame with good thermal break Double glazed, low-e with 90% argon	Uw 1.8 Ug 1,1

			SHGCg 27,4% VTg 58,8%
<b>IG</b>	<b>Internal window</b>	Generic clear 3 mm Air 6 mm Generic clear 3 mm	Ug 3,3 SHGCg 76% VTg 81%

Table 4: average U-value

Rooms	U-value external wall
4.7	0.13
4.1.6	0.14

### 1.2.3.2 Thermal bridge

Attention will be paid to the compliance of constructive nodes. Indeed, the insulation will be continuous, whether it is implemented from the inside or the outside. Where possible, the insulation will be extended at the ends of the walls to extend the path of least thermal resistance.

Thermal bridges are currently fixed and represent an additional loss of 10% to the values mentioned below.

### 1.2.3.3 Airtightness

A good airtightness is required. For the simulation a value has been set equal to 1 Vol/h at 50 Pa.

(NB for variant natural ventilation by windows airtightness is autosize)

### 1.2.4 Internal gain

The values of lighting, fixtures, and occupancy schedules (Fig 5.) related to the building, following the EN 16798-1:2019 standard, include:

Table 4: Internal gain

Parameter	Value	Schedule
<b>Occupancy</b>	10 m <sup>2</sup> /pers	7-18 h 5/7 day
<b>Metabolic rate</b>	123 W/pers	
<b>Internal Equipment</b>	12 W/m <sup>2</sup>	7-18 h 5/7 day
<b>Lighting</b>	7 W/m <sup>2</sup>	7-18 h 5/7 day
	500 lux	Daylight sensor
<b>Ventilation fresh air</b>	40 m <sup>3</sup> /h	CO <sub>2</sub> detector

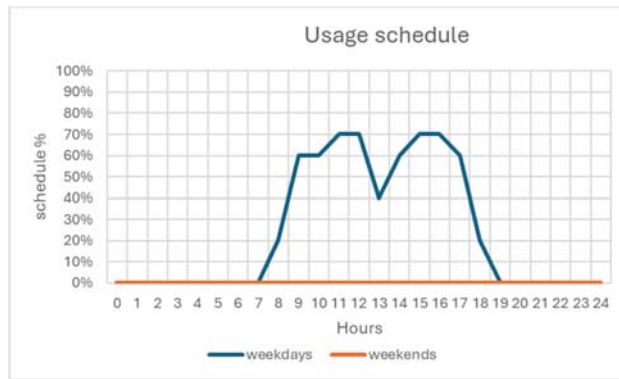


Figure 5: usage schedule

### 1.2.5 Temperature Setpoints

The temperature setpoints established in the different rooms are as follows:

Table 5: Set point

Parameter	Value
Heating set point temperature	21°C
Heating set back temperature	16°C
Cooling set point temperature	26°C
Cooling set back temperature	32°C

### 1.3 Strategies

The simulation has been carried out in a detailed way in Design builder.

#### 1.3.1 No strategies

##### 1.3.1.1 Baseline

The base case A does not present any active strategy.

The mechanical ventilation system includes a pre-heating battery to heat the incoming fresh air to 20°C. The zones are equipped with hot convector emitters capable of maintaining the winter setpoint temperature. An air heat pump powers the battery and convectors. The summer temperature is not controlled.

##### 1.3.1.2 50

This scenario corresponds to case A where low-emissivity double glazing is substituted with clearer double glazing having a higher solar factor of 49.9% and a light transmission of 70%.

Table 6: U-value

Code	Envelop	Description	U-value [W/m²K] Including bridges
EG2	Vertical Windows	Aluminum frame with good thermal break Double glazed, with 90% argon	Uw 1.8 Ug 1,1 SHGCg 49,4% VTg 71,1%

## 1.3.2 Passive cooling strategies

### 1.3.2.1 NNV

Night Natural ventilation NNV for pre-cooling of the office's rooms during nighttime. NNV is activated from 8:00 p.m. to 6:00 a.m., if all the following conditions are met simultaneously max air temperature exceed both the indoor set point of 24°C and the external temperature by min 2°C.

1. C : we have allowed all windows to be opened up to 30% of their surface
2. C2: we have allowed a limited number of windows to be opened corresponding to 5,2% of room's area

### 1.3.2.2 Shading

The screens on the southwest windows or both rooms were additionally provided with automatic store (when solar radiation > 250 W/m<sup>2</sup>). Store diffusing with solar reflectance 50% and transmittance 10%.

In this case the double glazing used is clearer with a solar factor of 49,4%.

## 1.3.3 Active Cooling Strategies

### 1.3.3.1 Cooling

In all cases, the Air Handling Unit (AHU) is equipped with additional features to maintain a relative humidity level between 40% and 60%.

Heating and cooling functions are carried out by a reversible heat pump (HP). This system can operate in both heating and cooling modes simultaneously. The Coefficient of Performance (COP) values are 3.3 and 3.2.

#### 1.3.3.1.1 Autosize

In the Autosize scenario, cooling is enabled to maintain the inner air temperature at 26°C. The initial cooling strategy involves the Air Handling Unit (AHU) that provides fresh air within a temperature range from 20°C up to 26°C, based on outside temperature conditions.

The FC fan coil unit covers the remaining cooling needs. AHU

In this scenario Cooling is exclusively allowed through the air pre-cooled by AHU. Rooms are equipped by radiators.

#### 1.3.3.1.2 Limited FC

In this variant the cooling power of the fan coil unit has been restricted.

### 1.3.3.2 MFC

Mechanical Free Cooling: This case is a combined the possibility for AHU to switch to free cooling mode when the outside temperature exceeds 15°C and the indoor temperature is above 24°C, with a maximum temperature difference of 2°C (limited to the maximum of Air flow per rooms).

#### 1.3.3.2.1 PO Power Outage

A 24-hour power outage scenario was examined on the day of the most severe heatwave, specifically on July 1, 2043, and July 30, 2051.



### 1.3.4 Variant Combinations

The other cases are a combination of various variants. A table below summarizes all the combinations:

Table 7: Variants

<b>OFFICE's ROOM (4.1.6 and 4.7)</b>	
<b>A</b>	<ul style="list-style-type: none"> <li>No strategies</li> </ul>
<b>B</b>	<ul style="list-style-type: none"> <li>Cooling (AHU + FC) Autosize</li> <li>Cooling (AHU + FC) Limited</li> <li>Cooling (AHU)</li> </ul>
<b>C</b>	<ul style="list-style-type: none"> <li>NNV</li> </ul>
<b>C2</b>	<ul style="list-style-type: none"> <li>NNV</li> </ul>
<b>D</b>	<ul style="list-style-type: none"> <li>NNV + Cooling (AHU + FC) Limited</li> <li>NNV + Cooling (AHU)</li> <li>NNV + Cooling (AHU + FC) Autosize</li> </ul>
<b>E</b>	<ul style="list-style-type: none"> <li>Shading</li> </ul>
<b>F</b>	<ul style="list-style-type: none"> <li>Shading + Cooling (AHU + FC) Limited</li> <li>Shading + Cooling (AHU)</li> <li>Shading + Cooling (AHU + FC) Autosize</li> </ul>
<b>G</b>	<ul style="list-style-type: none"> <li>Shading + NNV</li> </ul>
<b>H</b>	<ul style="list-style-type: none"> <li>Shading + NNV + Cooling (AHU + FC) Limited</li> <li>Shading + NNV + Cooling (AHU)</li> <li>Shading + NNV + Cooling (AHU + FC) Autosize</li> </ul>
<b>H2</b>	<ul style="list-style-type: none"> <li>Shading + NNV + Cooling (AHU + FC) Limited</li> <li>Shading + NNV + Cooling (AHU)</li> <li>Shading + NNV + Cooling (AHU + FC) Autosize</li> </ul>
<b>I</b>	<ul style="list-style-type: none"> <li>PO_Shading + MFC + Cooling (AHU)</li> <li>Shading + MFC + Cooling (AHU + FC) Limited</li> <li>Shading + MFC + Cooling (AHU)</li> <li>Shading + MFC + Cooling (AHU + FC) Autosize</li> </ul>

These 24 combinations were implemented for the entire building for the 2 HW weather data considered, by analyzing the two most problematic rooms, resulting in 100 cases.

## 1.4 Results

Several Pareto fronts have been established for the 100 cases:

- Pareto FRONT 1: CEP / EH28A
- Pareto FRONT 2: CP / EH28A
- Pareto FRONT 3: EH28A / EH28HW

These fronts allow for comparisons between the results of the present study.

In essence, a color highlighting of the points is used to emphasize the different variants (no strategies, passive cooling, and active cooling).

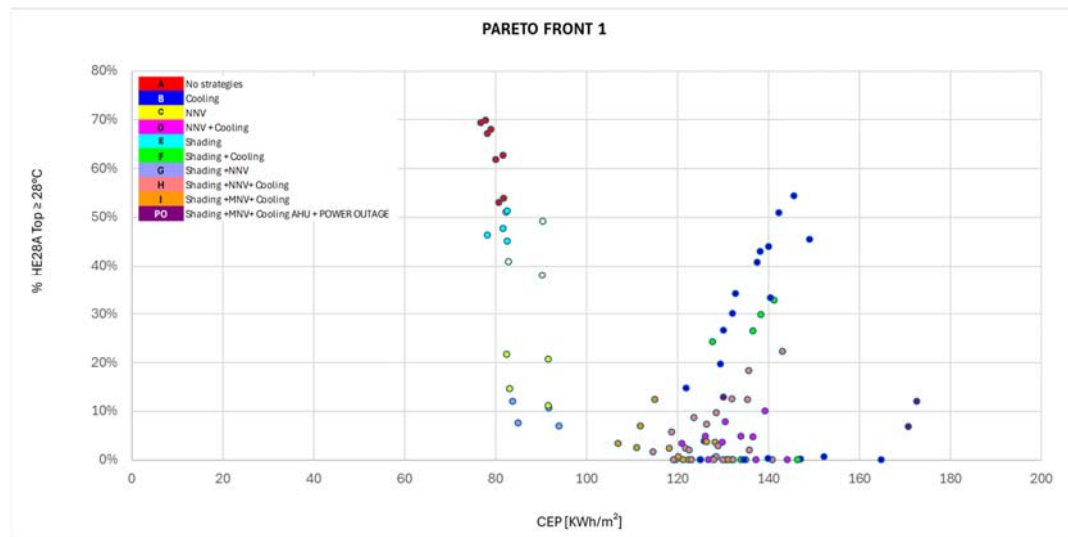


Figure 6: Pareto front 1

The image illustrates that without any strategy in place or with individual strategies such as shading, NNV with 5.2% of room’s surface window opening, or limited cooling, there is a significant increase in hourly exceedances exceeding 40%.

Solutions with autosize active cooling achieve total comfort but with a substantial increase in consumption (blue point at 0% of HE28A).

The combination of controlled automatic external shading with intensive natural nighttime ventilation (opening all fixtures by 30%) allows for a reduction in consumption and comfort (<20% HE28A) in this weather scenario without resorting to HVAC systems. It must be pointed out that there is a significant amount of incoming air, which in normalized climates could lead to a reversal of needs with increased consumption.

The optimal solutions depicted by the orange points on the graph represent the combination of shading and active cooling with mechanical free cooling. These solutions maintain average consumption values from 100 to 120 kWh/m<sup>2</sup> and EH28A below 10%.

This combination provides an effective balance between energy efficiency and comfort, showcasing a sustainable approach to managing temperature control within the HW climat.

This graph highlights the importance of implementing effective combined strategies to efficiently manage and control the temperature levels within the given environment.

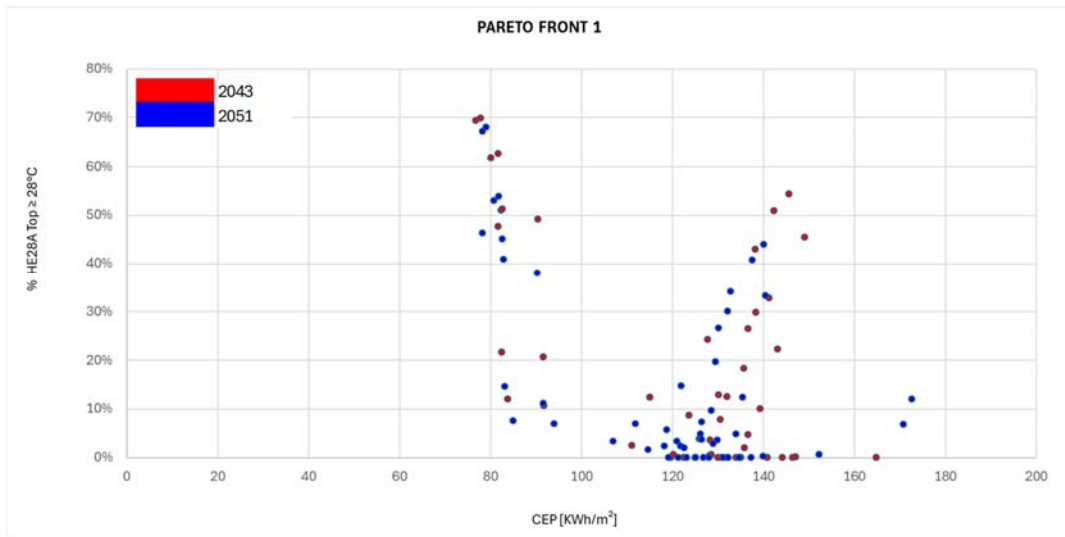


Figure 7: Pareto front 1 (HW in evidence)

This chart displays the Pareto front, with cases of HW 2043 represented in blue and HW 2051 in red.

Despite the higher peak temperatures in 2051, the weather conditions in 2043 exhibit a higher intensity, as reflected in the higher values of EH28A.

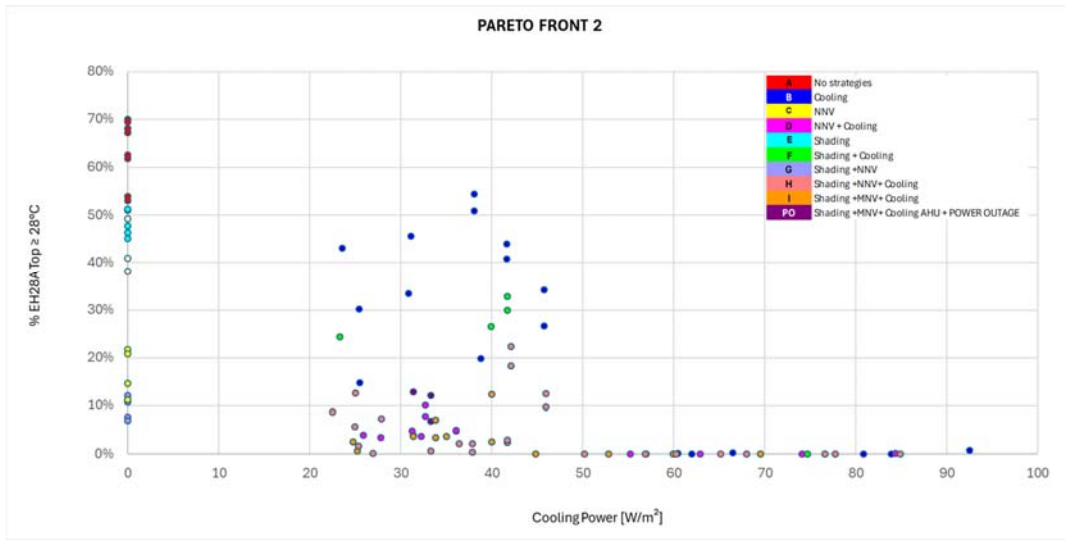


Figure 8: Pareto front 2

This image illustrates that for cooling powers exceeding 50 W/m<sup>2</sup>, EH28A values are below 0. Within the range of 20 to 50 W/m<sup>2</sup>, representing HVAC systems with lower power, EH values fluctuate between 0 and 60%. And for no cooling active strategy values fluctuate between 0 to 70%.

The graph emphasizes the importance of appropriately sizing the HVAC system and employing additional strategies to address increasingly hotter future climates.

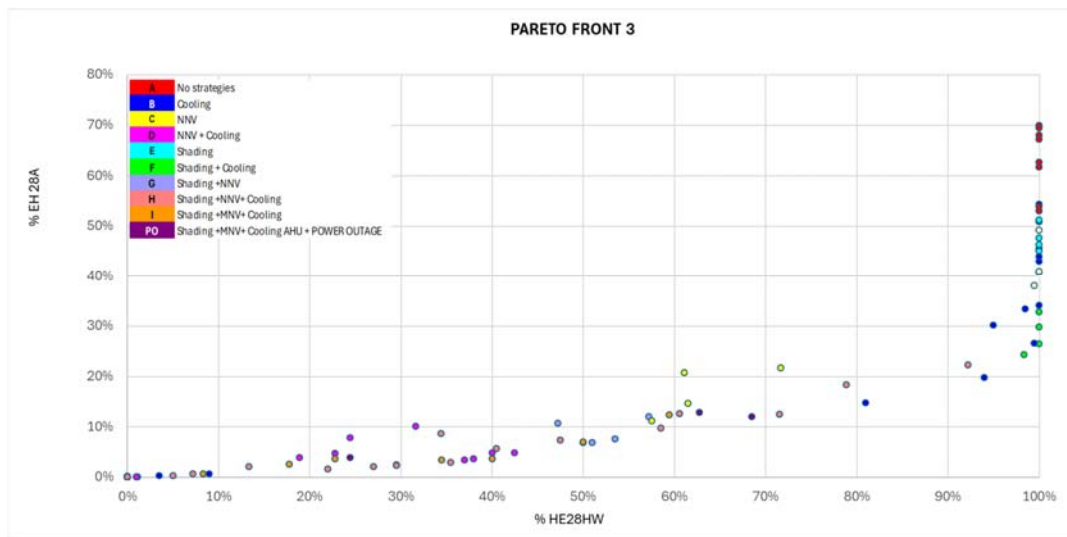


Figure 9: Pareto front 3

This graph showcases the correlation between annual excess hours and those specifically during the HW period. It effectively illustrates that any solutions surpassing an annual EH of 20% inevitably escalate to 100% during the hottest hours.

Optimal solutions corresponding to combined strategies with annual EH28A values below 20%, which equate to EH28HW values below 40%, typically involve a mix of energy-efficient HVAC systems and cooling passive strategy. By integrating these strategies judiciously, it is possible to maintain efficient thermal comfort levels while reducing energy consumption and environmental impact.

The table 8 provided includes various parameters related to different types of strategies (no strategies, passive cooling, and active cooling). Here is an explanation of each column in the table:

- Strategy: This column specifies the type of strategy being considered, such as "No Strategies," "Passive Cooling," and "Active Cooling" and combination between.
- HD Heat Demand: This column shows the average amount of heat required for each strategy.
- CD Cooling Demand: It presents the average cooling demand for each strategy.
- HP Heat Power: Indicates the maximum heat power required for each strategy.
- CP Cooling Power: Represents the maximum cooling power needed for each strategy.
- CEP Primary Energy Consumption: Displays the average annual primary energy consumption. CEP includes the consumption of auxiliaries (pumps), energy consumed by the heat pump, fan coil fan operation, air handling unit consumption, lighting consumption, and equipment consumption, as well as fan consumption for mechanical free cooling, motor consumption for window opening in cases of natural ventilation variations, and motor consumption for raising and lowering blinds for brightness control during shading.
- CO2 Emissions: Shows the average CO2 emissions, the source is electricity.
- Internal Air Temperature: Indicates the highest internal air temperature recorded for each strategy.
- Operative Air Temperature: Represents the highest operational air temperature observed for each strategy.
- %EW28A: represents the average number of hours in a year where the temperature exceeds 28°C. This parameter provides insight into how often the temperature rises above the

specified threshold throughout the year, indicating the frequency of high-temperature events. The annual occupancy hours is 2721 hours.

- EH28HW: specifically focuses on the average hours when the temperature exceeds 28°C during heatwave periods, corresponding to 200 hours for 2051 and 180 hours for 2043.

Each row in the table corresponds to a specific type of strategy, and the values provided under each column depict the characteristics or performance metrics associated with that particular strategy. The table serves as a reference for comparing and analyzing the outcomes of the study based on the different strategies employed.

Table 8: Results for groups of variants

Strategies	HD [kWh/m <sup>2</sup> ]	CD [kWh/m <sup>2</sup> ]	HP [W/m <sup>2</sup> ]	CP [W/m <sup>2</sup> ]	CEP [kWh/m <sup>2</sup> ]	GES [tCO <sub>2</sub> ]	Temperature air int max	Temperature operative max	% EH28 A	% EH28H W
No strategies	7.5	0.0	39.3	0.0	79.6	1.0	51.8	52.0	63%	100%
Cooling (AHU + FC) Autosize	14.6	55.0	48.9	92.5	151.1	1.8	26.1	28.2	0%	3%
Cooling (AHU + FC) Limited	15.7	23.7	48.9	31.2	140.0	1.7	34.1	34.9	38%	98%
Cooling (AHU)	18.8	19.6	38.0	41.7	141.4	1.7	35.7	36.5	48%	100%
NNV	11.0	0.0	40.1	0.0	86.9	1.0	37.9	37.6	31%	81%
NNV +Cooling (AHU + FC) Autosize	15.7	29.0	49.0	84.4	134.8	1.6	26.5	28.1	0%	0%
NNV + Cooling (AHU + FC) Limited	15.1	15.7	49.0	32.3	128.4	1.6	30.6	31.1	4%	29%
NNV + Cooling (AHU)	17.9	16.6	34.3	36.1	132.5	1.6	31.1	31.4	7%	35%
Shading	9.6	0.0	40.0	0.0	81.3	1.0	40.0	39.8	48%	100%
Shading +Cooling (AHU + FC) Autosize	16.3	39.7	47.7	80.9	135.1	1.6	26.0	27.7	0%	0%
Shading + Cooling (AHU + FC) Limited	16.4	20.2	47.7	40.0	129.0	1.6	31.5	32.3	21%	93%
Shading + Cooling (AHU)	20.3	20.7	38.0	45.8	135.7	1.7	33.4	34.1	31%	100%
Shading +NNV	12.7	0.0	40.1	0.0	88.6	1.1	32.7	32.0	9%	52%
Shading +NNV+Cooling (AHU + FC) Autosize	17.3	24.9	51.3	84.9	129.2	1.6	26.0	27.5	0%	0%
Shading +NNV+ Cooling (AHU + FC) Limited	16.2	13.5	51.3	36.5	123.4	1.5	30.6	31.0	5%	30%
Shading +NNV+ Cooling (AHU)	20.4	19.0	34.9	46.0	132.2	1.6	31.3	31.9	9%	48%
Shading +MFC+Cooling (AHU + FC) Autosize	15.7	22.9	49.8	69.6	126.8	1.5	26.0	27.6	0%	0%

Shading +MFC+ Cooling (AHU + FC) Limited	14.2	15.3	36.8	35.1	124.3	1.5	29.0	29.3	2%	16%
Shading +MFC+ Cooling (AHU)	17.0	15.6	49.8	40.0	115.0	1.4	31.1	31.5	5%	39%
PO_Shading +MFC+ Cooling (AHU)	16.6	16.1	38.0	33.4	150.0	1.9	34.7	34.7	9%	51%

Analyzing the table, it can be inferred that to achieve a comfortable operational temperature, the cooling power needs to be doubled compared to the restricted fan coil scenario “Cooling (AHU + FC) Limited”, leading to a light increase in energy consumption of 7%.

In situations with limited cooling capacity, the hours exceeding 28°C account for an average of 40% of total occupancy hours. These findings highlight that the current system design, without proper planning and incorporation of passive cooling methods, fails to meet the needs of the increasingly severe future climates.

We can notice from the table that passive solutions alone don’t reduce overheating hours without reaching acceptable comfort levels.

When examining a power outage scenario, configured as a comprehensive strategy utilizing a fusion of air-cooling AHU and free cooling alongside shading elements, it becomes evident that while the power demand for heating and cooling decreases, consumption rises by 23% to address the elevation in internal temperature and restore equilibrium. The surge in durations surpassing 28°C accounts for a 13% increment during the heating season and a 4% rise annually.

For completeness, all data related to the years, rooms, and variations are included in the tables below.

Table 9: Results for year and room

cases	HD [kWh/m <sup>2</sup> ]	CD [kWh/m <sup>2</sup> ]	HP [W/m <sup>2</sup> ]	CP [W/m <sup>2</sup> ]	CEP [kWh/m <sup>2</sup> ]	GES [tCO <sub>2</sub> ]	Temperature air int max	Temperature operative max	% EH28A	% EH28HW
<b>2043</b>	<b>14.8</b>	<b>17.7</b>	<b>46.4</b>	<b>83.9</b>	<b>121.7</b>	<b>1.5</b>	<b>49.8</b>	<b>50.1</b>	<b>19%</b>	<b>48%</b>
<b>4.7</b>	<b>18.0</b>	<b>19.1</b>	<b>46.4</b>	<b>83.9</b>	<b>125.6</b>	<b>0.5</b>	<b>49.8</b>	<b>50.1</b>	<b>20%</b>	<b>51%</b>
A	8.1	0.0	31.7	0.0	79.3	0.3	49.8	50.1	66%	100%
B	18.5	39.1	36.2	83.9	153.2	0.7	34.6	35.4	33%	67%
C	14.6	0.0	40.0	0.0	91.6	0.4	31.8	31.4	21%	61%
D	19.7	22.9	46.4	74.1	140.1	0.6	29.7	29.9	5%	18%
E	10.9	0.0	31.9	0.0	82.7	0.4	38.6	38.3	51%	100%
F	20.0	30.5	36.9	74.7	141.5	0.6	32.7	33.3	20%	67%
G	16.2	0.0	40.0	0.0	91.8	0.4	31.0	30.4	11%	47%
H	21.2	18.4	46.4	68.1	133.2	0.6	28.9	29.0	1%	7%
I	18.9	19.8	36.8	59.9	126.4	0.5	32.6	32.6	7%	36%
C2	13.6	0.0	40.0	0.0	90.4	0.4	35.6	35.5	49%	100%
H2	21.8	22.1	43.9	76.6	138.7	0.6	30.5	30.7	12%	51%
<b>4.1.6</b>	<b>11.5</b>	<b>16.4</b>	<b>20.8</b>	<b>60.5</b>	<b>117.9</b>	<b>2.4</b>	<b>48.6</b>	<b>48.9</b>	<b>18%</b>	<b>46%</b>
A	6.0	0.0	12.4	0.0	79.1	1.6	48.6	48.9	66%	100%
B	13.3	31.0	13.2	60.5	142.6	2.9	33.0	33.9	31%	67%
C	7.1	0.0	15.9	0.0	82.5	1.7	32.1	31.8	22%	72%
D	12.1	20.6	18.8	55.3	129.1	2.7	29.3	29.7	4%	14%
E	6.9	0.0	15.3	0.0	81.8	1.7	37.1	36.5	48%	100%
F	13.7	24.7	14.4	57.0	133.4	2.7	30.5	31.1	18%	66%

G	7.8	0.0	19.4	0.0	83.8	1.7	31.1	30.2	12%	57%
H	12.6	17.3	20.5	50.2	124.3	2.6	28.3	28.3	0%	2%
I	12.6	16.8	14.4	44.9	120.0	2.5	31.3	31.3	2%	13%
C2	7.0	0.0	15.9	0.0	82.3	1.7	35.7	35.6	51%	100%
H2	13.7	20.3	20.8	56.9	129.8	2.7	29.7	29.8	9%	38%
<b>2051</b>	<b>15.9</b>	<b>16.3</b>	<b>51.3</b>	<b>92.5</b>	<b>119.2</b>	<b>1.5</b>	<b>51.8</b>	<b>52.0</b>	<b>16%</b>	<b>51%</b>
<b>4.7</b>	<b>19.6</b>	<b>17.3</b>	<b>51.3</b>	<b>92.5</b>	<b>122.5</b>	<b>0.5</b>	<b>51.8</b>	<b>52.0</b>	<b>16%</b>	<b>53%</b>
A	9.2	0.0	39.3	0.0	80.0	0.3	51.8	52.0	60%	100%
B	20.0	33.0	48.9	92.5	144.3	0.6	35.7	36.5	26%	69%
C	15.9	0.0	40.1	0.0	91.7	0.4	33.9	33.7	11%	58%
D	20.7	19.6	49.0	84.4	133.8	0.6	31.1	31.4	3%	27%
E	12.9	0.0	40.0	0.0	78.2	0.3	40.0	39.8	46%	100%
F	22.5	28.7	47.7	80.9	132.3	0.6	33.4	34.1	18%	65%
G	18.1	0.0	40.1	0.0	94.0	0.4	32.4	31.9	7%	51%
H	23.1	17.3	51.1	77.7	126.6	0.5	29.9	30.0	2%	21%
I	20.3	17.9	49.8	69.6	135.6	0.6	34.7	34.7	6%	40%
C2	14.6	0.0	40.1	0.0	90.3	0.4	37.8	37.6	38%	100%
H2	23.5	21.3	51.3	84.9	131.4	0.6	31.3	31.9	7%	40%
<b>4.1.6</b>	<b>12.1</b>	<b>15.3</b>	<b>24.4</b>	<b>66.5</b>	<b>115.9</b>	<b>2.4</b>	<b>49.7</b>	<b>49.9</b>	<b>15%</b>	<b>49%</b>
A	6.5	0.0	20.7	0.0	79.9	1.6	49.7	49.9	61%	100%
B	13.7	27.8	21.3	66.5	136.6	2.8	33.4	34.3	24%	66%
C	7.6	0.0	20.8	0.0	83.1	1.7	34.5	34.2	15%	62%
D	12.3	18.6	21.5	63.0	124.7	2.6	30.6	31.2	3%	26%
E	7.8	0.0	23.4	0.0	82.6	1.7	38.4	37.8	45%	100%
F	14.6	23.7	22.8	62.0	125.8	2.6	31.1	31.8	14%	60%
G	8.6	0.0	23.1	0.0	85.0	1.7	32.7	32.0	8%	54%
H	13.4	16.5	24.3	60.3	118.6	2.4	29.2	29.3	1%	17%
I	13.1	15.6	24.2	52.9	129.4	2.7	33.6	33.6	3%	29%
C2	7.5	0.0	20.8	0.0	82.9	1.7	37.9	37.6	41%	100%
H2	14.6	19.8	24.4	65.2	123.5	2.5	30.4	30.9	5%	33%

## 2 CONCLUSION

In this article, a generic framework based on simulations has been developed to evaluate the impact of cooling strategies, especially the size of HVAC systems, on overheating due to climate change and future heatwaves.

The results demonstrate that:

- A system designed to combat high outdoor temperatures leads to a doubling of installed power and a significant increase in consumption.
- Restricting the installed cooling power is essential to decrease consumption but is not enough to tackle future climates.
- A blend of passive strategies such as external shading or night ventilation in conjunction with active systems is vital to uphold occupant comfort, managing consumption, and consequently, CO2 emissions.
- All of these considerations are relevant even in the event of power outage.
- The dimensions of rooms and openings proportionally impact the outcomes. Section 4.7 exhibits higher internal temperatures and increased consumption due to larger openings.

### 3 REFERENCES

In the text, references that are cited in a reference list should mention the author's surname and the year of publication. Example:

Attia et al. (2021), Resilient cooling of buildings to protect against heat waves and power outages: Key concepts and definition. *Energy & Buildings* 239 (2021) 110869

Crowe, K. (1974). *A History of the Original Peoples of Northern Canada*. Montreal: McGill/Queen's University Press for the Arctic Institute of North America.

Zaslow, M. (1988). The Northward Expansion of Canada. *The Journal of Canada*, 2(3), 216-222.



# Impact of solar shading & ventilative cooling control strategies on the resilience of residential buildings to overheating

Ivan Pollet<sup>\*1</sup>, Frederik Losfeld<sup>1</sup> and Steven Delrue<sup>1,2</sup>

*1 Renson Ventilation  
Maalbeekstraat 10  
Waregem, Belgium*

*\*Corresponding author: [ivan.pollet@renson.be](mailto:ivan.pollet@renson.be)*

*2 KU Leuven  
Faculty of Science, Kulak Kortrijk Campus  
Etienne Sabbelaan 53  
Kortrijk, Belgium*

## ABSTRACT

The Renson One residential concept focusses on the building envelope and the mechanical installations to ensure a climate-adaptive and resilient design throughout the year. Passive, renewable and energy-efficient elements are combined to address the total indoor environment and energy consumption, based on integrated control mechanisms. The high potential of external shading and ventilative cooling was proved to limit overheating and cooling consumption. Adding manual control of the windows to the simulations is a challenge to better approach reality.

## KEYWORDS

Overheating, resilience, passive cooling measures, simulations

## 1 INTRODUCTION

Summertime overheating is increasingly common in both new and existing homes, even in temperate climates (Lomas, 2001; Otaegi et al., 2022; Attia et al., 2023; Farrokhirad et al., 2024). As the demand for effective solutions and adapted regulations grows, it is crucial to address overheating in an energy-efficient manner. This is a key focus of the Renson One concept. This study examines the impact of external solar shading and ventilative cooling (VC) on thermal comfort during summer and the associated energy consumption in residential buildings.

## 2 RENSON ONE CONCEPT

Since 2000, Renson has been developing solutions aimed at "Creating Healthy Spaces" in the building sector. The Renson One concept initially centered around adaptive building envelope elements, such as natural ventilation, external solar shading, and ventilative cooling. Over time, energy-efficient HVAC systems with integrated control mechanisms were incorporated to enhance the concept for residential applications (see Fig. 1). A key component of the concept is air-water heat pump technology, which aligns well with renewable energy systems. Automated operation and cloud connectivity further simplify the complexity for inhabitants. To ensure optimal HVAC system performance, the entire process—design, installation, commissioning, and ongoing operation—must be managed with high quality (O’Hegarty et al., 2022; Mustakallio et al., 2023). The Renson concept is designed to support this comprehensive approach. While balancing energy consumption with comfort, the concept also enhances the

resilience and robustness of dwellings. The building envelope plays an equally crucial role as mechanical systems (e.g., heat pumps, fans):

- Energy demand for heating and cooling is minimized through reduced heat losses in winter and low solar gains in summer via solar shading, considering an appropriate window-to-wall ratio (WWR).
- Residents have the option to manually open façade elements for hygienic ventilation, intensive ventilation, or ventilative cooling, leveraging the outdoor environment to enhance living comfort at no additional cost.

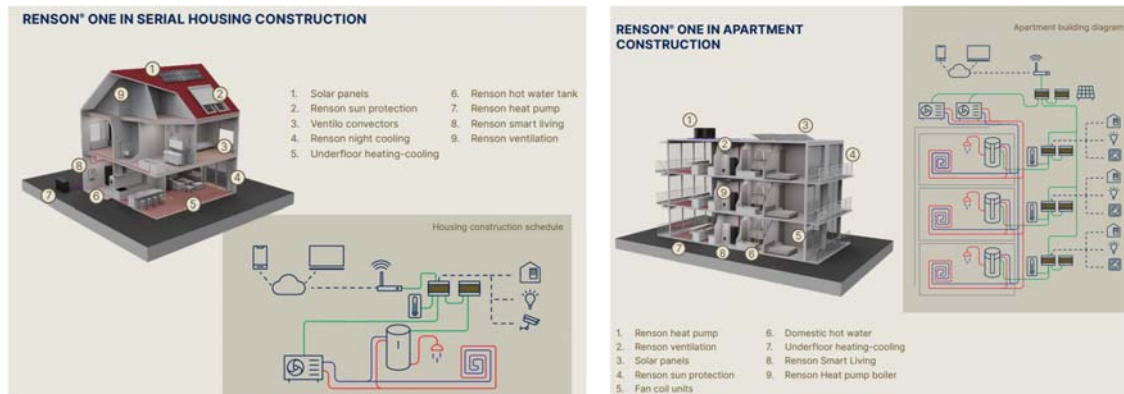


Figure 1: The Renson One concept applied in single- and multi-family buildings

This dual focus on the building envelope and mechanical installations ensures a climate-adaptive and resilient design that functions optimally throughout the year. The Renson One concept is founded on the following principles:

- Build tight, but allow for openings.
- Insulate right and protect from solar heat.
- Ventilate, heat, and cool intelligently and sustainably.

### 3 OVERHEATING

The Renson One concept encompasses the total indoor environment, addressing indoor air quality (IAQ), thermal comfort across all seasons, acoustic comfort, and visual comfort. Comfort is considered both in terms of time and space, focusing on providing comfort during periods of occupancy. Moreover, comfort is more critical in habitable spaces, where people spend more time, than in functional rooms (see Table 1).

Table 1: Comfort considerations by room type during occupancy

	Habitable rooms/Kitchen	Bathroom	WC/Laundry
<b>IAQ</b>	X	X	X
<b>Thermal comfort (heating period)</b>	X	X	
<b>Thermal comfort (cooling period)</b>	X		
<b>Acoustic comfort</b>	X	X	X
<b>Visual comfort</b>	X		

This study is limited to the resilience of the concept to overheating. Summer comfort in buildings is achieved through a dynamic balance between heat gains, heat losses, and heat

storage. Renson's approach to enhancing summer comfort involves three key strategies: minimizing solar heat gains, maximizing heat losses, and employing high-temperature cooling with minimal energy consumption.

Solar gains, often the most significant factor affecting indoor temperatures, are influenced by the solar irradiation  $I$  ( $\text{W}/\text{m}^2$ ), the glazing area  $A_g$  ( $\text{m}^2$ ), and the total solar factor  $g_{\text{tot}}$  (-) of the windows. To reduce these solar gains, Renson's building concept lowers the solar factor of transparent facade elements by incorporating external solar shading, particularly smart vertical blinds. Fixed horizontal overhangs, such as balconies, are less effective as they reduce solar gains in winter and limit daylight throughout the year.

The next step in the Renson approach is to remove any remaining internal heat passively through natural ventilative cooling. This strategy is complemented by active cooling methods, such as floor cooling or convectors, when necessary. Additionally, the building's total thermal capacity plays a crucial role in moderating indoor temperature fluctuations during both summer and winter. This capacity can be effectively utilized through surface cooling or heating systems to enhance overall comfort year-round.

### **3.1 Active heating & cooling**

Within Renson one, active heating and cooling in residential buildings utilize air-water heat pump (HP) technology with an inverter-driven approach. This technology allows for weather-dependent, controlled low-temperature heating and high-temperature cooling, enabling a wide modulation of heating and cooling capacity and ensuring high efficiency. The system includes an on/off controlled built-in circulation pump to maintain sufficient water flow. However, no built-in electrical backup is provided, so accurate heat loss calculations are essential during the building design phase to ensure that the maximum heating demand is met, unless an additional external backup is planned.

In the West-European climate, well-insulated, airtight dwellings can achieve seasonal heating efficiencies (SCOP) of 4 to 5 with current technologies. For buildings with a net heating demand ranging from 20 to 50  $\text{kWh}/\text{m}^2$  per year, the electricity consumption for space heating remains between 4.0 and 12.5  $\text{kWh}/\text{m}^2$  per year. When operating in cooling mode, the seasonal efficiency (SEER) is at least 3.

For surface heating, with a setpoint temperature of  $20^\circ\text{C}$  and a heat transfer coefficient of  $8 \text{ W}/(\text{m}^2\cdot\text{K})$ , the heating capacity can reach approximately  $90 \text{ W}/\text{m}^2$ . In cooling mode, with a setpoint temperature of  $24^\circ\text{C}$  and a heat transfer coefficient of  $6 \text{ W}/(\text{m}^2\cdot\text{K})$ , the cooling capacity is around  $30 \text{ W}/\text{m}^2$ .

In multi-family buildings, a cascade of heat pumps can be used to eliminate the need for central heat storage, which can otherwise result in space loss, heat loss, and higher investment costs. This cascade system allows for a high degree of capacity modulation.

For single-family homes, the heat pump solely produces sanitary hot water (SHW). In multi-family buildings, SHW is generated for each apartment using a separate SHW heat pump storage unit that is integrated into the two-pipes circuit of the heating/cooling system. This SHW unit operates in parallel with the floor heating/cooling system, providing hot water while slightly cooling the heating/cooling circuit. These functions complement each other during cooling periods but are non-complementary during heating periods.

In multi-family buildings, the hydraulic heating and cooling systems are controlled by a building management system at both collective and individual levels. This system uses a unique method called the critical path approach, where the control damper of the critical apartment—

determined by the current heating or cooling demand—is fully opened. This approach continuously monitors and minimizes water flow resistances to save energy. Additionally, the system allows for intelligent heating and cooling of different building areas, exposed to varying solar irradiation levels or internal heat gains.

This electrically-driven building concept is well-suited for integration with renewable electricity production, such as roof-installed or building-integrated photovoltaics (BIPV). This integration can significantly reduce both the final and primary energy consumption for HVAC systems.

### 3.2 Simulation of summer comfort and energy consumption

#### Methodology

A dynamic, zonal simulation using Dymola/Modelica/Ideas was conducted to evaluate the impact of solar shading and floor cooling on summer comfort and energy consumption (heating/cooling) in a single-family dwelling. The study focused on the existing Renson concept home, a detached two-story house completed in 2019 in Waregem, Belgium.

This residence, with a square layout, encompasses a total net floor area of 177 m<sup>2</sup> and includes two bedrooms, a polyvalent room, a bathroom, a living room with an open kitchen, and a technical room (as shown in Fig. 2). The house features a wall with a U-value of 0.15 W/m<sup>2</sup>·K, a window-to-wall ratio (WWR) of 0.27, and a building airtightness of 3 vol/h at 50 Pa. It has achieved a Belgian energy performance score of E13, corresponding to an A label.

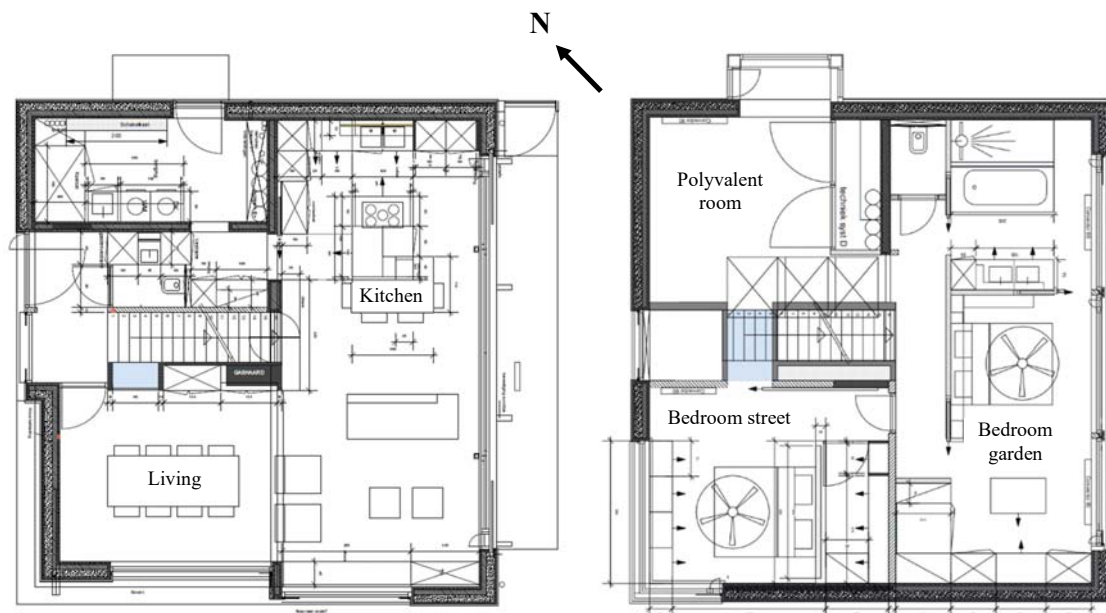


Figure 2: The building layout: left is ground floor, right is upper floor

The home is equipped with a demand-controlled mechanical extract ventilation system, the Healthbox 3.0 Smartzone, which locally adjusts airflow rates based on CO<sub>2</sub>, RH, and VOC levels. This system provides natural air supply in habitable rooms and extracts air from both wet and habitable spaces. All windows, including the roof windows in the night hall, are fitted with external blinds, achieving a total solar factor ( $g_{tot}$ ) of 0.1. Although the kitchen features a fixed horizontal overhang, it was not included in the simulation.

The simulated scenario involved a family of four, including two children, with the sensible heat generated by these occupants being the only internal heat source considered. For the purpose of the study, all windows were kept permanently closed, which is a deviation from real-life conditions. The effects of window use during both daytime and nighttime will be explored in subsequent studies.

### Controls and criteria

The control of climate systems in buildings can be managed manually or through automated methods, incorporating rules, predictions, models, and machine learning techniques (Peng et al., 2022). In the simulations conducted, specific temperature setpoints were maintained for different rooms: 20°C for the living room and kitchen, 18°C for the bedrooms, and 22°C for the bathroom. During active cooling, all rooms except the bathroom were cooled to an ideal setpoint of 24°C, which aligns with common practice. The demand-controlled mechanical extract ventilation (DC MEV) system was simulated as it operates in real-life scenarios, adjusting local air flow rates according to the needs.

HVAC systems typically utilize demand control, where system adjustments are made based on real-time needs. In contrast, solar shading is often automated solely based on outdoor climate conditions. Demand control represents a form of closed-loop control, where feedback is provided to ensure the desired outcome is achieved.

For the simulation, the standard ISO/FDIS 52016-3 (2023) was used to derive both automated and manual control strategies for external vertical blinds. Manual control was simulated based on a probabilistic model, where blinds were opened or closed linked to indoor and outdoor conditions when a person entered or left a room, with a minimum interval of four hours between actions. For rule-based automated controls, the following strategies were analyzed:

- Activation based on outdoor irradiation levels (250-300 W/m<sup>2</sup>) and a predicted maximum outdoor temperature of at least 21°C for the following day.
- Activation based on indoor temperature, implementing a demand-controlled approach.

As a reference, simulations were also conducted for scenarios where external blinds remained permanently up or down.

In this study, the windows were kept closed because accurately modelling real window control is challenging. However, to achieve results that are closer to reality, manual window control will be incorporated into the model, similar to the approach used for solar shading control.

To evaluate the effectiveness of these different control strategies, summer comfort at the room level was assessed using temperature-weighted exceedance hours, known as degree-hours in Kh, for temperatures exceeding 24°C and 26°C by a margin of +0.5°C (Fig. 3). This method provides a more accurate measure of overheating than simply counting hours above a temperature threshold, which can be misleading. Additionally, the yearly cooling demand required to maintain a set temperature of 24°C was calculated and compared with the heating demand (Fig. 4).

## Results

As illustrated in Fig. 3, without active cooling, temperature exceedances are relatively consistent across different habitable rooms. Minor variations are primarily due to differences in window-to-wall ratios (WWR), such as the reduced overheating observed in a bedroom with a low WWR on the west corner. In scenarios without cooling, solar shading, or openable windows, the degree-hours exceeding 24°C and 26°C are alarmingly high, around 56 kWh and 46 kWh respectively, indicating significant overheating. Under these conditions, indoor temperatures can rise to 35-40°C, even when outdoor temperatures are 10°C lower (25-30°C). This highlights the risk of overheating not just during summer but across at least 50% of the year, especially in energy-efficient homes with high glazing-to-wall ratios and no solar shading means.

Solar shading plays a crucial role in mitigating this overheating, especially when windows remain closed. The use of solar shading can reduce temperature exceedance by 50% to 67% at thresholds of 24°C and 26°C. The effectiveness of manual shading control is comparable to that of automated systems based on solar radiation and outdoor temperature. Inhabitants' ability to respond to indoor temperature changes in manual control scenarios and the presence of usually at least one person of the family, accounts for the relatively high performance of manual control. Even with solar shading, degree-hours still range between 15-25 kWh, corresponding to an average air temperature near 30°C during overheating. The well-insulated house with permanently closed windows and the quite high shading control levels of 250-300 W/m<sup>2</sup>, explain this high temperature exceedance. This result reflects and underscores the importance of addressing summer comfort in building design.

To explore the full potential of solar shading in reducing overheating, simulations were conducted with blinds permanently closed. This approach significantly improved summer comfort by virtually reducing the window area by 90%, thus minimizing solar gains. However, for optimal comfort, solar shading may need to be deployed more frequently than is typical in practice. A more responsive shading strategy could involve lower outdoor setpoints or demand-controlled mechanisms based on indoor temperature. Controlling shading in response to indoor comfort temperature (as indicated by a thermostat, for instance) also proved effective in maintaining summer comfort (Fig. 3). When shading is often fully closed, blinds are preferable to rolling shutters, for enhanced visual contact with the outdoors.

Additionally, the study analyzed the potential of floor cooling with a limited capacity of 30 W/m<sup>2</sup>. With a total available cooling capacity of approximately 4 kW or 70 W/m<sup>2</sup> window area, floor cooling can maintain summer comfort even without solar shading when outdoor temperatures are below 30°C. However, during heatwaves with temperatures reaching 35-40°C, the combination of solar shading and keeping windows closed during the day becomes essential to maintain a comfort temperature of 24°C.

While high-temperature floor cooling operates efficiently, its capacity is restricted to prevent condensation on the floor when the indoor air dew point is high. Increasing cooling capacity by lowering water temperature raises the risk of condensation, especially when windows are opened. Thus, to maintain the desired 24°C comfort level, solar shading is recommended to supplement the limited floor cooling capacity.

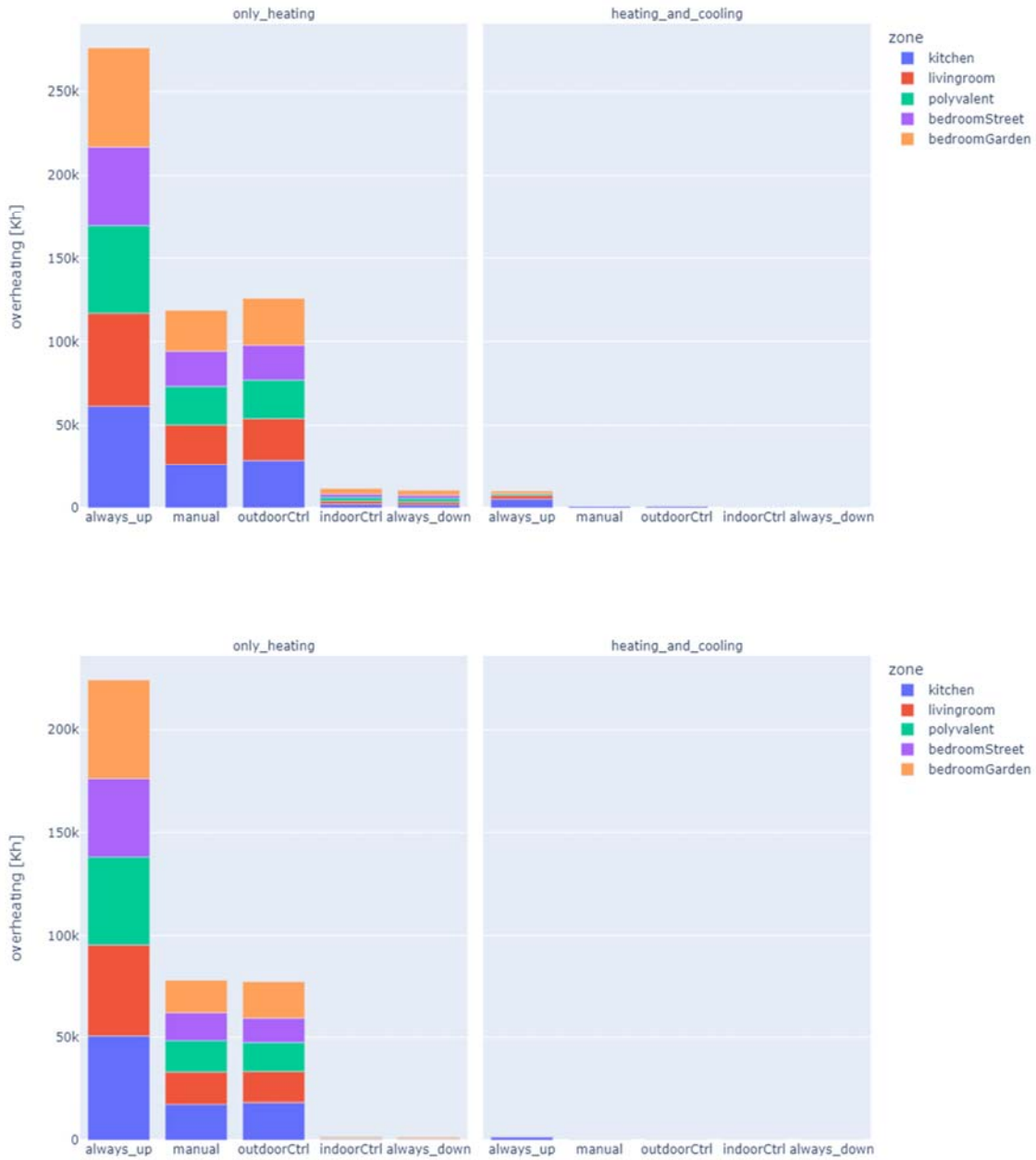


Figure 3: Overheating degree-hours (Kh) on room level above 24°C (top) and 26°C (bottom) for different external shading controls, without active cooling (left) and with active cooling (right)

Fig. 4 presents the energy demand for cooling and heating per conditioned floor area. The data clearly show the shift in new dwellings from heating challenges to cooling challenges. The energy required for heating is only half that needed for cooling. Without solar shading or openable windows, cooling demand is nearly four times that of heating. Implementing solar shading with suboptimal control almost halves the cooling demand to 40 kWh/m<sup>2</sup>. The total cooling demand is approximately 5000 kWh or 1500 kWh of final energy, which can be partially generated by PV systems.

The required heating demand is around 20 kWh/m<sup>2</sup> or 3000 kWh, equating to 600-750 kWh of annual heating consumption. Heat gains, whether solar or internal, significantly impact this demand, which can double if solar gains are reduced by obstructions near the dwelling or excessive use of solar shading. Although floor cooling can prevent remaining overheating, its cooling capacity is limited. Future simulations will explore the impact of heatwaves on overheating issues. Additionally, designing a cost-effective house could involve limiting WWR on solar-exposed façades to permanently reduce both capital and operational expenditures.

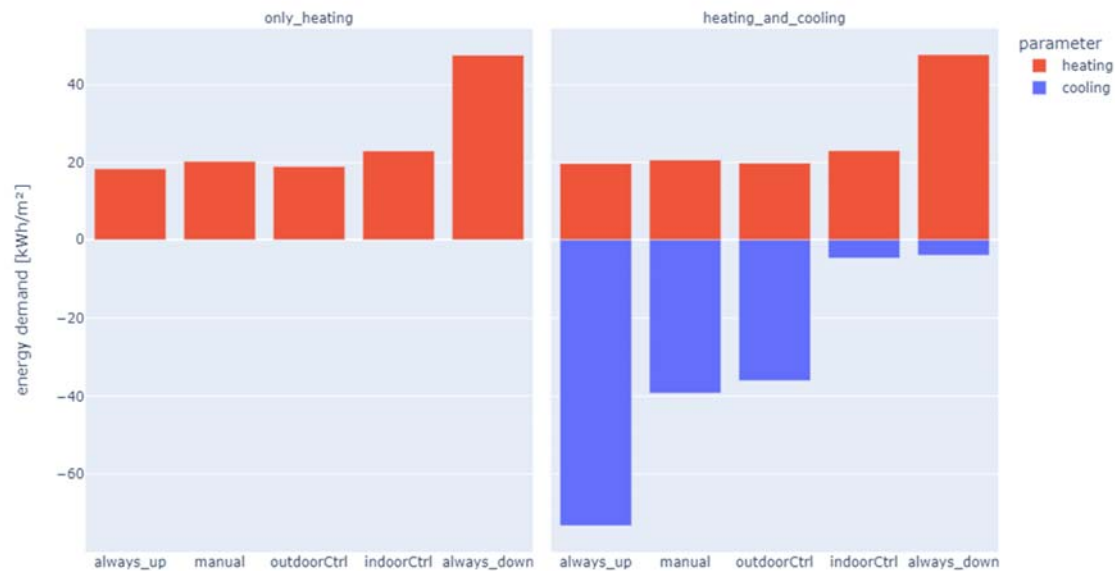


Figure 4: Heating and cooling demand (kWh/m<sup>2</sup>) on building level for different shading controls, without active cooling (left) and with active cooling (right)

### 3.3 Passive ventilative cooling (VC)

The impact of VC through openable windows, which are usually present in habitable rooms, can be substantial for maintaining summer comfort (Foldbjerg et al., 2014). This passive cooling method, driven by natural forces, is fully renewable and offers significant potential cooling capacity, though it is variable and uncertain across time and space. The cooling potential of VC is approximately 4 W/m<sup>2</sup> per air exchange, assuming an average outdoor-indoor temperature difference of 5°C. The effectiveness of this passive cooling is largely influenced by pressure differences, which average around ±1 Pa across facade ventilation elements. This pressure difference can facilitate a ventilation rate of about 30 m<sup>3</sup>/h/m<sup>2</sup> through a fully open window with a window-to-floor ratio (WFR) of 1%. While the WFR can be as high as 25%, the practical WFR for openable windows typically ranges between 5-10%.

Assuming a room height of 2.5 meters, the ventilation air renewal rate is about 60-120 air changes per hour (ACH). However, this rate can be significantly reduced by factors such as single-sided rather than cross-ventilation (by 50%), tilted versus fully open windows (by 95%), and the use of louvres (by 50%), potentially reducing the ACH to around 1. The maximum opening angle of the window is crucial in enhancing a building's resilience during heatwaves. Louvres also play a beneficial role by increasing the likelihood that VC openings will be effectively used. These multifunctional devices help prevent the entry of rain, insects, noise, and unauthorized persons, thereby encouraging the use of VC.



The presence or absence of active cooling systems greatly influences how frequently VC devices, such as windows, are utilized. Without an active cooling system, occupants are more likely to open windows to manage indoor temperatures. Therefore, summer comfort simulations that assume windows remain closed are unrealistic and will be the subject of further investigation. Similar to solar shading, the control conditions of VC devices are critical. Manual control of VC, without the need for actuators, provides an essential means of cooling, particularly if technical devices fail or during power outages.

#### 4 CONCLUSIONS

The Renson One concept approaches sustainable and resilient design through several key strategies:

- Implementing an efficient heating, cooling, and ventilation system.
- Combining passive and renewable cooling methods.
- Utilizing a single control system to integrate all climate control devices.
- Opting for cloud-based control over local systems to minimize the need for numerous detection mechanisms.
- Incorporating PV technology, partially integrated into building envelope products.

The dynamic control and behavior of the concept is simulated in detail. Generally, new residential buildings have a reduced heat demand due to improved building envelopes, greater compactness, and the impacts of climate change. This shift necessitates a focus on living comfort and energy efficiency during the non-heating months, particularly as this period extends for at least half of the year in Western Europe. Consequently, the challenge lies in preventing overheating during the design phase of well-insulated homes:

- A thorough use of external solar shading on all windows, allows to prevent cooling energy to maintain summer comfort, if no heat waves ( $>30^{\circ}\text{C}$ ) occur.
- High-temperature cooling methods can also significantly diminish overheating hours even without external shading. Nevertheless, solar shading is advisable for rooms oriented from east to west that feature substantial glazing. Ultimately, the key principle for ensuring summer comfort is to limit solar gains relative to floor area.
- During periods of extreme heat, a combination of external solar shading and high-temperature cooling becomes essential for maintaining a comfortable indoor environment, thereby significantly reducing electricity consumption, even from renewable sources.
- Manual control of solar shading can provide relatively good performance in case of conscious and present inhabitants.
- Additionally, openable windows usually present in habitable rooms can serve as a passive and renewable measure for ventilative cooling, enhancing the sustainability and heat resilience of residential buildings. Modelling of a real manual window control stays a challenge.
- Louvres improve the window performance in term of water tightness, insect-protection, and burglary resistance, increasing in that way the time in use of VC.

#### 5 ACKNOWLEDGEMENTS

This work has been supported by the Flanders Innovation and Entrepreneurship (VLAIO) in the flux 50 ICON-Project ‘ReCOVer++: Improving resilience of buildings to overheating.’

A more comprehensive discussion on the Renson One concept, including its broader implications for indoor environments, is available.

## 6 REFERENCES

- Attia, S., Caroline Benzidane, C., Rahif, R. et al. (2023). Overheating calculation methods, criteria, and indicators in European regulation for residential buildings. *Energy & Buildings*, 292, 2023, 113170. <https://doi.org/10.1016/j.enbuild.2023.113170>.
- Farrokhirad, E., Gao, Y., Pitts, A. & Chen, G. (2024). A Systematic review on the risk of overheating in passive houses. *Buildings* 2024, 14, 2501. <https://doi.org/10.3390/buildings14082501>.
- Foldbjerg, P., Asmussen, T., Fedkenheuer, M. & Holzer, P. (2014). Self-evaluated thermal comfort compared to measured temperatures during summer in three active houses where ventilative cooling is applied. 35<sup>th</sup> AIVC Conference, Poznań, Poland, 24-25 September 2014.
- ISO/FDIS 52016-3 (2023). Energy performance of buildings — Energy needs for heating and cooling, internal temperatures and sensible and latent heat loads — Part 3: Calculation procedures regarding adaptive building envelope elements.
- Lomas, K. J. (2021). Summertime overheating in dwellings in temperate climates. *Buildings and Cities*, 2(1), pp. 487–494. DOI: <https://doi.org/10.5334/bc.128>
- Mustakallio, P., Schild, P. & Ekberg, L. (2023). Challenges and needed remedies of demand controlled ventilation. *Rehva Journal*, April 2023, 13-17.
- O’Hegarty, R., Kinnane, O., Lennon, D. & Colclough, S. Air-to-water heat pumps: Review and analysis of the performance gap between in-use and product rated performance. *Renewable and Sustainable Energy Reviews* 155 (2022) 111887. <https://doi.org/10.1016/j.rser.2021.111887>
- Otaegi, J., Hernández, R.J., Oregi, X., Martín-Garín, A. & Rodríguez-Vidal, I. (2022) Comparative analysis of the effect of the evolution of energy saving regulations on the indoor summer comfort of five homes on the coast of the basque country. *Buildings* 2022, 12, 1047. <https://doi.org/10.3390/buildings12071047>.

# ReCOVer++ project: wrap up

Hilde Breesch<sup>1</sup>, Douaa Al Assaad<sup>1,2</sup>, Abantika Sengupta<sup>1,3</sup>, Marijke Steeman<sup>3</sup>

*1 KU Leuven  
9000 Gent, Belgium*

*2 TU Eindhoven  
5600 MB Eindhoven, The Netherlands*

*3 Ghent University, 9000 Gent, Belgium*

## SUMMARY

The increasing severity and duration of climate change is that extremes – notably heatwaves, increases the risk of human thermal stress in indoor environments where people spend most of their times. Recent field measurements have demonstrated significant overheating in the EU building stock in the EU, characterized by well-insulated and air-tight envelopes. This exposes vulnerable communities to increases mortality risks that is bound to only get worse with an ever-worsening climate warming. Moreover, heatwaves are often accompanied by other unexpected extreme events or “shocks” such as power outages, which can render some buildings uninhabitable even long after these shocks are over. Thus, it is critical to design future-proof buildings and systems. This performance characteristic of a building is known as resilience to overheating. Currently, in practice, designers and architects are under-equipped to deal with such events due to a lack of knowledge on resilience performance characteristics and building design parameters that influence them. There is a lack of a framework in current building standards to consider resilience and shock events in the design stage of a building. This includes the lack of straightforward and “easy-to-communicate” resilience key performance indicators. By bringing together academic and industrial partners, the VLAIO ICON project ReCOVer++ aims to bridge this knowledge gap and make resilience a more actionable concept for architects, engineering companies and manufacturers. ReCOVer++ defines a new holistic resilience indicator relating resilience performance characteristics to the building and systems’ most influential parameters which aims to improve resilience to overheating. This session aims to communicate the results of the ReCOVer++ project by presenting this novel indicator and discusses the implications of its use in practice.

## KEYWORDS

Thermal resilience, climate change, heatwaves, buildings, performance indicators

## 1 RESEARCH METHODOLOGY

The work plan of ReCOVer++ consists of 5 interacting work packages (WP) as seen in Figure 1 that aim to demonstrate the resilience indicators on real-use case study buildings. In WP1, the shocks that can cause overheating were defined, classified and quantified and each of the project partners selected representative case studies of different building typologies and HVAC systems. The selected case studies were an array of highly insulated and airtight residential and non-residential buildings equipped with different solar shading strategies and ventilative cooling technologies with different types of smart control. Note that WP1 eventually focused on heatwaves (HWs) as they were shown to challenge resilience at a higher level than system shocks (Sengupta, 2023). The HWs occurring during historical (2001-2020) and midterm future (2041-2060) were chosen. Future long-term (2081-2100) were not considered since it was assumed that by that time frame, building standards would be updated rendering current case study buildings non representative. HW weather data files were determined using the methodology of IEA EBC’s Annex 80 (Machard, 2024) using bias corrected CORDEX data and extracted according to the methodology of (Ouzeau, 2016), where regional temperature HW thresholds were defined.

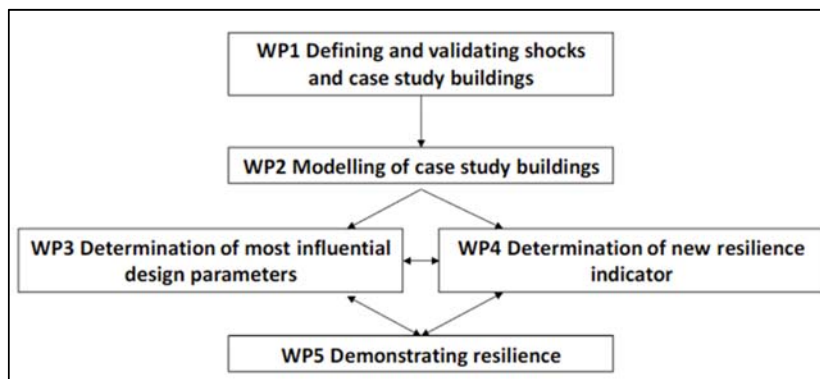


Figure 1. ReCOVer++ workflow overview

In WP2, the partners developed models of their case study buildings using various modelling tools such as Dymola (Modelica language), EnergyPlus and IDA-ICE. The partners verified the output comparativeness of the different tools by modelling and simulating a common building during a HW event. The case studies used by the partners were partially or fully validated against experimental data. In WP3, thermal resilience aspects (absorptive, adaptability and recovery capacities) were determined as representative aspects of the resilience response of a building. The Standard effective Temperature (SET) (based on the 2-node thermoregulation model of Gagge, 1972) degree.hours above 28°C was selected as an indicator that quantifies the degree of impact while integrating all three resilience aspects simultaneously. Subsequently, parametric studies were conducted under different HW events and different scenarios of building design and HVAC systems. The scenarios included the baseline case and variations of it. The outputs from simulations were used to calculate the SET degree.hours. WP4 was conducted in parallel to WP3 where KU Leuven & Ghent University conducted sensitivity analysis on reference apartment, educational and office buildings to determine via regression analysis a mathematical relation linking the SET degree.hours to the building's most influential parameters. WP4 showed that buildings' 4 most influential parameters were (by order of magnitude) the window to wall ratio, the cooling capacity and the operation of natural ventilation and solar shading. The validity of the indicator was verified based on the parametric study results from WP3. From insights gained from WP3 and 4, WP5 aimed to formulate best practices of resilient designs and strategies. For example, the architectural partners (i.e., archipelago) found that reducing the glazing ratio, providing shading, and adopting ventilative cooling strategies, with or without thermal mass, appear to be relevant strategies to reduce the energy demand for cooling, both under current and future typical meteorological year, and to improve the resilience to overheating.

## 2 REFERENCES

Sengupta, et al. Impact of heatwaves and system shocks on a nearly zero energy educational building: Is it resilient to overheating? *Building and Environment* 234 (2023): 110152.

<https://annex80.iea-ebc.org/>

Machard et al., Typical and extreme weather datasets for studying the resilience of buildings to climate change and heatwaves, *Scientific Data* 2024 11:1 11 (2024) 1–21. <https://doi.org/10.1038/s41597-024-03319-8>.

Ouzeau et al., Heat waves analysis over France in present and future climate: Application of a new method on the EURO-CORDEX ensemble, *Clim Serv* 4 (2016). <https://doi.org/10.1016/j.cliser.2016.09.002>.

Gagge et al., An effective temperature scale based on a simple model of human physiological regulatory response, *Memoirs of the Faculty of Engineering, Hokkaido University* 13 (1972) 21–36.

# How to design a resilient building? Lessons learnt from an architectural view

Joost Declercq\*<sup>1</sup>, Martijn Holvoet<sup>1</sup>

*1 archipelago architects  
1150 Brussels, Belgium  
\*jdeclercq@archipelago.be*

## SUMMARY

The EIA EBC Annex 80 Resilient Cooling program has focused on bringing together and extending the knowledge on the resilience of buildings to overheating (Holzer, 2024). In the context of the Annex 80 Resilient Cooling program a research project, Recover++, has been setup to define a new resilience indicator, based on the properties and behaviour of real-world building projects under extreme climatological condition and shocks, as heatwaves under current and future weather conditions. These extreme weather conditions will become a reality for the building stock in the near future. The real impact will depend upon the RCP-scenario. As the mean life expectancy of buildings in Europe is between 50 and 60 years, the building stock, which is being designed and built now, will be exposed to these future weather conditions, during its lifespan. And, as the main architectural design features such as the building envelope and the spatial concepts, are less prone to change during the lifetime of a building, it's relevant to take the impact of these future weather conditions in account, in the architectural design and conception of new buildings. Future weather conditions to which buildings will be exposed, can be both represented by Typical Meteorological Years (TMY), by Extreme Warm and Extreme Cold Years (EWY and ECY), and by weather data which include extreme events as heatwaves (Machard, 2024).

Up until now the impact of the architectural building features under future weather conditions have mainly been evaluated under typical future weather conditions (TMY, EWY and ECY) (Declercq, 2021, Machard, 2021, Ramon, 2023). These studies have suggested architectural strategies to reduce operational energy use for cooling under future climate conditions (Declercq, 2021 and Machard, 2021) and to reduce the embodied impacts over the full life cycle (Ramon, 2023). In this paper, parameters related to the architectural building properties have been explored which have an impact on the resilience of buildings under extreme weather conditions with shocks, such as heatwaves.

In this context two real-life buildings of different typology, from which one is under construction and the second one is due for construction, have been modelled and simulated under future weather conditions, including future weather conditions with shocks. Several architectural building features such as thermal mass, natural ventilative cooling strategies and different mechanical cooling strategies have been analysed.

The conclusions of (Machard, 2021 and Ramon, 2023) have been challenged towards the criteria of resilience to overheating. The case studies have confirmed that the main architectural drivers, influencing the resilience to overheating under extreme conditions, are the glazing ratio, the presence of shading, the thermal mass and the natural ventilative cooling. The design of one of the case studies was evaluated under typical future weather conditions (TMY 2070-2100 under RCP 8,5) (Declercq, 2021). This research has confirmed that the architectural design strategies, which were adopted to reduce the operational energy use for cooling under current and future climate conditions, also result in a high resilience to overheating of the building.

## KEYWORDS

Resilient Cooling; Overheating; Future Weather; Climate Change; Climate Responsive Design

## 1 INTRODUCTION

Climate change will result in higher stress on the built environment and higher efforts to guarantee a stable indoor climate, which is comfortable and healthy for its occupants. In most regions guaranteeing summer comfort will become more challenging and, in most cases, will increase the operational energy demand for cooling (Ramon, 2020). As the mean expected life spans of a building in the European context reaches from 50 to 60 years (Allacker, 2010), it is important to take these future conditions in consideration when designing new or refurbishing existing buildings.

Up until recent the impact of climate change upon summer comfort in buildings has mainly been studied from the perspective of changing energy demands. In this context, future weather data for Typical Meteorological Years (TMY) has been used. To inform current practise of climate responsive design towards future weather conditions, several studies have focused on the impact of the architectural building features, such as thermal mass, glazing ratio, air tightness, insulation level, natural ventilative cooling strategies, ... (Declercq, 2021, Machard, 2021 and Khosravi, 2023) and on the life cycle environmental impact (Ramon, 2023). Only recently also the behaviour of buildings under the new extremes induced by climate change is being studied. In this context, the EIA EBC Annex 80 Resilient Cooling program focuses on bringing together and extending the knowledge on the resilience of buildings to overheating (Holzer, 2024). In this paper the impact on indoor thermal comfort and energy use of extreme shocks, such as heatwaves and power outages, is evaluated.

This paper focuses on the double question, based upon real life case studies of two non-residential buildings:

- What is the impact of climate responsive design strategies on the resilience of buildings to overheating?
- To what extent can lessons learned from assessments under typical future climate weather data inform design strategies for improved resilience to overheating of buildings?

## 2 METHODOLOGY

### 2.1 The cases

Two non-residential buildings have been selected. Both are real life architectural projects whereof one is under construction and the second is due for construction. The data are acquired from the architectural office, archipelago architects (BE).

The first case consists of a low-tech duplex inner-city office building encompassing 940m<sup>2</sup> offices and architectural design studios in the city of Leuven (BE), designed by archipelago architects for their own use. The building design is orientated towards minimizing the need of operational energy and technical installations, through a set of climate responsive design strategies as automated natural ventilative cooling, exposed thermal mass, active shading and an equilibrated glazing ratio. The design team has made extensive use of thermal dynamic simulations during the design process to optimise the building design. The building, its design process and its performance under future TMY is extensively described in (Declercq, 2021 and Khosravi, 2024).

The second case is a freestanding community building on the outskirts of the city of Geel (BE). This project is an extensive refurbishment of an existing auditorium building, which is extended with a foyer and meeting and leisure spaces. This project also uses climate responsive design strategies as natural ventilative cooling and passive and active shading strategies. Thermal mass is to a lesser extent present, as the new foyer has a lightweight roof.

The existing auditorium only has accessible thermal mass in its walls, as the ceiling is closed with acoustical panels. The second case and its performance under future TMY is described in (Khosravi, 2023).

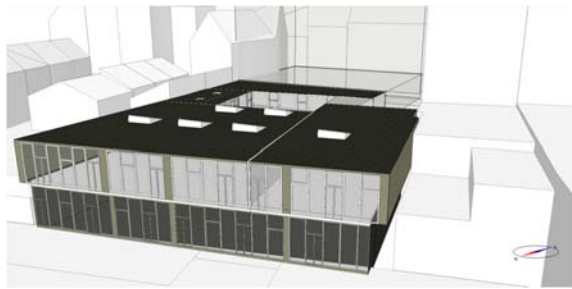


Figure 1: Case 1- IDA ICE model, viewed from the north-west facade

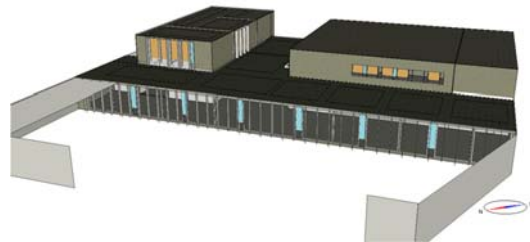


Figure 2: Case 2- IDA ICE model, viewed from the north-west facade

## 2.2 The resilience assessment

The two case studies have been modelled in the Building Energy Simulation software package IDA ICE v5.0 as a multi-zone model. In the simulation, different sets of TMY and heatwave data files have been used: one corresponding to the “historical severe heat wave,” spanning 25 days from July 6<sup>th</sup> to July 31<sup>st</sup>, and the other representing the “long-term severe heat wave,” lasting for 45 days from July 2<sup>nd</sup> to August 15<sup>th</sup>. For comparison reasons, weather data for the city of Brussels (BE) have been used in both cases. The weather datasets have been elaborated in the context of IEA EBC Annex 80 (Machard et al., 2024). The methodology has been aligned to (Zhang et al., 2021).

The resilience was assessed in the most relevant zones in the two buildings (see figure 3 and 4) through a dynamic simulation with an adaptive timestep, with a maximum of five minutes. The following resilience KPIs were assessed for the selected zones: Indoor Overheating Degree (IOD) and Overheating Escalation Factor (OEF) (Stern et al, 2024).

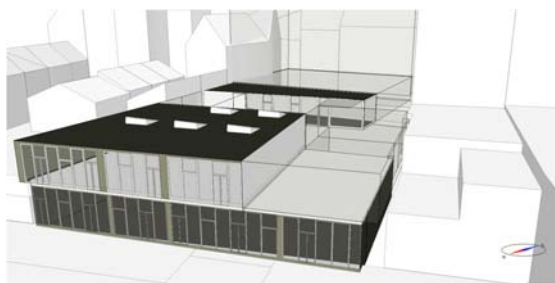


Figure 3: Case 1- zones evaluated: landscape office - 1 and 0, entrance lobby

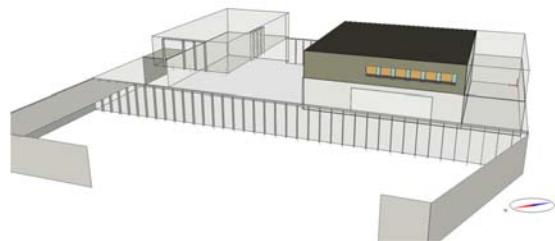


Figure 4: Case 2- zone evaluated: auditorium

For the first case six scenarios (Table 1) and for the second case three scenarios (Table 2) have been evaluated.

**Table 1** Case 1 – scenarios studied for landscape office -1 and 0, entrance lobby

Scenario	Automated shading	Mechanical ventilative cooling 24/7	Natural ventilative cooling 24/7	Thermal mass	Mechanical heating and cooling devices (zone level)
1	no	no	no	light	radiant panel
2	yes	no	no	light	radiant panel
3	yes	yes	no	light	radiant panel
4	yes	no	yes	light	radiant panel
5	yes	no	yes	heavy	radiant panel
6	yes	no	yes	heavy	TABS

**Table 2** Case 2 – scenarios studied for the auditorium

Scenario	Automated shading	Mechanical ventilative cooling 24/7	Natural ventilative cooling 24/7	Thermal mass	Mechanical heating and cooling devices (zone level)
1	yes	yes	yes	light	fan coil
2	yes	yes	yes	heavy	fan coil
3	yes	yes	no	heavy	fan coil

### 3 MAIN FINDINGS

#### 3.1 Evaluation of the resilience indicators

The results of calculation of the Overheating Escalation factor (OEF) and the Indoor Overheating Degree (IOD) under Historical Heatwave and under long-term future heatwave for the six scenarios of case 1 are shown in Figure 6. All scenarios have been simulated with and without mechanical cooling. For the second case similar results were found.

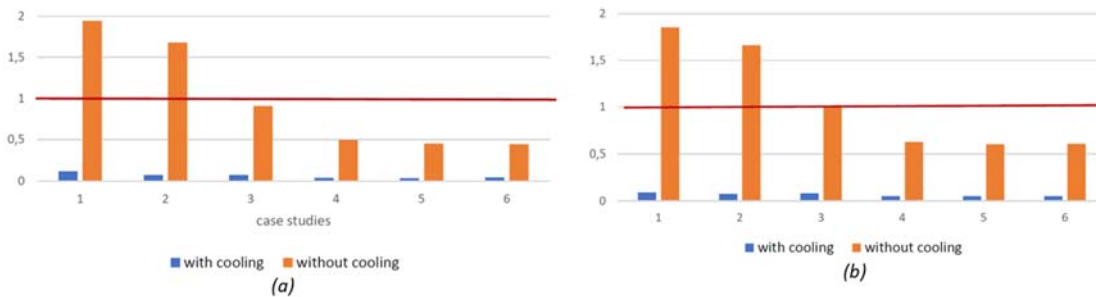


Figure 6: Case 1 (a) Overheating Escalation Factor (historical HW), (b) Overheating Escalation Factor (long-term future HW)

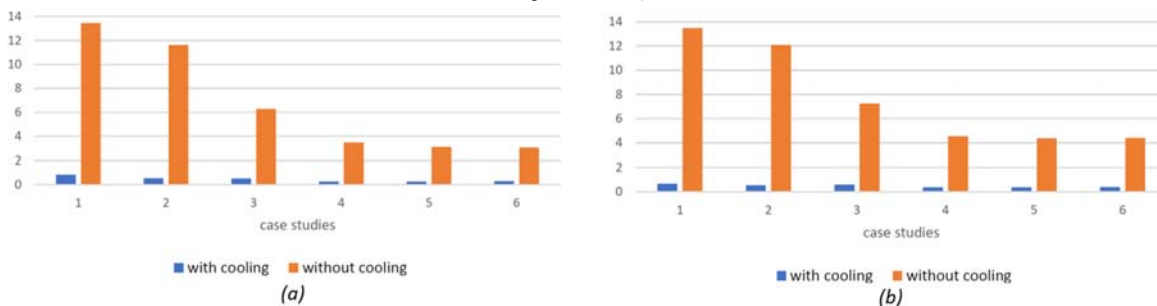


Figure 7: Case 1 (a) Indoor Overheating Degree (historical HW), (b) Indoor Overheating Degree (long-term future HW)



In both cases the effect of the climate responsive design strategies on the resilience indicator is clear. For case 1 the combination of shading with a ventilative cooling strategy, whether natural or mechanical results in an OEF  $< 1$ . An OEF greater than 1 means that indoor thermal conditions get worse when compared to outdoor stress. An OEF lower than 1 means that the dwelling can suppress some of the outdoor thermal stress (REHVA Task Force, 2024). The combination with a natural ventilative strategy results in an OEF  $< 0,5$ , which shows that this concept is even more robust. The impact of thermal mass is less significant. The results are similar under historical (Figure 6a and 7a) and future heatwave conditions (Figure 6b and 7b).

#### 4 DISCUSSION

(Machard, 2021) has identified thermal mass, free-cooling, a high-albedo, and a reduced glazing percentage as main strategies to reduce the cooling load under future climate conditions. (Ramon, 2024) evaluated the whole life cycle environmental impact under future climate conditions. She identified characteristics related to windows, with Window-To-Wall ratio as the most important and solar shading as one of the most important strategies. The main orientation of the windows also had a significant influence, with north-south orientated windows as more favorable than east-west. Thermal mass in combination with night cooling was considered in certain scenarios as a favorable strategy.

(Declercq, 2021) and (Khosravi, 2023) have identified similar strategies for the two case studies as favorable to reduce the energy use for cooling, both under current and under future climate conditions.

The resilience indicators OEF and IOD show a similar behavior. Shading and ventilative cooling prove to be good strategies to improve the resilience to overheating. The impact of thermal mass is less visible. The reason could be twofold. In first instance the high nocturnal ventilation rates reduce already significantly the risk to overheating. In second instance the resilience assessment is being performed with weather data with heatwaves of significant duration. During long heatwaves the thermal mass can get saturated. When the heatwave ends, the building needs more time to cool down and to regain its comfort status.

#### 5 CONCLUSION

Climate Responsive Design strategies, such as reducing the glazing ratio, providing shading, and adopting ventilative cooling strategies, with or without thermal mass, appear to be relevant strategies to reduce the energy demand for cooling, both under current and future typical meteorological year, and to improve the resilience to overheating under extreme weather conditions with shocks, such as heatwaves.

In current research, only a few cases are assessed. A more profound research could bring further insights. In these case studies some parameters have not been varied, such as the window-to-wall ratio and the overall orientation of the building. Also assessing the impact of these parameters on the resilience to overheating of a building can be an important added value to gain more insight and to further develop climate responsive design strategies, which make the building stock more robust towards the resilience of overheating.

The insights gained are already valuable to inform future building design. The impact of these building design related parameters on the resilience is significant. With the future climate challenges in mind it is worth considering the extent to which these design strategies should be applied to reach a more resilient building stock. That both reduces the energy demand for cooling and has greater resilience to shocks.

## 6 ACKNOWLEDGEMENTS

This research was funded through the VLAIO ICON Flux 50 research program of the Flemish Government.

The authors would like to thank Abantika Sengupta, Hilde Breesch and Shiva Khoshravi for their valuable contributions to this research.

## 7 REFERENCES

- Allacker, K. (2010). *Sustainable Building: The development of an evaluation method*. Dissertation, KU Leuven
- Declercq, J. et al. (2021). *The feasibility of natural ventilative cooling in an office building in a Flemish urban context and the impact of climate change*. Building Simulation 2021, International building performance simulation association (IBPSA), Sep 2021, Bruges, Belgium. DOI:10.26868/25222708.2021.30811
- Holzer, P. (2024). *International Energy Agency Resilient Cooling of Buildings – Project Summary Report (Annex 80)*. Institute of Building Research & Innovation
- Khosravi, S. et al. (2023). *Analyzing natural ventilation and cooling potential in a communal space building in Belgium under future climate conditions*. 43rd AIVC - 11th TightVent - 9th venticool Conference - Copenhagen, Denmark - 4-5 October 2023
- Khosravi, S. et al. (2024). *Chapter 10 – Developed Case Study II*. Resilient Cooling Design Guidelines. REHVA
- Machard, A. et al. (2021). *Adapting French buildings to future climate: passive design optimisation*. Building Simulation 2021, International building performance simulation association (IBPSA), Sep 2021, Bruges, Belgium. DOI:10.26868/25222708.2021.30718
- Machard, A., Salvati, A., Tootkaboni, M. et al. (2024). *Typical and extreme weather datasets for studying the resilience of buildings to climate change and heatwaves*. Sci Data 11, 531, May 2024. DOI:10.1038/s41597-024-03319-8
- Ramon, D. et al. (2020). *Future heating and cooling degree days for Belgium under a high-end climate change scenario*. Energ Buildings.
- Ramon, D. et al. (2023). *Optimizing building solutions in a changing climate: parameter-based analysis of embodied and operational environmental impacts*. Environ. Res.: Infrastruct. Sustain. 3 045010
- Stern, P. (ed.), Czarnecki, P. (ed) (2024). *Resilient cooling of buildings. Key Performance Indicators Report (Annex 80)*, International Energy Agency. DOI:10.52776/RHET5776
- REHVA Task Force (2024), *Resilient Cooling Design Guidelines*, REHVA and EBC
- Sengupta, A. et al. (2020). *Analysis of resilience of ventilative cooling technologies in a case study building*. iCRBE Procedia Volume 1: Issue 1 (2020) 1-10
- Zhang, C., et al. (2021). *IEA EBC Annex 80 – Dynamic simulation guideline for the performance testing of resilient cooling strategies*. Aalborg University.

# Indoor Thermal Resilience in Irish Schools, Office and Healthcare Buildings

Adam O' Donovan\*, Elahe Tavakoli, Paul D. O'Sullivan

*Department of Process, Energy & Transport Engineering  
Munster Technological University  
Rossa Avenue, Bishopstown, Cork, Ireland  
\*Corresponding author: adam.odonovan@mtu.ie*

## SUMMARY

There is an increasing need to consider and evaluate the effect of existing ambient warmth on current low energy buildings to determine if current guidelines and standards are robust or resilient in the face of projected future warming. Thus far there is a lack of empirical evidence from low energy non-residential spaces where resilience metrics are seldom explored. The purpose of this presentation is to present the status on overheating from over 30 different low energy non-residential buildings located in Ireland. The dataset includes data schools, office and educational buildings and healthcare buildings that were monitored over at least one cooling season between 2021 and 2023. The work will consider not only traditional overheating metrics but will also consider this overheating in the context of resilience metrics that have been adopted from previous work. The outcomes are expected to feed back into the future of non-residential building design in Ireland.

## KEYWORDS

Overheating, data, low energy buildings, resilience

## ACKNOWLEDGEMENTS

This research has been funded by the Sustainable Energy Authority of Ireland (SEAI) RD&D fund 2019, under grant number RDD/00496. We would like to thank all facilities management companies, data providers and study participants for their support for this project.

# Overall outcomes from the project and next steps

Adam O' Donovan\*, Paul D. O'Sullivan

*Department of Process, Energy & Transport Engineering  
Munster Technological University  
Rossa Avenue, Bishopstown, Cork, Ireland  
\*Corresponding author: adam.odonovan@mtu.ie*

## **SUMMARY**

Project RESILIENCE set out to examine overheating in a variety of building archetypes, but also examined several aspects of overheating related to the tools that are used, the weather data that has been employed in dynamic simulations and potential low-cost solutions to improving the resilience of the existing non-residential building stock that relies upon ventilative cooling. This presentation will discuss and synthesise the key outcomes from the project structured around evidence from: 1) existing measurement data, 2) reviews of the literature, 3) calibrated dynamic simulations, 4) subjective data from occupants' designers and 5) simplified ventilative cooling assessment methods. These five areas will contribute to a holistic assessment of overheating in non-residential buildings and what lessons can be learned to improve the policy regarding the resilience of buildings going forward.

## **KEYWORDS**

Overheating, summary, occupants, designers, modelling, future planning

## **ACKNOWLEDGEMENTS**

This research has been funded by the Sustainable Energy Authority of Ireland (SEAI) RD&D fund 2019, under grant number RDD/00496. We would like to thank all facilities management companies, data providers and study participants for their support for this project.

# Overheating Mitigation Policy: Current Trends & Future Outlook

Paul D. O'Sullivan\*, Adam O' Donovan

*Department of Process, Energy & Transport Engineering  
Munster Technological University  
Rossa Avenue, Bishopstown, Cork, Ireland  
\*Corresponding author: paul.osullivan@mtu.ie*

## SUMMARY

Project RESILIENCE set out to examine overheating risk in a variety of non-residential building archetypes, but also examined several aspects of both overheating risk metrics and indoor thermal resilience evaluation criteria. Assessing the future risk of overheating in new and retrofitted buildings is usually undertaken by applying national regulations and buildings codes where minimum criteria is typically published. The challenge for regulators is to ensure the adopted approaches are robust and ensure reliable evaluations of how a building will perform in the future under a range of different scenarios. Recent research work on resilient cooling and resilient indoor thermal environments has attempted to move beyond assessing the vulnerability of an indoor environment in isolation and instead include how the environment might adapt and recover from extreme events and failures in its basic functioning. In this workshop we intend to explore how regulatory approaches might evolve to incorporate new metrics in this regard. In particular the focus will look at the early stages of design and what regulatory or design based checks are in place to address vulnerability lock-in in future designs, i.e. are there planning stage checkpoints for stress testing building designs prior to detailed design stage. The work will also leverage results and insights from Project RESILIENCE, particularly regarding how different building designs performed in practice.

## KEYWORDS

Overheating, summary, occupants, designers, modelling, future planning

## ACKNOWLEDGEMENTS

This research has been funded by the Sustainable Energy Authority of Ireland (SEAI) RD&D fund 2019, under grant number RDD/00496. We would like to thank all facilities management companies, data providers and study participants for their support for this project.

# Effect of Personalized Environmental Control Systems on Occupants' Health, Comfort and Productivity

Mariya Bivolarova<sup>1</sup>, Dolaana Khovalyg<sup>2</sup>, Bjarne W. Olesen<sup>1\*</sup>

*1 Technical University of Denmark (DTU),  
International Center for Indoor Environment and  
Energy (ICIEE)  
Denmark*

*2 École polytechnique fédérale de Lausanne (EPFL),  
Laboratory of Integrated Comfort Engineering (ICE)  
Switzerland*

*\*Corresponding author: bwol@dtu.dk*

## SUMMARY

This summary highlights the benefits of PECS for occupants' health, comfort, and cognitive performance. A comprehensive literature review was conducted using databases such as Scopus, Web of Science, and Google Scholar, focusing on terms related to personalised conditioning, air quality, lighting, and acoustics. Relevant studies were identified and reviewed.

The session will present findings categorized into four topics: the relationship between thermal comfort and PECS performance, air quality and contaminant removal efficiency with PECS, cognitive performance and PECS, and overall health and well-being linked to PECS performance.

## KEYWORDS

Indoor Environment, Personalized Environmental Control Systems (PECS), Thermal Comfort, Air Quality, Occupant Health and Performance

## 1 INTRODUCTION

Indoor environment influences the health, comfort, and performance of building occupants (Wargocki et al., 2006; Sundell et al., 2011; Tang et al., 2020). Centralised heating, ventilation, and air-conditioning (HVAC) systems are the primary methods for controlling indoor air quality and the thermal conditions in buildings. These systems are designed to ventilate and condition the entire room air volume and provide uniform temperature and velocity distribution in the occupied zone at levels acceptable for an 'average occupant'. However, due to factors like gender, age, fitness, and personal preferences, it has been challenging for HVAC systems to maintain indoor temperature and humidity levels that meet everyone's thermal comfort needs (Indraganti, 2010). In addition, the method of ventilating an entire room based on total volume air distribution is often not efficient in providing pollutant-free air. Efficient transport, dilution, and removal of airborne contaminants in indoor environments are defined by air distribution. However, it is challenging to control the overall airflow pattern in rooms (Melikov, 2016). To overcome these disadvantages of HVAC systems, Personalized environmental control systems (PECS) have been extensively researched for their effectiveness in improving individual thermal comfort and providing high ventilation efficiency in the breathing zone of the occupants (Melikov, 2016; Vesely, M. and Zeiler, W., 2014). PECS are systems that can provide individually controlled thermal, air quality, acoustic or luminous environments in the immediate surroundings of an occupant without directly affecting the entire space and other occupants' environment.

There are several systematic literature reviews which describe the different PECS (Rawal et al., 2020). However, most existing literature review studies have focused primarily on the effectiveness of PECS in terms of human thermal comfort and energy-saving efficiency. The current summary will focus on the benefits of PECS in terms of occupants' health, comfort and cognitive performance.

## **2 METHODOLOGY**

The scientific databases Scopus, Web of Science, PubMed, Research Gate, Google Scholar, and Taylor and Francis were searched. A separate search was conducted for each domain. For the thermal and indoor air quality environmental domains, the search was done using the following keywords: personalised, local conditioning, heating and cooling in combination with thermal comfort/sensation, air quality, perceived air quality, cross-infection, exposure, airborne transmission, human-centred, occupant health, well-being, productivity, physiological response, human response and cognitive performance. For the visual domain, the following keywords were used: personal/personalized light, personalised façade, personalised shading/solar control/control in combination with human-centric, individual control, integrated/spectral/health lighting, and visual comfort. To search for relevant literature related to Acoustic PECS, the following keywords were used: personalized audio/sound, sound mask, noise mask in combination with headphones, earphones, headset, earmuff, earplug, and sound zone. Additionally, the keywords individual control, build environment, office, workplace, school, and home were used in the search strings for all domains. The resulting articles' abstracts were subsequently examined to ensure they aligned with the paper's objectives. After this step, the relevant papers were identified and reviewed.

## **3 RESULTS**

During the workshop on Advancing Personalised Environmental Control Systems, this session will present results based on the existing literature grouped into four topics:

- Link Thermal Sensation/Acceptability/Comfort votes/ with PECS performance and Background environment
- Link Perceived Air Quality votes/Contaminant removal efficiency with PECS performance and Background environment
- Link Performance/Cognition/Psychological tests with PECS performance and Background environment
- Link Health/Well-being with PECS performance and Background environment

## **4 ACKNOWLEDGEMENTS**

This work was conducted within the framework of IEA-EBC Annex 87.

## **5 REFERENCES**

- Wargocki, P., Seppanen, O., Andersson, J., Boerstra, A., Clements-Croome, D., Fitzner, K. and Hanssen, S.O. (2006) Indoor Climate and Productivity in Offices, REHVA Guidebook 6.
- Sundell, J., Levin, H., Nazaroff, W., Cain, W.S., Fisk, W.J., Grimsrud, D.T., Gyntelberg, F., Li, Y., Persily, A.K., Pickering, A.C., Samet, J.M., Spengler, J.D., Taylor, S.T. and Weschler, C.J. (2011) Ventilation rates and health: multidisciplinary review of the scientific literature, *Indoor Air*, 21, 191–204.

- H. Tang, Y. Ding, B. Singer, Interactions and comprehensive effect of indoor environmental quality factors on occupant satisfaction, *Build Environ* 167 (2020) 106462.
- M. Indraganti, K.D. Rao. (2010) Effect of age, gender, economic group and tenure on thermal comfort: A field study in residential buildings in hot and dry climate with seasonal variations, *Energ. Build.* 42 (3) (2010) 273–281.
- A. Melikov. (2016). Advanced air distribution: improving health and comfort while reducing energy use, *Indoor Air* 2016, 26: 112–124.
- Vesely, M. and Zeiler, W. (2014) Personalized conditioning and its impact on thermal comfort and energy performance – A review, *Renew. Sustain. Energy Rev.*, 34, 401–408.
- R. Rawal, M. Schweiker, O.B. Kazanci, V. Vardhan, Q. Jin, L. Duanmu, (2020) Personal comfort systems: A review on comfort, energy, and economics, *Energ Build* 214 (2020) 109858.



# Personalized environmental control systems (PECS): Overview of applications, technology classification and KPIs

Kai Rewitz\*<sup>1</sup>, Joyce Kim<sup>2</sup>, Fatemeh Nabilou<sup>1</sup>, Kehinde Bayode<sup>2</sup>, and Dirk Müller<sup>1</sup>

*1 RWTH Aachen University,  
E.ON Energy Research Center,  
Institute for Energy Efficient Buildings and Indoor  
Climate  
Mathieustraße 10, 52074 Aachen, Germany  
\*Corresponding author: kai.rewitz@eonerc.rwth-  
aachen.de*

*2 Department of Civil and Environmental  
Engineering, Faculty of Engineering  
University of Waterloo  
200 University Avenue West, CPH 3673  
Waterloo, Ontario, Canada, N2L 3G1  
\*Corresponding author: joyce.kim@uwaterloo.ca*

## SUMMARY

Personal Environmental Control Systems (PECS) enable to individually control the environment in the immediate surroundings of an occupant regarding the thermal, air quality, acoustic, and/or luminous domain without directly influencing the entire space and other occupants' environment. Although many studies on the influence on the respective comfort and acceptance in relation to the different domains already exist and estimates of energy savings have already been made, PECS have not yet established themselves on the market across the board. In this session we will propose how to classify PECS for the built environment and which KPIs can be used to evaluate different types of them. This is a first step towards a standardised qualitative and quantitative assessment of the benefits that PECS can provide.

## KEYWORDS

Indoor Environment, Personalized Environmental Control Systems (PECS), Thermal Comfort, Air Quality, KPI

## 1 INTRODUCTION

The application of PECS in buildings primarily enables an increase in comfort and user acceptance which is often also combined with healthier environments and increased productivity (Rawal et al. 2020; Luo et al. 2022; Song et al. 2022). These systems can be used for heating, cooling, ventilation, and air filtration as well as for adjusting the lighting and acoustic environment. PECS can also cover a combination of these application areas. In addition, studies of PECS often estimating a reduction in overall building energy demand as well as an economic advantage (Zhang et al. 2015; Hoyt et al. 2015).

However, PECS are not yet widespread and are used even less frequently in an overall building concept. The possibility of retrofitting often depends on the energy and media connection. For example, an electrically heated office chair is easier to retrofit than a personal ventilation system that has to be connected to a fresh air supply. Energy savings furthermore depend on the possibility of integrating PECS into the building automation system or taking it into account there. Planners and building operators therefore need an overview of the different types of PECS, their capabilities, and limitations to be able to use them in a more targeted way and answer the following questions, for example:

- Which PECS help to improve user satisfaction and comfort in certain domains?
- Which PECS help to decrease overall energy demand?

- Which PECS can be used for a certain building and can costs be saved when refurbishing with PECS compared to conventional approaches?
- How can PECS are integrated into the planning process for new buildings, e.g., through a smaller design or by avoiding conventional air handling units?

To help to answer these questions, this session will provide classification proposals and KPI of PECS for the different domains.

## 2 METHODOLOGY

Based on an extensive literature search within the framework of IEA-EBC Annex 87, in which the databases of Scopus, Web of Science, PubMed, Research Gate, Google Scholar, and Taylor and Francis were searched, classification proposals for different PECS are first developed. In addition to the already known categorizations regarding the thermal, air quality, acoustic and luminous domains, further relevant properties need to be identified to provide a better overview of the areas of application, implementation options and operation. For the implementation, a differentiation can be made regarding the general design as to whether the PECS are integrated into the building structure (“building attached”, e.g., a locally heated or cooled wall), can be used independently from the building structure (“building detached”, e.g., furniture-integrated device) or can be considered as building semi-detached (e.g., personalized ventilation with the supply duct connected to the central HVAC). Regarding implementation, a distinction can also be made between the media or energy supply (e.g., electricity, water or air-based) and the data connection (none, cable, wireless) as well as the communication protocol used. For operation, for example regarding the thermal domain, a difference can be made between the heat transport mechanisms (radiation, conduction, convection, evaporation), which have an influence on PECS efficiency. A distinction can also be made as to whether the PECS are operated in a stationary or transient mode.

In collaboration with the working group from Subtask-D of IEA-EBC ANNEX-87, relevant KPIs were analyzed based on the literature review. Firstly, the evaluation metrics for the individual domains were analyzed. For the thermal domain, for example, this includes the corrective power in the case of a change in the average room temperature, which represents the compensatory capacity of the PECS, which can be expressed either in K or in a shift in thermal sensation (Zhang et al. 2015). In addition, the degree of coverage of the PECS in relation to the body segments reached and the (specific) energy requirement are considered. Further KPIs are proposed with regard to the implementation effort for an evaluation of retrofitting in existing buildings and in terms of higher-level building automation with regard to the data and communication interfaces. Finally, economical KPI as well as indirect and overarching effects on productivity, well-being and health are summarized.

## 3 RESULTS AND DISCUSSION

During the workshop on PECS during the 44th AIVC – 12th TightVent & 10th venticool Conference, this session will propose the following:

- Extended classification approach for PECS regarding application, implementation, and operation in the built environment
- Summary of relevant KPI from literature and discussion of new KPI proposals
- Discussion of the results and new approaches

## 4 ACKNOWLEDGEMENTS

This work was conducted within the framework of IEA-EBC Annex 87. We gratefully acknowledge the financial support by the Federal Ministry for Economic Affairs and Climate Action (BMWK), promotional reference 03EN1081A.

Supported by:



on the basis of a decision  
by the German Bundestag

## 5 PUBLICATION BIBLIOGRAPHY

Hoyt, Tyler; Arens, Edward; Zhang, Hui (2015): Extending air temperature setpoints: Simulated energy savings and design considerations for new and retrofit buildings. In *Building and Environment* 88, pp. 89–96. DOI: 10.1016/j.buildenv.2014.09.010.

Luo, Wei; Kramer, Rick; Kort, Yvonne de; van Marken Lichtenbelt, Wouter (2022): Effectiveness of personal comfort systems on whole-body thermal comfort – A systematic review on which body segments to target. In *Energy and Buildings* 256, p. 111766. DOI: 10.1016/j.enbuild.2021.111766.

Rawal, Rajan; Schweiker, Marcel; Kazanci, Ongun Berk; Vardhan, Vishnu; Jin, Quan; Duanmu, Lin (2020): Personal comfort systems: A review on comfort, energy, and economics. In *Energy and Buildings* 214, p. 109858. DOI: 10.1016/j.enbuild.2020.109858.

Song, Wenfang; Zhang, Ziran; Chen, Zihao; Wang, Faming; Yang, Bin (2022): Thermal comfort and energy performance of personal comfort systems (PCS): A systematic review and meta-analysis. In *Energy and Buildings* 256, p. 111747. DOI: 10.1016/j.enbuild.2021.111747.

Zhang, Hui; Arens, Edward A.; Zhai, Yongchao (2015): A review of the corrective power of personal comfort systems in non-neutral ambient environments. In *Building and Environment* 91, pp. 15–41. DOI: 10.1016/j.buildenv.2015.03.013.

# Personalized environmental control systems (PECS): Overview of evaluation methods

Douaa Al Assaad\*<sup>1,2</sup>, Ilaria Pigliautile<sup>3</sup>

*1 KU Leuven  
Gebroeders de Smetstraat 1  
9000 Gent, Belgium*

*2 TU Eindhoven  
5600 MB Eindhoven, The Netherlands  
\*douaa.al-assaad@kuleuven.be*

*3 Engineering Department, University of Perugia  
Via G. Duranti, 93  
1626, Perugia (PG), Italy*

## SUMMARY

Nowadays, the building sector faces many challenges on occupant and resource levels. Given many indoor environmental quality (IEQ) complaints collected by field surveys, the first challenge is to provide comfort improvements. The second challenge is to be able to do so without unjustifiably increasing energy costs. The main reason why buildings face such issues is the implementation of IEQ management systems that target the entire space – even unoccupied zones. This doesn't guarantee comfort and wastes building resources. This led to the development of personalized environmental control systems (PECS) that aim to improve IEQ where it is needed – in the vicinity of occupants responding to individual needs while giving them the possibility of control. This not only improves comfort but can lead to energy savings with proper system design and operation. PECS have been extensively studied in the literature via diverse simulation or experimental methods with researchers reporting the performance using different indices and metrics. However, currently; there exists no standardized or universal ways of studying and reporting the performance of PECS. Thus, the aim of Subtask D of IEA EBC's Annex 87 on PECS is to develop such guidelines by first giving an overview of the existing methodological trends on PECS performance assessment. This summary gives an overview of the ongoing literature review with focus on thermal & IAQ PECS and presents some preliminary results.

## KEYWORDS

Personalized environmental control systems (PECS), performance assessment, simulations, chamber & field experiments

## 1 REVIEW METHODOLOGY

The scientific databases of Science Direct, Web of Science, Taylor & Francis, Wiley Online library were searched for terms related to PECS and their impact on thermal comfort, indoor air quality, energy. The search yielded 589 papers eligible for review that included PECS. From the 589 papers, and in line with the review objectives, reports pertaining to personal protective equipment, hospital environments, textiles with no active heating or cooling function were excluded yielding 530 papers. From these papers, 11.3% studied PECS using building simulation tools, 23.7% using computational fluid dynamics (CFD) simulations, 55.5% used chamber studies and 9.4% used field studies.

### 1.1 Simulation methods

With careful modelling and calibration, simulations allow testing a wide range of conditions at lower cost and complexity than experiments. Building simulations offer a better understanding on the balance between PECS performance and long-term power use under different typologies and climates. CFD offers a comprehensive visualization of the impact of PECS on the airflow field which helps to gain a deeper understanding into its performance and guiding its design. Out of 11.3% studies using building simulation methods, some integrate PECS directly into building simulation tools (EnergyPlus 20.6%, IES virtual environment 13.2%, Modelica 5.6%, ESP-r 5.6%, IDA-ICE 3.7%, TRNSYS 2%, other locally developed software 9.4%) (Shahzad,

2020) or develop their own simplified mathematical model of the PECS coupled with state space models or building simulation models of the space (39.6%) (Makhoul, 2013). The most simulated cases were offices (65.5%), residential (7%), educational (5%), commercial (3.5%) and others (19%). 96% of the PECS simulated were mostly heating and cooling personalized systems with no ventilation function (e.g., heated and cooled chairs, radiant panels). 4% had a ventilation function and assessed comfort, IAQ and energy performance or just energy performance. Out of 23.7% studies using CFD, all of them model PECS directly into the domain and use tools such as ANSYS Fluent (40.6%), Airpak (6%), COMSOL (3%), star-CCM+ (3%), own developed CFD code (2%) with most simulated cases being offices, vehicles and aircraft cabins and focused on ventilative PECS. 79.1% of the studies assessed the performance of personalized ventilation systems mounted in desks or chairs (Sekhar, 2018), while 6% studied local radiant panels for heating and cooling, 4% studied heated or cooled furniture (Shahzad, 2018), 4% ventilated clothing, 2% personalized exhaust and 2% thermal wearables (masks, jackets).

## 1.2 Experimental methods

Laboratory and field studies allow to determine the impact of a specific technology on human responses including physiological, perceptual, cognitive, and behavioural responses. Lab studies guarantee to examine the impact of PECS on occupants' responses under controlled environmental conditions. By varying both background system and PECS settings, most of the lab studies focus on determining physiological and perceptual changes of the average person. The sample size definition is thus of utmost importance to guarantee a great representativeness of the real population (Pasut, 2015). Moreover, it is quite common that lab experiments involve manikins, resembling a standard man and its physiological reactions, as for the 33% of the reviewed articles (Mustakallio, 2016). Field studies are mainly observational, further looking for occupants' acceptance of the proposed PECS that are generally introduced in the case study after an initial period of observation, representing the reference scenario without PECS. Most of the reviewed field studies took place in office spaces (63%) (Kim, 2019) and dealt with PECS not directly connected to the building structure, such as those associated to furniture elements (51%).

## 2 REFERENCES

- Shahzad, S. (2020). *Analysis of the Thermal Comfort and Energy Performance of a Thermal Chair for Open Plan Office*. Journal of Sustainable Development of Energy, Water and Environment Systems, 8(2), 373-395.
- Makhoul, A. (2013). *The energy saving potential and the associated thermal comfort of displacement ventilation systems assisted by personalised ventilation*. Indoor and Built Environment, 22(3), 508-519.
- Sekhar, C. (2018). *Study of an integrated personalized ventilation and local fan-induced active chilled beam air conditioning system in hot and humid climate*. In Building Simulation, 11, 787-801.
- Shahzad, S. (2018). *Advanced personal comfort system (APCS) for the workplace: A review and case study*. Energy and Buildings, 173, 689-709.
- Pasut, W. (2015). *Energy-efficient comfort with a heated/cooled chair: Results from human subject tests*. Building and Environment, 84, 10-21.
- Mustakallio, P., (2016). *Thermal environment in simulated offices with convective and radiant cooling systems under cooling (summer) mode of operation*. Building and Environment, 100, 82-91.
- Kim, J., (2019). *Occupant comfort and behavior: High-resolution data from a 6-month field study of personal comfort systems with 37 real office workers*. Building and Environment, 148, 348-360.

# Policy Strategies and Market Perspective of Personalized Environmental Control Systems

Rajan Rawal\*<sup>1</sup>, Bjarne Olesen<sup>2</sup>, Ongun Berk Kazanci<sup>2</sup>, and Arsen Krikor Melikov<sup>2</sup>

*1 CEPT University*

*Navarangpura*

*Ahmedabad 380 009 India*

*\*Corresponding author: rajanrawal@cept.ac.in*

*2 Technical University of Denmark (DTU),*

*Koppels Allé, 402, 220,*

*2800 Kgs. Lyngby, Denmark*

## SUMMARY

This session will begin with providing an overview of presence Personal Environmental Control Systems (PECS) related mention in various countries national codes and standards formulated by industry organizations. It will then articulate possible entry points for PECS in policy document such as building codes, health and safety code and voluntary building performance rating programs. Towards end, it will identify market barriers, market challenges and market opportunities that may aid widespread deployment of PECS.

## KEYWORDS

Indoor Environment, Personalized Environmental Control Systems (PECS), Technology Readiness Level (TRL), Policy intervention, market transformation, health and well being

## 1 INTRODUCTION

Personal Environment Control Systems (PECS) can generate a microenvironment within the buildings and around the building occupant that is in the control of the occupant and provides preferred thermal, luminous and aural environments. Apart from promoting desired environmental conditions, PECS is also known to provide higher energy efficiency and conducive healthy environments. Design, development and deployment of any technological advancements needs to have a suitable policy environment. Inclusive codes and standards towards modern approaches to gain comfort within the built environment provide a favourable market transformation environment for newer design approaches, technologies and products to flourish. Certain policy initiatives are also known to offer higher opportunities for industry to engage in newer areas and engage in economic activities. This session will provide an overview of reference codes and standards documents that deal with comfort concerning thermal comfort, lighting and acoustics. Extensive literature exists to understand the benefits of the PECS, further, available literature also provides suitable guidance to ideate, design and produce PECS in all three domains of thermal, lighting and acoustics. However, the inclusion of the PECS domain in codes and standards has not been advanced as expected. This session will discuss the possible entry points for codes and standards for the inclusion of PECS. The session will also elaborate on the possible market transformation pathways for the wider adoption of PECS, after discussing the barriers and challenges that must be overcome.

## 2 METHODOLOGY

The reference codes and standards document prepared by various countries as part of their national codes, best practices manuals prepared by industry organizations, actions plan such as cooling actions plans, and recommendations for ventilation and overheating risk mitigation

plans prepared by various countries were reviewed to find the possible reference to PECS, even the closest references that may have the possibility of PECS meeting the requirements were identified. The standards and guideline documents prepared by industry organizations such as the Federation of European Heating, Ventilation and Air Conditioning Associations (REHVA), The American Society of Heating, Refrigerating and Air-Conditioning Engineers (ASHRAE), and The Chartered Institution of Building Services Engineers (CIBSE) for thermal aspects, (International Association of Lighting Designers (IALD) and International Commission on Illumination (CIE) for lighting and Acoustical Society of America (ASA) for acoustics, as well as ISO and CEN were reviewed for likely PECS. The building codes, health-safety codes and voluntary rating program documents were reviewed. The mention was categorised into two broad categories, prescriptive and performance-based approaches. The strategy approaches were also studied from the perspective of PECS's reliance on building envelope systems, furniture systems, HVAC systems and stand-alone systems with a high degree of mobility. Toward the end, available PECS technologies were reviewed on their technology readiness level (TRL) to consider the suitable nature of policy intervention, possible policy entry points and means to achieve it.

### **3 RESULTS AND DISCUSSION**

During the workshop on PECS during the 44th AIVC – 12th Tight Vent & 10th Venti cool Conference, this session will propose the following

- Pathways and entry points for the inclusion of PECS in codes, standards and voluntary rating programs
- Ways and means to develop a roadmap for the industry to rely on available knowledge to develop technologies and products
- Identification of stakeholders, methods to inform them and outreach strategies to advocate PECS in practice.

### **4 ACKNOWLEDGEMENTS**

This work was conducted within the framework of IEA-EBC Annex 87.

### **5 BIBLIOGRAPHIC REFERENCES**

Shinoda, J., Technical University of Denmark, Technical University of Denmark, & Technical University of Denmark. (2022). *A qualitative evaluation of the resiliency of Personalized Environmental Control Systems (PECS)* (42nd AIVC Conference). <https://www.aivc.org/resource/qualitative-evaluation-resiliency-personalized-environmental-control-systems-pecs>

Rawal, R., Schweiker, M., Kazanci, O. B., Vardhan, V., Jin, Q., & Duanmu, L. (2020). Personal comfort systems: A review on comfort, energy, and economics. *Energy and Buildings*, 214, 109858. <https://doi.org/10.1016/j.enbuild.2020.109858>

*Transition to personal comfort systems*. (2022, June 10). Buildings and Cities. <https://www.buildingsandcities.org/insights/commentaries/transition-personal-comfort-systems.html>

*Mainstreaming Personal comfort systems (PCS)*. (2022, May 30). Buildings and Cities. <https://www.buildingsandcities.org/insights/commentaries/mainstreaming-personal-comfort-systems.html>

Rawal, R., Vardhan, V., Schweiker, M., Kazanci, O. B., (2021). *Guidelines for Personal Comfort Systems in Low Energy Buildings*. IEA EBC Annex 69: Strategy and Practice of Adaptive Thermal Comfort in Low Energy Buildings.



# Building ventilation requirements and inspection in Belgium

Arnold Janssens<sup>\*1</sup>, Laura De Jonge<sup>1</sup>, Maarten De Strycker<sup>2</sup>, Liesje Van Gelder<sup>2</sup>

*1 Research Group Building Physics  
Ghent University  
Gent, Belgium*

*2 Belgian Construction Certification Association  
Hermeslaan 9  
Diegem, Belgium*

*\*Corresponding author: [arnold.janssens@ugent.be](mailto:arnold.janssens@ugent.be)*

## ABSTRACT

In Belgium, the requirements for ventilation in buildings can be found in national ventilation standards, national health regulation and in regional environmental regulations and EPB regulations (Energy Performance and Indoor Climate). In 2006 the latter regulations were introduced for the first time including mandatory requirements for ventilation. From then on it was mandatory for all new and renovated, both residential and non-residential buildings for which a building permit is necessary to install a natural or mechanical ventilation system for acceptable indoor air quality. This paper further discusses the present ventilation requirements in buildings (both residential and non-residential), current trends in the Belgian building ventilation market, energy requirements, requirements for inspection of the systems, innovations in the market and the impact of Covid-19.

Although standards and guidelines are generally published at a national level in Belgium, building energy performance regulation is a regional matter, including ventilation requirements. This means that each of the three regions – Flemish, Brussels Capital and Walloon Region – can have a different approach. Although most regulations are similar, some parts of the regulation, for instance in relation to inspection, don't apply in all regions. The paper mentions the differences between the regions when this is the case.

## 1 NATIONAL TRENDS IN IAQ REQUIREMENTS AND MARKET

### 1.1 Requirements for the ventilation of dwellings

The Regional decrees on Energy Performance of Buildings in Flanders, Wallonia, and Brussels Capital Region (Energiebesluit 2010, Guide PEB 2015, Environnement Brussels 2024) refer to Annexes which specify the residential ventilation requirements. In general, these Annexes stipulate that ventilation in residential buildings must follow the Belgian standard NBN D50-001 (1991), and list the exceptions and additions to that standard. The standard contains guidelines for ventilation that were made mandatory through the decrees on Energy Performance of Buildings in 2006 in Flanders, and 2008 in Wallonia and Brussels Capital Region. Even though the standard was already 15 years old before it was integrated in the Regional Energy Performance Regulations, it didn't have a large impact in practice at the time. This changed in 2006, mainly as a result of the strictly enforced compliance framework of the Energy Performance Regulations, with declaration of performances after completion of construction works, and a fully operational fine system. As a consequence, the compliance rate of energy performance requirements and ventilation requirements is high.

The standard defines a general minimum rule of 3.6 m<sup>3</sup>/h/m<sup>2</sup> supply air for habitable spaces (also named dry rooms), which are the rooms where people typically spend most of their time, like living rooms, offices, or bedrooms. For extract spaces (also named wet rooms) such as kitchens, bathrooms, laundry rooms and toilets, the same general rule applies for the extract air. Additionally, minimum and permissible maximum flow rates are set for the various room types, as listed in Table 1. The total supply or exhaust flow rate of the system is equal to the sum of the minimum required flow rates per room. Application examples are given in Annex A.

Table 1: Minimum required flowrates in dwellings according to EPB based on NBN D50-001

General rule (supply, extract, transfer)	3.6 m <sup>3</sup> /h/m <sup>2</sup>
Living room (supply)	min: 75 m <sup>3</sup> /h, max: 150 m <sup>3</sup> /h
Bedroom, office, games room, etc. (supply)	min: 25 m <sup>3</sup> /h, max: 72 m <sup>3</sup> /h
Closed kitchen, bathroom, laundry rooms (extract)	min: 50 m <sup>3</sup> /h, max: 75 m <sup>3</sup> /h
Open kitchen (extract)	min: 75 m <sup>3</sup> /h
Toilet (extract)	25 m <sup>3</sup> /h

The standard also specifies that the habitable and the extract spaces should be connected through grilles or slots that can transfer an airflow of 25 m<sup>3</sup>/h (50 m<sup>3</sup>/h for kitchens) when a pressure difference of 2 Pa is applied to both sides of the connecting elements. In practice, the connections between zones are represented as openings of 70 cm<sup>2</sup> between zones (140 cm<sup>2</sup> for kitchens), which normally correspond to the typical gap of 1-2 cm that can be found between the interior doors and the floor in a dwelling.

The possible ventilation systems in the standard are systems with natural supply and natural exhaust (defined as system ‘A’ in the standard), systems with mechanical supply and natural exhaust (B), systems with natural supply and mechanical exhaust (C) and systems with mechanical supply and mechanical exhaust (D). If a ventilation system includes components for natural ventilation such as trickle ventilators or passive stacks, they are sized to achieve the nominal flow at 2 Pa. The EPB ventilation annexes also allow sizing these components at 10 Pa, if the room is served by a mechanical component, for instance if there is mechanical extraction in a room with supply through trickle ventilators.

The user is not obliged to achieve the required flow rates in each room at all times. It is allowed to reduce the flow rates according to the demands at a given moment. Control can be manually via a simple control mechanism (switch or button) or via an automatic control system in response to measurements of humidity, CO<sub>2</sub>,... Mechanical systems should however still maintain a permanent, although reduced, flow rate at all times.

## 1.2 Ventilation systems in residential building stock and market

In Belgium, the energy performance of new and renovated buildings is assessed at the moment of completion of the works by an EPB-assessor, who collects the as-built information, creates the necessary input in the EPB-software, and evaluates whether the building meets the requirements. The EPB-declarations with the results are uploaded to a database, managed by the regional authorities. The analysis of part of this data is publicly available, for instance for Flanders: <https://apps.energiesparen.be/energiekaart/vlaanderen>.

This database also contains extensive information about residential ventilation systems installed in the market, which allows to follow market evolutions. Most data relate to new residential buildings for which data are available since 2006. Although the ventilation requirements were also mandatory for renovation projects with building permit, they were only partially mandatory, depending on the extent of renovation works. As a consequence this data has not been systematically documented in the database. Since 2015 a ventilation system is also mandatory in residential buildings undergoing a deep energy renovation, for which financial benefits apply in Flanders. These data are also public.

Figure 1 shows the evolution of the distribution of residential ventilation systems since 2006 in Flanders. The mechanical extract (System C) and balanced mechanical systems (System D) dominate the market. Of all systems installed in the over 400.000 new dwellings constructed in between 2006 and 2021, 4% are natural ventilation systems (A), 55% are mechanical extract systems (C) and 41% are balanced mechanical systems (D). Since 2014 the share of balanced mechanical systems has gradually been increasing from 50% up to 66% in 2021. This is the result of an associated tightening of energy performance requirements during these years, which were easier to meet when balanced mechanical ventilation with heat recovery was installed.

This type of system is even slightly more prevailing in single family dwellings (67% in 2021), compared to multifamily dwellings (apartments, 60% in 2021). Also in deep energy renovation projects, the systems C and D dominate, with a share of respectively 56% and 42% of the projects constructed in between 2015 and 2021. The mechanical extract systems include systems with demand control, which can be taken into account in the energy performance calculation. However the share of these systems is not specifically documented in the regional analysis reports.

The figures shown in Figure 1 relate to newly constructed dwellings. The implementation of ventilation systems in the existing dwelling stock is much smaller. Analysis of the database of Energy Performance Certificates for dwellings that were for sale or for rent in between 2015 and 2018 showed that only 4% of existing dwellings were equipped with a mechanical ventilation system (B, C or D) (Van Hove et al. 2021).

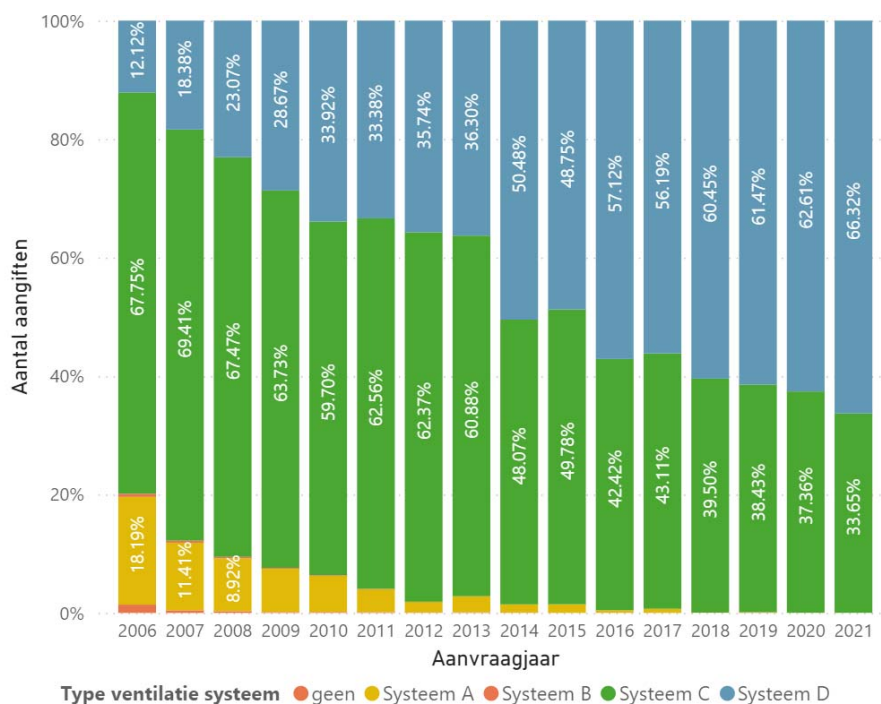


Figure 1: Evolution of the distribution of the type of ventilation systems in new dwellings in Flanders, Belgium between 2006 and 2021 (year of building permit), all dwellings combined

### 1.3 Requirements for the ventilation of non-residential buildings

Similar as for residential buildings, ventilation requirements for non-residential buildings are specified in separate Annexes to the Regional decrees on Energy Performance of Buildings in Flanders, Wallonia, and Brussels Capital Region. They also became mandatory for all types of new and renovated non-residential buildings with building permit, when the Energy Performance Regulations were introduced in 2006 in Flanders, and 2008 in Wallonia and Brussels Capital Region.

The Annexes refer to concepts and classes as defined in the standard NBN EN 13779 to express minimum requirements for the design and operation of ventilation systems. When sizing ventilation systems, the minimum flow rates corresponding to indoor air class IDA3 must be met. When specifying flow rates a difference is made between rooms serving for typical human

occupancy (offices, class rooms,...), and rooms not intended for long term human occupancy (corridors, toilets, storage rooms,...):

- In rooms for human occupancy a minimum flow rate of outdoor air need to be supplied depending on a flow rate per person (min. 22 m<sup>3</sup>/h per person), and the design occupation of the room. The design occupation follows from the design brief of the construction project, but should at least be equal to minimum design occupancies listed in the regulation, for a range of functions including restaurants, hotels, offices, theatres, shops, sport clubs, schools, prisons and hospitals.
- The required flow rates in rooms not for human occupancy depend on a minimum flow rate per unit of floor area (1.3 m<sup>3</sup>/h/m<sup>2</sup>), and the total floor area of the room. In case of sanitary facilities 25 m<sup>3</sup>/h per toilet needs to be provided. These flow rates may be met by transferring air from adjacent rooms and not necessarily by supplying outdoor air.

Application examples are given in Annex A.

Apart from specifying minimum flow rates, the regulation also imposes that a control system must be in place at least meeting class IDA-C3 (time control). This means that systems without control or with only a manually controlled switch are not allowed. Furthermore, supply and exhaust design flow rates don't need to be balanced, as long as an imbalance doesn't cause an underpressure larger than 5 Pa, or an overpressure larger than 10 Pa at building level. Finally, the regulation Annexes impose a maximum specific fan power that cannot be larger than class SFP-3 (< 0.4 W/(m<sup>3</sup>/h)). This requirement was abandoned in Flanders after 2014, since auxiliary energy use was already covered in the overall energy performance requirements (E-level, see §3).

In addition to the regional legislation on energy performance, there is a federal law "Codex on Well-Being at Work" (2017) which also imposes ventilation requirements, specifically for spaces where workers are employed. The requirements for ventilation came into force in 2020 for new buildings, and imposed the development of action plans for existing buildings to meet the requirements when planning renovations. As a result the Codex has had a stronger impact on the design of ventilation systems for non-residential buildings, than ventilation guidelines in older legislation for employment protection. In many non-residential buildings, the Codex leads to larger flow rates compared to the requirements for IDA3 in the energy performance regulations, thus in that case the Codex is decisive for the required design flow rates.

The Codex requires the employer to take the necessary measures to ensure that the CO<sub>2</sub>-level in the workspace remains below 900 ppm or to ensure a ventilation flow rate of 40 m<sup>3</sup>/h per person present in the workspace. The CO<sub>2</sub>-concentration requirement should be met during 95% of the occupation time, and assuming an outside concentration of 400 ppm. If the outdoor concentration is higher, the difference between 400 ppm and the actual outdoor concentration can be taken into account.

As an alternative, if the employer can demonstrate that pollution sources affecting indoor air quality have been eliminated or significantly reduced, e.g. by applying low-emission materials, the CO<sub>2</sub> requirement may be relaxed to 1200 ppm, or the minimum flow rate to be ensured amounts to 25m<sup>3</sup>/h per person present. The employer needs to seek advice from the relevant prevention adviser and committee in this case. The pollution sources mentioned in the Codex include building materials, flooring, finishing, furniture, equipment and cleaning of the workspace, among others. However, in practice, based on the methods and product information currently available in Belgium, it is sufficient that only floor coverings meet legal requirements for VOC-emissions, including formaldehyde (FOD WASO 2019, Belgian Government 2014).

## 2 NATIONAL TRENDS IN ENERGY REQUIREMENTS AND MARKET

### 2.1 Energy requirements

The energy requirements concern both energy efficiency of the building and indoor climate (summer comfort and ventilation), and are specified in a number of sub-requirements to which all new and renovated buildings have to comply:

- thermal insulation: maximum U-value of building envelope components and maximum overall heat loss coefficient
- maximum E-level (measure for total primary energy use of the project)
- minimum ventilation requirements
- maximum value of overheating indicator (summer comfort), only for residential buildings

The influence of ventilation is taken into account in the calculation of the heat loss coefficient of the building, and has an influence on the calculated E-level and overheating indicator. As a consequence energy performance requirements have an impact on ventilation system selection and design. There are two calculation procedures: one for residential buildings, and one for non-residential buildings. The following parameters, related to ventilation, can be taken into account (\* = residential only, \*\* = non-residential only):

- Design flow rate\*\* (for dwellings the flow rate is a function of the building volume only, regardless of design flow rates or system types)
- Building function\*\*: defines function specific operation time of ventilation, e.g. 100% for patient rooms in health care, 30% for offices or schools.
- Heat recovery: temperature efficiency, automatic flow control to balance air flow rates, summer by-pass
- Demand control (see §4)
- Fan energy use
- Ventilative cooling (opening of windows, increased mechanical ventilation rates\*\*, night ventilation\*\*, earth-to-air heat exchanger, evaporative cooling)
- Pressure controlled trickle ventilators\*
- Correctly commissioned flow rates\*
- Ductwork airtightness\*

As can be observed, these parameters not only involve system or product selection, made in the design stage, but also parameters that are a result of high quality installation and commissioning work. In between 2010 and 2021 the energy performance requirements saw a tightening to move towards nearly zero energy buildings, with the E-level to be achieved in new dwellings shifting from E100 to E30. As a consequence, energy efficient ventilation techniques received more and more attention.

### 2.2 Other drivers in energy performance

The recognition of EPB product data is a service that the Regions offer to all stakeholders with the aim of providing user-friendly product data that provides legal certainty for calculations in the context of the EPB regulations (Caillou 2017). The recognition of EPB product data is based on a voluntary scheme with procedures that ensure that the product data will be accepted without reservation by the administrations. This data is collected in a EPBD product database [www.epbd.be](http://www.epbd.be) and will never be questioned by the three Belgian regions when checking EPB declarations. It includes performance data of over 1000 ventilation components and systems:

- Trickle ventilators
- Air handling units and fans
- Demand controlled residential ventilation systems (DCV)

As an example Figure 2 shows the performance data of air handling units for balanced mechanical ventilation with heat recovery available in the database. There are data of units with a flow rate of up to 8000 m<sup>3</sup>/h, but since the majority of systems in the database are for residential applications the figure is restricted to units below 1500 m<sup>3</sup>/h. The comparison between systems with recognised data until 2023 and after 2024, don't show a systematic better performance for newer systems. The specific fan power was calculated as the ratio of maximum fan power (2 fans) and maximum ventilation flow rate documented in the database. The data show a large variation in SFP with only a small share meeting the SFP-3 class (< 0.4 W/(m<sup>3</sup>/h)).

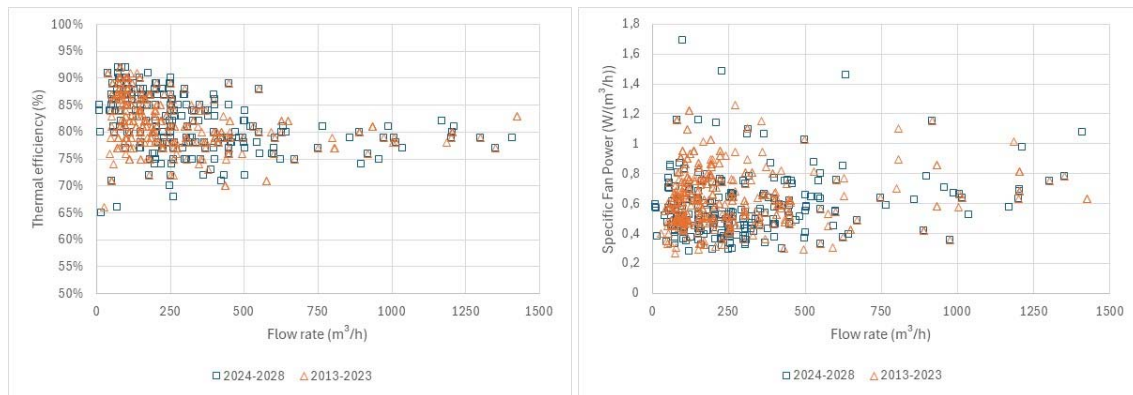


Figure 2: Performance data of air handling units for balanced mechanical ventilation with heat recovery: thermal efficiency of heat recovery system (left), and specific fan power (right) as a function of ventilation flow rate.

The performance of DCV is taken into account by means of a control factor which expresses the ratio between the ventilation heat loss in the DCV system and the ventilation heat loss in a reference system with constant air flow (CAV). In the energy performance calculation method for dwellings 60 different classes of DCV are described each with a predefined control factor varying in between 0.35 for systems with local CO<sub>2</sub>-control of supply flow rates and local control of extraction rates in all spaces, and 0.95 for systems without specific control of supply flow rates and with central control of extraction rates (Caillou et al. 2014, Flemish Government 2018). For non-residential buildings DCV control factors are related to the control classes defined in NBN EN 13779 with values ranging from 0.70 (IDA-C6, direct control e.g. CO<sub>2</sub>) to 1.00 (IDA-C3, time control).

### 3 NATIONAL TRENDS IN THE INSPECTION OF VENTILATION SYSTEMS

#### 3.1 Requirements on the inspection of ventilation systems

Since 2016, the Flemish government has been focusing on improving the quality of ventilation systems in residential buildings. As a result, two documents have been required [28] as of January 1st 2016: (1) a ventilation preliminary design (VPD) before the start of the construction works and (2) a ventilation performance report (VPR) after the construction works have been completed. Both are mandatory in Flanders for all new residential buildings and all residential buildings undergoing a deep energy renovation.

The preliminary design of the ventilation system comprises a floor plan with indication of all ventilation components, including the position of the ventilation unit, the position and the

indicative diameter of the ductwork. Details can be found in a separate document (STS Werkgroep 2017a).

The ventilation performance report is so far the only mandatory document that relates to the ventilation system after it has been installed and thus it is the only document requiring an inspection. The result is an objective overview of the as-built energy related performances of the installation which must be used as a reference in the energy performance reporting of the dwelling (STS Werkgroep 2017b).

There are no obligations about inspection of ventilation systems for non-residential buildings. Although in the Brussels Capital region and Walloon region a reporting of the ventilation performance is necessary as part of the energy performance reporting of the building, no formal inspection framework is implemented there.

The key document is the “unified technical specifications for ventilation in residential buildings” (STS-P 73-1 2015). In these STS-P, the criteria for ventilation systems that could be prescribed and could be reported are listed. STS-documents are edited by the Belgian Federal Public Service for Economy and can thus be applied in the three regions in Belgium. In complement to the STS-P, technical guidance for installers was developed (Caillou & Van den Bossche 2016).

The STS-P does not prescribe requirements for the ventilation system, but lists possible evaluation criteria for ventilation systems and how to prescribe and determine the performance of the ventilation system for each of the criteria. For example, the STS-P does not impose or advice a certain specific fan power of the system (SFPsystem), but it defines the formula for calculating the SFPsystem, the classes, and the method for measuring the power consumption of the ventilation unit. It is then up to the builder to define which class of SFPsystem should be reached and to the ventilation inspector to determine the actual class of SFPsystem.

Different levels of requirements may apply to a ventilation system, e.g. the energy performance regulation sets only minimal ventilation flows, but a builder could require better IAQ, so higher ventilation flows. Therefore the output of the ventilation inspection is not a declaration of conformity to a requirement, but a report (the VPR) with objective data and figures about the performance of the ventilation system such as (neither exhaustive, nor applicable to all):

- per room the measured air flow or the nominal air flow of air inlets,
- the efficiency of the heat recovery unit,
- the power consumption of the fan at nominal air flow,
- the description of the demand controlled ventilation system,

The main concern within the inspection framework is the correct reporting of the performances of the ventilation systems. There is a system of auditing the ventilation reporters, described more in detail by De Strycker et al. (2019) to guarantee that the content of the VPR is representing the actual situation of the ventilation system at the moment of inspection.

### **3.2 Inspection protocols**

The ventilation performance report must be compiled by one or more qualified ventilation reporters and delivered by a company, recognised by one of the organisers of a quality framework, which are recognised by the authorities.

The qualification procedure for the reporters includes:

- Optional theoretical training
- Theoretical exam for each component of the ventilation system
- For reporters qualified for measuring mechanical air flows a practical exam

Apart from passing the required exams and being recognised by an organiser of a quality framework there are no restrictions on who can compile the VPR. Mostly installers, energy performance reporters and airtightness measurers are acting as ventilation reporters.

In December 2017 and October 2020, the Flemish government has tightened the requirements for organisers of the quality framework for the inspection of residential ventilation systems. The organiser of a quality framework must have a qualification procedure for ventilation inspectors, which includes at least an optional training, and a mandatory theoretical and practical exam. The organiser must guarantee the reliability of the ventilation reporting by running desktop and on-site audits combined with effective enforcement. Minimal random annual desk and on-site audits is 10% each. Random checks are supplemented by targeted checks so that 90% of the active inspectors are checked at least once a year. He has to develop a database gathering all measurement data that can be consulted by the authorities. He should not have any members or directors who also carry out ventilation reporting in the context of the regulation.

Two types of measurement devices are necessary for the inspection: flow measurement devices and a power meter for the power consumption of the fan(s). The air flow measuring method used, must have a measurement deviation that does not exceed 15% of the measured flow value. The device must be calibrated every two years (BCCA 2024). The requirements for the power meter are defined by ministerial decree (Flemish Government 2018). It is not mandatory to measure and report the power of the fans, but it is strongly recommended and is done in the majority of cases. When the performance of the ventilation system is not conform the energy performance regulations, a penalty defined by the Flemish authorities is defined. Ventilation systems not conforming the requirements set by the builder are handled by contractual law.

#### **4 IMPACT OF THE COVID-19 PANDEMIC**

Belgium has passed a law in 2022 aiming to enhance the indoor air quality in publicly accessible spaces in the aftermath of the COVID-19 pandemic (FOD Health, 2022). Part of this legislation focusses on raising awareness about indoor air quality in the general population as they are often not aware of the risks linked to high pollutant concentrations indoors. This law, among other things, requires publicly accessible spaces to apply a CO<sub>2</sub> meter, defines two reference levels for IAQ based on the requirements of the Codex, and will provide an official label and underlying certification procedure that allows publicly accessible spaces to quantifiably showcase the efforts done to maintain good Indoor Air Quality (IAQ).

Since then, the Belgian Federal Public Health Service has been developing the more detailed, practical implementation of this new law, in consultation with stakeholders and research institutes. Originally it was the intention to have all necessary royal decrees ready to be able to bring into force all elements of the law by 2025. However a change in law has postponed the mandatory entry into force until 2038. Meanwhile, operators of publicly accessible spaces may implement elements of the law on a voluntary basis. To this end, Royal Decrees establishing requirements for CO<sub>2</sub>-meters and air cleaners have been published in 2024.

#### **5 ANNEX A: EXAMPLES OF MANDATORY FLOWRATES**

##### **5.1 Dwellings**

House of 90 m<sup>2</sup> (2.5m height), 1 main room (32 m<sup>2</sup>), 3 bedrooms (1 master (2 adults, 12 m<sup>2</sup>), 2 kids (10 m<sup>2</sup> each)), 1 kitchen (12 m<sup>2</sup>), 1 bathroom (4 m<sup>2</sup>) and 1 toilet (2 m<sup>2</sup>)

- Total minimum supply flow rate: 230 m<sup>3</sup>/h
  - Main room: 115 m<sup>3</sup>/h
  - Master bed room: 43 m<sup>3</sup>/h



- Children rooms: 36 m<sup>3</sup>/h each
- Total minimum extract flow rate: 125 m<sup>3</sup>/h
  - Kitchen: 50 m<sup>3</sup>/h
  - Bathroom: 50 m<sup>3</sup>/h
  - Toilet: 25 m<sup>3</sup>/h

Apartment of 50 m<sup>2</sup>, 1 main room (24 m<sup>2</sup>), 1 bedroom (12 m<sup>2</sup>), 1 kitchen open to the main room (8 m<sup>2</sup>), 1 bathroom with toilet (4 m<sup>2</sup>)

- Total minimum supply flow rate: 130 m<sup>3</sup>/h
  - Main room: 87 m<sup>3</sup>/h
  - Bedroom: 43 m<sup>3</sup>/h
- Total minimum extract flow rate: 125 m<sup>3</sup>/h
  - Open kitchen: 75 m<sup>3</sup>/h
  - Bathroom with toilet: 50 m<sup>3</sup>/h

## 5.2 Non-residential

A classroom of 50 m<sup>2</sup> with 25 students, 1 teacher:

- Based on ventilation requirements EPB: minimum ventilation rate = 572 m<sup>3</sup>/h (26 occupants with 22 m<sup>3</sup>/h/person; design occupation is larger than nominal occupation of 13 persons (50 m<sup>2</sup> with max. 4 m<sup>2</sup> per person), so the design occupation is decisive)
- Based on ventilation requirements Codex:
  - If low-emission class room: minimum ventilation rate = 650 m<sup>3</sup>/h (26 occupants with 25 m<sup>3</sup>/h/person)
  - Otherwise: minimum ventilation rate = 1040 m<sup>3</sup>/h (26 occupants with 40 m<sup>3</sup>/h/person)
    - Another flow rate can be estimated based on the requirement of maximum CO<sub>2</sub>-concentration of 900 ppm and an estimate of CO<sub>2</sub>-emission rate for the expected metabolism and age of occupants.

An office of 12 m<sup>2</sup> with 1 occupant:

- Based on ventilation requirements EPB: minimum ventilation rate = 22 m<sup>3</sup>/h (design occupation is equal to nominal occupation (12 m<sup>2</sup> with max. 15 m<sup>2</sup> per person))
  - If the office would be larger than 15m<sup>2</sup>, then the nominal occupation would become 2 persons and be decisive, even if the design occupation is 1. In this case the minimum flow rate would become 44 m<sup>3</sup>/h, and the EPB requirement would be larger than the Codex requirements.
- Based on ventilation requirements Codex:
  - If low-emission office: minimum ventilation rate = 25 m<sup>3</sup>/h
  - Otherwise: minimum ventilation rate = 40 m<sup>3</sup>/h
    - Another flow rate can be estimated based on the requirement of maximum CO<sub>2</sub>-concentration of 900 ppm and an estimate of CO<sub>2</sub>-emission rate for the expected metabolism and age of occupant.

## 6 REFERENCES

BCCA. (2024). Praktische uitdagingen bij het opmeten van ventilatiedebieten, versie 2.5.

[https://www.ikventileerverstandig.be/wp-content/uploads/2024/02/PraktischeUitdagingen\\_V025.pdf](https://www.ikventileerverstandig.be/wp-content/uploads/2024/02/PraktischeUitdagingen_V025.pdf)

Belgian Government (2014), *Royal Decree establishing the threshold levels for emissions to the indoor environment from construction products for certain intended uses*, C-2014/24239.

- Belgian Government (2017), Codex over het welzijn op het werk (Codex on well-being at work) <https://www.ejustice.just.fgov.be/eli/wet/2017/04/28/2017A10461/justel>
- Belgian Government (2022). Wet betreffende de verbetering van de binnenluchtkwaliteit in gesloten plaatsen die publiek toegankelijk zijn, C-2022/34199. [https://www.ejustice.just.fgov.be/cgi\\_loi/change\\_lg.pl?language=nl&la=N&cn=202210604&table\\_name=wet](https://www.ejustice.just.fgov.be/cgi_loi/change_lg.pl?language=nl&la=N&cn=202210604&table_name=wet)
- Caillou, S., Heijmans, N., Laverge, J., & Janssens, A. (2014). Development of an evaluation methodology to quantify the energy potential of demand controlled ventilation strategies. *35th AIVC Conference Proceedings*, 587–596. Poznan. AIVC.
- Caillou, S., Van den Bossche, P. (2016). TV 258 - Praktische gids voor de basisventilatie systemen voor woongebouwen. WTCB
- Caillou S. (2017), Voluntary scheme and database for compliant and easily accessible EPC product input data in Belgium, *Towards compliant building airtightness and ventilation systems*, AIVC Contributed Report 16.
- De Strycker, M., Van Gelder, L., Andrzejewicz, M., Leprince, V. (2019). Quality framework for residential ventilation systems in Flemish Region in Belgium – feedback after three years' experience. *40th AIVC Conference Proceedings*, 832-842. Ghent. AIVC.
- Energiebesluit (2010) (Flemish Region), <https://www.vlaanderen.be/epb-pedia/epb-regelgeving/energiebesluit-en-bijlagen>
- Environnement Brussels (2024) (Brussels Capital Region), <https://environnement.brussels/pro/reglementation/textes-de-loi/legislation-coordonnee-de-la-reglementation-travaux-peb>
- Flemish Government. (2018). Bijlagen bij het MB van 28 december 2018. <https://www.vlaanderen.be/epb-pedia/epb-regelgeving/ministeriele-besluiten-energieprestatieregelgeving/bijlagen-van-het-mb-van-28-december-2018>
- FOD WASO (2019), *Praktijkrichtlijn 'binnenluchtkwaliteit in werklokalen'* (Practical guideline 'indoor air quality in workrooms', Federal Public Service Employment, Labor and Social Dialogue, in Dutch) [https://werk.belgie.be/nl/themas/welzijn-op-het-werk/arbeidsplaatsen/basiseisen#toc\\_heading\\_3](https://werk.belgie.be/nl/themas/welzijn-op-het-werk/arbeidsplaatsen/basiseisen#toc_heading_3)
- Guide PEB (2015) (Walloon Region), <https://energie.wallonie.be/fr/guide-peb-2015.html?IDC=9491>
- Institut Belge de Normalisation (1991), *NBN D50-001 – Ventilation systems for housings*.
- Institut Belge de Normalisation (2004), *NBN EN 13779 - Ventilation for non-residential buildings – Performance requirements for ventilation and room-conditioning systems*.
- STS P 73-1 (2015). Systemen voor basisventilatie in residentiële toepassingen. [https://assets.vlaanderen.be/image/upload/v1664213769/STS-P-73-1-Systemen-basisventilatie-residentiele-toepassingen\\_sjmqxc.pdf](https://assets.vlaanderen.be/image/upload/v1664213769/STS-P-73-1-Systemen-basisventilatie-residentiele-toepassingen_sjmqxc.pdf)
- STS Werkgroep (2017a). Werkgroepdocument A, Ventilatievoorontwerp (VVO), Aanvulling op STS-P 73-1: Systemen voor basisventilatie in residentiële toepassingen. [https://assets.vlaanderen.be/image/upload/v1664214013/STS-P\\_73-1Ventilatie-WerkgroepdocumentA-ventilatievoorontwerp9februari2017\\_aaz0yi.pdf](https://assets.vlaanderen.be/image/upload/v1664214013/STS-P_73-1Ventilatie-WerkgroepdocumentA-ventilatievoorontwerp9februari2017_aaz0yi.pdf)
- STS Werkgroep (2017b). Werkgroepdocument B, Ventilatieprestatieverslag (VPV), Aanvulling op STS-P 73-1: Systemen voor basisventilatie in residentiële toepassingen. [https://assets.vlaanderen.be/image/upload/v1664214128/STS-P\\_73-1Ventilatie-WerkgroepdocumentB-ventilatieprestatieverslag\\_ch3xwh.pdf](https://assets.vlaanderen.be/image/upload/v1664214128/STS-P_73-1Ventilatie-WerkgroepdocumentB-ventilatieprestatieverslag_ch3xwh.pdf)
- Van Hove M., Delghust M. & Janssens A. (2021). *Analysis of the feasibility of statistical models that can predict energy use in homes based on building parameters*. Study ordered by Flemish Energy Agency (in Dutch). [https://assets.vlaanderen.be/image/upload/v1665674115/Analyse\\_haalbaarheid\\_statistische\\_modellen\\_die\\_energiegebruik\\_woningen\\_voorspellen\\_obv\\_gebouwparameters\\_guxvuv.pdf](https://assets.vlaanderen.be/image/upload/v1665674115/Analyse_haalbaarheid_statistische_modellen_die_energiegebruik_woningen_voorspellen_obv_gebouwparameters_guxvuv.pdf)

# Trends in building ventilation requirements and inspection in France

Valérie Leprince<sup>\*1</sup>, Gaëlle Guyot<sup>2</sup>, Laure Mouradian<sup>3</sup>

1 Cerema  
2 rue Antoine Charial  
69003 Lyon, France

\*Corresponding author: Valerie.leprince@cerema.fr

2 Cerema  
BPE research team  
46 rue St Théobald 38081  
L'Isle d'Abeau, France

3 Cetiat  
25 Avenue des arts  
69100 Villeurbanne, France

## SUMMARY

French regulation regarding residential ventilation dates from 1982. Almost every new residential buildings constructed since then are equipped with a mechanical ventilation system. For non-residential buildings, the regulation dates from 1979 and does not impose the installation of a ventilation system as a prescriptive requirement. Nevertheless, if air renewal relies only on windows opening, a significant windows area is necessary (according to the floor area) for the building to be considered compliant with the regulation. This paper is a short summary of a VIPaper that will be published on the AIVC website with the same title.

## KEYWORDS

Ventilation, regulation, France

## 1 RESIDENTIAL BUILDINGS

The French Regulation for residential buildings ventilation mainly relies on the « *Arrêté du 24 mars 1982 relatif à l'aération des logements* »<sup>1</sup>. This text gives requirements on ventilation system in every new dwelling since 1982.

Its main requirements are:

- Overall and continuous air renewal,
- Air inlets (natural or mechanical) in main rooms, which can be adjustable or self-adjustable but cannot be closed.
- Air exhausts in kitchen, bathroom(s), toilet and any utility room.
- Ventilation system must be able to reach given air flow rates
- Minimum flowrate must be maintained continuously depending on whether the system is demand-control (with a technical accreditation)

In practice, those requirements defined above have usually been achieved by using centralized-mechanical exhaust-only systems. Those systems have two-stages exhaust rates in kitchens (the user switch to maximum flowrate pushing a button, or pulling a string). Cooker-hood are not mandatory, they are assumed not to be needed thanks to this two-stages flowrate, usually recirculation cooker-hood are installed in order to comply with EP-requirements on airtightness.

---

<sup>1</sup> J.O., « Arrêté du 24 mars 1982 relatif à l'aération des logements » (1983).

Almost all new residential buildings with exhaust-only ventilation are equipped with a humidity-based demand control system. The humidity regulation is, most of the time, not done through sensors but mechanically, thanks to a humidity-sensible tress, inside inlets and exhaust devices, that adjusts their opening size.

Table 1 : Installed system in new dwellings in the last 10 years according to the French database of airtightness data<sup>2</sup>

	Single houses	Multi-family dwellings
None	0%	0%
Other	1%	1%
Heat recovery	3%	1%
Extract only (constant flowrate)	2%	4%
Extract only, HR -demand control on extraction	4%	3%
Extract only, HR demand control on extraction and inlet	89%	91%

Table 2: Ventilation systems in France Building Stocks (air.h 2007 + INSEE 2017)

	Total dwelling stock (in million)	Ratio
No ventilation	3560	10%
Room by room ventilation	10760	31%
Overall natural ventilation	6058	17%
Overall mechanical ventilation	14437	42%

Given the high rate of non-conformity observed, the energy performance regulation RE2020 imposes since January 2023 a mandatory inspection of the ventilation systems for every new residential buildings. This inspection shall be performed by a qualified tester (by qualification named “Qualibat 8741”).

The inspection is mandatory only once at commissioning.

Every control performed shall be recorded by the tester on an online platform<sup>3</sup> that provides general statics on the performance of ventilation systems.

## 2 NON-RESIDENTIAL BUILDINGS:

The French regulation about non-residential buildings ventilation mainly relies on the “code du travail” (work code) for building occupied with workers (article R.4212-1 until R. 4222-21) and on the “Règlement sanitaire Départemental Type” (named RSDT) article 62 to 66 linked to the “Code de la santé publique” (Public Health Code), for any buildings (inc. receiving public).

These two regulations (RSDT and Work code) define air flow rates. Work code applies in new or existing buildings if workers are in it. RSDT applies to any new building built after 1979 (including those with workers).

Those two codes make the distinction between rooms with no specific source of pollution such as classrooms, dormitories, offices, cinemas, restaurants, sports buildings etc. In those rooms there is a requirement on the supply air flow rate. And rooms with specific air pollution

<sup>2</sup> Bassam Moujalled, Valérie Leprince, et Adeline Bailly Mélois, « French database of building airtightness, statistical analyses of about 215,000 measurements: impacts of buildings characteristics and seasonal variations », in *Proceedings of the 39th AIVC conference « Smart ventilation for buildings »* (39th AIVC conference « Smart ventilation for buildings », Antibes Juan-Les-Pins, France, 2018).

<sup>3</sup> <https://www.observatoire-national-ventilation.developpement-durable.gouv.fr/>

sources such as bathrooms, showers, toilets, laundry, commercial kitchen. In those rooms there is a requirement on the extracted air flowrate.

Either a ventilation system is installed (mechanical or natural) or if the windows area in each room is sufficient it is considered that air replacement can be done through airing and the installation of a ventilation system is not required.

Table 3: Air flow rates for non residential buildings, required by health code and work code

Kind of enclosure	Qmin (m <sup>3</sup> /h) per occupant	
	Health code	Work code
School	15	-
High-school and university	18	-
Sleeping spaces (dormitory, etc.)	18	-
Office rooms	18	25
Meeting rooms	18	30
Shops	22	
Bar and restaurant	22	30
Gymnasium (per athlete)	25	
Swimming pool	22	
Gymnasium (per onlooker)	18	
Workshop and light physical work areas	-	45
Other workshops	-	60

AIR.H estimated in a 2007 study for ADEME that more than 57% of the square meter surface of the French stock of commercial buildings was equipped with an overall ventilation system or air handling unit.

About half of offices, shops and education buildings have as yet no ventilation system.

There is no mandatory inspection for non-residential buildings.

### 3 REFERENCES

J.O. Arrêté du 24 mars 1982 relatif à l'aération des logements (1983).

# Trends in building ventilation requirements and inspection in Ireland

Marie Coggins<sup>1</sup>, Brian McIntyre<sup>\*2</sup>, Simon Jones<sup>3</sup>, and James McGrath<sup>4</sup>

*School of Natural Sciences & Ryan Institute,  
University of Galway,  
Galway,  
H91TK33,  
Ireland*

*Sustainable Energy Authority of Ireland,  
Three Park Place, Hatch Street Upper,  
Dublin 2, D02 FX65,  
Ireland*

*Air Quality Matters,  
Crowsgrove, Kildavin,  
Bunclody,  
Wexford, Y21 RC67  
Ireland*

*Department of Experimental Physics,  
Maynooth University,  
Maynooth, Co. Kildare,  
W23 F2H6,  
Ireland*

## SUMMARY

This VIP paper provides a background regarding building ventilation regulations and inspection requirements in Ireland. Ventilation requirements for new buildings are provided in the National Building Regulations, which apply to the whole of the Republic of Ireland.

The Building Regulations came into force in Ireland on the 1st June 1992. The Building Regulations 1997 - 2022 set out the legal requirements in Ireland for the construction of new buildings (including houses), extensions to existing buildings as well as for material alterations and certain material changes of use to existing buildings. The Building Regulations are set out in a series of functional requirements, listed under the Second Schedule to the Regulations.

The related Technical Guidance Documents (Parts A - M respectively) provide technical guidance on how to comply with the Regulations in practical terms. Part L gives the requirements relating to the Conservation of Fuel and Energy in buildings and Part F gives the requirements relating to Ventilation.

The impetus for the amendments in 2019 were two fold, the increased focus on improving the energy performance of the building stock, and recognition of the important role of ventilation to optimise health and indoor air quality in energy-efficient buildings.

## 1 NATIONAL TRENDS

In Ireland, ventilation requirements for new buildings (and major renovations) are outlined in the Building Regulations, Part F (S.I. No. 263/2019 Building Regulations (Part F Amendment) Regulations 2019 (1) published by the Irish Department of Housing, Local Government and Heritage. Ventilation requirements for existing buildings, undergoing a retrofit are published by the National Standards Authority of Ireland in NSAI S.R. 54:2014&A2:2022 Code of Practice for the Energy Efficient Retrofit of Dwellings (2).

### 1.1 New Buildings

The Building Regulations apply to the design and construction of a new building or an extension, or a major renovation to an existing building. Part F of the Building Regulations applies to ventilation and was last revised in 2019 and has two Requirements, F1 and F2. F1 specifically refers to means of ventilation for people in buildings, and F2 refers to provisions to prevent excessive condensation in a roof.

A Technical Guidance Document F (TGD F) (1), provides guidance in relation to the application of Part F of the Building Regulations and the minimum provisions to meet ventilation requirements in non-complex buildings of normal design and construction with different ventilation strategies. Section 1.2 of TGD F deals with ventilation methods for new dwellings and extensions including continuous mechanical extract ventilation, mechanical ventilation with heat recovery and natural ventilation. Section 1.3 of TGD F deals with ventilation methods for buildings other than dwellings, in particular, offices and car parks.

An additional guidance document on the Installation and Commissioning of Ventilation Systems for Dwellings-Achieving Compliance with Part F 2019 (3) is referenced in TGD F. It provides installation guidance for ventilation systems as defined by TGD F and provides guidance on how to achieve compliance with Part F of the Building Regulations.

## **1.2 Existing Buildings**

In the case of material alterations or change of use of existing buildings, the adoption without modification of the guidance in TGD F may not, in all circumstances, be appropriate. In particular, the adherence to guidance, including codes, standards or technical specifications, intended for application to new work may be unduly restrictive or impracticable.

NSAI S.R. 54:2014 & a2:2022 is a Code of Practice for the Energy Efficient Retrofit of Dwellings that provides guidance for these dwellings (2). This guide provides specific guidance on ventilation in existing dwellings undergoing an energy retrofit.

## **2. REQUIREMENTS ON VENTILATION OF NON-RESIDENTIAL BUILDINGS**

Requirements for the ventilation of non-residential buildings are outlined in Part F of the Second Schedule to the Building Regulations (1), which provides for ventilation requirements in buildings other than dwellings. Such Regulations are mandatory.

A general ventilation rate of 10l/s per occupant for buildings is deemed appropriate where there are no significant pollutant levels. This rate is based on controlling body odours with low levels of other pollutants. Where there are significant levels of other pollutants, adequate outdoor air supply can be achieved by following the calculation method provided in CIBSE Guide A.

## **3. REQUIREMENTS ON THE INSPECTION OF VENTILATION SYSTEMS**

Requirements for inspection of ventilation systems are mandatory (for residential dwellings) and are covered in the National Standards Authority of Ireland Ventilation Validation Registration Scheme. Checks and measurement methods broadly follow the guidance given in I.S. EN 14134:2019 Ventilation for buildings – Performance testing and installation checks of residential ventilation systems.

### **KEYWORDS**

Ventilation Regulations Standards Guidance Inspection

## **2 REFERENCES**

1. Department of Housing, Local Government and Heritage, (Technical Guidance documents A-K <https://www.gov.ie/en/collection/d9729-technical-guidance-documents/?referrer=http://www.housing.gov.ie/housing/building-standards/tgd-part-d-materials-and-workmanship/Technical-guidance-documents#> (accessed February 2024)
2. S.R. 54:2014 Code of practice for energy efficient retrofit of dwellings (Amendment 2). [https://shop.standards.ie/en-ie/standards/s-r-54-2014-a2-2022-877610\\_saig\\_nsai\\_nsai\\_3214983/](https://shop.standards.ie/en-ie/standards/s-r-54-2014-a2-2022-877610_saig_nsai_nsai_3214983/) (accessed February 2024)

# Trends in building ventilation requirements and inspection in Spain

Pilar Linares-Alemparte<sup>1\*</sup>, Sonia García-Ortega<sup>1</sup>, Fernando Feldman<sup>2</sup>

*1 Instituto de las ciencias de la construcción  
Eduardo Torroja - CSIC  
4, Serrano Galvache St.  
Madrid, Spain  
\* Corresponding author*

*2 Aire Limpio  
143, Paseo de la Castellana.  
Madrid, Spain*

## ABSTRACT

In Spain, the construction sector has undergone significant changes over the last twenty years due to new ventilation standards driven by increased awareness of indoor air quality (IAQ) and energy efficiency, as well as environmental policies.

The *Código Técnico de la Edificación* (Building Code, CTE) (*Gobierno de España*, 2006) has been the main regulation governing the quality of buildings since 2006, addressing all related aspects, including energy efficiency and IAQ. The CTE includes provisions aimed at promoting adequate IAQ in residential buildings, while also limiting energy demand across all building types.

Furthermore, it is worth noting that since 1998, the *Reglamento de Instalaciones Térmicas de los Edificios* (Regulation on thermal systems in buildings, RITE) (*Gobierno de España*, 2021) has been setting the standards for IAQ in non-residential buildings.

It is important to acknowledge that both regulations are continuously evolving to keep up with advances in techniques and knowledge, as well as to ensure compliance with European Directives.

This paper is a summary of AIVCVIP 48.1 (Linares-Alemparte, P. et al, 2024) covering the following national trends:

- IAQ requirements and market,
- inspection of ventilation systems, and
- innovative systems and market.

## 1 NATIONAL TRENDS IN IAQ REQUIREMENTS AND MARKET

### 1.1 Requirements on ventilation of dwellings

As mentioned above, mandatory requirements on ventilation of dwellings are set in the CTE in Section HS 3 *Calidad del aire interior* (Indoor air quality). The current version dates from 2017.

Requirements for dwellings are established to be able to control pollutants generated by buildings' users, materials and furnishment. This way, indoor CO<sub>2</sub> concentration is set as the indicator of IAQ related to users' activities and, in addition to this, a minimum ventilation flow is required to extract pollutants derived from building materials, finishes and furnishment.



Therefore, taking CO<sub>2</sub> as an indicator, the following performance-based requirements must be fulfilled by means of simulation at design level (it is not required to demonstrate fulfilment via on site measurement) or by the use of minimum constant ventilation flows taken as accepted solutions:

- CO<sub>2</sub> average annual concentration in each room must not exceed 900 ppm,
- CO<sub>2</sub> annual accumulated over 1,600 ppm must not exceed 500,000 ppm·h, and
- minimum flow rate of 1.5 l/s per habitable room during periods of non-occupancy.

**Simulation** should be conducted under design conditions such as number of occupants, occupancy scenarios, weather conditions, CO<sub>2</sub> production rate, annual average outdoor CO<sub>2</sub> concentration, airtight envelope and doors in closed position. These design conditions are set out in Appendix C of Section HS 3.

For each room the minimum constant ventilation flowrates that perform as **accepted solutions** are displayed in Table 1, depending on the type of dwelling according to the number of bedrooms. These constant flowrates meet the performance-based requirements under the above design conditions.

Table 1. Minimum constant ventilation flowrates for dwellings (Table 2.1 of Section HS3, CTE)

Type of dwelling	Minimum constant ventilation flowrates (l/s)				
	Dry rooms			Wet rooms	
	Master bedroom	Bedrooms	Dining and living room	Global	Per room (kitchen and bathrooms)
0 or 1 bedrooms	8	-	6	12	6
2 bedrooms	8	4	8	24	7
≥ 3 bedrooms	8	4	10	33	8

Fresh air must be supplied to dry rooms and stale air must be extracted from wet rooms. Accordingly, two ventilation flows must be calculated using Table 1: total supply flow and total exhaust flow. Both flows must be balanced, so the biggest one is taken as the total ventilation flow for the design of the system.

## 1.2 Ventilation systems in residential buildings stock and market

According to population and housing census (INE, 2021) of the *Instituto Nacional de Estadística* (National Statistics Institute), in 2021 the total number of dwellings was 26,623,708, including 3,837,328 that were empty and 2,514,511 with sporadic use.

Regulations and standards in Spain have had a significant influence on the ventilation systems market, contributing to its sustained growth. In recent years, this market has experienced remarkable growth, driven mainly by increasing awareness of IAQ and regulatory updates.

Although there are not official statistics on the type of ventilation systems installed in dwellings, from 2006, when CTE was approved and came into force, all new dwellings must have a mechanical or hybrid ventilation system, with fully natural ventilation not allowed. In the DB HS3 hybrid ventilation is defined as a system designed to operate in accordance with the principles of natural ventilation when the atmospheric pressure and temperature conditions are favourable, and to function with a mechanical exhaust when they are unfavourable.

In general, the most widespread ventilation system in newly built dwellings in Spain consists of a hybrid centralised exhaust fan placed on the roof at the end of the vertical ventilation stack located in the wet rooms together with windows with micro-ventilation placed in the dry rooms to allow the inlet of fresh air. The micro-ventilation system is a device integrated into the window frame, usually tilt-and-turn, that is activated by the window handle leaving an opening of between 4 and 5 millimetres around the perimeter of the active window sash. It allows a small but permanent air flow.

Although air inlets such as trickle vents are also permitted in the CTE to supply fresh air, there is some rejection of their use because some of them do not have the means to be completely closed. In spite micro-ventilation not being the best way for delivering fresh air because it has to be operated manually and occupants are mostly unaware of its operation, developers and designers rather implement it because it does not arise as much rejection as air inlets.

The second most common ventilation system in newly built dwellings in Spain is the single-flow mechanical system. It usually consists of an exhaust fan which can be centralised, placed on the roof, or individual, placed in each dwelling in the suspended ceiling of one of the bathrooms. The fan is connected through ducts to all wet rooms. For the supply of fresh air, both micro-ventilation and air inlets can be used.

In more advanced cases, mechanical double-flow systems are used, where stale air is exhausted like in the previous system, but fresh air is taken from outside through a heat recovery unit and supplied to the dry rooms via a duct network. This latter system tends to be a smart and demand-controlled ventilation system (DCV). The deployment of DCV remains relatively uncommon, with the exception of humidity-controlled ventilation systems in dwellings.

In existing dwellings built before 2006, natural ventilation is the most widespread ventilation system. It is based on thermal buoyancy through a vertical ventilation stack in combination with airing, opening and closing windows, and infiltration through the building envelope, mainly joinery. The exploratory study carried out in recent years on the IAQ in traditionally ventilated dwellings based on natural ventilation (Garcia-Ortega, Sonia et al, 2023) has revealed that 50% of these existing dwellings would not satisfy the current IAQ parameters of the CTE.

For renovation, it is very common in Spain to install hybrid roof-mounted extractor fans at the top of vertical ventilation stacks.

The use of air filters and cleaners in dwellings is not generalized.

### **1.3 Requirements on ventilation of non-residential buildings**

Mandatory requirements on ventilation of non-residential buildings are set in the RITE.

These buildings must have a ventilation system for providing enough outdoor air flowrate that avoids, in rooms with human activity, the accumulation of high concentration of pollutants according to Table 2, that establishes four IAQ categories (IDA) depending on the use of the building. Procedure from EN 13779 (CEN, 2008) can be used to fulfil this requirement.

Table 2. IAQ categories (RITE)

IAQ categories	Examples
IDA 1 (optimal)	Hospitals, kindergardens
IDA 2 (good)	Offices, museums, classrooms
IDA 3 (average)	Shops, cinemas, restaurants, gyms
IDA 4 (poor)	Laundry rooms

In order to fulfil such categories, RITE establishes 5 different methods for the calculation of the needed outdoor rate:

- airflow per occupant indirect method,
- airflow per net floor area indirect method,
- perceived air quality direct method,
- CO<sub>2</sub> concentration direct method, and
- dilution method.

According to the airflow per occupant indirect method, for habitable rooms, minimum ventilation flow rates are set out for each IDA (See Table 3).

Table 3. Minimum ventilation flowrates for each IDA (Table 1.4.2.1 of RITE)

IDA Categories	dm <sup>3</sup> /(s per person)
IDA 1	20
IDA 2	12,5
IDA 3	8
IDA 4	5

According to the net floor area indirect method, for non-habitable rooms, minimum ventilation flowrates are set out for each IDA (See Table 4).

Table 4. Minimum ventilation flowrates for each IDA (Table 1.4.2.4 of RITE)

IDA Categories	dm <sup>3</sup> /(s m <sup>2</sup> )
IDA 1	Non applicable
IDA 2	0,83
IDA 3	0,55
IDA 4	0,28

The perceived air quality direct method is based on CR 1752 (CEN, 2008). It is hardly used due to its complexity.

The CO<sub>2</sub> concentration direct method can be used for premises with a high metabolic activity such as party halls, sport and leisure centres, as CO<sub>2</sub> is a good indicator of human bioeffluent emissions (See table 5).

Table 5. Indoor-outdoor CO<sub>2</sub> concentration difference for each IDA (Table 1.4.2.3 of RITE)

IDA Categories	ppm (*)
IDA 1	350
IDA 2	500
IDA 3	800
IDA 4	1.200

\* CO<sub>2</sub> concentration (in parts per million by volume) above CO<sub>2</sub> concentration in outside air

Dilution method follows the specifications established in EN 13779 (CEN, 2008). When there are known emissions of specific polluting materials, the dilution method shall be used.

In addition to this, RITE establishes filtration requirements based on outdoor (ODA) and indoor (IDA) air quality, requiring efficient filtration systems in areas with poor air quality (ODA3) or high indoor standards (IDA1/IDA2). Air filters and purifiers have become key to maintaining healthy spaces, reducing airborne contaminants.

#### **1.4 Ventilation systems in non-residential buildings stock and market**

According to the *Ministerio de Transportes, Movilidad y Agenda urbana* (Ministry of Transport, Mobility and Urban Agenda) the building stock in Spain for non-residential use is close to 2 million properties as stated by the statistics of the *Catastro* (Real Estate Cadastre).

Regulations and standards in Spain have had a considerable influence on the ventilation market, contributing to its sustained growth. During 2022, this market experienced a remarkable growth, mainly driven by the increasing awareness of indoor air quality and the regulatory updates in place.

There is no specific information on the number of buildings in Spain that are equipped with a ventilation system. However, there are several regulations and recommendations regarding ventilation systems, which suggests that there is a significant focus on ensuring adequate ventilation in buildings.

As per a market analysis carried out by AFEC (Air Conditioning Equipment Manufacturers Association) (AFEC, 2023):

- the market in air distribution and diffusion increased by 19.7% from 2021 to 2022,
- the Air Handling Units and Ventilation Units market also increased by approximately 10% from that same period,
- the residential ventilation market and the industrial/tertiary ventilation market increased 13.7% and 17.5% respectively. These categories represent 20.3% of the total revenue in 2022 from HVAC products.

Spain's market features mechanical filters such as HEPA, electronic filters (e.g., ionisers, precipitators), gas-phase filters (as activated carbon), and UVGI. The use of mechanical ventilation and autonomous equipment or filters in central air systems is encouraged in order to reduce the inhalation of aerosols in indoor spaces.

## **2 NATIONAL TRENDS IN THE INSPECTION OF VENTILATION SYSTEMS**

### **2.1 Requirements on the inspection of ventilation systems**

RITE regulates both initial and periodic assessments of ventilation systems. It is a mandatory regulation covering all buildings with thermal installations.

### **2.2 Inspection protocols**

In Spain, inspections of thermal installations must be carried out by authorised companies or inspection entities. Inspection entities may inspect their own installations (first party), act on behalf of the buyer (second party) or represent a third party like an insurance company or the government. Accredited entities, complying with the EN ISO/IEC 17020 (CEN-ISO, 2012) provide maximum assurance of technical competence.

These inspections evaluate the system's integrity, cleanliness design adequacy, operational efficiency, and various parameters such as airflow, pressure, ductwork airtightness, power consumption, indoor air quality, noise levels, and thermal comfort parameters.

Heating, ventilation, and air conditioning systems should undergo inspections every four years, with a comprehensive check of the thermal installation every fifteen years. Maintenance must align with established schedules and equipment specifications. Part of the maintenance involves indoor air pollution measurements per UNE 171330 (UNE, 2014) and hygienic assessments of duct networks as per UNE 100012 (UNE, 2005).

These inspections rely on precise measuring devices capable of assessing air flow type and velocity, and air contamination levels. These devices must be user-friendly and accurate for optimal system tuning.

Detected non-conformities are classified by severity and managed through a methodology that includes detection, immediate repair, cause analysis, corrective and preventive actions, follow-up, and verification for effective resolution.

### **3 NATIONAL TRENDS IN INNOVATIVE SYSTEMS AND MARKET**

In Spain, innovation in ventilation systems focuses on improving indoor air quality, energy efficiency, acoustics, thermal comfort, installation, maintenance, and cost reduction, with a special focus on smart ventilation. Trends indicate a strong focus on digitalisation and energy transition, as well as advanced metering and monitoring of systems. The adoption of smart ventilation systems helps buildings to become more sustainable and healthier, with optimised energy use and increased comfort for users.

Innovation in the ventilation sector faces regulatory barriers such as strict energy efficiency standards, complex and costly certification processes, regional differences in regulations and lack of standardisation. These challenges could limit flexibility in the adoption of new technologies and slow down the introduction of innovative products to the market.

The potential of these innovations lies in their ability to significantly transform both the energy performance of buildings and the well-being of their occupants (De Arriba Segurado, P., 2020)

#### **3.1 Innovative systems and Building Code**

The CTE contains the so-called *Documentos Básicos* (Basic Documents), which include deemed-to-satisfy solutions and performance-based requirements for compliance with the essential requirements established in CTE.

Innovative systems and solutions may deviate to a greater or lesser extent from the deemed-to-satisfy solutions of the DBs, but they must demonstrate compliance with the essential requirements. Compliance may be verified through a technical approval process.

In the case of innovative ventilation systems in dwellings, prior to the 2017 amendment to Section HS 3, compliance with the essential requirements could only be achieved by comparing its performance with the one provided by accepted solutions based on constant flow rates.

In 2017, the essential requirement was quantified as a function of CO<sub>2</sub> plus a minimum flow rate during non-occupancy. This made it easier for innovative systems to demonstrate compliance with CTE.

In the case of innovative ventilation systems in buildings other than dwellings, the RITE describes IAQ according to CO<sub>2</sub> concentration, so assessment can be conducted by comparing provided IAQ with it.

### **3.2 Procedure for the assessment of innovative systems: National Technical Approval**

In Spain, there are three organisations authorised by the competent Public Administrations to provide technical approval assessments of the performance of innovative products or systems that facilitate the application of the CTE. These are the *Instituto de ciencias de la construcción Eduardo Torroja* (Eduardo Torroja Construction Sciences Institute, IETcc), the *Institut de Tecnologia de la Construcció de Catalunya* (Catalonia Institute of Construction Technology, ITeC) and the *Fundación Tecnalia Research & Innovation* (Tecnalia).

The *Documento de Idoneidad Técnica* (National Technical Approval, DIT) is a voluntary document which is issued by the IETcc that contains a favourable technical assessment of the fitness for use of non-traditional or innovative materials, products, systems or procedures in building and/or civil engineering.

In the field of ventilation systems, there are currently three valid DITs on humidity-controlled ventilation systems in dwellings. This system automatically regulates the amount of air intake and exhaust based on the relative humidity of the indoor air (strongly influenced by human presence and activity) and optionally by occupancy detection, always ensuring a minimum level of ventilation. Intake vents are located in dry rooms (living rooms, dining rooms, bedrooms) and exhaust vents in wet rooms (kitchens, bathrooms, toilets and laundry rooms).

The verification of compliance with CO<sub>2</sub> quantification and minimum flow rate of Section HS 3 is carried out through simulation under design conditions. Occupancy criteria are established based on the parameters outlined in Appendix C of Section HS 3, while also considering variations in outdoor temperature and humidity.

## **4 CONCLUSION**

IAQ regulations in Spain are performance-based leading the most advanced regulations in the world. The IAQ requirement in dwellings is identified in terms of CO<sub>2</sub> concentration as an indicator. The main advantage of performance-based regulations is that they allow the use of innovative, energy efficient systems to fulfil the requirement. The requirements may be met through the utilisation of simulation or the implementation of minimum ventilation flow rates, which have been established as accepted solutions (see Table 1).

Ventilation market in Spain is a relatively recently arisen one but is strong and keeps increasing.

## **5 ACKNOWLEDGEMENTS**

This work was supported by the *Consejo Superior de Investigaciones Científicas* and the *Ministerio de Transportes, movilidad y agenda urbana* of Spain.

## **5 REFERENCES**

AFEC (2023). *Informe anual de mercado: Climatización y HVAC*.  
<https://www.afec.es/es/mercado-2023>

CEN. CR 1752:1998 IN Ventilation for buildings - Design criteria for the indoor environment

CEN-ISO. EN ISO/IEC 17020: 2012 Conformity assessment - Requirements for the operation of various types of bodies performing inspection.

De Arriba Segurado, Pilar (2020). Energy renovation of buildings in Spain and the EU. Odyssee-Mure. Enerdata.

<https://www.odyssee-mure.eu/publications/policy-brief/spanish-building-retrofitting-energy-efficiency.html#:~:text=Currently%2C%20the%20housing%20stock%20in,of%20the%20Real%20Estate%20Cadastre>

García-Ortega, S., & Linares-Alemparte, P. (2023). Calidad del aire interior en viviendas ventiladas de forma natural en España. *Informes De La Construcción*, 75(572), e519. <https://doi.org/10.3989/ic.6447>

Gobierno de España. *Real Decreto* 314/2006, March 17<sup>th</sup>.

<https://www.codigotecnico.org/DocumentosCTE/DocumentosCTE.html>

Gobierno de España. *Real Decreto* 178/2021, March 23<sup>rd</sup>.

<https://www.boe.es/eli/es/rd/2007/07/20/1027/con>

Instituto Nacional de Estadística, INE (2021). *Population and housing census*.

<https://www.ine.es/en/index.htm>

Linares-Alemparte, P., García-Ortega, S., Feldman, F., Romero-Fernández, A., Sorribes-Gil, M. and Villar-Burke, R. (2024). *AIVCVIP 48.1. Trends in building ventilation requirements and inspection in Spain*.

<https://www.aivc.org/resource/vip-481-trends-building-ventilation-requirements-and-inspection-spain?volume=33977>

UNE. UNE 171330-2: 2014 *Calidad ambiental en interiores. Parte 2: Procedimientos de inspección de calidad ambiental interior*.

UNE. UNE 100012: 2005 *Higienización de sistemas de climatización*.

# Design of ventilative cooling systems using Ventilative cooling standards; design steps and corresponding flow diagram

Beat Frei<sup>\*1</sup> and Paul D O'Sullivan<sup>2</sup>

*1 FREI WÜEST EXPERT  
Independent Consulting Engineer  
CH-6130 Willisau, Switzerland*

*2 Department of Process, Energy & Transport  
Engineering  
Munster Technological University  
Rossa Avenue, Bishopstown, Cork, Ireland*

*\*Corresponding author:  
[beat.frei@frei.expert](mailto:beat.frei@frei.expert)*

## SUMMARY

Ensuring an indoor environmental quality that is acceptable to the majority of users, while also being energy efficient is a challenge. In addition, both user demands and the climate change are making it even more difficult to ensure good indoor environmental quality. One of the solutions to combat climate change is free cooling systems, such as ventilative cooling.

One of the challenges for the design of ventilative cooling systems in general has been the lack of technical documents, such as standards dealing with the design process for free cooling systems such as Ventilative cooling. Another challenge has been that HVAC engineers have to get used to dealing with natural ventilation and ventilative cooling, as these technologies are not (only) based on mechanical principles. They may be reluctant to use these technologies because they threaten traditional fixed-fee design services and this needs to be addressed.

Therefore this article presents eight design steps to follow as part of the new forthcoming European Technical Specification "Ventilative Cooling Systems – Design" for the holistic design of ventilative cooling systems in buildings starting from the definition of performance criteria and requirements to the final definition of controls and operations. This design process should be used by e.g. HVAC engineers or architects.

## KEYWORDS

Design, ventilative cooling, performance-based, prescriptive, prevention, modulation, dissipation

## 1 INTRODUCTION AND BACKGROUND

Today's design processes are based on many years of experience with complex, multidisciplinary construction projects. The specialists involved are integrated sequentially. This makes it possible to implement classic core applications such as mechanical ventilation and/or mechanical cooling in a pre-defined design phase in any building.

90% of a person's life is spent in buildings, which account for 40% of primary energy consumption. At the same time, user requirements and the outside climate are constantly changing. Ensuring an indoor environment that is acceptable to the majority of users and can be provided in an energy efficient manner is a challenge. Reducing the primary energy consumption of buildings is a societal imperative.

The challenges described above are leading designers and system providers of HVAC solutions to offer their customers natural ventilation, hybrid ventilation and ventilative cooling. With these concepts, the building should provide the occupants with an acceptable and energy-efficient indoor environment. The building must therefore be able to respond to rapidly changing external climatic conditions with some delay.



Modern HVAC concepts do not start in the pre-project phase, but already in the feasibility study phase. The HVAC engineer therefore becomes part of an integral design team, involved from the start of the project according to the phases. This implies a holistic view of the building project, as the interaction with the building envelope is essential.

Knowledge of key terms such as thermal mass, solar shading, window area ratio and free-running temperature is essential for the HVAC engineer. Free-running temperature occurs when the building is occupied without heating or mechanical cooling.

Heating and cooling bring the room temperature into the contractually agreed comfort range. The HVAC engineer is used to assuming constant room temperatures over time, as this is the goal of conventional heating and cooling technologies. HVAC engineers need to adapt their thinking to variable temperature ranges rather than fixed values, and to dynamic rather than static processes.

They must learn to deal with uncertainty and combine it with criteria for acceptable deviations from target and contract values. In addition, the client needs to create a contractual framework that takes into account the fact that target values cannot be checked on the day the system is handed over.

The HVAC engineer needs to get used to dealing with natural ventilation and ventilative cooling, as these technologies are not (only) based on mechanical principles. They may be reluctant to use these technologies because they threaten traditional fixed fee design services. Furthermore, hybrid solutions are often the most energy efficient and cost-effective so a combination of ventilative cooling and mechanical cooling is a good solution for future buildings in the climate change scenarios we are looking at.

The effect of buoyancy and wind pressure, the daily variation of the external temperature, the overall dynamic processes and the handling of uncertainties are new challenges for HVAC engineers.

## 2 THE DESIGN PROCESS OF VENTILATIVE COOLING

The design process for ventilative cooling is iterative and integrative. In the forthcoming European Technical Specification called “Ventilative Cooling Systems – Design” the following design process for ventilative cooling is used:

1. Setting performance criteria and requirements
2. Specifying design assumptions, prevention and modulation strategies
3. Evaluate the ventilative cooling potential
4. Defining an ventilation principle and dissipation techniques
5. Develop a ventilation strategy (air flow distribution path) for ventilative cooling
6. Re-evaluate prevention and modulation interventions
7. Determine supplementary cooling for development during design
8. Defining controls and operation

The order of key decisions may depend on the building type or project specific requirements. Re-evaluate the thermal comfort performance of the building at each design stage. Once the ventilative cooling system has been designed, document the specifications and layout (e.g. drawings, plans). It is also important to define the project objectives in consultation with the client.

Below the eight design steps are detailed:

### 1. Setting performance criteria and requirements

Depending on the design assumptions the complexity level of the appropriate performance requirements might differ. In this point also the project objectives shall be defined in agreement with the client, together with the performance criteria and requirements.

- **Prescriptive approach** includes primary ventilation requirements expressed in the form of airflow rates and corresponding descriptive technical requirements (i.e. an air flow rate can be described/assessed by an opening area, fx. a window opening area)
- **Performance-based approach** includes primary ventilation requirements expressed in the form of airflow rates or in the form of thermal comfort criteria

Possible criteria for thermal comfort can be for example predicted mean vote and percentage of dissatisfied, exceedance hours or temperature ranges (weighted or non-weighted). Temperature ranges can be calculated using the adaptive comfort approach, which fully supports the use of ventilative cooling in buildings.

## **2. Specifying design assumptions, prevention and modulation strategies**

Parameters designers should make assumptions about or collect information about:

- Building typography and surroundings
- Outdoor environment (soundscape, air quality)
- Weather data (current (design) and future scenarios): Wind velocity and direction, temperature, humidity, solar irradiation
- Occupancy (user, usage schedule)
- Internal and external heat loads (internal gains, External window solar shading)
- Building thermal inertia (thermal mass)
- Spatial considerations (floor space, ceiling height)
- (Unobstructed) airflow paths/pattern
- Space demand for installations

## **3. Evaluate the ventilative cooling potential**

In the initial feasibility phase, the efficacy of ventilative cooling shall be evaluated. The design of a ventilative cooling system is an iterative process, and if the potential for ventilative cooling is limited and/or the thermal comfort requirements are not met, the initial design concept shall be reviewed in order to determine the optimal course of action prior to the installation of supplementary and/or mechanical cooling as part of the so-called cooling ladder, where passive measures are first explored before more energy-intensive active solutions are used.

## **4. Defining an ventilation principle and dissipation techniques**

A variety of ventilative cooling systems can be employed, with either a natural or mechanical driving force, or a combination of the two (i.e., hybrid). Dissipation techniques at the building level can be either ventilative cooling or supplementary cooling. Dissipation techniques at the room level, with user control, are preferable, such as ceiling fans, table fans, and wall switches to control windows/louvres.

## **5. Develop a ventilation strategy (air flow distribution path) for ventilative cooling**

The ventilation strategy is a comprehensive plan that defines the pathway of air within a building in order to achieve adequate ventilation and/or cooling. This is distinct from the field of hygienic ventilation. The aforementioned ventilation strategy is described in greater detail in the ventilation concept, which also outlines the potential ventilative cooling systems that could be implemented based on the specific requirements of the building in question. The ventilation concept is developed during the feasibility phase and presented to the client for discussion. In the subsequent design phase, the most suitable ventilative cooling system is selected in collaboration with the client.

## **6. Re-evaluate prevention and modulation interventions**

Ventilative Cooling+ (or VC+) should be clearly defined and refers to additional passive interventions in the architectural design beyond those that have a direct capacity effect on airflow rates, i.e. the ventilative cooling system itself could be operable windows, exhaust stacks or fans. However, additional interventions that minimise the need for cooling in the first place may reduce the target airflow rate. When assessing the potential for passive cooling, a core set of design choices should be evaluated before adding complexity to the solution/strategy.

## **7. Determine supplementary cooling for development during design**

The review should assess the need for interactions between ventilative cooling systems and other cooling systems, such as supplementary and/or mechanical cooling systems. This depends on an assessment of the cooling demand in a given building and the capacities of each type of cooling system. The number of cooling hours in a given building can be calculated using a simulation tool. If different types of cooling are designed in a given building, a combined control of all cooling systems is necessary. A priority list of cooling systems needs to be established for proper control.

## **8. Defining controls and operation**

Reasons for controlling a ventilative cooling system may include

- To match the (often lower) ventilation airflow rate to indoor air quality to meet primary ventilation requirements.
- To adapt the ventilation airflow rate to mitigate low humidity (heating season).
- To adjust the (often higher) ventilation airflow rate to mitigate high temperatures - overheating (cooling season).
- To achieve low energy consumption in the heating or cooling season.
- To reduce the energy consumption of fans.
- To limit pollutant infiltration during outdoor pollution peaks.

- To limit the heating-up power in intermittently heated spaces.
- To protect against weather conditions (e.g. rain) (open windows).
- To adapt the draught rate.

### **3 CONCLUSION**

Ventilative cooling design is a process that considers and investigates the cooling requirements of the building as a whole. Ideally, the free-running temperature of the occupied building should be within the contractually agreed comfort range of the room temperature. Architectural compromises and special use requirements can lead to an undesirable increase in the cooling requirements of the building. The design process for ventilative cooling using the proposed eight design steps can help to counteract and optimise this.

### **4 ACKNOWLEDGEMENTS**

We would like to thank Christoffer Plesner, Jannick Roth, Thomas Hartmann, Jaques Gandini, Jan Deklerck, and last but not least Annamaria Belleri for their excellent and inspiring collaboration in CEN/TC 156 WG 21 Task group "Ventilative Cooling Systems".

### **5 REFERENCES**

*"Ventilative Cooling Systems - Design,"* European Technical Specification (under drafting), European Committee for Standardization (CEN), Brussels, 2024

# A comprehensive overview of ventilative cooling and its role in the standardisation

Christoffer Plesner<sup>\*1</sup>, Jannick K. Roth<sup>2</sup>

1 VELUX A/S  
Ådalsvej 99  
2970 Hørsholm, Denmark

2 WindowMaster International A/S  
Skelstedet 13  
2950 Vedbæk, Denmark

*\*Corresponding author:*  
[christoffer.plesner@velux.com](mailto:christoffer.plesner@velux.com)

## SUMMARY

Ventilative cooling is a free cooling methodology, harnessing the cooling potential of the outdoor air to remove excess heat, without the use of thermodynamic process, thereby saving valuable cooling energy in buildings. In future zero energy buildings it is essential to lower the energy consumption for cooling and here ventilative cooling is one good option. Further, for airflows beyond the basic ventilation requirements to provide cooling can be considered part of the renewable energy calculation as indicated by EU 2022/759 Directive, hence underlining the sustainability aspects of ventilative cooling using outside air for cooling.

Further, in order for ventilative cooling to become an increasingly used technology it is essential to ensure integration into standards, legislation and compliance tools. In standards, this is further complicated by the fact that there are both performance, design and operation standards and here ventilative cooling is not yet present in “design standard”. There are specifically projects ongoing in CEN/TC 156 and ISO/TC 205, to make new “design standards”, ensuring a design methodology to design ventilative cooling systems in buildings. A new methodology for estimating the ventilative cooling potential in the early feasibility phase with 4 different Ventilative cooling modes (0-3), in order to estimate if the outdoor air can be used for cooling, which is presented in the forthcoming European Technical specification called “Ventilative cooling systems - design”.

For legislation and compliance tools there is lacking better integration of air flow predictions and the adaptive comfort approach supporting variable comfort temperatures, depending on the mean running outside temperature.

Ventilative cooling being a free cooling methodology needs to be better supported in standards, legislation and compliance tools and this is done with new standardisation projects and better awareness raising.

## KEYWORDS

Ventilative cooling, standards, legislation, compliance tools, sustainability, renewable energy

## 1 INTRODUCTION

Ventilative cooling is a sustainable and energy-efficient method of cooling buildings that utilizes natural, mechanical or hybrid means to remove excess heat. This process harnesses the cooling potential of outdoor air to reduce indoor temperatures, thereby decreasing the reliance on active cooling systems like air conditioning.

Ventilative cooling can be achieved through various techniques, such as natural means e.g. using cross ventilation, stack ventilation, and night-time cooling, each leveraging different natural forces and building designs to optimize airflow and temperature control. Also mechanical means can be used for ventilative cooling, e.g. through fans driving the air inside through ducts without thermodynamic processes and using the outside air at its current temperature.

Finally, the airflow that is increased beyond the basic ventilation requirements to provide cooling is considered part of the renewable energy calculation, as indicated by the Commission Delegated Regulation (EU) 2022/759 of 14 December 2021 amending Annex VII to Directive (EU) 2018/2001 as regards a methodology for calculating the amount of renewable energy used for cooling and district cooling. This information clearly underlines the sustainability aspects of ventilative cooling.

## 2 THE ROLE OF VENTILATIVE COOLING IN STANDARDS

### 2.1 General

Setting relevant KPI's for overheating targets and having calculation tools are essential for the assessment of ventilative cooling systems. Overheating refers to high indoor temperatures and can affect occupants' health, well-being and productivity. The calculation tools are in this case, tools used to assess the performance of the thermal comfort (overheating) in the building, where it is essential to both have a good early design stage design assessment, as well as a more detailed later on, to not waste time on a detailed concept design that has not been properly evaluated early on.

Standardisation plays a crucial role in promoting the adoption and effectiveness of ventilative cooling. By establishing clear guidelines and best practices, standardization helps ensure that ventilative cooling systems are designed, installed, and operated effectively. Further, standards can be the platform for setting criteria and assessment methods, if referred to in national legislations.

Below are listed some key areas of standardization, which could be split into performance, design and operational standards, as well as regulatory frameworks. Key standardisation types include:

- **Performance standards:** Standards establishing input parameters by setting key performance indicators for thermal comfort to be used for design and assessment of overheating in buildings. This is used to evaluate the performance of ventilative cooling systems and helps in assessing their effectiveness.
  - Example: Draft revision of **EN 16798-1:2019**, which currently is undergoing a revision into 5 parts (e.g. one part on thermal comfort) setting IEQ criteria
- **Design Standards/guidelines:** Standards for building design can incorporate guidelines for optimizing ventilative cooling systems, such as recommendations for design and how to estimate the potential.
  - Example 1: New Work Item (**Ventilative cooling systems – Design:2024, CEN/TS**); focusing on the design process of ventilative cooling systems for acceptable thermal comfort and among other things includes a method to estimate the ventilative cooling potential of the outdoor air in early feasibility phase
  - Example 2: Draft revision of **EN 15665:2024**; focusing on making a design framework for ventilation systems in residential buildings for acceptable IAQ
- **Operational Standards:** Standards for the operation and maintenance of ventilative cooling systems to ensure that they continue to perform efficiently over time. This includes protocols for managing indoor air quality and controlling ventilation based on outdoor conditions.
- **Regulatory Frameworks:** Governments and regulatory bodies can incorporate ventilative cooling standards into building codes and regulations, driving wider adoption and ensuring compliance.

The above shows differences in the types of standards, and the importance is the link and dependencies among each other, where one does not work, without the other. In CEN/TC 156 new Design standards are under development, to guide the designers using a design framework including approaches for design of ventilative cooling systems. The design framework also includes reference to performance standards, such as EN 16798-1 for thermal comfort criteria, e.g. using the categories of the adaptive comfort model for evaluation of ventilative cooling systems during the cooling season.

## **2.2 Identification and impact of missing elements in ventilative cooling systems (in standards and legislation)**

The situation of overheating calculations methods is very complex in Europe. There is a huge disparity between countries and almost no common approach to addressing overheating in residential buildings rigorously.

One of the areas of interest are how to predict the expected "thermal comfort and cooling requirements" when using ventilative cooling in buildings. These may be predicted by using "indicators", which may be based on either static models (e.g. Fanger PMV/PPD model) or adaptive models (e.g. Adaptive comfort model) as e.g. found in EN 16798-1 and others don't [2].

In a broad overheating study on legislations across Europe it was found that most countries heavily rely on the PMV/PPD model that requires active cooling systems, and this should be changed to also support the Adaptive comfort model. Further many countries models households as single zone and doesn't make a distinction between living and sleeping rooms [1].

A background report on status and recommendations to ventilative cooling in standards and legislation concludes that ventilative cooling is not sufficiently integrated in standards, legislation and compliance tools. It also shows that there is a broad field of evaluation methods for ventilative cooling, ranging from simple to detailed that can support a stronger integration of ventilative cooling in the near future [2].

There are many benefits associated with ventilative cooling that are acknowledged, but that still needs to be further implemented into standards, legislation and compliance tools [2]:

- The adequate modelling of natural ventilation and especially of air flows
- The share of the energy used for cooling to provide summer comfort and avoid the overheating risk tends to become equivalent to the energy consumption for heating in winter, depending on the climate
- The adequate prediction of the expected "thermal comfort and cooling requirements", as well as the "energy performance" when using ventilative cooling in buildings (this could be based on Static models e.g. Fanger PMV/PPD model using mechanical cooling or on Adaptive models e.g. adaptive comfort model using ventilative cooling

## **2.3 Status and developments of ventilative cooling (in standards)**

There has generally been missing good ventilative cooling design integration for "system design" and "performance" aspects in existing European standards and legislation and therefore new projects have started up in working groups under CEN/TC 156 and ISO/TC 205. These projects have the aim of developing new documents on ventilative cooling systems to foster motivation and raise awareness.

A new European technical specification (CEN/TS) called “**Ventilative cooling systems – design**” is under development and should be published in 2026 under CEN/TC 156/WG21 with the goal to be the go-to European technical document for how to design natural, mechanical and hybrid ventilative cooling systems. The aim of the new standard is to see how far the designer can get with using ventilative cooling, before going into other cooling solutions by following the eight design steps. In design step #3 the ventilative cooling potential shall be found in the early feasibility phase and here the Ventilative cooling potential method can estimate the cooling potential in 4 different Ventilative cooling modes (#0-3), where VC mode #1 uses Ventilative cooling at low air flow rates and mode #2 at high air flow rates. This method can be used prior to going into the detailed design phase.

When the standard is published it will be complimentary and hopefully become a relevant reference for ventilative cooling in the forthcoming revision of EN 16798-1, named EN 16798-1-3 (for thermal comfort).

### **3 CONCLUSION**

Free cooling solutions like ventilative cooling play a crucial role to address the challenge of increasing energy use in buildings, i.e. a projected 3 fold increase in the global energy consumption for space cooling towards 2030, leading to a 2 fold increase in CO<sub>2</sub> emissions related to cooling [3]. Ventilative cooling is further one of many cooling solutions and relies on the actual outdoor air temperature aiming at mitigating overheating, using natural, mechanical or hybrid means. Further ventilative cooling enhances thermal comfort, reduces cooling loads in buildings and doesn't use thermodynamic process like mechanical cooling.

Ventilative cooling represents a promising approach to enhance indoor environmental quality in buildings. Through effective standardisation, the implementation and optimisation of ventilative cooling systems can be facilitated, ensuring their benefits are realized across diverse building types and climates. As the push for sustainable building practices continues to grow, ventilative cooling will play an increasingly important role in creating energy-efficient and healthy indoor environments.

### **4 ACKNOWLEDGEMENTS**

Thanks to the Venticool (International platform for resilient cooling) for their support for facilitating this workshop [4].

Some of the material presented in this topical session has been collected and developed within IEA Annex 62 on "Ventilative cooling" of the IEA Technology Collaboration Programme: Energy in Buildings and Communities ending in 2018 and is the result of an international joint effort [5].

### **5 REFERENCES**

[1] Shady A. et al.. Overheating calculation methods, criteria, and indicators in European regulation for residential buildings, Energy and Buildings, Volume 292, 2023

[2] Venticool, “Status and recommendations for better implementation of ventilative cooling in standards, legislation and compliance tools (background report)”, 2018;  
[http://venticool.eu/wp-content/uploads/2018/09/venticool\\_ebc62\\_background\\_report.pdf](http://venticool.eu/wp-content/uploads/2018/09/venticool_ebc62_background_report.pdf)

[3] International Energy Agency (IEA), “The Future of Cooling”, 2018,  
[https://iea.blob.core.windows.net/assets/0bb45525-277f-4c9c-8d0c-9c0cb5e7d525/The\\_Future\\_of\\_Cooling.pdf](https://iea.blob.core.windows.net/assets/0bb45525-277f-4c9c-8d0c-9c0cb5e7d525/The_Future_of_Cooling.pdf)

[4] Venticool - the platform for resilient ventilative cooling, [www.venticool.eu](http://www.venticool.eu)

[5] IEA EBC Annex 62 - Ventilative cooling, <https://venticool.eu/information-on-annex-62/annex-62-home/>, 2018



# Early Stage Design of VC: A standardised approach to improve robustness and avoid vulnerability lock-in at the later design stages

Paul O'Sullivan

*1 School of Mechanical, Process & Electrical Engineering, Munster Technological University, Rossa Avenue, Bishopstown, Cork, Ireland*  
[Paul.osullivan@mtu.ie](mailto:Paul.osullivan@mtu.ie)

## SUMMARY

The global increase in building cooling demands poses a challenge for designers striving for net zero energy consumption. The prevalent use of mechanical cooling underscores the necessity for designers to consider Ventilative Cooling as a viable alternative in the early stages of building design. Recent research findings suggest that the pre-design stage has the same influence for promoting Ventilative Cooling strategies as the schematic and detailed design stages for practitioners, yet limited impactful decision making occurs at this stage. We present the latest process flow diagram for early stage evaluation of ventilative cooling strategies and discuss its implementation in terms of the iterative nature of design and the role of the proposed ventilative cooling potential method. We also discuss the different needs of architects and engineers at the early design stages of buildings.

## KEYWORDS

Calibration, modelling, ventilative cooling potential, early stage design

## 1 BACKGROUND

Evaluating design choices at the earliest possible time in the design cycle can reduce both the need for 'design churn' at the later detailed design stages as well as the risk of a 'lock-in' effect where poor design choices become difficult to reverse. Practitioners also have diverging needs where Architects prefer informative guidance and qualitative advice on choices whilst specialist consultants and engineers would be more comfortable with an approach that aims to quantify the performance of the particular design choice. Ventilative Cooling as a strategy for addressing occupant thermal comfort in indoor spaces is a low energy strategy that can be resilient to various external performance threats such as power outages. However its potential to meeting the cooling needs of indoor spaces is limited by the available cooling potential in the ambient air. Further, its performance is typically subject to various design choices linked to site design, building morphology, system and component selections and so on, therefore ensuring a successful design solution requires a multi-disciplinary approach involving Architects, Engineers and specialist designers, with an opportunity at the early design stages to have a strong influence over the adopted strategy. There is currently a lack of availability of 'easy to use' early stage design tools for Architects and Engineers that evaluate the potential for ventilative cooling. Further, any tool or method that might be employed at the early stages of design would need to be 'stress-tested' to ascertain its reliability in predicting the likely performance of a given strategy. While there is no requirement for high accuracy at the early stage there would need to be a reasonable level of robust advice so as not to result in a divergent finding when assessing a more complete version of the strategy at the detailed design stage with a tool such as dynamic whole building energy simulation software.

## 2 EARLY STAGE VENTILATIVE COOLING ASSESMENT

We qualitatively discuss the appropriateness of the VCPM tool as an early stage assessment method. We also present an early stage (or feasibility stage) design process flow diagram which incorporates the VCPM as well as a number of other steps linked to the overall design guidelines within the new European Technical Specification on designing ventilative cooling systems. The

proposed design process incorporates the iterative nature of defining a cooling and ventilation strategy, revising that with the addition of passive interventions (defined under the categories of preventative, modulating and dissipating effects) when the cooling demand prohibits ventilative cooling. It also assists the designers in making choices around supplementary cooling options when read in conjunction with the European Technical Specification document itself. This flow diagram and the corresponding steps shall ensure a coherent way of designing (passive) Ventilative cooling systems in the early design phase before needing to go into more energy consuming systems, such as mechanical cooling systems. The aim of this flow diagram for ventilative cooling design in the CEN/TS is that the designer in Europe will have a platform to actually design ventilative cooling systems, which currently has lacked in European standards and technical specifications.

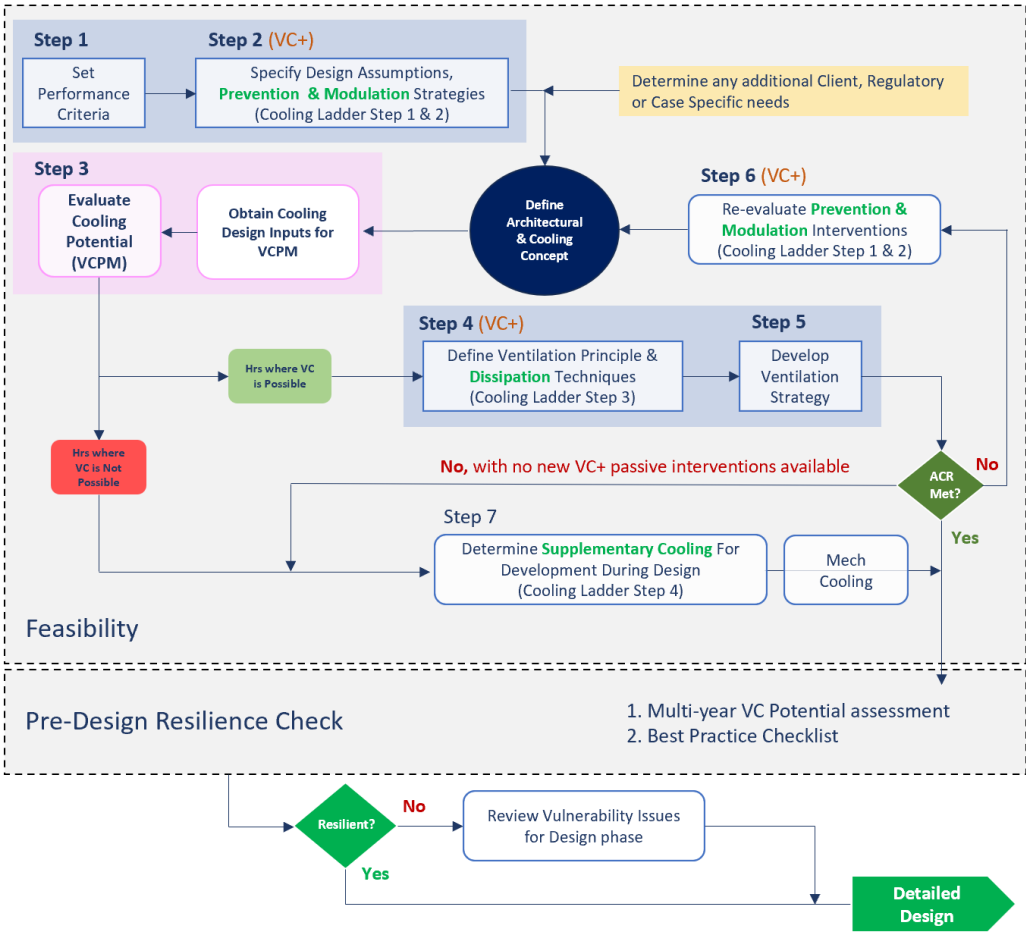


Figure 1: Early stage design process for evaluation of ventilative cooling potential

### 3 ACKNOWLEDGEMENTS

We acknowledge all the collaborative contributions from various participants in the ongoing writing group, namely; Beat Frei (Frei Wuest Expert), Jan Deklerck (Duco), Christoffer Plesner (VELUX A/S), Jannick Roth (WindowMaster International A/S), Thomas Hartmann (ITG Dresden) and others.

This research has been funded by the Sustainable Energy Authority of Ireland (SEAI) RD&D fund 2019, under grant number RDD/00496.